VOLUME 25 / NUMBER 17
SEPTEMBER 8, 1987
ACC. NOS. N87-23570 TO N87-24393

STAR

AN ABSTRACT JOURNAL

Scientific and Technical Aerospace Reports

PRODUCED BY THE
SCIENTIFIC AND TECHNICAL
INFORMATION
OFFICE

NASA

NATIONAL AERONAUTICS AND SPACE ADMINISTRATION

WHAT YOU CAN DO FOR *STAR*

All users of this abstract service are urged to forward reports to be considered for announcement in *STAR*. This will aid NASA in its efforts to provide the fullest possible coverage of all scientific and technical publications that might support aeronautics and space research and development. If you have prepared relevant reports (other than those that you will transmit to NASA, DoD, or DOE through the usual contract- or grant-reporting channels), please send them for consideration to the NASA Scientific and Technical Information Facility, P.O. Box 8757, B.W.I. Airport, Maryland 21240.

Reprints of journal articles, book chapters, and conference papers are also welcome. These will be considered for announcement in *STAR's* companion journal, *International Aerospace Abstracts.*

You may specify a particular source to be included in a report announcement if you wish; otherwise the report will be placed on public sale at the National Technical Information Service. Copyrighted publications will be announced but not distributed or sold.

PURCHASE OF *STAR*

The semimonthly issues are available for sale by the Superintendent of Documents, U.S. Government Printing Office, Washington, D.C. 20402.

PUBLISHED BY:

UNITED STATES GOVERNMENT
NATIONAL AERONAUTICS AND SPACE ADMINISTRATION
SCIENTIFIC AND TECHNICAL INFORMATION OFFICE
Scientific and Technical Aerospace Reports, Volume 25, is prepared by the NASA Scientific and Technical Information Facility operated for the National Aeronautics and Space Administration by RMS Associates.

The Administrator of the National Aeronautics and Space Administration has determined that the publication of this periodical is necessary in the transaction of the public business required by law of this Agency. Use of funds for printing this periodical has been approved by the Director of the Office of Management and Budget through March 22, 1988.

US ISSN 0036-8741

INTRODUCTION

Scientific and Technical Aerospace Reports (STAR) is a major component of a comprehensive National Aeronautics and Space Administration information system covering aeronautics, space, and supporting disciplines. *STAR* is issued on the 8th and 23rd of each month and announces current publications of the following types:

- NASA, NASA contractor, and NASA grantee reports
- Reports issued by other U.S. Government Agencies, domestic and foreign institutions, universities, and private firms
- Translations in report form
- NASA-owned patents and patent applications
- Dissertations and theses

Journal, book, and conference literature, cover-to-cover journal translations, and certain foreign dissertations are announced in a companion journal, *International Aerospace Abstracts (IAA)*, available on subscription from the American Institute of Aeronautics and Astronautics, Technical Information Service, 555 West 57th Street, 12th Floor, New York, New York 10019.

SUBJECT SCOPE

Subject scope of *STAR*, and *IAA* includes all aspects of aeronautics and space research and development, supporting basic and applied research, and applications. Aerospace aspects of earth resources, energy development, conservation, oceanography, environmental protection, urban transportation, and other topics of high national priority are also covered.

OTHER NASA PUBLICATIONS

Other NASA publications and information services are described in the publication, *The NASA Scientific and Technical Information System ... and How to Use It*, available without charge from the NASA Scientific and Technical Information Facility, P.O. Box 8757, B.W.I. Airport, Maryland 21240.

HOW TO USE *STAR* SUBJECT CATEGORIES

STAR is categorized by 10 major subject divisions divided into 76 specific subject categories and one general category/division. The major subject divisions are listed in the Table of Contents, together with a note for each that defines its scope and provides any cross-references. For example:

AERONAUTICS

Includes aeronautics (general); aerodynamics; air transportation and safety; aircraft communications and navigation; aircraft design, testing and performance; aircraft instrumentation; aircraft propulsion and power; aircraft stability and control; and research and support facilities (air).

For related information see also *Astronautics*.

Each major division is further divided into as many as nine specific categories, which are identified by category numbers.

Abstracts in *STAR* are grouped by specific category, the categories appearing in sequential order. Category breaks in the abstract section are identified by the category number and title, and a scope note. Cross-references to other categories are provided as appropriate. For example:

02 AERODYNAMICS

Includes aerodynamics of bodies, combinations, wings, rotors, and control surfaces; and internal flow in ducts and turbomachinery.

For related information see also *34 Fluid Mechanics and Heat Transfer.*

CROSS-REFERENCES

Individual *STAR* abstracts are not ordinarily cross-referenced, except for certain conference reports or book translations that have had separate abstracts written for their component papers or chapters. Citations and abstracts of the components follow immediately after those of the parent document. When the subject content of a component differs sufficiently from the general content of the parent, a cross-reference citation also is printed at the end of the category to which it normally would have been assigned if it were independent.

DOCUMENTS ON MICROFICHE

Documents on microfiche[1] are designated by a pound sign (#) following the accession number. The pound sign is used without regard to the source or quality of the microfiche.

AVAILABILITIES

One or more sources from which a document announced in *STAR* is available to the public is given in each citation. The most commonly indicated sources and their acronyms or abbreviations are listed below. If the publication is available from a source other than those listed, the publisher and his address will be displayed on the availability line or in combination with the corporate source line.

Avail: NTIS. Sold by the National Technical Information Service. Prices for hard copy (HC) and microfiche (MF) are indicated by a price code following the letters HC or MF in the *STAR* citation. Current values for the price codes are given in the tables on page vii.

Initially distributed microfiche under the NTIS SRIM (Selected Research in Microfiche) is available at greatly reduced unit prices. For this service and for information concerning subscription to NASA printed reports, consult the NTIS Subscription Section, Springfield, Va. 22161.

NOTE ON ORDERING DOCUMENTS: When ordering NASA publications (those followed by the * symbol), use the N accession number. NASA patent applications (only the specifications are offered) should be ordered by the US-Patent-Appl-SN number. Non-NASA publications (no asterisk) should be ordered by the AD, PB, or other *report* number shown on the last line of the citation, not by the N accession number. It is also advisable to cite the title and other bibliographic identification.

Avail: SOD (or GPO). Sold by the Superintendent of Documents, U.S. Government Printing Office, in hard copy. The current price and order number are given following the availability line. (NTIS will fill microfiche requests, as indicated above, for those documents identified by a # symbol.)

(1) A microfiche is a transparent sheet of film, 105 by 148 mm in size, containing as many as 60 to 98 pages of information reduced to micro images (not to exceed 26:1 reduction).

Avail: BLL (formerly NLL): British Library Lending Division, Boston Spa, Wetherby, Yorkshire, England. Photocopies available from this organization at the price shown. (If none is given, inquiry should be addressed to the BLL.)

Avail: DOE Depository Libraries. Organizations in U.S. cities and abroad that maintain collections of Department of Energy reports, usually in microfiche form, are listed in *Energy Research Abstracts*. Services available from the DOE and its depositories are described in a booklet, *DOE Technical Information Center - Its Functions and Services* (TID-4660), which may be obtained without charge from the DOE Technical Information Center.

Avail: ESDU. Pricing information on specific data, computer programs, and details on ESDU topic categories can be obtained from ESDU International Ltd. Requesters in North America should use the Virginia address while all other requesters should use the London address, both of which are on page vi.

Avail: Fachinformationszentrum, Karlsruhe. Sold by the Fachinformationszentrum Energie, Physik, Mathematik GMBH, Eggenstein Leopoldshafen, Federal Republic of Germany, at the price shown in deutschmarks (DM).

Avail: HMSO. Publications of Her Majesty's Stationery Office are sold in the U.S. by Pendragon House, Inc. (PHI), Redwood City, California. The U.S. price (including a service and mailing charge) is given, or a conversion table may be obtained from PHI.

Avail: NASA Public Document Rooms. Documents so indicated may be examined at or purchased from the National Aeronautics and Space Administration, Public Documents Room (Room 126), 600 Independence Ave., S.W., Washington, D.C. 20546, or public document rooms located at each of the NASA research centers, the NASA Space Technology Laboratories, and the NASA Pasadena Office at the Jet Propulsion Laboratory.

Avail: Univ. Microfilms. Documents so indicated are dissertations selected from *Dissertation Abstracts* and are sold by University Microfilms as xerographic copy (HC) and microfilm. All requests should cite the author and the Order Number as they appear in the citation.

Avail: US Patent and Trademark Office. Sold by Commissioner of Patents and Trademarks, U.S. Patent and Trademark Office, at the standard price of $1.50 each, postage free. (See discussion of NASA patents and patent applications below.)

Avail: (US Sales Only). These foreign documents are available to users within the United States from the National Technical Information Service (NTIS). They are available to users outside the United States through the International Nuclear Information Service (INIS) representative in their country, or by applying directly to the issuing organization.

Avail: USGS. Originals of many reports from the U.S. Geological Survey, which may contain color illustrations, or otherwise may not have the quality of illustrations preserved in the microfiche or facsimile reproduction, may be examined by the public at the libraries of the USGS field offices whose addresses are listed in this Introduction. The libraries may be queried concerning the availability of specific documents and the possible utilization of local copying services, such as color reproduction.

Avail: Issuing Activity, or Corporate Author, or no indication of availability. Inquiries as to the availability of these documents should be addressed to the organization shown in the citation as the corporate author of the document.

NASA PATENTS AND PATENT APPLICATIONS

Patents and patent applications owned by NASA are announced in *STAR* under appropriate subject categories and are referenced in the *STAR* indexes. In the Report/Accession Number Index, patents are indexed by the NASA Case Number (which appears in lieu of the report number in other indexes), the U.S. Patent Number, the U.S. Patent Application Serial Number, and the U.S. Patent Class. Patent applications for which patents have not yet been issued are indexed by the NASA Case Number and the U.S. Patent Application Serial Number.

NASA *patent application specifications* are sold in paper copy by the National Technical Information Service at price code A02. Microfiche are sold at price code A01. The US-Patent-Appl-SN- number should be used in ordering either paper copy or microfiche from NTIS. Printed copies of *patents* (which are not microfiched) are available for purchase at $1.50 per copy from:

Commissioner of Patents and Trademarks
U.S. Patent and Trademark Office
Washington, D.C. 20231

When ordering patents, the U.S. Patent Number should be used, and payment must be remitted in advance, preferably by money order or check payable to the Commissioner of Patents and Trademarks. Prepaid purchase coupons for ordering are also available from the Patent and Trademark Office. The patents and patent applications announced in *STAR* are owned by NASA and are available for royalty-free licensing. Requests for licensing terms and further information should be addressed to:

Assistant General Counsel for Patent Matters/Code GP
National Aeronautics and Space Administration
Washington, D.C. 20546

ELIGIBILITY AND REGISTRATION FOR NASA INFORMATION PRODUCTS AND SERVICES

A variety of services is available to organizations of the following types that have registered with NASA to receive specific services or products:

1. NASA offices, research centers, contractors, subcontractors, grantees, and consultants;
2. Other U.S. Government agencies and their contractors;
3. Libraries in the United States that have arrangements with NASA to maintain collections of NASA documents for public reference;
4. Other organizations in the United States having a need for NASA documents in work related to aeronautics and space research;
5. Organizations abroad that have established reciprocal document exchange arrangements with NASA.

Only the central service points or central points of document acquisition and control within qualified organizations are eligible to register for NASA products and services. Domestic organizations that may be eligible to receive various classes of NASA publications and services should address their requests for registration or for further information to:

NASA Scientific and Technical Information Facility
ATTN: Registration Activity
P.O. Box 8757
B.W.I. Airport, Maryland 21240

Organizations abroad should direct requests to the same address, but to the attention of: International Exchange Program.

AVAILABILITY OF *STAR* ABSTRACTS ON MICROFICHE

Microfiche of the abstract sections of this issue and other issues of *STAR* are available on annual subscription from NTIS, Attn: Subscriptions, 5285 Port Royal Road, Springfield, Virginia 22161. Annual subscription rates are $70.00 North America; $140.00 foreign. Abstract sections for previous years retroactive to 1964 are available at the current rates. Microfiche for individual *STAR* issue abstract sections are not available.

PUBLIC COLLECTIONS OF NASA DOCUMENTS

DOMESTIC: NASA and NASA-sponsored documents and a large number of aerospace publications are available to the public for reference purposes at the library maintained by the American Institute of Aeronautics and Astronautics, Technical Information Service, 555 West 57th Street, 12th Floor, New York, New York 10019

EUROPEAN: An extensive collection of NASA and NASA-sponsored publications is maintained by the British Library Lending Division, Boston Spa, Wetherby, Yorkshire, England for public access. The British Library Lending Division also has available many of the non-NASA publications cited in *STAR*. European requesters may purchase facsimile copy or microfiche of NASA and NASA-sponsored documents, those identified by both the symbols # and • from ESA - Information Retrieval Service European Space Agency, 8-10 rue Mario-Nikis, 75738 Paris CEDEX 15, France.

FEDERAL DEPOSITORY LIBRARY PROGRAM

In order to provide the general public with greater access to U.S. Government publications, Congress established the Federal Depository Library Program under the Government Printing Office (GPO), with 50 regional depositories responsible for permanent retention of material, inter-library loan, and reference services. At least one copy of nearly every NASA and NASA-sponsored publication, either in printed or microfiche format, is received and retained by the 50 regional depositories. A list of the regional GPO libraries, arranged alphabetically by state, appears on the inside back cover. These libraries are *not* sales outlets. A local library can contact a Regional Depository to help locate specific reports, or direct contact may be made by an individual.

ADDRESSES OF ORGANIZATIONS

American Institute of Aeronautics and Astronautics
Technical Information Service
555 West 57th Street, 12th Floor
New York, New York 10019

British Library Lending Division,
Boston Spa, Wetherby, Yorkshire,
England

Commissioner of Patents and Trademarks
U.S. Patent and Trademark Office
Washington, D.C. 20231

Department of Energy
Technical Information Center
P.O. Box 62
Oak Ridge, Tennessee 37830

ESA-Information Retrieval Service
ESRIN
Via Galileo Galilei
00044 Frascati (Rome) Italy

ESDU International, Ltd.
1495 Chain Bridge Road
McLean, Virginia 22101

ESDU International, Ltd.
251-259 Regent Street
London, W1R 7AD, England

Fachinformationszentrum Energie, Physik, Mathematik GMBH
7514 Eggenstein Leopoldshafen
Federal Republic of Germany

Her Majesty's Stationery Office
P.O. Box 569, S.E. 1
London, England

NASA Scientific and Technical Information Facility
P.O. Box 8757
B.W.I. Airport, Maryland 21240

National Aeronautics and Space Administration
Scientific and Technical Information Office (NTT-1)
Washington, D.C. 20546

National Technical Information Service
5285 Port Royal Road
Springfield, Virginia 22161

Pendragon House, Inc.
899 Broadway Avenue
Redwood City, California 94063

Superintendent of Documents
U.S. Government Printing Office
Washington, D.C. 20402

University Microfilms
A Xerox Company
300 North Zeeb Road
Ann Arbor, Michigan 48106

University Microfilms, Ltd.
Tylers Green
London, England

U.S. Geological Survey Library
National Center - MS 950
12201 Sunrise Valley Drive
Reston, Virginia 22092

U.S. Geological Survey Library
2255 North Gemini Drive
Flagstaff, Arizona 86001

U.S. Geological Survey
345 Middlefield Road
Menlo Park, California 94025

U.S. Geological Survey Library
Box 25046
Denver Federal Center, MS914
Denver, Colorado 80225

NTIS PRICE SCHEDULES

(Effective January 1, 1987)

Schedule A
STANDARD PRICE DOCUMENTS AND MICROFICHE

PRICE CODE	PAGE RANGE	NORTH AMERICAN PRICE	FOREIGN PRICE
A01	Microfiche	$ 6.50	$13.00
A02	001-025	9.95	19.90
A03	026-050	11.95	23.90
A04-A05	051-100	13.95	27.90
A06-A09	101-200	18.95	37.90
A10-A13	201-300	24.95	49.90
A14-A17	301-400	30.95	61.90
A18-A21	401-500	36.95	73.90
A22-A25	501-600	42.95	85.90
A99	601-up	*	*
NO1		45.00	80.00
NO2		48.00	80.00

Schedule E
EXCEPTION PRICE DOCUMENTS AND MICROFICHE

PRICE CODE	NORTH AMERICAN PRICE	FOREIGN PRICE
E01	$ 7.50	15.00
E02	10.00	20.00
E03	11.00	22.00
E04	13.50	27.00
E05	15.50	31.00
E06	18.00	36.00
E07	20.50	41.00
E08	23.00	46.00
E09	25.50	51.00
E10	28.00	56.00
E11	30.50	61.00
E12	33.00	66.00
E13	35.50	71.00
E14	38.50	77.00
E15	42.00	84.00
E16	46.00	92.00
E17	50.00	100.00
E18	54.00	108.00
E19	60.00	120.00
E20	70.00	140.00
E99	*	*

*Contact NTIS for price quote.

IMPORTANT NOTICE

NTIS Shipping and Handling Charges

U.S., Canada, Mexico — ADD $3.00 per TOTAL ORDER

All Other Countries — ADD $4.00 per TOTAL ORDER

Exceptions — Does NOT apply to:

ORDERS REQUESTING NTIS RUSH HANDLING

ORDERS FOR SUBSCRIPTION OR STANDING ORDER PRODUCTS *ONLY*

NOTE: Each additional delivery address on an order requires a separate shipping and handling charge.

VOLUME 25 NUMBER 17 / SEPTEMBER 8, 1987

TABLE OF CONTENTS

AERONAUTICS

Includes aeronautics (general); aerodynamics; air transportation and safety; aircraft communications and navigation; aircraft design, testing and performance; aircraft instrumentation; aircraft propulsion and power; aircraft stability and control; and research and support facilities (air).

For related information see also *Astronautics.*

01 AERONAUTICS (GENERAL) 2277

02 AERODYNAMICS 2279

Includes aerodynamics of bodies, combinations, wings, rotors, and control surfaces; and internal flow in ducts and turbomachinery.

For related information see also *34 Fluid Mechanics and Heat Transfer*

03 AIR TRANSPORTATION AND SAFETY 2282

Includes passenger and cargo air transport operations; and aircraft accidents.

For related information see also *16 Space Transportation* and *85 Urban Technology and Transportation.*

04 AIRCRAFT COMMUNICATIONS AND NAVIGATION 2283

Includes digital and voice communication with aircraft; air navigation systems (satellite and ground based); and air traffic control.

For related information see also *17 Space Communications, Spacecraft Communications, Command and Tracking* and *32 Communications and Radar.*

05 AIRCRAFT DESIGN, TESTING AND PERFORMANCE 2283

Includes aircraft simulation technology.

For related information see also *18 Spacecraft Design, Testing and Performance* and *39 Structural Mechanics.* For land transportation vehicles see *85 Urban Technology and Transportation.*

06 AIRCRAFT INSTRUMENTATION 2284

Includes cockpit and cabin display devices; and flight instruments.

For related information see also *19 Spacecraft Instrumentation* and *35 Instrumentation and Photography.*

07 AIRCRAFT PROPULSION AND POWER 2285

Includes prime propulsion systems and systems components, e.g., gas turbine engines and compressors; and onboard auxiliary power plants for aircraft.

For related information see also *20 Spacecraft Propulsion and Power, 28 Propellants and Fuels,* and *44 Energy Production and Conversion.*

08 AIRCRAFT STABILITY AND CONTROL 2287

Includes aircraft handling qualities; piloting; flight controls; and autopilots.

For related information see also *05 Aircraft Design, Testing and Performance.*

09 RESEARCH AND SUPPORT FACILITIES (AIR) 2288

Includes airports, hangars and runways; aircraft repair and overhaul facilities; wind tunnels; shock tubes; and aircraft engine test stands.

For related information see also *14 Ground Support Systems and Facilities (Space).*

ASTRONAUTICS

Includes astronautics (general); astrodynamics; ground support systems and facilities (space); launch vehicles and space vehicles; space transportation; space communications, spacecraft communications, command and tracking; spacecraft design, testing and performance; spacecraft instrumentation; and spacecraft propulsion and power.

For related information see also *Aeronautics*

12 ASTRONAUTICS (GENERAL) 2292

For extraterrestrial exploration see *lunar and planetary Exploration.*

13 ASTRODYNAMICS 2293

Includes powered and free-flight trajectories; and orbital and launching dynamics.

14 GROUND SUPPORT SYSTEMS AND FACILITIES (SPACE) 2293

Includes launch complexes, research and production facilities; ground support equipment, e.g., mobile transporters; and simulators.

For related information see also *09 Research and Support Facilities (Air).*

15 LAUNCH VEHICLES AND SPACE VEHICLES 2293

Includes boosters; operating problems of launch/space vehicle systems; and reusable vehicles.

For related information see also *20 Spacecraft Propulsion and Power.*

16 SPACE TRANSPORTATION 2294

Includes passenger and cargo space transportation, e.g., shuttle operations; and space rescue techniques.

For related information see also *03 Air Transportation and Safety* and *18 Spacecraft Design, Testing and Performance.* For space suits see *54 Man/System Technology and Life Support.*

17 SPACE COMMUNICATIONS, SPACECRAFT COMMUNICATIONS, COMMAND AND TRACKING N.A.

Includes telemetry; space communications networks; astronavigation and guidance; and radio blackout.

For related information see also *04 Aircraft Communications and Navigation* and *32 Communications and Radar.*

18 SPACECRAFT DESIGN, TESTING AND PERFORMANCE 2294

Includes satellites; space platforms; space stations; spacecraft systems and components such as thermal and environmental controls; and attitude controls.

For life support systems see *54 Man/System Technology and Life Support.* For related information see also *05 Aircraft Design, Testing and Performance, 39 Structural Mechanics,* and *16 Space Transportation.*

19 SPACECRAFT INSTRUMENTATION N.A.

For related information see also *06 Aircraft Instrumentation* and *35 Instrumentation and Photography.*

20 SPACECRAFT PROPULSION AND POWER 2296

Includes main propulsion systems and components, e.g. rocket engines; and spacecraft auxiliary power sources.

For related information see also *07 Aircraft Propulsion and Power, 28 Propellants and Fuels, 44 Energy Production and Conversion,* and *15 Launch Vehicles and Space Vehicles.*

CHEMISTRY AND MATERIALS

Includes chemistry and materials (general); composite materials; inorganic and physical chemistry; metallic materials; nonmetallic materials; propellants and fuels; and materials processing.

23 CHEMISTRY AND MATERIALS (GENERAL) 2299

24 COMPOSITE MATERIALS 2299

Includes physical, chemical, and mechanical properties of laminates and other composite materials.

For ceramic materials see *27 Nonmetallic Materials.*

25 INORGANIC AND PHYSICAL CHEMISTRY 2301

Includes chemical analysis, e.g., chromatography; combustion theory; electrochemistry; and photochemistry.

For related information see also *77 Thermodynamics and Statistical Physics.*

26 METALLIC MATERIALS 2303

Includes physical, chemical, and mechanical properties of metals, e.g., corrosion; and metallurgy.

27 NONMETALLIC MATERIALS 2305

Includes physical, chemical, and mechanical properties of plastics, elastomers, lubricants, polymers, textiles, adhesives, and ceramic materials.

For composite materials see *24 Composite Materials.*

28 PROPELLANTS AND FUELS 2309

Includes rocket propellants, igniters and oxidizers; their storage and handling procedures; and aircraft fuels.

For related information see also *07 Aircraft Propulsion and Power, 20 Spacecraft Propulsion and Power,* and *44 Energy Production and Conversion.*

29 MATERIALS PROCESSING N.A.

Includes space-based development of products and processes for commercial application.

For biological materials see *55 Space Biology.*

ENGINEERING

Includes engineering (general); communications and radar; electronics and electrical engineering; fluid mechanics and heat transfer; instrumentation and photography; lasers and masers; mechanical engineering; quality assurance and reliability; and structural mechanics.

For related information see also *Physics.*

31 ENGINEERING (GENERAL) 2320

Includes vacuum technology; control engineering; display engineering; cryogenics; and fire prevention.

32 COMMUNICATIONS AND RADAR 2320

Includes radar; land and global communications; communications theory; and optical communications.

For related information see also *04 Aircraft Communications and Navigation* and *17 Space Communications, Spacecraft Communications, Command and Tracking.* For search and rescue see *03 Air Transportation and Safety,* and *16 Space Transportation.*

33 ELECTRONICS AND ELECTRICAL ENGINEERING 2328

Includes test equipment and maintainability; components, e.g., tunnel diodes and transistors; microminiaturization; and integrated circuitry.

For related information see also *60 Computer Operations and Hardware* and *76 Solid-State Physics.*

34 FLUID MECHANICS AND HEAT TRANSFER 2333

Includes boundary layers; hydrodynamics; fluidics; mass transfer and ablation cooling.

For related information see aiso *02 Aerodynamics* and *77 Thermodynamics and Statistical Physics.*

35 INSTRUMENTATION AND PHOTOGRAPHY 2339

Includes remote sensors; measuring instruments and gages; detectors; cameras and photographic supplies; and holography.

For aerial photography see *43 Earth Resources and Remote Sensing.* For related information see also *06 Aircraft Instrumentation* and *19 Spacecraft Instrumentation.*

36 LASERS AND MASERS 2341

Includes parametric amplifiers.

For related information see also *76 Solid-State Physics.*

37 MECHANICAL ENGINEERING 2344

Includes auxiliary systems (nonpower); machine elements and processes; and mechanical equipment.

38 QUALITY ASSURANCE AND RELIABILITY 2347

Includes product sampling procedures and techniques; and quality control.

39 STRUCTURAL MECHANICS 2348

Includes structural element design and weight analysis; fatigue; and thermal stress.

For applications see *05 Aircraft Design, Testing and Performance* and *18 Spacecraft Design, Testing and Performance.*

GEOSCIENCES

Includes geosciences (general); earth resources and remote sensing; energy production and conversion; environment pollution; geophysics; meteorology and climatology; and oceanography.

For related information see also *Space Sciences.*

42 GEOSCIENCES (GENERAL) N.A.

43 EARTH RESOURCES AND REMOTE SENSING 2351

Includes remote sensing of earth resources by aircraft and spacecraft; photogrammetry; and aerial photography.

For instrumentation see *35 Instrumentation and Photography.*

44 ENERGY PRODUCTION AND CONVERSION 2352

Includes specific energy conversion systems, e.g., fuel cells; global sources of energy; geophysical conversion; and windpower.

For related information see also *07 Aircraft Propulsion and Power, 20 Spacecraft Propulsion and Power,* and *28 Propellants and Fuels.*

45 ENVIRONMENT POLLUTION 2355

Includes atmospheric, noise, thermal, and water pollution.

46 GEOPHYSICS 2355

Includes aeronomy; upper and lower atmosphere studies; ionospheric and magnetospheric physics; and geomagnetism.

For space radiation see *93 Space Radiation.*

47 METEOROLOGY AND CLIMATOLOGY 2357

Includes weather forecasting and modification.

48 OCEANOGRAPHY 2360

Includes biological, dynamic, and physical oceanography; and marine resources.

For related information see also *43 Earth Resources and Remote Sensing.*

LIFE SCIENCES

Includes life sciences (general); aerospace medicine; behavioral sciences; man/system technology and life support; and space biology.

51 LIFE SCIENCES (GENERAL) 2360

52 AEROSPACE MEDICINE 2361

Includes physiological factors; biological effects of radiation; and effects of weightlessness on man and animals.

53 BEHAVIORAL SCIENCES 2364

Includes psychological factors; individual and group behavior; crew training and evaluation; and psychiatric research.

54 MAN/SYSTEM TECHNOLOGY AND LIFE SUPPORT 2364

Includes human engineering; biotechnology; and space suits and protective clothing.

For related information see also *16 Space Transportation.*

55 SPACE BIOLOGY N.A.

Includes exobiology; planetary biology; and extraterrestrial life.

MATHEMATICAL AND COMPUTER SCIENCES

Includes mathematical and computer sciences (general); computer operations and hardware; computer programming and software; computer systems; cybernetics; numerical analysis; statistics and probability; systems analysis; and theoretical mathematics.

59 MATHEMATICAL AND COMPUTER SCIENCES (GENERAL) N.A.

60 COMPUTER OPERATIONS AND HARDWARE 2365

Includes hardware for computer graphics, firmware, and data processing.

For components see *33 Electronics and Electrical Engineering.*

61 COMPUTER PROGRAMMING AND SOFTWARE 2366

Includes computer programs, routines, algorithms, and specific applications, e.g., CAD/CAM.

62 COMPUTER SYSTEMS 2369

Includes computer networks and special application computer systems.

63 CYBERNETICS 2370

Includes feedback and control theory, artificial intelligence, robotics and expert systems.

For related information see also *54 Man/System Technology and Life Support.*

64 NUMERICAL ANALYSIS 2371

Includes iteration, difference equations, and numerical approximation.

65 STATISTICS AND PROBABILITY 2374

Includes data sampling and smoothing; Monte Carlo method; and stochastic processes.

66 SYSTEMS ANALYSIS 2375

Includes mathematical modeling; network analysis; and operations research.

67 THEORETICAL MATHEMATICS N.A.

Includes topology and number theory.

PHYSICS

Includes physics (general); acoustics; atomic and molecular physics; nuclear and high-energy physics; optics; plasma physics; solid-state physics; and thermodynamics and statistical physics.

For related information see also *Engineering.*

70 PHYSICS (GENERAL) 2376

For precision time and time interval (PTTI) see *35 Instrumentation and Photography;* for geophysics, astrophysics or solar physics see *46 Geophysics, 90 Astrophysics,* or *92 Solar Physics.*

71 ACOUSTICS 2376
Includes sound generation, transmission, and attenuation.
For noise pollution see *45 Environment Pollution.*

72 ATOMIC AND MOLECULAR PHYSICS 2377
Includes atomic structure, electron properties, and molecular spectra.

73 NUCLEAR AND HIGH-ENERGY PHYSICS 2378
Includes elementary and nuclear particles; and reactor theory.
For space radiation see *93 Space Radiation.*

74 OPTICS 2379
Includes light phenomena and optical devices.
For lasers see *36 Lasers and Masers.*

75 PLASMA PHYSICS 2381
Includes magnetohydrodynamics and plasma fusion.
For ionospheric plasmas see *46 Geophysics.* For space plasmas see *90 Astrophysics.*

76 SOLID-STATE PHYSICS 2383
Includes superconductivity.
For related information see also *33 Electronics and Electrical Engineering* and *36 Lasers and Masers.*

77 THERMODYNAMICS AND STATISTICAL PHYSICS 2387
Includes quantum mechanics; theoretical physics; and Bose and Fermi statistics.
For related information see also *25 Inorganic and Physical Chemistry* and *34 Fluid Mechanics and Heat Transfer.*

SOCIAL SCIENCES

Includes social sciences (general); administration and management; documentation and information science; economics and cost analysis; law, political science, and space policy; and urban technology and transportation.

80 SOCIAL SCIENCES (GENERAL) N.A.
Includes educational matters.

81 ADMINISTRATION AND MANAGEMENT 2387
Includes management planning and research.

82 DOCUMENTATION AND INFORMATION SCIENCE 2388
Includes information management; information storage and retrieval technology; technical writing; graphic arts; and micrography.
For computer documentation see *61 Computer Programming and Software.*

83 ECONOMICS AND COST ANALYSIS N.A.
Includes cost effectiveness studies.

84 LAW, POLITICAL SCIENCE AND SPACE POLICY 2390
Includes NASA appropriation hearings; aviation law; space law and policy; international law; international cooperation; and patent policy.

85 URBAN TECHNOLOGY AND TRANSPORTATION 2390
Includes applications of space technology to urban problems; technology transfer; technology assessment; and surface and mass transportation.
For related information see *03 Air Transportation and Safety, 16 Space Transportation,* and *44 Energy Production and Conversion.*

SPACE SCIENCES

Includes space sciences (general); astronomy; astrophysics; lunar and planetary exploration; solar physics; and space radiation.
For related information see also *Geosciences.*

88 SPACE SCIENCES (GENERAL) 2391

89 ASTRONOMY 2393
Includes radio, gamma-ray, and infrared astronomy; and astrometry.

90 ASTROPHYSICS 2411
Includes cosmology; celestial mechanics; space plasmas; and interstellar and interplanetary gases and dust.
For related information see also *75 Plasma Physics.*

91 LUNAR AND PLANETARY EXPLORATION 2414
Includes planetology; and manned and unmanned flights.
For spacecraft design or space stations see *18 Spacecraft Design, Testing and Performance.*

92 SOLAR PHYSICS 2414
Includes solar activity, solar flares, solar radiation and sunspots.
For related information see *93 Space Radiation.*

93 SPACE RADIATION 2415
Includes cosmic radiation; and inner and outer earth's radiation belts.
For biological effects of radiation see *52 Aerospace Medicine.* For theory see *73 Nuclear and High-Energy Physics.*

GENERAL

Includes aeronautical, astronautical, and space science related histories, biographies, and pertinent reports too broad for categorization; histories or broad overviews of NASA programs.

99 GENERAL 2417

Note: N.A. means that no abstracts were assigned to this category for this issue.

SUBJECT INDEX I-1
PERSONAL AUTHOR INDEX I-53
CORPORATE SOURCE INDEX I-61
CONTRACT NUMBER INDEX I-73
REPORT/ACCESSION NUMBER INDEX I-77

TYPICAL CITATION AND ABSTRACT

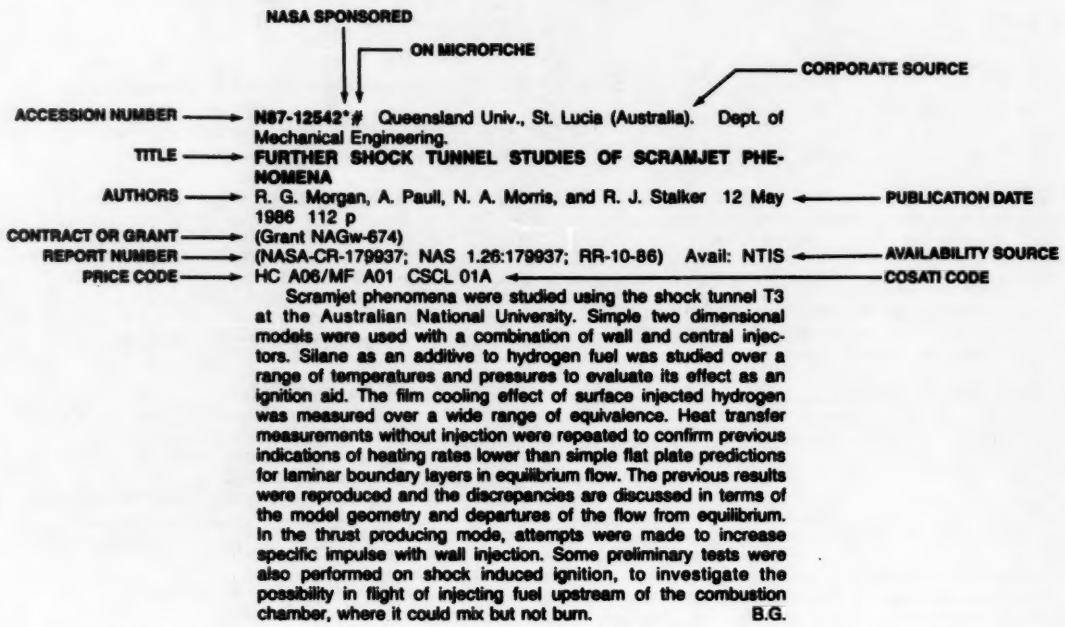
NASA SPONSORED
ON MICROFICHE
CORPORATE SOURCE
ACCESSION NUMBER
N87-12542*# Queensland Univ., St. Lucia (Australia). Dept. of Mechanical Engineering.
TITLE
FURTHER SHOCK TUNNEL STUDIES OF SCRAMJET PHENOMENA
AUTHORS
R. G. Morgan, A. Paull, N. A. Morris, and R. J. Stalker 12 May 1986 112 p
PUBLICATION DATE
CONTRACT OR GRANT
(Grant NAGw-674)
REPORT NUMBER
(NASA-CR-179937; NAS 1.26:179937; RR-10-86) Avail: NTIS
AVAILABILITY SOURCE
PRICE CODE
HC A06/MF A01 CSCL 01A
COSATI CODE
Scramjet phenomena were studied using the shock tunnel T3 at the Australian National University. Simple two dimensional models were used with a combination of wall and central injectors. Silane as an additive to hydrogen fuel was studied over a range of temperatures and pressures to evaluate its effect as an ignition aid. The film cooling effect of surface injected hydrogen was measured over a wide range of equivalence. Heat transfer measurements without injection were repeated to confirm previous indications of heating rates lower than simple flat plate predictions for laminar boundary layers in equilibrium flow. The previous results were reproduced and the discrepancies are discussed in terms of the model geometry and departures of the flow from equilibrium. In the thrust producing mode, attempts were made to increase specific impulse with wall injection. Some preliminary tests were also performed on shock induced ignition, to investigate the possibility in flight of injecting fuel upstream of the combustion chamber, where it could mix but not burn. B.G.

VOLUME 25 NUMBER 17 / SEPTEMBER 8, 1987

Scientific and Technical Aerospace Reports

A Semimonthly Publication of the National Aeronautics and Space Administration

01 AERONAUTICS (GENERAL)

N87-23570# Joint Publications Research Service, Arlington, Va.
USSR REPORT: ENGINEERING AND EQUIPMENT
9 Mar. 1987 106 p Transl. into ENGLISH from various Russian articles
(JPRS-UEQ-87-005) Avail: NTIS HC A06/MF A01

Articles and report abstracts are compiled which cover topics in various engineering fields including aeronautical and space technology, nuclear engineering, shipbuilding, construction, and turbine and engine design. For individual titles, see N87-23571 through N87-23582.

N87-23571# Joint Publications Research Service, Arlington, Va.
EFFECT OF SURFACE ROUGHNESS ON DRAG OF AIRCRAFT **c05**
R. I. Zukakishvili, A. M. Illarionov, and V. Ya. Belyayev *In its* USSR Report: Engineering and Equipment 9 Mar. 1987 p 1 Transl. into ENGLISH from Soobshcheniya Akademii Nauk Gruzinskoy SSR (Tbilisi, USSR), v. 122, no. 2, May 1986 p 358-360 Original language document was announced in IAA as A87-14717 (For primary document see N87-23570 17-01)
Avail: NTIS HC A06/MF A01

The effect of the roughness of a painted surface on the head resistance of an aircraft is investigated by using a physical model of flow past such a surface. It is found that a surface roughness of 2 to 10 microns has a noticeable effect on the head resistance of the aircraft and that the density of the surface projections determines the friction coefficient increment. It is further shown that the use of polyurethane coatings, rather than paint coatings, makes it possible to reduce the head resistance of the aircraft and its fuel consumption by 2%. IAA

N87-23572# Joint Publications Research Service, Arlington, Va.
PRINCIPLES OF DATA DISPLAY IN AVIATION INSTRUMENTS **c06**
P. A. Kovalenko and V. M. Kuznetsov *In its* USSR Report: Engineering and Equipment 9 Mar. 1987 p 2 Transl. into ENGLISH from Tekhnicheskaya Estetika (Moscow, USSR), no. 4, Apr. 1986 p 4-6 (For primary document see N87-23570 17-01)
Avail: NTIS HC A06/MF A01

Approaches to the ergonomical updating of aviation instrument displays are reviewed, and emphasis is given to the efficacious organization of data in composite instruments. The KI composite indicator which shows the positions of the elevators, rudder, stabilizer, ailerons, and spoilers is described. A redesign based on displaying the silhouette of the plane in foreshortened view (from behind) in such a way as to eliminate unnecessary explanatory text, with one optimum foreshortening of all control surfaces and one standard graphic language, has resulted in the modern MKI version of this instrument having faster readout, lower error rate, and ease of memorization. Author

N87-23573# Joint Publications Research Service, Arlington, Va.
EXPERIMENTAL STUDY OF SUPERSONIC STREAM SLIDING AT ANGLE PAST ONE-STEP WEDGE WITH JAWS **c02**
V. V. Duganov, N. N. Zakharov, and O. K. Ivanov *In its* USSR Report: Engineering and Equipment 9 Mar. 1987 p 2-3 Transl. into ENGLISH from Izvestiya Vysshikh Uchebnykh Zavedeniy: Aviatsionnaya Tekhnika (Kazan, USSR), no. 1, Jan. - Mar. 1986 p 107-110 Original language document was announced in IAA as A86-43404 (For primary document see N87-23570 17-01)
Avail: NTIS HC A06/MF A01

Experimental results are presented concerning flow around a single-stage wedge with side cheeks (a configuration typical for two-dimensional supersonic intakes) at sideslip angles of 0, 5, and 10 deg. Experiments were carried out in a wind tunnel at a Mach number of 2.1, a Reynolds number of 10 to the 8th (for a characteristic dimension of 1 m), and a stagnation temperature of 288 K. The pressure distributions are examined, and the shock wave configuration generated in the flow is discussed. IAA

N87-23574# Joint Publications Research Service, Arlington, Va.
STRUCTURAL ANALYSIS OF SUPERSONIC JET DISCHARGING FROM FREE-VORTEX NOZZLE BY METHOD OF HOLOGRAPHIC INTERFEROMETRY WITH PULSED LASER **c02**
V. I. Panchenko, A. A. Gilerson, and B. S. Vinogradov *In its* USSR Report: Engineering and Equipment 9 Mar. 1987 p 3 Transl. into ENGLISH from Izvestiya Vysshikh Uchebnykh Zavedeniy: Aviatsionnaya Tekhnika (Kazan, USSR), no. 1, Jan. - Mar. 1986 p 3 Original language document was announced in IAA as A86-43403 (For primary document see N87-23570 17-01)
Avail: NTIS HC A06/MF A01

Holographic interferometry was used to study the flow of a free-vortex jet beyond the nozzle in design conditions as well as when pressures on both boundaries of the jet differed from pressures on the nozzle section. The growth of the boundary layers on the jet boundaries is studied in both design and off-design conditions for different streamline curvatures of the ideal flow. IAA

N87-23575# Joint Publications Research Service, Arlington, Va.
MATHEMATICAL MODEL DESCRIBING INTERACTION OF SINGLE NONSTEADY SUPERSONIC JET AND MOVABLE BARRIER OF FINITE DIMENSIONS **c02**
A. V. Kuznetsov *In its* USSR Report: Engineering and Equipment 9 Mar. 1987 p 4 Transl. into ENGLISH from Izvestiya Vysshikh Uchebnykh Zavedeniy: Aviatsionnaya Tekhnika (Kazan, USSR), no. 1, Jan. - Mar. 1986 p 99-102 Original language document was announced in IAA as A86-43401 (For primary document see N87-23570 17-01)
Avail: NTIS HC A06/MF A01

The interaction of an unsteady supersonic jet with a moving barrier of finite size placed transverse to the flow is investigated with reference to the use of pulsating flows and gas-dynamic generators in various industrial processes to intensify mass transfer. A method is developed for determining the actual geometrical characteristics of the barrier, its motion in the jet, and its influence on the formation of the flow pattern. It is concluded that the proposed mathematical model is valid for arbitrary intrachamber processes and axisymmetric barriers of complex profile. IAA

N87-23576# Joint Publications Research Service, Arlington, Va.
SIMULTANEOUS RADIATIVE AND CONVECTIVE HEATING OF THIN BODY IN MEDIUM WITH VARIABLE TEMPERATURE **c34**
Yu. V. Vidin *In its* USSR Report: Engineering and Equipment

9 Mar. 1987 p 4 Transl. into ENGLISH from Izvestiya Vysshikh Uchebnykh Zavedeniy: Aviatsionnaya Tekhnika (Kazan, USSR), no. 1, Jan. - Mar. 1986 p 88-90 (For primary document see N87-23570 17-01)
Avail: NTIS HC A06/MF A01

Heating of a thermally thin body by a source at a variable temperature through a medium which transmits heat simultaneously by radiation and convection is described by a general transient-state equation for the rate of change of the body temperature with two terms, a Stefan-Boltzmann term and a Newton term, on the right-hand side. This first order differential equation is put in dimensionless form including the Fourier number as well as the Stark number and the Biot number, with retention of the body form factor (I = 1,2,3 for plate, cylinder, and sphere respectively). A rigorous analytical solution of this equation is shown to be possible when the heater temperature satisfies a certain fourth-order algebraic equation with ratio p = N(Bi)/N(Sk) and product m = N(Bi) x N(Fo) as parameters. Author

N87-23577# Joint Publications Research Service, Arlington, Va.
DEVELOPMENT OF MODEL DESCRIBING UNSTABLE OPERATION OF TURBOCOMPRESSOR AND DESIGN OF ANTISURGING PROTECTION FOR GAS TURBINE ENGINE **c07**
M. M. Shakiryanov *In its* USSR Report: Engineering and Equipment 9 Mar. 1987 p 5 Transl. into ENGLISH from Izvestiya Vysshikh Uchebnykh Zavedeniy: Aviatsionnaya Tekhnika (Kazan, USSR), no. 1, Jan. - Mar. 1986 p 61-66 (For primary document see N87-23570 17-01)
Avail: NTIS HC A06/MF A01

Unstable operation of an acoustical mechanical system which consists of a turbocompressor and a receiver with connecting pipes and a throttle is described by a mathematical model which includes four equations of state for air as an ideal gas in each of four locations within the system. On the basis of this model are established the surge characteristics of such a system, its stability region according to the Hurwitz criterion, and the conditions for gas dynamic stability. A pneumoelectronic system is then designed accordingly for protection of a gas turbine engine against surges. The system consists of three pressure transducers and one temperature transducer, two threshold devices, two computers and a function converter, and three final control elements between engine and guide vane array, engine and air bypass, and engine and fuel cutoff valve. Author

N87-23578# Joint Publications Research Service, Arlington, Va.
CATASTROPHIC BREAKUP OF LIQUID JET BY SUBSONIC TRANSVERSE GAS STREAM **c02**
M. Ye. Rudyak *In its* USSR Report: Engineering and Equipment 9 Mar. 1987 p 6 Transl. into ENGLISH from Izvestiya Vysshikh Uchebnykh Zavedeniy: Aviatsionnaya Tekhnika (Kazan, USSR), no. 1, Jan. - Mar. 1986 p 42-46 Original language document was announced in IAA as A86-43386 (For primary document see N87-23570 17-01)
Avail: NTIS HC A06/MF A01

An electric-contact method is used to study the catastrophic breakup of liquid jets in a subsonic transverse gas flow, with reference to the pneumatic atomization of liquid fuels. The special conditions of gas-liquid interaction are shown to determine the considerable increase in the breakup rate. It is recommended that catastrophic breakup be used to improve the operation of gas-liquid mixers. IAA

N87-23579# Joint Publications Research Service, Arlington, Va.
CALCULATION OF AXISYMMETRIC FLOW IN SWHIRLERS BY DIFFERENCE METHOD **c02**
V. N. Ignatyev *In its* USSR Report: Engineering and Equipment 9 Mar. 1987 p 6 Transl. into ENGLISH from Izvestiya Vysshikh Uchebnykh Zavedeniy: Aviatsionnaya Tekhnika (Kazan, USSR), no. 1, Jan. - Mar. 1986 p 25-29 (For primary document see N87-23570 17-01)
Avail: NTIS HC A06/MF A01

A difference scheme with exponential fitting is proposed for solution of the system of Navier-Stokes equations describing steady axisymmetric flow with rotation through a cylindrical swirler (vortex generator) with a parabolic radial profile of the flow function in the entrance section and with soft boundary conditions at the exit. Such a difference scheme is of highest-order precision and monotonic, designed for differential equations with a small parameter as coefficient of the highest-order derivatives. The scheme is implementable upon introduction of the difference Reynolds number on the basis of a theorem which ensures monotonicity at any value of the Reynolds number N(R) is greater than 0 when bar-r v(ij) h(j) is less than or equal to 1/N(R) (bar-r = discrete segment of radius, v(ij) = axial velocity). Calculations according to such a scheme with 10x20 or 20x40 grids and with stabilizing correction on a YeS-1033 computer indicate that this method is both efficient and accurate for low and high values of the Reynolds number. Author

N87-23580# Joint Publications Research Service, Arlington, Va.
EFFECTIVENESS OF BALANCING FLEXIBLE ROTARY COMPRESSOR VANES ON LOW-SPEED BALANCING MACHINE **c07**
A. I. Gleyzer and V. A. Bulychev *In its* USSR Report: Engineering and Equipment 9 Mar. 1987 p 7 Transl. into ENGLISH from Izvestiya Vysshikh Uchebnykh Zavedeniy: Aviatsionnaya Tekhnika (Kazan, USSR), no. 1, Jan. - Mar. 1986 p 15-19 Original language document was announced in IAA as A86-43379 (For primary document see N87-23570 17-01)
Avail: NTIS HC A06/MF A01

A method for calculating the efficiency of the low-cycle balancing of flexible rotors on acceleration-type balancing machines is proposed. The method includes a probabilistic estimation of the residual unbalance and a calculation of the limiting level of support vibrations or rotor deflections. The data obtained are compared with norms of residual vibrations permitted under low-cycle balancing. IAA

N87-23581# Joint Publications Research Service, Arlington, Va.
COMPRESSIBILITY OF SUBMERGED SUPERSONIC JETS **c02**
S. I. Baranovskiy, A. S. Nadvorskiy, and T. F. Savina *In its* USSR Report: Engineering and Equipment 9 Mar. 1987 p 7 Transl. into ENGLISH from Izvestiya Vysshikh Uchebnykh Zavedeniy: Aviatsionnaya Tekhnika (Kazan, USSR), no. 1, Jan. - Mar. 1986 p 11-15 Original language document was announced in IAA as A86-43378 (For primary document see N87-23570 17-01)
Avail: NTIS HC A06/MF A01

A compressibility function is considered which satisfactorily describes the mixing of supersonic submerged jets and provides an accurate measure of the potential-core length. The theoretical relationship has been confirmed experimentally. IAA

N87-23582# Joint Publications Research Service, Arlington, Va.
FLOW OF GAS THROUGH TURBINE STAGE WITH SPHERICAL NOZZLE SEGMENT **c07**
A. I. Arkhipov, M. K. Maksutova, and Yu. V. Strunkin *In its* USSR Report: Engineering and Equipment 9 Mar. 1987 p 8 Transl. into ENGLISH from Izvestiya Vysshikh Uchebnykh Zavedeniy: Aviatsionnaya Tekhnika (Kazan, USSR), no. 1, Jan. - Mar. 1986 p 8-11 Original language document was announced in IAA as A86-43377 (For primary document see N87-23570 17-01)
Avail: NTIS HC A06/MF A01

The characteristics of the structure behind the nozzle box are investigated. It is shown that the spherical flow-through part leads to a deflection of the flow from the periphery to the root, resulting in a greater energy loss in the peripheral zone. This flow deflection can lead to separation in this region, particularly for a large axial gap. Experimental results indicate that energy losses in the peripheral zone of a nozzle cascade are significantly greater than those in the root zone. IAA

02 AERODYNAMICS

Includes aerodynamics of bodies, combinations, wings, rotors, and control surfaces; and internal flow in ducts and turbomachinery.

For related information see also *34 Fluid Mechanics and Heat Transfer.*

N87-23583*# National Aeronautics and Space Administration, Washington, D.C.

HYPERSONIC AERODYNAMIC COEFFICIENTS AND CONVECTION FLOW ESTIMATION IN A HERMES TYPE PROJECT

C. Pollak May 1987 41 p Transl. into ENGLISH of "Prevision en Hypersonique des Coefficients Aerodynamiques et des Flux de Convection dans un Projet type HERMES" Les Mureaux (France) Presented at the 22nd AAAF Colloque d'Aerodynamique Appliquee, Lille (France), 13-15 Nov. 1985 Original language document was announced as N86-31540 Transl. by Kanner (Leo) Associates, Redwood City, Calif. Original doc. was prepared by Aerospatiale (Contract NASw-4005)

(NASA-TT-20019; NAS 1.77:20019) Avail: NTIS HC A03/MF A01 CSCL 01A

An analysis of all the experimental and computation requirements of the HERMES project is presented. The discussion includes the influence of the upper atmosphere composition and possible chemical reactions, the information collected in Orbiter experiments, the possibility of utilizing plasma generators and CF4 in wind tunnel tests, the development of parabolized Navier-Stokes models and solutions, and the computing capacity requirements.

ESA

N87-23584*# National Aeronautics and Space Administration. Ames Research Center, Moffett Field, Calif.

EVALUATION OF NAVIER-STOKES AND EULER SOLUTIONS FOR LEADING-EDGE SEPARATION VORTICES

K. Fujii, S. Gavali, and T. L. Holst Jun. 1987 14 p Prepared for presentation at the 5th International Conference on Numerical Methods in Laminar and Turbulent Flow, Montreal, Quebec, 6-10 Jul. 1987

(NASA-TM-89458; A-87202; NAS 1.15:89458) Avail: NTIS HC A02/MF A01 CSCL 01A

Extensive study on the numerical simulation of the vortical flow over a double delta wing is carried out using the thin layer Navier-Stokes and Euler equations. Two important flow characteristics, vortex interaction and vortex breakdown, are successfully simulated. Grid resolution is one of the most important factors associated with the vortex problem. Computations were performed on a series of grids with various levels of refinement, coarse, medium, and fine. Computations using either the coarse or medium grids fail to capture the proper physical phenomena. The computed result using a fine grid shows flow unsteadiness once the vortex breakdown takes place. The C sub L - alpha characteristics are well predicted up to the breakdown angle of attack for all the grid distributions. The Euler solutions show fairly good agreement with the experiment on the C sub L - alpha characteristics. However, other aspects of the solution at each angle of attack, such as the locus of the leading edge separation vortex, are not consistent with the experiment. Even for the fine grid Navier-Stokes computations, further grid resolution is required to obtain good quantitative agreement with the experiment.

Author

N87-23585# Ballistic Research Labs., Aberdeen Proving Ground, Md.

MEASUREMENT OF SURFACE PRESSURES CAUSED BY A PROJECTILE ROTATING BAND AT SUPERSONIC SPEEDS Final Report

James E. Danberg and Keith L. Palko (Delaware Univ., Newark.) Jul. 1986 44 p

(DA Proj. 1L1-62618-AH-80)

(AD-A171082; BRL-MR-3532) Avail: NTIS HC A03/MF A01 CSCL 01A

An experiment is described in which surface pressure distributions on a cone-cylinder model have been measured with and without a simulated rotating band. Measurements cover a Mach number range from 2.25 to 3.50 at an average Reynolds number of 1.3 X 10 to the 6th power. Increased resolution of the pressure distribution was achieved by using a movable band with only five orifices on the constant pressure cylindrical section of the model. The results show that the perturbation pressures caused by the band are independent of the actual band location. A second phase of the experiments concerned measuring the pressure changes caused by various band thicknesses which were produced by wrapping layers of tape around the model. The pressure disturbance of the band is found to correlate in terms of the maximum and minimum pressure coefficients and pressure interaction lengths. The interaction length ahead of the band is found to be nearly constant and the maximum pressure coefficient is inversely proportional to Beta =(M squared -1) sup 1/2. Behind the band the interaction length increases proportional to Beta whereas the minimum pressure coefficient is inversely proportional to Beta squared.

Author

N87-23586*# National Aeronautics and Space Administration. Langley Research Center, Hampton, Va.

ON MINIMIZING THE NUMBER OF CALCULATIONS IN DESIGN-BY-ANALYSIS CODES

Raymond L. Barger and Anutosh Moitra Jun. 1987 16 p

(NASA-TP-2706; L-16226; NAS 1.60:2706) Avail: NTIS HC A02/MF A01 CSCL 01A

A method is presented for aerodynamic design for a specified pressure distribution, using analysis codes only. The method requires a very conservative number of analysis runs, and therefore is appropriate when the analysis code is a large code in terms of storage and/or running time. Three model problems illustrate some capabilities and limitations of the method.

Author

N87-23587*# National Aeronautics and Space Administration. Langley Research Center, Hampton, Va.

CROSSFLOW VORTICITY SENSOR Patent Application

Bruce J. Holmes, inventor (to NASA), Debra L. Carraway, inventor (to NASA), Harlan K. Holmes, inventor (to NASA), and Thomas C. Moore, inventor (to NASA) 15 Jan. 1987 14 p

(NASA-Case-LAR-13436-1-CU; US-Patent-Appl-SN-003676) Avail: NTIS HC A02/MF A01 CSCL 01A

A crossflow vorticity sensor for the detection of crossflow vorticity characteristics is described. The sensor is comprised of crossflow sensors which are non-invasively adhered to a swept wing laminar surface either singularly, in multi-element strips, in polar patterns, or in orthogonal patterns. These crossflow sensors are comprised of hot-film sensor elements which operate as a constant temperature anemometer circuit to detect heat transfer rate changes. Accordingly, crossflow vorticity characteristics are determined via cross-correlation. In addition, the crossflow sensors have a thickness which does not exceed a maximum value h in order to avoid contamination of downstream crossflow sensors.

NASA

N87-23588# Naval Postgraduate School, Monterey, Calif.

APPLICATION OF THE VISCOUS-INVISCID INTERACTION METHOD TO THE ANALYSIS OF AIRFOIL FLOWS AT LOW REYNOLDS NUMBERS M.S. Thesis

Seung W. Paik Dec. 1986 88 p

(AD-A177948) Avail: NTIS HC A05/MF A01 CSCL 20D

This thesis shows the capability of strong viscous/inviscid interaction methods to predict airfoil flows at low Reynolds numbers. Cebeci's interactive program was applied to the Wortmann-Althaus FX 63-137 airfoil and the results were compared with the available experimental data. It was found that the boundary layer transition model has an important influence on the predictive capability of viscous/inviscid interaction methods.

GRA

N87-23589*# Ohio State Univ., Columbus. Aeronautical and Astronautical Research Lab.

TWO-DIMENSIONAL AERODYNAMIC CHARACTERISTICS OF THE AMES HI-120, HI-8, AND LOW-12 AIRFOILS Final Technical Report, Jun. - Sep. 1986

G. M. Gregorek and M. J. Berchak Jun. 1987 51 p
(Grant NAG2-401)
(NASA-CR-181018; NAS 1.26:181018) Avail: NTIS HC A04/MF A01 CSCL 01A

During the period between June and September 1986, the Aeronautical and Astronautical Engineering Research Laboratory (AARL) at the Ohio State University (OSU) in Columbus, Ohio, conducted tests in the 6'X22' Transonic Blowdown Wind Tunnel to determine the two-dimensional lift, drag, and pitching moment coefficients for three airfoils designated AMES HI-120, AMES LOW-12, and AMES HI-8. These tests covered a Mach number range of 0.20 to 0.86, Reynolds numbers between 2 x 10 to the 6th and 6 x 10 to the 6th powers, and angles of attack between 0 and 13 degs as directed by the NASA Project Engineer; each model was not run at every condition. This work was performed under NASA Grant NAG-2-401, Analysis of Two Advanced Transonic Airfoils. Author

N87-23590# Arnold Engineering Development Center, Arnold Air Force Station, Tenn.

LASER DOPPLER VELOCIMETER APPLICATION IN SUPERSONIC BOUNDARY-LAYER FLOW Final Report, 1 Oct. 1984 - 30 Sep. 1986

J. C. Donaldson Mar. 1987 55 p Prepared in cooperation with Calspan Corp., Arnold AFS, Tenn.
(AD-A178395; AEDC-TR-86-44) Avail: NTIS HC A04/MF A01 CSCL 17H

Laser Doppler velocimeter techniques have been investigated for nonintrusive measurements of cone boundary-layer mean-velocity profiles in supersonic flow. The investigation was performed in the AEDC Supersonic Wind Tunnel (A) at a free-stream Mach number of 4, using olive-oil droplets to seed the tunnel flow. The basis for the evaluation of the LDV results was a set of velocity profiles obtained using conventional probing techniques. Laminar, transitional, and turbulent boundary layers on a 7-deg (half-angle) sharp-cone model were included in this study. The results obtained in this investigation demonstrate that mean-velocity profiles can be obtained within acceptable limits of uncertainty provided: (1) seed particles of appropriate size are found in tunnel flow or can be added to the flow, and (2) a systematic editing procedure is available, when the results are evaluated, to eliminate velocities of relatively low probability and effects of spurious noise. Author (GRA)

N87-23591*# National Aeronautics and Space Administration. Lewis Research Center, Cleveland, Ohio.

ICING OF FLOW CONDITIONERS IN A CLOSED-LOOP WIND TUNNEL M.S. Thesis

James E. Newton Jun. 1987 13 p
(NASA-TM-89824; E-3474; NAS 1.15:89824) Avail: NTIS HC A02/MF A01 CSCL 01A

Described are the results of an experiment which determined whether flow conditioning screens and honeycombs would ice up in a closed-loop icing wind tunnel when placed downstream of the heat exchanger and upstream of the spray bars. The experiment was performed in the Icing Research Tunnel (IRT) at NASA Lewis Research Center. The investigation involved two separate tests: one to find the icing characteristics of flow conditioners in the IRT, and the second to find the icing characteristics of flow conditioners in the proposed rehabilitation of the Altitude Wind Tunnel (AWT). Both experiments showed that the heat exchanger removed nearly all of the icing cloud so that icing of the flow conditioners would cause no serious tunnel performance degradation during the course of a day's run. Only extremely cold conditions caused frost formation on the flow conditioners. The significance of this frost formation was minimized because frost buildup on the heat exchanger caused a much more severe pressure drop than did icing of the flow conditioners. Author

N87-23592*# National Aeronautics and Space Administration. Langley Research Center, Hampton, Va.

MACH 6 EXPERIMENTAL AND THEORETICAL STABILITY AND PERFORMANCE OF A CRUCIFORM MISSILE AT ANGLES OF ATTACK UP TO 65 DEGREES

Edward R. Hartman (Arnold Engineering Development Center, Arnold Air Force Station, Tenn.) and Patrick J. Johnston Jul. 1987 41 p
(NASA-TP-2733; L-16287; NAS 1.60:2733) Avail: NTIS HC A03/MF A01 CSCL 01A

An experimental and theoretical investigation of the longitudinal and lateral-directional stability and control of an axisymmetric cruciform-finned missile has been conducted at Mach 6. The angle-of-attack range extended from 20 to 65 deg to encompass maximum lift. Longitudinal stability, performance, and trim could be accurately predicted with the fins at a fin roll angle of 0 deg but not when the fins were at a fin roll angle of 45 deg. At this roll angle, windward fin choking occurred at angles of attack above 50 deg and reduced the effectiveness of the fins and caused pitch-up. Author

N87-23593*# National Aeronautics and Space Administration. Langley Research Center, Hampton, Va.

EFFECT OF A TRADE BETWEEN BOATTAIL ANGLE AND WEDGE SIZE ON THE PERFORMANCE OF A NONAXISYMMETRIC WEDGE NOZZLE

George T. Carson, Jr., E. Ann Bare, and James R. Burley, II Jul. 1987 67 p
(NASA-TP-2717; L-16248; NAS 1.60:2717) Avail: NTIS HC A04/MF A01 CSCL 01A

An investigation was conducted in the Langley 16-Foot Transonic Tunnel to determine the effect of a boattail angle and wedge-size trade on the performance of nonaxisymmetric wedge nozzles installed on a generic twin-engine fighter aircraft model. Test data were obtained at static conditions and at Mach numbers from 0.60 to 1.25. Angle of attack was held constant at 0 deg. High-pressure air was used to simulate jet exhaust, and the nozzle pressure ratio was varied from 1.0 (jet off) to slightly over 15.0. For the configurations studied, the results indicate that wedge size can be reduced without affecting aeropropulsive performance. Author

N87-23594*# National Aeronautics and Space Administration. Langley Research Center, Hampton, Va.

HIGH REYNOLDS NUMBER TESTS OF THE NASA SC(2)-0012 AIRFOIL IN THE LANGLEY 0.3-METER TRANSONIC CRYOGENIC TUNNEL

Raymond E. Mineck and Pierce L. Lawing Jul. 1987 58 p
(NASA-TM-89102; L-16259; NAS 1.15:89102) Avail: NTIS HC A04/MF A01 CSCL 01A

A wind-tunnel investigation of the NASA SC(2)-0012 airfoil has been conducted in the Langley 0.3-Meter Transonic Cryogenic Tunnel. This investigation supplements the two-dimensional airfoil studies of the Advanced Technology Airfoil Test Program. The Mach number was varied from 0.60 to 0.84. The stagnation temperature and pressure were varied to provide a Reynolds number range from 6 to 40 x 10 to the 6th power based on a 6.0-in. (15.24-cm) airfoil chord. No corrections for wind-tunnel wall interference have been made to the data. The aerodynamic results are presented as integrated force and moment coefficients and pressure distributions without any analysis. Author

N87-23595*# National Aeronautics and Space Administration. Ames Research Center, Moffett Field, Calif.

SOME ASPECTS OF VORTEX FLOWS DETERMINED FROM THE THIN-LAYER NAVIER-STOKES EQUATIONS

Unmeel Mehta Sep. 1986 7 p Presented at the 3rd Asian Congres of Fluid Mechanics, Tokyo, Japan, Sep. 1986
(NASA-TM-88375; A86409; NAS 1.15:88375) Avail: NTIS HC A02/MF A01 CSCL 01A

Vortex flows caused by a swept wing are described in some detail. The thin-shear-layer Navier-Stokes equations with an algebraic eddy-viscosity turbulence model are solved. An implicit,

factored numerical scheme is used. On the upper surface of the wing, flow is primarily along the free-stream and spanwise direction, respectively, at small and large angles of attack. Author

N87-23596*# McDonnell-Douglas Helicopter Co., Mesa, Ariz.
AEROELASTICITY AND MECHANICAL STABILITY REPORT, 0.27 MACH SCALE MODEL OF THE YAH-64 ADVANCED ATTACK HELICOPTER Final Report
F. K. Straub and R. A. Johnston May 1987 67 p Prepared in cooperation with Hughes Helicopters, Culver City, Calif.
(Contract NAS1-16475)
(NASA-CR-178284; NAS 1.26:178284; MDHC-150-V-1003) Avail: NTIS HC A04/MF A01 CSCL 01A

A 27% dynamically scaled model of the YAH-64 Advanced Attack Helicopter main rotor and hub has been designed and fabricated. The model will be tested in the NASA Langley Research Center V/STOL wind tunnel using the General Rotor Model System (GRMS). This report documents the studies performed to ensure dynamic similarity of the model with its full scale parent. It also contains a preliminary aeroelastic and aeromechanical substantiation for the rotor installation in the wind tunnel. From the limited studies performed no aeroelastic stability or load problems are projected. To alleviate a projected ground resonance problem, a modification of the roll characteristics of the GRMS is recommended. Author

N87-23597*# National Aeronautics and Space Administration. Langley Research Center, Hampton, Va.
STUDY OF LEE-SIDE FLOWS OVER CONICALLY CAMBERED DELTA WINGS AT SUPERSONIC SPEEDS, PART 1
Richard M. Wood and Carolyn B. Watson Jul. 1987 212 p
(NASA-TP-2660-Pt-1; L-16192; NAS 1.60:2660-Pt-1) Avail: NTIS HC A10/MF A01 CSCL 01A

An experimental investigation was performed in which surface pressure data, flow visualization data, and force and moment data were obtained on four conical delta wing models which differed in leading-edge camber only. Wing leading-edge camber was achieved through a deflection of the outboard 30% of the local wind semispan of a reference 75 degrees swept flat delta wing. The four wing models have leading-edge deflection angles delta sub F of 0, 5, 10, and 15 degrees measured streamwise. Data for the wings with delta sub F = 10 and 15 degrees showed that hinge-line separation dominated the lee-side wing loading and prohibited the develpment of leading-edge separation on the deflected portion of wing leading edge. However, data for the wing with delta sub F = 5 degrees, a vortex was positioned on the deflected leading edge with reattachment at the hinge line. Flow visualization results were presented which detail the influence of Mach number, angle of attack, and camber on the lee-side flow characteristics of conically cambered delta wings. Analysis of photgraphic data identified the existence of 12 distinctive lee-side flow types. In general, the aerodynamic force and moment data correlated well with the pressure and flow visualization data.
Author

N87-23598*# National Aeronautics and Space Administration. Lewis Research Center, Cleveland, Ohio.
COUPLED AERODYNAMIC AND ACOUSTICAL PREDICTIONS FOR TURBOPROPS
Bruce J. Clark and James R. Scott Mar. 1986 13 p Presented at the 107th Meeting of the American Acoustical Society, Norfolk, Va., 7-10 May 1984
(NASA-TM-87094; E-2688; NAS 1.15:87094) Avail: NTIS HC A02/MF A01 CSCL 01A

To predict the noise fields for proposed turboprop airplanes, an existing turboprop noise code by Farassat has been modified to accept blade pressure inputs from a three-dimensional aerodynamic code. A Euler-type code can handle the nonlinear transonic flow of these high-speed, highly swept blades. This turbofan code was modified to allow the calculation mesh to extend to about twice the blade radius and to apply circumferential periodicity rather than solid-wall boundary conditions on the blade in the region between the blade tip and the outer shroud. Outputs were added for input to the noise prediction program and for color contour plots of various flow variables. The Farassat input subroutines were modified to read files of blade coordinates and predicted surface pressures. Aerodynamic and acoustic results are shown for the SR-3 model blade. Comparison of the acoustic predicted results with measured data show good agreement.
Author

N87-23573# Joint Publications Research Service, Arlington, Va.
EXPERIMENTAL STUDY OF SUPERSONIC STREAM SLIDING AT ANGLE PAST ONE-STEP WEDGE WITH JAWS
V. V. Duganov, N. N. Zakharov, and O. K. Ivanov *In its* USSR Report: Engineering and Equipment 9 Mar. 1987 p 2-3 Transl. into ENGLISH from Izvestiya Vysshikh Uchebnykh Zavedeniy: Aviatsionnaya Tekhnika (Kazan, USSR), no. 1, Jan. - Mar. 1986 p 107-110 Original language document was announced in IAA as A86-43404 (For primary document see N87-23570 17-01)
Avail: NTIS HC A06/MF A01

N87-23574# Joint Publications Research Service, Arlington, Va.
STRUCTURAL ANALYSIS OF SUPERSONIC JET DISCHARGING FROM FREE-VORTEX NOZZLE BY METHOD OF HOLOGRAPHIC INTERFEROMETRY WITH PULSED LASER
V. I. Panchenko, A. A. Gilerson, and B. S. Vinogradov *In its* USSR Report: Engineering and Equipment 9 Mar. 1987 p 3 Transl. into ENGLISH from Izvestiya Vysshikh Uchebnykh Zavedeniy: Aviatsionnaya Tekhnika (Kazan, USSR), no. 1, Jan. - Mar. 1986 p 3 Original language document was announced in IAA as A86-43403 (For primary document see N87-23570 17-01)
Avail: NTIS HC A06/MF A01

N87-23575# Joint Publications Research Service, Arlington, Va.
MATHEMATICAL MODEL DESCRIBING INTERACTION OF SINGLE NONSTEADY SUPERSONIC JET AND MOVABLE BARRIER OF FINITE DIMENSIONS
A. V. Kuznetsov *In its* USSR Report: Engineering and Equipment 9 Mar. 1987 p 4 Transl. into ENGLISH from Izvestiya Vysshikh Uchebnykh Zavedeniy: Aviatsionnaya Tekhnika (Kazan, USSR), no. 1, Jan. - Mar. 1986 p 99-102 Original language document was announced in IAA as A86-43401 (For primary document see N87-23570 17-01)
Avail: NTIS HC A06/MF A01

N87-23578# Joint Publications Research Service, Arlington, Va.
CATASTROPHIC BREAKUP OF LIQUID JET BY SUBSONIC TRANSVERSE GAS STREAM
M. Ye. Rudyak *In its* USSR Report: Engineering and Equipment 9 Mar. 1987 p 6 Transl. into ENGLISH from Izvestiya Vysshikh Uchebnykh Zavedeniy: Aviatsionnaya Tekhnika (Kazan, USSR), no. 1, Jan. - Mar. 1986 p 42-46 Original language document was announced in IAA as A86-43386 (For primary document see N87-23570 17-01)
Avail: NTIS HC A06/MF A01

N87-23579# Joint Publications Research Service, Arlington, Va.
CALCULATION OF AXISYMMETRIC FLOW IN SWHIRLERS BY DIFFERENCE METHOD
V. N. Ignatyev *In its* USSR Report: Engineering and Equipment 9 Mar. 1987 p 6 Transl. into ENGLISH from Izvestiya Vysshikh Uchebnykh Zavedeniy: Aviatsionnaya Tekhnika (Kazan, USSR), no. 1, Jan. - Mar. 1986 p 25-29 (For primary document see N87-23570 17-01)
Avail: NTIS HC A06/MF A01

N87-23581# Joint Publications Research Service, Arlington, Va.
COMPRESSIBILITY OF SUBMERGED SUPERSONIC JETS
S. I. Baranovskiy, A. S. Nadvorskiy, and T. F. Savina *In its* USSR Report: Engineering and Equipment 9 Mar. 1987 p 7 Transl. into ENGLISH from Izvestiya Vysshikh Uchebnykh Zavedeniy: Aviatsionnaya Tekhnika (Kazan, USSR), no. 1, Jan. - Mar. 1986 p 11-15 Original language document was announced in IAA as A86-43378 (For primary document see N87-23570 17-01)
Avail: NTIS HC A06/MF A01

17-01)
Avail: NTIS HC A06/MF A01

03 AIR TRANSPORTATION AND SAFETY

Includes passenger and cargo air transport operations; and aircraft accidents.

For related information see also *16 Space Transportation* and *85 Urban Technology and Transportation.*

N87-23599# Calspan Field Services, Inc., Arnold AFS, Tenn.
BIRD IMPACT QUALIFICATION TEST FOR A-10 WINDSHIELD Final Report, 9 Dec. 1986
T. L. Buchanan Apr. 1987 22 p Prepared in cooperation with AEDC, Arnold AFS, Tenn.
(AD-A179263; AEDC-TSR-86-V57) Avail: NTIS HC A02/MF A01 CSCL 01C

One shot was made on the A-10's left side windshield for this program. The objective of this shot was to qualify the windshield. The shot was at a nominal velocity of 360 knots using a 4-lb bird. Descriptions of the test facility, test articles, and test procedures are presented. GRA

N87-23600# Transportation Systems Center, Cambridge, Mass.
US COAST GUARD SARSAT (SEARCH AND RESCUE SATELLITE-AIDED TRACKING). VOLUME 2. APPENDICES Final Evaluation Report, Feb. 1983 - Jan. 1985
J. Bellantoni Mar. 1987 455 p
(AD-A178307; DOT-TSC-CG-85-3-Vol-2; USCG-D-29-85-Vol-2) Avail: NTIS HC A20/MF A01 CSCL 06G

Appendices giving detailed information and data supporting the technical evaluation of the COSPAS/SARSAT satellite-aided search and rescue system are compiled. Specific section titles include: Controlled Tests; Controlled Test Error Analysis, Processing of Westwind Data; Exercises and Homing Tests; Further Analysis of Controlled Tests; Sar Case Analysis Tables; Narratives of Real Distress Cases; RCC Response Scenarios; Workload Assessments; Volume and Delays in the Sarsat Ground System; Number of Messages Routed to US Coast Guard with Real Maritime Positions; Distribution of Waiting Time; A Method of Estimating the Total Number of Distress Cases Involving an Actuated Elt or Epirb, and Cost Models for Scenarios 1 and 2. GRA

N87-23601# Transportation Systems Center, Cambridge, Mass.
US COAST GUARD SARSAT (SEARCH AND RESCUE SATELLITE-AIDED TRACKING). VOLUME 3. PROGRAMS AND DATA LISTINGS Final Evaluation Report, Feb. 1983 - Jan. 1985
J. Bellantoni Mar. 1987 229 p
(AD-A178308; DOT-TSC-CG-85-3-Vol-3; USCG-D-29-85-Vol-3) Avail: NTIS HC A11/MF A01 CSCL 06G

Volume I of this report, Technical Evaluation, presents the findings of the U.S. Coast Guard's two year demonstration and evaluation (D&E) of the COSPAS/SARSAT satellite-aided search and rescue system for locating distressed vessels and aircraft, a cooperative project of the US, USSR, France, and Canada. The report summarizes results of controlled tests and exercises; analyzes SARSAT's role in actual distress cases; discusses operations of the system's radio beacons; satellites, Cost Guard Rescue Coordination Centers, U.S. Mission Control Center, Local User Terminals, and ground communications; appraises the system's long-term economic costs and benefits; and assesses achievement of project objectives. GRA

N87-23602# Luftfahrt-Bundesamt, Brunswick (West Germany). Flugunfalluntersuchungsstelle.
RESULTS OF THE SPECIALIZED INVESTIGATION OF ACCIDENTS INVOLVING GERMAN AIRCRAFT AT HOME AND ABROAD, AND WITH FOREIGN AIRCRAFT AT HOME Annual Report, 1983 [ERGEBNISSE DER FACHLICHEN UNTERSUCHUNG VON UNFAELLEN BEI DEM BETRIEB DEUTSCHER LUFTFAHRZEUGE IM IN- UND AUSLAND SOWIE AUSLAENDISCHE LUFTFAHRZEUGE IM INLAND]
Jun. 1986 121 p In GERMAN
(ISSN-0178-8094; ETN-87-99668) Avail: NTIS HC A06/MF A01

Tables showing accidents of aircraft above 5.7 t, between 2 and 5.7 t, below 2 t, helicopters, sailplanes, powered gliders, parachutes, hang gliders and ultralight aircraft, balloons, and other aircraft, are given. For each type of aircraft, a short report is presented. ESA

N87-23603# National Transportation Safety Board, Washington, D. C. Bureau of Safety Programs.
AIRCRAFT ACCIDENT DATA: US AIR CARRIER OPERATIONS CALENDAR YEAR 1984 Annual Review
15 Apr. 1987 107 p
(PB87-183992; NTSB/ARC-87/02) Avail: NTIS HC A06/MF A01 CSCL 01C

This publication presents the record of aviation accidents involving revenue operations of U.S. Carriers including Commuter Air Carriers and on demand Air Taxis for calendar year 1984. The report is divided into three major sections according to the federal regulations under which the flight was conducted - 14 CFR 121, 125, 127, Scheduled 14 CFR 135, or Nonscheduled 14 CFR 135. In each section of the report tables are presented to describe the losses and characteristics of 1984 accidents to permit comparison with prior years. Author

N87-23604# National Transportation Safety Board, Washington, D. C. Bureau of Accident Investigation.
AIRCRAFT ACCIDENT REPORT: SOUTHERN AIR TRANSPORT LOGAIR FLIGHT 51, LOCKHEED L-382G, KELLY AIR FORCE BASE, TEXAS, OCTOBER 4, 1986
9 Apr. 1987 72 p
(PB87-910404; NTSB-AAR-87-04) Avail: NTIS HC A04/MF A01 CSCL 01C

Southern Air Transport's LOGAIR 15 flight, a Lockheed L-382G, was cleared for takeoff from Kelly Air Force Base, Texas, on an instrument flight plan to Warner Robbins Air Force Base, Georgia, at about 0405 on October 4, 1986. Visual meteorological conditions prevailed. There were three flightcrew members aboard the military contracted domestic cargo flight operating under 14 CFR Part 121. All communications with the air traffic control tower were routine. Radar recorded that the airplane reached an altitude of about 700 feet above ground level. Witnesses reported an abnormally steep climb attitude followed by a turn and/or bank to the left, after which the airplane continued to roll to the left and struck the ramp area at about a 90 deg angle to the departure runway in a near-inverted attitude between two hangars and exploded. A severe ground fire ensued. All three flight crew members were killed. The National Transportation Safety Board determines that the probable cause of this accident was the use by the carrier of a nonapproved device designed to raise the elevator during loading operations which was not properly stowed by the flightcrew and which lodged in the controls, preventing the flightcrew from controlling the aircraft during takeoff. Author

N87-23605# National Transportation Safety Board, Washington, D. C. Bureau of Safety Programs.
AIRCRAFT ACCIDENT DATA: US AIR CARRIER OPERATIONS CALENDAR YEAR 1983 Annual Review
13 Feb. 1987 111 p
(PB87-160628; NTSB/ARC-87/01) Avail: NTIS HC A06/MF A01 CSCL 01C

This publication presents the record of aviation accidents involving revenue operations of U.S. Air Carriers including

Commuter Air Carriers and On demand Air Taxis for calendar year 1983. The report is divided into three major sections according to the federal regulations under which the flight was conducted - 14 CFR 121, 125, 127, Scheduled 14 CFR 135, or Nonscheduled 14 CFR 135. In each section of the report tables are presented to describe the losses and characteristics of 1983 accidents to permit comparison with prior years. Author

N87-23606# National Transportation Safety Board, Washington, D. C.
ANNUAL REVIEW OF AIRCRAFT ACCIDENT DATA, US GENERAL AVIATION: CALENDAR YEAR 1984
11 May 1987 235 p
(PB87-194791; NTSB/ARG-87/02) Avail: NTIS HC A11/MF A01

This report presents a statistical compilation and review of general aviation accidents which occurred in 1984 in the United States, its territories and possessions, and in international waters. The accidents reported are all those involving U.S. registered aircraft not conducting air carrier revenue operations under 14 CFR 121, 14 CFR 125, 14 CFR 127, or 14 CFR 135. This report is divided into sections, each of which (except for the All Operations section) presents a review of a subset of all general aviation accidents. Each subset represents aircraft of similar types or aircraft being operated for particular purposes. Several tables present accident parameters for 1984 only, and each section includes tabulations which present comparative statistics for 1984 and the five-year period 1979-1983. Author

04 AIRCRAFT COMMUNICATIONS AND NAVIGATION

Includes digital and voice communication with aircraft; air navigation systems (satellite and ground based); and air traffic control.

For related information see also *17 Space Communications, Spacecraft Communications, Command and Tracking* and *Communications and Radar.*

N87-23607*# Mitre Corp., McLean, Va.
DEVELOPMENT OF AN AIR GROUND DATA EXCHANGE CONCEPT: FLIGHT DECK PERSPECTIVE Final Report
G. W. Flathers, II Jun. 1987 257 p
(Contract NAS1-17974)
(NASA-CR-4074; NAS 1.26:4074; MTR-87W21) Avail: NTIS HC A12/MF A01 CSCL 17B

The planned modernization of the U.S. National Airspace System (NAS) includes the development and use of a digital data link as a means to exchange information between aircraft and ground-based facilities. This report presents an operationally-oriented concept on how data link could be used for applications related directly to air traffic control. The specific goal is to establish the role that data link could play in the air-ground communications. Due regard is given to the unique characteristics of data link and voice communications, current principles of air traffic control, operational procedures, human factors/man-machine interfaces, and the integration of data link with other air and ground systems. The resulting concept is illustrated in the form of a paper-and-pencil simulation in which data link and voice communications during the course of a hypothetical flight are described. Author

N87-23608# Advisory Group for Aerospace Research and Development, Neuilly-Sur-Seine (France).
EFFICIENT CONDUCT OF INDIVIDUAL FLIGHTS AND AIR TRAFFIC OR OPTIMUM UTILIZATION OF MODERN TECHNOLOGY FOR THE OVERALL BENEFIT OF CIVIL AND MILITARY AIRSPACE USERS
Bernardo Furcolo 1987 16 p
(AGARD-AR-236) Avail: NTIS HC A02/MF A01

The AGARD Guidance and Control Panel 42nd Symposium was held in Brussels, Belgium, from 10 to 13 June 1986. The program presented at the symposium is appended to this report, and the Conference Proceedings are published separately. Author

05 AIRCRAFT DESIGN, TESTING AND PERFORMANCE

Includes aircraft simulation technology.

For related information see also *18 Spacecraft Design, Testing and Performance* and *39 Structural Mechanics.* For land transportation vehicles see *85 Urban Technology and Transportation.*

N87-23609# Advisory Group for Aerospace Research and Development, Neuilly-Sur-Seine (France). Structures and Materials Panel.
AIRCRAFT DYNAMIC RESPONSE TO DAMAGED AND REPAIRED RUNWAYS
Loughton, England Mar. 1987 45 p Meeting held in Oberammergau, West Germany, 8-13 Sep. 1985
(AGARD-R-739; ISBN-92-835-0409-7) Copyright Avail: NTIS HC A03/MF A01

The dynamic response of aircraft operating from damaged and repaired runways is examined. The response of a simplified representation of an aircraft to two discrete disturbances is analyzed to see how the second disturbance modifies system behavior caused by the first disturbance. A mathematical model is provided which can be used for calculation of the dynamic response of aircraft structures operating on rough surfaces; a comparison is made between theoretical predictions for a YF16 aircraft and typical measurements from frequency response tests. For individual titles, see N87-23610 through N87-23611.

N87-23610# Air Force Wright Aeronautical Labs., Wright-Patterson AFB, Ohio. Structures and Dynamics Div.
INTERPRETATION IN TERMS OF THE RESPONSE OF A ONE DEGREE-OF-FREEDOM OSCILLATOR TO TWO SUCCESSIVE DISTURBANCES
James J. Olsen *In* AGARD Aircraft Dynamic Response to Damaged and Repaired Runways Mar. 1987 22 p (For primary document see N87-23609 17-05)
Copyright Avail: NTIS HC A03/MF A01

The dynamic response of an aircraft that taxies over two arbitrary disturbances, under the assumption that the aircraft can be represented as a linear, one degree-of-freedom system is explained. That analysis produced the concept of the BUMP MULTIPLIER which explicitly and simply determines whether a second discrete disturbance will amplify or attenuate the response from a first disturbance. The BUMP MULTIPLIER also simplifies the understanding and presentation of the results. While the assumptions are very severe, the resulting formulas can be very useful to guide more elaborate nonlinear calculations or to plan test programs. Author

N87-23611# Deutsche Forschungs- und Versuchsanstalt fuer Luft- und Raumfahrt, Goettingen (West Germany). Inst. of Aeroelasticity.
AN EXPERIMENTAL-ANALYTICAL ROUTINE FOR THE DYNAMIC QUALIFICATION OF AIRCRAFT OPERATING ON ROUGH RUNWAY SURFACES
R. Freymann *In* AGARD Aircraft Dynamic Response to Damaged and Repaired Runways Mar. 1987 14 p (For primary document see N87-23609 17-05)
Copyright Avail: NTIS HC A03/MF A01

A mathematical model to be used as a basis for analytical investigations to predict the dynamic structural response of flexible aircraft operating on rough runway surfaces is presented. It is shown how the structural parameters included in the aircraft generalized equations of motion are determined in a ground vibration test on the real aircraft structure and in additional tests on components of the undercarriage. The validation of the developed mathematical model is achieved by a comparison of

typical results from frequency response tests and calculations performed on a YF-16 prototype fighter aircraft. Finally, the way in which the developed mathematical model can be used in combination with various systematic test procedures for the dynamic qualification process of aircraft operation on damages/repaired runways is indicated. Author

N87-23612# Air Force Inst. of Tech., Wright-Patterson AFB, Ohio. School of Engineering.
EVALUATION OF THE ANGLE OF ATTACK LIMITER OF THE F-16 C/D AIRCRAFT M.S. Thesis
Zeki Dikilitas Dec. 1986 311 p
(AD-A177941; AFIT/GE/ENG/86D-9) Avail: NTIS HC A14/MF A01 CSCL 01C

The angle-of-attack (AOA) limiter used in the present fighter aircraft can provide safe, head-up maneuvering capability up to full aerodynamic potential of the fighter. However, the F-16 aircraft flight control system limits the effective normal acceleration (g) command with the AOA. The AOA limiter utilized in the F-16 aircraft adversely impacts air-to-air tracking tasks. Therefore, it should be modified to improve this tracking capability. Two aircraft models are developed to evaluate current AOA limiter effects on the aircraft dynamics. The first model is a linear model which is developed in state space form for the F-16 from linearized aerodynamic data. This is accomplished at four points in the flight enveloped. The second model is a non-linear model which is developed using non-linear equations of motion and flight control system equations and then coded using PTRAN simulation language employed on SIMSTAR hybrid computer system at the Air Force Institute of Technology. After validation, these models are used for the evaluation of the AOA limiter. GRA

N87-23613# Cranfield Inst. of Tech., Bedford (England). Coll. of Aeronautics.
AN EXPERIMENTAL INVESTIGATION INTO METHODS FOR QUANTIFYING HANG GLIDER AIRWORITHNESS PARAMETERS Summary Report
M. V. Cook and E. A. Kilkenny May 1987 27 p
(Grant GR/B94953)
(CAR-8705; ISBN-0-947767-58-4) Avail: NTIS HC A03/MF A01

A three year program of research was completed in which the principle activity was an experimental investigation of those aerodynamic, stability and control parameters which influence the airworthiness of the hang glider. An experimental test rig was used which enabled aerodynamic measurements to be made on full scale hang glider wings. Early experiments were aimed at obtaining quantitative data for a number of wings, whereas later tests were concerned with flow visualization on the flexible wing surfaces. The principle objectives of the work were to provide a base of aerodynamic data for a representative selection of hang glider wings to improve the theoretical understanding of hang glider aerodynamics, stability and control and to assist in developing the test rig as a routine airworthiness test facility. M.G.

N87-23614*# National Aeronautics and Space Administration. Langley Research Center, Hampton, Va.
FLIGHT INVESTIGATION OF THE EFFECTS OF AN OUTBOARD WING-LEADING-EDGE MODIFICATION ON STALL/SPIN CHARACTERISTICS OF A LOW-WING, SINGLE-ENGINE, T-TAIL LIGHT AIRPLANE
H. Paul Stough, III, Daniel J. DiCarlo, and James M. Patton, Jr. Jul. 1987 117 p
(NASA-TP-2691; L-16243; NAS 1.60:2691) Avail: NTIS HC A06/MF A01 CSCL 01A

Flight tests were performed to investigate the change in stall/spin characteristics due to the addition of an outboard wing-leading-edge modification to a four-place, low-wing, single-engine, T-tail, general aviation research airplane. Stalls and attempted spins were performed for various weights, center of gravity positions, power settings, flap deflections, and landing-gear positions. Both stall behavior and wind resistance were improved compared with the baseline airplane. The latter would readily spin for all combinations of power settings, flap deflections, and aileron inputs, but the modified airplane did not spin at idle power or with flaps extended. With maximum power and flaps retracted, the modified airplane did enter spins with abused loadings or for certain combinations of maneuver and control input. The modified airplane tended to spin at a higher angle of attack than the baseline airplane. Author

N87-23615*# Hamilton Standard, Windsor Locks, Conn.
DYNAMIC RESPONSE OF TWO COMPOSITE PROP-FAN MODELS ON A NACELLE/WING/FUSELAGE HALF MODEL Final Report
Arthur F. Smith and Bennett M. Brooks Oct. 1986 157 p
(Contract NAS3-24088)
(NASA-CR-179589; NAS 1.26:179589; HSER-11058) Avail: NTIS HC A08/MF A01 CSCL 01C

Results are presented for blade response wind tunnel tests of two 62.2 cm diameter Prop-Fan (advanced turboprop) models with swept and unswept graphite/epoxy composite blades. Measurements of dynamic response were made with the rotors mounted on a simulated nacelle/wing/fuselage model, with varying tilt, at flow speeds up to 0.85 Mach number. The presence of the wing, downstream of the rotor, induced 1-P responses that were about twice those previously measured for an isolated nacelle installation. The swept blade had less 1-P response than the unswept (straight) blade. The 2-P response was significant for both blades, and was closely correlated to wing lift. Higher order response was not important for the straight blade, but possibly important for the swept blade near critical speeds, due to the proximity of the blade tips to the wing leading edge. Measurements are compared with theoretically based prediction. Correlations between calculated and measured 1-P response were good for the straight blade, and fair for the swept blade. Improvements to the calculation method were identified and implemented. Author

N87-23571# Joint Publications Research Service, Arlington, Va.
EFFECT OF SURFACE ROUGHNESS ON DRAG OF AIRCRAFT
R. I. Zukakishvili, A. M. Illarionov, and V. Ya. Belyayev *In its* USSR Report: Engineering and Equipment 9 Mar. 1987 p 1 Transl. into ENGLISH from Soobshcheniya Akademii Nauk Gruzinskoy SSR (Tbilisi, USSR), v. 122, no. 2, May 1986 p 358-360 Original language document was announced in IAA as A87-14717 (For primary document see N87-23570 17-01)
Avail: NTIS HC A06/MF A01

06 AIRCRAFT INSTRUMENTATION

Includes cockpit and cabin display devices; and flight instruments.

For related information see also *19 Spacecraft Instrumentation* and *35 Instrumentation and Photography.*

N87-23616*# National Aeronautics and Space Administration. Ames Research Center, Moffett Field, Calif.
HIGH-ANGLE-OF-ATTACK PNEUMATIC LAG AND UPWASH CORRECTIONS FOR A HEMISPHERICAL FLOW DIRECTION SENSOR
Stephen A. Whitmore, Jennifer Heeg, Terry J. Larson, L. J. Ehernberger, Floyd W. Hagen, and Richard V. DeLeo May 1987 21 p
(NASA-TM-86790; H-1314; NAS 1.15:86790) Avail: NTIS HC A02/MF A01 CSCL 01D

As part of the NASA F-14 high angle of attack flight test program, a nose mounted hemispherical flow direction sensor was calibrated against a fuselage mounted movable vane flow angle sensor. Significant discrepancies were found to exist in the angle of attack measurements. A two fold approach taken to resolve these discrepancies during subsonic flight is described. First, the sensing integrity of the isolated hemispherical sensor is established by wind tunnel data extending to an angle of attack of 60 deg. Second, two probable causes for the discrepancies, pneumatic lag and upwash, are examined. Methods of identifying and

compensating for lag and upwash are presented. The wind tunnel data verify that the isolated hemispherical sensor is sufficiently accurate for static conditions with angles of attack up to 60 deg and angles of sideslip up to 30 deg. Analysis of flight data for two high angle of attack maneuvers establishes that pneumatic lag and upwash are highly correlated with the discrepancies between the hemispherical and vane type sensor measurements. Author

N87-23617*# Charles River Analytics, Inc., Cambridge, Mass.
A DUAL-PROCESSOR MULTI-FREQUENCY IMPLEMENTATION OF THE FINDS ALGORITHM Final Report
Pankaj M. Godiwala and Alper K. Caglayan Apr. 1987 59 p
(Contract NAS1-17719)
(NASA-CR-178252; R-8610; NAS 1.26:178252; FR-2) Avail: NTIS HC A04/MF A01 CSCL 01D

This report presents a parallel processing implementation of the FINDS (Fault Inferring Nonlinear Detection System) algorithm on a dual processor configured target flight computer. First, a filter initialization scheme is presented which allows the no-fail filter (NFF) states to be initialized using the first iteration of the flight data. A modified failure isolation strategy, compatible with the new failure detection strategy reported earlier, is discussed and the performance of the new FDI algorithm is analyzed using flight recorded data from the NASA ATOPS B-737 aircraft in a Microwave Landing System (MLS) environment. The results show that low level MLS, IMU, and IAS sensor failures are detected and isolated instantaneously, while accelerometer and rate gyro failures continue to take comparatively longer to detect and isolate. The parallel implementation is accomplished by partitioning the FINDS algorithm into two parts: one based on the translational dynamics and the other based on the rotational kinematics. Finally, a multi-rate implementation of the algorithm is presented yielding significantly low execution times with acceptable estimation and FDI performance. Author

N87-23572# Joint Publications Research Service, Arlington, Va.
PRINCIPLES OF DATA DISPLAY IN AVIATION INSTRUMENTS
P. A. Kovalenko and V. M. Kuznetsov *In its* USSR Report: Engineering and Equipment 9 Mar. 1987 p 2 Transl. into ENGLISH from Tekhnicheskaya Estetika (Moscow, USSR), no. 4, Apr. 1986 p 4-6 (For primary document see N87-23570 17-01)
Avail: NTIS HC A06/MF A01

07 AIRCRAFT PROPULSION AND POWER

Includes prime propulsion systems and systems components, e.g., gas turbine engines and compressors; and onboard auxilliary power plants for aircraft.

For related information see also *20 Spacecraft Propulsion and Power, 28 Propellants and Fuels,* and *44 Energy Production and Conversion.*

N87-23618# Air Force Systems Command, Wright-Patterson AFB, Ohio. Foreign Technology Div.
ACTA AERONAUTICA ET ASTRONAUTICA SINICA
7 Apr. 1987 232 p Transl. into ENGLISH from Hang Kong Xuebao (China), v. 6, no. 3, 1985 p 201-300
(AD-A179673; FTD-ID(RS)T-1246-85) Avail: NTIS HC A11/MF A01 CSCL 13H

This paper reviews the current situation and the history of development of cast turbine blades of Chinese aircraft engines for nearly three decades since 1956 and sums up the cast high-temperature alloys and casting methods which were provided by the materials and casting scientific and technical personnel during this period which have met the demands of aircraft engines. Remarkable successes have been made in many fields such as cast rotor blades, ceramic cores for hollow blades, research into dispersion-strengthened alloys, and computer-based quality control, etc. With a view to future development of high performance engines this paper proposes research on ceramic and refractory materials to meet the following requirements: (1) increased operating temperature; (2) enhanced surface stability; and (3) superior mechanical properties. GRA

N87-23619*# National Aeronautics and Space Administration. Ames Research Center, Moffett Field, Calif.
HIGHLY INTEGRATED DIGITAL ELECTRONIC CONTROL: DIGITAL FLIGHT CONTROL, AIRCRAFT MODEL IDENTIFICATION, AND ADAPTIVE ENGINE CONTROL
Jennifer L. Baer-Riedhart and Robert J. Landy (McDonnell Aircraft Co., St. Louis, Mo.) Mar. 1987 16 p Presented at the AIAA Guidance and Control Conference, Snowmass, Colo., 19-21 Aug. 1985
(NASA-TM-86793; H-1318; NAS 1.15:86793; AIAA-Paper-85-1877)
Avail: NTIS HC A02/MF A01 CSCL 21E

The highly integrated digital electronic control (HIDEC) program at NASA Ames Research Center, Dryden Flight Research Facility is a multiphase flight research program to quantify the benefits of promising integrated control systems. McDonnell Aircraft Company is the prime contractor, with United Technologies Pratt and Whitney Aircraft, and Lear Siegler Incorporated as major subcontractors. The NASA F-15A testbed aircraft was modified by the HIDEC program by installing a digital electronic flight control system (DEFCS) and replacing the standard F100 (Arab 3) engines with F100 engine model derivative (EMD) engines equipped with digital electronic engine controls (DEEC), and integrating the DEEC's and DEFCS. The modified aircraft provides the capability for testing many integrated control modes involving the flight controls, engine controls, and inlet controls. This paper focuses on the first two phases of the HIDEC program, which are the digital flight control system/aircraft model identification (DEFCS/AMI) phase and the adaptive engine control system (ADECS) phase. Author

N87-23620# Vibration Inst., Clarendon Hills, Ill.
THE SHOCK AND VIBRATION DIGEST, VOLUME 19, NO. 5 Monthly Report
Judith Nagle-Eshleman May 1987 60 p
Avail: NTIS HC A04/MF A01

Abstracts are presented for the following areas: machines; structures; vehicles; mechanical components; structural components; experimental techniques; environments; mathematical methods; computational methods; and modeling techniques. Also contained is an article on turbomachine blade vibration. For individual titles, see N87-23621 through N87-23621.

N87-23621# Indian Inst. of Tech., New Delhi.
TURBOMACHINE BLADE VIBRATION
J. S. Rao *In* Vibration Inst. The Shock and Vibration Digest, Vol. 19, No. 5 May 1987 p 3-10 (For primary document see N87-23620 17-07)
Avail: NTIS HC A04/MF A01

Literature since 1983 is reviewed for free vibrations, excitation forces of blades, and blade response. Author

N87-23622*# Pratt and Whitney Aircraft Group, East Hartford, Conn. Engineering Div.
LIFE PREDICTION AND CONSTITUTIVE MODELS FOR ENGINE HOT SECTION ANISOTROPIC MATERIALS Annual Status Report
G. A. Swanson, I. Linask, D. M. Nissley, P. P. Norris, T. G. Meyer, and K. P. Walker Apr. 1987 166 p
(Contract NAS3-23939)
(NASA-CR-179594; NAS 1.26:179594; PWA-5968-47; ASR-2)
Avail: NTIS HC A08/MF A01 CSCL 21E

The results are presented of a program designed to develop life prediction and constitutive models for two coated single crystal alloys used in gas turbine airfoils. The two alloys are PWA 1480 and Alloy 185. The two oxidation resistant coatings are PWA 273, an aluminide coating, and PWA 286, an overlay NiCoCrAlY coating. To obtain constitutive and fatigue data, tests were conducted on uncoated and coated specimens loaded in the <100>, <110>, <111> and <123> crystallographic directions. Two constitutive models are being developed and evaluated for the single crystal

materials: a micromechanic model based on crystallographic slip systems, and a macroscopic model which employs anisotropic tensors to model inelastic deformation anisotropy. Based on tests conducted on the overlay coating material, constitutive models for coatings also appear feasible and two initial models were selected. A life prediction approach was proposed for coated single crystal materials, including crack initiation either in the coating or in the substrate. The coating initiated failures dominated in the tests at load levels typical of gas turbine operation. Coating life was related to coating stress/strain history which was determined from specimen data using the constitutive models. Author

N87-23623*# National Aeronautics and Space Administration. Lewis Research Center, Cleveland, Ohio.
PERFORMANCE OF TWO 10-LB/SEC CENTRIFUGAL COMPRESSORS WITH DIFFERENT BLADE AND SHROUD THICKNESSES OPERATING OVER A RANGE OF REYNOLDS NUMBERS
Gary J. Skoch (Army Aviation Research and Development Command, Cleveland, Ohio.) and Royce D. Moore 1987 25 p Presented at the 23rd Joint Propulsion Conference, San Diego, Calif., 29 Jun. - 2 Jul. 1987; sponsored by AIAA, SAE, ASME and ASEE
(NASA-TM-100115; E-3660; NAS 1.15:100115; AVSCOM-TR-87-C-21; AIAA-87-1745) Avail: NTIS HC A02/MF A01 CSCL 21E

Centrifugal compressors often cannot be directly scaled to very small flow sizes because of structural and manufacturing limitations. The inability to directly scale all design parameters leads to a performance loss other than that which can be associated with the lower Reynolds number. A 10-lb/sec centrifugal compressor was scaled down to 2-lb/sec where adjustments to blade and shroud thickness and fillet radii were required. The modified 2-lb/sec compressor was then directly scaled back up to 10 lb/sec so that the effect of the modifications could be determined. The performance of the two 10-lb/sec compressors is compared over a range of speed and mass flow. The effect of variations in Reynolds number, impeller tip clearance, and shroud thickness on compressor performance is also presented. Author

N87-23624*# National Aeronautics and Space Administration. Lewis Research Center, Cleveland, Ohio.
LINER COOLING RESEARCH AT NASA LEWIS RESEARCH CENTER
Waldo A. Acosta (Army Aviation Research and Development Command, Cleveland, Ohio.) 1987 18 p Presented at the 23rd Joint Propulsion Conference, San Diego, Calif., 29 Jun. - 2 Jul. 1987; sponsored by AIAA, SAE, ASME and ASEE
(NASA-TM-100107; E-3647; NAS 1.15:100107; AIAA-87-1828; AVSCOM-TR-87-C-8) Avail: NTIS HC A02/MF A01 CSCL 21E

Described are recently completed and current advanced liner research applicable to advanced small gas turbine engines. Research relating to the evolution of fuel efficient small gas turbine engines capable of meeting future commercial and military aviation needs is currently under way at NASA Lewis Research Center. As part of this research, a reverse-flow combustor geometry was maintained while different advanced liner wall cooling techniques were investigated and compared to a baseline combustor. The performance of the combustors featuring counterflow film-cooled (CFFC) panels, transpiration cooled liner walls (TRANS), and compliant metal/ceramic (CMC) walls was obtained over a range of simulated flight conditions of a 16:1 pressure ratio gas turbine engine and fuel/air ratios up to 0.034. All the combustors featured an identical fuel injection system, identical geometric configuration outline, and similar designed internal aerothermodynamics. Author

N87-23625*# National Aeronautics and Space Administration. Lewis Research Center, Cleveland, Ohio.
METHOD FOR THE DETERMINATION OF THE THREE-DIMENSIONAL AERODYNAMIC FIELD OF A ROTOR-STATOR COMBINATION TO COMPRESSIBLE FLOW
Sridhar M. Ramachandra, Lawrence J. Bober, and Suresh Khandelwal (Sverdrup Technology, Inc., Cleveland, Ohio.) Jul. 1987 32 p Presented at the 23rd Joint Propulsion Conference, San Diego, Calif., 29 Jun. - 2 Jul. 1987; cosponsored by AIAA, SAE, ASME and ASEE
(NASA-TM-100118; E-3662; NAS 1.15:100118; AIAA-87-1742) Avail: NTIS HC A03/MF A01 CSCL 21E

Using the lifting surface theory and the acceleration potential method for the flow field of an axial turbocompressor stage, a recursive and a direct method are presented that make use of the eigenfunction solutions of the isolated rotor and stator to solve for the rotor-stator interaction problem. The net pressure distribution on the rotor and stator blades is represented by modified Birnbaum series, whose coefficients are determined using a matrix procedure and satisfying the boundary conditions on the surface of the blades. The relation between the matrix operators of the recursive and the direct methods is also shown. Expressions have been given for the blade circulation, the axial and tangential forces on the blade, the rotor power required, and the induced upwash velocity of the stage. Author

N87-23626*# National Aeronautics and Space Administration. Lewis Research Center, Cleveland, Ohio.
THE SUPERSONIC THROUGH-FLOW TURBOFAN FOR HIGH MACH PROPULSION
Leo C. Franciscus Jul. 1987 14 p Presented at the 23rd Joint Propulsion Conference, San Diego, Calif., 29 Jun. - 2 Jul. 1987
(NASA-TM-100114; E-3659; NAS 1.15:100114; AIAA-87-2050) Avail: NTIS HC A02/MF A01 CSCL 21E

A study was done to evaluate the potential improvements in aircraft turbine engine performance by incorporating unique supersonic through-flow fans. Engine performance, weight, and mission studies were carried out for conventional turbofan engines using supersonic through-flow fans. A Mach 3 commercial transport mission was considered. The advantages of the supersonic fan engines were evaluated in terms of mission range comparisons between the supersonic fan engines and conventional engines. The installed specific fuel consumption of the supersonic fan engines was 12 percent better than the conventional engines and the installed weight was projected to be 25 percent lighter. For a takeoff gross weight of 550,000 lbs, the aircraft powered by supersonic fan engines had a range capability of 6600 nm compared to 5300 nm (a 25% improvement) for conventional engines. Author

N87-23577# Joint Publications Research Service, Arlington, Va.
DEVELOPMENT OF MODEL DESCRIBING UNSTABLE OPERATION OF TURBOCOMPRESSOR AND DESIGN OF ANTISURGING PROTECTION FOR GAS TURBINE ENGINE
M. M. Shakiryanov *In its* USSR Report: Engineering and Equipment 9 Mar. 1987 p 5 Transl. into ENGLISH from Izvestiya Vysshikh Uchebnykh Zavedeniy: Aviatsionnaya Tekhnika (Kazan, USSR), no. 1, Jan. - Mar. 1986 p 61-66 (For primary document see N87-23570 17-01)
Avail: NTIS HC A06/MF A01

N87-23580# Joint Publications Research Service, Arlington, Va.
EFFECTIVENESS OF BALANCING FLEXIBLE ROTARY COMPRESSOR VANES ON LOW-SPEED BALANCING MACHINE
A. I. Gleyzer and V. A. Bulychev *In its* USSR Report: Engineering and Equipment 9 Mar. 1987 p 7 Transl. into ENGLISH from Izvestiya Vysshikh Uchebnykh Zavedeniy: Aviatsionnaya Tekhnika (Kazan, USSR), no. 1, Jan. - Mar. 1986 p 15-19 Original language document was announced in IAA as A86-43379 (For primary document see N87-23570 17-01)
Avail: NTIS HC A06/MF A01

N87-23582# Joint Publications Research Service, Arlington, Va.
FLOW OF GAS THROUGH TURBINE STAGE WITH SPHERICAL NOZZLE SEGMENT
A. I. Arkhipov, M. K. Maksutova, and Yu. V. Strunkin *In its*

USSR Report: Engineering and Equipment 9 Mar. 1987 p 8 Transl. into ENGLISH from Izvestiya Vysshikh Uchebnykh Zavedeniy: Aviatsionnaya Tekhnika (Kazan, USSR), no. 1, Jan. - Mar. 1986 p 8-11 Original language document was announced in IAA as A86-43377 (For primary document see N87-23570 17-01)
Avail: NTIS HC A06/MF A01

08 AIRCRAFT STABILITY AND CONTROL

Includes aircraft handling qualities; piloting; flight controls; and autopilots.

For related information see also *05 Aircraft Design, Testing and Performance.*

N87-23627*# Stanford Univ., Calif. Joint Inst. for Aeronautics and Acoustics.
TWO BLOWING CONCEPTS FOR ROLL AND LATERAL CONTROL OF AIRCRAFT
D. A. Tavella, N. J. Wood, C. S. Lee, and L. Roberts Oct. 1986 107 p
(Contract NCC2-271)
(NASA-CR-180478; NAS 1.26:180478; JIAA-TR-75) Avail: NTIS HC A06/MF A01 CSCL 01C

Two schemes to modulate aerodynamic forces for roll and lateral control of aircraft have been investigated. The first scheme, called the lateral blowing concept, consists of thin jets of air exiting spanwise, or at small angle with the spanwise direction, from slots at the tips of straight wings. For this scheme, in addition to experimental measurements, a theory was developed showing the analytical relationship between aerodynamic forces and jet and wing parameters. Experimental results confirmed the theoretically derived scaling laws. The second scheme, which was studied experimentally, is called the jet spoiler concept and consists of thin jets exiting normally to the wing surface from slots aligned with the spanwise direction. Author

N87-23628# Air Force Inst. of Tech., Wright-Patterson AFB, Ohio. School of Engineering.
FAILURE DETECTION AND ISOLATION FOR AN ASYCHRONOUS DIGITAL FLIGHT CONTROL SYSTEM M.S. Thesis
Gursel Serpen Mar. 1987 192 p
(AD-A179210; AFIT/GE/ENG/87M-6) Avail: NTIS HC A09/MF A01 CSCL 01C

The purpose of this study was to design and test a failure detection and isolation subsystem for a triply redundant asychronous digital flight control system. The focus of the research was to analyze the time skew effect in an asychronous environment. A model to estimate the time skew and the time skew related interchannel difference was developed. The design was tested in a simulation environment where the YF-16 longitudinal dynamics and the AFTI/F-16 digital flight control system were modelled. GRA

N87-23629# Air Force Inst. of Tech., Wright-Patterson AFB, Ohio. School of Engineering.
FLIGHT TEST EVALUATION OF TECHNIQUES TO PREDICT LONGITUDINAL PILOT INDUCED OSCILLATIONS M.S. Thesis
Eileen A. Bjorkman Dec. 1986 186 p
(AD-A179229; AFIT/GAE/AA/86J-1) Avail: NTIS HC A09/MF A01 CSCL 05H

The purpose of this study was to determine if pilot induced oscillations (PIOs) can be predicted prior to flight using existing PIO prediction techniques. Two techniques to predict longitudinal PIO tendencies were studied analytically using an existing PIO data base. The two techniques were then applied to 18 aircraft/flight control system landing configurations. The 18 configurations were flight tested using a flared landing task with the USAF/Calspan variable stability NT-33A. The PIO tendencies and frequencies were correctly predicted provided the configuration was not sensitive to the pilot model used. A suggested modification of theory correctly predicted PIO ratings within an average of 0.6 rating. A suggested modification to the bandwidth method predicted PIO ratings within an average of 0.5 rating. The limited data base was too small to draw any definite conclusions. Recommendations for further study included collecting more PIO data and using existing data bases and simulator studies to better define the two techniques and to gain physical insights into PIO mechanization. GRA

N87-23630*# National Aeronautics and Space Administration. Langley Research Center, Hampton, Va.
HELICOPTER ANTI-TORQUE SYSTEM USING FUSELAGE STRAKES Patent Application
Henry L. Kelley, inventor (to NASA) and John C. Wilson, inventor (to NASA) 30 Jan. 1987 14 p
(NASA-Case-LAR-13630-1; US-Patent-Appl-SN-008895) Avail: NTIS HC A02/MF A01 CSCL 01C

This invention relates to helicopters, and particularly to the improvement of the helicopter torque control system. At low to medium forward speeds helicopter performance is limited by the effectiveness of the means for counter-acting main rotor torque and controlling sideslip airloads. These problems may be overcome by mounting strakes on the aft fuselage section. For single rotor helicopters whose main rotor rotates counter-clockwise as viewed from above, one of the strakes would be mounted in the upper left hand quadrant and the second in the lower left hand quadrant. The strakes alter the air flow around the fuselage by separating the flow so as to produce lateral air loads on the tail boom which oppose main-rotor torque. The upper strake operates in a right crosswind to oppose main rotor torque, and the lower strake has effect in left crosswinds. The novelty of this invention resides in the simple and economical manner in which the helicopter tail boom may be modified by the addition of strakes in order to increase torque control, and reduce the need for supplemental mechanical means of torque control. NASA

N87-23631* National Aeronautics and Space Administration. Ames Research Center, Moffett Field, Calif.
SWASHPLATE CONTROL SYSTEM Patent
Richard J. Peyran, Georgene H. Laub, and H. Andrew Morse 2 Jun. 1987 9 p Filed 31 Mar. 1986 Supersedes N86-24700 (24 - 15, p 2417)
(NASA-Case-ARC-11633-1; US-Patent-4,669,958; US-Patent-Appl-SN-846439; US-Patent-Class-416-114; US-Patent-Class-416-158)
Avail: US Patent and Trademark Office CSCL 01C

A mechanical system to control the position of a rotating swashplate is developed. This system provides independent lateral cyclic, longitudinal cyclic and collective pitch control of a helicopter rotor attached to the swashplate, without use of a mixer box. The system also provide direct, linear readout of cyclic and collective swashplate positions. NASA

N87-23632*# National Aeronautics and Space Administration. Ames Research Center, Moffett Field, Calif.
DEMONSTRATION OF FREQUENCY-SWEEP TESTING TECHNIQUE USING A BELL 214-ST HELICOPTER
Mark B. Tischler, Jay W. Fletcher, Vernon L. Diekmann, Robert A. Williams, and Randall W. Cason (Army Aviation Engineering Flight Activity, Edwards AFB, Calif.) Apr. 1987 83 p
(NASA-TM-89422; A-87073; AVSCOM-TM-87-A-1; NAS 1.15:89422) Avail: NTIS HC A05/MF A01 CSCL 01C

A demonstration of frequency-sweep testing using a Bell-214ST single-rotor helicopter was completed in support of the Army's development of an updated MIL-H-8501A, and an LHX (ADS-33) handling-qualities specification. Hover and level-flight (V sub a = 0 knots and V sub a = 90 knots) tests were conducted in 3 flight hours by Army test pilots at the Army Aviation Engineering Flight Activity (AEFA) at Edwards AFB, Calif. Bandwidth and phase-delay parameters were determined from the flight-extracted frequency responses as required by the proposed specifications. Transfer function modeling and verification demonstrates the validity of the

frequency-response concept for characterizing closed-loop flight dynamics of single-rotor helicopters -- even in hover. This report documents the frequency-sweep flight-testing technique and data-analysis procedures. Special emphasis is given to piloting and analysis considerations which are important for demonstrating frequency-domain specification compliance. Author

09 RESEARCH AND SUPPORT FACILITIES (AIR)

Includes airports, hangars and runways; aircraft repair and overhaul facilities; wind tunnels; shock tubes; and aircraft engine test stands.

For related information see also *14 Ground Support Systems and Facilities (Space).*

N87-23633# Advisory Group for Aerospace Research and Development, Neuilly-Sur-Seine (France). Flight Mechanics Panel.

FLIGHT SIMULATION

Loughton, England Sep. 1986 360 p In ENGLISH and FRENCH Symposium held in Cambridge, England, 30 Sep. - 3 Oct. 1985

(AGARD-CP-408; ISBN-92-835-0394-5) Copyright Avail: NTIS HC A16/MF A01

The objectives of the conference were to provide an up-to-date description of state-of-the-art technology and engineering for both ground-based and in-flight simulators, together with an indication of future possibilities; and to place the roles of ground-based and in-flight simulators into context with one another and within the aerospace industry. For individual titles, see N87-23634 through N87-23660.

N87-23634*# National Aeronautics and Space Administration. Ames Research Center, Moffett Field, Calif.

VISUAL AND MOTION CUEING IN HELICOPTER SIMULATION

Richard S. Bray *In* AGARD Flight Simulation Sep. 1986 16 p Previously announced as N86-11208 (For primary document see N87-23633 17-09)

Copyright Avail: NTIS HC A16/MF A01

The visual cues presented in the simulator are compared with those of flight in an attempt to identify deficiencies. For the low-amplitude maneuvering tasks normally associated with the hover mode, the unique motion capabilities of the Vertical Motion Simulator (VMS) at Ames Research Center permit nearly a full representation of vehicle motion. Especially appreciated in these tasks are the vertical-acceleration responses to collective control. For larger-amplitude maneuvering, motion fidelity must suffer diminution through direct attenuation through high-pass filtering washout of the computer cockpit accelerations or both. Experiments were conducted in an attempt to determine the effects of these distortions on pilot performance of height-control tasks. Author

N87-23635# Rediffusion Simulation Ltd., Crawley (England).

VISUAL DISPLAY RESEARCH TOOL

P. M. Murray and B. Barber *In* AGARD Flight Simulation Sep. 1986 8 p (For primary document see N87-23633 17-09)

Copyright Avail: NTIS HC A16/MF A01

The Visual Display Research Tool (VDRT) is a new concept in visual displays which utilizes area of interest approach by matching its display parameters to those of the human eye. Two fields of view are employed, a wide-angle field corresponding to the peripheral area and an area of interest field inset at its center. The combined field is coupled to head and eye movements such that the direction of gaze is followed and a detailed scene is apparent over the whole field of regard at all times. The specific design chosen for VDRT is based on helmet mounted projection of two full color rasters onto the interior surface of a spherical dome surrounding the cockpit. The VDRT has been designed to meet the specified performance in a manner which allows a great deal of flexibility in system performance under software control. It should enable a lot of experimental results to be obtained on the performance and suitability of a head mounted eye tracker area of interest system as a training device. Author

N87-23636# Singer-Link-Miles Ltd., Lancing (England). Visual Applications Group.

ADVANCED VISUALS IN MISSION SIMULATORS

D. A. Cowdrey *In* AGARD Flight Simulation Sep. 1986 10 p (For primary document see N87-23633 17-09)

Copyright Avail: NTIS HC A16/MF A01

Modern, sophisticated full mission flight systems trainers are capable of accurate representation of the actual aircraft in many areas including handling, controls, systems, etc. The major area of inadequacy to date has been the inability to produce a satisfactory visual representation of the outside world. To produce an image to match that of the pilot's field-of-view at the required resolution is beyond the capabilities of conventional visual system technology. Various alternative techniques of satisfying this demanding field-of-view/resolution requirement including the technique developed at the Link Flight Simulation Division of the Singer Company, based on an eye-slaved area-of-interest (AOI) concept are discussed. Author

N87-23637# Toronto Univ., Downsview (Ontario). Inst. for Aerospace Studies.

THE APPLICATION OF OPTIMAL CONTROL TECHNIQUES TO THE UTIAS RESEARCH SIMULATOR

L. D. Reid *In* AGARD Flight Simulation Sep. 1986 13 p Sponsored by the Natural Sciences and Engineering Research Council and the Transportation Development Centre (For primary document see N87-23633 17-09)

Copyright Avail: NTIS HC A16/MF A01

Optimal control has been useful in many aerospace applications in recent years. Two such applications to flight simulators are described. The first involves the generation of wind shear effects for use in training exercises. This work included simulator trails and an assessment of the process by a number of pilots. The second application is to the generation of simulator motion-base drive signals in a six degrees-of-freedom facility. In this case the optimal controller is composed of a series of filters that act much like a classical washout algorithm. Vestibular models which predict the sensation of motion by the pilot are incorporated within the optimal controller and are also used to evaluate its overall performance. Author

N87-23638# Avions Marcel Dassault-Breguet Aviation, Istres (France).

OASIS: A MODERN TOOL FOR REAL-TIME SIMULATION

J. Benoit *In* AGARD Flight Simulation Sep. 1986 13 p (For primary document see N87-23633 17-09)

Copyright Avail: NTIS HC A16/MF A01

The hardware and software of the OASIS real-time flight simulation system are discussed. Symbol generation, the performance of elementary graphic functions, the validation of system concepts, and training are briefly discussed. R.J.F.

N87-23639# Royal Aircraft Establishment, Bedford (England). FS(B)3 Div.

SIMULATOR MOTION CHARACTERISTICS AND PERCEPTUAL FIDELITY Progress Report

B. N. Tomlinson *In* AGARD Flight Simulation Sep. 1986 12 p Previously announced as X87-70218 (For primary document see N87-23633 17-09)

Copyright Avail: NTIS HC A16/MF A01

Information is given on a study, commissioned by the AGARD Flight Mechanics Panel, to review existing data and try to describe a relationship between certain motion system parameters, identified in an earlier AGARD Report (AR-144), and the fidelity of the pilot's perception of flight. Motion system characteristics as a whole are discussed, thus extending AR-144's treatment of motion mechanisms to include motion drive software and other features. Some of the key parameters of AR-144 are then examined in relation to total motion system fidelity. Finally, some proposals

are made for a common format data structure with which to summarise research results on motion cues. Author

N87-23640# British Aerospace Public Ltd. Co., Preston (England).
SIMULATION OF AIRCRAFT BEHAVIOUR ON AND CLOSE TO THE GROUND: SUMMARY OF AGARD(LC6)OGRAPH AG-285
A. G. Barnes *In* AGARD Flight Simulation Sep. 1986 4 p (For primary document see N87-23633 17-09)
Copyright Avail: NTIS HC A16/MF A01

A summary of a report on the simulation of aircraft characteristics on and near the ground is given. The benefits of good handling are noted. The components needed to put together a simulation - the data set, the computer, the visual system, the motion system, and other cueing devices - are considered. Modeling of the vehicle on the ground is discussed, as are visual system requirements. R.J.F.

N87-23641# Rediffusion Simulation Ltd., Crawley (England). Research and Development Dept.
USE OF VDU's BY FLIGHT SIMULATOR INSTRUCTORS
Mark A. Brunt *In* AGARD Flight Simulation Sep. 1986 6 p (For primary document see N87-23633 17-09)
Copyright Avail: NTIS HC A16/MF A01

The development of Visual Display Unit (VDU)-based simulator instructor stations with some ergonomics rules are compared. Design aims and practical experience are discussed. Further rules are developed to establish a baseline for designers, procurers and users of instructor stations. Author

N87-23642# Royal Aircraft Establishment, Bedford (England).
PROGRESS IN THE IMPLEMENTATION OF AGARD-AR-144 IN MOTION SYSTEM ASSESSMENT AND MONITORING
K. J. Staples, W. Love, and D. Parkinson (Singer-Link-Miles Ltd., Lancing, England) *In* AGARD Flight Simulation Sep. 1986 11 p (For primary document see N87-23633 17-09)
Copyright Avail: NTIS HC A16/MF A01

After a brief explanation of the techniques defined in AGARD-AR-144, a description is given of two systems which have been built and tested to satisfy the requirements of the AGARD Report. Each system is stand-alone and only requires the user to supply the sensors on the motion system itself. One system, from Singer Link Miles, is especially suited to six degree-of-freedom, synergistic motion systems, whereas the other, from Cranfield Institute of Technology, is more appropriate to systems with independent axes. The systems have each been used on several different motion systems and some examples of measured results are given. Author

N87-23643# National Aerospace Lab., Amsterdam (Netherlands).
FLEXIBLE AND HIGH QUALITY SOFTWARE ON A MULTIPROCESSOR COMPUTER SYSTEM CONTROLLING A RESEARCH FLIGHT SIMULATOR
A. P. L. A. Marsman *In* AGARD Flight Simulation Sep. 1986 11 p Previously announced as N87-18578 (For primary document see N87-23633 17-09)
Copyright Avail: NTIS HC A16/MF A01

The research environment and the multiprocessor computer system required for flexible software for flight simulation programs are described. The program incorporates all hardware options with different calibration tables as the most simple solution, since for example the drive laws trimming the primary control systems are different for each system. Modularity of the simulation program allows the usage of subsets of the hardware. Even the primary controls can be replaced by inputs from a file. This enables the flexibility of parallel maintenance of hardware, while testing modified modules in the software. It reduces the costs for projects which do not need all systems. Author

N87-23644# Messerschmitt-Boelkow-Blohm G.m.b.H., Munich (West Germany). Ergonomics and Cockpit System.
COMPUTER SIMULATION STUDIES ON HUMAN CONTROL RELIABILITY IN MANUAL AIRCRAFT CONTROL: THE ORIGIN OF PIO c54
K. Brauser and R. Seifert *In* AGARD Flight Simulation Sep. 1986 19 p (For primary document see N87-23633 17-09)
Copyright Avail: NTIS HC A16/MF A01

Pilot induced oscillations usually are defined as a sensitive indication of bad handling qualities. In the view of human performance reliability, PIO's are related to input errors with respect to the control characteristics of the controlled system. It is a general rule that man will make errors while performing arbitrary tasks under the influence of possible performance shaping factors (PSF's). A recently developed Task Taxonomy Method is used as a tool for the assessment of Human Error Probabilities (REP) depending quantitatively on the effects of performance shaping factors (PSF) like task dimensions and characteristics, operator characteristics, system characteristics and environment factors. Using this Task Taxonomy procedure, HEP values for the manual aircraft control task have been calculated. HEP values are drastically increased (0.5 to 0.9) by the influence of bad handling qualities, while good handling qualities may only reduce the HEP value to 0.1, because other PSF's may remain still active. Therefore PIO incidents remain possible, even in aircraft with good handling qualities. This has been demonstrated by means of SAINT computer simulations using appropriate HEP values. Author

N87-23645# Air Force Wright Aeronautical Labs., Wright-Patterson AFB, Ohio. Flight Control Div.
TRENDS IN GROUND-BASED AND IN-FLIGHT SIMULATORS FOR DEVELOPMENT APPLICATIONS
Paul E. Blatt and Don R. Gum *In* AGARD Flight Simulation Sep. 1986 13 p (For primary document see N87-23633 17-09)
Copyright Avail: NTIS HC A16/MF A01

Current capabilities and future trends for research and development simulators - both ground-based and in-flight are described. Engineering simulators are applied as design tools for synthesis and assessment of advanced aircraft, flight control systems, avionic system design, and cockpit man-machine integration. Real-time, piloted flight simulation for dynamic applications is discussed. No training simulation implications are intended. Author

N87-23646# Textron Bell Helicopter, Fort Worth, Tex.
PILOTED SIMULATION IN THE DEVELOPMENT OF THE XV-15 TILT ROTOR RESEARCH AIRCRAFT
Roger L. Marr and Gary B. Churchill (Army Aeromechanics Lab., Moffett Field, Calif.) *In* AGARD Flight Simulation Sep. 1986 15 p (For primary document see N87-23633 17-09)
Copyright Avail: NTIS HC A16/MF A01

The effective use of simulation in the XV-15 preliminary design was demonstrated. All primary program objectives were met. The initial simulation evaluation during the source evaluation board proceedings contributed significantly to performance and stability and control evaluations. Subsequent simulation periods provided major contributions in the areas of control concepts, cockpit configuraiton, handling qualities, pilot workload, failure effects and recovery procedures. The fidelity of the simulation also provided a valuable pilot training aid as well as a means of evaluating the tilt rotor concept for various military and civil missions. Simulation continues to provide valuable design data for refinement of automatic flight control systems and design support for future tilt rotor applications. Throughout, fidelity has been a prime issue and has resulted in unique data and methods to validate and update the tilt rotor math model. Researchers participation from contractor and government agencies in the development of this simulation effort has led to a generic tilt rotor simulation capability on numerous facilities. Author

N87-23647# Centre d'Essais en Vol, Istres (France).
SIMULATION OF FLY-BY-WIRE CONTROL FOR CIVIL TRANSPORT AIRCRAFT AT THE FRENCH CENTRE d'ESSAIS EN VOL [SIMULATION DES COMMANDES DE VOL ELECTRIQUES AU CENTRE D'ESSAIS EN VOL FRANCAIS (CEV) POUR LES AVIONS DE TRANSPORT CIVIL]
R. Vadrot *In* AGARD Flight Simulation Sep. 1986 13 p In FRENCH; In FRENCH (For primary document see N87-23633 17-09)
Copyright Avail: NTIS HC A16/MF A01

A review of the facilities and projects of the flight simulation center at Istres is presented. In particular, a joint program of the Centre d'Essais en Vol and Aerospatiale to develop simulation capabilities and conduct studies in civil aviation fly-by-wire control is discussed. The two phase project covered real-time image generation, cabin motion simulation, and control law development for the Airbus A-300 and A320 aircraft. M.G.

N87-23648# Industrieanlagen-Betriebsgesellschaft m.b.H., Ottobrunn (West Germany).
MANNED AIR TO AIR COMBAT SIMULATION
Paul A. Patzner *In* AGARD Flight Simulation Sep. 1986 7 p (For primary document see N87-23633 17-09)
Copyright Avail: NTIS HC A16/MF A01

The design and the development of modern fighter aircraft weapon systems has created an ever growing need for simulation activities. Especially manned simulation of combat missions in real time can provide invaluable information to the design engineers as well as to potential users of such weapon systems. The ground based Dual Flight Simulator (DFS) described here simulates air to air combat missions in real time for two different manned aircraft including avionics and armament. Each aircraft is flown by a pilot. The type of aircraft, its avionics and armament, can be modelled by exchangeable programs. In order to enlarge realism, the simulation covers a multiple target environment both in the visible range and beyond by infrared radiation radar sensors. The engagement scenario includes short range and medium range air to air missiles as well as the gun. The task area of the simulation covers mission performance assessments as well as the investigation of technical components during the research and development phase of future fighter aircraft systems. Author

N87-23649# Grumman Aerospace Corp., Bethpage, N.Y. Flight Test Dept.
UTILIZATION OF SIMULATION TO SUPPORT F-14A LOW ALTITUDE HIGH ANGLE OF ATTACK FLIGHT TESTING
P. Conigliaro and R. Goodman *In* AGARD Flight Simulation Sep. 1986 15 p (For primary document see N87-23633 17-09)
Copyright Avail: NTIS HC A16/MF A01

Ground-based flight simulation has been used successfully to support low altitude, asymmetric thrust, high angle of attack flight testing of the Grumman/Navy F-14A. The high risk nature of this flight testing, while representing a prime example of the application of simulation in the flight test environment, nonetheless generated particular problems regarding simulation fidelity and utilization requirements. As a result, new simulation capabilities were developed specifically for flight test support applications and were fully integrated into existing flight test computing/data analysis facilities. Results from the F-14 high angle of attack flight testing are used to illustrate how simulation can significantly enhance overall flight test safety and productivity. Using simulation support, an efficient test program was completed on time and allowed the F-14's departure characteristics to be safely demonstrated at angles of attack greater than 60 degrees with full engine thrust asymmetry at altitudes below 10,000 ft (3030 m). Author

N87-23650# Aeritalia S.p.A., Torino (Italy). Combat Aircraft Group.
THE USE OF AERITALIA FLIGHT SIMULATOR FOR THE DEVELOPMENT OF THE AM-X WEAPON SYSTEM
Armando Armando and Maurizio Spinoni *In* AGARD Flight Simulation Sep. 1986 12 p (For primary document see N87-23633 17-09)
Copyright Avail: NTIS HC A16/MF A01

The use of the Aeritalia flight simulator in the development of the AM-X weapon system is discussed. A brief discription of simulator components is given. Flight mechanics, flight controls simulation, cockpit development, head-up display symbology, air-to-air gun attack simulation, in-flight refueling simulation, and aircraft formation lights positioning are among the topics covered. R.J.F.

N87-23651# Thomson-CSF, Trappes (France).
RADAR SIMULATORS
J. C. Pietrement *In* AGARD Flight Simulation Sep. 1986 5 p (For primary document see N87-23633 17-09)
Copyright Avail: NTIS HC A16/MF A01

The diversity of on-board radars, the required training in their use and the need for preliminary testing prior to their definition led to the development of a multifunction radar simulator architecture offering maximum flexibility. This modular architecture makes possible a wide variety of products from simple training equipment to the most sophisticated research simulators. In addition, it can be adapted as radar techniques develop. Author

N87-23652# Air Force Flight Test Center, Edwards AFB, Calif. 6520 Test Group.
THE DEVELOPMENT OF THE T-46 NEXT GENERATION TRAINER MANNED ENGINEERING SIMULATOR AT THE US AIR FORCE FLIGHT TEST CENTER
Jonathan C. Pick *In* AGARD Flight Simulation Sep. 1986 12 p (For primary document see N87-23633 17-09)
Copyright Avail: NTIS HC A16/MF A01

The development and structure of the T-46A flight test simulation at the U.S. Air Force Flight Test Center is described. Two interesting aspects of the simulation are emphasized: (1) An electrohydraulic force-feel system is driven by a digital computer to model a reversible flight control system. This led to some force-feel system instabilities that had to be eliminated. (2) Data for extremely high angles-of-attack are incorporated into the simulation in order to simulate aircraft stall, departure, spin, and recovery. As a tool for supporting flight test operations, the T-46 simulation will be used for planning, practice flying of flight tests, and to facilitate the development and evaluation of aircraft modifications (especially those involving the flight control system). This necessitates the use of very versatile software which can be changed daily to support daily flight operations. In addition, a simulation that can accurately model flight conditions on the edges of the flight envelope greatly enhances the safety and efficiency of flight tests. Since handling qualities is the primary area of interest in this simulation, certain elements of the simulation are of key importance. One of these is control stick feel. The use of an electrohydraulic force-feel system with digital control caused a number of challenges related to force-feel system stability, which are described along with the solutions implemented. Author

N87-23653# Dornier-Werke G.m.b.H., Friedrichshafen (West Germany).
OPERATIONAL TRAINING: APPLICATION AND EXPERIENCE
Heinz Friedrich *In* AGARD Flight Simulation Sep. 1986 8 p (For primary document see N87-23633 17-09)
Copyright Avail: NTIS HC A16/MF A01

Possible applications and experience gained in the simulation of missions are described. At first, activities involving operational flight simulation are presented which are performed in the Dornier simulation laboratory and on the Alpha Jet simulator. Following a brief description of the simulator, typical examples are explained. Then a specific task on the simulator is detailed - the development of an air-to-air mode for the Heads Up Display (HUD). In the final section some aspects of operational training on flight simulators in the German air force are discussed. Author

N87-23654# Air Force Flight Test Center, Edwards AFB, Calif. 6520 Test Group.

A METHOD FOR AIRCRAFT SIMULATION VERIFICATION AND VALIDATION DEVELOPED AT THE UNITED STATES AIR FORCE FLIGHT SIMULATION FACILITY

G. R. Anderson *In* AGARD Flight Simulation Sep. 1986 7 p (For primary document see N87-23633 17-09)

Copyright Avail: NTIS HC A16/MF A01

The flight simulators at the United States Air Force Flight Test Center (AFFTC), Aircraft Flight Simulation Facility (AFSF) are primarily used for performance and flying qualities studies. These high-fidelity, real-time simulators are used as an engineering tool during the flight development of new or modified aircraft. Emphasis is placed on fully developing, verifying and validating a simulation before the actual aircraft begins flight testing. The flexibility, accuracy and ease with which the facility's method of verification and validation can be learned and implemented are a few of its advantages. This is demonstrated by the number of simulations which have been developed using it. The F-16 A/B, B-1B, Shuttle, F-15 C/D, AFTI (Advanced Fighter Technology Integration) F-16, F-16 C/D, and the T-46 are examples of simulations presently operational at the facility which were developed using the AFSF's method. The philosophy of developing a simulation before flight test allows the most to be learned about the aircraft before testing begins. The test smarter approach taken at the AFFTC requires that aircraft simulations be built quickly and be used to make flight testing more efficient and safer. The method for verifying and validating simulations used at the AFSF assures that these requirements are fulfilled. Author

N87-23655# National Aerospace Lab., Amsterdam (Netherlands).

CORRELATION BETWEEN FLIGHT SIMULATION AND PROCESSING OF FLIGHT TESTS BASED ON INERTIAL MEASUREMENTS

A. M. H. Nieuwpoort, J. H. Breeman, L. J. J. Erkelens, and P. J. J. vanderGeest *In* AGARD Flight Simulation Sep. 1986 18 p Previously announced as N87-10863 (For primary document see N87-23633 17-09)

Copyright Avail: NTIS HC A16/MF A01

Flight tests and simulations were performed using conventional and dynamic techniques based on inertial measurements. The use of inertial sensors in flight testing implies that specific forces and body rates are determined which are directly employed in the flight path reconstruction procedure. This procedure uses the equations of motion governing flight. After this step, aerodynamics model identification can take place. In flight simulation, the opposite process occurs. From the available aerodynamic and engine model, specific forces and angular accelerations can be computed. Then the equations of motion can be integrated in order to determine the flight path. Consequently there is a strong similarity in the way flight test results are processed and reduced in order to obtain aerodynamic information and the way simulations are executed using a given model. Author

N87-23656# Calspan Advanced Technology Center, Buffalo, N.Y.

UNUSUAL AIRBORNE SIMULATOR APPLICATIONS

Philip A. Reynolds *In* AGARD Flight Simulation Sep. 1986 14 p (For primary document see N87-23633 17-09)

Copyright Avail: NTIS HC A16/MF A01

Airborne simulation was conceived as a general purpose flying qualities research technique. Many diverse uses, forecast for the Total In-Flight Simulator (TIFS) while it was being developed, have come to pass, but diversity of application has exceeded even the most imaginative predictions. Some of the most unusual TIFS projects since it became active in 1971 are described. The objective is to help define and illustrate the role of airborne simulation in aerospace research and development as it interfaces with analysis, ground simulation, and flight test. Author

N87-23657# Deutsche Forschungs- und Versuchsanstalt fuer Luft- und Raumfahrt, Brunswick (West Germany). Inst. fuer Flugmechanik.

DFVLR IN-FLIGHT SIMULATORS ATTAS AND ATTHES FOR FLYING QUALITIES AND FLIGHT CONTROL RESEARCH

Dietrich Hanke and Gerd Bouwer *In* AGARD Flight Simulation Sep. 1986 13 p (For primary document see N87-23633 17-09)

Copyright Avail: NTIS HC A16/MF A01

Two new in-flight simulators have been developed by DFVLR in recent years. These are the advanced airborne simulator Advanced Technologies Testing Aircraft System (ATTAS) based on a modified VFW-614 jet transport aircraft which will be operational in 1986, and the helicopter silulator ATTHeS (Advanced Technologies Testing Helicopter System) based on a BO 105 helicopter, which has operated since 1984. The application potential, the design requirements, the vehicle modifications, the overall system performance and the simulation capabilities as well as the used model-following-control methods, showing that good simulation fidelity could be achieved are among the types discussed. Author

N87-23658# Royal Aircraft Establishment, Bedford (England). FS(B)1 Div.

DEVELOPMENT OF IN-FLIGHT SIMULATION AIRCRAFT FOR RESEARCH AND TRAINING APPLICATIONS IN UK

O. P. Nicholas, J. A. Giles, and D. A. Williams (Cranfield Inst. of Tech., Bedford, England) *In* AGARD Flight Simulation Sep. 1986 13 p (For primary document see N87-23633 17-09)

Copyright Avail: NTIS HC A16/MF A01

The objectives and the aircraft experimental system for the Vectored thrust Aircraft Advanced Flight Control (VAAC) research program are discussed. The VAAC program studies control laws, displays and cockpit controls for advanced STOL aircraft. The objective is to develop concepts and design and assessment techniques through ground based piloted simulation, mathematical studies, and flight in a two-seat fly-by-wire research Harrier aircraft. This work seeks to free the designer from some of the traditioned stability and control constraints and to maximise operational effectiveness throughout the flight envelope VSTOL aircraft.

Author

N87-23659# National Aeronautical Establishment, Ottawa (Ontario). Airborne Simulation Facility.

AIRBORNE SIMULATION AT THE NATIONAL AERONAUTICAL ESTABLISHMENT OF CANADA

J. M. Morgan *In* AGARD Flight Simulation Sep. 1986 16 p Sponsored in part by the Canadian Department of National Defence (For primary document see N87-23633 17-09)

Copyright Avail: NTIS HC A16/MF A01

The present Airborne Simulator operated by the Flight Research Laboratory (FRL) of the National Aeronautical Establishment (NAE), is based on a Bell 205A-1 host vehicle, and is the third generation of such simulators at the laboratory, the previous two being based on Bell 47 models. This aircraft was acquired by the NAE in 1969, first saw service in the simulation of variable stability role in 1971, and since then has undergone and is still undergoing a process of evolutionary development. This paper will concentrate on the operational aspects of airborne simulation using this aircraft, specifically addressing its limitations and the flight safety implications of operating in a single channel fly-by-wire mode in close proximity to the surface and obstacles. The implications of such operations, encompassing such flight phases as landing and Nap of the Earth (NOE) flight on future generations of airborne simualtion are also mentioned. Recent trends in flight mechanics research at the FRL have tended to remove emphasis from classical handling qualities experiments to a more system oriented field, and following this the Airborne Simuator has, of late, been used for investigations of the inherent aspects of fly-by-wire systems and as a general research tool in the investigation of various aspects of the glass cockpit and high technology pilot/machine interfacing. Author

N87-23660# Systems Technology, Inc., Hawthorne, Calif.
COLLECTED FLIGHT AND SIMULATION COMPARISONS AND CONSIDERATIONS
Irving L. Ashkenas *In* AGARD Flight Simulation Sep. 1986 34 p (For primary document see N87-23633 17-09)
Copyright Avail: NTIS HC A16/MF A01

Government-sponsored research at Systems Technology, Inc. dealing with simulation fidelity and utility is reviewed, starting with some generic effects of motion and vision system characteristics and computational artifacts. Diagnostic methods and tools useful in discovering and delineating significant qualitative and quantitative differences between simulation and flight are then exposed and illustrated. Finally, examples of both fixed and moving simulation successes and shortcomings are reviewed and examined as to root causes of either. The research-simulator equipment involved in the above comparisons ranges from modern large-scale motion systems and computer-generated imagery to fixed-base with simple CRT-generated displays. Author

N87-23661# Army Construction Engineering Research Lab., Champaign, Ill.
CONSEQUENCE OF LAYER SEPARATION ON PAVEMENT PERFORMANCE Final Report
Mohamed Y. Shahin, Eleanor W. Blackmon, Thomas VanDam, and Keith Kirchner Apr. 1987 59 p
(DOT/FAA/PM-86/48) Avail: NTIS HC A04/MF A01

Asphalt concrete (AC) and portland cement concrete (PCC) pavements were investigated to determine the consequence of overlay separation on pavement behavior. Available methods of detection and rehabilitation of layer separation were addressed. Stresses and strains resulting from aircraft loading in an AC pavement section were computed by layered elastic theory. Layer slippage and consequent separation generates large tensile strains at the bottom of the slipped layer, resulting in reduced fatigue life. Horizontal tangential loads due to braking or turning generate high tensile strains at the top of the overlay just outside the wheel imprint which are likely to be critical even when layer separation is not present. A finite element model was used to evaluate PCC pavement response to load, and Westergaard/Bradbury equations were used to determine curling stresses. It was found that loss of bond adversely affects maximum pavement tensile stress and maximum pavement deflections. Detection of bond loss may be possible using corner deflections determined by nondestructive testing. Author

N87-23662*# National Aeronautics and Space Administration. Lewis Research Center, Cleveland, Ohio.
EXPERIMENTAL EVALUATION OF HONEYCOMB/SCREEN CONFIGURATIONS AND SHORT CONTRACTION SECTION FOR NASA LEWIS RESEARCH CENTER'S ALTITUDE WIND TUNNEL
Richard R. Burley and Douglas E. Harrington May 1987 30 p
(NASA-TP-2692; E-3142; NAS 1.60:2692) Avail: NTIS HC A03/MF A01 CSCL 14B

An experimental investigation was conducted in the high speed leg of the 0.1 scale model of the proposed Altitude Wind Tunnel to evaluate flow conditioner configurations in the settling chamber and their effect on the flow through the short contraction section. The lowest longitudinal turbulence intensity measured at the contraction-section entrance, 1.2%, was achieved with a honeycomb plus three fine-mesh screens. Turbulence intensity in the test section was estimated to be between 0.1 and 0.2% with the honeycomb plus three fine mesh screens in the settling chamber. Adding screens, however, adversely affected the total pressure profile, causing a small defect near the centerline at the contraction section entrance. No significant boundary layer separation was evident in the short contraction section. Author

N87-23663*# Cryolab, Inc., San Luis Obispo, Calif.
COST EFFECTIVE USE OF LIQUID NITROGEN IN CRYOGENIC WIND TUNNELS
Glen E. McIntosh, David S. Lombard, David L. Martindale, and Robert P. Dunn Apr. 1987 63 p
(Contract NAS1-18216)
(NASA-CR-178279; NAS 1.26:178279) Avail: NTIS HC A04/MF A01 CSCL 14B

A method of reliquefying from 12 to 19% of the nitrogen exhaust gas from a cryogenic wind tunnel has been developed. Technical feasibility and cost effectiveness of the system depends on performance of an innovative positive displacement expander which requires scale model testing to confirm design studies. The existing cryogenic system at the 0.3-m transonic cryogenic tunnel has been surveyed and extensive upgrades proposed. Upgrades are generally cost effective and may be implemented immediately since they are based on established technology. Author

N87-23664*# National Aeronautics and Space Administration. Lewis Research Center, Cleveland, Ohio.
REACTIVATION STUDY FOR NASA LEWIS RESEARCH CENTER'S HYPERSONIC TUNNEL FACILITY
Jeffrey E. Haas Jul. 1987 14 p Presented at the 23rd Joint Propulsion Conference, San Diego, Calif., 29 Jun. - 2 Jul. 1987; cosponsored by AIAA, SAE, ASME, and ASEE
(NASA-TM-89918; E-3614; NAS 1.15:89918; AIAA-87-1886) Avail: NTIS HC A02/MF A01 CSCL 14B

The Hypersonic Tunnel Facility (HTF) at NASA Lewis Research Center's Plum Brook Station is a blowdown, free-jet, nonvitiated propulsion facility capable of Mach 5, 6, and 7 with true temperature, altitude, and air composition simulation. The facility has been in a deactivated status for 13 years. Discussed are the capabilities of HTF, and the results of a deactivation study recently conducted to determine the cost, schedule, and technical effort required to restore HTF to its original design operating capabilities are summarized. Author

N87-23665# Duits-Nederlandse Windtunnel, North East Polder (Netherlands).
[ACTIVITIES REPORT OF THE GERMAN-DUTCH WIND TUNNEL] Annual Report, 1984
1985 12 p Original document contains color illustrations
(B8677593; JE535; ETN-87-99590) Avail: NTIS HC A02/MF A01

Wind tunnel tests on aircraft and automobiles are described. Support interference and ground proximity effects; blockage correction for automotive testing; and helicopter rotor noise were studied. ESA

N87-23666# Duits-Nederlandse Windtunnel, North East Polder (Netherlands).
[ACTIVITIES REPORT OF THE GERMAN-DUTCH WIND TUNNEL] Annual Report, 1985
7 Jan. 1987 18 p Original document contains color illustrations
(B8677594; JE535; ETN-87-99591) Avail: NTIS HC A02/MF A01

Wind tunnel tests on aircraft and automobiles are described. Correction of thermal effects on an internal gage balance; flow visualization with a sweeping laser beam; and acoustical calibration are summarized. ESA

12 ASTRONAUTICS (GENERAL)

For extraterrestrial exploration see *91 Lunar and Planetary Exploration.*

N87-23667# Dayton Univ., Ohio.
POTENTIAL APPLICATIONS OF BIOTECHNOLOGY TO AEROSPACE MATERIALS Final Conference Report
Rebecca Schiavone Nov. 1986 17 p Workshop held in Dayton, Ohio, 27-29 Aug. 1986
(Grant AF-AFOSR-0183-86)
(AD-A177875; AFOSR-87-0168TR) Avail: NTIS HC A02/MF A01 CSCL 06B

This report of a three-day workshop on the applications of biotechnology to aerospace materials held in Dayton, Ohio, 27 to 29 August 1986. The workshop was organized by the University

of Dayton Research Institute and received support from AFOSR-NC and AFWAL/MLBC. Areas covered included biotech approaches to the synthesis of chemicals, bioelectronics, biomining, and biodegradation of materials. Participants included representatives from AFOSR and the Air Force Laboratories, and the biotech and aerospace industries. GRA

13 ASTRODYNAMICS

Includes powered and free-flight trajectories; and orbital and launching dynamics.

N87-23668# Air Force Inst. of Tech., Wright-Patterson AFB, Ohio. School of Engineering.
OPTIMAL CONTINUOUS THRUST ORBITAL EVASIVE MANEUVERS FROM GEOSYNCHRONOUS ORBIT M.S. Thesis
Robert D. Preissinger Dec. 1986 78 p
(AD-A179413; AFIT/GA/AA/86D-12) Avail: NTIS HC A05/MF A01 CSCL 22C

A satellite under attack by another orbiting body relying on an explosive device to effect a kill has the problem of avoiding a volume space, in which its destruction is highly likely. To avoid this volume, the attackee could use continuous low thrust, such as that provided by electric propulsion or attitude control thrusters, if its warning time and orbital parameters were appropriate. A model is developed using optimal control theory and the thrust direction is solved numerically using various magnitudes of thrust. The model progresses from a one satellite solution (where the threat is a fixed sphere in space) to a two satellite solution in which the distance between the threat and the target satellite is maximized. A minimum time solution for the single satellite problem is included. The results are given for several values of thrust, several maneuvering times, the optimized time-of-maneuver, and for circular and non-circular end orbits. GRA

14 GROUND SUPPORT SYSTEMS AND FACILITIES (SPACE)

Includes launch complexes, research and production facilities; ground support equipment, e.g., mobile transporters; and simulators.

For related information see also *09 Research and Support Facilities (Air).*

N87-23669# California Univ., Berkeley. Lawrence Berkeley Lab.
EXPERIMENTS AND PROSPECTS FOR INDUCTION LINAC DRIVERS
D. Keefe Dec. 1986 14 p Presented at the Symposium on Heavy Ion Inertial Fusion, Washington, D.C., 27 May 1986
(Contract DE-AC03-76SF-00098)
(DE87-006144; LBL-21345-Rev; CONF-860510-17-Rev) Avail: NTIS HC A02/MF A01

In the last three years, the US program in Heavy Ion Fusion has concentrated on understanding the induction linac approach to a power-plant driver. In this method it is important that the beam current be maximized throughout the accelerator. Consequently, it is crucial to understand the space-charge limit in the AG transport system in the linac and, also, to achieve current amplification during acceleration to keep pace with the kinematical increase of this limit with energy. Experimental results on both these matters and also on the use of multiple beams (inside the same accelerating structure) will be described. A new examination of the most attractive properties of the induction linac for a fusion driver has clearly pointed to the advantage of using heavy ions with a charge-state greater than unity - perhaps q = 3 may be an optimum. This development places even greater importance on understanding space-charge limits and mechanisms for emittance growth; also, it will require a new emphasis on the development of a suitable ion source. DOE

N87-23670*# Catholic Univ. of America, Washington, D.C. School of Engineering and Architecture.
THE DEVELOPMENT OF A CONTAINMENT VESSEL AND DEWAR FOR THE PARTICLE ASTROPHYSICS MAGNET FACILITY (ASTROMAG)
28 May 1985 37 p
(Grant NAG5-848)
(NASA-CR-181016; NAS 1.26:181016) Avail: NTIS HC A03/MF A01 CSCL 14B

The ASTROMAG facility is the heart of a large charged particle detection and resolution system. ASTROMAG utilizes a superconducting magnet consisting of a large superconducting magnet coil with a stored magnetic energy of approximately 15 MJ. The active coil will have a mass of 1200 kg. This magnet will be cooled by a cryostat using a liquid helium Dewar for storage. The cryostat will have a series of gas-cooled shields with an external guard vacuum shield and an internal Dewar. The magnet and cryostat will be designed for shuttle or Delta launch and will be designed to withstand the internal pressure of expanded helium under full quench conditions when venting is prevented. The external guard vacuum shell is required to maintain a vacuum for Earth based testing and for cold launch of the cryostat and magnet. The magnet is designed to operate at 4.4 K with a peak field of 7.0 tesla. The superconducting material within the magnet is niobium titanium in a conductive matrix. Author

15 LAUNCH VEHICLES AND SPACE VEHICLES

Includes boosters; operating problems of launch/space vehicle systems; and reusable vehicles.

For related information see also *20 Spacecraft Propulsion and Power.*

N87-23671*# National Aeronautics and Space Administration. Goddard Space Flight Center, Greenbelt, Md.
COSPAS-SARSAT SATELLITE ORBIT PREDICTOR, VOLUME 9 Technical Memorandum, Apr. - Oct. 1987
Morton L. Friedman Apr. 1987 105 p
(NASA-TM-85015; Rept-87-B-0289; NAS 1.15:85015) Avail: NTIS HC A06/MF A01 CSCL 22A

The satellite orbit predictor is a graphical aid for determining the relationship between the satellite (SARSAT or COSPAS) orbit, antenna coverage of the spacecraft and coverage of the Local User Terminal (LUTs). The predictor allows the user to quickly visualize if a selected position will probably be detected and is composed of a base map and a satellite track overlay for each satellite. Additionally, a table of equator crossings for each satellite is included. The table of satellite equator crossings contains the zulu date/time group that a satellite will cross the equator northbound, the orbit number, and the longitude that it will cross the equator. B.G.

N87-23672# Hokenson (Gustave J.), Los Angeles, Calif.
OPTIMAL AERODYNAMIC SHAPES FOR HYPERVELOCITY PROJECTILES Final Report, 31 Jul. 1986 - 31 Jan. 1987
Gustave J. Hokenson 28 Feb. 1987 62 p
(Contract DASG60-86-C-0082)
(AD-A178367; THC-02GH87021A) Avail: NTIS HC A04/MF A01 CSCL 20D

Phase 1 of this research was to demonstrate the feasibility of establishing optimal shapes for hypervelocity projectiles, considering simultaneously the effects of drag, internal volume distribution and impact effectiveness. Utilizing classical optimization analysis and hypersonic inviscid flow theory, minimum pressure drag bodies were obtained subject to various constraints. It was then assumed that the shapes so obtained corresponded to the solid body plus a viscous displacement. Utilizing state-of-the-art turbulent boundary layer theory in an iterative mode, the solid body shape was then determined along with the skin friction drag. Relative to any specified reference penetrator shape, the internal volume distribution effectiveness may then be characterized.

Subsequently, the loss in kinetic energy of the projectile along its trajectory is computed and the initial stage of impact is computed from a Navier-Stokes numerical simulation in order to quantify the target damage. As a result of this procedure, various candidate hypervelocity projectile shapes may compete against one another from an overall mission point of view. GRA

N87-23673# Los Alamos National Lab., N. Mex.
RF CONTROL SYSTEM FOR A ROCKET-BORNE ACCELERATOR
M. T. Lynch, L. N. Sorum, and D. R. Keffeler 1987 4 p Presented at the Particle Accelerator Conference, Washington, D.C., 16 Mar. 1987
(Contract W-7405-eng-36)
(DE87-007459; LA-UR-87-416; CONF-870302-45) Avail: NTIS HC A02/MF A01

The Beam Experiments Aboard Rockets (BEAR) accelerator experiment imposes several nonstandard requirements on the rf control system. The experiment is entirely hands-off and must operate under local computer control. The rf control system must be extremely reliable, which implies excellence in design and fabrication as well as redundancy whenever possible. This paper describes the design of the frequency-source, frequency-control, and amplitude-control systems for the BEAR experiment. DOE

N87-23674*# National Aeronautics and Space Administration. Lewis Research Center, Cleveland, Ohio.
SPECULATIONS ON FUTURE OPPORTUNITIES TO EVOLVE BRAYTON POWERPLANTS ABOARD THE SPACE STATION
Robert E. English 1987 29 p Presented at the 4th Symposium on Space Nuclear Power Systems, Albuquerque, N. Mex., 12-16 Jan. 1987; sponsored by Sandia National Labs.
(NASA-TM-89863; E-3530; NAS 1.15:89863) Avail: NTIS HC A03/MF A01 CSCL 10B

The Space Station provides a unique, low-risk environment in which to evolve new capabilities. In this way, the Space Station will grow in capacity, in its range of capabilities, and its economy of operation as a laboratory and as a center for space operations. Although both Rankine and Brayton cycles, two concepts for solar dynamic power generation, now compete to power the station, this paper confines its attention to the Brayton cycle using a mixture of He and Xe as its working fluid. Such a Brayton powerplant to supply the station's increasing demands for both electric power and heat has the potential to gradually evolve higher and higher performance by exploiting already-evolved materials (ASTAR-811C and molten-Li heat storage), its peak cycle temperature rising ultimately to 1500 K. Adapting the station to exploit long tethers (200 to 300 km long) could yield increases in payloads to LEO, to GEO, and to distant destinations in the solar system. Such tethering of the Space Station would not only require additional power for electric propulsion but also would so increase nuclear safety that nuclear powerplants might provide this power. From an 8000-kWt SP-100 reactor, thermoelectric power generation could produce 300 kWe, or adapted solar-Brayton cycle, 2400 to 2800 kWe.
Author

16 SPACE TRANSPORTATION

Includes passenger and cargo space transportation, e.g., shuttle operations; and space rescue techniques.

For related information see also *03 Air Transportation and Safety* and *18 Spacecraft Design, Testing and Performance.* For space suits see *54 Man/System Technology and Life Support.*

N87-23675*# National Aeronautics and Space Administration. John F. Kennedy Space Center, Cocoa Beach, Fla.
ICE/FROST/DEBRIS ASSESSMENT FOR SPACE SHUTTLE MISSION STS-32 (61-C)
Charles G. Stevenson, Gregory N. Katnik, and Robert F. Speece 20 Jan. 1986 96 p
(NASA-TM-89192; NAS 1.15:89192) Avail: NTIS HC A05/MF A01 CSCL 22D

An Ice/Frost/Debris assessment was conducted for Space Shuttle Mission STS-32 (61-C). This assessment begins with debris inspections of the flight elements and launch facilities before and after launch. Ice/Frost formations are calculated during cryogenic loading of the external tank followed by an on-pad assessment of the Shuttle vehicle and pad at T-3 hours in the countdown. High speed films are reviewed after launch to identify Ice/Frost/Debris sources and investigate potential vehicle damage. The Ice/Frost/Debris conditions and their effects on the Space Shuttle are documented. Author

N87-23676*# National Aeronautics and Space Administration, Washington, D.C.
ACTIONS TO IMPLEMENT THE RECOMMENDATIONS OF THE PRESIDENTIAL COMMISSION ON THE SPACE SHUTTLE CHALLENGER ACCIDENT: EXECUTIVE SUMMARY
14 Jul. 1986 11 p Previously announced as N86-27352
Avail: NTIS HC A02/MF A01 CSCL 22A

The status of the implementation of the recommendations of the Presidential Commission on the Space Shuttle Challenger Accident is reported. The implementation of recommendations in the following areas is detailed: (1) solid rocket motor design; (2) shuttle management structure, including the shuttle safety panel and astronauts in management; (3) critical item review and hazard analysis; (4) safety organization; (5) improved communication; (6) landing safety; (7) launch abort and crew escape; (8) flight rate; and (9) maintenance safeguards. Supporting memoranda and communications from NASA are appended. Author

17 SPACE COMM., SPACECRAFT COMM., COMMAND & TRACKING

Includes telemetry; space communications networks; astronavigation and guidance; and radio blackout.

For related information see also *04 Aircraft Communications and Navigation* and *32 Communications and Radar.*

No abstracts in this category.

18 SPACECRAFT DESIGN, TESTING AND PERFORMANCE

Includes satellites; space platforms; space stations; spacecraft systems and components such as thermal and environmental controls; and attitude controls.

For life support systems see *54 Man/System Technology and Life Support.* For related information see also *05 Aircraft Design, Testing and Performance, 39 Structural Mechanics,* and *16 Space Transportation.*

N87-23677# Air Force Inst. of Tech., Wright-Patterson AFB, Ohio. School of Engineering.
A QUANTITATIVE COMPARISON OF SEVERAL ORBITAL MANEUVERING VEHICLE CONFIGURATIONS FOR SATELLITE REPAIR/REPLENISHMENT M.S. Thesis
Joseph H. Cavallaro 16 Jun. 1987 75 p
(AD-A179106; AFIT/GSO/AA/86D-2) Avail: NTIS HC A04/MF A01 CSCL 22A

The history of spaceflight is full of examples of astronaut crewmembers returning damaged/malfunctioning spacecraft to an operational status. The recent Space Shuttle rescues of Solar Max, Westar and Palapa B-11 are perhaps the most dramatic of these. The current operational concept of servicing the target vehicle on board the shuttle however limits the potential number of spacecraft which can be reached. A potential solution is to use the Orbital Maneuvering Vehicle (OMV) that NASA is developing

as a multi-role spacecraft. Use of the OMV has the potential of extending the reach of servicing to spacecraft beyond the range of the Shuttle. This paper examines three OMV/Servicer configurations, including both telepresence and manned version. The Analytic Hierarchy Process is used to rank order the alternatives for further study. A computer program was used to solve for the weights of the various measures of the effectiveness, and resulting priority vector was calculated. Preliminary results show the telepresence servicer rated highest, followed by the full environment manned system. GRA

N87-23678# TRW Space Technology Labs., Redondo Beach, Calif. System Integration Lab.

SPACECRAFT ENVIRONMENT INTERACTION INVESTIGATION Final Report, Oct. 1983 - Sep. 1986

N. J. Stevens and Marc E. Kirkpatrick Oct. 1986 175 p

(Contract F19628-84-C-0038)

(AD-A179183; TRW-43543-6011-UE-00; AFGL-TR-86-0214) Avail: NTIS HC A08/MF A01 CSCL 22B

This report summarizes the results of the spacecraft environment interaction investigation. The objectives of this investigation were to characterize environmental interaction technology and to determine the adequacy of present military standards and handbooks for future, large AF missions. The characterization of the technology status was accomplished by literature searches and key-expert questionnaires. The determination of military standard adequacy was accomplished by considering interactions with five concepts synthesized from those available in the MSSTP. Based on these concepts studies, critical interactions were identified. The available military documentation was searched for applicability. A recommended document development plan was prepared along with a discussion of technology gaps. GRA

N87-23679# Air Force Inst. of Tech., Wright-Patterson AFB, Ohio. School of Engineering.

DETUMBLING OF TWO INTER-CONNECTED RIGID BODIES USING LIAPUNOV METHODS FOR FEEDBACK CONTROL M.S. Thesis

Michael P. Paquette Dec. 1986 95 p

(AD-A179207; AFIT/GA/AA/86D-11) Avail: NTIS HC A05/MF A01 CSCL 22A

A satellite is modeled as two rigid bodies interconnected by a joint with one degree of freedom. In a tumbling situation, the satellite is brought to a condition of stabilized spin about its maximum moment of inertia axis. This is accomplished by a torque applied to the internal joint by an electronic motor. The control law which supplies the input to the torque motor is derived using both nonlinear and linear feedback. Liapunov stability theory is used to develop both methods. Various models are devised with varying rigid body physical properties in order to draw comparisons, and results are presented for each case. While the nonlinear control law was unsuccessful for the case presented, due to a violation in theory, the linear feedback approach produced favorable outcome for a variety of linear control law cases. Author (GRA)

N87-23680# Air Force Inst. of Tech., Wright-Patterson AFB, Ohio. School of Engineering.

A SYSTEMS ANALYSIS OF EMERGENCY ESCAPE AND RECOVERY SYSTEMS FOR THE US SPACE STATION M.S. Thesis

Brian K. Kelly Dec. 1986 115 p

(AD-A179233; AFIT/GSO/AA/86D-5) Avail: NTIS HC A06/MF A01 CSCL 06G

Recent designs for the U.S. manned space station have crews on board the space station without any means of emergency escape for periods of up to 90 days. This investigation analyzes emergency escape recovery systems for use on the space station in an effort to find the best escape device. Initially, the objectives to be met by an effective escape device were identified along with the corresponding measures of effectiveness (MOE) for each objective. Fifteen alternative escape systems were found that could be used on the manned core portion of the space station complex. A preliminary analysis reduced the number of alternatives considered for more detailed analysis to six. These final six, The Maneuverable Entry Research Vehicle (MERV), Emergency Astronaut Re-entry Parachute System, Manned Orbital Escape System (MOSES), MOOSE (Man out of Space Easiest), and Apollo Command Module, were compared on the basis of their calculated MOEs using multi-attribute utility theory. The overall utilities for each of the final six alternatives were calculated for two crew sizes, 3-man and 8-man. MOSES was found to consistently rate the highest overall utility for both manning scenarios. The next best alternative was the Apollo Command Module. GRA

N87-23681# Air Force Inst. of Tech., Wright-Patterson AFB, Ohio. School of Engineering.

AN ANALYSIS OF SPACE STATION MOTION SUBJECT TO THE PARAMETRIC EXCITATION OF PERIODIC ELEVATOR MOTION M.S. Thesis

John D. Chan Dec. 1986 83 p

(AD-A179235; AFIT/GA/AA/86D-2) Avail: NTIS HC A05/MF A01 CSCL 06S

This study will derive the equations of attitude motion for a gravity gradient stabilized space station whose moments of inertia are varying with time. The equations are then linearized, after which an analytical solution of the pitch equation is developed. An examination of the stability of motion for the resulting Hill equation is presented and then compared to the solution obtained from numerical integration of the nonlinear equations. The results show that for elevator frequencies on the order of the orbit rate, motion can grow unboundedly with time. Consequently, the shape of the classical Lagrange stability region is altered. GRA

N87-23682# Air Force Inst. of Tech., Wright-Patterson AFB, Ohio. School of Engineering.

A MULTIPLE ATTRIBUTE DECISION ANALYSIS OF MANNED AIRLOCK SYSTEMS M.S. Thesis

Dennis P. Jeanes Dec. 1986 128 p

(AD-A179241; AFIT/GSO/ENS/86D-3) Avail: NTIS HC A07/MF A01 CSCL 22B

This study is a multiple attribute decision analysis involving five manned airlock alternatives. The five alternatives are the present shuttle airlock system augmented with additional consumable gas tanks, four variations of the Crewlock, a new airlock design concept proposed by Mr. William Haynes of the Aerospace Corporation. The purpose was to identify which airlock system can best support both the normal shuttle mission extravehicular activity (EVA) and the shuttle's EVA requirements during construction of the space station. Only physical characteristics and performance parameters are included in the analysis. Cost factors are not addressed. The analytic hierarchy process (AHP) was used to structure the problem and helped identify and rate ten airlock attributes, safety, reliability, weight, size, volume, transit time, depressurization time, repressurization time, expendable gas usage, and number of EVA periods per mission. Compromise programming was used to identify the airlock system closest to the ideal solution using the AHP-derived weights. GRA

N87-23683# California Univ., Berkeley. Electronics Research Lab.

AN INTEGRATED, OPTIMIZATION-BASED APPROACH TO THE DESIGN AND CONTROL OF LARGE SPACE STRUCTURES Final Technical Report, 1 Oct. 1983 - 30 Sep. 1986

Elijah Polak, Karl S. Pister, and Robert L. Taylor 30 Sep. 1986 10 p

(Grant AF-AFOSR-0361-83)

(AD-A179459; AFOSR-87-0402TR) Avail: NTIS HC A02/MF A01 CSCL 20K

This research was aimed at laying the groundwork for a long term project on the integrated, optimization-based design of large, flexible structures and their control systems. Research was carried out in four areas: (1) modeling the dynamic behavior of simple flexible structures; (2) development of a theory of nondifferentiable optimization algorithms for the solution of problems with max

function type inequality constraints; (3) exploration of the use of optimization in optimization-based design of large, flexible structures and their control systems; and (4) interactive software for optimization-based control system design. GRA

N87-23684# Air Force Inst. of Tech., Wright-Patterson AFB, Ohio. School of Engineering.
AN ANALYSIS OF GEOPOTENTIAL EFFECTS ON SATELLITE CONSTELLATIONS M.S. Thesis
Mark J. Buechter Dec. 1986 58 p
(AD-A179507; AFIT/GSO/AA/86D-1) Avail: NTIS HC A04/MF A01 CSCL 08E

Current plans for systems to be used for ballistic missile defense sometimes call for using satellites that are placed so as to form a constellation that can continuously monitor specified areas of the Earth's surface or direct weapons against attacking missiles and warheads. This study analyzes the relative motion between satellites within such a constellation under gravitational perturbations caused by the Earth's equatorial bulge (oblateness). Relative motion is calculated using a system of equations which describes the variation of relative orbital elements between two satellites. The cases studied simulate the position of two satellites that are located within a constellation containing ten orbits with ten satellites in each orbit. The orbits investigated were all circular with altitudes ranging from 300 km to 1000 km and inclinations ranging from 40 degrees to 80 degrees. Range between the satellites was oscillatory with deviations from the average range of up to 5 km. The results vary only slightly with changes in orbital inclination or altitude. These results show that the relative motion between satellites in a low altitude constellations caused by the Earth's oblateness does not significantly affect the initial geometry of the constellation. GRA

N87-23685*# National Aeronautics and Space Administration. Lewis Research Center, Cleveland, Ohio.
DESIGN, DEVELOPMENT AND TEST OF SHUTTLE/CENTAUR G-PRIME CRYOGENIC TANKAGE THERMAL PROTECTION SYSTEMS
Richard H. Knoll, Peter N. MacNeil, and James E. England (General Dynamics Corp., San Diego, Calif.) May 1987 42 p Presented at the 22nd Thermophysics Conference, Honolulu, Hawaii, 8-10 Jun. 1987; sponsored by AIAA
(Contract NAS3-22901)
(NASA-TM-89825; E-3473; NAS 1.15:89825; AIAA-87-1557) Avail: NTIS HC A03/MF A01 CSCL 22B

The thermal protection systems for the shuttle/Centaur would have had to provide fail-safe thermal protection during prelaunch, launch ascent, and on-orbit operations as well as during potential abort. The thermal protection systems selected used a helium-purged polyimide foam beneath three rediation shields for the liquid-hydrogen tank and radiation shields only for the liquid-oxygen tank (three shields on the tank sidewall and four on the aft bulkhead). A double-walled vacuum bulkhead separated the two tanks. The liquid-hydrogen tank had one 0.75-in-thick layer of foam on the forward bulkhead and two layers on the larger area sidewall. Full scale tests of the flight vehicle in a simulated shuttle cargo bay that was purged with gaseous nitrogen gave total prelaunch heating rates of 88,500 Btu/hr and 44,000 Btu/hr for the liquid-hydrogen and -oxygen tanks, respectively. Calorimeter tests on a representative sample of the liquid-hydrogen tank sidewall thermal protection system indicated that the measured unit heating rate would rapidly decrease from the prelaunch rate of approx. 100 Btu/hr/sq ft to a desired rate of less than 1.3 Btu/-hr/sq ft once on orbit. Author

N87-23686# Institut Franco-Allemand de Recherches, St. Louis (France).
THE FREEZING OF FLOW DEFLECTION IN PRANDTL-MEYER EXPANSION TO VACUUM
K. W. Naumann 20 Aug. 1986 14 p Presented at the 15th International Symposium on Rarefied Gas Dynamics, Grado, Italy, 16-20 Jun. 1986
(ISL-CO-226/86; ETN-87-99643) Avail: NTIS HC A02/MF A01

The flow from satellite attitude control thrusters with laminar boundary layer is discussed. Experiments on the highly underexpanded exhaust plume from a conical nozzle with thick laminar boundary layer show that the streamline deflection in the plume flow vanishes according to rarefaction effects. The suitable formulation of Bird's (1976) continuum-breakdown parameter provides the possibility to approximately describe the flowfield streamline by streamline from the conditions in the nozzle aperture and the nozzle geometry. This includes the direction of the frozen streamline and the state parameters along it. Comparison with experiments shows good agreement, particularly for gases having a great number of internal degrees of freedom. In this case the freezing of the expansion deflection takes place at quite small Mach numbers. It causes the plume to get significantly closer packed than is suggested by the continuum expansion laws. ESA

N87-23687*# National Aeronautics and Space Administration. Langley Research Center, Hampton, Va.
OPTIMIZATION OF PAYLOAD MASS PLACEMENT IN A DUAL KEEL SPACE STATION
Melvin J. Ferebee, Jr. and Robert B. Powers Mar. 1987 23 p
(NASA-TM-89051; NAS 1.15:89051) Avail: NTIS HC A02/MF A01 CSCL 22B

In order to keep a Space Station in a stable low-Earth orbit, angular momentum storage and translational attitude control systems will have to be used. In order to minimize the size of these attitude control systems, the induced gravity gradient torque effects will have to be minimized. This can be done by minimizing the cross-products of inertia of the Station through the management of payload placement with the Station geometry. A derived and automated methodology is presented which utilizes mathematical nonlinear programming techniques. An optimal arrangement of a set of five payloads on a Dual Keel Space Station was found that minimized the cross products of inertia and thus the required controllability resources. Author

19 SPACECRAFT INSTRUMENTATION

For related information see also *06 Aircraft Instrumentation* and *35 Instrumentation and Photography.*

No abstracts in this category.

20 SPACECRAFT PROPULSION AND POWER

Includes main propulsion systems and components, e.g., rocket engines; and spacecraft auxilliary power sources.

For related information see also *07 Aircraft Propulsion and Power, 28 Propellants and Fuels, 44 Energy Production and Conversion,* and *15 Launch Vehicles and Space Vehicles.*

N87-23688# Air Force Systems Command, Wright-Patterson AFB, Ohio. Foreign Technology Div.
AN APPROACH OF PREVENTING COMBUSTION VIBRATIONS OF ROCKET ENGINE WITH LATERAL BAFFLE
Di Lianshun and Xing Fuyuan 25 Mar. 1987 26 p Transl. into ENGLISH from Yuhang Xuebao (China), no. 2, 1986 p 72-80
(AD-A179222; FTD-ID(RS)T-0012-87) Avail: NTIS HC A03/MF A01 CSCL 21H

In the process of developing the variable thrust rocket engine, combustion vibrations are encountered in the low end of the operating conditions. We used a lateral baffle to satisfactorily solve the problem. This paper mainly introduces the experimental results

and qualitative analysis. The approach is novel. It can be used as a reference. GRA

N87-23689# New Mexico State Univ., Las Cruces.
ENGINEERING AND INSTRUMENTATION SUPPORT OF THE AFGL (AIR FORCE GEOPHYSICS LABORATORY) ROCKET RESEARCH PROGRAM Final Report, 8 Jun. 1982 - 31 Mar. 1986
Dwight M. Bawcom, Harold Shaw, and Larry Cunningham 7 Nov. 1986 46 p
(Contract F19628-82-C-0111)
(AD-A179257; AFGL-TR-86-242) Avail: NTIS HC A03/MF A01 CSCL 09F

The Physical Science Laboratory (PSL) of New Mexico State University provided technical support to AFGL over a four year period in the testing, firing, and collection of telemetry data involving sounding rocket payloads. In addition PSL provided software system analysis in support of the CIRRIS project and designed specialized hardware for telemetry ground systems. The hardware included a PCM Bit Synchronizer, PCM Decommutator, and a Portable PCM Ground Station. Software was developed for the system which PSL designed, assembled, and tested. GRA

N87-23690*# National Aeronautics and Space Administration. Lewis Research Center, Cleveland, Ohio.
CONTROL CONSIDERATIONS FOR HIGH FREQUENCY, RESONANT, POWER PROCESSING EQUIPMENT USED IN LARGE SYSTEMS
J. W. Mildice, K. E. Schreiner, and F. Wolff 1987 8 p Prepared for presentation at the 22nd Intersociety Energy Conversion Engineering Conference, Philadelphia, Pa., 10-14 Aug. 1987; cosponsored by AIAA, ANS, ASME, SAE, IEEE, ACS, and AIChE
(NASA-TM-89926; E-3629; NAS 1.15:89926; AIAA-87-9353) Avail: NTIS HC A02/MF A01 CSCL 10B

Addressed is a class of resonant power processing equipment designed to be used in an integrated high frequency (20 KHz domain), utility power system for large, multi-user spacecraft and other aerospace vehicles. It describes a hardware approach, which has been the basis for parametric and physical data used to justify the selection of high frequency ac as the PMAD baseline for the space station. This paper is part of a larger effort undertaken by NASA and General Dynamics to be sure that all potential space station contractors and other aerospace power system designers understand and can comfortably use this technology, which is now widely used in the commercial sector. In this paper, we will examine control requirements, stability, and operational modes; and their hardware impacts from an integrated system point of view. The current space station PMAD system will provide the overall requirements model to develop an understanding of the performance of this type of system with regard to: (1) regulation; (2) power bus stability and voltage control; (3) source impedance; (4) transient response; (5) power factor effects, and (6) limits and overloads. Author

N87-23691*# National Aeronautics and Space Administration. Lewis Research Center, Cleveland, Ohio.
LOW POWER ARCJET THRUSTER PULSE IGNITION
Charles J. Sarmiento and Robert P. Gruber 1987 29 p Presented at the 23rd Joint Propulsion Conference, San Diego, Calif., 29 Jun. - 2 Jul. 1987; sponsored by AIAA, SAE, ASME and ASEE
(NASA-TM-100123; E-3645; NAS 1.15:100123) Avail: NTIS HC A03/MF A01 CSCL 21C

An investigation of the pulse ignition characteristics of a 1 kW class arcjet using an inductive energy storage pulse generator with a pulse width modulated power converter identified several thruster and pulse generator parameters that influence breakdown voltage including pulse generator rate of voltage rise. This work was conducted with an arcjet tested on hydrogen-nitrogen gas mixtures to simulate fully decomposed hydrazine. Over all ranges of thruster and pulser parameters investigated, the mean breakdown voltages varied from 1.4 to 2.7 kV. Ignition tests at elevated thruster temperatures under certain conditions revealed occasional breakdowns to thruster voltages higher than the power converter output voltage. These post breakdown discharges sometimes failed to transition to the lower voltage arc discharge mode and the thruster would not ignite. Under the same conditions, a transition to the arc mode would occur for a subsequent pulse and the thruster would ignite. An automated 11 600 cycle starting and transition to steady state test demonstrated ignition on the first pulse and required application of a second pulse only two times to initiate breakdown. Author

N87-23692*# National Aeronautics and Space Administration. Lewis Research Center, Cleveland, Ohio.
NUCLEAR POWERED MARS CARGO TRANSPORT MISSION UTILIZING ADVANCED ION PROPULSION
Diane L. Galecki (Sverdrup Technology, Inc., Cleveland, Ohio.) and Michael J. Patterson 1987 29 p Presented at the 23rd Joint Propulsion Conference, San Diego, Calif., 29 Jun. - 2 Jul. 1987; sponsored by AIAA, SAE, ASME and ASEE
(NASA-TM-100109; E-3641; NAS 1.15:100109; AIAA-87-1903) Avail: NTIS HC A03/MF A01 CSCL 21F

Nuclear-powered ion propulsion technology was combined with detailed trajectory analysis to determine propulsion system and trajectory options for an unmanned cargo mission to Mars in support of manned Mars missions. A total of 96 mission scenarios were identified by combining two power levels, two propellants, four values of specific impulse per propellant, three starting altitudes, and two starting velocities. Sixty of these scenarios were selected for a detailed trajectory analysis; a complete propulsion system study was then conducted for 20 of these trajectories. Trip times ranged from 344 days for a xenon propulsion system operating at 300 kW total power and starting from lunar orbit with escape velocity, to 770 days for an argon propulsion system operating at 300 kW total power and starting from nuclear start orbit with circular velocity. Trip times for the 3 MW cases studied ranged from 356 to 413 days. Payload masses ranged from 5700 to 12,300 kg for the 300 kW power level, and from 72,200 to 81,500 kg for the 3 MW power level. Author

N87-23693*# National Aeronautics and Space Administration. Lewis Research Center, Cleveland, Ohio.
IN-SITU ANALYSIS OF HYDRAZINE DECOMPOSITION PRODUCTS
Francis M. Curran and Margaret V. Whalen Jul. 1987 16 p Presented at the 23rd Joint Propulsion Conference, San Diego, Calif., 29 Jun. - 2 Jul. 1987; cosponsored by AIAA, SAE, ASME, and ASEE
(NASA-TM-89916; E-3609; NAS 1.15:89916; AIAA-87-2122) Avail: NTIS HC A02/MF A01 CSCL 21I

A gas analyzer utilizing a nondispersive infrared (NDIR) detection system was used to monitor the ammonia and water vapor content of the products of a previously unused hydrazine gas generator. This provided an in-situ measurement of the generator's efficiency difficult to obtain by other means. The analyzer was easily installed in both the calibration and hydrazine systems, required no maintenance other than periodic zero adjustments, and performed well for extended periods in the operating range tested. The catalyst bed operated smoothly and repeatably during the 28 hr of testing. No major transients were observed on startup or during steady state operation. The amount of ammonia in the output stream of the gas generator was found to be a strong function of temperature at catalyst bed temperatures below 450 C. At temperatures above this, the efficiency remained nearly constant. On startup the gas generator efficiency was found to decrease with time until a steady state value was attained. Elevated catalyst bed temperatures in the periods before steady state operation was found to be responsible for this phenomenon. Author

N87-23694# Air Force Geophysics Lab., Hanscom AFB, Mass.
EIRMA: AN ENERGETIC ION RETARDING MASS ANALYZER FOR THE BERT-1 (BEAM EMISSION ROCKET TEST ONE) Final Technical Report
A. D. Bailey and C. Sherman 19 May 1986 65 p
(AD-A178231; AFGL-TR-860109; AFGL-IP-332) Avail: NTIS HC A04/MF A01 CSCL 20H

(AD-A178231; AFGL-TR-860109; AFGL-IP-332) Avail: NTIS HC A04/MF A01 CSCL 20H

The AFGL Beam Emission Rocket Test-One (BERT-1) launched in June 1985, included in its instrumentation an Energetic Ion Retarding Mass Analyzer (EIRMA) to study the mass and energy distribution of positive ions in the return current to the spacecraft from which energetic ion and electron beams are emitted. The EIRMA is a quadrupole mass filter scannable over the 1 to 100 amu range with programmable resolution delta m/m to less than 1/15. The filter was biased by programs over a -100v to +4.5 kv range, allowing a retarding analysis of individual ion species in the return current. The report is a summary description of the instrument design, performance testing results and flight performance. GRA

N87-23695*# Rockwell International Corp., Canoga Park, Calif. Rocketdyne Div.

SPACE STATION WP-04 POWER SYSTEM. VOLUME 1: EXECUTIVE SUMMARY Final Study Report

G. J. Hallinan 19 Jan. 1987 92 p

(Contract NAS3-24666)

(NASA-CR-179587; NAS 1.26:179587; FSR-DR-15) Avail: NTIS HC A05/MF A01 CSCL 14B

Major study activities and results of the phase B study contract for the preliminary design of the space station Electrical Power System (EPS) are summarized. The areas addressed include the general system design, man-tended option, automation and robotics, evolutionary growth, software development environment, advanced development, customer accommodations, operations planning, product assurance, and design and development phase planning. The EPS consists of a combination photovoltaic and solar dynamic power generation subsystem and a power management and distribution (PMAD) subsystem. System trade studies and costing activities are also summarized. M.G.

N87-23696*# Rockwell International Corp., Canoga Park, Calif. Rocketdyne Div.

SPACE STATION WP-04 POWER SYSTEM. VOLUME 2: STUDY RESULTS Final Study Report

G. J. Hallinan 19 Jan. 1987 556 p

(Contract NAS3-24666)

(NASA-CR-179587; NAS 1.26:179587; FSR-DR-15) Avail: NTIS HC A24/MF A01 CSCL 14B

Results of the phase B study contract for the definition of the space station Electric Power System (EPS) are presented in detail along with backup information and supporting data. Systems analysis and trades, preliminary design, advanced development, customer accommodations, operations planning, product assurance, and design and development phase planning are addressed. The station design is a hybrid approach which provides user power of 25 kWe from the photovoltaic subsystem and 50 kWe from the solar dynamic subsystem. The electric power is distributed to users as a utility service; single phase at a frequency of 20 kHz and voltage of 440VAC. The solar array NiH2 batteries of the photovoltaic subsystem are based on commonality to those used on the co-orbiting and solar platforms. M.G.

N87-23758# Morton Thiokol, Brigham City, Utah.

ACOUSTIC WAVEFORMS IN STATICALLY TESTED SPACE SHUTTLE SOLID ROCKET MOTORS (SRM)

B. Hussey *In* Johns Hopkins Univ., The 23rd JANNAF Combustion Meeting, Volume 1 Oct. 1986 p 1-7 (For primary document see N87-23757 17-28)

Avail: CPIA, Laurel, Md. 20707 HC $70.00

N87-23759# Johns Hopkins Univ., Laurel, Md. Lab. for Computational Physics.

NUMERICAL STUDY OF ACOUSTIC REFRACTION AND FLOW TURNING

Joseph D. Baum and Jay N. Levine (Air Force Rocket Propulsion Lab., Edwards AFB, Calif.) *In* Johns Hopkins Univ., The 23rd JANNAF Combustion Meeting, Volume 1 Oct. 1986 p 9-31 Prepared in cooperation with Air Force Rocket Propulsion Lab., Edwards AFB, Calif. Sponsored in part by Air Force (For primary document see N87-23757 17-28)

Avail: CPIA, Laurel, Md. 20707 HC $70.00

N87-23761# Pennsylvania State Univ., State College.

STOCHASTIC EXCITATION OF ACOUSTIC WAVES IN A COMBUSTION CHAMBER

Vigor Yang and Fred E. C. Culick *In* Johns Hopkins Univ., The 23rd JANNAF Combustion Meeting, Volume 1 Oct. 1986 p 45-50 Prepared in cooperation with California Inst. of Tech., Pasadena (For primary document see N87-23757 17-28)

Avail: CPIA, Laurel, Md. 20707 HC $70.00

N87-23763# Naval Weapons Center, China Lake, Calif.

TTCP NON-LINEAR INSTABILITY PROGRAM: US MOTOR TEST DATA

H. B. Mathes *In* Johns Hopkins Univ., The 23rd JANNAF Combustion Meeting, Volume 1 Oct. 1986 p 59-64 (For primary document see N87-23757 17-28)

Avail: CPIA, Laurel, Md. 20707 HC $70.00

N87-23767# Morton Thiokol, Brigham City, Utah.

NEW IGNITION PARAMETER CORRELATIONS FOR PREDICTING SOLID ROCKET MOTOR IGNITION TRANSIENTS

James D. Rozanski *In* Johns Hopkins Univ., The 23rd JANNAF Combustion Meeting, Volume 1 Oct. 1986 p 101-108 (For primary document see N87-23757 17-28)

Avail: CPIA, Laurel, Md. 20707 HC $70.00

N87-23768# Morton Thiokol, Brigham City, Utah.

STUDY OF THE SUPPRESSION OF ROCKET PLUME AFTERBURNING BY CHEMICAL ADDITIVES

L. G. McMillion and E. Miller *In* Johns Hopkins Univ., The 23rd JANNAF Combustion Meeting, Volume 1 Oct. 1986 p 109-117 Prepared in cooperation with Nevada Univ.,Reno. (For primary document see N87-23757 17-28)

Avail: CPIA, Laurel, Md. 20707 HC $70.00

N87-23769# Naval Postgraduate School, Monterey, Calif.

MEASUREMENTS OF PARTICULATES IN SOLID PROPELLANT ROCKET MOTORS

T. Edwards, K. G. Horton, D. Redman, J. S. Rosa, J. B. Rubin, S. C. Yoon, J. P. Powers, and D. W. Netzer *In* Johns Hopkins Univ., The 23rd JANNAF Combustion Meeting, Volume 1 Oct. 1986 p 119-132 (For primary document see N87-23757 17-28) (Contract F04611-86-X-0008)

Avail: CPIA, Laurel, Md. 20707 HC $70.00

N87-23777# Sandia Labs., Livermore, Calif.

INFLUENCE OF TWO-PHASE FLOW IN THE DEFLAGRATION OF HOMOGENEOUS SOLIDS

Stephen B. Margolis, Forman A. Williams, and Robert C. Armstrong *In* Johns Hopkins Univ., The 23rd JANNAF Combustion Meeting, Volume 1 Oct. 1986 p 203-211 Prepared in cooperation with Princeton Univ., N.J. Sponsored in part by DOE and Army (For primary document see N87-23757 17-28)

Avail: CPIA, Laurel, Md. 20707 HC $70.00

N87-23795# California Inst. of Tech., Pasadena.

LINEAR COUPLING OF ACOUSTICS AND ENTROPY AND ACOUSTIC STABILITY IN RAMJET COMBUSTION CHAMBERS CONTAINING A PLANE FLAME

Joseph W. Humphrey and F. E. C. Culick *In* Johns Hopkins Univ., The 23rd JANNAF Combustion Meeting, Volume 1 Oct. 1986 p 435-448 (For primary document see N87-23757 17-28) (Contract N00014-84-K-0434)

Avail: CPIA, Laurel, Md. 20707 HC $70.00

N87-23796# California Inst. of Tech., Pasadena.

ANALYSIS OF PRESSURE OSCILLATIONS IN RAMJETS. REVIEW OF RESEARCH: 1985-1986

F. E. C. Culick *In* Johns Hopkins Univ., The 23rd JANNAF Combustion Meeting, Volume 1 Oct. 1986 p 449-457 (For primary document see N87-23757 17-28)

(Contract N00014-84-K-0434)
Avail: CPIA, Laurel, Md. 20707 HC $70.00

N87-23809* National Aeronautics and Space Administration. Lewis Research Center, Cleveland, Ohio.
EXPERIMENTAL THRUST PERFORMANCE OF A HIGH AREA-RATIO ROCKET NOZZLE
A. J. Pavli, K. J. Kacynski, and T. A. Smith *In* Johns Hopkins Univ., The 23rd JANNAF Combustion Meeting, Volume 1 Oct. 1986 p 585-599 Previously announced as N87-20381 (For primary document see N87-23757 17-28)
Avail: CPIA, Laurel, Md. 20707 HC $70.00 CSCL 21H

N87-23810# Illinois Univ., Chicago.
ANALYTICAL PREDICTION OF COMBUSTION PERFORMANCE CHARACTERISTICS OF BIPROPELLANT LIQUID ROCKET ENGINE COMBUSTOR
H. H. Chiu, T. L. Jiang, G. F. Berry, and E. J. Croke *In* Johns Hopkins Univ., The 23rd JANNAF Combustion Meeting, Volume 1 Oct. 1986 p 601-610 (For primary document see N87-23757 17-28)
(Contract W-31-109-eng-38)
Avail: CPIA, Laurel, Md. 20707 HC $70.00

N87-23811# Remtech, Inc., Huntsville, Ala.
MEASUREMENTS FOR ROCKET ENGINE PERFORMANCE CODE VERIFICATION
S. C. Praharaj and R. L. Palko *In* Johns Hopkins Univ., The 23rd JANNAF Combustion Meeting, Volume 1 Oct. 1986 p 611-622 (For primary document see N87-23757 17-28)
(Contract NAS8-36548)
Avail: CPIA, Laurel, Md. 20707 HC $70.00

N87-23812# Rockwell International Corp., Canoga Park, Calif. Rocketdyne Div.
NUMERICAL AND EXPERIMENTAL STUDIES OF ATOMIZATION AND MIXING FROM A COAXIAL INJECTOR ELEMENT
P. Y. Liang and M. Varma *In* Johns Hopkins Univ., The 23rd JANNAF Combustion Meeting, Volume 1 Oct. 1986 p 623-631 (For primary document see N87-23757 17-28)
Avail: CPIA, Laurel, Md. 20707 HC $70.00

23 CHEMISTRY AND MATERIALS (GENERAL)

N87-23697# Oak Ridge National Lab., Tenn.
METALS AND CERAMICS DIVISION Progress Report, period ending 30 Sep. 1986
Mar. 1987 172 p
(Contract DE-AC05-84OR-21400)
(DE87-008548; ORNL-6358) Avail: NTIS HC A08/MF A01
This report is divided into the following sections: engineering materials, high-temperature materials, materials science, program activities, collaborative research facilities, and appendixes. DOE

N87-23698* National Aeronautics and Space Administration. Ames Research Center, Moffett Field, Calif.
PREPARATION OF B-TRICHLOROBORAZINE Patent
Salvatore R. Riccitiello, Ming-Ta S. Hsu, and Timothy S. Chen, 03inventors (to NASA) (Chem, H. C. Research and Service Corp., San Jose, Calif) 30 Jun. 1987 6 p Filed 28 Aug. 1986 Supersedes N87-15275 (25 - 7, p 877)
(NASA-Case-ARC-11643-1-SB; US-Patent-4,676,962; US-Patent-Appl-SN-901496; US-Patent-Class-423-284; US-Patent-Class-423-276) Avail: US Patent and Trademark Office CSCL 07A
The present invention relates to a method of preparing B-trichloroborazine. Generally, the method includes the combination of gaseous boron trichloride in an anhydrous aprotic organic solvent followed by addition of excess gaseous ammonia at ambient temperature or below. The reaction mixture is heated to about 100 to 140 C followed by cooling, removal of the solid ammonium chloride at ambient temperature, distillation of the solvent under vacuum if necessary at a temperature of up to about 112 C, and recovery of the B-trichloroborazine. Solvents include toluene, benzene, xylene, chlorinated hydrocarbons, chlorinated aromatic compounds, or mixtures thereof. Toluene is a preferred solvent. The process provides a convenient synthesis of a material which often decomposes on standing. B-trichloroborazine is useful in a number of chemical reactions, and particularly in the formation of high temperature inorganic polymers and polymer precursors.
NASA

24 COMPOSITE MATERIALS

Includes physical, chemical, and mechanical properties of laminates and other composite materials.
For ceramic materials see *27 Nonmetallic Materials.*

N87-23699# United Kingdom Atomic Energy Authority, Harwell (England). Materials Development Div.
CERAMIC FIBRE/GLASS MATRIX COMPOSITES WITH OUTSTANDING MECHANICAL PERFORMANCE
D. M. Dawson, R. F. Preston, A. Briggs, and R. W. Davidge Oct. 1986 10 p
(AERE-R-12025) Avail: NTIS HC A01/MF A01
The performance of most engineering ceramics, when used under conditions of stress, is limited by their tensile strength. The introduction of fibers into a ceramic matrix offers the possibility of a significant increase in fracture energy associated with the fibrous nature of the fracture. Samples were prepared with unidirectional fiber reinforcement. Particular attention was given to good fiber alignment, even glass distribution during impregnation and winding, and to time/temperature/pressure cycle in the hot pressing stage so as to fully optimize the mechanical properties. The work of fracture was estimated from the area under the stress/strain curves and from notched impact testing. It should be noted in addition that unlike in many other brittle matrix systems there was no evidence of significant, permanent, matrix cracking except at stresses very near the ultimate failure stress. This effect and the very high work of fracture both suggest that the interfacial shear strength between fiber and matrix is very high, but not so high that the fiber is completely bonded to the matrix. B.G.

N87-23700# Air Force Inst. of Tech., Wright-Patterson AFB, Ohio. School of Engineering.
MATERIAL DAMPING MEASUREMENTS OF 2D CARBON-CARBON COMPOSITE BEAMS M.S. Thesis
Ernest S. Muller Dec. 1986 117 p
(AD-A179109; AFIT/GAE/AA/86D-10) Avail: NTIS HC A06/MF A01 CSCL 11D
Thermal protective materials for space systems and advanced jet engines are investigated. The use of an advanced carbon-carbon composite material (ACCM) to build critical components that must operate in very high temperature regimes is examined. The potential use of ACCM in these applications must address the problems of vibration that might occur during system operations. Vibrations can cause severe performance degradations. One method of control, called passive damping, relies on the material's inherent damping characteristics. This study evaluates ACCM's damping characteristics, important to passive damping understanding. Modal analysis techniques using an impact hammer to excite sinuseidal free vibration were used to find the damping natural frequencies for 2-D ACCM beams. The logarithmic decrement technique was applied to the fundamental modes to verify the frequency and damping data derived by the modal analysis. Additionally, the logarithmic decrement technique was used to evaluate atmopheric drag influences on damping. It was shown that for small amplitudes, less than the beam's thickness, the damping effects of atmospheric drag were minimized and considered negligible. Cantilevered beam specimens were studied for the first three modes in test conditions at room temperature and atmospheric pressure. GRA

N87-23701# Air Force Inst. of Tech., Wright-Patterson AFB, Ohio. School of Engineering.
COLLAPSE ANALYSIS OF CYLINDRICAL COMPOSITE PANELS WITH LARGE CUTOUTS UNDER AN AXIAL LOAD M.S. Thesis
Thomas W. Tisler, Jr. Dec. 1986 129 p
(AD-A179112; AFIT/GAE/AA/86D-18) Avail: NTIS HC A07/MF A01 CSCL 11D

In order to better understand the collapse properties of composite shells, an analysis of cylindrical panels with large cutouts (11 and 18% of panel area) was conducted using a finite element program (STAGSC-1). These results were then compared to experimental findings. Cutout size, loading methods, vertical boundary conditions, and imperfections were varied to see how each affected the collapse load. In addition, the release of residual strain due to placing the cutout within the panel was evaluated. It was found the panel collapsed at a lower value when the applied force was a uniform load as compared to a uniform displacement. The decrease in collapse load with increased cutout size is less dramatic for the displacement condition. Initial imperfections were found to reduce the collapse load, but not to the extent seen for panels without cutouts. Fixing circumferential freedom along the vertical boundaries resulted in increased collapse loads as compared to leaving it free. Compared to experimental findings, STAGSC-1 was seen to progressively underestimate collapse load as cutout size increases. GRA

N87-23702# Sandia National Labs., Albuquerque, N. Mex.
MECHANICAL PROPERTIES OF UNDIRECTIONAL AND FABRIC GRAPHITE/EPOXY COMPOSITES
T. R. Guess Jun. 1986 26 p
(Contract DE-AC04-76DP-00789)
(SAND-86-0784) Avail: NTIS HC A03/MF A01

Room-temperature tension, compression, flexural, short beam shear, and inplane shear test results are presented for unidirectional and fabric reinforced graphite/epoxy composites. The reinforcement was 34 million psi modulus graphite fibers: Celion 12K in a unidirectional material and Thornel 300 in a fabric composite of 24 x 23 ends/inch eight-harness satin weave fabric. Both composites used a 350 F epoxy resin, CE-9000, for the matrix material. The elastic and strength properties of the unidirectional specimens were in good agreement with analytical predictions and with literature values for similar materials. The tensile stress-strain curves of the unidirectional and fabric composites were linear elastic to failure; whereas, the compression curves exhibited some nonlinearity near failure. A slight degree of anisotropy (less than 5%) was observed between the properties in the warp and fill directions of a fabric composite in which the individual plies of fabric were warp aligned. This anisotropy is attributed to the fact that there is about 4% more fiber reinforcement in the warp direction than in the fill direction of the fabric. Author

N87-23703# Sandia National Labs., Albuquerque, N. Mex.
SPIN-CAST CARBON FILMS FROM POLYACRYLONITRILE
C. L. Renschler and A. P. Sylwester 1987 2 p Presented at the 193rd National Meeting of the American Chemical Society, Denver, Colo., 5 Apr. 1987
(Contract DE-AC04-76DP-00789)
(DE87-002489; SAND-86-2535C; CONF-870410-3) Avail: NTIS HC A02/MF A01

Carbon films have been made by a variety of techniques, including evaporation, sputtering, and laser or thermal pyrolysis of organic polymers. Polyacrylonitrile (PAN) is often used as a carbon precursor, since low-temperature thermo-oxidative pretreatment produces a material which can be pyrolyzed without loss of shape. This is the basis for the production of carbon fibers with good mechanical properties. We report here the formation of very thin films of carbon (500 to 1500 A) by pyrolysis of spin-cast PAN. Using this technique, large, conductive films can be made which are sufficiently robust to allow intact lift-off and transfer of the films from one substrate to another. Such films are chemically inert, but can be photolithographically patterned and etched with an oxygen plasma. DOE

N87-23704# Lawrence Livermore National Lab., Calif.
WHITE PAPER ON NANOCOMPOSITES AS HARMONIC GENERATION MEDIA
D. Eimerl and S. Velsko 30 Oct. 1986 45 p
(Contract W-7405-eng-48)
(DE87-008337; UCID-20907) Avail: NTIS HC A03/MF A01

Nanocomposites (composites containing 5 to 50 nm particles) may be a flexible and inexpensive way to make large area harmonic generators, and may also provide noncritically phase-matched harmonic generators at wavelengths where none are currently available. There does not appear to be any extreme optical requirements on either the matrix or the microcrystallites. Scattering may well be significant, and reducing it to acceptable levels will require the use of either very small microparticles or strongly nonlinear microparticles, depending on the degree of long range order in the nanostructure of the nanocomposite. DOE

N87-23705# Northrop Corp., Hawthorne, Calif. Aircraft Div.
CERTIFICATION TESTING METHODOLOGY FOR COMPOSITE STRUCTURE. VOLUME 1: DATA ANALYSIS Final Report
R. S. Whitehead, H. P. Kan, R. Cordero, and E. S. Saether Oct. 1986 94 p Prepared in cooperation with Naval Air Development Center, Warminster, Pa. and Federal Aviation Agency, Atlantic City, N.J.
(Contract N62269-84-C-0243)
(NADC-87042-60-Vol-1; DOT/FAA/CT-86/39-Vol-1) Avail: NTIS HC A05/MF A01

This research developed a certification testing methodology for composite structures. The existing composite static strength and fatigue life data are analyzed statistically to determine the influence of test parameters on the scatter of composite data. Guidelines to use the composite data scatter in structural certification are recommended. Various approaches to composite structures certification are analytically evaluated. The approaches evaluated are: scatter factor approach, load enhancement factor approach, ultimate strength approach,and change in spectrum approach. The capability, advantages and disadvantages of each approach to determine the minimum life and/or strength are discussed. Volume 1 contains Data Analysis. Author

N87-23706# Northrop Corp., Hawthorne, Calif. Aircraft Div.
CERTIFICATION TESTING METHODOLOGY FOR COMPOSITE STRUCTURE. VOLUME 2: METHODOLOGY DEVELOPMENT Final Report
R. S. Whitehead, H. P. Kan, R. Cordero, and E. S. Saether Oct. 1986 286 p
(Contract N62269-84-C-0243)
(NADC-87042-60-Vol-2; DOT/FAA/CT-86/39-Vol-2) Avail: NTIS HC A13/MF A01

This research developed a certification testing methodology for composite structures. The existing composite static strength and fatigue life data are analyzed statistically to determine the influence of test parameters on the scatter of composite data. Guidelines to use the composite data scatter in structural certification are recommended. Various approaches to composite structures certification are analytically evaluated. The approaches used are: scatter factor, load enhancement, ultimate strength, and change in spectrum. The capability, advantages and disadvantages of each approach to determine the minimum life and/or strength are discussed. Volume 2 traces Methodology Development.
Author

25 INORGANIC AND PHYSICAL CHEMISTRY

Includes chemical analysis, e.g., chromatography; combustion theory; electrochemistry; and photochemistry.

For related information see also *77 Thermodynamics and Statistical Physics.*.

N87-23707# Utah State Univ., Logan. Center for Space Engineering.

A STUDY OF THE MAXIMUM ENTROPY METHOD OF POWER SPECTRUM ESTIMATION AS APPLIED TO INTERFEROMETER DATA

A. S. Zachor and D. S. Smith 17 Nov. 1986 68 p Prepared in cooperation with Atmospheric Radiation Consultants, Inc., Action, Mass.

(Contract F19628-83-C-0056)

(AD-A179403; CSE/86-108; AFGL-TR-86-0162; SR-18) Avail: NTIS HC A04/MF A01 CSCL 07D

Maximum entropy method (MEM) computer experiments were conducted on synthetic CO2 and OH input signals. They compared the power spectra which MEM produced with the given, exactly known, line spectra as well as with spectra produced by transitional Fourier methods. ARC scientists concluded from their study that MEM produces power spectra which are characterized by: (1) far higher resolution (narrower line widths) than that produced by Fourier methods, (2) errors in frequency (line positions) which are about 2 orders of magnitude smaller than those of Fourier methods, and (3) when the frequencies have been determined by locating maxima in the MEM or Fourier spectra, finding the amplitudes is a linear least squares problem. The errors in the MEM amplitude are about two orders of magnitude smaller than those of the Fourier methods. In the case of the quasiregular spectra, the implied very high resolution and accuracy provided by the MEM is contingent on an interferogram length equal to at least the reciprocal of the minimum line separation, and equivalent to at least four independent samples for each spectrum line. GRA

N87-23708# Utah State Univ., Bedford, Mass. Radiance Lab.

MEDIUM- AND LONG-WAVE INFRARED ABSORPTION SPECTRA OF CARBON DIOXIDE NITROUS OXIDE AT 800K

William M. Barowy, Mark P. Esplin, George A. Vanasse, and Ronald J. Huppi 8 Jan. 1987 63 p

(Contract F19628-83-C-0056)

(AD-A179430; AFGL-TR-87-0016; SR-21) Avail: NTIS HC A04/MF A01 CSCL 07D

A high resolution interferometer was used to measure the medium- and long-wave infrared absorption spectra of carbon dioxide and nitrous oxide heated to 800K. Modifications were made to the instrument to improve its wavelength accuracy and reliability. In the 4.3 micrometer region, 5 bands of 12c16O18O were identified and the corresponding spectral constants were reduced. The constants reproduce the position of the spectral lines to within 0.0005/cm. Absorption spectra of N20 and CO2 in the 7.8 micrometer and 15 micrometer regions respectively, have been recorded and their preliminary analysis has been completed. GRA

N87-23709# Yale Univ., New Haven, Conn. High Temperature Chemical Reaction Engineering Lab.

TRANSPORT PHENOMENA AND INTERFACIAL KINETICS IN MULTIPHASE COMBUSTION SYSTEMS Annual Report, 1 Dec. 1985 - 31 Dec. 1986

Daniel E. Rosner Jan. 1987 11 p

(Grant AF-AFOSR-0034-84)

(AD-A179544; AFOSR-87-0523TR) Avail: NTIS HC A02/MF A01 CSCL 21B

This annual report summarizes Yale High Temperature Chemical Reaction Engrg. Laboratory research methods/results for the one year period ending 12/31/86. Our techniques and results are outlined in the areas of: (1) laser based real time optical techniques for measuring soot particle thermophoretic diffusivities, and vapor and/or particle-deposition rates onto cooled surfaces in combustion gases, (2) role of thermophoresis in the capture of soot particles and the use of this phenomenon to infer both local soot volume fractions and logical gas temperatures, (3) boundary layer computational methods and correlations for thermophoretically-modified vapor and small particle transport, including high mass-loading and dopant redistribution effects, and (4) use of a micro-wave-induced plasma emission spectroscopic (MIPES) method to follow boron surface gasification kinetics in stream containing oxygen (g). Presentation and archive publications describing these techniques/findings are documented, including the publication of a more comprehensive textbook: Transport Processes in Chemically Reacting Flow Systems (Butter-worths, Stoneham MA) by the Principal Investigator. GRA

N87-23710# National Bureau of Standards, Washington, D.C. Center for Chemical Physics.

LASER STUDIES OF CHEMICAL DYNAMICS AT THE GAS-SOLID INTERFACE Progress Report

R. R. Cavanagh and D. S. King Sep. 1986 12 p

(Contract DE-AI05-84ER-13150)

(DE87-005950; DOE/ER-13150/3) Avail: NTIS HC A02/MF A01

Experiments during this period have focused on the thermal desorption of NO from Pt(111). Emphasis was placed on the relative importance of adsorbate-substrate vs adsorbate-adsorbate interactions. Both mass spectrometric and laser diagnostic techniques were used. The influence of coadsorption of CO was studied. Laser-induced thermal desorption of NO from platinum foil was studied. DOE

N87-23711# Geological Survey, Menlo Park, Calif.

INELASTIC PROPERTIES OF ICE I/SUB h/ AT LOW TEMPERATURES AND HIGH PRESSURES

S. H. Kirby, W. B. Durham, M. L. Beeman, H. C. Heard, and M. A. Daley Jan. 1987 8 p Presented at the 7th Symposium on the Physics and Chemistry of Ice, Grenoble, France, 1 Sep. 1986 Prepared in cooperation with Lawrence Livermore National Lab., Calif. and Cornell Univ., Ithaca, N.Y.

(Contract W-7405-eng-48)

(DE87-007334; UCRL-95941; CONF-8609269-1) Avail: NTIS HC A02

The aim was to explore the rheological behavior of H2O ices under conditions appropriate to the interiors of the icy satellites of the outer planets in order to give insight into their deformation. To this end, we have performed over 100 constant-strain-rate compression tests at pressures to 500 MPa and temperatures as low as 77 K. The effect of increasing confining pressure on stress-strain behavior and deformation mechanisms depends on the test temperature. At a strain rate of 3.5 x 10(-5)/s, ice I sub h fails catastrophically at temperatures below 165 K at all pressures tested (0.1 to 350 MPa). Failure strength increases sharply with increasing pressure. At P greater than 30 MPa, ice I sub h fails by a shear instability producing faults in the maximum shear stress orientation and failure strength typically is independent of pressure. We have also studied the frictional sliding characteristics of ice I sub h by shortening cylindrical specimens sawn and ground at 45 deg to the cylindrical axis. We observed sudden (stick slip) frictional sliding with the maximum shear strength necessary to overcome static friction tau obeying the simple law tau (MPa) = 8.5 + 0.2 sigma(sub n) (MPa) where sigma(sub n) is the normal stress on the sliding surface. This law was determined over the range 17 less than or equal to sigma(sub n) less than or equal to 240 MPa and is insensitive to temperature and sliding rate over the range of conditions we explored. Stress-strain curves under ductile conditions typically display a linear quasi-elastic stage followed by macroscopic yield, strain softening and finally a flat steady state flow. Optical study of thin sections of samples taken to various strains shows that macroscopic yield corresponds to the first optical evidence of internal plastic deformation, that nucleation and rapid growth of new grains accompanies strain softening and that steady-state flow corresponds to the attainment of a steady-state recrystallization structure. DOE

N87-23712# Du Pont de Nemours (E. I.) and Co., Aiken, S.C.
FINITE-DIFFERENCE PROGRAM FOR HYDROGEN DIFFUSION: EXAMPLE PROBLEMS MANUAL
K. E. Kain Jan. 1987 320 p
(Contract DE-AC09-76SR-00001)
(DE87-007515; DPST-87-203) Avail: NTIS HC A14

The finite-difference program DIFF.BAS calculates hydrogen and helium concentration profiles for hydrogen systems. The program can be used to determine the possibility of hydrogen/helium embrittlement and estimate the health hazards associated with tritium permeation. For these safety analyses, a computer program has been written for special applications of interest to the Savannah River Laboratory and the Department of Energy complex. Over 160 possible combinations of structure shape, isotope calculations, material properties and boundary conditions are available. This does not include the infinite variations in fill data, exposure sequences, time, temperatures and structure sizes which the program can accommodate. The example manual cannot address all of these possibilities. However, all options have been investigated and are included in this manual containing 61 example problems. DOE

N87-23713*# National Aeronautics and Space Administration. Langley Research Center, Hampton, Va.
APPARATUS AND PROCEDURE TO DETECT A LIQUID-SOLID INTERFACE DURING CRYSTAL GROWTH IN A BRIDGMAN FURNACE Patent Application
Patrick G. Barber, inventor (to NASA), Roger K. Crouch, inventor (to NASA), Archibald L. Fripp, Jr., inventor (to NASA), Robert F. Berry, Jr., inventor (to NASA), William J. Debnam, Jr., inventor (to NASA), and Richard T. Simchick, inventor (to NASA) (PRC Kentron, Inc., Hampton, Va.) 29 Jan. 1987 10 p
(NASA-Case-LAR-13597-1-CU; US-Patent-Appl-SN-008199) Avail: NTIS HC A02/MF A01 CSCL 07D

This invention relates to a method and apparatus for detecting a liquid-solid interface of a substance. In particular, the invention detects the liquid-solid interface of a semiconductor crystal grown in a Bridgman furnace. A substance, such as germanium, in a Bridgman furnace is irradiated by solid-penetrating energy from a radiation source. The solid penetrating energy is detected by a radiation detector. Differences in the intensity of the detected energy indicate the shape of the liquid-solid interface. In the case of germanium, X-rays can be used as the solid penetrating energy, while in the case of a substance such as lead tin telluride, gamma rays are perferable. The invention enables detection of the shape of the liquid-solid interface of a semiconductor substance during growth of a crystal formed from the substance. Variations in several characteristics of semiconductor crystals are believed to be related to the shape of the liquid-solid interface, but previously there was no means to detect the shape of the liquid-solid interface during growth of the crystal. NASA

N87-23714# Sandia National Labs., Albuquerque, N. Mex.
SANDIA COOPERATIVE GROUP ON THE AEROTHERMOCHEMISTRY OF TURBULENT COMBUSTION
R. W. Dibble, R. W. Carling, and S. C. Johnston Mar. 1987 54 p
(Contract DE-AC04-76DR-00789)
(DE87-008345; SAND-87-8213) Avail: NTIS HC A04/MF A01

A turbulent reacting flow working group has been established through the Department of Energy/Office of Basic Energy Sciences. The purpose of this group is to establish and maintain a strong interaction and active dialogue between workers currently involved in modeling turbulent reacting flows and those involved in related experiments. One objective of this collaboration is to develop an increased understanding of the fundamental interaction between the chemical and fluid dynamical processes occurring in chemically reacting flows and to utilize this understanding to improve predictive capabilities for turbulent combustion. Regular members, who represent academia, private industry, and national laboratories, and guests participate in the meetings. Several guests are invited to each meeting to provide an influx of different ideas and opinions to the discussions. This document is a summary of the discussions that took place during the seventh and eighth meetings, which were held at California Institute of Technology, Pasadena, Calif., March 25 to 26, 1986 and Yale University, New Haven, Conn., October 13 to 14, 1986, respectively. DOE

N87-23715# Indiana Univ., Bloomington.
METAL ALKOXIDES: MODELS FOR METAL OXIDES: ALKOXIDE LIGANDS IN EARLY TRANSITION METAL ORGANOMETALLIC CHEMISTRY Progress Report
M. H. Chisholm 1986 14 p
(Contract DE-FG02-86ER-13570)
(DE87-007309; DOE/ER-13570/1) Avail: NTIS HC A02/MF A01

Alkoxide clusters of molybdenum and tungsten provide structural models for the oxides of these elements in their lower valencies. The steric bulk of a given alkoxide ligand allows for the molecular design of unsaturated species which may model surface sites. The organometallic chemistry of these alkoxides clusters is being investigated. Activation of alkynes and carbon monoxide by these clusters leads to alkylidyne and carbido species. This 6 electron reduction of the substrate parallels surface chemistry wherein chemisorbed X identical to Y molecules (X, Y = C, N, O) are cleaved leading to surface bound carbido, nitrodo, alkylidyne and oxo ligands. Addition of RO-H to certain tungsten clusters leads to hydridoalkoxide clusters which have been found to be catalytically active in olefin isomerization. Current work is aimed at studying the reactivity of these alkoxide clusters as models for heterogeneous catalysts. This work provides a new dimension to organometallic cluster chemistry and is expected to yield mechanistic information of fundamental importance in the understanding of the activation of small molecules. DOE

N87-23716# Georgia Univ., Athens. Dept. of Chemistry.
NOVEL APPLICATION OF TOPOLOGICAL INDICES. 2. PREDICTION OF THE THRESHOLD SOOT INDEX FOR HYDROCARBON FUELS
Milton P. Hanson and D. H. Rouvray 6 Mar. 1987 28 p
(Contract N00014-84-K-0365)
(AD-A178001; TR-40) Avail: NTIS HC A03/MF A01 CSCL 21D

The propensity of hydrocarbons to form soot in a diffusion flame is correlated here for the first time against various topological indices. Two of the indices, the hydrogen deficiency index and the Balaban distance sum connectivity index, were found to be especially valuable for correlational purposes. For a total of 98 hydrocarbon fuel molecules, of differing types, regression analyses yielded good correlations between the threshold soot indices (TSIs) for diffusion flames and these two indices. An equation which can be used to estimate TSI values in fuel molecules is presented. GRA

N87-23717*# Alabama Univ., Huntsville. Dept. of Chemistry.
CELLULAR MONOTECTIC MODEL SOLIDIFICATION Semiannual Report
William F. Kaukler Jun. 1987 10 p
(Grant NAG8-069)
(NASA-CR-181027; NAS 1.26:181027) Avail: NTIS HC A02/MF A01 CSCL 07D

Succinonitrile (sn) was purified to a superior level using a fractional recrystallization method. The melting point of the best twice recrystallized sn was not raised by following with double distillation. This was tested using differential scanning calorimetry. The peak shape on melting also proved that double distillation after double recrystallization did not improve the quality. Stability and phase diagrams for succinonitrile and glycerol are presented. M.G.

N87-23718*# National Aeronautics and Space Administration. Lewis Research Center, Cleveland, Ohio.
ELECTROCHEMICAL PERFORMANCE AND TRANSPORT PROPERTIES OF A NAFION MEMBRANE IN A HYDROGEN-BROMINE CELL ENVIRONMENT
Richard S. Baldwin Jun. 1987 27 p

(NASA-TM-89862; E-3529; NAS 1.15:89862) Avail: NTIS HC A03/MF A01 CSCL 07D

The overall energy conversion efficiency of a hydrogen-bromine energy storage system is highly dependent upon the characteristics and performance of the ion-exchange membrane utilized as a half-cell separator. The electrochemical performance and transport properties of a duPont Nafion membrane in an aqueous HBr-Br2 environment were investigated. Membrane conductivity data are presented as a function of HBr concentration and temperature for the determination of ohmic voltage losses across the membrane in an operational cell. Diffusion-controlled bromine permeation rates and permeabilities are presented as functions of solution composition and temperature. Relationships between the degree of membrane hydration and the membrane transport characteristics are discussed. The solution chemistry of an operational hydrogen-bromine cell undergoing charge from 45% HBr to 5% HBr is discussed, and, based upon the experimentally observed bromine permeation behavior, predicted cell coulombic losses due to bromine diffusion through the membrane are presented as a function of the cell state-of-charge. M.G.

N87-23792 United Technologies Research Center, East Hartford, Conn.

CARS APPROACHES TO SIMULTANEOUS MEASUREMENTS OF H2 AND H2O CONCENTRATION AND TEMPERATURE IN H2-AIR COMBUSTION SYSTEMS

Alan C. Eckbreth, Torger J. Anderson, and Gregory M. Dobbs *In* Johns Hopkins Univ., The 23rd JANNAF Combustion Meeting, Volume 1 Oct. 1986 p 405-415 (For primary document see N87-23757 17-28)

Avail: CPIA, Laurel, Md. 20707 HC $70.00

N87-23798# Naval Weapons Center, China Lake, Calif.

PASSIVE SHEAR-FLOW CONTROL TO MINIMIZE RAMJET COMBUSTION INSTABILITIES

K. C. Schadow, E. Gutmark, T. P. Parr, D. M. Parr, and K. J. Wilson *In* Johns Hopkins Univ., The 23rd JANNAF Combustion Meeting, Volume 1 Oct. 1986 p 469-484 (For primary document see N87-23757 17-28)

Avail: CPIA, Laurel, Md. 20707 HC $70.00

N87-23803# Georgia Inst. of Tech., Atlanta.

COMBUSTION INSTABILITIES IN DUMP TYPE RAMJET COMBUSTORS

U. G. Hegde, D. Reuter, B. T. Zinn, and B. R. Daniel *In* Johns Hopkins Univ., The 23rd JANNAF Combustion Meeting, Volume 1 Oct. 1986 p 533-544 (For primary document see N87-23757 17-28)

(Contract N00014-84-K-0470)

Avail: CPIA, Laurel, Md. 20707 HC $70.00

N87-23805# California Univ., Irvine.

SPRAY COMBUSTION: A DRIVING MECHANISM FOR RAMJET COMBUSTION INSTABILITY

W. A. Sirignano, G. Riva, A. Tong, B. Abramzon, and K. Molavi *In* Johns Hopkins Univ., The 23rd JANNAF Combustion Meeting, Volume 1 Oct. 1986 p 551-559 (For primary document see N87-23757 17-28)

(Contract N00014-85-K-0658)

Avail: CPIA, Laurel, Md. 20707 HC $70.00

N87-23806# California Univ., Davis. Dept. of Mechanical Engineering.

COMBUSTION, VAPORIZATION, AND MICROEXPLOSION OF DROPLETS OF ORGANIC AZIDES

C. K. Law, A. Lee, S. Deevi, A. Ganji, and A. Makino *In* Johns Hopkins Univ., The 23rd JANNAF Combustion Meeting, Volume 1 Oct. 1986 p 561-572 (For primary document see N87-23757 17-28)

(Contract N00014-84-K-0700)

Avail: CPIA, Laurel, Md. 20707 HC $70.00

N87-23808* National Aeronautics and Space Administration. Langley Research Center, Hampton, Va.

MULTISPECIES CARS MEASUREMENTS IN TURBULENT COMBUSTION

Richard R. Antcliff, Olin Jarrett, Jr., R. Clayton Rogers, and Thomas VanOverbeck *In* Johns Hopkins Univ., The 23rd JANNAF Combustion Meeting, Volume 1 Oct. 1986 p 577-583 Prepared in cooperation with NASA- Lewis Research Center, Cleveland, Ohio. (For primary document see N87-23757 17-28)

Avail: CPIA, Laurel, Md. 20707 HC $70.00 CSCL 07D

26 METALLIC MATERIALS

Includes physical, chemical, and mechanical properties of metals, e.g., corrosion; and metallurgy.

N87-23719# Naval Surface Weapons Center, Silver Spring, Md.

GALVANIC CORROSION OF Al-7075-T6 AND STEEL-4340 COUPLED TO BRASS QQ-B-626, 360 AND Al-7075-T6 COUPLED TO STEEL-4130 AND STEEL-4340: EXPOSURE TO AQUEOUS NaCl AND SALT-FOG ENVIRONMENTS Technical Report, Jun. - Dec. 1985

J. F. McIntyre, S. M. Hoover, and K. A. Musselman 30 Jun. 1986 57 p

(AD-A179121; NSWC/TR-86-26) Avail: NTIS HC A04/MF A01 CSCL 11F

For this investigation, laboratory studies on the corrosion behavior of four galvanic couples is discussed; the four couples include: Al-7075-T6/Brass QQ-B-626, 360, Al-7075-T6/Steel-4340, Al-7075-T6/Steel-4130, and Steel-4340/Brass QQ-B-626, 360. Test samples were exposed to aqueous 3.5% NaCl and to a salt-fog environment. A measurement of the galvanic current generated for each couple tested was used to determine the magnitude of galvanic interaction. Results indicated that the corrosion rate of Al-7075-T6 was significantly accelerated when galvanically coupled to brass or the steel samples. In addition, it was discovered that Steel-4130 and Steel 4340 corroded when coupled to Al-7075-T6, however, at a reduced rate when compared to the uncoupled steel samples. In contrast, brass samples revealed no signs of corrosion when coupled to either Al-7075-T6 or Steel-4340. For the Steel-4340/Brass galvanic couple, it was found that the corrosion rate of Steel-4340 was significantly increased while the brass sample remained unaffected. In addition to the discussion of experimental results, a theoretical treatment relating galvanic currents to observed corrosion rates are presented for each of the four couples. GRA

N87-23720# Southwest Research Inst., San Antonio, Tex.

STUDY OF THE INFLUENCE OF METALLURGICAL FACTORS ON FATIGUE AND FRACTURE OF AEROSPACE STRUCTURAL MATERIALS Annual Report, 1 Jan. - 31 Dec. 1986

James Lankford, David L. Davidson, Kwai S. Chan, and Gerald R. Leverant 30 Jan. 1987 37 p

(Contract F49620-86-C-0024)

(AD-A179268; SWRI-06-8972; AFOSR-87-0310TR) Avail: NTIS HC A03/MF A01 CSCL 11F

Summarized are the results of a two-phase study involving: (1) experimental characterization and analytical modeling of fatigue crack tip micromechanics in aerospace structural Aluminum alloys, and (2) identification and modeling of key microstructural factors controlling fracture in Al-Iron-X alloys. Dynamic load cycling within the Scanning Electron Microscopy and stereoimaging strain analysis were used to characterize crack opening loads and crack opening modes for 7091-T7E69 Al alloy. Relationships between Delta K, Delta k sub eff, Delta k sub th, and R are defined. These data are used to determine compressive residual stresses within the near crack tip region. It was found that at the threshold, crack tips are able to open only in Mode 2, i.e., the threshold corresponds to an absence at Mode 1 crack opening. A model was developed which relates the threshold stress intensity factor to the length of a microstructure-related dominant slip line length. The validity of the model was tested experimentally, with reasonable

agreement between predicted and measured results. The fracture behavior of Al-Fe-X alloys was investigated with the objectives of identifying the micromechanisms of fracture and establishing microstructure/property relationships in this series of dispersoid-strengthened, powder-metallurgy aluminum alloys. Tensile and fracture toughness tests were performed at room temperature to obtain the yield stress, strain hardening exponent, and local fracture strain. GRA

N87-23721# Illinois Univ., Urbana. Dept. of Metallurgy and Mining Engineering.
Al AND Mg ALLOYS FOR AEROSPACE APPLICATIONS USING RAPID SOLIDIFICATION AND POWDER METALLURGY PROCESSING Annual Report, 15 May 1986 - 15 May 1987
Fraser May 1987 13 p
(Grant AF-AFOSR-0191-85)
(AD-A179547; AFOSR-87-0421TR) Avail: NTIS HC A02/MF A01 CSCL 11F

The first section of the progress report is concerned with the development of rapidly solidified Al-8Fe-2Mo-Si alloys for elevated temperature applications. Rapidly solidified Al-8FE-2Mo alloys containing silicon in the range of 0 to 1 wt pct were produced by melt spinning. In the second annual report, preliminary results of the effect of Si on the formation of the Sone A microstructure and on subsequent changes of this structure during heat-treatment were described. It was shown that addition of Si has a dramatic effect on the transformation behavior and microstructure of heat-treated ribbons. In contrast to the thermally unstable, multiphase precipitate distribution in the ternary Al-8FE-2Mo alloy, quarternary Si-containing alloys showed a uniform dispersion of fine cuboidal/polygonal precipitates, which displayed a remarkable resistance to coarsening. A typical TEM micrograph portraying this effect is shown for a Al-8Fe-2Mo0-0.5Si alloy heat treated at 450 C for 50 hrs. To identify the nature of the precipitates, X-ray and electron diffraction were used, and these results are reported. GRA

N87-23722# Mound Lab., Miamisburg, Ohio.
CORROSION OF GOLD BRIDGEWIRE IN ELECTRONIC COMPONENTS
G. L. Downs, J. D. Braun, and E. E. Tibbitts 1986 20 p Presented at the International Metallographic Society Conference on Microstructural Science, Boston, Mass., 3 Aug. 1986
(Contract DE-AC04-76DP-00053)
(DE87-000922; MLM-3393(OP); CONF-8608153-3) Avail: NTIS HC A02/MF A01

Accelerated aging tests on gold bridgewired detonator assemblies to determine compatibility of the Au and Pd-In-Sn solder with the organic explosive, PETN, have revealed an unusual corrosion process. These tests, conducted at 74 C and 54 C indicated a preferential attack of the gold. A matrix of corrosion test units was established to study this corrosion problem with accelerating temperatures up to 100 C. Scanning electron microscopy (SEM), energy dispersive x-ray (EDX), and x-ray diffraction techniques were used to determine the extent of the corrosion and identify the corrosion products. Results indicate the preferential attack of the gold was due to HCN formed by decomposition of the explosive powder (PETN) at high temperatures. Other associated reactions were also observed including subsequent attack of the solder by the gold corrosion product and degradation of the plastic header. DOE

N87-23723# Sandia National Labs., Albuquerque, N. Mex.
CORROSION SENSING WITH ACOUSTIC WAVE DEVICES
S. J. Martin, A. J. Ricco, and N. R. Sorensen 1987 9 p Presented at the 171st Electrochemical Society Meeting, Philadelphia, Pa., 10 May 1987
(Contract DE-AC04-76DP-00789)
(DE87-003516; SAND-86-2714C; CONF-870513-3) Avail: NTIS HC A02/MF A01

Corrosion of thin metal films has been monitored (real-time) both in gaseous environments and in solution using acoustic wave sensors. A surface acoustic wave (SAW) was used to monitor corrosion in gaseous environments, while a horizontally polarized shear wave (HPSW) allowed measurement in liquid environments. The devices, which have 32 micron transducer periodicity, were fabricated on ST-cut quartz substrates. DOE

N87-23724# Sandia National Labs., Albuquerque, N. Mex.
PLASMA DEPOSITION OF TUNGSTEN
K. E. Greenberg Dec. 1986 9 p Presented at the Materials Research Society Fall Meeting, Boston, Mass., 1 Dec. 1986
(Contract DE-AC04-76DP-00789)
(DE87-007390; SAND-86-1299C; CONF-861207-93) Avail: NTIS HC A02/MF A01

Tungsten films were plasma-deposited using an abnormal glow discharge through a mixture of tungsten hexafluoride, hydrogen, and argon. The films adhered well to silicon, silicon dioxide, gallium arsenide, and aluminum substrates placed directly on the discharge cathode. Typical deposition rates were on the order of 160 Angstroms/minute with as-deposited film resistivities of 40 to 70 microohm-cm. The tungsten was analyzed using a number of techniques including X-ray diffraction, scanning electron microscopy, and Auger spectroscopy. Low-resistivity (less than 10 microohm-cm) films that adhered well to silicon dioxide were obtained with a two-step process utilizing plasma deposition and conventional chemical vapor deposition. DOE

N87-23725# Los Alamos National Lab., N. Mex.
THE USE OF MOLECULAR DYNAMICS FOR THE THERMODYNAMIC PROPERTIES OF SIMPLE AND TRANSITION METALS
G. K. Straub Apr. 1987 36 p
(Contract W-7405-eng-36)
(DE87-007718; LA-10959-MS) Avail: NTIS HC A03/MF A01

The technique of computer simulation of the molecular dynamics in metallic systems to calculate thermodynamic properties is discussed. The nature of a metal as determined by its electronic structure is used to determine the total adiabatic potential. The effective screened ion-ion interaction can then be used in a molecular dynamics simulation. The method for the construction of a molecular dynamics ensemble, its relation to the canonical ensemble, and the definition of thermodynamic functions from the Helmholtz free energy is given. The method for the analysis of the molecular dynamics results from quasiharmonic lattice dynamics and the decomposition in terms of harmonic and anharmonic contributions is given for solids. For fluid phase metals, procedures for calculating the thermodynamics and determining the constant of entropy are presented. The solid-fluid phase boundary as a function of pressure and temperature is determined using the results of molecular dynamics. Throughout, examples and results for metallic sodium are used. The treatment of the transition metal electronic d-states in terms of an effective pair-wise interaction is also discussed and the phonon dispersion curves of Al, Ni, and Cu are calculated. DOE

N87-23726# Sandia National Labs., Albuquerque, N. Mex.
THE CORROSION OF Al 7075-T6 ALLOY COUPLED TO Ti 6A 1-4V IN WET AIR
M. W. Mote Mar. 1987 9 p
(Contract DE-AC04-76DR-00789)
(DE87-008347; SAND-87-8208) Avail: NTIS HC A02/MF A01

Titanium coupled to aluminum alloy 7075-T6 did not accelerate the corrosion of the aluminum in a condensing moist air environment. DOE

N87-23727# Michigan State Univ., East Lansing.
STUDIES ON AGE-HARDENING IN SPINODALLY MODULATED ALLOYS: EXPERIMENTAL AND THEORETICAL Final Report, 1 Jul. 1981 - 30 Apr. 1986
Jan. 1987 44 p
(Contracts DE-AC02-81ER-10942; DE-FG02-84ER-45060)
(DE87-008361; DOE/ER-10942/T1) Avail: NTIS HC A03/MF A01

In-situ straining of homogeneous as well as spinodally modulated specimens of Cu-10Ni-6Sn alloy was carried out in the

High Voltage Electron Microscope. Dislocations reoriented themselves continuously during their motion. Dislocation motion was smooth in homogeneous specimens and discontinuous in modulated specimens. These dislocations existed in screw orientation in homogenized specimens and in specimens that have undergone early stages of decomposition. However, extensive modulation due to longer aging causes these dislocations to possess a mixed character having Burgers vector at about 60 deg to their line direction. The deformation structure in homogenized as well as spinodally modulated specimens of Cu-10Ni-6Sn alloy was also investigated by transmission electron microscopy. Tensile tests on Cu-10Ni-6Sn spinodal alloy were carried out on polycrystalline samples in as-quenched and aged conditions at various temperatures ranging from 77 K to 353 K.
DOE

N87-23728# Pennsylvania State Univ., University Park. Coll. of Earth and Minerals Sciences.
NONUNIFORM GRAIN BOUNDARY CORROSION AND THE LOCAL ELECTRODE POTENTIAL IN CREVICING
R. N. Iyer, A. Valdes, and H. W. Pickering Feb. 1987 41 p
(Contract N00014-84-K-0201)
(AD-A177889; AD-E950921) Avail: NTIS HC A03/MF A01 CSCL 11F

This Technical Report consists of three papers to be presented at the upcoming Conference on Environmental Degradation of Engineering Materials III to be held April 13-15, 1987 at The Pennsylvania State University, University Park, PA. The first two papers are on precipitation induced grain boundary corrosion, with a particular emphasis on sensitization in stainless steel. The third paper is on the importance of the local electrical potential on crack formation and pit growth.
GRA

N87-23729*# Sverdrup Technology, Inc., Cleveland, Ohio.
THE T55-L-712 TURBINE ENGINE COMPRESSOR HOUSING REFURBISHMENT PROJECT Final Report
George W. Leissler, Cliff Darling, and George Gilchrist (Corpus Christi Army Depot, Tex.) May 1987 23 p Prepared in cooperation with Army Aviation Research and Development Command, Cleveland, Ohio
(Contract NAS3-24105; DA Proj. 1L1-61102-AH-45)
(NASA-CR-179624; E-3571; NAS 1.26:179624; AVSCOM-TR-87-C-20) Avail: NTIS HC A02/MF A01 CSCL 11F

A study was conducted to access the feasibility of reclaiming T55-L-712 turbine engine compressor housings with an 88 wt % aluminum – 12 wt % silicon alloy applied by the plasma spray processes. Tensile strength testing was conducted on as-sprayed and thermally cycled test specimens which were plasma sprayed from 0.020 to 0.100 in. Satisfactory tensile strength valves were observed in the as-sprayed tensile specimens. There was essentially no decrease in tensile strength after thermally cycling the tensile specimens.
Author

27 NONMETALLIC MATERIALS

Includes physical, chemical, and mechanical properties of plastics, elastomers, lubricants, polymers, textiles, adhesives, and ceramic materials.

For composite materials see *24 Composite Materials*.

N87-23730# Arizona Univ., Tucson. Dept. of Chemistry.
FABRICATION OF POLYMERS FOR USE UNDER EXTREME CONDITIONS Final Report, 1 Jan. 1982 - 31 Dec. 1986
C. S. Marvel, N. N. Malder, and Dan Zuber 31 Dec. 1986 8 p
(Grant AF-AFOSR-0007-82)
(AD-A179458; AFOSR-87-0409TR) Avail: NTIS HC A02/MF A01 CSCL 07C

Several naturally occurring polyacetylenes have been synthesized and preliminary tests made for their polymerization. Results follow.
GRA

N87-23731# Sandia National Labs., Albuquerque, N. Mex.
FOAM RHEOLOGY: THE LINEAR VISCOELASTIC RESPONSE OF A SPATIALLY PERIODIC MODEL
A. M. Kraynik 1987 3 p Presented at the 11th Canadian Congress of Applied Mechanics, Edmonton, Canada, 31 May 1987
(Contract DE-AC04-76DP-00789)
(DE87-000960; SAND-86-2169C; CONF-870533-2) Avail: NTIS HC A02/MF A01

Foam is considered to be a dispersion of gas cells in a continuous network of thin liquid films. The interfacial properties that are essential to foam stability are equally important to foam rheology. This is illustrated by the linear viscoelastic response of a model foam. Spatially periodic models of foam rheology have provided insight into the cell-level mechanisms that are responsible for such properties as a finite shear modulus, yield stress, non-Newtonian viscosity, normal stresses, and shear strength. The analysis described here extends previous work by considering several new features: linear viscoelastic behavior, Gibbs' elasticity, and interfacial viscosity.
DOE

N87-23732# Sandia National Labs., Albuquerque, N. Mex.
THREE-DIMENSIONAL MODEL FOR THE LINEAR ELASTIC PROPERTIES OF A FOAM
W. E. Warren and A. M. Kraynik Oct. 1986 7 p Presented at the 11th Canadian Congress of Applied Mechanics, Edmonton, Canada, 31 May 1987
(Contract DE-AC04-76DP-00789)
(DE87-000984; SAND-86-2347C; CONF-870533-3) Avail: NTIS HC A02/MF A01

Tetrahedral strut junctions are predominant in foams whose synthesis route involves a liquid state. A general analysis of tetrahedral-joint mechanics is presented which is based upon a recent analysis of 2-D spatially periodic cellular materials. The deformation of an arbitarily oriented joint in uniaxial strain and pure shear is analyzed. Averaging the stresses over all possible joint orientations provides a consistent set of relations for determining the effective isotropic elastic constants for this 3-D foam model.
DOE

N87-23733# Sandia National Labs., Albuquerque, N. Mex.
A MODEL FOR SILICON DENDRITE GROWTH DURING LASER/PLASMA DEPOSITION FROM A SILANE DISCHARGE
H. M. Anderson and P. J. Hargis, Jr. 1986 9 p Presented at the Materials Research Society Fall Meeting, Boston, Mass., 1 Dec. 1986 Prepared in cooperation with New Mexico Univ., Albuquerque
(Contract DE-AC04-76DP-00789)
(DE87-007579; SAND-86-1169C; CONF-861207-94) Avail: NTIS HC A02

A model for dendrite growths in polycrystalline Si films formed during laser/plasma deposition with a silane discharge and a pulsed KrF laser has been developed. The model assumes a thin (less than 10 nm) amorphous silicon (a-Si) film is deposited on a substrate prior to phase transformation due to laser heating. The observed dendritic structure of the overall polycrystalline Si films is attributed to Si crystals shooting from an excessively supercooled Si liquid bath. Supercooled liquid forms since the melting point for a-Si can be reached at relatively low KrF laser fluences. Latent heat evolved at the solid-liquid interface induces an interface temperature higher than that of the melt and the requisite negative temperature gradient for absolute bath supercooling. Since the formation of an undercooled liquid by fast melting a-Si is also an important first step in explosive crystal regrowth studies, these results may have important implications for crystal growth and transient annealing. A conical approximation model is used in this study to characterize the stability of the dendrite tip in terms of local temperature gradients, i.e., the degree of undercooling at the tip of the parabolic dendrite. The degree of undercooling and hence the tip radius appears to be significantly affected by small changes in the laser fluence. Stability criteria lead to a relationship between regrowth velocity, V, and the tip radius, R, of the form VR^2 = constant. The size and stability of the dendrite tip is

determined from a balance between the destabilizing force due to thermal diffusion and the stabilizing capillary force. Based on the observed tip radii formed at laser fluences from 0.13 to 0.25 J/sq cm, the model predicts regrowth velocities in a range between 2.0 and 20 m/s -- values consistent with transient annealing studies of a-Si. DOE

N87-23734# Sandia National Labs., Albuquerque, N. Mex.
A MECHANISTIC STUDY OF THE INTERACTION OF ULTRAVIOLET LASER RADIATION WITH LOW DENSITY POLYMERS
P. J. Hargis, Jr. 1986 9 p Presented at the Materials Research Society Fall Meeting, Boston, Mass., 1 Dec. 1986
(Contract DE-AC04-76DP-00789)
(DE87-007846; SAND-86-1290C; CONF-861207-96) Avail: NTIS HC A02/MF A01

Ultraviolet laser radiation at 248 nm and 266 nm was used to ablate low density (0.04 to 0.14 g/cu cm) microcellular polystyrene and TPX foams at laser fluences between 0.1 and 1000 J/sq cm. The dependence of the etch rate on laser fluence and foam density is consistent with a linear absorption mechanism for the initial stages of the ablation process. Studies of the morphology and chemical composition of the ablated foams as a function of laser fluence and foam density show that the degree of melting increases at the higher foam densities. Blackbody and radical species contributions to optical emission from the ablated foam were readily resolved for correlation with laser fluence, foam density, absorption spectra, and etch depth. Temperatures in excess of 3000 K are calculated from emission spectra observed during the ablation of polystyrene foams. From this data we conclude that chemical and thermal changes in the ablated foam are influenced by the absorption spectrum as well as the density of the foam. DOE

N87-23735# Rockwell International Corp., Thousand Oaks, Calif. Science Center.
IMPROVED BETA" -ALUMINA OXIDE ELECTROLYTES THROUGH TRANSFORMATION TOUGHENING Final Report
F. F. Lange and K. T. Miller Oct. 1986 61 p
(Contract DE-AC03-76SF-00098)
(DE87-007897; LBL-22353) Avail: NTIS HC A04/MF A01

A colloidal method which ensures phase homogeneity has been developed for processing Beta double prime-Al2O3/ZrO2 composites. Pressure filtration kinetics and mechanics were examined for flocced and dispersed Al2O3 slurries over the applied pressure range of 0.04 to 80 MPa. DOE

N87-23736* National Aeronautics and Space Administration. Lewis Research Center, Cleveland, Ohio.
OXIDATION PROTECTION COATINGS FOR POLYMERS Patent
James S. Sovey, inventor (to NASA), Bruce A. Banks, inventor (to NASA), and Michael J. Mirtich, inventor (to NASA) 12 May 1987 7 p Filed 27 Feb. 1986 Supersedes N86-26434 (24 - 17, p 2709) Division of US-Patent-4,604,181, Patent-Appl-SN-761235, which is a division of US-Patent-4,560,577, US-Patent-Appl-SN-649330
(NASA-Case-LEW-14072-3; US-Patent-4,664,980; US-Patent-Appl-SN-834977; US-Patent-Class-428-421; US-Patent-Class-428-422; US-Patent-Class-428-447; US-Patent-Class-428-473.5; US-Patent-Class-428-702) Avail: US Patent and Trademark Office CSCL 11B

A polymeric substrate is coated with a metal oxide film to provide oxidation protection in low Earth orbital environments. The film contains about four volume percent polymer to provide flexibility. NASA

N87-23737*# National Aeronautics and Space Administration. Ames Research Center, Moffett Field, Calif.
CERAMIC HONEYCOMB STRUCTURES AND THE METHOD THEREOF Patent Application
Salvatore R. Riccitiello, inventor (to NASA) and Domenick E. Cagliostro, inventor (to NASA) 29 Jan. 1987 17 p
(NASA-Case-ARC-11652-1; NAS 1.71:ARC-11652-1; US-Patent-Appl-SN-008242) Avail: NTIS HC A02/MF A01 CSCL 11B

The subject invention pertains to a method of producing an improved composite-composite honeycomb structure for aircraft or aerospace use. Specifically, the subject invention relates to a method for the production of a lightweight ceramic-ceramic composite honeycomb structure, which method comprises: (1) pyrolyzing a loosely woven fabric/binder having a honeycomb shape and having a high char yield and geometric integrity after pyrolysis at between about 700 and 1,100 C; (2) substantially evenly depositing at least one layer of ceramic material on the pyrolyzed fabric/binder of step (1); (3) recovering the coated ceramic honeycomb structure; (4) removing the pyrolyzed fabric/binder of the structure of step (3) by slow pyrolysis at between 700 and 1000 C in between about a 2 to 5% by volume oxygen atmosphere for between about 0.5 and 5 hr.; and (5) substantially evenly depositing on and within the rigid hollow honeycomb structure at least one additional layer of the same or a different ceramic material by chemical vapor deposition and chemical vapor infiltration. The honeycomb shaped ceramic articles have enhanced physical properties and are useful in aircraft and aerospace uses. NASA

N87-23738# Sandia National Labs., Albuquerque, N. Mex.
FUNDAMENTALS OF SOL-GEL THIN FILM FORMATION
C. J. Brinker, A. J. Hurd, and K. J. Ward 1987 23 p Presented at the 3rd International Conference on Ultrastructure Processing of Ceramics, Glasses and Composites, San Diego, Calif., 23 Feb. 1987
(Contract DE-AC04-76DP-00789)
(DE87-007387; SAND-87-0402C; CONF-870254-3) Avail: NTIS HC A02/MF A01

It is shown that the structure of sol-gel-derived thin films depends on the precursor structure and deposition conditions. Weakly branched precursors (reduced D) applied under reaction-limited conditions result in the densest films, whereas branching or aggregation (increased D) combined with transport-limited deposition conditions result in the most porous films. A complete spectrum of microstructures is achievable by independent control of both precursor size and structure and the condensation rate or sticking probability. Application of shear during deposition is shown to restructure tenous, fractal structures and align weakly branched precursors. DOE

N87-23739# Florida Univ., Gainesville. Dept. of Chemistry.
SYNTHESIS OF MODEL POLYMERS AND RELATED STRUCTURES IN SUPPORT OF VINYL MONOMER GRAFTING STUDIES Progress Report, 1 Jul. 1986 - 30 Jun. 1987
T. E. Hogen-Esch 25 Mar. 1987 14 p
(Contract DE-FG05-84ER-45104)
(DE87-007406; DOE/ER-45104/3) Avail: NTIS HC A02/MF A01

The objectives of the present program include the synthesis, structural characterization and properties, of cellulose-based water-soluble graft copolymers capable of effectively enhancing the viscosity of their aqueous solutions. In support of this program we plan the synthesis of a number of water-soluble well defined block- or star block copolymers capable of effectively viscosifying their aqueous solutions through reversible crosslinking. In order to understand the effects on rheology of branching or cyclization in the above systems, we also plan the synthesis of water-soluble cyclic- and star polymers. DOE

N87-23740# Oak Ridge National Lab., Tenn.
CERAMIC TECHNOLOGY FOR ADVANCED HEAT ENGINES PROJECT Semiannual Progress Report, Apr. - Sep. 1986
Mar. 1987 362 p
(Contract DE-AC05-84OR-21400)
(DE87-008538; ORNL/TM-10308) Avail: NTIS HC A16/MF A01

An assessment of needs was completed, and a five-year project plan was developed with extensive input from private industry. The objective is to develop the industrial technology base required

for reliable ceramics for application in advanced automotive heat engines. The project approach includes determining the mechanisms controlling reliability, improving processes for fabricating existing ceramics, developing new materials with increased reliability, and testing these materials in simulated engine environments to confirm reliability. Although this is a generic materials project, the focus is on structural ceramics for advanced gas turbine and diesel engines, ceramic bearings and attachments, and ceramic coatings for thermal barrier and wear applications in these engines. DOE

N87-23741# Sandia National Labs., Albuquerque, N. Mex.
DIELECTRIC PROPERTIES OF STYRENE/ACRYLATE COPOLYMER COATINGS FORMED BY ELECTROPHORETIC DEPOSITION ON GOLD, ALUMINUM ALLOY, AND POROUS ANODIZED ALUMINUM ALLOY SUBSTRATES
J. K. G. Panitz, D. J. Sharp, and F. E. Martinez Apr. 1987 64 p
(Contract DE-AC04-76DP-00789)
(DE87-008885; SAND-85-2873) Avail: NTIS HC A04/MF A01

Styrene/acrylate copolymer coatings were electrophoretically deposited on four types of substrates. Processing characteristics were observed including cell voltage vs time for current densities of 0.05 to 4 mA/sq cm; polymer coating thickness vs cell voltage; and polymer coating thickness vs Coulombic consumption. Properties of the resultant polymer coatings were evaluated including breakdown voltage vs thickness; capacitance and dielectric constant; composition (from Fourier transform infrared spectroscopy); and morphology (from Scanning Electron Microscopy). Little polymeric coating deposition occurs if the current density is low. Defective coating growth occurs at high current density. The relationship between polymer thickness and cell voltage depends on the type of substrate coated and the current density used. After the initial stages of deposition, coating formation proceeds at a rate of 0.2 microns/(mA sq cm/sec). Anodization occurs during electrophoretic deposition onto the aluminum alloy and the anodized aluminum alloy substrates; more anodization occurs at lower current densities and at the beginning of electrolysis. The dielectric constants and the intrinsic breakdown strength exhibited by the coatings depend on the coating thickness and on substrate type. The release of water from the coatings during the curing cycle allows coatings exhibiting breakdown a strength as high as 1000 V/microns to form at cell voltages of 4 to 14 V per micron polymer coating thickness. DOE

N87-23742# Battelle Pacific Northwest Labs., Richland, Wash.
MANUFACTURING PROCESSES FOR HIGH-TEMPERATURE STRUCTURAL CERAMICS: A PATENT TREND ANALYSIS Topical Report, Jul. 1985 - Jul. 1986
L. O. Levine Dec. 1986 104 p
(Contract GRI-5085-800-1191)
(PB87-178059; GRI-86/0195) Avail: NTIS HC A06/MF A01 CSCL 11B

The current state of art in production techniques for high-temperature structural ceramics was characterized using analysis of patent data to clarify major technical development trusts. Natural gas is used for slightly more than 50% of the total energy needs of the high-temperature structural ceramics industry. Indications are that a high level of research and development is ongoing in this industry. Changes resulting from process or materials research and development in the ceramics industry could affect gas use or impose new requirements on gas technologies. The level of inventive effort, as indicated by patent activity increased until 1977 and was maintained at a moderate level through 1982. Since 1983, the level of effort has again increased. No major shifts in emphasis have occurred for the last 5 to 10 years among types of materials or process technologies. Also, there seems to be no major breakthroughs to address the principal barriers to much faster adoption of high-temperature structural ceramics: reproducibility, reliability, and cost. Primarily, there was an intensification of the research and development effort along the lines of previous approaches to key technical issues. GRA

N87-23743# Naval Air Development Center, Warminster, Pa. Aircraft and Crew Systems Technology Directorate.
POLY (PYRROLIUM ANION) STUDIES: ELECTROCHEMICAL SYNTHESIS AND PHYSICAL BEHAVIOR Phase Report, Oct. 1985 - Oct. 1986
Leonard J. Buckley and James J. Katilaus 1 Oct. 1986 32 p
(AD-A178097; NADC-86117-60) Avail: NTIS HC A03/MF A01 CSCL 07C

Conductive polymers exhibit many unique physical property combinations that lead to a variety of applications which include coatings, sensors, and thin film devices. Conductive polypyrrole has shown the most promise with respect to enviromental stability and mechanical integrity. Various poly (pyrrolium anion) materials have been synthesized electronically using novel dopant counterions. The counterions (substituted benzenesulfonates) were prepared as tetraethylammonium salts from the acids and ranged in size from small (8 angstroms) to large (25 angstroms) with varying degrees of symmetry. Depending on the dopant anion used in the synthesis, the electrical conductivity, tensile strength and tensile modulus varied greatly. X-ray diffraction studies have shown varying peak breadths indicating a difference in molecular order among the polymers. Interrelationships between molecular structure, electrical conductivity, and mechanical behavior have been addressed. GRA

N87-23744# Cambridge Univ. (England). Cavendish Lab.
INVESTIGATION OF THE IMPACT PERFORMANCE OF VARIOUS GLASS AND CERAMIC SYSTEMS Annual Report, Jul. 1985 - Jul. 1986
D. Townsend and J. E. Field 27 Jan. 1987 54 p
(Contract DAJA45-85-C-0021; DA Proj. 1L1-61102-BH-57)
(AD-A178115) Avail: NTIS HC A04/MF A01 CSCL 11B

A study of the strength impact and fracture behavior of a range of ceramic materials is described. One part of the research is concerned with ceramics which have applications as radomes or infra-red transmitting window materials, the other with ceramics with potential application in body armour. Ceramics included in the study include zinc sulphide, various glass ceramics and aluminas, silicon carbide, silicon nitride, titanium diboride and boron carbide. One series of experiments measured post-impact (i.e., residual) strength curves. These experiments involve impacting specimens at chosen velocities and then measuring the residual strengths after impact. Strength is plotted as a function of velocity. Such curves give: (1) the threshold velocity above which strength degradation following impact occurs; (2) the fall in strength above the threshold; (3) a ready comparison with other materials or between different batches of the same material which have had, for example, different surface preparations. From these strength curves, it is possible to estimate the size of the flaws controlling the damage. Microscopy studies of the fracture faces have been made to locate the nucleating flaws so that there is a crosscheck with the flaw sizes calculated. In cases where physical property data were not available, they were measured. Tables give data on hardness, fracture toughness, elastic moduli, stress wave and fracture velocities. GRA

N87-23745# Washington State Univ., Pullman. Shock Dynamics Lab.
COMPRESSION AND SHEAR WAVE PROPAGATION IN PLAIN AND FILLED ELASTOMERS Final Report, 1 Dec. 1982 - 31 May 1986
Y. M. Gupta 30 Sep. 1986 30 p
(Contract N00014-81-K-0840)
(AD-A178153; WSU-SDL-0106-FTR) Avail: NTIS HC A03/MF A01 CSCL 11J

Experimental results from several research tasks designed to address fundamental issues related to the shock response of energetic materials are summarized and discussed. Shock response of a recently synthesized energetic elastomer (BAMO/THF) and a composite (CdS/BAMO:THF) have been determined experimentally. Bulk and shear moduli, and viscosity of the elastometer were measured for different shock compressions. The elastomer behaves as a viscous fluid and no thermal decomposition

was detected. The composite results can be modeled using a simple mixture model. The experimental results show that the Cadmium Sulfide particles experience a nearly hydrodynamic compression and no strength effects appear to be present. The measured end states are in agreement with the Wurtzite to rock salt transition observed in hydrostatically compressed CdS. Experimental techniques have been developed to examine shock induced phase transformation in CdS single crystals. Preliminary results suggest that prior to transformation the CdS remains elastic. GRA

N87-23746# Texas Univ., Arlington. Dept. of Chemistry.
ELECTRONICS AND IONIC TRANSPORT IN POLYMERS Quarterly Technical Report, 16 Dec. 1986 - 15 Mar. 1987
Martin Pomerantz, John R. Reynolds, Krishnan Rajeshwar, Dennis S. Marynick, and Timothy D. Shaffer 15 Mar. 1987 8 p
(Contract N00014-86-K-0769)
(AD-A178227; QTR-2) Avail: NTIS HC A02/MF A01 CSCL 07D

Ion transport studies of the self-doped copolymer, poly(pyrrole-co-3-(pyrrol-1-yl)propane sulfonate have shown that lithium mobility is 50% higher than butyl nitride. Polymerizaton of 3-(pyrrol-1-yl) propane sulfonate with ferric chloride has provided a water soluble polymer. A study of anodic polymerization of pyrrole using a quartz crystal microbalance, set up to be used in solution, shows poor polymerization efficiency at the beginning but improves as the reaction proceeds. The band gap of poly(1,2-dithienylethylene) has been measured as 1.77eV. Ion exchange in self-standing films of polypyrrole has been measured with bathing medium composition, pH and counter-diffusing ion charge as variables and the data show good adherence to the Heifferich and Plesset diffusion model. PRDDO calculations on a number of thiophene systems have provided information about HOMO-LUMO gaps, conformations, spin densities in radical cations and ease of polymerizations. Copolymerization of 1,3-cyclohexadiene and 2-chloroacrylonitrile has been shown to give mainly 1,2-polymerization with smaller amounts of 1,4-polymerization. Thermotropic liquid crystalline behavior has been observed in molecules containing square planar Cu(II) metal chelates of bis(2,5-dihydroxybenzaldehyde) ethylenediimine. Two polymers have been prepared from this system, neither of which appears to show liquid crystalline behavior. GRA

N87-23747# Sandia National Labs., Albuquerque, N. Mex.
HIGH TEMPERATURE ELECTRICALLY CONDUCTIVE ADHESIVES
R. J. Martinez, C. Allen, C. Kerr, and P. Walker 23 Jun. 1987 17 p Presented at the SAMPE Electronics Materials and Processes Conference, Santa Clara, Calif., 23 Jun. 1987 Prepared in cooperation with Atomic Weapons Research Establishment, Aldermaston, England
(Contract DE-AC04-76DP-00789)
(DE87-007020; SAND-87-0295C; CONF-870674-2) Avail: NTIS HC A02/MF A01

A non-proprietary electrically conductive, high-temperature adhesive has been developed. The base resin is a commercial bismaleimide resin with silver particles added to produce electrical conductivity. This adhesive has been formulated for use in our microelectronic area as a die-attach adhesive. Following a typical chip processing cycle (350°C for one hour), the adhesive has a strength of 8.3 MPa and a volume resistivity of .00005 ohm cm. DOE

N87-23748# Sandia National Labs., Albuquerque, N. Mex.
POLYMER DYNAMICS AND GELATION
J. E. Martin 1987 27 p
(Contract DE-AC04-76DP-00789)
(DE87-007578; SAND-87-0691C) Avail: NTIS HC A03/MF A01

This talk reviews some of the recent advances in the study of the sol-gel transition and in the dynamics of the sol clusters. Emphasis is on the experimental literature, but theory is discussed where it is needed to interpret the data. The first part of this lecture focuses on the kinetics of growth of the sol beneath the gel point, and on a few purely static issues, such as the fractal structure of the sol and the observation of a spatial correlation length in undiluted gels. The second part of this lecture discusses the relaxation of concentration fluctuations from the diluted and undiluted sol. DOE

N87-23749# Pennsylvania State Univ., University Park. Materials Research Lab.
NEW LOW TEMPERATURE (HYDROXYLATED) MATERIALS Progress Report
R. Roy Dec. 1986 13 p
(Contract DE-FG02-85ER-45204)
(DE87-008530; DOE/ER-45204/T1) Avail: NTIS HC A02/MF A01

Hydroxylated and hydrated phases are more stable than most anhydrous ceramic phases at temperatures below 250°C in the presence of water. In fact, high-temperature phases such as glass react to form hydroxylated or hydrated phases at low temperatures in the presence of water. While there is a great deal of research on the synthesis of high-temperature glasses and ceramics, there is but little research on the low-temperature hydroxylated and hydrated materials. Thus, the main objective of this research is to synthesize and characterize new low-temperature hydroxylated or hydrated materials preferably by topotaxy and epitaxy which could serve as useful hosts for immobilization of ions at the typical repository temperatures that are contemplated at present for hazardous (including nuclear) wastes. DOE

N87-23750*# National Aeronautics and Space Administration. Lewis Research Center, Cleveland, Ohio.
SOL-GEL SYNTHESIS OF MgO-SiO2 GLASS COMPOSITIONS HAVING STABLE LIQUID-LIQUID IMMISCIBILITY
Narottam P. Bansal Apr. 1987 23 p Presented at the 89th Annual Meeting and Exposition of the American Ceramic Society, Pittsburgh, Pa., 26-30 Apr. 1987
(NASA-TM-89905; E-3599; NAS 1.15:89905) Avail: NTIS HC A02/MF A01 CSCL 11B

MgO-SiO2 glasses containing up to 15 mol % MgO, which could not have been prepared by the conventional glass melting method due to the presence of stable liquid-liquid immiscibility, were synthesized by the sol-gel technique. Clear and transparent gels were obtained from the hydrolysis and polycondensation of silicon tetraethoxide (TEOS) and magnesium nitrate hexahydrate when the water/TEOS mole ratio was four or more. The gelling time decreased with increase in magnesium content, water/TEOS ratio, and reaction temperature. Magnesium nitrate hexahydrate crystallized out of the gels containing 15 and 20 mol % MgO on slow drying. This problem was partially alleviated by drying the gels quickly at higher temperatures. Monolithic gel samples were prepared using glycerol as the drying control additive. The gels were subjected to various thermal treatments and characterized by several methods. No organic groups could be detected in the glasses after heat treatments to approx. 800 C, but trace amounts of hydroxyl groups were still present. No crystalline phase was found from X-ray diffraction in the gel samples to approx. 890 C. At higher temperatures, alpha quartz precipitated out as the crystalline phase in gels containing up to 10 mol % MgO. The overall activation energy for gel formation in 10MgO-90SiO2 (mol %) system for water/TEOS mole ratio of 7.5 was calculated to be 58.7 kJ/mol. M.G.

N87-23751* National Aeronautics and Space Administration. Ames Research Center, Moffett Field, Calif.
FIRE AND HEAT RESISTANT LAMINATING RESINS BASED ON MALEMEIDO AND CITRACONIMIDO SUBSTITUTED 1 ((DIORGANO OXYPHOSPHONYL) METHYL) -2,4- AND -2,6-DIAMINOBENZENES Patent
John A. Mikroyannidis (National Academy of Sciences - National Research Council, Washington, D. C.) and Demetrius A. Kourtides, 02inventors (to NASA) 2 Jun. 1987 11 p Filed 16 Aug. 1984 Supersedes N85-21364 (23 - 12, p 1812) Continuation-in-part of US-Patent-Appl-SN-522629, filed 12 Aug.

1983, abandoned
(NASA-Case-ARC-11533-1; US-Patent-4,670,565; US-Patent-Appl-SN-641147; US-Patent-Class-548-413) Avail: US Patent and Trademark Office CSCL 11B

A novel class of fire and heat resistant bisimide resins prepared by thermal polymerization of maleimido or citraconimido substituted 1-(dialkox phosphonyl) methyl-2-4 and -2,6-diamino benzenes was presented. The polymer precursors are prepared by reacting 1-(diorgano oxyphosphonyl) methyl-2-4- and -2,6-diamino benzenes with maliec anhydride or citraconic anhydride in a mole ratio 1:2. Chain extension of the monomers is achieved by reacting the mono-N-maleimido derivaties of 1 oxyphosphonyl) methyl• -2,4- and -2,6-diamino benzenes with aryl tetracarboxylic dianhydrides, such as benzophenone tetracarboxylic dianhydride, or aryl diisocyanates, such as methylene bis(4-phenyl isocyanate), in a mole ratio 2:1. The polymerization of the monomers is studied by diferential scanning calorimetry and the thermal stability of the polymers is ascertained by thermogravimetric analysis. NASA

N87-23752*# National Aeronautics and Space Administration. Langley Research Center, Hampton, Va.
ADHESIVE EVALUATION OF WATER-SOLUBLE LARC-TPI
Donald J. Progar and Roscoe A. Pike Jun. 1987 29 p
(NASA-TM-89152; NAS 1.15:89152) Avail: NTIS HC A03/MF A01 CSCL 11A

The water-soluble polyimide, identified as TPI(MTC)/H2O, was evaluated as a high temperature thermoplastic adhesive for bonding Ti-6Al-4V and comparing those results primarily with results reported in earlier work with the polyamic-acid/diglyme material. The lap shear strength test was the primary test performed to evaluate the adhesive before (controls) and after thermal exposure in air at 204 C for up to 5000 hours and after a 72 hour water-boil exposure. Lap shear strengths were determined at RT, 177, 204, and 232 C. The adhesive was also characterized after fracture by determining the glass transition temperature as well as defining the mode of failure by visual observation. In general, the results indicate that the TPI(MTC)/H2O retains high lap shear strengths after thermal exposure but had reduced strengths after the water-boil exposure. All failures were cohesive. The TPI(MTC)/H2O compared very well with previous data reported for the standard polyamic-acid/diglyme LARC-TPI results, and therefore, shows promise as a water-soluble adhesive for use in various applications. Author

28 PROPELLANTS AND FUELS

Includes rocket propellants, igniters, and oxidizers; their storage and handling procedures; and aircraft fuels.

For related information see also *07 Aircraft Propulsion and Power, 20 Spacecraft Propulsion and Power,* and *44 Energy Production and Conversion.*

N87-23753# Midwest Research Inst., Golden, Colo. Solar Energy Research Inst.
FUELS FROM MICROALGAE: TECHNOLOGY STATUS, POTENTIAL AND RESEARCH REQUIREMENTS
B. Neenan, D. Feinberg, A. Hill, R. McIntosh, and K. Terry Aug. 1986 171 p
(Contract DE-AC02-83CH-10093)
(DE86-010739; SERI/SP-231-2550) Avail: NTIS HC A08/MF A01

Although numerous options for the production of fuels from microalgae have been proposed, our analysis indicates that only two qualify for extensive development - gasoline and ester fuel. In developing the comparisons that support this conclusion, we have identified the major areas of microalgae production and processing that require extensive development. Technology success requires developing and testing processes that fully utilize the polar and nonpolar lipids produced by microalgae. Process designs used in these analyses were derived from fragmented, preliminary laboratory data. These results must be substantiated and integrated processes proposed, tested, and refined to be able to evaluate the commercial feasibility from microalgae. The production of algal feedstocks for processing to gasoline or ester fuel requires algae of high productivity and high lipid content that efficiently utilize saline waters. Species screening and development suggest that algae can achieve required standards taken individually, but algae that can meet the integrated requirements still elude researchers. Effective development of fuels from microalgae technology requires that R and D be directed toward meeting the integrated standards set out in the analysis. DOE

N87-23754# Mound Lab., Miamisburg, Ohio.
LOW ENERGY IGNITION OF HMX USING A FOIL BRIDGE
D. W. Ewick 1986 11 p Presented at the 13th Symposium on Explosives and Pyrotechnics, Hilton Head Island, S.C., 2 Dec. 1986
(Contract DE-AC04-76DP-00053)
(DE87-004211; MLM-3413(OP); CONF-861230-6) Avail: NTIS HC A02/MF A01

The use of an etched foil bridge to initiate the deflagration of high-density HMX is described. Two foil bridges were evaluated, each having a cross-sectional area approximately equal to that of a 0.0034-in. diameter bridgewire. One foil was 0.11 in. wide and 0.0008 in. thick; the other was 0.022 in. wide and 0.0004 in. thick. The all-fire current for the 0.022-in. wide foil bridge was roughly 15% greater than that of the 0.011-in. wide foil, which in turn was approximately 7% greater than the round wire bridge. The no-fire current for the 0.022-in. wide foil bridge was roughly 26% greater than that of the 0.011-in. wide foil, which in turn was approximately 10% greater than the round wire bridge. DOE

N87-23755# IIT Research Inst., Bartlesville, Okla. National Inst. for Petroleum and Energy Research.
TRENDS OF PETROLEUM FUELS: TOPICAL REPORT
C. L. Dickson, P. W. Woodward, and P. L. Bjugstad May 1987 36 p
(Contract DE-FC22-83FE-60149)
(DE87-001237; NIPER-224) Avail: NTIS HC A03/MF A01

Trends in properties of motor gasolines for 1942 through 1986; diesel fuels for 1950 through 1986; aviation fuels for 1947 through 1986; and heating oils for 1955 through 1986, have been evaluated based on data contained in surveys prepared and published by the National Institute for Petroleum and Energy Research (NIPER) and its predecessor organizations. The surveys for motor gasolines were conducted under a cooperative agreement with the Coordinating Research Council (CRC) and the Bureau of Mines from 1935 through 1948 and in cooperation with the American Petroleum Institute (API) since 1948 for all surveys. Other surveys prepared in cooperation with the API and the Bureau of Mines, the Energy Research and Development Administration, the Department of Energy, and currently the National Institute for Petroleum and Energy Research were aviation gasolines beginning in 1947, diesel fuels in 1950, aviation turbine fuels in 1951, and heating oils, formerly burner fuel oils, in 1955. Various companies throughout the country obtain samples of motor gasolines from retail outlets and refinery samples for the other surveys, and analyze the samples using American Society for Testing and Materials (ASTM) procedures. DOE

N87-23756# Maryland Univ., College Park. Inst. for Physical Science and Technology.
VISCOSITY OF SYNFUEL COMPOUNDS AND MIXTURES Quarterly Progress Report, 1 Jan. - 31 Mar. 1987
J. Kestin 1987 5 p
(Contract DE-FG22-85PC-80505)
(DE87-008696; DOE/PC-80505/T6; QPR-6) Avail: NTIS HC A02/MF A01

During this report period, the kinematic viscosity of transdecalin and tetralin and their mixtures were measured. Papers on the viscosity of liquid toluene and on the experimental feasibility of measuring both the viscosity and density of liquids with our oscillating-disk viscometer were completed. DOE

N87-23757 Johns Hopkins Univ., Laurel, Md. Chemical Propulsion Information Agency.
THE 23RD JANNAF COMBUSTION MEETING, VOLUME 1
Dorothy L. Becker, ed. Oct. 1986 772 p Meeting held in Hampton, Va., 20-24 Oct. 1986
(Contract N00024-85-C-5301)
(AD-A179158; CPIA-Publ-457) Avail: CPIA, Laurel, Md. 20707 HC $70.00

This volume, the first of four, is a collection of 60 papers which were presented at this conference. Specific subjects discussed include: advanced diagnostic equipment; combustion instability in rocket motors and ramjets; thermal degradation and ignition of nitramine propellants; combustion of rocket motors, rocket engines, and ramjet propellants; and chemistry and kinetics of solid propellants. Subject, author and source indexes for all four volumes are included, as is the list of meeting attendees. For individual titles, see N87-23758 through N87-23813.

N87-23758# Morton Thiokol, Brigham City, Utah.
ACOUSTIC WAVEFORMS IN STATICALLY TESTED SPACE SHUTTLE SOLID ROCKET MOTORS (SRM) **c20**
B. Hussey *In* Johns Hopkins Univ., The 23rd JANNAF Combustion Meeting, Volume 1 Oct. 1986 p 1-7 (For primary document see N87-23757 17-28)
Avail: CPIA, Laurel, Md. 20707 HC $70.00

Dynamic pressure transducers and dynamic strain gages were used to measure the axial dependence of oscillating chamber pressure within several statically tested Space Shuttle solid rocket motors. Plots of the low level, axially dependent pressure oscillation amplitudes (acoustic waveforms) were created and compared for two motors at selected times during burn. The first and second longitudinal modes (15 Hz and 30 Hz, respectively) were the main modes investigated. The results of the analysis are presented, and the implications on classic acoustic wave theory are discussed. Author

N87-23759# Johns Hopkins Univ., Laurel, Md. Lab. for Computational Physics.
NUMERICAL STUDY OF ACOUSTIC REFRACTION AND FLOW TURNING **c20**
Joseph D. Baum and Jay N. Levine (Air Force Rocket Propulsion Lab., Edwards AFB, Calif.) *In* Johns Hopkins Univ., The 23rd JANNAF Combustion Meeting, Volume 1 Oct. 1986 p 9-31 Prepared in cooperation with Air Force Rocket Propulsion Lab., Edwards AFB, Calif. Sponsored in part by Air Force (For primary document see N87-23757 17-28)
Avail: CPIA, Laurel, Md. 20707 HC $70.00

An attempt is made to understand the physical mechanisms by which energy is exchanged between the mean and acoustic flow fields in resonant combustion chambers. These processes may alter the balance between sources and sinks of oscillatory energy in the combustor significantly and thus are critical to the ability to predict the stability characteristics of proposed motor designs. The description and analysis of the computational results obtained to date of acoustic refraction and flow turning phenomena is given. Three studies were conducted. The time dependent compressible Navier-Stokes equations were solved utilizing an implicit, non-iterative Linearized Block Implicit scheme. To help discriminate between acoustic energy loss due to artificial numerical dissipation and energy loss due to physical processes, a second study was conducted in which acoustic wave propagation in a tube with no mean flow was investigated. The third study investigated acoustic wave propagation in a tube with a coexisting mean flow, where the mean flow is injected into the tube through its lateral boundary. Author

N87-23760# Georgia Inst. of Tech., Atlanta. School of Aerospace Engineering.
BEHAVIOR OF SIMULATED SOLID PROPELLANT FLAMES IN AXIAL ACOUSTIC FIELDS
S. V. Sankar, J. I. Jagoda, B. R. Daniel, and B. T. Zinn *In* Johns Hopkins Univ., The 23rd JANNAF Combustion Meeting, Volume 1 Oct. 1986 p 33-44 (For primary document see N87-23757 17-28)
(Grant AF-AFOSR-0082-84)
Avail: CPIA, Laurel, Md. 20707 HC $70.00

An experimental setup developed to simulate solid propellant flames experiencing axial instability was used to investigate the oscillatory heat release rate behavior of the simulated flames. Oscillatory radiation from C-H and C-C species present in the flame was measured. The magnitude of this radiation oscillation is an indicator of the magnitude of the heat release rate and are reported. These phase differences are such that Rayleigh's criterion for driving acoustic waves is always satisfied in regions away from pressure minima provided the flame is stabilized at some distance away from the burner surface. Theoretical studies of the oscillatory heat release rates were also conducted using simulated flame data. The flame model predictions are in good qualitative agreement with the measured data. The results obtained strongly suggest that oscillatory heat transfer to the propellant surface could play an important role in the driving of axial instabilities. Author

N87-23761# Pennsylvania State Univ., State College.
STOCHASTIC EXCITATION OF ACOUSTIC WAVES IN A COMBUSTION CHAMBER **c20**
Vigor Yang and Fred E. C. Culick *In* Johns Hopkins Univ., The 23rd JANNAF Combustion Meeting, Volume 1 Oct. 1986 p 45-50 Prepared in cooperation with California Inst. of Tech., Pasadena (For primary document see N87-23757 17-28)
Avail: CPIA, Laurel, Md. 20707 HC $70.00

An analytical analysis dealing with stochastic excitation of acoustic waves in a combustion chamber was developed. The model treats nonlinear self-oscillation with linear random motion. As a specific example, the response of longitudinal pressure oscillations to stationary white noise was studied. It was shown that the time evolution of acoustic mode consists of a periodic function and a narrow band noise term centered at the frequency of self-oscillation. The influences of random excitation on periodic motion appear in the d.c. shift of oscillation. Acoustic energy associated with random oscillations may be transferred among modes through periodic motions. Author

N87-23762# Pennsylvania State Univ., University Park.
WORKSHOP REPORT: METHODS FOR MEASURING SOLID PROPELLANT COMBUSTION RESPONSE
Michael M. Micci *In* Johns Hopkins Univ., The 23rd JANNAF Combustion Meeting, Volume 1 Oct. 1986 p 51-57 (For primary document see N87-23757 17-28)
Avail: CPIA, Laurel, Md. 20707 HC $70.00

The objective of the workshop was to critically review and assess the validity of available methods for experimentally determining solid propellant combustion responses. Accurate response data is a necessity for the predictive programs and models that would afford a fast and inexpensive means for comparison/evaluation of condidate propellant formulations during motor development programs. Three issues were identified to be specifically addressed by the workshop: (1) Arrive at a consensus from the propulsion community as to what is the optimum method for determining solid propellant combustion response with respect to the imposed constraints of cost, time accuracy, response frequency, pressure vs. velocity coupling, etc.; (2) Determine the status of the available combustion response data base that focuses on data collected for identical propellant formulations within different experimental devices; and (3) Determine what future work needs to be performed, where should efforts and money be best spent, and what methods are the most promising. E.R.

N87-23763# Naval Weapons Center, China Lake, Calif.
TTCP NON-LINEAR INSTABILITY PROGRAM: US MOTOR TEST DATA **c20**
H. B. Mathes *In* Johns Hopkins Univ., The 23rd JANNAF Combustion Meeting, Volume 1 Oct. 1986 p 59-64 (For primary document see N87-23757 17-28)
Avail: CPIA, Laurel, Md. 20707 HC $70.00

Combustion instability specialists in Australia, Canada, the United Kingdom, and the United States, under the Technical

Cooperation Program (TTCP), are engaged in an effort to better understand nonlinear combustion instability. One aspect of the program involves firing a number of specially instrumented rocket motors which will be pulsed several times during firing. Results are presented from the first TTCP motor firing at the Naval Weapons Center. Topics discussed include motor geometry, pulsing and effect on motor stability, instability waveforms, and details of instrumentation. Author

N87-23764# Sandia Labs., Livermore, Calif. Combustion Research Facility.
ASYMPTOTIC MODELS FOR SOLID PROPELLANT COMBUSTION AND THE ONSET OF INTRINSIC INSTABILITY
Stephen B. Margolis and Robert C. Armstrong *In* Johns Hopkins Univ., The 23rd JANNAF Combustion Meeting, Volume 1 Oct. 1986 p 65-79 (For primary document see N87-23757 17-28)
Avail: CPIA, Laurel, Md. 20707 HC $70.00

Two different asymptotic models were derived which describe the nonsteady, nonplanar burning of certain types of homogeneous solid propellants. Motivated in part by recent work on ammonium perchlorate deflagration, it is assumed, in the first model, that a fraction of the propellant is pyrolyzed directly to product gases at a solid/gas interface, while the remainder sublimes and burns in the gas phase. In the second model, there is a thin liquid layer between the solid and gas, with combustion occurring in both the liquid and gas phases. The analysis exploits the largeness of activation energies to derive flame sheet models analogous to those derived for strictly gaseous and strictly condensed deflagrations. For the special case of steady, planar burning, expressions were obtained for the regression rate eigenvalue as a function of the various parameters in the problem. However, a linear stability analysis of this basic solution shows that, for sufficiently large values of a certain grouping of parameters, it is unstable to small perturbations which correspond to pulsating, cellular modes of burning. Author

N87-23765# Cohen (Norman S.) Professional Services, Inc., Redlands, Calif.
ROLE OF COMBUSTION IN THE NONLINEAR COMBUSTION INSTABILITY OF COMPOSITE SOLID PROPELLANTS
Norman S. Cohen and Gary L. Vogt *In* Johns Hopkins Univ., The 23rd JANNAF Combustion Meeting, Volume 1 Oct. 1986 p 81-88 Prepared in cooperation with Air Force Rocket Propulsion Lab., Edwards AFB, Calif. (For primary document see N87-23757 17-28)
(Contract F04611-84-C-0024)
Avail: CPIA, Laurel, Md. 20707 HC $70.00

It is argued that the multipeaked response function curves of Ammonium Perchlorate/composite propellants are responsible for triggering and driving nonlinear instability in the axial modes. The background for this assertion is briefly reviewed. The importance of the multipeaked response lies in the ability to drive harmonics, which is believed crucial to the instability. The simplified combustion model in the Levine and Baum nonlinear instability computer program was modified in an artificial way to provide for a double peaked response. Computed combustion waves resulting from input nonlinear pressure waves are shown. New insight on the role of combustion may be available from this approach. Author

N87-23766# Sandia Labs., Livermore, Calif. Combustion Research Facility.
MODIFICATION OF SOLID PROPELLANT DEFLAGRATION RATES DUE TO RANDOM NONHOMOGENEITIES
Robert C. Armstrong and Stephen B. Margolis *In* Johns Hopkins Univ., The 23rd JANNAF Combustion Meeting, Volume 1 Oct. 1986 p 89-100 Sponsored in part by DOE and Army (For primary document see N87-23757 17-28)
Avail: CPIA, Laurel, Md. 20707 HC $70.00

A nonlinear response theory is employed to obtain the modification of the mean burning rate of a nonhomogeneous solid propellant. Although the methods use are quite general, attention is focused on the interaction between the three dimensional structure of the deflagration and the constitutive model. Based on a calculation of the mean burning rate as a function of the correlation length of a random nonhomogeneity, it is shown that the mean burning rate is greater than that of homogeneous burning for small correlation lengths, and is less for larger correlation lengths. Thus, it is indicated that a solid composed of particles of two different propellants would burn more slowly than their mean rate if the size of the particles were large, and more quickly if their size were small. As many of the methods used are new to this application, some comments is also made on the utility of this approach in computing mean burning rate statistics for random media. Author

N87-23767# Morton Thiokol, Brigham City, Utah.
NEW IGNITION PARAMETER CORRELATIONS FOR PREDICTING SOLID ROCKET MOTOR IGNITION TRANSIENTS **c20**
James D. Rozanski *In* Johns Hopkins Univ., The 23rd JANNAF Combustion Meeting, Volume 1 Oct. 1986 p 101-108 (For primary document see N87-23757 17-28)
Avail: CPIA, Laurel, Md. 20707 HC $70.00

The three primary models required for the prediction of solid rocket motor ignition transients are grain preheating, grain ignition, and flame propagation. The difficult task for the ignition analyst, when asked to predict the ignition of a new or unique motor configuration, is the assignment of values to the empirical free constants in these models without the benefit of a database of measured transients for similar motors on which to base these values. An approach is described for dealing with this problem which eliminates some of these free constants and establishes a technique for correlating those that remain. The first part entails reconstructing the ignition characteristics of a diverse group of solid rocket motors using a volume filling computer code. The next phase described is the normalization and correlation of the heat transfer models and their free constants, which were established during the reconstruction. A relationship is presented between the calculated heating level required for first grain ignition, and the measured heat flux from steady state propellant ignitability tests. Finally, a methodology is suggested which incorporates these correlations in a grain heating model for an ignition transient prediction. Author

N87-23768# Morton Thiokol, Brigham City, Utah.
STUDY OF THE SUPPRESSION OF ROCKET PLUME AFTERBURNING BY CHEMICAL ADDITIVES **c20**
L. G. McMillion and E. Miller *In* Johns Hopkins Univ., The 23rd JANNAF Combustion Meeting, Volume 1 Oct. 1986 p 109-117 Prepared in cooperation with Nevada Univ.,Reno. (For primary document see N87-23757 17-28)
Avail: CPIA, Laurel, Md. 20707 HC $70.00

An attempt is made to identify alternative additives for prevention of inhibition of the signatures produced by afterburning. Methyl bromide, phosphorus pentoxide, and anhydrous ammonia were evaluated for their effects on the afterburning reactions by introducing them into flat diffusion flames of H2-CO-N2/O2-N2 and CH4-N2/O2-N2 and scanning the flame zone incrementally to examine the infrared spectral emission. An opposed jet diffusion burner adapted from one described by Hahn, Wendt, and Tyson was used. The burner configuration permitted study of the inhibition of afterburning under conditions simulating those in the plume. A Beckman infrared spectrometer was modified with an external optical system and staged slit permitting examinations of the spectra from the narrow segments of the flat opposed jet diffusion flame. Author

N87-23769# Naval Postgraduate School, Monterey, Calif.
MEASUREMENTS OF PARTICULATES IN SOLID PROPELLANT ROCKET MOTORS **c20**
T. Edwards, K. G. Horton, D. Redman, J. S. Rosa, J. B. Rubin, S. C. Yoon, J. P. Powers, and D. W. Netzer *In* Johns Hopkins Univ., The 23rd JANNAF Combustion Meeting, Volume 1 Oct. 1986 p 119-132 (For primary document see N87-23757 17-28)
(Contract F04611-86-X-0008)
Avail: CPIA, Laurel, Md. 20707 HC $70.00

An investigatin was conducted to develop techniques for obtaining quantitative data that can be used to relate solid rocket propellant composition and operating environment to the behavior of solid particulates within the grain port and exhaust nozzle. The techniques employed are high speed motion pictures of propellant strand burners and slab burners in a cross flow environment, SEM analysis of post fire residue, determination of D sub 32 across the exhaust nozzle using measurements of scattered laser light, and holograms of burning propellant strands, slabs, and motors. In addition, techniques are being developed for automatic retrieval of particle size distributions from holograms taken of the combustion of solid propellants. Results are presented on (1) the measurement of particle size changes across an exhaust nozzle, (2) holograms obtained at the grain exit plane and (3) progress on the automatic retrieval of particle data from the holograms. Author

N87-23770# Naval Weapons Center, China Lake, Calif.
MEASUREMENT OF SOLID-PROPELLANT BURN RATE USING MILLIMETER-WAVE TECHNIQUES
J. W. Battles, C. J. Bicker, H. B. Mathes, and F. S. Blomshield *In* Johns Hopkins Univ., The 23rd JANNAF Combustion Meeting, Volume 1 Oct. 1986 p 6 (For primary document see N87-23757 17-28)
Avail: CPIA, Laurel, Md. 20707 HC $70.00

Equations are developed that describe the reflected microwave/millimeter wave Doppler signal from a burning solid propellant test sample. The resulting equations are used in a simulation to determine the instrumentation requirements for a solid propellant burn rate measuring system using Doppler techniques. Author

N87-23771# United Technologies Research Center, East Hartford, Conn.
NEW CONCEPTS FOR CARS DIAGNOSTICS OF SOLID PROPELLANT COMBUSTION
J. H. Stufflebeam and A. C. Eckbreth *In* Johns Hopkins Univ., The 23rd JANNAF Combustion Meeting, Volume 1 Oct. 1986 p 139-148 (For primary document see N87-23757 17-28)
Avail: CPIA, Laurel, Md. 20707 HC $70.00

There is a current need in solid propellant combustion for more information of a microscopic nature, i.e., high spatial and temporal resolution measurements of species concentration and temperature above the combusting propellant. Of the various optical techniques, Coherent Anti-Stokes Ramen Spectroscopy (CARS) is best suited to solid propellant combustion. CARS is fast, spatially precise, remote and nonperturbing. The very difficult experimental problems posed by solid propellant combustion environments challenge even the most modern diagnostic techniques. In response to these challenges, new concepts are proposed for the application of CARS to measure temperature and species concentrations in solid propellant combustion. The experiments utilize a new advance, dual broadband CARS, that excites multiple species simultaneously, so that their signatures can be recorded with each laser shot. Techniques to acquire all signatures with each laser pulse are discussed and include laser selection, phase matching considerations, detectors and alternate spectrograph configurations. Author

N87-23772# Purdue Univ., West Lafayette, Ind. School of Aeronautics and Astronautics.
TWO TECHNIQUES FOR MEASURING AP IGNITION DELAY
R. A. Frederick, Jr. and J. R. Osborn *In* Johns Hopkins Univ., The 23rd JANNAF Combustion Meeting, Volume 1 Oct. 1986 p 149-156 (For primary document see N87-23757 17-28)
(Contract F04611-84-0019)
Avail: CPIA, Laurel, Md. 20707 HC $70.00

The ignition delay of coarse Ammonium Perchlorate particles is influenced by minor formulation changes in wide distribution propellants. The long range objective of this research is to develop techniques for actually measuring, in situ, the ignition delay of individual, 400 micron oxidizer particles. In this effort, the effect of increasing combustion pressures on the performance of two optical distance measurement techniques was evaluated by burning propellant strands at pressure levels from 0 to 3.4 MPa (0 to 500 psig). Both techniques detect the propellant surface height by sensing the position of a laser spot which is reflected off of the propellant surface. The techniques tested had a linear distance resolution of 200 micron and a range of 25 mm. Author

N87-23773# Morton Thiokol, Brigham City, Utah.
CHEMICAL KINETICS COMBUSTION MODEL OF THE NG/BINDER SYSTEM
R. L. Hatch *In* Johns Hopkins Univ., The 23rd JANNAF Combustion Meeting, Volume 1 Oct. 1986 p 157-165 (For primary document see N87-23757 17-28)
Avail: CPIA, Laurel, Md. 20707 HC $70.00

A steady state one dimensional combustion model was developed which treats the detailed kinetics of the chemically reacting flow from a burning monopropellant. Numerical techniques are used to solve the differential equations which describe the conservation of species and energy. The use of experimental elementary reaction rate data from the kinetics literature and experimental thermochemical data for each gaseous species eliminates the free or adjustable parameters present in most models. The model was applied to the nitroglycerine/binder system. The calculated temperature profile away from the propellant surface exhibits the three distinct zones seen experimentally in the combustion of double base propellants, the fizz zone near the propellant surface, the dark or induction zone of near constant temperature, and the final flame zone. The calculation of burn rate is found to be very sensitive to which published reaction set is chosen, but the calculated values bracket the experimental results. Selected chemical species were added to the propellant to investigate the feasibility of burn rate acceleration through gas phase reactions. The hydrogen free radical was found to be very effective in gas phase acceleration reactions and, consequently, the burn rate of the propellant. Author

N87-23774# Wayne State Univ., Detroit, Mich.
THE INHIBITION EFFECTS OF H2/O2/N2 FLAMES SEEDED BY POTASSIUM
Trilochan Singh and David P. Weaver *In* Johns Hopkins Univ., The 23rd JANNAF Combustion Meeting, Volume 1 Oct. 1986 p 167-180 Prepared in cooperation with Air Force Rocket Propulsion Lab., Edwards AFB, Calif. Sponsored in part by Air Force (For primary document see N87-23757 17-28)
Avail: CPIA, Laurel, Md. 20707 HC $70.00

The phenomenon in rocket and missile plumes that results from the reignition of the fuel rich exhaust products mixing with the ambient atmosphere is described. This secondary flame zone, called afterburning, occurs some distance downstream in the exhaust plume, and generates temperatures typically higher than that of the nozzle exhaust plane. Over the past two decades a variety of substances have been added to rocket and gun propellants in an effort to eliminate or reduce afterburning, and a variety of compounds have been found to be effective to a greater or lesser extent. However, the specific physical and/or chemical mechanisms of afterburning suppression are not as yet completely understood. The results of analytical investigations into the afterburning suppression issue are summarized. The analyses were performed using potassium as suppressant material. In particular, an investigation into the inhibition effects of KOH on H2-O2-N2 flames are described. E.R.

N87-23775# Air Force Rocket Propulsion Lab., Edwards AFB, Calif.
CN RADICAL DISTRIBUTIONS IN SOLID PROPELLANT FLAMES
T. Edwards, D. P. Weaver, D. H. Campbell, and F. Frederick, II *In* Johns Hopkins Univ., The 23rd JANNAF Combustion Meeting, Volume 1 Oct. 1986 p 181-195 Prepared in cooperation with Dayton Univ., Ohio. Sponsored in part by Air Force (For primary document see N87-23757 17-28)
Avail: CPIA, Laurel, Md. 20707 HC $70.00

The application of laser induced fluorescence of the CN radical to the study of high pressure solid propellant flame chemistry is described. Propellants based on AP, HMX, and AN were examined. The propellant flame structure, as shown by the distribution of CN, was examined for the propellants at pressures between atmospheric and 3.5 MPa. The relationship between the CN distribution and the reaction mechanisms in the various flames is discussed. The influence of changes in stoichiometry in HMX propellants on the propellant flame structure was shown to be important. Author

N87-23776# Naval Weapons Center, China Lake, Calif.
AP/HMX COMPOSITE PROPELLANT MODELING
F. S. Blomshield *In* Johns Hopkins Univ., The 23rd JANNAF Combustion Meeting, Volume 1 Oct. 1986 p 197-202 (For primary document see N87-23757 17-28)
Avail: CPIA, Laurel, Md. 20707 HC $70.00

Considerable past effort has been spent theoretically modeling solid propellants that consist of binder and AP but without HMX or other nitramine based high energy ingredients. The statistically based multiple flame Petite Ensemble Model (PEM) is such a model. Work has also been done modeling HMX combustion. Progress is presented on a steady state theoretical propellant combustion model which attempts to model AP/HMX/HTPB composite propellants. The approach uses a PEM method which allows different distributions of both AP and HMX particles to be present in the propellant. Hence, the name of the combustion model is HYPEM (High Energy Petite Ensemble Model). The AP portion of the model uses a modified Beckstead, Derr, Price (BDP) model while the HMX portion of the model uses a time averaged approach. This time averaged approach is able to deal with the intermittent aspect of HMX crystals burning in a binder medium. The BDP space averaged approach is unable to handle this nonsteady burning of the HMX crystals since the monopropellant burning rates of HMX and the binder are significantly different. Author

N87-23777# Sandia Labs., Livermore, Calif.
INFLUENCE OF TWO-PHASE FLOW IN THE DEFLAGRATION OF HOMOGENEOUS SOLIDS **c20**
Stephen B. Margolis, Forman A. Williams, and Robert C. Armstrong *In* Johns Hopkins Univ., The 23rd JANNAF Combustion Meeting, Volume 1 Oct. 1986 p 203-211 Prepared in cooperation with Princeton Univ., N.J. Sponsored in part by DOE and Army (For primary document see N87-23757 17-28)
Avail: CPIA, Laurel, Md. 20707 HC $70.00

Theoretical analyses are developed for the deflagration of solids such as nitramines that experience exothermic reactions in liquid layers at their surfaces. Relative motion of gas and liquid in a two phase region at the surface is considered, with influences of pressure gradients and of surface tension gradients taken into account for the drops and bubbles. It is shown that these influences tend to produce gas velocities in excess of liquid velocities. Burning rate expressions are derived by activation energy asymptotics, with special attention paid to the role of interphase heat transfer. Author

N87-23778# Sandia Labs., Livermore, Calif. Combustion Research Facility.
A THEORETICAL AND NUMERICAL STUDY OF RADIATIVE IGNITION AND DERADIATIVE EXTINCTION IN SOLID PROPELLANTS
M. L. Koszykowski and Robert C. Armstrong *In* Johns Hopkins Univ., The 23rd JANNAF Combustion Meeting, Volume 1 Oct. 1986 p 10 Sponsored in part by DOE and Army (For primary document see N87-23757 17-28)
Avail: CPIA, Laurel, Md. 20707 HC $70.00

Time dependent processes of solid propellant deflagration are modeled and a numerical simulation of ignition and extinction is undertaken. Since the analytic theory of ignition is well developed, it is relied upon to verify the ability of the numerical algorithm to track stiff, time dependent features of an ignition event. The verification of the numerical method provides a degree of confidence for the subsequent study of deradiation. An activation energy asymptotic theory for deradiation is developed, which predicts that an influx of radiation on the order of the steady heat release of the exothermic reaction will, at near term, extinguish the propellant. Beyond this, conduction processes inherited from the thermal profile at the instant of deradiation may, or may not, cause resumption of pyrolysis, and presumably, the deflagration as a whole. The analytic theory ignores the subsequent impact of a possible gas phase flame that is detached many conductive diffusive lengths away from the gas-solid surface. The assumption is based on the observation that for most physical systems the gas density and hence its thermal capacitance is many times smaller than that of the solid and thus lacks the potential to alter the surface temperature after deradiation. The simulation is used to verify more complicated and more physical situations than those accessible via the theory, including deradiation with a detached flame and in the presence of an instability. Author

N87-23779# Army Armament Research and Development Command, Dover, N. J.
FORCE-FIELD PARAMETERS AND MOLECULAR MECHANICS CALCULATIONS FOR NITRAMINES
T. Vladimiroff *In* Johns Hopkins Univ., The 23rd JANNAF Combustion Meeting, Volume 1 Oct. 1986 p 223-229 (For primary document see N87-23757 17-28)
Avail: CPIA, Laurel, Md. 20707 HC $70.00

Over the past fifteen years, molecular mechanics has developed into a powerful tool for the calculation of structure, energies, dipole moments, as well as other properties of molecules. Originally the method was developed for hydrocarbons and it has subsequently been extended to many other functionalized kinds of molecules. The molecular force field was extended to cover nitramine type chemical compounds. Dipole moments and geometries of simple nitramines were fit and the method was then applied to more complicated molecules like RDX and HMX. A heat of formation scheme was developed based on available data for nitramine compounds. In general, the results are fair with respect to structures, dipole moments, and heat of formation when compared to available experimental data. Author

N87-23780# Sandia Labs., Livermore, Calif. Combustion Research Facility.
SIMULTANEOUS THERMOGRAVIMETRIC MODULATED BEAM MASS SPECTROMETRY AND TIME-OF-FLIGHT VELOCITY SPECTRA MEASUREMENTS OF THERMAL DECOMPOSITION PRODUCTS FROM RDX AND HMX
Richard Behrens, Jr. *In* Johns Hopkins Univ., The 23rd JANNAF Combustion Meeting, Volume 1 Oct. 1986 p 231-240 Sponsored in part by DOE and Army (For primary document see N87-23757 17-28)
Avail: CPIA, Laurel, Md. 20707 HC $70.00

Simultaneous thermogravimetric modulated beam mass spectrometry (STMBMS) and time of flight (TOF) velocity spectra measurements of the thermal decomposition products from HMX and RDX show several reaction mechanisms. The STMBMS and TOF measurements as a function of mass spectrometer electron energy show substantial ion dissociation of HMX down to 12.4 eV. This implies that appearance potential measurements cannot discriminate between ion dissociation fragments from HMX and its possible large ring segment thermal decomposition products. The thermal decomposition of HMX at 212 C shows an autocatalytic behavior with two different reaction mechanisms, both occurring in the condensed phase. One produces N-nitroformimine, N2O, H2CO, and a substituted hydrocarbone residue. The other produces an intermediate product with a molecular weight between 250 and 296 which may lead to HCN formation. The thermal decomposition of RDX between 160 and 220 C shows both gas phase and condensed phase decomposition. The gas phase reaction starts at 187 C and produces H2O, NO, N2O, NO2, H2CO, HCN, and hydroxy-s-triazine. A bimolecular hydrogen abstraction reaction may lead to the formation of the gas phase products. The condensed phase reaction produces a product with a slightly lower molecular weight than RDX and forms a 132+ ion in the

mass spectrometer. This is similar to one of the HMX condensed phase reactions. Author

N87-23781# Sandia Labs., Livermore, Calif.
QUANTUM CHEMICAL CALCULATIONS OF THE DECOMPOSITION OF NITRAMINES: THERMOCHEMISTRY AND REACTION PATHWAYS
C. F. Melius and J. S. Binkley *In* Johns Hopkins Univ., The 23rd JANNAF Combustion Meeting, Volume 1 Oct. 1986 p 241-248 Sponsored in part by DOE and DoD (For primary document see N87-23757 17-28)
Avail: CPIA, Laurel, Md. 20707 HC $70.00

The gas phase decomposition of nitramines was studied theoretically using the quantum chemical Bond Additivity Corrected Moeller Plesset fourth order perturbation theory method (BAC-MP4). The BAC-MP4 method provides accurate thermochemical properties, such as bond energies, heats of formation, entropies and free energies, for gas phase molecular species. The nitramine decomposition process was treated by examining prototype chemical building blocks such as nitramine (H2NNO2) and methylnitramine (CH3H2NNO2) and the various intermediates formed from these molecules. Using the various heats of formation as well as activation energies of activated complexes, the various bond energies in the nitramines were determined as well as possible dissociation pathways. A new gas phase decomposition mechanism is proposed involving attack by autocatalytically generated H atoms. The H atoms arise from the dissociation of H2CN which is formed from the unzipping of the cyclic nitramines such as RDX and HMX. These proposed mechanisms are constrained to be thermodynamically consistent with the calculated BAC-MP4 heats of formation and activation energies. The H atoms, which assist the gas phase decomposition process, also are proposed to play an important role in propagating the secondary flame. The competition for the H atoms between these two processes can lead to the spatial separation of the two flames. Author

N87-23782# Naval Weapons Center, China Lake, Calif.
THE APPLICATION OF IMAGING LASER INDUCED FLUORESCENCE TO THE MEASUREMENT OF HMX AND ALUMINIZED PROPELLANT IGNITION AND DEFLAGRATION FLAME STRUCTURE
T. P. Parr and D. M. HansonParr *In* Johns Hopkins Univ., The 23rd JANNAF Combustion Meeting, Volume 1 Oct. 1986 p 249-267 (For primary document see N87-23757 17-28)
(N00014-86-WR-2C034)
Avail: CPIA, Laurel, Md. 20707 HC $70.00

Experiments using imaging Planar Laser Induced Fluorescence (PLIF) to measure species profiles during CO2 laser ignition and steady state deflagration of HMX and aluminized nitramine high energy propellant (HEPs) are described. All experiments were done at one atmosphere. Time resolved PLIF images were obtained for NO2, NO, CN, NH, and OH during ignition of both HMX and HEPs. CN and NH form at reasonably large heights off the sample surface in gas phase ignition kernels at finite delays, and reform into relatively thin flame sheets which snap back towards the sample surface. NO2 and NO are initial products during laser ignition, beginning to form at minimum delay times and producing tall plumes until ignition occurs in the gas phase. The NO2 and NO PLIF signals are then confined to an expanding spherical shell plus a steady state solid core between the sample surface and the CN or NH flame sheet. Thus it appears that NO2 and NO are early decomposition products which are consumed in a flame separated significantly from the surface. The CN and NH are produced in this flame as transient radicals. OH is produced at the same delay as CN and NH but extends very far beyond the thin CN/NH flame front. Author

N87-23783# Pennsylvania State Univ., University Park. Dept. of Mechanical Engineering.
THERMAL DECOMPOSITION AND IGNITION OF A SERIES OF NEW NITRAMINE LOVA PROPELLANTS BY CO2 LASER
J. U. Kim, T. Torikai, and K. K. Kuo *In* Johns Hopkins Univ., The 23rd JANNAF Combustion Meeting, Volume 1 Oct. 1986 p 269-279 (For primary document see N87-23757 17-28)
(Contract N00014-79-C-0762)
Avail: CPIA, Laurel, Md. 20707 HC $70.00

The thermal decomposition and ignition characteristics of a series of RDX based composite propellants was studied. A high powered CO2 laser was used to provide the radiative energy to test samples. Three different types of cameras were used to record the ignition events. A near infrared photodiode was also used to detect light emission from the ignition site. Generally, the delay time based upon the onset of light emission decreases monotonically with the increase of incident laser energy flux. The slope was found to be affected by the oxygen concentration in the ambient gas. The effect is prominent when the sample contains volatile energetic binder. The effects of oxygen concentration are greater in the gas phase ignition of nitramine propellants than in conventional AP based composite propellants. The flame structure of nitramine propellants are also found to depend strongly upon the ambient gas conditions. At a higher oxygen concentration, the flame is much closer to the sample surface than is the flame at a low oxygen concentration; this implies that gas phase reaction with ambient oxygen plays an important role in the initial phase of laser ignition of this series of nitramine propellants. Author

N87-23784# Gough (Paul) Associates, Inc., Portsmouth, N.H.
THEORETICAL INFLUENCE OF PROPELLANT PACKAGING ON TUBE EROSION: MODEL FORMULATION AND ALGORITHM DEVELOPMENT
P. S. Gough and K. D. Fickie *In* Johns Hopkins Univ., The 23rd JANNAF Combustion Meeting, Volume 1 Oct. 1986 p 281-294 Prepared in cooperation with Ballistic Research Labs., Aberdeen Proving Ground, Md. (For primary document see N87-23757 17-28)
(Contracts DAAK11-83-C-0051; DAAA14-85-C-0014)
Avail: CPIA, Laurel, Md. 20707 HC $70.00

Although the problem of thermal erosion of gun tubes has received considerable attention from theoreticians, even the most elaborate models have not yet attempted to account for the influence of the details of packaging and ignition of the charge. A first attempt to construct a model is described, which addresses the influence of packaging and ignition on tube erosion. The model is an extension of an existing two dimensional flamespreading code, TDNOVA, which simulates the details of packaging and ignition. TDNOVA is extended by linking it to an implicit Navier Stokes solver, LADIS, to determine the flow in the region of ullage around the charge. The content of TDNOVA is reviewed and its scope of applicability is discussed. The details of LADIS are described and the linkages between the two algorithms are considered. Author

N87-23785# Pennsylvania State Univ., University Park. Dept. of Mechanical Engineering.
NUMERICAL SIMULATION OF COMBUSTION PROCESSES OF MOBILE STICK-PROPELLANT BUNDLES
K. C. Hsieh and K. K. Kuo *In* Johns Hopkins Univ., The 23rd JANNAF Combustion Meeting, Volume 1 Oct. 1986 p 295-306 (For primary document see N87-23757 17-28)
(Contract DAAK29-83-K-0081)
Avail: CPIA, Laurel, Md. 20707 HC $70.00

Flame-spreading, combustion, and grain-deformation phenomena associated with unslotted stick propellant bundles were studied both theoretically and experimentally. Calculated pressure-time variations during the initial period before grain rupture are in reasonable agreement with test results. Recovered propellant samples exhibit numerous small shattered pieces and several long integral pieces with slits. Mechanical damage of grains at the breech end is significantly less than that at the projectile end. Observed coning phenomena of the internal surfaces on both ends of recovered samples suggest the importance of erosive buring. Stick propellant grains were found to move slowly in the cartridge. This could cause excessively high temperatures near the breech end. Author

N87-23786# Lawrence Livermore National Lab., Calif.
A HYBRID CLOSED BOMB-STRAND BURNER FOR VERY HIGH PRESSURE BURNING RATE MEASUREMENTS
Marc Costantino and Donald Ornellas *In* Johns Hopkins Univ., The 23rd JANNAF Combustion Meeting, Volume 1 Oct. 1986 p 307-316 (For primary document see N87-23757 17-28)
(Contract W-7405-eng-48)
Avail: CPIA, Laurel, Md. 20707 HC $70.00

A hybrid closed bomb-strand burner, suitable for burning rate measurements at pressures in excess of 1 GPa (150,000 PSI) is described. The device is a cylindrical pressure vessel having an internal volume of about 50 cc and a means of extracting up to fifteen electrical or fiber optic signals. The sample is a right circular cylinder 6.35 mm in diameter and 10 cm long with an epoxy coating on the outside surface as an inhibitor. The sample fits in a fixture which prevents its motion during the burn and provides mounting points for the diagnostics that detect the arrival of the burning surface. A variety of break wires and ionization probes were used to trigger the timing electronics. At the burning rates of present interest (less than 1 m/s), the pressure was measured using an external load cell. An experiment consists of a pre-pressurizing the vessel with argon, igniting the sample at one end, and measuring the pressure and the time of arrival at each probe. The average burning rate between wire locations n-1 and n, over the pressure range (P sub n-1 and P sub n), is r sub n-1,n = (x sub n - x sub n-1)/(t sub n - t sub n-1), giving a large portion of the burning rate-pressure curve in a single experiment. Author

N87-23787# Naval Postgraduate School, Monterey, Calif.
SOLID FUEL RAMJET FUEL REGRESSION RATE/THRUST MODULATION
W. H. Campbell, Jr., B. N. Ko, S. R. Lowe, and D. W. Netzer *In* Johns Hopkins Univ., The 23rd JANNAF Combustion Meeting, Volume 1 Oct. 1986 p 339-352 (For primary document see N87-23757 17-28)
(Contracts N00019-84-WR-41049; N00019-85-WR-51139; N60530-86-WR-30021)
Avail: CPIA, Laurel, Md. 20707 HC $70.00

An experimental investigation was conducted to examine the effects of inlet air swirl and secondary gas injection on the combustion properties in a solid fuel ramjet. Tests were conducted with 18818, HTPB, and PMM fuels. Inlet swirl characteristics were measured in nonreacting flows. The swirl tests were conducted at high and low air mass fluxes with equivalence ratios between 0.5 and 1.8. Swirl was found effective for increasing the fuel regression rate but the magnitude was hgihly dependent upon motor geometry, fuel type, and operating environment. The gas injection tests included hydrogen at low equivalence ratios, and nitric oxide and nitrous oxide at high equivalence ratios. Secondary injection generally resulted in increases in combustion pressure in agreement with equilibrium, adiabatic combustion expectations. Author

N87-23788# Naval Postgraduate School, Monterey, Calif.
METALLIZED FUEL BURNING CHARACTERISTICS IN THE SOLID FUEL RAMJET
C. K. Scott, II and D. W. Netzer *In* Johns Hopkins Univ., The 23rd JANNAF Combustion Meeting, Volume 1 Oct. 1986 p 353-364 (For primary document see N87-23757 17-28)
(Contract N60530-86-WR-30021)
Avail: CPIA, Laurel, Md. 20707 HC $70.00

An experimental investigation was conducted with highly metallized (approximately 70% by weight) solid fuels burned in a two-dimensional solid fuel ramjet (SFRJ). Highspeed motion pictures were taken of the combustion process through viewing windows located at two locations along the fuel slab length. Films revealed various ejection events ranging from small particle ejections to large flakes of burning and nonburning material leaving the surface. Nine different fuels were tested at air mass fluxes of 0.2 and 0.5 pounds pass per inch squared per second and pressures ranging from 35 to 200 psia. There was evidence that both minor binder ingredient changes (polymer and curative) and the inclusion of magnesium resulted in larger required inlet step heights to sustain combustion. Most of the metallized fuels did not burn well at pressures below approximately 40 psia. Low air mass fluxes generally resulted in larger metallic surface agglomerations, larger particles in the gas phase and more dominate shedding of surface layers. Author

N87-23789* National Aeronautics and Space Administration. Langley Research Center, Hampton, Va.
PLASMA TORCH IGNITER FOR SCRAMJETS
Timothy C. Wagner, Walter F. OBrien, G. Burton Northam, and James M. Eggers *In* Johns Hopkins Univ., The 23rd JANNAF Combustion Meeting, Volume 1 Oct. 1986 p 365-376 Prepared in cooperation with Virginia Polytechnic Inst. and State Univ., Blacksburg (For primary document see N87-23757 17-28)
Avail: CPIA, Laurel, Md. 20707 HC $70.00 CSCL 21I

A small, uncooled plasma torch was developed and used in combination with an injector designed to study ignition and flameholding in hydrogen-fueled supersonic flows. The plasma torch was operated on mixtures of hydrogen and argon with total flows of 10 to 70 scfh. The fuel injector design consisted of five small upstream pilot fuel injectors, a rearward facing step for recirculation, and three main fuel injectors downstream of the step. The plasma torch was located in the recirculation region, and all injection was perpendicular to the Mach 2 stream. Both semi-freejet and ducted tests were conducted. The experimental results indicate that a low power plasma torch operating on a 1:1 volumetric mixture of hygrogen and argon and located in the recirculation zone fueled by the upstream pilot fuel injectors is a good igniter for flow conditions simulating a flight Mach number of 3.7. The total temperature required to autoignite the hydrogen fuel for this injector geometry was 2640 R. The injector configuration was shown to be a good flameholder over a wide range of total temperature. Spectroscopic measurements were used to verify the presence of air total temperatures below 1610 R. Author

N87-23790* National Aeronautics and Space Administration. Langley Research Center, Hampton, Va.
EFFECTS OF TEST FACILITY CONTAMINANTS ON SUPERSONIC HYDROGEN-AIR DIFFUSION FLAMES
R. Clayton Rogers *In* Johns Hopkins Univ., The 23rd JANNAF Combustion Meeting, Volume 1 Oct. 1986 p 377-390 (For primary document see N87-23757 17-28)
Avail: CPIA, Laurel, Md. 20707 HC $70.00 CSCL 21I

Results are presented from an analytical assessment of the effects of NO and H2O in air on the ignition and reaction of hydrogen. Three flow models of the burning process were used, each including a 32 reaction chemistry mechanism. These models were a plug flow reactor to determine ignition and reaction times; a well-stirred reactor to assess flame stability or blow-off; and a parabolic Navier-Stokes code to examine the diffusion flame combustion. The diffusion flame was computed for a cold supersonic H2 jet coaxial with a supersonic air stream at a static temperature of 1100 K and a pressure of 1 atmosphere. Author

N87-23791* National Aeronautics and Space Administration. Langley Research Center, Hampton, Va.
OPPOSED JET BURNER STUDIES OF SILANE-METHANE, SILANE-HYDROGEN AND HYDROGEN DIFFUSION FLAMES WITH AIR
G. L. Pellett, Rosemary Guerra, L. G. Wilson, and G. B. Northam *In* Johns Hopkins Univ., The 23rd JANNAF Combustion Meeting, Volume 1 Oct. 1986 p 391-404 Previously announced in IAA as A87-23259 (For primary document see N87-23757 17-28)
Avail: CPIA, Laurel, Md. 20707 HC $70.00 CSCL 21I

An atmospheric pressure tubular opposed jet burner technique was used to characterize certain diffusion-flame transitions and associated burning rates for N2-diluted mixtures of highly-reactive fuels. Presented are: (1) details of the technique, with emphasis on features permitting the study of flames involving pyrophoric gases and particle-forming combustion reactions: (2) discoveries on the properties of these flames which correspond to physically and chemically distinct stages of silane and hydrogen combustion;

and (3) unburnt gas velocity data obtained from flames based on SiH4-CH4-N2, SiH4-H2-N2, and H2-N2 fuel mixtures, and plotted as functions of combustible-fuel mole fraction and fuel/oxygen molar input flow ratios. In addition, these burning velocity results are analyzed and interpreted. IAA

N87-23792 United Technologies Research Center, East Hartford, Conn.
CARS APPROACHES TO SIMULTANEOUS MEASUREMENTS OF H2 AND H2O CONCENTRATION AND TEMPERATURE IN H2-AIR COMBUSTION SYSTEMS **c25**
Alan C. Eckbreth, Torger J. Anderson, and Gregory M. Dobbs *In* Johns Hopkins Univ., The 23rd JANNAF Combustion Meeting, Volume 1 Oct. 1986 p 405-415 (For primary document see N87-23757 17-28)
Avail: CPIA, Laurel, Md. 20707 HC $70.00

An approach to Coherent Anti-Stokes Raman Spectroscopy (CARS) capable of providing simultaneous measurements of major H2/air combustion constituents with potential as a diagnostic for advanced air-breathing propulsion concepts, is described and demonstrated. The technique employs both a broadband and a narrowband Stokes beam to generate CARS via two, two-color and two, three-color wave mixing processes. Temperature and concentration information are simultaneously available from N2, H2, and H2O. This permits the disappearance of fuel and appearance of product to be monitored. An analysis of the technique's capabilities and future improvements are discussed. Author

N87-23793# McDonnell-Douglas Corp., St. Louis, Mo.
RESPONSE OF TRANSONIC DIFFUSER FLOWS TO ABRUPT INCREASES OF BACK PRESSURE: WALL PRESSURE MEASUREMENTS **c34**
T. J. Bogar and M. Sajben *In* Johns Hopkins Univ., The 23rd JANNAF Combustion Meeting, Volume 1 Oct. 1986 p 417-424 (For primary document see N87-23757 17-28)
(Contract N60530-83-C-0186)
Avail: CPIA, Laurel, Md. 20707 HC $70.00

The propagation of compression pulses in a supercritically operated transonic diffuser was investigated by use of pressure measurements along the top wall of the model. The pulses were generated at the downstream end of the diffuser by the abrupt injection of a secondary flow of air. Two types of waves were observed: (1) an upstream-traveling acoustic wave and (2) a downstream-traveling convective wave which resulted from the impingement of the acoustic wave on the shock. Wave speeds were determined for a range of diffuser pressure ratios including separated, strong-shock flows and fully attached, weak-shock flows. Streamwise distributions of initial and reflected pulse amplitudes were determined for one weak and one strong-shock case over a 3-to-1 range of initial pulse strengths. Author

N87-23794# Naval Surface Weapons Center, Silver Spring, Md.
DOWNSTREAM BOUNDARY EFFECTS ON THE FREQUENCY OF SELF-EXCITED OSCILLATIONS IN TRANSONIC DIFFUSER FLOWS **c34**
T. Hsieh *In* Johns Hopkins Univ., The 23rd JANNAF Combustion Meeting, Volume 1 Oct. 1986 p 425-434 (For primary document see N87-23757 17-28)
Avail: CPIA, Laurel, Md. 20707 HC $70.00

Investigation of downstream boundary effects on the frequency of self-excited oscillations in two-dimensional, separated transonic diffuser flows were conducted numerically by solving the compressible, Reynolds-averaged, thin-layer Navier-Stokes equation with two equation turbulence models. It was found that the flow fields are very sensitive to the location of the downstream boundary. Extension of the diffuser downstream boundary significantly reduces the frequency and amplitude of oscillations for pressure, velocity, and shock. The existence of a suction slot in the experimental setpup obscures the physical downstream boundary and therefore presents a difficulty for quantitative comparisons between computation and experiment. Author

N87-23795# California Inst. of Tech., Pasadena.
LINEAR COUPLING OF ACOUSTICS AND ENTROPY AND ACOUSTIC STABILITY IN RAMJET COMBUSTION CHAMBERS CONTAINING A PLANE FLAME **c20**
Joseph W. Humphrey and F. E. C. Culick *In* Johns Hopkins Univ., The 23rd JANNAF Combustion Meeting, Volume 1 Oct. 1986 p 435-448 (For primary document see N87-23757 17-28)
(Contract N00014-84-K-0434)
Avail: CPIA, Laurel, Md. 20707 HC $70.00

A one-dimensional analytical model is presented for calculating the longitudinal acoustic modes of idealized dump-type ramjet engines. The model contains the matching required to place an oscillating flame sheet in the interior of a combustion chamber with mean flow. The linear coupling of the acoustic and entropy waves at the inlet shock, flame sheet, and exit nozzle along with acoustic admittances at the inlet and exit are combined to determine the stability of the system as well as the acoustic modes. Since the acoustic and entroy waves travel at different velocities, the geometry is a critical factor in determining stability. Typical values of the admittances will produce damped solutions when the entropy is neglected, but, as the ratio of the entropy to acoustic fluctuations is increased, the coupling can either feed acoustic energy into or out of different modes independently. This transfer of energy has a destabilizing or stabilizing effect on the acoustic modes of the system depending upon the phase of the energy transfer. Author

N87-23796# California Inst. of Tech., Pasadena.
ANALYSIS OF PRESSURE OSCILLATIONS IN RAMJETS. REVIEW OF RESEARCH: 1985-1986 **c20**
F. E. C. Culick *In* Johns Hopkins Univ., The 23rd JANNAF Combustion Meeting, Volume 1 Oct. 1986 p 449-457 (For primary document see N87-23757 17-28)
(Contract N00014-84-K-0434)
Avail: CPIA, Laurel, Md. 20707 HC $70.00

Unsteady motions in ramjet engines are studied. The program comprises analytical work devoted generally to the question: what causes unsteady motions in ramjet engines to grow and reach the limiting amplitudes observed in practice? The effort therefore encompasses both the causes or mechanisms of instabilities; and the linear and nonlinear processes influencing the time evolution of the motions. The application of approximate analysis, in contrast to numerical analysis carried out, to produce solution of complete equations of motion was of primary concern. Subjects covered here include progress in the linear and nonlinear analysis of acoustics with entropy waves; application of the method of averaging to problems having arbitrary distributions of modal frequencies; and the excitation of nonlinear acoustic waves by random sources. Author

N87-23797# San Diego State Univ., Calif.
TONES GENERATED DUE TO THE IMPINGEMENT OF TWO JETS ON EACH OTHER **c71**
Nagy Nosseir, Uri Peled, and Gregory Hildebrand *In* Johns Hopkins Univ., The 23rd JANNAF Combustion Meeting, Volume 1 Oct. 1986 p 459-467 (For primary document see N87-23757 17-28)
Avail: CPIA, Laurel, Md. 20707 HC $70.00

The impingement of two, axisymmetric turbulent jets on each other is investigated experimentally. The angle of impingement is equal to 180 degrees, and the jets are issued from large flat plates. Characteristics of the flow field, and pressure disturbances generated in the impinging region and amplified by feedback mechanisms are discussed. Author

N87-23798# Naval Weapons Center, China Lake, Calif.
PASSIVE SHEAR-FLOW CONTROL TO MINIMIZE RAMJET COMBUSTION INSTABILITIES **c25**
K. C. Schadow, E. Gutmark, T. P. Parr, D. M. Parr, and K. J. Wilson *In* Johns Hopkins Univ., The 23rd JANNAF Combustion Meeting, Volume 1 Oct. 1986 p 469-484 (For primary document see N87-23757 17-28)
Avail: CPIA, Laurel, Md. 20707 HC $70.00

Passive shear-flow control methods to avoid combustion instabilites in a ramjet dump combustor were developed in cold nonreacting flows and verified in combustion processes. All control methods, which are based on the detailed understanding of flow instability mechanisms in shear layers, were used to change the initial conditions of the air flow issued from the inlet duct into dump combustor, in an attempt to decouple combustion from the large-scale structures in the flow. Four different jet nozzles located at the dump plane are discussed to augment fine-scale mixing and, at the same time, reduce large-scale mixing: jet nozzles having sharp corners, tapered-elliptical nozzles with a special inner transition section which induces axial vorticity into the flow, multiple-step nozzle with numerous sources for turbulence production yielding highly turbulent homogeneous incoherent flow fields, and secondary high speed axial and radial injection which simulates fuel injection and is aimed to use rationally the fuel injection for a desired flow management. All methods were shown to be able to modify the flow field mixing patterns and inner eddy structure and to provide the potential for minimizing combustion instabilites. Author

N87-23799# Georgia Inst. of Tech., Atlanta.
ACOUSTIC RESPONSE OF TURBULENT REACTING RECIRCULATORY FLOWS **c71**
J. A. Davis, N. L. Sankar, and W. C. Strahle *In* Johns Hopkins Univ., The 23rd JANNAF Combustion Meeting, Volume 1 Oct. 1986 p 485-497 (For primary document see N87-23757 17-28)
(Contract N00014-83-G-0047)
Avail: CPIA, Laurel, Md. 20707 HC $70.00

Experiment and analysis are reported upon concerning two dimensional plane turbulent cold flow behind a backward facing step which is acoustically forced. Numerically, the axisymmetric configuration was also examined. At issue is the interaction between vorticity and acoustics. It is shown experimentally that a lock-in between the shear layer behind the step and the acoustic potential field can occur at distinct frequencies. Furthermore, there is a significant alteration of the potential field when this occurs. In addition, the lock-in is removed when the recirculation zone is removed by a wind tunnel insert. Full numerical Navier-Stokes solution of the problem has shown that this phenomena is heavily dependent upon the boundary conditions of the problem and shows that inviscid treatments of the problem are likely to give misleading results. Author

N87-23800# California Univ., Berkeley. Dept. of Mechanical Engineering.
VORTEX-NOZZLE INTERACTIONS IN RAMJET COMBUSTORS **c34**
K. Yu, S. Lee, H. E. Stewart, and J. W. Daily *In* Johns Hopkins Univ., The 23rd JANNAF Combustion Meeting, Volume 1 Oct. 1986 p 499-508 (For primary document see N87-23757 17-28)
(Grant N00014-84-K-0372)
Avail: CPIA, Laurel, Md. 20707 HC $70.00

A facility designed to study the role of vortex-nozzle interactions in promoting low frequency instabilities in ramjet combustors is described. The design issues are outlined, as are potential instabilities. Preliminary data are reported which indicate the possibility of a recirculation vortex instability being an important mode. Author

N87-23801# Naval Research Lab., Washington, D. C. Lab. for Computational Physics.
COMPUTATIONAL STUDIES OF THE EFFECTS OF ACOUSTICS AND CHEMISTRY ON THE FLOW FIELD IN AN AXISYMMETRIC RAMJET COMBUSTOR **c34**
K. Kailasanath, J. H. Gardner, E. S. Oran, and J. P. Boris *In* Johns Hopkins Univ., The 23rd JANNAF Combustion Meeting, Volume 1 Oct. 1986 p 509-520 (For primary document see N87-23757 17-28)
Avail: CPIA, Laurel, Md. 20707 HC $70.00

A potentially important source of large pressure oscillations in compact ramjets is a combustion instability induced by the interaction of large-scale vortex structures with acoustic modes in the combustion chamber. To study these interactions numerical simulations were performed using the Flux Corrected Transport technique. The highlights are presented of the work to date on the chemical-acoustic-vortex interactions in an idealized axisymmetric ramjet combustor. The results of a number of cold flow calculations are presented in which the length of the combustion chamber and the acoustic forcing function were systematically varied. These simulations indicate a strong coupling between the acoustic modes and the frequency of formation of large vortical structures near the entrance to the combustion chamber. They also show the presence of a low frequency oscillation which does not directly depend on the acoustics of the combustor but depends on the acoustics of the inlet. The effects of energy release from chemical reactions on the flow field in the combustor and the low frequecy oscillations are discussed. Author

N87-23802# Flow Research, Inc., Kent, Wash.
NUMERICAL SIMULATIONS OF COLD FLOW IN A RAMJET DUMP COMBUSTOR WITH A CHOKED EXIT NOZZLE **c34**
S. Menon and W.-H. Jou *In* Johns Hopkins Univ., The 23rd JANNAF Combustion Meeting, Volume 1 Oct. 1986 p 521-531 (For primary document see N87-23757 17-28)
(Contract N00014-84-C-0359)
Avail: CPIA, Laurel, Md. 20707 HC $70.00

Simulations of the flow field were performed in a ramjet dump combustor equipped with an exit nozzle. The flow through the nozzle is choked numerically to simulate a realistic ramjet configuration. This also removes any ambiguities associated with the imposed outflow boundary conditions. The method of numerical choking is described. Large-scale motions similar to those in unchoked flow simulations are observed. The interaction between these large vortices and the choked throat is studied. Two simulations at Mach numbers 0.32 and 0.44 are discussed. Spectral analysis of the pressure and vorticity fluctuations in the combustor indicate a much richer spectral content when compared to unchoked flow results. Both convective-wave-dominated oscillations and acoustic oscillations appear to be present in the flow. Some preliminary results are presented. Author

N87-23803# Georgia Inst. of Tech., Atlanta.
COMBUSTION INSTABILITIES IN DUMP TYPE RAMJET COMBUSTORS **c25**
U. G. Hegde, D. Reuter, B. T. Zinn, and B. R. Daniel *In* Johns Hopkins Univ., The 23rd JANNAF Combustion Meeting, Volume 1 Oct. 1986 p 533-544 (For primary document see N87-23757 17-28)
(Contract N00014-84-K-0470)
Avail: CPIA, Laurel, Md. 20707 HC $70.00

Combustion instability problems often occur in coaxial dump type ramjet combustors. A potentially severe type of instability is characterized by low frequency pressure and velocity oscillations. The coupling between cone shaped flames, often encountered in dump type ramjet combustors and the longitudinal acoustic fields associated with the low frequency instability are investigated. Specifically the unsteady behavior of a V-shaped flame, stabilized in a rectangular combustor, in various longitudinal acoustic fileds is studied. A variety of experimental techniques were employed. It is found that the shear layer formed by the flame exhibits a marked fluid dynamical instability at low frequencies resulting in the formation of burning vortical structures that are convected along the flame front. The resulting unsteady combustion process acts as a strong acoustic source resulting in longitudinal pressure oscillations. This problem, therefore, presents an intricate coupling among the three basic modes of fluid motion. A simple model developed to predict flame generated acoustic spectra from measurements of the unsteady heat release rate yields the coupling between the thermal and acoustic modes. The unsteady vortical behavior of the flame is extremely complicated and exhibits many nonlinear features, in particular the presence of subharmonics and harmonics of the main repsonse frequency. Author

N87-23804# Stanford Univ., Calif. Dept. of Mechanical Engineering.
EFFECTS ON FUEL SPRAY CHARACTERISTICS AND VAPORIZATION ON ENERGY RELEASE RATES AND FLOW FIELD STRUCTURE IN A DUMP COMBUSTOR **c34**
C. T. Bowman, R. K. Hanson, U. Vandsburger, M. G. Allen, and K. R. McManus *In* Johns Hopkins Univ. 23rd JANNAF Combustion Meeting, Volume 1 Oct. 1986 p 545-550 (For primary document see N87-23757 17-28)
(Contract N00014-84-K-0383)
Avail: CPIA, Laurel, Md. 20707 HC $70.00

An experimental investigation of the effects of fuel spray characteristics, specifically droplet size and extent of prevaporization, on energy release rate and flow field structure in a liquid-fueled dump combustor is in progress. Visualization and measurment of the spray characteristics and of the reacting flow field are carried out using high-speed schlieren photography and planar imaging techniques. An important element of the research is development of these imaging techniques for two-phase reacting flows. Progress to date is described in the development of several imaging techniques and initial results from experiments in the dump combustor. Author

N87-23805# California Univ., Irvine.
SPRAY COMBUSTION: A DRIVING MECHANISM FOR RAMJET COMBUSTION INSTABILITY **c25**
W. A. Sirignano, G. Riva, A. Tong, B. Abramzon, and K. Molavi *In* Johns Hopkins Univ., The 23rd JANNAF Combustion Meeting, Volume 1 Oct. 1986 p 551-559 (For primary document see N87-23757 17-28)
(Contract N00014-85-K-0658)
Avail: CPIA, Laurel, Md. 20707 HC $70.00

Analytical and computational studies of liquid-fueled ramjet combustion instability are made. The vaporization rate of droplets in an oscillatory gaseous environment are determined; heat conduction and convection within the droplet interior are considered and shown to have very significant effects compared to the infinite-conductivity or rapid-mixing models of the past. The gain or response function associated with the oscillatory vaporization rate component in phase with the pressure is shown to be sufficiently large to sustain instability. A one-dimensional analysis of longitudinal mode instability indicates that limit cycle oscillations do result after a perturbation is applied. An axisymmetric analysis is concerned on improved numerical methods to reduce numerical diffusion and dispersion. Author

N87-23806# California Univ., Davis. Dept. of Mechanical Engineering.
COMBUSTION, VAPORIZATION, AND MICROEXPLOSION OF DROPLETS OF ORGANIC AZIDES **c25**
C. K. Law, A. Lee, S. Deevi, A. Ganji, and A. Makino *In* Johns Hopkins Univ., The 23rd JANNAF Combustion Meeting, Volume 1 Oct. 1986 p 561-572 (For primary document see N87-23757 17-28)
(Contract N00014-84-K-0700)
Avail: CPIA, Laurel, Md. 20707 HC $70.00

An experimental investigation was conducted on the vaporization, combustion, and microexplosion characteristics of freely-falling droplets of organic azides and their mixtures with conventional hydrocarbon fuels in hot oxidizing or inert environments. The droplet burning rate and the state of microexplosion were measured. Results show that, compared with the conventional hydrocarbon fuels, droplets of azido fuels gasify faster and microexplode earlier in the droplet lifetime. The effect is especially strong for n-alkyl diazides whose gasification rates can exceed those of the corresponding n-alkanes by several hundred percent. Such strong responses are believed to be caused by the exothermic decomposition of the azides either in the liquid phase or upon gasification. Effects of OH-substitution, molecular branching, and the proximity and number of the azide groups on the gasification behavior were studied while the potential of inducing droplet microexplosion by doping JP-10 with various diazides was also explored. A theoretical model was formulated; the predictions qualitatively agree with the experimental observations. Author

N87-23807# Illinois Univ., Chicago.
FUNCTIONALIZATION OF CUBANE USING HYPERVALENT IODINE
Robert M. Moriarty and Jaffar S. Khosrowshani *In* Johns Hopkins Univ., The 23rd JANNAF Combustion Meeting, Volume 1 Oct. 1986 p 573-575 (For primary document see N87-23757 17-28)
(Contract ONR-2-538403-SDI-1986)
Avail: CPIA, Laurel, Md. 20707 HC $70.00

The hypervalent iodine oxidative decarboxlyation reaction upon homocubyl and cubyl mono and dicarboxylic acids is examined. Specifically the appropriate carboxylic acid is treated with C6H5I(OCOCH3)2/CCl4/I2 under irradiation conditions and 80 to 90% of the derived iodo compound is obtained. These derivatives are of key importance because they serve as starting materials for subsequent displacement reactions using hypervalent iodine methodology. Thus azido analogs are synthetically accessible. The cubylaryliodonium salt is also accessible using these methods.
Author

N87-23808* National Aeronautics and Space Administration. Langley Research Center, Hampton, Va.
MULTISPECIES CARS MEASUREMENTS IN TURBULENT COMBUSTION **c25**
Richard R. Antcliff, Olin Jarrett, Jr., R. Clayton Rogers, and Thomas VanOverbeck *In* Johns Hopkins Univ., The 23rd JANNAF Combustion Meeting, Volume 1 Oct. 1986 p 577-583 Prepared in cooperation with NASA- Lewis Research Center, Cleveland, Ohio. (For primary document see N87-23757 17-28)
Avail: CPIA, Laurel, Md. 20707 HC $70.00 CSCL 07D

A coherent anti-Stokes Raman scattering (CARS) instrument was upgraded to more accurately measure the number density of oxygen molecules. This instrument is designed to simultaneously measure nitrogen number density, oxygen number density, and the ro-vibrational temperature of nitrogen. The CARS is a nonintrusive diagnostic technique which utilizes a pulsed Nd:YAG laser, broadband dye lasers, a complex optical system, and an intensified photodiode array detector to sample hostile combustion environments. Measurements were made in a flame produced by a coaxial subsonic diffusion hydrogen-air burner. These data were used as a data base for comparison with the results of two separate computational fluid dynamics calculations. Complications which had arisen in previous studies with regard to interpretation of the oxygen data were eliminated. Author

N87-23809* National Aeronautics and Space Administration. Lewis Research Center, Cleveland, Ohio.
EXPERIMENTAL THRUST PERFORMANCE OF A HIGH AREA-RATIO ROCKET NOZZLE **c20**
A. J. Pavli, K. J. Kacynski, and T. A. Smith *In* Johns Hopkins Univ., The 23rd JANNAF Combustion Meeting, Volume 1 Oct. 1986 p 585-599 Previously announced as N87-20381 (For primary document see N87-23757 17-28)
Avail: CPIA, Laurel, Md. 20707 HC $70.00 CSCL 21H

An experimental investigation was conducted to determine the thrust performance attainable from high-area-ratio rocket nozzles. A modified Rao-contoured nozzle with an expansion area of 1030 was test fired with hydrogen-oxygen propellants at altitude conditions. The nozzle was also tested as a truncated nozzle, at an expansion area ratio of 428. Thrust coefficient and thrust coefficient efficiency values are presented for each configuration at various propellant mixture ratios (oxygen/fuel). Several procedural techniques were developed permitting improved measurement of nozzle performance. The more significant of these were correcting the thrust for the aneroid effects, determining the effective chamber pressure, and referencing differential pressure transducers to a vacuum reference tank. Author

N87-23810# Illinois Univ., Chicago.
ANALYTICAL PREDICTION OF COMBUSTION PERFORMANCE CHARACTERISTICS OF BIPROPELLANT LIQUID ROCKET ENGINE COMBUSTOR c20
H. H. Chiu, T. L. Jiang, G. F. Berry, and E. J. Croke *In* Johns Hopkins Univ., The 23rd JANNAF Combustion Meeting, Volume 1 Oct. 1986 p 601-610 (For primary document see N87-23757 17-28)
(Contract W-31-109-eng-38)
Avail: CPIA, Laurel, Md. 20707 HC $70.00

Theories of conjugate and group combustion and the associated numerical code were developed to aid in the analytical prediction of combustion performance and to establish the theoretical base of engine efficiency optimization by the technique of optimum-sized-droplet (OSD) sprays. The numerical simulation and performance synthesis of a cylindrical combustor with a pair of concentric annular ring injectors for fuel and oxidizer reveals that existence of a pronounced efficiency peak in a droplet size region termed mixing and vaporization controlled group conjugate and normal combustion region (MVGCN) and an symptotic efficiency plateau broadly based in a fine-spray region termed Priem-Heidmann vaporization controlled combustion region (PHVC). The mechanisms and the generic characteristics of enhanced efficiency in MVGCN peak and PHVC plateau are identified, and the criteria for design of the optimum injector and injector assembly, together with reduction of combustor size, based on the combustor efficency profile are discussed. The conventional design concept linked with the corollary the finer the spray, the better the efficiency is reassessed in light of the present theoretical predictions. Areas for future research are also discussed. Author

N87-23811# Remtech, Inc., Huntsville, Ala.
MEASUREMENTS FOR ROCKET ENGINE PERFORMANCE CODE VERIFICATION c20
S. C. Praharaj and R. L. Palko *In* Johns Hopkins Univ., The 23rd JANNAF Combustion Meeting, Volume 1 Oct. 1986 p 611-622 (For primary document see N87-23757 17-28)
(Contract NAS8-36548)
Avail: CPIA, Laurel, Md. 20707 HC $70.00

The various performance losses are currently calculated by the JANNAF procedure using codes such as CICM, SDER, TDK, BLIMPJ and BLM. Systematic measurements to verify the calculated losses individually hardly exist and are associated with high degrees of uncertainity. This effort attempts to establish a general directory which will help the engineer to select the appropriate parameter to measure, necessary test set-up, uncertainty evaluation of the measured data, and required instrumentation with associated accuracy and operation complexity. Author

N87-23812# Rockwell International Corp., Canoga Park, Calif. Rocketdyne Div.
NUMERICAL AND EXPERIMENTAL STUDIES OF ATOMIZATION AND MIXING FROM A COAXIAL INJECTOR ELEMENT c20
P. Y. Liang and M. Varma *In* Johns Hopkins Univ., The 23rd JANNAF Combustion Meeting, Volume 1 Oct. 1986 p 623-631 (For primary document see N87-23757 17-28)
Avail: CPIA, Laurel, Md. 20707 HC $70.00

The mixing efficiency of coaxial injectors is an important performance parameter in oxygen/hydrogen liquid rocket engines. A numerical study is described which was carried out to analyze the liquid mass flux distribution profiles downstream of a coaxial injector and results compared with cold-flow experiments. The actual experiment was done using water and a gaseous mixture of nitrogen and helium, the latter being added to achieve sufficently high gaseous injection velocities at reduced pressures as well as to help differentiate between the injector flow and the faceplate flow. Sampling probes and pitot tubes are used for measurement. The numerical simulation was done using the three-phase Advanced Rocket Injector Combustion Code (ARICC). Although the chemistry model was not turned on, the code still provides a capability to describe the entire atomization, drop dispersion, and drop-gas interaction processes. Transverse mixture ratio profiles were evaluated and the experimental and numerical data compare favorably with each other. The parameters thus investigated include the initial drop Sauter mean diameter, the initial drop radial velocities, and the turbulence time scale of the stochastic drop turbulence model. Author

N87-23813# Rockwell International Corp., Canoga Park, Calif. Rocketdyne Div.
NONINTRUSIVE TEMPERATURE MEASUREMENTS IN SSME PREBURNER ELEMENT FLOWFIELDS c34
R. J. Jensen and S. C. Fisher *In* Johns Hopkins Univ., The 23rd JANNAF Combustion Meeting, Volume 1 Oct. 1986 p 633-640 (For primary document see N87-23757 17-28)
Avail: CPIA, Laurel, Md. 20707 HC $70.00

Combustion gas temperatures in a coaxial Space Shuttle Main Engine (SSME) preburner element were measured nonintrusively using OH emission spectroscopy. Low resolution spectra of 1 Sigma + to 2 Pi electronic transition obtained experimentally were compared with theoretical predictions to indicate temperatures in the axisymmetric flame. Emission spectra were taken of the flame at three axial locations for a range of mixture ratios from 0.39 to 1.24. The lower end of the mixture ratio range was near the ignition limit for this configuration. Measured flame temperatures were found to be insensitive to overall mixture ratio. The measured temperatures indicate a diffusion flame structure characterized by local flame mixture ratios less than stoichiometric but larger than the overall (well-mixed) element mixture ratio. The OH band intensity for the lower mixture ratios tended to decrease from a maximum at ignition to a much lower steady state value over a time period of seconds. Considering the volume of the combustor and the fact that the ignition sequence includes an oxidizer lead, the decreasing intensity is suspected to be related to a depletion of oxygen in the recirculating chamber gases. Author

N87-23814# Naval Surface Weapons Center, Silver Spring, Md.
EFFECT OF PARTICLE SIZE ON THE SHOCK SENSITIVITY OF PURE POROUS HE (HIGH EXPLOSIVE)
Donna Price Sep. 1986 35 p
(AD-A178206; NSWC/TR-86-336) Avail: NTIS HC A03/MF A01 CSCL 19A

The literature shows that in the gap tests, coarse porous High Explosive seems more shock sensitive than fine whereas in most wedge tests, the reverse is true. It is proposed that gap tests measure threshold for ignition, and that the reversal occurs because the time to ignition is shorter and the time of buildup of chemical reaction is longer for the coarse than the fine material. In other words, for any pair of fine and coarse HE in any specific experiment, there is a pressure (P sub r) at and above which ignition for the fine and coarse is simultaneous. At and above this pressure, the finer material appears more sensitive than the coarse. GRA

N87-23815# Federal Aviation Agency, Atlantic City, N.J.
AUTOGAS IN GENERAL AVIATION AIRCRAFT Final Report
H. Stewart Byrnes, William C. Cavage, and Augusto M. Ferrara Mar. 1987 58 p
(DOT/FAA/CT-87/05) Avail: NTIS HC A04/MF A01

A series of aircraft engine tests was conducted on a dynamometer which compared the vapor lock tendency of selected automobile gasolines against aviation gasolines. The effects of fuel temperature, the technique for heating the fuel used in vapor lock studies, the engine cooling air temperature, the fill level in the tanks, and fuel system configuration were investigated. The tendency for automobile gasoline to detonate in and aircraft engine was investigated, and the results show a strong correlation with the Motor Octane Number. Flight data is presented which shows the effect of the mode of operation on fuel system temperatures in two typical general aviation aircraft. Select results from a fuel aging study demonstrate the effects of long-range storage of automobile gasoline in typical general aviation wing tanks. Based on these results, a number of considerations pertaining to certification of general aviation aircraft fuel systems with automobile gasoline are identified. Author

N87-23816# General Electric Co., Cincinnati, Ohio. Aircraft Engine Business Group.
ANTIMISTING FUEL (AMK) FLIGHT DEGRADER DEVELOPMENT AND AIRCRAFT FUEL SYSTEM INVESTIGATION Final Report, Mar. 1983 - Dec. 1985
George A. Coffinberry and Thomas M. Tucker Feb. 1987 209 p
(Contract DTFA03-83-C-00018)
(DOT/FAA/CT-86/6; R86AEB565) Avail: NTIS HC A10/MF A01

Results from an effort involving the design, fabrication and evaluation of an Antimisting Kerosene (AMK) degrader are summarized. The principal objective was to demonstrate the feasibility of employing a high speed centrifugal pump to condition AMK fuel for use in an aircraft turbine engine. The effects of AMK fuel on the engine/airframe fuel system as well as any effect the flight environment might have had on the fire preventive characteristics of the AMK were also investigated. Five functionally identical degrader systems were produced. The first system was installed on the No. 3 engine of a CV880 aircraft with a dedicated AMK fuel tank. The remaining four degrader systems were installed on a B720 aircraft that was used in the Full Scale Transport Controlled Impact Demonstration (CID). The degrader system performed well and met the objectives of both the CV880 and the CID programs. Aside from the intermittent occurrence of gel, little difference in performance could be distinguished between the No. 3 engine, operating on AMK, and the No. 2 reference engine, operating on Jet A. Author

29 MATERIALS PROCESSING

Includes space-based development of products and processes for commercial applications.

For biological materials see *55 Space Biology.*

No abstracts in this category.

31 ENGINEERING (GENERAL)

Includes vacuum technology; control engineering; display engineering; cryogenics; and fire prevention.

N87-23817# California Univ., Berkeley. Lawrence Berkeley Lab.
IN SITU HREM OBSERVATION OF INTERPHASE BOUNDARY MOTION IN 95Pb-5Sn SOLDER
J. B. Posthill, D. Frear, and J. W. Morris, Jr. Jan. 1987 6 p Presented at the Annual Joint Meeting of the Electron Microscopy Society of America and the Microbeam Analysis Society, Albuquerque, N. Mex., 10 Aug. 1986
(Contract DE-AC03-76SF-00098)
(DE87-007616; LBL-22879; CONF-860829-41) Avail: NTIS HC A02/MF A01

The micrographs clearly show precipitate dissolution occurring only at the top interface and the tip. These regions of the boundary contain ledges of different sizes. One region contains ledges approx. 4 nm in height that appear to have rounded corners. Smaller ledges of approx. 0.6 nm can be seen after further heating in a thinner area of the foil. Their spacing along the boundary is of the order of 8 nm. The lower interface does not appear to contain similar ledges and has not moved during observation. In conclusion, precipitate dissolution has been observed at high-resolution to occur by a ledge mechanism. DOE

N87-23818# Vibration Inst., Clarendon Hills, Ill.
THE SHOCK AND VIBRATION DIGEST, VOLUME 19, NO. 4 Monthly Report
Judith Nagle-Eshleman, ed. Apr. 1987 72 p
Avail: NTIS HC A04/MF A01

Recent advances in the nonlinear analysis of laminated composite plates and shells and various aspects of automobile suspension and steering systems are discussed in detail. Abstracts of articles dealing with machine tools, fans, electric motors, turbine blades, building foundations, ships, helicopters, and bearings are given. For individual titles, see N87-23819 through N87-23820.

N87-23819# Virginia Polytechnic Inst. and State Univ., Blacksburg. Dept. of Engineering Science and Mechanics.
RECENT ADVANCES IN THE NONLINEAR ANALYSIS OF LAMINATED COMPOSITE PLATES AND SHELLS c39
J. N. Reddy and K. Chandrashekhara (Missouri Univ., Rolla.) *In* Vibration Inst., The Shock and Vibration Digest, Volume 19, No. 4 Apr. 1987 p 3-9 Sponsored in part by Navy and Army (For primary document see N87-23818 17-31)
Avail: NTIS HC A04/MF A01

Progress in the nonlinear analysis of laminated composite plates and shells is discussed. Emphasis is on literature that deals with the development of material modeling and simultaneous treatment of geometric and material nonlinear effects in the analysis of fiber reinforced composites. R.J.F.

N87-23820# Iowa State Univ. of Science and Technology, Ames. Dept. of Mechanical Engineering.
RECENT DEVELOPMENTS IN VEHICLE DYNAMICS c37
J. Bernard, M. Vanderploeg, and J. Shannan *In* Vibration Inst., The Shock and Vibration Digest, Volume 19, No. 4 Apr. 1987 p 10-16 (For primary document see N87-23818 17-31)
Avail: NTIS HC A04/MF A01

Recent developments in vehicle dynamics are discussed. Vehicle suspension systems, applications of multi-body dynamics problems in vehicle dynamics, rear steer, and special aspects of commercial vehicle dynamics are discussed. R.J.F.

N87-23821*# National Aeronautics and Space Administration. Lewis Research Center, Cleveland, Ohio.
PRELIMINARY PERFORMANCE CHARACTERIZATIONS OF AN ENGINEERING MODEL MULTIPROPELLANT RESISTOJET FOR SPACE STATION APPLICATION
W. Earl Morren, Stuart S. Hay (Purdue Univ., West Lafayette, Ind.), Thomas W. Haag, and James S. Sovey Jul. 1987 24 p Presented at the 23rd Joint Propulsion Conference, San Diego, Calif., 29 Jun. - 2 Jul. 1987; cosponsored by AIAA, SAE, ASME, and ASEE (NASA-TM-100113; E-3657; NAS 1.15:100113; AIAA-87-2120)
Avail: NTIS HC A02/MF A01 CSCL 20H

Presented are the results of a program to describe the operational characteristics of an engineering model multipropellant resistojet for application as an auxiliary propulsion system for the space station. Performance was measured on hydrogen, helium, methane, water (steam), nitrogen, air, argon, and carbon dioxide. Thrust levels ranged form 109 to 355 mN, power levels ranged from 167 to 506 W, and specific impulse values ranged from 93 to 385 sec, depending on the propellant, chamber pressure, and heater current level selected. Detailed thermal maps of the heater and heat exchanger were also obtained for operation with carbon dioxide. Author

32 COMMUNICATIONS AND RADAR

Includes radar; land and global communications; communications theory; and optical communications.

For related information see also *04 Aircraft Communications and Navigation* and *17 Space Communications, Spacecraft Communications, Command and Tracking.* For search and rescue see *03 Air Transportation and Safety,* and *16 Space Transportation.*

N87-23822# Naval Ocean Systems Center, San Diego, Calif.
A NEW VERSION OF MODESRCH USING INTERPOLATED VALUES OF THE MAGNETOIONIC REFLECTION COEFFICIENTS Interim Technical Report, Aug. 1980 - Jul. 1986

C. H. Shellman Aug. 1986 29 p
(AD-A179094; NOSC/TR-1143) Avail: NTIS HC A03/MF A01 CSCL 20N

For low frequency cases of nighttime propagation, an elevated antenna, or distances close to the transmitter, the propagation constants for a large number of modes must be found to adequately represent the fields in the earth-ionosphere waveguide. Most of the cost in using MODESRCH to obtain these mode constants has been in performing full wave integrations to obtain the approximate reflection matrix, R. Until recently it had been necessary to carry out several fullwave integrations each for R and its derivative with respect to the angle of incidence, theta, for each waveguide mode. As a result of this present effort it has become possible to obtain interpolated values of R which are more than adequate to describe the earth-ionosphere mode constants. The approach used is to transform the reflection matrix, R, obtained from a fullwave integration, into magnetoionic reflection coefficients, R sup oe. Each coefficient represents the complex amplitude of the ordinary or extraordinary. The equations defining the magnetoionic eigenvectors, which are required for this transformation, have been derived for the free space limit, so that they are applicable to a height that is below most of the ionization. GRA

N87-23823# Rome Air Development Center, Griffiss AFB, N.Y.
RECTANGULAR MICROSTRIP PATCH ANTENNA ARRAYS
Daniel A. Mullinix and Daniel T. McGrath Oct. 1986 60 p
(AD-A179170; RADC-TR-86-151) Avail: NTIS HC A04/MF A01 CSCL 09A

This report is oriented toward designing rectangular microstrip patch antenna arrays with corporate feed networks. It includes an explanation of the transmission line model for designing inset feed rectangular patch antennas and presents some very accurate results that were achieved in spite of the relative simplicity of the model. In addition, it presents a reactive power divider design that doesn't require much space, yet was near ideal in minimizing the input VSWR and providing equal phase and amplitude between the output ports. Finally, it presents a 4x4 array designed for 8 GHz which achieved near maximum gain with very little phase or amplitude error. Author (GRA)

N87-23824# Teledyne Geotechnical, Alexandria, Va.
FINITE DIFFERENCE SIMULATIONS OF RAYLEIGH WAVE SCATTERING BY 2-D ROUGH TOPOGRAPHY
K. L. McLaughlin and R. S. Jih Nov. 1986 63 p
(Contract F19628-85-C-0035)
(AD-A179190; TGAL-86-9; AFGL-TR-86-0269; SR-3) Avail: NTIS HC A04/MF A01 CSCL 08K

Rayleigh waves normally incident upon 2 D simple or rough topographic structures are simulated by the linear finite difference method to study the attenuation, transmission, and reflection of Rayleigh waves and to measure the Rayleigh-to-P and -SV bodywave conversion. For simple ramp structures, transmission, reflection, and scattering depend on the sign of change of slope of the topographic feature, as well as the ratio of the ramp height to the wavelength, h/lambda. Simple ramp structures produce back-scattered body-waves h greater than lambda, and forward-scattered body-waves for h less than lambda. The radiation patterns of P and S bodywaves are roughly consistent with the model of equivalent point forces along the free surface. More complicated topographic features generated by random Markov sequences have been characterized by the Rayleigh wave spatial Q(f). As expected, rougher topography attenuates Rayleigh waves more than smooth topography. P and S amplitudes ratios are consistent with radiation from equivalent point forces near the surface, but distribution of slownesses generated is greater than from the simple ramp structures. Reflection of Rayleigh waves by topographic slopes and by random topography is an inefficient process and the bulk of the energy that is not transmitted as Rayleigh waves is converted to bodywaves. Fundamental Rayleigh-to-Lg scattering and generation of teleseismic P coda by short period Rayleigh should be observable. GRA

N87-23825# Electronics Research Lab., Adelaide (Australia).
A NEW APPROACH TO MULTITARGET TRACKING USING PROBABILISTIC DATA ASSOCIATION
C. B. Colegrove Sep. 1986 38 p
(AD-A179437; ERL-0381-TR) Avail: NTIS HC A03/MF A01 CSCL 17I

This report develops the theory for a multitarget tracking algorithm based on Probabilistic Data Association with new selection rules for assigning sensor measurements to target track and for forming multitrack clusters. These new rules remove the requirement to form a gate about each target's predicted position for the selection of sensor measurements. The resultant algorithm is the same for all target tracks and clutter conditions. The algorithm adapts to the sensor measurements via probability terms which model the environment and sensor processing. GRA

N87-23826# Southern Methodist Univ., Dallas, Tex. Dept. of Electrical Engineering.
SPREAD SPECTRUM MOBILE RADIO COMMUNICATIONS Interim Report, 1 Apr. 1986 - 28 Feb. 1987
S. C. Gupta and S. S. Soliman 28 Feb. 1987 73 p
(Grant AF-AFOSR-0309-82)
(AD-A179446; AFOSR-87-0512TR) Avail: NTIS HC A04/MF A01 CSCL 17B

This report is made up of two parts. In the first part we present additional results on the performance of random access protocols for mobile packet radio networks. The effect of three different types of diversity reception in Nakagami fading environment on the channel throughput and the average packet delay of nonpersistent carrier sense multiple access (NPCSMA) protocol is considered. Expressions for the probability of packet error with diversity receptions are newly obtained for both independent and correlated diversity branches. A noncoherent frequency shift keying modulation scheme is assumed. In the second part a comprehensive study of the problem of synchronization over fading dispersive channels is presented. Synchronization is a fundamental problem in digital communications as used in mobile radio. In the first chapter, we consider a simple binary detection problem. The effect of receiver mismatch is investigated. A closed form expression for the probability of false alarm and probability of detection are given, also a set of curves are provided to demonstrate the amount of degradation for under-spread channels with some special scattering. GRA

N87-23827# Army Engineer Topographic Labs., Fort Belvoir, Va.
AUTOMATED RADAR IMAGE ANALYSIS RESEARCH IN SUPPORT OF MILITARY NEEDS
Frederick W. Rohde, Pi-Fuay Chen, and Richard A. Hevenor Oct. 1986 10 p
(AD-A179615; USAETL-R-092) Avail: NTIS HC A02/MF A01 CSCL 17I

Synthetic aperture radars (SAR) are high resolution radars that can be used for reconnaissance, surveillance, and terrain analysis. The high resolution in range and azimuth is achieved by pulse compression and phase history processing, respectively. SAR images have much in common with optical images such as aerial photographs. Both are characterized by tones, patterns, shapes, and shadows. There are, however, significant differences between SAR and optical images due to the differences in the wavelengths and in the illumination and reflection of the targets. Cloud cover presents an obstacle to optical imagery but not to SAR imagery because radar waves can penetrate cloud cover. Optical imagery provides more detailed information than SAR imagery because of its higher resolution. The resolution of optical imagery decreases with distance whereas the resolution of SAR imagery is independent of distance. For large distances, for example from satellites to the surface of the Earth, the resolution of SAR imagery approaches the resolution of optical imagery. These properties make SAR a very useful tool for military purposes. SAR systems can collect large quantities of imagery. For the timely and economic analysis and interpretation of SAR imagery there is a need for the development of automated and interactive capabilities that will

reduce the dependency on and requirements for highly trained image analysts. GRA

N87-23828*# Jet Propulsion Lab., California Inst. of Tech., Pasadena.
THE TELECOMMUNICATIONS AND DATA ACQUISITION REPORT Progress Report, Jan. - Mar. 1987
E. C. Posner, ed. 15 May 1987 123 p
(NASA-CR-181010; JPL-TDA-PR-42-89; NAS 1.26:181010) Avail: NTIS HC A06/MF A01 CSCL 17B

Archival reports on developments in programs managed by JPL's Office of Telecommunications and Data Acquisition (TDA) are provided. Activities of the Deep Space Network (DSN) in space communications, radio navigation, radio science, and ground-based radio astronomy are reported. Also included are the plans, supporting research and technology, implementation and operations for the Ground Communications Facility (GCF). In geodynamics, the publication reports on the application of radio interferometry at microwave frequencies for geodynamic measurements. In the search for extraterrestrial intelligence (SETI), it reports on implementation and operations for searching the microwave spectrum. For individual titles, see N87-23829 through N87-23840.

N87-23829*# Jet Propulsion Lab., California Inst. of Tech., Pasadena.
DSS 13 FREQUENCY STABILITY TESTS
T. Y. Otoshi and M. M. Franco *In its* The Telecommunications and Data Acquisition Report 15 May 1987 p 1-20 (For primary document see N87-23828 17-32)
Avail: NTIS HC A06/MF A01 CSCL 17B

In a previous article, the results of frequency stability tests at DSS 13 were presented in table form for tau = 1000 s for the test period May 1985 through March 1986. This article is a continuation of that initial report and presents specially selected Allan sigma (square root of variance) plots of each of the subsystem test previously reported. An additional result obtained from tests performed during July 1986 was included for completeness. The Allan sigma plots are useful in that frequency stability information is not only given for tau = 1000 s, but for tau values in the regions of 1, 100, 500, and 2000 s as well. Author

N87-23830*# Jet Propulsion Lab., California Inst. of Tech., Pasadena.
SPACECRAFT MASS TRADE-OFFS VERSUS RADIO-FREQUENCY POWER AND ANTENNA SIZE AT 8 GHz AND 32 GHz
C. E. Gilchriest *In its* The Telecommunications and Data Acquisition Report 15 May 1987 p 21-33 (For primary document see N87-23828 17-32)
Avail: NTIS HC A06/MF A01 CSCL 17B

The purpose of this analysis is to help determine the relative merits of 32 GHz over 8 GHz for future deep space communications. This analysis is only a piece of the overall analysis and only considers the downlink communication mass, power, and size comparisons for 8 and 32 GHz. Both parabolic antennas and flat-plate arrays are considered. The Mars Sample Return mission is considered in some detail as an example of the tradeoffs involved; for this mission the mass, power, and size show a definite advantage of roughly 2:1 in using the 32 GHz over 8 GHz.
Author

N87-23831*# Jet Propulsion Lab., California Inst. of Tech., Pasadena.
USE OF A 2.3-GHz TRAVELING-WAVE MASER ON THE USUDA 64-METER ANTENNA **c36**
D. Neff *In its* The Telecommunications and Data Acquisition Report 15 May 1987 p 34-40 (For primary document see N87-23828 17-32)
Avail: NTIS HC A06/MF A01 CSCL 20E

A 2.3 GHz traveling-wave maser/closed-cycle refrigeration system was installed on the 64 m antenna at Usuda, Japan. This was done to evaluate the beam-waveguide antenna noise performance, and to support the International Cometary Explorer's (ICE's) comet flyby mission. System noise temperature at 2270 MHz was measured to be 15 K, including the maser noise contribution of 2.5 K. Maser installation and noise performance are described. The Usuda 64 m antenna is of high quality with a system operating noise temperature better than the DSN 64 m antennas. Author

N87-23832*# Jet Propulsion Lab., California Inst. of Tech., Pasadena.
A VLSI SINGLE CHIP (255,223) REED-SOLOMON ENCODER WITH INTERLEAVER **c33**
I. S. Hsu, L. J. Deutsch, T. K. Truong, and I. S. Reed (University of Southern California, Los Angeles.) *In its* The Telecommunications and Data Acquisition Report 15 May 1987 p 41-47 (For primary document see N87-23828 17-32)
Avail: NTIS HC A06/MF A01 CSCL 09C

A single-chip implementation of a Reed-Solomon encoder with interleaving capability is described. The code used was adapted by the CCSDS (Consulative Committee on Space Data Systems). It forms the outer code of the NASA standard concatenated coding system which includes a convolutional inner code of rate 1/2 and constraint length 7. The architecture, leading to this single VLSI chip design, makes use of a bit-serial finite field multiplication algorithm due to E.R. Berlekamp. Author

N87-23833*# Jet Propulsion Lab., California Inst. of Tech., Pasadena.
DSN ADVANCED RECEIVER: BREADBOARD DESCRIPTION AND TEST RESULTS
D. H. Brown and W. J. Hurd *In its* The Telecommunications and Data Acquisition Report 15 May 1987 p 48-66 (For primary document see N87-23828 17-32)
Avail: NTIS HC A06/MF A01 CSCL 17B

A breadboard Advanced Receiver for use in the Deep Space Network was designed, built, and tested in the laboratory. Field testing was also performed during Voyager Uranus encounter at DSS-13. The development of the breadboard is intended to lead towards implementation of the new receiver throughout the network. The receiver is described on a functional level and then in terms of more specific hardware and software architecture. The results of performance tests in the laboratory and in the field are given. Finally, there is a discussion of suggested improvements for the next phase of development. Author

N87-23834*# Jet Propulsion Lab., California Inst. of Tech., Pasadena.
RESULTS OF USING THE GLOBAL POSITIONING SYSTEM TO MAINTAIN THE TIME AND FREQUENCY SYNCHRONIZATION IN THE DEEP SPACE NETWORK **c35**
P. A. Clements, A. Kirk, and R. Unglaub *In its* The Telecommunications and Data Acquisition Report 15 May 1987 p 67-72 (For primary document see N87-23828 17-32)
Avail: NTIS HC A06/MF A01 CSCL 14B

There are two hydrogen maser clocks located at each signal processing center (SPC) in the DSN. Close coordination of the time and frequency of the SPC clocks is needed to navigate spacecraft to the outer planets. A recent example was the Voyager spacecraft's encounter with Uranus in January 1986. The clocks were adjusted with the goal of minimizing time and frequency offsets between the SPCs at encounter. How time and frequency at each SPC is estimated using data acquired from the Global Positioning System Timing Receivers operating on the NBS-BIH (National Bureau of Standards-Bureau International de l'Heure) tracking schedule is described. These data are combined with other available timing receiver data to calculate the time offset estimates. The adjustment of the clocks is described. It was determined that long range hydrogen maser drift is quite predictable and adjustable within limits. This enables one to minimize time and frequency differences between the three SPCs for many months by matching the drift rates of the three standards. Data acquisition and processing techniques using a Kalman filter to make estimates of time and frequency offsets between the clocks

at the SPCs and UTC(NBS) (Coordinated Universal Time realized at NBS) are described. Author

N87-23835*# Jet Propulsion Lab., California Inst. of Tech., Pasadena.
MICROWAVE COMPONENT TIME DELAYS FOR THE 70-METER ANTENNAS
R. Hartop *In its* The Telecommunications and Data Acquisition Report 15 May 1987 p 73-76 (For primary document see N87-23828 17-32)
Avail: NTIS HC A06/MF A01 CSCL 17B

The X-band feed assemblies in the 64 meter antennas were redesigned to accommodate the upgrading to 70 meters and the associated surface reshaping. To maintain time delay data logs, new calculations were made of the microwave component delays for the XRO Mod IV X-band (8.4 to 8.45 GHz) feed assembly that was installed at DSS-63, and will soon be implemented at DSS-43 and DSS-14. Author

N87-23836*# Jet Propulsion Lab., California Inst. of Tech., Pasadena.
Z-CORRECTIONS FOR DSN 70-METER ANTENNA RANGING CALIBRATION
A. G. Cha *In its* The Telecommunications and Data Acquisition Report 15 May 1987 p 77-82 (For primary document see N87-23828 17-32)
Avail: NTIS HC A06/MF A01 CSCL 17B

The Z-corrections of the DSN 70 m dual-shaped reflector antennas are documented. These corrections to the group delay time measured by the translator are required before the 70 m antennas can be used for ranging. Author

N87-23837*# Jet Propulsion Lab., California Inst. of Tech., Pasadena.
BLOCK 3 X-BAND RECEIVER-EXCITER
C. E. Johns *In its* The Telecommunications and Data Acquisition Report 15 May 1987 p 83-93 (For primary document see N87-23828 17-32)
Avail: NTIS HC A06/MF A01 CSCL 17B

The development of an X-band exciter, for use in the X-Band Uplink Subsystem, was completed. The exciter generates the drive signal for the X-band transmitter and also generates coherent test signals for the S- and X-band Block 3 translator and a Doppler reference signal for the Doppler extractor system. In addition to the above, the exciter generates other reference signals that are described. Also presented is an overview of the exciter design and some test data taken on the prototype. A brief discussion of the Block 3 Doppler extractor is presented. Author

N87-23838*# Jet Propulsion Lab., California Inst. of Tech., Pasadena.
DUAL-POLARIZATION 8.45 GHz TRAVELING-WAVE MASER c36
R. B. Quinn *In its* The Telecommunications and Data Acquisition Report 15 May 1987 p 94-100 (For primary document see N87-23828 17-32)
Avail: NTIS HC A06/MF A01 CSCL 20E

An 8.5 GHz dual-channel, dual-polarization traveling-wave maser (TWM) amplifier was installed in the XKR solar system radar cone at DSS 14. The TWM is based on the Blk IIA 8.45 GHz maser structure, with two of the four maser stages being used for each channel, and each maser half then followed by a high-performance GaAs FET amplifier to achieve the desired net gain. A shortened low-noise input waveguide and an orthogonal-mode junction which is cooled to 4.5 K feeds each amplifier chain. The rotation of an external polarizer permits the polarization of each channel to be defined as either linear or circular. A circular waveguide switch was also developed to provide for noise calibration and to protect the maser from incident transmitter power. Author

N87-23839*# Jet Propulsion Lab., California Inst. of Tech., Pasadena.
AN INTERACTIVE WIRE-WRAP BOARD LAYOUT PROGRAM c33
A. Schlutsmeyer *In its* The Telecommunications and Data Acquisition Report 15 May 1987 p 101-107 (For primary document see N87-23828 17-32)
Avail: NTIS HC A06/MF A01 CSCL 09C

An interactive computer-graphics-based tool for specifying the placement of electronic parts on a wire-wrap circuit board is presented. Input is a data file (currently produced by a commercial logic design system) which describes the parts used and their interconnections. Output includes printed reports describing the parts and wire paths, parts counts, placement lists, board drawing, and a tape to send to the wire-wrap vendor. The program should reduce the engineer's layout time by a factor of 3 to 5 as compared to manual methods. Author

N87-23840*# Jet Propulsion Lab., California Inst. of Tech., Pasadena.
AN EVALUATION OF THE COMMUNICATION SYSTEM FOR THE TAU MISSION STUDY
B. D. Metscher *In its* The Telecommunications and Data Acquisition Report 15 May 1987 p 108-117 (For primary document see N87-23828 17-32)
Avail: NTIS HC A06/MF A01 CSCL 17B

The requirements for possible microwave and optical frequency communication systems to return 20 kbps from 1000 AU are compared and sample telemetry links are calculated. Microwave systems were found to have impractical parameter requirements, while the required optical system parameters are much more feasible. A first-level design of an optical communication link is presented; this design can be implemented with conservatively projected technology development. Optical background noise can be either tolerated or eliminated and it was found that TAU could detect a laser beacon from Earth even if Earth were in front of the Sun. Author

N87-23841# Sandia National Labs., Albuquerque, N. Mex.
MICROWAVE COUPLING INSIDE COMPLEX SYSTEMS
R. P. Toth and L. D. Bacon 1986 4 p Presented at the 3rd National Conference on High Power Microwave Technology for Defense Applications, Albuquerque, N. Mex., 1 Dec. 1986
(Contract DE-AC04-76DP-00789)
(DE87-003505; SAND-86-1785C; CONF-861240-15) Avail: NTIS HC A02/MF A01

In order to understand the parameters which contribute to microwave coupling phenomenon in complex systems, it is first necessary to investigate the problem using simple, easily modeled systems. To that goal, we define the term complex systems to mean hollow, cylindrically shaped test objects with one or more apertures and an internal sensor of known characteristics. Our objective in this work is to determine the effect of complex clutter inside a weapon system on the propagation of microwaves from their entry point to the terminals of vulnerable electronic subsystems. Our approach is to measure the response of representative geometries, using low-power CW illumination over the frequency range of 100 MHz to 18 GHz. We were particularly interested in the effect of lossy materials on the interaction of multiple apertures. DOE

N87-23842# Lawrence Livermore National Lab., Calif.
SCATTERING FROM AN OPEN SPHERICAL SHELL HAVING A CIRCULAR APERTURE AND ENCLOSING A CONCENTRIC DIELECTRIC SPHERE
R. W. Ziolkowski, D. P. Marsland, L. F. Libelo, and G. Pisane Feb. 1987 33 p Prepared in cooperation with Harry Diamond Labs., Adelphi, Md.
(Contract W-7405-eng-48)
(DE87-007099; UCRL-96074) Avail: NTIS MF A01

The generalized dual series solution to the scattering of an arbitrary plane wave from an open spherical shell having a circular aperture and enclosing a concentric, homogeneous dielectric

sphere is presented. This solution explicitly exhibits the correct edge behavior, and it can handle spheres that are electrically small or large without special considerations. A variety of cross-section results are presented for the normally incident case. It is shown that effects corresponding to the presence of the interior cavity dominate all of the scattering data. In particular, the cross-sections exhibit new resonance features that are due to the cavity-backed nature of the aperture and depend on the characteristics of the interior sphere. The results demonstrate that interior information is contained in the exterior scattering data.
DOE

N87-23843# Sandia National Labs., Albuquerque, N. Mex. Electromagnetic Applications Div.
SINGLE AND MULTIPLE ELECTROMAGNETIC SCATTERING BY DIELECTRIC OBSTACLES FROM A RESONANCE PERSPECTIVE
D. J. Riley Mar. 1987 127 p
(Contract DE-AC04-76DP-00789)
(DE87-007347; SAND-87-0011) Avail: NTIS HC A07/MF A01

A new application of the singularity expansion method (SEM) is explored. This application combines the classical theory of wave propagation through a multiple-scattering environment and the SEM. Because the SEM is generally considered to be a theory for describing surface currents on conducting scatterers, extensions are made which permit, under certain conditions, a singularity expansion representation for the electromagnetic field scattered by a dielectric scatterer. Application of this expansion is then made to the multiple-scattering case using both single and multiple interactions. A resonance scattering tensor form is used for the SEM description which leads to an associated tensor form for the solution to the multiple-scattering problem with each SEM pole effect appearing explicitly. The coherent field is determined for both spatial and SEM parameter random variations. A numerical example for the case of an ensemble of dielectric spheres which possess frequency-dependent loss is also made. Accurate resonance expansions for the single-scattering problem are derived, and resonance trajectories based on the Debye relaxation model for the refractive index are introduced. Application of these resonance expansions is then made to the multiple-scattering results for a slab containing a distribution of spheres with varying radii. Conditions are discussed which describe when the hybrid theory is appropriate.
DOE

N87-23844# Air Force Inst. of Tech., Wright-Patterson AFB, Ohio. School of Engineering.
ANALYSIS OF JITTER IN A DIGITAL TRANSMISSION SYSTEM M.S. Thesis
Michael R. Ownby Dec. 1986 92 p
(AD-A177945; AFIT/GE/ENG/86D-54) Avail: NTIS HC A05/MF A01 CSCL 17B

This work outlines a method for predicting the accumulation of timing jitter in a digital transmission system. Earlier works have concentrated on regenerative repeators or pulse-stuffing multiplexer/demultiplexers, as the sole source of jitter, without regard to the digital transmission system as a whole. Here, the timing jitter accumulation is evaluated from source to sink with almost any sequence of repeater chains, multiplexers, switches and demultiplexers in between. The basic model for the jitter accumulation are taken from earlier works, such as the 1963 paper by Bryne et al, Systematic Jitter in a Chain of Digital Repeaters and the 1972 paper by Duttweiller, Waiting Time Jitter. These models have been reworked to some degree to reflect more recent timing extraction circuitry, but are basically unchanged from their original derivations. The digital transmission system is treated as a series of jitter transfer and jitter generation components which can be analyzed sequentially. The jitter is assumed to be an additive, random process whose spectrum is peak-to-peak, unit intervals versus frequency.
GRA

N87-23845# Communications Research Centre, Ottawa (Ontario).
ANALYSIS OF SPACE-BASED RADAR CLUTTER SPECTRA OVER DIFFERENT TYPES OF TERRAIN AND THEIR EFFECTS ON DETECTION PERFORMANCE
D. Faubert, B. J. Rook, and W. Tam 21 Nov. 1986 47 p
(AD-A178066; CRC-1408) Avail: NTIS HC A03/MF A01 CSCL 17I

A computer model was used to make a detailed analysis of the clutter spectra received by real aperture Space-Based Radars orbiting over different types of terrain. The influence of terrain on L-band SBR detection performance has also been studied. It was found that the clutter spectra tend to become narrower as the grazing range of the antenna increases but that they broaden as the antenna points progressively more away from the direction of motion of the satellite. The interference caused by the clutter background is progressively higher for ice covered ground but smaller for a snow-covered terrain and the smallest for an ocean background. The minimum detectable velocities of the SBR were found to vary by a factor of up to three according to the terrain type.
GRA

N87-23846# Technology Service Corp., Silver Spring, Md.
RESULTS OF NEAR FIELD PROBE SCANNING TESTS FOR ULTRALOW SIDELOBE ARRAYS Final Report, 6 Jun. 1983 - Mar. 1986
Kenneth R. Grimm, John B. Hoffman, Allen C. Newell, and Michael H. Francis May 1986 194 p
(Contracts N00014-83-C-0671; N00014-83-F-0180)
(AD-A178141; TSC-W41-405/KKS) Avail: NTIS HC A09/MF A01 CSCL 20N

This report documents a unique Navy research program regarding fundamental measurement accuracy issues of near field antenna scanning. This work has accomplished both analytic studies and demonstration testing with very low sidelobe antennas. The program results have affirmed known relations between near field scanning errors and the resulting inaccuracies of the transformed far field sidelobe patterns. An existing planar near field scanner at the National Bureau of Standards in Boulder, Colorado has been modified to accept the large test antennas, and subsequently used for scanning tests with the AWACS phased array as well as a second experimental ultralow sidelobe slotted waveguide array. Results show that far field sidelobe accuracy is ultimately limited by uncontrollable random near field measurement error, multipath, and probe pattern directivity. A novel mainbeam nulling probe has been shown to increase measurement accuracy of wide angle sidelobes by greatly minimizing the error gain in the coupling product during scanning. Classical probe correction post-processing is then necessary to recover the improved sidelobe pattern, but with degraded accuracy in mainbeam directions. The new probe radiates a fixed-direction null aligned with test antennas steered mainbeam. Catalogs of available data and results from unclassified antenna scanning tests are given in appendices.
Author (GRA)

N87-23847# Massachusetts Inst. of Tech., Cambridge. Research Lab. of Electronics.
TIME DOMAIN WAVE PROPAGATION IN MULTILAYERED INTEGRATED CIRCUITS Semiannual Report, 1 Aug. 1986 - 31 Jan. 1987
J. A. Kong Jan. 1987 6 p
(Contract N00014-86-K-0533)
(AD-A178180) Avail: NTIS HC A02/MF A01 CSCL 09E

During this period, we have (1) modeled and calculated the impedance parameters and propagation characteristics of simple structures, (2) analyzed the transient response of signal transmission on strip lines with perpendicularly crossing strips geometry and (3) analyzed the transient response of point and line sources excitation in two-layer media, (4) generalized the method of characteristics for signal propagation on nonuniformly coupled transmission lines, and (5) studied the models for vias for interchip connections. Many integrated circuits contain strip lines at different heights that run parallel or perpendicular to each

other. First the capacitances associated with two offset parallel strips at different heights between ground planes are computed using the conformal mapping approach. As an extension, a simplified circuit of parallel-plate lines with transverse ridges is introduced to model two parallel strips with perpendicularly crossing strips on top. It was treated as a distributed circuit of transmission lines segments with periodical capacitive loading. In order to calculate the coupling between two lines, this structure was reduced to two equivalent single line circuits. GRA

N87-23848# Rit Research Corp., Rochester, N.Y.
IMPULSIVE EMI (ELECTROMAGNETIC INTERFERENCE) RADIATED BY ELECTROSTATIC DISCHARGES (ESD)
Perambur S. Neelakantaswamy Jan. 1987 25 p
(Contract N00014-84-K-0532)
(AD-A178213; RITRC-009; TR-9) Avail: NTIS HC A02/MF A01 CSCL 20N

Failure of equipment mounted devices due to indirect (noninvasive) energy transfer from the ESD via transient electromagnetic coupling/interference warrants a unique modeling as detailed in this report. GRA

N87-23849# Aerospace Corp., El Segundo, Calif. Space Sciences Lab.
AN ELF (EXTREMELY-LOW-FREQUENCY) TRANSMITTER EXPERIMENT FOR THE SPACE SHUTTLE. (THE NASC-201 (NAVAL AIR SPACE COMMAND) EXPERIMENT). VOLUME 1
Harry C. Koons 30 Sep. 1986 73 p
(Contract F04701-85-C-0086)
(AD-A178237; TR-0086(6940-06)-10-Vol-1; SD-TR-87-03-Vol-1) Avail: NTIS HC A04/MF A01 CSCL 17B

This report describes the design for a spaceborne ELF/VLF transmitter. The transmitter could be used for experiments to obtain the radiation data in a space plasma required to determine the feasibility of an ELF downlink communications system from a satellite to a subsurface antenna. The antenna is designed to be deployed by the Remote Manipulator Arm on the Space Shuttle. GRA

N87-23850# Michigan Univ., Ann Arbor. Radiation Lab.
MAGNETOSTATIC SURFACE FIELD MEASUREMENT FACILITY Final Report, Oct. 1982 - Jun. 1984
V. V. Liepa, D. L. Sengupta, and T. B. Senior Dec. 1986 137 p
(Contract F29601-82-K-0024)
(AD-A178258; AFWL-TN-86-29) Avail: NTIS HC A07/MF A01 CSCL 14B

This report presents the analysis, design, and performance characteristics of a Radio Frequency Helmholtz coil facility. The facility was developed to measure the magnetic response of models up to two feet in size. Test measurements were made on metallic spheres and cylinders, and on a model F 106 aircraft over a 1-25 MHz frequency range corresponding to 20-520 kHz full scale. A large portion of the report is devoted to the relevant theoretical studies that include studies of the magnetostatic response of canonical shapes, both perfectly and imperfectly conducting. GRA

N87-23851# Massachusetts Inst. of Tech., Cambridge. Lincoln Lab.
ADAPTIVE NOISE REDUCTION IN AIRCRAFT COMMUNICATION SYSTEMS
Jeffrey J. Rodriguez 20 Jan. 1987 56 p
(Contract F19628-85-C-0002)
(AD-A178267; TR-756; ESD-T-86-096) Avail: NTIS HC A04/MF A01 CSCL 01C

In many military environments, such as fighter jet cockpits, the increasing use of digital communication systems has created a need for robust vocoders and speech recognition systems. However, the high level of ambient noise in such environments makes vocoders less intelligible and makes reliable speech recognition more difficult. One method of enhancing the noise-corrupted speech is adaptive noise cancellation. In previous research, this method was tested in a simulated cockpit environment, yielding impressive results. However, in new simulations, reflecting more realistic conditions, adaptive noise cancellation has been less successful. Spectral analysis of the data shows that the spectral concentration of the ambient noise, along with the microphone characteristics, has a significant effect on the performance of adaptive noise cancellation. GRA

N87-23852# Illinois Univ., Urbana. Coordinated Science Lab.
SCATTERING BY A TRUNCATED PERIODIC ARRAY
W. L. Ko and R. Mittra Mar. 1987 54 p
(Contract N00014-84-C-0149)
(AD-A178285; UILU-ENG-87-2217) Avail: NTIS HC A04/MF A01 CSCL 20N

The scattering characteristics of a doubly periodic array of metallic patches is investigated in this paper from the point of view of determining the effect of truncating such a screen. The induced surface current on each patch of the array as well as the scattered far-field pattern of the truncated array are computed using the spectral-Galerkin method. The usefulness of the results for the truncated screen problem for the design of frequency selective surfaces (FSS) is discussed. GRA

N87-23853# Massachusetts Inst. of Tech., Cambridge. Lab. for Computer Science.
COMMUNICATION-EFFICIENT PARALLEL GRAPH ALGORITHMS
Charles E. Leiserson and Bruce M. Maggs Dec. 1986 28 p
(Contract N00014-80-C-0622)
(AD-A178286; MIT/LCS/TM-318) Avail: NTIS HC A03/MF A01 CSCL 09B

Communication bandwidth is a resource ignored by most parallel random-access machine (PRAM) models. This paper shows that many graph problems can be solved in parallel, not only with polylogarithmic performance, but with efficient communication at each step of the computation. We measure the communication requirements of an algorithm in a model called the distributed random-access machine (DRAM), in which communication cost is measured in terms of the congestion of memory accesses across cuts of an underlying network. The algorithms are based on a communication-efficient variant of the tree contraction technique. Author (GRA)

N87-23854# Virginia Univ., Charlottesville. Dept. of Electrical Engineering.
A MULTI USER RANDOM ACCESS COMMUNICATION SYSTEM FOR USERS WITH DIFFERENT PRIORITIES Technical Report, 1 Sep. 1986 - 31 Mar. 1987
P. P. Kazakos 11 Mar. 1987 33 p
(Contract N00014-86-K-0742)
(AD-A178372; UVA/525415/EE87/104) Avail: NTIS HC A03/MF A01 CSCL 17B

A multi user random access communication system with a population of two classes of users is considered. It is assumed that packets generated by users from different classes have different priorities. Fast moving users in a mobile communication system, or high priority users in a static environment, might be members of the high priority class. A binary feed back collision resolution algorithm is developed and both throughput and delay analysis are performed. Analytical results show that for the operation region of practical interest, the high priority class experiences significantly shorter delays, compared to the low priority one which maintains good delay characteristics. Author (GRA)

N87-23855*# Harvard Coll. Observatory, Cambridge, Mass.
ATMOSPHERIC PROPAGATION EFFECTS ON RADIO INTERFEROMETRY
J. L. Davis Apr. 1986 285 p
(Grants NAG5-538; NAG5-27571)
(AD-A178405; AFGL-TR-86-0243; SR-1) Avail: NTIS HC A13/MF A01 CSCL 20N

Very-long-baseline interferometry (VLBI) offers estimates of distances on the Earth of several thousand kilometers with

uncertainties of a few centimeters or less. Since the completion of the Mark III VLBI system, combining group-delay measurements at two widely separated frequency bands to estimate ionospheric refraction, the source of error that limits this accuracy has been thought to be refraction by the neutral atmosphere. The largest component of the radio refractive index of air is due to the dry atmosphere. The integrated effect of this component can be estimated accurately from the surface pressure for a signal arriving at the site from the zenith direction. For a signal arriving from other directions, a model for the atmosphere must be combined with surface meteorological measurements to estimate the propagation delay. The accuracy of this estimation is limited by the accuracy of the atmospheric model. The remaining component of the radio refractive index of air is due to water vapor, which in the lower troposphere is unmixed, and its effect on the group delay can vary from 0 to 20% of the effect of the dry atmosphere. The wet delay is very difficult to model using surface meteorological parameters. GRA

N87-23856*# Boeing Commercial Airplane Co., Seattle, Wash.
AIRCRAFT ELECTROMAGNETIC COMPATIBILITY Final Report, Sep. 1985 - Jun. 1987
Clifton A. Clarke and William E. Larsen (Federal Aviation Administration, Moffett Field, Calif.) Jun. 1987 146 p
(Contract NAS2-12261)
(NASA-CR-181051; NAS 1.26:181051; DOT/FAA/CT-86/40; D6-53840) Avail: NTIS HC A07/MF A01 CSCL 20N

Illustrated are aircraft architecture, electromagnetic interference environments, electromagnetic compatibility protection techniques, program specifications, tasks, and verification and validation procedures. The environment of 400 Hz power, electrical transients, and radio frequency fields are portrayed and related to thresholds of avionics electronics. Five layers of protection for avionics are defined. Recognition is given to some present day electromagnetic compatibility weaknesses and issues which serve to reemphasize the importance of EMC verification of equipment and parts, and their ultimate EMC validation on the aircraft. Proven standards of grounding, bonding, shielding, wiring, and packaging are laid out to help provide a foundation for a comprehensive approach to successful future aircraft design and an understanding of cost effective EMC in an aircraft setting. Author

N87-23857# Sandia National Labs., Albuquerque, N. Mex.
EVALUATION OF A THIN-SLOT FORMALISM FOR FINITE-DIFFERENCE TIME-DOMAIN ELECTROMAGNETICS CODES
C. D. Turner and L. D. Bacon Mar. 1987 22 p
(Contract DE-AC04-76DP-00789)
(DE87-008078; SAND-86-2196) Avail: NTIS HC A02/MF A01

A thin-slot formalism for use with finite-difference time-domain (FDTD) electromagnetics codes has been evaluated in both two and three dimensions. This formalism allows narrow slots to be modeled in the wall of a scatterer without reducing the space grid size to the gap width. In two dimensions, the evaluation involves the calculation of the total fields near two infinitesimally thin coplanar strips separated by a gap. A method-of-moments (MoM) solution of the same problem is used as a benchmark for comparison. Results in two dimensions show that up to 10% error can be expected in total electric and magnetic fields both near (lambda/40) and far (1 lambda) from the slot. In three dimensions, the evaluation is similar. The finite-length slot is placed in a finite plate and an MoM surface patch solution is used for the benchmark. These results, although less extensive than those in two dimensions, show that slightly larger errors can be expected. Considering the approximations made near the slot in incorporating the formalism, the results are very promising. Possibilities also exist for applying this formalism to wall of arbitrary thickness and to other types of slots, such as overlapping joints. DOE

N87-23858*# Georgia Inst. of Tech., Atlanta.
RESEARCH IN MILLIMETER WAVE TECHNIQUES Final Report
R. W. McMillan 17 Jun. 1987 83 p
(Grant NsG-5012)
(NASA-CR-181026; A-1642; NAS 1.26:181026) Avail: NTIS HC A05/MF A01 CSCL 20N

The areas of millimeter wave (MMW) research include atmospheric propagation and radiometry, advanced MMW component design with emphasis on quasi-optical techniques, and the development of MMW receivers, especially those using subharmonic mixers. Calculations of atmospheric attenuation and radiometric antenna temperature were made in the range 100 to 700 GHz, together with measurements of atmospheric antenna temperature near 95 and 183 GHz. Quasi-optical components designed include lenses, mirrors, and wire grid devices, as well as feedhorns for interference with waveguide components. Subharmonic mixers with state-of-the-art performance at 183 GHz were also developed. Each of these areas of research is summarized. B.G.

N87-23859# Advisory Group for Aerospace Research and Development, Neuilly-Sur-Seine (France). Avionics Panel.
MICROWAVE ANTENNAS FOR AVIONICS
Apr. 1987 161 p Lectures held in Rome, Italy, 7-8 May 1987; in Guenzburg, West Germany, 11-12 May 1987; and in Ankara, Turkey, 14-15 May 1987
(AGARD-LS-151; ISBN-92-835-1547-1) Copyright Avail: NTIS HC A08/MF A01

Even though considerable advances have been made in digital technology and signal processing, antennas continue to play a key role and their performance is often a dominating factor in defining the overall effectiveness of a system. New system requirements, and the need to provide electronic scanning cababilities have presented major challenges to the technology that require substantial improvements over what is currently available. Over the last decade there have been notable advances in antenna and radome design, particularly in sidelobe reduction, electronic scanning, conformal arrays, printed circuit arrays, adaptive control and millimeter wave antennas. Many of these issues are addressed. Future trends and new directions for technological innovation are subjects for round table discussions. For individual titles, see N87-23860 through N87-23867.

N87-23860# Rome Air Development Center, Hanscom AFB, Mass. Electromagnetics Directorate.
BASIC PARAMETERS OF ANTENNAS FOR AIRCRAFT, SATELLITES AND MISSILES
Robert J. Mailloux *In* AGARD Microwave Antennas for Avionics Apr. 1987 17 p (For primary document see N87-23859 17-32)
Copyright Avail: NTIS HC A08/MF A01

System requirements for airborne, satellite and missile antennas continue to place increasingly severe demands upon antenna technology. In general these requirements push toward the increased capability to control and modify antenna patterns, and away from the use of small antennas with broad radiation patterns. Increased control can imply several levels of added sophistication. At the lowest level it implies mechanical or electronic scanning of an antenna directive pattern, at the next level there are needs to produce precise low sidelobe radiation patterns, and at the highest level of complexity there is the need to actively suppress jammer interference through the use of adaptive control of a full array or an antenna with sidelobe cancellers. In addition to increased control, there is also a trend toward higher frequencies, even to EHF frequencies where arrays of several thousand elements are necessary for some applications. These needs and applications of antenna technology are examined. Author

N87-23861# Westinghouse Electric Corp., Baltimore, Md. Advisory Engineer-Antenna Development.
AIRCRAFT RADAR ANTENNAS
Helmut E. Schrank *In* AGARD Microwave Antennas for Avionics Apr. 1987 7 p (For primary document see N87-23859 17-32)
Copyright Avail: NTIS HC A08/MF A01

Many changes have taken place in airborne radar antennas since their beginnings over forty years ago. A brief historical review of the advances in technology is presented, from mechanically scanned reflectors to modern multiple function phased arrays.

However, emphasis is not on history but on the state-of-the-art technology and trends for future airborne radar systems. The status of rotating surveillance antennas is illustrated by the AN/APY-1 Airborne Warning and Control System (AWACS) slotted waveguide array, which achieved a significant breakthrough in sidelobe suppression. Gimballed flat plate arrays in nose radomes are typified by the AN/APG-66 (F-16) antenna. Multifunction phased arrays are presented by the Electronically Agile Radar (EAR) antenna, which has achieved significant advances in performance versatility and reliability. Trends toward active aperture, adaptive, and digital beamforming arrays are briefly discussed. Antennas for future aircraft radar systems must provide multiple functions in less aperture space, and must perform more reliably. Author

N87-23862# AEG-Telefunken, Ulm (West Germany). Radar Subdivision.
AIRCRAFT ANTENNAS/CONFORMAL ANTENNAS MISSILE ANTENNAS
Klaus Solbach *In* AGARD Microwave Antennas for Avionics Apr. 1987 16 p (For primary document see N87-23859 17-32)
Copyright Avail: NTIS HC A08/MF A01

Three major areas of airborne microwave antennas are examined. The basic system environment for missile telemetry/telecommand and fuze functions is sketched and the basic antenna design together with practical examples are discussed. The principle requirements of modern nose radar flat plate antennas are shown to result from missile/aircraft system requirements. Basic principles of slotted waveguide antenna arrays are sketched and practical antenna designs are discussed. The present early warning system designs are sketched to point out requirements and performance of practical radar warning and jamming antennas (broadband spiral antennas and horn radiators). With respect to newer developments in the ECM scenario, some demonstrated and proposed antenna systems (lens fed arrays, phased array, active array) are discussed. Author

N87-23863# TICRA A/S, Copenhagen (Denmark).
SPACECRAFT MULTI-BEAM AND CONTOURED-BEAM ANTENNAS
P. Balling *In* AGARD Microwave Antennas for Avionics Apr. 1987 23 p Sponsored in part by INTELSAT (For primary document see N87-23859 17-32)
Copyright Avail: NTIS HC A08/MF A01

High gain spacecraft antennas with multiple beams and contoured beams are key components in satellite communications and direct broadcast systems. This is reflected on the latest generation of communications satellites, where the antenna subsystem is the largest subsystem with its weight of more than 300 kg. The antennas achieved a large communications capacity through multiple frequency reuses and may be reconfigured to serve different coverage areas. The current multi-beam and contoured-beam antenna technology is reviewed. Different implementation, reflector or lens with feed array or direct radiating array, are considered. The emphasis is placed upon systems with offset paraboloidal reflectors. The limitations of the offset reflector with respect to beam scanning and cross polarization are reviewed. Computer aided design procedures and design examples are presented. Author

N87-23864# Army Communications-Electronics Command, Fort Monmouth, N.J.
MILLIMETER WAVE ANTENNAS FOR AVIONICS
Felix K. Schwering *In* AGARD Microwave Antennas for Avionics Apr. 1987 8 p (For primary document see N87-23859 17-32)
Copyright Avail: NTIS HC A08/MF A01

An overview of the area of mm-wave antennas is presented with emphasis on possible avionics applications. For the purpose of the review, mm-wave radiating structures are grouped into two classes: antennas of conventional configuration and antennas based on new design concepts. The first class is composed of well known antennas such as reflector, lens, horn and slotted waveguide antennas. The second class includes radiating structures such as printed circuit mm-wave antennas, antennas derived from open mm-waveguides, and integrated antennas. Some of these antennas have microwave counterparts, others are new with no microwave heritage. Millimeter wave antennas are usually of very reasonable size and weight, and some of these antennas are suitable for rapid mechanical scanning. They should be sufficiently versatile to satisfy most avionics requirements. Atmospheric propagation conditions vary strongly throughout the mm-wave band and have to be taken into account in the design of mm-wave systems and their antennas. A brief summary of these effects is included. Author

N87-23865# Standard Telephones and Cables Ltd., Paignton (England).
ADAPTIVE ANTENNAS
P. Barton *In* AGARD Microwave Antennas for Avionics Apr. 1987 21 p (For primary document see N87-23859 17-32)
Copyright Avail: NTIS HC A08/MF A01

The basic principles of adaptive antennas are outlined in terms of the Wiener-Hopf expression for maximising signal to noise ratio in an arbitrary noise environment; the analogy with generalised matched filter theory provides a useful aid to understanding. For many applications, there is insufficient information to achieve the above solution and thus non-optimum constrained null steering algorithms are also described, together with a summary of methods for preventing wanted signals being nulled by the adaptive system. The three generic approaches to adaptive weight control are discussed; correlation steepest descent, weight perturbation and direct solutions based on sample matrix conversion. The tradeoffs between hardware complexity and performance in terms of null depth and convergence rate are outlined. The sidelobe cancellor technique is described. Performance variation with jammer power and angular distribution is summarized and the key performance limitations identified. The configuration and performance characteristics of both multiple beam and phase scan array antennas are covered, with a brief discussion of performance factors. Author

N87-23866# Communications Research Centre, Ottawa (Ontario).
MIC TECHNOLOGY FOR PHASED ARRAYS
R. Douville *In* AGARD Microwave Antennas for Avionics Apr. 1987 19 p (For primary document see N87-23859 17-32)
Copyright Avail: NTIS HC A08/MF A01

The technology and performance of typical transmit receive (T/R) modules which include the basic elements of a phase shifter, a low noise amplifier, and a high power amplifier is emphasized. An overview is given of microwave integrated circuits (MICs) technology with respect to its use in phased array systems for military applications. Historically, the term MIC has been used to refer to planar microwave circuits using one or more different forms of printed transmission lines, all characterized by their ability to be photoetched on a suitable dielectric substrate. Active and passive discrete components such as transistors, chip capacitors and resistors are then attached. This technology is more precisely referred to as hybrid MIC (HMIC). The field of MIC design is currently undergoing a major revolution due to the rapid emergence of monolithic MIC (MMIC) design. In this latter, all components, including the active devices, are fabricated using deposition and etching processes, thereby eliminating the need for attachment of discrete components. These technologies are discussed with respect to their potential in phased array antennas. E.R.

N87-23867# Massachusetts Univ., Amherst. Dept. of Electrical and Computer Engineering.
PRINTED CIRCUIT ANTENNA TECHNOLOGY **c33**
Daniel H. Schaubert *In* AGARD Microwave Antennas for Avionics Apr. 1987 15 p (For primary document see N87-23859 17-32)
Copyright Avail: NTIS HC A08/MF A01

Printed circuit antennas are being used on a variety of spacecraft, aircraft, and projectiles where their low profile and conformability minimize interference with the structural and aerodynamic properties of the vehicle. The basic microstrip antenna has been studied extensively, but some important aspects of its

performance are not yet characterized by the analyses that are available to the designer. Furthermore, new applications in millimeter wave monolithic phased arrays are forcing the designer to use substrates that are electrically thick and that may have a high permittivity. Several characteristics of microstrip antennas are described and some that are being studied with the aim of improving antenna performance are identified. A brief description of analysis techniques available to the designer and researcher are presented. Finally, several aspects of monolithic and integrated phased arrays are considered. General properties of these arrays are discussed, and then several architectures and their associated printed circuit radiators are presented. Author

33 ELECTRONICS AND ELECTRICAL ENGINEERING

Includes test equipment and maintainability; components, e.g., tunnel diodes and transistors; microminiaturization; and integrated circuitry.

For related information see also *60 Computer Operations and Hardware* and *76 Solid-State Physics.*

N87-23868# Stanford Univ., Calif. Labs. of Physics.
PICOSECOND OPTICAL ELECTRONICS Final Report, 1 Jul. 1984 - 30 Jun. 1985
D. M. Bloom Apr. 1986 50 p
(Grant AF-AFOSR-0139-84)
(AD-A179061; AFOSR-87-0294TR) Avail: NTIS HC A03/MF A01 CSCL 17E

An electrooptic (EO) sampling system suitable for high speed measurements on gallium arsenide (GaAs) integrated circuits (IC's) was developed. This measurement technique is based on the linear electrooptic effect in GaAs. Using a longitudinal probing geometry, sub bandgap energy infrared light is passed through the substrate of a GaAs IC, reflected off some circuit metallization, and passed through a polarizer, resulting in an intensity change of the light past the polarizer proportional to the voltage across the substrate. GRA

N87-23869# Air Force Inst. of Tech., Wright-Patterson AFB, Ohio. School of Engineering.
VHDL (VHSIC (VERY HIGH SPEED INTEGRATED CIRCUITS) HARDWARE DESCRIPTIVE LANGUAGES) PROTOTYPE SIMULATOR M.S. Thesis
William L. Lynch, Jr. Dec. 1986 143 p
(AD-A179073; AFIT/GCS/ENG/86D-15) Avail: NTIS HC A07/MF A01 CSCL 09B

This research effort studied, modeled and implemented a prototype simulator kernel for VHDL in a UNIX environment. The prototype simulator was written in the C programming language. The detailed design of the prototype simulator includes an installation guide, users manual, and design description. The simulation program, called VSIM for VHDL simulator, does not support the full capabilities of VHDL. It implements the simple signal assignment statement and models transport and inertial delay. Requirement specifications are given for both the prototype and a fully implemented VHDL simulator. GRA

N87-23870# Energy Research Corp., Danbury, Conn.
AIRCRAFT BATTERY STATE OF CHARGE AND CHARGE CONTROL SYSTEM Interim Report, 1 Jul. 1985 - 30 Jun. 1986
Sivaswamy Viswanathan and Allen Charkey Apr. 1987 71 p
(Contract F33615-84-C-2435)
(AD-A179086; AFWAL-TR-86-2114) Avail: NTIS HC A04/MF A01 CSCL 10B

This Interim Report describes work done by Energy Research Corporation (ERC) in developing an aircraft battery state-of-charge indicator and charge control system. The basis for this system, developed by ERC, is a nickel-oxygen (NiO2) pilot cell (0.374 Ah). This pilot cell is cycled in tandem with a nickel-cadmium battery. The oxygen pressure of the pilot cell is used to determine and control the state-of-charge of the nickel-cadmium battery. Nickel-cadmium batteries from different manufacturers were cycled using this pilot cell charge indication and control system. The performance of the pilot cell and a nickel-cadmium battery as a function of temperature were separately determined. GRA

N87-23871# Air Force Inst. of Tech., Wright-Patterson AFB, Ohio. School of Engineering.
INVESTIGATION OF ELECTROMIGRATION IN THIN FILM ALUMINUM AT LOW TEMPERATURES M.S. Thesis
David W. Banton 19 Dec. 1986 109 p
(AD-A179110; AFIT/GE/ENG/86D-21) Avail: NTIS HC A06/MF A01 CSCL 09A

Collected are electromigration induced time to failure data from unglassed and glassed one percent silicon doped aluminum test patterns at four current densities: 4.5, 4.75, 5.5, and 6.25 mega-amps/sq cm. At 4.5 mega-amps/sq cm, unglassed pattern time to failure data is collected between -13 and 70 C. The activation energy is calculated to be approx 0.3 electron-volts. At 4.75 mega-amps/sq cm, unglassed pattern time to failure data is collected between -50 and 80 C. The activation energy is calculated to be approx 0.3 electron-volts between 10 and 80 C. At 5.5 mega-amps/sq cm, unglassed pattern time to failure data is collected between -50 and 20 C. The activation energy is calculated to be between 0.35 and 0.43 volts for temperatures between -7 and 20 C. At 6.25 mega-amps/sq cm, glassed pattern time to failure data is collected between -13 and 80 C. The activiation energy is calculated to be approx 0.3 electronvolts at temperatures between 20 and 80 C. These ranges of activation energies indicate that surface electromigration is the dominant failure mechanism. GRA

N87-23872# Stanford Univ., Calif. Center for Integrated Systems.
RESEARCH IN VLSI SYSTEMS Technical Progress Report, Apr. - Dec. 1986
John Hennessy Dec. 1986 63 p
(Contracts MDA903-84-K-0062; MDA903-83-C-0335; MDA903-80-C-0432; DARPA Order-3773-6)
(AD-A179227) Avail: NTIS HC A04/MF A01 CSCL 09B

This report summarizes progress in the DARPA funded VLSI Systems Research Projects. The major areas under investigation have included: analysis and synthesis design aids, applications of VSLI, special purpose chip design, VLSI computer architectures, reliability studies, hardware specification and verification, and VLSI fabrication. The major research problems are introduced and progress is discussed; the Appendix contains a list of published research papers from these projects. GRA

N87-23873# Texas Univ., Austin. Microwave Lab.
FINITE ELEMENT ANALYSIS OF SLOW-WAVE SCHOTTKY CONTACT PRINTED LINES Technical Report, 1 Nov. 1985 - 1 Nov. 1986
Ching-Kuang C. Tzuang, Dean P. Neikirk, and Tatsuo Itoh 16 Feb. 1987 54 p
(Grant AF-AFOSR-0036-86)
(AD-A179259; CMW-87-P-2; AFOSR-87-0481TR) Avail: NTIS HC A04/MF A01 CSCL 09C

Extensive finite element analyses on MMIC (monolithic microwave integrated circuit) slow wave structures with both localized and layered models are presented. Good agreement is achieved for results obtained in this paper with other theoretical results and experiments. Higher order elements that improve accuracy are discussed. The comparative studies for the Schottky contact microstrip and the coplanar waveguide with localized and layered models are presented. Potential applications of the localized models to more general and practical slow wave circuits are also discussed. GRA

N87-23874# Kimball Physics, Inc., Wilton, N.H.
HIGH-CURRENT ELECTRON GUN FOR SPACE FLIGHT Final Technical Report, 17 Sep. 1985 - 31 Aug. 1986
G. Dyer 31 Aug. 1986 37 p
(Contract F19628-85-C-0101)

(AD-A179287; AFGL-TR-86-0217) Avail: NTIS HC A03/MF A01 CSCL 09A

The feasibility of a conventional triode electron gun and the construction of a duoplasmatron electron gun for use on rocket and space shuttle flights. The ideal gun would be capable of modulation up to 50 kHz, capable of beam currents of several tens of amperes, and capable of beam energies from 1 keV to 50 keV. A module of such a triode electron gun was tested in a configuration as close to the flight arrangement as possible, keeping in mind the need for flexibility and experimentation. The structure was a triode arrangement with four separate cathodes and control grids. The results indicate that this type of approach is ultimately limited by fundamental space charge and current density considerations, rather than by the mechanical difficulties of gun design. The triode gun was able to deliver from one of its four cathodes pulses of electrons with an energy beam of 5 KeV and a fully or partially modulated current from 1.5 A down to 4mA. One of the four cathodes was operated continuously in a tetrode configuration with a 1 keV beam energy while the current was square-wave modulated from 0 to 500 kHz producing from 1 mA to 450 mA. GRA

N87-23875# Kimball Physics, Inc., Wilton, N.H.
HIGH CURRENT ELECTRON GUN FOR SPACE FLIGHT Final Technical Report, Sep. 1985 - May 1986
G. Dyer Dec. 1986 26 p
(Contract F19628-85-C-0090)
(AD-A178467; RADC-TR-86-184) Avail: NTIS HC A03/MF A01 CSCL 09A

The purpose of this project is to develop a high energy, high current electron gun capable of modulation up to 100 kHz for use in rocket and space shuttle flights. The energy capability ideally should cover the 1 keV to 50 KeV range while the current capability should be several tens of amperes. A module of such an electron gun was constructed on a 4.5 inch Conflat flange. The configuration was as close to the final flight arrangement as possible, keeping in mind the need for flexibility and experimentation. The structure was a triode arrangement with four separate cathodes and control grids. This was changed to a tetrode after early experiments. Results indicate that this type of approach is ultimately limited by fundamental space charge and current density considerations, rather than by the mechanical difficulties of gun design. At 1 keV beam energy, the maximum beam current density possible within the gun was 0.3 A/sq. cm. Delivery of this beam onto a target of more than 1 cm away proved impossible. GRA

N87-23876# Department of Energy, Washington, D. C.
WORLDWIDE NICKEL/IRON BATTERY DEVELOPMENT FOR ELECTRIC VEHICLE APPLICATIONS
P. G. Patil, W. J. Walsh, and J. F. Miller 1986 5 p Presented at the 8th International Electric Vehicle Symposium, Washington, D.C., 20 Oct. 1986 Prepared in cooperation with Argonne National Lab., Ill.
(Contract W-31-109-eng-38)
(DE87-004822; CONF-8610122-11) Avail: NTIS HC A02/MF A01

Worldwide efforts to develop Ni/Fe batteries for EV applications are summarized. Research, development, and testing activities in the United States, France, West Germany, Sweden, Czechoslovakia, Russia, Taiwan and Japan are described. Recent technology advances are discussed, and the present state-of-art capability is summarized. Advanced Ni/Fe batteries have exhibited good performance and a service life of 50,000 to 100,000 miles is expected by most developers. Ni/Fe batteries have been tested extensively in electric vehicles in the USA, Japan, Western Europe, and the USSR with generally good results. The present R and D directions of the various developers are described. DOE

N87-23877# Los Alamos National Lab., N. Mex.
A PULSED ELECTRON INJECTOR USING A METAL PHOTOCATHODE IRRADIATED BY AN EXCIMER LASER
T. J. Kauppila, L. A. Builta, J. K. Crutcher, J. C. Elliott, and D. C. Moir 1987 3 p Presented at the Particle Accelerator Conference, Washington, D.C., 16 Mar. 1987
(Contract W-7405-eng-36)
(DE87-007499; LA-UR-87-810; CONF-870302-61) Avail: NTIS HC A02

The hot cathode of an electron gun is replaced by a metallic photocathode driven by an excimer laser. The current, current density, and emittance of the 500-kV electron beam produced by the photoelectron source are presented. In addition, the temperature of the photocathode is varied to study the possibility of a hybrid source. DOE

N87-23878# Colorado Univ., Boulder.
INVESTIGATIONS ON THE IMPACT OF VOLTAGE AND CURRENT HARMONICS ON END-USE DEVICES AND THEIR PROTECTION Summary Report, 1 Jan. 1980 - 30 Jun. 1986
E. F. Fuchs Jan. 1987 14 p
(Contract DE-AC02-80RA-50150)
(DE87-008018; DOE/RA-50150/23) Avail: NTIS HC A02

After defining the relation between harmonic voltages and currents through harmonic impedances, the impact of harmonics on electromagnetic end-use devices such as transformers and machines is formulated based on analytical and experimental investigations. A harmonic factor representing the square of a weighted total harmonic distortion factor provides a mechanism for estimating the reduction of lifetime of electromagnetic end-use devices due to additional losses generated by sets of harmonics of frequencies below 2000 Hz. The forces and torques of saturable three-phase induction machines during starting and steady-state operation are computed from magnetic field solutions. Within the above frequency range the accuracy of induction watthour meters is reduced and the impact of harmonics or fractional harmonics (which exhibit a frequency other than those of harmonics and subharmonics) on distribution system relays can be severe. Also, the performance of television sets deteriorates for fractional harmonics below 2000 Hz. The impact of harmonics on shunt capacitors limits the harmonic amplitudes with frequencies above 2000 Hz. Depending upon the size of the system impedance either the harmonic voltages or the harmonic currents will be predominant. For small impedances the values of the harmonic currents will be limited by the permissible harmonic current loading of pole and substation transformers, whereas for large impedances the harmonic voltage amplitudes will be limited by the permissible additional losses in parallel connected electromagnetic end-use devices. The propagation of harmonics within a distribution feeder is such that for dispersed harmonic sources of the same kind no significant canceling of harmonic amplitudes occurs. Under certain circumstances the propagation of harmonics within a distribution feeder can cause resonances. DOE

N87-23879* National Aeronautics and Space Administration. Pasadena Office, Calif.
FLOATING EMITTER SOLAR CELL Patent
Sah Chih, inventor (to NASA) and Li-Jen Cheng, inventor (to NASA) (Jet Propulsion Lab., California Inst. of Tech., Pasadena.) 12 May 1987 12 p Filed 11 Mar. 1986 Supersedes N86-24908 (24 - 15, p 2450)
(NASA-Case-NPO-16467-1-CU; US-Patent-4,665,277; US-Patent-Appl-SN-838648; US-Patent-Class-136-255; US-Patent-Class-136-249; US-Patent-Class-357-30; US-Patent-Class-357-35) Avail: US Patent and Trademark Office CSCL 09A

A front surface contact floating emitter solar cell transistor is provided in a semiconductor body (n-type), in which floating emitter sections (p-type) are diffused or implanted in the front surface. Between the emitter sections, a further section is diffused or implanted in the front surface, but isolated from the floating emitter sections, for use either as a base contact to the n-type semiconductor body, in which case the section is doped n+, or as a collector for the adjacent emitter sections. NASA

N87-23880# Argonne National Lab., Ill.
LOW-RESISTIVITY GLASS ELECTROLYTES FOR SODIUM-SULFUR CELLS

I. Bloom, G. H. Kucera, J. Bradley, P. A. Nelson, and M. F. Roche 1986 17 p Presented at the Electrochemical Society Fall Meeting, San Diego, Calif., 19 Oct. 1986
(Contract W-31109-eng-38)
(DE87-004837; CONF-861068-18) Avail: NTIS HC A02/MF A01

Twenty-three glasses in the soda-alumina-zirconia-silica system were prepared and characterized in terms of resistivity, activation energy for conduction, and glass transition temperature. In the high-soda region of the system, 40 to 42 mol % soda, the glasses were found to possess resistivities in the range of 130 to 160 ohm-cm at 300 C. The additives, Al2O3 and ZrO2, were found to improve the conductivity of the glasses as well as their chemical stability toward Na, Na2S4, S, and Na2S4 (400 C for 1000 h). The high-soda quaternary glasses were found to have chemical stabilities comparable to those of the Dow borate glass and Ceramatec beta' -alumina. Thermal expansion coefficients of selected high-soda glasses are in the range of 16 to 19 x 10 to the 6th power deg C. Based on these results, the following glass composition has been selected for further testing (in mol %): 42 Na2O, 8 Al2O3, 5 ZrO2, and 45 SiO2. Using this glass, preliminary cell performance calculations indicate the potential for very high specific power and specific energy. DOE

N87-23881# Sandia National Labs., Albuquerque, N. Mex.
COST REDUCTIONS IN THE NICKEL/HYDROGEN BATTERY
R. L. Beauchamp and J. F. Sindorf 1987 14 p Presented at the Space Electrochemical Research and Technology Conference, Cleveland, Ohio, 14 Apr. 1987 Prepared in cooperation with Johnson Controls, Inc., Milwaukee, Wis.
(Contract DE-AC04-76DP-00789)
(DE87-007576; SAND-87-7100C; CONF-8704101-2) Avail: NTIS HC A02/MF A01

Significant progress has been made toward the development of a commercially marketable hydrogen/nickel oxide battery. The costs projected for this battery are remarkably low when one considers where we are on the learning curve for commercialization of this system. Further developmental efforts on this project are warranted as the H2/NiO battery is already cost competitive with other battery systems. DOE

N87-23882# Chrysler Corp., Huntsville, Ala. Military-Public Electronic Systems Div.
ADVANCED DC MOTOR CONTROLLER Final Report
1987 277 p
(Contract DE-AC08-83NV-10336)
(DE87-007756; DOE/NV-10336/1) Avail: NTIS HC A13

This report has been prepared to document the work conducted under a Department of Energy contract wherein a high frequency, filtered, DC Motor Controller (DCMC) has been developed which includes facilities for complete electric vehicle systems control. The system features a microprocessor controlled, high frequency, filtered, transistorized motor controller which includes RUN, REGENERATION and CHARGER functions. Also included are all necessary controls and sensors for complete control of an electric vehicle. The unit is totally contained in a 90 pound enclosure. This report details the design and test results of the DCMC system. DOE

N87-23883# Sandia National Labs., Albuquerque, N. Mex.
WETTING PROPERTIES OF Au/Sn SOLDERS FOR MICROELECTRONICS
K. A. Peterson and C. B. Williams 1987 9 p Presented at the 3d Annual Electronic Packaging Conference, Minneapolis, Minn., 27 Apr. 1987
(Contract DE-AC04-76DP-00789)
(DE87-008519; SAND-86-1904C; CONF-870486-2) Avail: NTIS HC A02

Hermetic sealing of microelectronic packages with Au/Sn solder is critically dependent upon good wetting. In studying specific problems in hermetic sealing, a solderability test based on ASTM standard F-357-78 has proven useful. The test has helped isolate and quantify the effects of contamination due to epoxy die attach and related handling, thermal preconditioning of packages, gold plating thickness, time and temperature during sealing, and solder alloy composition as they affect wetting. Some differences in hardware have been documented between manufacturing lots, but the overriding factors have been contamination which occurs during packaging process flows and thermal preconditioning during processing. The paper includes a review of metallurgical aspects of soldering to a non-inert surface and an examination of microstructural differences in seal joints. The results also quantify the conventional wisdom that alloys which are on the tin-rich side of the eutectic composition offer superior wetting properties. DOE

N87-23884# Severn Communications Corp., Severna Park, Md.
COMPARISON OF CREME (COSMIC RAY EFFECTS ON MICROELECTRONICS) MODEL LET (LINEAR ENERGY TRANSFER) SPACEFLIGHT DOSIMETRY DATA
John R. Letaw and James H. Adams, Jr. 15 Jul. 1986 26 p
(Contract N00014-85-C-2200)
(AD-A177873; SCC-86-01) Avail: NTIS HC A03/MF A01 CSCL 18F

The galactic cosmic radiation (GCR) component of space radiation is the dominant cause of single event phenomena in microelectronic circuits when Earth's magnetic shielding is low. Spaceflights outside the magnetosphere and in high inclination orbits are examples of such circumstances. In high inclination orbits, low energy (high LET) particles are transmitted through the field only at extreme !atitudes, but can dominate the orbit-averaged dose. GCR is an important part of the radiation dose to astronauts under the same conditions. As a test of the CREME environmental model and particle transport codes used to estimate single event upsets, we have compiled existing measurements of HZE doses where GCR is expected to be important: Apollo 16 and 17, Skylab, Apollo Soyuz Test Project, and Kosmos 782. The LET spectra, due to direct ionization from GCR, for each of these missions has been estimated. The resulting comparisons with data validate the CREME model predictions of high LET galactic cosmic ray fluxes to within a factor of two. Some systematic differences between the model and data are identified. GRA

N87-23885# Stanford Univ., Calif. Electronics Lab.
JSEP (JOINT SERVICES ELECTRONICS PROGRAM) Final Annual Report, 1 May 1985 - 30 Apr. 1986
James S. Harris 30 Apr. 1986 39 p
(Contract DAAG29-85-K-0048)
(AD-A177881; AD-E950921) Avail: NTIS HC A03/MF A01 CSCL 20L

A report of the Joint Services Electronics Program contains the following items: Quantum Well and Reduced Dimensional Semiconductor Systems; The Chemical and Electronic Structure of Refractory Metal GaAs Interfaces; The Study of Crystal Properties using Channeling Radiation; Ultra-Submicron Devices; Complementary MOS Device and Material Physics at 77K; and Real Time Signal Processing. GRA

N87-23886# Stanford Univ., Calif. Computer Systems Lab.
A SINGLE CHIP LSI HIGH-SPEED FUNCTIONAL TESTER
Jun-ichi Miyamoto and Mark A. Horowitz 16 Sep. 1986 8 p
(Contract MDA903-83-C-0335)
(AD-A177886; AD-E950921) Avail: NTIS HC A02/MF A01 CSCL 09E

A new architecture for the single chip tester, DGR, will be proposed. It generates test vectors designated by the internal memory data, and simultaneously detects the Device Under Test (DUT) data, being overwritten on that memory. A prototype chip, designed in a 3-micron CMOS technology, contains 64.5K transistors in a die size of 9.2mm by 7.9mm, and dissipates less than 300mW at an operating frequency of 10MHz. GRA

N87-23887# Stanford Univ., Calif. Computer Systems Lab.
A VLSI CMOS CIRCUIT DESIGN TECHNIQUE TO AID TEST GENERATION
Dick L. Liu and Edward J. McCluskey 1986 5 p

(Contract MDA903-83-C-0335)
(AD-A177934) Avail: NTIS HC A02/MF A01 CSCL 09E

This paper describes a new design technique for fully-testable CMOS combinational circuits and a 3-pattern test scheme to detect switch-level (stuck-open and stuck-on) faults. A fully-testable combinational circuit is implemented with specially designed gates that have no undetectable stuck-on faults. Switch-level faults in this type of combinational circuit can be detected with a 3-pattern test scheme. These 3-pattern tests are easy to generate with a gate-level automatic test pattern generator (ATPG) that offers better performance than a switch-level ATPG. GRA

N87-23888# Naval Underwater Systems Center, New London, Conn.
THREE-DIMENSIONAL ELECTRIC FIELD PREDICTIONS OF AN IRON-COPPER GALVANIC COUPLE Final Report, Oct. 1985 - Oct. 1986
Rolf G. Kasper 18 Feb. 1987 31 p
(AD-A178040; NUSC-TR-7849) Avail: NTIS HC A03/MF A01 CSCL 20C

Based on completed experimental electric field scans and the corresponding finite element field predictions, it appears that the finite element numerical technique presents a strong analytical tool in calculating the nearfield electric intensity distributions about active microcells. These calculations were analytically achieved with the new double membrane finite element configuration representing nonlinear polarization and with a local tangent slope (impedance) definition dependent on the local potential difference. The experimental determination of the multidimensional current density structure was realized with a newly developed scanning vibrating electrode technique (SVET). The finite element model developed in this paper uses a priori measured uncoupled polarization curves for pure iron and pure copper. The current densities and the electric field intensities were calculated in the X, Y, and Z directions within specific regions of the electrolyte and on its boundaries. Results appear to indicate that first-order anodic mass loss can be predicated using (1) numerically predicted current density distributions on the anodic surface and (2) Faraday's law. The electric field correlation established in this work for the three-dimensional current density components provides the confidence to proceed in the evaluation of time-dependent effects of electric fields and multipolarized surfaces associated with pitting and crevice corrosion. GRA

N87-23889# Illinois Univ., Urbana. Coordinated Science Lab.
COMPLEXITIES OF LAYOUTS IN THREE-DIMENSIONAL VLSI (VERY LARGE-SCALE INTEGRATION) CIRCUITS
Mokhtar A. Aboelaze and Benjamin W. Wah Feb. 1987 26 p
(Contract N00014-84-C-0149)
(AD-A178150; UILU-ENG-87-2212; CSG-63) Avail: NTIS HC A03/MF A01 CSCL 09E

Recent advances in Very Large-Scale Integration (VLSI) fabrication technologies have demonstrated the feasibility of three-dimensional (3-D) circuits in a single chip. Due to the ability and flexibility to connect non-adjacent circuits using the third dimension, the cost of mapping non-planar circuits to two-dimensional (2-D) systems can be reduced. In this report, we examine the complexities in volume and maximum wire length of mapping circuits represented as undirected graphs to 3-D systems. Tighter bounds than those previously known are shown for various families of graphs, in both the one-active-layer and the unrestricted layouts. Finally, we develop a cost model to reflect the cost implementation in the third dimension and present an optimization model on the number of layers to minimize the overall cost. GRA

N87-23890# Rit Research Corp., Rochester, N.Y.
ESD (ELECTROSTATIC DISCHARGE)/EOS (ELECTRICAL OVERSTRESS) SUSCEPTIBILITY OF A CLASS OF BIPOLAR RF POWER TRANSISTORS: EXPERIMENTAL STUDIES ON STRIPLINE-OPPOSED EMITTER TRANSISTORS Technical Report, 1 Jan. - 31 Dec. 1986
Perambur S. Neelakantaswamy and Ibrahim R. Turkman Dec. 1986 118 p
(Contract N00014-84-K-0532)
(AD-A178212; RITRC-002; TR-2) Avail: NTIS HC A06/MF A01 CSCL 09A

Susceptibility of a class of bipolar RF power transistors (stripline-opposed emitter (SOE) devices) to electrical overstressing (EOS) is studied. Having unique packaging compatible for RF/stripline applications, SOE devices pose prominent/extended exteriors for static propensity and hence are critically vulnerable to degradation as predictable by the charge-device modeling. As such, contrary to the popular notion that rugged bipolar devices are not excessively prone to ESD-based detrimental effects, SOE transistors, on the other hand, are severely vulnerable. It is not just the Wunsch Bell limit of catastrophy due to PN junction burnout (under high-level zaps) that dictates the damages in the devices like SOE transistors. The entire device configuration, i.e., active junction, metallization, bonding, etc., as well as the external packaging, decide the device lethality. This is demonstrated by experimental studies on a family of SOE devices by subjecting them to ESD zaps using a Human Body Simulator. The results positively indicate that their vulnerability is in excess of Class II limit and require specific handling precautions, lest they pose quality control and/or field failure problems. Especially, considering these devices being extremely costly, specific ESD control efforts are rather imminent. Author (GRA)

N87-23891# Rit Research Corp., Rochester, N.Y.
INFLUENCE OF IONIZING RADIATIONS AND ELECTRICAL OVERSTRESSINGS ON MOS (METAL-OXIDE SEMICONDUCTORS) DEVICES: A COMPARISON
Perambur S. Neelakantaswamy and Ibrahim R. Turkman Jan. 1987 23 p
(Contract N00014-84-K-0532)
(AD-A178214; RITRC-011; TR-11) Avail: NTIS HC A02/MF A01 CSCL 18F

Primary mode of failure and/or degradation of MOSFETs due to oxide charge and surface effects can result either from ionizing radiations or from electrical overstressings. In either case, the resulting damage can be characterized by a global parametric degradation specified in terms of device noise characteristics. That is, the net effect of charge trapping and the associated occupation of surface states can be viewed as random/fluctuation phenomena which manifest as the device noise. Thus a common noise model can be prescribed to represent tha analogous influence of ionizing radiations and electrical overstressings. Relevant theoretical results and measured data are presented. GRA

N87-23892# Rit Research Corp., Rochester, N.Y.
NOISE CHARACTERISTICS OF MOS (METAL-OXIDE SEMICONDUCTORS) DEVICES DEGRADED BY ELECTRICAL OVERSTRESSINGS
Perambur S. Neelakantaswamy and Ibrahim R. Turkman Jan. 1987 10 p
(Contract N00014-84-K-0532)
(AD-A178217; RITRC-010; TR-10) Avail: NTIS HC A02/MF A01 CSCL 20C

The endochronic degradation of MOS devices arising from the global response of the device parameters collectively deteriorating under the repetitive influence of electrical overstresses (at subcatastrophic levels) such as electrostatic discharge (ESD), electromagnetic pulsing (EMP), etc., is quantified in terms of noise characteristics. Life-time studies depicting the degradation of a test device are presented. Computer and experimental data are furnished. Author (GRA)

N87-23893*# National Aeronautics and Space Administration. Marshall Space Flight Center, Huntsville, Ala.
AUTOMATIC DETECTION OF ELECTRIC POWER TROUBLES (AI APPLICATION)
Caroline Wang, Hugh Zeanah, Audie Anderson, and Clint Patrick Apr. 1987 80 p
(NASA-TM-86593; NAS 1.15:86593) Avail: NTIS HC A05/MF A01 CSCL 09C

The design goals for the Automatic Detection of Electric Power Troubles (ADEPT) were to enhance Fault Diagnosis Techniques in a very efficient way. ADEPT system was designed in two modes of operation: (1) Real time fault isolation, and (2) a local simulator which simulates the models theoretically. Author

N87-23894# Sandia National Labs., Albuquerque, N. Mex.
REMOVABLE ENCAPSULANTS FOR ELECTRONIC DEVICES
K. B. Wischmann 1987 13 p Presented at the SAMPE Electronics Materials and Processes Conference, Santa Clara, Calif., 23 Jun. 1987
(Contract DE-AC04-76DP-00789)
(DE87-005869; SAND-87-0077C; CONF-870674-1) Avail: NTIS HC A02/MF A01

Expensive and complex electronic hardware that has been encapsulated for mechanical and electrical protection often necessitates a rework capability. Unfortunately, most encapsulants are difficult to penetrate either by mechanical means or solvent attack. Usually, these approaches result in component damage. This paper describes the development of three different solvent-removable thermoplastic encapsulants that exhibit varying upper use temperatures (80 to 130 C) and physical properties. Two materials are based on expandable bead foam technology, while the third is a polyurethane casting resin. Functional electronic components have been successfully potted and depotted, a capability which has resulted in sizeable cost savings in production situations. DOE

N87-23895# Sandia National Labs., Albuquerque, N. Mex.
THE EFFECT OF REINFORCEMENT ON THE TEAR PROPERTIES OF FLEXIBLE CIRCUITS
A. E. Acton 1987 16 p Presented at the SAMPE Electronics Materials and Processes Conference, Santa Clara, Calif., 23 Jun. 1987
(Contract DE-AC04-76DP-00789)
(DE87-007022; SAND-87-0296C; CONF-870674-3) Avail: NTIS MF A01

The tear properties of Kapton flexible circuitry are very poor. To better understand the properties of flex circuits and how to reinforce them, four different reinforcing materials were applied to a typical flex circuit and the tear properties were measured. Teflon film, nylon fabric, glass fabric and Kevlar fabric were all laminated to a flex circuit with Pyralux (a Dupont tradename) adhesive. The fabrics were laminated in both a 0/90 and a + or - 45 configuration. Five tests wereperformed, Graves, crescent, trousers, tensile and single edge notch (SEN). Of the four materials used for reinforcement, Kevlar clearly showed the greatest overall improvement in tear properties. However, Kevlar also provided the greatest processing difficulties. All of the reinforced circuits had an increase in thickness which resulted in an unacceptable loss of flexibility. DOE

N87-23896# Los Alamos National Lab., N. Mex.
HIGH-POWERED, SOLID-STATE rf SYSTEMS
D. W. Reid 1987 5 p Presented at the Particle Accelerator Conference, Washington, D.C., 16 Mar. 1987
(Contract W-7405-eng-36)
(DE87-007457; LA-UR-87-502; CONF-870302-49) Avail: NTIS HC A02/MF A01

Over the past two years, the requirement to supply megawatts of rf power for space-based applications at uhf and L-band frequencies has caused dramatic increases in silicon solid-state power capabilities in the frequency range from 10 to 3000 MHz. Radar and communications requirements have caused similar increases in gallium arsenide solid-state power capabilities in the frequency ranges from 3000 to 10,000 MHz. The present state of the art is reviewed for solid-state rf amplifiers for frequencies from 10 to 10,000 MHz. Information regarding power levels, size, weight, and cost will be given. Technical specifications regarding phase and amplitude stability, efficiency, and system architecture will be discussed. Solid-stage rf amplifier susceptibility to radiation damage will also be examined. DOE

N87-23897# Los Alamos National Lab., N. Mex.
COMPUTER SIMULATION OF THE LASERTRON WITH A RING MODEL
P. J. Tallerico and J. P. Coulon 16 Mar. 1987 4 p Presented at the Particle Accelerator Conference, Washington, D.C., 16 Mar. 1987 Prepared in cooperation with Paris-II Univ., Orsay, France
(Contract W-7405-eng-36)
(DE87-007461; LA-UR-87-517; CONF-870302-30) Avail: NTIS HC A02

The lasertron is more efficient, lighter, and smaller than a klystron, especially at outputs below 2 GHz. Higher peak output powers are possible with the lasertron, and a separate modulator is not required. These advantages are useful for rf accelerators and linear colliders. The electron dynamics are simulated to estimate the device performance limits and to design an experimental lasertron. The relativistic electron dynamics are followed from the photocathode through the acceleration region and through the output region. The total fields are the sum of the space-charge, external magnetic, and acceleration or output-cavity fields. Wake fields are ignored, and the steady-state output fields are found. Lasertron performance as a function of acceleration field, charge per pulse and frequency is calculated, showing its avantages and limitations. A preliminary design for the first Orsay lasertron experiment is presented. DOE

N87-23898# Los Alamos National Lab., N. Mex.
PRELIMINARY THERMAL ANALYSIS OF TRANSISTOR PACKAGES
L. M. Ross and G. A. Bennett Apr. 1987 21 p
(Contract W-7405-eng-36)
(DE87-007708; LA-10905-MS) Avail: NTIS HC A02/MF A01

Efficient thermal design of microwave power transistors is critical for realizing reliable operation of high-power modern electronic circuitry. In an effort to improve thermal performance and enhance reliability, a systematic study is made to quantify transistor package thermal behavior. A series of two-dimensional finite element thermal analyses was completed of a transistor side view. These analyses provide trends for the temperature field and internal thermal resistance components as functions of material properties and geometry. Results from the analyses are shown as isothermal contour plots, plots of temperature drop across the flange and carrier, and plots of temperature versus time. DOE

N87-23899# Sandia National Labs., Albuquerque, N. Mex.
TWO-STAGE HYBRID MICROCIRCUIT AMPLIFIER
M. L. Pyo Apr. 1987 24 p
(Contract DE-AC04-76DP-00789)
(DE87-009092; SAND-86-2904) Avail: NTIS HC A02/MF A01

This report documents the design, development, and fabrication of a two-stage amplifier operating at 400 to 600 MHz. Included are characterization data, predictions generated during design, and measured performance. DOE

N87-23900*# National Aeronautics and Space Administration. Lewis Research Center, Cleveland, Ohio.
OPTICALLY CONTROLLED MICROWAVE DEVICES AND CIRCUITS: EMERGING APPLICATIONS IN SPACE COMMUNICATIONS SYSTEMS
Kul B. Bhasin and Rainee N. Simons Jul. 1987 11 p Prepared for presentation at the International Microwave Symposium, Rio de Janeiro, Brazil, 27-30 Jul. 1987; cosponsored by Brazilian Microwave Society and the IEEE-MTT
(NASA-TM-89869; E-3543; NAS 1.15:89869) Avail: NTIS HC A02/MF A01 CSCL 09A

Optical control of microwave devices and circuits by an optical fiber has the potential to simplify signal distribution networks in high frequency communications systems. The optical response of two terminal and three terminal (GaAs MESFET, HEMT, PBT) microwave devices are compared and several schemes for controlling such devices by modulated optical signals examined. Monolithic integration of optical and microwave functions on a single semiconductor substrate is considered to provide low power,

low loss, and reliable digital and analog optical links for signal distribution. Author

N87-23901*# National Aeronautics and Space Administration. Lewis Research Center, Cleveland, Ohio.
ISSUES IN SPACE PHOTOVOLTAIC RESEARCH AND TECHNOLOGY
Dennis J. Flood 30 May 1987 16 p Presented at the 19th Photovoltaic Specialists Conference, New Orleans, La., 4-8 May 1987; sponsored by IEEE
(NASA-TM-89922; E-3620; NAS 1.15:89922) Avail: NTIS HC A02/MF A01 CSCL 09C

Key issues and opportunities in space photovoltaic research and technology are addressed relative to future NASA mission requirements and drivers. Examples are given of future space missions and/or operational capabilities that are on NASA's planning horizon presenting major tachnology challenges to the use of photovoltaic power generation in space. A brief description of the capabilities ascribed to the competing technologies of nuclear and solar thermal power systems are given. The performance goals that space photovoltaic power systems must meet to remain competitive are described. Author

N87-23902*# National Aeronautics and Space Administration. Lewis Research Center, Cleveland, Ohio.
SYNCHRONIZATION TRIGGER CONTROL SYSTEM FOR FLOW VISUALIZATION
K. S. Chun Feb. 1987 18 p Presented at the International Congress and Exposition, Detroit, Mich., 23-27 Feb. 1987; sponsored by SAE
(NASA-TM-89902; E-3449; SAE-Paper-870450; NAS 1.15:89902) Avail: NTIS HC A02/MF A01 CSCL 09A

The use of cinematography or holographic interferometry for dynamic flow visualization in an internal combustion engine requires a control device that globally synchronizes camera and light source timing at a predefined shaft encoder angle. The device is capable of 0.35 deg resolution for rotational speeds of up to 73 240 rpm. This was achieved by implementing the shaft encoder signal addressed look-up table (LUT) and appropriate latches. The developed digital signal processing technique achieves 25 nsec of high speed triggering angle detection by using direct parallel bit comparison of the shaft encoder digital code with a simulated angle reference code, instead of using angle value comparison which involves more complicated computation steps. In order to establish synchronization to an AC reference signal whose magnitude is variant with the rotating speed, a dynamic peak followup synchronization technique has been devised. This method scrutinizes the reference signal and provides the right timing within 40 nsec. Two application examples are described. Author

N87-23903*# National Aeronautics and Space Administration. Lewis Research Center, Cleveland, Ohio.
A STUDY OF SCHWARZ CONVERTERS FOR NUCLEAR POWERED SPACECRAFT
Thomas A. Stuart and Gene E. Schwarze 1987 11 p Prepared for Presentation at the 22nd Intersociety Energy Conversion Engineering Conference, Philadelphia, Pa., 10-14 Aug. 1987; cosponsored by AIAA, ANS, ASME, SAE, IEEE, ACS, and AIChE
(NASA-TM-89911; E-3588; NAS 1.15:89911; AIAA-87-9314) Avail: NTIS HC A02/MF A01 CSCL 10B

High power space systems which use low dc voltage, high current sources such as thermoelectric generators, will most likely require high voltage conversion for transmission purposes. This study considers the use of the Schwarz resonant converter for use as the basic building block to accomplish this low-to-high voltage conversion for either a dc or an ac spacecraft bus. The Schwarz converter has the important assets of both inherent fault tolerance and resonant operation; parallel operation in modular form is possible. A regulated dc spacecraft bus requires only a single stage converter while a constant frequency ac bus requires a cascaded Schwarz converter configuration. If the power system requires constant output power from the dc generator, then a second converter is required to route unneeded power to a ballast load. Author

N87-23904* National Aeronautics and Space Administration. Goddard Space Flight Center, Greenbelt, Md.
RECIPROCATING LINEAR MOTOR Patent
Michael P. Goldowsky, inventor (to NASA) (North American Philips Co., Inc., Tarrytown, N.Y.) 23 Jun. 1987 10 p Filed 17 Dec. 1985 Continuation of US-Patent-Appl-SN-437914, filed 29 Oct. 1982, abandoned
(NASA-Case-GSC-12773-2; US-Patent-4,675,563; US-Patent-Appl-SN-809851; US-Patent-Class-310-15; US-Patent-Class-290-1-R; US-Patent-Class-310-30) Avail: US Patent and Trademark Office CSCL 09A

A reciprocating linear motor is formed with a pair of ring-shaped permanent magnets having opposite radial polarizations, held axially apart by a nonmagnetic yoke, which serves as an axially displaceable armature assembly. A pair of annularly wound coils having axial lengths which differ from the axial lengths of the permanent magnets are serially coupled together in mutual opposition and positioned with an outer cylindrical core in axial symmetry about the armature assembly. One embodiment includes a second pair of annularly wound coils serially coupled together in mutual opposition and an inner cylindrical core positioned in axial symmetry inside the armature radially opposite to the first pair of coils. Application of a potential difference across a serial connection of the two pairs of coils creates a current flow perpendicular to the magnetic field created by the armature magnets, thereby causing limited linear displacement of the magnets relative to the coils.
Official Gazette of the U.S. Patent and Trademark Office

N87-23832*# Jet Propulsion Lab., California Inst. of Tech., Pasadena.
A VLSI SINGLE CHIP (255,223) REED-SOLOMON ENCODER WITH INTERLEAVER
I. S. Hsu, L. J. Deutsch, T. K. Truong, and I. S. Reed (University of Southern California, Los Angeles.) *In its* The Telecommunications and Data Acquisition Report 15 May 1987 p 41-47 (For primary document see N87-23828 17-32)
Avail: NTIS HC A06/MF A01 CSCL 09C

N87-23839*# Jet Propulsion Lab., California Inst. of Tech., Pasadena.
AN INTERACTIVE WIRE-WRAP BOARD LAYOUT PROGRAM
A. Schlutsmeyer *In its* The Telecommunications and Data Acquisition Report 15 May 1987 p 101-107 (For primary document see N87-23828 17-32)
Avail: NTIS HC A06/MF A01 CSCL 09C

N87-23867# Massachusetts Univ., Amherst. Dept. of Electrical and Computer Engineering.
PRINTED CIRCUIT ANTENNA TECHNOLOGY
Daniel H. Schaubert *In* AGARD Microwave Antennas for Avionics Apr. 1987 15 p (For primary document see N87-23859 17-32)
Copyright Avail: NTIS HC A08/MF A01

34 FLUID MECHANICS AND HEAT TRANSFER

Includes boundary layers; hydrodynamics; fluidics; mass transfer; and ablation cooling.

For related information see also *02 Aerodynamics* and *77 Thermodynamics and Statistical Physics.*

N87-23905# Air Force Inst. of Tech., Wright-Patterson AFB, Ohio. School of Engineering.
UNSTEADY HEAT TRANSFER RESULTING FROM THE RAPID CHARGING OF AN EVACUATED TANK WITH CONDUCTING WALLS M.S. Thesis
Dennis E. Lileikis Dec. 1986 76 p

(AD-A179206; AFIT/GA/AA/86D-9) Avail: NTIS HC A05/MF A01 CSCL 20M

The two classical problems of charging a tank with an ideal gas concern themselves only with the initial and final states of the gas. The first problem involves an insulated tank. From initial conditions, the final temperature of the gas in the tank can be determined. The second problem involves a tank with conducting walls. In this case, it is the total heat transferred from the gas to the tank walls which can be found. This study went beyond these equilibrium analyses to acquire a fundamental understanding of the transient phenomenon involved in charging a tank. By way of experimentation, transient pressure and heat flux measurement were made on an evacuated cylindrical tank as it was charged by sudden exposure to the atmosphere. Then, an average convection coefficient and driving temperature potential for the tank was found. A method was then developed for estimating heating rates for other tanks and different ambient conditions. Also, information about the transient flow dynamics occurring within the tank was gleaned from the heat transfer data. This information includes rates of kinetic, internal, and thermal energy generation and dissipation as well as rates of entropy creation in the gas. GRA

N87-23906# Air Force Inst. of Tech., Wright-Patterson AFB, Ohio. School of Engineering.

EFFECTS OF CORONA ON HEAT TRANSFER IN AN ENCLOSURE M.S. Thesis

Donald D. Dyer, Jr. Dec. 1986 79 p

(AD-A179209; AFIT/GA/AA/86D-4) Avail: NTIS HC A05/MF A01 CSCL 20M

Experiments were conducted to determine the effects of corona wind on heat transfer rates for enclosures. Tests were performed with an enclosed cavity heated on the bottom and cooled on the top (and vice versa). A corona wind was established inside the cavity by applying high voltages to 0.004 inch diameter chromel wires placed along the hot and cold surfaces of the cavity. Tests were conducted using both positive voltage potential and negative voltage potential to create the corona discharge. Different wiring configurations were used to establish a variety of flow patterns inside the cavity. The heated surface heat transfer rates were calculated for each of the test configurations with and without corona. These heat transfer rates were determined when the corona discharge was present and compared to the rates found when the discharge was not present. Comparing these transfer rates revealed how much the corona wind augmented the heat transfer process. Results showed corona wind can increase heat transfer rates inside an enclosure by almost four times the rates attained without the corona discharge for the wire configurations investigated. GRA

N87-23907# Massachusetts Inst. of Tech., Cambridge. Fluid Dynamics Research Lab.

TURBULENT BOUNDARY LAYER STRUCTURE, DRAG REDUCTION Annual Report, 12 Nov. 1984 - 11 Nov. 1985

Marten T. Landahl and Joseph H. Haritonidis 19 Nov. 1986 14 p

(Contract F49620-83-C-0019)
(AD-A179246; AFOSR-87-0315TR) Avail: NTIS HC A02/MF A01 CSCL 20D

The research work has progressed along the following lines: (1) continuation of theoretical work on the effects of large-eddy breakup devices on turbulent eddies; (2) theoretical study of the role of pressures in the wall turbulence generation process; (3) application of a theoretical model for designing smart wall boundary layer control; (4) use of a new bursting model for predicting the mean velocity profile near a wall; (5) development and application of a new skin friction probe, and (6) initial design of a smart wall producing a controlled travelling disturbance. GRA

N87-23908# Virginia Polytechnic Inst. and State Univ., Blacksburg. Dept. of Engineering Science and Mechanics.

THREE-DIMENSIONAL STRUCTURE OF BOUNDARY LAYERS IN TRANSITION TO TURBULENCE Annual Report, Feb. 1985 - Feb. 1986

Thorwald Herbert Dec. 1986 12 p

(Contract F49620-84-K-0002)
(AD-A179247; AFOSR-87-0316TR) Avail: NTIS HC A02/MF A01 CSCL 20D

A unified theory of secondary instability in wall-bound shear flows has been developed. This theory rests on Floquet systems of stability equations and permits classification and quantitative analysis of different modes of secondary instability in the three-dimensional stage of laminar-turbulent transition. The catalog of solutions is consistent with observations and predicts other phenomena that have not been identified in experiments. The theoretical results have been used to reproduce patterns in flow visualizations by computer animation. Analysis of the energy balance has shown a feedback loop between mean flow, two-dimensional, and three-dimensional disturbances that is considered key to the process of self-sustained transition. Various techniques are currently applied to shed more light on this nonlinear process. GRA

N87-23909# Rutgers - The State Univ., New Brunswick, N. J. Dept. of Mechanical Industrial and Aerospace Engineering.

THEORETICAL INVESTIGATION OF 3-D SHOCK WAVE-TURBULENT BOUNDARY LAYER INTERACTIONS, PART 5 Final Report, 1 Oct. 1985 - 30 Sep. 1986

Doyle D. Knight 24 Feb. 1987 20 p

(Grant AF-AFOSR-0040-82)
(AD-A179455; RU-TR-165-MAE-F; AFOSR-87-0395TR) Avail: NTIS HC A02/MF A01 CSCL 20D

The research concerns the understanding of three dimensional shock wave turbulent boundary layer interactions. The focus was on theoretical and experimental investigations of the three dimensional swept compression corner at Mach 3 for compression angle of 24 deg sweep angle of 60 deg, and two different Reynolds numbers. The flowfield is computed utilizing the three dimensional Reynolds averaged compressible Navier Stokes equations, with turbulence incorporated through the Baldwin Lomax algebraic turbulent eddy viscosity model. Studies are also performed on the flowfield, and the same configuration is computed using the Jones Launder turbulence model. The computed surface pressure profiles at the lower Reynolds number display significant disagreement with experiment. The computed surface pressure and boundary layer profiles of pitot pressure and yaw angle are in good agreement with experiment at the high Reynolds number. On the basis of particle pathlines, the principal flowfield is observed to be a large vortical structure aligned approximately with the compression corner. This structure is qualitatively identical to that observed for the 3-D sharp fin under the same flow conditions. GRA

N87-23910# Arizona Univ., Tucson. Engineering Experiment Station.

EXPERIMENTAL AND NUMERICAL INVESTIGATION OF COHERENT STRUCTURES Annual Report, 5 Feb. 1985 - 6 Feb. 1986

F. H. Champagne and H. Fasel 30 Aug. 1986 14 p

(Grant AF-AFOSR-0146-85)
(AD-A179456; AFOSR-87-0424TR) Avail: NTIS HC A02/MF A01 CSCL 20D

Several significant tasks were accomplished during the first year of the grant period. The first involved completing the Reynolds stress measurements behind various wake generators and demonstrating that the previously observed variation in the spreading rate of the mean flow field could be confirmed by the Reynolds stress results. This provides convincing evidence for the lack of universality of the turbulent structure of two dimensional small deficit wakes. The model decomposition work, initiated to investigate possible cause for the lack of universality, was completed. Varicose disturbances were successfully generated using a two flap mechanism to investigate the significance of the varicose mode. The amplitude ratio of the two modes, sinuous and varicose, appear to approach an asymptotic value in the far wake. Finally, varicose effects were accounted for in the model decomposition work by solving the Orr Sommerfeld equation. The varicose mode appears to be more affected by viscosity than the

sinuous mode. Numerical simulations based on the complete Navier Stokes equation are under development for a somewhat simpler flow geometry than the wake, namely the free shear layer. Considerable progress has been made toward the development of numerical methods that are applicable to such simulations. For simplicity, the temporal model is being used first. A computer program based on the spatial model is nearly finished. GRA

N87-23911# Air Force Inst. of Tech., Wright-Patterson AFB, Ohio. School of Engineering.
INVESTIGATION OF SHROUDED NOZZLE EXIT PRESSURE CHANGES M.S. Thesis
Douglas C. Rodgers Dec. 1986 104 p
(AD-A179477; AFIT/GAE/AA/86D-15) Avail: NTIS HC A06/MF A01 CSCL 20D

Shrouded two- and three-dimensional, supersonic, cold flow nozzles were investigated. Altitudes up to 87,000 feet were simulated and nozzle inlet to ambient pressure ratios up to 400 were used. Pressure measurements were made along the nozzle exit plane and the shroud walls to determine the effect shrouding has on exit base pressure and the pressure distribution along the shroud walls. Comparisons were made in the blowdown wind tunnel using a variety of nozzle types, nozzle area ratios, and shroud lengths. Study results reveal that the pressure fields in the base region of the nozzle and along the shroud walls are dependent upon the geometry of configuration and operating altitude. Shroud wall pressures were found to act in the same manner as the base pressures by first maintaining a fairly constant pressure value until the chamber to ambient pressure ratio reached some critical value. When this condition occurred, the flow separated from the shroud with a resulting increase in the shroud wall pressures. Potential increases in nozzle assembly performance are possible from changing effective nozzle exit area and the resulting changes in the flow gas dynamics. GRA

N87-23912# Colorado Univ., Boulder. Dept. of Aerospace Engineering Sciences.
UNSTEADY SEPARATED FLOWS: VORTICITY AND TURBULENCE Final Report
M. Luttges 6 Apr. 1987 36 p
(Contract F49620-83-K-0009)
(AD-A179500; AFOSR-87-0384TR) Avail: NTIS HC A03/MF A01 CSCL 20D

Throughout a wide combination of initial pitch angles, pitch amplitudes and pitch rates for a NACA 0015 airfoil section, several unsteady flow initiation and development trends have been documented. The effects of mean angle of attack and reduced frequency, and the interactions between them, are generally linear (for the ranges studied). Incremental changes in reduced frequency and mean pitch angle resulted in later or earlier vortex initiation, respectively, within the pitch cycle. Other notable features of the flowfield development include the initiation of a prominent trailing edge vortex as the leading edge vortex sheds, and the convection velocity of the leading edge vortex. Similar tests employing a flat plate produced somewhat different results. The vortices were more coherent and convected at higher velocities. In general, however, the developmental trends across the parameters tested followed those of the airfoil model. GRA

N87-23913# Air Force Inst. of Tech., Wright-Patterson AFB, Ohio. School of Engineering.
SURFACE ROUGHNESS: ITS EFFECTS ON THE PERFORMANCE OF A TWO-DIMENSIONAL COMPRESSOR CASCADE M.S. Thesis
J. R. Poulin Dec. 1986 214 p
(AD-A179506; AFIT/GAE/AA/86D-13) Avail: NTIS HC A10/MF A01 CSCL 20D

The effects of surface roughness on the losses in the flow through a two-dimensional compressor cascade were studied. The cascade consisted of 7 NACA 65-A506 airfoils with 2-in. chords and aspect ratio of 1. The blades were mounted with a stagger angle of 16 deg, an angle of attack of 15 deg and a solidity of 1.5. The Reynolds number/foot was in excess of 2 million. Three blade configurations were evaluated: one smooth and two with different degrees of roughness applied to the first quarter chord. Hot wire/film anemometers measured velocities and turbulence intensities both in the wake and along the suction surface of the center blade. Surface roughness is shown to increase both boundary layer edge velocities and boundary layer thickness towards the trailing edge while advancing the transition point towards the leading edge. It is also shown to increase wake full thickness, momentum thickness, form factor, and total pressure loss coefficient while decreasing the velocity recovery immediately downstream of the trailing edge. Wake characteristics are most sensitive to an initial increase in roughness but the majority of the changes occur within the first half chord length distance downstream. GRA

N87-23914# Air Force Inst. of Tech., Wright-Patterson AFB, Ohio. School of Engineering.
A REDEFINED HYDRAULIC DIAMETER FOR LAMINAR FLOW Final Report, Jul. 1985 - Dec. 1986
Bruce J. Sutherland 1 Dec. 1986 114 p
(AD-A179511; AFIT/GAE/AA/86D-17) Avail: NTIS HC A06/MF A01 CSCL 20D

For laminar, steady flow in ducts, the current definition of hydraulic diameter, Dh, does not accurately depict the non-uniform wall shear stress distribution around the perimeter of non-circular duct shapes. In this investigation, a new hydraulic diameter Dh(1), was empirically determined. It correlated friction factor data for many non-circular shapes to within approximately 2.4 % of the circular duct value. An experiment, using the AFIT oil Flow Rig Set-Up, was run to determine the effect of transition Reynolds number, Re(tr), and hydrodynamic entrance length, L(+), of replacing Dh with Dh(1). Transition Reynolds number and L(+) were determined, based on Dh and Dh(1) for a circular, square, and concentric annular duct. Transition Reynolds numbers, based on Dh, for the square and concentric annular ducts were approximately 12.5% lower than the circular duct Re(tr). The Re(tr), based on Dh(1), did not correlate well for the concentric annulus, but did correlate for the square duct. GRA

N87-23915# Tel-Aviv Univ. (Israel).
ON THE BREAKDOWN OF THE WAVE PACKET TRAILING A TURBULENT SPOT IN A LAMINAR LAYER Interim Report, 1984 - 85
A. Glezer, Y. Katz, and I. Wygnanski Jan. 1986 42 p
(Grant AF-AFOSR-0333-84)
(AD-A179607; AE-85-2; AFOSR-87-0388TR) Avail: NTIS HC A03/MF A01 CSCL 20D

The evolution of two oblique wave packets trailing the transitional spot was investigated in order to determine the extent of the interaction between the packets and the spot. The experimental investigation, carried out in two slightly different laminar boundary layers characterized by Falkner-Skan parameters of 0 and 0.2, revealed the importance of miniscule pressure gradients on the stability of the laminar boundary layer and the rate at which it can be contaminated by a turbulent spot. Some simple statistical procedures for treating the data were developed and were used to accentuate the understanding of the physical processes governing transition to turbulence. GRA

N87-23916*# Colorado Univ., Boulder. Dept. of Mathematics.
SELECTION PRINCIPLES AND PATTERN FORMATION IN FLUID MECHANICS AND NONLINEAR SHELL THEORY Final Technical Report
Duane P. Sather 1987 3 p
(Grant NAG2-278)
(NASA-CR-180941; NAS 1.26:180941) Avail: NTIS HC A02/MF A01 CSCL 20D

Research accomplishments are summarized and publications generated under the contract are listed. The general purpose of the research was to investigate various symmetry breaking problems in fluid mechanics by the use of structure parameters and selection principles. Although all of the nonlinear problems studied involved systems of partial differential equations, many of

these problems led to the study of a single nonlinear operator equation of the form F(w, lambda, gamma) = 0, (w is an element of H), (lambda is an element of R1), (gamma is an element of R1). Instead of varying only the load parameter lambda, as is often done in the study of such equations, one of the main ideas used was to vary the structure parameter gamma in such a way that stable solutions were obtained. In this way one determines detailed stability results by making use of the structure of the model equations and the known physical parameters of the problem. The approach was carried out successfully for Benard-type convection problems, Taylor-like problems for short cylinders, rotating Couette-Poiseuille channel flows, and plane Couette flows. The main focus of the research was on wave theory of vortex breakdown in a tube. A number of preliminary results for inviscid axisymmetric flows were obtained. M.G.

N87-23917# Illinois Univ., Urbana-Champaign. Dept. of Mechanical and Industrial Engineering.

FLOW REGIMES OF REFRIGERANT MIXTURES CONDENSING INSIDE TUBES

E. Kornota and W. F. Stoecker Jun. 1985 136 p

(Contract DE-AC05-84OR-21400)

(ORNL/sub/81-7762/4 and 01; UILU-ENG-86-4004) Avail: NTIS HC A07/MF A01

In order to take full advantage of the energy-conservation potential of refrigerant mixtures, the heat-transfer coefficients should be maintained high. More insight was sought into the condensation process by observing and photographing the flow regimes of the nonazeotropic mixed refrigerants condensing in a single-tube glass condenser. Measurements of pressure and temperature profiles through the condenser as well as chromatographic analysis of samples at several points along the condenser were taken. The four principal flow regimes from the entrance to the exit of the condenser are: annular flow, stratified flow, slug flow, and bubble flow. The most significant reduction in heat-transfer coefficient occurred in the midrange of the condenser on the operating system, and the regime was shown in the glass condenser to be stratified flow. Several explanations for the reduction in heat-transfer coefficient are selective diffusivity, temperature and concentration gradients, and vapor-liquid slip. Slip was prominent in the region where the major reduction in heat-transfer coefficient occurred, so inhibiting this slip may prevent at least some of the heat-transfer degradation. Author

N87-23918# Sandia National Labs., Albuquerque, N. Mex. Fluid and Thermal Sciences Dept.

ONSET OF TAYLOR VORTICES IN FLOWS WITH A CIRCUMFERENTIAL PRESSURE GRADIENT: APPLICATION TO THE HELICAL SCREW RHEOMETER

N. E. Bixler and A. M. Kraynik 1987 6 p Presented at the 11th Canadian Congress of Applied Mechanics, Edmonton, Canada, 31 May 1987

(Contract DE-AC04-76DP-00789)

(DE87-000453; SAND-86-2281C; CONF-870533-1) Avail: NTIS HC A02/MF A01

Taylor vortex flows are analyzed for the stability of flow between two rotating, concentric cylinders. The study is pertinent to the helical screw rheometer. Relative stability is given for four configurations: (1) high pressure, (2) chemically reacting fluids, (3) multiphase fluids, and (4) on-line measurements. DOE

N87-23919# Pittsburgh Univ., Pa.

PHYSICS OF PATTERN FORMATION AT LIQUID INTERFACES Final Report, Aug. 1984 - Dec. 1986

J. V. Maher 1987 37 p

(Contract DE-FG02-84ER-45131)

(DE87-007540; DOE/ER-45131/4) Avail: NTIS HC A03/MF A01

Viscous fingering experiments have been performed in both flat and circular interface geometries. The interest has been to study the early stages of the flow from the linear regime on through to the non-linear pattern formation. DOE

N87-23920# Texas Univ., Austin. Inst. for Fusion Studies.

EFFECTIVE DIFFUSION IN LAMINAR CONVECTIVE FLOWS

M. N. Rosenbluth, H. L. Berk, I. Doxas, and W. Horton Mar. 1987 42 p

(Contract DE-FG05-80ET-53088)

(DE87-008054; DOE/ET-53088/261; IFSR-261) Avail: NTIS HC A03/MF A01

The effective diffusion coefficient D* of a passive component, such as test particles, dye, temperature, magnetic flux, etc., is derived for motion in periodic two-dimensional incompressible convective flow with characteristic velocity v and size d in the presence of an intrinsic local diffusivity D. Asymptotic solutions for effective diffusivity D*(P) in the large P limit, with P approx. vd/D, are shown to be of the form D* = cDP(sup 1/2) with c being a coefficient that is determined analytically. The constant c depends on the geometry of the convective cell and on an average of the flow speed along the separatrix. The asymptotic method of evaluation applies to both free boundary and rough boundary flow patterns and it is shown that the method can be extended to more complicated patterns such as the flows generated by rotating cylinders, as in the problem considered by Nadim, Cox, and Brenner. The diffusivity D* is readily calculated for small P, but the evaluation for arbitrary P requires numerical methods. Monte Carlo particle simulation codes are used to evaluate D* at arbitrary P, and thereby describe the transition for D* between the large and small P limits. DOE

N87-23921*# National Aeronautics and Space Administration. Lewis Research Center, Cleveland, Ohio.

THREE-STEP LABYRINTH SEAL FOR HIGH-PERFORMANCE TURBOMACHINES

Robert C. Hendricks Jun. 1987 75 p

(NASA-TP-1848; E-3186; NAS 1.60:1848) Avail: NTIS HC A04/MF A01 CSCL 20D

A three-step labyrinth seal with 12, 11, and 10 labyrinth teeth per step, respectively, was tested under static (nonrotating) conditions. The configuration represented the seal for a high-performance turbopump (e.g., the space shuttle main engine fuel pump). The test data included critical mass flux and pressure profiles over a wide range of fluid conditions at concentric, partially eccentric, and fully eccentric seal positions. The seal mass fluxes (leakage rates) were lower over the entire range of fluid conditions tested than those for data collected for similar straight and three-step cylindrical seals, and this conformed somewhat to expectations. However, the pressure profiles for the eccentric positions indicated little, if any, direct stiffness for this configuration in contrast to significant direct stiffness reported for the straight and three-step cylindrical seals over the range of test conditions. Seal dynamics depend on geometric configuration, inlet and exit parameters, fluid phase, and rotation. The method of corresponding states was applied to the mass flux data, which were found to have a pressure dependency for helium. Author

N87-23922# Integral Technologies, Inc., Westmont, Ill.

MULTIDIMENSIONAL MODELING OF CONVECTIVE HEAT TRANSFER WITH APPLICATION TO I.C. ENGINES Technical Progress Report

M. J. Jennings and T. Morel 30 Nov. 1986 9 p

(Contract DE-AC04-86AL-33183)

(DE87-002939; DOE/AL-33183/T1) Avail: NTIS HC A02/MF A01

The objective is to develop a more comprehensive understanding of the convective heat transfer process in complex, unsteady turbulent reacting flows, typical of those which occur in internal combustion engines. The area of research will be the representation of heat transfer in multi-dimensional Navier-Stokes models, and modeling of turbulent transport mechanisms. The tasks will include a review of relevant prior work. Based on this review, and original work done under this contract, several modeling approaches will be formulated, studied and tested. The tests will be carried out on flow cases which have relevance to engine flows, and for which reliable experimental data exist. Such data will be sought and identified. The analytical studies will lead to

the determination of the best modeling approaches to be used for heat transfer simulation in internal combustion engines. Following that, a study will be carried out of spatial and temporal heat flux distribution in a representative engine. This will be complemented by a parametric study of engine heat transfer dependence on intake flow details, combustion chamber geometry, engine speed, and engine load. DOE

N87-23923# Argonne National Lab., Ill.
MOTION-DEPENDENT FLUID FORCES ACTING ON A TUBE ROW IN CROSSFLOW
J. A. Jendrzejczyk and S. S. Chen Oct. 1986 32 p
(Contract W-31109-eng-38)
(DE87-005574; ANL-86-48) Avail: NTIS HC A03/MF A01

Motion-dependent fluid forces acting on a tube row with a pitch-to-diameter ratio of 1.35 are measured for several flow velocities and a series of oscillation frequencies. Fluid-damping and fluid-stiffness coefficients are obtained from motion-dependent fluid forces as a function of reduced flow velocity. Fluid-force coefficients agree reasonably with published data. Based on the fluid-force coefficients, the critical flow velocity and instability characteristics of tube arrays in crossflow can be predicted. DOE

N87-23924# Iowa Univ., Iowa City. Inst. of Hydraulic Research.
VISCOUS-INVISCID INTERACTION WITH HIGHER-ORDER VISCOUS-FLOW EQUATIONS: APPLICATIONS TO THREE-DIMENSIONAL BODIES Technical Report, Sep. 1986 - Mar. 1987
Sungyul Yoo, Frederick Stern, and Virendra C. Patel Mar. 1987 45 p
(Contract N00014-83-K-0136)
(AD-A178264; IIHR-307) Avail: NTIS HC A03/MF A01 CSCL 20D

A viscous inviscid interaction method for three dimensional flows, in which the partially parabolic Reynolds equations are coupled with an inviscid flow solution procedure in an interactive and iterative manner, is applied to two simple three dimensional bodies for which experimental data are available for comparison. The relative merits of interactive and global solution procedures are evaluated by comparing the viscous inviscid interaction solutions with noninteractive large domain solutions of only the viscous flow equations. Both methods yield satisfactory results, although the interaction solutions are found to be computationally more efficient for the cases considered. GRA

N87-23925*# Virginia Polytechnic Inst. and State Univ., Blacksburg. Turbomachinery Research Group.
THERMODYNAMIC EVALUATION OF TRANSONIC COMPRESSOR ROTORS USING THE FINITE VOLUME APPROACH Final Report, 20 Dec. 1984 - 19 Dec. 1986
John Moore, Stephen Nicholson, and Joan G. Moore 19 Dec. 1986 83 p
(Grant NAG3-593)
(NASA-CR-180587; NAS 1.26:180587; JM/87-4) Avail: NTIS HC A05/MF A01 CSCL 20D

The development of a computational capability to handle viscous flow with an explicit time-marching method based on the finite volume approach is summarized. Emphasis is placed on the extensions to the computational procedure which allow the handling of shock induced separation and large regions of strong backflow. Appendices contain abstracts of papers and whole reports generated during the contract period. For individual titles, see N87-23926 through N87-23929.

N87-23926*# Virginia Polytechnic Inst. and State Univ., Blacksburg.
DEVELOPMENT OF AN EXPLICIT TIME MARCHING PROCEDURE FOR LAMINAR AND TURBULENT FLOW
In its Thermodynamic Evaluation of Transonic Compressor Rotors Using the Finite Volume Approach 19 Dec. 1986 p 4-46 (For primary document see N87-23925 17-34)
Avail: NTIS HC A05/MF A01 CSCL 20D

A finite-volume based, time-marching method for turbulent and laminar flows is described. Extensions to the computational procedure to allow the handling of shock induced separation and large regions of strong backflow are emphasized. Two test cases are considered, the United Technologies Research Center (UTRC) separated and reattached turbulent boundary layer and the strong shock case in the McDonnell Douglas Research Lab (MDRL) transonic diffuser G. The extended method worked well on the UTRC flow with a boundary layer blockage of 58% and a maximum backflow velocity of 37% of the local maximum free-stream velocity. It also worked well on the MDRL diffuser with a shock Mach number of 1.353 and a maximum backflow velocity of -71.7 m/s. A Mach number dependent interpolation formula for effective pressure was developed for use in density-update time-marching methods. M.G.

N87-23927*# Virginia Polytechnic Inst. and State Univ., Blacksburg. Dept. of Mechanical Engineering.
DEVELOPMENT OF A FINITE VOLUME TIME MARCHING METHOD
Stephen Nicholson *In its* Thermodynamic Evaluation of Transonic Compressor Rotors Using the Finite Volume Approach 19 Dec. 1986 p 47-48 (For primary document see N87-23925 17-34)
(JM/85-3) Avail: NTIS HC A05/MF A01 CSCL 20D

Progress made in the development of a time-marching finite volume method from September 1984 to December 1984 is reported. The objective of the work is to develop and demonstrate a Navier-Stokes approach for transonic flow which includes viscous terms in the finite volume method. The accuracy of the computational method will be verified using a transonic diffuser as a test case. The computational goal is to calculate the flow in sufficient detail and with sufficient accuracy that the loss generating mechanisms can be studied to assess the sources of inefficiency in the transonic diffuser. Author

N87-23928*# Virginia Polytechnic Inst. and State Univ., Blacksburg. Dept. of Mechanical Engineering.
AN EXPLICIT FINITE-VOLUME TIME-MARCHING PROCEDURE FOR TURBULENT FLOW CALCULATIONS
Stephen Nicholson, Joan G. Moore, and John Moore *In its* Thermodynamic Evaluation of Transonic Compressor Rotors Using the Finite Volume Approach 19 Dec. 1986 p 59-70 (For primary document see N87-23925 17-34)
Avail: NTIS HC A05/MF A01 CSCL 20D

A method was developed which calculates two-dimensional, transonic, viscous flow in ducts. The finite-volume, time-marching formulation is used to obtain steady flow solutions of the Reynolds-averaged form of the Navier-Stokes equations. The entire calculation is performed in the physical domain. Control volumes are chosen so that smoothing of flow properties, typically required for stability, is not required. Different time steps are used in the different governing equations. A new pressure interpolation scheme is introduced which improves the shock capturing ability of the method. A multi-volume method for pressure changes in the boundary layer allows calculations which use very long and thin control volumes (length/height - 1000). The method is compared with two test cases. Essentially incompressible turbulent boundary layer flow in an adverse pressure gradient is calculated and the computed distributions of mean velocity and shear are in good agreement with the measurements. Transonic viscous flow in a converging diverging nozzle is calculated; the Mach number upstream of the shock is approximately 1.25. The agreement between the calculated and measured shock strength and total pressure losses is good. M.G.

N87-23929*# Virginia Polytechnic Inst. and State Univ., Blacksburg. Dept. of Mechanical Engineering.
EXPLICIT FINITE-VOLUME TIME-MARCHING CALCULATIONS OF TOTAL TEMPERATURE DISTRIBUTIONS IN TURBULENT FLOW
Stephen Nicholson, Joan G. Moore, and John Moore *In its* Thermodynamic Evaluation of Transonic Compressor Rotors Using the Finite Volume Approach 19 Dec. 1986 p 71-82 (For

primary document see N87-23925 17-34)
Avail: NTIS HC A05/MF A01 CSCL 20D

A method was developed which calculates two-dimensional, transonic, viscous flow in ducts. The finite volume, time-marching formulation is used to obtain steady flow solutions of the Reynolds-averaged form of the Navier-Stokes equations. The entire calculation is performed in the physical domain. This paper investigates the introduction of a new formulation of the energy equation which gives improved transient behavior as the calculation converges. The effect of variable Prandtl number on the temperature distribution through the boundary layer is also investigated. A turbulent boundary layer in an adverse pressure gradient (M = 0.55) is used to demonstrate the improved transient temperature distribution obtained when the new formulation of the energy equation is used. A flat plate turbulent boundary layer with a supersonic free-stream Mach number of 2.8 is used to investigate the effect of Prandtl number on the distribution of properties through the boundary layer. The computed total temperature distribution and recovery factor agree well with the measurements when a variable Prandtl number is used through the boundary layer.
M.G.

N87-23930# Los Alamos National Lab., N. Mex.
REZONE: A METHOD FOR AUTOMATIC REZONING IN TWO-DIMENSIONAL LAGRANGIAN HYDRODYNAMICS PROBLEMS
K. B. Wallick Mar. 1987 114 p
(Contract W-7405-eng-36)
(DE87-006324; LA-10829-MS) Avail: NTIS HC A06/MF A01

A method for automatic rezoning in two-dimensional Lagrangian hydrodynamics problems is described. This method conserves mass, internal energy, and directed kinetic energy as these quantities are transferred from one zone to another. The general procedure is to run the problem hydrodynamically while monitoring the mesh for distortion. When the distortion becomes severe, the problem is interrupted and the REZONE code takes over to clear up the mesh distortion. This process is continued as needed during the entire run of the problem. Only those areas of the mesh that show distortion are rezoned. The purpose of this method is to keep hydrodynamic problems running while disturbing the normal calculations as little as possible. With this method the overall shape of the mesh will still indicate the natural flow of the hydrodynamics problems.
DOE

N87-23931# Lawrence Livermore National Lab., Calif.
GASPS: A TIME-DEPENDENT, ONE-DIMENSIONAL, PLANAR GAS DYNAMICS COMPUTER CODE
R. E. Pierce, S. B. Sutton, and W. J. Comfort, III Dec. 1986 33 p
(Contract W-7405-eng-48)
(DE87-008338; UCID-21029) Avail: NTIS HC A03/MF A01

GASP is a transient, one-dimensional planar gas dynamic computer code that can be used to calculate the propagation of a shock wave. GASP, developed at LLNL, solves the one-dimensional planar equations governing momentum, mass and energy conservation. The equations are cast in an Eulerian formulation where the mesh is fixed in space, and material flows through it. Thus it is necessary to account for convection of material from one cell to its neighbor.
DOE

N87-23932# Argonne National Lab., Ill.
MODELING OF DILUTE TWO-PHASE MULTISPECIES SOLID/GAS FLOWS
E. D. Doss, M. G. Srinivasan, and A. C. Raptis Jun. 1986 64 p
(Contract W-31109-eng-38)
(DE87-009254; ANL/FE-86-5) Avail: NTIS HC A04/MF A01

The report gives a detailed description of the analytical modeling that underlies the numerical code for predicting the flow of dilute solid/gas flows in pipes. The model is two-phase multispecies. Particles of one size are treated as one species and the equations of particle dynamics include terms to account for momentum transfer between species and the wall friction on each species of particles. New expressions for particle/particle interaction and wall friction for multispecies flow are derived. Results of parametric studies based on the new expressions are described. The predictions of this model for gas/powder flow through a venturi are compared with experimental measurements. The model's capability for predicting the flow in Argonne's Solid/Gas Flow Test Facility will be the subject of a companion report.
DOE

N87-23933*# National Aeronautics and Space Administration. Lewis Research Center, Cleveland, Ohio.
DIRECT NUMERICAL SIMULATIONS OF A TEMPORALLY EVOLVING MIXING LAYER SUBJECT TO FORCING
Russell W. Claus 1986 22 p Presented at the 10th Symposium on Turbulence, Rolla, Mo., 22-24 Sep. 1986; sponsored by ONR and Missouri Univ.
(NASA-TM-88896; E-3313; NAS 1.15:88896) Avail: NTIS HC A02/MF A01 CSCL 20D

The vortical evolution of mixing layers subject to various types of forcing is numerically simulated using pseudospectral methods. The effect of harmonic forcing and random noise in the initial conditions is examined with some results compared to experimental data. Spanwise forcing is found to enhance streamwise vorticity in a nonlinear process leading to a slow, secondary growth of the shear layer. The effect of forcing on a chemical reaction is favorably compared with experimental data at low Reynolds numbers. Combining harmonic and subharmonic forcing is shown to both augment and later destroy streamwise vorticity.
Author

N87-23934*# National Aeronautics and Space Administration. Lewis Research Center, Cleveland, Ohio.
COMPUTATION OF FULL-COVERAGE FILM-COOLED AIRFOIL TEMPERATURES BY TWO METHODS AND COMPARISON WITH HIGH HEAT FLUX DATA
H. J. Gladden, F. C. Yeh, and P. J. Austin, Jr. Jun. 1987 18 p Presented at the 32nd International Gas Turbine Conference and Exhibition, Anaheim, Calif., 31 May - 4 Jun. 1987; sponsored by ASME
(NASA-TM-88931; E-3372; NAS 1.15:88931) Avail: NTIS HC A02/MF A01 CSCL 20D

Two methods were used to calculate the heat flux to full-coverage film cooled airfoils and, subsequently, the airfoil wall temperatures. The calculated wall temperatures were compared to measured temperatures obtained in the Hot Section Facility operating at real engine conditions. Gas temperatures and pressures up to 1900 K and 18 atm with a Reynolds number up to 1.9 million were investigated. Heat flux was calculated by the convective heat transfer coefficient adiabatic wall method and by the superposition method which incorporates the film injection effects in the heat transfer coefficient. The results of the comparison indicate the first method can predict the experimental data reasonably well. However, superposition overpredicted the heat flux to the airfoil without a significant modification of the turbulent Prandtl number. The results suggest that additional research is required to model the physics of full-coverage film cooling where there is significant temperature/density differences between the gas and the coolant.
Author

N87-23935# Institut Franco-Allemand de Recherches, St. Louis (France).
LIGHT SHEET VISUALIZATION AND VELOCITY FIELD MEASUREMENTS IN SEEDED FLOWS
J. Haertig and P. Smigielski 11 Aug. 1986 7 p Presented at the Third International Symposium on Applications of Laser Anemometry to Fluid Mechanics, Lisbon, Portugal, 7-9 Jul. 1986
(ISL-CO-225/86; ETN-87-99642) Avail: NTIS HC A02/MF A01

A double frequency YAG laser giving pairs of triggered pulses and able to operate at high repetition rates was used for chrono-tomography of seeded flows. In addition to the flow visualization, velocity fields were deduced by processing double-exposure pictures. Photography is still necessary, but a video camera of poor resolution compared with pictures can be used if tracer concentration is low and if only a small region of the flow is of interest. Such methods are computer time consuming

and more complicated to handle than usual local methods. Nevertheless, multiexposure methods can give valuable results when investigating unstationary flow with medium scale such that vortical flows where spatial information on instantaneous velocities are very important but difficult to obtain with classical means.
ESA

N87-23936*# National Aeronautics and Space Administration. Lewis Research Center, Cleveland, Ohio.
STRAIGHT CYLINDRICAL SEAL FOR HIGH-PERFORMANCE TURBOMACHINES
Robert C. Hendricks Jun. 1987 76 p
(NASA-TP-1850; E-3184; NAS 1.60:1850) Avail: NTIS HC A05/MF A01 CSCL 20D

A straight cylindrical seal configuration representing the seal for a high-performance turbopump (e.g., the space shuttle main engine fuel pump) was tested under static (nonrotating) conditions. The test data included critical mass flux and pressure profiles over a wide range of inlet temperatures and pressures for fluid nitrogen and fluid hydrogen with the seal in concentric and fully eccentric positions. The critical mass fluxes (or leakage rates) for the concentric and fully eccentric configurations were nearly the same when based on stagnation conditions upstream of the seal. The fully eccentric configuration pressure profiles of the gas and liquid were different. Further, the pressure differences between the maximum and the minimum clearance positions were highly dependent on the geometric conditions, the temperature, and the absolute pressure at both the inlet and the exit. The pressure differences were greatest in the inlet region. The results, although complex, tend to follow the corresponding-states principles for critical flows. Gaseous injection near the seal exit plane significantly altered the pressure profiles and could be used to control turbomachine instabilities. Author

N87-23576# Joint Publications Research Service, Arlington, Va.
SIMULTANEOUS RADIATIVE AND CONVECTIVE HEATING OF THIN BODY IN MEDIUM WITH VARIABLE TEMPERATURE
Yu. V. Vidin *In its* USSR Report: Engineering and Equipment 9 Mar. 1987 p 4 Transl. into ENGLISH from Izvestiya Vysshikh Uchebnykh Zavedeniy: Aviatsionnaya Tekhnika (Kazan, USSR), no. 1, Jan. - Mar. 1986 p 88-90 (For primary document see N87-23570 17-01)
Avail: NTIS HC A06/MF A01

N87-23793# McDonnell-Douglas Corp., St. Louis, Mo.
RESPONSE OF TRANSONIC DIFFUSER FLOWS TO ABRUPT INCREASES OF BACK PRESSURE: WALL PRESSURE MEASUREMENTS
T. J. Bogar and M. Sajben *In* Johns Hopkins Univ., The 23rd JANNAF Combustion Meeting, Volume 1 Oct. 1986 p 417-424 (For primary document see N87-23757 17-28)
(Contract N60530-83-C-0186)
Avail: CPIA, Laurel, Md. 20707 HC $70.00

N87-23794# Naval Surface Weapons Center, Silver Spring, Md.
DOWNSTREAM BOUNDARY EFFECTS ON THE FREQUENCY OF SELF-EXCITED OSCILLATIONS IN TRANSONIC DIFFUSER FLOWS
T. Hsieh *In* Johns Hopkins Univ., The 23rd JANNAF Combustion Meeting, Volume 1 Oct. 1986 p 425-434 (For primary document see N87-23757 17-28)
Avail: CPIA, Laurel, Md. 20707 HC $70.00

N87-23800# California Univ., Berkeley. Dept. of Mechanical Engineering.
VORTEX-NOZZLE INTERACTIONS IN RAMJET COMBUSTORS
K. Yu, S. Lee, H. E. Stewart, and J. W. Daily *In* Johns Hopkins Univ., The 23rd JANNAF Combustion Meeting, Volume 1 Oct. 1986 p 499-508 (For primary document see N87-23757 17-28)
(Grant N00014-84-K-0372)
Avail: CPIA, Laurel, Md. 20707 HC $70.00

N87-23801# Naval Research Lab., Washington, D. C. Lab. for Computational Physics.
COMPUTATIONAL STUDIES OF THE EFFECTS OF ACOUSTICS AND CHEMISTRY ON THE FLOW FIELD IN AN AXISYMMETRIC RAMJET COMBUSTOR
K. Kailasanath, J. H. Gardner, E. S. Oran, and J. P. Boris *In* Johns Hopkins Univ., The 23rd JANNAF Combustion Meeting, Volume 1 Oct. 1986 p 509-520 (For primary document see N87-23757 17-28)
Avail: CPIA, Laurel, Md. 20707 HC $70.00

N87-23802# Flow Research, Inc., Kent, Wash.
NUMERICAL SIMULATIONS OF COLD FLOW IN A RAMJET DUMP COMBUSTOR WITH A CHOKED EXIT NOZZLE
S. Menon and W.-H. Jou *In* Johns Hopkins Univ., The 23rd JANNAF Combustion Meeting, Volume 1 Oct. 1986 p 521-531 (For primary document see N87-23757 17-28)
(Contract N00014-84-C-0359)
Avail: CPIA, Laurel, Md. 20707 HC $70.00

N87-23804# Stanford Univ., Calif. Dept. of Mechanical Engineering.
EFFECTS ON FUEL SPRAY CHARACTERISTICS AND VAPORIZATION ON ENERGY RELEASE RATES AND FLOW FIELD STRUCTURE IN A DUMP COMBUSTOR
C. T. Bowman, R. K. Hanson, U. Vandsburger, M. G. Allen, and K. R. McManus *In* Johns Hopkins Univ. 23rd JANNAF Combustion Meeting, Volume 1 Oct. 1986 p 545-550 (For primary document see N87-23757 17-28)
(Contract N00014-84-K-0383)
Avail: CPIA, Laurel, Md. 20707 HC $70.00

N87-23813# Rockwell International Corp., Canoga Park, Calif. Rocketdyne Div.
NONINTRUSIVE TEMPERATURE MEASUREMENTS IN SSME PREBURNER ELEMENT FLOWFIELDS
R. J. Jensen and S. C. Fisher *In* Johns Hopkins Univ., The 23rd JANNAF Combustion Meeting, Volume 1 Oct. 1986 p 633-640 (For primary document see N87-23757 17-28)
Avail: CPIA, Laurel, Md. 20707 HC $70.00

35 INSTRUMENTATION AND PHOTOGRAPHY

Includes remote sensors; measuring instruments and gages; detectors; cameras and photographic supplies; and holography.

For aerial photography see *43 Earth Resources and Remote Sensing.* For related information see also *06 Aircraft Instrumentation,* and *19 Spacecraft Instrumentation.*

N87-23937# Michigan Univ., Ann Arbor. Dept. of Electrical and Computer Engineering.
HOLOGRAPHIC OPTICAL ELEMENTS FORMED IN LIGHT OF REDUCED COHERENCE Annual Report, 1 Dec. 1985 - 31 Nov. 1986
E. Leith 21 Feb. 1987 117 p
(Grant AF-AFOSR-0012-85)
(AD-A179372; AFOSR-87-0478TR) Avail: NTIS HC A06/MF A01 CSCL 14E

A new type of interferometer for producing fringes with spatially incoherent light was invented, which can be used for construction of Holographic Optical Elements (HOEs). A method for forming HOEs of very high diffraction efficiency and low noise was developed. THe new superresolution discovery was explored, and significant experimental verification was carried out. A new method of image formation through inhomogeneities was discovered and experimentally verified. This method is based on the technique of superresolution by incoherent conversion. An incoherent spatial filtering technique was developed for use with spatially incoherent white light. This technique was extended to the use of real world, reflecting, three-dimensional objects. GRA

N87-23938# Oklahoma State Univ., Stillwater. Electronics Lab.
INTER-VEHICLE RANGING SYSTEM
T. G. Bertenshaw and W. A. Holloway 1 Jan. 1987 15 p
(Contract F19628-85-C-0006)
(AD-A179492; AFGL-TR-87-0030; SR-2) Avail: NTIS HC A02/MF A01 CSCL 17I

The inter-vehicle ranging system is a simple and inexpensive device designed to provide the relative distance between two bodies. It is an active system in that receive/transmit transponders are employed in a master/slave relationship. The system can accommodate several transponders operating in differing frequency bands with range resolution of less than 30 meters. Resolution improves to LSB accuracy, or 10 meters, if one pair of transponders is used. The system is designed such that inter-vehicle ranging can readily be incorporated in a PCM data stream. GRA

N87-23939# Rockwell International Corp., Golden, Colo. Space Operations.
SPECIAL APPLICATIONS OF THE DEBYE MICRODIFFRACTOMETER
P. A. Steinmeyer 27 May 1986 14 p
(Contract DE-AC04-76DP-03533)
(RFP-3906) Avail: NTIS HC A02/MF A01

The Debye microdiffractometer utilizes powder camera-type X-ray optics to detect a large fraction of a Debye ring, making possible the use of very small primary beams. Suggested here are applications of this instrument to several types of analysis, including preferred orientation studies and simple nondispersive XRF (X-ray fluorescence). Author

N87-23940# Rochester Univ., N. Y. Lab. for Laser Energetics.
DOUBLE-DIFFRACTION X-RAY IMAGING CAMERA Final Report
Apr. 1987 12 p
(Contract DE-AS08-84DP-40197)
(DE87-007936; DOE/DP-40197/1) Avail: NTIS MF A01

A device designed for obtaining monochromatic images of laser-plasma X-ray sources via the double diffraction process has been constructed. Such imaging, which is monochromatic and of high resolution, could for the first time make possible a study of the hydrodynamic stability of laser-target implosions. As a first step in the realization of such a possibility, a camera had to be designed and fabricated, for the precise alignment of doubly-diffracting crystals in the OMEGA tank. The design constraints were: the instrument has to be positioned as close to the target as possible (which will maximize the imaging resolution), while avoiding damage from the target explosion as well as avoiding interference with neighboring laser beams and other measuring devices in the OMEGA tank. This called for a miniaturized X-ray camera. To enable multi-shot operation without the need to extract the instrument from the vacuum tank between successive shots, a motorized, remotely-controlled operation was called for. In the following we briefly describe the finished instrument and its testing. We enclose photographs and drawings pertaining to the imaging camera. DOE

N87-23941*# National Aeronautics and Space Administration. Langley Research Center, Hampton, Va.
RAPID QUANTIFICATION OF AN INTERNAL PROPERTY Patent Application
John Companion, inventor (to NASA), Joseph S. Heyman, inventor (to NASA), Al Cavalier, inventor (to NASA), Beth Mineo, inventor (to NASA), and Travis Blalock, inventor (to NASA) 13 Nov. 1986 19 p
(NASA-Case-LAR-13689-1-NP; NAS 1.71:LAR-13689-1; US-Patent-Appl-SN-929869) Avail: NTIS HC A02/MF A01 CSCL 14B

A device and method for the rapid quantification of an internal property of a material are described which are typified by embodiments for rapidly quantifying the amount of urine in the bladder of a human subject. An ultrasonic transducer, which is positioned on the subject in proximity to the bladder, is excited by a logic-controlled pulser/receiver to introduce an acoustic wave into the patient. This wave interacts with the bladder walls and is reflected back to the ultrasonic transducer, whence it is amplified and processed by the pulser/receiver. The resulting signal is digitized by an analog-to-digital converter under the command of the logic system and is stored in a memory. The software in the logic system determines the amount of urine in the bladder as a function of propagated ultrasonic energy based on programmed scientific measurements and past history of the specific subject. The system then sends out a signal to turn on any or all of the audible alarm, the visible alarm, the tactile alarm, and the remote wireless alarm. NASA

N87-23942 British Broadcasting Corp., Kingswood (England). Engineering Div.
SPECOL: A COLORIMETRIC MEASUREMENT SYSTEM
A. Roberts Apr. 1987 26 p
(BBC-RD-1987/4) Avail: Issuing Activity

A spectroradiometric colorimeter system, SpeCol, comprising a light detector and a microcomputer is described. The light detector is a monochromator which can be tuned over the entire wavelength range of visible light so that spectral energy distributions of all types of light sources can be measured. The computer has direct control over the monochromator and can derive the chromacity coordinates of the light source by calculation. The equipment has many modes of operation and can measure the properties of absorptive and reflective filters as well as those of self luminous sources such as lamps and television displays. For measurements of tricolor television displays the performance of the display can be analyzed for conformity with the relevant EBU (European Broadcasting Union) specification. Using this equipment, measurement can be made rapidly and with good accuracy. Author

N87-23943# Sandia National Labs., Albuquerque, N. Mex.
PALLADIUM-SILVER AND GOLD ALLOYS AS CATALYTIC GATES ON MIS GAS SENSORS
R. C. Hughes, T. E. Zipperian, W. K. Schubert, T. A. Plut, and J. L. Rodriguez 1987 5 p Presented at the 4th International Conference on Solid-State Sensors and Actuators, Tokyo, Japan, 2 Jun. 1987
(Contract DE-AC04-76DP-00789)
(DE87-006959; SAND-87-0582C; CONF-870676-1) Avail: NTIS HC A02

The addition of Ag or Au to Pd to form an alloy gate metal of a metal-oxide-semiconductor (MOS) gas sensing diode can improve the performance and change the selectivity of the sensors for a variety of gas mixtures. The basic sensitivity to molecular hydrogen is not lost for alloy compositions below 40% Ag or Au. The signal from the diodes to mixtures of H2 with the oxidizing gases, NO2 and Cl2, is quite different for Pd gated diodes than for Pd-Ag alloy gated diodes. DOE

N87-23944* National Aeronautics and Space Administration. Marshall Space Flight Center, Huntsville, Ala.
APPARATUS AD METHOD FOR QUIESCENT CONTAINERLESS PROCESSING OF HIGH TEMPERATURE METALS AND ALLOYS IN LOW GRAVITY Patent
Michael B. Robinson, inventor (to NASA) and Lewis L. Lacy, inventor (to NASA) 30 Jun. 1987 8 p Filed 5 Dec. 1985 Supersedes N86-23899 (24 - 14, p 2285)
(NASA-Case-MFS-28087-1; US-Patent-4,677,642; US-Patent-Appl-SN-805010; US-Patent-Class-373-10; US-Patent-Class-373-15)
Avail: US Patent and Trademark Office CSCL 14B

The electron bombardment furnace consists of two confinement grid sections which may be moved and separated from each other. Inside the bombardment furnace, a tungsten element is enclosed. The material specimen is located within the tungsten element and grounded by means of grounded support wires connected to the respective sections of the furnace. The material specimen is supported on the ground wires and heated by electron bombardment until melt occurs. The furnace sections are separated in opposite directions causing the ground wires to pull from the

surfaces of the specimen, leaving the specimen freely suspended in the process chamber without the action of external forces. The specimen remains in its melt condition in the processing chamber where it can be undercooled without external forces acting on the specimen, which would cause dynamic nucleation.
Official Gazette of the U.S. Patent and Trademark Office

N87-23834*# Jet Propulsion Lab., California Inst. of Tech., Pasadena.
RESULTS OF USING THE GLOBAL POSITIONING SYSTEM TO MAINTAIN THE TIME AND FREQUENCY SYNCHRONIZATION IN THE DEEP SPACE NETWORK
P. A. Clements, A. Kirk, and R. Unglaub *In its* The Telecommunications and Data Acquisition Report 15 May 1987 p 67-72 (For primary document see N87-23828 17-32)
Avail: NTIS HC A06/MF A01 CSCL 14B

36 LASERS AND MASERS

Includes parametric amplifiers.
For related information see also *76 Solid-State Physics.*

N87-23945# Army Environmental Hygiene Agency, Aberdeen Proving Ground, Md.
LASER HAZARDS BIBLIOGRAPHY, 12 EDITION
David H. Sliney, Penelope K. Galoff, Anita Robinson, and Jody Rush 31 Oct. 1986 220 p
(AD-A179220) Avail: NTIS HC A10/MF A01 CSCL 06R

The Laser Hazards Bibliography consists of 2,979 references in the open literature broken into subject categories which relate to general biological effects, the eye, the skin, laser safety, laser propagation in the atmosphere, and laser measurements. GRA

N87-23946# Hughes Research Labs., Malibu, Calif.
EXPERIMENTAL AND THEORETICAL STUDIES OF LASER COOLING AND EMITTANCE CONTROL OF NEUTRAL BEAMS Final Report, 1 Nov. 1981 - 31 Jan. 1987
J. F. Lam, R. A. McFarlane, A. J. Palmer, D. G. Steel, and R. S. Turley 31 Jan. 1987 130 p
(Contract F49620-82-C-0004)
(AD-A179226; HAC-REF-E9915; AFOSR-87-0339TR) Avail: NTIS HC A07/MF A01 CSCL 20H

Experimental and theoretical studies are made of issues relevant to laser cooling and emittance control of neutral beams. Experimental accomplishments include development of a technique for state specific velocity selection in atomic beams, observation of the Optical Kapitza Dirac Effect, construction of sodium and atomic hydrogen beam facilities, and initial development of a tunable, transform limited, Vacuum Ultraviolet source. Theoretical accomplishments include development of a theory of pi pulse cooling, a theory of two photon ionization in atomic hydrogen resonant with the Lyman alpha transition, and an incorporation of the effects of intense fields in the theory of the Optical Kapitza Dirac Effect. GRA

N87-23947# Rochester Univ., N. Y. Lab. for Laser Energetics.
UNIVERSITY OF ROCHESTER, LABORATORY FOR LASER ENERGETICS Annual Report, 1 Oct. 1985 - 30 Sep. 1986
Jan. 1987 224 p
(Contract DE-FC08-85DP-40200)
(DE87-005920; DOE/DP-40200/37) Avail: NTIS HC A10/MF A01

In FY86 the Laboratory has produced a list of accomplishments in which it takes pride. LLE has met every laser-fusion program milestone to date in a program of research for direct-drive ultraviolet laser fusion originally formulated in 1981. LLE scientists authored or co-authored 135 scientific papers during 1985 to 1986. The collaborative experiments with NRL, LANL, and LLNL have led to a number of important ICF results. The cryogenic target system developed by KMS Fusion for LLE will be used in future high-density experiments on OMEGA to demonstrate the compression of thermonuclear fuel to 100 to 200 times that of solid (20 to 40 g/cm³) in a test of the direct-drive concept, as noted in the National Academy of Sciences' report. The excellence of the advanced technology efforts at LLE is illustrated by the establishment of the Ultrafast Science Center by the Department of Defense through the Air Force Office of Scientific Research. Research in the Center will concentrate on bridging the gap between high-speed electronics and ultrafast optics by providing education, research, and development in areas critical to future communications and high-speed computer systems. The Laboratory for Laser Energetics continues its pioneering work on the interaction of intense radiation with matter. This includes inertial-fusion and advanced optical and optical electronics research; training people in the technology and applications of high-power, short-pulse lasers; and interacting with the scientific community, business, industry, and government to promote the growth of laser technology. DOE

N87-23948# Defense Advanced Research Projects Agency, Arlington, Va. Information Science and Technology Office.
FUTURE DIRECTIONS OF C3 RESEARCH AT DARPA (DEFENSE ADVANCED RESEARCH PROJECTS AGENCY)
D. G. Perry and J. S. Dahmann 1987 11 p Presented at the European AFCEA Meeting, Brussels, Belgium, 16 Feb. 1987 Prepared in cooperation with Los Alamos National Lab., N. Mex. and Mitre Corp., Bedford, Mass.
(Contract W-7405-eng-36)
(DE87-007501; LA-UR-87-805; CONF-870271-1) Avail: NTIS HC A02/MF A01

Research into C3 related problems is a major effort of the Information Science and Technology Office of the Defense Advanced Research Projects Agency. The major thrusts of projects are in the area of future, high-risk efforts, often resulting in the development of a conceptual model or prototype. Some of these prototypes are then further developed to provide an infrastructure for future research. The programs can be divided into two groups: base technology research programs and testbed programs. The testbeds provide a focus for the technology programs. DOE

N87-23949# Los Alamos National Lab., N. Mex.
DEVELOPMENT OF A HIGH TEMPERATURE CERAMIC-TO-METAL SEAL FOR AIR FORCE WEAPONS LABORATORY LASER
R. E. Honnell and S. D. Stoddard Mar. 1987 17 p
(Contract W-7405-eng-36)
(DE87-007711; LA-10884-MS) Avail: NTIS HC A02/MF A01

Procedures were developed for fabricating vacuum tight metal-to-ceramic ring seals between Inconel 625 and MgO-3 wt % Y2O3 tubes metallized with a calcia-alumina-silica glass (CaO-29 wt % Al2O3-35 wt % SiO2) containing 50 vol % molybdenum filler. Palniro No. 1 (Au-25 wt % Pd-25 wt % Ni) was found to be the most reliable braze for joining Inconel to metallized MgO-3 wt % Y2O3 bodies. The reliabilities of the processing procedures and the material systems were demonstrated. A prototype electrical feedthrough was fabricated for 1173 K operation in air or vacuum. DOE

N87-23950# Texas Univ., Austin. Dept. of Physics.
KINETIC STUDIES FOLLOWING STATE-SELECTIVE LASER EXCITATION Annual Performance Report, 15 Mar. 1986 - 31 Mar. 1987
J. W. Keto Oct. 1986 53 p
(Contract DE-FG05-84ER-13191)
(DE87-007938; DOE/ER-13191/7) Avail: NTIS HC A04/MF A01

Three general areas of energy transfer are discussed: (1) the direct measurement of state-to-state reaction rates by measuring time dependent loss of reactants and products, (2) studies of rovibrationally resolved spectral studies in supersonic beams, and (3) laser assisted collisions. Specifically, results are presented for reactions of Xe*(5p5 6p) with Cl2, optical collisions of Xe*6p(1/2) sub O, and high resolution of xenon and cesium dimers. DOE

N87-23951# Illinois Univ., Chicago. Dept. of Physics.
ORDERED MANY-ELECTRON MOTIONS IN ATOMS AND X-RAY LASERS
C. K. Rhodes 1986 28 p Presented at the NATO Advanced Study Conference, Les Houche, France, 16 Jun. 1986
(Contract DE-AC02-83ER-13137)
(DE87-004731; CONF-8606157-4) Avail: NTIS HC A03/MF A01

Subpicosecond ultraviolet laser technology is enabling the exploration of nonlinear atomic interactions with electric field strengths considerably in excess of an atomic unit. As this regime is approached, experiments studying multiple ionization, photoelectron energy spectra, and harmonically produced radiation all exhibit strong nonlinear coupling. Peak total energy transfer rates on the order of approx 2 x 10 to the -4 W/atom have been observed at an intensity of approx. 10 to the 16th W/cu cm, and it is expected that energy transfer rates approaching approx. 0.1 to 1 W/atom will occur under more extreme conditions for which the ultraviolet electric field E is significantly greater than e/sup 3 sub 0. In this high intensity regime, a wide range of new nonlinear phenomena will be open to study. These will include the possibility of ordered driven motions in atoms, molecules, and plasmas, mechanisms involving collisions, and relativistic processes such as electron-positron pair production. An understanding of these physical interactions may provide a basis for the generation of stimulated emission in the x-ray range. DOE

N87-23952# Los Alamos National Lab., N. Mex.
TIME-RESOLVED PICOSECOND REFLECTIVITY STUDY OF LASER-EXCITED LAYERED COMPOUNDS
C. Y. Huang, A. M. Malvezzi, N. Bloembergen, and F. J. DiSalvo, Jr. 1986 7 p Presented at the Materials Research Society Fall Meeting, Boston, Mass., 1 Dec. 1986 Prepared in cooperation with Harvard Univ., Cambridge, Mass.; Bell Telephone Labs., Inc., Murray Hill, N.J.
(Contract W-7405-eng-36)
(DE87-005115; LA-UR-87-72; CONF-861207-97) Avail: NTIS HC A02/MF A01

The pump-and-probe technique is employed to perform picosecond time resolved measurements of the reflectivity changes in two archetypal layered compounds, 1T-TiS2 and 1T-TiSe2 probed at 1.064 microns after pumping by 20 ps, 0.532 micron laser pulses. At the threshold fluence, approx. 40 mJ/sq cm, the reflectivity drops sharply, marking the occurrence of a phase transformation on the surface of the sample. Above threshold, the reflectivity reaches a value as low as approx. 0.1 at high fluences, strongly suggesting that, as in graphite, the high temperature phase is not metallic. DOE

N87-23953# Northwestern Univ., Evanston, Ill. Midwest Bio-Laser Inst.
MIDWEST FREE-ELECTRON LASER PROGRAM Annual Report, 1 Mar. 1986 - 28 Feb. 1987
L. J. Cerullo, M. Epstein, M. E. Marhic, W. Z. Rymer, and K. G. Spears 1 Mar. 1987 12 p
(Contract N00014-86-K-0188)
(AD-A178106) Avail: NTIS HC A02/MF A01 CSCL 20E

Developments in infrared waveguides for laser beam delivery include liquid core fibers, germanium coated brass guides, whisper gallery waveguides, Bragg fibers and waveguides with periodic structures. Studies of interaction of laser radiation with tissue over a broad range of wavelengths include absorption of radiant energy by chromophores in a light scattered matrix, effects of heating with pulsed Nd-YAG lasers and the use of the diffusion model of radiative transfer to optical dosimetry in clinical phototherapy. The development of picosecond laser instrumentation for neuroscience research allows for the simulation of the FEL in pulse duration, energy and wavelengths. The effects of laser-beam energy in neural tissue were investigated. These studies included the effects of CO2 laser energy on the rat spinal cord as determined by the evoked potentials recorded from dorsal white matter in the mid-thoracic cord. The latter showed no discernable effects for levels below those causing visible damage to the dorsal column white matter. These studies indicate minimal thermal effects at levels corresponding to the onset of breakdown. GRA

N87-23954# Naval Ocean Systems Center, San Diego, Calif.
HORIZONTAL VARIATION OF ATMOSPHERIC EXTINCTION/-BACKSCATTER COEFFICIENTS Final Report, Oct. 1985 - Sep. 1986
Douglas R. Jensen Dec. 1986 51 p
(AD-A178298; NOSC/TD-1042) Avail: NTIS HC A04/MF A01 CSCL 20F

This document describes the evaluation of aerosol data to determine the horizontal homogeneity of atmospheric extinction and backscatter coefficients as it applies to the inversion technique for deducing extinction from lidar returns. GRA

N87-23955# Lawrence Livermore National Lab., Calif.
THERMAL IGNITION OF PYROTECHNICS WITH LASERS
C. T. S. Chow and J. H. Mohler 1987 11 p Presented at the 3rd International Conference of the Groupe de Travail de Pyrotechnic Spatiale and 12th International Pyrotechnics Seminar, Paris, France, 8 Jun. 1987 Prepared in cooperation with Mound Lab., Miamisburg, Ohio
(Contracts W-7405-eng-48; DE-AC04-76DP-00053)
(DE87-006245; UCRL-94740; CONF-870668-1) Avail: NTIS HC A02/MF A01

We are studying the transient phenomena of thermal ignition using laser energy. Present-day infrared scanning and recording techniques enable us to determine the heat content based on the thermal profiles, during ignition, with spatial and temporal resolution. Thus, we can actually observe the laser heating and onset of self-sustained combustion in the sample pellet, and we can use the data obtained with existing theory to characterize pyrotechnic materials and to develop more-precise kinetic models of the ignition process. The results demonstrate the viability of our methods for studying the pyrotechnic ignition process. The whole ignition process consists of two stages. In the first stage, a laser acts as an external heat source that heats the surface of a pellet, an inert body. When the temperature reaches a certain level, a second-stage chemical reaction occurs. The two stages are separated by the inflection point of the temperature-vs-time trace. We present a formula derived from the thermal-explosion theory that allows one to determine the kinetic constants, with the surface-heat flux and the inflection temperature as the only parameters. In addition, we also report the ignition delay time as a function of the heat flux and describe the experimental apparatus used. We investigated three reactions: Fe3O4/Al, Fe2O3/Al, and Ti/2B. For our test samples, we used several kinds of powders, including spherical and flaked aluminum powders and medium and fine iron-oxide powders, with various compact densities. DOE

N87-23956# Los Alamos National Lab., N. Mex.
ON-LINE ELECTRON BEAM MEASUREMENTS FOR THE LOS ALAMOS FREE-ELECTRON LASER
A. H. Lumpkin, R. B. Feldman, D. W. Feldman, and W. E. Stein 1987 15 p Presented at the Particle Accelerator Conference, Washington, D.C., 16 Mar. 1987
(Contract W-7405-eng-36)
(DE87-007452; LA-UR-87-925; CONF-870302-48) Avail: NTIS HC A02/MF A01

Recent developments in the electron beam diagnostics used on the Los Alamos Free-Electron Laser (FEL) have extended our on-line, quantitative analysis capability to extraction efficiency and micropulse temporal duration. The FEL's 20-MeV electron beam is 100 microns in length and consists of approx 2000 micropulses of 20-ps duration and 46-ns separation. This extreme range of time scales is addressed by employing a combination of synchronized beam deflectors, an electron spectrometer, intensified video cameras, real-time video digitizers, and microcomputers. The tapered wiggler result for extraction efficiency (2%) and results for pulse duration measurements (10 to 15 ps) by two techniques are presented. DOE

N87-23957# Oak Ridge National Lab., Tenn.
LASER-ENHANCED ELECTRON ATTACHMENT AND ITS POSSIBLE APPLICATION FOR OPTICAL SWITCHING
L. A. Pinnaduwage, L. G. Christophorou, and S. R. Hunter 1987 7 p Presented at the 5th International Symposium on Gaseous Dielectrics, Knoxville, Tenn., 3 May 1987
(Contract DE-AC05-84OR-21400)
(DE87-008787; CONF-870516-7) Avail: NTIS HC A02/MF A01

Observation of enhanced electron attachment to electronically excited thiophenol (C6H5SH) and thioanisole (C6H5SCH3) molecules produced by excimer laser irradiation is reported. The potential significance of this finding for high-power diffuse discharge opening switches is indicated. DOE

N87-23958# Oak Ridge National Lab., Tenn.
CONTROLLED NUCLEATION AND GROWTH STUDIES IN METAL OXIDE AND ALKOXIDE SYSTEMS BY DYNAMIC LASER-LIGHT-SCATTERING METHODS
C. H. Byers, R. R. Brunson, M. T. Harris, and D. F. Williams Apr. 1987 49 p
(Contract DE-AC05-84OR-21400)
(DE87-009103; ORNL/TM-10285) Avail: NTIS HC A03/MF A01

A method for studying the dynamics of crystallization by using an in situ crystallizer in a dynamic laser-light-scattering system has been developed. Results for growing systems in the size range of 0.005 to 1 micron may be monitored nondestructively using this method. In a series of tests, homogeneous precipitation techniques provide reproducible, controlled nucleation and growth of oxides such as hematite and silica. The effects of driving force and homogeneous and heterogeneous seeding were compared with a theoretical treatment of crystal formation and growth. The hydrolysis of tetraethoxysilicate (TEOS) in ethanol, n-butanol, and tert-butyl alcohol was investigated as a function of initial water and ammonia contents. Ethanol concentration, particle size, and number concentration were studied as a function of time. Preliminary results indicate that in the presence of excess water the growth rate of silica particles has a first-order dependence on TEOS concentration. DOE

N87-23959*# National Aeronautics and Space Administration. Marshall Space Flight Center, Huntsville, Ala.
SHUTTLE COHERENT ATMOSPHERIC LIDAR EXPERIMENT (SCALE)
J. Bilbro, R. Beranek, D. Fitzjarrald, and J. Mabry Jun. 1987 275 p
(NASA-TM-100307; NAS 1.15:100307) Avail: NTIS HC A12/MF A01 CSCL 20E

The results of a study to design and accommodate a simplified version of a coherent lidar system capable of performing tropospheric wind measurements are outlined. The following topics are addressed: system sensitivity, orbital analysis, science experiments, preliminary system design, accommodations, and the space qualification of a 2J CO2 laser. Author

N87-23960* National Aeronautics and Space Administration. Pasadena Office, Calif.
MEANS FOR PHASE LOCKING THE OUTPUTS OF A SURFACE EMITTING LASER DIODE ARRAY Patent
James R. Lesh, inventor (to NASA) (Jet Propulsion Lab., California Inst. of Tech., Pasadena.) 30 Jun. 1987 7 p Filed 30 Sep. 1985 Supersedes N86-20780 (24 - 11, p 1780)
(NASA-Case-NPO-16542-1-CU; US-Patent-4,677,629; US-Patent-Appl-SN-781812; US-Patent-Class-372-18; US-Patent-Class-372-103; US-Patent-Class-372-43; US-Patent-Class-350-3.73; US-Patent-Class-350-3.81) Avail: US Patent and Trademark Office CSCL 20E

An array of diode lasers, either a two-dimensional array of surface emitting lasers, or a linear array of stripe lasers, is phase locked by a diode laser through a hologram which focuses the output of the diode laser into a set of distinct, spatially separated beams, each one focused onto the back facet of a separate diode laser of the array. The outputs of the diode lasers thus form an emitted coherent beam out of the front of the array.
Official Gazette of the U.S. Patent and Trademark Office

N87-23961* National Aeronautics and Space Administration. Pasadena Office, Calif.
MULTIPLEX ELECTRIC DISCHARGE GAS LASER SYSTEM Patent
James B. Laudenslager, inventor (to NASA) and Thomas J. Pacala, inventor (to NASA) (Jet Propulsion Lab., California Inst. of Tech., Pasadena.) 30 Jun. 1987 12 p Filed 23 Oct. 1985 Supersedes N86-20778 (24 - 11, p 1780)
(NASA-Case-NPO-16433-1; US-Patent-4,677,636; US-Patent-Appl-SN-790594; US-Patent-Class-372-68; US-Patent-Class-372-81) Avail: US Patent and Trademark Office CSCL 20E

A multiple pulse electric discharge gas laser system is described in which a plurality of pulsed electric discharge gas lasers are supported in a common housing. Each laser is supplied with excitation pulses from a separate power supply. A controller, which may be a microprocessor, is connected to each power supply for controlling the application of excitation pulses to each laser so that the lasers can be fired simultaneously or in any desired sequence. The output light beams from the individual lasers may be combined or utilized independently, depending on the desired application. The individual lasers may include multiple pairs of discharge electrodes with a separate power supply connected across each electrode pair so that multiple light output beams can be generated from a single laser tube and combined or utilized separately.
Official Gazette of the U.S. Patent and Trademark Office

N87-23962*# National Aeronautics and Space Administration, Washington, D.C.
LASA (LIDAR ATMOSPHERIC SOUNDER AND ALTIMETER) EARTH OBSERVING SYSTEM. VOLUME 2D: INSTRUMENT PANEL REPORT
1987 103 p Original contains color illustrations
(NASA-TM-89356; NAS 1.15:89356) Avail: NTIS HC A06/MF A01 CSCL 20E

The Earth Observing System (Eos) will provide an ideal forum in which the stronly synergistic characteristics of the lidar systems can be used in concert with the characteristics of a number of other sensors to better understand the Earth as a system. Progress in the development of more efficient and long-lasting laser systems will insure their availability in the Eos time frame. The necessary remote-sensing techniques are being developed to convert the Lidar Atmospheric Sounder and Altimeter (LASA) observations into the proper scientific parameters. Each of these activities reinforces the promise that LASA and GLRS will be a reality in the Eos era. Author

N87-23831*# Jet Propulsion Lab., California Inst. of Tech., Pasadena.
USE OF A 2.3-GHz TRAVELING-WAVE MASER ON THE USUDA 64-METER ANTENNA
D. Neff *In its* The Telecommunications and Data Acquisition Report 15 May 1987 p 34-40 (For primary document see N87-23828 17-32)
Avail: NTIS HC A06/MF A01 CSCL 20E

N87-23838*# Jet Propulsion Lab., California Inst. of Tech., Pasadena.
DUAL-POLARIZATION 8.45 GHz TRAVELING-WAVE MASER
R. B. Quinn *In its* The Telecommunications and Data Acquisition Report 15 May 1987 p 94-100 (For primary document see N87-23828 17-32)
Avail: NTIS HC A06/MF A01 CSCL 20E

37 MECHANICAL ENGINEERING

Includes auxiliary systems (nonpower); machine elements and processes; and mechanical equipment.

N87-23963# California Univ., Berkeley. Dept. of Civil Engineering.
A CONSISTENT FINITE ELEMENT FORMULATION OF NONLINEAR FRICTIONAL CONTACT PROBLEMS Final Report, Mar. 1986 - Feb. 1987
Jiann-Wen Ju, Robert L. Taylor, and Louis Y. Cheng Mar. 1987 25 p
(Contracts N62583-86-M-T167; YR0-2303)
(AD-A179179; NCEL-CR-87.008) Avail: NTIS HC A02/MF A01 CSCL 20K

A perturbed Lagrangian-based variational formulation is proposed for the finite element solution of fully nonlinear frictional contact problems. In the spirit of an operator splitting methodology, an analogy exists between the proposed treatment for the stick-slip motion and the corresponding treatment in elastoplasticity. Within the context of discrete formulations arising from a finite element approximation, explicit expressions for the frictional consistent contact tangent stiffness and residual are derived from variational equations by using a consistent linearization procedure for both the sliding and adhesion phases. The consistent tangent operator is always non-symmetric for the case of frictional sliding owing to the nature of the Coulomb's friction law employed. For two-dimensional applications, a three-node contact element is employed in the finite element discretization. Numerical examples are also presented that illustrate the performance of the proposed formulation. GRA

N87-23964# Louisiana State Univ., Baton Rouge. Dept. of Computer Science.
ON AUTONOMOUS TERRAIN MODEL ACQUISITION BY A MOBILE ROBOT
N. S. V. Rao, S. S. Iyengar, and C. R. Weisbin 20 Jan. 1987 7 p Presented at the Workshop on Space Telerobotics, Pasadena, Calif., 20 Jan. 1987 Prepared in cooperation with ORNL, Tenn.
(Contract DE-AC05-84OR-21400)
(DE87-005719; CONF-870134-2; CESAR-86/59) Avail: NTIS HC A02

The following problem is considered: A point robot is placed in a terrain populated by unknown number of polyhedral obstacles of varied sizes and locations in two/three dimensions. The robot is equipped with a sensor capable of detecting all the obstacle vertices and edges that are visible from the present location of the robot. The robot is required to autonomously navigate and build the complete terrain model using the sensor information. It is established that the necessary number of scanning operations needed for complete terrain model acquisition by any algorithm that is based on scan from vertices strategy is given by the summation of i = 1 (sup n) N(O sub i)-n and summation of i = 1 (sup n) N(O sub i)-2n in two and three dimensional terrains respectively, where O = (O sub 1, O sub 2,....O sub n) set of the obstacles in the terrain, and N(O sub i) is the number of vertices of the obstacle O sub i. DOE

N87-23965# Oak Ridge National Lab., Tenn.
ANALYSIS OF A MECHANICALLY SIMPLE EXTERNAL COMBUSTION ENGINE WITH AN UNUSUAL CYCLE
N. C. J. Chen and C. D. West Mar. 1987 30 p
(DE87-007788; ORNL/TM-10351) Avail: NTIS HC A03/MF A01

A single-cylinder, single-piston heat engine with no valves is described. Heat is supplied from an external source, so that a wide variety of heat sources or fuels could be used. The ideal performance of the thermodynamic cycle is calculated; a reasonable power output and indicated efficiency appears to be attainable from a machine of practicable size, operating under very modest conditions of temperature and pressure. DOE

N87-23966# Wisconsin Univ., Madison.
A COMPARISON OF UNBURNED FUEL AND ALDEHYDE EMISSIONS FROM A METHANOL-FUELED STRATIFIED CHARGE AND HOMOGENEOUS CHARGE ENGINE
D. E. Foster, C. Kim, and N. Scull Mar. 1987 53 p Prepared in cooperation with ORNL, Tenn.
(Contract DE-AC05-84OR-21400)
(DE87-007793; ORNL/Sub-86-97366/1) Avail: NTIS HC A04/MF A01

This paper presents the results of an experimental program in which a Texaco L-163S engine was fueled with methanol and operated in its traditional stratified charge mode and then modified to run as a homogeneous charge spark ignited engine. The primary data taken were the aldehyde and unburned fuel emissions (UBF). Those data were taken using a continuous time-averaging sampling probe at the exhaust tank and at the exhaust port and with a rotary time-resolving sampling valve located at the exhaust port. The data are for two loads, 138.1 kPa (20 psi) and 207.1 kPa (30 psi) BMEP and three speeds, 1000, 1400 and 1800 rpm. The data indicate that for both the stratified charge and the homogeneous charge modes of operation formaldehyde was the only aldehyde detected in the exhaust and it primarily originated in the cylinder. Over the load and speed ranges tested, the unburned fuel emissions were higher and the formaldehyde emissions lower when comparing the stratified charge to the homogeneous charge operation. Time resolved data at the exhaust port for the two modes of operation are compared. The homogeneous charge operation had a uniform concentration of both unburned fuel and formaldehyde over the exhaust stroke. The stratified charge data shows large changes in the unburned fuel and moderate changes in the aldehyde concentrations during the exhaust stroke. DOE

N87-23967# Sandia National Labs., Albuquerque, N. Mex.
PULSED Nd:YAG LASER CLOSURE WELDING OF THE MC3593/3594 RELAY
P. W. Fuerschbach Mar. 1987 27 p
(Contract DE-AC04-76DP-00789)
(DE87-007825; SAND-87-0354) Avail: NTIS HC A03/MF A01

The pulsed Nd:YAG laser welding process is often chosen today for closure welding of small hermetically sealed electrical devices. This is because it is a high power density welding process that can minimize total heat input and therefore is less likely to damage heat sensitive components. The effect of the pulsed Nd:YAG laser welding parameters on the incidence of glass-to-metal seal cracking and on the weld fusion zone dimensional parameters for the MC 3593/3594 relays has been determined. Fluctuations in weld penetration in production relays have been attributed to variability in sharp focus positioning. A large increase in blowholes and porosity in the fusion zone has been traced to the inadvertent substitution of 304 stainless steel for 304L stainless steel header material. The blowholes and porosity are thought to result from a carbon-oxygen gas reaction in the weld pool due to the presence of a 4% oxygen atmosphere and the increased carbon content of the 304 stainless steel. DOE

N87-23968# Department of Energy, Washington, D. C.
ELECTRIC AND HYBRID VEHICLES PROGRAM: 10TH ANNUAL REPORT TO CONGRESS FOR FISCAL YEAR 1986
Apr. 1987 34 p
(DE87-008350; DOE/CE-0179; AR-10) Avail: NTIS HC A03/MF A01

This tenth annual report on the implementation of the Electric and Hybrid Vehicle Research, Development and Demonstration Act of 1976 (Public Law 94-413, as amended by Public Law 95-238, and Public Law 96-185), referred to as the Act, complies with the reporting requirements established in Section 14 of the Act. In addition to informing Congress of the progress and plans of the Department of Energy Electric and Hybrid Vehicles Program, this report is intended to serve as a communication link between the Department and all of the public and private interests involved in making the program a success. During FY 1986, significant progress was made toward fulfilling the intent of the Congress in the Act.

There has been continuing interest shown by both the automobile manufacturing and supply sectors of our economy in electric and hybrid vehicles. Research and development efforts in batteries and propulsion components continue to achieve significant progress in providing industry with technology options that will result in vehicles that will be more economically competitive and more acceptable to the public. DOE

N87-23969*# Cincinnati Univ., Ohio.
COMPUTER AIDED DESIGN AND ANALYSIS OF GEAR TOOTH GEOMETRY Final Report
S. H. Chang and R. L. Huston May 1987 84 p
(Grant NsG-3188)
(NASA-CR-179611; NAS 1.26:179611; AVSCOM-TR-87-C-13) Avail: NTIS HC A05/MF A01 CSCL 13I

A simulation method for gear hobbing and shaping of straight and spiral bevel gears is presented. The method is based upon an enveloping theory for gear tooth profile generation. The procedure is applicable in the computer aided design of standard and nonstandard tooth forms. An inverse procedure for finding a conjugate gear tooth profile is presented for arbitrary cutter geometry. The kinematic relations for the tooth surfaces of straight and spiral bevel gears are proposed. The tooth surface equations for these gears are formulated in a manner suitable for their automated numerical development and solution. Author

N87-23970* National Aeronautics and Space Administration. Pasadena Office, Calif.
ROTARY STEPPING DEVICE WITH MEMORY METAL ACTUATOR Patent
Robert S. Jamieson, inventor (to NASA) 12 May 1987 7 p
Filed 26 Aug. 1983 Supersedes N83-36484 (21 - 24, p 3978)
(NASA-Case-NPO-15482-1; US-Patent-4,665,334; US-Patent-Appl-SN-526739; US-Patent-Class-310-306; US-Patent-Class-337-393)
Avail: US Patent and Trademark Office CSCL 13I

A rotary stepping device includes a rotatable shaft which is driven by means of a coiled spring clutch which is alternately tightened to grip and rotate the shaft and released to return it to a resting position. An actuator formed of a memory metal is used to pull the spring clutch to tighten it and rotate the shaft. The actuator is activated by heating it above its critical temperature and is returned to an elongated configuration by means of the force of the spring cloth. NASA

N87-23971# National Academy of Sciences - National Research Council, Washington, D. C. National Materials Advisory Board.
CONTROL OF WELDING PROCESSES Final Report, Jan. 1985 - Jan. 1987
Jan. 1987 59 p
(Contract MDA903-86-K-0220)
(AD-A177893; AD-E950921; NMAB-421) Avail: NTIS HC A04/MF A01 CSCL 13H

Increased automatic welding processes has led to an increased requirement for close control of the process. The objectives of welding control and the problems involved with such control are addressed. Because welding is such a complicated process, control strategies are needed to close the gap between what desire and practice. Some of the variables in the process include the base material, joint preparation, controllability of the automated system, consistency of consumables, and welding environment. The importance of understanding the basic processes--arc physics, heat and fluid flow, solidification, and process disturbances, etc,--is emphasized. The state of the art in welding process modeling and the feasibility and need for adaptive control are described. At present, empirically derived models for some processes have been verified, systems based on fully integrated computer-aided design and manufacturing and adaptive controls can be achieved. Such a welding process simulation could permit the design engineer to know in advance the interaction of weldment preparation, fixture design, distortion, and mechanical properties and thus do a much better job of optimizing the entire process. GRA

N87-23972# Solar Turbines International, San Diego, Calif.
INTERCOOLED GAS TURBINE Final Report, Feb. 1985 - Feb. 1987
K. W. Karstensen May 1986 169 p
(Contract GRI-5084-233-1039)
(PB87-178042; ER-6129; GRI-86/0166) Avail: NTIS HC A08/MF A01 CSCL 13I

The simple addition of an intercooler to the Solar 5650 gas turbine increases its maximum output from 3600 to 4700 horsepower and its maximum thermal efficiency from 34.1 to 37.6%. Concurrent improvements under development can boost thermal efficiency to 43%. The optimum near-term intercooler is liquid cooled and is available in four months' lead time from the heat exchanger industry based on an existing heat transfer surface and associated production tooling. Air cooled intercoolers of conventional construction are prohibitively large. Air-to-air intercooling offers attractive advantages if a suitable size can be achieved. GRA

N87-23973# Mechanical Technology, Inc., Latham, N. Y.
SQUEEZE FILM DAMPER TECHNOLOGY. PART 4. DESIGN AND APPLICATION OF SQUEEZE FILM DAMPERS Final Report, Aug. 1979 - Mar. 1985
J. Walton, O. Pinkus, J. Tecza, and W. Parker Sep. 1986 53 p
(Contract F33615-79-C-2050)
(AD-A177996; MTI-87TR17-Pt-4; AFWAL-TR-82-2112-Pt-4) Avail: NTIS HC A04/MF A01 CSCL 13H

Based on the previous three parts of this series, procedures are outlined for the interaction of damper analysis with rotordynamic requirements in order to arrive at an operationally viable system incorporating squeeze film dampers. The design considerations include the various practical aspects of rotating machinery such as spacing, damper location, spring supports, the proximity of various critical, manufacturing tolerances, etc. The procedures are then applied to the fan of a TF-41 engine, resulting in a new design which promises substantially better performance than the one presently used. Author (GRA)

N87-23974# Mechanical Technology, Inc., Latham, N. Y.
SQUEEZE FILM DAMPER TECHNOLOGY. PART 2. EXTENSION OF ANALYSIS AND PARAMETRIC STUDY Final Report, Aug. 1979 - Mar. 1985
J. Walton, O. Pinkus, J. Walowit, J. Tecza, and C. Lee Sep. 1986 87 p
(Contract F33615-79-C-2050)
(AD-A178094; MTI-87TR15-Pt-2; AFWAL-TR-82-2112-Pt-2) Avail: NTIS HC A05/MF A01 CSCL 13G

This report provides refinements and extensions to the analytical treatment of squeeze film dampers reported in Part 1. Specifically, it incorporates the effects of squeeze film damper cavitation on performance based on short-bearing theory and particularly on the damping properties. The analysis also provides means of a more accurate evaluation of the flow resistance in the feeding holes by taking account of the stagnation pressures at the entrance to the clearance space. With these modifications introduced into the computer program, a parametric study is then conducted on the effects of the many variables on the operation of sealed and unsealed dampers, both hole- and groove-fed. Among the variables considered are clearance, size, eccentricity ratio, supply pressure and system frequency. Conclusions are drawn as to the optimum values of these parameters with regard to best damper performance. GRA

N87-23975# Mechanical Technology, Inc., Latham, N. Y.
SQUEEZE FILM DAMPER TECHNOLOGY. PART 3. EXPERIMENTAL INVESTIGATION OF SQUEEZE FILM DAMPERS Final Report, Aug. 1979 - Mar. 1985
J. Walton, O. Pinkus, E. Zorzi, J. Tecza, and J. Giordano Sep. 1986 145 p
(Contract F33615-79-C-2050)
(AD-A178095; MTI-87TR16-Pt-3; AFWAL-TR-82-2112-Pt-3) Avail: NTIS HC A07/MF A01 CSCL 13G

A test rig was constructed and proper instrumentation provided for measuring the performance of squeeze film dampers. The tests provided both conceptual understanding of the mechanism of damper operation by providing data on the viscous and inertia components of the fluid film, and on the modalities of oil delivery via the feeding holes and grooves, for both sealed and unsealed dampers. Quantitative data were then provided for the entire gamut of variables attending the design of squeeze film dampers and these were then compared with theoretical predictions. A particularly important part of the test was the visual documentation via both still and motion pictures of cavitation which is still not a fully understood phenomenon under dynamic conditions. Failure tests were conducted to simulate damper response to extreme loadings such as resulting form loss of a turbine blade. While the correlation with theory was shown to be generally valid up to the upper ranges of speeds, the quality of correlation was much affected by the encountered variation of boundary conditions in the feed grooves. The latter thus emerge as an aspect of squeexe film damper mechanics which needs further study. GRA

N87-23976# Lawrence Livermore National Lab., Calif.
APPLICATION OF A 100-kV ELECTRIC GUN FOR HYPERVELOCITY IMPACT STUDIES
J. E. Osher, H. H. Chau, G. R. Gathers, R. S. Lee, and R. C. Weingart Oct. 1986 10 p Presented at the Hypervelocity Impact Symposium, San Antonio, Tex., 21 Oct. 1986
(Contract W-7405-eng-48)
(DE87-008730; UCRL-95464; CONF-8610268-1) Avail: NTIS HC A02

The Lawrence Livermore National Laboratory 100-kV electric gun has been used to launch flat-plate projectiles for use in studies of spall and hypervelocity impact penetration of thin plates. Impactors were 0.3-mm thick Kapton with dimensions and velocities ranging from 100 sq mm at 4 km/s to 10 sq mm at 18 km/s. A Fabry-Perot laser velocimeter, an electronic streak camera, and a flash x ray were used as diagnostics of the flyer-plate impact on the selected specimen. Experiments generally included the recovery of the remnant specimen and fragments for detailed examination, permitting a study of incipient spall, onset of melting, and fraction fragmented. Experiments to be described include spall measurements on simple and composite target walls at normal and oblique incidence and reverse ballistics impacts of the thin-plate impactor on a stationary penetrator (e.g., Kapton impactors at 15 km/s incident on rods of steel, aluminum, and lead) for calibration of hypervelocity impact codes. DOE

N87-23977*# Northwestern Univ., Evanston, Ill.
A SIMPLIFIED COMPUTER SOLUTION FOR THE FLEXIBILITY MATRIX OF CONTACTING TEETH FOR SPIRAL BEVEL GEARS Final Report
C. Y. Hsu and H. S. Cheng Jun. 1987 73 p
(Grant NAG3-3143)
(NASA-CR-179620; NAS 1.26:179620; AVSCOM-TR-87-C-16) Avail: NTIS HC A04/MF A01 CSCL 13I

A computer code, FLEXM, was developed to calculate the flexibility matrices of contacting teeth for spiral bevel gears using a simplified analysis based on the elementary beam theory for the deformation of gear and shaft. The simplified theory requires a computer time at least one order of magnitude less than that needed for the complete finite element method analysis reported earlier by H. Chao, and it is much easier to apply for different gear and shaft geometries. Results were obtained for a set of spiral bevel gears. The teeth deflections due to torsion, bending moment, shearing strain and axial force were found to be in the order 10(-5), 10(-6), 10(-7), and 10(-8) respectively. Thus, the torsional deformation was the most predominant factor. In the analysis of dynamic load, response frequencies were found to be larger when the mass or moment of inertia was smaller or the stiffness was larger. The change in damping coefficient had little influence on the resonance frequency, but has a marked influence on the dynamic load at the resonant frequencies. M.G.

N87-23978*# National Aeronautics and Space Administration. Lewis Research Center, Cleveland, Ohio.
THE IMPACT DAMPED HARMONIC OSCILLATOR IN FREE DECAY
G. V. Brown and C. M. North 1987 23 p Prepared for presentation at the Vibrations Conference, Boston, Mass., 27-30 Sep. 1987; sponsored by the ASME
(NASA-TM-89897; E-3587; NAS 1.15:89897) Avail: NTIS HC A02/MF A01 CSCL 13I

The impact-damped oscillator in free decay is studied by using time history solutions. A large range of oscillator amplitude is covered. The amount of damping is correlated with the behavior of the impacting mass. There are three behavior regimes: (1) a low amplitude range with less than one impact per cycle and very low damping, (2) a useful middle amplitude range with a finite number of impacts per cycle, and (3) a high amplitude range with an infinite number of impacts per cycle and progressively decreasing damping. For light damping the impact damping in the middle range is: (1) proportional to impactor mass, (2) additive to proportional damping, (3) a unique function of vibration amplitude, (4) proportional to 1-epsilon, where epsilon is the coefficient of restitution, and (5) very roughly inversely proportional to amplitude. The system exhibits jump phenomena and period doublings. An impactor with 2 percent of the oscillator's mass can produce a loss factor near 0.1. Author

N87-23979*# Dartmouth Coll., Hanover, N.H. School of Engineering.
THERMOMECHANICAL EFFECTS IN HIGH-SPEED SEAL RUBS Final Report, 26 Feb. 1979 - 31 Dec. 1984
Francis E. Kennedy, Jr. Jun. 1987 9 p
(Grant NsG3-253)
(NASA-CR-180418; NAS 1.26:180418) Avail: NTIS HC A02/MF A01 CSCL 11A

The analytical effort was aimed at development of numerical model of thermal and mechanical phenomena which occur during seal rub. Finite element programs were develped for studying the temperatures that result from frictional heating during rubs, and the plastic deformation which is caused by rub forces. The experiment phase was originally intended to aid in verification of the results of the analytical model. Experimental techniques were developed for measuring surface temperatures and deformations during single pass rubs. Modifications were made to the device to permit testing at both high and cryogenic temperatures. The results from the experiments are discussed. B.G.

N87-23980*# Catholic Univ. of America, Washington, D.C. Dept. of Mechanical Engineerining.
MODIFIED INDEPENDENT MODAL SPACE CONTROL METHOD FOR ACTIVE CONTROL OF FLEXIBLE SYSTEMS
A. Baz and S. Poh Jul. 1987 32 p
(Grants NAG5-520; NAG5-749)
(NASA-CR-181065; NAS 1.26:181065) Avail: NTIS HC A03/MF A01 CSCL 13I

A modified independent modal space control (MIMSC) method is developed for designing active vibration control systems for large flexible structures. The method accounts for the interaction between the controlled and residual modes. It incorporates also optimal placement procedures for selecting the optimal locations of the actuators in the structure in order to minimize the structural vibrations as well as the actuation energy. The MIMSC method relies on an important feature which is based on time sharing of a small number of actuators, in the modal space, to control effectively a large number of modes. Numerical examples are presented to illustrate the application of the method to generic flexible systems. The results obtained suggest the potential of the devised method in designing efficient active control systems for large flexible structures. Author

N87-23981* National Aeronautics and Space Administration. Lyndon B. Johnson Space Center, Houston, Tex.
METHOD OF MAKING A FLEXIBLE DIAPHRAGM Patent
Guillermo Lerma, inventor (to NASA) (Rockwell International Corp.,

Canoga Park, Calif.) 30 Jun. 1987 8 p Filed 30 Aug. 1985 Supersedes N86-20806 (24 - 11, p 1784)
(NASA-Case-MSC-20797-1; US-Patent-4,676,853; US-Patent-Appl-SN-771537; US-Patent-Class-156-87; US-Patent-Class-156-286; US-Patent-Class-156-289; US-Patent-Class-156-298; US-Patent-Class-156-307.1; US-Patent-Class-156-307.3; US-Patent-Class-156-307.7) Avail: US Patent and Trademark Office CSCL 13I

A diaphragm suitable for extreme temperature usage, such as encountered in critical aerospace applications, is fabricated by a unique method, and of a unique combination of materials, which include multilayered lay-ups of diaphragm materials sandwiched between layers of bleeder fabrics which, after being formed in the desired shape on a mold, are vacuum sealed and then cured under pressure, in a heated autoclave, to produce a bond capable of withstanding extreme temperatures.

Official Gazette of the U.S. Patent and Trademark Office

N87-23982* National Aeronautics and Space Administration. Langley Research Center, Hampton, Va.
ADJUSTABLE MOUNT FOR ELECTRO-OPTIC TRANSDUCERS IN AN EVACUATED CRYOGENIC SYSTEM Patent
Edward A. Crossley, Jr., David P. Haynes, Howard C. Jones, and Irby W. Jones, 04inventors (to NASA) 9 Jun. 1987 10 p Filed 20 Feb. 1986 Supersedes N86-24993 (24 - 15, p 2463
(NASA-Case-LAR-13100-1; US-Patent-4,672,202; US-Patent-Appl-SN-831377; US-Patent-Class-250-238; US-Patent-Class-250-352; US-Patent-Class-62-514•R) Avail: US Patent and Trademark Office CSCL 13I

The invention is an adjustable mount for positioning an electro-optic transducer in an evacuated cryogenic environment. Electro-optic transducers are used in this manner as high sensitivity detectors of gas emission lives of spectroscopic analysis. The mount is made up of an adjusting mechanism and a transducer mount. The adjusting mechanism provided five degrees of freedom, linear adjustments and angular adjustments. The mount allows the use of an internal lens to focus energy on the transducer element thereby improving the efficiency of the detection device. Further, the transducer mount, although attached to the adjusting mechanism, is isolated thermally such that a cryogenic environment can be maintained at the transducer while the adjusting mechanism remains at room temperature. Radiation shields also are incorporated to further reduce heat flow to the transducer location. NASA

N87-23983* National Aeronautics and Space Administration. Langley Research Center, Hampton, Va.
FULLY REDUNDANT MECHANICAL RELEASE ACTUATOR Patent
Melvin H. Lucy, inventor (to NASA) 2 Jun. 1987 9 p Filed 2 May 1985 Supersedes N85-29287 (23 - 18, p 3116)
(NASA-Case-LAR-13198-1; US-Patent-4,669,354; US-Patent-Appl-SN-729704; US-Patent-Class-89-1.14; US-Patent-Class-60-634; US-Patent-Class-60-638) Avail: US Patent and Trademark Office CSCL 13I

A system is described for performing a mechanical release function exhibiting low shock. This system includes two pyrotechnic detents fixed mounted in opposing axial alignment within a cylindrical housing having two mechanical bellows. Two mechanical bellow assemblies, each having one end hermetically bonded to the housing and the other to the respective actuator pin extending from either end of the housing, ensure that all outgassing and contamination from the operation of the pyrotechnic devices will be contained within the housing and bellows. The pin on one end of the assembly is fixed mounted and supported, via a bolt or ball-and-socket joint so that when the charge corresponding to that pin ignites, the entire assembly will exhibit rectilinear movement, including the opposing pin providing the unlatching motion. The release detent pin is supported by a linear bearing and when its corresponding pyrotechnic charge ignites the pin is retracted within the housing producing the same unlatching motion without movement of the entire assembly, thus providing complete mechanical, electrical and pyrotechnic redundancy for the unlatching pin.

Official Gazette of the U.S. Patent and Trademark Office

N87-23984*# National Aeronautics and Space Administration. Lewis Research Center, Cleveland, Ohio.
EXPERIMENTS ON DYNAMIC STIFFNESS AND DAMPING OF TAPERED BORE SEALS
David P. Fleming 1987 13 p Prepared for presentation at the Vibrations Conference, Boston, Mass., 27-30 Sep. 1987; sponsored by ASME
(NASA-TM-89895; E-3552; NAS 1.15:89895) Avail: NTIS HC A02/MF A01 CSCL 11A

Stiffness and damping were measured in tapered bore ring seals with air as the sealed fluid. Excitation was provided by a known unbalance in the shaft which rotated in the test seals. Results were obtained for various seal supply pressures, clearances, unbalance amounts, and shaft speeds. Stiffness and damping varied little with unbalance level, indicating linearity of the seal. Greater variation was observed with speed and particularly supply pressure. A one-dimensional analysis predicted stiffness fairly well, but considerably overestimated damping. Author

N87-23820# Iowa State Univ. of Science and Technology, Ames. Dept. of Mechanical Engineering.
RECENT DEVELOPMENTS IN VEHICLE DYNAMICS
J. Bernard, M. Vanderploeg, and J. Shannan *In* Vibration Inst., The Shock and Vibration Digest, Volume 19, No. 4 Apr. 1987 p 10-16 (For primary document see N87-23818 17-31)
Avail: NTIS HC A04/MF A01

38 QUALITY ASSURANCE AND RELIABILITY

Includes product sampling procedures and techniques; and quality control.

N87-23985# Pacific Northwest Labs., Richland, Wash.
FEDERAL LABORATORY NONDESTRUCTIVE TESTING RESEARCH AND DEVELOPMENT APPLICABLE TO INDUSTRY
S. A. Smith and N. L. Moore Feb. 1987 259 p
(Contract DE-AC06-76RL-01830)
(DE87-008351; PNL-6143) Avail: NTIS HC A12/MF A01

This document presents the results of a survey of nondestructive testing (NDT) and related sensor technology research and development (R and D) at selected federal laboratories. The objective was to identify and characterize NDT activities that could be applied to improving energy efficiency and overall productivity in US manufacturing. Numerous federally supported R and D programs were identified in areas such as acoustic emissions, eddy current, radiography, computer tomography and ultrasonics. A Preliminary Findings Report was sent to industry representatives, which generated considerable interest. DOE

N87-23986# Oak Ridge National Lab., Tenn.
ULTRASONIC TECHNIQUES FOR THE EVALUATION OF CERAMIC JOINTS
W. A. Simpson, Jr. and R. W. McClung Apr. 1987 56 p
(Contract DE-AC05-84OR-21400)
(DE87-009104; ORNL-6350) Avail: NTIS HC A04/MF A01

The increasing use of structural ceramics in high-temperature applications has led to the need for nondestructive evaluation techniques to ensure the integrity of the ceramic materials and the quality of joints consisting of ceramics bonded to ceramics or to metals. We describe the development of ultrasonic techniques for the characterization of ceramic materials and for the detection of flaws in these materials and at ceramic joints. This has led to the ability to determine which face of a 60-micron-thick layer of braze filler material is unbonded, thus providing information about the integrity of the ceramic-filler metal bond. We also describe the development of a rapid technique using Lamb waves to probe the bond between alumina coupons in flexure-strength specimens,

whose geometry makes conventional ultrasonic evaluation of the bond difficult. DOE

N87-23987*# National Aeronautics and Space Administration. Lewis Research Center, Cleveland, Ohio.
APPLICATION OF SCANNING ACOUSTIC MICROSCOPY TO ADVANCED STRUCTURAL CERAMICS
Alex Vary and Stanley J. Klima Jul. 1987 14 p Prepared for presentation at the Symposium on Characterization of Advanced Materials, Monterey, Calif., 27-28 Jul. 1987; sponsored by International Metallographic Society
(NASA-TM-89929; E-3632; NAS 1.15:89929) Avail: NTIS HC A02/MF A01 CSCL 14D

A review is presentod of research investigations of several acoustic microscopy techniques for application to structural ceramics for advanced heat engines. Results obtained with scanning acoustic microscopy (SAM), scanning laser acoustic microscopy (SLAM), scanning electron acoustic microscopy (SEAM), and photoacoustic microscopy (PAM) are compared. The techniques were evaluated on research samples of green and sintered monolithic silicon nitrides and silicon carbides in the form of modulus-of-rupture bars containing deliberately introduced flaws. Strengths and limitations of the techniques are described with emphasis on statistics of detectability of flaws that constitute potential fracture origins. Author

39 STRUCTURAL MECHANICS

Includes structural element design and weight analysis; fatigue; and thermal stress.

For applications see *05 Aircraft Design, Testing and Performance* and *18 Spacecraft Design, Testing and Performance.*

N87-23988# Air Force Inst. of Tech., Wright-Patterson AFB, Ohio. School of Engineering.
IMPROVED MODELING OF STRUCTURAL JOINT DAMPING M.S. Thesis
Gregory L. Leiker Dec. 1986 123 p
(AD-A179111; AFIT/GAE/AA/86D-9) Avail: NTIS HC A06/MF A01 CSCL 13M

The purpose of this thesis is to develop a better model of damping that occurs in structural joints due to Coulomb friction when rotational slip occurs in the joints. A one-dimensional, indirect formulation, of the Boundary Element Method (BEM) is developed to calculate the displacement, rotation, moment and shear in beams which obey the assumptions of simple beam theory. This BEM code is then modified to account for friction damping at the joint of two beams due to a relative rotation between them. A gross slip model of the friction in the joint is used to establish basic behavior of the beam joint with friction damping. Next, a micro-slip model of friction is developed. The micro-slip model, depending on the applied moment, allows for the elastic rotation of the joint up to some threshold moment where partial slip begins. As the applied moment increases the region of partial slip expands until the entire joint is slipping and the gross slip condition exists. GRA

N87-23989# SRI International Corp., Menlo Park, Calif.
INFLUENCE OF MICROSTRUCTURE AND MICRODAMAGE PROCESSES ON FRACTURE AT HIGH LOADING RATES Annual Report, No. 1, Feb. 1986 - Jan. 1987
J. H. Giovanola and D. A. Shockey 27 Feb. 1987 21 p
(Contract F49620-86-K-0010)
(AD-A179264; AFOSR-87-0313TR) Avail: NTIS HC A02/MF A01 CSCL 11F

The optimal use of advanced beta and near-beta titanium alloys, in cases of dynamic or shock loading, requires an understanding of how both microstructure and loading rate influence the fracture behavior. Dynamic crack initiation and propagation experiments on Ti-10V-2Fe-3Al are performed in three microstructural conditions, varying the loading rate to establish the rate-dependence of the fracture toughness. A new experimental method and advanced instrumentation techniques are used to measure the dynamic initiation and propagation toughness. The Fracture Surface Topography Analysis (FRASTS) technique, a novel quantitative fractography process, is applied to the fractured specimens to elucidate the microstructural failure mechanisms controlling fracture in each of the investigated microstructures. Summarized is the progress made during the first year of the program. A metallurgical investigation has been completed to determine the appropriate heat treatments to produce three microstructures with 0%, 12%, and 40% of primary alpha phase, and with a strength level of about 1300 MPa. An optical technique to measure crack opening displacements (COD) during dynamic fracture experiments is developed. GRA

N87-23990# National Aeronautical Establishment, Ottawa (Ontario).
THE INFLUENCE OF TURBULENCE AND DECK SECTION GEOMETRY ON THE AEROELASTIC BEHAVIOUR OF A CABLE-STAYED BRIDGE MODEL
S. J. Zan, H. Yamada, and H. Tanaka Aug. 1986 101 p
(NAE-AN-40; NRC-26190) Avail: NTIS HC A06/MF A01

The results of a full aeroelastic model test of a cable-stayed bridge at a geometric scale of 1:75 are given. Nine deck section configurations were tested in three different flows, two of which were properly scaled atmospheric turbulence, and the third smooth flow. R.J.F.

N87-23991*# National Aeronautics and Space Administration. Langley Research Center, Hampton, Va.
ENERGY-ABSORPTION CAPABILITY AND SCALABILITY OF SQUARE CROSS SECTION COMPOSITE TUBE SPECIMENS
Gary L. Farley (Army Aviation Research and Development Command, Hampton, Va.) Mar. 1987 18 p
(NASA-TM-89087; NAS 1.15:89087; AVSCOM-TM-87-B-3) Avail: NTIS HC A02/MF A01 CSCL 20K

Static crushing tests were conducted on graphite/epoxy and Kevlar/epoxy square cross section tubes to study the influence of specimen geometry on the energy-absorption capability and scalability of composite materials. The tube inside width-to-wall thickness (W/t) ratio was determined to significantly affect the energy-absorption capability of composite materials. As W/t ratio decreases, the energy-absorption capability increases nonlinearly. The energy-absorption capability of Kevlar epoxy tubes was found to be geometrically scalable, but the energy-absorption capability of graphite/epoxy tubes was not geometrically scalable. Author

N87-23992# Sandia National Labs., Albuquerque, N. Mex.
FORCED VIBRATION AS A METHOD FOR DETERMINING STRUCTURAL INTEGRITY
J. D. Rogers 1987 4 p Presented at the 14th Department of Energy Compatibility, Aging and Service Life Conference, Amarillo, Tex., 28 Apr. 1987
(Contract DE-AC04-76DP-00789)
(DE87-005878; SAND-87-0336C; CONF-870482-2) Avail: NTIS HC A02/MF A01

This work presents a method for determining material damping from forced vibration tests by measuring the driving force required at resonance. The force measurement is broken into its various frequency components which allowed the investigation of the harmonic frequency generation associated with specific flaws. DOE

N87-23993# Sandia National Labs., Albuquerque, N. Mex.
PRONTO 2D: A TWO-DIMENSIONAL TRANSIENT SOLID DYNAMICS PROGRAM
L. M. Taylor and D. P. Flanagan Mar. 1987 225 p
(Contract DE-AC04-76DP-00789)
(DE87-007823; SAND-86-0594) Avail: NTIS MF A01

PRONTO 2D is a two-dimensional transient solid dynamics code for analyzing large deformations of highly nonlinear materials subjected to extremely high strain rates. This Lagrangian finite element program uses an explicit time integration operator to

integrate the equations of motion. Four node uniform strain quadrilateral elements are used in the finite element formulation. A number of new numerical algorithms which have been developed for the code are described in this report. An adaptive time step control algorithm is described which greatly improves stability as well as performance in plasticity problems. A robust hourglass control scheme which eliminates hourglass distortions without disturbing the finite element solution is included. All constitutive models in PRONTO are cast in an unrotated configuration defined using the rotation determined from the polar decomposition of the deformation gradient. An accurate incremental algorithm was developed to determine this rotation and is described in detail. A robust contact algorithm was developed which allows for the impact and interaction of deforming contact surfaces of quite general geometry. A number of numerical examples are presented to demonstrate the utility of these algorithms. DOE

N87-23994*# National Aeronautics and Space Administration. Ames Research Center, Moffett Field, Calif.
THERMAL STRESS ANALYSIS OF SPACE SHUTTLE ORBITER WING SKIN PANEL AND THERMAL PROTECTION SYSTEM
William L. Ko and Jerald M. Jenkins Mar. 1987 26 p
(NASA-TM-88276; H-1382; NAS 1.15:88276) Avail: NTIS HC A03/MF A01 CSCL 20K

Preflight thermal stress analysis of the space shuttle orbiter wing skin panel and the thermal protection system (TPS) was performed. The heated skin panel analyzed was rectangular in shape and contained a small square cool region at its center. The wing skin immediately outside the cool region was found to be close to the state of elastic instability in the chordwise direction based on the conservative temperature distribution. The wing skin was found to be quite stable in the spanwise direction. The potential wing skin thermal instability was not severe enough to tear apart the strain isolation pad (SIP) layer. Also, the preflight thermal stress analysis was performed on the TPS tile under the most severe temperature gradient during the simulated reentry heating. The tensile thermal stress induced in the TPS tile was found to be much lower than the tensile strength of the TPS material. The thermal bending of the TPS tile was not severe enough to cause tearing of the SIP layer. Author

N87-23995*# National Aeronautics and Space Administration. Ames Research Center, Moffett Field, Calif.
INELASTIC STRAIN ANALOGY FOR PIECEWISE LINEAR COMPUTATION OF CREEP RESIDUES IN BUILT-UP STRUCTURES
Jerald M. Jenkins Apr. 1987 13 p
(NASA-TM-86813; H-1355; NAS 1.15:86813) Avail: NTIS HC A02/MF A01 CSCL 20K

An analogy between inelastic strains caused by temperature and those caused by creep is presented in terms of isotropic elasticity. It is shown how the theoretical aspects can be blended with existing finite-element computer programs to exact a piecewise linear solution. The creep effect is determined by using the thermal stress computational approach, if appropriate alterations are made to the thermal expansion of the individual elements. The overall transient solution is achieved by consecutive piecewise linear iterations. The total residue caused by creep is obtained by accumulating creep residues for each iteration and then resubmitting the total residues for each element as an equivalent input. A typical creep law is tested for incremental time convergence. The results indicate that the approach is practical, with a valid indication of the extent of creep after approximately 20 hr of incremental time. The general analogy between body forces and inelastic strain gradients is discussed with respect to how an inelastic problem can be worked as an elastic problem. Author

N87-23996# Vibration Inst., Clarendon Hills, Ill.
THE SHOCK AND VIBRATION DIGEST, VOLUME 19, NO. 3 Monthly Report
Judith Nagle-Eshleman, ed. Mar. 1987 72 p
Avail: NTIS HC A04/MF A01

Abstracts are included for the following areas: machines; structures; vehicles; testing systems; human response; mechanical components; structural components; electric components; materials; experimental techniques; mathematical methods; computational methods; and modeling techniques. Also included are two articles: Random Vibration of Nonlinear Systems, and Recent Studies in Plate Vibration. For individual titles, see N87-23997 through N87-23998.

N87-23997# University of Western Ontario, London. Dept. of Engineering Science.
RANDOM VIBRATION OF NONLINEAR SYSTEMS
C. W. S. To *In* Vibration Inst., The Shock and Vibration Digest, Volume 19, No. 3 Mar. 1987 p 3-9 (For primary document see N87-23996 17-39)
(Grant U0230)
Avail: NTIS HC A04/MF A01

Recently developed techniques for the analysis of general nonlinear mechanical and structural systems excited by random vibration are reviewed. Emphasis is on the applicability of these techniques to multi-degree-of-freedom nonlinear systems subjected to nonstationary random excitations and their adaptability to finite element analysis of systems with many degrees of freedom. Author

N87-23998# Air Force Academy, Colo. Dept. of Engineering Mechanics.
RECENT STUDIES IN PLATE VIBRATIONS: 1981-1985. PART 2: COMPLICATING EFFECTS
A. W. Leissa *In* Vibration Inst., The Shock and Vibration Digest, Volume 19, No. 3 Mar. 1987 p 10-24 (For primary document see N87-23996 17-39)
Avail: NTIS HC A04/MF A01

Two hundred and thirteen publications which appeared during the most recent five year period (1981 to 1985) for plates not governed by classical theory are briefly summarized. Thus, the effects of anisotropy, inplane stresses, variable thickness, nonhomogeneity, surrounding media, large deflection, large thickness, nonhomogeneous elastic foundation, initial imperfection, and transverse magnetic field are encompassed. Author

N87-23999# Polish Academy of Sciences, Warsaw. Dept. of Structural Mechanics.
RETARDATION EFFECT IN FATIGUE CRACK GROWTH UNDER STATIONARY STOCHASTIC LOADING
Krzysztof Dolinski 1986 43 p
(Rept-43/1986; ISSN-0208-5658) Avail: NTIS HC A03/MF A01

The crack propagation under Gaussian stationary stochastic loading in the presence of crack growth retardation effects is considered. The Wheeler retardation model is applied. The crack growth process is modeled by Markovian diffusion processes. Some properties of envelope and clustering effect of the load process are taken into account in the calculation of parameters of the Kolmogorov diffusion equation. The mean time to failure when the crack reaches its critical length is determined. The analysis of the mean life-time equation and the results of an example show that the stochastic fluctuations of the stationary load process alone do not significantly affect random variation of the life-time. A quasi-deterministic relationship is allowed between the feature of the fatigue fracture and some material and load parameters. It gives a potential to consider effectively the fatigue crack propagation with retardation effects as an additional failure mode in reliability analysis. Author

N87-24000# Naval Ship Research and Development Center, Annapolis, Md. Ship Materials Engineering Dept.
INVESTIGATION OF TEARING INSTABILITY PHENOMENA IN ASTM STEEL Final Report
Richard E. Link and Richard A. Hays Nov. 1986 28 p
(AD-A177993; DTNSRDC/SME-86-31) Avail: NTIS HC A03/MF A01 CSCL 11F

An experimental investigation was performed to evaluate tearing instability theory by varying the applied tearing modulus, T(applied), so that fracture instability would be initiated at various levels of stable crack extension. This is an extension of past investigations of tearing instability theory in that crack extension was monitored continuously using the D.C. potential drop technique, enabling the applied and material tearing moduli to be calculated at the point of instability. The results of this investigation indicate that, in most cases, fracture instability occurred when the difference between the applied and material tearing moduli was on the order of 10%. Variations in the load versus displacement records of the specimens near maximum load due to local instabilities and friction in the load train precluded measurement of a smooth applied tearing modulus curve. GRA

N87-24001# Defence Research Establishment Atlantic, Dartmouth (Nova Scotia).
THIN-WALLED BEAM THEORIES AND THEIR APPLICATIONS IN THE TORSIONAL STRENGTH ANALYSIS OF SHIP HULLS
Thomas A. Vernon and Y. Nadeau Jan. 1987 73 p
(AD-A178296; DREA-TM-87/202) Avail: NTIS HC A04/MF A01 CSCL 13J

Unified developments of the St-Venant and warping-based thin-walled beam theories and their application in the torsional analysis of ship structures are presented. Open cell, closed cell and multi-cell configurations are treated. The warping-based torsional theory, which accounts for out-of-plane displacements and displacement restraints, provides axial stress distributions resulting from bimoments and in general offers improved predictions of shear stress distribution in thin-walled beams over the St-Venant theory; however, the use of that theory necessitates a more detailed cross sectional property evaluation. The generalization of the warping function to a displacement field independent of the twist is discussed, as are several iterative methods of including warping shear deformations. The application of the prismatic warping theory to the analysis of non-prismatic beams is discussed, and the flexural torsional beam method proposed by Pedersen is developed. This method, in conjunction with a computer program to calculate the required cross sectional properties, has been integrated into a general torsional stress analysis capability within Defence Research Establishment Atlantic (DREA). The DREA system, which can account for geometric discontinuities in a structure, has been developed as an alternative to finite element methods, and is evaluated here via comparison with detailed finite element analyses for several prismatic beams with discontinuities. GRA

N87-24002# Sandia National Labs., Albuquerque, N. Mex.
TECHNIQUES FOR IMPLEMENTING STATICALLY COMPLETE COMPONENT MODE SYNTHESIS FOR FORCED RESPONSE
J. J. Allen 1987 8 p Presented at the 5th International Modal Analysis Conference, London, England, 6 Apr. 1987
(Contract DE-AC04-76DP-00789)
(DE87-002698; SAND-86-1589C; CONF-870446-1) Avail: NTIS HC A02

The Component Mode Synthesis (CMS) method is a Raleigh-Ritz technique, which allows structural models to be reduced in size and coupled with other analytical or experimental components. The CMS transformation uses combinations of static and dynamic trial vectors. Static trial vectors (constraint modes) for all component interface degrees of freedom (DOF) and externally loaded DOF need to be included in the CMS transformation to produce a statically complete CMS transformation. This requirement for aerospace models with surface pressure loads would be restrictive. This study will investigate techniques for producing a statically complete solution using a CMS method, which has a statically incomplete set of constraint modes. The study will also investigate the additional problems involved with the multi-level CMS. The study will be conducted by modifying the transient and frequency response solution sequences of NASTRAN. DOE

N87-24003# Sandia National Labs., Albuquerque, N. Mex.
MATERIAL DAMPING FROM FREQUENCY ANALYSIS OF DRIVING POINT MEASUREMENTS
J. D. Rogers and K. G. McConnell 1987 45 p Presented at the Society for Experimental Mechanics Spring Meeting, Houston, Tex., 14 Jun. 1987
(Contract DE-AC04-76DP-00789)
(DE87-005873; SAND-87-0014C; CONF-870665-1) Avail: NTIS HC A03

An experimental method for determining material damping from the forced vibration of beam specimens has been developed. In this method, the damping was determined from measurements of the driving point force and driving point acceleration. Tests were performed on 2024-T351 aluminum and an aluminum particle filled epoxy. The material damping loss factor was extracted from the test results and compared with results obtained from another test method for the same materials. The loss factor determined for the aluminum specimen was also compared with the loss factor predicted by the Zener Thermal Relaxation Theory. The tests were conducted in atmospheric air and in a reduced pressure environment to observe the effect of air damping. The effects of system nonlinearities and friction damping were also considered. DOE

N87-24004# Sandia National Labs., Albuquerque, N. Mex.
RECONSTRUCTION OF DYNAMIC STRUCTURAL INPUTS IN THE PRESENCE OF NOISE
V. I. Bateman and O. M. Solomon, Jr. 1987 25 p Presented at the Society for Experimental Mechanics Spring Meeting, Houston, Tex., 14 Jun. 1987
(Contract DE-AC04-76DP-00789)
(DE87-006701; SAND-86-1607C; CONF-870665-3) Avail: NTIS HC A02

This report describes a technique to reconstruct dynamic structural inputs by deconvolution of measured data. The structure to which this technique has been applied is a mild steel bar (76.2 mm diameter and 1.524 m long) with a conical nose which provides some geometric simulation of penetrating structures which are used in field test. The deconvolution technique successfully reconstructs dynamic inputs to the bar with and without additive white noise present in the measured response. DOE

N87-24005# Sandia National Labs., Albuquerque, N. Mex.
DYNAMIC BRITTLE FRACTURE ANALYSIS BASED ON CONTINUUM DAMAGE MECHANICS
E. P. Chen 26 Mar. 1987 24 p Presented at the 20th National Fracture Mechanics: Prospectives and Directions, Leheigh, Pa., 23 Jun. 1987
(Contract DE-AC04-76DP-00789)
(DE87-006704; SAND-86-1431C; CONF-870697-1) Avail: NTIS HC A02/MF A01

The dynamic response of materials with existing flaw structures is the subject of the present investigation. In this paper, the cracked solid is described by a constitutive model based on continuum damage mechanics. The purpose of the analysis is to show that the constitutive model can predict many of the experimentally observed phenomena in these materials. This is demonstrated by treating a sample problem. The geometry and loading condition selected for this sample problem is that of a 45 degree inclined crack, centrally situated in a concrete panel and subjected to the action of a step tensile pulse. Damage localization and tension-softening have been observed. These results and their implications are discussed. DOE

N87-24006*# National Aeronautics and Space Administration. Lewis Research Center, Cleveland, Ohio.
IDENTIFICATION OF STRUCTURAL INTERFACE CHARACTERISTICS USING COMPONENT MODE SYNTHESIS
A. A. Huckelbridge (Case Western Reserve Univ., Cleveland, Ohio.) and C. Lawrence 1987 14 p Prepared for presentation at the Vibrations Conference, Boston, Mass., 27-30 Sep. 1987; sponsored by ASME
(NASA-TM-88960; E-3415; NAS 1.15:88960) Avail: NTIS HC A02/MF A01 CSCL 20K

(NASA-TM-88960; E-3415; NAS 1.15:88960) Avail: NTIS HC A02/MF A01 CSCL 20K

The inability to adequately model connections has limited the ability to predict overall system dynamic response. Connections between structural components are often mechanically complex and difficult to accurately model analytically. Improved analytical models for connections are needed to improve system dynamic predictions. This study explores combining Component Mode synthesis methods for coupling structural components with Parameter Identification procedures for improving the analytical modeling of the connections. Improvements in the connection properties are computed in terms of physical parameters so the physical characteristics of the connections can be better understood, in addition to providing improved input for the system model. Two sample problems, one utilizing simulated data, the other using experimental data from a rotor dynamic test rig are presented. Author

N87-24007*# National Aeronautics and Space Administration. Lewis Research Center, Cleveland, Ohio.

ENVIRONMENTAL DEGRADATION OF 316 STAINLESS STEEL IN HIGH TEMPERATURE LOW CYCLE FATIGUE

Sreeramesh Kalluri, S. Stanford Manson, and Gary R. Halford Apr. 1987 17 p Presented at the 3rd International Conference on Environmental Degradation of Engineering Materials, University Park, Pa., 13-15 Apr. 1987; sponsored by the Pennsylvania State Univ.

(Grants NAG3-337; NAG3-553)

(NASA-TM-89931; E-3636; NAS 1.15:89931) Avail: NTIS HC A02/MF A01 CSCL 20K

Procedures based on modification of the conventional Strainrange Partitioning method are proposed to characterize the time-dependent degradation of engineering alloys in high-temperature, low-cycle fatigue. Creep-fatigue experiments were conducted in air using different waveforms of loading on 316 stainless steel at 816 C (1500 F) to determine the effect of exposure time on cyclic life. Reductions in the partitioned cyclic lives were observed with an increase in the time of exposure (or with the corresponding decrease in the steady-state creep rate) for all the waveforms involving creep strain. Excellent correlations of the experimental data were obtained by modifying the Conventional Strainrange Partitioning life relationships involving creep strain using a power-law term of either: (1) time of exposure, or (2) steady-state creep rate of the creep-fatigue test. Environmental degradation due to oxidation, material degradation due to the precipitation of carbides along the grain boundaries and detrimental deformation modes associated with the prolonged periods of creep were observed to be the main mechanisms responsible for life reductions at long exposure times. Author

N87-24008# Technische Univ., Hanover (West Germany). Inst. fuer Statik.

INVESTIGATION OF THE BUCKLING SENSITIVITY OF HEMISPHERICAL CONTAINERS WITH ARBITRARY LIQUID CONTENT Thesis

A. Menzel Apr. 1986 78 p In GERMAN; ENGLISH summary (MITT-31; ISSN-0073-0300; ETN-87-99645) Avail: NTIS HC A05/MF A01

The stability of hemispherical containers filled with a liquid was investigated, with particular attention to the influence of geometrical imperfections. The nonlinear geometrical formulation of the problem is based upon the general shell theory of Wlassov. The filling of the container is of particular importance since conditions of high buckling sensitivity are always given for partial filling. Based on a two-parameter description of the loading, the critical buckling parameters which represent an upper limit for the stability of the shell during the complete filling operation were calculated. The postbuckling behavior of a perfect shell can be related to a disturbance sensitivity. The influence of various imperfections and prebuckling depths was demonstrated by load-deformation curves. For poor prebuckling modes, percentage decreases of the critical buckling parameters were computed. On this basis, suggestions as to the form of the buckling-safety check are given. ESA

N87-23819# Virginia Polytechnic Inst. and State Univ., Blacksburg. Dept. of Engineering Science and Mechanics.

RECENT ADVANCES IN THE NONLINEAR ANALYSIS OF LAMINATED COMPOSITE PLATES AND SHELLS

J. N. Reddy and K. Chandrashekhara (Missouri Univ., Rolla.) *In* Vibration Inst., The Shock and Vibration Digest, Volume 19, No. 4 Apr. 1987 p 3-9 Sponsored in part by Navy and Army (For primary document see N87-23818 17-31)

Avail: NTIS HC A04/MF A01

42 GEOSCIENCES (GENERAL)

No abstracts in this category.

43 EARTH RESOURCES AND REMOTE SENSING

Includes remote sensing of earth resources by aircraft and spacecraft; photogrammetry; and aerial photography.

For instrumentation see *35 Instrumentation and Photography.*

N87-24009# Massachusetts Inst. of Tech., Cambridge. Research Lab. of Electronics.

ACTIVE AND PASSIVE REMOTE SENSING OF ICE Semiannual Report, 1 Aug. 1986 - 31 Jan. 1987

Jin A. Kong 31 Jan. 1987 9 p

(Contract N00014-83-K-0258)

(AD-A179461) Avail: NTIS HC A02/MF A01 CSCL 17I

During the period August 1, 1986 to January 31, 1987, we have studied the volume scattering effects of snow-covered sea ice with a three-layer random medium model for microwave remote sensing. The strong fluctuation theory and the bilocal approximation are applied to calculate the effective permittivities for snow and sea ice. The wave scattering theory in conjunction with the distorted Born approximation is then used to compute bistatic coefficients and backscattering cross sections. Theoretical results are illustrated by matching experimental data for dry snow-covered thick first-year sea ice at Point Barrow. The radar backscattering cross sections are seen to increase with snow cover for snow-covered sea ice, due to the increased scattering effects in the snow layer. The results derived can also be applied to the passive remote sensing by calculating the emissivity from the bistatic scattering coefficients. GRA

N87-24010*# National Aeronautics and Space Administration. Lyndon B. Johnson Space Center, Houston, Tex.

ERROR ANALYSIS OF LEAF AREA ESTIMATES MADE FROM ALLOMETRIC REGRESSION MODELS

A. H. Feiveson and R. S. Chhikara 14 Jul. 1986 44 p

(NAG5-548)

(NASA-TM-89220; NAS 1.15:89220) Avail: NTIS HC A03/MF A01 CSCL 02F

Biological net productivity, measured in terms of the change in biomass with time, affects global productivity and the quality of life through biochemical and hydrological cycles and by its effect on the overall energy balance. Estimating leaf area for large ecosystems is one of the more important means of monitoring this productivity. For a particular forest plot, the leaf area is often estimated by a two-stage process. In the first stage, known as dimension analysis, a small number of trees are felled so that their areas can be measured as accurately as possible. These leaf areas are then related to non-destructive, easily-measured features such as bole diameter and tree height, by using a regression model. In the second stage, the non-destructive features are measured for all or for a sample of trees in the plots and

then used as input into the regression model to estimate the total leaf area. Because both stages of the estimation process are subject to error, it is difficult to evaluate the accuracy of the final plot leaf area estimates. This paper illustrates how a complete error analysis can be made, using an example from a study made on aspen trees in northern Minnesota. The study was a joint effort by NASA and the University of California at Santa Barbara known as COVER (Characterization of Vegetation with Remote Sensing).
Author

N87-24011# Los Alamos National Lab., N. Mex.
AN ATMOSPHERIC CORRECTION ALGORITHM FOR REMOTE IDENTIFICATION OF NON-LAMBERTIAN SURFACES AND ITS RANGE OF VALIDITY
A. Gratzki and S. A. W. Gerstl 20 Feb. 1987 6 p Presented at IGARSS '87, Ann Arbor, Mich., 18 May 1987
(Contract W-7405-eng-36)
(DE87-006059; LA-UR-87-571; CONF-870576-2) Avail: NTIS HC A02

The usefulness of remotely sensed surface data depends on the ability to correct for atmospheric pertubations on the image. An atmospheric correction algorithm has been proposed which removes atmospheric pertubations from off-nadir measured radiances at the top of the atmosphere in the visible and near-infrared wavelength region. The ability of the model to reproduce radiance distributions at the surface from radiances at the top of the atmosphere is tested and found to be better than 15%. The correction formalism requires as minimum information the total optical depth of the atmosphere and the surface albedo. In this study the accuracy of the model to assumptions about the aerosol phase function, the single-scattering albedo and the vertical profile of the optical depth is also tested. DOE

N87-24012*# National Marine Fisheries Service, Miami, Fla. Southeast Fisheries Center.
UTILIZING REMOTE SENSING OF THEMATIC MAPPER DATA TO IMPROVE OUR UNDERSTANDING OF ESTUARINE PROCESSES AND THEIR INFLUENCE ON THE PRODUCTIVITY OF ESTUARINE-DEPENDENT FISHERIES Semiannual Progress Report
Joan A. Browder, L. Nelson May, Jr., Alan Rosenthal, Robert H. Baumann, and James G. Gosselink 10 Jun. 1987 21 p
(NASA Order S-56107-D)
(NASA-CR-180984; NAS 1.26:180984; SAPR-4) Avail: NTIS HC A02/MF A01 CSCL 08B

A stochastic spatial computer model addressing coastal resource problems in Lousiana is being refined and validated using thematic mapper (TM) imagery. The TM images of brackish marsh sites were processed and data were tabulated on spatial parameters from TM images of the salt marsh sites. The Fisheries Image Processing Systems (FIPS) was used to analyze the TM scene. Activities were concentrated on improving the structure of the model and developing a structure and methodology for calibrating the model with spatial-pattern data from the TM imagery. B.G.

N87-24013# Geological Survey, Reston, Va. National Mapping Div.
RADAR AS A COMPLEMENT TO TOPOGRAPHIC MAPS FOR DELINEATING MARINE TERRACES Open File Report
J. L. Place Dec. 1986 15 p
(PB87-154597; USGS/OFR-86/010) Avail: NTIS HC A02/MF A01 CSCL 08B

In special situations, side-looking airborne radar images can be used to complement topographic maps for locating and mapping marine terraces on mountainous coasts. When a radar image and a topographic map are superimposed in a Zoom Transfer Scope, the two data sources enhance each other to provide more information than is available from either alone. For locating marine terraces on mountainous coasts, a radar view that is parallel with the coast of looking offshore apparently produces a more interpretable image than a view straight in toward the land. This technique has not proven to be equal to field work for terrace mapping, but it should be faster and less expensive for a preliminary terrace delineation. Radar images form the SEASAT satellite were also tested, but without notable success; the side-looping airborne radar images were generally superior for terrace delineation.
GRA

N87-24014# Los Alamos National Lab., N. Mex.
MODELLING OF ATMOSPHERIC EFFECTS ON THE ANGULAR DISTRIBUTION OF A BACKSCATTERING PEAK
B. J. Powers and S. A. W. Gerstl 20 Feb. 1987 5 p Presented at the IGARSS '87, Ann Arbor, Mich., 18 May 1987
(Contract W-7405-eng-36)
(DE87-006060; LA-UR-87-572; CONF-870576-1) Avail: NTIS HC A02/MF A01

If off-nadir satellite sensing of vegetative surfaces is considered, understanding the angular distribution of the radiance exiting the atmosphere in all upward directions is of interest. Of particular interest is the discovery of those reflectance features which are invariant to atmospheric perturbations. When mono-directional radiation is incident on a vegetative scene a characteristic angular signature called the hot-spot is produced in the solar retro-direction. The remotely sensed hot-spot is modified by atmospheric extinction of the direct and reflected solar radiation, atmospheric backscattering, and the diffuse sky irradiance incident on the surface. It is demonstrated, however, by radiative transfer calculations through model atmospheres that at least one parameter which characterizes the canopy hot-spot, namely its angular half width, is invariant to atmospheric perturbations.
DOE

44 ENERGY PRODUCTION AND CONVERSION

Includes specific energy conversion systems, e.g., fuel cells; global sources of energy; geophysical conversion; and windpower.

For related information see also *07 Aircraft Propulsion and Power, 20 Spacecraft Propulsion and Power,* and *28 Propellants and Fuels.*

N87-24015# Midwest Research Inst., Golden, Colo. Solar Energy Research Inst.
WIND ENERGY SYSTEMS: PROGRAM SUMMARY, FISCAL YEAR 1984 AND 1985
Dec. 1986 135 p
(Contract DE-AC02-83CH-10093)
(DE87-001109; DOE/CH-10093/3) Avail: NTIS HC A07/MF A01

This document summarizes the research and development activities sponsored by the Wind/Ocean Technologies Division of DOE during fiscal years (FY) 1984 and 1985. The summary is organized into the following sections: an introduction to the Federal Wind Energy Program, its history, and current research directions; the program's organization for FY 1984 and FY 1985; the program's budget; highlighted accomplishments of the DOE field laboratories in FY 1984 and FY 1985; the program's future role; an index to and summaries of individual projects and contracts managed by each laboratory; and a bibliography of major publications produced by DOE and its laboratories in FY 1984 and FY 1985. DOE

N87-24016# Sandia National Labs., Albuquerque, N. Mex.
SANDIA NATIONAL LABORATORIES 34-METER DIAMETER VERTICAL AXIS WIND TURBINE TEST BED
P. C. Klimas 1987 5 p Presented at the ASME/JSME/ISES Solar Energy Conference, Honolulu, Hawaii, 22 Mar. 1987
(Contract DE-AC04-76DP-00789)
(DE87-003096; SAND-86-1222C; CONF-870307-16) Avail: NTIS HC A02/MF A01

Sandia National Laboratories has designed, procured, and is erecting a 34-meter diameter vertical axis wind turbine test bed. The turbine incorporates many innovative features to investigate possible reductions in the cost-of-energy produced by wind energy

conversion systems. These features include: blade element airfoil sections designed specifically for wind turbines, variable chord-variable section modular blades, stress reducing discontinuous slope blades, and variable speed-constant frequency generation capabilities. The modular blades allow for relatively simple partial configurational changes. Based on Sandia's twelve years of wind turbine research and testing, the test bed is heavily instrumented. The data acquisition and analysis system is capable of rapidly treating large amounts of information on both attended and unattended bases. A comprehensive test plan has been formulated. The turbine is intended to be the primary Department of Energy vehicle for validating concepts intended to improve vertical axis wind energy conversion systems. DOE

N87-24017# Sandia National Labs., Albuquerque, N. Mex.
TEST PLAN FOR THE 34 METER VERTICAL AXIS WIND TURBINE TEST BED LOCATED AT BUSHLAND, TEXAS
W. A. Stephenson Dec. 1986 75 p
(Contract DE-AC04-76DP-00789)
(DE87-004777; SAND-86-1623) Avail: NTIS HC A04/MF A01

A plan is presented for the testing and evaluation of a new 500 kW vertical axis wind turbine test bed. The plan starts with the initial measurements made during construction, proceeds through evaluation of the design, the development of control methods, and finally to the test bed phase where new concepts are evaluated and in-depth studies are performed. DOE

N87-24018*# Pennsylvania Univ., Philadelphia. School of Electrical Engineering.
DEVELOPMENT AND ANALYSIS OF SILICON SOLAR CELLS NEAR 20% EFFICIENCY IN THE FLAT PLATE SOLAR ARRAY PROJECT Final Report
M. Wolf and M. Newhouse 22 Oct. 1986 228 p
(Contracts NAS7-100; JPL-956290)
(NASA-CR-181005; DOE/JPL-7006117; NAS 1.26:181005; DE87-006117) Avail: NTIS HC A11/MF A01 CSCL 10A

The project reported consisted of two phases. The objective of the first was, through a multi-variable experiment, to determine those process parameters in CVD epitaxial deposition which would yield adequate minority carrier lifetimes in the deposited layers to make them suitable for use in crystalline silicon solar cells. A second task was to develop a method for the measurement of these lifetimes which could not be accessed with the commonly applied methods. The objective of the second phase was to refine the lifetime measuring method called Absolute Light Beam Induced Current (ASLBIC), establish its reliability and transportability, perform a comparative assessment of other potentially applicable methods, and possible select or develop a better method. The study on minority carrier lifetimes obtainable in CVD layers is summarized. The ASLBIC method is described, followed by a theoretical discussion of dynamic techniques, applications and implementations. The merits and limitations of the various experimental methods are compared. DOE

N87-24019# Pacific Northwest Labs., Richland, Wash.
CHARACTERIZATION OF SOLAR THERMAL CONCEPTS FOR ELECTRICITY GENERATION. VOLUME 1: ANALYSES AND EVALUATION
T. A. Williams, J. A. Dirks, D. R. Brown, M. K. Drost, Z. A. Antoniac, and B. A. Ross Mar. 1987 219 p
(Contract DE-AC06-76RL-01830)
(DE87-007161; PNL-6128-Vol-1) Avail: NTIS HC A10/MF A01

This study is aimed at providing a relative comparison of the thermodynamic and economic performance in electric applications of several concepts that have been studied and developed in the DOE solar thermal program. Since the completion of earlier systems comparison studies in the late 1970's, there have been a number of years of progress in solar thermal technology. This progress has included development of new solar components, improvements in component and system design detail, construction of working systems, and collection of operating data on the systems. This study provides an updating of the expected performance and cost of the major components and the overall system energy cost for the concepts evaluated. The projections in this study are for the late 1990's time frame, based on the capabilities of the technologies that could be expected to be achieved with further technology development. DOE

N87-24020# North Carolina Univ., Chapel Hill.
ENERGY CONVERSION PROCESSES BASED ON MOLECULAR EXCITED STATES Progress Report, 1 Aug. 1986 - 31 Jul. 1987
T. J. Meyer Mar. 1987 6 p
(Contract DE-FG05-86ER-13633)
(DE87-007408; DOE/ER-13633/1) Avail: NTIS HC A02/MF A01

The major emphasis of our DOE-supported research efforts remains the use of molecular excited states in energy conversion processes. In the past year we have made significant progress in the distinct areas of: (1) electronic structure, photophysical and photochemical properties of MLCT-based excited states, (2) design and characterization of metallopolymeric films as a basis for photoelectrodes containing MLCT-based chromophores, and (3) excited state photoelectrochemical cells based on excited state redox quenching. We have continued to develop synthetic routes to new MLCT excited states, most recently to a series of complexes. Systematic variations (from electron-donating to electron-withdrawing properties) allow control to be gained over changes in emission energies (E sub em), excited state redox potentials, ground state absorption energies, and radiative and nonradiative decay rate constants and perhaps, most importantly, open up two new families of excited states for photoredox application. DOE

N87-24021# Oak Ridge National Lab., Tenn.
APPLICATION OF THERMAL AND FLYWHEEL ENERGY STORAGE IN ORBITING NUCLEAR BURST POWER SYSTEMS
R. P. Wichner and M. Olszewski Mar. 1987 145 p
(Contract DE-AC05-84OR-21400)
(DE87-007882; ORNL/TM-10194) Avail: NTIS HC A07/MF A01

A survey was conducted of currently available thermal energy storage and flywheel energy storage technology and development programs as they may apply to nuclear-based, burst power systems. The manner in which such storage systems may be used in closed cycle, regenerable burst systems is described for a number of cases utilizing the Boiling Potassium Rankine and Dual Loop Lithium Cooled LMRs and the Direct Cycle Brayton HTGR. In general, energy storage devices for such systems enable use of smaller power system components by allowing continuous operation over the duration of both the bursts and the regeneration time. The degree of size reduction depends principally on the required regeneration time. DOE

N87-24022# Washington Univ., St. Louis, Mo. Dept. of Mechanical Engineering.
ANALYSIS AND TEST RESULTS FOR AN IMPROVED CONSTANT SPEED PASSIVE CYCLIC PITCH WIND TURBINE Final Subcontract Report
K. H. Hohenemser Jan. 1987 62 p Prepared in cooperation with Midwest Research Inst., Golden, Colo.
(Contract DE-AC02-83CH-10093)
(DE87-001135; SERI/STR-217-3002) Avail: NTIS HC A04/MF A01

This report describes research conducted at Washington University to address whether or not conventional blade-pitch control of wind turbines can be replaced by rotor yaw control. The test equipment consisted of a horizontal-axis wind turbine, mounted on a 60-ft tower, with an upwind, vane-controlled, passive-cyclic-pitch (PCP) rotor 25 ft in diameter. The automatic rotor-control system was passive. Some erratic yawing at low-speed, power-on operation was corrected with a larger-area tail vane and a longer tail boom. The turbine was tested at gusts of up to 60 mph. The power-off rotor speed was always kept fairly constant. The results would indicate smooth low-load storm survival. Generator cut-in and cut-out were achieved with a digital

controller responding to rotor speed. Torque was found to peak at twice the value predicted by the conventional prop code. Overall, the PCP rotor continued to function very well, even at high yaw rates and wind velocities. However, the combination of the passive furl control system and a fast-reacting, wind-following tail vane caused some problems that could not be corrected at the time.
DOE

N87-24023# Midwest Research Inst., Golden, Colo. Solar Energy Research Inst.
HEAT TRANSFER RESEARCH FOR OCEAN THERMAL ENERGY CONVERSION
F. Kreith and D. Bharathan Mar. 1987 24 p Presented at the 2nd ASME/JSME Thermal Engineering Conference, Honolulu, Hawaii, 22 Mar. 1987
(Contract DE-AC02-83CH-10093)
(DE87-001155; SERI/TP-250-3119; CONF-870304-5) Avail: NTIS HC A02

In this lecture an overview of the heat- and mass-transfer phenomena of importance in ocean thermal energy conversion (OTEC) is presented with particular emphasis on open-cycle OTEC systems. Also included is a short historical review of OTEC developments in the past century and a comparison of open- and closed-cycle thermodynamics. Finally, results of system analyses, showing the effect of plant size on cost and the near-term potential of using OTEC for combined power production and desalination systems are briefly discussed.
DOE

N87-24024# Midwest Research Inst., Golden, Colo. Solar Energy Research Inst.
REVIEW OF INTERACTIONS OF LARGE SOLAR FLUXES WITH MATERIALS
H. H. Harris Mar. 1987 36 p
(Contract DE-AC02-83CH-10093)
(DE87-001156; SERI/SP-255-3046) Avail: NTIS HC A03/MF A01

This report contains a survey of the scientific literature relevant to materials that are candidates for use in receivers of very highly concentrated solar energy. This review includes literature up to 1985. Over one hundred references were found that bear on the high-flux (greater than or equal to 1 MW/sq m), high-temperature (greater than or equal to 700 C) behavior of candidate materials or the fundamental physics and chemistry of the high-flux environment. The majority of them suggest the direction of further work. There is no combination of materials that, on the basis of current knowledge, with certainty would prove practical in such an environment.
DOE

N87-24025# Naval Postgraduate School, Monterey, Calif.
SOLAR CELL CONCENTRATOR SYSTEM M.S. Thesis
Nevsan Sengil Dec. 1986 53 p
(AD-A177981; NPS72-86-002) Avail: NTIS HC A04/MF A01 CSCL 10B

If solar cells are exposed to charged particle radiation, efficiency decreases. Also solar cell efficiency is increased by concentrated solar light. A solar cell concentrator system includes shielding against particle radiation and provides concentrated solar light, with increased efficiency. A solar cell concentrator system was constructed using a GaAs solar cell. Using a heat pipe, heat was transferred to a radiator. Cell operating temperature (77 C) and under concentrated solar light (Concentration Ration = or approx. 130) solar cell efficiency was measured. Observed efficiency was 18.18. + or - 0.18 (%). These results were used to calculate the performance of an array, consisting of small concentrators. The performance of the concentrator array was compared with a conventional array, and demonstrated the higher efficiency advantages.
GRA

N87-24026*# National Aeronautics and Space Administration. Lewis Research Center, Cleveland, Ohio.
FLUORIDE SALTS AND CONTAINER MATERIALS FOR THERMAL ENERGY STORAGE APPLICATIONS IN THE TEMPERATURE RANGE 973 TO 1400 K
Ajay K. Misra (Case Western Reserve Univ., Cleveland, Ohio.) and J. Daniel Whittenberger 1987 23 p Proposed for presentation at the 22nd Intersociety Energy Conversion Engineering Conference, Philadelphia, Pa., 10-14 Aug. 1987; sponsored by AIAA, ANS, ASME, SAE, IEEE, ACS and AIChE
(NASA-TM-89913; E-3563; NAS 1.15:89913; AIAA-87-9226) Avail: NTIS HC A02/MF A01 CSCL 10C

Multicomponent fluoride salt mixtures were characterized for use as latent heat of fusion heat storage materials in advanced solar dynamic space power systems with operating temperatures in the range of 973 to 1400 K. The melting points and eutectic composition for many systems with published phase diagrams were verified, and several new eutectic compositions were identified. Additionally, the heats of fusion of several binary and ternary eutectics and congruently melting intermediate compounds were measured by differential scanning calorimetry. The extent of corrosion of various metals by fluoride melts was estimated from thermodynamic considerations, and equilibrium conditions inside a containment vessel were calculated as functions of the initial moisture content of the salt and free volume above the molten salt. Preliminary experimental data on the corrosion of commercial, high-temperature alloys in LiF-19.5CaF2 and NaF-27CaF2-36MgF2 melts are presented and compared to the thermodynamic predictions.
Author

N87-24027# Midwest Research Inst., Golden, Colo. Solar Energy Research Inst.
SOLAR THERMAL TECHNOLOGY PROGRAM BIBLIOGRAPHY, 1973-1985
Dec. 1986 191 p
(Contract DE-AC02-83CH-10093)
(DE86-010728; SERI/SP-272-3008) Avail: NTIS HC A09/MF A01

This bibliography contains citations of technical publications that have emerged from the US Department of Energy's Solar Thermal Technology (STT) Program. The entries include research performed at the Federal laboratories and at various universities and other organizations under subcontract to the US Department of Energy or its laboratories from 1973 through 1985. The types of references include journal articles, papers presented in conference proceedings, monographs, chapters in monographs, technical reports, and patents. The citations are divided into chapters by federal laboratory where the research was performed or where the subcontract was monitored. Although there may be some crossover among the laboratories, each one has traditionally had certain areas of responsibility. The first chapter contains citations from the Jet Propulsion Laboratory, which directed most of the parabolic dish technology research. The second chapter, Sandia National Laboratory/Albuquerque, lists documents primarily for distributed receiver technology as well as documents pertaining to the Central Receiver Test Facility (CRTF), which is located in Albuquerque. The third chapter, Sandia National Laboratory/Livermore, contains references for central receiver technology. The documents on central receiver technology that resulted from contracts managed by the US Deapartment of Energy San Francisco Operations Office are also included in the third chapter. The fourth chapter, Solar Energy Research Institute, contains citations documenting advanced research concepts.
DOE

N87-24028# Oak Ridge National Lab., Tenn.
APPLICATION OF ADVANCED FLYWHEEL TECHNOLOGY FOR ENERGY STORAGE ON SPACE STATION
M. Olszewski Apr. 1987 11 p Presented at the Space Electrochemical Research and Technology Conference, Cleveland, Ohio, 14 Apr. 1987
(Contract DE-AC05-84OR-21400)
(DE87-007657; CONF-8704101-1) Avail: NTIS HC A02/MF A01

In space power applications where solar inputs are the primary thermal source, energy storage is necessary to provide a continuous power supply during the eclipse portion of the orbit. Because of their potentially high storage density, flywheels are

being considered for use as the storage system on the proposed orbiting space station. During the past several years graphite fiber technology has advanced, leading to significant gains in flywheel storage density. Use of these improved fibers in experimental flywheel rims has resulted in ultimate storage densities of 878 kJ/kg. With these high-strength graphite fibers, operational storage densities for flywheel storage modules applicable to the space station power storage could reach 200 kJ/kg. This module would also be volumetrically efficient occupying only about 1 cu m. Because the size and mass of the flywheel storage module are controlled by the storage density, improvements in fiber strength can have a significant impact on these values. With the improvements anticipated within the next five years, operational storage density on the order of 325 kJ/kg may be possible for the flywheel module. DOE

N87-24029*# National Aeronautics and Space Administration. Lewis Research Center, Cleveland, Ohio.
TEST RESULTS OF A 60 VOLT BIPOLAR NICKEL-HYDROGEN BATTERY
Russell L. Cataldo, Olga Gonzalez-Sanabria, Randall F. Gahn, Michelle A. Manzo, and Russel P. Gemeiner 1987 7 p Prepared for presentation at the 22nd Intersociety Energy Conversion Engineering Conference, Philadelphia, Pa., 10-14 Aug. 1987; cosponsored by AIAA, ANS, ASME, SAE, IEEE, ACS, and AIChE
(NASA-TM-89927; E-3631; NAS 1.15:89927; AIAA-87-9262) Avail: NTIS HC A02/MF A01 CSCL 10C

In July, 1986, a high-voltage nickel-hydrogen battery was assembled at the NASA Lewis Research Center. This battery incorporated bipolar construction techniques to build a 50-cell stack with approximately 1.0 A-hr capacity (C) and an open-circuit voltage of 65 V. The battery was characterized at both low and high current rates prior to pulsed and nonpulsed discharges. Pulse discharges at 5 and 10 C were performed before placing the battery on over 1400, 40% depth-of-discharge, low-earth-orbit cycles. The successful demonstration of a high-voltage bipolar battery in one containment vessel has advanced the technology to where nickel-hydrogen high-voltage systems can be constructed of several modules instead of hundreds of individual cells.
Author

45 ENVIRONMENT POLLUTION

Includes atmospheric, noise, thermal, and water pollution.

N87-24030# Oak Ridge National Lab., Tenn.
STORAGE AND PRESERVATION OF ENVIRONMENTAL SAMPLES
M. P. Maskarinec and R. L. Moody 1987 11 p Presented at the 193rd National Meeting of the American Chemical Society, Denver, Colo., 5 Apr. 1987
(Contract DE-AC05-84OR-21400)
(DE87-004271; CONF-870410-11) Avail: NTIS HC A02/MF A01

The chemical analysis of environmental samples is complicated by the lack of a definitive data base establishing the allowable preanalytical holding times for such samples. This study is designed to establish the preanalytical holding times for volatile organic compounds in water and soil, and explosives in water and soil, under various storage conditions. Procedures are also being developed to reproducibly prepare the large number of samples necessary to create such a data base. These sample preparation procedures and the data base also will make it possible to produce materials for reference and quality assurance purposes. DOE

N87-24031*# National Aeronautics and Space Administration. Goddard Space Flight Center, Greenbelt, Md.
SPATIAL CHARACTERIZATION OF ACID RAIN STRESS IN CANADIAN SHIELD LAKES Progress Report, 1 Aug. 1985 - 1 Feb. 1986
Fred J. Tanis 1986 9 p
(Contract NAS5-28779)
(NASA-CR-180983; NAS 1.26:180983; ERIM-198400-19-L) Avail: NTIS HC A02/MF A01 CSCL 13B

The acidification of lake waters from airborne pollutants is of continental proportions both in North America and Europe. A major concern of the acid rain problem is the cumulative ecosystem damage to lakes and forest. The number of lakes affected in northeastern United States and on the Canadian Shield is though to be enormous. The principle objective is to examine how seasonal changes in lake water transparency are related to annual acidic load. Further, the relationship between variations in lake acidification and ecophysical units is being examined. Finally, the utility of Thematic Mapper (TM) based observations to measure seasonal changes in the optical transparency in acid lakes is being investigated.
Author

N87-24032*# National Aeronautics and Space Administration. Goddard Space Flight Center, Greenbelt, Md.
SPATIAL CHARACTERIZATION OF ACID RAIN STRESS IN CANADIAN SHIELD LAKES Progress Report, 1 Feb. - 1 Aug. 1986
Fred J. Tanis 1986 19 p
(Contract NAS5-28779)
(NASA-CR-180982; NAS 1.26:180982; ERIM-189400-21-L) Avail: NTIS HC A02/MF A01 CSCL 13B

A major concern of the acid rain problem is the cumulative ecosystem damage to lakes and forests. The number of lakes affected in northeastern United States and on the Canadian Shield is thought to be enormous. Seasonal changes in lake transparency are examined relative to annual acidic load. The relationship between variations in lake acidification and ecophysical units is being examined. Finally, the utility of Thematic Mapper (TM) based observations is being used to measure seasonal changes in the optical transparency in acid lakes. B.G.

N87-24033# Gesellschaft fuer Strahlen- und Umweltforschung m.b.H., Munich (West Germany).
SURVEY OF ENVIRONMENT RELATED MONITORING PROGRAMS OF INTERNATIONAL ORGANIZATIONS AND THEIR CONTRIBUTION TO INTERNATIONAL ORGANIZATIONS
Dec. 1986 39 p Submitted for publication
(ETN-87-99913) Avail: NTIS HC A03/MF A01

Atmospheric and water pollution monitoring by international organizations is described. Project independent standardization and data handling is discussed. ESA

46 GEOPHYSICS

Includes aeronomy; upper and lower atmosphere studies; inospheric and magnetospheric physics; and geomagnetism.

For space radiation see *93 Space Radiation.*

N87-24034# Aerospace Corp., El Segundo, Calif. Lab. Operations.
GENERATION OF BROADBAND NOISE IN THE MAGNETOTAIL
P. B. Dusenbery and Lawrence R. Lyons 1 Mar. 1987 29 p
(Contract F04701-85-C-0086)
(AD-A179136; TR-0086(6940-06)-12; SD-TR-87-12) Avail: NTIS HC A03/MF A01 CSCL 04A

The generation of electrostatic noise in the geomagnetic tail by ion beams is evaluated. A stationary plasma-sheet electron distribution and streaming ion distributions is assumed. Both warm ion streams, as observed within the plasma sheet boundary layer, and cold ion streams, as expected from upward flowing ionospheric ions, are considered. Warm ion streams by themselves are found to be stable, whereas a cold ion stream by itself is unstable to the beam acoustic model. However, wave growth is increased if both cold and warm streams are simultaneously present. These results suggest that the interaction between the warm and cold

ion streams is responsible for the peak in electrostatic wave intensities observed within the plasma sheet boundary layer. For cold and warm ions streaming in the same direction, we find wave growth peaks for wave normal angles theta = O deg and wave frequencies about 0.1 x the electron plasma frequency. However, for anti-parallel streaming cold and warm ions, wave growth peaks near theta approx = 90 deg and wave frequencies are an order of magnitude smaller. Including counter streaming warm ions in addition to a cold ion stream in wave growth that is a superposition of that for the above two cases. GRA

N87-24035# Utah State Univ., Logan.
ATMOSPHERIC RADIANCE PROFILE CODES
B. K. Yap 17 Sep. 1986 52 p Prepared in cooperation with Yap Analytics, Inc., Lexington, Mass.
(Contract F19628-83-C-0056)
(AD-A179258; CSE/86-120; AFGL-TR-87-0009; SR-19) Avail: NTIS HC A04/MF A01 CSCL 04A

This report presents and describes the computer codes developed to generate atmospheric radiance profiles for various molecules, species, and rotational bands. Researchers extracted radiance profiles from the standard NLTE program output files and transferred them from the Cyber system to the Apollo system. Efforts include a routine to plot the radiance profiles' sum total and SPIRE program measured data. GRA

N87-24036# Utah State Univ., Logan. Center for Atmospheric and Space Sciences.
A COMPARISON OF IONOSPHERIC MODEL PREDICTIONS WITH MITHRAS OBSERVATIONS Final Scientific Report, 14 Nov. 1983 - 14 Nov. 1986
Robert W. Schunk 14 Jan. 1987 11 p
(Grant AF-AFOSR-0029-84)
(AD-A179374; AFOSR-87-0522TR) Avail: NTIS HC A02/MF A01 CSCL 04A

MITHRAS is a coordinated multiradar program to study the interactions between the magnetosphere, ionosphere, and thermosphere, as well as the phenomena that result from these interactions. The program is based on a data set acquired by the Chatanika, Millstone Hill, and Eiscat incoherent scatter radars. A large portion of the data is unique in that it was the only time when the radars, well separated in local and magnetic time, simultaneously probed the high latitude ionosphere. Our effect concerned model data comparisons. Specifically, we compared the predictions of our three-dimensional, time dependent model of the high latitude ionosphere with MITHRAS data sets. Of particular interest were the variations of the ionosphere with altitude, latitude, longitude, universal time, season, and magnetic activity. Model data comparisons enabled us to determine the adequacy of our current understanding of high latitude ionosphere dynamics as well as certain magnetosphere ionosphere atmosphere coupling processes. GRA

N87-24037# Utah State Univ., Logan. Center for Space Engineering.
STUDIES OF INFRARED AURORAE
Jane L. Fox 3 Nov. 1986 51 p Prepared in cooperation with Smithsonian Institution, Cambridge, Mass.
(Contract F19628-83-C-0056)
(AD-A179539; CSE/86-139; AFGL-TR-87-0010; SR-20) Avail: NTIS HC A04/MF A01 CSCL 04A

Smithsonian researchers began their studies of infrared aurorae by computing the rate of vibrational excitation of N2 by the impact of energetic electrons. Although the radiative lifetime of vibrationally excited N2 is long, infrared emission may appear as a result of V-V transfer from N2 to molecules which may radiate, such as CO2 and NO. A complete set of cross sections was compiled for electron impact excitation of vibrational levels v = 1 through v = 6 for the impact of electrons with energies from 2 to 200 eV. They found that for high electron energies and low fractional ionizations, about 6% of the total energy of the electron appears as vibrational excitation. GRA

N87-24038*# Massachusetts Inst. of Tech., Cambridge. Dept. of Earth, Atmospheric, and Planetary Sciences.
THE INTERPRETATION OF CRUSTAL DYNAMICS DATA IN TERMS OF PLATE MOTIONS AND REGIONAL DEFORMATION NEAR PLATE BOUNDARIES Semiannual Status Report, 22 Sep. 1986 - 21 Mar. 1987
Sean C. Solomon 15 Jun. 1987 141 p
(Grant NAG5-814)
(NASA-CR-180938; NAS 1.26:180938; SASR-1) Avail: NTIS HC A07/MF A01 CSCL 08G

The nature and dynamics of time-dependent deformation along major seismic zones including the influence of irregularities in fault geometry on the earthquake cycle, and the processes contributing to the state of stress and rates of strain in plate interior regions were studied. The principle findings of the research are discussed. B.G.

N87-24039*# National Aeronautics and Space Administration. Goddard Space Flight Center, Greenbelt, Md.
THE MAGSAT BIBLIOGRAPHY
R. A. Langel and B. J. Benson Jun. 1987 67 p Prepared in cooperation with Maryland Univ., College Park
(NASA-TM-87822; Rept-87-B-0293; NAS 1.15:87822) Avail: NTIS HC A04/MF A01 CSCL 08G

Publications related to the Magsat project number 228, as of March 1987 are listed. Of these, 34 deal with analysis of the Earth's main magnetic field, 125 with analysis of the Earth's crustal field, and 42 with analysis of the magnetic field originating external to the Earth. The remainder document the Magsat program, satellite, instruments or data are review papers. The bibliography is divided into two parts. The first lists all papers by first author; the second is subdivided by topic. Author

N87-24040*# ST Systems Corp., Hampton, Va.
TRANSPORT AND PHOTOCHEMICAL MODELING. STUDIES OF ATMOSPHERIC SPECIES
M. Natarajan Mar. 1987 28 p Prepared for NASA Langley Research Center, Hampton, Va.
(Contract NAS1-16456)
(NASA-CR-178311; NAS 1.26:178311) Avail: NTIS HC A03/MF A01 CSCL 04A

A program of research studies related to the photochemistry, radiative transfer, and dynamics of the stratosphere is described. Investigations were conducted in two broad areas: (1) studies of the stratospheric processes and their response to external perturbations, and (2) analysis of satellite measurements in conjunction with theoretical models. Contemporary one dimensional photochemical, radiative-convective model was used to assess the impact of perturbations such as solar flux variability, increases in atmospheric carbon dioxide, chlorofluoromethanes and other greenhouse gases. Data from satellite experiments such as LIMS and SBUV, were used along with theoretical models to develop a climatology of trace species in the stratosphere. The consistency of contemporary ozone photochemistry was examined in the light of LIMS data. Research work also includes analysis of stratospheric nitrogen dioxide distributions from different satellite experiments, investigation of the wintertime latitudinal gradients in NO2, estimation of the stratospheric odd nitrogen level and its variability, and studies related to the changes in ozone in the Antarctic, and mid latitude Southern Hemisphere. Author

N87-24041# Lawrence Livermore National Lab., Calif.
THE REALITY OF THE GREENHOUSE EFFECT
M. C. MacCracken Oct. 1986 22 p Presented at the 12th World Petroleum Congress, Houston, Tex., 26 Apr. 1987
(Contract W-7405-eng-48)
(DE87-002383; UCRL-95580; CONF-870414-1) Avail: NTIS HC A02/MF A01

The Earth's surface absorbs solar radiation, to which the atmosphere is mostly transparent, and re-emits infrared radiation that is absorbed primarily by carbon dioxide and water vapor. Without the consequent warming, or greenhouse effect, the Earth's mean surface temperature of 15 C would be well below freezing.

Changes in the concentration of CO2 and other greenhouse gases can perturb the present climate. Theoretical models constructed to generate quantitative estimates of these changes suggest that a doubling of the CO2 concentration could raise global-average temperatures by 1.5 to 4.5 C. Global temperatures appear to have risen about 0.5 C over the past hundred years, in part probably due to the 25% rise in CO2 concentration. There are important questions, however, regarding the rate and history of the warming and the spatial pattern of the changes. The projected climatic changes could induce significant societal impacts, especially if society is viewed as unresponsive. Sea level rise, reduced water resources, and stressed agricultural systems may be the most important consequences, but uncertainties in the estimated climatic effects and the long lead time make assessment difficult. Developing and evaluating options for slowing the rate and magnitude of and adapting to the projected changes require accelerated research. DOE

N87-24042*# Texas Univ., Austin. Center for Space Research.
SIMULATION AND ANALYSIS OF A GEOPOTENTIAL RESEARCH MISSION Semiannual Status Report
B. E. Schutz Jun. 1987 19 p
(Grant NAG5-528)
(NASA-CR-180695; NAS 1.26:180695) Avail: NTIS HC A02/MF A01 CSCL 08E

Computer simulations were performed for a Geopotential Research Mission (GRM) to enable the study of the gravitational sensitivity of the range rate measurements between the two satellites and to provide a set of simulated measurements to assist in the evaluation of techniques developed for the determination of the gravity field. The simulations were conducted with two satellites in near circular, frozen orbits at 160 km altitudes separated by 300 km. High precision numerical integration of the polar orbits were used with a gravitational field complete to degree and order 360. The set of simulated data for a mission duration of about 32 days was generated on a Cray X-MP computer. The results presented cover the most recent simulation, S8703, and includes a summary of the numerical integration of the simulated trajectories, a summary of the requirements to compute nominal reference trajectories to meet the initial orbit determination requirements for the recovery of the geopotential, an analysis of the nature of the one way integrated Doppler measurements associated with the simulation, and a discussion of the data set to be made available. Author

N87-24043# Texas Univ., Austin. Bureau of Economic Geology.
LANDSAT-BASED LINEAMENT ANALYSIS, EAST TEXAS BASIN, AND STRUCTURAL HISTORY OF THE SABINE UPLIFT AREA, EAST TEXAS AND NORTH LOUISIANA Topical Report, Mar. 1984 - Nov. 1986
R. W. Baumgardner and M. L. W. Jackson 2 Mar. 1987 128 p
(Contract GRI-5082-211-0708)
(PB87-176327; GRI-87/0077) Avail: NTIS HC A07/MF A01 CSCL 08G

The relationship between subsurface structure and lineaments was examined. More than 2,200 lineaments were mapped from 1:250,000-scale LANDSAT images. Vector sums of greater-than-average values of length-weighted frequency define significant peaks of lineament orientation. For all lineaments, significant peaks occur at 325 degrees and 21 degrees. The northwest peak parallels mean azimuth of borehole elongations in Cotton Valley sandstone wells throughout East Texas. Lineament density delineates major fault zones. These results suggest that lineaments and subsurface structures results from like-oriented stresses. Identification of the timing, extent, and orientation of arching episodes in the Sabine Uplift areas is important in developing a structural history of the area. GRA

N87-24044# Boston Univ., Mass. Dept. of Astronomy.
A MODEL FOR THE LOW-LATITUDE IONOSPHERE WITH COEFFICIENTS FOR DIFFERENT SEASONAL AND SOLAR CYCLE CONDITIONS Final Report, 1 Oct. 1981 - 30 Jun. 1986
Michael Mendillo and Bruce Herniter 1 Nov. 1986 46 p
(Contract F19628-81-K-0051)
(AD-A178207; AFGL-TR-86-0260) Avail: NTIS HC A03/MF A01 CSCL 04A

A new ionospheric model for the low latitude ionosphere has been constructed to provide easy access to electron density profiles (Ne(h)), total electron content (TEC) and 6300A airglow under a variety of conditions. The results from the rigorous theoretical calculations for ionospheric structure at a given time and a site were parameterized to a set of six coefficients that reproduce the individual Ne(h) profiles using a simple algebraic formula. In this report we summarize the rationale for such a model, describe the input parameters and methods used to generate the coefficients, and provide a comprehensive set of coefficients. The model covers the low latitude ionosphere (24 N to 24 S every 4 deg of dip latitude), over the altitude range 180km to 1000km, for every hour of local time. The tabulated coefficients, TEC and 6300 airglow are presented for three seasons (Equinox, June solstice and December solstice) and two solar cycles (solar maximum and solar minimum). GRA

N87-24249*# National Oceanic and Atmospheric Administration, Boulder, Colo. Space Environment Lab.
AURORAL PARTICLES
David S. Evans *In* NASA Goddard Space Flight Center, Greenbelt, Md. Essays in Space Science Jun. 1987 p 19-45 Prepared in cooperation with Lockheed Missiles and Space Co., Palo Alto, Calif. (For primary document see N87-24247 17-88)
Avail: NTIS HC A18/MF A01 CSCL 04A

47 METEOROLOGY AND CLIMATOLOGY

Includes weather forecasting and modification.

N87-24045# Transportation Systems Center, Cambridge, Mass.
OTIS ANGB (AIR NATIONAL GUARD BASE) VISIBILITY SENSOR FIELD TEST STUDY Final Report, Dec. 1983 - Jan. 1986
D. Schwartz and D. Burnham Feb. 1987 186 p
(AF Proj. 2688)
(AD-A179176; AFGL-TR-86-0011; ESD-5-606) Avail: NTIS HC A09/MF A01 CSCL 04B

Forward scatter meters (FSMs) are evaluated for use as visibility sensors in Automatic Observing Systems (AOS) and as possible replacements for transmissometers to measure Runway Visual Range (RVR) at airports. Data collected from three FSMs at the Otis Air National Guard Base during a 17-month period starting in 1983 is analyzed. Two of the FSMs use chopped incandescent light sources and have a large scatter volume. The other uses a modulated light emitting diode (LED) light source and has a small scatter volume. Two analysis procedures are included: (1) a statistical analysis of the entire data set disaggregated according to the obstruction to vision (fog, rain, snow, etc.) and the magnitude of the extinction coefficient; and (2) detailed analysis of selected reduced visibility events. Most of the time extinction coefficients measured by the FSMs and the transmissometers agreed to within 16.5 percent for RVR values between 400 and 6000 feet and within one reporting increment for AOS visibility. Most of the cases of large disagreement were traced to problems such as sensors being clogged by snow, which affected both FSMs and the transmissometers. The large volume FSMs gave more stable readings, but those with LED were more reliable. Author (GRA)

N87-24046# Lowell Univ., Mass. Dept. of Earth Science.
THE SPECIFICATION OF LATERAL BOUNDARY CONDITIONS IN THREE-DIMENSIONAL MESOSCALE NUMERICAL MODELS Final Report, 22 Oct. 1984 - 21 Jan. 1987
Keith L. Seitter 21 Jan. 1987 138 p
(Contract F19628-85-K-0008)
(AD-A179185; AFGL-TR-87-0015) Avail: NTIS HC A07/MF A01 CSCL 04B

The specification of lateral boundary conditions in meso-beta scale models is investigated with the use of a one dimensional shallow water model and a full three dimensional atmospheric model. A large number of boundary condition schemes and variations on these schemes are tested in the one dimensional model using initial conditions which are not in geostrophic balance to determine the ability of the boundary condition to allow geostrophic adjustment to proceed in the model. The radiation type boundary conditions tested are found to be superior to all other schemes, with the flow relaxation scheme also producing acceptable results. Initial conditions similar to those used in the one dimensional model are used to test the sponge, flow relaxation, one dimensional radiation and multi dimensional radiation conditions in the three dimensional model. While all conditions had certain strengths and weaknesses depending on the specific form of the initial condition, the one dimensional radiation condition gave the best overall results. The one-dimensional model was further used to investigate the geostrophic adjustment of the model to large scale imbalances and to test some methods of nesting the mesoscale model. It is found that while the pressure or height fields rapidly adjust to the winds for disturbances within the domain, the adjustment to imposed large scale gradients takes place in the wind field on the much slower time scale given by the inertial period. GRA

N87-24047# Air Force Environmental Technical Applications Center, Scott AFB, Ill.

STATION CLIMATIC SUMMARIES, ANTARCTICA, AUSTRALIA AND OCEANIA Data Summary Report

William F. Sjoberg Mar. 1987 52 p Supersedes USAFETAC/DS-81-060, AD-A118453

(Contract USAFETAC/DS-87-038)

(AD-A179242; USAFETAC/DS-81-060) Avail: NTIS HC A04/MF A01 CSCL 04B

A collection of summarized monthly and annual climatic data for specific locations in Antarctica, Australia, and Oceania. Summarized climatological elements are: percent frequency of occurrence of ceiling and visibility; means, extremes and number of days with specified values of temperature, precipitation, and snowfall; means of relative humidity, vapor pressure, dew point pressure altitude, and cloud cover; prevailing wind direction, with mean and extreme speeds; and number of days with thunderstorms and fog. GRA

N87-24048# Science Applications International Corp., Monterey, Calif.

MID-LATITUDE WIND PROBABILITY MODEL Final Report, 12 Sep. 1984 - 11 May 1986

Jerry D. Jarrell Nov. 1986 38 p

(Contract N00228-84-C-3142; DA Proj. W05-13-CC)

(AD-A179256; NEPRF-CR-86-06) Avail: NTIS HC A03/MF A01 CSCL 04B

A model to estimate the probability of a strike on a point by a mid-latitude storm was developed and tested. This model was based on a vortex tracking program operational for quality control at the Fleet Numerical Oceanography Center, Monterey, Calif. An extension of this model to assess the probability of a mid-latitude storm causing 30 kt winds also was developed and tested. Both developments followed successful comparable probability estimation models for tropical cyclones. Model development is described and the test methodology and results are described and interpreted. GRA

N87-24049# Stanford Univ., Calif. Center for Large Scale Scientific Computation.

ADAPTIVE GRID REFINEMENT FOR NUMERICAL WEATHER PREDICTION

William Skamarock, Joseph Oliger, and Robert L. Street Feb. 1987 42 p

(Contracts N00014-84-K-0267; N00014-82-K-0335)

(AD-A179393; CLASSIC-87-15) Avail: NTIS HC A03/MF A01 CSCL 04B

An adaptive atmospheric flow model is described and results of integrations with this model are presented. The adaptive technique employed is that of Berger and Oliger. The technique uses a finite difference method to integrate the dynamical equations first on a cargo grid and then on finer grids which have been placed based on a Richardson type estimate of the truncation error in the coarse grid solution. By correctly coupling the integrations on the various grids, periodically reestimating the error and recreating the finer grids, uniformly accurate solutions are economically producted. The primitive hydrostatic equations of meteorology are solved for the advection of a barotropic cyclone and for the development of a baroclinic disturbance which results from the perturbation of an unstable jet. These integrations demonstrate the feasibility of using multiple, rotated, overlapping fine grids. Direct computations of the truncation error are used to confirm the accuracy of the Richardson type truncation error estimates. GRA

N87-24050# Consultants Choice, Inc., Atlanta, Ga.

TACTICAL WEATHER EXPERT SYSTEM Final Report, 18 Sep. 1986 - 18 Mar. 1987

H. B. Teates, Paul D. Lampru, and Michael D. Condon 18 Mar. 1987 55 p

(Contract DAAD07-86-C-0100)

(AD-A178605) Avail: NTIS HC A04/MF A01 CSCL 04B

The objective of this project was to assess the feasibility of developing an expert system for tactical weather prediction. Using WILLARD, an expert system developed to predict severe thunderstorms in the Great Plains Regions of the United States, as a point of departure, the project undertook the modification of WILLARD to assess the feasibility of its being adapted to diverse, division-size geographical areas and improving its robustness by increasing its scope of meteorological data sources, including satellite imagery data. A Lisp algorithm, using gyxels rather than pixels to represent satellite grey scale images, was used to explore the feasibility of representing relevant cloud formations symbolically. The results of this research indicate that intelligent interpretations of cloud formations can be made. These inferences can then be automatically passed to the expert system for processing as another piece of information. It is anticipated that this technology will significantly reduce the dependence of the expert system on a meteorologist to visually interpret satellite weather data. The project not only demonstrated feasibility, but indicated that fielding of an initial capability within the next three to four years is technically realistic. Based upon these encouraging results, it is recommended that the application of expert system technology to the tactical weather forecasting domain be continued in Phase 2.

Author (GRA)

N87-24051# Pacific Northwest Labs., Richland, Wash.

A PRELIMINARY EVALUATION OF THE PERFORMANCE OF WIND TUNNEL AND NUMERICAL MODELING SIMULATIONS OF THE WIND FLOW OVER A WIND FARM

J. C. Barnard and H. L. Wegley Jan. 1987 30 p

(Contract DE-AC06-76RL-01830)

(DE87-004634; PNL-6105) Avail: NTIS HC A03/MF A01

This report is an analysis of physical and numerical model simulations of the wind flow over complex terrain. The specific area to which these models were applied is a wind farm in the Altamont Pass area of California. The physical model results were obtained from wind tunnel flow simulations, and the numerical model used was the optimizing version of the NOABL model. The goals of this analysis were: (1) to evaluate the relative performance of the two models, and (2) to uncover any clues that would point toward improvement of the wind tunnel modeling. The performances of the models were gauged by comparing model simulations to wind observations taken over the modeled area. DOE

N87-24052# Lawrence Livermore National Lab., Calif.

THE DETECTION OF CO2-INDUCED CLIMATE CHANGE

M. C. MacCracken and S. L. Grotch Jan. 1987 12 p Presented at the Commission of European Communities Symposium on

CO/sub 2/ and Other Greenhouse: Climate and Associated Impacts, Brussels, Belgium, 3 Nov. 1986
(Contract W-7405-eng-48)
(DE87-006085; UCRL-95914; CONF-8611146-1) Avail: NTIS HC A02

Theoretical projections suggest that the global average temperature will rise and other climatic characteristics will shift as a result of the increasing CO2 and trace gas concentrations. There are important uncertainties, however, regarding the amount and spatial distribution of the changes and the rate at which they will occur. Improving computer simulations is a possible and necessary step. However, both the identification of the actual changes in the observational record and convincing attribution of them to the increasing CO2 and trace gas concentrations are essential steps for providing the impetus for what may prove costly adaptative, ameliorative, or preventative steps. The observed rises of global average temperature and of sea level over the past century are suggestive that the 25% increase in CO2 concentration in this period is, in fact, perturbing the climate. Unexplained discrepancies in magnitude and pattern between theoretical calculations and the observations, however, must be resolved if we are to become able to make the accurate projections needed for determining the appropriate societal responses. DOE

N87-24053# Washington Univ., Seattle. Dept. of Atmospheric Sciences.
GLOBAL DISTRIBUTION OF TOTAL CLOUD COVER AND CLOUD TYPE AMOUNTS OVER LAND
S. G. Warren, C. J. Hahn, J. London, R. M. Chervin, and R. L. Jenne Oct. 1986 468 p Prepared in cooperation with Colorado Univ., Boulder; National Center for Atmospheric Research, Boulder, Colo.
(Contract DE-AI01-82ER-60085)
(DE87-006903; DOE/ER-60085/H1; NCAR-TN/STR-273) Avail: NTIS HC A20

The atlas describes, for the land areas of the Earth, the average total cloud cover and the amounts of each cloud type, and their geographical, diurnal, seasonal, and interannual variations, as well as the average base heights of the low clouds. DOE

N87-24054# Alaska Univ., Fairbanks. Inst. of Marine Science.
CLIMATOLOGICAL OBSERVATIONS IN THE PHILIP SMITH MOUNTAINS OF THE NORTH SLOPE, ALASKA Climatology Report Series No. 2
J. J. Kelley and D. Foster Oct. 1986 348 p
(Contract DE-FG06-84ER-60269)
(DE87-008179; DOE/ER-60269/5) Avail: NTIS MF A01

Climatological data from an automatic weather station (Aanderaa) located at the Alyeska Pipeline Service Company Material Site 117 (MS-117) are presented in this report. Data are listed for hourly averages daily. The data report covers the period 1 August 1985 to 31 May 1986. Observations in this report include wind speed and direction, temperature and barometric pressure. Descriptions of the instrumentation and estimates of reliability are included in the text. Various analyses of the data are presented in the appendices. A summary of the wind and temperature regime is presented through displays of cumulative frequencies of hourly temperatures and wind speeds for the 12-month period, June 1985 to May 1986. DOE

N87-24055# Air Force Global Weather Central, Offutt AFB, Nebr.
TAF (TERMINAL AERODROME FORECAST) VERIFICATION Final Report
Sherwin W. Jamison 30 Nov. 1986 32 p
(AD-A177931; AFGWC/TN-86/002) Avail: NTIS HC A03/MF A01 CSCL 04B

The Terminal Aerodrome Forecast Verification (TAFVER) system gives AWS a means to monitor its performance in a cost-effective manner. This technical note will provide AWS personnel with the necessary information to effectively use the TAFVER system. The TAFVER system will perform the following tasks: (a) Retrieve decoded and validated observations and store selected elements in the TAFVER database; (b) Retrieve decoded TAFs and store them in the TAFVER database; (c) Send TAFVER receipt messages (AX bulletins) for observations and TAFs twice a day; (d) Prepare end-of-month summary reports of forecast verification for Headquarters Air Weather Service and for each wing. The TAFVER database includes a TAF section, an observations section, and an information section. The TAF section can contain up to 31 days of TAFs per station. The observations section can contain up to 32 days of observations per station. Stored TAFs and observations contain ceiling and visibility information. Only hourly observations are stored; special observations and TAF amendments are not stored. GRA

N87-24056# National Oceanic and Atmospheric Administration, Boulder, Colo. Air Resources Lab.
GEOPHYSICAL MONITORING FOR CLIMATIC CHANGE NUMBER 14 Summary Report, 1985
R. C. Schnell Dec. 1986 158 p
(PB87-162533) Avail: NTIS HC A08/MF A01 CSCL 04B

At MLO, the major facilities change was construction of lava diversion embankments. The diversion system, which hopefully will never be tested, was designed to divert a flowing lava stream around the observatory. Upgrade of the lidar system continued. It detected an enhanced stratospheric aerosol layer late in the year, presumably the result of the November eruption of Nevada del Ruiz in Columbia. A new solar radiation program was begun cooperatively with the University of Arizona. The program goal is to study 22-year variability in solar constant as measurable at ground level. The programs include measurements of CO2 from the flask network and observatories, total column ozone, ozone vertical distribution by ECC sonde and Umkehr technique, surface ozone, stratospheric water vapor by balloon soundings at Boulder, CFC-11 and -12 and N2O from flask samples, stratospheric aerosols at MLO using lidar, aerosol light scattering and CN concentration, direct and diffuse solar radiation, meteorological variables, and chemistry of precipitation. GRA

N87-24057# Air Force Inst. of Tech., Wright-Patterson AFB, Ohio.
MESO GAMMA-SCALE KINETIC ENERGY BUDGETS OF A THUNDERSTORM WITHIN A SQUALL-LINE DERIVED FROM SESAME DUAL-DOPPLER DATA M.S. Thesis
John A. Coover, Jr. 1986 155 p
(AD-A178119; AFIT/CI/NR-87-28T) Avail: NTIS HC A08/MF A01 CSCL 04B

A lack of reliable mesoscale data within convective cells has hampered the meteorologist's understanding of the inner workings of thunderstorms. Researchers have realized that convection impacts larger scale features, Maddox (1980), but past studies of energetics of convective storms have focused on the storm environment using rawinsonde data: see studies by Fuelberg and Scoggins (1978), Vincent and Schlatter (1979), and Fuelberg and Printy (1984). Kinematic features and dynamic processes within the convective cell were generally inferred from these studies. This study will utilize highly reliable retrieved thermodynamic variables, Gal-Chen (1978), for investigating the kinematic and dynamic features of a convective cell at time periods 1630 and 1634 CST. The goal is an ehanced understanding of the energetic processes within the convective cell. GRA

N87-24058# Pacific Northwest Labs., Richland, Wash.
USER'S MANUAL FOR THE CONVECTIVE CLOUD MODULE VERSION 1.0
B. C. Scott Apr. 1987 172 p
(Contract DE-AC06-76RL-01830)
(DE87-008343; PNL-6188) Avail: NTIS HC A08/MF A01

Described is a convective cloud model and guidance for users. The convective cloud model is assumed to provide a time-averaged distribution of data from a population of precipitating, convective clouds in different stages of development. This model was designed to characterize a scavenging environment using meteorological conditions provided by a regional-scale meteorological code. This meteorological code explicitly simulates processes related to cloud

microphysics. The cloud model predicts the vertical profiles of condensed water that correspond to specified surface precipitation rates and cloud top and freezing level heights. The cloud model also predicts profiles of various microphysical constituents, such as fall velocity and accretion rates that exist in conjunction with the condensed water profiles. Descriptions of routines written to solve mass conservation equations for air, cloud, and precipitation water are presented. The solutions are appropriate for precipitating convective clouds with a horizontal spacing on the order of 10 km. Routines are also provided for generating tables of profiles for many discrete input conditions. Once tables are generated, additional routines may be used to interpolate between the tables and to rapidly determine values at levels other than the discrete input levels. DOE

48 OCEANOGRAPHY

Includes biological, dynamic, and physical oceanography; and marine resources.

For related information see also *43 Earth Resources and Remote Sensing.*

N87-24059# Sandia National Labs., Albuquerque, N. Mex.
DESIGN OF THE SHELL PROJECT SEAFLOOR EARTHQUAKE MEASUREMENT SYSTEM (SEMS)
J. P. Hickerson and A. A. Lopez Mar. 1987 106 p
(Contract DE-AC04-76DP-00789)
(DE87-007946; SAND-85-2604) Avail: NTIS HC A06/MF A01

A new generation system which measures strong motion in marine sediments has been developed and deployed. The system consists of three subsystems: a seafloor data acquisition package and two shipboard packages that command and record data from the seafloor package. Communication between the two systems is via an acoustic telemetry system. The seafloor unit is powered by lithium batteries and has an operational life of four years. The seafloor unit is microprocessor controlled and uses a three-axis accelerometer package to continuously measure sediment motions from .001 to 10 g's. These data are digitized at a 100 hertz rate and, if they meet the preestablished event selection criterion, they are stored in an eight-million bit, nonvolatile, magnetic bubble memory. In addition to recording seismic data, the shipboard subsystem can monitor the status of the seafloor package and change the operating characteristics, if necessary. The paper describes the design, development, and deployment of the Seafloor Earthquake Measurement System. DOE

N87-24060# National Oceanic and Atmospheric Administration, Miami, Fla. Atlantic Oceanographic and Meteorological Labs.
MIXED LAYER AND THERMOCLINE DEPTH CLIMATOLOGIES IN THE WESTERN INDIAN OCEAN
R. L. Molinari, J. F. Festa, and J. C. Swallow Oct. 1986 46 p
(PB87-154613; NOAA-TM-ERL-AOML-64) Avail: NTIS HC A03/MF A01 CSCL 08C

Mean monthly distributions of the mixed layer depth (defined as the first depth at which the temperature is 0.5 C less than the sea-surface temperature) and thermocline depth (defined as the depth of the 20 C isotherm) are derived from data collected between 1948 and 1981. Approximately 50,000 temperature profiles are available to generate the climatologies. Amplitude and phase distributions for the annual and semi-annual signals are computed from the monthly time series. The mixed layer depth distributions are compared to the thermocline depth distributions to identify possible regions where thermocline displacements influence mixed layer displacement. GRA

N87-24061# Naval Ocean Research and Development Activity, Bay St. Louis, Miss.
OCEAN WIND AND WAVE MODEL COMPARISONS WITH GEOSAT (GEODESY SATELLITE) SATELLITE DATA Final Report
R. L. Pickett, D. A. Burns, and R. D. Broome Dec. 1986 11 p
(AD-A178302; NORDA-168) Avail: NTIS HC A02/MF A01 CSCL 08C

By comparing operational wind and wave models to GEOSAT, we found that on 10 March 1986, the Federal Republic of Germany had the best skill score for a regional wind analysis, NOAA had the best score for a global wind analysis, the Netherlands had the best score for a regional wave analysis and the U.S. Navy had the best score for a global wave analysis. GRA

51 LIFE SCIENCES (GENERAL)

N87-24062# Midwest Research Inst., Golden, Colo. Solar Energy Research Inst.
PROCEEDINGS OF THE TENTH DOE SOLAR PHOTOCHEMISTRY RESEARCH CONFERENCE
1986 245 p Conference held in Ontario, Canada, 8 Jun. 1986 Prepared in cooperation with Windsor Univ., Ontario
(Contract DE-AC02-83CH-10093)
(DE87-006421; SERI/CP-233-2959; CONF-8606279) Avail: NTIS HC A11/MF A01

The Tenth DOE Solar Photochemistry Research conference cosponsored by the Division of Chemical Sciences, Office of Basic Energy Sciences, US Department of Energy and the Natural Sciences and Engineering Research Council of Canada was held on June 8-12, 1986, at the Pillar and Post Conference Center in Niagara-on-the-Lake, Ontario, Canada. This volume contains the program of the meeting, the abstracts of 29 formal presentations and 46 posters. In commemoration of the 10th anniversary of this conference, a special session was held in which James R. Bolton of the University of Western Ontario presented an overview of past accomplishments and served as moderator for a panel comprised of Melvin Calvin, Nick Serpone, Michael Wasielewski and Mark Wrighton, who discussed future directions of solar photochemical conversion research. A transcript of these proceedings is included in this volume. DOE

N87-24063*# National Aeronautics and Space Administration, Washington, D.C.
THE 1986-87 NASA SPACE/GRAVITATIONAL BIOLOGY ACCOMPLISHMENTS
Thora W. Halstead, ed. Jun. 1987 223 p Prepared in cooperation with George Washington Univ., Washington, D.C.
(Contract NASw-3165)
(NASA-TM-89951; NAS 1.15:89951) Avail: NTIS HC A10/MF A01 CSCL 06B

This report consists of individual technical summaries of research projects of NASA's Space/Gravitational Biology program, for research conducted during the period January 1986 to April 1987. This program utilizes the unique characteristics of the space environment, particularly microgravity, as a tool to advance knowledge in the biological sciences; understanding how gravity has shaped and affected life on Earth; and understanding how the space environment affects both plant and animal species. The summaries for each project include a description of the research, a list of accomplishments, an explanation of the significance of the accomplishments, and a list of publications. Author

N87-24064*# National Aeronautics and Space Administration. Ames Research Center, Moffett Field, Calif.
HUMAN FACTORS IN SPACE STATION ARCHITECTURE 2. EVA ACCESS FACILITY: A COMPARATIVE ANALYSIS OF 4 CONCEPTS FOR ON-ORBIT SPACE SUIT SERVICING
Marc M. Cohen and Steven Bussolari (Massachusetts Inst. of Tech., Cambridge.) Apr. 1987 25 p
(NASA-TM-86856; A-86037; NAS 1.15:86856) Avail: NTIS HC A02/MF A01 CSCL 05H

Four concepts for on-orbit spacesuit donning, doffing, servicing, check-out, egress and ingress are presented. These are: the Space Transportation System (STS) Type (shuttle system enlarged), the

Transit Airlock (Shuttle Airlock with suit servicing removed from the pump-down chamber), the Suitport (a rear-entry suit mates to a port in the airlock wall), and the Crewlock (a small, individual, conformal airlock). Each of these four concepts is compared through a series of seven steps representing a typical Extra Vehicular Activity (EVA) mission: (1) Predonning suit preparation; (2) Portable Life Support System (PLSS) preparation; (3) Suit Donning and Final Check; (4) Egress/Ingress; (5) Mid-EVA rest period; (6) Post-EVA Securing; (7) Non-Routine Maintenance. The different characteristics of each concept are articulated through this step-by-step approach. Recommendations concerning an approach for further evaluations of airlock geometry, anthropometrics, ergonomics, and functional efficiency are made. The key recommendation is that before any particular airlock can be designed, the full range of spacesuit servicing functions must be considered, including timelines that are most supportive of EVA human productivity. Author

52 AEROSPACE MEDICINE

Includes physiological factors; biological effects of radiation; and effects of weightlessness on man and animals.

N87-24065# Wisconsin Univ., Madison.
PULMONARY ADAPTATION TO HIGH ALTITUDE Annual Progress Report, 14 Nov. 1984 - 1 Feb. 1986
Jerome A. Dempsey Nov. 1986 6 p
(Contract DAMD17-82-C-2259; DA Proj. 3M1-61102-BS-10)
(AD-A179139) Avail: NTIS HC A02/MF A01 CSCL 06S

Studies demonstrate the causes and consequences of periodic breathing during sleep at high altitudes, showed the susceptibility of the highly trained athlete to development of hypoxemia during heavy exercise at even very moderately high altitudes, and tested the effect of exercise in hypoxia on respiratory muscle fatigue. GRA

N87-24066# Baylor Univ., Dallas, Tex. Research Foundation.
BIOMEDICAL APPLICATIONS OF THE FREE ELECTRON LASER Annual Report, Jan. - Dec. 1986
J. L. Matthews, M. M. Judy, Michael V. Dennis, David Vandermuelen, and Don Nealon 14 Apr. 1987 121 p
(Contract N00014-86-K-0186)
(AD-A179182; Rept-87-1) Avail: NTIS HC A06/MF A01 CSCL 06L

This study involves seven separate projects. The areas approached are the: modeling of porphyrin uptake, sequestration and photoxicity genetic in identical genetic cell lines, the photosensitizing properties of merocyanine, the modeling of sustained triplet population by FEL radiation in photoexcited porphyrins, tissue optical property measurements, thermal effects of laser irradiation on tissue, the near-ultraviolet effects on celluar tissue and the optical studies of protein flexibility using pulsed and modulated laser sources. Utilizing reverse-transforming techniques, a model system for porphyrin uptake and sequestration has been developed utilizing the commercially available porphyrin preparation, PHOTOFRIN II. Efficient photodynamical killing of the human promyelocytic leukemia HL-60 cell line under aerobic conditions after exposure to MC540 was demonstrated. A significant increase in the efficiency of HPD mediated photodynamical killing of a tumor by use pulse trained laser has occurred. Other than for skin and for blood, there appears to have been little systematic determination for the optical scattering and absorption coefficients of biological tissues. Measures are being taken to extend measurements of the scattering and absorption coefficients to a broad spectrum of major biological tissues. Histological and histochemical staining capabilities were developed for evaluating the tissue and cellular and subcellular level of thermally induced damage upon absorption of laser light. GRA

N87-24067# Duke Univ., Durham, N. C. Dept. of Psychiatry.
INVESTIGATION OF BIOCHEMICAL VARIATION IN OPERATIONAL AIRCREW Final Report, Feb. - Dec. 1983
Redford B. Williams, Jr., John C. Barefoot, and Thomas L. Haney Dec. 1986 23 p
(Contract F33615-82-D-0627)
(AD-A179223; USAFSAM-TR-85-56) Avail: NTIS HC A02/MF A01 CSCL 06S

Principal-components analyses of biochemical values obtained on a sample of operational aircrew revealed two factors that appear to reflect stress levels: Factor 1--positive loadings for Red Blood Cell sedimentation rate, serum uric acid, triglycerides, and cholesterol/HDL ratio; and Factor 4--a negative loading for serum calcium and positive loadings for 0900 plasma cortisol, fasting blood sugar, and Sodium/Potassiam ratio. High Factor-1 scores could result from increased sympathetic nervous system activity, and high Factor 4 scores could reflect heightened arousal of the pituitary-adrenocortical axis. Both are logical consequences of stress, whether due to chronic environmental pressures, individual characteristics predisposing to reduced stress tolerance, or some combination. The pattern of relationship between scores on these factors and individual variables such as command status and environmental variables such as aircraft type suggests that scores on Factors 1 and 4 are indeed valid indicators of stress. If further studies strengthen these conclusions, scores on these two factors may be useful measures of pilot attributes that should be routinely screened for, so as to select personnel with highest proficiency but least possible health risks. GRA

N87-24068# Northeastern Univ., Boston, Mass.
MULTIPURPOSE VISUAL DISPLAY AND EYE MOVEMENT RECORDING SYSTEM Final Report, 15 Sep. 1984 - 15 Mar. 1986
Alexander A. Skavenski 5 Feb. 1987 3 p
(Grant AF-AFOSR-0312-84)
(AD-A179620; AFOSR-87-0533TR) Avail: NTIS HC A02/MF A01 CSCL 14C

The instrumentation to build a complete eye movement recording and visual display facility is centered on a Generation V, SDI Double Purkinje Image Eye Tracker which permits high resolution 2 dimensional eye movement recording in a 20 deg arc field without contacting the human subject's eye. Visual stimulation is produced on a high resolution color monitor which is driven by a video tape recorder or by digitally stored and processed images from the computer. Eye movement data from the tracker are digitized for storage, analysis and plotting by a PDP 11/73 computer. The system is presently operational and we are beginning experimental work. The first experiments involve finding out why an accurate eye position signal is available for localization judgements requiring that the body be pointed at the target but not when judgements are made solely within the visual modality. Details are found in the original proposal. Equipment cost breakdown is included. GRA

N87-24069# New York Univ., New York. Dept. of Psychology.
THE PERCEPTION OF THE HIGHER DERIVATIVES OF VISUAL MOTION Final Report, 30 Sep. 1985 - 1 Oct. 1986
L. Kaufman 5 Mar. 1987 18 p
(Grant AF-AFOSR-0329-85)
(AD-A179627; AFOSR-87-0435TR) Avail: NTIS HC A02/MF A01 CSCL 06P

This final report provides a brief overview of work conducted prior to the final hear of this project, as more complete descriptions have been published. The overview covers work done on the sensitivity of the perceptual system to changing speed. The stimuli were sinusoidal gratings drifting normal to the lengths of their bars, and speed was modulated. Threshold modulation of speed was about 12% of average speed, although performance was better for higher spatial frequencies and higher average speeds. To avoid effects of contour change, we adopted a random dot approach in which threshold for motion of dots was determined as a function of the proportion of dots exhibiting correlated motion. Thus, threshold is expressed as a signal to noise ratio. For the

detection of uniform motion of moderate speed, the percent correlation was about 5.7, i.e., 5 or 6 dots out of 100 had to move together, with all the other dots in random motion. There was approximately a 47% increase in threshold for change in direction of motion where the change in direction was about 30 deg. However, in a parametric experiment it was found that there was a monotonic decrease in threshold with amount of change in direction. Where the change in direction was only 2 deg, it could not be detected even with 100% correlation. At 3 deg 96% correlation was required. Only 14% correlation required at 30 deg. GRA

N87-24070# Advisory Group for Aerospace Research and Development, Neuilly-Sur-Seine (France). Aerospace Medical Panel.

SHORT COURSE ON CARDIOPULMONARY ASPECTS OF AEROSPACE MEDICINE

Loughton, England Mar. 1987 130 p Course held in Fuerstenfeldbruck, West Germany, 18-20 May 1987, in Athens, Greece, 21-23 May 1987, in Copenhagen, Denmark, 9-11 Jun. 1987, and in Eskisehir, Turkey, 15-17 Jun. 1987

(AGARD-R-758; ISBN-92-835-1544-7) Copyright Avail: NTIS HC A07/MF A01

Lectures and case presentations delivered as part of a course on the cardiopulmonary aspects of aerospace medicine are compiled. The major thrust of the course was directed toward aeromedical decision making. Medical problems such as arrhythmias, coronary disease, valvular disease, hypertension, and bronchiopulmonary disease are addressed. Diagnostic and screening techniques are also discussed. For individual titles, see N87-24071 through N87-24079.

N87-24071# Advisory Group for Aerospace Research and Development, Neuilly-Sur-Seine (France).

AEROMEDICAL EVALUATION AND DISPOSITION OF ELECTROCARDIOGRAPHIC ABNORMALITIES

William B. Kruyer *In* AGARD Short Course on Cardiopulmonary Aspects of Aerospace Medicine Mar. 1987 8 p (For primary document see N87-24070 17-52)

Avail: NTIS HC A07/MF A01

Electrocardiographic abnormalities are discussed with regard to their aeromedical significance, evaluation, and disposition. Sinus bradycardia, sinus and ventricular tachycardia, atrioventricular block, axis deviation, right and left bundle branch block, ventricular hypotrophy, tachyarrhythmias, atrial abnormalities, and short PR syndromes are addressed. Evaluation of the significance of these abnormalities is based on aviator cardiographic records in the USAF Central Electrocardiographic Library. The importance of natural history follow-up studies is emphasized. M.G.

N87-24072# Advisory Group for Aerospace Research and Development, Neuilly-Sur-Seine (France). Clinical Sciences Div.

NONINVASIVE METHODS FOR THE DETECTION OF CORONARY ARTERY DISEASE IN AVIATORS: A STRATIFIED BAYESIAN APPROACH

James R. Hickman, Jr. *In* AGARD Short Course on Cardiopulmonary Aspects of Aerospace Medicine Mar. 1987 11 p (For primary document see N87-24070 17-52)

Avail: NTIS HC A07/MF A01

The detection of asymptomatic coronary disease is a major goal of most aeromedical services, especially those associated with high-performance aircraft. Unfortunately, the pursuit of silent coronary artery disease with contemporary noninvasive diagnostic methods has been disappointing. This lecture discusses the epidemiological principles which underlie this rather poor performance of contemporary diagnostic tools in a population where coronary artery disease is of low prevalence. The underlying statistical problem is best explained by analysis of Bayes' theorem, which applies conditional probability analysis to diagnostic tests which are not perfect. The predictive power of a positive diagnostic test is very heavily dependent upon the prevalence of the disease in the population being tested. Unlike sensitivity and specificity, which are independent of disease prevalence, predictive value is strongly influenced by stratification of the test population into subsets with high pretest probability of disease. Strategies to improve the poor performance of contemporary noninvasive tools in the testing of otherwise healthy individuals are discussed. The USAF School of Aerospace Medicine Risk Index is offered as a theoretical, but unvalidated, stratification tool. M.G.

N87-24073# Advisory Group for Aerospace Research and Development, Neuilly-Sur-Seine (France).

VALVULAR AND CONGENITAL HEART DISEASE IN THE AVIATOR

William B. Kruyer and Robert S. Schwartz *In* AGARD Short Course on Cardiopulmonary Aspects of Aerospace Medicine Mar. 1987 12 p (For primary document see N87-24070 17-52)

Avail: NTIS HC A07/MF A01

Many valvular and congenital heart lesions can have major impact in the aviation environment. In the flying population, such lesions are typically asymptomatic and may be subtle enough that their presence can be detected only by very careful physical or laboratory examination. Thus, valvular or congenital cardiac disease is often found in a flier in whom there is a great deal of time, effort, and monetary investment. The loss of such an individual from flying status should thus be avoided if at all possible. As in all aeromedical decisions, these considerations must be weighed against the likelihood of significant impairment while performing aviation duties resulting either directly or indirectly from the cardiac lesion of concern. In light of these conflicting considerations, a discussion of regulations and medical aspects of specific valvular and congenital problems as approached by the USAF School of Aerospace Medicine is presented. Author

N87-24074# Advisory Group for Aerospace Research and Development, Neuilly-Sur-Seine (France). Clinical Sciences Div.

AEROMEDICAL ASPECTS OF MITRAL VALVE PROLAPSE

James R. Hickman, Jr. *In* AGARD Short Course on Cardiopulmonary Aspects of Aerospace Medicine Mar. 1987 7 p (For primary document see N87-24070 17-52)

Avail: NTIS HC A07/MF A01

Mitral valve prolapse (MVP) continues to be a major aeromedical problem. Current issues revolve around diagnostic criteria, aeromedical thresholds for disqualification and the lack of definitive natural history studies upon which to base aeromedical decisions. Currently, there are no existing natural history studies of incidentally discovered mitral valve prolapse in the asymptomatic male. The USAF School of Aerospace Medicine is following over 300 mitral valve prolapse subjects on a recurrent basis in order to determine this natural history. The comparison of this natural history group with age-matched controls should be completed in approximately 1988. Preliminary data offered in this report enumerate the most common grounding causes of mitral valve prolapse in the first 202 aviators with prolapse in the study. A suggested scheme for clinical evaluation, aeromedical disposition of MVP and suggested aeromedical diagnostic criteria are offered. Author

N87-24075# Advisory Group for Aerospace Research and Development, Neuilly-Sur-Seine (France).

PULMONARY PHYSIOLOGY AND PULMONARY FUNCTION TESTING IN AEROSPACE MEDICINE

G. W. Gray *In* AGARD Short Course on Cardiopulmonary Aspects of Aerospace Medicine Mar. 1987 8 p (For primary document see N87-24070 17-52)

Avail: NTIS HC A07/MF A01

Respiratory diseases may have serious consequences in the aviation environment, ranging from life threatening incapacitation (e.g., tension pneumothorax) to aggravation of hypoxia, acceleration atelectasis and perhaps lowered G tolerance in individuals with relatively minor degrees of small airways disease. Some concepts of respiratory physiology which are of particular relevance in the aviation environment are reviewed and current methods of pulmonary function testing which can be applied to detect asymptomatic disease in aircrew are discussed. Author

N87-24076# Advisory Group for Aerospace Research and Development, Neuilly-Sur-Seine (France). Central Medical Establishment.

AEROMEDICAL DISPOSITION OF PULMONARY SARCOIDOSIS, CHRONIC OBSTRUCTIVE LUNG DISEASE, REACTIVE AIRWAY DISEASE AND SPONTANEOUS PNEUMOTHORAX

David H. Hull *In* AGARD Short Course on Cardiopulmonary Aspects of Aerospace Medicine Mar. 1987 5 p (For primary document see N87-24070 17-52)

Avail: NTIS HC A07/MF A01

Four respiratory diseases are described in relation to aviation medicine: sarcoidosis, chronic obstructive lung disease, reactive airway disease, and spontaneous pneumothorax. Each is discussed in the context of flying safety, operational efficiency, and problems of treatment. Guidelines are offered for decisions on management and disposal of aircrew candidates and of trained aircrew who have a history of one of these diseases or who develop the disease during their flying career. Author

N87-24077# Advisory Group for Aerospace Research and Development, Neuilly-Sur-Seine (France).

HYPERTENSION IN THE AVIATOR

William B. Kruyer *In* AGARD Short Course on Cardiopulmonary Aspects of Aerospace Medicine Mar. 1987 3 p (For primary document see N87-24070 17-52)

Avail: NTIS HC A07/MF A01

Systemic hypertension is one of the most commonly encountered medical problems for both the general medical practitioner and the specialist in aerospace medicine. Its frequent occurrence, its contribution to the risk of cardiovascular events, and problems with early detection and compliance with therapy all make hypertension a health problem of significant concern. It is clear from the literature that therapy for moderate and severe hypertension significantly reduces morbidity and mortality. However, much study and debate has occurred regarding the benefit of mild hypertension. The appropriateness of therapy for mild hypertension is discussed based on a review of several major studies from the world literature. Detrimental effects of thiazide diuretics have been reported, prompting interest in the use of smaller doses of thiazide diuretics as well as interest in the use of other agents as first line therapeutic choices. Current USAF policies regarding the treatment of hypertension in aviation are discussed as well as considerations that must be addressed in the study of new medications for use in the aviator population. Author

N87-24078# Advisory Group for Aerospace Research and Development, Neuilly-Sur-Seine (France). Clinical Sciences Div.

CORONARY RISK FACTORS IN AEROSPACE MEDICINE

James R. Hickman, Jr. *In* AGARD Short Course on Cardiopulmonary Aspects of Aerospace Medicine Mar. 1987 8 p (For primary document see N87-24070 17-52)

Avail: NTIS HC A07/MF A01

Coronary risk factors may be used in the aeromedical setting to identify aviators who are at high risk for the development of coronary artery disease and are, therefore, at a higher risk for sudden incapacitation. Coronary risks may be used to identify those aviators who need additional testing in an attempt to discover asymptomatic coronary disease. Coronary risk factor analysis should also be applied to the entire aviator population in order to identify those aviators who need routine or intensive risk factor modification. Certain lipid patterns, especially familial hyperlipidemia patterns, may be used to identify younger trainees who do not represent a good long-term training investment because of high risk of subsequent development of coronary artery disease. Author

N87-24079# Advisory Group for Aerospace Research and Development, Neuilly-Sur-Seine (France).

CARDIOPULMONARY SCREENING FOR HIGH-PERFORMANCE FLYING: SELECTION AND RETENTION ISSUES

G. W. Gray *In* AGARD Short Course on Cardiopulmonary Aspects of Aerospace Medicine Mar. 1987 4 p (For primary document see N87-24070 17-52)

Avail: NTIS HC A07/MF A01

Detection methods used in the cardiopulmonary screening of aircrew are discussed with reference to candidate selection standards and retention of older experienced pilots. Aircrew candidate screening emphasizes the diagnosis of mostly asymtomatic diseases and disorders. It is designed to identify structural cardiac abnormalities and cardiac arrhythmias that may be a problem in the high +G(z) environment. Screening should also be directed toward pulmonary disorders which may compromise human effectiveness in rapid onset high G (ROHG) and high sustained G (HSG) fighter operations. In experienced aircrew, screening emphasis shifts to the detection of abnormalities which develop with age, particularly, coronary heart disease and small airways disease. Current issues including tobacco smoking, the effects of repetative HSG on the heart and lungs, minimal coronary heart disease, and coronary angioplasty are also discussed. M.G.

N87-24080# Brookhaven National Lab., Upton, N. Y.

INTERNATIONAL SYMPOSIUM ON IN VIVO BODY COMPOSITION STUDIES: PROGRAM AND ABSTRACTS

1986 97 p Symposium held at Upton, N.Y., 28 Sep. 1986

(Contract DE-AC02-76CH-00016)

(DE87-006750; BNL-39428; CONF-8609203) Avail: NTIS HC A05/MF A01

This booklet contains the program and individual abstracts for papers presented at the International Symposium on In Vivo Body Composition Studies. The presentations were divided into five sessions. Individual abstracts were indexed for the Energy Data Base. DOE

N87-24081# Lawrence Livermore National Lab., Calif.

HAZARDS EVALUATION OF RADIOFREQUENCY AND MICROWAVE RADIATION

G. C. Miller Mar. 1987 74 p

(Contract W-7405-eng-48)

(DE87-008536; UCID-20978) Avail: NTIS HC A04/MF A01

This manual is primarily for Industrial Hygienists. The basic concepts of protection from radiofrequency and microwave radiation (RFMW) are presented here to help readers recognize and evaluate RFMW-associated potential health hazards and to understand the technical issues in public debates about RFMW. This manual contains the technical background for understanding and measuring RFMW. The control of RFMW radiation is not covered, requiring as it does a degree of familiarity with electrical engineering. The appendices are designed for use by RFMW surveyors in the field. Included are a summary of bioeffects studies, common RFMW sources, field survey protocols, and formulas for field measurement calculations. Upon completion of this manual, industrial hygienists should be in a position to handle most radiofrequency and microwave emergencies and should know when to call for assistance. While essentially a classroom training aid, the manual can also stand alone as a guide. DOE

N87-24082# Army Research Inst. of Environmental Medicine, Natick, Mass.

OPERATION EVEREST 2: IMPORTANCE OF VENTILATION IN DEFENSE OF MAXIMAL OXYGEN UPTAKE AT EXTREME ALTITUDES

Allen Cymerman, Paul B. Rock, John R. Sutton, John T. Reeves, and Bertron M. Groves Nov. 1986 36 p

(AD-A177874) Avail: NTIS HC A03/MF A01 CSCL 06S

The role of ventilation in the reduction of maximal aerobic power was studied in 8 subjects exposed to progressive simulated altitudes of 3962, 6096, 7468, and 8839 m (barometric pressures of 464, 347, 289, 240 Torr, respectively), as members of Operation Everest 2, a 40-day simulated ascent of Mt. Everest. The mean (+ or - SEM) maximal oxygen uptake (VO2 max) was decreased from 4.13 + or - 0.20 at sea level (SL) to 1.2 + or - 0.08 l/min at P sub B 240 Torr. Maximal heart rate also decreased while arterial oxygen saturation was reduced. Maximal exercise ventilation at all barometric pressures compared to SL with a significant

increase occurring at 464 Torr. Both frequency (f) and tidal volume (TV) contributed to the increase in VE (with f tending to be higher and TV lower for any VE at SL). A higher correlation was found between SaO2 and VO2 max than with heart rate and VO2 max. The rank order of subjects for VE/VO2 at SL was essentially the same as that at 240 Torr. VO2 max was reduced in all subjects 2 days after return to SL reaching 82% of the original mean while associated values for VE, f and TV were not different, suggesting that responses which improve or maintain exercise performance at altitude persist for at least several days after return to SL to the detriment of VO2 max. It was concluded that ventilatory control is not lost under severe, progressive hypoxia; that a strong response is paramount to maintaining VO2 max; and that ventilation may be more critical than circulation in preserving VO2 max. GRA

N87-24083# Naval Submarine Medical Research Lab., Groton, Conn.
THE REVIEW OF A RESEARCH PROPOSAL TO STUDY THE EFFECTS OF 130 torr OXYGEN ON SUBMARINES HELD AT GROTON, CONNECTICUT ON SEPTEMBER 4, 1986
Douglas R. Knight and Arthur B. Callahan 29 Jan. 1987 18 p
(AD-A177976; NSMRL-MR-87-1) Avail: NTIS HC A02/MF A01 CSCL 06S

The extinguishments for fire aboard patroling submarines relies on crew action and speed of response. Therefore, anything that slows the growth of fires will assist crews in bringing fires under control. Submarines routinely operate with oxygen concentrations close to 19%. Snorkeling rarely drops a ship's internal pressure below 700 torr, but accidental circumstances could create a partial vacuum of -5 inches mercury. The effects of reduced oxygen concentration and partial vacuums can be studied in an altitude chamber. The selection of physiological and psychological tests is appropriate, except for collecting blood samples which attempt to measure arterial oxygen content and detect damage to organs such as the liver. The exposure time of 8 days is appropriate in the absence of data showing that longer exposure at 5,000 ft altitude cause delayed onset of mountain sickness. GRA

N87-24084# Texas A&M Univ., College Station.
POTENTIAL ELECTRON BEAM INDUCED FLASHBLINDNESS IN PILOTS Final Report, Oct. 1985 - Aug. 1986
Norma D. Miller and Thomas G. Wheeler Nov. 1986 26 p
(Contract F33615-83-D-0602)
(AD-A178002; USAFSAM-TR-86-31) Avail: NTIS HC A03/MF A01 CSCL 06R

A simplified but representative situation of a flat windscreen and visor in front of a pilot's eyes has been defined to evaluate the potential for flashblindness caused by Cerenkov radiation, produced by a 1-sec exposure to relativistic electrons with velocities of about 0.95 c. The spectral and spatial distribution of the Cerenkov radiation in the windscreen and visor from the electron beam has been calculated to find the additional retinal illumination contributed by them. On the basis of the calculations performed and of a brief survey of existing data, the following five estimates can be made: (1) Absolute threshold for the Cerenkov radiation from the windscreen and that produced in the eye is equivalent to a 3-Microrad beam of 0.95 c electrons. (2) Cone threshold for the Cerenkov radiation produced in the eye is equivalent to 0.8 rads; and, for that produced in the windscreen, 0.09 rad. (3) Extrapolating from foveal and parafoveal data, a 10-rad beam would cause a 2.5-sec interruption in visibility for low contrast targets in the mid-scotopic adaptation range in the region of the windscreen arcs. (4) Insufficient data exist for proper evaluation of the flashblindness effect in the periphery at scotopic levels, so the estimate in item 3 may be conservative by a large factor. (5) No possibility exists for flashblindness from Cerenkov radiation in the mid-photopic range at sublethal doses. GRA

N87-24085# Tufts Univ., Medford, Mass. Dept. of Anatomy and Cellular Biology.
TRAINING, MUSCLE FATIGUE, AND STRESS FRACTURES Annual Report, 15 Nov. 1985 - 14 Nov. 1986
Clinton T. Rubin 15 Dec. 1986 13 p
(Contract DAMD17-86-C-6088; DA Proj. 3M1-61102-BS-10)
(AD-A178350) Avail: NTIS HC A02/MF A01 CSCL 06P

The abrupt increase in physical activity required during basic training frequently leads to stress fractures in the lower limbs of new recruits. During peacetime, stress fractures are the most common physical injury in military populations. The objective of this three year research program is to study the etiology of the stress fracture lesion for which purpose, two parallel experimental protocols were begun: (1) the effect of muscle fatigue on bone strain distributions and, (2) the effect of repetitive cyclic loading on bone remodeling. The summation of these two protocols will provide unique insight towards the effect of new strain regimens on skeletal remodeling. The development of an experimental protocol in 4 horses to determine the effect of fatigue and uncoordinated muscle activity on the distribution, magnitude and rate of change of strains developed in vivo within the cannon bone. Experimental methodology includes bone-bonded rosette strain gauges, liquid metal strain gages attached to tendon, surface and muscle embedded electro-myographs, heart and ventilation frequencies, blood lactate production, maximum oxygen consumption, and carbon dioxide production. GRA

53 BEHAVIORAL SCIENCES

Includes psychological factors; individual and group behavior; crew training and evaluation; and psychiatric research.

N87-24086# Ecole Nationale Superieure des Telecommunications, Paris (France). Dept. Systemes et Communications.
PERCEPTION AND STRUCTURAL ANALYSIS OF MORPHOLOGIES
Claudie Faure Aug. 1986 36 p
(ENST-86D004; ISSN-0751-1345; ETN-87-99608) Avail: NTIS HC A03/MF A01

For seismic signals, human perception of analogy between signals; and for speech spectrogram segmentation, expert decisions which include high level knowledge, are compared to automatic decisions. Automatic decisions quite often fit human decisions and disagree when high level knowledge, which is used by subjects, is not included in the pattern recognition system, but, also, automatic decisions are made by using information that is disregarded by the subjects. Hence, automatic processing cannot be considered to be a bad imitation of human process but as a different process which has its own behavior. Adaptation to the context is one of the most difficult problems to solve for automatic interpretation of patterns. ESA

54 MAN/SYSTEM TECHNOLOGY AND LIFE SUPPORT

Includes human engineering; biotechnology; and space suits and protective clothing.

For related information see also *16 Space Transportation.*

N87-24087# Army Construction Engineering Research Lab., Champaign, Ill.
FULL-SCALE TEST PROGRAM FOR A SHOWER WASTEWATER RECYCLING SYSTEM: TECHNICAL EVALUATION Interim Report
Richard J. Scholze, John T. Bandy, Donald K. Jamison, James A. Morgan, and Vincent J. Ciccone Jan. 1987 39 p
(AD-A178061; CERL-N-87/06) Avail: NTIS HC A03/MF A01 CSCL 13B

A shower wastewater recycling system is investigated for potential military use under conditions of limited water supply. Results are reported for laboratory tests on the proposed system. Parameters measured in the tests include those specified by the Office of the Surgeon General (OTSG) in the Interim Quality Criteria

for direct reuse of water as well as several others of concern. The laboratory test results show that the wastewater recycling system merits further investigation and development. The proposed system is compatible with existing Army facilities and equipment and is portable. Wastewater can be treated to a quality meeting OTSG standards. Several recycles are possible, with 85 percent of the wastewater recoverable for reuse. No harmful contaminants were detected in any of the test samples. GRA

N87-24088# Army Construction Engineering Research Lab., Champaign, Ill.

THE FIELD SHOWER WASTEWATER RECYCLING SYSTEM: DEVELOPMENT OF A PROGRAM OF INSTRUCTION AND PRELIMINARY ANALYSIS OF ITS POTENTIAL HEALTH IMPLICATIONS Final Report

Richard J. Scholze, John T. Bandy, William P. Gardiner, Winifred Curley, and Ed D. Smith Feb. 1987 70 p

(AD-A178112; CERL-TR-N-87/07) Avail: NTIS HC A04/MF A01 CSCL 13B

Discussed is the development of a suggested program of instruction for operators of a Field Shower Wastewater Recycling System (FSWRS)--a system designed to recycle water used in showers in the field. A 40-hour training course is recommended. These operations will emphasize water treatment procedures and water sampling and testing. Analysis of field needs indicated that water quality testing can be limited to measurements of pH, turbidity, and residual chlorine and that these measurements can be made with relatively unsophisticated equipment. It was found that most constituents of shower wastewater that could pose health hazards will be removed during FSWRS recycling operations. However, basic procedures should be followed, such as avoiding ingestion of recycled shower waters and ensuring that FSWRS operators take appropriate precautions in handling sulfuric acid and untreated waters. Although no health hazards are anticipated to result from components such as soaps and shampoos, there is concern about the hazard potential of volatile organic compounds, heavy metals, chlorinated compounds, and chlorination byproducts. The most likely health effects would be skin and eye irritations. GRA

N87-24089# Naval Submarine Medical Research Lab., Groton, Conn.

MEDICAL RESEARCH PROGRAMS, PAST AND FUTURE, FOR DESIGNING ATMOSPHERES TO RETARD FIRES

Douglas R. Knight 7 Feb. 1987 14 p

(AD-A178354; NSMRL-MEMO-87-2) Avail: NTIS HC A02/MF A01 CSCL 13L

One method of improving submarine fire safety is to retard the flammability of combustible materials with atmospheres containing less than or = 19% oxygen. This should only be done if it is known that crews can effectively perform their occupation in the oxygen-lean environment. The purpose of this report is to summarize the history of research in this special topic of submarine medicine. The report is concluded with an outline of work needed to provide nuclear submarine commanders the option of using fire-retardant atmospheres aboard patroling submarines. GRA

N87-23644# Messerschmitt-Boelkow-Blohm G.m.b.H., Munich (West Germany). Ergonomics and Cockpit System.

COMPUTER SIMULATION STUDIES ON HUMAN CONTROL RELIABILITY IN MANUAL AIRCRAFT CONTROL: THE ORIGIN OF PIO

K. Brauser and R. Seifert *In* AGARD Flight Simulation Sep. 1986 19 p (For primary document see N87-23633 17-09)

Copyright Avail: NTIS HC A16/MF A01

55 SPACE BIOLOGY

Includes exobiology; planetary biology; and extraterrestrial life.

No abstracts in this category.

59 MATHEMATICAL AND COMPUTER SCIENCES (GENERAL)

No abstracts in this category.

60 COMPUTER OPERATIONS AND HARDWARE

Includes hardware for computer graphics, firmware, and data processing.

For components see *33 Electronics and Electrical Engineering.*

N87-24090# Massachusetts Univ., Amherst.

INTERMEDIATE LEVEL COMPUTER VISION PROCESSING ALGORITHM DEVELOPMENT FOR THE CONTENT ADDRESSABLE ARRAY PARALLEL PROCESSOR Progress Report, Dec. 1986 - Feb. 1987

Riseman 29 Nov. 1986 38 p

(Contract F49620-86-C-0041)

(AD-A179515; AFOSR-87-0453TR) Avail: NTIS HC A03/MF A01 CSCL 09B

During this quarter the low to intermediate level interface hardward design for the IUA has been finalized. Various network topologies for communications within the intermediate level of the IUA have also been examined. At the minimum a mesh with an overlain hypercube will be supported. However, a fully programmable network topology is under consideration that will allow us to experiment with different processor interconnection schemes. GRA

N87-24091# Royal Inst. of Tech., Stockholm (Sweden). Dept. of Numerical Analysis and Computing Science.

HARDWARE SYNTHESIS FROM SPECIFICATION WITH POLYNOMIALS

Bjoern Lisper 1987 90 p

(TRITA-NA-8506) Avail: NTIS HC A05/MF A01

A theoretical framework for synthesis of hardware, given a description of the desired outputs, is developed. Outputs are specified as polynomials in the inputs over some universal, possibly heterogeneous algebra. Given these output specifications, an algorithm specified by formal expressions for the polynomials can be derived and a set of cell actions, computations, can be determined. The set of computations can be mapped into a space-time, that is a model of the events in the target hardware, by a mapping fulfilling certain conditions. The result is a description of where and when the different steps in the algorithm are performed. This description contains the information of what the different parts of the hardware are able to do, as well as the information about timing of the data sent between different events. The generality of the synthesis approach is discussed, and it is shown that the action of any Turing machine can be described by a set of polynomials. The methodology seems, however, to have its widest applicability for synthesizing hardware for solving problems for which algorithms with a fixed number of steps exist, which is not the case for algorithms performed by Turing machines in general. M.G.

N87-24092# California Inst. of Tech., Pasadena.
THE HYPERCUBE AS A SUPERCOMPUTER
G. C. Fox 1987 22 p Presented at the 2nd International Conference on Supercomputing, San Francisco, Calif., 1 May 1987
(Contracts DE-FG03-85ER-25009; DE-AC03-81ER-40050)
(DE87-005029; DOE/ER-25009/391; CONF-870567-1) Avail: NTIS HC A02/MF A01

We show that a hypercomputer is a relatively general purpose supercomputer that can address a wide variety of fields. We describe both the general issues and specific examples that have been developed at Caltech. We review some of the software tools that can help the development of code for such concurrent computers. DOE

N87-24093# Oak Ridge National Lab., Tenn.
GAUSSIAN ELIMINATION WITH PARTIAL PIVOTING AND LOAD BALANCING ON A MULTIPROCESSOR
A. George and E. Chu Mar. 1987 18 p
(Contract DE-AC05-84OR-21400)
(DE87-007784; ORNL/TM-10323) Avail: NTIS HC A02/MF A01

A row-oriented implementation of Gaussian elimination with partial pivoting on a local-memory multiprocessor is described. In the absence of pivoting, the initial data loading of the node processors leads to a balanced computation. However, if interchanges occur, the computational loads on the processors may become unbalanced, leading to inefficiency. A simple load balancing scheme is described which is inexpensive and which maintains computational balance in the presence of pivoting. Using some reasonable assumptions about the probability of pivoting occurring, an analysis of the communication costs of the algorithm is developed, along with an analysis of the computation performed in each node processor. This model is then used to derive the expected speed-up of the algorithm. Finally, experiments using an Intel iPSC hypercube are presented in order to demonstrate the extent to which the analytical model predicts the performance. DOE

N87-24094# Sandia National Labs., Albuquerque, N. Mex.
DATA: A COMPREHENSIVE DATA ANALYSIS ENVIRONMENT FOR HP1000 COMPUTERS
W. D. Drotning Mar. 1987 42 p
(Contract DE-AC04-76DP-00789)
(DE87-007824; SAND-87-0369) Avail: NTIS HC A03/MF A01

DATA was designed to accomplish a wide variety of tasks related to analysis of data stored in files on Hewlett-Packard HP 1000 minicomputer systems. As a data analysis tool, DATA provides a number of often-used mathematical analysis and data manipulation functions which may be employed. Flexible file structures, on both input and output, are allowed. An editor is included which allows DATA to serve as a binary file editor for data; search routines based on numeric, rather than string, values are incorporated. Graphical plotting of data and functions, cursor selection of specific data regions, and other graphics features are also included. DATA also serves as a shell operating system, with direct interface to the RTE operating system. Commonly-used file management functions are incorporated or enhanced for operator convenience. DATA is both command and menu (softkey) driven, and on-line help facilities are included. Finally, DATA serves as a common framework for future expansion, such as incorporation of the IMSL library or additional user-defined functions. DOE

61 COMPUTER PROGRAMMING AND SOFTWARE

Includes computer programs, routines, alogorithms, and specific applications, e.g., CAD/CAM.

N87-24095# Air Force Inst. of Tech., Wright-Patterson AFB, Ohio. School of Engineering.
A PROGRAM MAINTENANCE AID USING STATIC DATA FLOW ANALYSIS TECHNIQUES M.S. Thesis
Timothy S. Weber Mar. 1987 65 p
(AD-A179108; AFIT/GCS/ENG/87M-1) Avail: NTIS HC A04/MF A01 CSCL 09B

Data flow and data dependencies in a program significantly contribute to its complexity. However, data dependency research has produced only single-valued measures of that complexity; those complexity measures provide little to help the maintenance programmer understand data flow in a program. Needed is a maintenance tool that will reveal to the programmer sources of the data flow complexity. This thesis presents a specification for a static intraprocedural data flow analysis tool. It computes six data flow properties of programs: definition without a corresponding use, possible use without a corresponding definition, two distinct uses of a variable, dependency slice of a variable, influence slice of a variable, and influence of a predicate. The first three properties reveal potential program errors and the last three show how statements in a program influence the outcome of other statements. A modified Generalized Program Graph is used to model the program control flow and data flow information needed to compute the properties. Algorithms are presented to compute each property from the Generalized Program Graph. GRA

N87-24096# Illinois Univ., Urbana. Coordinated Science Lab.
RECOVERING THE ORIENTATION OF TEXTURED SURFACES IN NATURAL SCENES Ph.D. Thesis
Dorothea Blostein Apr. 1987 148 p
(Grant AF-AFOSR-0317-82)
(AD-A179360; UILU-ENG-87-2219) Avail: NTIS HC A07/MF A01 CSCL 09D

A perspective view of a slanted textured surface shows systematic changes in the density, area and aspect-ratio of texture elements. These apparent changes in texture element properties can be analyzed to recover information about the physical layout of the scene. However, in practice it is difficult to identify texture elements, especially in images where the texture elements are partially occluded or are themselves textured at a finer scale. To solve this problem, it is necessary to integrate the extraction of texture elements with the recognition of scene layout. This thesis presents a method for recovering the orientation of textured surfaces while simultaneously identifying texture elements. Candidate texture elements are constructed from overlapping circular regions of relatively uniform gray-level. The uniform circular regions are found by convolving the image with Laplacian-of-Gaussian masks over a range of scales, and comparing the convolution output to that expected for a circular disk of constant gray level. True texture elements are selected from the set of candidate texture elements by finding the planar surface that best predicts the properties of the candidate texture elements. Each planar fit is evaluated by comparing the predicted texture-element areas to the actual areas of the candidate texture elements. The planar fit receiving support from the most regions is chosen as the correct interpretation. GRA

N87-24097# Naval Postgraduate School, Monterey, Calif.
RESEARCH ASPECTS OF RAPID PROTOTYPING
Luqi Mar. 1987 20 p
(AD-A179007; NPS52-87-006) Avail: NTIS HC A02/MF A01 CSCL 09B

The objectives of the proposed research are to develop specification methods for identifying and retrieving reusable software components, to develop implementation techniques for the prototyping language PSDL, and to extend the language and

techniques to a multiprocessor model for the prototype. Our approach to component specification will be based on term rewriting systems and the concept of generalization per category. We will seek component specifications that admit effective reductions to a canonical or normal form to aid component retrieval. The attributes of reusable software components will be abstracted to support the design of a software base schema, which will be structured using generalization per category to aid component retrieval. The relation between the specification language and the software base operators will be established. The proposed research will solve some key problems in automated prototyping based on reusable software. Validating software requirements by rapid prototyping depends on three major components: a prototyping language, a software base, and a prototyping method. The objectives of the proposed research contribute to the software base and the prototyping language. GRA

N87-24098*# National Aeronautics and Space Administration. Goddard Space Flight Center, Greenbelt, Md.
THE DEVELOPMENT OF A PROTOTYPE INTELLIGENT USER INTERFACE SUBSYSTEM FOR NASA'S SCIENTIFIC DATABASE SYSTEMS
William J. Campbell, Larry H. Roelofs, and Nicholas M. Short, Jr. (Science Applications Research, Lanham, Md.) Jun. 1987 57 p
(NASA-TM-87821; Rept-87-B-0266; NAS 1.15:87821) Avail: NTIS HC A04/MF A01 CSCL 09B

The National Space Science Data Center (NSSDC) has initiated an Intelligent Data Management (IDM) research effort which has as one of its components the development of an Intelligent User Interface (IUI).The intent of the latter is to develop a friendly and intelligent user interface service that is based on expert systems and natural language processing technologies. The purpose is to support the large number of potential scientific and engineering users presently having need of space and land related research and technical data but who have little or no experience in query languages or understanding of the information content or architecture of the databases involved. This technical memorandum presents prototype Intelligent User Interface Subsystem (IUIS) using the Crustal Dynamics Project Database as a test bed for the implementation of the CRUDDES (Crustal Dynamics Expert System). The knowledge base has more than 200 rules and represents a single application view and the architectural view. Operational performance using CRUDDES has allowed nondatabase users to obtain useful information from the database previously accessible only to an expert database user or the database designer. Author

N87-24099# Royal Inst. of Tech., Stockholm (Sweden). Dept. of Numerical Analysis and Computing Science.
EDGE FOCUSING
Fredrik Bergholm 1987 36 p
(TRITA-NA-8518; INTEGRAL-46) Avail: NTIS HC A03/MF A01

Edge detection in a gray-scale image at a fine resolution typically yields noise and unnecessary detail, whereas edge detection at a coarse resolution distorts edge contours. It is shown that edge focusing, i.e., a coarse-to-fine tracking in a continuous manner, combines high positional accuracy with good noise reduction. This is of vital interest in several applications. Junctions of different kinds are in this way restored with high precision, which is a basic requirement when performing (projective) geometric analysis of an image for the purpose of restoring the three-dimensional scene. Segmentation of a scene using geometric clues like parallelism is also facilitated by the algorithm, since unnecessary detail has been filtered away. The focusing scheme furthermore offers a possibility to classify edge contours with respect to fuzziness. Illumination phenomena like (diffuse) shadow edges could be extracted to some extent, using an extended focusing algorithm. The edge focusing algorithm contains only one essential parameter, namely the courseness of the resolution in the initially blurred image. Author

N87-24100# Oak Ridge National Lab., Tenn.
LU FACTORIZATION ALGORITHMS ON DISTRIBUTED-MEMORY MULTIPROCESSOR ARCHITECTURES
G. A. Geist and C. H. Romine Mar. 1987 31 p
(Contract DE-AC05-84OR-21400)
(DE87-007794; ORNL/TM-10383) Avail: NTIS HC A03

In this paper, we consider the effect that the data storage scheme and pivoting scheme have on the efficiency of LU factorization on a distributed-memory multiprocessor. Our presentation will focus on the hypercube architecture, but most of our results are applicable to distributed-memory architectures generally. We restrict our attention to two commonly used storage schemes (storage by rows and by columns) and investigate partial pivoting both by rows and by columns, yielding four factorization algorithms. The goal is to determine which of these four algorithms admits the most efficient parallel implementation. We analyze factors such as load distribution, pivoting cost, and potential for pipelining. We conclude that, in the absence of loop unrolling, LU factorization with partial pivoting is most efficient when pipelining is used to mask the cost of pivoting. The two schemes that can be pipelined are pivoting by interchanging rows when the coefficient matrix is distributed to the processors by columns, and pivoting by interchanging columns when the matrix is distributed to the processors by rows. DOE

N87-24101# Argonne National Lab., Ill.
AN EXTENDED SET OF FORTRAN BASIC LINEAR ALGEBRA SUBPROGRAMS: MODEL IMPLEMENTATION AND TEST PROGRAMS
J. J. Dongarra, J. DuCroz, S. Hammarling, and R. J. Hanson Jan. 1987 18 p
(Contract W-31-109-eng-38)
(DE87-007913; ANL/MCS-TM-81) Avail: NTIS HC A02/MF A01

This paper describes a model implementation and test software for the Level 2 Basic Linear Algebra Subprograms (Level 2 BLAS). The Level 2 BLAS are targeted at matrix-vector operations with the aim of providing more efficient, but portable, implementations of algorithms on high-performance computers. The model implementation provides a portable set of FORTRAN 77 Level 2 BLAS for machines where specialized implementations do not exist or are not required. The test software aims to verify that specialized implementations meet the specification of the Level 2 BLAS and that implementations are correctly installed. DOE

N87-24102# Sandia National Labs., Albuquerque, N. Mex.
CADCAM-005: AN INTRODUCTION TO THE DATA EXCHANGE PROCESS USING IGES
J. C. Kelly, R. E. Parks, and D. B. Saylors Mar. 1987 36 p
(Contract DE-AC04-76DP-00789)
(DE87-008079; SAND-86-2564) Avail: NTIS HC A03/MF A01

This introductory report deals with some of the ingredients of the data exchange process. Current vendor interactive graphics CAD/CAM systems (Applicon, Calma, Computervision, CD-2000, ANVIL-4000, etc.) are discussed from a generic point of view. Also discussed is the data format given in the Initial Graphics Exchange Specification, which is intended to be a standardized format for the communication of data between interactive graphics CAD/CAM systems. DOE

N87-24103*# Stanford Univ., Calif. Knowledge Systems Lab.
RESEARCH ON KNOWLEDGE REPRESENTATION, MACHINE LEARNING, AND KNOWLEDGE ACQUISITION Final Report, 1 Oct. 1983 - 31 Jan. 1987
Bruce G. Buchanan 23 Jun. 1987 11 p
(Contract NCC2-274)
(NASA-CR-180408; NAS 1.26:180408) Avail: NTIS HC A02/MF A01 CSCL 09B

Research in knowledge representation, machine learning, and knowledge acquisition performed at Knowledge Systems Lab. is summarized. The major goal of the research was to develop flexible, effective methods for representing the qualitative knowledge

necessary for solving large problems that require symbolic reasoning as well as numerical computation. The research focused on integrating different representation methods to describe different kinds of knowledge more effectively than any one method can alone. In particular, emphasis was placed on representing and using spatial information about three dimensional objects and constraints on the arrangement of these objects in space. Another major theme is the development of robust machine learning programs that can be integrated with a variety of intelligent systems. To achieve this goal, learning methods were designed, implemented and experimented within several different problem solving environments. E.R.

N87-24104# Lawrence Livermore National Lab., Calif.
THREE DIMENSIONAL GRAPHICS IN THE STATISTICAL ANALYSIS OF SCIENTIFIC DATA
S. L. Grotch May 1986 9 p Presented at the 13th International Biometric Conference, Seattle, Wash., 28 Jul. 1986
(Contract W-7405-eng-48)
(DE87-008151; UCRL-94113; CONF-860758-2) Avail: NTIS HC A02

In scientific data analysis, the two-dimensional plot has become an indispensable tool. As the scientist more commonly encounters multivariate data, three dimensional graphics will form the natural extension of these more traditional representations. There can be little doubt that as the accessibility to ever more powerful graphics tools increases, their use will expand dramatically. In using three dimensional graphics in routine data analysis for nearly a decade, they have proved to be a powerful means for obtaining insights into data simply not available with traditional 2D methods. Examples of this work, taken primarily from chemistry and meteorology, are presented to illustrate a variety of 3D graphics found to be practically useful. Some approaches for improving these presentations are also highlighted. DOE

N87-24105# Sandia National Labs., Albuquerque, N. Mex.
MVSE (MINIMIZES VARIANCE SQUARED ERROR) ADAPTIVE FILTERING SUBJECT TO A CONSTRAINT ON MSE (MEAN SQUARED ERROR)
Jerry D. Gibson (Texas A&M Univ., College Station.) and Steven D. Gray 1987 6 p Presented at the Conference on Information Sciences and Systems, Baltimore, Md., 25-27 Mar. 1987
(Contract DE-AC04-76DP-00789)
(DE87-007859; SAND-87-0823C; CONF-8703110-1) Avail: NTIS HC A02/MF A01

A new adaptive filtering algorithm which minimizes the variance of the squared error subject to a constraint on the mean squared error (MSE) is proposed and studied. For the adaptive linear combiner signal processing configuration, this algorithm, called the LVCMS algorithm for least variance subject to a constraint on mean squared error, has a gradient that is a weighted linear combination of the least mean square (LMS) and least mean fourth (LMF) algorithm gradients. Theoretical expressions are derived for the LVCMS algorithm convergence factor and misadjustment, and comparisons are made with the LMS and LMF adaptation rules for Gaussian, Laplacian, and uniform plant noise and driving term distributions. DOE

N87-24106# Air Force Inst. of Tech., Wright-Patterson AFB, Ohio. School of Engineering.
A RAPID PROTOTYPING APPROACH TO SOFTWARE VALIDATION M.S. Thesis
Richard L. Rogers Dec. 1986 110 p
(AD-A177939; AFIT/GCE/ENG/86D-10) Avail: NTIS HC A06/MF A01 CSCL 09B

The purpose of this study was to investigate the use of rapid prototyping for software validation. The expected benefits of this approach are reduced time and cost over the software development life cycle. These benefits are derived from the establishment and validation of software requirements at the beginning of the development rather than waiting until the end to validate them. An examination of nine case studies was done to compare the effects of using a rapid prototyping approach to software development and using a conventional approach. The projects for the case studies were selected from current thesis projects at the Air Force Institute of Technology. Analysis of these case studies was based on criteria used in an earlier, similar experiment. While the results were not conclusive they did suggest further research would be beneficial. GRA

N87-24107*# National Aeronautics and Space Administration. Langley Research Center, Hampton, Va.
SOLVING THE CAUCHY-RIEMANN EQUATIONS ON PARALLEL COMPUTERS Final Report
Raad A. Fatoohi and Chester E. Grosch (Old Dominion Univ., Norfolk, Va.) May 1987 38 p Submitted for publication
(Contracts NAS1-17070; NAS1-18107)
(NASA-CR-178307; ICASE-87-34; NAS 1.26:178307) Avail: NTIS HC A03/MF A01 CSCL 09B

Discussed is the implementation of a single algorithm on three parallel-vector computers. The algorithm is a relaxation scheme for the solution of the Cauchy-Riemann equations; a set of coupled first order partial differential equations. The computers were chosen so as to encompass a variety of architectures. They are: the MPP, and SIMD machine with 16K bit serial processors; FLEX/32, an MIMD machine with 20 processors; and CRAY/2, an MIMD machine with four vector processors. The machine architectures are briefly described. The implementation of the algorithm is discussed in relation to these architectures and measures of the performance on each machine are given. Simple performance models are used to describe the performance. These models highlight the bottlenecks and limiting factors for this algorithm on these architectures. Conclusions are presented. Author

N87-24108# Massachusetts Inst. of Tech., Cambridge. Microsystems Research Center.
COMPUTER-AIDED FABRICATION SYSTEM IMPLEMENTATION Semiannual Technical Report, 1 Apr. - 30 Sep. 1986
Paul Penfield, Jr., Dimitri A. Antoniadis, Stanley B. Gershwin, and Donald E. Troxel 30 Sep. 1986 55 p
(Contract N00014-85-K-0213)
(AD-A178225) Avail: NTIS HC A04/MF A01 CSCL 09B

A hierarchical model for scheduling integrated-circuit manufacturing facilities has been developed. In this model, the higher-level modules deal with a longer characteristic time. Faster events are modeled by their statistics (means and variances) and slower events are modeled by their actual values, taken to be constant. The communication patterns modules remain to be worked out. The process development system MASTIF was ported to a workstation, the VAXstation-II. The process simulation program SUPREM was modified to account for impurity clustering and precipitation in silicon. A generalized Boundary Element Method (BEM) was developed for modeling linear viscoelastic materials. This approached was based on Kelvin's solution modified for viscoelastic flow. It can handle a wide range of relaxation time, dealing with elastostatic deformation and viscous in flow. Proposals for a wafer profile interchange format and a binary form suitable for internal use were developed. This document contains three articles: Stochastic Scheduling and Set-Ups in Flexible Manufacturing Systems; A Proposal for a Profile Interchange Format, Part I: Syntax, and A Proposal for a Profile Interchange Format, Part II: Semantics. GRA

N87-24109# Massachusetts Inst. of Tech., Cambridge. Lab. for Computer Science.
EFFICIENT PARALLEL ALGORITHMS FOR (DELTA + 1)-COLORING AND MAXIMAL INDEPENDENT SET PROBLEMS
Andrew V. Goldberg and Serge A. Plotkin Jan. 1987 28 p
(Contracts N00014-80-C-0622; N00014-75-C-0661)
(AD-A178287; MIT/LCS/TM-320) Avail: NTIS HC A03/MF A01 CSCL 12A

We described an efficient technique for breaking symmetry in parallel. The technique works especially well on rooted trees and on graphs with a small maximum degree. In particular, we can find a maximal independent set on a constant-degree graph in

O(lg*n) time on an EREW PRAM using a linear number of processors. We show how to apply this technique to construct more efficient parallel algorithms for several problems, including coloring of planar graphs and (delta + 1)-coloring of constant-degree graphs. We also prove lower bounds for two related problems. Author (GRA)

N87-24110# Massachusetts Inst. of Tech., Cambridge. Lab. for Computer Science.
EFFICIENT GRAPH ALGORITHMS FOR SEQUENTIAL AND PARALLEL COMPUTERS Ph.D. Thesis
Andrew V. Goldberg Feb. 1987 126 p
(Contract N00014-80-C-0622)
(AD-A178403; MIT/LCS/TR-374) Avail: NTIS HC A07/MF A01 CSCL 09B

Graph algorithms are studied, both in sequential and parallel contexts. Algorithm complexities are stated in terms of the number of vertices n, the number of edges m, the largest absolute value of capacities U, and the largest absolute value of costs C. Chapter 1 introduces a new approach to the maximum flow problem that leads to better algorithms for the problem. Chapter 2 is devoted to the minimum cost flow problem, which is a generalization of the maximum flow problem. Chapter 3 addresses implementation of parallel algorithms through a case-study of an implementation of a parallel maximum flow algorithm. Parallel prefix operations play an important role in our implementation. Present experimental results achieved by the implementation are presented. Present Parallel symmetry-breaking techniques are the main topic of Chapter 4. GRA

N87-24111# Ecole Nationale Superieure des Telecommunications, Paris (France). Dept. Informatique.
COLORED STOCHASTIC PETRI NETS
Alexandre Zenie 1986 14 p Presented at the International Workshop on Timed Petri Nets, Torino, Italy, 1-3 Jul. 1985; ACM, IEEE, AEI, IEEE Computer Society Order No. 674, p 262-271
(ENST-86C001; ISSN-0751-1337; ETN-87-99606) Avail: NTIS HC A02/MF A01

Colored stochastic Petri nets are presented as an extension of the stochastic Petri nets model in which the tokens, the transitions, and the corresponding probability measurement are colored. The development leads to a simplification of the basic model and the corresponding stochastic process, while achieving results identical to those obtained with stochastic Petri nets. ESA

62 COMPUTER SYSTEMS

Includes computer networks and special application computer systems.

N87-24112# California Univ., Berkeley. Dept. of Computer Sciences.
USING EXPERT SYSTEMS TO MANAGE DISTRIBUTED COMPUTER SYSTEMS Technical Report, 7 Aug. 1984 - 6 Aug. 1987
Joseph Pasquale 16 Jun. 1987 13 p
(Contract N00039-84-C-0089; ARPA Order 4871)
(AD-A179329) Avail: NTIS HC A02/MF A01 CSCL 09B

Expert systems can be used effectively to manage distributed computer systems which are based on decentralized control of shared resources. These distributed systems can exhibit high reliability and performance. Yet, designing such systems pose formidable problems. These problems involve real-time distributed decision-making where decision-makers do not know with full certainty the state of remote nodes. We identify what characteristics an intelligent decision-making agent must possess to successfully attack these problems, and argue that expert systems share these characteristics. We also present the architecture of an Expert Manager, an experimental system which uses expert system techniques to manage a distributed computer system. GRA

N87-24113# Air Force Inst. of Tech., Wright-Patterson AFB, Ohio. School of Engineering.
ARCHITECTURAL IMPLICATIONS OF A PARALLEL COMPUTATIONAL APPROACH TO THE VECTOR WAVE EQUATION M.S. Thesis
Jack L. Strauss Mar. 1987 111 p
(AD-A179510; AFIT/GE/ENG/87M-5) Avail: NTIS HC A06/MF A01 CSCL 09B

An algorithm has been specified for the hardware implementation of the numerical solution of the electromagnetic fields of an arbitrary current source. The algorithm, defined as the Vector Wave Equation (VWE), solves for the magnetic and electric fields, as well as the vector potential of a finite length arbitrary current source. The specified algorithm has been verified through FORTRAN simulation to produce results accurate to within 2 decimal places for a 500 sub-element dipole. The VWE forms a model which is algorithmically symmetric with respect to the Cartesian coordinate system. As such, the VWE lends itself to highly parallel and concurrent computational techniques. This property of the algorithm makes it an excellent candidate for implementation by a Very High Speed Integrated Circuit (VHSIC) class processor. Investigation of a parallel, highly concurrent architectural implementation has yielded preliminary results that computational savings of a factor of 3 and a throughput rate increase of 5 orders of magnitude is attainable. This research has shown that an application specific VHSIC-class processor array has sufficient computing power to support interactive calculation of a set of equations which solve for the magnetic and electric fields, as well as the vector potential of an arbitrarily current source. GRA

N87-24114# Royal Inst. of Tech., Stockholm (Sweden). Dept. of Numerical Analysis and Computing Science.
INVESTIGATIONS INTO THE PATTERN PROCESSING CAPABILITIES OF ASSOCIATIVE NETS
Anders Lansner 1987 158 p
(TRITA-NA-8601) Avail: NTIS HC A08/MF A01

Pattern processing capabilities of associative nets were investigated by means of computer simulations. Using a simulation program with biologically reasonably realistic model neurons it was shown that Hebbian cell assemblies are likely to form in the cortical network. They may thereafter serve as internal representations of concepts. Pattern completion and sequential association could be demonstrated. These results have later on been scaled up using nets with more abstract nodes and connections. In a model with binary connections, earlier results on the storage capacity of associative nets could be verified. An iterative algorithm for associative recall was designed and the reliability and speed of associative recall using this algorithm was studied. Furthermore, it was shown that an associative net with more than one bit per connection is capable of extracting prototypes of an unknown number of classes, given as input only a set of instances from the classes. Results of the computational complexity analysis show that a parallel implementation with one processor for each node in the net (N processors) is capable of performing associative recall in time 0(log N)squared. This is expected to allow real time performance in many realistic pattern processing tasks. The relevance of associative nets as models of the brain and the role for associative pattern processing in artificial intelligence research is also discussed. Finally, the need for and directions of future research are addressed. Important research areas include short-term memory mechanisms, generation of coordinated and timed output activity, goal direction and motivation, and non-conventional hardware for the implementation of associative pattern processing algorithms. M.G.

N87-24115# Argonne National Lab., Ill.
BEYOND SPEEDUP: PERFORMANCE ANALYSIS OF PARALLEL PROGRAMS
K. W. Dritz and J. M. Boyle Feb. 1987 34 p
(Contract W-31109-eng-38)
(DE87-007954; ANL-87-7) Avail: NTIS HC A03/MF A01

This paper addresses the problem of measuring and analyzing the performance of fine-grained parallel programs running on shared-memory multiprocessors. Such processors use locking (either directly in the application program, or indirectly in a subroutine library or the operating system) to serialize accesses to global variables. Given sufficiently high rates of locking, the chief factor preventing linear speedup (besides lack of adequate inherent parallelism in the application) is lock contention - the blocking of processes that are trying to acquire a lock currently held by another process. We show how a high-resolution, low-overhead clock may be used to measure both lock contention and lack of parallel work. Several ways of presenting the results are covered, culminating in a method for calculating, in a single multiprocessing run, both the speedup actually achieved and the speedup lost to contention for each lock and to lack of parallel work. The speedup losses are reported in the same units, processor-equivalents, as the speedup achieved. Both are obtained without having to perform the usual one-process comparison run. We chronicle also a variety of experiments motivated by actual results obtained with our measurement method. The insights into program performance that we gained from these experiments helped us to refine the parts of our programs concerned with communication and synchronization. Ultimately these improvements reduced lock contention to a negligible amount and yielded nearly linear speedup in applications not limited by lack of parallel work. We describe two generally applicable strategies (code motion out of critical regions and critical-region fissioning) for reducing lock contention and one (lock/variable fusion) applicable only on certain architectures. DOE

N87-24116# California Univ., Berkeley. Lawrence Berkeley Lab.

THE FUTURE OF INTERSITE NETWORKING

Nov. 1986 361 p Presented at the 1st Annual Energy Research Workshop on Interlaboratory Computing, Berkeley, Calif., 27 Oct. 1986

(Contract DE-AC03-76SF-00098)

(DE87-007912; LBL-22460; CONF-8610138) Avail: NTIS HC A16

Copies of viewgraphs and summaries of three discussion groups are presented. The purpose of the workshop was to identify strategies for meeting the computer networking needs of the scientists under the Office of Energy Research. DOE

N87-24117# California Univ., Berkeley. Lawrence Berkeley Lab.

THE EFFECT OF DISTRIBUTED COMPUTING TECHNOLOGY ON WIDE AREA NETWORK CAPACITY REQUIREMENTS

D. Hall, W. Johnston, M. Hutchinson, M. Rosenblum, and D. Robertson Feb. 1987 12 p Presented at the Federal Coordinating Council on Science, Engineering and Technology, San Diego, Calif., 17 Feb. 1987

(Contract DE-AC03-76SF-00098)

(DE87-008229; LBL-22948; CONF-870277-1) Avail: NTIS HC A02/MF A01

This report identifies a need to increase wide area network capacity by as much as three orders of magnitude over the next ten years. These increases are necessary to support new distributed computing products. Such products increase productivity, but are currently available only on local area networks. There is no technical reason for limiting these products to tightly constrained geographical areas, however. They can operate perfectly well over any terrestrial distance provided sufficient bandwidth is available. Such bandwidth is available today with fiber optics. To quantify capacity requirements, network traffic generated by this newer technology is compared with traditional traffic in a local network environment. An extrapolation to wide area networks is made. Speculation about the long term future of distributed computing technology and its effect on network capacity requirements is offered. It is argued that an increase of network capacity by one order of magnitude is sufficient to accommodate new distributed computing technology on existing wide area networks. Two orders of magnitude are needed to accommodate a fully integrated distributed system such as interactive graphics. Three orders of magnitude are needed to accommodate increases in hardware speed anticipated in the next five to ten years. Availability of highly integrated, nationwide distributed computing service would significantly increase the competitive edge of the United States in science and computing. DOE

63 CYBERNETICS

Includes feedback and control threory, artificial intelligence, robotics and expert systems.

For related information see also *54 Man/System Technology and Life Support.*

N87-24118# Carnegie-Mellon Univ., Pittsburgh, Pa. Robotics Inst.

CHOOSING SAMPLING RATES FOR ROBOT CONTROL Interim Report

Pradeep K. Khosla Mar. 1987 21 p

(AD-A179447; CMU-RI-TR-87-5) Avail: NTIS HC A02/MF A01 CSCL 13I

In previous research, the author experimentally implemented and evaluated the effect of dynamics compensation in model-based control algorithms. In this paper, he evaluates the effect of changing the control sampling period on the performance of the computed-torque and independent joint control schemes. While the former utilizes the complete dynamics model of the manipulator, the latter assumes a decoupled and linear model of the manipulator dynamics. The author discusses the design of controller gains for both the computed-torque and the independent joint control schemes and establishes a framework for comparing their trajectory tracking performance. The experiments show that within each scheme the trajectory tracking accuracy varies slightly with the change of the sampling rate. However, at low sampling rates the computed-torque scheme outperforms the independent joint control scheme. Based on experimental results, also conclusively established is the importance of high sampling rates as they result in an increased stiffness of the system. GRA

N87-24119# Carnegie-Mellon Univ., Pittsburgh, Pa. Robotics Inst.

EXPERIMENTAL EVALUATION OF NONLINEAR FEEDBACK AND FEEDFORWARD CONTROL SCHEMES FOR MANIPULATORS Interim Report

Pradeep K. Khosla and Takeo Kanade Mar. 1987 28 p

(Grant NSF ECS-83-20364)

(AD-A179449; CMU-RI-TR-87-4) Avail: NTIS HC A03/MF A01 CSCL 13I

The manipulator trajectory tracking control problem revolves around computing the torques to be applied to achieve accurate tracking. While this problem has been extensively studied in simulations, the real-time results have been lacking in the robotics literature. This paper presents the experimental results of the real-time performance of model-based control algorithms. It compares the computed-torque control scheme with the feedforward dynamics compensation scheme. The feedforward scheme compensates for the manipulator dynamics in the feedforward path while the computed-torque scheme uses the dynamics in the feedback loop for linearization and decoupling. The manipulator control schemes have been implemented on the CMU DD Arm II with a sampling period of 2 ms. GRA

N87-24120# Air Force Inst. of Tech., Wright-Patterson AFB, Ohio. School of Engineering.

CONTENT-ADDRESSABLE MEMORY: APPLICATIONS, ALGORITHMS, AND SIMULATION M.S. Thesis

Ronald W. Brower 8 Dec. 1986 158 p

(AD-A177944; AFIT/GCE/ENG/86D-1) Avail: NTIS HC A08/MF A01 CSCL 09B

A number of algorithms supporting artificial intelligence (AI), database management, and pattern recognition have been developed at the Air Force Institute of Technology (AFIT). These

algorithms exploit an innovative peripheral-memory architecture, also developed at AFIT, which uses content-addressable memory (CAM). Algorithms for LISP garbage collection, database searching, and pattern recognition have been developed. This thesis analyzes the algorithms and the supporting CAM hardware using both computer simulation (N.2 and VHDL) as well as mathematical models of algorithmic complexity. Included in this study are CAM algorithms for performing: (1) real-time LISP garbage collection in a virtual memory environment, and (2) associatively searching through a database whose records are many times longer than the CAM's basic word size. In contrast to classical garbage-collection algorithms, the algorithm described in this thesis reclaims storage in real time. Program interruptions are limited to 1/100th of a second for memory utilizations beyond 99% in a 100 Megaword address space. The simple expedience of a free-page table extends this utilization limit to 100%. Unlike previous CAM-based schemes, the new algorithm operates in a virtual memory environment and requires much less total CAM. For databases searches, it is shown that, by avoiding indices, the higher cost of CAM is offset by decreased memory needs. The AFIT CAM is shown to be more flexible than previous CAMs in adapting to different database record widths. GRA

N87-24121# Oak Ridge National Lab., Tenn.
PROPOSAL FOR CONTINUED RESEARCH IN INTELLIGENT MACHINES AT THE CENTER FOR ENGINEERING SYSTEMS ADVANCED RESEARCH (CESAR) FOR FY 1988 TO FY 1991
C. R. Weisbin Mar. 1987 143 p
(Contract DE-AC05-84OR-21400)
(DE87-007789; ORNL/TM-10388; CESAR-87/09P) Avail: NTIS HC A07/MF A01

This document reviews research accomplishments achieved by the staff of the Center for Engineering Systems Advanced Research (CESAR) during the fiscal years 1984 through 1987. The manuscript also describes future CESAR objectives for the 1988-1991 planning horizon, and beyond. As much as possible, the basic research goals are derived from perceived Department of Energy (DOE) needs for increased safety, productivity, and competitiveness in the United States energy producing and consuming facilities. Research areas covered include the HERMIES-II Robot, autonomous robot navigation, hypercube computers, machine vision, and manipulators. DOE

N87-24122*# National Aeronautics and Space Administration. Langley Research Center, Hampton, Va.
STRONG CONVERGENCE AND CONVERGENCE RATES OF APPROXIMATING SOLUTIONS FOR ALGEBRAIC RICCATI EQUATIONS IN HILBERT SPACES Final Report
Kazufumi Ito (Brown Univ., Providence, R. I.) May 1987 21 p
Prepared for presentation at the 3rd International Conference on Control and Identification of Distributed Parameter Systems, Vorau, Austria, 6-12 Jul. 1986 Submitted for publication
(Contracts NAS1-17070; NAS1-18107; Grants NAG1-517; AF-AFOSR-0398-84; AF-AFOSR-0303-85)
(NASA-CR-178302; ICASE-87-31; NAS 1.26:178302) Avail: NTIS HC A02/MF A01 CSCL 09B

The linear quadratic optimal control problem on infinite time interval for linear time-invariant systems defined on Hilbert spaces is considered. The optimal control is given by a feedback form in terms of solution pi to the associated algebraic Riccati equation (ARE). A Ritz type approximation is used to obtain a sequence pi sup N of finite dimensional approximations of the solution to ARE. A sufficient condition that shows pi sup N converges strongly to pi is obtained. Under this condition, a formula is derived which can be used to obtain a rate of convergence of pi sup N to pi. The results of the Galerkin approximation is demonstrated and applied for parabolic systems and the averaging approximation for hereditary differential systems. Author

64 NUMERICAL ANALYSIS

Includes iteration, difference equations, and numerical approximation.

N87-24123# Stanford Univ., Calif. Center for Large Scale Scientific Computation.
FAR FIELD BOUNDARY CONDITIONS FOR TIME-DEPENDENT HYPERBOLIC SYSTEMS
Bertil Gustafsson Feb. 1987 21 p
(Contracts N00014-84-K-0267; N00014-82-K-0335)
(AD-A179361; CLASSIC-87-16) Avail: NTIS HC A02/MF A01 CSCL 12A

For problems defined on infinite domains, the most common computational methods use an artificial boundary gamma in order to make the computation finite. Since data are usually not available at this boundary, conditions must be used that somehow are related to the behavior of the solution outside the computational domain omega. This means that some apriori knowledge of the solution is necessary. In particular, if the system of differential equations has variable coefficients or is non-linear, then we shall make the coefficients constant outside omega. In this way there is a possibility to compute the solution exactly, or to compute it approximately in a simple way outside omega, such that boundary conditions can be derived on gamma. The one-dimensional case was analyzed thoroughly, and it was shown under what conditions it is possible to derive accurate conditions at the artificial boundary. A two-dimensional example was also treated, and a method leading to exact conditions for steady state solutions was presented. This paper treats hyperbolic systems in two space-dimensions with non-zero initial data also outside omega. GRA

N87-24124# New Mexico Univ., Albuquerque. Dept. of Mathematics and Statistics.
SYMBOL MANIPULATION AND APPLIED MATHEMATICS Interim Report
Stanly Steinberg Mar. 1986 5 p
(Grant AF-AFOSR-0092-85)
(AD-A179571; AFOSR-87-0405TR) Avail: NTIS HC A02/MF A01 CSCL 09B

The purpose of this project is to reveal the region of validity of perturbation methods in Hamiltonian mechanics. A canonical Lie series method was implemented to calculate perturbations of systems close to those encountered in celestial mechanics. The classical perturbation methods do not result in good approximations in the whole phase space, that is, both far from and close to the resonances. A perturbation theory with extended validity is now being sought. In the course of this study some problems encountered in algebraic manipulations in MACSYMA were corrected. This allowed a fast and efficient algorithm for canonical perturbation theory to be implemented. GRA

N87-24125# Vibration Inst., Clarendon Hills, Ill.
THE SHOCK AND VIBRATION DIGEST, VOLUME 19, NO. 6
Judith Nagle-Eshleman, ed. Jun. 1987 76 p
Avail: NTIS HC A05/MF A01

Abstracts from the current literature are presented in the following fields: machines; structures; vehicles; testing systems; mechanical components; structural components; electric components; materials; experimental techniques; environments; mathematical models; computational methods; modeling techniques; and design. Also included is the article On Integrating a Logarithmic or Semilogarithmic Piecewise Linear PSD Plot of a Random Variable X(T). For individual titles, see N87-24126 through N87-24126.

N87-24126# Wyle Labs., Inc., Huntsville, Ala.
ON INTEGRATING A LOGARITHMIC OR SEMILOGARITHMIC PIECEWISE LINEAR PSD PLOT OF A RANDOM VARIABLE X(T): PART 1
R. E. Doyle *In* VI The Shock and Vibration Digest, Volume 19, No. 6 Jun. 1987 p 3-10 (For primary document see N87-24125 17-64)
Avail: NTIS HC A05/MF A01

Formulas for integrating a piecewise linear power spectral density (PSD) plot to obtain the composite rms values are derived and tabulated. Case 1 shows a plot on logarithmic paper (both scales logarithmic). Cases 2 and 3 contain plots on semilogarithmic paper with the PSD scale logarithmic and the frequency scale uniform and semilogarithmic paper with the PSD scale uniform and the frequency scale logarithmic respectively. Numerical examples illustrate the three cases along with a comparative study of the results, which provide insight into PSD plots in general. Integration errors and the effect of different scales on the composite rms value are examined. The treatment is general, expository, and applicable to the design and analysis of structures and equipment subjected to random vibration environments. Author

N87-24127# Royal Inst. of Tech., Stockholm (Sweden). Dept. of Numerical Analysis and Computing Science.

APPROXIMATION ERRORS AND PERCEIVED SIMILARITY BETWEEN APPROXIMATED POLYGONS

Hans Marmolin 1987 17 p

(TRITA-NA-8505; INTEGRAL-35) Avail: NTIS HC A02/MF A01

Numerous techniques for fitting polygons to curves have been suggested in the literature. These methods are used in three different contexts: (1) keeping visually important features of contours displayed on a low resolution device; (2) image analysis; and (3) reducing the number of datapoints in map databases. The present study was designed to visually evaluate a polygon approximation method, suggested by Pavlides, and further developed by Eklundh and Howako. Specifically, the study addresses the problem of choosing the stepsize and the error thresholds (systematic deviations and variable deviations) by using perceived similarity between the original curve and the approximating polygon as a criteria of the goodness of approximation. M.G.

N87-24128# Argonne National Lab., Ill.

UNIQUENESS OF NON-NEGATIVE SOLUTIONS OF A CLASS OF SEMI-LINEAR ELLIPTIC EQUATIONS

H. G. Kaper and M. K. Kwong 1986 12 p Presented at the Microprogram on Nonlinear Diffusion Equations and their Equilibrium States, Berkeley, Calif., 25 Aug. 1986

(Contract W-31-109-eng-38)

(DE87-006966; CONF-8608164-1) Avail: NTIS HC A02

This article is concerned with boundary value problems (BVP) of the type u'' + g(r)u' + f(u) = 0, r is greater than 0; u'(0) = 0, lim(sub r) approaches infinity/u(r) = 0; where f(0) = 0. Such problems arise in the study of semi-linear elliptic differential equations in R(sup n). It is shown that (BVP) has at most one non-negative non-trival solution under appropriate conditions on f and g. The conditions are weaker than those given by Peletier and Serrin who considered the special case g(r) = (n-1)/r, n = 2,3,... DOE

N87-24129# Los Alamos National Lab., N. Mex.

INTEGRAL APPROXIMANTS FOR FUNCTIONS OF HIGHER MONODROMIC DIMENSION

G. A. Baker, Jr. 1987 30 p Presented at the Nonlinear Numerical Methods and Rational Approximation Conference, Antwerp, Belgium, 20 Apr. 1987

(Contract W-7405-eng-36)

(DE87-007508; LA-UR-87-1036; CONF-870492-1) Avail: NTIS HC A03/MF A01

In addition to the description of multiform, locally analytic functions as covering a many-sheeted version of the complex plane, Riemann also introduced the notion of considering them as describing a space whose monodromic dimension is the number of linearly independent coverings by the monogenic analytic function at each point of the complex plane. I suggest that this latter concept is natural for integral approximants (sub-class of Hermite-Pade approximants) and discuss results for both horizontal and diagonal sequences of approximants. Some theorems are now available in both cases and make clear that the natural domain of convergence of the horizontal sequences is a disk centered on the origin and that of the diagonal sequences is a suitably cut complex-plane together with its identically cut pendant Riemann sheets. Some numerical examples have also been computed. DOE

N87-24130# Sandia National Labs., Albuquerque, N. Mex.

NUMERICAL PREDICTION OF 1-D ABLATION USING A FINITE CONTROL VOLUME PROCEDURE WITH EXPONENTIAL DIFFERENCING

B. F. Blackwell Apr. 1987 32 p

(Contract DE-AC04-76DP-00789)

(DE87-007947; SAND-87-0206) Avail: NTIS HC A03/MF A01

The exponential differencing scheme of Spalding, which has been used for convection problems, is adapted to solve one-dimensional ablation problems by using a grid attached to the receding surface. Using the Finite Control Volume approach, element conduction, convection, and storage matrices are developed. The method is applied to a steady state ablation problem for which an analytical solution is known; comparisons are also made with upwind differencing for the convection terms and central differencing for the conduction terms. An example of a realistic ablation problem is presented. DOE

N87-24131# Ballistic Research Labs., Aberdeen Proving Ground, Md.

ASYMPTOTIC ANALYSIS OF THE ROOTS OF A CERTAIN TRANSCENDENTAL EQUATION Final Report

Raymond Sedney and Nathan Gerber Apr. 1986 34 p Supersedes IMR-843 (Mar. 1985)

(DA Proj. 1L1-61102-AF-43)

(AD-A168315; BRL-TR-2727) Avail: NTIS HC A03/MF A01 CSCL 12A

The spatial eigenvalues that occurred first in the Stewartson-Wedemeyer theory and then in later theories consist of a denumerable basic set which are 0(1) for Re yields infinity. In this report the existence of an additional single, isolated eigenvalue that is 0(Re sup 1/2) is demonstrated. The former were used in several reports on liquid-filled projectiles; the latter was detected in previous work. Asymptotic analysis for Re yields infinity is used to give accurate estimates for the new eigenvalue. Numerically it is shown that for 10 less than Re less than 1000 and 0.1 less than or equal to tau 1.0 the formulas from asymptotic analysis must be used rather than those in the original CDC program. The limiting case of nutational frequency approaching spin frequency is also discussed. The effect of the new eigenvalue on previous results, for Re greater than 1000, is negligible but for Re less than 1000 the effect is significant. Author

N87-24132*# National Aeronautics and Space Administration. Lewis Research Center, Cleveland, Ohio.

A GENERALIZED PROCEDURE FOR CONSTRUCTING AN UPWIND BASED TVD SCHEME

Meng-Sing Liou Jan. 1987 27 p Presented at the 25th Aerospace Sciences Meeting, Reno, Nev., 12-15 Jan. 1987; sponsored by AIAA

(NASA-TM-88926; E-3364; NAS 1.15:88926; AIAA-87-0355) Avail: NTIS HC A03/MF A01 CSCL 12A

A generalized formulation for constructing second- and higher-order accurate TVD (total variation diminishing) schemes is presented. A given scheme is made TVD by limiting antidiffusive flux differences with some linear functions, so-called limiters. The general idea of the formulation and its mathematical proof of Harten's TVD conditions is shown by applying the Lax-Wendroff method to scalar nonlinear equations and a constant-coefficient system of conservation laws. For the system of equations, several definitions are derived for the argument used in the limiter function and present their performance in numerical experiments. The formulation is extended to the nonlinear system. It is demonstrated that the present procedure can easily convert existing central or upwind, and second- or higher-order differencing schemes to preserve monotonicity and yield physically admissible solutions. The formulation is simple mathematically as well as numerically; both matrix-vector multiplication and Riemann solver are avoided. Although the notion of TVD is based on the initial value problem,

application to the steady Euler equations of the formulation is also made. Author

N87-24133# Allied Bendix Aerospace, Kansas City, Mo.
COMPUTER PROGRAMS FOR NONLINEAR LEAST SQUARES ANALYSIS OF VARIOUS THREE-DIMENSIONAL GEOMETRICAL ELEMENTS
S. R. Drake Apr. 1987 149 p
(Contract DE-AC04-76DP-00613)
(DE87-008046; BDX-613-3741) Avail: NTIS HC A07/MF A01

The nonlinear mathematics and the corresponding computer programs are presented for least squares fitting a line, plane, circular cylinder, circular cone, ring, and toroid all in three dimensions where the perpendicular residuals were minimized. The computer programs also include self-checking routines. DOE

N87-24134# Columbia Univ., New York.
SINGULARITY STRUCTURE OF NONLINEAR ORDINARY AND PARTIAL DIFFERENTIAL EQUATIONS Progress Report
1986 4 p
(Contract DE-FG02-84ER-13190)
(DE87-008242; DOE/ER-13190/3) Avail: NTIS HC A02/MF A01

Brief descriptions are given for results of the analyses of the Painleve property for the KdV and AKNS hierarchies. DOE

N87-24135# Sandia National Labs., Albuquerque, N. Mex.
CALCULATION OF EIGENVECTOR DERIVATIVES FOR STRUCTURES WITH REPEATED EIGENVALUES
W. C. Mills-Curran Mar. 1987 31 p
(DE87-008399; SAND-87-0050) Avail: NTIS HC A03/MF A01

In structural optimization and system identification, eigenvector derivatives provide important information for updating design/model parameters. When the current parameter values yield repeated eigenvalues, it has not been possible previously to calculate unique eigenvector derivatives. Recent work has provided a method for determining unique eigenvalue derivatives for this case, but methods for calculating the eigenvector sensitivities have been incomplete. In this work, a method is shown which allows efficient calculation of eigenvector derivatives. As an example, the repeated root eigenvector sensitivities are calculated for a simple three degree of freedom beam grillage. Comparisons of linear approximations (using these derivatives) to the calculated eigenvectors demonstrate the accuracy of the formulation. DOE

N87-24136# Air Force Inst. of Tech., Wright-Patterson AFB, Ohio. School of Engineering.
A PASCAL IMPLEMENTATION OF THE IMAGE ALGEBRA M.S. Thesis
Christopher J. Titus Dec. 1986 126 p
(AD-A177943; AFIT/GE/ENG/86D-59) Avail: NTIS HC A07/MF A01 CSCL 09B

This study produced an image processing algorithm development tool on a VAX computer system using the recent advances in an Image Algebra developed by G. Ritter et al at the University of Florida. The image algebra provides the basis for a hardware and software independent environment for the expression of practically all image processing algorithms. The goals of this project were twofold. The first goal was the implementation of the image algebra operators in a high level language to achieve hardware independence. The second goal was the design and implementation of a flexible preprocessor that could translate image processing algorithms, written in the image algebra language, into a high level computer language which could be compiled and executed on the VAX computer. The implementation was achieved in the PASCAL computer language. All of the basic image algebra operators and the preprocessor were successfully programmed on the VAX computer, but a complete software independence of the image algebra was not achieved. This version also produces very large blocks of executable code for relatively simple algorithms. Examples of the power and simplicity of the image algebra language and preprocessor environment are included. GRA

N87-24137# Naval Postgraduate School, Monterey, Calif.
THE DECOMPOSITION OF AN ARBITRARY THREE-DIMENSIONAL PLANAR POLYGON INTO A SET OF CONVEX POLYGONS M.S. Thesis
Jeffrey H. Potts Dec. 1986 77 p
(AD-A177947) Avail: NTIS HC A05/MF A01 CSCL 12A

This study presents a three step algorithm for the decomposition of arbitrary, three dimensional, planar polygons into convex polygons. Through a series of translations and rotations, an arbitrary polygon is mapped onto the x-y plane, then broken into a set of convex polygons, and finally mapped back to the polygon's original coordinate system for filling and display by special graphics hardware. GRA

N87-24138# Portland State Univ., Oreg. Dept. of Psychology.
ESTIMATION OF PARAMETERS IN LATENT CLASS MODELS WITH CONSTRAINTS ON THE PARAMETERS
James A. Paulson Jun. 1986 42 p
(Contract N00014-81-K-0564)
(AD-A178196; TR-86-1) Avail: NTIS HC A03/MF A01 CSCL 05J

This paper reviews the application of the EM Algorithm to marginal maximum likelihood estimation of parameters in the latent class model and extends the algorithm to the case where there are monotone homogeneity constraints on the item parameters. A likelihood ratio test of the hypothesis monotone homogeneity is proposed. The hypothesis is of interest because all standard item response theory models assume that it holds. GRA

N87-24139# Colorado State Univ., Fort Collins. Dept. of Mathematics.
AMG (ALGEBRAIC MULTIGRID): BASIC DEVELOPMENT, APPLICATIONS AND THEORY Final Report
Stephen F. McCormick 7 Jan. 1987 8 p
(Grant AF-AFOSR-0240-82)
(AD-A178222; AFOSR-87-0234TR) Avail: NTIS HC A02/MF A01 CSCL 12A

The central focus was the study of algebraic multigrid (AMG), which was in fact developed under this project. Conventional or geometric multigrid algorithms depend on knowledge of the underlying geometry for a given problem (e.g., a partial differential equation). This knowledge is used to predetermine coarser grids and the attendant operators and intergrid transfer. Although very efficient solvers can be developed in this way, the dissemination and use of geometric multigrid have been impeded by the need to tailor the algorithm to each application. A fairly general black box solver based on multigrid principles would be useful in overcoming these difficulties, thereby promoting multigrid applications. GRA

N87-24140# Pennsylvania State Univ., State College. Applied Research Lab.
A UNIFIED DIRECT-INVERSE PROCEDURE FOR TWO-DIMENSIONAL BOUNDARY LAYERS USING SPLINE/FINITE DIFFERENCE DISCRETIZATION M.S. Thesis
K. C. Kaufman and G. H. Hoffman Feb. 1987 167 p
(AD-A178223; TR-87-001) Avail: NTIS HC A08/MF A01 CSCL 12A

A unified approach is presented for solving the two dimensional incompressible boundary layer equations. Solutions are obtained for direct and inverse options using the same equation formulation by a simple interchange of boundary conditions. A modified form of the mechul function scheme obtains inverse solutions with specification of transformed wall shear, skin friction coefficient, or displacement thickness distributions. Turbulent flow is treated using a two piece algebraic eddy viscosity model, with the modified Levy Lees transformation applied to capture the growth of laminar and turbulent layers. Fourth order spline discretization approximates normal derivatives with three and two point backward differences approximating streamwise derivatives, yielding a fully implicit solution method. The resulting spline/finite difference equations are solved by Newton Raphson iteration together with partial

pivoting. Numerical solutions are presented for several nonsimilar flows and compared with published results. GRA

N87-24141# Maryland Univ., College Park. Inst. for Physical Science and Technology.
INFORMATION BASED NUMERICAL PRACTICE
I. Babuska Feb. 1987 27 p
(Contract N00014-85-K-0169)
(AD-A178362; BN-1059) Avail: NTIS HC A03/MF A01 CSCL 12A

The paper is a survey of some aspects of information based selection of numerical methods. Some theoretical ideas on how to deal with uncertain information are discussed and the example of a universal quadrature formula is introduced. Certain aspects of the selection of finite element method and adaptive mesh construction are discussed. Numerical examples illustrate the theoretical aspects. GRA

N87-24142# Maryland Univ., College Park. Inst. for Physical Science and Technology.
ESTIMATE FOR THE ERRORS IN EIGENVALUE AND EIGENVECTOR APPROXIMATION BY GALERKIN METHODS, WITH PARTICULAR ATTENTION TO THE CASE OF MULTIPLE EIGENVALUES Final Report
I. Babuska and J. E. Osborn Nov. 1986 58 p
(Contract N00014-85-K-0169; Grants NSF DMS-85-16191; NSF DMS-84-10324)
(AD-A178390; BN-1056) Avail: NTIS HC A04/MF A01 CSCL 12A

Refined estimates for the errors in eigenvalue and eigenvector approximation by finite element, or, more generally, Galerkin methods, as they apply to self-adjoint problems, are presented. Particular attention is given to the case of multiple eigenvalues. The results are new in this case. The proof is based on a novel approach which yields the known results for simple eigenvalues in a simple way. Numerical computations are presented and analyzed in light of the theoretical results. GRA

N87-24143# Pacific Northwest Labs., Richland, Wash.
STATUS OF PHENOMENOLOGICAL MODELING
L. A. Braby Dec. 1986 4 p Presented at the DOE/CEC Workshop on Mechanisms of Radiation Interaction With DNA, San Diego, Calif., 21 Jan. 1987
(Contract DE-AC06-76RL-01830)
(DE87-004922; PNL-SA-14591; CONF-870163-1) Avail: NTIS HC A02/MF A01

Mathematical models serve two primary functions, to provide the means for estimating the effects of exposures which fall outside the range which can be investigated directly, and to form a framework for organizing observations so that the patterns and eventually the underlying mechanisms can be determined. The response of cells to acute irradiation as a function of dose can be described rather easily. Many different mathematical expressions fit the observed data within the experimental uncertainties. However, the regions of dose and dose rate which are of concern in radiation protection are far below those generally used in experimental studies. The small errors remaining in even the best experiments translate into large uncertainties at the doses of interest. Thus purely phenomenological models (avoiding explanation or interpretation) cannot be totally successful in justifying the extrapolation. One is forced to look at general characteristics of mechanisms in order to justify the use of the models. If the model can be established independently then the shape of the dose response curve is known and extrapolations can be made with confidence even though some uncertainty remains about the values of coefficients. DOE

N87-24144# Lawrence Livermore National Lab., Calif.
ADAPTIVE MOVING GRID STRATEGIES FOR ONE-DIMENSIONAL SYSTEMS OF PARTIAL DIFFERENTIAL EQUATIONS
L. R. Petzold 23 Feb. 1987 9 p Presented at the 6th IMACS International Symposium on Computer Methods for Partial Differential Equations, Bethlehem, Pa., 23 Jun. 1987
(Contract W-7405-eng-48)
(DE87-006824; UCRL-96190; CONF-870677-1) Avail: NTIS HC A02

A scheme was proposed recently for choosing a moving mesh based on minimizing the time rate of change of the solution in the moving coordinates for one-dimensional systems of PDEs. It is shown how to apply this idea to systems where the time derivatives cannot be solved for explicitly, writing the moving mesh equations in an implicit form. We give a geometrical interpretation of the scheme which exposes some of its weaknesses, and suggest some modifications based on this interpretation which increases the efficiency of the scheme. We show how changing the error estimate for time step selection from the usual strategy can significantly reduce the computation time. We discuss how to apply this moving mesh method to elliptic-parabolic systems. Finally, we present some numerical experiments which illustrate how well the resulting method works. DOE

N87-24145*# National Aeronautics and Space Administration. Ames Research Center, Moffett Field, Calif.
UPWIND AND SYMMETRIC SHOCK-CAPTURING SCHEMES
H. C. Yee May 1987 130 p
(NASA-TM-89464; A-87236; NAS 1.15:89464) Avail: NTIS HC A07/MF A01 CSCL 12A

The development of numerical methods for hyperbolic conservation laws has been a rapidly growing area for the last ten years. Many of the fundamental concepts and state-of-the-art developments can only be found in meeting proceedings or internal reports. This review paper attempts to give an overview and a unified formulation of a class of shock-capturing methods. Special emphasis is on the construction of the basic nonlinear scalar second-order schemes and the methods of extending these nonlinear scalar schemes to nonlinear systems via the extact Riemann solver, approximate Riemann solvers, and flux-vector splitting approaches. Generalization of these methods to efficiently include real gases and large systems of nonequilibrium flows is discussed. The performance of some of these schemes is illustrated by numerical examples for one-, two- and three-dimensional gas dynamics problems. Author

N87-24146*# National Aeronautics and Space Administration. Ames Research Center, Moffett Field, Calif.
SMOOTHING AND THE SECOND LAW
Marshal L. Merriam Sep. 1986 23 p Presented at the 1st World Congress on Computational Mechanics, Austin, Tex., 22-25 Sep. 1986
(NASA-TM-88371; A-86424; NAS 1.15:88371) Avail: NTIS HC A02/MF A01 CSCL 12A

The technique of obtaining second order, oscillation free, total variation diminishing (TVD), scalar difference schemes by adding a limited diffusion flux (smoothing) to a second order centered scheme is explored. It is shown that such schemes do not always converge to the correct physical answer. The approach presented here is to construct schemes that numerically satisfy the second law of thermodynamics on a cell by cell basis. Such schemes can only converge to the correct physical solution and in some cases can be shown to be TVD. An explicit scheme with this property and second order spatial accuracy was found to have an extremely restrictive time step limitation (Delta t less than Delta x squared). Switching to an implicit scheme removed the time step limitation. Author

65 STATISTICS AND PROBABILITY

Includes data sampling and smoothing; Monte Carlo method; and stochastic processes.

N87-24147# Washington Univ., Seattle. Dept. of Statistics.
MIN-MAX BIAS ROBUST M-ESTIMATES OF SCALE Technical Report, 1 Dec. 1986 - 30 Nov. 1987
R. D. Martin and Ruben H. Zamar Dec. 1986 40 p

(Contract N00014-84-C-0169)
(AD-A179255; TR-72) Avail: NTIS HC A03/MF A01 CSCL 12A

Min-max bias robust M-estimates of scale are obtained for positive random variables which have epsilon-contaminated distributions. Any such estimate is a scaled order statistic, with the order statistic determined by epsilon. As epsilon approaches limit of 0.5 the min-max bias robust estimate becomes a scaled sample median, which thereby enjoys both high breakdown point of 0.5 and min-max bias robustness. Furthermore, for a wide range of epsilon, min-max estimate is quite close to the scaled median in terms of both structure and min-max bias behavior. Results are also obtained for random variables whose distribution is F = (epsilon)sub 0 + epsilon H with F sub o symmetric about an unknown location parameter. In particular we show that when F sub o is normal and less than or = epsilon less than or = .35, the min-max bias M-estimate of scale is a scaled order statistic applied to the absolute value of centered data, with the median as the centering estimate. This estimate is extremely close to a scaled median absolute deviation about the median, in terms of both structure and bias behavior. GRA

N87-24148# North Carolina Univ., Chapel Hill. Center for Stochastic Processes.
ON THE EXISTENCE AND CONVERGENCE OF PROBABILITY MEASURES ON CONTINUOUS SEMI-LATTICES
Tommy Norberg Aug. 1986 62 p
(Contract F49620-85-C-0144)
(AD-A179267; TR-148; AFOSR-87-0338TR) Avail: NTIS HC A04/MF A01 CSCL 12A

This paper studies probability measures on continuous lattices and, more generally, continuous semi-lattices. It characterizes probability measures by distribution functions, it characterizes weak convergence of probability measures by pointwise convergence of distribution functions and it provides a Levy-Khinchin representation of all infinitely divisible distributions. By applying the general results to special cases this paper extends some well-known results for random closed sets in locally compact second countable Hausdorff spaces to non-Hausdorff spaces. It also provides some new results for random compact sets and random compact convex sets in Euclidean spaces. GRA

N87-24149# Oklahoma State Univ., Stillwater.
CHANGING TIME SERIES Final Report
Lyle Broemeling 26 Aug. 1986 4 p
(Contract N00014-82-K-0292)
(AD-A178030) Avail: NTIS HC A02/MF A01 CSCL 12A

The statistical analysis of time series data is a challenging and fascinating topic. Much has appeared in the statistical and engineering literature concerning time series analysis, however very few people have attempted the Bayesian approach, but this approach by the principal investigator has been quite successful. Virtually nothing from the Bayesian paradigm had been used until the principal investigator began to investigate this area in the early 1980's. The motivation for using the Bayesian method was to eliminate some of the problems left unresolved by the Box-Jenkins approach. The objectives of the proposed research were quite ambitious because the Bayesian methods of analyzing non-changing time series (such as with the ARMA process) had not been tried, thus the first order of business was to try a Bayesian solution on ARMA processes. Later, processes the time changing parameters were analyzed, thus satisfying the objectives of the proposed research. GRA

N87-24150# Naval Postgraduate School, Monterey, Calif.
NONPARAMETRIC ESTIMATION OF THE PROBABILITY OF A LONG DELAY IN THE M/G/1 QUEUE
Donald P. Gaver and Patricia A. Jacobs Nov. 1986 32 p
(AD-A178259; NPS55-86-022) Avail: NTIS HC A03/MF A01 CSCL 12A

An M/G/1 queue is approached by stationary Poisson traffic with known arrival rate. Observations of service times are all that is known about the service distribution. Nonparametric estimates of the probability of a long customer delay are given. The estimates include the solution of an equation involving the empirical transform of the service times. Asymptotic properties of the estimates are derived. Simulation studies of the small sample behavior of the estimates are reported. The jackknife is used to provide error assessment of the estimates and to construct confidence intervals in the simulation studies of small sample behavior. GRA

N87-24151# Center for Naval Analyses, Alexandria, Va. Information Sciences Research Dept.
CONFIDENCE INTERVAL FOR PARAMETER n IN A BINOMIAL DISTRIBUTION
Victor K. Tang and Ronald B. Sindler Jan. 1987 20 p
(Contract N00014-87-C-0001)
(AD-A178325; CRM-86-265) Avail: NTIS HC A02/MF A01 CSCL 12A

Consider the binomial distribution b(n,p), where the parameter n represents the number of trials and the parameter p represents the probability of success. When n is fixed in advance after observing k successes, the usual problem is to estimate the probability of success p in the experiment. Situations may also arise when n becomes the unknown parameter of interest. If p is assumed to be known and k successes have been observed, the experimenter would be interested in estimating n instead. When some threats have been detected in a certain region, the total number of threats in that region becomes a major concern. An estimate of the unknown quantity would be an important consideration in the decision-making process. The next section presents the background and recent development of the problem of estimating n in a binomial distribution. The third section derives the procedure of estimating n in the form of a confidence interval. The last section consists of some concluding remark. A simulation procedure, an interactive computer program, and selected tables are included in the appendices. GRA

66 SYSTEMS ANALYSIS

Includes mathematical modeling; network analysis; and operations research.

N87-24152# California Univ., Berkeley. Dept. of Computer Sciences.
DECAYING CONFIDENCE FUNCTIONS FOR AGING KNOWLEDGE IN EXPERT SYSTEMS
Joseph Pasquale Jan. 1987 10 p
(Contract N00039-84-C-0089)
(AD-A179328) Avail: NTIS HC A02/MF A01 CSCL 09B

Expert systems which maintain knowledge objects whose attributes are time-variant must have an awareness of time. This awareness can be made manifest by incorporating time in the quantification of uncertainty of aging knowledge about such objects. Many expert systems use some method to quantify the degree of belief, or uncertainty, of their knowledge. Examples of these methods include Bayesian probability theory certainty factors of EMYCIN, the Dempster-Shafer theory, and fuzzy logic. These methods offer different representations for measures of confidence, and different calculi for combining these measures. We describe an extension to such confidence measures by adding a dimension of time. We propose the concept of Decaying Confidence Functions to express the time-varying uncertainty of aging knowledge. Decaying confidence functions specify how confidence in knowledge should decrease as the knowledge gets older. We describe how this can lead to efficiencies in expert systems which must deal with time-varying information, such as expert systems used for monitoring real-time systems. GRA

N87-24153# California Univ., Los Angeles. Management Science Inst.
AN INTRODUCTION TO STRUCTURED MODELING, REVISION
Arthur M. Geoffrion Feb. 1987 79 p
(Contract N00014-75-C-0570)

(AD-A179355; WP-338-Rev) Avail: NTIS HC A05/MF A01 CSCL 12B

The discipline of modeling has advanced only slowly compared to disciplines concerned with analyzing and solving models once they are brought into being. Structured Modeling is an attempt to redress this imbalance. Structured Modeling aims to provide a formal mathematical framework, and computer-based environment for conceiving, representing, and manipulating a wide variety of models. The framework uses a hierarchically organized, partitioned, and attributed acyclic graph to represent the semantic as well as mathematical structure of a model. The computer-based environment is evolving via experimental prototypes that provide for ad hoc query, immediate expression evaluation, solving simultaneous systems, and optimization. If successful, Structured Modeling will enable model-based work to be done with greater productivity and acceptance by non-specialists, will exploit important developments in small computers, and will cross-fertilize management science/operations research, artificial intelligence, database management, programming language design, and software engineering. This paper is an introduction and status report on a long term project. The presentation is based largely on examples; rigorous development and details are left to a series of technical reports. Author (GRA)

N87-24154# Lawrence Livermore National Lab., Calif.
SDI (STRATEGIC DEFENSE INITIATIVE) AND THE US DEFENSE POSTURE
M. M. May 1 Jul. 1986 20 p Presented at the Aspen Strategy Group Summer Workshop on Strategic Defense Initiative and American Security, Aspen, Colo., 10 Aug. 1986
(Contract W-7405-eng-48)
(DE87-008731; UCRL-94835; CONF-8608172-1) Avail: NTIS HC A02/MF A01

Issues surrounding the Strategic Defense Initiative are discussed. Comments are made on the research and development program and the effect of this program on the defensive posture of the United States. DOE

N87-24155# Los Alamos National Lab., N. Mex.
SATELLITE ALLOCATION FOR BOOST-PHASE MISSILE INTERCEPTS
G. H. Canavan and A. G. Petschek Apr. 1987 32 p
(Contract W-7405-eng-36)
(DE87-007719; LA-10926-MS) Avail: NTIS HC A03/MF A01

An essential component of the debate over strategic defense is the size of the defensive constellations needed to counter given threats. Although computer simulations can give accurate estimates, analytic calculations can led to greater insight and sensitivity. Limiting estimates have been published in which missiles are assumed to be launched from either an enormous area or a point; neither assumption corresponds to current threats. The combined solution derived here obtains the optimal solution for all areas. The resulting constellations are both smaller and less sensitive to parameters than those derived for the two published limits. DOE

N87-24156*# National Aeronautics and Space Administration. Ames Research Center, Moffett Field, Calif.
ON THE RELIABLE AND FLEXIBLE SOLUTION OF PRACTICAL SUBSET REGRESSION PROBLEMS
M. H. Verhaegen Mar. 1987 7 p
(NASA-TM-89442; A-87158; NAS 1.15:89442) Avail: NTIS HC A02/MF A01 CSCL 12B

A new algorithm for solving subset regression problems is described. The algorithm performs a QR decomposition with a new column-pivoting strategy, which permits subset selection directly from the originally defined regression parameters. This, in combination with a number of extensions of the new technique, makes the method a very flexible tool for analyzing subset regression problems in which the parameters have a physical meaning. Author

67 THEORETICAL MATHEMATICS

Includes topology and number theory.

No abstracts in this category.

70 PHYSICS (GENERAL)

For precision time and time interval (PTTI) see *35 Instrumentation and Photography;* for geophysics, astrophysics or solar physics see *46 Geophysics, 90 Astrophysics,* or *92 Solar Physics.*

N87-24157*# Rensselaer Polytechnic Inst., Troy, N.Y.
RADIATION TRANSPORT IN DUST IN DISK GEOMETRY Final Technical Report, 15 Apr. 1984 - 16 Oct. 1986
Ming Leung Chun Oct. 1986 9 p
(Grant NAGw-577)
(NASA-CR-180995; NAS 1.26:180995) Avail: NTIS HC A02/MF A01 CSCL 20C

The main objective of the research program is twofold: (1) to develop a computer code to solve the problem of scattering, absorption and emission of photons by dust grains in a dusty medium with 2 dimensional disk geometry, and (2) to study the various physical and geometrical effects of 2 dimensional radiation transport on the thermal structure and radiation field. These tasks were accomplished and are briefly summarized. The method for solving the radiation transport problem in disk geometry is a generalization of the quasi-diffusion method (QDM) previously developed by the author. Author

N87-24158# Military Academy, West Point, N. Y. Dept. of Electrical Engineering.
AN ALTERNATIVE LAPLACIAN ELECTROSTATIC FIELD FINITE ELEMENT FORMULATION
P. F. Barber and T. S. Lauber 1987 6 p Prepared in cooperation with Rensselaer Polytechnic Inst., Troy, N.Y.
(Contract DE-AS05-80RA-50159)
(DE87-007031; DOE/RA-50159/T2) Avail: NTIS HC A02/MF A01

An alternative finite element method for calculating three-dimensional electrostatic fields is described. The matrix equation is assembled using linear tetrahedral elements and an electrical network solution techniques known as impedance matrix building with axis discarding. The solutions of sample problems are described. DOE

71 ACOUSTICS

Includes sound generation, transmission and attenuation. For noise pollution see *45 Environmental Pollution.*

N87-24159# California Inst. of Tech., Pasadena.
MICROSCOPIC MODELING OF SOUND WAVES IN GRANULAR MATERIAL Quarterly Progress Report, 1 Jan. - 31 Mar. 1987
P. K. Haff 1987 4 p
(Contract DE-FG22-86PC-90959)
(DE87-007400; DOE/PC-90959/T1) Avail: NTIS HC A02/MF A01

As a preliminary to the study of sound waves themselves, we have looked at test cases of particles contained within vibrating boxes. The vibration amplitudes were larger than would occur in most sound-wave problems, but observed particle behavior could be compared against behavior seen in similar calculations performed with a completely independent particle-dynamics code [Haff and Werner, 1986]. These comparisons provide one line of argument supporting the notion that the present code is correctly computing the motion of particles in the presence of an external energy source. Some comparisons have also been made against

particle motion observed in the laboratory in a two-dimensional shaking box, with satisfactory agreement. A one-dimensional array of particles is being constructed which will be driven acoustically with a piezoelectric transducer. This will allow us to compare code predictions with one of the simplest possible particle configurations capable of transmitting acoustic waves. These and similar comparisons will also allow a calibration of the simulation model, and will help us determine allowable ranges of material constants which cannot otherwise easily be pinned down. We will begin some simple acoustic simulations in which a sample of approx. 100 particles is enclosed in a container at known pressure and a periodic elastic wave signal is fed into the system at one boundary and detected at another. This simple system will suffice for preliminary studies of the effects on wave speeds and attenuation of external variables such as pressure, and internal variables, such as grain properties, packing-geometry, and so forth. DOE

N87-24160*# National Aeronautics and Space Administration. Langley Research Center, Hampton, Va.
EXTENSION OF KIRCHHOFF'S FORMULA TO RADIATION FROM MOVING SURFACES
F. Farassat and M. K. Myers (Joint Inst. for Advancement of Flight Sciences, Hampton, Va.) May 1987 24 p Submitted for publication
(NASA-TM-89149; NAS 1.15:89149) Avail: NTIS HC A02/MF A01 CSCL 20A

Kirchhoff's formula for radiation from a closed surface has been used recently for prediction of the noise of high speed rotors and propellers. Because the closed surface on which the boundary data are prescribed in these cases is in motion, an extension of Kirchhoff's formula to this condition is required. In this paper such a formula, obtained originally by Morgans for the interior problem, is derived for regions exterior to surfaces moving at speeds below the wave propagation speed by making use of some results of generalized function theory. It is shown that the usual Kirchhoff formula is a special case of the main result of the paper. The general result applies to a deformable surface. However, the special form it assumes for a rigid surface in motion is also noted. In addition, Morgans' result is further extended by showing that edge line integrals appear in the formula when applied to a surface that is piecewise smooth. Some possible areas of application of the formula to problems of current interest in aeroacoustics are discussed. Author

N87-24161*# National Aeronautics and Space Administration. Langley Research Center, Hampton, Va.
ANNOYANCE RESPONSE TO SIMULATED ADVANCED TURBOPROP AIRCRAFT INTERIOR NOISE CONTAINING TONAL BEATS
Jack D. Leatherwood Jul. 1987 28 p
(NASA-TP-2689; L-16184; NAS 1.60:2689) Avail: NTIS HC A03/MF A01 CSCL 20A

A study is done to investigate the effects on subjective annoyance of simulated advanced turboprop (ATP) interior noise environments containing tonal beats. The simulated environments consisted of low-frequency tones superimposed on a turbulent-boundary-layer noise spectrum. The variables used in the study included propeller tone frequency (100 to 250 Hz), propeller tone levels (84 to 105 dB), and tonal beat frequency (0 to 1.0 Hz). Results indicated that propeller tones within the simulated ATP environment resulted in increased annoyance response that was fully predictable in terms of the increase in overall sound pressure level due to the tones. Implications for ATP aircraft include the following: (1) the interior noise environment with propeller tones is more annoying than an environment without tones if the tone is present at a level sufficient to increase the overall sound pressure level; (2) the increased annoyance due to the fundamental propeller tone frequency without harmonics is predictable from the overall sound pressure level; and (3) no additional noise penalty due to the perception of single discrete-frequency tones and/or beats was observed. Author

N87-24162*# National Academy of Sciences - National Research Council, Washington, D. C. Committee on Hearing, Bioacoustics, and Biomechanics.
GUIDELINES FOR NOISE AND VIBRATION LEVELS FOR THE SPACE STATION
Jun. 1987 39 p
(NASA Order L-76724-B)
(NASA-CR-178310; NAS 1.26:178310) Avail: NTIS HC A03/MF A01 CSCL 20A

Human habitability noise and vibration guidelines for the Space Station are presented. These were developed by a working group of experts established by the Committee on Hearing, Bioacoustics, and Biomechanics (CHABA) of the National Research Council's Commission on Behavioral and Social Science and Education. Noise exposure limits are suggested that will permit adequate speech communication, sleep, and hearing safety. Vibration exposure limits are suggested which will provide adequate comfort and permit adequate task performance. These are provided for guidance only for setting criteria. The exact criteria will depend on Space Station design and duty cycles. Author

N87-23797# San Diego State Univ., Calif.
TONES GENERATED DUE TO THE IMPINGEMENT OF TWO JETS ON EACH OTHER
Nagy Nosseir, Uri Peled, and Gregory Hildebrand *In* Johns Hopkins Univ., The 23rd JANNAF Combustion Meeting, Volume 1 Oct. 1986 p 459-467 (For primary document see N87-23757 17-28)
Avail: CPIA, Laurel, Md. 20707 HC $70.00

N87-23799# Georgia Inst. of Tech., Atlanta.
ACOUSTIC RESPONSE OF TURBULENT REACTING RECIRCULATORY FLOWS
J. A. Davis, N. L. Sankar, and W. C. Strahle *In* Johns Hopkins Univ., The 23rd JANNAF Combustion Meeting, Volume 1 Oct. 1986 p 485-497 (For primary document see N87-23757 17-28)
(Contract N00014-83-G-0047)
Avail: CPIA, Laurel, Md. 20707 HC $70.00

72 ATOMIC AND MOLECULAR PHYSICS

Includes atomic structure, electron properties, and molecular spectra.

N87-24163# Rome Univ. (Italy). Dipt. di Fisica.
STUDY OF MINIMUM BIAS TRIGGER EVENTS IN THE p(p-) COLLIDER FOR THE SQUARE ROOT OF s = 0.2 TO 0.9 TeV [STUDIO DEGLI EVENTI MINIMUM-BIAS TRIGGER AL COLLIDER SPP (-) S DEL CERN A S SQ ROOT = 0.2 AL 0.9 TeV]
Carla Zaccardelli 4 Dec. 1986 23 p In ITALIAN; In ITALIAN Presented at the 72nd Congress Nazionale della Societa Italiana di Fisica, Padua, Italy, 2-7 Oct. 1986
(Nota-Interna-874; ETN-87-99767) Avail: NTIS HC A02/MF A01

Results to complement the analysis of the effects found in high energy proton-proton collision studies are presented. The UA1 detector and magnetic and calorimetric analysis are used. The charged particle multiplicity distribution and the transversal impulse distribution are presented and related to the s sq root. The study of the jet and no-jet sets in which data was classified may explain phenomena observed in signal onset from jets. ESA

N87-24164# Toledo Univ., Ohio. Dept. of Physics and Astronomy.
SEMIEMPIRICAL STUDIES OF ATOMIC STRUCTURE Progress Report, 2 Apr. 1986 - 15 Feb. 1987
L. J. Curtis Mar. 1987 5 p
(Contract DE-AS05-80ER-10676)
(DE87-007320; DOE/ER-10676/9) Avail: NTIS HC A02/MF A01

Studies of the structure and properties of highly ionized many electron atoms are proceeding through a combination of experimental measurements, semiempirical modeling and systematizations, and ab initio theoretical calculations. Atomic systems which have both many electrons stripped away and many electrons remaining often occur as contaminants or controlled impurities in high temperature plasmas, but information on their spectroscopic properties remains fragmentary. Spectroscopic classifications require accuracies exceeding parts per million, which cannot be achieved by standard ab initio methods for these complex systems. Semiempirical systematizations of high precision data can provide these accuracies, and an increasing base of this data is becoming available through studies utilizing fast ion beam excitation, laser and Tokamak produced plasmas, astrophysical sources, and conventional spectroscopic sources. This program seeks to acquire, systematize, and parametrize large blocks of data along, e.g., isoelectronic, homologous, isoionic, isonuclear, Rydberg, and yrast series for the exposition of predictive empirical regularities. Trends revealed are then tested through well chosen experimental measurements, and ab initio methods are used to seek quantitative understanding of the empirical regularities. DOE

N87-24165# Los Alamos National Lab., N. Mex.
AXCEL: INTERACTIVE SIMULATION PROGRAM TO COMPUTE TWO-DIMENSIONAL POTENTIAL DISTRIBUTIONS OF ELECTROSTATIC ARRANGEMENTS AND OF ION PATHS IN ELECTROSTATIC FIELDS UNDER CONSIDERATION OF SPACE CHARGING
P. Spedtke 1987 66 p Prepared in cooperation with Gesellschaft fuer Schwerionenforschung m.b.H., Darmstadt, West Germany
(Contract W-7405-eng-36)
(DE87-007760; LA-tr-87-5) Avail: NTIS HC A04/MF A01

The AXCEL program optimizes transport paths for charged particles and extraction geometries for ion sources with planar or cylindrical symmetry. In the first iteration the Laplace equation is solved, and in later iterations the Poisson equation is solved. After each iteration the charge distribution is determined anew. If the solution of the Poisson equation converges to the solution of the time-constant Vlasov equation, then a self-consistent solution is obtained for the potential problem with space charging. DOE

N87-24166*# Maryland Univ., College Park. Dept. of Physics and Astronomy.
THE JOINT NASA/GODDARD-UNIVERSITY OF MARYLAND RESEARCH PROGRAM IN CHARGED PARTICLE AND HIGH ENERGY PHOTON DETECTOR TECHNOLOGY Semiannual Progress Report, Sep. 1986 - Mar. 1987
25 Jun. 1987 13 p
(Grant NgR21-002-316)
(NASA-CR-180996; NAS 1.26:180996) Avail: NTIS HC A02/MF A01 CSCL 20H

The first measurements of Fe charge states in two coronal hole-association high speed streams, using the sensor on ISEE-3, are presented. Eight event intervals from the January to June 1983 timeframe were chosen for the study of magnetotail dynamics and its relationship to substorm activity and the possible formation of plasmoids. Techniques are being explored for measurement of secondary electrons which are characteristically emitted when ions hit a target material. Efforts are continuing to understand kilometer wavelength shock associated radio events. An all-sky survey of fast X-ray transients of duration of 5 to 10,000 s was completed. Research using high resolution gamma-ray spectroscopy of celestial sources in the 20 keV to 20 MeV range to search for and study narrow lines in low-energy gamma-ray spectrum continues. Research in high energy radiation from pulsars is being conducted. B.G.

N87-24167# Illinois Inst. of Tech., Chicago.
THEORETICAL STUDIES IN ELEMENTARY PARTICLE PHYSICS Progress Report, Jun. 1986 - Feb. 1987
J. C. Collins 1987 10 p
(Contract DE-FG02-85ER-40235)
(DE87-005895; DOE/ER-40235/T2) Avail: NTIS HC A02/MF A01

Theoretical research on elementary particles is reported, with progress discussed in these areas: heavy quark production, the cosmic rays observed from Cygnus X-3, hadron-hadron collisions at small values of x, Monte Carlo event generators for hadron-hadron collisions, review of perturbative QCD theorems, direct computation of helicity amplitudes for tree diagrams, and application of the factorization of helicity amplitudes to the effective W approximation. DOE

N87-24168# Virginia Univ., Charlottesville. Dept. of Physics.
SYMMETRY PROBLEMS IN PARTICLE PHYSICS Progress Report, 1 Jun. 1986 - 31 May 1987
P. K. Kabir and P. M. Fishbane Mar. 1987 6 p
(Contract DE-FG05-84ER-40157)
(DE87-006369; DOE/ER-40157/T1) Avail: NTIS HC A02/MF A01

Particle physics symmetry problems progress is reported in these areas: review of symmetry limits in neutral kaon decays, effects of interposing matter on the departure from reciprocity, radiative processes accompanying tau lepton decays, analysis of angular correlations in sequential radiative transitions between and from heavy quark-antiquark bound states, consequences of heavy isosinglet fermions, dynamics of confinement, and quark degrees of freedom in threshold annihilation of nucleons. DOE

N87-24169# Kansas Univ., Lawrence.
RESEARCH IN THEORETICAL PARTICLE PHYSICS Progress Report, 1 May 1986 - 30 Apr. 1987
D. W. McKay, H. J. Munczek, and J. P. Ralston Mar. 1987 15 p
(Contract DE-FG02-85ER-40214)
(DE87-008240; DOE/ER-40214/2) Avail: NTIS HC A02/MF A01

Research is reported on seven different topics. The topics include dynamical symmetry breaking and confinement, dynamical symmetry breaking and technicolor, small x-behavior of structure functions and applications in astrophysics and collider physics, chiral soliton physics, new approximation methods in quantum mechanics and field theory, dynamical polarization effects in QCD, and improved development of the effective-W approximation with new applications to collider physics. The infrared singular part of the gluon propagator produces confined behavior in the quark propagator. New techniboson production and decay rates were calculated which would be detectable at supercollider energies. Simple, analytic expressions were developed for gluon and quark structure functions at small x and large Q(2) , and it was shown that nu N-scattering is greatly enhanced at astrophysical energies, that b-quark production estimates are unreliable because input values at small x, small Q(2) are unknown, and showed how different input at small x, small Q(2) feeds through to large Q(2) regions. Detailed soliton wavefunctions were developed in a field theory context, and applied to show evaluation of matrix elements of hadronic currents. The effect of energy dependence of phases in elastic p-p collisions affected Farrar's program is shown. DOE

73 NUCLEAR AND HIGH-ENERGY PHYSICS

Includes elementary and nuclear particles; and reactor theory.

For space radiation see *93 Space Radiation.*

N87-24170# Los Alamos National Lab., N. Mex.
THE PHYSICS AND A PLAN FOR A 45 GeV FACILITY THAT EXTENDS THE HIGH-INTENSITY CAPABILITY IN NUCLEAR AND PARTICLE PHYSICS
May 1986 284 p Original document contains color illustrations
(Contract W7405-eng-36)
(LA-10720-MS) Avail: NTIS HC A13/MF A01

A proposed program of physics research to be carried out at a 45 GeV high-intensity proton accelerator is discussed. In addition to a general discussion of the potentially most productive research directions, specific experiments in flavor and strong physics are presented. The proposed strong interaction studies deal with the investigation of nonperturbative quantum chromodynamics (QCD) through the study of exotic hadrons and measurement of nuclear medium effects on flavor-specific quark momentum distributions. The major part of the proposed program in flavor interaction physics probes possible physics beyond the minimal standard model. A design using two synchrotrons produces a 45 GeV proton beam by increasing the energy of the present LAMPF 800 MeV beam. A booster operating at 60 Hz accelerates 144 mu-A from 800 MeV to 6 GeV while the main ring operating at 3.33 Hz accelerates 32 mu-A from 6 GeV to 45 GeV. The 112 mu-A at 6 GeV which is not further accelerated is used to create intense beams of neutrinos and pulsed muons. The 32 mu-A of 45 GeV beam is slow extracted into an existing experimental area in which a large number of high-intensity, high-purity kaon and other secondary beams will be produced. A proposed layout of the experimental areas along with the characteristics of the secondary beams is also presented. Finally, a cost estimate for the construction of such a facility at Los Alamos is provided. Author

N87-24171# Sandia National Labs., Albuquerque, N. Mex.
DEVELOPMENT OF ULTRASONIC THERMOMETRY FOR HIGH-TEMPERATURE HIGH-RESOLUTION TEMPERATURE PROFILING APPLICATIONS IN LMFBR SAFETY RESEARCH
M. E. Field May 1986 74 p Sponsored in part by US Nuclear Regulatory Commission, Washington, D.C.; EURATOM JRC; and Japanese PNC
(Contract DE-AC04-76DP-00789)
(SAND-84-1341) Avail: NTIS HC A04/MF A01

Ultrasonic thermometry was developed as a high temperature profiling diagnostic for use in the Liquid Metal Fast Breeder Reactor (LMFBR) Debris Coolability Program at Sandia National Laboratories. These instruments were used successfully in the DC series experiments and the D10 experiment. Temperatures approaching 3000 C with spatial resolution of 10 mm and indicated temperature gradients of 700 C/cm were measured. Instruments were operated in molten sodium, molten steel, and molten UO2 environments. Up to 14 measurement zones on a single instrument in molten sodium were used with 12 mm and 15 mm spatial resolution. Hermetically sealed units operating at elevated temperatures were used. Post-test examination revealed very little systematic calibration drifts (less than 10 C) with random drifts occuring with less than 40 C standard deviation in a 10 to 12 mm measured zone. The stability of the system varies from +/- 1 C to +/- 15 C depending on the sensor design constraints for a particular application. Doped tungsten sensors were developed to permit operation of total measurement zone length of 30 cm at temperatures above 2500 C. M.G.

N87-24172# Maryland Univ., College Park. Lab. for Plasma and Fusion Energy Studies.
HIGH-CURRENT BEAM DYNAMICS AND TRANSPORT, THEORY AND EXPERIMENT
M. Reiser 1986 5 p Presented at the Linear Accelerator Conference, Stanford, Calif., 2 Jun. 1986
(Contract DE-AC05-85ER-40216)
(DE87-006154; CONF-860629-69) Avail: NTIS MF A01

Recent progress in the understanding of beam physics and technology factors determining the current and brightness of ion and electron beams in linear accelerators are reviewed. Topics to be discussed include phase-space density constraints of particle sources, low-energy beam transport including charge neutralization, emittance growth due to mismatch, energy exchange, instabilities, nonlinear effects, and longitudinal bunching. DOE

74 OPTICS

Includes light phenomena; and optical devices.
For lasers see *36 Lasers and Masers.*

N87-24173# Air Force Inst. of Tech., Wright-Patterson AFB, Ohio. School of Engineering.
HOLOGRAPHIC CORRECTION OF ABERRATIONS IN OPTICAL SYSTEMS EMPLOYING SYNTHETIC APERTURES M.S. Thesis
Charles W. Gill Mar. 1987 85 p
(AD-A179107; AFIT/GNE/ENP/87M-3) Avail: NTIS HC A05/MF A01 CSCL 14E

The effectiveness of using holograms to correct aberrated wavefronts exiting a misaligned synthetic aperture is investigated. Negative transparency, photographic plate holograms were used as corrector plates for eliminating aberrations in a three lens synthetic aperture system built from commercially available components. In addition, holograms created within a lithium niobate crystal in near real time (less than 1 1/2 hours) were used to correct aberrations in a misaligned single lens system. The effectiveness of each aberration correction was qualitatively evaluated by comparing the impulse response of an unaberrated, aligned system to the impulse response of the corrected, misaligned system. These evaluations were made by comparing photographs of the corrected impulse response to computer generated plots of the unaberrated response predicted by Fourier optics. The holographic corrections made to the synthetic aperture were found to transform an aberrated impulse response into one that did resemble the computer prediction. However, the diffraction efficiency of the correction hologram was very low, and the impulse response obtained from it was very dim. GRA

N87-24174# Electronics Research Lab., Adelaide (Australia).
FABRY-PEROT TYPE OPTICAL INTERFERENCE FILTERS
M. A. Folkard and J. Ward Aug. 1986 92 p
(AD-A179394; ERL-0300-TR) Avail: NTIS HC A05/MF A01 CSCL 20F

The formulae and theory describing the optical properties of a classical Fabry Perot interferometer are stated in terms of the reflection, transmission, absorption and phase angle. The appropriate boundary conditions and experimental limitations are defined. The theory is extended to the production of vacuum deposited, all dielectric, multilayer thin film systems for use as Fabry Perot type, narrow spectral band filters. GRA

N87-24175# Brown Univ., Providence, R. I. Div. of Engineering.
NOVEL FIBER PREFORMS: RARE EARTH DOPING Final Report, 31 Aug. 1985 - 31 Oct. 1986
T. F. Morse 31 Mar. 1987 31 p
(Grant AF-AFOSR-0304-85)
(AD-A179454; AFOSR-87-0556TR) Avail: NTIS HC A03/MF A01 CSCL 20F

Optical fibers doped with rare earth elements have potential application as passive fiber devices through their ability to rotate the plane of polarization in the presence of a magnetic field. Such devices have use not only as sensors of electric and magnetic fields but also as fiber lasers for a host of applications. The Laboratory for Lightwave Technology, in conjunction with the Dept. of Chemistry, has engaged in a program of the study of rare earth elements in fibers, and in bulk glasses as well. Some of the first rare earth glasses made with the sol-gel technique come from this research. GRA

N87-24176# Air Force Inst. of Tech., Wright-Patterson AFB, Ohio. School of Engineering.
COHERENT MULTIPLE APERTURE OPTICAL IMAGING SYSTEMS: ANALYSIS AND DESIGN M.S. Thesis
Dana J. Bergey Mar. 1987 110 p
(AD-A179476; AFIT/GE/ENG/87M-1) Avail: NTIS HC A06/MF A01 CSCL 20F

The imaging of simple objects through coherent multiple aperture optical imaging systems was investigated. Multiple aperture telescopes are a candidate technology for the Strategic Defense Initiative missions of surveillance, tracking, and kill

assessment. Multiaperture images of edges, slits, rectangles, and circles are theoretically predicted and experimentally produced. Photographs of the actual images produced in the lab were compared to the theoretical images, and the analytical and computer prediction techniques were found to be accurate. The results were analyzed to determine how different multiaperture geometries affected the images. It was found that multiaperture imaging produces edge enhancement. The position of a single edge could be found exactly, while multiple edges sometimes produced slight edge shifts. A computer program was developed predicting edge shifts that will be observed when imaging through a given multiple aperture. Larger subaperture spacings were found to exhibit better resolution but produced more ringing about the edges. The possibility of rotating the multiple aperture system to gather more infomation was discussed, as well as designs including a central subaperture. GRA

N87-24177# Arizona Univ., Tucson. Optical Sciences Center.
SIGNAL PROCESSING WITH DEGENERATE 4-WAVE MIXING Annual Report, Sep. 1985 - Oct. 1986
G. I. Stegeman 17 Mar. 1987 16 p
(Grant AF-AFOSR-0277-84)
(AD-A179679; AFOSR-87-0548TR) Avail: NTIS HC A02/MF A01 CSCL 20F

The effort of the past year has been a continuation of research into the semiconductor-doped glass material system. Bulk DFWM and photoluminescence experiments on these materials determined that they have a large nonlinear index of refraction (n(2) approx 10 to the minus 14th power sq m) with fast response times (r less than 16 psec) required for high speed optical signal processing. Along with collaborators in the University of Galsgow we successfully developed a successful ion-exchange (Na+:K+) technique for producing low-loss optical waveguides in these materials, the details of which follow. GRA

N87-24178# Air Force Inst. of Tech., Wright-Patterson AFB, Ohio. School of Engineering.
TARGET SEGMENTATION AND IMAGE ENHANCEMENT THROUGH MULTISENSOR DATA FUSION M.S. Thesis
Carl W. Tong Dec. 1986 402 p
(AD-A178875; AFIT/GE/ENG/86D-55) Avail: NTIS HC A18/MF A01 CSCL 17E

This thesis effort develops a data fusion process for laser radar and forward looking infrared sensors. The process contains an algorithm which segments man-made objects away from a variety of backgrounds. Importantly, the segmentation algorithm does not use pre-stored templates. Other algorithms within the process also enhance and extract target features from both laser radar and infrared images. The overall process provides target details which were not easily found in either one of the sensors by themselves. Furthermore, key algorithms within the overall process have possible optical implementations. Author (GRA)

N87-24179# Brookhaven National Lab., Upton, N. Y.
REPORT OF THE SECOND WORKSHOP ON SYNCHROTRON RADIATION SOURCES FOR X-RAY LITHOGRAPHY
M. Q. Barton, ed., B. Craft, ed., and G. P. Williams, ed. 1986 52 p Workshop held at Upton, N.Y., 25 Aug. 1986
(Contract DE-AC02-76CH-00016)
(DE87-002155; BNL-38789; CONF-8608102-Summ) Avail: NTIS HC A04/MF A01

The reported workshop is part of an effort to implement a US-based X-ray lithography program. Presentations include designs for three storage rings (one superconducting and two conventional) and an overview of a complete lithography program. The background of the effort, the need for synchrotron radiation, and the international competition in the area are discussed briefly. The technical feasibility of X-ray lithography is discussed, and synchrotron performance specifications and construction options are given, as well as a near-term plan. It is recommended that a prototype synchrotron source be built as soon as possible, and that a research and development plan on critical technologies which could improve cost effectiveness of the synchrotron source be established. It is further recommended that a small number of second generation prototype synchrotrons be distributed to IC manufacturing centers to expedite commercialization. DOE

N87-24180# Oak Ridge National Lab., Tenn.
THE FIBER OPTIC REFRIGERATION CYCLE MONITOR
L. N. Klatt, D. T. Bostick, and H. Perez-Blanco 1987 6 p Presented at the Technical Symposium Southeast on Optics, Electro-Optics and Sensors, Orlando, Fla., 17 May 1987
(Contract DE-AC05-84OR-21400)
(DE87-006632; CONF-870584-1) Avail: NTIS HC A02

The measurement of absorbent concentration is a key control parameter in operating and assessing the performance of absorption heat pump systems. Because most refrigerant absorbent fluids are binary mixtures, the measurement of refractive index has been used routinely to directly determine the concentration of absorbent fluid components. Until recently, this measurement has been limited to the analysis of samples withdrawn from the absorption machine after system shut-down. The Fiber Optic Refrigeration Cycle Monitor (FORCM) is capable of making multiple and in-situ, real-time measurements of refractive index at user-definable points within operating absorption machines. The refractive index of the solution is determined by measuring light loss from an unclad segment of an optical fiber that is immersed in the absorption fluid. Changes in fluid refractive index alter the angle at which the light rays are totally internally reflected at the core-fluid interface, thereby altering the light transmission efficiency of the fiber. The unclad portion of the fiber is placed at a point within the absorption vessel for which the fluid composition measurement is desired. Any number of modified optical fibers can be installed within a system. A thermocouple junction adjacent to each fiber measures the local fluid temperature. The combination of local concentration and temperature measurements allows in-line monitoring and control of the system, as well as provides a detailed study of heat and mass transfer processes occurring within these machines. The operating characteristics of the FORCM are described in this paper. DOE

N87-24181# Sandia National Labs., Livermore, Calif.
A FIBER OPTIC LINK FOR AN INFRARED IMAGING CAMERA SYSTEM
M. T. Stewart Mar. 1987 39 p
(Contract DE-AC04-76DR-00789)
(DE87-008346; SAND-87-8205) Avail: NTIS HC A03/MF A01

Discussed are the design, implementation and testing of a fiber optic link for an infrared imaging camera system. Specifically, the link consisted of a data link and a control link. The data link transmitted pixel and sensor data from a movable camera structure to a main processor. The control link transmitted control information from the processor to the camera. Special design requirements included low power, low volume, and low noise electronics, as well as a 8.0 Mbs data rate. DOE

N87-24182# University of Southern California, Los Angeles. Signal and Image Processing Inst.
NONLINEAR REAL-TIME OPTICAL SIGNAL PROCESSING Annual Technical Report, 1 Jul. 1985 - 30 Jun. 1986
A. A. Sawchuk and B. K. Jenkins 18 Sep. 1986 33 p
(Grant AF-AFOSR-0181-84)
(AD-A178169; AFOSR-87-0082TR) Avail: NTIS HC A03/MF A01 CSCL 20F

During the period 1 July 1985 to 30 June 1986, the research under Grant AFOSR-84-0181 has concentrated on various aspects of optical digital computing. We have continued detailed studies of a sequential optical parallel computing architecture whose wiring is implemented by computer-generated holograms. We have studied the implementation of various specialized processors such as cellular logic processors on this architecture and have examined high space-bandwidth interconnection holograms that serve this purpose. The implementation of some architectures such as cellular hypercubes and pyramids are not feasible for electronic VLSI, but are more easily suited to the page-oriented architecture of a 2-D digital optical array. We have also examined mathematical

morphology as a basic image algebra for cellular logic image processing, and found that three fundamental image operations: complement; union (or intersection); dilation (or erosion) are sufficient to implement any binary morphological function. A final area of study has been the investigation of abstract parallel computing models in the context of the physical constraints and technology of optical computing. These models include shared memory and graph/network models. Author (GRA)

N87-24183# Lawrence Livermore National Lab., Calif.
PARAMETRIC FREQUENCY UPCONVERSION, OPTICAL FIBER TRANSMISSION AND STREAK CAMERA RECORDING
M. E. Lowry and M. D. Rotter 30 Jan. 1987 8 p Presented at the Society of Photo-Optical Instrumentation Advanced Institute on Broadband Photonic Sensors, Howey-in-the-Hills, Fla., 7 Apr. 1986
(Contract W-7405-eng-48)
(DE87-005841; UCRL-95999; CONF-8604292-2) Avail: NTIS HC A02/MF A01

The use of optical fiber for the transmission of information over relatively long distances is being recognized as the only viable solution to many data transmission problems, particularly those requiring high information density and faithful temporal content. This necessary reliance upon the optical carrier has meant that the image-tube based optical streak camera is often the instrument of choice for recording single-shot multi-parameter events with high temporal resolution. However, current photocathode technology is incompatible with the trend of the optical fiber industry toward the use of the 1300 to 1600 nm wavelength regime. To retain the advantages of optical streak-camera recording and optical fiber transmission, a way must be found to upconvert the optical carrier to higher energy. This report describes the use of an intense laser pump beam coincident with the IR signal into a non-linear crystal (LiIO3) to increase the signal's frequency. A beam splitter is used to separate the signal from the pump beam at the detector. The physical theory underlying this process is described. DOE

N87-24184*# Electro-Optics Consultants, Inc., Huntsville, Ala.
CORNEA OPTICAL TOPOGRAPHICAL SCAN SYSTEM (COTSS) Final Report
11 Aug. 1986 39 p
(Contract NAS8-34659)
(NASA-CR-179012; NAS 1.179012) Avail: NTIS HC A03/MF A01 CSCL 20F

The Cornea Optical Topographical Scan System (COTSS) is an instrument designed for use by opthalmologist to aid in performing surgical procedures such as radial keratotomy and to provide quick accurate data to aid in prescribing contact lenses and eyeglasses. A breadboard of the system was built and demonstrated in June of 1984. Additional refinements to the breadboard are needed to meet systems requirements prior to proceeding with prototype development. The present status of the COTSS instrument is given and the areas in which system refinements are required, are defined. Author

75 PLASMA PHYSICS

Includes magnetohydrodynamics and plasma fusion.

For ionospheric plasmas see *46 Geophysics*. For space plasmas see *90 Astrophysics*.

N87-24185# Royal Inst. of Tech., Stockholm (Sweden). Dept. of Plasma Physics.
EXTENDED POTENTIAL DROPS PRECEDING DOUBLE LAYER FORMATION IN A TRIPLE PLASMA DEVICE
Martin Bohm and Staffan Torven Dec. 1986 9 p Sponsored by the Swedish Natural Sciences Research Council
(TRITA-EPP-86-11; ISSN-0348-7539: ETN-87-99785) Avail: NTIS HC A02/MF A01

Experiments showing that the formation of a double layer may be preceded by an extended potential drop (EPD), much thicker than the double layer are reported. When a step voltage is applied between the 2 sources of a triple plasma device, the potential in the EPD varies quasi-linearly between the sources for time intervals up to 50 ion plasma periods. For larger times the initially prevailing ion density distribution becomes significantly modified and the EPD then steepens to a double layer. Measurements with high frequency probes show a broad spectrum of electric field fluctuations. When the EPD exists, the power level is between one and two orders of magnitude larger than the level at the end of the time interval when a double layer has formed. These fluctuations are invoked to explain how quasi-neutrality is maintained in the EPD. ESA

N87-24186# Air Force Inst. of Tech., Wright-Patterson AFB, Ohio. School of Engineering.
RADIAL DENSITY DISTRIBUTION OF NEGATIVE ATOMIC OXYGEN IN THE OXYGEN POSITIVE COLUMN: AN EXPERIMENT M.S. Thesis
J. Mark DelGrande Dec. 1986 83 p
(AD-A179212; AFIT/GEP/ENP/86D-3) Avail: NTIS HC A05/MF A01 CSCL 20I

This thesis develops the foundation for an experiment to determine the radial distribution of the negative atomic oxygen ion in the positive column of a plasma discharge. Lee's theory is modified to apply to a discharge of square cross-section. A new design for a discharge tube is presented. The operating characteristics of this tube are investigated: current-voltage measurements are made showing operating regimes of the T-form and H-form of the discharge, and acoustic waves are shown to exist in the T-form region. Three experimental designs are presented to determine the radial density of the oxygen anion, each involving photodetachment. GRA

N87-24187# Maryland Univ., College Park. Lab. for Plasma and Fusion Energy Studies.
FORMATION AND STABILITY OF PARTIALLY-NEUTRALIZED PLASMA CLUMPS Annual Technical Report, 1 Jan. - 15 Dec. 1986
John Guillory 1 Jan. 1987 73 p
(Grant AF-AFOSR-0055-86)
(AD-A179444; AFOSR-87-0477TR) Avail: NTIS HC A04/MF A01 CSCL 20I

A University of Maryland group has made an experimental investigation of neutralized electron beam propagation in nonconducting vacuum drift tubes (to eliminate image currents and a clear return path for the electrons) and investigated a significant new way of increasing the ion velocity (and therefore the propagation distance) in such systems. This program constructed a microscopic equilibrium for such a propagating electron/ion beam in which both species are in radial force balance, and numerical simulation studies of beam and ion propagation in such a system. GRA

N87-24188# Oak Ridge Associated Universities, Inc., Tenn.
FUSION ENERGY POSTDOCTORAL RESEARCH PROGRAM AND PROFESSIONAL DEVELOPMENT PROGRAM Annual Report, FY 1986
Jan. 1987 23 p
(Contract DE-AC05-76OR-00033)
(DE87-006350; DOE/OR-00033/T285) Avail: NTIS MF A01

During FY 1986, Oak Ridge Associated Universities (ORAU) initiated two new programs for the US Department of Energy (DOE), and Office of Fusion Energy (OFE). The Fusion Energy Postdoctoral Research Program and the Fusion Energy Professional Development Program provide opportunities to conduct collaborative research in magnetic fusion energy research and development programs at DOE laboratories and contractor sites. Participants become trained in advanced fusion energy research, interact with outstanding professionals, and become familiar with energy-related national issues while making personal contributions to the search for solutions. Both programs enhance the national fusion energy research and development effort by providing channels for the exchange of scientists and engineers, the diffusion of ideas and knowledge, and the transfer of relevant technologies.

These programs complement the Magnetic Fusion Energy Science and Technology Fellowship Programs already administered by ORAU for DOE/OFE. DOE

N87-24189# North Carolina Univ., Chapel Hill. Dept. of Chemistry.
HEATS OF FORMATION, STRUCTURE AND HETEROATOM ((17)O, (33)S) NMR STUDIES OF ORGANOSULFUR MOLECULES, RADICALS AND IONS Progress Report
Tomas Baer and Slayton Evans 1986 18 p
(Contract DE-AS05-80ER-10641)
(DE87-006361; DOE/ER-10641/5) Avail: NTIS MF A01

Such organosulfur compounds as sulfoxides, thiolsufonates, thiolsulfinates and sulfones will be prepared and investigated by photoionization and photoelectron photoion coincidence (PEPICO) in order to determine the gas phase structures and ground state energies of these molecules and the fragments and ions derived from them. The experimental results will be supplemented by ab initio molecular orbital calculations. A new threshold electron energy analyzer will also be constructed and tested. The application of O-17 and S-33 NMR spectroscopy to problems in organosulfur chemistry is described with major emphasis on the evaluation and identification of organosulfur constituents of coal and petroleum based materials. An important focus of the research is to determine in a semiquantitative manner the effects of substituents on O-17 and S-33 NMR shifts. Continued development of lanthanide shift reagents in O-17 NMR spectroscopy as an analytical tool for determination of oxidized organosulfur components in solution coal samples is also proposed. During this granting period, we will integrate our solution C-13 NMR results with those obtained in the solid-state using cross polarization (CP)-magic angle spinning (MAS) techniques. We will also make attempts to observe organosulfur components directly in the solid state using CP-MAS techniques. DOE

N87-24190# California Univ., Berkeley. Electronics Research Lab.
COMPUTER SIMULATION OF BOUNDED PLASMA SYSTEMS
W. S. Lawson Mar. 1987 39 p
(Contract DE-AS03-76ET-53064)
(DE87-008193; UCB/ERL-M-87/14) Avail: NTIS HC A03/MF A01

The physical and numerical problems of kinetic simulation of a bounded electrostatic plasma system in one planar dimension are examined, and solutions to them are presented. These problems include particle absorption, reflection and emission at boundaries, the solution of Poisson's equation under non-periodic boundary conditions, and the treatment of an external circuit connecting the boundaries. Some comments are also made regarding the problems of higher dimensions. The methods which are described here are implemented in a code named PDW1. DOE

N87-24191# California Univ., Berkeley. Electronics Research Lab.
LINEAR MAGNETIZED PLASMA RESPONSE TO AN OBLIQUE ELECTROSTATIC WAVE
W. S. Lawson 15 Dec. 1986 25 p
(Contract DE-AS03-76ET-53064)
(DE87-008194; UCB/ERL-M-86/94) Avail: NTIS HC A02/MF A01

The linear response of a spatially periodic magnetized Vlasov plasma distribution function is computed to second order in the electric field. The results for a specific electric field are then compared with the results of computer simulation for different amplitudes of the electric field. Both trapping and resonant heating are observed, and both appear to contribute (for the chosen parameters) to limiting the validity of linear theory at larger electric field amplitudes. DOE

N87-24192# California Univ., Los Angeles. Dept. of Physics.
ROLE OF CAVITONS IN LASER-PLASMA INTERACTIONS Final Report, 15 Aug. 1984 - 14 Aug. 1985
A. Y. Wong and T. Tanikawa Sep. 1986 43 p Prepared in cooperation with Lawrence Livermore National Lab., Calif.
(Contract W-7405-eng-48)
(DE87-008485; UCRL-15900) Avail: NTIS HC A03/MF A01

We have observed three new phenomena associated with cavitons generated at the critical layer in an inhomogeneous plasma. Half-harmonic electromagnetic (em) radiation, accompanying the resonant absorption of the high-power microwave at omega(0) by an inhomogeneous plasma, appears to originate from the cavitons. Double layers have been found to develop near the locations of cavitons. Acceleration of ions by these double layers has also been observed. The evolution of resonantly excited electron plasma waves and density profile modification at the critical layer has been studied in detail. Conditions under which the role of cavitons becomes significant in em wave-plasma interactions are discussed. DOE

N87-24193# Maryland Univ., College Park. Inst. for Fluid Dynamics and Applied Mathematics.
INVESTIGATION OF UNIVERSAL PLASMA INSTABILITIES Annual Progress Report
H. Lashinsky Mar. 1987 9 p
(Contract AT(40-1)-3405)
(DE87-008276; DOE/NBM-7008276; APR-2) Avail: NTIS HC A02/MF A01

It is the purpose of this program to carry out an experimental investigation of universal or drift plasma instabilities in a thermal plasma device or Q machine with the hope that the results will be useful in evaluating various instability loss mechanisms in connection with the diffusion of plasma across magnetic fields in controlled thermonuclear devices. The effect of instabilities on plasma transport across magnetic fields is perhaps one of the most pressing problems in plasma confinement. Two of the important questions in this field of research at the present time are the relative roles of collisional and collisionless instabilities and the importance of linear and nonlinear phenomena, especially in connection with plasma turbulence. DOE

N87-24194# Lawrence Livermore National Lab., Calif.
MICROWAVE PRODUCTION FROM A PLASMA DRIVEN BY A HIGH POWER RELATIVISTIC ELECTRON BEAM
M. S. DiCapua, E. S. Fulkerson, D. Meeker, and J. DeGroot 1 Dec. 1986 7 p Presented at the 3rd National Conference on High Power Microwave Technology for Defense Applications, Albuquerque, N. Mex., 1 Dec. 1986 Prepared in cooperation with California Univ., Davis
(Contract W-7405-eng-48)
(DE87-003518; UCRL-94639; CONF-861240-16) Avail: NTIS HC A02/MF A01

Microwave emission from an unmagnetized, electron beam driven plasma has been measured. Argon, contained in a Lucite tube, is pre-ionized by a 90 microsec, 90 A electron source. The electron current is then injected into the tube. A diode is placed over the tube's aperture as the electron source for the microwave radiation. A spectrometer measures the output from 2 to 47 GHz in 3 bands. The emission takes place in two distinct phases. The 2 to 6 GHz output rises promptly with current pulse and then decays. For 6 GHz and above, there appears a low level microwave prepulse simultaneous with the 2 to 6 GHz output. This output rises sharply 25 ns after the current pulse begins, and includes frequencies beyond 40 GHz. The radio frequency output falls off before the current pulse ends. The microwave intensity decays monotonically with frequency. DOE

N87-24195# Spectra Technology, Inc., Bellevue, Wash.
COMPACT TOROID GENERATION, LIFETIME, AND STABILITY STUDIES IN LINEAR REVERSE FIELD THETA PINCH GEOMETRIES (TRX-2): FINAL REPORT
J. T. Slough, E. A. Crawford, A. L. Hoffman, R. D. Milroy, and L. C. Steinhauer 30 Jan. 1987 142 p
(Contract DE-AC06-80ER-53096)
(DE87-005094; DOE/ER-53096/T1) Avail: NTIS HC A07/MF A01

Separate abstracts were prepared for each of the 4 included sections. DOE

N87-24196# Los Alamos National Lab., N. Mex.
COLLECTIVE ACCELERATION OF PROTONS BY THE PLASMA WAVES IN A COUNTERSTREAMING ELECTRON BEAM
Y. T. Yan Mar. 1987 8 p Presented at the Particle Accelerator Conference, Washington, D.C., 16 Mar. 1987
(Contract W-7405-eng-36)
(DE87-007493; LA-UR-87-870; CONF-870302-63) Avail: NTIS HC A02/MF A01

A novel advanced accelerator is proposed. The counterstreaming electron beam accelerator relies on the same physical mechanism as that of the plasma accelerator but replaces the stationary plasma in the plasma accelerator by a magnetized relativistic electron beam, drifting antiparallel to the driving source and the driven particles, as the wave supporting medium. The plasma wave in a counterstreaming electron beam can be excited either by a density-ramped driving electron beam or by properly beating two laser beams. The fundamental advantages of the counterstreaming electron beam accelerator over the plasma accelerator are a longer and tunable plasma wavelength, a longer pump depletion length or a larger transformer ratio, and easier pulse shaping for the driving source and the driven beam. Thus the energy gain of the driven particles can be greatly enhanced whereas the trapping threshold can be dramatically reduced so as to admit the possibility for proton acceleration. DOE

N87-24197# GA Technologies, Inc., San Diego, Calif.
REPORT TO DOE OF THE FUSION PROGRAMS IN APPLIED PLASMA PHYSICS AND DEVELOPMENT AND TECHNOLOGY AT GA TECHNOLOGIES, INCORPORATED Annual Report, fiscal 1986
D. O. Overskei Dec. 1986 107 p
(Contract DE-AC03-84ER-53158)
(DE87-008882; GA-A-18692) Avail: NTIS HC A06/MF A01

Highlights of the fusion theory effort described in this report include investigations of high beta limit disruptions in the DIII-D device, Tokamak transport code simulations with electrostatic drift wave models, theoretical investigation of electromagnetic emissions from neutral beam injected plasmas, and results of a design study of the ellipsoidal shell Tokamak. Experimental plasma research efforts are addressing several important issues in fusion research. Neutron and alpha particle spectroscopy and triton confinement diagnostics are being developed to enable fusion researchers to understand alpha particle confinement and slowdown in burning plasmas. Development of Li beam diagnostic systems continued and has shown a capability for measuring both magnetic field pitch angle and relative current density profiles. Experiments on ergodic magnetic divertor (EMD) phenomena on the Texas Experimental Tokamak (TEXT) continued to demonstrate low plasma edge temperatures and impurity reduction that make the concept attractive for reactor applications. GA led efforts continuing the Helical Resonant Island Divertor (HRID) experiments on TEXT using the EMD as a controlled magnetic perturbation. Other research included reactor systems design studies, development of an advanced antenna for radiofrequency heating of plasma ions, and development of ferritic steels suitable for use as a structural material in fusion reactors. DOE

N87-24198# Nagoya Univ. (Japan). Inst. of Plasma Physics.
WAVELENGTHS OF K X-RAYS OF IRON IONS
Takako Kato, Shigeru Morita, and Hiroyuki Tawara Mar. 1987 126 p
(IPPJ-AM-49) Avail: NTIS HC A07/MF A01

Wavelengths of K X-rays of iron ions in all ionization stages are presented. Wavelengths and configurations for each transition are tabulated together with references. Available data for transition probabilities are also tabulated. Author

N87-24199# FOM-Inst. voor Plasmafysica, Rijnhuizen, Jutphaas (Netherlands).
[ACTIVITIES REPORT IN PLASMA PHYSICS] Annual Status Report, 31 Dec. 1985
Oct. 1986 126 p Sponsored by Euratom, and Nederlandse Organisatie voor Zuiver-Wetenschappelijk Onderzoek
(ETN-87-99588) Copyright Avail: NTIS HC A07/MF A01

Experiments on plasma pinches; turbulent heating in TORTUR; and diagnostical studies, electron cyclotron resonance heating; and diagnostics are described. Theoretical studies of magnetohydrodynamics, wave dynamics, and transport problems are summarized. ESA

76 SOLID-STATE PHYSICS

Includes superconductivity.

For related information, see also *33 Electronics and Electrical Engineering* and *36 Lasers and Masers.*

N87-24200# Westinghouse Research and Development Center, Pittsburgh, Pa.
SUPERCONDUCTING ELECTRONIC FILM STRUCTURES Annual Report, 1 Jan. - 31 Dec. 1986
A. I. Braginski and J. R. Gavaler 20 Jan. 1987 24 p
(Contract F49620-85-C-0043)
(AD-A179134; Rept-87-909-SUPER-R1; AFOSR-87-0314TR) Avail: NTIS HC A02/MF A01 CSCL 20L

Bulk samples of the newly discovered La-Sr-Cu-O Superconductors have been made which have critical onset temperatures over 38 K. The greater effectiveness of impurities (oxygen) compared to epitaxy for the stabilization of stoichiometric A15 Nb-Ge was demonstrated. The positive effect of oxides on the formation of A15 Nb-Al was also shown. Experiments involving the deliberate addition of a contaminant (methane) during barrier deposition provided a major advance in the understanding of the processes required for producing high quality NbN-MgO-NbN junctions. A model for predicting the orientation of single crystal Nb and Nb-Sn films on sapphire was experimentally verified. Results were obtained which indicate that epitaxy is essential for NbN-MgO-NbN trilayer processing if the junction is to be operated above 4.2 K. GRA

N87-24201# Air Force Inst. of Tech., Wright-Patterson AFB, Ohio. School of Engineering.
FABRICATION OF AlGaAs/InGaAs PSEUDOMORPHIC MODULATION DOPED FIELD EFFECT TRANSISTORS WITH p-DOPED SURFACE LAYERS M.S. Thesis
Thomas E. McLaughlin Dec. 1986 145 p
(AD-A179230; AFIT/GE/ENG/86D-11) Avail: NTIS HC A07/MF A01 CSCL 09A

Modulation doped field-effect transistors (MODFETs) are fabricated, incorporating two recently developed improvements to the MODFET structure to produce a unique electronic device. Highly p-doped surface layers were incorporated under the gate contact of the device. These layers have been shown to increase the Schottky barrier height at the MODFETs. Pseudomorphic AlGaAs/InGaAs technology was also incorporated for its proven unsurpassed electron saturation velocity and resulting high speed of operation. To evaluate the response of these ES pseudomorphic devices, their characteristics were measured and compared directly with those of reference samples fabricated at the same time from the same substrate material. The p-layers of the reference transistors were etched off chemically just before deposition of gate contact metal. The peak transconductance, threshold voltage, contact resistance and barrier height of all devices were measured at direct current (dc). Also, microwave S-parameters were measured over the range of 2 to 12 gigahertz (GHz). GRA

N87-24202# Air Force Inst. of Tech., Wright-Patterson AFB, Ohio. School of Engineering.

EVALUATION OF TERSOFF'S REVISED SILICON POTENTIAL IN A MOLECULAR DYNAMIC SIMULATION OF SOLID SILICON M.S. Thesis

William D. Metzler Mar. 1987 82 p
(AD-A179231; AFIT/GNE/ENP/87M-5) Avail: NTIS HC A05/MF A01 CSCL 20B

The goal was to provide an initial testing of a new silicon potential proposed by Tersoff. Molecular Dynamic (MD) simulations were performed at four temperatures below the melting point of silicon to evaluate the new potential's ability to reproduce the characteristics of diamond-Si. A constant enthalpy ensemble composed of 64 atoms was used. Although the Tersoff potential does identify the diamond structure as the lowest energy crystal at absolute zero, problems were noted at higher temperatures. At all temperatures above zero, the calculational cell showed a marked decrease in volume. The amount of system shrinkage increased with increasing simulation temperature. Because of this shrinkage, the Tersoff potential is unusable in MD simulations. It was noted that as the bonding environment became more favorable (stronger bonding), the bonding radius of minimum energy decreased. Since the potential relies primarily on coordination number to stabilize the diamond structure, it is postulated that there exists an as-yet unidentified four-bond configuration that provides a lower energy and as a result has a shorter rest bond length than the tetrahedral diamond structure. GRA

N87-24203# Air Force Inst. of Tech., Wright-Patterson AFB, Ohio. School of Engineering.

ELECTRICAL BEHAVIOR OF Ge AND (Ge+As) IMPLANTED GALLIUM ARSENIDE M.S. Thesis

Bryan L. Kelchner Dec. 1986 75 p
(AD-A179505; AFIT/GEP/ENP/86D-6) Avail: NTIS HC A04/MF A01 CSCL 20L

The amphoteric electrical properties of single implants of Ge and dual implants of Ge and As into semi-insulating Cr-doped GaAs have been studied using the Hall-effect/sheet-resistivity measurement method. Room temperature implantation was performed at an ion energy of 120 keV with a dose ranging from 5 x 10 to the 12th power to 3 x 10 to the 15th power per sq cm. The implanted samples were annealed at 900 C for 15 minutes. The results of carrier profile measurements show the amphoteric behavior of Ge, and the Ga-site occupancy by the Ge ions are significantly enhanced by the addition of As ions. In general, the carrier depth profiles show relatively flat but considerably fluctuating distributions. Capacitance-voltage (C-V) measurements were also made on some samples with low enough carrier concentrations, and the Hall profiles corrected for surface depletion widths were compared with the C-V profiles. SIMS atomic distributions of Ge have also been measured, and the results show that the Ge atomic profiles of the as-implanted samples do not follow the LSS Gaussian distribution. The SIMS profile for annealed samples show very little redistribution of the Ge ions. A comparison of the Hall and SIMS data shows that carrier concentrations are much less than the number of Ge ions in most of the implanted region. This is probably due to the unannealed implantation damage and/or electrical self-compensation. Author (GRA)

N87-24204# Massachusetts Inst. of Tech., Cambridge.

STUDY OF QUANTUM MECHANICAL EFFECTS IN DEEP SUBMICRON, GRATING-GATE FIELD EFFECT TRANSISTORS Annual Technical Report, 30 Sep. 1985 - 29 Sep. 1986

Dimitri A. Antoniadis and Henry I. Smith 30 Dec. 1986 8 p
(Grant AF-AFOSR-0376-85)
(AD-A179617; AFOSR-85-0376-001; AFOSR-87-0433TR) Avail: NTIS HC A02/MF A01 CSCL 09A

This research program investigates the effect of extreme submicron spatial modulation of the electrostatic potential on the transport of electrons in silicon and in III-V compound semiconductor devices. The test vehicle is the so called grating gate FET (GGFET). When made to move in a direction perpendicular to the potential modulation, i.e., perpendicular to the grating gate, electrons experience a surface superlattice (SSL) effect. When moving along the potential modulation electrons are restricted to only one degree of freedom and thus constitute a one dimensional system. The major accomplishments to date are in process technology and design of the devices. They are: (1) Double X ray/deep UV exposure of PMMA to simultaneously define fine and coarse patterns; (2) High temperature (950 C) anneal of Silicon wafer after delineation of tungsten conductor patterns, to eliminate X ray damage of silicon dioxide; and (3) Design of Gallium/Gallium Aluminum Arsenide structure for the implementation of the III-V GGFET. GRA

N87-24205# Aerospace Corp., El Segundo, Calif. Space Sciences Lab.

HEAVY ION INDUCED UPSETS IN SEMICONDUCTOR DEVICES

R. Koga, W. A. Kolasinski, and S. Imamoto 15 Aug. 1986 28 p
(ATR-86(8139)-3) Avail: NTIS HC A03/MF A01

Heavy ions produced at various accelerator facilities have been employed to measure the effect of cosmic rays on semiconductor devices in space. An ion transmission counter, a solid state detector, and a position sensitive detector constitute the beam-monitor system used to measure the flux in real time and to monitor the spatial beam uniformity. An LSI 11/23 computer exercises the semiconductor devices under test. The experimental technique and test results are discussed. Author

N87-24206# California Univ., Berkeley. Lawrence Berkeley Lab.

THE STRUCTURE OF Al/GaAs INTERFACES

Z. Liliental-Weber, C. Nelson, R. Gronsky, J. Washburn, and R. Ludeke Dec. 1986 8 p Presented at the Materials Research Society Fall Meeting, Boston, Mass., 1 Dec. 1986 Prepared in cooperation with IBM Corp., Yorktown Heights, N.Y.
(Contract DE-AC03-76SF-00098)
(DE87-007181; LBL-22581; CONF-861207-95) Avail: NTIS HC A02

The structure of Al/GaAs interfaces was investigated by high resolution electron microscopy. The Al layers were deposited in a molecular beam epitaxy chamber with a vacuum base pressure of less than 1 x 10 to the -8 Pa. The GaAs substrate temperature varied during Al deposition from -30 C to 400 C. Deposition of Al on cold substrates less than or equal to 25 C resulted in epitaxial growth of (001) Al on (001) GaAs. Droplets of Ga were observed in samples with the substrate temperature at -30 C (1 x 2) and 0°C (c(2 x 8)). Postannealing of the last sample caused formation of the AlGaAs phase. Deposition of Al on hot substrates (150 C and 400 C) resulted in the formation of the AlGaAs phase, which separated (110) oriented Al from (001) GaAs. DOE

N87-24207# Oak Ridge National Lab., Tenn.

TRANSIENT ENHANCED DIFFUSION IN ION-IMPLANTED SILICON

S. J. Pennycook and R. J. Culbertson Mar. 1987 10 p Presented at the SPIE Conference on Growth of Compound Semiconductors, Bay Point, Fla., 22 Mar. 1987
(Contract DE-AC05-84OR-21400)
(DE87-007659; CONF-870385-7) Avail: NTIS HC A02

We discuss the transient-enhanced diffusion of Sb, As, P, In, Ga, and B in ion-implanted Si, where the near-surface region has been amorphized by the dopant or by a self-implantation process. With Sb, a large transient diffusion enhancement is observed proportional to dopant concentration. For Sb, As, P, and In, the enhancement follows the relative interstitialcy diffusion coefficient. We believe this behavior is caused by stable implantation-induced point defects present in the amorphous surface layer, which decay during thermal processing to release high concentrations of self-interstitials. This process occurs in competition with the solid phase epitaxial (SPE) growth process, and for high dopant concentrations can occur in the amorphous phase ahead of the crystallization front. We believe this may be the origin of the dopant redistribution which can occur during SPE growth, which sets the upper limit to the dopant concentration which can be incorporated

in the lattice by SPE growth. These effects are reduced for Ga and are absent for B, although transient enhanced diffusion of these species can still occur from defects emitted from the damaged crystal underlying the original amorphous/crystalline interface. DOE

N87-24208# Harvard Univ., Cambridge, Mass.
DRIFT MOBILITIES BY TIME-OF-FLIGHT METHODS AND TIME-DEPENDENT PHOTOTRANSPORT IN THE NANOSECOND REGIME IN AMORPHOUS SEMICONDUCTORS Annual Report, 1 May 1985 - 30 Apr. 1986
W. Paul and J. R. Eggert Mar. 1987 98 p
(Contract DE-FG02-84ER-45070)
(DE87-008021; DOE/ER-45070/2) Avail: NTIS HC A05/MF A01

The general purpose of this work has been to clarify the steady-state photoelectronic properties of amorphous hydrogenated silicon and related semiconductors, and to contribute to understanding the underlying electronic band structure. The first phase of this work concentrated on transient phototransport measured on samples of doped and undoped a-Si:H. In the second year of this contract, we have concentrated on the examination of the possibility of investigating the doping of a-Si:H by P through neutron transmutation doping, examination of the theory of photoluminescence, completion of a study on the effect of carrier loss to deep traps during dispersive transport, and an experimental study of optical absorption involving states near mid-gap, caused by carrier injection at contacts. DOE

N87-24209# Lawrence Livermore National Lab., Calif.
THERMAL FRACTURE IN SELECTED NONLINEAR OPTICAL MATERIALS
D. Eimerl, J. Marion, and E. K. Graham 2 Mar. 1987 11 p Presented at the LASE-13: Pulse Power for Lasers Conference, Los Angeles, Calif., 11 Jan. 1987 Prepared in cooperation with Pennsylvania State Univ., University Park
(Contract W-7405-eng-48)
(DE87-008213; UCRL-96256; CONF-870132-102) Avail: NTIS HC A02/MF A01

The fracture temperature is a figure of merit describing the resistance of a crystal to thermal fracture. It has been determined as function of orientation of the normal to the plate surface for three common nonlinear and electrooptic materials (KDP, LiIO3, LiNbO3), and for the new material, barium borate. For the first three materials, the fracture temperature is small, between 3 and 20 C. However, barium borate appears to be about an order of magnitude more resistant to thermal fracture than the other three. DOE

N87-24210# California Univ., Berkeley. Lawrence Berkeley Lab.
THE STRUCTURE AND ELECTRICAL PROPERTIES OF METAL CONTACTS ON GaAs
Z. Liliental-Weber Jan. 1987 39 p Presented at the Conference on Physics and Chemistry of Semiconductor Interfaces, Salt Lake City, Utah, 27 Jan. 1987
(Contract DE-AC03-76SF-00098)
(DE87-008217; LBL-23016; CONF-870167-1) Avail: NTIS HC A03/MF A01

This paper reports a study of the structural and analytical properties of Au and Al contacts on GaAs and their change in the range of temperatures where the Schottky barrier height changed. The annealing of Au contacts above 290 C caused the Schottky barrier height to decrease, an effect opposite to that of Al, where the Schottky barrier height increased upon annealing. An increase in As in the GaAs under the as-deposited metal was consistently found in both cases, whereas annealing seems to change the As/Ga ratio in an opposite way for Au and Al. The orientation relationship of the Au contacts changed upon annealing, which was not observed with the annealed Al. The orientation relationship depended strongly on the surface preparation before the metal deposition and on the annealing environment. It was proposed that the presence of As at the interface can determine the orientation relationship between metals and GaAs. DOE

N87-24211*# Catholic Univ. of America, Washington, D.C.
DEVELOPMENT OF A THEORETICAL MODEL FOR ANNEALING OF RADIATION DAMAGE IN SEMICONDUCTOR DEVICES Quarterly Report, 8 Mar. - 8 Jun. 1987
V. Litovchenko Jun. 1987 5 p
(Grant NAG5-864)
(NASA-CR-180394; NAS 1.26:180394; Q-2) Avail: NTIS HC A02/MF A01 CSCL 20L

The radiation response of Metal Oxide Semiconductor (MOS) devices and Integrated Circuits (ICs) was studied theoretically. The case of short-term annealing and the rebound effect are modeled mathematically using the linear response theory. B.G.

N87-24212# Sandia National Labs., Albuquerque, N. Mex.
EPITAXIAL SEMICONDUCTOR OPTICAL INTERFERENCE DEVICES
P. L. Gourley, R. M. Biefeld, T. J. Drummond, and T. E. Zipperian 1987 23 p Presented at the SPIE Conference on Growth of Compound Semiconductors, Bay Point, Fla., 22 Mar. 1987
(Contract DE-AC04-76DP-00789)
(DE87-006890; SAND-87-0386C; CONF-870385-4) Avail: NTIS HC A02/MF A01

A new class of single-crystal, semiconductor optical interference devices is described. The basic physics governing their operation and materials and growth methods to implement them are summarized. Recent experimental results for epitaxial optical filters, monolithic integration, and tunability are discussed. DOE

N87-24213# Lawrence Livermore National Lab., Calif.
EXPERIMENTAL OBSERVATION OF THE QUANTUM BEHAVIOR OF A MACROSCOPIC DEGREE OF FREEDOM
M. H. Devoret, J. M. Martinis, D. Esteve, and J. Clarke May 1986 34 p Presented at the Les Houches Summer School on Theoretical Physics, Les Houches, France, 30 Jun. 1986 Prepared in cooperation with Commissariat a l'Energie Atomique, Gif-sur-Yvette, France
(Contract DE-AC03-76SF-00098)
(DE87-008228; LBL-23119; CONF-8606292-1) Avail: NTIS HC A03/MF A01

Our measurements of the lifetime of the zero-voltage state of a current biased Josephson junction agree quantitatively with predictions based on quantum theory, all the relevant parameters being measured in situ. This shows that the phase difference across a Josephson junction behaves as a macroscopic quantum variable. DOE

N87-24214# Oak Ridge National Lab., Tenn.
THIN FILM CHARACTERIZATION USING A MECHANICAL PROPERTIES MICROPROBE
W. C. Oliver, C. J. McHargue, and S. J. Zinkle 1987 29 p Presented at the International Conference on Metallurgical Coatings, San Diego, Calif., 23 Mar. 1987
(Contract DE-AC05-84OR-21400)
(DE87-008593; CONF-870388-5) Avail: NTIS HC A03/MF A01

A new ultra-low load microindentation system has been acquired in the ORNL Metals and Ceramics Division. The system's spatial resolution and its data acquisition capabilities allow the determination of several mechanical properties from volumes of material with submicron dimension; hence, the term Mechanical Properties Microprobe (MPM). Research with the MPM at Oak Ridge has led to improved techniques for determining the plastic and elastic properties of materials using microindentation experiments. The techniques have been applied to thin films created by ion implanting metals and ceramics, radiation damaged materials, and thin hard coatings of TiN. Changes in the strength (hardness) and modulus have been measured in films as thin as 200 nm. DOE

N87-24215# Air Force Inst. of Tech., Wright-Patterson AFB, Ohio. School of Engineering.
THE DEVELOPMENT OF A PROTOTYPE CMOS (COMPLEMENTARY METAL OXIDE SEMICONDUCTOR) CIRCUIT SIMULATOR M.S. Thesis
Thomas K. Shuminsky Dec. 1986 248 p
(AD-A177942; AFIT/GE/ENG/86D-39) Avail: NTIS HC A11/MF A01 CSCL 09E

This thesis effort designed and developed a prototype CMOS circuit simulator written in FORTRAN 77. The program is totally interactive, and prompts the user for all required information to generate the circuit and input vector files. Output is in the form of two text files, one detailed, and the other, tailored by the user to provide only specific information. The prototype was designed and implemented to model CMOS circuits of up to 100 components, with four basic component types defined. Circuit timing is also simulated, with a variable transistor switching delay capability. Analysis of the simulator was performed on a DEC VAX 11/785 using the UNIX operating system and the UNIX F77 FORTRAN compiler. Tests were run on two types of circuits, constructed from basic logic gates, and varying in size from two to 68 components. Overall execution times of 37 to 78 msec per component were experienced. GRA

N87-24216# Washington Univ., Seattle. Lab. for Chemometrics.
MULTICOMPONENT ANALYSIS USING AN ARRAY OF PIEZOELECTRIC CRYSTAL SENSORS Interim Report
W. P. Carey, Kenneth R. Beebe, and Bruce R. Kowalski 20 Feb. 1987 32 p
(Contract N00014-75-C-0536)
(AD-A178012; AD-E950935; TR-35) Avail: NTIS HC A03/MF A01 CSCL 07D

An array of nine piezoelectric quartz crystals, each coated with a different partially selective coating material, was constructed for multicomponent analysis of organic vapors. The usefulness of this array was evaluated by quantitating known mixture samples in both two and three component cases using two calibration techniques, multiple linear regression (MLR) and partial least squares (PLS). With the use of microsensors such as coated piezoelectric crystals, a high degree of collinearity between the sensors may exist which has an effect on the regression results. In the two component cases, the PLS method yielded a four to six fold improvement in prediction capability over MLR. Although the individual sensors produce a 3 to 6% relative error in response, the average relative prediction error using an array of sensors and the PLS method was 4.6% in the two component cases, while in the three component case the effect of collinearity decreases prediction capability. Author

N87-24217# European Research Office, London (England).
ASSEMBLY AND FUNCTIONALIZATION OF SUPRAMOLECULAR STRUCTURES STUDIED BY LUMINESCENCE TECHNIQUES Final Report
F. C. DeSchryver 15 Jan. 1987 26 p
(Contract DAJA45-84-C-0012)
(AD-A178064) Avail: NTIS HC A03/MF A01 CSCL 07C

Species of colloidal dimensions like micelles, inverted micelles or microemulsions are formed in aqueous or non-aqueous media when a certain concentration of monomers also called tensides, amphiphiles or detergents, has been exceeded. This concentration is called the CMC or critical micellar concentration. This aggregation of monomers is a result of the typical structure of a detergent molecule, that combines a hydrophilic part (the polar headgroup) with a hydrophobic part (the apolar tail). The size and shape of the aggregates formed is strongly dependent upon the molecular structure of the monomers that are building up such a micelle and even so upon the medium used and upon the presence or absence of additives. One of the most important features, which is also the subject of study in this project; is the stability of the aggregates formed, and more especially the factors that account for the differences in structure and stability of the known inverse micellar system. Within the framework of this project new detergents were synthesized and probe/quencher systems, used for fluorescence studies, are evaluated to see in how far they can provide a better understanding of the aggregation behavior and of the structure aspects that determine aggregate stabilization. GRA

N87-24218# Massachusetts Inst. of Tech., Cambridge. Dept. of Materials Science and Engineering.
MICROSCALE DEFECT KINETICS IN MELT-GROWN GaAs Final Technical Report, 1 Aug. 1983 - 31 Aug. 1986
Harry C. Gatos and Jacek Logowski 31 Aug. 1986 10 p
(Contract N00014-83-K-0581)
(AD-A178158) Avail: NTIS HC A02/MF A01 CSCL 20L

Our research on the kinetics of defects in melt-grown GaAs involved crystal growth experiments and post-growth treatments of crystals combined with extensive characterization of electronic properties related to defects. In our crystal growth experiments we used an especially constructed Czochralski-type puller equipped with a vertical magnetic field for the growth of GaAs under conditions of suppressed convection. We have identified for the first time a beneficial effect of the magnetic field for the compensation ratio and electron mobility (Ref. 1). Experiments on doping with oxygen of GaAs crystals grown by the Horizontal Bridgman technique have revealed an anomalous silicon segregation behavior governed by chemical reactions in a closed growth ampul rather than standard impurity distribution during the solidification (Refs. 2 and 3). Experiments on fast growth of GaAs by the LEC technique using pulling rates of up to 2 inch/h showed a significant decrease of EL2 concentration with increasing the pulling rate. We have shown that this effect originates from fast cooling of the crystal grown under high pulling rates (Ref. 4). We have essentially completed a detailed study on the effects of plastic deformation on deep levels in GaAs (Refs. 5, 6). This study combined electrical and optical characterization of crystals subjected to plastic deformation at 400 C. GRA

N87-24219# Air Force Inst. of Tech., Wright-Patterson AFB, Ohio. School of Engineering.
SURFACE PASSIVATION OF AN IMPLANTABLE SEMICONDUCTOR MULTIELECTRODE ARRAY M.S. Thesis
Steven P. Ernst Dec. 1986 111 p
(AD-A178175; AFIT/GE/ENG/86D-5) Avail: NTIS HC A06/MF A01 CSCL 20L

An effective passivation material was needed for the protection of a semiconductor multielectrode array during long-term bio-implantations. The following properties were required: a large electrical resistivity, a small relative dielectric constant, good adhesion to silicon dioxide and aluminum, impermeability to water and ionic contaminants, chemical stability in water, and a thermal coefficient of expansion compatible with those of aluminum and silicon dioxide. Three materials were examined: Du Pont PI-2555, Accuglass 407, and Diffusion Technology U-1A. The first is a polyimide, and the latter two are polysiloxanes. The latter were found to be permeable to ionic contaminants and eliminated. The polyimide possesses all of the desired properties. Several multielectrode arrays were passivated with polyimide using conventional photolithography and wet etching techniques. These arrays were tested in vitro in a saline solution for thirty days. The aluminum metallization on the multielectrode array was heavily corroded by the saline solution, resulting in changes in the integrated circuits's electrical parameters. GRA

N87-24220# Wright State Univ., Dayton, Ohio.
CHARACTERIZATION OF MATERIAL DEVICE STRUCTURES Final Report, Jan. 1984 - Sep. 1986
David C. Look, Phil W. Yu, George E. Norris, Dennis C. Walters, and William M. Theis 11 Feb. 1987 82 p
(Contract F33615-84-C-1423)
(AD-A178262; AFWAL-TR-86-1181) Avail: NTIS HC A05/MF A01 CSCL 20L

Impurities and defects in semiconducting and semi-insulating GaAs and other III-V compounds have been investigated by electrical, optical, and mass spectroscopic techniques.

Modulation-doped field-effect transistors have been fabricated and tested. A CAE/CAD environment has been implemented for the design, development, and evaluation of electronic circuitry. GRA

N87-24221# Massachusetts Inst. of Tech., Lexington. Lincoln Lab.
SOLID STATE RESEARCH Quarterly Technical Report, 1 May - 31 Jul. 1986
Alan L. McWhorter 7 Jan. 1987 79 p
(Contract F19628-85-C-0002)
(AD-A178394; Rept-1986-3; ESD-TR-86-99) Avail: NTIS HC A05/MF A01 CSCL 09C

This report on solid state research contains articles on the following: High-Speed Photoconductive Switches Fabricated on Ti Doped Semi-insulating InP; Diode Lasers with Cylindrical Mirror Facets; Ti:Al2O3 Laser Development; Electro Optic Tuning of a Ti:Al2O3 Laser; Er:YAG Laser Development; Laser Frequency Conversion; Tracer Gas Studies for OMVPE Reactor Design; Radiation Effects on CMOS Circuits Fabricated in SOI Films; MBE Grown Insulating GaAs Used as MESFET Buffers; Charge Coupled Device Imagers; Wafer Thinning Process; Attainment of 0.13 micrometers Lines and Spaces by Excimer-Laser Projection Lithography; Observation of Millimeter Wave Oscillation from Resonant-Tunneling Diodes and Some Theoretical Considerations of Oscillation Frequency Limits; High Performance Superconductive Chirp Filters; Superconductive Delay Line with Integral MOSFET Taps; and Further Assessment of Nonlinear Associative Memory for Detecting Lines in Images. GRA

N87-24222# Lawrence Livermore National Lab., Calif.
ELECTRICAL RESISTIVITY RESPONSE DUE TO ELASTIC-PLASTIC DEFORMATIONS
R. B. Stout Jan. 1987 47 p Presented at the Summer Meeting of the American Society of Mechanical Engineers, Cincinnati, Ohio, 14 Jun. 1987
(Contract W-7405-eng-48)
(DE87-006826; UCRL-94738; CONF-870637-2) Avail: NTIS HC A03/MF A01

The electrical resistivity of many materials is sensitive to changes in the electronic band configurations surrounding the atoms, changes in the electron-phonon interaction cross-sections, and changes in the density of intrinsic defect structures. These changes are most directly dependent on interatomic measures of relative deformation. For this reason, a model for resistivity response is developed in terms of interatomic measures of relative deformation. The relative deformation consists of two terms, a continuous function to describe the recoverable displacement between two atoms in the atomic lattice structure and a functional to describe the nonrecoverable displacement between two atoms as a result of interatomic discontinuities from dislocation kinetics. This model for resistivity extends the classical piezoresistance representation and relates electric resistance change directly to physical mechanisms. An analysis for the resistivity change of a thin foil ideally embedded in a material that undergoes elastic-plastic deformation is presented. DOE

N87-24223# Utah Univ., Salt Lake City.
THEORETICAL AND EXPERIMENTAL STUDY OF SOLID PHASE MISCIBILITY GAPS IN 3/5 QUATERNARY ALLOYS Progress Report
G. B. Stringfellow 16 Mar. 1987 6 p
(Contract DE-FG02-84ER-45061)
(DE87-008942; DOE/ER-45061/1) Avail: NTIS HC A02/MF A01

During the last year, a systematic study was completed of the effects of growth temperature and substrate orientation on the growth and properties of metastable GaInAsSb alloys. Work on the ordering of GaInAs and GaInAsSb alloys was also done. DOE

77 THERMODYNAMICS AND STATISTICAL PHYSICS

Includes quantum mechanics; theoretical physics; and Bose and Fermi statistics.

For related information see also *25 Inorganic and Physical Chemistry* and *34 Fluid Mechanics and Heat Transfer.*

N87-24224# Florida Univ., Gainesville.
THEORETICAL AND EXPERIMENTAL INVESTIGATIONS OF FLUCTUATION THERMODYNAMIC PROPERTIES OF LIQUID SOLUTIONS Technical Progress Report, 15 Apr. 1986 - 14 Apr. 1987
J. P. OConnell 1987 3 p
(Contract DE-FG05-85ER-13362)
(DE87-005681; DOE/ER-13362/2) Avail: NTIS HC A02/MF A01

Work has continued in the three activities of theory, correlation, and experiment. Results have been obtained for the thermodynamic properties of both nonelectrolyte and electrolyte liquids. DOE

N87-24225# Naval Research Lab., Washington, D. C.
NUMERICAL SIMULATION OF A RANDOMLY HEATED, THERMALLY UNSTABLE FLUID
R. B. Dahlburg, J. M. Picone, and J. T. Mariska 31 Dec. 1986 27 p
(AD-A177888; AD-E950921; NRL-MR-5911) Avail: NTIS HC A03/MF A01 CSCL 03B

Numerical simulations examine the response of a radiation driven thermally unstable fluid medium to randomization of the heating rate. Condensed structures develop more quickly as the heating becomes more spatially and temporally variable. Furthermore, the duration and intensity of the radiation events are altered. An analysis is presented which indicates that increasing the amplitude of temperature perturbations will lead to increases in radiated energy output. GRA

N87-24226# Lawrence Livermore National Lab., Calif.
GAUGE INVARIANT QUANTUM COSMOLOGY
B. K. Berger 16 Jun. 1986 10 p Presented at the 26th Liege International Astrophysical Colloquium, Liege, Belgium, 1 Jul. 1986 Prepared in cooperation with Oakland Univ., Rochester, Mich.
(Contract W-7405-eng-48)
(DE87-006685; UCRL-94746; CONF-8607121-1; CONF-8607113-2) Avail: NTIS MF A01

Path integral quantization of minisuperspace models allows study of boundary conditions, the Hamiltonian constraint, reparameterization invariance, and quantum dynamics. DOE

80 SOCIAL SCIENCES (GENERAL)

Includes educational matters.

N87-24285*# Hawaii Univ., Honolulu. Inst. for Astronomy.
STAR FORMATION IN NORMAL GALAXIES
C. G. Wynn-Williams *In* NASA, Washington Star Formation in Galaxies May 1987 p 125-131 (For primary document see N87-24266 17-89)
(Grant NSF AST-84-18197)
Avail: NTIS HC A99/MF E03 CSCL 03B

81 ADMINISTRATION AND MANAGEMENT

Includes management planning and research.

N87-24227# Assistant Secretary of Defense (Comptroller), Washington, D. C.
DOD (DEPARTMENT OF DEFENSE) PROCEDURES FOR MANAGEMENT OF INFORMATION REQUIREMENTS

R. Drake Nov. 1986 112 p
(PB87-155495; DOD-7750.5-M) Avail: NTIS HC A06/MF A01 CSCL 05A

The Manual guides action officers who need to establish reports or obtain information from the public, other Federal agencies, or DoD Components and provides them with the necessary information to license their information requirements. In addition, it contains information to assist program managers in the operation of their reports management programs. GRA

N87-24228# Bundesministerium fuer Forschung und Technologie, Bonn (West Germany).
RESULTS OF THE ENCOURAGEMENT OF BASIC RESEARCH (1982-1986) [BILANZ DER FOERDERUNG VON GRUNDLAGENFORSCHUNG (1982-1986)]
1986 105 p In GERMAN
(ETN-87-99665) Avail: NTIS HC A06/MF A01

The results of the stimulation of fundamental research work by the German Federal Ministry of Research and Technology are reviewed. The research-political framework and the general trends are outlined, including the financial development. The main points of research effort supported by the Ministry are presented. ESA

82 DOCUMENTATION AND INFORMATION SCIENCE

Includes information management; information storage and retrieval technology; technical writing; graphic arts; and micrography.

For computer documentation see *61 Computer Programming and Software.*

N87-24229# Carlow Associates, Inc., Fairfax, Va.
TEXT EDITING PERFORMANCE AS A FUNCTION OF SCREEN SIZE Final Report, 7 Apr. - 31 Dec. 1986
Clifford C. Baker 31 Dec. 1986 49 p
(Contract DAAA15-86-D-0005; DA Proj. 1L1-62716-AH-70)
(AD-A179067) Avail: NTIS HC A03/MF A01 CSCL 09B

A pilot study was performed to experimentally assess the implications of CRT screen size and definition on text editing performance. The study manipulated line length (16, 32, and 64 characters displayed per line), window height (1, 4, 8, and 19 line text pages) and edit field location (text to be edited was located at the beginning, middle, or end of text messages) to measure effects on text editing performance as measured by edit field location time, editing time, and errors. Of these, text location time and location errors (as measured by vertical scroll reversals) were significantly influenced by line length and edit field location. GRA

N87-24230# California Univ., Berkeley. Electronics Research Lab.
OPTIMIZATION OF EXTENDED RELATIONAL DATABASE SYSTEMS
S. L. Graham and Timoleon K. Sellis 23 Jul. 1986 172 p
(Contract N00039-84-C-0089; ARPA Order 4871)
(AD-A179308; UCB/ERL-M86/58) Avail: NTIS HC A08/MF A01 CSCL 09B

Current relational Database Management Systems must be extended to function well in Engineering and Artificial Intelligence applications. Various additional functionalities have been proposed and in this thesis we study the optimization of one extended environment. Specifically, we consider the optimization of a version of the QUEL query language extended with two new features: the repetitive execution of commands; and the execution of relation fields in which collections of QUEL commands are stored. An extended query processing algorithm based on the original INGRES decomposition algorithm is first presented and then various modifications aiming to improve its performance are suggested. Caching of query results is also considered as another means to improve the performance of the processing engine. We analyze and suggest solutions to the various problems related to the design of a query result cache (replacement policies, invalidation techniques, etc). Based on the above extensions, a relation field may contain more than one QUEL commands. Accessing such a field triggers the execution of all these commands. We present a set of tactics that can be to reduce the cost of processing multiple commands using some interquery analysis. Special cases amenable to different kind of processing are also identified and studied. GRA

N87-24231# California Univ., Berkeley. Dept. of Computer Sciences.
AUTOMATING INDEX PREPARATION Technical Report, 7 Aug. 1984 - 6 Aug. 1987
Pehong Chen and Michael Harrison 23 Mar. 1987 27 p
(Contract N00039-84-C-0089; ARPA Order 4871)
(AD-A179327) Avail: NTIS HC A03/MF A01 CSCL 05B

This paper shows how the indexing process can be automated in a way which is largely independent of a specific typesetting system and independent of the format being used. Specifically, we describe a framework for placing index commands in the document and a general purpose index processor which transforms a raw index into an alphabetized version. These concepts have been implemented as apart of an extensive authoring environment. This includes a suite of Lisp programs for the index placing facility and a C program for the index processor. The resulting system has been successfully used in producing indexes for a book and a number of technical manuals. We focus on issues under both language-based and direct manipulation paradigms. In a language-based system, the user specifies the document with interspersed commands which is then passed to a formatter and the output is obtained. In a direct manipulation environment sometimes referred to as a WYSIWYG (what-you-see-is-what-you-get) system the user manipulates the document output appearance directly by invoking built-in commands available through menus and buttons. There is no such concept as the document specification language in direct manipulation systems. GRA

N87-24232# Lawrence Livermore National Lab., Calif.
LIVERMORE RISK ANALYSIS METHODOLOGY: A QUANTITATIVE APPROACH TO MANAGEMENT OF THE RISK ASSOCIATED WITH THE OPERATION OF INFORMATION SYSTEMS
S. B. Guarro, A. A. Garcia, C. C. Wood, and P. G. Prassinos 14 Aug. 1986 18 p Presented at the Computer and Communications Security Conference, New York, N.Y., 7 Oct. 1986
(Contract W-7405-eng-48)
(DE87-006828; UCRL-95133; CONF-8610255-1) Avail: NTIS HC A02/MF A01

Risk assessment methods vary in nature and depth. Their application to the evaluation of information security issues should be decided on the basis of their capability to provide answers to practical and fundamental questions concerning the design and implementation of security controls in specific information systems. Quantitative risk analysis provides an objectively based approach to the problem of assessing and managing risk. As a decision making and risk assessment tool, it is not only capable of identifying potential losses that could be unacceptable for a given system, but it can be used to determine which specific security controls and countermeasures can be effective and cost justifiable. The Livermore Risk Analysis Methodology (LRAM) was developed to cover these objectives in a balanced and comprehensive way. Its model and procedures, from the identification of valuable assets to the prioritization and budgeting of proposed controls, are examined and discussed both from the technical and from the decision making/risk management perspectives. DOE

N87-24233# Oak Ridge National Lab., Tenn.
THE SUCCESS OR FAILURE OF MANAGEMENT INFORMATION SYSTEMS: A THEORETICAL APPROACH
T. R. Curlee and B. T. Tonn Mar. 1987 29 p
(Contract DE-AC05-84OR-21400)
(DE87-007802; ORNL/TM-10320) Avail: NTIS HC A03/MF A01

(DE87-007802; ORNL/TM-10320) Avail: NTIS HC A03/MF A01

Work has been done by various disciplines to address the reasons why modern, computerized management information systems either succeed or fail. However, the studies are not based on a well-defined conceptual framework and the focus has been narrow. This report presents a comprehensive conceptual framework of how an information system is used within an organization. This framework not only suggests how the use of an information system may translate into productivity improvements for the implementing organization but also helps to identify why a system may succeed or fail. A major aspect of the model is its distinction between the objectives of the organization in its decision to implement an information system and the objectives of the individual employees who are to use the system. A divergence between these objectives can lead to system under-utilization or misuse at the expense of the organization's overall productivity. DOE

N87-24234# Oak Ridge National Lab., Tenn.
USE OF A DBMS TO AID IN THE SOFTWARE CONVERSION PROCESS
A. F. Huntley, R. A. Bryant, M. A. Buhrmaster, J. L. Christian, and R. Hume Feb. 1987 25 p
(Contract DE-AC05-84OR-21400)
(DE87-007883; ORNL-6365) Avail: NTIS HC A02/MF A01

Procedures are described that provide for the automated conversion of a screen library containing over a thousand screen display definitions to a new screen definition software package. The first step is to extract the screen definition information from the original screen package. This information is then loaded into a data base management system (DBMS). The information is manipulated as necessary and output in a format that can be utilized by the new screen package. A major benefit of the procedures developed is that a DBMS allows bulk updates of multiple screen definitions to be performed. Both the source and target screen packages provide only for the updating of individual screens. Although the procedures described apply to the problem of converting screen definitions for a specific application using the two specific screen definition software packages, the flexibility inherent in a DBMS allows its use in solving many such complex problems. The concept can be modified to allow possibilities limited only by the creativity of the DBMS users and the information contained in the data base. DOE

N87-24235# Department of Energy, Oak Ridge, Tenn.
ENERGY DATA BASE: SUBJECT CATEGORIES AND SCOPE, A REFERENCE MANUAL
M. C. Grissom, ed. Apr. 1987 68 p
(DE87-005547; DOE/TIC-4584-R7) Avail: NTIS HC A04/MF A01

The subject scope of the Energy Data Base (EDB) is defined, encompassing all technological aspects of energy production, conversion, and efficient utilization, and the economic, social, and political aspects as well. Coverage also includes the basic sciences as applicable. The subject areas within the scope of EDB are defined and hierarchically numbered, and scope notes are provided to define the extent of interest in certain areas, particularly areas of basic research. DOE

N87-24236# California Univ., Berkeley. Lawrence Berkeley Lab.
DATA MANAGEMENT FOR HIGH ENERGY PHYSICS EXPERIMENTS: PRELIMINARY PROPOSALS
F. Olken, S. C. Loken, D. Rotem, A. Shoshani, and T. G. Trippe Jan. 1987 9 p Presented at the Computing High Energy Physics, Pacific Grove, Calif., 2 Feb. 1987
(Contract DE-AC03-76SF-00098)
(DE87-006940; LBL-22883; CONF-870249-4) Avail: NTIS HC A02/MF A01

Currently HEP experimental data are reduced as they become available. We propose instead a demand driven approach to data analysis. Full analysis will be performed only as needed, in response to user queries which specify the subset of events for which reduced data is needed. To support this approach we propose to partition the datasets on the cross product of several trigger inputs, instead of storing the data in chronological order. Queries will be automatically decomposed into a set of requests against several partitions. Indexing, physically clustering the data on the logical partitions, and caching of partitions will be employed for efficiency. DOE

N87-24237# Massachusetts Inst. of Tech., Cambridge. Center for Information Systems Research.
TIME SLICE MANIPULATION IN INFORMATION HIERARCHY
Meichun Hsu and Stuart E. Madnick Feb. 1987 15 p
(Contracts N00039-85-C-0571; N00039-83-C-0463)
(AD-A177949; CISR-M010-8702-21) Avail: NTIS HC A02/MF A01 CSCL 09D

This paper presents theoretical results on a generalized form of partial order, called hierarchical partial order, for enforcing serializability that takes advantage of transaction analysis in database systems. Transaction analysis partitions the database into data partitions that may assume a hierarchy of priorities, such that transactions primarily updating less critical data partitions will not interfere with transactions primarily updating the more critical data partitions, or will do so to a lesser extent than those in conventional systems. This results from the ability for transactions in the system to access different data partitions using different synchronization protocols. The rules governing the different protocols are presented and their corrections with respect to serializability is proven. GRA

N87-24238# Rutgers - The State Univ., New Brunswick, N. J.
EXPERIMENTS ON THE COGNITIVE ASPECTS OF INFORMATION SEEKING AND INFORMATION RETRIEVING Final Report, 1985-1987
Tefko Saracevic, Paul Kantor, Alice Chamis, and Donna Trivison (Case Western Reserve Univ., Cleveland, Ohio.) Jan. 1987 584 p
(Grant NSF IST-87-05411)
(PB87-157699) Avail: NTIS HC A25/MF A01 CSCL 05B

The aim of the study was to contribute to the formal, scientific characterization of the elements involved in information seeking and retrieving, particularly in relation to the cognitive decisions and human interactions involved. The objectives were to conduct experiments and observations under as real-life conditions as possible relative to: user context of questions in information retrieval; the structure and classification of questions; cognitive traits and decision making of searchers; and different searches of the same question. The study involved 40 users with 1 question each, 39 searchers, 360 searchers, and 5411 unique documents evaluated by users. The final report contains detailed descriptions of model, methods, procedures, and results obtained. An appendix contains the raw data, question, and forms used. GRA

N87-24239# Naval Safety Center, Norfolk, Va.
STANDARDIZED PROCEDURE FOR SYSTEM SAFETY INPUT TO THE DEFENSE TECHNICAL INFORMATION CENTER (DTIC)
R. P. Kinzey and N. Kniepp Jan. 1987 10 p
(AD-A178246; TR-1-JSSC) Avail: NTIS HC A02/MF A01 CSCL 15E

Currently, there are no standardized key words for system safety reports being submitted to the Defense Technical Information Center (DTIC). Retrieval of this data without key words requires DTIC to conduct extensive text searches to locate specific hazard analyses or other system safety reports. This procedure creates considerable time delays in obtaining historical data and generates excessive costs. To reduce costs and time, this technical report has been prepared to standardize key words and phrases for inputting system safety related data to DTIC. System Safety is defined by MIL-STD-882B, System Safety Program Requirements, as the application of engineering and management principles, criteria, and techniques to optimize safety within the constraints of operational effectiveness, time, and cost throughout all phases

of the system life cycle. A system is a composite, at any level of complexity, of personnel, procedures, materials, tools, equipment, facilities, and software. The elements of this composite entity are used together in the intended operational support environment to perform a given task or achieve a specific production, support, or mission requirement. GRA

83 ECONOMICS AND COST ANALYSIS

Includes cost effectiveness studies.

No abstracts in this category.

84 LAW, POLITICAL SCIENCE AND SPACE POLICY

Includes NASA appropriation hearings; aviation law; space law and policy; international law; international cooperation; and patent policy.

N87-24240# Committee on Commerce, Science, and Transportation (U. S. Senate).
NATIONAL AERONAUTICS AND SPACE ADMINISTRATION AUTHORIZATION ACT
Washington GPO 1987 47 p A bill, S. 1164, referred to the Committee on Commerce, Science and Transportation, 100th Congress, 1st Session, 7 May 1987
(S-Rept-100-87) Avail: US Capitol, Senate Document Room

Appropriations for the National Aeronautics and Space Administration for research and development, space flight, control and data communication, construction of facilities, and research and program management are discussed. B.G.

N87-24241# Committee on Appropriations (U. S. House).
DEPARTMENT OF HOUSING AND URBAN DEVELOPMENT - INDEPENDENT AGENCIES APPROPRIATIONS BILL, 1988
Boland Washington GPO 25 Jun. 1987 78 p Report to accompany H.R. 2783 presented by the Committee on Appropriations, 100th Congr., 1st Sess., 25 Jun. 1987
(H-Rept-100-189; GPO-74-463) Avail: Document Room, House of Representatives, Washington, D.C. 20515 HC free

House bill H.R. 2783 which covers the appropriations for the Department of Housing and Urban Development, and for sundry independent agencies, boards, commissions, and offices is described. Comparative statements of the budget authority for fiscal year 1987 and budget estimates and amounts recommended in the bill for fiscal year 1988 are provided. For individual titles, see N87-24242 through N87-24242.

N87-24242# Committee on Appropriations (U. S. House).
NATIONAL AERONAUTICS AND SPACE ADMINISTRATION
In its Department of Housing and Urban Development - Independent Agencies Appropriations Bill, 1988 25 Jun. 1987 p 39-43 (For primary document see N87-24241 17-84)
Avail: Document Room, House of Representatives, Washington, D.C. 20515 HC free

The section of House bill H.R. 2783 which deals with the appropriations for the National Aeronautics and Space Administration is summarized. Appropriations cover research and development, space flight control and data communications, construction of facilities, and research and program management. The 1987 appropriation amounts, 1988 estimates, and the amounts recommended in the bill are provided. M.G.

N87-24243# Committee on Commerce, Science, and Transportation (U. S. Senate).
NATIONAL AERONAUTICS AND SPACE ADMINISTRATION AUTHORIZATION ACT, 1988
Washington GPO 1987 114 p A report on S.1164 submitted by the Committee on Commerce, Science and Transportation, 100th Congress, 1st Session, 24 Jun. 1987
(S-Rept-100-87; GPO-74-470) Avail: US Capitol, Senate Document Room

The major provisions and legislative history of Senate bill S. 1164 authorizing appropriations to the National Aeronautics and Space Administration for research and development, space flight, control and data communications, construction of facilities, and research and program management are summarized. A section-by-section analysis of the bill is also presented. The various amendments to the bill include the language of S. 1173 (the Office of Space Transportation FY-1988 Authorization), S. 502 (Technical Amendments to the Land Remote-Sensing Commercialization Act of 1984), S. 752 (the Space Grant College and Fellowship Program), and others. M.G.

85 URBAN TECHNOLOGY AND TRANSPORTATION

Includes applications of space technology to urban problems; technology transfer; technology assessment; and surface and mass transportation.

For related information see also *03 Air Transportation and Safety, 16 Space Transportation,* and *44 Energy Production and Conversion.*

N87-24244# Los Alamos National Lab., N. Mex.
FUEL CELL POWERED PROPULSION SYSTEMS FOR HIGHWAY VEHICLES
J. R. Huff, N. E. Vanderborgh, J. F. Roach, and H. S. Murray 1987 18 p Presented at the 14th Annual Energy Technology Conference and Exposition, Washington, D.C., 14 Apr. 1987
(Contract W-7405-eng-36)
(DE87-007497; LA-UR-87-820; CONF-870416-5) Avail: NTIS HC A02/MF A01

Over the past thirty-five years, the transportation sector has accounted for approx. 25% of the total gross energy consumption in the US. Transportation's share of petroleum use in this time frame has ranged from 50 to 55%. Therefore, the use of fuel cell power plants that could possibly operate more efficiently than internal combustion engines in this type of application has been examined. In addition, these fuel cell power plants can operate on methanol produced from indigenous, non-petroleum sources and thereby reduce US dependency on petroleum resources. Fuel cell power plant use in city buses and automobiles has been explored and feasibility determined from both performance and cost viewpoints. Fuel cell systems for transportation applications have been selected on the basis of state-of-development, performance (both present and projected), and fuel considerations. In the last 25 years, most of the development work by research organizations and industrial firms has focused on five types of fuel cells, classified according to the electrolyte used. In terms of the overall state-of-development of systems, the ranking is as follows: (1) phosphoric acid, (2) alkaline, (3) proton exchange membrane, (4) molten carbonate, and (5) solid oxide. DOE

N87-24245# Santa Fe Corp., Alexandria, Va.
SYSTEMS MODEL FOR NATURAL GAS VEHICLE FLEETS Final Report, Jan. - Dec. 1986
W. M. Georgen and W. A. Meyer Jan. 1987 87 p
(Contract GRI-5086-410-1230)
(PB87-178083; GRI-87/0019) Avail: NTIS HC A05/MF A01 CSCL 13F

A computer-based systems model for natural gas vehicle (NGV) fleets is described. The model uses the Lotus 1-2-3 worksheet program to analyze the economic characteristics of the dual-fuel NGV fleets and assess the impact of research and development efforts. Operating, maintenance, capital, and annualized life-cycle costs for the entire NGV system are calculated from vehicle and refueling station component cost inputs and system operating parameters. The benefits of NGV component research and development are readily evaluated from sensitivity analysis of

system cost factors. A derivative model designed to broaden the focus of the basic model to evaluate fleet conversion options is also described. A diskette containing the model software is available from the Gas Research Institute, Technology Applications Department. GRA

N87-24246# Environmental Research Inst. of Michigan, Ann Arbor. Sensor Systems Div.
IMAGE SENSOR DATA BASE FOR THE DARPA ALV (DEFENSE ADVANCED RESEARCH PROJECTS AGENCY AUTONOMOUS LAND VEHICLE) PROGRAM Final Report, 1 Sep. 1984 - 30 Sep. 1986
C. Miller Oct. 1986 74 p
(AD-A178117; ERIM-193600-1-F) Avail: NTIS HC A04/MF A01 CSCL 17E

This report describes the acquisition of imaging sensor data for the DARPA Autonomous Land Vehicle (ALV) Program. Data were acquired during four seasonal measurement periods from September 1984 through June 1986 at the Martin Marietta ALV Test Site near Denver Colorado. Passive Multispectral, 3-D Imaging, and color TV sensors were installed on an instrumented van and operated over road networks and various fixed locations at the Martin site. The report presents the specifications for the sensors and describes each measurement period including site locations on map overlays. Data format for the sensors is described and field logs are included as appendices. GRA

88 SPACE SCIENCES (GENERAL)

N87-24247*# National Aeronautics and Space Administration. Goddard Space Flight Center, Greenbelt, Md.
ESSAYS IN SPACE SCIENCE
Reuven Ramaty, ed., Thomas L. Cline, ed., and Jonathan F. Ormes, ed. Jun. 1987 424 p Symposium held in Greenbelt, Md., 23 Apr. 1985
(NASA-CP-2464; Rept-87B0055; NAS 1.55:2464) Avail: NTIS HC A18/MF A01 CSCL 03B

The papers presented cover a broad segment of space research and are an acknowledgement of the personal involvement of Frank McDonald in many of these efforts. The totality of the papers were chosen so as to sample the scientific areas influenced by him in a significant manner. Three broad areas are covered: particles and fields of the solar system; cosmic ray astrophysics; and gamma ray, X-ray, and infrared astronomics. For individual titles, see N87-24248 through N87-24264.

N87-24248*# Iowa Univ., Iowa City. Dept. of Physics and Astronomy.
MAGNETOSPHERES OF THE OUTER PLANETS c91
James A. VanAllen *In* NASA Goddard Space Flight Center, Greenbelt, Md. Essays in Space Science Jun. 1987 p 1-17
(For primary document see N87-24247 17-88)
(Contracts NAS2-11125; N00014-76-C-0016)
Avail: NTIS HC A18/MF A01 CSCL 03B

The five qualitatively different types of magnetism that a planet body can exhibit are outlined. Potential sources of energetic particles in a planetary magnetosphere are discussed. The magnetosphere of Uranus and Neptune are then described using Pioneer 10 data. B.G.

N87-24249*# National Oceanic and Atmospheric Administration, Boulder, Colo. Space Environment Lab.
AURORAL PARTICLES c46
David S. Evans *In* NASA Goddard Space Flight Center, Greenbelt, Md. Essays in Space Science Jun. 1987 p 19-45 Prepared in cooperation with Lockheed Missiles and Space Co., Palo Alto, Calif. (For primary document see N87-24247 17-88)
Avail: NTIS HC A18/MF A01 CSCL 04A

The problems concerning the aurora posed prior to the war are now either solved in principle or were restated in a more fundamental form. The pre-war hypothesis concerning the nature of the auroral particles and their energies was fully confirmed, with the exception that helium and oxygen ions were identified as participating in the auroral particle precipitation in addition to the protons. The nature of the near-Earth energization processes affecting auroral particles was clarified. Charged particle trajectories in various electric field geometries were modeled. The physical problems have now moved from determining the nature and geometry of the electric fields, which accelerate charged particles near the Earth, to accounting for the existence of these electric fields as a natural consequence of the solar wind's interaction with Earth. Ultimately the reward in continuing the work in auroral and magnetospheric particle dynamics will be a deeper understanding of the subtleties of classical electricity and magnetism as applied to situations not blessed with well-defined and invariant geometries. B.G.

N87-24250*# National Aeronautics and Space Administration. Goddard Space Flight Center, Greenbelt, Md.
PARTICLE ACCELERATION IN SOLAR FLARES c93
R. Ramaty and M. A. Forman (State Univ. of New York, Stony Brook.) *In its* Essays in Space Science Jun. 1987 p 47-73
(For primary document see N87-24247 17-88)
Avail: NTIS HC A18/MF A01 CSCL 03B

The most direct signatures of particle acceleration in flares are energetic particles detected in interplanetary space and in the Earth atmosphere, and gamma rays, neutrons, hard X-rays, and radio emissions produced by the energetic particles in the solar atmosphere. The stochastic and shock acceleration theories in flares are reviewed and the implications of observations on particle energy spectra, particle confinement and escape, multiple acceleration phases, particle anistropies, and solar atmospheric abundances are discussed. Author

N87-24251*# Chicago Univ., Ill. Dept. of Physics.
THE ENERGY SOURCE OF THE INTERPLANETARY MEDIUM AND THE HELIOSPHERE c90
Eugene N. Parker *In* NASA Goddard Space Flight Center, Greenbelt, Md. Essays in Space Science Jun. 1987 p 75-85
(For primary document see N87-24247 17-88)
(Grant NGL-14-001-001)
Avail: NTIS HC A18/MF A01 CSCL 03B

The activity of the interplanetary medium arises from occasional transient outbursts of the active corona and, for the most part, from the interaction of fast and slow streams in the solar wind. The basic driver is the heat input to the corona, both transient and steady. The fast streams issue from coronal holes where the heat input may be Alfven waves with root mean squared (rms) fluid velocities of nearly 100 km/sec or may be wholly or in part the waves refracted into the hole from neighboring active regions. If the latter, then the character of the wind from the coronal hole depends upon the proximity and vigor of active regions, with significant differences between the polar and low altitude solar wind. In any case, there is no observational support for any of these ideas, so that the primary cause of the wind from the Sun, as well as any other similar star is not without mystery. It is to be hoped that ground-based observations together with the input from the Solar Optical Telescope and the International Solar Polar Mission may in time succeed in clearing up some of the basic questions. Author

N87-24252*# California Univ., Berkeley. Space Sciences Lab.
PARTICLE PROPAGATION CHANNELS IN THE SOLAR WIND c92
K. A. Anderson and W. M. Dougherty *In* NASA Goddard Space Flight Center, Greenbelt, Md. Essays in Space Science Jun. 1987 p 87-98 (For primary document see N87-24247 17-88)
(Grant NAG5-376)
Avail: NTIS HC A18/MF A01 CSCL 03B

The intensities of low energy solar-interplanetary electrons and ions at 1 AU occasionally change in a square wave manner. The changes may be increases or decreases and they typically have durations of from one hour to a few hours. In some cases these

channels are bounded by discontinuities in the interplanetary field and the plasma properties differ from the surrounding solar wind. In one case solar flare particles were confined to a channel of width 3 x 10 to the 6th km at Earth. At the Sun this dimension extrapolates to about 12,000 km, a size comparable to small flares. Author

N87-24253*# National Aeronautics and Space Administration. Goddard Space Flight Center, Greenbelt, Md.
STUDIES OF THE INTERPLANETARY MAGNETIC FIELD: IMP'S TO VOYAGER c90
Norman F. Ness *In its* Essays in Space Science Jun. 1987 p 99-121 (For primary document see N87-24247 17-88)
Avail: NTIS HC A18/MF A01 CSCL 03B

During the last two decades, spacecraft projects and individual experiments for which Frank McDonald was a leader have contributed very significantly to the current understanding of the structure of interplanetary space and the correlation between solar and interplanetary disturbances. Studies on the IMP, HELIOS, and Pioneer spin-stabilized spacecraft and the larger attitude-stabilized Voyager spacecraft have provided data sets from which the modern view of the heliosphere has evolved. That concept in which the inner solar system is shown to be dominated by individual streams associated with specific source regions on the Sun is illustrated. As these high-speed streams overtake the preexisting solar plasma, they coalesce and modify the characteristics so that at larger heliocentric distances, these disturbances appear as radially propagating concentric shells of compressed magnetic fields and enhanced fluctuations B.G.

N87-24254*# New Hampshire Univ., Durham. Dept. of Physics.
COSMIC RAYS IN THE HELIOSPHERE c93
William R. Webber *In* NASA Goddard Space Flight Center, Greenbelt, Md. Essays in Space Science Jun. 1987 p 125-154 (For primary document see N87-24247 17-88)
Avail: NTIS HC A18/MF A01 CSCL 03B

The different types of cosmic ray particles and their role in the heliosphere are briefly described. The rates of various energetic particles were examined as a function of time and used to derive various differential energy gradients. The Pioneer and Voyager cosmic ray observations throughout the heliosphere are indeed giving a perspective on the three-dimensional character and size of the heliosphere. Most clearly the observations are emphasizing the role that transient variations in the outer heliosphere, and most likely the heliospheric boundary shock, play in the 11 year solar cycle modulation of cosmic rays. B.G.

N87-24255*# National Aeronautics and Space Administration. Goddard Space Flight Center, Greenbelt, Md.
ANTIPROTONS IN COSMIC RAYS c93
V. K. Balasubrahmanyan, J. F. Ormes, and R. E. Streitmatter *In its* Essays in Space Science Jun. 1987 p 155-172 (For primary document see N87-24247 17-88)
Avail: NTIS HC A18/MF A01 CSCL 03B

Recent experimental observations and results are discussed. It was found that the approximately 50 antiprotons collected in balloon experiments to date have generated considerable theoretical interest. Clearly, confirmatory experiments and measurements over an extended energy range are required before definite conclusions are drawn. Antiproton measurements have a bearing on astrophysical problems ranging from cosmic ray propagation to issues of cosmological import. The next generation of balloon experiments and the Particle Astrophysics Magnet Facility being discussed for operation on NASA's space station should provide data and insights of highest interest. B.G.

N87-24256*# Washington Univ., St. Louis, Mo. Dept. of Physics and the McDonnell Center for the Space Sciences.
MEASUREMENTS OF ULTRAHEAVY COSMIC RAYS WITH HEAO-3 c93
W. R. Binns, M. H. Israel, J. Klarmann, T. L. Garrard, E. C. Stone, and C. J. Waddington (Minnesota Univ., Minneapolis.) *In* NASA Goddard Space Flight Center, Greenbelt, Md. Essays in Space Science Jun. 1987 p 173-189 (For primary document see N87-24247 17-88)
(Contracts NAS8-27976; NAS8-27977; NAS8-27978; Grants NAG8-498; NAG8-500; NAG8-502; NgR05-002-160; NgR24-005-050; NgR26-008-001)
Avail: NTIS HC A18/MF A01 CSCL 03B

The HEAO-3 Heavy Nuclei Experiment has measured abundances of elements from Ar-18 to U-92 in the cosmic rays. The results on the ultraheavy elements, those with atomic numbers greater than 30, indicate that the source of the cosmic rays contain a mixture of r-process and s-process material similar to that found in the solar system. This result is at variance with previous indications that the sources are greatly enhanced with freshly synthesized r-process material. Apparent discrepancies between the results and the accepted solar-system abundance have led to a reexamination of data on photospheric abundances of Ge and Pb, resulting in suggested reductions in their values. Author

N87-24257*# National Aeronautics and Space Administration. Goddard Space Flight Center, Greenbelt, Md.
ORIGIN AND PROPAGATION OF GALACTIC COSMIC RAYS c93
Catherine J. Cesarsky (Commissariat a l'Energie Atomique, Gif-sur-Yvette, France) and Jonathan F. Ormes *In its* Essays in Space Science Jun. 1987 p 191-223 (For primary document see N87-24247 17-88)
Avail: NTIS HC A18/MF A01 CSCL 03B

The study of systematic trends in elemental abundances is important for unfolding the nuclear and/or atomic effects that should govern the shaping of source abundances and in constraining the parameters of cosmic ray acceleration models. In principle, much can be learned about the large-scale distributions of cosmic rays in the galaxy from all-sky gamma ray surveys such as COS-B and SAS-2. Because of the uncertainties in the matter distribution which come from the inability to measure the abundance of molecular hydrogen, the results are somewhat controversial. The leaky-box model accounts for a surprising amount of the data on heavy nuclei. However, a growing body of data indicates that the simple picture may have to be abandoned in favor of more complex models which contain additional parameters. Future experiments on the Spacelab and space station will hopefully be made of the spectra of individual nuclei at high energy. Antiprotons must be studied in the background free environment above the atmosphere with much higher reliability and presion to obtain spectral information. B.G.

N87-24258*# National Aeronautics and Space Administration. Goddard Space Flight Center, Greenbelt, Md.
HIGH ENERGY GAMMA RAY ASTRONOMY c89
Carl E. Fichtel *In its* Essays in Space Science Jun. 1987 p 227-274 (For primary document see N87-24247 17-88)
Avail: NTIS HC A18/MF A01 CSCL 03A

High energy gamma ray astronomy has evolved with the space age. Nonexistent twenty-five years ago, there is now a general sketch of the gamma ray sky which should develop into a detailed picture with the results expected to be forthcoming over the next decade. The galactic plane is the dominant feature of the gamma ray sky, the longitude and latitude distribution being generally correlated with galactic structural features including the spiral arms. Two molecular clouds were already seen. Two of the three strongest gamma ray sources are pulsars. The highly variable X-ray source Cygnus X-3 was seen at one time, but not another in the 100 MeV region, and it was also observed at very high energies. Beyond the Milky Way Galaxy, there is seen a diffuse radiation, whose origin remains uncertain, as well as at least one quasar, 3C 273. Looking to the future, the satellite opportunities for high energy gamma ray astronomy in the near term are the GAMMA-I planned to be launched in late 1987 and the Gamma Ray Observatory, scheduled for launch in 1990. The Gamma Ray Observatory will carry a total of four instruments covering the entire energy range from 30,000 eV to 3 x 10 to the 10th eV with over an order of magnitude increase in sensitivity relative to previous satellite instruments. Author

N87-24259*# Jet Propulsion Lab., California Inst. of Tech., Pasadena.
NUCLEOSYNTHESIS AND ASTROPHYSICAL GAMMA RAY SPECTROSCOPY **c93**
Allan S. Jacobson *In* NASA Goddard Space Flight Center, Greenbelt, Md. Essays in Space Science Jun. 1987 p 275-294 (For primary document see N87-24247 17-88)
Avail: NTIS HC A18/MF A01 CSCL 03B

The HEAO-3 gamma ray spectrometer has provided evidence in the quest for the understanding of complex element formation in the universe with the discovery of Al-26 in the interstellar medium. It has demonstrated that the synthesis of intermediate mass nuclei is currently going on in the galaxy. This discovery was confirmed by the Solar Maximum Mission. The flux is peaked near the galactic center and indicates about 3 solar masses of Al-26 in the interstellar medium, with an implied ratio of Al-26/Al-27 = .00001. Several possible distributions were studied but the data gathered thus far do not allow discrimination between them. It is felt that only the spaceflight of a high resolution gamma ray spectrometer with adequate sensitivity will ultimately resolve the issue of the source of this material. B.G.

N87-24260*# National Aeronautics and Space Administration. Goddard Space Flight Center, Greenbelt, Md.
GAMMA RAY TRANSIENTS **c93**
Thomas L. Cline *In its* Essays in Space Science Jun. 1987 p 295-316 (For primary document see N87-24247 17-88)
Avail: NTIS HC A18/MF A01 CSCL 03B

The discovery of cosmic gamma ray bursts was made with systems designed at Los Alamos Laboratory for the detection of nuclear explosions beyond the atmosphere. HELIOS-2 was the first gamma ray burst instrument launched; its initial results in 1976, seemed to deepen the mystery around gamma ray transients. Interplanetary spacecraft data were reviewed in terms of explaining the behavior and source of the transients. B.G.

N87-24261*# Space Telescope Science Inst., Baltimore, Md.
DISCRETE X-RAY SOURCES AND THE X-RAY BACKGROUND **c93**
Riccardo Giacconi *In* NASA Goddard Space Flight Center, Greenbelt, Md. Essays in Space Science Jun. 1987 p 317-338 (For primary document see N87-24247 17-88)
Avail: NTIS HC A18/MF A01 CSCL 03B

Since the discovery of a highly uniform X-ray background (XRB) in the 2 to 10 keV range, its nature is not yet fully explained. It appears clear from the results of Einstein medium and deep surveys that at least 50% of the XRB is due to individual extragalactic sources when their contribution is integrated to Z = 3. This includes contribution from Quasi Stellar Objects (QSOs), Active Galactic Nuclei (AGNs), galaxies, and clusters of galaxies. The average spectrum of each of the individual contributing sources is softer than that of the observed XRB. Therefore, the remaining contribution must have a rather hard spectrum of alpha nearly equal to 0.0 to 0.2. It is unlikely that this spectrum can be produced by diffuse processes. Therefore, the remainder of the XRB must be due to individual sources with the appropriate spectrum. This requires either that the spectrum of the already identified sources changes at early epochs or a new class of objects. Advanced X-ray Astrophysics Facility (AXAF) observations will extend survey sensitivity to limiting fluxes of order of 3 x 10 to the minus 16 erg/sq cm/s, some 50 times fainter than any previous survey. There will be sufficient sensitivity and angular resolution to permit identification and study of these objects. Author

N87-24262*# National Aeronautics and Space Administration. Goddard Space Flight Center, Greenbelt, Md.
THE COSMIC X-RAY BACKGROUND **c93**
Elihu A. Boldt *In its* Essays in Space Science Jun. 1987 p 339-378 (For primary document see N87-24247 17-88)
Avail: NTIS HC A18/MF A01 CSCL 03B

The present knowledge about the overall spectrum of the isotropic extragalactic background of electromagnetic radiation is summarized. The role of the HEAO program is discussed. Spectral measurements from HEAO are examined. B.G.

N87-24263*# National Aeronautics and Space Administration. Goddard Space Flight Center, Greenbelt, Md.
X-RAY ASTRONOMICAL SPECTROSCOPY **c89**
Stephen S. Holt *In its* Essays in Space Science Jun. 1987 p 379-394 (For primary document see N87-24247 17-88)
Avail: NTIS HC A18/MF A01 CSCL 03A

The contributions of the Goddard group to the history of X-ray astronomy are numerous and varied. One role that the group has continued to play involves the pursuit of techniques for the measurement and interpretation of the X-ray spectra of cosmic sources. The latest development is the selection of the X-ray microcalorimeter for the Advanced X-ray Astrophysics Facility (AXAF) study payload. This technology is likely to revolutionize the study of cosmic X-ray spectra. Author

N87-24264*# National Aeronautics and Space Administration. Goddard Space Flight Center, Greenbelt, Md.
INFRARED ASTRONOMY **c89**
Michael G. Hauser *In its* Essays in Space Science Jun. 1987 p 395-401 (For primary document see N87-24247 17-88)
Avail: NTIS HC A18/MF A01 CSCL 03A

The role and contributions of Frank McDonald in extending high energy astrophysics to the sub-eV photon energy range (in putting infrared astronomy into orbit) are discussed. B.G.

89 ASTRONOMY

Includes radio, gamma-ray, and infrared astronomy, and astrometry.

N87-24265# Columbia Univ., New York. Astrophysics Lab.
A PROGRAM OF GROUND-BASED ASTRONOMY TO COMPLEMENT EINSTEIN OBSERVATIONS Final Report, 1 Oct. 1981 - 30 Sep. 1986
David J. Helfand Dec. 1986 14 p
(Grant AF-AFOSR-0014-82)
(AD-A179331; CAL-1629; AFOSR-87-0503TR) Avail: NTIS HC A02/MF A01 CSCL 03A

Our program of multiwavelength observational investigations and their attendant interpretive studies concerning problems in stellar coronae, supernova, remnants, and neutron star astrophysics continued in FY 86. A variety of important projects have been undertaken, several of which reached completion in the last year of the five-year period (1 October 1981 to 30 September 1986), including the compilation of the complete X-ray flux-limited sample of M stars, a study of small scale anisotropy of the extragalactic X-ray background, and a definitive paper on the new class of composite SNRs. A total of 26 papers presenting the results of the program were published or accepted for publication in the technical literature, as well as six review articles for conference proceedings. A total of 35 presentations were given at regional, national, and international meetings by the principal investigator, two co-investigators, and/or the six graduate students supported under this program. In addition, radio and optical observations under several existing proposals were conducted and more than twenty new proposals were prepared, the majority of which have already been accepted. Author (GRA)

N87-24266*# National Aeronautics and Space Administration, Washington, D.C.
STAR FORMATION IN GALAXIES
May 1987 755 p Conference held in Pasadena, Calif., 16-19 Jun. 1986
(NASA-CP-2466; NAS 1.55:2466) Avail: NTIS HC A99/MF E03 CSCL 03A

Topics addressed include: star formation; galactic infrared emission; molecular clouds; OB star luminosity; dust grains; IRAS observations; galactic disks; stellar formation in Magellanic clouds; irregular galaxies; spiral galaxies; starbursts; morphology of galactic

centers; and far-infrared observations. For individual titles, see N87-24267 through N87-24376.

N87-24267*# California Inst. of Tech., Pasadena. Dept. of Astronomy.
HIGH MASS STAR FORMATION IN THE GALAXY c90
N. Z. Scoville and J. C. Good *In* NASA, Washington Star Formation in Galaxies May 1987 p 3-20 (For primary document see N87-24266 17-89)
(Grant NSF AST-84-12473)
Avail: NTIS HC A99/MF E03 CSCL 03B

The Galactic distributions of HI, H2, and HII regions are reviewed in order to elucidate the high mass star formation occurring in galactic spiral arms and in active galactic nuclei. Comparison of the large scale distributions of H2 gas and radio HII regions reveals that the rate of formation of OB stars depends on (n sub H2) sup 1.9 where (n sub H2) is the local mean density of H2 averaged over 300 pc scale lengths. In addition the efficiency of high mass star formation is a decreasing function of cloud mass in the range 200,000 to 3,000,000 solar mass. These results suggest that high mass star formation in the galactic disk is initiated by cloud-cloud collisions which are more frequent in the spiral arms due to orbit crowding. Cloud-cloud collisions may also be responsible for high rates of OB star formation in interacting galaxies and galactic nuclei. Based on analysis of the Infrared Astronomy Satellite (IRAS) and CO data for selected GMCs in the Galaxy, the ratio L sub IR/M sub H2 can be as high as 30 solar luminosity/solar mass for GMCs associated with HII regions. The L sub IR/M sub H2 ratios and dust temperature obtained in many of the high luminosity IRAS galaxies are similar to those encountered in galactic GMCs with OB star formation. High mass star formation is therefore a viable explanation for the high infrared luminosity of these galaxies. Author

N87-24268*# Ecole Normale Superieure, Paris (France). Radioastronomie.
DIFFUSE INFRARED EMISSION OF THE GALAXY: LARGE SCALE PROPERTIES Abstract Only c93
J. L. Puget, M. Perault, F. Boulanger, and E. Falgarone *In* NASA, Washington Star Formation in Galaxies May 1987 p 21 (For primary document see N87-24266 17-89)
Avail: NTIS HC A99/MF E03 CSCL 03B

A quantitative analysis of Infrared Astronomy Satellite (IRAS) data in the galactic plane shows that: about 66% of the power radiated in the 100 micron band comes from the diffuse medium, the other 33% coming from well identified luminous sources. The diffuse emission has almost constant colors throughout the Galaxy, similar to the local cirrus colors. The sources have a much lower 12 micron/25 micron and a much high 60 micron/100 micron emission ratio than the diffuse component, giving a very striking anticorrelation in the color-color diagrams. The separation between one narrow and a second broader component shows that the molecular component does not provide much more than one half of the diffuse emission in the molecular ring: this implies a 4 pi nul(nu) emissivity at 100 microns for the atomic component of about 2.4 x 10 to the minus 30th watts per H atom, 10 times higher than the emissivity of the molecular component at the same galactocentric radius. The atomic component emissivity measures the interstellar radiation field density. The temperature distribution of the 2 components is discussed comparing IRAS data with measures of the 900 micron emission of the galactic plane, which appears to be dominated by cold dust in the narrow component. Author

N87-24269*# Max-Planck-Inst. fuer Radioastronomie, Bonn (West Germany).
THE ORIGIN OF THE DIFFUSE GALACTIC IR/SUBmm EMISSION: REVISITED AFTER IRAS c93
P. Cox and P. G. Mezger *In* NASA, Washington Star Formation in Galaxies May 1987 p 23-35 (For primary document see N87-24266 17-89)
Avail: NTIS HC A99/MF E03 CSCL 03B

Balloon observations are compared with Infrared Astronomy Satellite observations. There was good agreement for the longitudinal profiles. However, the dust emission observed by IRAS, contrary to the balloon observations which show dust emission only within the absolute value of b is equal to or less than 3 degrees, extends all the way to the galactic pole. The model fits were repeated using more recent parameters for the distribution of interstellar matter in the galactic disk and central region. The IR luminosities are derived for the revised galactic distance scale of solar radius - 8.5 Kpc. A total IR luminosity of 1.2 E10 solar luminosity is obtained, which is about one third of the estimated stellar luminosity of the Galaxy. The dust emission spectrum lambdal(sub lambda) attains it maximum at 100 microns. A secondary maximum in the dust emission spectrum occurs at 10 microns, which contains 15% of the total IR luminosity of the Galaxy. The galactic dust emission spectrum was compared with the dust emission spectra of external IRAS galaxies. The warm dust luminosity relates to the present OB star formation rate, while flux densities observed at longer submm wavelengths are dominated by cold dust emission and thus can be used to estimate gas masses. B.G.

N87-24270*# State Univ. of New York, Stony Brook. Astronomy Program.
MASSES, LUMINOSITIES AND DYNAMICS OF GALACTIC MOLECULAR CLOUDS c90
P. M. Solomon, A. R. Rivolo, T. J. Mooney, J. W. Barrett, and L. J. Sage *In* NASA, Washington Star Formation in Galaxies May 1987 p 37-59 (For primary document see N87-24266 17-89)
Avail: NTIS HC A99/MF E03 CSCL 03B

Star formation in galaxies takes place in molecular clouds and the Milky Way is the only galaxy in which it is possible to resolve and study the physical properties and star formation activity of individual clouds. The masses, luminosities, dynamics, and distribution of molecular clouds, primarily giant molecular clouds in the Milky Way are described and analyzed. The observational data sets are the Massachusetts-Stony Brook CO Galactic Plane Survey and the IRAS far IR images. The molecular mass and infrared luminosities of glactic clouds are then compared with the molecular mass and infrared luminosities of external galaxies. Author

N87-24271*# Washington Univ., Seattle. Dept. of Astronomy.
IRAS COLORS OF VLA IDENTIFIED OBJECTS IN THE GALAXY
Michel Fich and Susan Terebey (National Center for Atmospheric Research, Boulder, Colo.) *In* NASA, Washington Star Formation in Galaxies May 1987 p 63-66 (For primary document see N87-24266 17-89)
Avail: NTIS HC A99/MF E03 CSCL 03A

Infrared Astronomy Satellite (IRAS) sources found within 4 degrees of l = 125 deg, b = 2 deg on the 3rd HCON 60 micron Sky Brightness Images were observed at the Very Large Array (VLA). Regions were to be identified where massive stars are forming by looking for small areas of radio continuum emissions. The IRAS sources could be divided into three groups by their IRAS 12 micron/25 micron and 60 micron/100 micron color. The group identified with star forming regions contained essentially all of the objects with extended radio emission. In all of these cases the extended radio emission showed a morphology consistent with the identification of these objects as HII regions. The conclusion drawn is that star formation regions can be distinguished from other objects by their infrared colors. Author

N87-24272*# National Aeronautics and Space Administration. Goddard Inst. for Space Studies, New York, N.Y.
STAR FORMATION IN CARINA OB1: OBSERVATIONS OF A GIANT MOLECULAR CLOUD ASSOCIATED WITH THE ETA CARINAE NEBULA c90
D. A. Grabelsky, R. S. Cohen (Columbia Univ., New York.), and P. Thaddeus *In* NASA, Washington Star Formation in Galaxies May 1987 p 67-70 (For primary document see N87-24266 17-89)
Avail: NTIS HC A99/MF E03 CSCL 03B

17-89)
Avail: NTIS HC A99/MF E03 CSCL 03B

A giant molecular cloud associated with the eta Carinae nebula was fully mapped in CO with the Columbia Millimeter-Wave Telescope at Cerro Tololo. The cloud comples has a mass of roughly 700,000 solar mass and extends about 140 pc along the Galactic plane, with the giant Carina HII region situated at one end of the complex. Clear evidence of interaction between the HII region and the molecular cloud is found in the relative motions of the ionized gas, the molecular gas, and the dust; simple energy and momentum considerations suggest that the HII region is responsible for the observed motion of a cloud fragment. The molecular cloud complex appears to be the parent material of the entire Car OB1 Association which, in addition to the young clusters in the Carine nebula, includes the generally older cluster NGC 3325, NGC 3293, and IC 2581. The overall star formation efficiency in the cloud complex is estimated to be approximately 0.02.
Author

N87-24273*# Jet Propulsion Lab., California Inst. of Tech., Pasadena.
STAR FORMING REGIONS OF THE SOUTHERN GALAXY c90
T. B. H. Kuiper, J. B. Whiteoak, and J. W. Fowler (California Inst. of Tech., Pasadena.) *In* NASA, Washington Star Fromation in Galaxies May 1987 p 71-74 Sponsored by JPL (For primary document see N87-24266 17-89)
Avail: NTIS HC A99/MF E03 CSCL 03B

A catalog of southern dust cloud properties is being compiled to aid in the planning and analysis of radio spectral line surveys in the southern hemisphere. Ultimately, images of dust temperature and column density will be produced. For the interim, a list of the 60 and 100 micron fluxes was prepared for the cores and adjacent backgrounds of 65 prominent dust clouds. Dust temperatures and column densities were derived.
Author

N87-24274*# National Aeronautics and Space Administration. Goddard Space Flight Center, Greenbelt, Md.
ON THE REDISTRIBUTION OF OB STAR LUMINOSITY AND THE WARMING OF NEARBY MOLECULAR CLOUDS
D. Leisawitz *In* NASA, Washington Star Formation in Galaxies May 1987 p 75-78 (For primary document see N87-24266 17-89)
Avail: NTIS HC A99/MF E03 CSCL 03A

Infrared Astronomy Satellite (IRAS) observations of the neighborhoods of six outer-Galaxy HII regions were combined with CO observations to show that most of the far infrared (FIR) luminosity from within approximately 25 to 75 pc of the ionizing stars is contributed by dust in molecular clouds, not by dust in the low-density ionized gas. Dust associated with the clouds is warmed by absorption of UV and visible light from the cluster of stars responsible for the ionization. Most of the OB cluster starlight is not absorbed locally. A fraction of the order of 10% of the OB cluster luminosity is absorbed by nearby molecular clouds and reradiated as FIR light. The luminosity per unit mass for the heated clouds is approximately 3 to 13 solar luminosity/solar mass, approximately one order of magnitude greater than the corresponding ratio for clouds found near clusters without O stars, and two orders of magnitude greater than the ratio for dark clouds heated primarily by the interstellar radiation field. If the observations of clouds near outer-Galaxy HII regions are used to characterize the molecular clouds heated by HII regions in the inner-Galaxy, then at most 30% of the Galaxy's molecular cloud mass is actively engaged in the formation of massive stars at the present time.
Author

N87-24275*# California Inst. of Tech., Pasadena. Div. of Physics, Mathematics and Astronomy.
MAPS OF MILLIMETER WAVE EMISSION FROM THREE GALACTIC STAR-FORMING REGIONS c93
Mary Barsony *In* NASA, Washington Star Formation in Galaxies May 1987 p 79-82 (For primary document see N87-24266 17-89)
(Grants NSF AST-84-12473; NSF AST-84-03054)
Avail: NTIS HC A99/MF E03 CSCL 03B

In order to investigate the gas dynamics around young stellar objects, three sources were mapped which exhibit supersonic velocities in the 115 GHZ, J = 1-0 transition of CO. The maps, made with the Owens Valley Radio Observatory Millimeter Interferometer, are the highest spatial resolution images currently available of millimeter-wave continuum and line emission from the sources S106, S87, and LkHalpha101. Observations were made in the CS (J = 2-1) and C-13O (J = 1-0) transitions. In all the sources, the observations indicate that the ionized stellar wind is sweeping up ambient molecular gas. The molecular gas is found adjacent to the outer edges of the ionized winds, which originate in embedded infrared sources. From the observations presented, it may be inferred that the outflowing ionized winds are channeled by the surrounding dense, neutral gas.
Author

N87-24276*# Groningen Rijksuniversiteit (Netherlands). Lab. for Space Research.
SHOCK HEATED DUST IN L1551: L(IR) GREATER THAN 20 SOLAR LUMINOSITIES c90
F. O. Clark, R. J. Laureijs, G. Chlewicki, C. Y. Zhang, W. vanOosterom, and D. Kester *In* NASA, Washington Star Formation in Galaxies May 1987 p 83-86 (For primary document see N87-24266 17-89)
Avail: NTIS HC A99/MF E03 CSCL 03B

The infrared bolometric luminosity of the extended emission from the L1551 flow exceeds 20 solar luminosities. Ultraviolet radiation from the shock associated with the flow appears to heat the dust requiring shock temperatures from 10,000 to 90,000 K in L1551, velocities of approximately 50 km/s near the end of the flow, and a minimum mechanical luminosity of approximately 40 solar luminosities. The total energy requirement of the infrared emission over a 10,000 year lifetime is 10 to the 46th to 47th ergs, two orders of magnitude higher than previous estimates for L1551. Infrared radiation offers a method of probing interstellar shocks, by sampling the untraviolet halo surrounding the shock. At least one current model for bipolar flows is capable of meeting the energetic requirements.
Author

N87-24277*# Illinois Univ., Urbana-Champaign. Dept. of Physics.
MECHANISMS FOR THE CIRCULAR POLARIZATION OF ASTROPHYSICAL OH MASERS IN STAR-FORMING REGIONS AND THE INFERRED MAGNETIC FIELDS c90
Shuji Deguchi and William D. Watson *In* NASA, Washington Star Formation in Galaxies May 1987 p 87-90 Sponsored by NSF (For primary document see N87-24266 17-89)
Avail: NTIS HC A99/MF E03 CSCL 03B

Results of further calculations to explore the cause for the circular polarization of astrophysical OH masers in regions of star formation are presented. Calculations are given for both the nonlinear, Zeeman overlap mechanishm, and the Cook mechanism. The previous result that magnetic field strengths of a few milligauss or greater are required, still survives.
Author

N87-24278*# Centre National de la Recherche Scientifique, Toulouse (France). Centre d'Etude Spatiales des Rayonnements.
SURVEY OF THE GALACTIC DISK FROM 1 = -150 DEG TO 1 = 82 DEG IN THE SUBMILLIMETER RANGE c93
Emmanuel Caux and Guy Serra *In* NASA, Washington Star Formation in Galaxies May 1987 p 93-96 Original language document was announced in IAA as A87-17077 (For primary document see N87-24266 17-89)
Avail: NTIS HC A99/MF E03 CSCL 03B

The first almost complete survey of the galactic disk from 1 = -150 deg to 1 = 82 deg in the submillimeter range (effective wavelength = 380 microns), performed with the AGLAE balloon-borne instrument modified to include a submillimeter channel, is reported. The instrumentation and observational procedures are described, as are the signal processing and calibration. The results are presented as a profile of the submillimeter brightness of the galactic disk displayed as a function

of the galactic longitude. This profile exhibits diffuse emission all along the disk with bright peaks associated with resolved sources. The averaged galactic spectrum is in agreement with a temperature distribution of the interstellar cold dust. IAA

N87-24279*# Ecole Normale Superieure, Paris (France). Radioastronomie

DIFFUSE INFRARED EMISSION OF THE GALAXY: LARGE SCALE PROPERTIES **c93**

M. Perault, F. Boulanger, E. Falgarone, and J. L. Puget *In* NASA, Washington Star Formation in Galaxies May 1987 p 97 Prepared in cooperation with California Inst. of Tech., Pasadena (For primary document see N87-24266 17-89)

Avail: NTIS HC A99/MF E03 CSCL 03B

The Infrared Astronomy Satellite (IRAS) survey is used to study large scale properties and the origin of the diffuse emission of the Galaxy. A careful subtraction of the zodiacal light enables longitude profiles of the galactic emission at 12, 25, 60, and 100 microns to be presented. Author

N87-24280*# National Aeronautics and Space Administration. Goddard Space Flight Center, Greenbelt, Md.

THE LARGE SCALE GAS AND DUST DISTRIBUTION IN THE GALAXY: IMPLICATIONS FOR STAR FORMATION **c90**

T. J. Sodroski, E. Dwek, M. G. Hauser, and F. J. Kerr (Maryland Univ., College Park.) *In* NASA, Washington Star Formation in Galaxies May 1987 p 99-102 (For primary document see N87-24266 17-89)

Avail: NTIS HC A99/MF E03 CSCL 03B

Infrared Astronomy Observations are presented for the diffuse infrared (IR) emissions from the galactic plane at wavelengths of 60 and 100 microns and the total far infrared intensity and its longitudinal variations in the disk were derived. Using available CO, 5 GHz radio-continuum, and HI data, the IR luminosity per hydrogen mass and the ingrared excess (IRE) ratio in the Galaxy were derived. The longitudinal profiles of the 60 and 100 micron emission were linearly decomposed into three components that are associated with molecular (H2), neutral (HI), and ionized (HII) phases in the interstellar medium (ISM), and the relevant dust properties were derived in each phase. Implications of the findings for various models of the diffuse IR emisison and for star formation in the galactic disk are discussed. Author

N87-24281*# National Center for Atmospheric Research, Boulder, Colo. High Altitude Observatory.

A CORRELATION BETWEEN THE IRAS INFRARED CIRRUS AT 60 OR 100 MICRONS AND NEUTRAL ATOMIC HYDROGEN IN THE OUTER GALAXY

Susan Terebey and Michel Fich (Washington Univ., Seattle.) *In* NASA, Washington Star Formation in Galaxies May 1987 p 103-105 (For primary document see N87-24266 17-89)

Avail: NTIS HC A99/MF E03 CSCL 03A

A linear correlation was found between the infrared cirrus at 100 or 60 microns and neutral atomic hydrogen near the galactic plane. Infrared Astronomy Satellite (IRAS) Sky Brightness images were compared to the 0.5 deg resolution Weaver-Williams HI survey in two regions of the outer Galaxy near $l = 125$ deg and $l = 215$ deg. The dust temperature inferred is nearly uniform and in reasonable agreement with theoretical predictions of thermal dust emission. Author

N87-24282*# Rutherford High Energy Lab., Chilton (England).

THE ARP RING: GALACTIC OR EXTRAGALACTIC?

J. A. Abolins and W. L. Rice (California Inst. of Tech., Pasadena.) *In* NASA, Washington Star Formation in Galaxies May 1987 p 107-110 (For primary document see N87-24266 17-89)

Avail: NTIS HC A99/MF E03 CSCL 03A

The Arp Ring is a faint, loop-like structure around the northern end of M81 which becomes apparent only on deep optical photographs of the galaxy. The nature of the Ring and its proximity to M81 are uncertain. Is it simply foreground structure, part of this galaxy, or is it within the M81 system? Infrared Astronomy Satellite (IRAS) maps of the region show a far-infrared counterpart of the Ring. The infrared data are compared with previous optical and radio observations to try to ascertain its physical nature. The poor correlation found between the common infrared/optical structure and the distribution of extragalactic neutral hydrogen, and the fact that its infrared properties are indistinguishable from those of nearby galactic cirrus, imply that the Arp Ring is simply a ring structure in the galactic cirrus. Author

N87-24283*# Groningen Rijksuniversiteit (Netherlands). Lab. for Space Research.

INFRARED PROPERTIES OF DUST GRAINS DERIVED FROM IRAS OBSERVATIONS

G. Chlewicki, R. J. Laureijs, I. O. Clark (Kentucky Univ., Lexington.), and P. R. Wesselius *In* NASA, Washington Star Formation in Galaxies May 1987 p 113-116 (For primary document see N87-24266 17-89)

Avail: NTIS HC A99/MF E03 CSCL 03A

The analysis of several diffuse interstellar clouds observed by the Infrared Astronomy Satellite (IRAS) is presented. The 60/100 micron flux ratios appear to be nearly constant in clouds with up to 1 sup m visual extinction at the center. Observations of a highly regular cloud in Chamaeleon show that the 12/100 micron ratio peaks at an intermediate radial distance and declines towards the center of the cloud. These observations indicate that nonequilibrium emission accounts only for the 12 and 25 micron bands; strong emission observed at the 60 micron band is probably due to equilibrium thermal radiation. The correlation of the 12 micron emission with a red excess observed for a high latitude cloud, L1780, is shown to be consistent with the assumption that both features are due to fluorescence by the same molecular species. Author

N87-24284*# Max-Planck-Inst. fuer Radioastronomie, Bonn (West Germany).

IRAS OBSERVATIONS OF THE PLEIADES

P. Cox and A. Leene (Kapteyn Astronomical Lab., Groningen, Netherlands) *In* NASA, Washington Star Formation in Galaxies May 1987 p 117-121 (For primary document see N87-24266 17-89)

Avail: NTIS HC A99/MF E03 CSCL 03A

The Infrared Astronomy Satellite (IRAS) observations of the Pleiades region are reported. The data show large flux densities at 12 and 25 microns, extended over the optical nebulosity. This strong excess emission, implying temperatures of a few hundred degrees Kelvin, indicates a population of very small grains in the Pleiades. It is suggested that these grains are similar to the small grains needed to explain the surface brightness measurements made in the ultraviolet. Author

N87-24285*# Hawaii Univ., Honolulu. Inst. for Astronomy.

STAR FORMATION IN NORMAL GALAXIES **c80**

C. G. Wynn-Williams *In* NASA, Washington Star Formation in Galaxies May 1987 p 125-131 (For primary document see N87-24266 17-89)

(Grant NSF AST-84-18197)

Avail: NTIS HC A99/MF E03 CSCL 03B

The ways in which recent infrared observations, particularly by the Infrared Astronomy Satellite (IRAS), have influenced ideas about star formation in normal galaxies, are discussed. B.G.

N87-24286*# London Univ. (England). Theoretical Astronomy Unit.

MODELS FOR INFRARED EMISSION FROM IRAS GALAXIES **c93**

M. Rowan-Robinson *In* NASA, Washington Star Formation in Galaxies May 1987 p 133-152 (For primary document see N87-24266 17-89)

Avail: NTIS HC A99/MF E03 CSCL 03B

Models for the infrared emission from Infrared Astronomy Satellite (IRAS) galaxies by Rowan-Robinson and Crawford, by deJong and Brink, and by Helou, are reviewed. Rowan-Robinson and Crawford model the 12 to 100 micron radiation from IRAS galaxies in terms of 3 components: a normal disk component,

due to interstellar cirrus; a starburst component, modeled as hot stars in an optically thick dust cloud; and a Seyfert component, modeled as a power-law continuum immersed in an n(r) variation r sup -1 dust cloud associated with the narrow-line region of the Seyfert nucleus. The correlations between the luminosities in the different components, the blue luminosity, and the X-ray luminosity of the galaxies are consistent with the model. Spectra from 0.1 to 1000 microns are predicted and compared with available observations. The de Jong and Brink, and Helou, model IRAS non-Seyfert galaxies in terms of a cool (cirrus) component and a warm (starburst) component. The de Jong and Brink estimate the face-on internal extinction in the galaxies and find that it is higher in galaxies with more luminous starbursts. In Helou's model the spectrum of the warm component varies strongly with the luminosity in that component. The three models are briefly compared.
Author

N87-24287*# California Inst. of Tech., Pasadena. Infrared Processing and Analysis Center.
ON THE ORIGIN OF THE 40-120 MICRON EMISSION OF GALAXY DISKS: A COMPARISON WITH H-ALPHA FLUXES **c90**
Carol J. Lonsdale Persson and George Helou *In* NASA, Washington Star Formation in Galaxies May 1987 p 153-160 Sponsored by JPL (For primary document see N87-24266 17-89)
Avail: NTIS HC A99/MF E03 CSCL 03B
A comparison of 40 to 120 micron Infrared Astronomy Satellite (IRAS) fluxes with published H alpha and UBV photometry shows that the far infrared emission of galaxy disks consists of at least two components: a warm one associated with OB stars in HII-regions and young star-forming complexes, and a cooler one from dust in the diffuse, neutral interstellar medium, heated by the more general interstellar radiation field of the old disk population (a cirrus-like component). Most spiral galaxies are dominated by emission from the cooler component in this model. A significant fraction of the power for the cool component must originate with non-ionizing stars. For a normal spiral disk there is a substantial uncertainty in a star formation rate derived using either the H alpha or the far infrared luminosity. Author

N87-24288*# Kitt Peak National Observatory, Tucson, Ariz.
STAR FORMATION IN THE MAGELLANIC CLOUDS **c90**
Jay A. Frogel *In* NASA, Washington Star Formation in Galaxies May 1987 p 161-166 (For primary document see N87-24266 17-89)
Avail: NTIS HC A99/MF E03 CSCL 03B
Because of their proximity, the Magellanic Clouds provide the opportunity to conduct a detailed study of the history and current state of star formation in dwarf irregular galaxies. There is considerable evidence that star formation in the Clouds was and is proceeding in a manner different from that found in a typical well-ordered spiral galaxy. Star formation in both Clouds appears to have undergone a number of relatively intense bursts. There exist a number of similarities and differences in the current state of star formation in the Magellanic Clouds and the Milky Way. Examination of Infrared Astronomy Satellite (IRAS) sources with ground based telescopes allows identification of highly evolved massive stars with circumstellar shells as well as several types of compact emission line objects. Author

N87-24289*# Kitt Peak National Observatory, Tucson, Ariz.
MEASURING STAR FORMATION RATES IN BLUE GALAXIES **c90**
John S. Gallagher, III and Deidre A. Hunter (Carnegie Institution of Washington, D. C.) *In* NASA, Washington Star Formation in Galaxies May 1987 p 167-177 Sponsored in part by JPL (For primary document see N87-24266 17-89)
Avail: NTIS HC A99/MF E03 CSCL 03B
The problems associated with measurements of star formation rates in galaxies are briefly reviewed, and specific models are presented for determinations of current star formation rates from H alpha and Far Infrared (FIR) luminosities. The models are applied to a sample of optically blue irregular galaxies, and the results are discussed in terms of star forming histories. It appears likely that typical irregular galaxies are forming stars at nearly constant rates, although a few examples of systems with enhanced star forming activity are found among HII regions and luminous irregular galaxies. Author

N87-24290*# Tokyo Univ. (Japan). Dept. of Astronomy.
CO OBSERVATIONS OF GALAXIES WITH THE NOBEYAMA 45-M TELESCOPE
Y. Sofue, T. Handa, M. Hayashi, and N. Nakai (Nobeyema Solar Radio Observatory, Japan) *In* NASA, Washington Star Formation in Galaxies May 1987 p 179-196 (For primary document see N87-24266 17-89)
Avail: NTIS HC A99/MF E03 CSCL 03A
High-resolution (15 inch), filled aperture maps of the CO (J = 1-0) line emission were obtained for several nearby, CO-bright galaxies like M82, M83, IC342, and NGC891 in order to study star forming activity in these galaxies. Author

N87-24291*# Massachusetts Univ., Amherst. Dept. of Physics and Astronomy.
CO OBSERVATIONS OF NEARBY GALAXIES AND THE EFFICIENCY OF STAR FORMATION
Judith S. Young *In* NASA, Washington Star Formation in Galaxies May 1987 p 197-215 Sponsored by JPL (For primary document see N87-24266 17-89)
(Grant NSF AST-82-12252)
Avail: NTIS HC A99/MF E03 CSCL 03A
The CO distributions and total molecular content of 160 galaxies were observed using the 14 meter millimeter telescope of the FCRAO. For the luminous, relatively face-on Sc galaxies, the azimuthally averaged CO distributions are centrally peaked, while for the Sb and Sa galaxies the Co distributions often exhibit central CO holes up to 5 kpc across. None of the Sc galaxies have CO distributions which resemble the Milky Way. A general correlation was found between total CO and IR luminosities in galaxies. The scatter in this relation is highly correlated with dust temperature. No strong correlation of IR luminosities was found with HI masses, and it was thereby concluded that the infrared emission is more directly tied to the molecular content of galaxies. It is suggested that galaxies which have high Star Formation Effiencies (SFEs) produce more stars per unit molecular mass, thereby increasing the average temperature of the dust in the star forming regions. Irregular galaxies and galaxies previously identified as mergers have the highest observed star formation efficiencies. For the mergers, evidence was found that the IR/CO luminosity ratio increases with the merger age estimated by Joseph and Wright (1985). Author

N87-24292*# Max-Planck-Inst. fuer Radioastronomie, Bonn (West Germany).
SUBmm OBSERVATIONS OF IRAS GALAXIES Abstract Only
R. Chini, E. Kreysa, E. Kruegel, and P. G. Mezger *In* NASA, Washington Star Formation in Galaxies May 1987 p 217 (For primary document see N87-24266 17-89)
Avail: NTIS HC A99/MF E03 CSCL 03A
Twenty-six galaxies from the Infrared Astronomy Satellite (IRAS) point source catalog were observed at 250 and 1300 microns. The Far Infrared (FIR) spectra from 25 to 1300 microns are interpreted in terms of two dust components of about 16 and 53 K. Flux densities at 1300 microns are used to estimate the total gas mass M sub g. The warm dust luminosity L sup W is considered to be proportional to M sub g sup 0.9 in the mass range 3 x 10 to the 8th is equal to or less than M sub g/solar mass is equal to or less than 10 to the 12th power. The efficiency of star formation seems to be four times higher in barred and peculiar galaxies than in Sc types. Author

N87-24293*# Hawaii Univ., Honolulu. Inst. for Astronomy.
STELLAR BARS AND THE SPATIAL DISTRIBUTION OF INFRARED LUMINOSITY
Nicholas Devereux *In* NASA, Washington Star Formation in

Galaxies May 1987 p 219-226 (For primary document see N87-24266 17-89)
Avail: NTIS HC A99/MF E03 CSCL 03A

Ground-based 10 micron observations of the central region of over 100 infrared luminous galaxies are presented. A first order estimate of the spatial distribution of infrared emission in galaxies is obtained through a combination of ground-based and Infrared Astronomy Satellite (IRAS) data. The galaxies are nearby and primarily noninteracting, permitting an unbiased investigation of correlations with Hubble type. Approximately 40% of the early-type barred galaxies in this sample are associated with enhanced luminosity in the central (approximately 1 kpc diameter) region. The underlying luminosity source is attributed to both Seyfert and star formation activity. Late-type spirals are different in that the spatial distribution of infrared emission and the infrared luminoisty are not strongly dependent on barred morphology. Author

N87-24294*# Ohio State Univ., Columbus. Dept. of Physics.
STAR FORMATION AND SPIRAL STRUCTURE IN M81 c90
Michele Kaufman and Frank N. Bash (Texas Univ., Austin.) *In* NASA, Washington Star Formation in Galaxies May 1987 p 227-233 (For primary document see N87-24266 17-89)
Avail: NTIS HC A99/MF E03 CSCL 03B

High resolution digitized images of M81 in the radio continuum, H alpha, H I, and I band are used to see how well various density wave models agree in detail with observations. It was found that the observed width of the nonthermal radio arms favors a cloudy version of a density wave model. The radial distribution of the set of giant radio H II regions disagrees with the simple expression of Shu and Visser for star formation by a density wave. The observed displacements of the giant radio H II regions from the spiral velocity shock indicate that some revisions in the details of the ballistic particle model of Leisawitz and Bash are necessary. Author

N87-24295*# Netherlands Foundation for Radio Astronomy, Dwingelo.
THE HII REGIONS IN M51: RADIO AND OPTICAL OBSERVATIONS
J. M. vanderHulst and R. C. Kennicutt, Jr. (Minnesota Univ., Minneapolis.) *In* NASA, Washington Star Formation in Galaxies May 1987 p 235-238 (For primary document see N87-24266 17-89)
(Grants NSF AST-84-20374; NATO-82-0592)
Avail: NTIS HC A99/MF E03 CSCL 03A

High resoluton, dual frequency radio observations and calibrated H alpha surface photometry of the spiral galaxy M51 are used to determine the physical properties of the 40 brightest HII region complexes. M51 appears to have a normal HII region population when compared with other nearby Sc galaxies for which good data exist. The radio and H alpha data were used to measure the extinction toward the HII regions. The extinction is very patchy but appears to have a weak trend to become on the average smaller toward large galactocentric radii. This trend is consistent with a possible metallicity gradient in M51. The radio determined extinctions were compared with Balmer decrement extinctions and good agreement was found between the two, contrary to previous studies of M51 and other galaxies. Author

N87-24296*# California Inst. of Tech., Pasadena. Dept. of Physics.
IRAS AND GROUND-BASED OBSERVATIONS OF STAR FORMATION REGIONS IN THE MAGELLANIC CLOUDS c90
Jonathan H. Elias and Jay A. Frogel (Kitt Peak National Observatory, Tucson, Ariz.) *In* NASA, Washington Star Formation in Galaxies May 1987 p 241-246 Sponsored in part by NSF (For primary document see N87-24266 17-89)
Avail: NTIS HC A99/MF E03 CSCL 03B

The Infrared Astronomy Satellite (IRAS) detected several hundred individual regions of star formation in the Large and Small Magellanic Clouds. Nearly two dozen of the brightest such sources were searched for from the ground at 10 microns; most of these were located and measured at wavelengths from 0.6 to 20 microns. Three principle results emerge from this study: First, the IRAS data show that star formation is considerably less active in the SMC than in the LMC, relative either to mass, luminosity, or H I content. The reduced activity in the SMC is consistent with the smaller amount of molecular material inferred from CO observations. Second, the sizes of the objects range from less than a few arcsecs (objects which look like extremely compact HII regions, with little or no extended radio, optical, or infrared emission) to some tens of arcsecs across (giant HII regions, of which the largest and brightest is 30 Doradus). Third, there are no obvious differences in the characteristics of the central portions of the LMC and SMC sources; all look like Galactic H II regions of similar luminosity. Author

N87-24297*# Minnesota Univ., Minneapolis.
STAR FORMATION IN THE LARGE MAGELLANIC CLOUD c90
Terry Jay Jones, A. R. Hyland, and Paul M. Harvey (Texas Univ., Austin.) *In* NASA, Washington Star Formation in Galaxies May 1987 p 245-246 (For primary document see N87-24266 17-89)
Avail: NTIS HC A99/MF E03 CSCL 03B

What role the Large Magellanic Cloud (LMC), a dwarf irregular galaxy, plays in understanding infrared luminous galaxies is discussed. There are two main reasons the LMC may prove helpful. One, the LMC is only 55 kpc away, very nearby compared to much rarer high luminosity systems. Second, the environment in the LMC is distinctly different than in the Milky Way, at least those parts of the Milky Way interior to the sun, where most of the studies of massive star formation were concentrated. The LMC is an interacting system with a large amount of neutral hydrogen that is pushed around by the galaxy's encounter with the Milky Way. Perhaps a good understanding of star formation process in the LMC will provide guidance in the study of the infrared luminous galaxies. Two questions which will be addressed are: how is star formation in the LMC similar to the Milky Way Galaxy, and how is it different? B.G.

N87-24298*# Groningen Rijksuniversiteit (Netherlands). Space Research.
INFRARED EMISSION AND EXCITATION IN LMC HII REGIONS c93
V. Ungerer and F. Viallefond (Observatoire de Paris-Meudon, France) *In* NASA, Washington Star Formation in Galaxies May 1987 p 247-251 (For primary document see N87-24266 17-89)
Avail: NTIS HC A99/MF E03 CSCL 03B

The infrared excess (IRE) of the Large Magellanic Cloud (LMC) HII nebulae is found to correlate positively with the temperature of the ambient radiation field or with the He(+)/H(+) abundance ratio. This result is discussed in terms of a selective absorption of the photons in the range 504 to 912 A relative to the He ionizing photons. This interpretation may explain the paradox of finding highly excited nebulae with only relatively moderate equivalent width of their Balmer lines. Author

N87-24299*# Carnegie Institution of Washington, D. C. Dept. of Terrestrial Magnetism.
IRAS OBSERVATIONS OF IRREGULAR GALAXIES
D. Hunter, W. Rice, J. Gallagher, and F. Gillett (Kitt Peak National Observatory, Tucson, Ariz.) *In* NASA, Washington Star Formation in Galaxies May 1987 p 253-256 Sponsored in part by NASA (For primary document see N87-24266 17-89)
Avail: NTIS HC A99/MF E03 CSCL 03A

Normal irregular galaxies seem to be unusual in having vigorous star formation yet lacking the many dark nebulae typical of spirals. The Infrared Astronomy Satellite (IRAS) observations of a large sample of irregulars are used to explore the dust contents of these galaxies. Compared to normal spirals, the irregulars generally have higher L sub IR/L sub B ratios, warmer f(100)/f(60) dust color temperatures, and lower globally-averaged dust/gas ratios. The relationship between the infrared data and various global optical properties of the galaxies is discussed. Author

N87-24300*# Lowell Observatory, Flagstaff, Ariz.
ERRATUM: IRAS OBSERVATIONS OF IRREGULAR GALAXIES
D. A. Hunter and J. S. Gallagher *In* NASA, Washington Star Formation in Galaxies May 1987 p 257 (For primary document see N87-24266 17-89)
Avail: NTIS HC A99/MF E03 CSCL 03A

In Infrared Astronomy Satellite (IRAS) observations of irregular galaxies, galactic blue luminosities were based on standard optical definitions. The blue luminosities (L sub B) were derived from the blue absolute magnitude (M sub B) or form the in band flux. However, the L sub B system for spiral galaxies was based on quasi-bolometric (rather than in band) fluxes. The formulation and resulting statements are corrected. B.G.

N87-24301*# National Aeronautics and Space Administration, Washington, D.C.
IUE OBSERVATIONS OF LUMINOUS BLUE STAR ASSOCIATIONS IN IRREGULAR GALAXIES
S. A. Lamb, D. A. Hunter, and J. S. Gallagher, III (Kitt Peak National Observatory, Tucson, Ariz.) *In* NASA, Washington Star Formation in Galaxies May 1987 p 259-262 (For primary document see N87-24266 17-89)
(Grant NAG5-404)
Avail: NTIS HC A99/MF E03 CSCL 03A

Two regions of recent star formation in blue irregular galaxies were observed with the IUE in the short wavelength, low dispersion mode. The spectra indicate that the massive star content is similar in these regions and is best fit by massive stars formed in a burst and now approximately 2.5 to 3.0 million years old. Author

N87-24302*# Netherlands Foundation for Radio Astronomy, Dwingelo.
NEUTRAL HYDROGEN AND STAR FORMATION IN IRREGULAR GALAXIES **c90**
Evan D. Skillman *In* NASA, Washington Star Formation in Galaxies May 1987 p 263-266 Sponsored in part by the Netherlands Organization for the Advancement of Pure Research (For primary document see N87-24266 17-89)
Avail: NTIS HC A99/MF E03 CSCL 03B

The Very Large Array and WSTR H I synthesis observations of seven irregular galaxies are presented. The total H I images of four Local Group dwarf irregular galaxies and three larger more distant irregular galaxies are constructed at the identical resolution of 500 pc. When compared to H II region distributions derived from H alpha images, all galaxies studied show an excellent correlation between the H I surface density and the presence of H II regions. This correlation is most easily interpreted in terms of a requisite threshold H I surface density for massive star formation. This threshold is 1 x 10 to the 21st power H I atoms/sq cm for a resolution of 500 pc. Giant extragalactic H II regions are only found near H I surface densities of a factor of 3 to 5 times this threshold level. The observed threshold implies a Jeans length of 150 pc, which is the same as the size scale at which the structure in the H I complexes correlates well with the H II region distribution. This, combined with the fact that in none of the galaxies observed is there H I above the threshold level with concomitant H II regions, implies an exclusively gravitational origin for the star formation events. That is, there is no need to involve a trigger as in the SSPSF theory (Seiden 1983) or feedback as in Dopita (1985). Author

N87-24303*# Wyoming Univ., Laramie. Infrared Observatory.
CARBON MONOXIDE EMISSION FROM SMALL GALAXIES **c93**
Harley A. Thronson, Jr. and John Bally (Bell Telephone Labs., Inc., Murray Hill, N. J.) *In* NASA, Washington Star Formation in Galaxies May 1987 p 267-270 (For primary document see N87-24266 17-89)
(Grant NAG2-134)
Avail: NTIS HC A99/MF E03 CSCL 03B

A search was conducted for J = 1 yields 0 CO emission from 22 galaxies, detecting half, as part of a survey to study star formation in small to medium size galaxies. Although substantial variation was found in the star formation efficiencies of the sample galaxies, there is no apparent systematic trend with galaxy size. Author

N87-24304*# California Inst. of Tech., Pasadena. Infrared Processing and Analysis Center.
CHARACTERISTICS OF UGC GALAXIES DETECTED BY IRAS
Carol J. Lonsdale Persson, W. Rice, and G. D. Bothun *In* NASA, Washington Star Formation in Galaxies May 1987 p 273-276 (For primary document see N87-24266 17-89)
Avail: NTIS HC A99/MF E03 CSCL 03A

Infrared Astronomy Satellite (IRAS) detection rates at 60 microns were determined for the Uppsala General Catalog of Galaxies (Nilson 1973; the UCG). Late-type spirals, characterized by a normal IR/B ratio of approximately 0.6, are detected to a velocity of approximately 6000 km/s for L sub B = L sub *. Contrary to the situation for IRAS-selected galaxy samples, little evidence was found for a correlation between IR/B and 60/100 microns in this large optically-selected sample. Thus a significant fraction of the IRAS-measured far-infrared flux from normal spirals must originate in the diffuse interstellar medium, heated by the interstellar radiation field. Support was not found for Burstein and Lebofsky's (1986) conclusion that spiral disks are optically thick in the far-infrared. Author

N87-24305*# Arecibo Ionospheric Observatory, Puerto Rico.
FAR-INFRARED PROPERTIES OF CLUSTER GALAXIES **c93**
M. D. Bicay and R. Giovanelli (Stanford Univ., Calif.) *In* NASA, Washington Star Formation in Galaxies May 1987 p 277-281 (For primary document see N87-24266 17-89)
(Contract NAS7-918)
Avail: NTIS HC A99/MF E03 CSCL 03B

Far-infrared properties are derived for a sample of over 200 galaxies in seven clusters: A262, Cancer, A1367, A1656 (Coma), A2147, A2151 (Hercules), and Pegasus. The IR-selected sample consists almost entirely of IR normal galaxies, with Log of L(FIR) = 9.79 solar luminosities, Log of L(FIR)/L(B) = 0,79, and Log of S(100 microns)/S(60 microns) = 0.42. None of the sample galaxies has Log of L(FIR) greater than 11.0 solar luminosities, and only one has a FIR-to-blue luminosity ratio greater than 10. No significant differences are found in the FIR properties of HI-deficient and HI-normal cluster galaxies. Author

N87-24306*# Institut d'Astrophysique, Paris (France).
PRESENT STAR FORMATION IN SPRIALS OF THE VIRGO CLUSTER **c90**
B. Guiderdoni *In* NASA, Washington Star Formation in Galaxies May 1987 p 283-286 (For primary document see N87-24266 17-89)
Avail: NTIS HC A99/MF E03 CSCL 03B

From a study of spiral galaxies in the Virgo Cluster (VC), it is shown that the RDDO anemics with smooth arms and no sign of present formation of (massive) stars have HI surface densities below a threshold value of 2 to 5 x 10 to the 20th power atoms/sq cm. This value is very consistent with predictions of theoretical models. It is likely that the HI disks of VC HI-deficient RDDO anemics were deeply affected by ram pressure stripping in the gaseous intracluster medium, while VC HI deficient RDDO spirals were only peripherally stripped. Author

N87-24307*# Massachusetts Univ., Amherst. Dept. of Physics and Astronomy.
MOLECULAR GAS AND STAR FORMATION IN HI-DEFICIENT VIRGO CLUSTER GALAXIES **c90**
Jeffrey D. Kenney and Judith S. Young *In* NASA, Washington Star Formation in Galaxies May 1987 p 287-292 (For primary document see N87-24266 17-89)
Avail: NTIS HC A99/MF E03 CSCL 03B

Mapping of the CO emission line in 42 Virgo cluster galaxies reveals that the molecular gas contents and distributions are roughly normal in severaly HI-deficient Virgo spirals. The survival of the molecular component mitigates the impact of the HI-stripping on star formation and subsequent galactic evolution. For spirals

which are deficient in HI by a factor of 10, far-infrared, H alpha line, and nonthermal radio continuum luminosities are lower by no more than a factor of 2. The fact that the inner galactic disks are stripped of HI, while CO is normal, suggests that the lifetime of the molecular phase is approximately one billion years in the inner regions of luminous spirals. Author

N87-24308*# Arizona State Univ., Tempe. Dept. of Physics.
STAR FORMATION RATES AS A FUNCTION OF GALAXY MASS **c90**
W. Romanishin *In* NASA, Washington Star Formation in Galaxies May 1987 p 293-296 (For primary document see N87-24266 17-89)
(Contract JPL-957317)
Avail: NTIS HC A99/MF E03 CSCL 03B

Correlations were found between the colors and absolute magnitudes of spiral galaxies. Using optical and/or near IR (1.6 micron) colors, it was found that lower luminosity spirals are systematically bluer than higher luminosity spirals. Infrared Astronomy Satellite (IRAS) far IR luminosities were used to investigate the suggestion that one prime cause of these color-absolute magnitude correlations is a systematic variation with galaxy mass of the current star formation rate (SFR) per unit mass. To the extent that the IRAS fluxes actually measure disk SFR, no correlation of SFR/unit mass and galaxy mass was found. Other possible explanations of the color-absolute magnitude correlations are discussed, as well as caveats on the use of IRAS fluxes as a means of comparing SFRs in galaxies of differing mass. Author

N87-24309*# California Inst. of Tech., Pasadena. Infrared Processing and Analysis Center.
GLOBAL PROPERTIES OF THE NEARBY SPIRAL M101 **c90**
C. Beichman, F. Boulanger, W. Rice, Carol J. Lonsdale Persson, and F. Viallefond (Institut d'Astrophysique, Paris, France) *In* NASA, Washington Star Formation in Galaxies May 1987 p 297-302 Prepared in cooperation with JPL, California Inst. of Tech., Pasadena (For primary document see N87-24266 17-89)
Avail: NTIS HC A99/MF E03 CSCL 03B

M101 (NGC 5457) is a classic Sc I spiral galaxy located suffiently nearby, 6.8 Mpc, that its structure can be studied even with the coarse angular resolution of the Infrared Astronomy Satellite (IRAS). The global infrared properties of M101 are addressed including the radial dependence of its infrared emission. Author

N87-24310*# Massachusetts Univ., Amherst. Dept. of Physics and Astronomy.
EFFICIENT STAR FORMATION IN THE BRIGHT BAR OF M83 **c90**
S. D. Lord, S. E. Strom, and J. S. Young *In* NASA, Washington Star Formation in Galaxies May 1987 p 303-307 (For primary document see N87-24266 17-89)
(Grant NSF AST-82-12252)
Avail: NTIS HC A99/MF E03 CSCL 03B

The bright molecular bar in M83 was detected standing out as a 100% enhancement of molecular emission with respect to the off-bar emission at the same radii. The spatial variations in the star formation efficiency, as traced by H alpha emission and the surface density of the interstellar gas, in M83 and M51 were compared. Both the central bar of M83 and the spiral arms of M51 are regions characterized by high massive star formation rates. For M83, it is ascribed that both the gas surface density and the star formation efficiency are high to the hydrodynamics of the central region. Author

N87-24311*# Illinois Univ., Urbana. Dept. of Astronomy.
LARGE SCALE DISSOCIATION OF MOLECULAR GAS IN THE SPRIAL ARMS OF M51 **c90**
R. P. J. Tilanus and R. J. Allen *In* NASA, Washington Star Formation in Galaxies May 1987 p 309-313 Sponsored in part by the Netherlands Organization for the Advancement of Pure Research (For primary document see N87-24266 17-89)
Avail: NTIS HC A99/MF E03 CSCL 03B

The distribution of the atomic and ionized hydrogen along the inner spiral arms of M51 are compared. As is the case in M83, the location of both these phases of the interstellar medium with respect to the major dust lanes suggests that molecular hydrogen is dissociated on kpc scales in active star-forming regions, and that this dissociation process may strongly affect the observed morphology of atomic hydrogen in spiral arms. Author

N87-24312*# Onsala Space Observatory (Sweden).
STRUCTURE AND KINEMATICS OF THE MOLECULAR SPIRAL ARMS IN M51 **c90**
G. Rydbeck, A. Hjalmarson, L. E. B. Johansson, O. E. H. Rydbeck, and T. Wiklind *In* NASA, Washington Star Formation in Galaxies May 1987 p 315-317 Sponsored by JPL (For primary document see N87-24266 17-89)
Avail: NTIS HC A99/MF E03 CSCL 03B

Mapping of the CO(1-0) emission from the spiral galaxy was made with the Onsala 20 m antenna. The observations show that the emission is considerably enhanced in spiral arms which appear to originate as intense ridges of emission about 1 kpc from the nucleus. One of the main objectives for the 1986 observations was to study the variations of the tangential velocity component of molecular gas across a spiral arm. The radial velocity was found to have a velocity shift similar to that predicted by the density wave theory. The present (1986) observations of the inner southern spiral arm of M51 show that the tangential velocity component also behaves in a way which conforms with the density wave model. The molecular arms were compared with the H alpha ionized gas arms of Tully (1974) and it was found that the ionized gas appears to have its maximum intensity slightly outside the molecular arm. B.G.

N87-24313*# California Inst. of Tech., Pasadena. Infrared Processing and Analysis Center.
MODELLING THE IRAS COLORS OF GALAXIES
George Helou *In* NASA, Washington Star Formation in Galaxies May 1987 p 319-322 Sponsored by JPL (For primary document see N87-24266 17-89)
Avail: NTIS HC A99/MF E03 CSCL 03A

A physical interpretation is proposed for the color-color diagram of galaxies which are powered only by star formation. The colors of each galaxy result from the combination of two components: cirrus-like emission from the neutral disk, and warmer emission from regions directly involved in on-going star formation. This approach to modelling the emission is based on dust properties, but independent evidence for it is found in the relation between the color sequence and the luminosity sequence. Implications of data and interpretations are discussed and possible tests mentioned for the model. Author

N87-24314*# Amsterdam Univ. (Netherlands). Astronomical Inst.
A SIMPLE TWO-COMPONENT MODEL FOR THE FAR-INFRARED EMISSION FROM GALAXIES **c93**
T. deJong and K. Brink *In* NASA, Washington Star Formation in Galaxies May 1987 p 323-328 Sponsored by the Netherlands Foundation for Astronomical Research and the Netherlands Organization for the Advancement of Pure Research (For primary document see N87-24266 17-89)
Avail: NTIS HC A99/MF E03 CSCL 03B

A simple model was constructed to calculate the far-infrared emission of galaxies made up of a disk component containing cool dust heated by the general interstellar radiation field and of a molecular cloud component containing warm dust heated by recently formed massive stars. This model is fitted to the optical and far-infrared data of 120 Shapley-Ames galaxies and of 20 optically studied mini-survey galaxies, resulting in the determination of blue face-on extinctions and of the total luminosities of recently born massive stars and disk stars. The ratio of these two luminosities is a more reliable star formation activity index than the previously used ratio L sub IR/L sub B. The results show that infrared selected galaxies are on the average almost three times more dusty than optically selected ones. Only about 10% of the

mini-survey galaxies exhibits strongly enhanced star formation.
Author

N87-24315*# Onsala Space Observatory (Sweden).
DETECTION OF CO (J=1-0) IN THE DWARF ELLIPTICAL GALAXY NGC 185
Tommy Wiklind and Gustaf Rydbeck *In* NASA, Washington Star Formation in Galaxies May 1987 p 331-332 Original language document was announced in IAA as A87-16880 (For primary document see N87-24266 17-89)
Avail: NTIS HC A99/MF E03 CSCL 03A

The detection of CO (J = 1-0) emission in the dwarf elliptical galaxy NGC 185 is reported. The presence of massive molecular clouds in this early-type galaxy supports the idea of recent or ongoing stellar formation indicated by the population of blue stars in the center. The CO was detected in two positions in the galaxy, the center, and a prominent dustcloud. The emission profile has two peaks, roughly centered around the systemic velocity. It is found that NGC 185 is overluminous in blue light for its CO luminosity compared with Sc galaxies. This might indicate a higher star-formation efficiency for NGC 185 than for the late-type galaxies. Author

N87-24316*# Lick Observatory, Mount Hamilton, Calif.
STAR FORMING REGIONS IN GAS-RICH SO GALAXIES c90
Richard W. Pogge and Paul B. Eskridge (Washington Univ., Seattle.) *In* NASA, Washington Star Formation in Galaxies May 1987 p 333-336 (For primary document see N87-24266 17-89)
Avail: NTIS HC A99/MF E03 CSCL 03B

The first results of an H alpha imaging survey of HI rich SO galaxies, which were searched for HII regions and other sources of emission, are presented. The charge coupled device H alpha interference filter images were made of 16 galaxies. Eight of these galaxies show evidence for on-going star formation, one has nuclear emission but no HII regions, and the remaining seven have no emissions detected within well defined upper limits. With the exception of one notably peculiar galaxy in which the emission from HII regions appears pervasive, the HII regions are either organized into inner-disk rings or randomly distributed throughout the disk. A few of these galaxies are found to be clearly not SO's; or peculiar objects atypical of the SO class. Using simple models star formation rates (SFRs) and gas depletion times from the observed H alpha fluxes were estimated. In general, the derived SFRs are much lower than those found in isolated field spiral galaxies and the corresponding gas depletion time scales are also longer. Author

N87-24317*# Space Telescope Science Inst., Baltimore, Md.
A SIMPLE THEORY OF BIMODAL STAR FORMATION c90
Rosemary F. G. Wyse and J. Silk (California Univ., Berkeley.) *In* NASA, Washington Star Formation in Galaxies May 1987 p 339-342 Sponsored in part by Calspace (For primary document see N87-24266 17-89)
Avail: NTIS HC A99/MF E03 CSCL 03B

A model of bimodal star formation is presented, wherein massive stars form in giant molecular clouds (GNC), at a rate regulated by supernovae energy feedback through the interstellar medium, the heat input also ensuring that the initial mass function (IMF) remains skewed towards massive stars. The low mass stars form at a constant rate. The formation of the GMC is governed by the dynamics of the host galaxy through the rotation curve and potential perturbations such as a spiral density wave. The characteristic masses, relative normalizations, and rates of formation of the massive and low mass modes of star formation may be tightly constrained by the requirements of the chemical evolution in the Solar Neighborhood. Good fits were obtained for the age metallicity relation and the metallicity structure of thin disk and spheroid stars only for a narrow range of these parameters. Author

N87-24318*# Arizona Univ., Tucson. Dept. of Planetary Sciences.
THE HISTORY OF GAS IN SPRIAL GALAXIES c90
Philip Maloney *In* NASA, Washington Star Formation in Galaxies May 1987 p 343-347 (For primary document see N87-24266 17-89)
Avail: NTIS HC A99/MF E03 CSCL 03B

The general association of luminous young stars with spiral arms in galaxies has led to widespread acceptance of the idea that the formation of massive stars, at least, is somehow triggered by the interaction of interstellar gas clouds with a spiral density wave. A very simple model for the gas in a spiral galaxy, with a specified initial surface density and angular velocity is examined. Typical results from this simple model, with parameters appropriate to NGC 6946, are shown. The accuracy of the presumption that the molecular gas distributions in galaxies is based upon observations of CO J = 1-0 emission, is discussed. B.G.

N87-24319*# Pennsylvania State Univ., University Park. Dept. of Astronomy.
STARBURST GALAXIES c90
Daniel W. Weedman *In* NASA, Washington Star Formation in Galaxies May 1987 p 351-361 (For primary document see N87-24266 17-89)
Avail: NTIS HC A99/MF E03 CSCL 03B

The infrared properties of star-forming galaxies, primarily as determined by the Infrared Astronomy Satellite (IRAS), are compared to X-ray, optical, and radio properties. Luminosity functions are reviewed and combined with those derived from optically discovered samples using 487 Markarian galaxies with redshifts and published IRAS 60 micron fluxes, and 1074 such galaxies in the Center for Astrophysics redshift survey. It is found that the majority of infrared galaxies which could be detected are low luminosity sources already known from the optical samples, but non-infrared surveys have found only a very small fraction of the highest luminosity sources. Distributions of infrared to optical fluxes and available spectra indicate that the majority of IRAS-selected galaxies are starburst galaxies. Having a census of starburst galaxies and associated dust allow severl important global calculations. The source counts are predicted as a function of flux limits for both infrared and radio fluxes. These galaxies are found to be important radio sources at faint flux limits. Taking the integrated flux to z = 3 indicates that such galaxies are a significant component of the diffuse X-ray background, and could be the the dominant component depending on the nature of the X-ray spectra and source evolution. Author

N87-24320*# Northeastern Univ., Boston, Mass.
INFRARED SPECTROSCOPY OF STAR FORMATION IN GALAXIES
Sara C. Beck, Paul T. P. Ho, and Jean L. Turner (Harvard-Smithsonian Center for Astrophysics, Cambridge, Mass.) *In* NASA, Washington Star Formation in Galaxies May 1987 p 363-366 Sponsored in part by NASA (For primary document see N87-24266 17-89)
(Grant NSF AST-86-09907)
Avail: NTIS HC A99/MF E03 CSCL 03A

The Brackett alpha and beta lines with 7.2 seconds angular and 350 km/s velocity resolution were observed in 11 infrared-bright galaxies. From these measurements extinctions, Lyman continuum fluxes, and luminosities due to OB stars were derived. The galaxies observed to date are NGC3690, M38, NGC 5195, Arp 220, NGC 520, NGC660, NGC1614, NGC 3079, NGC 6946, NGC 7714, and Maffei 2, all of which were suggested at some time to be starburst ogjects. The contributions of OB stars to the luminosities of these galaxies can be quantified from the measurements and range from insignificant to sufficient to account for the total energy output. The OB stellar luminosities observed are as high as 10 to the 12th solar luminosities in the galaxy NGC 1614. It is noteworthy that star formation can play very different roles in the infrared energy output of galaxies of similar luminosity, as for example Arp 220 and NGC 1614. In addition to probing the star formation process in these galaxies, the Brackett line measurements, when compared to radio and infrared continuum results, have revealed some unexpected and at present imperfectly understood phenomena: in some very luminous sources the radio continuum appears to be suppressed relative to the infrared recombination

lines; in many galaxies there is a substantial excess of 10 micron flux over that predicted from simple models of Lyman alpha heating of dust if young stars are the only significant energy source. Author

N87-24321*# California Inst. of Tech., Pasadena.
MOLECULAR GAS IN THE STARBURST NUCLEUS OF M82 **c90**
K. Y. Lo *In* NASA, Washington Star Formation in Galaxies May 1987 p 367-382 (For primary document see N87-24266 17-89)
Avail: NTIS HC A99/MF E03 CSCL 03B

The 7' resolution CO observations of the central 1 kpc of M82 have resolved 2 components of molecular gas: (1) a high concentration in the central 700 pc x 200 pc, and (2) extended features that may be gas expelled from the central concentration. The central concentration of molecular gas falls in the same confines as the other tracers of recent star formation, and may be identified directly with the star burst region. The molecular gas in the star burst nucleus of M82 appears to be highly disturbed and has high kinetic temperature, likely consequences of the high density of young star clusters. Stellar winds and subsequent supernovae from the star clusters can effectively sweep up the interstellar medium. The spatial distribution and kinematics of the nuclear concentration of the molecular gas, as well as the 2 micron light distribution, suggest the presence of a stellar bar in M82. Comparisons of the M82 star burst nucleus to a sample of IR luminous galaxies suggest that star burst regions in general may have a higher gas temperature and much higher L sub IR/M sub H2 that the galactic disk, and that the L sub IR of the star burst regions may be essentially proportional to their area. Author

N87-24322*# Harvard-Smithsonian Center for Astrophysics, Cambridge, Mass.
NUCLEAR STAR FORMATION ON 100 PARSEC SCALES: 10' RESOLUTION RADIO CONTINUUM, HI AND CO OBSERVATIONS **c90**
Jean L. Turner, Paul T. P. Ho, and Robert N. Martin (Arizona Univ., Tucson.) *In* NASA, Washington Star Formation in Galaxies May 1987 p 383-386 (For primary document see N87-24266 17-89)
(Grants NATO-83/584; NSF AST-85-09907)
Avail: NTIS HC A99/MF E03 CSCL 03B

A program of radio line and continuum studies of star formation in nearby spiral galaxies is reported. The objective is a search for hot gas and peculiar dynamics in spiral nuclei with 10' to 30' angular resolution. Vigorous star formation is found to be a common phenomenon in the inner kpc of spirals. Arcsecond resolution observations of radio continuum emission at 6 and 2 cm were used to separate the thermal and nonthermal radio components. It was found that thermal and nonthermal emission are well mixed even on sizescales of 10 pc. To understand the reason for the increased level of star formation activity in spiral nuclei, HI and CO emission in these galaxies is studied. The CO transition was detected in M51, M82, NGC 253, NGC 6946 and IC 342 with T sub a approx. 0.5 to 2.0 K, at 20' angular resolution. The dynamics and spatial distribution of nuclear gas are being studied using VLA HI maps with 30' synthesized beams. Evidence for noncircular motions in HI was found in the nucleus of IC 342. Author

N87-24323*# National Aeronautics and Space Administration. Goddard Space Flight Center, Greenbelt, Md.
EXTREMELY LUMINOUS FAR-INFRARED SOURCES (ELFS)
Martin Harwit, James R. Houck, B. Thomas Soifer (California Inst. of Tech., Pasadena.), and Giorgio G. C. Palumbo *In* NASA, Washington Star Formation in Galaxies May 1987 p 387-393 (For primary document see N87-24266 17-89)
(Grant NAGw-761)
Avail: NTIS HC A99/MF E03 CSCL 03A

The Infrared Astronomical Satellite (IRAS) survey uncovered a class of Extremely Luminous Far Infrared Sources (ELFS), exhibiting luminosities up to and occasionally exceeding 10 to the 12th power L sub 0. Arguments are presented to show that sources with luminosities L equal to or greater than 3 x 10 to the 10th power L sub 0 may represent gas rich galaxies in collision. The more conventional explanation of these sources as sites of extremely active star formation fails to explain the observed low optical luminosities of ELFS as well as their high infrared excess. In contrast, a collisional model heats gas to a temperature of approx. 10 to the 6th power K where cooling takes place in the extreme ultraviolet. The UV is absorbed by dust and converted into far infrared radiation (FIR) without generation of appreciable optical luminosity. Gas recombination as it cools generates a Lyman alpha photon only once for every two extreme ultraviolet approx. 50eV photons emitted by the 10 to the 6th power gas. That accounts for the high infrared excess. Finally, the model also is able to explain the observed luminosity distribution of ELFS as well as many other traits. Author

N87-24324*# Johns Hopkins Univ., Baltimore, Md.
STAR FORMATION AND DYNAMICS IN STARBURST NUCLEI **c90**
Colin A. Norman *In* NASA, Washington Star Formation in Galaxies May 1987 p 395-400 Prepared in cooperation with Space Telescope Science Inst.,Baltimore, Md. (For primary document see N87-24266 17-89)
Avail: NTIS HC A99/MF E03 CSCL 03B

A simple model is presented for gas inflow through a disk galaxy driven by interacting galaxies through the action of a non-axisymmetric disturbance acting on the disk whose gas is modelled as an ensemble of gas clouds. Cloud collisions, as well as being a vital process in forcing gas inflow to the center of the disk, are also assumed to generate massive stars. This ever increasing rate of gas flow toward the center of the galaxy and the associated rapid increase in cloud collisions lead to a centrally concentrated starburst. Starbursts have important consequences for the immediate environment of galaxjes. Mildly collimated outflows can be driven by a combination of multiple supernovae and OB star winds. Jets associated with activity in the galactic nucleus can interact strongly with a starburst environment. Author

N87-24325*# Minnesota Univ., Minneapolis. Dept. of Astronomy.
INDUCED STAR FORMATION IN INTERACTING GALAXIES **c90**
R. C. Kennicutt, K. A. Roettiger, W. C. Keel, J. M. vanderHulst, and E. Hummel (Max-Planck-Inst. fuer Radioastronomie, Bonn, West Germany) *In* NASA, Washington Star Formation in Galaxies May 1987 p 401-408 (For primary document see N87-24266 17-89)
(Contract JPL-957243; Grants NATO-0592/82; NSF AST-81-11711)
Avail: NTIS HC A99/MF E03 CSCL 03B

Measurements of H alpha emission line fluxes and FIR fluxes in approx. 100 interacting spirals were used to investigate the effects of close tidal interactions on the disk and nuclear star formation rates in galaxies. Two samples of interacting spirals were studied, a complete sample of close pairs, and a set of strongly perturbed systems from the Arp atlas. Both the integrated H alpha luminosities and FIR luminosities are enhanced in the interacting galaxies, indicating that the encounters indeed trigger massive star formation in many cases. The response of individual galaxies is highly variable, however. A majority of the interacting spirals exhibit normal star formation rates, while a small fraction are undergoing bursts with luminosities which are rarely, if ever, observed in noninteracting systems. Virtually all of the latter are in the Arp sample, indicating that the Arp atlas is heavily biased to the most active star forming systems. Author

N87-24326*# Arizona Univ., Tucson.
THE FREQUENCY OF ENHANCED STAR FORMATION IN INTERACTING AND ISOLATED GALAXIES Abstract Only **c90**
Roc M. Cutri *In* NASA, Washington Star Formation in Galaxies May 1987 p 409 (For primary document see N87-24266 17-89)
Avail: NTIS HC A99/MF E03 CSCL 03B

17-89)
Avail: NTIS HC A99/MF E03 CSCL 03B

To probe the sensitivity of the star formation rate and extent in galaxies to gravitational encounters, ground based near and mid-infrared and IRAS far-infrared measurements of complete samples of isolated and interacting pairs of galaxies were obtained. The observed infrared properties of the isolated galaxies are used to gauge the magnitude of star formation in galaxies free from external influences, and to define the relationships between morphological type and infrared luminosity. These properties were contrasted with those of the interacting sample to examine the extent to which interactions can enhance or alter the nature of star formation. The mechanisms by which interactions influence activity such as star formation are investigated through correlations of the infrared characteristics with radio and optical measurements, and with morphological and physical parameters such as galaxy types, separations, encounter velocities and interaction types. Limits to the physical extent of the star formation are obtained by comparing the large aperture measurements of IRAS with the small aperture ground based photometry. Author

N87-24327*# California Inst. of Tech., Pasadena.
ULTRALUMINOUS INFRARED GALAXIES
D. B. Sanders, B. T. Soifer, G. Neugebauer, N. Z. Scoville, B. F. Madore, G. E. Danielson, J. H. Elias, K. Matthews, C. J. Persson, and S. E. Persson (Mount Wilson Observatory, Pasadena, Calif.) *In* NASA, Washington Star Formation in Galaxies May 1987 p 411-420 Sponsored in part by NSF Prepared in cooperation with Las Campanas Observatory, Chile (For primary document see N87-24266 17-89)
Avail: NTIS HC A99/MF E03 CSCL 03A

The IRAS survey of the local universe has revealed the existence of a class of ultraluminous infrared galaxies with L(8 to 1000 micrometer) greater than 10 to the 12th L sub 0 that are slightly more numerous, and as luminous as optically selected quasars at similar redshift. Optical CCD images of these infrared galaxies show that nearly all are advanced mergers. Millimeter wave CO observations indicate that these interacting systems are extremely rich in molecular gas with total H2 masses 1 to 3 x 10 to the 10th power M sub 0. Nearly all of the ultraluminous infrared galaxies show some evidence in their optical spectra for nonthermal nuclear activity. It is proposed that their infrared luminosity is powered by an embedded active nucleus and a nuclear starburst both of which are fueled by the tremendous reservoir of molecular gas. Once these merger nuclei shed their obscuring dust, allowing the AGN to visually dominate the decaying starburst, they become the optically selected quasars. Author

N87-24328*# Imperial Coll. of Science and Technology, London (England).
EXTRAGALACTIC INFRARED SPECTROSCOPY
R. D. Joseph, G. S. Wright, R. Wade, J. R. Graham, I. Gatley (United Kingdom Infrared Telescope Unit, Hilo, Hawaii.), and A. H. Prestwich *In* NASA, Washington Star Formation in Galaxies May 1987 p 421-433 (For primary document see N87-24266 17-89)
Avail: NTIS HC A99/MF E03 CSCL 03A

The spectra of galaxies in the near infrared atmospheric transmission windows are explored. Emission lines were detected due to molecular hydrogen, atomic hydrogen recombination lines, a line attributed to FEII, and a broad CO absorption feature. Lines due to H2 and FEII are especially strong in interacting and merging galaxies, but they were also detected in Seyferts and normal spirals. These lines appear to be shock excited. Multi-aperture measurements show that they emanate from regions as large as 15 kpc. It is argued that starbursts provide the most plausible and consistent model for the excitation of these lines, but the changes of relative line intensity of various species with aperture suggest that other excitation mechanisms are also operating in the outer regions of these galaxies. Author

N87-24329*# Iowa State Univ. of Science and Technology, Ames. Astronomy Program.
CLOUD FLUID MODELS OF GAS DYNAMICS AND STAR FORMATION IN GALAXIES **c90**
Curtis Struck-Marcell, John M. Scalo (Texas Univ., Austin.), and P. N. Appleton *In* NASA, Washington Star Formation in Galaxies May 1987 p 435-460 (For primary document see N87-24266 17-89)
Avail: NTIS HC A99/MF E03 CSCL 03B

The large dynamic range of star formation in galaxies, and the apparently complex environmental influences involved in triggering or suppressing star formation, challenges the understanding. The key to this understanding may be the detailed study of simple physical models for the dominant nonlinear interactions in interstellar cloud systems. One such model is described, a generalized Oort model cloud fluid, and two simple applications of it are explored. The first of these is the relaxation of an isolated volume of cloud fluid following a disturbance. Though very idealized, this closed box study suggests a physical mechanism for starbursts, which is based on the approximate commensurability of massive cloud lifetimes and cloud collisional growth times. The second application is to the modeling of colliding ring galaxies. In this case, the driving processes operating on a dynamical timescale interact with the local cloud processes operating on the above timescale. The results is a variety of interesting nonequilibrium behaviors, including spatial variations of star formation that do not depend monotonically on gas density. Author

N87-24330*# Maryland Univ., College Park. Astronomy Program.
STARBURST-DRIVEN SUPERWINDS FROM INFRARED GALAXIES **c90**
Timothy M. Heckman, Lee Armus, Patrick McCarthy, Wil vanBreugel, and George K. Miley (Space Telescope Science Inst., Baltimore, Md.) *In* NASA, Washington Star Formation in Galaxies May 1987 p 461-469 (For primary document see N87-24266 17-89)
Avail: NTIS HC A99/MF E03 CSCL 03B

New data is presented that indicate that strong far infrared galaxies commonly have largescale emission line nebulae whose properties are suggestive of mass outflows (superwinds), presumably driven by the high supernova rate associated with the central starburst. These data include longslit spectra of M82 which show that the radial variation of the gas pressure in the emission line nebula is in excellent agreement with a previous wind model. The M82 nebula also has a LINER spectrum, consistent with shock heating. Morphologically and spectroscopically similar emission line nebulae were found in NGC253, and Arp 220 and NGC6240. A longslit spectroscopic investigation was conducted of 20 additional very powerful far-infrared galaxies and found that they generally have spatially extended emission line nebulae whose spectra closely resemble that of the M82 nebula. If the superwind interpretation is correct, it could have many important consequences in extragalactic astronomy. Author

N87-24331*# California Inst. of Tech., Pasadena. Div. of Physics, Mathematics and Astronomy.
INTERFEROMETRIC CO OBSERVATIONS OF THE ULTRALUMINOUS IRAS GALAXIES ARP 220, IC 694/NGC 3690, NGC 6420 AND NGC 7469
A. I. Sargent, D. B. Sanders, N. Z. Scoville, and B. T. Soifer *In* NASA, Washington Star Formation in Galaxies May 1987 p 471-475 Sponsored in part by NASA (For primary document see N87-24266 17-89)
(Grant NSF AST-84-12473)
Avail: NTIS HC A99/MF E03 CSCL 03A

High resolution CO observations of the IRAS galaxies Arp 220, IC 694/NGC 3690, NGC 6240 and NGC 7469 were made with the Millimeter Wave Interferometer of the Owen Valley Radio Observatory. These yield spatial information on scales of 1 to 5 kpc and allow the separation of compact condensations from the more extended emission in the galaxies. In the case of the obviously interacting system IC 694/NGC 3690 the contributions of each

component can be discerned. For that galaxy, and also for Arp 220, the unusually high lumonisities may be produced by nonthermal processes rather than by intense bursts of star formation. Author

N87-24332*# Harvard Univ., Cambridge, Mass. Center for Astrophysics.
THE INITIAL MASS FUNCTION IN HII GALAXIES
Alison W. Campbell *In* NASA, Washington Star Formation in Galaxies May 1987 p 479-482 (For primary document see N87-24266 17-89)
Avail: NTIS HC A99/MF E03 CSCL 03A

Observation of a large sample of HII galaxies shows that the emission line ratios of the youngest objects change systematically with gaseous oxygen abundance, which was interpreted as resulting from changes in the initial mass function (IMF) of the ionizing cluster. Comparison with cluster/nebula models shows that both the slope and the upper mass limit of the cluster IMF vary with abundance. In HII galaxies with oxygen abundance about 1/10 that of Orion, the IMF for massive stars must have a slope which is about a factor of 2 smaller than in the Solar Neighborhood. Author

N87-24333*# Universidad Nacional Autonoma de Mexico, Ensenada. Inst. de Astronomia.
VLA CONTINUUM OBSERVATIONS OF BARRED SPIRAL GALAXIES
J. Antonio Garcia-Barreto and P. Pismis (Universidad Nacional Autonoma de Mexico, Mexico City.) *In* NASA, Washington Star Formation in Galaxies May 1987 p 483-484 (For primary document see N87-24266 17-89)
Avail: NTIS HC A99/MF E03 CSCL 03A

Observations of NGC 613, NGC 1300, NGC 4314 and NGC 5383 using the VLA at frequencies of 1464.9 and 4885.1 MHz are reported. These objects are a subset of galaxies from which radio emission were searched. The selection criteria were: (1) they are barred spiral galaxies preferentially with different Hubble type; (2) they have a peculiar or hot spot nucleus; (3) they have been observed at far infrared wavelengths by IRAS; and (4) they are observable from the northern hemisphere. Their radio and far infrared properties are summarized and their composite spectra are shown. Author

N87-24334*# Massachusetts Inst. of Tech., Cambridge.
A DUST SCATTERED HALO IN STARBURST GALAXY M82?
c90
Michael Rohan, Philip Morrison, and Alberto Sadun *In* NASA, Washington Star Formation in Galaxies May 1987 p 485-489 (For primary document see N87-24266 17-89)
Avail: NTIS HC A99/MF E03 CSCL 03B

The source of the halo about M82 has been under discussion for several years. One explanation for it is the dust model of Solinger, Morrison and Markert in which they propose a diffuse cloud of dust through the M81 group, with M82 traveling through the group holding a denser cloud of dust around it. The feasibility of the dust theory is examined in the X-ray range, using the halo in the X-ray image of M82 taken by the Einstein Observatory. To this end the X-ray cross section for dust is presented, along with the single scattered image of an X-ray source surrounded by a dust cloud; multiply scattered images were simulated with a Monte Carlo program; profiles of the halo along the major and minor axes of M82 are presented. Also presented is an accounting for line spectrographs of M82 that show unusual splitting, using the dust model. The final model proposed for the X-ray image requires dust of radius 50 to 300 A, with density on the order of 10 to the -7th power cu cm, out to a distance of about 9 kpc for some regions. Author

N87-24335*# Five-College Astronomy Dept., Amherst, Mass.
THE AZIMUTHAL AND RADIAL DISTRIBUTIONS OF HI AND H2 IN NGC 6946
Linda J. Tacconi-Garman and Judith S. Young *In* NASA, Washington Star Formation in Galaxies May 1987 p 491-495 (For primary document see N87-24266 17-89)
Avail: NTIS HC A99/MF E03 CSCL 03A

A study was completed of the atomic and molecular components of the ISM in NGC 6946. The distribution of molecular clouds was determined from a fully sampled CO map of the inner disk using the 14-meter telescope of the FCRAO. The distribution of atomic gas was derived from VLA observations at 40' resolution in the D configuration. When comparing the global CO and HI properties with other components of the galaxy, it was found that the azimuthally averaged radial distributions of CO, H-alpha, radio continuum and blue light all exhibit similar roughly exponential falloffs, while the azimuthally averaged HI surface densities vary by only a factor of 2 out to R = 16 kpc. This indicates that while the H-alpha/CO ratio is approximately constant with radius, the CO/HI ratio decreases by a factor of 30 from the center of the galaxy to R = 10 kpc. Author

N87-24336*# National Aeronautics and Space Administration. Marshall Space Flight Center, Huntsville, Ala.
THE INFRARED MORPHOLOGY OF GALACTIC CENTERS
C. M. Telesco, R. Decher, B. D. Ramsey, R. D. Wolstencroft, and S. G. Leggett (Royal Observatory, Edinburgh, Scotland) *In* NASA, Washington Star Formation in Galaxies May 1987 p 497-500 (For primary document see N87-24266 17-89)
Avail: NTIS HC A99/MF E03 CSCL 03A

Initial results are presented of a program to map the centers of galaxies in the mid-infrared using the NASA-MSFC 20 pixel bolometer array. Maps at 10.8 micrometer of the galaxies NGC 5236 (M82), NGC 1808, NGC 4536, and NGC 4527 reveal complex emitting regions ranging in size from 500 pc to 2 kpc. The infrared spatial distributions generally resemble those in the visible and radio. In all cases a large fraction of the IRAS 12 micrometer flux originates in spatial structures prominent in the maps. Author

N87-24337*# Institut d'Astrophysique, Paris (France).
FAR-INFRARED ACTIVITY AND STARBURST GALAXIES
P. Belfort, R. Mochkovitch, and M. Dennefeld *In* NASA, Washington Star Formation in Galaxies May 1987 p 501-505 (For primary document see N87-24266 17-89)
Avail: NTIS HC A99/MF E03 CSCL 03A

After the IRAS discovery of galaxies with large far-infrared to blue luminosity ratio, it has been proposed that an enhanced star formation could be the origin of the far-infrared emission through dust heating. Whether a simple photometric model is able to account for the FIR and optical properties of IRAS galaxies was investigated. The L sub IR/L sub B ratio, (B-V) color and H sub alpha equivalent width of normal spirals are well reproduced with smooth star formation histories. In the case of starburst galaxies, several theoretical diagrams allow us to estimate the burst strength and extinction. L sub IR/L sub B ratio up to 100 can be rather easily reached, whereas extreme values probably require IMF truncated at the low end. Author

N87-24338*# New Mexico State Univ., Las Cruces. Dept. of Astronomy.
IRAS OBSERVATIONS OF STARBURST GALAXIES
Kazuhiro Sekiguchi *In* NASA, Washington Star Formation in Galaxies May 1987 p 507-511 (For primary document see N87-24266 17-89)
Avail: NTIS HC A99/MF E03 CSCL 03A

Far infrared properties of Starburst galaxies were analyzed using IRAS observations at 25, 60, and 100 micrometers. Seventy-nine of 102 Starburst galaxies from the list of Balzano were detected. These galaxies have high IR luminosities of up to a few 10 to the 12th power L sub 0 and concentrate in a small area of the IR color - color diagram. The IR power law spectral indices, alpha, lie within the ranges -2.5 $<$alpha(60,25)$<$ -1.5 and -1.5 $<$alpha(100,60)$<$ 0. These observed indices can be interpreted in terms of a cold disk component and a warm component. More than 80% of the 60 micrometer emission comes from the warm component. The fraction of the 60 micrometer emission attributable to the warm component can be used as an activity indicator. Author

N87-24339*# Texas Univ., Austin. Dept. of Astronomy.
A NEAR-INFRARED STUDY OF THE LUMINOUS MERGING GALAXIES NGC 2623 AND ARP 148
Marshall Joy and Paul M. Harvey *In* NASA, Washington Star Formation in Galaxies May 1987 p 515 Submitted for publication (For primary document see N87-24266 17-89)
Avail: NTIS HC A99/MF E03 CSCL 03A

As part of an investigation of the physical mechanisms which produce large infrared luminosities in interacting systems, multicolor near-infrared maps were obtained of the long tailed galaxy NGC 2623 and the ring galaxy Arp 148. The near-infrared broadband spectrum was decomposed to obtain the contribution of four processes: emission from evolved stars, nebular continuum emission, thermal reradiation, and extinction. This multicolor analysis, along with 2 micrometer maps and 10 micrometer measurements, is used to determine the structure of these interacting galaxies and to delineate regions of star formation.
Author

N87-24340*# California Univ., Berkeley. Lawrence Berkeley Lab.
STAR FORMATION IN THE MERGING GALAXY NGC3256
James R. Graham, G. S. Wright, R. D. Joseph, J. A. Frogel, M. M. Phillips, and W. P. S. Meikle (Iowa State Univ. of Science and Technology, Ames.) *In* NASA, Washington Star Formation in Galaxies May 1987 p 517-519 Sponsored in part by the Royal Commission for the Exhibition of 1851 and the United Kingdom SERC (For primary document see N87-24266 17-89)
(Contract DE-AC03-76SF-00098)
Avail: NTIS HC A99/MF E03 CSCL 03A

The central 5 kpc of the ultra-luminous merging galaxy NGC 3256 was mapped at J, H, K, L, and 10 micrometer, and a 2 micrometer spectra of the nuclear region was obtained. This data was used to identify and characterize the super starburst which has apparently been triggered and fuelled by the merger of two gas rich galaxies. It is also shown that the old stellar population has relaxed into a single spheroidal system, and that a supernova driven wind might eventually drive any remaining gas from the system to leave a relic which will be indistinguishable from an elliptical galaxy.
Author

N87-24341*# California Inst. of Tech., Pasadena.
THE LUMINOSITY FUNCTION OF THE BRIGHTEST GALAXIES IN THE IRAS SURVEY
B. T. Soifer, D. B. Sanders, B. F. Madore, G. Neugebauer, C. J. Persson, S. E. Persson (Mount Wilson Observatory, Pasadena, Calif.), and W. L. Rice *In* NASA, Washington Star Formation in Galaxies May 1987 p 523-530 Prepared in cooperation with Las Campanas Observatory, Chile (For primary document see N87-24266 17-89)
Avail: NTIS HC A99/MF E03 CSCL 03A

Results from a study of the far infrared properties of the brightest galaxies in the IRAS survey are described. There is a correlation between the infrared luminosity and the infrared to optical luminosity ratio and between the infrared luminosity and the far infrared color temperature in these galaxies. The infrared bright galaxies represent a significant component of extragalactic objects in the local universe, being comparable in space density to the Seyferts, optically identified starburst galaxies, and more numerous than quasars at the same bolometric luminosity. The far infrared luminosity in the local universe is approximately 25% of the starlight output in the same volume.
Author

N87-24342*# Hawaii Univ., Honolulu. Inst. for Astronomy.
VLA OBSERVATIONS OF A SAMPLE OF GALAXIES WITH HIGH FAR-INFRARED LUMINOSITIES
S. A. Eagles, C. G. Wynn-Williams, and C. A. Beichman (California Inst. of Tech., Pasadena.) *In* NASA, Washington Star Formation in Galaxies May 1987 p 531-536 (For primary document see N87-24266 17-89)
(Grant NSF AST-84-18197)
Avail: NTIS HC A99/MF E03 CSCL 03A

Preliminary results are presented from a radio survey of galaxies detected by the IRAS minisurvey. It was found that the main difference between galaxies selected in the far infrared and those selected in the optical is that the former have higher radio luminosities and that the radio emission is more centrally concentrated. There is some evidence that the strong central radio sources in the galaxies selected in the infrared are due to star formation, the star formation rate divided by the volume in which the star formation is occuring is 100 to 1000 times greater in the galaxies selected in the infrared than in the disks of normal galaxies.
Author

N87-24343*# Royal Observatory, Edinburgh (Scotland).
SYSTEMATIC IDENTIFICATION OF IRAS POINT SOURCES
A. Savage, R. G. Clowes, H. T. MacGillivray, R. D. Wolstencroft, S. K. Leggett, and P. J. Puxley (Edinburgh Univ., Scotland) *In* NASA, Washington Star Formation in Galaxies May 1987 p 537-545 (For primary document see N87-24266 17-89)
Avail: NTIS HC A99/MF E03 CSCL 03A

A large scale program was initiated to identify IRAS point sources. At ROE the ideal facilities are at hand to undertake such a large program, viz. the rapid scanning capabilities of the COSMOS measuring machine to exploit the depth and resolution of the U.K. Schmidt Telescope J survey plates. Sources in 44 Schmidt plate areas were identified including 1300 sources and covering 1100 square degrees. The identification comprise 700 galaxy identifications and 600 stellar identifications. There are also about 40 sources with no obvious identification but which can be most easily explained by cirrus, confusion between two sources or sources just outside the 2 sigma error box. A major aim with the galaxy identification is to provide a data base from which sound statistical analyses can be made. Accurate blue magnitudes and morphological classifications for each identification were produced.
E.R.

N87-24344*# Cornell Univ., Ithaca, N.Y. Center for Radiophysics and Space Research.
A VERY DEEP IRAS SURVEY AT l(II) = 97 DEG, b(II) = +30 DEG
Perry Hacking and James R. Houck *In* NASA, Washington Star Formation in Galaxies May 1987 p 547-552 (For primary document see N87-24266 17-89)
Avail: NTIS HC A99/MF E03 CSCL 03A

A deep far-infrared survey is presented using over 1000 scans made of a 4 to 6 sq. deg. field at the north ecliptic pole by the IRAS. Point sources from this survey are up to 100 times fainter than the IRAS point source catalog at 12 and 25 micrometers, and up to 10 times fainter at 60 and 100 micrometers. The 12 and 25 micrometer maps are instrumental noise-limited, and the 60 and 100 micrometer maps are confusion noise-limited. The majority of the 12 micrometer point sources are stars within the Milky Way. The 25 micrometer sources are composed almost equally of stars and galaxies. About 80% of the 60 micrometer sources correspond to galaxies on Palomar Observatory Sky Survey (POSS) enlargements. The remaining 20% are probably galaxies below the POSS detection limit. The differential source counts are presented and compared with what is predicted by the Bahcall and Soneira Standard Galaxy Model using the B-V-12 micrometer colors of stars without circumstellar dust shells given by Waters, Cote and Aumann. The 60 micrometer source counts are inconsistent with those predicted for a uniformly distributed, nonevolving universe. The implications are briefly discussed.
Author

N87-24345*# California Univ., Berkeley. Dept. of Astronomy.
WHAT ARE CIRRUS POINT SOURCES?
Carl Heiles, Patrick J. McCarthy, William Reach, and Michael A. Strauss *In* NASA, Washington Star Formation in Galaxies May 1987 p 553-558 Sponsored in part by NSF (For primary document see N87-24266 17-89)
Avail: NTIS HC A99/MF E03 CSCL 03A

Most cirrus point sources are associated with interstellar gas. A subset of these was isolated, together with other sources showing

large band 4 to 3 flux density ratios, that are not associated with interstellar gas. Most of the point sources are associated with diffuse cirrus emissions. The sources appear to be distributed randomly on the sky, with the exception of six clusters, one of which is not associated with any known object. Six sources out of seventeen that were observed for redshifted H I at Arecibo were found to be associated with relatively nondescript external galaxies. Most of the sources do not appear on the Palomar Sky Survey. Deep optical observations of eight fields revealed some fairly distant galaxies, one object with a very peculiar optical spectrum, and several blank fields. Author

N87-24346*# Massachusetts Univ., Amherst. Dept. of Physics and Astronomy.
PROPERTIES OF THE UNUSUAL GALAXY PSC 09104+4109
S. G. Kleinmann and W. G. Keel (Leiden Univ., Netherlands) *In* NASA, Washington Star Formation in Galaxies May 1987 p 559-562 (For primary document see N87-24266 17-89)
Avail: NTIS HC A99/MF E03 CSCL 03A

The IRAS source PSC 09104+4109 is tentatively identified with a faint emission line galaxy having z = 0.442. Assuming this identification is correct, the total infrared luminosity of this galaxy is estimated to be 5 x 10 to the 12th power L sub 0, among the highest for galaxies detected by IRAS. This energy is concentrated at wavelengths less than 30 micrometers, and is approx. 50 times greater than the estimated optical luminosity. The serendipitous way in which this source was found in the PSC catalog suggests that many more similar objects may be found at the lowest levels of the IRAS survey. Author

N87-24347*# Five-College Astronomy Dept., Amherst, Mass.
A REDSHIFT SURVEY OF IRAS GALAXIES
Beverly J. Smith, S. G. Kleinmann, J. P. Huchra, and F. J. Low (Arizona Univ., Tucson.) *In* NASA, Washington Star Formation in Galaxies May 1987 p 565-568 (For primary document see N87-24266 17-89)
(Grant AF-AFOSR-0057-85)
Avail: NTIS HC A99/MF E03 CSCL 03A

Results are presented from a redshift survey of all 72 galaxies detected by IRAS in Band 3 at flux levels equal to or greater then 2 Jy. The luminosity function at the high luminosity end is proportional to L sup -2, however, a flattening was observed at the low luminosity end indicating that a single power law is not a good description of the entire luminosity function. Only three galaxies in the sample have emission line spectra indicative of AGN's, suggesting that, at least in nearby galaxies, unobscured nuclear activity is not a strong contributor to the far infrared flux. Comparisons between the selected IRAS galaxies and an optically complete sample taken from the CfA redshift survey show that they are more narrowly distributed than those optically selected, in the sence that the IRAS sample includes few galaxies of low absolute blue luminosity. It was also found that the space distributions of the two samples differ: the density enhancement or IRAS galaxies is only approx. 1/3 that of the optically selected galaxies in the core of the Coma cluster. Author

N87-24348*# Yale Univ., New Haven, Conn. Dept. of Astronomy.
OPTICAL AND IR LUMINOSITY FUNCTIONS OF IRAS GALAXIES
J. Patricia Vader and M. Simon (State Univ. of New York, Stony Brook.) *In* NASA, Washington Star Formation in Galaxies May 1987 p 569-572 Submitted for publication (For primary document see N87-24266 17-89)
Avail: NTIS HC A99/MF E03 CSCL 03A

The optical and infrared luminosity functions are determined for a 60 micron flux-limited sample of 68 IRAS galaxies covering a total area of 150 deg sq. The IR function is in good agreement with that obtained by other authors. The shape of the optical luminosity function is similar to that of optically selected galaxy samples. The integrated light of most objects in the sample have (NII) to H alpha line flux ratios characteristic of HII-region galaxies. In the absolute magnitude range M sub J = -18, -22 about 14% of late-type galaxies are IRAS galaxies. The apparent companionship frequency is about twice as large as that for a comparable sample of non-IRAS late-type galaxies. Author

N87-24349*# Minnesota Univ., Minneapolis. Dept. of Astronomy.
THE CORRELATION BETWEEN FAR-IR AND RADIO CONTINUUM EMISSION FROM SPIRAL GALAXIES c93
John M. Dickey, Robert W. Garwood, and George Helou (California Inst. of Tech., Pasadena.) *In* NASA, Washington Star Formation in Galaxies May 1987 p 575-578 (For primary document see N87-24266 17-89)
Avail: NTIS HC A99/MF E03 CSCL 03B

A sample of 30 galaxies selected for their intense IRAS flux at 60 and 100 micron using the Arecibo telescope at 21 cm to measure the continuum and HI line luminosities were observed. The centimeter wave continuum correlates very well with the far-infrared flux, with a correlation coefficient as high as that found for other samples, and the same ratio between FIR and radio luminosities. Weaker correlations are seen between the FIR and optical luminosity and between the FIR and radio continuum. There is very little correlation between the FIR and the HI mass deduced from the integral of the 21 cm line. The strength of the radio continuum correlation suggests that there is little contribution to either the radio and FIR from physical processes not affecting both. If they each reflect time integrals of the star formation rate then the time constants must be similar, or the star formation rate must change slowly in these galaxies. Author

N87-24350*# Rice Univ., Houston, Tex. Dept. of Space Physics and Astronomy.
RADIO AND INFRARED OBSERVATIONS OF (ALMOST) ONE HUNDRED NON-SEYFERT MARKARIAN GALAXIES
Linda L. Dressel *In* NASA, Washington Star Formation in Galaxies May 1987 p 579-582 Sponsored by NASA (For primary document see N87-24266 17-89)
Avail: NTIS HC A99/MF E03 CSCL 03A

The 13 cm flux densities of 96 non-Seyfert Markarian galaxies were measured at Arecibo Observatory. Far infrared flux densities have been published for 78 of these galaxies in the IRAS catalog. The radio, infrared, and optical fluxes of these galaxies and of a magnitude limited sample of normal galaxies were compared to clarify the nature of the radio emission in Markarian galaxies. It was found that Markarian galaxies of a given apparent magnitude and Hubble type generally have radio fluxes several times higher that the fluxes typical of normal galaxies of the same magnitude and type. Remarkably, the ratio of radio flux to far infrared flux is nearly the same for most of these starburst galaxies and for normal spiral disks. However, the compact and peculiar Markarian galaxies consistently have about 60% more radio flux per unit infrared flux than the other Markarian galaxies and the normal spirals. It is not clear whether this difference reflects a difference in the evolution of the starbursts in these galaxies or whether there is excess radio emission of nonstellar origin. Author

N87-24351*# Bonn Univ. (West Germany). Radioastronomisches Inst.
THE RADIO-FAR INFRARED CORRELATION: SPIRAL AND BLUE COMPACT DWARF GALAXIES OPPOSED
U. Klein and E. Wunderlich (Max-Planck-Inst. fuer Radioastronomie, Bonn, West Germany) *In* NASA, Washington Star Formation in Galaxies May 1987 p 583-588 (For primary document see N87-24266 17-89)
Avail: NTIS HC A99/MF E03 CSCL 03A

The recently established correlation between radio continuum and far infrared emission in galaxies was further investigated by comparing normal spiral and blue compact dwarf galaxies. The puzzling result is that the ratio of radio to far infrared luminosity and its dispersion is the same for both samples, although their ratios of blue to far infrared luminosity, their radio spectral indices and their dust temperatures exhibit markedly different mean values and dispersions. This suggests that the amount of energy radiated in the two regimes is enhanced in the same way although the

mechanisms responsible for the two components are rather different and complex. The fact that the blue light does not increase at the same proportion shows that both the radio and the far infrared emission are connected with the recent star formation history. Author

N87-24352*# Max-Planck-Inst. fuer Radioastronomie, Bonn (West Germany).
RADIO CONTINUUM, FAR INFRARED AND STAR FORMATION c93

R. Wielebinski, E. Wunderlich, U. Klein (Bonn Univ., West Germany), and E. Hummel *In* NASA, Washington Star Formation in Galaxies May 1987 p 589-593 (For primary document see N87-24266 17-89)
Avail: NTIS HC A99/MF E03 CSCL 03B

A very tight correlation was found between the radio emission and the far infrared emission from galaxies. This has been found for various samples of galaxies and is explained in terms of recent star formation. The tight correlation would imply that the total radio emission is a good tracer of star formation. The correlation between the radio power at 5 GHz and the far infrared luminosity is shown. The galaxies are of various morphological types and were selected from the various IRAS circulars, hence the sample is an infrared selected sample. The far infrared luminosities were corrected for the dust temperature. This is significant because it decreases the dispersion in the correlation. Author

N87-24353*# Observatoire de Paris-Meudon (France).
EXTRAGALACTIC OH MEGAMASERS IN STRONG IRAS SOURCES

L. Bottinelli, H. Dennefeld, L. Gouguenheim, J. M. Martin, G. Paturel (Observatoire de Lyon, France), and A. M. LeSqueren *In* NASA, Washington Star Formation in Galaxies May 1987 p 597-600 (For primary document see N87-24266 17-89)
Avail: NTIS HC A99/MF E03 CSCL 03A

From the OH and HI survey of the strongest far infrared IRAS sources, 3 new powerful OH megamasers were discovered in Arp 143, IRAS 1510+0724 and in the uncatalogued IRAS source, IRAS 17208-0014. The HI line, the OH 1667 and 1665 MHz main lines and the 21 cm continuum observations were made with Nancy radio telescope. The optical spectra and images were obtained at the European Southern Observatory. The spectra are displayed in figures together with the main IR and OH properties of the 8 megamasers detected up to now, including IC 4553, NGC 3690 and Mrk 231, Mrk 273 and III ZW35. Author

N87-24354*# California Inst. of Tech., Pasadena.
NEAR-INFRARED OBSERVATIONS OF IRAS MINISURVEY GALAXIES

David P. Carico, B. T. Soifer, J. H. Elias, K. Matthews, G. Neugebauer, C. Beichman, C. J. Persson, and S. E. Persson (Mount Wilson Observatory, Pasadena, Calif.) *In* NASA, Washington Star Formation in Galaxies May 1987 p 601-604 Prepared in cooperation with Las Campanas Observatory, Chile (For primary document see N87-24266 17-89)
(Grant NSF AST-83-12699)
Avail: NTIS HC A99/MF E03 CSCL 03A

Near infrared photometry at J, H, and K was obtained for 82 galaxies from the IRAS minisurvey. The near infrared colors of these galaxies cover a larger range in J-H and H-K than do normal field spiral galaxies, and evidence is presented of a tighter correlation between the near and far infrared emission in far infrared bright galaxies than exists between the far infrared and the visible emission. These results suggest the presence of dust in the far infrared bright galaxies, with hot dust emission contributing to the 2.2 micron emission, and extinction by dust affecting both the near infrared colors and the visible luminosities. In addition, there is some indication that the infrared emission in many of the minisurvey galaxies is coming from a strong nuclear component. Author

N87-24355*# Institut d'Astrophysique, Paris (France).
GROUND-BASED FOLLOW UP OF IRAS GALAXIES

M. Dennefeld, H. Karoji, P. Bouchet, L. Bottinelli, and L. Gouguenheim (Observatoire de Paris-Meudon, France) *In* NASA, Washington Star Formation in Galaxies May 1987 p 605-609 (For primary document see N87-24266 17-89)
Avail: NTIS HC A99/MF E03 CSCL 03A

Optical, near infrared, radio continuum and HI observations were undertaken of the galaxies identified with IRAS sources in a few fields roughly of the size of a sky survey plate. Results are presented from two fields at galactic latitude +27 and +43 deg over a total area of 100 sq. deg. These regions contained 115 IRAS point sources, out of which 26 were identified with stars and 81 with faint galaxies, 10 of which were difficult to recognize on the Schmidt plates. Spectroscopy was obtained with the ESO telescopes at a resolution of about 10 A. The vast majority of galaxies have low excitation spectra dominated by low ionization lines. The spectra are typical of HII region type galaxies, however of much lower excitation that other starbursts galaxies. The importance of the reddening as determined from the H alpha/H beta ratio is stressed: the visual absorption A sub v ranges from 2 to 6 magnitudes and as a consequence the corrected L sub IR/L sub B ratios are considerably reduced if those reddenings apply to the whole galaxy. Author

N87-24356*# Hawaii Univ., Honolulu. Inst. for Astronomy.
NUCLEAR INFRARED EMISSION AND THE COLORS OF IRAS GALAXIES c93

Gary J. Hill *In* NASA, Washington Star Formation in Galaxies May 1987 p 611-617 (For primary document see N87-24266 17-89)
(Grant NSF AST-84-18197)
Avail: NTIS HC A99/MF E03 CSCL 03B

J, H, K, L', and N observations of galaxies detected at 12 microns by IRAS are combined with IRAS flux densities to investigate the relationship between the infrared sizes and colors of galaxian infrared sources. It is found that typical IRAS galaxies have 10 micron radii of 0.5 to 2.0 kpc, while active galaxies and galaxies with higher 25 to 60 micron color temperatures are smaller. One unusal object, 23060+0505, is at high redshift and has an infrared luminosity of 1.5 x 10 to the 12th power L sub 0. Its 1 to 100 micron energy distribution resembles that of a Seyfert 1 galaxy, but it shows very little sign of broad line emission in the visible. Its properties suggest that it may be a prototype for a class of highly obscured active galaxy. Author

N87-24357*# Edinburgh Univ. (Scotland). Dept. of Astronomy.
ENHANCED STAR FORMATION: THE IMPORTANCE OF BARS IN SPIRAL GALAXIES c90

P. J. Puxley, T. G. Hawarden, C. M. Mountain (Royal Observatory, Edinburgh, Scotland), and S. K. Leggett *In* NASA, Washington Star Formation in Galaxies May 1987 p 619-622 (For primary document see N87-24266 17-89)
Avail: NTIS HC A99/MF E03 CSCL 03B

It was found that among an IR luminous subset of nearby spiral galaxies, nearly all of the systems with IRAS colors and luminosities indicative of enhanced star formation are barred. Radio continuum and IR spectroscopic results support the hypothesis that this emission originates within the central 2 kpc; possibly in a circumnuclear ring. It was also found that outer rings are over represented among these barred systems and suggest possible reasons for this phenomena. Author

N87-24358*# Royal Observatory, Edinburgh (Scotland).
THE PROPERTIES OF HIGHLY LUMINOUS IRAS GALAXIES c90

R. D. Wolstencroft, P. J. Puxley, J. N. Heasley, S. K. Leggett (Edinburgh Univ., Scotland), A. Savage, H. T. MacGillivray, and R. G. Clowes *In* NASA, Washington Star Formation in Galaxies May 1987 p 623-627 (For primary document see N87-24266 17-89)
Avail: NTIS HC A99/MF E03 CSCL 03B

From a complete sample of 154 galaxies identified with IRAS sources in a 304 sq deg area centered on the South Galactic Pole, a subsample of 58 galaxies with L sub IR/L sub B > 3 was

chosen. Low resolution spectra were obtained for 30% of the subsample and redshifts and relative emission line intensities were derived. As a class these galaxies are very luminous with < L sub IR > = 2.9 x 10 to the 11th power L sub 0 and (L sub IR) max = 1.3 x 10 to the 12th power L sub 0. CCD images and JHK photometry were obtained for many of the subsample. The galaxies are for the most part newly identified and are optically faint, with a majority showing evidence of a recent interaction. Radio continuum observations of all galaxies of the subsample were recently obtained at 20 cm VLA with about 75% being detected in a typical integration time of about 10 minutes.

Author

N87-24359*# University of Southern California, Los Angeles. Dept. of Astronomy.

USING SIRTF TO STUDY EXTRAGALACTIC STAR FORMATION

Edward L. Wright *In* NASA, Washington Star Formation in Galaxies May 1987 p 629 (For primary document see N87-24266 17-89)

(Grant NAG2-315)

Avail: NTIS HC A99/MF E03 CSCL 03A

SIRTF, the Space Infrared Telescope Facility, is a NASA mission to provide a long lifetime, sensitive and flexible infrared observatory in space. SIRTF will be able to study selected objects with a sensitivity over 5,000 time better than the IRAS survey limits, and will provide photometric and low to medium resolution spectroscopic data over almost nine octaves from 1.8 to 700 micron wavelength. The baseline SIRTF design has an 85 cm telescope with optics and control system designed for diffraction limited operation at 4 micron and longer wavelengths. SIRTF will be able to measure important cooling lines from neutral regions, such as the 157 micron line, and lines from H II regions such as the 88 micron line. SIRTF will also be able to survey small areas of the sky to the confusion limit in the 3 to 700 micron region. Author

N87-24360*# Arizona Univ., Tucson.

THE RELATION BETWEEN STAR FORMATION AND ACTIVE NUCLEI **c90**

G. H. Rieke *In* NASA, Washington Star Formation in Galaxies May 1987 p 633-641 Sponsored by NSF (For primary document see N87-24266 17-89)

Avail: NTIS HC A99/MF E03 CSCL 03B

Three questions relevant to the relation between an active nucleus and surrounding star formation are discussed. The infrared stellar CO absorption bands can be used to identify galaxies with large populations of young, massive stars and thus can identify strong starburst unambiguously, such as in NGC 6240, and can help identify composite active/starburst systems such as Arp 220. An active nucleus is probably not required for LINER spectral characteristics; dusty starburst galaxies, particularly if they are nearly edge-on, can produce LINER spectra through the shock heating of their interstellar media by supernovae combined with the obscuration of their nuclei in the optical. The Galactic Center would be an ideal laboratory for studying the interaction of starbursts and active nuclei, if both could be demonstrated to occur there. Failure to detect a cusp in the stellar distribution raises questions about the presence of an active nucleus, which should be answered by additional observations in the near future.

Author

N87-24361*# Hawaii Univ., Honolulu. Inst. for Astronomy.

GROUND-BASED 1- TO 32-MICRONS OBSERVATIONS OF ARP 220: EVIDENCE FOR A DUST-EMBEDDED AGN?

E. E. Becklin and C. G. Wynn-Williams *In* NASA, Washington Star Formation in Galaxies May 1987 p 643-650 (For primary document see N87-24266 17-89)

(Grant NSF AST-84-18197)

Avail: NTIS HC A99/MF E03 CSCL 03A

New observations of the 10 and 20 micron size of the emission region in Arp 220 are presented. Also given are ground based photometry from 1 to 32 micron including measurements of the strength of the silicate feature at 10 micron. The results show that the 20 micron size of Arp is smaller than 1.5 arcsec (500 pc); comparison of IRAS and ground based observations show that IRAS 12 micron flux measured with a large arcmin beam is the same as that seen from the ground with a 3 arcsec aperture. At 10 micron a deep silicate absorption feature is seen that corresponds to a visual extinction of about 50 mag. These results suggest that a very significant portion of the 10 to the 12th power L sub 0 infrared luminosity from Arp 220 comes from a region less than or of the order of 500 pc in diameter. When these results are combined with recent measurement of a broad Brackett alpha line by DePoy and an unresolved 2.2 micron source by Neugebauer, Matthews and Scoville, a very attractive possibility for the primary luminosity source Arp 220 is a dust embedded compact Seyfert type nucleus. Author

N87-24362*# Arizona Univ., Tucson.

SPATIAL DECONVOLUTION OF IRAS GALAXIES AT 60 UM

Frank J. Low *In* NASA, Washington Star Formation in Galaxies May 1987 p 651-660 Sponsored by NASA (For primary document see N87-24266 17-89)

Avail: NTIS HC A99/MF E03 CSCL 03A

Using IRAS in a slow scan observing mode to increase the spatial sampling rate and a deconvolution analysis to increase the spatial resolution, several bright galaxies were resolved at 60 micron. Preliminary results for M 82, NGC 1068, NGC 3079 and NGC 2623 show partially resolved emission from 10 to 26 arcsec., full width at half maximum, and extended emission from 30 to 90 arcsec. from the center. In addition, the interacting system, Arp 82, along with Mark 231 and Arp 220 were studied using the program ADDSCAN to average all available survey mode observations. The Arp 82 system is well resolved after deconvolution and its brighter component is extended; the two most luminous objects are not resolved with an upper limit of 15 arcsec. for Arp 220. Author

N87-24363*# Leiden Univ. (Netherlands). Sterrewacht.

STAR FORMATION AROUND ACTIVE GALACTIC NUCLEI **c90**

William C. Keel *In* NASA, Washington Star Formation in Galaxies May 1987 p 661-667 (For primary document see N87-24266 17-89)

Avail: NTIS HC A99/MF E03 CSCL 03B

Active galactic nuclei (Seyfert nuclei and their relatives) and intense star formation can both deliver substantial amounts of energy to the vicinity of a galactic nucleus. Many luminous nuclei have energetics dominated by one of these mechanisms, but detailed observations show that some have a mixture. Seeing both phenomena at once raises several interesting questions: (1) Is this a general property of some kinds of nuclei? How many AGNs have surround starbursts, and vice versa? (2) As in 1, how many undiscovered AGNs or starbursts are hidden by a more luminous instance of the other? (3) Does one cause the other, and by what means, or do both reflect common influences such as potential well shape or level of gas flow? (4) Can surrounding star formation tell us anything about the central active nuclei, such as lifetimes, kinetic energy output, or mechanical disturbance of the ISM? These are important points in the understanding of activity and star formation in galactic nuclei. Unfortunately, the observational ways of addressing them are as yet not well formulated. Some preliminary studies are reported, aimed at clarifying the issues involved in study of the relationships between stellar and nonstellar excitement in galactic nuclei. Author

N87-24364*# European Southern Observatory, La Silla (Chile).

STAR FORMATION IN SEYFERT GALAXIES **c90**

J. M. Rodriguez Espinosa, Richard J. Rudy, and Barbara Jones (California Univ., San Diego.) *In* NASA, Washington Star Formation in Galaxies May 1987 p 669-674 (For primary document see N87-24266 17-89)

Avail: NTIS HC A99/MF E03 CSCL 03B

An analysis of the IRAS data for a sample of classical (optically selected) Seyfert galaxies is presented. The IRAS fluxes at 25 micron, 60 micron, and 100 micron are found to be uncorrelated

or only very weakly correlated with the UV/Optical continuum flux and the near and mid IR flux at 3.5 and 10 microns. To investigate the possibility that star formation accounts for the far IR flux, the IRAS measurements for the Seyfert galaxies are compared to IRAS observations of a sample of normal spiral galaxies, and a sample of Starburst galaxies. It is shown that the far IR luminosities and far IR colors of Seyfert galaxies are indistinguishable from those of the Starburst galaxies. Besides, normal galaxies are an order of magnitude less luminous than both the Seyfert and the Starburst galaxies. This indicates that star formation produces the bulk of the far infrared emission in Seyfert galaxies. Author

N87-24365*# Maryland Univ., College Park. Astronomy Program.

CIRCUMNUCLEAR STARBURSTS IN SEYFERT GALAXIES

Andrew S. Wilson *In* NASA, Washington Star Formation in Galaxies May 1987 p 675-691 (For primary document see N87-24266 17-89)

Avail: NTIS HC A99/MF E03 CSCL 03A

Observational diagnostics for the recognition of circumnuclear star formation in Seyfert galaxies are described and illustrated. These methods include: (1) spatially resolved optical spectroscopy, which allows the emission lines for HII regions to be separated from those originating in gas ionized by the Seyfert nucleus; (2) radio continuum mapping, where the linear radio sources characteristic of the nuclear activity may be distinguished from the diffuse morphology of multiple supernova remnants generated in a starburst; (3) infrared spectroscopic searches for emission features of dust, which are seen in starbursts but not in Seyfert nuclei; (4) the shape of the IRAS spectrum. These various diagnostics agree well as to the presence or absence of ongoing star formation. The IRAS spectra of a significant fraction of Seyferts are dominated by emission from dust heated by stars, not the Seyfert nucleus itself. In these cases, the spectrum is curved, being steep between 25 and 60 microns and flatter between 60 and 100 microns. When the Seyfert nucleus dominates, the 25 to 100 micron spectrum is much flatter. It is suggested that the location of a Seyfert galaxy in the IRAS color-color diagram reflects primarily the relative contributions of the active nucleus and dust heated by stars to the infrared fluxes. Author

N87-24366*# Leiden Univ. (Netherlands). Sterrewacht.

IRAS OBSERVATIONS OF AGN CANDIDATES AT LOW FLUX LEVELS

Marinus H. K. deGrijp, William C. Keel, and George K. Miley (Space Telescope Science Inst., Baltimore, Md.) *In* NASA, Washington Star Formation in Galaxies May 1987 p 693-698 (For primary document see N87-24266 17-89)

Avail: NTIS HC A99/MF E03 CSCL 03A

IRAS additional observations were used to obtain a sample of point sources at much fainter flux levels than hitherto available through the IRAS Point Source Catalogue. This sample is being used to compile an incomplete but representative catalogue of faint IRAS candidate Active Galactic Nuclei (AGNs) and to study the evolution of the infrared bright galaxies. Ground based follow up observations (optical spectroscopy) are mainly hampered by identification confusion. Author

N87-24367*# Hawaii Univ., Honolulu. Inst. for Astronomy.

SPECTROPHOTOMETERY OF BRACKETT LINES IN VERY LUMINOUS IRAS GALAXIES

D. L. DePoy *In* NASA, Washington Star Formation in Galaxies May 1987 p 701-705 (For primary document see N87-24266 17-89)

Avail: NTIS HC A99/MF E03 CSCL 03A

Observation of the Brackett-alpha and Brackett-gamma hydrogen recombination lines were made in a sample of galaxies chosen from the IRAS catalog to have high luminosities at infrared wavelengths. Most have strong Brackett line emission indicating large numbers of high mass stars; the formation of these stars may hence be the underlying source for the galaxies' luminosities. However, there are at least two exceptions that may not be explained in this manner: NGC 6240 and Arp 220. Additional evidence indicates that each of these exceptions may be more closely related to Seyfert-type galaxies or other active galactic nuclei. Author

N87-24368*# Imperial Coll. of Science and Technology, London (England).

EVIDENCE FOR EXTENDED IR EMISSION IN NGC2798 AND NGC6240 **c93**

G. S. Wright, R. D. Joseph, P. A. James, and N. A. Robertson *In* NASA, Washington Star Formation in Galaxies May 1987 p 707-710 (For primary document see N87-24266 17-89)

Avail: NTIS HC A99/MF E03 CSCL 03B

Extended emission at 10 and 20 microns can be used to distinguish starbursts from monsters as the underlying energy source driving the luminous infrared emission in the central regions of galaxies. The spatial extent of the mid infrared emission in the interacting galaxy NCG 2798 and the merger NGC 6240 were investigated. The 10 and 20 micron profiles of the IR source in NGC 2798 are significantly wider than beam profiles measured on a standard star, supporting a starburst interpretation of its IR luminosity. For NGC 6240 there is marginal evidence for an extended 10 micron source, suggesting that a significant fraction of its IR luminosity could be produced by a burst of star formation. Author

N87-24369*# Manchester Univ. (England).

MODELS RELATING THE RADIO EMISSION AND IONISED GAS IN SEYFERT NUCLEI **c93**

A. Pedlar, S. W. Unger, D. J. Axon, and J. E. Dyson *In* NASA, Washington Star Formation in Galaxies May 1987 p 711-715 (For primary document see N87-24266 17-89)

Avail: NTIS HC A99/MF E03 CSCL 03B

Possible models are discussed in which the radio emitting components in Seyfert II nuclei can compress and accelerate the ambient nuclear medium to produce the characteristics of the narrow line region. A first order model, which considers only the expansion of the radio components, is briefly described. However, in many Seyfert nuclei it appears that the linear motion of the radio components is also important. This can result in shock heating of the ambient medium, and if the cooling time is long enough, can lead to a displacement between the radio component and the associated emission lines. This effect may be present in NGC 1068 and NGC 5929 and by considering ram pressure balance and the cooling length it is possible to estimate lobe velocities and ambient densities. Author

N87-24370*# National Aeronautics and Space Administration. Goddard Space Flight Center, Greenbelt, Md.

STRUCTURE IN THE NUCLEUS OF NGC 1068 AT 10 MICRONS **c90**

R. Tresch-Fienberg, G. G. Fazio, D. Y. Gezari, W. F. Hoffmann, G. M. Lamb, P. K. Shu, and C. R. McCreight (National Aeronautics and Space Administration. Ames Research Center, Moffett Field, Calif.) *In* NASA, Washington Star Formation in Galaxies May 1987 p 717-721 Previously announced in IAA as A87-30957 (For primary document see N87-24266 17-89)

Avail: NTIS HC A99/MF E03 CSCL 03B

New 8 to 13 micron array camera images of the central kiloparsec of Seyfert 2 galaxy NGC 1068 resolve structure that is similar to that observed at visible and radio wavelengths. The images reveal an infrared source which is extended and asymmetric, with its long axis oriented at P.A. 33 deg. Maps of the spatial distribution of 8 to 13 micron color temperature and warm dust opacity are derived from the multiwavelength infrared images. The results suggest that there exist two pointlike luminosity sources in the central regions of NGC 1068, with the brighter source at the nucleus and the fainter one some 100 pc to the northeast. This geometry strengthens the possibility that the 10 micron emission observed from grains in the nucleus is powered by a nonthermal source. In the context of earlier visible and radio studies, these results considerably strengthen the case for jet induced star formation in NGC 1068. Author

N87-24371*# Owens Valley Radio Observatory, Pasadena, Calif.
FAR-INFRARED PROPERTIES OF OPTICALLY-SELECTED QUASARS AND SEYFERT GALAXIES
R. A. Edelson and M. A. Malkan (California Univ., Los Angeles.) *In* NASA, Washington Star Formation in Galaxies May 1987 p 723-725 (For primary document see N87-24266 17-89)
Avail: NTIS HC A99/MF E03 CSCL 03A

Pointed IRAS observations and ground based observations are used to determine the infrared properties of optically selected galaxies and quasars. The use of complete, unbiased, optically selected samples means that statistical tests can be applied to probe the underlying properties of active galactic nuclei (AGNs). The near infrared to millimeter spectral energy distributions (SEDs) were studied of the CfA Seyfert galaxies, a well defined, unbiased sample of 25 Type 1 and 23 Type 2 Seyfert galaxies selected by optical spectroscopy. Data given show strong trends in the infrared SEDs. Strong evidence is also given that the infrared spectra of Seyfert 2 galaxies are dominated by thermal emission from warm dust, while nonthermal emission is more important in the spectra of quasars and luminous Seyfert 1 nuclei. Author

N87-24372*# California Univ., Los Angeles. Dept. of Astronomy.
INFRARED-ULTRAVIOLET SPECTRA OF ACTIVE GALACTIC NUCLEI
M. A. Malkan and R. A. Edelson (Owens Valley Radio Observatory, Pasadena, Calif.) *In* NASA, Washington Star Formation in Galaxies May 1987 p 727-729 (For primary document see N87-24266 17-89)
Avail: NTIS HC A99/MF E03 CSCL 03A

Data from IRAS and IUE were combined with ground based optical and infrared spectrophotometry to derive emission line free spectral energy distributions (SEDs) for 29 active galactic nuclei (AGNs) between 0.1 and 100 microns. The IRAS data were scaled down to account for extended emission. These correction factors, determined by comparing small aperture ground based 10.6 micron data with large aperture IRAS 12 micron fluxes, were usually less than 25%. These corrected SEDs are shown. Author

N87-24373*# California Inst. of Tech., Pasadena.
IRAS OBSERVATIONS OF BL LAC OBJECTS
C. Impey, G. Neugebauer, and G. Miley (Space Telescope Science Inst., Baltimore, Md.) *In* NASA, Washington Star Formation in Galaxies May 1987 p 731-735 Sponsored by NASA (For primary document see N87-24266 17-89)
(Contract JPL-97582)
Avail: NTIS HC A99/MF E03 CSCL 03A

IRAS data was analyzed for 35 BL Lac objects selected from a complete 5 GHz radio sample, using the coadded survey database. The detection rate is 50% with more than 40% detected in more than one band. This compares with only 15% of these sources that are included in the IRAS Point Source Catalog. High luminosity BL Lac objects generally have smooth energy spectra over four or five decades in frequency, consistent with incoherent synchrotron emission from 1 cm to 1 micron. However, many low luminosity BL Lac objects have discontinuous spectra, with a large range in the spectral index at IRAS wavelengths. For BL Lacs with a total luminosity of less than 10 to the 44th power ergs/-s, most of the far infrared energy probably originates from dust heated near the galaxy nucleus. The energy budget shows that the majority of the power per unit bandwidth emerges in the infrared (1 to 100 microns). Author

N87-24374*# Lick Observatory, Mount Hamilton, Calif.
SPECTRAL CLASSIFICATION OF EMISSION-LINE GALAXIES
Sylvain Veilleux and Donald E. Osterbrock *In* NASA, Washington Star Formation in Galaxies May 1987 p 737-740 (For primary document see N87-24266 17-89)
Avail: NTIS HC A99/MF E03 CSCL 03A

A revised method of classification of narrow line active galaxies and H II region-like galaxies is proposed. It involves the line ratios (O III) lambda 5007/H beta, (N II) lambda 6583/H alpha, (S II) (lambda lambda 6716 = 6731)/H alpha, and (O I) lambda 6300/H alpha. These line ratios take full advantage of the physical distinction between the two types of objects and minimize the effects of reddening correction and errors in the flux calibration. Large sets of internally consistent data are used including new previously unpublished measurements. Prediction of recent photoionization models by power law spectra and by hot stars are compared with the observations. The classification is based on the observational data interpreted on the basis of these models. Author

N87-24375*# California Univ., Berkeley. Dept. of Astronomy.
SUMMARY OF SYMPOSIUM: LOW LUMINOSITY SOURCES
Frank H. Shu *In* NASA, Washington Star Formation in Galaxies May 1987 p 743-752 (For primary document see N87-24266 17-89)
Avail: NTIS HC A99/MF E03 CSCL 03A

The author summarized certain aspects of the conference. He shares this task with another colleague thereby breaking the task into more manageable proportions. The author covers the low luminosity sources. He begins his review with a summary of some major themes of the conference and ends with a few speculations on possible theoretical mechanisms. E.R.

N87-24376*# Hawaii Univ., Honolulu. Inst. for Astronomy.
MORPHOLOGY OF LUMINOUS IRAS GALAXIES: SUMMARY TALK
E. E. Becklin *In* NASA, Washington Star Formation in Galaxies May 1987 p 753-756 (For primary document see N87-24266 17-89)
Avail: NTIS HC A99/MF E03 CSCL 03A

The author discusses the morphology of luminous Infrared Astronomy Satellite (IRAS) galaxies. A few comments are made about the direction to be taken in future observations of luminous IRAS galaxies. E.R.

N87-24377*# National Aeronautics and Space Administration. Goddard Space Flight Center, Greenbelt, Md.
FIFTY YEAR CANON OF SOLAR ECLIPSES: 1986-2035
Fred Espenak Nov. 1986 262 p
(NASA-TM-89346; NAS 1.15:89346) Avail: NTIS HC A12/MF A01 CSCL 03A

A reference of moderately detailed eclipse predictions and maps for use by the professional astronomical community is provided. The general characteristics of every solar eclipse and a detailed set of cylindrical project world maps which show the umbral paths of every solar eclipse from 1901 to 2100 are presented. The geodetic path coordinates and local circumstance on the center line, and a series of orthographic projection maps which show the regions of visibility of both partial and central phases for every eclipse from 1986 through 2035 are also provided. B.G.

N87-24378*# National Aeronautics and Space Administration. Ames Research Center, Moffett Field, Calif.
DETECTOR ARRAYS FOR LOW-BACKGROUND SPACE INFRARED ASTRONOMY
C. R. McCreight, M. E. McKelvey, J. H. Goebel, G. M. Anderson, and J. H. Lee Sep. 1986 13 p Presented at the SPIE 30th Annual International Technical Symposium, San Diego, Calif., 17-22 Aug. 1986
(NASA-TM-88344; NAS 1.15:88344) Avail: NTIS HC A02/MF A01 CSCL 03A

The status of development and characterization tests of integrated infrared detector array technology for astronomy applications is described. The devices under development include intrinsic, extrinsic silicon, and extrinsic germanium detectors, with hybrid silicon multiplexers. Laboratory test results and successful astronomy imagery have established the usefulness of integrated arrays in low-background astronomy applications. Author

N87-24258*# National Aeronautics and Space Administration. Goddard Space Flight Center, Greenbelt, Md.
HIGH ENERGY GAMMA RAY ASTRONOMY

Carl E. Fichtel *In its* Essays in Space Science Jun. 1987 p 227-274 (For primary document see N87-24247 17-88)
Avail: NTIS HC A18/MF A01 CSCL 03A

N87-24263*# National Aeronautics and Space Administration. Goddard Space Flight Center, Greenbelt, Md.
X-RAY ASTRONOMICAL SPECTROSCOPY
Stephen S. Holt *In its* Essays in Space Science Jun. 1987 p 379-394 (For primary document see N87-24247 17-88)
Avail: NTIS HC A18/MF A01 CSCL 03A

N87-24264*# National Aeronautics and Space Administration. Goddard Space Flight Center, Greenbelt, Md.
INFRARED ASTRONOMY
Michael G. Hauser *In its* Essays in Space Science Jun. 1987 p 395-401 (For primary document see N87-24247 17-88)
Avail: NTIS HC A18/MF A01 CSCL 03A

90 ASTROPHYSICS

Includes cosmology; celestial mechanics; space plasmas; and interstellar and interplanetary gases and dust.
For related information see also *75 Plasma Physics*.

N87-24379# Los Alamos National Lab., N. Mex.
NEUTRON STARS AS COSMIC NEUTRON MATTER LABORATORIES
D. Pines 1986 8 p Presented at the Texas Symposium, Chicago, Ill., 14 Dec. 1986 Prepared in cooperation with Illinois Univ., Urbana
(Contract W-7405-eng-36)
(DE87-007468; LA-UR-87-709; CONF-861264-2) Avail: NTIS HC A02/MF A01

Recent developments which have radically changed our understanding of the dynamics of neutron star superfluids and the free precession of neutron stars are summarized, and the extent to which neutron stars are cosmic neutron matter laboratories is discussed. DOE

N87-24380# Los Alamos National Lab., N. Mex.
OBSERVATIONS OF HEAVY ENERGETIC IONS FOR UPSTREAM FROM COMET HALLEY
T. R. Sanderson, K. P. Wenzel, P. W. Daly, S. W. H. Cowley, R. J. Hynds, I. G. Richardson, E. J. Smith, S. J. Bame, and R. D. Zwickl 1986 6 p Presented at the 20th ESLAB Symposium, Heidelberg, West Germany, 27 Oct. 1986 Prepared in cooperation with ESA, European Space Research and Technology Centre, Noordwijk, Netherlands, Max-Planck-Inst. fuer Aeronomie, Katlenburg-Lindau, West Germany; Imperial Coll. of Science and Tech., London, England and JPL, Pasadena, Calif.
(Contract W-7405-eng-36)
(DE87-003752; LA-UR-86-4331; CONF-8610207-3) Avail: NTIS HC A02

On March 25, 1986, the ICE spacecraft came within 28 x 10^4 km of the nucleus of comet Halley. For several days around this time, bursts of heavy ions were observed by the ICE energetic ion experiment. These bursts were observed only during periods when the solar wind velocity was considerably higher than its nominal value. We examine the characteristics of these ions, in particular their anisotropies. Using the well known formulae for transformation of distributions from the solar wind frame of reference to the spacecraft frame, we examine the angular distributions expected from either protons, or heavy ions from the water group, and show that the measurements are consistent with heavy ions, and not with protons. We discuss other sources of heavy ions and conclude that the most likely source of these ions is comet Halley. DOE

N87-24251*# Chicago Univ., Ill. Dept. of Physics.
THE ENERGY SOURCE OF THE INTERPLANETARY MEDIUM AND THE HELIOSPHERE
Eugene N. Parker *In* NASA Goddard Space Flight Center, Greenbelt, Md. Essays in Space Science Jun. 1987 p 75-85 (For primary document see N87-24247 17-88)
(Grant NGL-14-001-001)
Avail: NTIS HC A18/MF A01 CSCL 03B

N87-24253*# National Aeronautics and Space Administration. Goddard Space Flight Center, Greenbelt, Md.
STUDIES OF THE INTERPLANETARY MAGNETIC FIELD: IMP'S TO VOYAGER
Norman F. Ness *In its* Essays in Space Science Jun. 1987 p 99-121 (For primary document see N87-24247 17-88)
Avail: NTIS HC A18/MF A01 CSCL 03B

N87-24267*# California Inst. of Tech., Pasadena. Dept. of Astronomy.
HIGH MASS STAR FORMATION IN THE GALAXY
N. Z. Scoville and J. C. Good *In* NASA, Washington Star Formation in Galaxies May 1987 p 3-20 (For primary document see N87-24266 17-89)
(Grant NSF AST-84-12473)
Avail: NTIS HC A99/MF E03 CSCL 03B

N87-24270*# State Univ. of New York, Stony Brook. Astronomy Program.
MASSES, LUMINOSITIES AND DYNAMICS OF GALACTIC MOLECULAR CLOUDS
P. M. Solomon, A. R. Rivolo, T. J. Mooney, J. W. Barrett, and L. J. Sage *In* NASA, Washington Star Formation in Galaxies May 1987 p 37-59 (For primary document see N87-24266 17-89)
Avail: NTIS HC A99/MF E03 CSCL 03B

N87-24272*# National Aeronautics and Space Administration. Goddard Inst. for Space Studies, New York, N.Y.
STAR FORMATION IN CARINA OB1: OBSERVATIONS OF A GIANT MOLECULAR CLOUD ASSOCIATED WITH THE ETA CARINAE NEBULA
D. A. Grabelsky, R. S. Cohen (Columbia Univ., New York.), and P. Thaddeus *In* NASA, Washington Star Formation in Galaxies May 1987 p 67-70 (For primary document see N87-24266 17-89)
Avail: NTIS HC A99/MF E03 CSCL 03B

N87-24273*# Jet Propulsion Lab., California Inst. of Tech., Pasadena.
STAR FORMING REGIONS OF THE SOUTHERN GALAXY
T. B. H. Kuiper, J. B. Whiteoak, and J. W. Fowler (California Inst. of Tech., Pasadena.) *In* NASA, Washington Star Fromation in Galaxies May 1987 p 71-74 Sponsored by JPL (For primary document see N87-24266 17-89)
Avail: NTIS HC A99/MF E03 CSCL 03B

N87-24276*# Groningen Rijksuniversiteit (Netherlands). Lab. for Space Research.
SHOCK HEATED DUST IN L1551: L(IR) GREATER THAN 20 SOLAR LUMINOSITIES
F. O. Clark, R. J. Laureijs, G. Chlewicki, C. Y. Zhang, W. vanOosterom, and D. Kester *In* NASA, Washington Star Formation in Galaxies May 1987 p 83-86 (For primary document see N87-24266 17-89)
Avail: NTIS HC A99/MF E03 CSCL 03B

N87-24277*# Illinois Univ., Urbana-Champaign. Dept. of Physics.
MECHANISMS FOR THE CIRCULAR POLARIZATION OF ASTROPHYSICAL OH MASERS IN STAR-FORMING REGIONS AND THE INFERRED MAGNETIC FIELDS
Shuji Deguchi and William D. Watson *In* NASA, Washington Star Formation in Galaxies May 1987 p 87-90 Sponsored by NSF (For primary document see N87-24266 17-89)
Avail: NTIS HC A99/MF E03 CSCL 03B

N87-24280*# National Aeronautics and Space Administration. Goddard Space Flight Center, Greenbelt, Md.
THE LARGE SCALE GAS AND DUST DISTRIBUTION IN THE GALAXY: IMPLICATIONS FOR STAR FORMATION

T. J. Sodroski, E. Dwek, M. G. Hauser, and F. J. Kerr (Maryland Univ., College Park.) *In* NASA, Washington Star Formation in Galaxies May 1987 p 99-102 (For primary document see N87-24266 17-89)
Avail: NTIS HC A99/MF E03 CSCL 03B

N87-24287*# California Inst. of Tech., Pasadena. Infrared Processing and Analysis Center.
ON THE ORIGIN OF THE 40-120 MICRON EMISSION OF GALAXY DISKS: A COMPARISON WITH H-ALPHA FLUXES
Carol J. Lonsdale Persson and George Helou *In* NASA, Washington Star Formation in Galaxies May 1987 p 153-160 Sponsored by JPL (For primary document see N87-24266 17-89)
Avail: NTIS HC A99/MF E03 CSCL 03B

N87-24288*# Kitt Peak National Observatory, Tucson, Ariz.
STAR FORMATION IN THE MAGELLANIC CLOUDS
Jay A. Frogel *In* NASA, Washington Star Formation in Galaxies May 1987 p 161-166 (For primary document see N87-24266 17-89)
Avail: NTIS HC A99/MF E03 CSCL 03B

N87-24289*# Kitt Peak National Observatory, Tucson, Ariz.
MEASURING STAR FORMATION RATES IN BLUE GALAXIES
John S. Gallagher, III and Deidre A. Hunter (Carnegie Institution of Washington, D. C.) *In* NASA, Washington Star Formation in Galaxies May 1987 p 167-177 Sponsored in part by JPL (For primary document see N87-24266 17-89)
Avail: NTIS HC A99/MF E03 CSCL 03B

N87-24294*# Ohio State Univ., Columbus. Dept. of Physics.
STAR FORMATION AND SPIRAL STRUCTURE IN M81
Michele Kaufman and Frank N. Bash (Texas Univ., Austin.) *In* NASA, Washington Star Formation in Galaxies May 1987 p 227-233 (For primary document see N87-24266 17-89)
Avail: NTIS HC A99/MF E03 CSCL 03B

N87-24296*# California Inst. of Tech., Pasadena. Dept. of Physics.
IRAS AND GROUND-BASED OBSERVATIONS OF STAR FORMATION REGIONS IN THE MAGELLANIC CLOUDS
Jonathan H. Elias and Jay A. Frogel (Kitt Peak National Observatory, Tucson, Ariz.) *In* NASA, Washington Star Formation in Galaxies May 1987 p 241-246 Sponsored in part by NSF (For primary document see N87-24266 17-89)
Avail: NTIS HC A99/MF E03 CSCL 03B

N87-24297*# Minnesota Univ., Minneapolis.
STAR FORMATION IN THE LARGE MAGELLANIC CLOUD
Terry Jay Jones, A. R. Hyland, and Paul M. Harvey (Texas Univ., Austin.) *In* NASA, Washington Star Formation in Galaxies May 1987 p 245-246 (For primary document see N87-24266 17-89)
Avail: NTIS HC A99/MF E03 CSCL 03B

N87-24302*# Netherlands Foundation for Radio Astronomy, Dwingelo.
NEUTRAL HYDROGEN AND STAR FORMATION IN IRREGULAR GALAXIES
Evan D. Skillman *In* NASA, Washington Star Formation in Galaxies May 1987 p 263-266 Sponsored in part by the Netherlands Organization for the Advancement of Pure Research (For primary document see N87-24266 17-89)
Avail: NTIS HC A99/MF E03 CSCL 03B

N87-24306*# Institut d'Astrophysique, Paris (France).
PRESENT STAR FORMATION IN SPRIALS OF THE VIRGO CLUSTER
B. Guiderdoni *In* NASA, Washington Star Formation in Galaxies May 1987 p 283-286 (For primary document see N87-24266 17-89)
Avail: NTIS HC A99/MF E03 CSCL 03B

N87-24307*# Massachusetts Univ., Amherst. Dept. of Physics and Astronomy.
MOLECULAR GAS AND STAR FORMATION IN HI-DEFICIENT VIRGO CLUSTER GALAXIES
Jeffrey D. Kenney and Judith S. Young *In* NASA, Washington Star Formation in Galaxies May 1987 p 287-292 (For primary document see N87-24266 17-89)
Avail: NTIS HC A99/MF E03 CSCL 03B

N87-24308*# Arizona State Univ., Tempe. Dept. of Physics.
STAR FORMATION RATES AS A FUNCTION OF GALAXY MASS
W. Romanishin *In* NASA, Washington Star Formation in Galaxies May 1987 p 293-296 (For primary document see N87-24266 17-89)
(Contract JPL-957317)
Avail: NTIS HC A99/MF E03 CSCL 03B

N87-24309*# California Inst. of Tech., Pasadena. Infrared Processing and Analysis Center.
GLOBAL PROPERTIES OF THE NEARBY SPIRAL M101
C. Beichman, F. Boulanger, W. Rice, Carol J. Lonsdale Persson, and F. Viallefond (Institut d'Astrophysique, Paris, France) *In* NASA, Washington Star Formation in Galaxies May 1987 p 297-302 Prepared in cooperation with JPL, California Inst. of Tech., Pasadena (For primary document see N87-24266 17-89)
Avail: NTIS HC A99/MF E03 CSCL 03B

N87-24310*# Massachusetts Univ., Amherst. Dept. of Physics and Astronomy.
EFFICIENT STAR FORMATION IN THE BRIGHT BAR OF M83
S. D. Lord, S. E. Strom, and J. S. Young *In* NASA, Washington Star Formation in Galaxies May 1987 p 303-307 (For primary document see N87-24266 17-89)
(Grant NSF AST-82-12252)
Avail: NTIS HC A99/MF E03 CSCL 03B

N87-24311*# Illinois Univ., Urbana. Dept. of Astronomy.
LARGE SCALE DISSOCIATION OF MOLECULAR GAS IN THE SPRIAL ARMS OF M51
R. P. J. Tilanus and R. J. Allen *In* NASA, Washington Star Formation in Galaxies May 1987 p 309-313 Sponsored in part by the Netherlands Organization for the Advancement of Pure Research (For primary document see N87-24266 17-89)
Avail: NTIS HC A99/MF E03 CSCL 03B

N87-24312*# Onsala Space Observatory (Sweden).
STRUCTURE AND KINEMATICS OF THE MOLECULAR SPIRAL ARMS IN M51
G. Rydbeck, A. Hjalmarson, L. E. B. Johansson, O. E. H. Rydbeck, and T. Wiklind *In* NASA, Washington Star Formation in Galaxies May 1987 p 315-317 Sponsored by JPL (For primary document see N87-24266 17-89)
Avail: NTIS HC A99/MF E03 CSCL 03B

N87-24316*# Lick Observatory, Mount Hamilton, Calif.
STAR FORMING REGIONS IN GAS-RICH SO GALAXIES
Richard W. Pogge and Paul B. Eskridge (Washington Univ., Seattle.) *In* NASA, Washington Star Formation in Galaxies May 1987 p 333-336 (For primary document see N87-24266 17-89)
Avail: NTIS HC A99/MF E03 CSCL 03B

N87-24317*# Space Telescope Science Inst., Baltimore, Md.
A SIMPLE THEORY OF BIMODAL STAR FORMATION
Rosemary F. G. Wyse and J. Silk (California Univ., Berkeley.) *In* NASA, Washington Star Formation in Galaxies May 1987 p 339-342 Sponsored in part by Calspace (For primary document see N87-24266 17-89)
Avail: NTIS HC A99/MF E03 CSCL 03B

N87-24318*# Arizona Univ., Tucson. Dept. of Planetary Sciences.
THE HISTORY OF GAS IN SPRIAL GALAXIES
Philip Maloney *In* NASA, Washington Star Formation in

Galaxies May 1987 p 343-347 (For primary document see N87-24266 17-89)
Avail: NTIS HC A99/MF E03 CSCL 03B

N87-24319*# Pennsylvania State Univ., University Park. Dept. of Astronomy.
STARBURST GALAXIES
Daniel W. Weedman *In* NASA, Washington Star Formation in Galaxies May 1987 p 351-361 (For primary document see N87-24266 17-89)
Avail: NTIS HC A99/MF E03 CSCL 03B

N87-24321*# California Inst. of Tech., Pasadena.
MOLECULAR GAS IN THE STARBURST NUCLEUS OF M82
K. Y. Lo *In* NASA, Washington Star Formation in Galaxies May 1987 p 367-382 (For primary document see N87-24266 17-89)
Avail: NTIS HC A99/MF E03 CSCL 03B

N87-24322*# Harvard-Smithsonian Center for Astrophysics, Cambridge, Mass.
NUCLEAR STAR FORMATION ON 100 PARSEC SCALES: 10' RESOLUTION RADIO CONTINUUM, HI AND CO OBSERVATIONS
Jean L. Turner, Paul T. P. Ho, and Robert N. Martin (Arizona Univ., Tucson.) *In* NASA, Washington Star Formation in Galaxies May 1987 p 383-386 (For primary document see N87-24266 17-89)
(Grants NATO-83/584; NSF AST-85-09907)
Avail: NTIS HC A99/MF E03 CSCL 03B

N87-24324*# Johns Hopkins Univ., Baltimore, Md.
STAR FORMATION AND DYNAMICS IN STARBURST NUCLEI
Colin A. Norman *In* NASA, Washington Star Formation in Galaxies May 1987 p 395-400 Prepared in cooperation with Space Telescope Science Inst.,Baltimore, Md. (For primary document see N87-24266 17-89)
Avail: NTIS HC A99/MF E03 CSCL 03B

N87-24325*# Minnesota Univ., Minneapolis. Dept. of Astronomy.
INDUCED STAR FORMATION IN INTERACTING GALAXIES
R. C. Kennicutt, K. A. Roettiger, W. C. Keel, J. M. vanderHulst, and E. Hummel (Max-Planck-Inst. fuer Radioastronomie, Bonn, West Germany) *In* NASA, Washington Star Formation in Galaxies May 1987 p 401-408 (For primary document see N87-24266 17-89)
(Contract JPL-957243; Grants NATO-0592/82; NSF AST-81-11711)
Avail: NTIS HC A99/MF E03 CSCL 03B

N87-24326*# Arizona Univ., Tucson.
THE FREQUENCY OF ENHANCED STAR FORMATION IN INTERACTING AND ISOLATED GALAXIES Abstract Only
Roc M. Cutri *In* NASA, Washington Star Formation in Galaxies May 1987 p 409 (For primary document see N87-24266 17-89)
Avail: NTIS HC A99/MF E03 CSCL 03B

N87-24329*# Iowa State Univ. of Science and Technology, Ames. Astronomy Program.
CLOUD FLUID MODELS OF GAS DYNAMICS AND STAR FORMATION IN GALAXIES
Curtis Struck-Marcell, John M. Scalo (Texas Univ., Austin.), and P. N. Appleton *In* NASA, Washington Star Formation in Galaxies May 1987 p 435-460 (For primary document see N87-24266 17-89)
Avail: NTIS HC A99/MF E03 CSCL 03B

N87-24330*# Maryland Univ., College Park. Astronomy Program.
STARBURST-DRIVEN SUPERWINDS FROM INFRARED GALAXIES
Timothy M. Heckman, Lee Armus, Patrick McCarthy, Wil vanBreugel, and George K. Miley (Space Telescope Science Inst., Baltimore, Md.) *In* NASA, Washington Star Formation in Galaxies May 1987 p 461-469 (For primary document see N87-24266 17-89)
Avail: NTIS HC A99/MF E03 CSCL 03B

N87-24334*# Massachusetts Inst. of Tech., Cambridge.
A DUST SCATTERED HALO IN STARBURST GALAXY M82?
Michael Rohan, Philip Morrison, and Alberto Sadun *In* NASA, Washington Star Formation in Galaxies May 1987 p 485-489 (For primary document see N87-24266 17-89)
Avail: NTIS HC A99/MF E03 CSCL 03B

N87-24357*# Edinburgh Univ. (Scotland). Dept. of Astronomy.
ENHANCED STAR FORMATION: THE IMPORTANCE OF BARS IN SPIRAL GALAXIES
P. J. Puxley, T. G. Hawarden, C. M. Mountain (Royal Observatory, Edinburgh, Scotland), and S. K. Leggett *In* NASA, Washington Star Formation in Galaxies May 1987 p 619-622 (For primary document see N87-24266 17-89)
Avail: NTIS HC A99/MF E03 CSCL 03B

N87-24358*# Royal Observatory, Edinburgh (Scotland).
THE PROPERTIES OF HIGHLY LUMINOUS IRAS GALAXIES
R. D. Wolstencroft, P. J. Puxley, J. N. Heasley, S. K. Leggett (Edinburgh Univ., Scotland), A. Savage, H. T. MacGillivray, and R. G. Clowes *In* NASA, Washington Star Formation in Galaxies May 1987 p 623-627 (For primary document see N87-24266 17-89)
Avail: NTIS HC A99/MF E03 CSCL 03B

N87-24360*# Arizona Univ., Tucson.
THE RELATION BETWEEN STAR FORMATION AND ACTIVE NUCLEI
G. H. Rieke *In* NASA, Washington Star Formation in Galaxies May 1987 p 633-641 Sponsored by NSF (For primary document see N87-24266 17-89)
Avail: NTIS HC A99/MF E03 CSCL 03B

N87-24363*# Leiden Univ. (Netherlands). Sterrewacht.
STAR FORMATION AROUND ACTIVE GALACTIC NUCLEI
William C. Keel *In* NASA, Washington Star Formation in Galaxies May 1987 p 661-667 (For primary document see N87-24266 17-89)
Avail: NTIS HC A99/MF E03 CSCL 03B

N87-24364*# European Southern Observatory, La Silla (Chile).
STAR FORMATION IN SEYFERT GALAXIES
J. M. Rodriguez Espinosa, Richard J. Rudy, and Barbara Jones (California Univ., San Diego.) *In* NASA, Washington Star Formation in Galaxies May 1987 p 669-674 (For primary document see N87-24266 17-89)
Avail: NTIS HC A99/MF E03 CSCL 03B

N87-24370*# National Aeronautics and Space Administration. Goddard Space Flight Center, Greenbelt, Md.
STRUCTURE IN THE NUCLEUS OF NGC 1068 AT 10 MICRONS
R. Tresch-Fienberg, G. G. Fazio, D. Y. Gezari, W. F. Hoffmann, G. M. Lamb, P. K. Shu, and C. R. McCreight (National Aeronautics and Space Administration. Ames Research Center, Moffett Field, Calif.) *In* NASA, Washington Star Formation in Galaxies May 1987 p 717-721 Previously announced in IAA as A87-30957 (For primary document see N87-24266 17-89)
Avail: NTIS HC A99/MF E03 CSCL 03B

91 LUNAR AND PLANETARY EXPLORATION

Includes planetology; and manned and unmanned flights.

For spacecraft design or space stations see *18 Spacecraft Design, Testing and Performance.*

N87-24381*# National Academy of Sciences - National Research Council, Washington, D. C. Space Science Board.
STRATEGY FOR EXPLORATION OF THE OUTER PLANETS: 1986-1996 Interim Report
Dec. 1986 110 p Sponsored by NASA, Washington
(NASA-CR-181021; NAS 1.26:181021; PB87-158556) Avail: NTIS HC A06/MF A01 CSCL 03B

Over the past decade COMPLEX has published three strategy reports which, taken together, encompass the entire planetary system and recommend a coherent program of planetary exploration. The highest priority for outer planet exploration during the next decade is intensive study of Saturn (the planet, satellites, rings, and magnetosphere) as a system. The Committee additionally recommends that NASA engage in the following supporting activities: increased support of laboratory and theoretical studies; pursuit of earth-based and earth-orbital observations; commitment to continued operation of productive spacecraft; implementation of the instrument development plan as appropriate for the outer solar system; studies of deep atmospheric probes; development of penetrators or other hard landers; development of radiation-hardened spacecraft; and development of low-thrust propulsion systems. Longer-term objectives include exploration and intensive study of: the Uranus and Neptune systems; planetology of the Galilean satellites and Titan; and the inner Jovian system. GRA

N87-24248*# Iowa Univ., Iowa City. Dept. of Physics and Astronomy.
MAGNETOSPHERES OF THE OUTER PLANETS
James A. VanAllen *In* NASA Goddard Space Flight Center, Greenbelt, Md. Essays in Space Science Jun. 1987 p 1-17
(For primary document see N87-24247 17-88)
(Contracts NAS2-11125; N00014-76-C-0016)
Avail: NTIS HC A18/MF A01 CSCL 03B

92 SOLAR PHYSICS

Includes solar activity, solar flares, solar radiation and sunspots.

For related information see *93 Space Radiation.*

N87-24382# Colorado Univ., Boulder. Dept. of Astrophysical Planetary and Atmospheric Sciences.
VECTOR ARRAY PROCESSOR COMPUTER EQUIPMENT Final Report, 1 Jan. - 31 Dec. 1985
Juri Toomre 6 Feb. 1987 16 p
(Grant AF-AFOSR-0070-85)
(AD-A179545; AFOSR-87-0497TR) Avail: NTIS HC A02/MF A01 CSCL 03A

To support the on-going research on Solar Oscillations and Convective Flows as Probes of Structure in the Subphotosphere, a vector array processor system was acquired to augment the existing DEC VAX-11/750 computer system. The fifty-fold average increase in computing speed offered by the array processor would make it feasible to invert solar oscillation data on a regular basis, and thereby permit us to use the five-minutes oscillations of the Sun to probe the turbulent convection zone below the surface of this star. The array processor would also permit us to carry out detailed numerical experiments with compressible convection in the presence of magnetic fields, for the speed and memory of the machine makes it a formidable tool for direct numerical simulations of two- and three-dimensional fluid dynamics. Such theoretical simulations are also needed to study the solar dynamo and its ability to build and transform magnetic fields, an issue central to solar-terrestrial variability and predictions of solar activity. Attached as Appendix A is a cover article in Science Magazine that describes the importance of the work on the Seismology of the Sun that is beginning to emerge from the class of array processors. GRA

N87-24383# South Carolina Univ., Columbia.
EXPERIMENTAL BOUNDS ON BETA BETA-DECAY, COLD DARK MATTER AND SOLAR AXIONS WITH AN ULTRALOW BACKGROUND Ge DETECTOR
F. T. Avignone, III, S. P. Ahlen, R. L. Brodzinski, S. Dimopolous, A. K. Drukier, G. Gelmini, B. W. Lynn, H. S. Miley, J. H. Reeves, D. N. Spergel et al. Oct. 1986 21 p Presented at the 7th Vanderbilt High Energy Physics Conference, Nashville, Tenn., 15 May 1986 Prepared in cooperation with Boston Univ., Mass., Pacific Northwest Lab., Richland, Wash., Stanford Univ., Calif., Harvard-Smithsonian Astrophysics Center, Cambridge, Mass. and Harvard Univ., Cambridge, Mass.
(Contracts DE-AC03-76SF-00515; DE-AC06-76RL-01830; Grants NSF PHY-84-05654; NSF PHY-83-10654; NSF PHY-83-06693; NSF PHY-82-15249)
(DE87-002065; PNL-SA-14385; CONF-8605182-4) Avail: NTIS HC A02/MF A01

The PNL/USC ultralow background prototype Ge detector in the Homestake goldmine is being applied to searches for 0 nu beta beta-decay, dark matter candidates and solar axions. An upper bound of 2.2 eV has been placed on the Majorana mass of the electron neutrino. The low energy data exclude particles with spin independent Z deg exchange interactions having masses between 20 GeV and 5 TeV as significant contributors to the cold dark matter of the halo of our galaxy. The existence of stable Dirac neutrinos more massive than 20 GeV is also excluded except for a narrow region around the Z deg resonance. Finally, Dine-Fischler-Srednicki (DFS) axion models with F/2x (sup 1)(sub e) less than or equal to 0.5 x 10 to the 7th GeV are ruled out by the maximum count rate attributable to solar axions. DOE

N87-24384# National Oceanic and Atmospheric Administration, Boulder, Colo. Space Environment Lab.
PERSONAL COMPUTER BASED GOES DATA ARCHIVE
H. H. Sauer Jan. 1987 15 p
(PB87-157517; NOAA-TM-ERL-SEL-74) Avail: NTIS HC A02/MF A01 CSCL 03B

An archive of space environment monitor data obtained from the GOES geosynchronous satellite operated by the National Oceanic and Atmospheric Administration was developed. The data archived consist of GOES observations of solar X-rays integrated over the solar disk, the geosynchronous energetic particle populations. The structure and content of the archive data base is described, as are associated plot programs by which the date may be examined. GRA

N87-24385# National Geophysical Data Center, Boulder, Colo.
SOLAR-GEOPHYSICAL DATA NUMBER 509, JANUARY 1987. PART 1: (PROMPT REPORTS). DATA FOR DECEMBER 1986, NOVEMBER 1986
H. E. Coffey Jan. 1987 100 p
(Contract N00014-86-F-0049)
(PB87-162574; SGD-509-Pt-1) Avail: NTIS HC A05/MF A01 CSCL 03B

Data included consist of detailed index for 1986; data for December 1986 (advanced and worldwide IUWDS alert periods, solar activity indices, solar flares, solar radio emission, and Standard mean solar magnetic field); data for November 1986 (solar active regions, sudden ionospheric disturbances, solar radio spectral observations, cosmic ray measurements by neutral monitor, geomagnetic indices, radio propagation indices); and late data (cosmic ray measurements by neutron monitor, geomagnetic indices, calcium plage data July-August 1986). GRA

N87-24386# National Geophysical Data Center, Boulder, Colo.
SOLAR-GEOPHYSICAL DATA NUMBER 509, JANUARY 1987. PART 2: (COMPREHENSIVE REPORTS). DATA FOR JULY 1986

H. E. Coffey Jan. 1987 79 p
(Contract N00014-86-F-0049)
(PB87-162582; SGD-509-Pt-2) Avail: NTIS HC A05/MF A01 CSCL 03B

Data included are: a detailed index for 1986; data for July 1986 (Meudon carte synoptique, solar flares, solar radio bursts at fixed frequencies; solar X-ray radiation from GOES satellite, mass ejections from the sun, and active prominences and filaments); and miscellaneous data (interplanetary solar plasma). GRA

N87-24387*# Smithsonian Astrophysical Observatory, Cambridge, Mass.
PHYSICS OF THE INNER HELIOSPHERE: MECHANISMS, MODELS AND OBSERVATIONAL SIGNATURES Semiannual Progress Reports, 1 May 1986 - 30 Apr. 1987
George L. Withbroe Jun. 1987 22 p
(Grant NAGw-249)
(NASA-CR-181063; NAS 1.26:181063; SAPR-10; SAPR-11) Avail: NTIS HC A02/MF A01 CSCL 03B

Selected problems concerned with the important physical processes that occur in the corona and solar wind acceleration region, particularly time dependent phenomena were studied. Both the physics of the phenomena and the resultant effects on observational signatures, particularly spectroscopic signatures were also studied. Phenomena under study include: wave motions, particularly Alfven and fast mode waves; the formation of standing shocks in the inner heliosphere as a result of momentum and/or heat addition to the wind; and coronal transient phenomena where momentum and/or heat are deposited in the corona to produce transient plasma heating and/or mass ejection. The development of theoretical models for the inner heliosphere, the theoretical investigation of spectroscopic plasma diagnostics for this region, and the analysis of existing skylab and other relevant data are also included. B.G.

N87-24252*# California Univ., Berkeley. Space Sciences Lab.
PARTICLE PROPAGATION CHANNELS IN THE SOLAR WIND
K. A. Anderson and W. M. Dougherty *In* NASA Goddard Space Flight Center, Greenbelt, Md. Essays in Space Science Jun. 1987 p 87-98 (For primary document see N87-24247 17-88)
(Grant NAG5-376)
Avail: NTIS HC A18/MF A01 CSCL 03B

93 SPACE RADIATION

Includes cosmic radiation; and inner and outer earth's radiation belts.

For biological effects of radiation see *52 Aerospace Medicine*. For theory see *73 Nuclear and High-Energy Physics*.

N87-24388# Chicago Univ., Ill. Enrico Fermi Inst.
PARTICLE PHYSICS AND COSMOLOGY Technical Progress Report
M. S. Turner and D. N. Schramm Jan. 1987 13 p
(Contract DE-FG02-85ER-40234)
(DE87-007308; DOE/ER-40234/2) Avail: NTIS HC A02/MF A01

A brief summary of research carried out since January 1985 is given. Topics covered include inflationary universe models; cosmology in extra dimensions/superstrings; particle emission from the direction of Cygnus X-3; ultra-high energy cosmic ray physics; astrophysical/cosmological constraints on particle physics; quantum fields in curved space-time, dark matter, exotic relics, and structure formation in the universe; and resonant neutrino oscillations (RNO). A list of publications resulting from this research during the period from 1985 through 1986 is also included. DOE

N87-24389# Severn Communications Corp., Severna Park, Md.
SATELLITE OBSERVATION OF ATMOSPHERIC NUCLEAR GAMMA RADIATION
J. R. Letaw, G. H. Share, R. L. Kinzer, R. Silberberg, and C. H. Tsao Jan. 1987 32 p
(Contract N00014-85-C-2200)
(AD-A177937) Avail: NTIS HC A03/MF A01 CSCL 18H

A satellite observation of the spectrum of gamma radiation from the Earth's atmosphere is presented in the energy interval from 300 keV to 8.5 MeV. The data were accumulated by the Gamma Ray Spectrometer on the Solar Maximum Mission over three and one-half years. The excellent statistical accuracy of the data set allows 20 atmosphere line features to be distinguished. All observed lines are consistent with production by secondary neutron interactions with atmospheric N-14 and O-16. Although no evidence was found for other production mechanisms, direct excitation or spallation by primary protons cannot be ruled out as a source of atmospheric line radiation. Line intensities are in rough agreement with theoretical models which are presently limited by cross section availability. The intensity and spectrum of scattered photons at energies below the 0.511 MeV line can be accounted for by Compton scattering in a 21 g/sq cm slab of atmosphere. GRA

N87-24250*# National Aeronautics and Space Administration. Goddard Space Flight Center, Greenbelt, Md.
PARTICLE ACCELERATION IN SOLAR FLARES
R. Ramaty and M. A. Forman (State Univ. of New York, Stony Brook.) *In its* Essays in Space Science Jun. 1987 p 47-73 (For primary document see N87-24247 17-88)
Avail: NTIS HC A18/MF A01 CSCL 03B

N87-24254*# New Hampshire Univ., Durham. Dept. of Physics.
COSMIC RAYS IN THE HELIOSPHERE
William R. Webber *In* NASA Goddard Space Flight Center, Greenbelt, Md. Essays in Space Science Jun. 1987 p 125-154 (For primary document see N87-24247 17-88)
Avail: NTIS HC A18/MF A01 CSCL 03B

N87-24255*# National Aeronautics and Space Administration. Goddard Space Flight Center, Greenbelt, Md.
ANTIPROTONS IN COSMIC RAYS
V. K. Balasubrahmanyan, J. F. Ormes, and R. E. Streitmatter *In its* Essays in Space Science Jun. 1987 p 155-172 (For primary document see N87-24247 17-88)
Avail: NTIS HC A18/MF A01 CSCL 03B

N87-24256*# Washington Univ., St. Louis, Mo. Dept. of Physics and the McDonnell Center for the Space Sciences.
MEASUREMENTS OF ULTRAHEAVY COSMIC RAYS WITH HEAO-3
W. R. Binns, M. H. Israel, J. Klarmann, T. L. Garrard, E. C. Stone, and C. J. Waddington (Minnesota Univ., Minneapolis.) *In* NASA Goddard Space Flight Center, Greenbelt, Md. Essays in Space Science Jun. 1987 p 173-189 (For primary document see N87-24247 17-88)
(Contracts NAS8-27976; NAS8-27977; NAS8-27978; Grants NAG8-498; NAG8-500; NAG8-502; NgR05-002-160; NgR24-005-050; NgR26-008-001)
Avail: NTIS HC A18/MF A01 CSCL 03B

N87-24257*# National Aeronautics and Space Administration. Goddard Space Flight Center, Greenbelt, Md.
ORIGIN AND PROPAGATION OF GALACTIC COSMIC RAYS
Catherine J. Cesarsky (Commissariat a l'Energie Atomique, Gif-sur-Yvette, France) and Jonathan F. Ormes *In its* Essays in Space Science Jun. 1987 p 191-223 (For primary document see N87-24247 17-88)
Avail: NTIS HC A18/MF A01 CSCL 03B

N87-24259*# Jet Propulsion Lab., California Inst. of Tech., Pasadena.
NUCLEOSYNTHESIS AND ASTROPHYSICAL GAMMA RAY SPECTROSCOPY
Allan S. Jacobson *In* NASA Goddard Space Flight Center, Greenbelt, Md. Essays in Space Science Jun. 1987 p 275-294 (For primary document see N87-24247 17-88)
Avail: NTIS HC A18/MF A01 CSCL 03B

N87-24260*# National Aeronautics and Space Administration. Goddard Space Flight Center, Greenbelt, Md.
GAMMA RAY TRANSIENTS
Thomas L. Cline *In its* Essays in Space Science Jun. 1987 p 295-316 (For primary document see N87-24247 17-88)
Avail: NTIS HC A18/MF A01 CSCL 03B

N87-24261*# Space Telescope Science Inst., Baltimore, Md.
DISCRETE X-RAY SOURCES AND THE X-RAY BACKGROUND
Riccardo Giacconi *In* NASA Goddard Space Flight Center, Greenbelt, Md. Essays in Space Science Jun. 1987 p 317-338 (For primary document see N87-24247 17-88)
Avail: NTIS HC A18/MF A01 CSCL 03B

N87-24262*# National Aeronautics and Space Administration. Goddard Space Flight Center, Greenbelt, Md.
THE COSMIC X-RAY BACKGROUND
Elihu A. Boldt *In its* Essays in Space Science Jun. 1987 p 339-378 (For primary document see N87-24247 17-88)
Avail: NTIS HC A18/MF A01 CSCL 03B

N87-24268*# Ecole Normale Superieure, Paris (France). Radioastronomie.
DIFFUSE INFRARED EMISSION OF THE GALAXY: LARGE SCALE PROPERTIES Abstract Only
J. L. Puget, M. Perault, F. Boulanger, and E. Falgarone *In* NASA, Washington Star Formation in Galaxies May 1987 p 21 (For primary document see N87-24266 17-89)
Avail: NTIS HC A99/MF E03 CSCL 03B

N87-24269*# Max-Planck-Inst. fuer Radioastronomie, Bonn (West Germany).
THE ORIGIN OF THE DIFFUSE GALACTIC IR/SUBmm EMISSION: REVISITED AFTER IRAS
P. Cox and P. G. Mezger *In* NASA, Washington Star Formation in Galaxies May 1987 p 23-35 (For primary document see N87-24266 17-89)
Avail: NTIS HC A99/MF E03 CSCL 03B

N87-24275*# California Inst. of Tech., Pasadena. Div. of Physics, Mathematics and Astronomy.
MAPS OF MILLIMETER WAVE EMISSION FROM THREE GALACTIC STAR-FORMING REGIONS
Mary Barsony *In* NASA, Washington Star Formation in Galaxies May 1987 p 79-82 (For primary document see N87-24266 17-89)
(Grants NSF AST-84-12473; NSF AST-84-03054)
Avail: NTIS HC A99/MF E03 CSCL 03B

N87-24278*# Centre National de la Recherche Scientifique, Toulouse (France). Centre d'Etude Spatiales des Rayonnements.
SURVEY OF THE GALACTIC DISK FROM 1 = -150 DEG TO 1 = 82 DEG IN THE SUBMILLIMETER RANGE
Emmanuel Caux and Guy Serra *In* NASA, Washington Star Formation in Galaxies May 1987 p 93-96 Original language document was announced in IAA as A87-17077 (For primary document see N87-24266 17-89)
Avail: NTIS HC A99/MF E03 CSCL 03B

N87-24279*# Ecole Normale Superieure, Paris (France). Radioastronomie
DIFFUSE INFRARED EMISSION OF THE GALAXY: LARGE SCALE PROPERTIES
M. Perault, F. Boulanger, E. Falgarone, and J. L. Puget *In* NASA, Washington Star Formation in Galaxies May 1987 p 97 Prepared in cooperation with California Inst. of Tech., Pasadena (For primary document see N87-24266 17-89)
Avail: NTIS HC A99/MF E03 CSCL 03B

N87-24286*# London Univ. (England). Theoretical Astronomy Unit.
MODELS FOR INFRARED EMISSION FROM IRAS GALAXIES
M. Rowan-Robinson *In* NASA, Washington Star Formation in Galaxies May 1987 p 133-152 (For primary document see N87-24266 17-89)
Avail: NTIS HC A99/MF E03 CSCL 03B

N87-24298*# Groningen Rijksuniversiteit (Netherlands). Space Research.
INFRARED EMISSION AND EXCITATION IN LMC HII REGIONS
V. Ungerer and F. Viallefond (Observatoire de Paris-Meudon, France) *In* NASA, Washington Star Formation in Galaxies May 1987 p 247-251 (For primary document see N87-24266 17-89)
Avail: NTIS HC A99/MF E03 CSCL 03B

N87-24303*# Wyoming Univ., Laramie. Infrared Observatory.
CARBON MONOXIDE EMISSION FROM SMALL GALAXIES
Harley A. Thronson, Jr. and John Bally (Bell Telephone Labs., Inc., Murray Hill, N. J.) *In* NASA, Washington Star Formation in Galaxies May 1987 p 267-270 (For primary document see N87-24266 17-89)
(Grant NAG2-134)
Avail: NTIS HC A99/MF E03 CSCL 03B

N87-24305*# Arecibo Ionospheric Observatory, Puerto Rico.
FAR-INFRARED PROPERTIES OF CLUSTER GALAXIES
M. D. Bicay and R. Giovanelli (Stanford Univ., Calif.) *In* NASA, Washington Star Formation in Galaxies May 1987 p 277-281 (For primary document see N87-24266 17-89)
(Contract NAS7-918)
Avail: NTIS HC A99/MF E03 CSCL 03B

N87-24314*# Amsterdam Univ. (Netherlands). Astronomical Inst.
A SIMPLE TWO-COMPONENT MODEL FOR THE FAR-INFRARED EMISSION FROM GALAXIES
T. deJong and K. Brink *In* NASA, Washington Star Formation in Galaxies May 1987 p 323-328 Sponsored by the Netherlands Foundation for Astronomical Research and the Netherlands Organization for the Advancement of Pure Research (For primary document see N87-24266 17-89)
Avail: NTIS HC A99/MF E03 CSCL 03B

N87-24349*# Minnesota Univ., Minneapolis. Dept. of Astronomy.
THE CORRELATION BETWEEN FAR-IR AND RADIO CONTINUUM EMISSION FROM SPIRAL GALAXIES
John M. Dickey, Robert W. Garwood, and George Helou (California Inst. of Tech., Pasadena.) *In* NASA, Washington Star Formation in Galaxies May 1987 p 575-578 (For primary document see N87-24266 17-89)
Avail: NTIS HC A99/MF E03 CSCL 03B

N87-24352*# Max-Planck-Inst. fuer Radioastronomie, Bonn (West Germany).
RADIO CONTINUUM, FAR INFRARED AND STAR FORMATION
R. Wielebinski, E. Wunderlich, U. Klein (Bonn Univ., West Germany), and E. Hummel *In* NASA, Washington Star Formation in Galaxies May 1987 p 589-593 (For primary document see N87-24266 17-89
Avail: NTIS HC A99/MF E03 CSCL 03B

N87-24356*# Hawaii Univ., Honolulu. Inst. for Astronomy.
NUCLEAR INFRARED EMISSION AND THE COLORS OF IRAS GALAXIES
Gary J. Hill *In* NASA, Washington Star Formation in Galaxies May 1987 p 611-617 (For primary document see N87-24266 17-89)
(Grant NSF AST-84-18197)
Avail: NTIS HC A99/MF E03 CSCL 03B

N87-24368*# Imperial Coll. of Science and Technology, London (England).
EVIDENCE FOR EXTENDED IR EMISSION IN NGC2798 AND NGC6240
G. S. Wright, R. D. Joseph, P. A. James, and N. A. Robertson *In* NASA, Washington Star Formation in Galaxies May 1987

p 707-710 (For primary document see N87-24266 17-89)
Avail: NTIS HC A99/MF E03 CSCL 03B

N87-24369*# Manchester Univ. (England).
MODELS RELATING THE RADIO EMISSION AND IONISED GAS IN SEYFERT NUCLEI
A. Pedlar, S. W. Unger, D. J. Axon, and J. E. Dyson *In* NASA, Washington Star Formation in Galaxies May 1987 p 711-715 (For primary document see N87-24266 17-89)
Avail: NTIS HC A99/MF E03 CSCL 03B

99 GENERAL

N87-24390*# National Aeronautics and Space Administration. Langley Research Center, Hampton, Va.
ENGINEER IN CHARGE: A HISTORY OF THE LANGLEY AERONAUTICAL LABORATORY, 1917-1958
James R. Hansen (Maine Univ., Orono.) Washington, D.C. 1986 643 p NASA History Series
(Contract NASw-3502)
(NASA-SP-4305; NAS 1.21:4305) Avail: SOD HC $30.00 as 033-000-00999-2; NTIS MF A01 CSCL 05B

A history is presented by using the most technologically significant research programs associated with the Langley Aeronautical Laboratory from 1917 to 1958 and those programs that, after preliminary research, seemed best to illustrate how the laboratory was organized, how it works, and how it cooperated with industry and the military. B.G.

N87-24391*# National Aeronautics and Space Administration. Ames Research Center, Moffett Field, Calif.
RESEARCH AND TECHNOLOGY Annual Report, 1986
Apr. 1987 184 p
(NASA-TM-89411; A-87031; NAS 1.15:89411) Avail: NTIS HC A09/MF A01 CSCL 05D

Selected achievements at the Ames-Moffett and Ames-Dryden sites of the Ames Research Center are illustrated. The challenging work that was accomplished in the past year is presented for the following areas: engineering and technical services, aerospace systems, flight operations and research, aerophysics, and space research. B.G.

N87-24392*# National Aeronautics and Space Administration. John F. Kennedy Space Center, Cocoa Beach, Fla.
RESEARCH AND TECHNOLOGY Annual Report, 1986
Dec. 1986 66 p
(NASA-TM-89193; NAS 1.15:89193) Avail: NTIS HC A04/MF A01 CSCL 05D

As the NASA Center responsible for assembly, checkout, servicing, launch, recovery, and operational support of Space Transportation System elements and payloads, Kennedy Space Center is placing increasing emphasis on the Center's research and technology program. In addition to strengthening those areas of engineering and operations technology that contribute to safer, more efficient, and more economical execution of our current mission, we are developing the technological tools needed to execute the Center's mission relative to future programs. The Engineering Development Directorate encompasses most of the laboratories and other Center resources that are key elements of research and technology program implementation, and is responsible for implementation of the majority of the projects in this Kennedy Space Center 1986 Annual Report. Author

N87-24393# Air Force Systems Command, Wright-Patterson AFB, Ohio. Foreign Technology Div.
HISTORY OF SPACEFLIGHT
Yu. Lin 4 Mar. 1987 18 p Transl. into ENGLISH from Hangkong Zhishi (China), no. 7, Jul. 1986 p 20-22
(AD-A178381; FTD-ID(RS)T-1218-86) Avail: NTIS HC A02/MF A01 CSCL 22A

Ever since the opening of a new chapter of spaceflight activity on October 4, 1957, the Soviet Union and the United States had launched a total of nine scientific satellites in a little over one year's time and had obtained preliminary understanding of some conditions outside the Earth's atmosphere to set the ground for further spaceflight activities. At that time, out of military necessity and for practical civilian applications, in addition to continuing the development of scientific satellites and thoroughly studying outer space, the manufacturing of satellites that have practical value had become a pressing matter. GRA

Typical Subject Index Listing

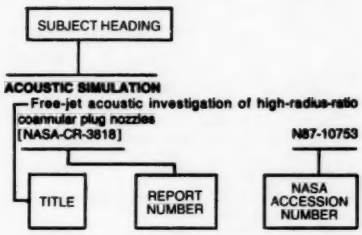

The subject heading is the key to the subject content of the document. Titles, report numbers, and accession numbers of pertinent documents are provided under each subject heading. When the title is insufficiently descriptive of the document content, a title extension has been added, separated from the title by three hyphens. The report number helps to indicate the type of document cited (e.g., NASA report, NASA translation, NASA contractor report). The NASA accession number is the number by which the document abstracts are arranged in this journal and by which the document is sold or requested. The titles, with title extensions if present, are arranged under each subject heading in ascending accession number order. The subject headings have been selected from the latest revision of the *NASA Thesaurus* (NASA SP-7053).

A

A-300 AIRCRAFT
Simulation of fly-by-wire control for civil transport aircraft at the French Centre d'Essais en Vol N87-23647
A-320 AIRCRAFT
Simulation of fly-by-wire control for civil transport aircraft at the French Centre d'Essais en Vol N87-23647
ABERRATION
Holographic correction of aberrations in optical systems employing synthetic apertures
[AD-A179107] N87-24173
ABLATION
A mechanistic study of the interaction of ultraviolet laser radiation with low density polymers
[DE87-007846] N87-23734
Numerical prediction of 1-D ablation using a finite control volume procedure with exponential differencing
[DE87-007947] N87-24130
ABNORMALITIES
Aeromedical evaluation and disposition of electrocardiographic abnormalities N87-24071
ABSORBENTS
The fiber optic refrigeration cycle monitor
[DE87-006632] N87-24180
ABSORPTION SPECTRA
Medium- and long-wave infrared absorption spectra of carbon dioxide nitrous oxide at 800K
[AD-A179430] N87-23708
ABSTRACTS
The Shock and Vibration Digest, Volume 19, No. 6 N87-24125
Nonlinear real-time optical signal processing
[AD-A178169] N87-24182
ABUNDANCE
Antiprotons in cosmic rays N87-24255
Measurements of ultraheavy cosmic rays with HEAO-3 N87-24256
Origin and propagation of galactic cosmic rays N87-24257
Neutral hydrogen and star formation in irregular galaxies N87-24302
Star forming regions in gas-rich SO galaxies N87-24316
ACCELERATED LIFE TESTS
Corrosion of gold bridgewire in electronic components
[DE87-000922] N87-23722
ACCELERATION (PHYSICS)
The perception of the higher derivatives of visual motion
[AD-A179627] N87-24069
ACCEPTABILITY
Bird impact qualification test for A-10 windshield
[AD-A179263] N87-23599
ACCIDENT PREVENTION
Actions to implement the recommendations of the Presidential Commission on the Space Shuttle Challenger accident: Executive summary N87-23676
ACCLIMATIZATION
Pulmonary adaptation to high altitude
[AD-A179139] N87-24065
ACCURACY
Inter-vehicle ranging system
[AD-A179492] N87-23938
Erratum: IRAS observations of irregular galaxies N87-24300
ACID RAIN
Spatial characterization of acid rain stress in Canadian Shield lakes
[NASA-CR-180983] N87-24031
Spatial characterization of acid rain stress in Canadian Shield lakes
[NASA-CR-180982] N87-24032
ACOUSTIC EXCITATION
Stochastic excitation of acoustic waves in a combustion chamber N87-23761
ACOUSTIC MEASUREMENT
Coupled aerodynamic and acoustical predictions for turboprops
[NASA-TM-87094] N87-23598
Corrosion sensing with acoustic wave devices
[DE87-003516] N87-23723
Rapid quantification of an internal property — ultrasonic determination of bladder urine quantity
[NASA-CASE-LAR-13689-1-NP] N87-23941
Development of ultrasonic thermometry for high-temperature high-resolution temperature profiling applications in LMFBR safety research
[SAND-84-1341] N87-24171
ACOUSTIC MICROSCOPES
Application of scanning acoustic microscopy to advanced structural ceramics
[NASA-TM-89929] N87-23987
ACOUSTIC PROPAGATION
Microscopic modeling of sound waves in granular material
[DE87-007400] N87-24159
ACOUSTICS
Acoustic waveforms in statically tested space shuttle Solid Rocket Motors (SRM) N87-23758
ACRYLATES
Dielectric properties of styrene/acrylate copolymer coatings formed by electrophoretic deposition on gold, aluminum alloy, and porous anodized aluminum alloy substrates
[DE87-006885] N87-23741
ACRYLIC RESINS
Dielectric properties of styrene/acrylate copolymer coatings formed by electrophoretic deposition on gold, aluminum alloy, and porous anodized aluminum alloy substrates
[DE87-006885] N87-23741
ACRYLONITRILES
Spin-cast carbon films from polyacrylonitrile
[DE87-002489] N87-23703
ACTIVATION
Reactivation study for NASA Lewis Research Center's hypersonic tunnel facility
[NASA-TM-89918] N87-23664
ACTIVATION ENERGY
Asymptotic models for solid propellant combustion and the onset of intrinsic instability N87-23764
A theoretical and numerical study of radiative ignition and deradiative extinction in solid propellants N87-23778
ACTIVE CONTROL
Modified independent modal space control method for active control of flexible systems
[NASA-CR-181065] N87-23980
ACTUATORS
Rotary stepping device with memory metal actuator
[NASA-CASE-NPO-15482-1] N87-23970
Modified independent modal space control method for active control of flexible systems
[NASA-CR-181065] N87-23980
Fully redundant mechanical release actuator
[NASA-CASE-LAR-13198-1] N87-23983
ADAPTATION
Adaptive noise reduction in aircraft communication systems
[AD-A178267] N87-23851
Adaptive grid refinement for numerical weather prediction
[AD-A179393] N87-24049
Pulmonary adaptation to high altitude
[AD-A179139] N87-24065
ADAPTIVE CONTROL
Highly integrated digital electronic control: Digital flight control, aircraft model identification, and adaptive engine control
[NASA-TM-86793] N87-23619
Adaptive antennas N87-23865
Control of welding processes
[AD-A177893] N87-23971
Adaptive moving grid strategies for one-dimensional systems of partial differential equations
[DE87-006824] N87-24144
ADAPTIVE FILTERS
MVSE (Minimizes Variance Squared Error) adaptive filtering subject to a constraint on MSE (Mean Squared Error)
[DE87-007859] N87-24105
ADDITIVES
Low-resistivity glass electrolytes for sodium-sulfur cells
[DE87-004837] N87-23880
ADHESION
Plasma deposition of tungsten
[DE87-007390] N87-23724
ADHESIVE BONDING
Adhesive evaluation of water-soluble LARC-TPI
[NASA-TM-89152] N87-23752
ADHESIVES
High temperature electrically conductive adhesives
[DE87-007020] N87-23747
ADJUSTING
Adjustable mount for electro-optic transducers in an evacuated cryogenic system
[NASA-CASE-LAR-13100-1] N87-23982
ADSORPTION
Laser studies of chemical dynamics at the gas-solid interface
[DE87-005950] N87-23710
AERIAL PHOTOGRAPHY
Automated radar image analysis research in support of military needs
[AD-A179615] N87-23827
AERODYNAMIC CHARACTERISTICS
Effect of surface roughness on drag of aircraft N87-23571
Experimental study of supersonic stream sliding at angle past one-step wedge with jaws N87-23573
Two-dimensional aerodynamic characteristics of the AMES HI-120, HI-8, and LOW-12 airfoils
[NASA-CR-181018] N87-23589
An experimental investigation into methods for quantifying hang glider airworthiness parameters
[CAR-8705] N87-23613
Method for the determination of the three-dimensional aerodynamic field of a rotor-stator combination to compressible flow
[NASA-TM-100118] N87-23625

AERODYNAMIC CONFIGURATIONS
On minimizing the number of calculations in design-by-analysis codes
[NASA-TP-2706] N87-23586
Optimal aerodynamic shapes for hypervelocity projectiles
[AD-A178367] N87-23672
AERODYNAMIC FORCES
Two blowing concepts for roll and lateral control of aircraft
[NASA-CR-180478] N87-23627
AERODYNAMIC STABILITY
An experimental investigation into methods for quantifying hang glider airworthiness parameters
[CAR-8705] N87-23613
AERODYNAMIC STALLING
Flight investigation of the effects of an outboard wing-leading-edge modification on stall/spin characteristics of a low-wing, single-engine, T-tail light airplane
[NASA-TP-2691] N87-23614
AERODYNAMICS
Coupled aerodynamic and acoustical predictions for turboprops
[NASA-TM-87094] N87-23598
Evaluation of the angle of attack limiter of the F-16 C/D aircraft
[AD-A177941] N87-23612
AEROELASTICITY
The influence of turbulence and deck section geometry on the aeroelastic behaviour of a cable-stayed bridge model
[NAE-AN-40] N87-23990
AERONAUTICAL ENGINEERING
Engineer in charge: A history of the Langley Aeronautical Laboratory, 1917-1958
[NASA-SP-4305] N87-24390
Research and Technology
[NASA-TM-89411] N87-24391
AEROSOLS
Horizontal variation of atmospheric extinction/backscatter coefficients
[AD-A178298] N87-23954
AEROSPACE ENGINEERING
USSR report: Engineering and equipment
[JPRS-UEQ-87-005] N87-23570
High current electron gun for space flight
[AD-A178467] N87-23675
AEROSPACE ENVIRONMENTS
Spacecraft environment interaction investigation
[AD-A179183] N87-23678
High-current electron gun for space flight
[AD-A179287] N87-23674
Method of making a flexible diaphragm
[NASA-CASE-MSC-20797-1] N87-23661
Test results of a 60 volt bipolar nickel-hydrogen battery
[NASA-TM-89827] N87-24029
The 1986-87 NASA space/gravitational biology accomplishments
[NASA-TM-89951] N87-24063
AEROSPACE MEDICINE
An analysis of space station motion subject to the parametric excitation of periodic elevator motion
[AD-A179235] N87-23681
Short Course on Cardiopulmonary Aspects of Aerospace Medicine
[AGARD-R-758] N87-24070
Aeromedical evaluation and disposition of electrocardiographic abnormalities N87-24071
Noninvasive methods for the detection of coronary artery disease in aviators: A stratified Bayesian approach N87-24072
Valvular and congenital heart disease in the aviator N87-24073
Aeromedical aspects of mitral valve prolapse N87-24074
Pulmonary physiology and pulmonary function testing in aerospace medicine N87-24075
Aeromedical disposition of pulmonary sarcoidosis, chronic obstructive lung disease, reactive airway disease and spontaneous pneumothorax N87-24076
Hypertension in the aviator N87-24077
Coronary risk factors in aerospace medicine N87-24078
Cardiopulmonary screening for high-performance flying: Selection and retention issues N87-24079
AEROSPACE SAFETY
Actions to implement the recommendations of the Presidential Commission on the Space Shuttle Challenger accident: Executive summary N87-23676
AEROSPACE SYSTEMS
Potential Applications of Biotechnology to Aerospace Materials
[AD-A177875] N87-23667
Spacecraft environment interaction investigation
[AD-A179183] N87-23678
Al and Mg alloys for aerospace applications using rapid solidification and powder metallurgy processing
[AD-A179547] N87-23721
AEROSPACE VEHICLES
Study of the influence of metallurgical factors on fatigue and fracture of aerospace structural materials
[AD-A179268] N87-23720
AEROTHERMOCHEMISTRY
Sandia cooperative group on the aerothermochemistry of turbulent combustion
[DE87-008345] N87-23714
AFTERBURNING
Study of the suppression of rocket plume afterburning by chemical additives N87-23768
The inhibition effects of H2/O2/N2 flames seeded by potassium N87-23774
AGE FACTOR
Cardiopulmonary screening for high-performance flying: Selection and retention issues N87-24079
AGING (METALLURGY)
Studies on age-hardening in spinodally modulated alloys: Experimental and theoretical
[DE87-008361] N87-23727
AIR COOLING
Intercooled gas turbine
[PB87-178042] N87-23972
AIR FLOW
Application of the viscous-inviscid interaction method to the analysis of airfoil flows at low Reynolds numbers
[AD-A177948] N87-23588
AIR INTAKES
Experimental study of supersonic stream sliding at angle past one-step wedge with jaws N87-23573
AIR LOCKS
A multiple attribute decision analysis of manned airlock systems
[AD-A178241] N87-23682
AIR POLLUTION
Spatial characterization of acid rain stress in Canadian Shield lakes
[NASA-CR-180983] N87-24031
Survey of environment related monitoring programs of international organizations and their contribution to international organizations
[ETN-87-99913] N87-24033
The reality of the greenhouse effect
[DE87-002383] N87-24041
AIR TO AIR MISSILES
Manned air to air combat simulation N87-23648
AIR TRAFFIC CONTROL
Development of an air ground data exchange concept: Flight deck perspective
[NASA-CR-4074] N87-23607
Efficient conduct of individual flights and air traffic or optimum utilization of modern technology for the overall benefit of civil and military airspace users
[AGARD-AR-236] N87-23608
AIRCRAFT ACCIDENT INVESTIGATION
Results of the specialized investigation of accidents involving German aircraft at home and abroad, and with foreign aircraft at home
[ISSN-0178-8094] N87-23602
Aircraft accident data: US air carrier operations calendar year 1984
[PB87-183992] N87-23603
Aircraft accident report: Southern Air Transport LOGAIR Flight 51, Lockheed L-382G, Kelly Air Force Base, Texas, October 4, 1986
[PB87-910404] N87-23604
Aircraft accident data: US air carrier operations calendar year 1983
[PB87-160628] N87-23605
AIRCRAFT ACCIDENTS
Results of the specialized investigation of accidents involving German aircraft at home and abroad, and with foreign aircraft at home
[ISSN-0178-8094] N87-23602
Annual review of aircraft accident data, US general aviation: Calendar year 1984
[PB87-194791] N87-23606
AIRCRAFT ANTENNAS
Basic parameters of antennas for aircraft, satellites and missiles N87-23660
Aircraft radar antennas N87-23661
Aircraft antennas/conformal antennas missile antennas N87-23662
AIRCRAFT COMMUNICATION
Adaptive noise reduction in aircraft communication systems
[AD-A178267] N87-23651
AIRCRAFT COMPARTMENTS
Annoyance response to simulated advanced turboprop aircraft interior noise containing tonal beats
[NASA-TP-2689] N87-24161
AIRCRAFT CONSTRUCTION MATERIALS
Potential Applications of Biotechnology to Aerospace Materials
[AD-A177875] N87-23667
AIRCRAFT CONTROL
Computer simulation studies on human control reliability in manual aircraft control: The origin of PIO N87-23644
AIRCRAFT DESIGN
Trends in ground-based and in-flight simulators for development applications N87-23645
Piloted simulation in the development of the XV-15 tilt rotor research aircraft N87-23646
Aircraft electromagnetic compatibility
[NASA-CR-181051] N87-23656
Engineer in charge: A history of the Langley Aeronautical Laboratory, 1917-1958
[NASA-SP-4305] N87-24390
AIRCRAFT ENGINES
Acta aeronautica et astronautica sinica
[AD-A179673] N87-23618
Highly integrated digital electronic control: Digital flight control, aircraft model identification, and adaptive engine control
[NASA-TM-86793] N87-23619
AIRCRAFT FUEL SYSTEMS
Antimisting Fuel (AMK) flight degrader development and aircraft fuel system investigation
[DOT/FAA/CT-86/8] N87-23616
AIRCRAFT FUELS
Autogas in general aviation aircraft
[DOT/FAA/CT-87/05] N87-23615
AIRCRAFT INSTRUMENTS
Principles of data display in aviation instruments N87-23572
AIRCRAFT LANDING
Aircraft Dynamic Response to Damaged and Repaired Runways
[AGARD-R-739] N87-23609
Interpretation in terms of the response of a one degree-of-freedom oscillator to two successive disturbances N87-23610
Flight test evaluation of techniques to predict longitudinal pilot induced oscillations
[AD-A179229] N87-23629
Simulation of aircraft behaviour on and close to the ground: Summary of AGARD-Ic6)ograph AG-285 N87-23640
AIRCRAFT MANEUVERS
Utilization of simulation to support F-14A low altitude high angle of attack flight testing N87-23649
AIRCRAFT MODELS
Highly integrated digital electronic control: Digital flight control, aircraft model identification, and adaptive engine control
[NASA-TM-86793] N87-23619
Magnetostatic surface field measurement facility
[AD-A178258] N87-23650
AIRCRAFT NOISE
Annoyance response to simulated advanced turboprop aircraft interior noise containing tonal beats
[NASA-TP-2689] N87-24161
AIRCRAFT PILOTS
Aeromedical evaluation and disposition of electrocardiographic abnormalities N87-24071
Noninvasive methods for the detection of coronary artery disease in aviators: A stratified Bayesian approach N87-24072
Valvular and congenital heart disease in the aviator N87-24073
Aeromedical aspects of mitral valve prolapse N87-24074
Pulmonary physiology and pulmonary function testing in aerospace medicine N87-24075
Aeromedical disposition of pulmonary sarcoidosis, chronic obstructive lung disease, reactive airway disease and spontaneous pneumothorax N87-24076
Hypertension in the aviator N87-24077
Coronary risk factors in aerospace medicine N87-24078
Cardiopulmonary screening for high-performance flying: Selection and retention issues N87-24079
AIRCRAFT SPIN
Utilization of simulation to support F-14A low altitude high angle of attack flight testing N87-23649
AIRFOILS
Application of the viscous-inviscid interaction method to the analysis of airfoil flows at low Reynolds numbers
[AD-A177948] N87-23588
Two-dimensional aerodynamic characteristics of the AMES HI-120, HI-8, and LOW-12 airfoils
[NASA-CR-181018] N87-23589
High Reynolds Number tests of the NASA SC(2)-0012 airfoil in the Langley 0.3-meter transonic cryogenic tunnel
[NASA-TM-89102] N87-23594

Life prediction and constitutive models for engine hot section anisotropic materials
[NASA-CR-179594] N87-23622
Unsteady separated flows: Vorticity and turbulence
[AD-A179500] N87-23912
Computation of full-coverage film-cooled airfoil temperatures by two methods and comparison with high heat flux data
[NASA-TM-88931] N87-23934

AIRGLOW
A model for the low-latitude ionosphere with coefficients for different seasonal and solar cycle conditions
[AD-A178207] N87-24044

AIRPORTS
Otis ANGB (Air National Guard Base) visibility sensor field test study
[AD-A179176] N87-24045

ALASKA
Climatological observations in the Philip Smith Mountains of the North Slope, Alaska
[DE87-008179] N87-24054

ALBEDO
An atmospheric correction algorithm for remote identification of non-Lambertian surfaces and its range of validity
[DE87-006059] N87-24011

ALGAE
Fuels from microalgae: Technology status, potential and research requirements
[DE86-010739] N87-23753

ALGEBRA
An extended set of FORTRAN basic linear algebra subprograms: Model implementation and test programs
[DE87-007913] N87-24101
Strong convergence and convergence rates of approximating solutions for algebraic Riccati equations in Hilbert spaces
[NASA-CR-178302] N87-24122
AMG (Algebraic Multigrid): Basic development, applications and theory
[AD-A178222] N87-24139

ALGORITHMS
A dual-processor multi-frequency implementation of the FINDS algorithm
[NASA-CR-178252] N87-23617
An integrated, optimization-based approach to the design and control of large space structures
[AD-A179459] N87-23683
Communication-efficient parallel graph algorithms
[AD-A178286] N87-23853
An atmospheric correction algorithm for remote identification of non-Lambertian surfaces and its range of validity
[DE87-006059] N87-24011
Intermediate level computer vision processing algorithm development for the content addressable array parallel processor
[AD-A179515] N87-24090
Gaussian elimination with partial pivoting and load balancing on a multiprocessor
[DE87-007784] N87-24093
LU factorization algorithms on distributed-memory multiprocessor architectures
[DE87-007794] N87-24100
MVSE (Minimizes Variance Squared Error) adaptive filtering subject to a constraint on MSE (Mean Squared Error)
[DE87-007859] N87-24105
Solving the Cauchy-Riemann equations on parallel computers
[NASA-CR-178307] N87-24107
Efficient parallel algorithms for (delta+1)-coloring and maximal independent set problems
[AD-A178287] N87-24109
Efficient graph algorithms for sequential and parallel computers
[AD-A178403] N87-24110
Content-addressable memory: Applications, algorithms, and simulation
[AD-A177944] N87-24120
A PASCAL implementation of the image algebra
[AD-A177943] N87-24136
The decomposition of an arbitrary three-dimensional planar polygon into a set of convex polygons
[AD-A177947] N87-24137
AMG (Algebraic Multigrid): Basic development, applications and theory
[AD-A178222] N87-24139
Time slice manipulation in information hierarchy
[AD-A177949] N87-24237

ALIGNMENT
Adjustable mount for electro-optic transducers in an evacuated cryogenic system
[NASA-CASE-LAR-13100-1] N87-23982

ALKYNES
Metal alkoxides: Models for metal oxides: Alkoxide ligands in early transition metal organometallic chemistry
[DE87-007309] N87-23715

ALLOCATIONS
Department of Housing and Urban Development - Independent Agencies Appropriations Bill, 1988
[H-REPT-100-189] N87-24241

ALTIMETERS
LASA (Lidar Atmospheric Sounder and Altimeter) Earth observing system. Volume 2D: Instrument panel report
[NASA-TM-89356] N87-23962

ALTITUDE SIMULATION
Investigation of shrouded nozzle exit pressure changes
[AD-A179477] N87-23911
Operation Everest 2: Importance of ventilation in defense of maximal oxygen uptake at extreme altitudes
[AD-A177874] N87-24082

ALUMINUM
Investigation of electromigration in thin film aluminum at low temperatures
[AD-A179110] N87-23871
The structure of Al/GaAs interfaces
[DE87-007181] N87-24206

ALUMINUM ALLOYS
Galvanic corrosion of Al-7075-T6 and Steel-4340 coupled to brass QQ-B-626, 360 and Al-7075-T6 coupled to Steel-4130 and Steel-4340: Exposure to aqueous NaCl and salt-fog environments
[AD-A179121] N87-23719
Al and Mg alloys for aerospace applications using rapid solidification and powder metallurgy processing
[AD-A179547] N87-23721
The corrosion of Al 7075-T6 alloy coupled to Ti 6A 1-4V in wet air
[DE87-008347] N87-23726

ALUMINUM GALLIUM ARSENIDES
Fabrication of AlGaAs/InGaAs pseudomorphic modulation doped field effect transistors with p-doped surface layers
[AD-A179230] N87-24201

AMMONIUM PERCHLORATES
Two techniques for measuring AP ignition delay N87-23772
AP/HMX composite propellant modeling N87-23776

AMORPHOUS SEMICONDUCTORS
Drift mobilities by time-of-flight methods and time-dependent phototransport in the nanosecond regime in amorphous semiconductors
[DE87-008021] N87-24208

AMPLIFIERS
Dual-polarization 8.45 GHz traveling-wave maser N87-23838
Two-stage hybrid microcircuit amplifier
[DE87-009092] N87-23899

ANALYSIS (MATHEMATICS)
Results of near field probe scanning tests for ultralow sidelobe arrays
[AD-A178141] N87-23846

ANALYTIC FUNCTIONS
Integral approximants for functions of higher monodromic dimension
[DE87-007506] N87-24129

ANGIOGRAPHY
Noninvasive methods for the detection of coronary artery disease in aviators: A stratified Bayesian approach N87-24072

ANGLE OF ATTACK
Mach 6 experimental and theoretical stability and performance of a cruciform missile at angles of attack up to 65 degrees
[NASA-TP-2733] N87-23592
Evaluation of the angle of attack limiter of the F-16 C/D aircraft
[AD-A177941] N87-23612
High-angle-of-attack pneumatic lag and upwash corrections for a hemispherical flow direction sensor
[NASA-TM-86790] N87-23616
Utilization of simulation to support F-14A low altitude high angle of attack flight testing N87-23649

ANGULAR DISTRIBUTION
Modelling of atmospheric effects on the angular distribution of a backscattering peak
[DE87-006060] N87-24014
Observations of heavy energetic ions for upstream from comet Halley
[DE87-003752] N87-24380

ANISOTROPIC SHELLS
Recent advances in the nonlinear analysis of laminated composite plates and shells N87-23819

ANISOTROPY
Recent studies in plate vibrations: 1981-1985. Part 2: Complicating effects N87-23998
Observations of heavy energetic ions for upstream from comet Halley
[DE87-003752] N87-24360

ANNEALING
The structure and electrical properties of metal contacts on GaAs
[DE87-008217] N87-24210

ANNIHILATION REACTIONS
Antiprotons in cosmic rays N87-24255

ANNUAL VARIATIONS
Global distribution of total cloud cover and cloud type amounts over land
[DE87-006903] N87-24053
Geophysical monitoring for climatic change number 14
[PB87-162533] N87-24056

ANTARCTIC REGIONS
Station climatic summaries, Antarctica, Australia and Oceania
[AD-A179242] N87-24047

ANTENNA ARRAYS
Rectangular microstrip patch antenna arrays
[AD-A179170] N87-23823
Spacecraft mass trade-offs versus radio-frequency power and antenna size at 8 GHz and 32 GHz N87-23830
Basic parameters of antennas for aircraft, satellites and missiles N87-23860
Adaptive antennas N87-23865
MIC technology for phased arrays N87-23866

ANTENNA DESIGN
The Telecommunications and Data Acquisition Report
[NASA-CR-181010] N87-23828
Spacecraft mass trade-offs versus radio-frequency power and antenna size at 8 GHz and 32 GHz N87-23830
Use of a 2.3-GHz traveling-wave maser on the Usuda 64-meter antenna N87-23831
Microwave component time delays for the 70-meter antennas N87-23835
Z-corrections for DSN 70-meter antenna ranging calibration N87-23836
Microwave Antennas for Avionics
[AGARD-LS-151] N87-23859
Aircraft radar antennas N87-23861
Aircraft antennas/conformal antennas missile antennas N87-23862
Spacecraft multi-beam and contoured-beam antennas N87-23863
Millimeter wave antennas for avionics N87-23864
Adaptive antennas N87-23865
MIC technology for phased arrays N87-23866
Printed circuit antenna technology N87-23867

ANTENNA FEEDS
Rectangular microstrip patch antenna arrays
[AD-A179170] N87-23823

ANTENNA RADIATION PATTERNS
Rectangular microstrip patch antenna arrays
[AD-A179170] N87-23823
An ELF (Extremely-Low-Frequency) transmitter experiment for the space shuttle. (The NASC-201 (Naval Air Space Command) experiment). Volume 1
[AD-A178237] N87-23849
Basic parameters of antennas for aircraft, satellites and missiles N87-23860
Aircraft radar antennas N87-23861
Spacecraft multi-beam and contoured-beam antennas N87-23863
Millimeter wave antennas for avionics N87-23864
Adaptive antennas N87-23865

ANTENNAS
Microwave coupling inside complex systems
[DE87-003505] N87-23841
Results of near field probe scanning tests for ultralow sidelobe arrays
[AD-A178141] N87-23846

ANTIMISSILE DEFENSE
An analysis of geopotential effects on satellite constellations
[AD-A179507] N87-23684
SDI (Strategic Defense Initiative) and the US defense posture
[DE87-006731] N87-24154
Coherent multiple aperture optical imaging systems: Analysis and design
[AD-A179476] N87-24178

ANTIMISTING FUELS
Antimisting Fuel (AMK) flight degrader development and aircraft fuel system investigation
[DOT/FAA/CT-86/6] N87-23816

ANTIPROTONS
Antiprotons in cosmic rays N87-24255

APERTURES
Microwave coupling inside complex systems
[DE87-003505] N87-23841

Scattering from an open spherical shell having a circular aperture and enclosing a concentric dielectric sphere [DE87-007099] N87-23842
Coherent multiple aperture optical imaging systems: Analysis and design [AD-A179476] N87-24176

APPLICATIONS PROGRAMS (COMPUTERS)
US Coast Guard SARSAT (Search and Rescue Satellite-Aided Tracking). Volume 3. Programs and data listings [AD-A178308] N87-23601
Interpretation in terms of the response of a one degree-of-freedom oscillator to two successive disturbances N87-23610
Numerical simulation of combustion processes of mobile stick-propellant bundles N87-23785
Measurements for rocket engine performance code verification N87-23811
PRONTO 2D: A two-dimensional transient solid dynamics program [DE87-007823] N87-23993
An extended set of FORTRAN basic linear algebra subprograms: Model implementation and test programs [DE87-007913] N87-24101
Computer programs for nonlinear least squares analysis of various three-dimensional geometrical elements [DE87-006046] N87-24133
AXCEL: Interactive simulation program to compute two-dimensional potential distributions of electrostatic arrangements and of ion paths in electrostatic fields under consideration of space charging [DE87-007760] N87-24165
Systems model for natural gas vehicle fleets [PB87-178083] N87-24245
Personal computer based GOES data archive [PB87-157517] N87-24384

APPROPRIATIONS
National Aeronautics and Space Administration Authorization Act [S-REPT-100-87] N87-24240
National Aeronautics and Space Administration — appropriations bill H.R. 2783 N87-24242
National Aeronautics and Space Administration Authorization Act, 1988 [S-REPT-100-87] N87-24243

APPROXIMATION
On minimizing the number of calculations in design-by-analysis codes [NASA-TP-2706] N87-23586
Strong convergence and convergence rates of approximating solutions for algebraic Riccati equations in Hilbert spaces [NASA-CR-178302] N87-24122
Approximation errors and perceived similarity between approximated polygons [TRITA-NA-8505] N87-24127
Integral approximants for functions of higher monodromic dimension [DE87-007506] N87-24129
Estimate for the errors in eigenvalue and eigenvector approximation by Galerkin methods, with particular attention to the case of multiple eigenvalues [AD-A178390] N87-24142

ARC JET ENGINES
Low power arcjet thruster pulse ignition [NASA-TM-100123] N87-23691

ARCHITECTURE (COMPUTERS)
Radar simulators N87-23651
LU factorization algorithms on distributed-memory multiprocessor architectures [DE87-007794] N87-24100
Content-addressable memory: Applications, algorithms, and simulation [AD-A177944] N87-24120
Nonlinear real-time optical signal processing [AD-A178169] N87-24182

ARCTIC REGIONS
Climatological observations in the Philip Smith Mountains of the North Slope, Alaska [DE87-008179] N87-24054

AREA
Experimental thrust performance of a high area-ratio rocket nozzle N87-23809

ARRAYS
Scattering by a truncated periodic array [AD-A178285] N87-23852
Surface passivation of an implantable semiconductor multielectrode array [AD-A178175] N87-24219
Detector arrays for low-background space infrared astronomy [NASA-TM-88344] N87-24378

ARTIFICIAL INTELLIGENCE
Tactical weather expert system [AD-A178605] N87-24050
The development of a prototype intelligent user interface subsystem for NASA's scientific database systems [NASA-TM-87821] N87-24098
Investigations into the pattern processing capabilities of associative nets [TRITA-NA-8601] N87-24114
Proposal for continued research in intelligent machines at the Center for Engineering Systems Advanced Research (CESAR) for FY 1988 to FY 1991 [DE87-007789] N87-24121
Optimization of extended relational database systems [AD-A179308] N87-24230

ARTIFICIAL SATELLITES
An analysis of geopotential effects on satellite constellations [AD-A179507] N87-23684
History of spaceflight [AD-A178381] N87-24393

ASPHALT
Consequence of layer separation on pavement performance [DOT/FAA/PM-86/48] N87-23661

ASSEMBLIES
Fully redundant mechanical release actuator [NASA-CASE-LAR-13198-1] N87-23983

ASSOCIATIVE PROCESSING (COMPUTERS)
Investigations into the pattern processing capabilities of associative nets [TRITA-NA-8601] N87-24114

ASTHMA
Aeromedical disposition of pulmonary sarcoidosis, chronic obstructive lung disease, reactive airway disease and spontaneous pneumothorax N87-24076

ASTRONAUTS
Comparison of CREME (Cosmic Ray Effects on Microelectronics) model LET (Linear Energy Transfer) spaceflight dosimetry data [AD-A177873] N87-23884

ASTRONOMICAL CATALOGS
Star forming regions of the southern galaxy N87-24273
Submm observations of IRAS galaxies N87-24292
Characteristics of UGC galaxies detected by IRAS N87-24304
Fifty year canon of solar eclipses: 1986-2035 [NASA-TM-89346] N87-24377

ASTRONOMICAL MAPS
The properties of highly luminous IRAS galaxies N87-24358
Structure in the nucleus of NGC 1068 at 10 microns N87-24370

ASTRONOMICAL MODELS
Gauge invariant quantum cosmology [DE87-006685] N87-24226
Antiprotons in cosmic rays N87-24255
X-ray astronomical spectroscopy N87-24263
The origin of the diffuse galactic IR/submm emission: Revisited after IRAS N87-24269
Masses, luminosities and dynamics of galactic molecular clouds N87-24270
Models for infrared emission from IRAS galaxies N87-24286
On the origin of the 40-120 micron emission of galaxy disks: A comparison with H-alpha fluxes N87-24287
Measuring star formation rates in blue galaxies N87-24289
Star formation and spiral structure in M81 N87-24294
Erratum: IRAS observations of irregular galaxies N87-24300
Present star formation in sprials of the Virgo cluster N87-24306
Modelling the IRAS colors of galaxies N87-24313
A simple two-component model for the far-infrared emission from galaxies N87-24314
The history of gas in sprial galaxies N87-24318
Physics of the inner heliosphere: Mechanisms, models and observational signatures [NASA-CR-181063] N87-24387

ASTRONOMICAL PHOTOMETRY
Near-infrared observations of IRAS minisurvey galaxies N87-24354

ASTROPHYSICS
The joint NASA/Goddard-University of Maryland research program in charged particle and high energy photon detector technology [NASA-CR-180996] N87-24166
Essays in Space Science [NASA-CP-2464] N87-24247
Particle acceleration in solar flares N87-24250
Origin and propagation of galactic cosmic rays N87-24257
Nucleosynthesis and astrophysical gamma ray spectroscopy N87-24259
Gamma ray transients N87-24260
The cosmic X-ray background N87-24262
Infrared astronomy N87-24264
A program of ground-based astronomy to complement Einstein observations [AD-A179331] N87-24265
Mechanisms for the circular polarization of astrophysical OH masers in star-forming regions and the inferred magnetic fields N87-24277

ASYMPTOTIC METHODS
Asymptotic models for solid propellant combustion and the onset of intrinsic instability N87-23764
A theoretical and numerical study of radiative ignition and deradiative extinction in solid propellants N87-23778
Effective diffusion in laminar convective flows [DE87-008054] N87-23920
Asymptotic analysis of the roots of a certain transcendental equation [AD-A166315] N87-24131
Nonparametric estimation of the probability of a long delay in the M/G/1 queue [AD-A178259] N87-24150

ASYMPTOTIC SERIES
Nonparametric estimation of the probability of a long delay in the M/G/1 queue [AD-A178259] N87-24150

ATELECTASIS
Pulmonary physiology and pulmonary function testing in aerospace medicine N87-24075

ATMOSPHERIC ATTENUATION
Research in millimeter wave techniques [NASA-CR-181026] N87-23858
Horizontal variation of atmospheric extinction/backscatter coefficients [AD-A178298] N87-23954

ATMOSPHERIC CHEMISTRY
Medical research programs, past and future, for designing atmospheres to retard fires [AD-A178354] N87-24089

ATMOSPHERIC COMPOSITION
Hypersonic aerodynamic coefficients and convection flow estimation in a HERMES type project [NASA-TT-20019] N87-23583
LASA (Lidar Atmospheric Sounder and Altimeter) Earth observing system. Volume 2D: Instrument panel report [NASA-TM-89356] N87-23962
The detection of CO2-induced climate change [DE87-006085] N87-24052
Geophysical monitoring for climatic change number 14 [PB87-162533] N87-24056

ATMOSPHERIC CORRECTION
An atmospheric correction algorithm for remote identification of non-Lambertian surfaces and its range of validity [DE87-006059] N87-24011

ATMOSPHERIC HEATING
The reality of the greenhouse effect [DE87-002383] N87-24041
The detection of CO2-induced climate change [DE87-006085] N87-24052

ATMOSPHERIC MODELS
Modelling of atmospheric effects on the angular distribution of a backscattering peak [DE87-006060] N87-24014
A comparison of ionospheric model predictions with MITHRAS observations [AD-A179374] N87-24036
A model for the low-latitude ionosphere with coefficients for different seasonal and solar cycle conditions [AD-A178207] N87-24044
The specification of lateral boundary conditions in three-dimensional mesoscale numerical models [AD-A179185] N87-24046
Adaptive grid refinement for numerical weather prediction [AD-A179393] N87-24049
User's manual for the convective cloud module version 1.0 [DE87-008343] N87-24058
Ocean wind and wave model comparisons with GEOSAT (GEOdesy SATellite) satellite data [AD-A178302] N87-24061
Auroral particles N87-24249

ATMOSPHERIC PHYSICS
Atmospheric radiance profile codes [AD-A179258] N87-24035

ATMOSPHERIC PRESSURE
Climatological observations in the Philip Smith Mountains of the North Slope, Alaska [DE87-008179] N87-24054
Operation Everest 2: Importance of ventilation in defense of maximal oxygen uptake at extreme altitudes [AD-A177874] N87-24082

ATMOSPHERIC RADIATION
Transport and photochemical modeling. Studies of atmospheric species [NASA-CR-178311] N87-24040

Satellite observation of atmospheric nuclear gamma radiation
[AD-A177937] N87-24389

ATMOSPHERIC REFRACTION
Atmospheric propagation effects on radio interferometry
[AD-A178405] N87-23855

ATMOSPHERIC SOUNDING
LASA (Lidar Atmospheric Sounder and Altimeter) Earth observing system. Volume 2D: Instrument panel report
[NASA-TM-89356] N87-23962

ATMOSPHERIC STRATIFICATION
Horizontal variation of atmospheric extinction/backscatter coefficients
[AD-A178298] N87-23954

ATMOSPHERIC TEMPERATURE
The reality of the greenhouse effect
[DE87-002363] N87-24041
The detection of CO2-induced climate change
[DE87-006085] N87-24052
Climatological observations in the Philip Smith Mountains of the North Slope, Alaska
[DE87-008179] N87-24054

ATOMIC BEAMS
Experimental and theoretical studies of laser cooling and emittance control of neutral beams
[AD-A179226] N87-23946

ATOMIC SPECTRA
Semiempirical studies of atomic structure
[DE87-007320] N87-24164

ATOMIC STRUCTURE
Semiempirical studies of atomic structure
[DE87-007320] N87-24164

ATOMIZING
Catastrophic breakup of liquid jet by subsonic transverse gas stream N87-23578
Numerical and experimental studies of atomization and mixing from a coaxial injector element N87-23812

ATOMS
Ordered many-electron motions in atoms and X-ray lasers
[DE87-004731] N87-23951

ATTENUATION COEFFICIENTS
Horizontal variation of atmospheric extinction/backscatter coefficients
[AD-A178298] N87-23954

ATTITUDE CONTROL
Optimal continuous thrust orbital evasive maneuvers from geosynchronous orbit
[AD-A179413] N87-23668

ATTITUDE STABILITY
An analysis of space station motion subject to the parametric excitation of periodic elevator motion
[AD-A179235] N87-23681

AURORAL TEMPERATURE
Atmospheric radiance profile codes
[AD-A179258] N87-24035

AURORAS
Studies of infrared aurorae
[AD-A179539] N87-24037
Auroral particles N87-24249

AUSTRALIA
Station climatic summaries, Antarctica, Australia and Oceania
[AD-A179242] N87-24047

AUTOMATIC CONTROL
Efficient conduct of individual flights and air traffic or optimum utilization of modern technology for the overall benefit of civil and military airspace users
[AGARD-AR-236] N87-23608
A new approach to multitarget tracking using probabilistic data association
[AD-A179437] N87-23825
Automatic detection of electric power troubles (AI application)
[NASA-TM-86593] N87-23893
Control of welding processes
[AD-A177893] N87-23971
Automating index preparation
[AD-A179327] N87-24231

AUTOMOBILE FUELS
Autogas in general aviation aircraft
[DOT/FAA/CT-87/05] N87-23815

AUTOMOBILES
Activities report of the German-Dutch wind tunnel
[B8677593] N87-23665
Activities report of the German-Dutch wind tunnel
[B8677594] N87-23666
Recent developments in vehicle dynamics N87-23820

AUXILIARY PROPULSION
Preliminary performance characterizations of an engineering model multipropellant resistojet for space station application
[NASA-TM-100113] N87-23821

AVIONICS
Millimeter wave antennas for avionics N87-23864

AWACS AIRCRAFT
Results of near field probe scanning tests for ultralow sidelobe arrays
[AD-A178141] N87-23846

AXIAL LOADS
Collapse analysis of cylindrical composite panels with large cutouts under an axial load
[AD-A179112] N87-23701

AXIAL MODES
Behavior of simulated solid propellant flames in axial acoustic fields N87-23760
Role of combustion in the nonlinear combustion instability of composite solid propellants N87-23765

AXIAL STRAIN
A simplified computer solution for the flexibility matrix of contacting teeth for spiral bevel gears
[NASA-CR-179620] N87-23977

AXISYMMETRIC BODIES
Effect of a trade between boattail angle and wedge size on the performance of a nonaxisymmetric wedge nozzle
[NASA-TP-2717] N87-23593

AXISYMMETRIC FLOW
Calculation of axisymmetric flow in swirlers by difference method N87-23579

AZIDES (ORGANIC)
Combustion, vaporization, and microexplosion of droplets of organic azides N87-23806

B

B STARS
High mass star formation in the galaxy N87-24267
On the origin of the 40-120 micron emission of galaxy disks: A comparison with H-alpha fluxes N87-24287
Infrared spectroscopy of star formation in galaxies N87-24320

BACKGROUND RADIATION
The cosmic X-ray background N87-24262
Detector arrays for low-background space infrared astronomy
[NASA-TM-88344] N87-24378

BACKSCATTERING
Horizontal variation of atmospheric extinction/backscatter coefficients
[AD-A178298] N87-23954
Modelling of atmospheric effects on the angular distribution of a backscattering peak
[DE87-006060] N87-24014

BACKWARD FACING STEPS
Acoustic response of turbulent reacting recirculatory flows N87-23799

BALLOON-BORNE INSTRUMENTS
Survey of the galactic disk from 1 = -150 deg to 1 = 82 deg in the submillimeter range N87-24278

BANDWIDTH
Flight test evaluation of techniques to predict longitudinal pilot induced oscillations
[AD-A179229] N87-23629
Communication-efficient parallel graph algorithms
[AD-A178286] N87-23853

BARRED GALAXIES
Stellar bars and the spatial distribution of infrared luminosity N87-24293
VLA continuum observations of barred spiral galaxies N87-24333
Enhanced star formation: The importance of bars in spiral galaxies N87-24357

BARRIER LAYERS
The structure and electrical properties of metal contacts on GaAs
[DE87-008217] N87-24210

BARRIERS
Mathematical model describing interaction of single nonsteady supersonic jet and movable barrier of finite dimensions N87-23575

BATHS
The field shower wastewater recycling system: Development of a program of instruction and preliminary analysis of its potential health implications
[AD-A178112] N87-24088

BATTERY CHARGERS
Aircraft battery state of charge and charge control system
[AD-A179086] N87-23870

BAYES THEOREM
Noninvasive methods for the detection of coronary artery disease in aviators: A stratified Bayesian approach N87-24072
Changing time series
[AD-A178030] N87-24149
Decaying confidence functions for aging knowledge in expert systems
[AD-A179328] N87-24152

BEAMS (RADIATION)
Rf control system for a rocket-borne accelerator
[DE87-007459] N87-23673
Means for phase locking the outputs of a surface emitting laser diode array
[NASA-CASE-NPO-16542-1-CU] N87-23960
High-current beam dynamics and transport, theory and experiment
[DE87-006154] N87-24172
Formation and stability of partially-neutralized plasma clumps
[AD-A179444] N87-24187

BEAMS (SUPPORTS)
Material damping measurements of 2D carbon-carbon composite beams
[AD-A179109] N87-23700
Thin-walled beam theories and their applications in the torsional strength analysis of ship hulls
[AD-A178296] N87-24001

BELL AIRCRAFT
Airborne simulation at the National Aeronautical Establishment of Canada N87-23659

BENDING MOMENTS
A simplified computer solution for the flexibility matrix of contacting teeth for spiral bevel gears
[NASA-CR-179620] N87-23977

BIAS
Min-max bias robust M-estimates of scale
[AD-A179255] N87-24147

BIBLIOGRAPHIES
Laser hazards bibliography, 12 edition
[AD-A179220] N87-23945
Solar Thermal Technology Program bibliography, 1973-1985
[DE86-010728] N87-24027
The Magsat Bibliography
[NASA-TM-87822] N87-24039
A program of ground-based astronomy to complement Einstein observations
[AD-A179331] N87-24265

BINARY MIXTURES
Physics of pattern formation at liquid interfaces
[DE87-007540] N87-23919

BINARY SYSTEMS (MATERIALS)
Cellular monotectic model solidification
[NASA-CR-181027] N87-23717

BINOMIALS
Confidence interval for parameter n in a binomial distribution
[AD-A178325] N87-24151

BIOCHEMISTRY
Investigation of biochemical variation in operational aircrew
[AD-A179223] N87-24067

BIOCONVERSION
Fuels from microalgae: Technology status, potential and research requirements
[DE86-010739] N87-23753

BIOLOGICAL EFFECTS
Laser hazards bibliography, 12 edition
[AD-A179220] N87-23945

BIOMASS
Error analysis of leaf area estimates made from allometric regression models
[NASA-TM-89220] N87-24010

BIOMETRICS
Rapid quantification of an internal property — ultrasonic determination of bladder urine quantity
[NASA-CASE-LAR-13689-1-NP] N87-23941
International Symposium on In Vivo Body Composition Studies: Program and abstracts
[DE87-006750] N87-24060

BIOTECHNOLOGY
Potential Applications of Biotechnology to Aerospace Materials
[AD-A177875] N87-23667

BIPOLAR TRANSISTORS
ESD (Electrostatic Discharge)/EOS (Electrical OverStress) susceptibility of a class of bipolar RF power transistors: Experimental studies on stripline-opposed emitter transistors
[AD-A178212] N87-23890

BIRD-AIRCRAFT COLLISIONS
Bird impact qualification test for A-10 windshield
[AD-A179263] N87-23599

BIREFRINGENCE
White paper on nanocomposites as harmonic generation media
[DE87-008337] N87-23704

BISTATIC REFLECTIVITY
Active and passive remote sensing of ice
[AD-A179461] N87-24009

BL LACERTAE OBJECTS
IRAS observations of BL Lac objects N87-24373

BLADDER
Rapid quantification of an internal property — ultrasonic determination of bladder urine quantity
[NASA-CASE-LAR-13689-1-NP] N87-23941
BLADES
Performance of two 10-lb/sec centrifugal compressors with different blade and shroud thicknesses operating over a range of Reynolds numbers
[NASA-TM-100115] N87-23623
BLOOD
Investigation of biochemical variation in operational aircrew
[AD-A179223] N87-24067
BLOWDOWN WIND TUNNELS
Two-dimensional aerodynamic characteristics of the AMES HI-120, HI-8, and LOW-12 airfoils
[NASA-CR-181018] N87-23589
BO-105 HELICOPTER
DFVLR in-flight simulators ATTAS and ATTHES for flying qualities and flight control research N87-23657
BOATTAILS
Effect of a trade between boattail angle and wedge size on the performance of a nonaxisymmetric wedge nozzle
[NASA-TP-2717] N87-23593
BODY COMPOSITION (BIOLOGY)
International Symposium on In Vivo Body Composition Studies: Program and abstracts
[DE87-006750] N87-24080
BOMBER AIRCRAFT
Bird impact qualification test for A-10 windshield
[AD-A179263] N87-23599
BONES
Training, muscle fatigue, and stress fractures
[AD-A178350] N87-24065
BORON CHLORIDES
Preparation of B-trichloroborazine
[NASA-CASE-ARC-11643-1-SB] N87-23698
BOUNDARIES
In situ HREM observation of interphase boundary motion in 95Pb-5Sn solder
[DE87-007616] N87-23817
The specification of lateral boundary conditions in three-dimensional mesoscale numerical models
[AD-A179185] N87-24046
Far field boundary conditions for time-dependent hyperbolic systems
[AD-A179361] N87-24123
Computer simulation of bounded plasma systems
[DE87-008193] N87-24190
BOUNDARY ELEMENT METHOD
Improved modeling of structural joint damping
[AD-A179111] N87-23988
BOUNDARY LAYER COMBUSTION
Transport phenomena and interfacial kinetics in multiphase combustion systems
[AD-A179544] N87-23709
BOUNDARY LAYER CONTROL
Turbulent boundary layer structure, drag reduction
[AD-A179246] N87-23907
BOUNDARY LAYER FLOW
Laser Doppler velocimeter application in supersonic boundary-layer flow
[AD-A178395] N87-23590
BOUNDARY LAYER SEPARATION
Unsteady separated flows: Vorticity and turbulence
[AD-A179500] N87-23912
BOUNDARY LAYER TRANSITION
Crossflow vorticity sensor
[NASA-CASE-LAR-13436-1-CU] N87-23587
Application of the viscous-inviscid interaction method to the analysis of airfoil flows at low Reynolds numbers
[AD-A177948] N87-23588
Three-dimensional structure of boundary layers in transition to turbulence
[AD-A179247] N87-23908
On the breakdown of the wave packet trailing a turbulent spot in a laminar layer
[AD-A179607] N87-23915
BOUNDARY LAYERS
Direct numerical simulations of a temporally evolving mixing layer subject to forcing
[NASA-TM-88896] N87-23933
BOUNDARY VALUE PROBLEMS
Combustion instabilities in dump type ramjet combustors N87-23803
Uniqueness of non-negative solutions of a class of semi-linear elliptic equations
[DE87-006966] N87-24126
BRASSES
Galvanic corrosion of Al-7075-T6 and Steel-4340 coupled to brass QQ-B-626, 360 and Al-7075-T6 coupled to Steel-4130 and Steel-4340: Exposure to aqueous NaCl and salt-fog environments
[AD-A179121] N87-23719
BRAYTON CYCLE
Speculations on future opportunities to evolve Brayton powerplants aboard the space station
[NASA-TM-89863] N87-23674
Intercooled gas turbine
[PB87-178042] N87-23972
BRAZING
Development of a high temperature ceramic-to-metal seal for Air Force Weapons Laboratory Laser
[DE87-007711] N87-23949
BREADBOARD MODELS
DSN advanced receiver: Breadboard description and test results N87-23833
BREMSSTRAHLUNG
High energy gamma ray astronomy N87-24258
BRIDGES (STRUCTURES)
The influence of turbulence and deck section geometry on the aeroelastic behaviour of a cable-stayed bridge model
[NAE-AN-40] N87-23990
BRIDGMAN METHOD
Apparatus and procedure to detect a liquid-solid interface during crystal growth in a bridgman furnace
[NASA-CASE-LAR-13597-1-CU] N87-23713
BRIGHTNESS TEMPERATURE
A correlation between the IRAS infrared cirrus at 60 or 100 microns and neutral atomic hydrogen in the outer galaxy N87-24281
IRAS observations of the Pleiades N87-24284
BRITTLENESS
Dynamic brittle fracture analysis based on continuum damage mechanics
[DE87-006704] N87-24005
BROADBAND
Demonstration of frequency-sweep testing technique using a Bell 214-ST helicopter
[NASA-TM-89422] N87-23632
Generation of broadband noise in the magnetotail
[AD-A179136] N87-24034
BROKEN SYMMETRY
Research in theoretical particle physics
[DE87-008240] N87-24169
BROMINE
Electrochemical performance and transport properties of a Nafion membrane in a hydrogen-bromine cell environment
[NASA-TM-89662] N87-23718
BUCKLING
Investigation of the buckling sensitivity of hemispherical containers with arbitrary liquid content
[MITT-31] N87-24008
BUNDLES
Numerical simulation of combustion processes of mobile stick-propellant bundles N87-23785
BURNERS
A hybrid closed bomb-strand burner for very high pressure burning rate measurements N87-23786
BURNING RATE
The 23rd JANNAF Combustion Meeting, volume 1
[AD-A179158] N87-23757
Acoustic waveforms in statically tested space shuttle Solid Rocket Motors (SRM) N87-23758
Modification of solid propellant deflagration rates due to random nonhomogeneities N87-23766
Measurement of solid-propellant burn rate using millimeter-wave techniques N87-23770
Two techniques for measuring AP ignition delay N87-23772
Influence of two-phase flow in the deflagration of homogeneous solids N87-23777
Quantum chemical calculations of the decomposition of nitramines: Thermochemistry and reaction pathways N87-23781
A hybrid closed bomb-strand burner for very high pressure burning rate measurements N87-23786
Solid fuel ramjet fuel regression rate/thrust modulation N87-23787
BURNING TIME
Measurement of solid-propellant burn rate using millimeter-wave techniques N87-23770

C

CABLES (ROPES)
The influence of turbulence and deck section geometry on the aeroelastic behaviour of a cable-stayed bridge model
[NAE-AN-40] N87-23990
CALCULUS OF VARIATIONS
A generalized procedure for constructing an upwind based TVD scheme
[NASA-TM-88926] N87-24132
CALIBRATING
Z-corrections for DSN 70-meter antenna ranging calibration N87-23838
Otis ANGB (Air National Guard Base) visibility sensor field test study
[AD-A179176] N87-24045
CALIFORNIA
Radar as a complement to topographic maps for delineating marine terraces
[PB87-154597] N87-24013
CAMERAS
Double-diffraction X-ray imaging camera
[DE87-007936] N87-23940
A fiber optic link for an infrared imaging camera system
[DE87-006346] N87-24181
CANADIAN SHIELD
Spatial characterization of acid rain stress in Canadian Shield lakes
[NASA-CR-180983] N87-24031
Spatial characterization of acid rain stress in Canadian Shield lakes
[NASA-CR-180982] N87-24032
CANOPIES (VEGETATION)
Error analysis of leaf area estimates made from allometric regression models
[NASA-TM-89220] N87-24010
CANTILEVER BEAMS
Material damping measurements of 2D carbon-carbon composite beams
[AD-A179109] N87-23700
CAPACITANCE-VOLTAGE CHARACTERISTICS
Electrical behavior of Ge and (Ge+As) implanted gallium arsenide
[AD-A179505] N87-24203
CARBON
Spin-cast carbon films from polyacrylonitrile
[DE87-002489] N87-23703
CARBON DIOXIDE
Medium- and long-wave infrared absorption spectra of carbon dioxide nitrous oxide at 800K
[AD-A179430] N87-23708
CARBON DIOXIDE CONCENTRATION
The reality of the greenhouse effect
[DE87-002383] N87-24041
The detection of CO2-induced climate change
[DE87-006085] N87-24052
CARBON DIOXIDE LASERS
Thermal decomposition and ignition of a series of new nitramine lova propellants by CO2 laser N87-23783
Shuttle Coherent Atmospheric Lidar Experiment (SCALE)
[NASA-TM-100307] N87-23959
CARBON MONOXIDE
Laser studies of chemical dynamics at the gas-solid interface
[DE87-005950] N87-23710
Carbon monoxide emission from small galaxies N87-24303
Detection of CO (J=1-0) in the dwarf elliptical galaxy NGC 185 N87-24315
Molecular gas in the starburt nucleus of M82 N87-24321
Interferometric CO observations of the ultraluminous IRAS galaxies ARP 220, IC 694/NGC 3690, NGC 6420 and NGC 7469 N87-24331
CARBON-CARBON COMPOSITES
Material damping measurements of 2D carbon-carbon composite beams
[AD-A179109] N87-23700
CARBONIZATION
Spin-cast carbon films from polyacrylonitrile
[DE87-002489] N87-23703
CARDIOGRAPHY
Short Course on Cardiopulmonary Aspects of Aerospace Medicine
[AGARD-R-758] N87-24070
Valvular and congenital heart disease in the aviator N87-24073
Aeromedical aspects of mitral valve prolapse N87-24074
CARDIOLOGY
Aeromedical evaluation and disposition of electrocardiographic abnormalities N87-24071
Valvular and congenital heart disease in the aviator N87-24073
CARGO AIRCRAFT
Aircraft accident report: Southern Air Transport LOGAIR Flight 51, Lockheed L-382G, Kelly Air Force Base, Texas, October 4, 1986
[PB87-910404] N87-23604
CARGO SPACECRAFT
Nuclear powered Mars cargo transport mission utilizing advanced ion propulsion
[NASA-TM-100109] N87-23692

CARRIER INJECTION
Drift mobilities by time-of-flight methods and time-dependent phototransport in the nanosecond regime in amorphous semiconductors
[DE87-008021] N87-24206
CARRIER LIFETIME
Development and analysis of silicon solar cells near 20% efficiency in the Flat Plate Solar Array Project
[NASA-CR-181005] N87-24018
CASCADE FLOW
Surface roughness: Its effects on the performance of a two-dimensional compressor cascade
[AD-A179506] N87-23913
CASSEGRAIN ANTENNAS
Z-corrections for DSN 70-meter antenna ranging calibration N87-23836
CAST ALLOYS
Acta aeronautica et astronautica sinica
[AD-A179673] N87-23618
CATALYSIS
Palladium-silver and gold alloys as catalytic gates on MIS gas sensors
[DE87-006959] N87-23943
CATHODE RAY TUBES
OASIS: A modern tool for real-time simulation N87-23638
Text editing performance as a function of screen size
[AD-A179067] N87-24229
CAUCHY-RIEMANN EQUATIONS
Solving the Cauchy-Riemann equations on parallel computers
[NASA-CR-178307] N87-24107
CAVITATION FLOW
Squeeze film damper technology. Part 2. Extension of analysis and parametric study
[AD-A178094] N87-23974
Squeeze film damper technology. Part 3. Experimental investigation of squeeze film dampers
[AD-A178095] N87-23975
CAVITONS
Role of cavitons in laser-plasma interactions
[DE87-008485] N87-24192
CAVITY RESONATORS
Scattering from an open spherical shell having a circular aperture and enclosing a concentric dielectric sphere
[DE87-007099] N87-23842
CEILINGS (METEOROLOGY)
Station climatic summaries, Antarctica, Australia and Oceania
[AD-A179242] N87-24047
CELLULOSE
Synthesis of model polymers and related structures in support of vinyl monomer grafting studies
[DE87-007406] N87-23739
CEMENTS
Consequence of layer separation on pavement performance
[DOT/FAA/PM-86/48] N87-23661
CENTAUR LAUNCH VEHICLE
Design, development and test of shuttle/Centaur G-prime cryogenic tankage thermal protection systems
[NASA-TM-89825] N87-23685
CENTRIFUGAL COMPRESSORS
Performance of two 10-lb/sec centrifugal compressors with different blade and shroud thicknesses operating over a range of Reynolds numbers
[NASA-TM-100115] N87-23623
CENTRIFUGAL PUMPS
Antimisting Fuel (AMK) flight degrader development and aircraft fuel system investigation
[DOT/FAA/CT-86/6] N87-23816
CERAMIC BONDING
Ceramic technology for advanced heat engines project
[DE87-008538] N87-23740
Development of a high temperature ceramic-to-metal seal for Air Force Weapons Laboratory Laser
[DE87-007711] N87-23949
CERAMIC COATINGS
Ceramic technology for advanced heat engines project
[DE87-008538] N87-23740
CERAMIC HONEYCOMBS
Ceramic honeycomb structures and the method thereof
[NASA-CASE-ARC-11652-1] N87-23737
CERAMIC MATRIX COMPOSITES
Ceramic technology for advanced heat engines project
[DE87-008538] N87-23740
CERAMICS
Metals and Ceramics Division
[DE87-008548] N87-23697
Ceramic fibre/glass matrix composites with outstanding mechanical performance
[AERE-R-12025] N87-23699
Ceramic technology for advanced heat engines project
[DE87-008538] N87-23740
Manufacturing processes for high-temperature structural ceramics: A patent trend analysis
[PB87-178059] N87-23742
Investigation of the impact performance of various glass and ceramic systems
[AD-A178115] N87-23744
New low temperature (hydroxylated) materials
[DE87-008530] N87-23749
Ultrasonic techniques for the evaluation of ceramic joints
[DE87-009104] N87-23986
Application of scanning acoustic microscopy to advanced structural ceramics
[NASA-TM-89929] N87-23987
CEREBRAL VASCULAR ACCIDENTS
Hypertension in the aviator N87-24077
CERENKOV RADIATION
Potential electron beam induced flashblindness in pilots
[AD-A178002] N87-24084
CERTIFICATION
Certification testing methodology for composite structure. Volume 1: Data analysis
[NADC-87042-60-VOL-1] N87-23705
Certification testing methodology for composite structure. Volume 2: Methodology development
[NADC-87042-60-VOL-2] N87-23706
CHALLENGER (ORBITER)
Actions to implement the recommendations of the Presidential Commission on the Space Shuttle Challenger accident: Executive summary N87-23676
CHANNEL FLOW
Laser Doppler velocimeter application in supersonic boundary-layer flow
[AD-A178395] N87-23590
Response of transonic diffuser flows to abrupt increases of back pressure: Wall pressure measurements N87-23793
Selection principles and pattern formation in fluid mechanics and nonlinear shell theory
[NASA-CR-180941] N87-23916
CHARGE CARRIERS
Drift mobilities by time-of-flight methods and time-dependent phototransport in the nanosecond regime in amorphous semiconductors
[DE87-008021] N87-24206
CHARGE COUPLED DEVICES
Solid state research
[AD-A178394] N87-24221
CHARGE EFFICIENCY
Aircraft battery state of charge and charge control system
[AD-A179086] N87-23870
CHARGED PARTICLES
The development of a containment vessel and Dewar for the particle astrophysics magnet facility (ASTROMAG)
[NASA-CR-181018] N87-23670
The joint NASA/Goddard-University of Maryland research program in charged particle and high energy photon detector technology
[NASA-CR-180996] N87-24166
CHEMICAL ANALYSIS
Storage and preservation of environmental samples
[DE87-004271] N87-24030
The field shower wastewater recycling system: Development of a program of instruction and preliminary analysis of its potential health implications
[AD-A178112] N87-24088
CHEMICAL COMPOSITION
Measurements of particulates in solid propellant rocket motors N87-23769
New concepts for cars diagnostics of solid propellant combustion N87-23771
Two techniques for measuring AP ignition delay N87-23772
Geophysical monitoring for climatic change number 14
[PB87-162533] N87-24056
Investigation of biochemical variation in operational aircrew
[AD-A179223] N87-24067
Multicomponent analysis using an array of piezoelectric crystal sensors
[AD-A178012] N87-24216
CHEMICAL REACTIONS
Preparation of B-trichloroborazine
[NASA-CASE-ARC-11643-1-SB] N87-23698
Sandia cooperative group on the aerothermochemistry of turbulent combustion
[DE87-008345] N87-23714
Thermal ignition of pyrotechnics with lasers
[DE87-006245] N87-23955
Microscale defect kinetics in melt-grown GaAs
[AD-A178158] N87-24218
CHEMOTHERAPY
Hypertension in the aviator N87-24077
CHIPS (ELECTRONICS)
A VLSI single chip (255,223) Read-Solomon encoder with interleaver N87-23632
CHIPS (MEMORY DEVICES)
A single chip LSI high-speed functional tester
[AD-A177886] N87-23886
CHOLESTEROL
Coronary risk factors in aerospace medicine N87-24078
CHRONOLOGY
LANDSAT-based lineament analysis, East Texas Basin, and structural history of the Sabine Uplift area, East Texas and North Louisiana
[PB87-176327] N87-24043
IUE observations of luminous blue star associations in irregular galaxies N87-24301
CIRCUIT BOARDS
An interactive wire-wrap board layout program N87-23639
CIRCUIT PROTECTION
Investigations on the impact of voltage and current harmonics on end-use devices and their protection
[DE87-008018] N87-23878
CIRCUIT RELIABILITY
Time domain wave propagation in multilayered integrated circuits
[AD-A178180] N87-23847
CIRCUITS
The effect of reinforcement on the tear properties of flexible circuits
[DE87-007022] N87-23895
CIRCULAR ORBITS
An analysis of geopotential effects on satellite constellations
[AD-A179507] N87-23684
CIRCULAR POLARIZATION
Dual-polarization 8.45 GHz traveling-wave maser N87-23638
Mechanisms for the circular polarization of astrophysical OH masers in star-forming regions and the inferred magnetic fields N87-24277
CIVIL AVIATION
Results of the specialized investigation of accidents involving German aircraft at home and abroad, and with foreign aircraft at home
[ISSN-0178-8094] N87-23602
CLIMATE
The reality of the greenhouse effect
[DE87-002383] N87-24041
The detection of CO2-induced climate change
[DE87-006085] N87-24052
Climatological observations in the Philip Smith Mountains of the North Slope, Alaska
[DE87-008179] N87-24054
Geophysical monitoring for climatic change number 14
[PB87-162533] N87-24056
CLIMATOLOGY
Station climatic summaries, Antarctica, Australia and Oceania
[AD-A179242] N87-24047
Mixed layer and thermocline depth climatologies in the western Indian Ocean
[PB87-154613] N87-24060
CLINICAL MEDICINE
Midwest free-electron laser program
[AD-A178106] N87-23953
CLOUD COVER
Global distribution of total cloud cover and cloud type amounts over land
[DE87-006903] N87-24053
CLOUDS (METEOROLOGY)
Global distribution of total cloud cover and cloud type amounts over land
[DE87-006903] N87-24053
CLUMPS
Metal alkoxides: Models for metal oxides: Alkoxide ligands in early transition metal organometallic chemistry
[DE87-007309] N87-23715
Formation and stability of partially-neutralized plasma clumps
[AD-A179444] N87-24187
CLUTCHES
Rotary stepping device with memory metal actuator
[NASA-CASE-NPO-15482-1] N87-23970
CLUTTER
Analysis of space-based radar clutter spectra over different types of terrain and their effects on detection performance
[AD-A178066] N87-23845

CMOS
A VLSI CMOS circuit design technique to aid test generation
[AD-A177934] N87-23887
The development of a prototype CMOS (Complementary Metal Oxide Semiconductor) circuit simulator
[AD-A177942] N87-24215
Solid state research
[AD-A178394] N87-24221
COASTS
Utilizing remote sensing of thematic mapper data to improve our understanding of estuarine processes and their influence on the productivity of estuarine-dependent fisheries
[NASA-CR-180984] N87-24012
Radar as a complement to topographic maps for delineating marine terraces
[PB87-154597] N87-24013
COATING
Consequence of layer separation on pavement performance
[DOT/FAA/PM-86/48] N87-23661
Dielectric properties of styrene/acrylate copolymer coatings formed by electrophoretic deposition on gold, aluminum alloy, and porous anodized aluminum alloy substrates
[DE87-006885] N87-23741
COATINGS
Dielectric properties of styrene/acrylate copolymer coatings formed by electrophoretic deposition on gold, aluminum alloy, and porous anodized aluminum alloy substrates
[DE87-006885] N87-23741
COCKPITS
Visual and motion cueing in helicopter simulation N87-23634
OASIS: A modern tool for real-time simulation N87-23638
Trends in ground-based and in-flight simulators for development applications N87-23645
CODING
A method for aircraft simulation verification and validation developed at the United States Air Force Flight Simulation Facility N87-23654
A VLSI single chip (255,223) Reed-Solomon encoder with interleaver N87-23832
GASPS: A time-dependent, one-dimensional, planar gas dynamics computer code
[DE87-008338] N87-23931
Atmospheric radiance profile codes
[AD-A179258] N87-24035
COGNITION
Experiments on the cognitive aspects of information seeking and information retrieving
[PB87-157699] N87-24238
COHERENT LIGHT
Coherent multiple aperture optical imaging systems: Analysis and design
[AD-A179476] N87-24176
COHERENT RADAR
Shuttle Coherent Atmospheric Lidar Experiment (SCALE)
[NASA-TM-100307] N87-23959
COLD FLOW TESTS
Numerical simulations of cold flow in a ramjet dump combustor with a choked exit nozzle N87-23802
COLD PLASMAS
Generation of broadband noise in the magnetotail
[AD-A179136] N87-24034
COLLAPSE
Collapse analysis of cylindrical composite panels with large cutouts under an axial load
[AD-A179112] N87-23701
COLLISIONS
Kinetic studies following state-selective laser excitation
[DE87-007938] N87-23950
COLLOIDS
Assembly and functionalization of supramolecular structures studied by luminescence techniques
[AD-A178064] N87-24217
COLOR
Multipurpose visual display and eye movement recording system
[AD-A179620] N87-24068
Modelling the IRAS colors of galaxies N87-24313
COLOR CODING
Colored stochastic Petri nets
[ENST-86C001] N87-24111
COLOR-MAGNITUDE DIAGRAM
Star formation in the Magellanic clouds N87-24288
COLORIMETRY
SPECOL: A colorimetric measurement system
[BBC-RD-1987/4] N87-23942
COMBAT
Manned air to air combat simulation N87-23648
The use of Aeritalia flight simulator for the development of the AM-X weapon system N87-23650
Operational training: Application and experience N87-23653
COMBUSTION CHAMBERS
Liner cooling research at NASA Lewis Research Center
[NASA-TM-100107] N87-23624
Stochastic excitation of acoustic waves in a combustion chamber N87-23761
Linear coupling of acoustics and entropy and acoustic stability in ramjet combustion chambers containing a plane flame N87-23795
Vortex-nozzle interactions in ramjet combustors N87-23800
Computational studies of the effects of acoustics and chemistry on the flow field in an axisymmetric ramjet combustor N87-23801
Numerical simulations of cold flow in a ramjet dump combustor with a choked exit nozzle N87-23802
COMBUSTION CHEMISTRY
New concepts for cars diagnostics of solid propellant combustion N87-23771
Chemical kinetics combustion model of the NG/binder system N87-23773
COMBUSTION CONTROL
Passive shear-flow control to minimize ramjet combustion instabilities N87-23798
COMBUSTION EFFICIENCY
Metallized fuel burning characteristics in the solid fuel ramjet N87-23788
Plasma torch igniter for scramjets N87-23789
Analytical prediction of combustion performance characteristics of bipropellant liquid rocket engine combustor N87-23810
Synchronization trigger control system for flow visualization
[NASA-TM-89902] N87-23902
A comparison of unburned fuel and aldehyde emissions from a methanol-fueled stratified charge and homogeneous charge engine
[DE87-007793] N87-23966
COMBUSTION PHYSICS
Sandia cooperative group on the aerothermochemistry of turbulent combustion
[DE87-006345] N87-23714
The 23rd JANNAF Combustion Meeting, volume 1
[AD-A179158] N87-23757
COMBUSTION PRODUCTS
Transport phenomena and interfacial kinetics in multiphase combustion systems
[AD-A179544] N87-23709
Study of the suppression of rocket plume afterburning by chemical additives N87-23768
A comparison of unburned fuel and aldehyde emissions from a methanol-fueled stratified charge and homogeneous charge engine
[DE87-007793] N87-23966
COMBUSTION STABILITY
The 23rd JANNAF Combustion Meeting, volume 1
[AD-A179158] N87-23757
Behavior of simulated solid propellant flames in axial acoustic fields N87-23760
Stochastic excitation of acoustic waves in a combustion chamber N87-23761
Workshop report: Methods for measuring solid propellant combustion response N87-23762
TTCP non-linear instability program: US motor test data N87-23763
Asymptotic models for solid propellant combustion and the onset of intrinsic instability N87-23764
Role of combustion in the nonlinear combustion instability of composite solid propellants N87-23765
A theoretical and numerical study of radiative ignition and deradiative extinction in solid propellants N87-23778
Downstream boundary effects on the frequency of self-excited oscillations in transonic diffuser flows N87-23794
Tones generated due to the impingement of two jets on each other N87-23797
Passive shear-flow control to minimize ramjet combustion instabilities N87-23798
Computational studies of the effects of acoustics and chemistry on the flow field in an axisymmetric ramjet combustor N87-23801
Combustion instabilities in dump type ramjet combustors N87-23803
Spray combustion: A driving mechanism for ramjet combustion instability N87-23805
COMBUSTION TEMPERATURE
New concepts for cars diagnostics of solid propellant combustion N87-23771
Quantum chemical calculations of the decomposition of nitramines: Thermochemistry and reaction pathways N87-23781
COMBUSTION VIBRATION
An approach of preventing combustion vibrations of rocket engine with lateral baffle
[AD-A179222] N87-23688
TTCP non-linear instability program: US motor test data N87-23763
COMMAND AND CONTROL
Future directions of C3 research at DARPA (Defense Advanced Research Projects Agency)
[DE87-007501] N87-23948
COMMERCIAL AIRCRAFT
Aircraft accident data: US air carrier operations calendar year 1984
[PB87-183992] N87-23603
Aircraft accident data: US air carrier operations calendar year 1983
[PB87-160628] N87-23605
Aircraft electromagnetic compatibility
[NASA-CR-181051] N87-23856
COMMUNICATION NETWORKS
Communication-efficient parallel graph algorithms
[AD-A178286] N87-23853
Future directions of C3 research at DARPA (Defense Advanced Research Projects Agency)
[DE87-007501] N87-23948
COMMUNICATION SATELLITES
Spacecraft multi-beam and contoured-beam antennas N87-23863
COMPARISON
A quantitative comparison of several orbital maneuvering vehicle configurations for satellite repair/replenishment
[AD-A179106] N87-23677
COMPENSATORY TRACKING
Choosing sampling rates for robot control
[AD-A179447] N87-24118
COMPLEX SYSTEMS
Microwave coupling inside complex systems
[DE87-003505] N87-23841
COMPONENT RELIABILITY
Techniques for implementing statically complete component mode synthesis for forced response
[DE87-002698] N87-24002
COMPOSITE MATERIALS
Acta aeronautica et astronautica sinica
[AD-A179673] N87-23618
Material damping measurements of 2D carbon-carbon composite beams
[AD-A179109] N87-23700
White paper on nanocomposites as harmonic generation media
[DE87-008337] N87-23704
Energy-absorption capability and scalability of square cross section composite tube specimens
[NASA-TM-89087] N87-23991
Material damping from frequency analysis of driving point measurements
[DE87-005873] N87-24003
COMPOSITE PROPELLANTS
Role of combustion in the nonlinear combustion instability of composite solid propellants N87-23765
Modification of solid propellant deflagration rates due to random nonhomogeneities N87-23766
Two techniques for measuring AP ignition delay N87-23772
AP/HMX composite propellant modeling N87-23776
Thermal decomposition and ignition of a series of new nitramine lova propellants by CO2 laser N87-23783
COMPOSITE STRUCTURES
Collapse analysis of cylindrical composite panels with large cutouts under an axial load
[AD-A179112] N87-23701
Certification testing methodology for composite structure. Volume 1: Data analysis
[NADC-87042-60-VOL-1] N87-23705
Certification testing methodology for composite structure. Volume 2: Methodology development
[NADC-87042-60-VOL-2] N87-23706
Ceramic honeycomb structures and the method thereof
[NASA-CASE-ARC-11652-1] N87-23737
COMPRESSIBILITY EFFECTS
Compressibility of submerged supersonic jets N87-23581
COMPRESSIBLE BOUNDARY LAYER
Theoretical investigation of 3-D shock wave-turbulent boundary layer interactions, part 5
[AD-A179455] N87-23909
COMPRESSIBLE FLOW
Method for the determination of the three-dimensional aerodynamic field of a rotor-stator combination to compressible flow
[NASA-TM-100118] N87-23625
Theoretical investigation of 3-D shock wave-turbulent boundary layer interactions, part 5
[AD-A179455] N87-23909

COMPRESSING
Compression and shear wave propagation in plain and filled elastomers
[AD-A178153] N87-23745

COMPRESSION TESTS
Inelastic properties of ice I/sub h/ at low temperatures and high pressures
[DE87-007334] N87-23711

COMPRESSOR BLADES
Surface roughness: Its effects on the performance of a two-dimensional compressor cascade
[AD-A179506] N87-23913

COMPRESSOR ROTORS
Effectiveness of balancing flexible rotary compressor vanes on low-speed balancing machine N87-23580
Thermodynamic evaluation of transonic compressor rotors using the finite volume approach
[NASA-CR-180587] N87-23925

COMPRESSORS
The T55-L-712 turbine engine compressor housing refurbishment project
[NASA-CR-179624] N87-23729

COMPTON EFFECT
Satellite observation of atmospheric nuclear gamma radiation
[AD-A177937] N87-24389

COMPUTATION
Computation of full-coverage film-cooled airfoil temperatures by two methods and comparison with high heat flux data
[NASA-TM-88931] N87-23934
Inelastic strain analogy for piecewise linear computation of creep residues in built-up structures
[NASA-TM-86813] N87-23995
The hypercube as a supercomputer
[DE87-005029] N87-24092
Gaussian elimination with partial pivoting and load balancing on a multiprocessor
[DE87-007784] N87-24093
An extended set of FORTRAN basic linear algebra subprograms: Model implementation and test programs
[DE87-007913] N87-24101
Efficient parallel algorithms for (delta+1)-coloring and maximal independent set problems
[AD-A178287] N87-24109
Symbol manipulation and applied mathematics
[AD-A179571] N87-24124
Estimate for the errors in eigenvalue and eigenvector approximation by Galerkin methods, with particular attention to the case of multiple eigenvalues
[AD-A178390] N87-24142

COMPUTATIONAL FLUID DYNAMICS
Mathematical model describing interaction of single nonsteady supersonic jet and movable barrier of finite dimensions N87-23575
Calculation of axisymmetric flow in swirlers by difference method N87-23579
Compressibility of submerged supersonic jets N87-23581
Some aspects of vortex flows determined from the thin-layer Navier-Stokes equations
[NASA-TM-88375] N87-23595
Multispecies CARS measurements in turbulent combustion N87-23608
Selection principles and pattern formation in fluid mechanics and nonlinear shell theory
[NASA-CR-180941] N87-23916
Onset of Taylor vortices in flows with a circumferential pressure gradient: Application to the helical screw rheometer
[DE87-000453] N87-23918
Viscous-inviscid interaction with higher-order viscous-flow equations: Applications to three-dimensional bodies
[AD-A178264] N87-23924
Thermodynamic evaluation of transonic compressor rotors using the finite volume approach
[NASA-CR-180587] N87-23925
Development of an explicit time marching procedure for laminar and turbulent flow N87-23926
Development of a finite volume time marching method
[JM/85-3] N87-23927
An explicit finite-volume time-marching procedure for turbulent flow calculations N87-23928
Explicit finite-volume time-marching calculations of total temperature distributions in turbulent flow N87-23929
Upwind and symmetric shock-capturing schemes
[NASA-TM-89484] N87-24145

COMPUTATIONAL GRIDS
Some aspects of vortex flows determined from the thin-layer Navier-Stokes equations
[NASA-TM-88375] N87-23595
Adaptive grid refinement for numerical weather prediction
[AD-A179393] N87-24049
Information based numerical practice
[AD-A178362] N87-24141
Adaptive moving grid strategies for one-dimensional systems of partial differential equations
[DE87-006824] N87-24144

COMPUTER AIDED DESIGN
OASIS: A modern tool for real-time simulation N87-23638
Piloted simulation in the development of the XV-15 tilt rotor research aircraft N87-23646
An interactive wire-wrap board layout program N87-23839
Computer aided design and analysis of gear tooth geometry
[NASA-CR-179611] N87-23969
CADCAM-005: An introduction to the data exchange process using IGES
[DE87-006079] N87-24102

COMPUTER AIDED MANUFACTURING
CADCAM-005: An introduction to the data exchange process using IGES
[DE87-006079] N87-24102
Computer-aided fabrication system implementation
[AD-A178225] N87-24108

COMPUTER COMPONENTS
Vector array processor computer equipment
[AD-A179545] N87-24382

COMPUTER DESIGN
Hardware synthesis from specification with polynomials
[TRITA-NA-8506] N87-24091
The hypercube as a supercomputer
[DE87-005029] N87-24092

COMPUTER GRAPHICS
OASIS: A modern tool for real-time simulation N87-23638
An interactive wire-wrap board layout program N87-23839
CADCAM-005: An introduction to the data exchange process using IGES
[DE87-006079] N87-24102
Three dimensional graphics in the statistical analysis of scientific data
[DE87-006151] N87-24104
The decomposition of an arbitrary three-dimensional planar polygon into a set of convex polygons
[AD-A177947] N87-24137

COMPUTER INFORMATION SECURITY
Livermore risk analysis methodology: A quantitative approach to management of the risk associated with the operation of information systems
[DE87-006828] N87-24232

COMPUTER NETWORKS
Future directions of C3 research at DARPA (Defense Advanced Research Projects Agency)
[DE87-007501] N87-23948
Using expert systems to manage distributed computer systems
[AD-A179329] N87-24112
The future of intersite networking
[DE87-007912] N87-24116
The effect of distributed computing technology on wide area network capacity requirements
[DE87-008229] N87-24117

COMPUTER PROGRAMMING
A program maintenance aid using static data flow analysis techniques
[AD-A179108] N87-24095
Research aspects of rapid prototyping
[AD-A179007] N87-24097
Use of a DBMS to aid in the software conversion process
[DE87-007883] N87-24234

COMPUTER PROGRAMS
Finite-difference program for hydrogen diffusion: Example problems manual
[DE87-007515] N87-23712
Evaluation of a thin-slot formalism for finite-difference time-domain electromagnetics codes
[DE87-008078] N87-23857
GASPS: A time-dependent, one-dimensional, planar gas dynamics computer code
[DE87-008338] N87-23931
Atmospheric radiance profile codes
[AD-A179258] N87-24035
Mid-latitude wind probability model
[AD-A179256] N87-24048
Research aspects of rapid prototyping
[AD-A179007] N87-24097
The Shock and Vibration Digest, Volume 19, No. 6 N87-24125
Radiation transport in dust in disk geometry
[NASA-CR-180995] N87-24157
Automating index preparation
[AD-A179327] N87-24231

COMPUTER SYSTEMS DESIGN
Flexible and high quality software on a multiprocessor computer system controlling a research flight simulator N87-23643
An introduction to structured modeling, revision
[AD-A179355] N87-24153
Vector array processor computer equipment
[AD-A179545] N87-24382

COMPUTER SYSTEMS PERFORMANCE
Flexible and high quality software on a multiprocessor computer system controlling a research flight simulator N87-23643
Using expert systems to manage distributed computer systems
[AD-A179329] N87-24112
Beyond Speedup: Performance analysis of parallel programs
[DE87-007954] N87-24115
An introduction to structured modeling, revision
[AD-A179355] N87-24153
The success or failure of management information systems: A theoretical approach
[DE87-007802] N87-24233
Vector array processor computer equipment
[AD-A179545] N87-24382

COMPUTER SYSTEMS PROGRAMS
OASIS: A modern tool for real-time simulation N87-23638
DATA: A comprehensive data analysis environment for HP1000 computers
[DE87-007824] N87-24094
A rapid prototyping approach to software validation
[AD-A177939] N87-24106
Use of a DBMS to aid in the software conversion process
[DE87-007883] N87-24234

COMPUTER SYSTEMS SIMULATION
The success or failure of management information systems: A theoretical approach
[DE87-007802] N87-24233

COMPUTER TECHNIQUES
Tactical weather expert system
[AD-A178605] N87-24050
TAF (Terminal Aerodrome Forecast) verification
[AD-A177931] N87-24055
Recovering the orientation of textured surfaces in natural scenes
[AD-A179360] N87-24096
A PASCAL implementation of the image algebra
[AD-A177943] N87-24136
An introduction to structured modeling, revision
[AD-A179355] N87-24153
Nonlinear real-time optical signal processing
[AD-A178169] N87-24182

COMPUTER VISION
Intermediate level computer vision processing algorithm development for the content addressable array parallel processor
[AD-A179515] N87-24090

COMPUTERIZED SIMULATION
Evaluation of the angle of attack limiter of the F-16 C/D aircraft
[AD-A177941] N87-23612
Computer simulation studies on human control reliability in manual aircraft control: The origin of PIO N87-23644
Piloted simulation in the development of the XV-15 tilt rotor research aircraft N87-23646
Manned air to air combat simulation N87-23648
Utilization of simulation to support F-14A low altitude high angle of attack flight testing N87-23649
The use of molecular dynamics for the thermodynamic properties of simple and transition metals
[DE87-007718] N87-23725
Computer simulation of the lasertron with a ring model
[DE87-007461] N87-23897
Computer aided design and analysis of gear tooth geometry
[NASA-CR-179611] N87-23969
A simplified computer solution for the flexibility matrix of contacting teeth for spiral bevel gears
[NASA-CR-179620] N87-23977
Simulation and analysis of a geopotential research mission
[NASA-CR-180695] N87-24042
Computer-aided fabrication system implementation
[AD-A178225] N87-24108
Investigations into the pattern processing capabilities of associative nets
[TRITA-NA-8601] N87-24114
Content-addressable memory: Applications, algorithms, and simulation
[AD-A177944] N87-24120
Satellite allocation for boost-phase missile intercepts
[DE87-007719] N87-24155

AXCEL: Interactive simulation program to compute two-dimensional potential distributions of electrostatic arrangements and of ion paths in electrostatic fields under consideration of space charging
[DE87-007760] N87-24165
Computer simulation of bounded plasma systems
[DE87-006193] N87-24190
Systems model for natural gas vehicle fleets
[PB87-178083] N87-24245
CONCATENATED CODES
A VLSI single chip (255,223) Reed-Solomon encoder with interleaver N87-23832
CONCENTRATION (COMPOSITION)
CARS approaches to simultaneous measurements of H2 and H2O concentration and temperature in H2-air combustion systems N87-23792
The review of a research proposal to study the effects of 130 torr oxygen on submarines held at Groton, Connecticut on September 4, 1986
[AD-A177976] N87-24083
CONCENTRATORS
Solar cell concentrator system
[AD-A177981] N87-24025
CONCENTRIC CYLINDERS
Onset of Taylor vortices in flows with a circumferential pressure gradient: Application to the helical screw rheometer
[DE87-000453] N87-23918
CONCENTRIC SPHERES
Scattering from an open spherical shell having a circular aperture and enclosing a concentric dielectric sphere
[DE87-007099] N87-23842
CONCRETE STRUCTURES
Consequence of layer separation on pavement performance
[DOT/FAA/PM-86/48] N87-23661
CONCURRENT PROCESSING
The hypercube as a supercomputer
[DE87-005029] N87-24092
CONDENSERS
Flow regimes of refrigerant mixtures condensing inside tubes
[ORNL/SUB/81-7762/4 AND 01] N87-23917
CONDUCTION
Numerical prediction of 1-D ablation using a finite control volume procedure with exponential differencing
[DE87-007947] N87-24130
CONFERENCES
Flight Simulation
[AGARD-CP-408] N87-23633
Proceedings of the Tenth DOE Solar Photochemistry Research Conference
[DE87-006421] N87-24062
Short Course on Cardiopulmonary Aspects of Aerospace Medicine
[AGARD-R-758] N87-24070
International Symposium on In Vivo Body Composition Studies: Program and abstracts
[DE87-006750] N87-24080
The future of intersite networking
[DE87-007912] N87-24116
Essays in Space Science
[NASA-CP-2464] N87-24247
Star Formation in Galaxies
[NASA-CP-2466] N87-24266
CONFIDENCE LIMITS
Nonparametric estimation of the probability of a long delay in the M/G/1 queue
[AD-A178259] N87-24150
Confidence interval for parameter n in a binomial distribution
[AD-A178325] N87-24151
Decaying confidence functions for aging knowledge in expert systems
[AD-A179328] N87-24152
CONFORMAL MAPPING
Time domain wave propagation in multilayered integrated circuits
[AD-A178180] N87-23847
CONGENITAL ANOMALIES
Valvular and congenital heart disease in the aviator N87-24073
CONGRESSIONAL REPORTS
Electric and Hybrid Vehicles Program: 10th annual report to Congress for Fiscal Year 1986
[DE87-006350] N87-23966
National Aeronautics and Space Administration Authorization Act
[S-REPT-100-87] N87-24240
Department of Housing and Urban Development - Independent Agencies Appropriations Bill, 1988
[H-REPT-100-189] N87-24241
National Aeronautics and Space Administration --- appropriations bill H.R. 2783 N87-24242
National Aeronautics and Space Administration Authorization Act, 1988
[S-REPT-100-87] N87-24243
CONICAL CAMBER
Study of lee-side flows over conically cambered delta wings at supersonic speeds, part 1
[NASA-TP-2660-PT-1] N87-23597
CONSERVATION
The field shower wastewater recycling system: Development of a program of instruction and preliminary analysis of its potential health implications
[AD-A178112] N87-24088
CONSERVATION LAWS
A generalized procedure for constructing an upwind based TVD scheme
[NASA-TM-88926] N87-24132
Upwind and symmetric shock-capturing schemes
[NASA-TM-89464] N87-24145
CONSOLES
Use of VDU's by flight simulator instructors N87-23641
CONSTANTS
Medium- and long-wave infrared absorption spectra of carbon dioxide nitrous oxide at 800K
[AD-A179430] N87-23708
CONTACT LOADS
A simplified computer solution for the flexibility matrix of contacting teeth for spiral bevel gears
[NASA-CR-179620] N87-23977
CONTAINERLESS MELTS
Apparatus ad method for quiescent containerless processing of high temperature metals and alloys in low gravity
[NASA-CASE-MFS-28087-1] N87-23944
CONTAMINANTS
Storage and preservation of environmental samples
[DE87-004271] N87-24030
CONTINUUM MECHANICS
Dynamic brittle fracture analysis based on continuum damage mechanics
[DE87-006704] N87-24005
CONTROL
A fiber optic link for an infrared imaging camera system
[DE87-008346] N87-24181
CONTROL EQUIPMENT
Use of VDU's by flight simulator instructors N87-23641
Optically controlled microwave devices and circuits: Emerging applications in space communications systems
[NASA-TM-89669] N87-23900
CONTROL SIMULATION
Control of welding processes
[AD-A177893] N87-23971
CONTROL STICKS
Flight test evaluation of techniques to predict longitudinal pilot induced oscillations
[AD-A179229] N87-23629
The development of the T-46 next generation trainer manned engineering simulator at the US Air Force Flight Test Center N87-23652
CONTROL SYSTEMS DESIGN
Rf control system for a rocket-borne accelerator
[DE87-007459] N87-23673
Synchronization trigger control system for flow visualization
[NASA-TM-89902] N87-23902
Modified independent modal space control method for active control of flexible systems
[NASA-CR-181065] N87-23980
CONTROL THEORY
Development of in-flight simulation aircraft for research and training applications in UK N87-23658
Optimal continuous thrust orbital evasive maneuvers from geosynchronous orbit
[AD-A179413] N87-23668
CONTROLLABILITY
Visual and motion cueing in helicopter simulation N87-23634
Computer simulation studies on human control reliability in manual aircraft control: The origin of PIO N87-23644
Utilization of simulation to support F-14A low altitude high angle of attack flight testing N87-23649
CONTROLLERS
The application of optimal control techniques to the UTIAS research simulator N87-23637
Advanced DC Motor Controller
[DE87-007756] N87-23882
CONVECTION
Numerical prediction of 1-D ablation using a finite control volume procedure with exponential differencing
[DE87-007947] N87-24130
CONVECTION CLOUDS
User's manual for the convective cloud module version 1.0
[DE87-008343] N87-24058
CONVECTIVE FLOW
Effective diffusion in laminar convective flows
[DE87-008054] N87-23920
Vector array processor computer equipment
[AD-A179545] N87-24382
CONVECTIVE HEAT TRANSFER
Simultaneous radiative and convective heating of thin body in medium with variable temperature N87-23576
Effects of corona on heat transfer in an enclosure
[AD-A179209] N87-23906
Multidimensional modeling of convective heat transfer with application to I.C. engines
[DE87-002939] N87-23922
CONVERGENCE
Strong convergence and convergence rates of approximating solutions for algebraic Riccati equations in Hilbert spaces
[NASA-CR-178302] N87-24122
On the existence and convergence of probability measures on continuous semi-lattices
[AD-A179267] N87-24148
CONVERTERS
A study of Schwarz converters for nuclear powered spacecraft
[NASA-TM-89911] N87-23903
COOLING
Liner cooling research at NASA Lewis Research Center
[NASA-TM-100107] N87-23624
COPOLYMERIZATION
Synthesis of model polymers and related structures in support of vinyl monomer grafting studies
[DE87-007406] N87-23739
COPOLYMERS
Synthesis of model polymers and related structures in support of vinyl monomer grafting studies
[DE87-007406] N87-23739
Dielectric properties of styrene/acrylate copolymer coatings formed by electrophoretic deposition on gold, aluminum alloy, and porous anodized aluminum alloy substrates
[DE87-008885] N87-23741
Electronics and ionic transport in polymers
[AD-A178227] N87-23746
CORNEA
Cornea Optical Topographical Scan System (COTSS)
[NASA-CR-179012] N87-24184
CORONARY ARTERY DISEASE
Noninvasive methods for the detection of coronary artery disease in aviators: A stratified Bayesian approach N87-24072
Coronary risk factors in aerospace medicine N87-24078
CORRELATION COEFFICIENTS
The correlation between far-IR and radio continuum emission from spiral galaxies N87-24349
CORROSION
Corrosion of gold bridgewire in electronic components
[DE87-000922] N87-23722
Corrosion sensing with acoustic wave devices
[DE87-003516] N87-23723
The corrosion of Al 7075-T6 alloy coupled to Ti 6A 1-4V in wet air
[DE87-008347] N87-23726
Nonuniform grain boundary corrosion and the local electrode potential in crevicing
[AD-A177889] N87-23728
CORROSION PREVENTION
Oxidation protection coatings for polymers
[NASA-CASE-LEW-14072-3] N87-23736
CORROSION TESTS
Corrosion of gold bridgewire in electronic components
[DE87-000922] N87-23722
The corrosion of Al 7075-T6 alloy coupled to Ti 6A 1-4V in wet air
[DE87-008347] N87-23726
COSMIC DUST
Radiation transport in dust in disk geometry
[NASA-CR-180995] N87-24157
A dust scattered halo in starburst galaxy M82? N87-24334
What are cirrus point sources? N87-24345
Ground-based 1- to 32-microns observations of ARP 220: Evidence for a dust-embedded AGN? N87-24361
COSMIC RAYS
Heavy ion induced upsets in semiconductor devices
[ATR-86(8139)-3] N87-24205
Essays in Space Science
[NASA-CP-2464] N87-24247
Studies of the interplanetary magnetic field: IMP's to Voyager N87-24253
Cosmic rays in the heliosphere N87-24254
Antiprotons in cosmic rays N87-24255
Measurements of ultraheavy cosmic rays with HEAO-3 N87-24256
High energy gamma ray astronomy N87-24258

Solar-geophysical data number 509, January 1987. Part 1: (Prompt reports). Data for December 1986, November 1986
[PB87-162574] N87-24385

COSMOLOGY
Gauge invariant quantum cosmology
[DE87-006685] N87-24226
Particle physics and cosmology
[DE87-007308] N87-24388

COSPAS
COSPAS-SARSAT satellite orbit predictor, volume 9
[NASA-TM-85015] N87-23671

COST ANALYSIS
Systems model for natural gas vehicle fleets
[PB87-178083] N87-24245

COST EFFECTIVENESS
Cost effective use of liquid nitrogen in cryogenic wind tunnels
[NASA-CR-178279] N87-23663
Aircraft electromagnetic compatibility
[NASA-CR-181051] N87-23656
A rapid prototyping approach to software validation
[AD-A177939] N87-24106

COST ESTIMATES
Characterization of solar thermal concepts for electricity generation. Volume 1: Analyses and evaluation
[DE87-007161] N87-24019
A rapid prototyping approach to software validation
[AD-A177939] N87-24106

COST REDUCTION
Cost reductions in the nickel/hydrogen battery
[DE87-007576] N87-23881

COUETTE FLOW
Selection principles and pattern formation in fluid mechanics and nonlinear shell theory
[NASA-CR-180941] N87-23916

COUNTERMEASURES
Satellite allocation for boost-phase missile intercepts
[DE87-007719] N87-24155
Livermore risk analysis methodology: A quantitative approach to management of the risk associated with the operation of information systems
[DE87-006828] N87-24232

COUPLING
Galvanic corrosion of Al-7075-T6 and Steel-4340 coupled to brass QQ-B-626, 360 and Al-7075-T6 coupled to Steel-4130 and Steel-4340: Exposure to aqueous NaCl and salt-fog environments
[AD-A179121] N87-23719
Results of near field probe scanning tests for ultralow sidelobe arrays
[AD-A178141] N87-23846

CRACK ARREST
Retardation effect in fatigue crack growth under stationary stochastic loading
[REPT-43/1986] N87-23999

CRACK INITIATION
Nonuniform grain boundary corrosion and the local electrode potential in crevicing
[AD-A177889] N87-23728

CRACK PROPAGATION
Influence of microstructure and microdamage processes on fracture at high loading rates
[AD-A179264] N87-23969
Retardation effect in fatigue crack growth under stationary stochastic loading
[REPT-43/1986] N87-23999
Investigation of tearing instability phenomena in ASTM steel
[AD-A177993] N87-24000

CRACKS
Study of the influence of metallurgical factors on fatigue and fracture of aerospace structural materials
[AD-A179268] N87-23720
Dynamic brittle fracture analysis based on continuum damage mechanics
[DE87-006704] N87-24005

CREEP ANALYSIS
Inelastic strain analogy for piecewise linear computation of creep residues in built-up structures
[NASA-TM-86813] N87-23995

CREWS
A systems analysis of emergency escape and recovery systems for the US space station
[AD-A179233] N87-23680

CROSS FLOW
Crossflow vorticity sensor
[NASA-CASE-LAR-13436-1-CU] N87-23587
Measurements of particulates in solid propellant rocket motors N87-23769
Motion-dependent fluid forces acting on a tube row in crossflow
[DE87-005574] N87-23923

CROSS SECTIONS
Energy-absorption capability and scalability of square cross section composite tube specimens
[NASA-TM-89087] N87-23991

CRUCIFORM WINGS
Mach 6 experimental and theoretical stability and performance of a cruciform missile at angles of attack up to 65 degrees
[NASA-TP-2733] N87-23592

CRYOGENIC ROCKET PROPELLANTS
Design, development and test of shuttle/Centaur G-prime cryogenic tankage thermal protection systems
[NASA-TM-89825] N87-23685

CRYOGENIC STORAGE
Design, development and test of shuttle/Centaur G-prime cryogenic tankage thermal protection systems
[NASA-TM-89825] N87-23685

CRYOGENIC WIND TUNNELS
High Reynolds Number tests of the NASA SC(2)-0012 airfoil in the Langley 0.3-meter transonic cryogenic tunnel
[NASA-TM-89102] N87-23594
Cost effective use of liquid nitrogen in cryogenic wind tunnels
[NASA-CR-178279] N87-23663

CRYOSTATS
The development of a containment vessel and Dewar for the particle astrophysics magnet facility (ASTROMAG)
[NASA-CR-181016] N87-23670

CRYSTAL DEFECTS
Microscale defect kinetics in melt-grown GaAs
[AD-A178158] N87-24218

CRYSTAL GROWTH
Apparatus and procedure to detect a liquid-solid interface during crystal growth in a bridgman furnace
[NASA-CASE-LAR-13597-1-CU] N87-23713
A model for silicon dendrite growth during laser/plasma deposition from a silane discharge
[DE87-007579] N87-23733
Polymer dynamics and gelation
[DE87-007578] N87-23748
Controlled nucleation and growth studies in metal oxide and alkoxide systems by dynamic laser-light-scattering methods
[DE87-009103] N87-23958
Microscale defect kinetics in melt-grown GaAs
[AD-A178158] N87-24218
Theoretical and experimental study of solid phase miscibility gaps in 3/5 quaternary alloys
[DE87-008942] N87-24223

CRYSTAL OPTICS
White paper on nanocomposites as harmonic generation media
[DE87-008337] N87-23704

CRYSTAL STRUCTURE
Evaluation of Tersoff's revised silicon potential in a molecular dynamic simulation of solid silicon
[AD-A179231] N87-24202

CRYSTALLIZATION
Controlled nucleation and growth studies in metal oxide and alkoxide systems by dynamic laser-light-scattering methods
[DE87-009103] N87-23958

CUBANE
Functionalization of cubane using hypervalent iodine N87-23807

CURRENT DENSITY
Investigation of electromigration in thin film aluminum at low temperatures
[AD-A179110] N87-23871
Three-dimensional electric field predictions of an iron-copper galvanic couple
[AD-A178040] N87-23888

CURRENT SHEETS
Studies of the interplanetary magnetic field: IMP's to Voyager N87-24253

CURVE FITTING
Approximation errors and perceived similarity between approximated polygons
[TRITA-NA-8505] N87-24127

CURVES (GEOMETRY)
Computer aided design and analysis of gear tooth geometry
[NASA-CR-179611] N87-23969

CYANIDES
Cellular monotectic model solidification
[NASA-CR-181027] N87-23717
CN radical distributions in solid propellant flames N87-23775

CYBERNETICS
Investigations into the pattern processing capabilities of associative nets
[TRITA-NA-8601] N87-24114

CYCLIC LOADS
Environmental degradation of 316 stainless steel in high temperature low cycle fatigue
[NASA-TM-89931] N87-24007

CYLINDRICAL BODIES
Collapse analysis of cylindrical composite panels with large cutouts under an axial load
[AD-A179112] N87-23701
Straight cylindrical seal for high-performance turbomachines
[NASA-TP-1850] N87-23936

D

DAMAGE
Dynamic brittle fracture analysis based on continuum damage mechanics
[DE87-006704] N87-24005
Study of quantum mechanical effects in deep submicron, grating-gate field effect transistors
[AD-A179617] N87-24204

DAMAGE ASSESSMENT
Forced vibration as a method for determining structural integrity
[DE87-005878] N87-23992
Spatial characterization of acid rain stress in Canadian Shield lakes
[NASA-CR-180982] N87-24032
Coherent multiple aperture optical imaging systems: Analysis and design
[AD-A179476] N87-24176

DAMPING
Motion-dependent fluid forces acting on a tube row in crossflow
[DE87-005574] N87-23923
Squeeze film damper technology. Part 2. Extension of analysis and parametric study
[AD-A178094] N87-23974
Squeeze film damper technology. Part 3. Experimental investigation of squeeze film dampers
[AD-A178095] N87-23975
The impact damped harmonic oscillator in free decay
[NASA-TM-89897] N87-23978
Improved modeling of structural joint damping
[AD-A179111] N87-23988
Material damping from frequency analysis of driving point measurements
[DE87-005873] N87-24003

DARK MATTER
Experimental bounds on beta beta-decay, cold dark matter and solar axions with an ultralow background Ge detector
[DE87-002065] N87-24383

DATA ACQUISITION
Correlation between flight simulation and processing of flight tests based on inertial measurements N87-23655
Engineering and instrumentation support of the AFGL (Air Force Geophysics Laboratory) Rocket Research Program
[AD-A179257] N87-23689
The Telecommunications and Data Acquisition Report
[NASA-CR-181010] N87-23828
On autonomous terrain model acquisition by a mobile robot
[DE87-005719] N87-23964
Design of the shell project Seafloor Earthquake Measurement System (SEMS)
[DE87-007946] N87-24059
Research on knowledge representation, machine learning, and knowledge acquisition
[NASA-CR-180408] N87-24103

DATA BASE MANAGEMENT SYSTEMS
TAF (Terminal Aerodrome Forecast) verification
[AD-A177931] N87-24055
The development of a prototype intelligent user interface subsystem for NASA's scientific database systems
[NASA-TM-87821] N87-24096
CADCAM-005: An introduction to the data exchange process using IGES
[DE87-008079] N87-24102
Content-addressable memory: Applications, algorithms, and simulation
[AD-A177944] N87-24120
An introduction to structured modeling, revision
[AD-A179355] N87-24153
Text editing performance as a function of screen size
[AD-A179067] N87-24229
Optimization of extended relational database systems
[AD-A179308] N87-24230
Use of a DBMS to aid in the software conversion process
[DE87-007883] N87-24234
Time slice manipulation in information hierarchy
[AD-A177949] N87-24237

DATA BASES
Energy Data Base: Subject categories and scope, a reference manual
[DE87-005547] N87-24235
Image sensor data base for the DARPA ALV (Defense Advanced Research Projects Agency Autonomous Land Vehicle) program
[AD-A178117] N87-24246
Personal computer based GOES data archive
[PB87-157517] N87-24384

DATA FLOW ANALYSIS
A program maintenance aid using static data flow analysis techniques
[AD-A179108] N87-24095

DATA LINKS
Development of an air ground data exchange concept: Flight deck perspective
[NASA-CR-4074] N87-23607
A fiber optic link for an infrared imaging camera system
[DE87-006346] N87-24181

DATA MANAGEMENT
DATA: A comprehensive data analysis environment for HP1000 computers
[DE87-007824] N87-24094
Data management for high energy physics experiments: Preliminary proposals
[DE87-006940] N87-24236
Image sensor data base for the DARPA ALV (Defense Advanced Research Projects Agency Autonomous Land Vehicle) program
[AD-A178117] N87-24246

DATA PROCESSING
A program maintenance aid using static data flow analysis techniques
[AD-A179108] N87-24095
Personal computer based GOES data archive
[PB87-157517] N87-24384

DATA TRANSMISSION
Analysis of jitter in a digital transmission system
[AD-A177945] N87-23844

DEBRIS
Ice/frost/debris assessment for space shuttle Mission STS-32 (61-C)
[NASA-TM-89192] N87-23675

DEBYE-SCHERRER METHOD
Special applications of the Debye Microdiffractometer
[RFP-3906] N87-23939

DECAY RATES
Kinetic studies following state-selective laser excitation
[DE87-007938] N87-23950
The impact damped harmonic oscillator in free decay
[NASA-TM-89897] N87-23978

DECIDUOUS TREES
Error analysis of leaf area estimates made from allometric regression models
[NASA-TM-89220] N87-24010

DECISION MAKING
A multiple attribute decision analysis of manned airlock systems
[AD-A179241] N87-23682
Mid-latitude wind probability model
[AD-A179256] N87-24048
Short Course on Cardiopulmonary Aspects of Aerospace Medicine
[AGARD-R-758] N87-24070
Confidence interval for parameter n in a binomial distribution
[AD-A178325] N87-24151
Livermore risk analysis methodology: A quantitative approach to management of the risk associated with the operation of information systems
[DE87-006828] N87-24232
Experiments on the cognitive aspects of information seeking and information retrieving
[PB87-157699] N87-24238

DECOMPOSITION
In-situ analysis of hydrazine decomposition products
[NASA-TM-89916] N87-23693
The decomposition of an arbitrary three-dimensional planar polygon into a set of convex polygons
[AD-A177947] N87-24137

DEEP SPACE NETWORK
The Telecommunications and Data Acquisition Report
[NASA-CR-181010] N87-23828
DSS 13 frequency stability tests N87-23829
DSN advanced receiver: Breadboard description and test results N87-23833
Results of using the global positioning system to maintain the time and frequency synchronization in the Deep Space Network N87-23834
Microwave component time delays for the 70-meter antennas N87-23835
Block 3 X-band receiver-exciter N87-23837
Dual-polarization 8.45 GHz traveling-wave maser N87-23838

DEFECTS
Investigation of the impact performance of various glass and ceramic systems
[AD-A178115] N87-23744
Characterization of material device structures
[AD-A178262] N87-24220

DEFENSE PROGRAM
SDI (Strategic Defense Initiative) and the US defense posture
[DE87-006731] N87-24154
Image sensor data base for the DARPA ALV (Defense Advanced Research Projects Agency Autonomous Land Vehicle) program
[AD-A178117] N87-24246

DEFLAGRATION
Modification of solid propellant deflagration rates due to random nonhomogeneities N87-23766
Influence of two-phase flow in the deflagration of homogeneous solids N87-23777
A theoretical and numerical study of radiative ignition and deradiative extinction in solid propellants N87-23778
The application of imaging laser induced fluorescence to the measurement of HMX and aluminized propellant ignition and deflagration flame structure N87-23782

DEFLECTION
The freezing of flow deflection in Prandtl-Meyer expansion to vacuum
[ISL-CO-226/86] N87-23686
A simplified computer solution for the flexibility matrix of contacting teeth for spiral bevel gears
[NASA-CR-179620] N87-23977

DEFORMATION
PRONTO 2D: A two-dimensional transient solid dynamics program
[DE87-007823] N87-23993
The interpretation of crustal dynamics data in terms of plate motions and regional deformation near plate boundaries
[NASA-CR-180938] N87-24038

DEGRADATION
Nonuniform grain boundary corrosion and the local electrode potential in crevicing
[AD-A177889] N87-23728
Spread spectrum mobile radio communications
[AD-A179446] N87-23826
Influence of ionizing radiations and electrical overstressings on MOS (Metal-Oxide Semiconductors) devices: A comparison
[AD-A178214] N87-23891
Noise characteristics of MOS (Metal-Oxide Semiconductors) devices degraded by electrical overstressings
[AD-A178217] N87-23892
Environmental degradation of 316 stainless steel in high temperature low cycle fatigue
[NASA-TM-89931] N87-24007

DEGREES OF FREEDOM
Experimental observation of the quantum behavior of a macroscopic degree of freedom
[DE87-006228] N87-24213

DELAY
Two techniques for measuring AP ignition delay N87-23772
Nonparametric estimation of the probability of a long delay in the M/G/1 queue
[AD-A178259] N87-24150

DELTA WINGS
Evaluation of Navier-Stokes and Euler solutions for leading-edge separation vortices
[NASA-TM-89458] N87-23584
Study of lee-side flows over conically cambered delta wings at supersonic speeds, part 1
[NASA-TP-2660-PT-1] N87-23597

DEMULTIPLEXING
Analysis of jitter in a digital transmission system
[AD-A177945] N87-23844

DENDRITIC CRYSTALS
A model for silicon dendrite growth during laser/plasma deposition from a silane discharge
[DE87-007579] N87-23733

DENSITY (NUMBER/VOLUME)
Multispecies CARS measurements in turbulent combustion N87-23808

DENSITY DISTRIBUTION
Three-dimensional electric field predictions of an iron-copper galvanic couple
[AD-A178040] N87-23888
Radial density distribution of negative atomic oxygen in the oxygen positive column: An experiment
[AD-A179212] N87-24186

DENSITY WAVE MODEL
Star formation and spiral structure in M81 N87-24294
Large scale dissociation of molecular gas in the spiral arms of M51 N87-24311
Structure and kinematics of the molecular spiral arms in M51 N87-24312
A simple theory of bimodal star formation N87-24317
The history of gas in spiral galaxies N87-24318

DEPLETION
Star forming regions in gas-rich SO galaxies N87-24316

DEPOSITION
Plasma deposition of tungsten
[DE87-007390] N87-23724
A model for silicon dendrite growth during laser/plasma deposition from a silane discharge
[DE87-007579] N87-23733
Superconducting electronic film structures
[AD-A179134] N87-24200
The structure of Al/GaAs interfaces
[DE87-007181] N87-24206

DEPTH
Mixed layer and thermocline depth climatologies in the western Indian Ocean
[PB87-154613] N87-24060

DESIGN ANALYSIS
Principles of data display in aviation instruments N87-23572
On minimizing the number of calculations in design-by-analysis codes
[NASA-TP-2706] N87-23586
A systems analysis of emergency escape and recovery systems for the US space station
[AD-A179233] N87-23680
Design, development and test of shuttle/Centaur G-prime cryogenic tankage thermal protection systems
[NASA-TM-89825] N87-23685
Space station WP-04 power system. Volume 1: Executive summary
[NASA-CR-179587] N87-23695
Space station WP-04 power system. Volume 2: Study results
[NASA-CR-179587] N87-23696
Microwave Antennas for Avionics
[AGARD-LS-151] N87-23859
A VLSI CMOS circuit design technique to aid test generation
[AD-A177934] N87-23887
Hardware synthesis from specification with polynomials
[TRITA-NA-8506] N87-24091

DESORPTION
Laser studies of chemical dynamics at the gas-solid interface
[DE87-005950] N87-23710

DETECTION
Corrosion sensing with acoustic wave devices
[DE87-003516] N87-23723
Automatic detection of electric power troubles (AI application)
[NASA-TM-86593] N87-23893

DETERGENTS
Assembly and functionalization of supramolecular structures studied by luminescence techniques
[AD-A178064] N87-24217

DETONATORS
Corrosion of gold bridgewire in electronic components
[DE87-000922] N87-23722

DIAGNOSIS
Short Course on Cardiopulmonary Aspects of Aerospace Medicine
[AGARD-R-758] N87-24070
Noninvasive methods for the detection of coronary artery disease in aviators: A stratified Bayesian approach N87-24072
Valvular and congenital heart disease in the aviator N87-24073
Aeromedical aspects of mitral valve prolapse N87-24074
Pulmonary physiology and pulmonary function testing in aerospace medicine N87-24075
Coronary risk factors in aerospace medicine N87-24078
Cardiopulmonary screening for high-performance flying: Selection and retention issues N87-24079

DIAMETERS
A redefined hydraulic diameter for laminar flow
[AD-A179511] N87-23914

DIAMONDS
Evaluation of Tersoff's revised silicon potential in a molecular dynamic simulation of solid silicon
[AD-A179231] N87-24202

DIAPHRAGMS (MECHANICS)
Method of making a flexible diaphragm
[NASA-CASE-MSC-20797-1] N87-23981

DIELECTRIC PROPERTIES
Dielectric properties of styrene/acrylate copolymer coatings formed by electrophoretic deposition on gold, aluminum alloy, and porous anodized aluminum alloy substrates
[DE87-008885] N87-23741
DIELECTRICS
Electronics and ionic transport in polymers
[AD-A178227] N87-23746
Single and multiple electromagnetic scattering by dielectric obstacles from a resonance perspective
[DE87-007347] N87-23843
DIESEL FUELS
Trends of petroleum fuels: Topical report
[DE87-001237] N87-23755
DIFFERENCE EQUATIONS
A generalized procedure for constructing an upwind based TVD scheme
[NASA-TM-88926] N87-24132
A unified direct-inverse procedure for two-dimensional boundary layers using spline/finite difference discretization
[AD-A178223] N87-24140
DIFFERENTIAL EQUATIONS
Strong convergence and convergence rates of approximating solutions for algebraic Riccati equations in Hilbert spaces
[NASA-CR-178302] N87-24122
Singularity structure of nonlinear ordinary and partial differential equations
[DE87-008242] N87-24134
DIFFRACTOMETERS
Special applications of the Debye Microdiffractometer
[RFP-3906] N87-23939
DIFFUSE RADIATION
High energy gamma ray astronomy N87-24258
Infrared astronomy N87-24264
Diffuse infrared emission of the galaxy: Large scale properties N87-24268
The origin of the diffuse galactic IR/submm emission: Revisited after IRAS N87-24269
Diffuse infrared emission of the galaxy: Large scale properties N87-24279
A correlation between the IRAS infrared cirrus at 60 or 100 microns and neutral atomic hydrogen in the outer galaxy N87-24281
The Arp Ring: Galactic or extragalactic? N87-24282
Infrared properties of dust grains derived from IRAS observations N87-24283
Characteristics of UGC galaxies detected by IRAS N87-24304
DIFFUSION
Finite-difference program for hydrogen diffusion: Example problems manual
[DE87-007515] N87-23712
Effective diffusion in laminar convective flows
[DE87-008054] N87-23920
Midwest free-electron laser program
[AD-A178106] N87-23953
DIFFUSION FLAMES
Novel application of topological indices. 2. Prediction of the threshold soot index for hydrocarbon fuels
[AD-A178001] N87-23716
Effects of test facility contaminants on supersonic hydrogen-air diffusion flames N87-23790
Opposed jet burner studies of silane-methane, silane-hydrogen and hydrogen diffusion flames with air N87-23791
DIFFUSION THEORY
Radiation transport in dust in disk geometry
[NASA-CR-180995] N87-24157
DIGITAL ELECTRONICS
Highly integrated digital electronic control: Digital flight control, aircraft model identification, and adaptive engine control
[NASA-TM-86793] N87-23619
DIGITAL SYSTEMS
Failure detection and isolation for an asychronous digital flight control system
[AD-A179210] N87-23628
Analysis of jitter in a digital transmission system
[AD-A177945] N87-23844
DIGITAL TECHNIQUES
DSN advanced receiver: Breadboard description and test results N87-23833
DILUTION
Modeling of dilute two-phase multispecies solid/gas flows
[DE87-009254] N87-23932
DIMENSIONS
Adaptive moving grid strategies for one-dimensional systems of partial differential equations
[DE87-006824] N87-24144
DIPOLE MOMENTS
Force-field parameters and molecular mechanics calculations for nitramines N87-23779
DIRECT CURRENT
Investigation of electromigration in thin film aluminum at low temperatures
[AD-A179110] N87-23871
Advanced DC Motor Controller
[DE87-007756] N87-23882
DISCRETE FUNCTIONS
A unified direct-inverse procedure for two-dimensional boundary layers using spline/finite difference discretization
[AD-A178223] N87-24140
DISK GALAXIES
The azimuthal and radial distributions of HI and H2 in NGC 6946 N87-24335
IRAS observations of starburst galaxies N87-24338
DISKS (SHAPES)
Recovering the orientation of textured surfaces in natural scenes
[AD-A179360] N87-24096
DISPLACEMENT MEASUREMENT
Thin film characterization using a mechanical properties microprobe
[DE87-008593] N87-24214
DISPLAY DEVICES
Principles of data display in aviation instruments N87-23572
Visual display research tool N87-23635
Advanced visuals in mission simulators N87-23636
Use of VDU's by flight simulator instructors N87-23641
Collected flight and simulation comparisons and considerations N87-23660
DISTORTION
Holographic correction of aberrations in optical systems employing synthetic apertures
[AD-A179107] N87-24173
DISTRIBUTED PROCESSING
Using expert systems to manage distributed computer systems
[AD-A179329] N87-24112
The effect of distributed computing technology on wide area network capacity requirements
[DE87-006229] N87-24117
DISTRIBUTION FUNCTIONS
Optical and IR luminosity functions of IRAS galaxies N87-24348
DIURNAL VARIATIONS
Global distribution of total cloud cover and cloud type amounts over land
[DE87-006903] N87-24053
DOMAINS
Time domain wave propagation in multilayered integrated circuits
[AD-A178180] N87-23847
DOPED CRYSTALS
Fabrication of AlGaAs/InGaAs pseudomorphic modulation doped field effect transistors with p-doped surface layers
[AD-A179230] N87-24201
DOPPLER EFFECT
Laser Doppler velocimeter application in supersonic boundary-layer flow
[AD-A178395] N87-23590
Measurement of solid-propellant burn rate using millimeter-wave techniques N87-23770
DRAG REDUCTION
Turbulent boundary layer structure, drag reduction
[AD-A179246] N87-23907
DROPS (LIQUIDS)
Combustion, vaporization, and microexplosion of droplets of organic azides N87-23806
DUCTED FLOW
A redefined hydraulic diameter for laminar flow
[AD-A179511] N87-23914
An explicit finite-volume time-marching procedure for turbulent flow calculations N87-23928
Explicit finite-volume time-marching calculations of total temperature distributions in turbulent flow N87-23929
DUST
Diffuse infrared emission of the galaxy: Large scale properties N87-24268
Star forming regions of the southern galaxy N87-24273
On the redistribution of OB star luminosity and the warming of nearby molecular clouds N87-24274
Shock heated dust in L1551: L(IR) greater than 20 solar luminosities N87-24276
A correlation between the IRAS infrared cirrus at 60 or 100 microns and neutral atomic hydrogen in the outer galaxy N87-24281
Infrared properties of dust grains derived from IRAS observations N87-24283
IRAS observations of the Pleiades N87-24284
Models for infrared emission from IRAS galaxies N87-24286
On the origin of the 40-120 micron emission of galaxy disks: A comparison with H-alpha fluxes N87-24287
IRAS observations of irregular galaxies N87-24299
Large scale dissociation of molecular gas in the spiral arms of M51 N87-24311
Modelling the IRAS colors of galaxies N87-24313
A simple two-component model for the far-infrared emission from galaxies N87-24314
DWARF GALAXIES
Neutral hydrogen and star formation in irregular galaxies N87-24302
Detection of CO (J=1-0) in the dwarf elliptical galaxy NGC 185 N87-24315
The initial mass function in HII galaxies N87-24332
The radio-far infrared correlation: Spiral and blue compact dwarf galaxies opposed N87-24351
DYNAMIC CHARACTERISTICS
Demonstration of frequency-sweep testing technique using a Bell 214-ST helicopter
[NASA-TM-89422] N87-23632
An integrated, optimization-based approach to the design and control of large space structures
[AD-A179459] N87-23683
Squeeze film damper technology. Part 3. Experimental investigation of squeeze film dampers
[AD-A178095] N87-23975
Influence of microstructure and microdamage processes on fracture at high loading rates
[AD-A179264] N87-23989
Reconstruction of dynamic structural inputs in the presence of noise
[DE87-006701] N87-24004
Adaptive grid refinement for numerical weather prediction
[AD-A179393] N87-24049
Meso gamma-scale kinetic energy budgets of a thunderstorm within a squall-line derived from sesame dual-doppler data
[AD-A178119] N87-24057
Experimental evaluation of nonlinear feedback and feedforward control schemes for manipulators
[AD-A179449] N87-24119
Evaluation of Tersoff's revised silicon potential in a molecular dynamic simulation of solid silicon
[AD-A179231] N87-24202
DYNAMIC CONTROL
Choosing sampling rates for robot control
[AD-A179447] N87-24118
DYNAMIC LOADS
Study of the influence of metallurgical factors on fatigue and fracture of aerospace structural materials
[AD-A179268] N87-23720
Influence of microstructure and microdamage processes on fracture at high loading rates
[AD-A179264] N87-23989
PRONTO 2D: A two-dimensional transient solid dynamics program
[DE87-007823] N87-23993
DYNAMIC MODELS
A comparison of ionospheric model predictions with MITHRAS obeservations
[AD-A179374] N87-24036
DYNAMIC MODULUS OF ELASTICITY
Compression and shear wave propagation in plain and filled elastomers
[AD-A178153] N87-23745
DYNAMIC PRESSURE
Acoustic waveforms in statically tested space shuttle Solid Rocket Motors (SRM) N87-23758
DYNAMIC RESPONSE
Aircraft Dynamic Response to Damaged and Repaired Runways
[AGARD-R-739] N87-23609
Interpretation in terms of the response of a one degree-of-freedom oscillator to two successive disturbances N87-23610
An experimental-analytical routine for the dynamic qualification of aircraft operating on rough runway surfaces N87-23611
Dynamic response of two composite prop-fan models on a nacelle/wing/fuselage half model
[NASA-CR-179589] N87-23615
PRONTO 2D: A two-dimensional transient solid dynamics program
[DE87-007823] N87-23993
Dynamic brittle fracture analysis based on continuum damage mechanics
[DE87-006704] N87-24005
DYNAMIC STRUCTURAL ANALYSIS
An integrated, optimization-based approach to the design and control of large space structures
[AD-A179459] N87-23683
The influence of turbulence and deck section geometry on the aeroelastic behaviour of a cable-stayed bridge model
[NAE-AN-40] N87-23990

Inelastic strain analogy for piecewise linear computation of creep residues in built-up structures
[NASA-TM-86813] N87-23995
Reconstruction of dynamic structural inputs in the presence of noise
[DE87-006701] N87-24004
Identification of structural interface characteristics using component mode synthesis
[NASA-TM-88960] N87-24006

DYNAMICAL SYSTEMS
High-current beam dynamics and transport, theory and experiment
[DE87-006154] N87-24172

E

EARTH ATMOSPHERE
Modelling of atmospheric effects on the angular distribution of a backscattering peak
[DE87-006060] N87-24014
Particle acceleration in solar flares N87-24250
Satellite observation of atmospheric nuclear gamma radiation
[AD-A177937] N87-24389

EARTH IONOSPHERE
A comparison of ionospheric model predictions with MITHRAS observations
[AD-A179374] N87-24036

EARTH ORBITS
Optimization of payload mass placement in a dual keel space station
[NASA-TM-89051] N87-23687

EARTHQUAKES
The interpretation of crustal dynamics data in terms of plate motions and regional deformation near plate boundaries
[NASA-CR-180938] N87-24038
Design of the shell project Seafloor Earthquake Measurement System (SEMS)
[DE87-007946] N87-24059

ECHOCARDIOGRAPHY
Cardiopulmonary screening for high-performance flying: Selection and retention issues N87-24079

ECONOMIC ANALYSIS
Fuels from microalgae: Technology status, potential and research requirements
[DE86-010739] N87-23753
Automated radar image analysis research in support of military needs
[AD-A179615] N87-23827
Cost reductions in the nickel/hydrogen battery
[DE87-007576] N87-23881
Characterization of solar thermal concepts for electricity generation. Volume 1: Analyses and evaluation
[DE87-007161] N87-24019
Systems model for natural gas vehicle fleets
[PB87-176083] N87-24245

ECOSYSTEMS
Spatial characterization of acid rain stress in Canadian Shield lakes
[NASA-CR-180982] N87-24032

EDGES
Edge focusing
[TRITA-NA-8518] N87-24099
Coherent multiple aperture optical imaging systems: Analysis and design
[AD-A179476] N87-24176

EDITING
Text editing performance as a function of screen size
[AD-A179067] N87-24229

EDUCATION
Short Course on Cardiopulmonary Aspects of Aerospace Medicine
[AGARD-R-758] N87-24070
The field shower wastewater recycling system: Development of a program of instruction and preliminary analysis of its potential health implications
[AD-A178112] N87-24088
Fusion Energy Postdoctoral Research Program and Professional Development Program
[DE87-006350] N87-24188

EIGENVALUES
Asymptotic analysis of the roots of a certain transcendental equation
[AD-A168315] N87-24131
Calculation of eigenvector derivatives for structures with repeated eigenvalues
[DE87-008399] N87-24135
Estimate for the errors in eigenvalue and eigenvector approximation by Galerkin methods, with particular attention to the case of multiple eigenvalues
[AD-A178390] N87-24142

EIGENVECTORS
Calculation of eigenvector derivatives for structures with repeated eigenvalues
[DE87-008399] N87-24135
Estimate for the errors in eigenvalue and eigenvector approximation by Galerkin methods, with particular attention to the case of multiple eigenvalues
[AD-A178390] N87-24142

EJECTA
Solar-geophysical data number 509, January 1987. Part 2: (Comprehensive reports). Data for July 1986
[PB87-162582] N87-24386

ELASTIC ANISOTROPY
Life prediction and constitutive models for engine hot section anisotropic materials
[NASA-CR-179594] N87-23622

ELASTIC DEFORMATION
Three-dimensional model for the linear elastic properties of a foam
[DE87-000984] N87-23732
A simplified computer solution for the flexibility matrix of contacting teeth for spiral bevel gears
[NASA-CR-179620] N87-23977
Electrical resistivity response due to elastic-plastic deformations
[DE87-006826] N87-24222

ELASTIC PROPERTIES
Three-dimensional model for the linear elastic properties of a foam
[DE87-000984] N87-23732

ELASTIC WAVES
Numerical study of acoustic refraction and flow turning N87-23759
Stochastic excitation of acoustic waves in a combustion chamber N87-23761
Theoretical influence of propellant packaging on tube erosion: model formulation and algorithm development N87-23784

ELECTRIC AUTOMOBILES
Fuel cell powered propulsion systems for highway vehicles
[DE87-007497] N87-24244

ELECTRIC BATTERIES
Aircraft battery state of charge and charge control system
[AD-A179086] N87-23870
Cost reductions in the nickel/hydrogen battery
[DE87-007576] N87-23881

ELECTRIC BRIDGES
Low energy ignition of HMX using a foil bridge
[DE87-004211] N87-23754

ELECTRIC CHARGE
Influence of ionizing radiations and electrical overstressings on MOS (Metal-Oxide Semiconductors) devices: A comparison
[AD-A178214] N87-23891

ELECTRIC CONDUCTORS
Investigation of electromigration in thin film aluminum at low temperatures
[AD-A179110] N87-23871

ELECTRIC CONTACTS
The structure and electrical properties of metal contacts on GaAs
[DE87-008217] N87-24210

ELECTRIC CONTROL
The development of the T-46 next generation trainer manned engineering simulator at the US Air Force Flight Test Center N87-23652

ELECTRIC CORONA
Effects of corona on heat transfer in an enclosure
[AD-A179209] N87-23906

ELECTRIC CURRENT
Investigations on the impact of voltage and current harmonics on end-use devices and their protection
[DE87-008018] N87-23878

ELECTRIC DISCHARGES
Impulsive EMI (Electromagnetic Interference) radiated by Electrostatic Discharges (ESD)
[AD-A178213] N87-23848

ELECTRIC EQUIPMENT
Investigations on the impact of voltage and current harmonics on end-use devices and their protection
[DE87-008018] N87-23878

ELECTRIC FIELDS
Three-dimensional electric field predictions of an iron-copper galvanic couple
[AD-A178040] N87-23888
An alternative Laplacian electrostatic field finite element formulation
[DE87-007031] N87-24158
AXCEL: Interactive simulation program to compute two-dimensional potential distributions of electrostatic arrangements and of ion paths in electrostatic fields under consideration of space charging
[DE87-007790] N87-24165
Linear magnetized plasma response to an oblique electrostatic wave
[DE87-008194] N87-24191

ELECTRIC HYBRID VEHICLES
Electric and Hybrid Vehicles Program: 10th annual report to Congress for Fiscal Year 1986
[DE87-008350] N87-23968
Fuel cell powered propulsion systems for highway vehicles
[DE87-007497] N87-24244

ELECTRIC MOTOR VEHICLES
Worldwide nickel/iron battery development for electric vehicle applications
[DE87-004822] N87-23876
Advanced DC Motor Controller
[DE87-007756] N87-23882
Electric and Hybrid Vehicles Program: 10th annual report to Congress for Fiscal Year 1986
[DE87-008350] N87-23968
Fuel cell powered propulsion systems for highway vehicles
[DE87-007497] N87-24244

ELECTRIC MOTORS
Advanced DC Motor Controller
[DE87-007756] N87-23882
Reciprocating linear motor
[NASA-CASE-GSC-12773-2] N87-23904

ELECTRIC POTENTIAL
Investigations on the impact of voltage and current harmonics on end-use devices and their protection
[DE87-008018] N87-23878
An alternative Laplacian electrostatic field finite element formulation
[DE87-007031] N87-24158

ELECTRIC PROPULSION
Optimal continuous thrust orbital evasive maneuvers from geosynchronous orbit
[AD-A179413] N87-23668

ELECTRIC RELAYS
Pulsed Nd:YAG laser closure welding of the MC3593/3594 relay
[DE87-007825] N87-23967

ELECTRICAL FAULTS
Automatic detection of electric power troubles (AI application)
[NASA-TM-86593] N87-23893

ELECTRICAL PROPERTIES
Electrical behavior of Ge and (Ge+As) implanted gallium arsenide
[AD-A179505] N87-24203
The structure and electrical properties of metal contacts on GaAs
[DE87-008217] N87-24210
Epitaxial semiconductor optical interference devices
[DE87-006890] N87-24212
Surface passivation of an implantable semiconductor multielectrode array
[AD-A178175] N87-24219

ELECTRICAL RESISTANCE
Electrical behavior of Ge and (Ge+As) implanted gallium arsenide
[AD-A179505] N87-24203

ELECTRICAL RESISTIVITY
High temperature electrically conductive adhesives
[DE87-007020] N87-23747
Surface passivation of an implantable semiconductor multielectrode array
[AD-A178175] N87-24219
Electrical resistivity response due to elastic-plastic deformations
[DE87-006826] N87-24222

ELECTRO-OPTICS
Picosecond optical electronics
[AD-A179061] N87-23668
Adjustable mount for electro-optic transducers in an evacuated cryogenic system
[NASA-CASE-LAR-13100-1] N87-23982
Novel fiber preforms: Rare earth doping
[AD-A179454] N87-24175
Cornea Optical Topographical Scan System (COTSS)
[NASA-CR-179012] N87-24184
Thermal fracture in selected nonlinear optical materials
[DE87-006213] N87-24209
Solid state research
[AD-A178394] N87-24221

ELECTROCARDIOGRAPHY
Aeromedical evaluation and disposition of electrocardiographic abnormalities N87-24071
Noninvasive methods for the detection of coronary artery disease in aviators: A stratified Bayesian approach N87-24072
Cardiopulmonary screening for high-performance flying: Selection and retention issues N87-24079

ELECTROCHEMICAL CELLS
Energy conversion processes based on molecular excited states
[DE87-007408] N87-24020
ELECTROCHEMICAL CORROSION
Galvanic corrosion of Al-7075-T6 and Steel-4340 coupled to brass QQ-B-626, 360 and Al-7075-T6 coupled to Steel-4130 and Steel-4340: Exposure to aqueous NaCl and salt-fog environments
[AD-A179121] N87-23719
ELECTROCHEMISTRY
Electrochemical performance and transport properties of a Nafion membrane in a hydrogen-bromine cell environment
[NASA-TM-89662] N87-23718
Poly (pyrrolium anion) studies: Electrochemical synthesis and physical behavior
[AD-A178097] N87-23743
ELECTRODEPOSITION
Dielectric properties of styrene/acrylate copolymer coatings formed by electrophoretic deposition on gold, aluminum alloy, and porous anodized aluminum alloy substrates
[DE87-006885] N87-23741
ELECTRODES
Nonuniform grain boundary corrosion and the local electrode potential in crevicing
[AD-A177889] N87-23728
Surface passivation of an implantable semiconductor multielectrode array
[AD-A178175] N87-24219
ELECTROLYTES
Theoretical and experimental investigations of fluctuation thermodynamic properties of liquid solutions
[DE87-005681] N87-24224
ELECTROMAGNETIC COMPATIBILITY
Aircraft electromagnetic compatibility
[NASA-CR-181051] N87-23856
ELECTROMAGNETIC FIELDS
Computer simulation of the lasertron with a ring model
[DE87-007461] N87-23897
Architectural implications of a parallel computational approach to the vector wave equation
[AD-A179510] N87-24113
ELECTROMAGNETIC INTERACTIONS
Magnetostatic surface field measurement facility
[AD-A178258] N87-23850
ELECTROMAGNETIC INTERFERENCE
Microwave coupling inside complex systems
[DE87-003505] N87-23841
Impulsive EMI (Electromagnetic Interference) radiated by Electrostatic Discharges (ESD)
[AD-A178213] N87-23848
Aircraft electromagnetic compatibility
[NASA-CR-181051] N87-23856
ELECTROMAGNETIC NOISE
Generation of broadband noise in the magnetotail
[AD-A179136] N87-24034
ELECTROMAGNETIC RADIATION
Impulsive EMI (Electromagnetic Interference) radiated by Electrostatic Discharges (ESD)
[AD-A178213] N87-23848
Magnetostatic surface field measurement facility
[AD-A178258] N87-23850
Evaluation of a thin-slot formalism for finite-difference time-domain electromagnetics codes
[DE87-008078] N87-23857
ELECTROMAGNETIC SCATTERING
Single and multiple electromagnetic scattering by dielectric obstacles from a resonance perspective
[DE87-007347] N87-23843
ELECTROMAGNETIC WAVE TRANSMISSION
Atmospheric propagation effects on radio interferometry
[AD-A178405] N87-23855
Formation and stability of partially-neutralized plasma clumps
[AD-A179444] N87-24187
ELECTROMAGNETISM
Evaluation of a thin-slot formalism for finite-difference time-domain electromagnetics codes
[DE87-008078] N87-23857
ELECTROMIGRATION
Investigation of electromigration in thin film aluminum at low temperatures
[AD-A179110] N87-23871
ELECTRON ACCELERATION
Computer simulation of the lasertron with a ring model
[DE87-007461] N87-23897
ELECTRON ATTACHMENT
Laser-enhanced electron attachment and its possible application for optical switching
[DE87-008787] N87-23957
ELECTRON BEAMS
On-line electron beam measurements for the Los Alamos Free-Electron Laser
[DE87-007452] N87-23956
High-current beam dynamics and transport, theory and experiment
[DE87-006154] N87-24172
Formation and stability of partially-neutralized plasma clumps
[AD-A179444] N87-24187
Collective acceleration of protons by the plasma waves in a counterstreaming electron beam
[DE87-007493] N87-24196
ELECTRON BOMBARDMENT
Apparatus ad method for quiescent containerless processing of high temperature metals and alloys in low gravity
[NASA-CASE-MFS-28087-1] N87-23944
ELECTRON DENSITY PROFILES
A model for the low-latitude ionosphere with coefficients for different seasonal and solar cycle conditions
[AD-A178207] N87-24044
ELECTRON ENERGY
Studies of infrared aurorae
[AD-A179539] N87-24037
Wavelengths of K X-rays of iron ions
[IPPJ-AM-49] N87-24198
ELECTRON FLUX DENSITY
Particle propagation channels in the solar wind
N87-24252
ELECTRON GUNS
High-current electron gun for space flight
[AD-A179287] N87-23874
High current electron gun for space flight
[AD-A178467] N87-23875
A pulsed electron injector using a metal photocathode irradiated by an excimer laser
[DE87-007499] N87-23877
ELECTRON IMPACT
Studies of infrared aurorae
[AD-A179539] N87-24037
ELECTRON MICROSCOPY
In situ HREM observation of interphase boundary motion in 95Pb-5Sn solder
[DE87-007616] N87-23817
ELECTRON MOBILITY
Ordered many-electron motions in atoms and X-ray lasers
[DE87-004731] N87-23951
ELECTRON PLASMA
Microwave production from a plasma driven by a high power relativistic electron beam
[DE87-003518] N87-24194
ELECTRON SCATTERING
Satellite observation of atmospheric nuclear gamma radiation
[AD-A177937] N87-24389
ELECTRON TRANSITIONS
Wavelengths of K X-rays of iron ions
[IPPJ-AM-49] N87-24198
ELECTRONIC EQUIPMENT
Research in VLSI systems
[AD-A179227] N87-23872
Removable encapsulants for electronic devices
[DE87-005869] N87-23894
Superconducting electronic film structures
[AD-A179134] N87-24200
ELECTRONIC EQUIPMENT TESTS
Aircraft electromagnetic compatibility
[NASA-CR-181051] N87-23856
A VLSI CMOS circuit design technique to aid test generation
[AD-A177934] N87-23887
ELECTROPHORESIS
Dielectric properties of styrene/acrylate copolymer coatings formed by electrophoretic deposition on gold, aluminum alloy, and porous anodized aluminum alloy substrates
[DE87-006885] N87-23741
ELECTROPHYSICS
JSEP (Joint Services Electronics Program)
[AD-A177881] N87-23885
ELECTROSTATIC CHARGE
Impulsive EMI (Electromagnetic Interference) radiated by Electrostatic Discharges (ESD)
[AD-A178213] N87-23848
ELECTROSTATIC WAVES
Generation of broadband noise in the magnetotail
[AD-A179136] N87-24034
Linear magnetized plasma response to an oblique electrostatic wave
[DE87-008194] N87-24191
ELECTROSTATICS
ESD (Electrostatic Discharge)/EOS (Electrical OverStress) susceptibility of a class of bipolar RF power transistors: Experimental studies on stripline-opposed emitter transistors
[AD-A178212] N87-23890
An alternative Laplacian electrostatic field finite element formulation
[DE87-007031] N87-24158
AXCEL: Interactive simulation program to compute two-dimensional potential distributions of electrostatic arrangements and of ion paths in electrostatic fields under consideration of space charging
[DE87-007760] N87-24165
ELEMENTARY PARTICLES
Theoretical studies in elementary particle physics
[DE87-005895] N87-24167
Symmetry problems in particle physics
[DE87-006369] N87-24168
Particle physics and cosmology
[DE87-007306] N87-24388
ELLIPTIC DIFFERENTIAL EQUATIONS
Uniqueness of non-negative solutions of a class of semi-linear elliptic equations
[DE87-006966] N87-24128
ELLIPTICAL GALAXIES
Detection of CO (J=1-0) in the dwarf elliptical galaxy NGC 185 N87-24315
EMBEDDING
Complexities of layouts in three-dimensional VLSI (Very Large-Scale Integration) circuits
[AD-A178150] N87-23889
EMERGENCIES
A systems analysis of emergency escape and recovery systems for the US space station
[AD-A179233] N87-23880
EMISSION SPECTRA
Studies of infrared aurorae
[AD-A179539] N87-24037
Diffuse infrared emission of the galaxy: Large scale properties N87-24268
Models for infrared emission from IRAS galaxies N87-24286
Carbon monoxide emission from small galaxies N87-24303
Global properties of the nearby spiral M101 N87-24309
Efficient star formation in the bright bar of M83 N87-24310
Interferometric CO observations of the ultraluminous IRAS galaxies ARP 220, IC 694/NGC 3690, NGC 6420 and NGC 7469 N87-24331
The initial mass function in HII galaxies N87-24332
VLA continuum observations of barred spiral galaxies N87-24333
Spectral classification of emission-line galaxies N87-24374
EMPHYSEMA
Aeromedical disposition of pulmonary sarcoidosis, chronic obstructive lung disease, reactive airway disease and spontaneous pneumothorax N87-24078
EMULSIONS
Assembly and functionalization of supramolecular structures studied by luminescence techniques
[AD-A178064] N87-24217
ENCAPSULATING
Removable encapsulants for electronic devices
[DE87-005869] N87-23894
ENERGETIC PARTICLES
EIRMA: An Energetic Ion Retarding Mass Analyzer for the BERT-1 (Beam Emission Rocket Test one)
[AD-A178231] N87-23894
Magnetospheres of the outer planets N87-24248
Particle acceleration in solar flares N87-24250
Cosmic rays in the heliosphere N87-24254
Origin and propagation of galactic cosmic rays N87-24257
ENERGY ABSORPTION
Energy-absorption capability and scalability of square cross section composite tube specimens
[NASA-TM-89067] N87-23991
ENERGY CONSERVATION
Flow regimes of refrigerant mixtures condensing inside tubes
[ORNL/SUB/81-7762/4 AND 01] N87-23917
REZONE: A method for automatic rezoning in two-dimensional Lagrangian hydrodynamics problems
[DE87-006324] N87-23930
ENERGY CONVERSION
Energy conversion processes based on molecular excited states
[DE87-007408] N87-24020
ENERGY CONVERSION EFFICIENCY
Development and analysis of silicon solar cells near 20% efficiency in the Flat Plate Solar Array Project
[NASA-CR-181005] N87-24018

Characterization of solar thermal concepts for electricity generation. Volume 1: Analyses and evaluation
[DE87-007161] N87-24019
Solar cell concentrator system
[AD-A177981] N87-24025

ENERGY DISTRIBUTION
Cosmic rays in the heliosphere N87-24254
IRAS and ground-based observations of star formation regions in the Magellanic clouds N87-24296
Infrared emission and excitation in LMC HII regions N87-24298

ENERGY LEVELS
Drift mobilities by time-of-flight methods and time-dependent photoltransport in the nanosecond regime in amorphous semiconductors
[DE87-006021] N87-24208

ENERGY SPECTRA
IRAS observations of BL Lac objects N87-24373

ENERGY STORAGE
Application of thermal and flywheel energy storage in orbiting nuclear burst power systems
[DE87-007882] N87-24021
Application of advanced flywheel technology for energy storage on space station
[DE87-007657] N87-24028

ENERGY TECHNOLOGY
USSR report: Engineering and equipment
[JPRS-UEQ-87-005] N87-23570
Solar Thermal Technology Program bibliography, 1973-1985
[DE86-010728] N87-24027
Fusion Energy Postdoctoral Research Program and Professional Development Program
[DE87-006350] N87-24188
Energy Data Base: Subject categories and scope, a reference manual
[DE87-005547] N87-24235

ENERGY TRANSFER
Numerical study of acoustic refraction and flow turning N87-23759
REZONE: A method for automatic rezoning in two-dimensional Lagrangian hydrodynamics problems
[DE87-006324] N87-23930
Experimental and theoretical studies of laser cooling and emittance control of neutral beams
[AD-A179226] N87-23946
Kinetic studies following state-selective laser excitation
[DE87-007938] N87-23950
Magnetospheres of the outer planets N87-24248

ENGINE CONTROL
Highly integrated digital electronic control: Digital flight control, aircraft model identification, and adaptive engine control
[NASA-TM-86793] N87-23619

ENGINE DESIGN
TTCP non-linear instability program: US motor test data N87-23763
Analysis of a mechanically simple external combustion engine with an unusual cycle
[DE87-007788] N87-23965

ENGINE MONITORING INSTRUMENTS
Development of model describing unstable operation of turbocompressor and design of antisurging protection for gas turbine engine N87-23577

ENGINE PARTS
Ceramic technology for advanced heat engines project
[DE87-006538] N87-23740

ENGINE TESTS
TTCP non-linear instability program: US motor test data N87-23763
Measurements for rocket engine performance code verification N87-23811
Synchronization trigger control system for flow visualization
[NASA-TM-89902] N87-23902
A comparison of unburned fuel and aldehyde emissions from a methanol-fueled stratified charge and homogeneous charge engine
[DE87-007793] N87-23966

ENGINEERING
USSR report: Engineering and equipment
[JPRS-UEQ-87-005] N87-23570

ENGINEERING MANAGEMENT
Preliminary performance characterizations of an engineering model multipropellant resistojet for space station application
[NASA-TM-100113] N87-23821

ENTROPY
Linear coupling of acoustics and entropy and acoustic stability in ramjet combustion chambers containing a plane flame N87-23795
Analysis of pressure oscillations in ramjets. Review of research: 1985-1986 N87-23796

ENVIRONMENT EFFECTS
Scattering by a truncated periodic array
[AD-A178285] N87-23852
The reality of the greenhouse effect
[DE87-002383] N87-24041

ENVIRONMENTAL CHEMISTRY
Environmental degradation of 316 stainless steel in high temperature low cycle fatigue
[NASA-TM-89931] N87-24007

ENVIRONMENTAL MONITORING
Storage and preservation of environmental samples
[DE87-004271] N87-24030

EPIDEMIOLOGY
Noninvasive methods for the detection of coronary artery disease in aviators: A stratified Bayesian approach N87-24072

EPITAXY
New low temperature (hydroxylated) materials
[DE87-008530] N87-23749
Floating emitter solar cell
[NASA-CASE-NPO-16467-1-CU] N87-23879
Superconducting electronic film structures
[AD-A179134] N87-24200

EQUATIONS OF MOTION
PRONTO 2D: A two-dimensional transient solid dynamics program
[DE87-007823] N87-23993

EQUATORIAL REGIONS
A model for the low-latitude ionosphere with coefficients for different seasonal and solar cycle conditions
[AD-A178207] N87-24044

EQUIPMENT SPECIFICATIONS
Use of a 2.3-GHz traveling-wave maser on the Usuda 64-meter antenna N87-23831
Double-diffraction X-ray imaging camera
[DE87-007936] N87-23940
LASA (Lidar Atmospheric Sounder and Altimeter) Earth observing system. Volume 2D: Instrument panel report
[NASA-TM-89356] N87-23962
X-ray astronomical spectroscopy N87-24263

ERROR ANALYSIS
Error analysis of leaf area estimates made from allometric regression models
[NASA-TM-89220] N87-24010
Adaptive grid refinement for numerical weather prediction
[AD-A179393] N87-24049
On integrating a logarithmic or semilogarithmic piecewise linear PSD plot of a random variable X(T): Part 1 N87-24126

ESCAPE SYSTEMS
A systems analysis of emergency escape and recovery systems for the US space station
[AD-A179233] N87-23680

ESTIMATES
A study of the maximum entropy method of power spectrum estimation as applied to interferometer data
[AD-A179403] N87-23707
Estimation of parameters in latent class models with constraints on the parameters
[AD-A178196] N87-24138
Nonparametric estimation of the probability of a long delay in the M/G/1 queue
[AD-A178259] N87-24150

ETCHING
Surface passivation of an implantable semiconductor multielectrode array
[AD-A178175] N87-24219

ETHYLENE COMPOUNDS
Cellular monotectic model solidification
[NASA-CR-181027] N87-23717

ETIOLOGY
Coronary risk factors in aerospace medicine N87-24078
Training, muscle fatigue, and stress fractures
[AD-A178350] N87-24085

EULER EQUATIONS OF MOTION
Evaluation of Navier-Stokes and Euler solutions for leading-edge separation vortices
[NASA-TM-89458] N87-23584

EUROPEAN SPACE PROGRAMS
Hypersonic aerodynamic coefficients and convection flow estimation in a HERMES type project
[NASA-TT-20019] N87-23583

EUTECTICS
Review of interactions of large solar fluxes with materials
[DE87-001156] N87-24024

EXCIMER LASERS
A pulsed electron injector using a metal photocathode irradiated by an excimer laser
[DE87-007499] N87-23877

EXCITATION
Kinetic studies following state-selective laser excitation
[DE87-007938] N87-23950
Time-resolved picosecond reflectivity study of laser-excited layered compounds
[DE87-005115] N87-23952
Studies of infrared aurorae
[AD-A179539] N87-24037
Satellite observation of atmospheric nuclear gamma radiation
[AD-A177937] N87-24389

EXHAUST DIFFUSERS
Response of transonic diffuser flows to abrupt increases of back pressure: Wall pressure measurements N87-23793
Downstream boundary effects on the frequency of self-excited oscillations in transonic diffuser flows N87-23794

EXHAUST EMISSION
A comparison of unburned fuel and aldehyde emissions from a methanol-fueled stratified charge and homogeneous charge engine
[DE87-007793] N87-23966

EXHAUST GASES
Cost effective use of liquid nitrogen in cryogenic wind tunnels
[NASA-CR-178279] N87-23663
A comparison of unburned fuel and aldehyde emissions from a methanol-fueled stratified charge and homogeneous charge engine
[DE87-007793] N87-23966

EXHAUST NOZZLES
Numerical simulations of cold flow in a ramjet dump combustor with a choked exit nozzle N87-23802

EXOBIOLOGY
The 1986-87 NASA space/gravitational biology accomplishments
[NASA-TM-89951] N87-24063

EXOTHERMIC REACTIONS
Influence of two-phase flow in the deflagration of homogeneous solids N87-23777

EXPERIMENTATION
Mach 6 experimental and theoretical stability and performance of a cruciform missile at angles of attack up to 65 degrees
[NASA-TP-2733] N87-23592

EXPERT SYSTEMS
Automatic detection of electric power troubles (AI application)
[NASA-TM-86593] N87-23893
Tactical weather expert system
[AD-A178605] N87-24050
The development of a prototype intelligent user interface subsystem for NASA's scientific database systems
[NASA-TM-87821] N87-24098
Using expert systems to manage distributed computer systems
[AD-A179329] N87-24112
Decaying confidence functions for aging knowledge in expert systems
[AD-A179328] N87-24152

EXPLODING WIRES
Corrosion of gold bridgewire in electronic components
[DE87-000922] N87-23722

EXPLOSIONS
Combustion, vaporization, and microexplosion of droplets of organic azides N87-23806

EXPLOSIVES
Effect of particle size on the shock sensitivity of pure porous HE (High Explosive)
[AD-A178206] N87-23814

EXTERNAL COMBUSTION ENGINES
Analysis of a mechanically simple external combustion engine with an unusual cycle
[DE87-007788] N87-23965

EXTERNAL STORES
Utilization of simulation to support F-14A low altitude high angle of attack flight testing N87-23649

EXTINCTION
Horizontal variation of atmospheric extinction/backscatter coefficients
[AD-A178298] N87-23954

EXTRAGALACTIC RADIO SOURCES
Discrete X-ray sources and the X-ray background N87-24261
The luminosity function of the brightest galaxies in the IRAS survey N87-24341
Extragalactic OH megamasers in strong IRAS sources N87-24353

EXTRATERRESTRIAL MATTER
Neutron stars as cosmic neutron matter laboratories
[DE87-007468] N87-24379
Experimental bounds on beta beta-decay, cold dark matter and solar axions with an ultralow background Ge detector
[DE87-002065] N87-24383

EXTRAVEHICULAR ACTIVITY
A multiple attribute decision analysis of manned airlock systems
[AD-A179241] N87-23682
Human factors in space station architecture 2. EVA access facility: A comparative analysis of 4 concepts for on-orbit space suit servicing
[NASA-TM-86856] N87-24064
EXTREMELY HIGH FREQUENCIES
Basic parameters of antennas for aircraft, satellites and missiles N87-23860
EXTREMELY LOW FREQUENCIES
An ELF (Extremely-Low-Frequency) transmitter experiment for the space shuttle. (The NASC-201 (Naval Air Space Command) experiment). Volume 1
[AD-A178237] N87-23849
EYE MOVEMENTS
Multipurpose visual display and eye movement recording system
[AD-A179620] N87-24068

F

F-14 AIRCRAFT
Utilization of simulation to support F-14A low altitude high angle of attack flight testing N87-23649
F-15 AIRCRAFT
Highly integrated digital electronic control: Digital flight control, aircraft model identification, and adaptive engine control
[NASA-TM-86793] N87-23619
F-16 AIRCRAFT
Evaluation of the angle of attack limiter of the F-16 C/D aircraft
[AD-A177941] N87-23612
FABRICATION
Aeroelasticity and mechanical stability report, 0.27 Mach scale model of the YAH-64 advanced attack helicopter
[NASA-CR-178284] N87-23596
Spin-cast carbon films from polyacrylonitrile
[DE87-002489] N87-23703
Plasma deposition of tungsten
[DE87-007390] N87-23724
Fabrication of polymers for use under extreme conditions
[AD-A179458] N87-23730
Development and analysis of silicon solar cells near 20% efficiency in the Flat Plate Solar Array Project
[NASA-CR-181005] N87-24018
Computer-aided fabrication system implementation
[AD-A178225] N87-24106
Fabrication of AlGaAs/InGaAs pseudomorphic modulation doped field effect transistors with p-doped surface layers
[AD-A179230] N87-24201
Epitaxial semiconductor optical interference devices
[DE87-006890] N87-24212
FABRICS
Mechanical properties of undirectional and fabric graphite/epoxy composites
[SAND-86-0784] N87-23702
FABRY-PEROT INTERFEROMETERS
Fabry-Perot type optical interference filters
[AD-A179394] N87-24174
FACTORIZATION
Gaussian elimination with partial pivoting and load balancing on a multiprocessor
[DE87-007784] N87-24093
LU factorization algorithms on distributed-memory multiprocessor architectures
[DE87-007794] N87-24100
FACULAE
Solar-geophysical data number 509, January 1987. Part 1: (Prompt reports). Data for December 1986, November 1986
[PB87-162574] N87-24385
FAIL-SAFE SYSTEMS
Failure detection and isolation for an asychronous digital flight control system
[AD-A179210] N87-23628
FAILURE
Influence of microstructure and microdamage processes on fracture at high loading rates
[AD-A179264] N87-23989
FAILURE ANALYSIS
A dual-processor multi-frequency implementation of the FINDS algorithm
[NASA-CR-178252] N87-23617
Failure detection and isolation for an asychronous digital flight control system
[AD-A179210] N87-23628
Ceramic fibre/glass matrix composites with outstanding mechanical performance
[AERE-R-12025] N87-23699
Adhesive evaluation of water-soluble LARC-TPI
[NASA-TM-89152] N87-23752
ESD (Electrostatic Discharge)/EOS (Electrical OverStress) susceptibility of a class of bipolar RF power transistors: Experimental studies on stripline-opposed emitter transistors
[AD-A178212] N87-23890
FAINT OBJECTS
A very deep IRAS survey at l(II) = 97 deg, b(II) = +30 deg N87-24344
Properties of the unusual galaxy PSC 09104+4109 N87-24346
IRAS observations of AGN candidates at low flux levels N87-24366
FAR FIELDS
Scattering by a truncated periodic array
[AD-A178285] N87-23852
Far field boundary conditions for time-dependent hyperbolic systems
[AD-A179361] N87-24123
FAR INFRARED RADIATION
Survey of the galactic disk from l = -150 deg to l = 82 deg in the submillimeter range N87-24278
Far-infrared properties of cluster galaxies N87-24305
Extremely Luminous Far-infrared Sources (ELFS) N87-24323
Starburst-driven superwinds from infrared galaxies N87-24330
Far-infrared activity and starburst galaxies N87-24337
IRAS observations of starburst galaxies N87-24338
The luminosity function of the brightest galaxies in the IRAS survey N87-24341
VLA observations of a sample of galaxies with high far-infrared luminosities N87-24342
A very deep IRAS survey at l(II) = 97 deg, b(II) = +30 deg N87-24344
A redshift survey of IRAS galaxies N87-24347
The correlation between far-IR and radio continuum emission from spiral galaxies N87-24349
Radio and infrared observations of (almost) one hundred non-Seyfert Markarian galaxies N87-24350
The radio-far infrared correlation: Spiral and blue compact dwarf galaxies opposed N87-24351
Radio continuum, far infrared and star formation N87-24352
Extragalactic OH megamasers in strong IRAS sources N87-24353
Far-infrared properties of optically-selected quasars and Seyfert galaxies N87-24371
FATIGUE (MATERIALS)
Study of the influence of metallurgical factors on fatigue and fracture of aerospace structural materials
[AD-A179268] N87-23720
Retardation effect in fatigue crack growth under stationary stochastic loading
[REPT-43/1986] N87-23999
Environmental degradation of 316 stainless steel in high temperature low cycle fatigue
[NASA-TM-89931] N87-24007
FAULT TOLERANCE
A dual-processor multi-frequency implementation of the FINDS algorithm
[NASA-CR-178252] N87-23617
FEASIBILITY ANALYSIS
Tactical weather expert system
[AD-A178605] N87-24050
Fuel cell powered propulsion systems for highway vehicles
[DE87-007497] N87-24244
FEDERAL BUDGETS
National Aeronautics and Space Administration Authorization Act
[S-REPT-100-87] N87-24240
Department of Housing and Urban Development - Independent Agencies Appropriations Bill, 1988
[H-REPT-100-189] N87-24241
National Aeronautics and Space Administration --- appropriations bill H.R. 2783 N87-24242
National Aeronautics and Space Administration Authorization Act, 1988
[S-REPT-100-87] N87-24243
FEEDBACK
A multi user random access communication system for users with different priorities
[AD-A178372] N87-23854
FEEDBACK CONTROL
Flight test evaluation of techniques to predict longitudinal pilot induced oscillations
[AD-A179229] N87-23629
Airborne simulation at the National Aeronautical Establishment of Canada N87-23659
Collected flight and simulation comparisons and considerations N87-23660
Detumbling of two inter-connected rigid bodies using Liapunov methods for feedback control
[AD-A179207] N87-23679
Experimental evaluation of nonlinear feedback and feedforward control schemes for manipulators
[AD-A179449] N87-24119
FIBER COMPOSITES
Ceramic fibre/glass matrix composites with outstanding mechanical performance
[AERE-R-12025] N87-23699
FIBER OPTICS
Optically controlled microwave devices and circuits: Emerging applications in space communications systems
[NASA-TM-89869] N87-23900
Novel fiber preforms: Rare earth doping
[AD-A179454] N87-24175
The fiber optic refrigeration cycle monitor
[DE87-006632] N87-24180
A fiber optic link for an infrared imaging camera system
[DE87-006346] N87-24181
Parametric frequency upconversion, optical fiber transmission and streak camera recording
[DE87-005841] N87-24183
FIBER REINFORCED COMPOSITES
Ceramic fibre/glass matrix composites with outstanding mechanical performance
[AERE-R-12025] N87-23699
Mechanical properties of undirectional and fabric graphite/epoxy composites
[SAND-86-0784] N87-23702
Recent advances in the nonlinear analysis of laminated composite plates and shells N87-23819
FIELD EFFECT TRANSISTORS
Influence of ionizing radiations and electrical overstressings on MOS (Metal-Oxide Semiconductors) devices: A comparison
[AD-A178214] N87-23891
Fabrication of AlGaAs/InGaAs pseudomorphic modulation doped field effect transistors with p-doped surface layers
[AD-A179230] N87-24201
Study of quantum mechanical effects in deep submicron, grating-gate field effect transistors
[AD-A179617] N87-24204
Solid state research
[AD-A178394] N87-24221
FIELD OF VIEW
Advanced visuals in mission simulators N87-23636
FIELD STRENGTH
Three-dimensional electric field predictions of an iron-copper galvanic couple
[AD-A178040] N87-23668
FIELD THEORY (PHYSICS)
Force-field parameters and molecular mechanics calculations for nitramines N87-23779
Research in theoretical particle physics
[DE87-008240] N87-24189
FIGHTER AIRCRAFT
Manned air to air combat simulation N87-23648
The use of Aeritalia flight simulator for the development of the AM-X weapon system N87-23650
Activities report of the German-Dutch wind tunnel
[B8677593] N87-23665
Activities report of the German-Dutch wind tunnel
[B8677594] N87-23666
FILM COOLING
Computation of full-coverage film-cooled airfoil temperatures by two methods and comparison with high heat flux data
[NASA-TM-88931] N87-23934
FILTRATION
Improved beta" -alumina oxide electrolytes through transformation toughening
[DE87-007897] N87-23735
FINE STRUCTURE
Semiempirical studies of atomic structure
[DE87-007320] N87-24164
FINITE DIFFERENCE THEORY
Turbomachine blade vibration N87-23621
Finite-difference program for hydrogen diffusion: Example problems manual
[DE87-007515] N87-23712
Numerical simulation of combustion processes of mobile stick-propellant bundles N87-23785
Finite difference simulations of Rayleigh wave scattering by 2-D rough topography
[AD-A179190] N87-23824
Evaluation of a thin-slot formalism for finite-difference time-domain electromagnetics codes
[DE87-008078] N87-23857
Numerical prediction of 1-D ablation using a finite control volume procedure with exponential differencing
[DE87-007947] N87-24130

A unified direct-inverse procedure for two-dimensional boundary layers using spline/finite difference discretization
[AD-A178223] N87-24140
FINITE ELEMENT METHOD
Turbomachine blade vibration N87-23621
Collapse analysis of cylindrical composite panels with large cutouts under an axial load
[AD-A179112] N87-23701
Recent advances in the nonlinear analysis of laminated composite plates and shells N87-23819
Finite element analysis of slow-wave Schottky contact printed lines
[AD-A179259] N87-23873
Three-dimensional electric field predictions of an iron-copper galvanic couple
[AD-A178040] N87-23888
Preliminary thermal analysis of transistor packages
[DE87-007706] N87-23898
A consistent finite element formulation of nonlinear frictional contact problems
[AD-A179179] N87-23963
A simplified computer solution for the flexibility matrix of contacting teeth for spiral bevel gears
[NASA-CR-179620] N87-23977
Thermomechanical effects in high-speed seal rubs
[NASA-CR-180418] N87-23979
Influence of microstructure and microdamage processes on fracture at high loading rates
[AD-A179264] N87-23989
PRONTO 2D: A two-dimensional transient solid dynamics program
[DE87-007823] N87-23993
The Shock and Vibration Digest, Volume 19, No. 3 N87-23996
Random vibration of nonlinear systems N87-23997
Recent studies in plate vibrations: 1981-1985. Part 2: Complicating effects N87-23998
Architectural implications of a parallel computational approach to the vector wave equation
[AD-A179510] N87-24113
An alternative Laplacian electrostatic field finite element formulation
[DE87-007031] N87-24158
FINITE VOLUME METHOD
Thermodynamic evaluation of transonic compressor rotors using the finite volume approach
[NASA-CR-180587] N87-23925
Development of an explicit time marching procedure for laminar and turbulent flow N87-23926
Development of a finite volume time marching method
[JIM/85-3] N87-23927
An explicit finite-volume time-marching procedure for turbulent flow calculations N87-23928
Explicit finite-volume time-marching calculations of total temperature distributions in turbulent flow N87-23929
FIRE PREVENTION
Medical research programs, past and future, for designing atmospheres to retard fires
[AD-A178354] N87-24089
FLAME PROPAGATION
Behavior of simulated solid propellant flames in axial acoustic fields N87-23760
Asymptotic models for solid propellant combustion and the onset of intrinsic instability N87-23764
Role of combustion in the nonlinear combustion instability of composite solid propellants N87-23765
New ignition parameter correlations for predicting solid rocket motor ignition transients N87-23767
CN radical distributions in solid propellant flames N87-23775
The application of imaging laser induced fluorescence to the measurement of HMX and aluminized propellant ignition and deflagration flame structure N87-23782
Thermal decomposition and ignition of a series of new nitramine lova propellants by CO2 laser N87-23783
Theoretical influence of propellant packaging on tube erosion: model formulation and algorithm development N87-23784
A hybrid closed bomb-strand burner for very high pressure burning rate measurements N87-23786
Thermal ignition of pyrotechnics with lasers
[DE87-006245] N87-23955
FLAME RETARDANTS
Antimisting Fuel (AMK) flight degrader development and aircraft fuel system investigation
[DOT/FAA/CT-86/6] N87-23816
Medical research programs, past and future, for designing atmospheres to retard fires
[AD-A178354] N87-24089
FLAME STABILITY
Effects of test facility contaminants on supersonic hydrogen-air diffusion flames N87-23790
FLAME TEMPERATURE
Nonintrusive temperature measurements in SSME preburner element flowfields N87-23813
FLAMEOUT
A theoretical and numerical study of radiative ignition and deradiative extinction in solid propellants N87-23778
FLAPS (CONTROL SURFACES)
Experimental and numerical investigation of coherent structures
[AD-A179456] N87-23910
FLASH BLINDNESS
Potential electron beam induced flashblindness in pilots
[AD-A178002] N87-24084
FLAT PLATES
Tones generated due to the impingement of two jets on each other N87-23797
Spacecraft mass trade-offs versus radio-frequency power and antenna size at 8 GHz and 32 GHz N87-23830
FLAVOR (PARTICLE PHYSICS)
The physics and a plan for a 45 GeV facility that extends the high-intensity capability in nuclear and particle physics
[LA-10720-MS] N87-24170
FLEXIBILITY
The effect of reinforcement on the tear properties of flexible circuits
[DE87-007022] N87-23895
A simplified computer solution for the flexibility matrix of contacting teeth for spiral bevel gears
[NASA-CR-179620] N87-23977
Method of making a flexible diaphragm
[NASA-CASE-MSC-20797-1] N87-23981
On the reliable and flexible solution of practical subset regression problems
[NASA-TM-89442] N87-24156
FLEXIBLE BODIES
Effectiveness of balancing flexible rotary compressor vanes on low-speed balancing machine N87-23580
An integrated, optimization-based approach to the design and control of large space structures
[AD-A179459] N87-23683
Modified independent modal space control method for active control of flexible systems
[NASA-CR-181065] N87-23960
FLIGHT CHARACTERISTICS
Flight Simulation
[AGARD-CP-408] N87-23633
Simulation of aircraft behaviour on and close to the ground: Summary of AGARD-lc6)ograph AG-285 N87-23640
Unusual airborne simulator applications N87-23656
DFVLR in-flight simulators ATTAS and ATTHES for flying qualities and flight control research N87-23657
Airborne simulation at the National Aeronautical Establishment of Canada N87-23659
FLIGHT CONTROL
Evaluation of the angle of attack limiter of the F-16 C/D aircraft
[AD-A177941] N87-23612
A dual-processor multi-frequency implementation of the FINDS algorithm
[NASA-CR-178252] N87-23617
Highly integrated digital electronic control: Digital flight control, aircraft model identification, and adaptive engine control
[NASA-TM-86793] N87-23619
Failure detection and isolation for an asychronous digital flight control system
[AD-A179210] N87-23628
Flight test evaluation of techniques to predict longitudinal pilot induced oscillations
[AD-A179229] N87-23629
Trends in ground-based and in-flight simulators for development applications N87-23645
The use of Aeritalia flight simulator for the development of the AM-X weapon system N87-23650
The development of the T-46 next generation trainer manned engineering simulator at the US Air Force Flight Test Center N87-23652
Unusual airborne simulator applications N87-23656
DFVLR in-flight simulators ATTAS and ATTHES for flying qualities and flight control research N87-23657
FLIGHT CREWS
Investigation of biochemical variation in operational aircrew
[AD-A179223] N87-24067
FLIGHT INSTRUMENTS
Principles of data display in aviation instruments N87-23572
FLIGHT MANAGEMENT SYSTEMS
Efficient conduct of individual flights and air traffic or optimum utilization of modern technology for the overall benefit of civil and military airspace users
[AGARD-AR-236] N87-23608
FLIGHT MECHANICS
The use of Aeritalia flight simulator for the development of the AM-X weapon system N87-23650
FLIGHT SIMULATION
Flight test evaluation of techniques to predict longitudinal pilot induced oscillations
[AD-A179229] N87-23629
Flight Simulation
[AGARD-CP-408] N87-23633
Visual and motion cueing in helicopter simulation N87-23634
Visual display research tool N87-23635
The application of optimal control techniques to the UTIAS research simulator N87-23637
OASIS: A modern tool for real-time simulation N87-23638
Simulator motion characteristics and perceptual fidelity N87-23639
Progress in the implementation of AGARD-AR-144 in motion system assessment and monitoring N87-23642
Flexible and high quality software on a multiprocessor computer system controlling a research flight simulator N87-23643
Trends in ground-based and in-flight simulators for development applications N87-23645
Piloted simulation in the development of the XV-15 tilt rotor research aircraft N87-23646
Simulation of fly-by-wire control for civil transport aircraft at the French Centre d'Essais en Vol N87-23647
Manned air to air combat simulation N87-23648
The development of the T-46 next generation trainer manned engineering simulator at the US Air Force Flight Test Center N87-23652
A method for aircraft simulation verification and validation developed at the United States Air Force Flight Simulation Facility N87-23654
Correlation between flight simulation and processing of flight tests based on inertial measurements N87-23655
Unusual airborne simulator applications N87-23656
DFVLR in-flight simulators ATTAS and ATTHES for flying qualities and flight control research N87-23657
Development of in-flight simulation aircraft for research and training applications in UK N87-23658
Airborne simulation at the National Aeronautical Establishment of Canada N87-23659
Collected flight and simulation comparisons and considerations N87-23660
FLIGHT SIMULATORS
Flight Simulation
[AGARD-CP-408] N87-23633
Visual and motion cueing in helicopter simulation N87-23634
Visual display research tool N87-23635
Advanced visuals in mission simulators N87-23636
The application of optimal control techniques to the UTIAS research simulator N87-23637
OASIS: A modern tool for real-time simulation N87-23638
Simulation of aircraft behaviour on and close to the ground: Summary of AGARD-lc6)ograph AG-285 N87-23640
Use of VDU's by flight simulator instructors N87-23641
Progress in the implementation of AGARD-AR-144 in motion system assessment and monitoring N87-23642
Flexible and high quality software on a multiprocessor computer system controlling a research flight simulator N87-23643
Trends in ground-based and in-flight simulators for development applications N87-23645
Piloted simulation in the development of the XV-15 tilt rotor research aircraft N87-23646
Simulation of fly-by-wire control for civil transport aircraft at the French Centre d'Essais en Vol N87-23647
Manned air to air combat simulation N87-23648
Utilization of simulation to support F-14A low altitude high angle of attack flight testing N87-23649
The use of Aeritalia flight simulator for the development of the AM-X weapon system N87-23650
The development of the T-46 next generation trainer manned engineering simulator at the US Air Force Flight Test Center N87-23652
Operational training: Application and experience N87-23653
A method for aircraft simulation verification and validation developed at the United States Air Force Flight Simulation Facility N87-23654
DFVLR in-flight simulators ATTAS and ATTHES for flying qualities and flight control research N87-23657
Airborne simulation at the National Aeronautical Establishment of Canada N87-23659
Collected flight and simulation comparisons and considerations N87-23660
FLIGHT TEST INSTRUMENTS
Correlation between flight simulation and processing of flight tests based on inertial measurements N87-23655

FLIGHT TESTS
Flight investigation of the effects of an outboard wing-leading-edge modification on stall/spin characteristics of a low-wing, single-engine, T-tail light airplane
[NASA-TP-2691] N87-23614
High-angle-of-attack pneumatic lag and upwash corrections for a hemispherical flow direction sensor
[NASA-TM-86790] N87-23616
Highly integrated digital electronic control: Digital flight control, aircraft model identification, and adaptive engine control
[NASA-TM-86793] N87-23619
Flight test evaluation of techniques to predict longitudinal pilot induced oscillations
[AD-A179229] N87-23629
Demonstration of frequency-sweep testing technique using a Bell 214-ST helicopter
[NASA-TM-89422] N87-23632
Utilization of simulation to support F-14A low altitude high angle of attack flight testing N87-23649
The development of the T-46 next generation trainer manned engineering simulator at the US Air Force Flight Test Center N87-23652
Correlation between flight simulation and processing of flight tests based on inertial measurements N87-23655
Unusual airborne simulator applications N87-23656
Collected flight and simulation comparisons and considerations N87-23660

FLOAT ZONES
Floating emitter solar cell
[NASA-CASE-NPO-16467-1-CU] N87-23879

FLOCCULATING
Improved beta" -alumina oxide electrolytes through transformation toughening
[DE87-007897] N87-23735

FLOW CHARACTERISTICS
Flow of gas through turbine stage with spherical nozzle segment N87-23582
Icing of flow conditioners in a closed-loop wind tunnel
[NASA-TM-89824] N87-23591
Effects of test facility contaminants on supersonic hydrogen-air diffusion flames N87-23790
Response of transonic diffuser flows to abrupt increases of back pressure: Wall pressure measurements N87-23793

FLOW DISTRIBUTION
Study of lee-side flows over conically cambered delta wings at supersonic speeds, part 1
[NASA-TP-2680-PT-1] N87-23597
High-angle-of-attack pneumatic lag and upwash corrections for a hemispherical flow direction sensor
[NASA-TM-86790] N87-23616
Method for the determination of the three-dimensional aerodynamic field of a rotor-stator combination to compressible flow
[NASA-TM-100118] N87-23625
The freezing of flow deflection in Prandtl-Meyer expansion to vacuum
[ISL-CO-226/86] N87-23686
Numerical study of acoustic refraction and flow turning N87-23759
Computational studies of the effects of acoustics and chemistry on the flow field in an axisymmetric ramjet combustor N87-23801
Numerical simulations of cold flow in a ramjet dump combustor with a choked exit nozzle N87-23802
Effects of corona on heat transfer in an enclosure
[AD-A179209] N87-23906
Theoretical investigation of 3-D shock wave-turbulent boundary layer interactions, part 5
[AD-A179455] N87-23909
Experimental and numerical investigation of coherent structures
[AD-A179456] N87-23910
Unsteady separated flows: Vorticity and turbulence
[AD-A179500] N87-23912

FLOW EQUATIONS
Mathematical model describing interaction of single nonsteady supersonic jet and movable barrier of finite dimensions N87-23575
Calculation of axisymmetric flow in swirlers by difference method N87-23579
Three-dimensional structure of boundary layers in transition to turbulence
[AD-A179247] N87-23908
Upwind and symmetric shock-capturing schemes
[NASA-TM-89464] N87-24145

FLOW MEASUREMENT
Crossflow vorticity sensor
[NASA-CASE-LAR-13436-1-CU] N87-23587

FLOW RESISTANCE
Effect of surface roughness on drag of aircraft N87-23571

FLOW STABILITY
Physics of pattern formation at liquid interfaces
[DE87-007540] N87-23919
Double-diffraction X-ray imaging camera
[DE87-007936] N87-23940

FLOW VELOCITY
Workshop report: Methods for measuring solid propellant combustion response N87-23782
Influence of two-phase flow in the deflagration of homogeneous solids N87-23777
Combustion instabilities in dump type ramjet combustors N87-23803
Surface roughness: Its effects on the performance of a two-dimensional compressor cascade
[AD-A179506] N87-23913
An explicit finite-volume time-marching procedure for turbulent flow calculations N87-23928
Light sheet visualization and velocity field measurements in seeded flows — YAG laser
[ISL-CO-225/86] N87-23935
Structure and kinematics of the molecular spiral arms in M51 N87-24312

FLOW VISUALIZATION
Structural analysis of supersonic jet discharging from free-vortex nozzle by method of holographic interferometry with pulsed laser N87-23574
Effects on fuel spray characteristics and vaporization on energy release rates and flow field structure in a dump combustor N87-23804
Synchronization trigger control system for flow visualization
[NASA-TM-89902] N87-23902
Light sheet visualization and velocity field measurements in seeded flows — YAG laser
[ISL-CO-225/86] N87-23935

FLOWMETERS
Crossflow vorticity sensor
[NASA-CASE-LAR-13436-1-CU] N87-23587

FLUID BOUNDARIES
Squeeze film damper technology. Part 3. Experimental investigation of squeeze film dampers
[AD-A178095] N87-23975

FLUID DYNAMICS
Sandia cooperative group on the aerothermochemistry of turbulent combustion
[DE87-008345] N87-23714

FLUID FILLED SHELLS
Onset of Taylor vortices in flows with a circumferential pressure gradient: Application to the helical screw rheometer
[DE87-000453] N87-23918

FLUID FILMS
Squeeze film damper technology. Part 2. Extension of analysis and parametric study
[AD-A178094] N87-23974
Squeeze film damper technology. Part 3. Experimental investigation of squeeze film dampers
[AD-A178095] N87-23975

FLUID FLOW
Physics of pattern formation at liquid interfaces
[DE87-007540] N87-23919
Motion-dependent fluid forces acting on a tube row in crossflow
[DE87-005574] N87-23923

FLUID JETS
Catastrophic breakup of liquid jet by subsonic transverse gas stream N87-23578

FLUID MECHANICS
Selection principles and pattern formation in fluid mechanics and nonlinear shell theory
[NASA-CR-180941] N87-23916

FLUORIDES
Fluoride salts and container materials for thermal energy storage applications in the temperature range 973 to 1400 K
[NASA-TM-89913] N87-24026

FLUX DENSITY
IRAS observations of the Pleiades N87-24284
Radio and infrared observations of (almost) one hundred non-Seyfert Markarian galaxies N87-24350
Nuclear infrared emission and the colors of IRAS galaxies N87-24356

FLUX VECTOR SPLITTING
Upwind and symmetric shock-capturing schemes
[NASA-TM-89464] N87-24145

FLY BY WIRE CONTROL
Simulation of fly-by-wire control for civil transport aircraft at the French Centre d'Essais en Vol N87-23647
Development of in-flight simulation aircraft for research and training applications in UK N87-23658
Airborne simulation at the National Aeronautical Establishment of Canada N87-23659

FLYWHEELS
Application of thermal and flywheel energy storage in orbiting nuclear burst power systems
[DE87-007882] N87-24021
Application of advanced flywheel technology for energy storage on space station
[DE87-007657] N87-24028

FOAMS
Foam rheology: The linear viscoelastic response of a spatially periodic model
[DE87-000960] N87-23731
Three-dimensional model for the linear elastic properties of a foam
[DE87-000964] N87-23732
A mechanistic study of the interaction of ultraviolet laser radiation with low density polymers
[DE87-007846] N87-23734

FOLIAGE
Error analysis of leaf area estimates made from allometric regression models
[NASA-TM-89220] N87-24010

FORCED VIBRATION
Forced vibration as a method for determining structural integrity
[DE87-005878] N87-23992
Material damping from frequency analysis of driving point measurements
[DE87-005873] N87-24003

FORESTS
Error analysis of leaf area estimates made from allometric regression models
[NASA-TM-89220] N87-24010

FORMALDEHYDE
A comparison of unburned fuel and aldehyde emissions from a methanol-fueled stratified charge and homogeneous charge engine
[DE87-007793] N87-23966

FORMALISM
Evaluation of a thin-slot formalism for finite-difference time-domain electromagnetics codes
[DE87-006078] N87-23857

FORMAT
Image sensor data base for the DARPA ALV (Defense Advanced Research Projects Agency Autonomous Land Vehicle) program
[AD-A178117] N87-24246

FORMULATIONS
A model for the low-latitude ionosphere with coefficients for different seasonal and solar cycle conditions
[AD-A178207] N87-24044

FORWARD SCATTERING
Otis ANGB (Air National Guard Base) visibility sensor field test study
[AD-A179176] N87-24045

FOURIER ANALYSIS
A study of the maximum entropy method of power spectrum estimation as applied to interferometer data
[AD-A179403] N87-23707

FRACTOGRAPHY
Influence of microstructure and microdamage processes on fracture at high loading rates
[AD-A179264] N87-23989

FRACTURE MECHANICS
Ceramic fibre/glass matrix composites with outstanding mechanical performance
[AERE-R-12025] N87-23699
Study of the influence of metallurgical factors on fatigue and fracture of aerospace structural materials
[AD-A179268] N87-23720
Adhesive evaluation of water-soluble LARC-TPI
[NASA-TM-89152] N87-23752
Dynamic brittle fracture analysis based on continuum damage mechanics
[DE87-006704] N87-24005

FRACTURE STRENGTH
Investigation of the impact performance of various glass and ceramic systems
[AD-A178115] N87-23744
Influence of microstructure and microdamage processes on fracture at high loading rates
[AD-A179264] N87-23989

FRACTURES (MATERIALS)
Investigation of tearing instability phenomena in ASTM steel
[AD-A177993] N87-24000
Training, muscle fatigue, and stress fractures
[AD-A178350] N87-24085

FRACTURING
Thermal fracture in selected nonlinear optical materials
[DE87-006213] N87-24209

FREE ELECTRON LASERS
Midwest free-electron laser program
[AD-A178106] N87-23953
On-line electron beam measurements for the Los Alamos Free-Electron Laser
[DE87-007452] N87-23956
Biomedical applications of the free electron laser
[AD-A179182] N87-24066

FREE JETS
Tones generated due to the impingement of two jets on each other N87-23797
FREE RADICALS
CN radical distributions in solid propellant flames N87-23775
Heats of formation, structure and heteroatom ((17)O, (33)S) NMR studies of organosulfur molecules, radicals and ions [DE87-006361] N87-24189
FREE VIBRATION
Recent studies in plate vibrations: 1981-1985. Part 2: Complicating effects N87-23996
FREQUENCIES
Material damping from frequency analysis of driving point measurements [DE87-005873] N87-24003
FREQUENCY CONVERTERS
Parametric frequency upconversion, optical fiber transmission and streak camera recording [DE87-005841] N87-24183
FREQUENCY STABILITY
DSS 13 frequency stability tests N87-23829
FREQUENCY SYNCHRONIZATION
Results of using the global positioning system to maintain the time and frequency synchronization in the Deep Space Network N87-23834
FRICTION DRAG
Effect of surface roughness on drag of aircraft N87-23571
FRICTION FACTOR
A consistent finite element formulation of nonlinear frictional contact problems [AD-A179179] N87-23963
FROST
Icing of flow conditioners in a closed-loop wind tunnel [NASA-TM-89824] N87-23591
Ice/frost/debris assessment for space shuttle Mission STS-32 (61-C) [NASA-TM-89192] N87-23675
FUEL CELLS
Fuel cell powered propulsion systems for highway vehicles [DE87-007497] N87-24244
FUEL COMBUSTION
Effects of test facility contaminants on supersonic hydrogen-air diffusion flames N87-23790
Spray combustion: A driving mechanism for ramjet combustion instability N87-23805
Combustion, vaporization, and microexplosion of droplets of organic azides N87-23806
Multispecies CARS measurements in turbulent combustion N87-23808
A comparison of unburned fuel and aldehyde emissions from a methanol-fueled stratified charge and homogeneous charge engine [DE87-007793] N87-23966
FUEL INJECTION
Numerical and experimental studies of atomization and mixing from a coaxial injector element N87-23812
FUEL OILS
Trends of petroleum fuels: Topical report [DE87-001237] N87-23755
FUEL PRODUCTION
Fuels from microalgae: Technology status, potential and research requirements [DE86-010739] N87-23753
FUEL PUMPS
Three-step labyrinth seal for high-performance turbomachines [NASA-TP-1848] N87-23921
Straight cylindrical seal for high-performance turbomachines [NASA-TP-1850] N87-23936
FUEL SYSTEMS
Autogas in general aviation aircraft [DOT/FAA/CT-87/05] N87-23815
FUEL TESTS
Opposed jet burner studies of silane-methane, silane-hydrogen and hydrogen diffusion flames with air N87-23791
FUEL-AIR RATIO
Opposed jet burner studies of silane-methane, silane-hydrogen and hydrogen diffusion flames with air N87-23791
FUNCTIONAL DESIGN SPECIFICATIONS
Hardware synthesis from specification with polynomials [TRITA-NA-8506] N87-24091
FURNACES
Apparatus ad method for quiescent containerless processing of high temperature metals and alloys in low gravity [NASA-CASE-MFS-28087-1] N87-23944
FUSELAGES
Effect of surface roughness on drag of aircraft N87-23571
Helicopter anti-torque system using fuselage strakes [NASA-CASE-LAR-13630-1] N87-23630
FUSION REACTORS
Fusion Energy Postdoctoral Research Program and Professional Development Program [DE87-006350] N87-24188

G

GALACTIC CLUSTERS
Far-infrared properties of cluster galaxies N87-24305
Systematic identification of IRAS point sources N87-24343
What are cirrus point sources? N87-24345
GALACTIC COSMIC RAYS
Comparison of CREME (Cosmic Ray Effects on Microelectronics) model LET (Linear Energy Transfer) spaceflight dosimetry data [AD-A177873] N87-23884
Origin and propagation of galactic cosmic rays N87-24257
Particle physics and cosmology [DE87-007306] N87-24388
GALACTIC EVOLUTION
High mass star formation in the galaxy N87-24267
IUE observations of luminous blue star associations in irregular galaxies N87-24301
Present star formation in sprials of the Virgo cluster N87-24306
Molecular gas and star formation in HI-deficient Virgo cluster galaxies N87-24307
A very deep IRAS survey at l(II) = 97 deg, b(II) = +30 deg N87-24344
IRAS observations of AGN candidates at low flux levels N87-24366
GALACTIC NUCLEI
Discrete X-ray sources and the X-ray background N87-24261
The cosmic X-ray background N87-24262
Star formation and dynamics in starburst nuclei N87-24324
The infrared morphology of galactic centers N87-24336
Star formation in the merging Galaxy NGC3256 N87-24340
Nuclear infrared emission and the colors of IRAS galaxies N87-24356
The relation between star formation and active nuclei N87-24360
Ground-based 1- to 32-microns obeservations of ARP 220: Evidence for a dust-embedded AGN? N87-24361
Spatial deconvolution of IRAS galaxies at 60 UM N87-24362
Star formation around active galactic nuclei N87-24363
Star formation in Seyfert galaxies N87-24364
Circumnuclear starbursts in Seyfert galaxies N87-24365
IRAS observations of AGN candidates at low flux levels N87-24366
Spectrophotometery of Brackett lines in very luminous IRAS galaxies N87-24367
Evidence for extended IR emission in NGC2798 and NGC6240 N87-24368
Models relating the radio emission and ionised gas in Seyfert nuclei N87-24369
Structure in the nucleus of NGC 1068 at 10 microns N87-24370
Far-infrared properties of optically-selected quasars and Seyfert galaxies N87-24371
Infrared-ultraviolet spectra of active galactic nuclei N87-24372
Spectral classification of emission-line galaxies N87-24374
Summary of symposium: Low luminosity sources N87-24375
Morphology of luminous IRAS galaxies: Summary talk N87-24376
GALACTIC RADIATION
The luminosity function of the brightest galaxies in the IRAS survey N87-24341
VLA observations of a sample of galaxies with high far-infrared luminosities N87-24342
A redshift survey of IRAS galaxies N87-24347
Radio continuum, far infrared and star formation N87-24352
Near-infrared observations of IRAS minisurvey galaxies N87-24354
GALACTIC STRUCTURE
Star Formation in Galaxies [NASA-CP-2466] N87-24266
High mass star formation in the galaxy N87-24267
The origin of the diffuse galactic IR/submm emission: Revisited after IRAS N87-24269
Masses, luminosities and dynamics of galactic molecular clouds N87-24270
On the redistribution of OB star luminosity and the warming of nearby molecular clouds N87-24274
Maps of millimeter wave emission from three galactic star-forming regions N87-24275
Survey of the galactic disk from 1 = -150 deg to 1 = 82 deg in the submillimeter range N87-24278
Diffuse infrared emission of the galaxy: Large scale properties N87-24279
The large scale gas and dust distribution in the galaxy: Implications for star formation N87-24280
The Arp Ring: Galactic or extragalactic? N87-24282
Infrared properties of dust grains derived from IRAS observations N87-24283
Star formation in normal galaxies N87-24285
Star formation in the Magellanic clouds N87-24288
CO observations of galaxies with the Nobeyama 45-M telescope N87-24290
CO observations of nearby galaxies and the efficiency of star formation N87-24291
Submm observations of IRAS galaxies N87-24292
Stellar bars and the spatial distribution of infrared luminosity N87-24293
Star formation and spiral structure in M81 N87-24294
The HII regions in M51: Radio and optical observations N87-24295
Star formation in the large Magellanic cloud N87-24297
Carbon monoxide emission from small galaxies N87-24303
Characteristics of UGC galaxies detected by IRAS N87-24304
Far-infrared properties of cluster galaxies N87-24305
Star formation rates as a function of galaxy mass N87-24306
Global properties of the nearby spiral M101 N87-24309
Large scale dissociation of molecular gas in the sprial arms of M51 N87-24311
Structure and kinematics of the molecular spiral arms in M51 N87-24312
Modelling the IRAS colors of galaxies N87-24313
Star forming regions in gas-rich SO galaxies N87-24316
The history of gas in sprial galaxies N87-24318
Starburst galaxies N87-24319
Infrared spectroscopy of star formation in galaxies N87-24320
The frequency of enhanced star formation in interacting and isolated galaxies N87-24326
The infrared morphology of galactic centers N87-24336
A near-infrared study of the luminous merging galaxies NGC 2623 and ARP 148 N87-24339
Systematic identification of IRAS point sources N87-24343
Radio continuum, far infrared and star formation N87-24352
Structure in the nucleus of NGC 1068 at 10 microns N87-24370
Morphology of luminous IRAS galaxies: Summary talk N87-24376
GALAXIES
Star Formation in Galaxies [NASA-CP-2466] N87-24266
Diffuse infrared emission of the galaxy: Large scale properties N87-24268
GALERKIN METHOD
Estimate for the errors in eigenvalue and eigenvector approximation by Galerkin methods, with particular attention to the case of multiple eigenvalues [AD-A178390] N87-24142
GALLIUM ARSENIDES
Electrical behavior of Ge and (Ge + As) implanted gallium arsenide [AD-A179505] N87-24203
The structure of Al/GaAs interfaces [DE87-007181] N87-24206
The structure and electrical properties of metal contacts on GaAs [DE87-008217] N87-24210
Microscale defect kinetics in melt-grown GaAs [AD-A178158] N87-24218
Characterization of material device structures [AD-A178262] N87-24220
Solid state research [AD-A178394] N87-24221
GAMMA RAY ASTRONOMY
The joint NASA/Goddard-University of Maryland research program in charged particle and high energy photon detector technology [NASA-CR-180996] N87-24166

Essays in Space Science
[NASA-CP-2464] N87-24247
High energy gamma ray astronomy N87-24258
Nucleosynthesis and astrophysical gamma ray spectroscopy N87-24259
Gamma ray transients N87-24260

GAMMA RAY BURSTS
Gamma ray transients N87-24260

GAMMA RAYS
Nucleosynthesis and astrophysical gamma ray spectroscopy N87-24259

GAS ANALYSIS
In-situ analysis of hydrazine decomposition products
[NASA-TM-89916] N87-23693
Palladium-silver and gold alloys as catalytic gates on MIS gas sensors
[DE87-006959] N87-23943

GAS COMPOSITION
Star forming regions in gas-rich SO galaxies N87-24316

GAS DENSITY
A theoretical and numerical study of radiative ignition and deradiative extinction in solid propellants N87-23778
Star formation and spiral structure in M81 N87-24294
Efficient star formation in the bright bar of M83 N87-24310
The history of gas in sprial galaxies N87-24318

GAS DETECTORS
Palladium-silver and gold alloys as catalytic gates on MIS gas sensors
[DE87-006959] N87-23943

GAS DISCHARGE TUBES
Radial density distribution of negative atomic oxygen in the oxygen positive column: An experiment
[AD-A179212] N87-24186

GAS DISCHARGES
Multiplex electric discharge gas laser system
[NASA-CASE-NPO-16433-1] N87-23961

GAS DYNAMICS
Investigation of shrouded nozzle exit pressure changes
[AD-A179477] N87-23911
GASPS: A time-dependent, one-dimensional, planar gas dynamics computer code
[DE87-008338] N87-23931
Maps of millimeter wave emission from three galactic star-forming regions N87-24275
Cloud fluid models of gas dynamics and star formation in galaxies N87-24329

GAS FLOW
Catastrophic breakup of liquid jet by subsonic transverse gas stream N87-23578
Flow of gas through turbine stage with spherical nozzle segment N87-23582
Influence of two-phase flow in the deflagration of homogeneous solids N87-23777
Investigation of shrouded nozzle exit pressure changes
[AD-A179477] N87-23911
Star formation and dynamics in starburst nuclei N87-24324

GAS GENERATORS
In-situ analysis of hydrazine decomposition products
[NASA-TM-89916] N87-23693

GAS PRESSURE
Unsteady heat transfer resulting from the rapid charging of an evacuated tank with conducting walls
[AD-A179206] N87-23905

GAS TURBINE ENGINES
Development of model describing unstable operation of turbocompressor and design of antisurging protection for gas turbine engine N87-23577
Flow of gas through turbine stage with spherical nozzle segment N87-23582
Life prediction and constitutive models for engine hot section anisotropic materials
[NASA-CR-179594] N87-23622
Liner cooling research at NASA Lewis Research Center
[NASA-TM-100107] N87-23624

GAS TURBINES
Computation of full-coverage film-cooled airfoil temperatures by two methods and comparison with high heat flux data
[NASA-TM-88931] N87-23934
Intercooled gas turbine
[PB87-178042] N87-23972
Squeeze film damper technology. Part 2. Extension of analysis and parametric study
[AD-A178094] N87-23974

GAS-LIQUID INTERACTIONS
Catastrophic breakup of liquid jet by subsonic transverse gas stream N87-23578

GAS-SOLID INTERACTIONS
Laser studies of chemical dynamics at the gas-solid interface
[DE87-005950] N87-23710

GAS-SOLID INTERFACES
Laser studies of chemical dynamics at the gas-solid interface
[DE87-005950] N87-23710

GASOLINE
Fuels from microalgae: Technology status, potential and research requirements
[DE86-010739] N87-23753
Trends of petroleum fuels: Topical report
[DE87-001237] N87-23755
Autogas in general aviation aircraft
[DOT/FAA/CT-87/05] N87-23815

GATES (CIRCUITS)
Palladium-silver and gold alloys as catalytic gates on MIS gas sensors
[DE87-006959] N87-23943
Study of quantum mechanical effects in deep submicron, grating-gate field effect transistors
[AD-A179617] N87-24204
The development of a prototype CMOS (Complementary Metal Oxide Semiconductor) circuit simulator
[AD-A177942] N87-24215

GAUGE INVARIANCE
Gauge invariant quantum cosmology
[DE87-006685] N87-24226

GEAR TEETH
Computer aided design and analysis of gear tooth geometry
[NASA-CR-179611] N87-23969
A simplified computer solution for the flexibility matrix of contacting teeth for spiral bevel gears
[NASA-CR-179620] N87-23977

GEARS
A simplified computer solution for the flexibility matrix of contacting teeth for spiral bevel gears
[NASA-CR-179620] N87-23977

GELS
Polymer dynamics and gelation
[DE87-007578] N87-23748
Sol-Gel synthesis of MgO-SiO2 glass compositions having stable liquid-liquid immiscibility
[NASA-TM-89905] N87-23750

GENERAL AVIATION AIRCRAFT
Annual review of aircraft accident data, US general aviation: Calendar year 1984
[PB87-194791] N87-23606
Autogas in general aviation aircraft
[DOT/FAA/CT-87/05] N87-23815

GENETICS
Biomedical applications of the free electron laser
[AD-A179182] N87-24066

GEOLOGICAL FAULTS
The interpretation of crustal dynamics data in terms of plate motions and regional deformation near plate boundaries
[NASA-CR-180938] N87-24038
LANDSAT-based lineament analysis, East Texas Basin, and structural history of the Sabine Uplift area, East Texas and North Louisiana
[PB87-176327] N87-24043

GEOLOGICAL SURVEYS
Radar as a complement to topographic maps for delineating marine terraces
[PB87-154597] N87-24013

GEOMAGNETISM
The Magsat Bibliography
[NASA-TM-87822] N87-24039
Auroral particles N87-24249

GEOMETRY
Z-corrections for DSN 70-meter antenna ranging calibration N87-23836
Physics of pattern formation at liquid interfaces
[DE87-007540] N87-23919
Compact toroid generation, lifetime, and stability studies in linear reverse field theta pinch geometries (TRX-2): Final report
[DE87-005094] N87-24195
Studies of the interplanetary magnetic field: IMP's to Voyager N87-24253

GEOPHYSICS
Engineering and instrumentation support of the AFGL (Air Force Geophysics Laboratory) Rocket Research Program
[AD-A179257] N87-23689
Geophysical monitoring for climatic change number 14
[PB87-162533] N87-24056
Solar-geophysical data number 509, January 1987. Part 1: (Prompt reports). Data for December 1986, November 1986
[PB87-162574] N87-24385
Solar-geophysical data number 509, January 1987. Part 2: (Comprehensive reports). Data for July 1986
[PB87-162582] N87-24386

GEOPOTENTIAL
An analysis of geopotential effects on satellite constellations
[AD-A179507] N87-23684
Simulation and analysis of a geopotential research mission
[NASA-CR-180695] N87-24042

GEOSTROPHIC WIND
The specification of lateral boundary conditions in three-dimensional mesoscale numerical models
[AD-A179185] N87-24046

GEOSYNCHRONOUS ORBITS
Optimal continuous thrust orbital evasive maneuvers from geosynchronous orbit
[AD-A179413] N87-23668

GERT
Three dimensional graphics in the statistical analysis of scientific data
[DE87-008151] N87-24104

GIRDERS
The influence of turbulence and deck section geometry on the aeroelastic behaviour of a cable-stayed bridge model
[NAE-AN-40] N87-23990

GLASS
Investigation of the impact performance of various glass and ceramic systems
[AD-A178115] N87-23744
New low temperature (hydroxylated) materials
[DE87-008530] N87-23749
Sol-Gel synthesis of MgO-SiO2 glass compositions having stable liquid-liquid immiscibility
[NASA-TM-89905] N87-23750
Low-resistivity glass electrolytes for sodium-sulfur cells
[DE87-004837] N87-23880

GLOBAL POSITIONING SYSTEM
Results of using the global positioning system to maintain the time and frequency synchronization in the Deep Space Network N87-23834

GLOW DISCHARGES
Plasma deposition of tungsten
[DE87-007390] N87-23724

GOLD
Corrosion of gold bridgewire in electronic components
[DE87-000922] N87-23722

GOLD ALLOYS
Wetting properties of Au/Sn solders for microelectronics
[DE87-008519] N87-23883

GOVERNMENT/INDUSTRY RELATIONS
Federal laboratory nondestructive testing research and development applicable to industry
[DE87-008351] N87-23985

GRADIENTS
The specification of lateral boundary conditions in three-dimensional mesoscale numerical models
[AD-A179185] N87-24046

GRAFTING
Synthesis of model polymers and related structures in support of vinyl monomer grafting studies
[DE87-007406] N87-23739

GRAIN BOUNDARIES
Nonuniform grain boundary corrosion and the local electrode potential in crevicing
[AD-A177889] N87-23728

GRAIN SIZE
Modification of solid propellant deflagration rates due to random nonhomogeneities N87-23766
Infrared properties of dust grains derived from IRAS observations N87-24283

GRANULAR MATERIALS
Microscopic modeling of sound waves in granular material
[DE87-007400] N87-24159

GRAPH THEORY
Efficient parallel algorithms for (delta+1)-coloring and maximal independent set problems
[AD-A178287] N87-24109

GRAPHITE-EPOXY COMPOSITES
Dynamic response of two composite prop-fan models on a nacelle/wing/fuselage half model
[NASA-CR-179589] N87-23615
Mechanical properties of undirectional and fabric graphite/epoxy composites
[SAND-86-0784] N87-23702

GRAPHS (CHARTS)
Three dimensional graphics in the statistical analysis of scientific data
[DE87-008151] N87-24104

GRATINGS (SPECTRA)
Study of quantum mechanical effects in deep submicron, grating-gate field effect transistors
[AD-A179617] N87-24204

GRAVITATION
The 1986-87 NASA space/gravitational biology accomplishments
[NASA-TM-89951] N87-24063
GRAVITATIONAL FIELDS
Simulation and analysis of a geopotential research mission
[NASA-CR-180695] N87-24042
GRAY SCALE
Recovering the orientation of textured surfaces in natural scenes
[AD-A179360] N87-24096
GREENHOUSE EFFECT
The reality of the greenhouse effect
[DE87-002383] N87-24041
GROUND STATE
Heats of formation, structure and heteroatom ((17)O, (33)S) NMR studies of organosulfur molecules, radicals and ions
[DE87-006361] N87-24189
GROUND STATIONS
Engineering and instrumentation support of the AFGL (Air Force Geophysics Laboratory) Rocket Research Program
[AD-A179257] N87-23689
GROUND-AIR-GROUND COMMUNICATION
Development of an air ground data exchange concept: Flight deck perspective
[NASA-CR-4074] N87-23607
GROWTH
Generation of broadband noise in the magnetotail
[AD-A179136] N87-24034

H

H ALPHA LINE
Measuring star formation rates in blue galaxies N87-24289
Optical and IR luminosity functions of IRAS galaxies N87-24348
HALL EFFECT
Influence of microstructure and microdamage processes on fracture at high loading rates
[AD-A179264] N87-23989
Electrical behavior of Ge and (Ge+As) implanted gallium arsenide
[AD-A179505] N87-24203
Characterization of material device structures
[AD-A178282] N87-24220
HALLEY'S COMET
Observations of heavy energetic ions for upstream from comet Halley
[DE87-003752] N87-24380
HALOS
A dust scattered halo in starburst galaxy M82? N87-24334
HANG GLIDERS
An experimental investigation into methods for quantifying hang glider airworithness parameters
[CAR-8705] N87-23613
HARMONIC ANALYSIS
Forced vibration as a method for determining structural integrity
[DE87-005878] N87-23992
HARMONIC OSCILLATION
The impact damped harmonic oscillator in free decay
[NASA-TM-89897] N87-23978
HARMONICS
Investigations on the impact of voltage and current harmonics on end-use devices and their protection
[DE87-008018] N87-23878
HARRIER AIRCRAFT
Development of in-flight simulation aircraft for research and training applications in UK N87-23658
HEAD-UP DISPLAYS
Evaluation of the angle of attack limiter of the F-16 C/D aircraft
[AD-A177941] N87-23612
Operational training: Application and experience N87-23653
HEALTH
Investigation of biochemical variation in operational aircrew
[AD-A179223] N87-24067
The field shower wastewater recycling system: Development of a program of instruction and preliminary analysis of its potential health implications
[AD-A178112] N87-24088
HEART DISEASES
Short Course on Cardiopulmonary Aspects of Aerospace Medicine
[AGARD-R-758] N87-24070
Valvular and congenital heart disease in the aviator N87-24073
Aeromedical aspects of mitral valve prolapse N87-24074
Hypertension in the aviator N87-24077
Cardiopulmonary screening for high-performance flying: Selection and retention issues N87-24079
HEART FUNCTION
Aeromedical evaluation and disposition of electrocardiographic abnormalities N87-24071
HEART VALVES
Valvular and congenital heart disease in the aviator N87-24073
Aeromedical aspects of mitral valve prolapse N87-24074
HEAT FLUX
Computation of full-coverage film-cooled airfoil temperatures by two methods and comparison with high heat flux data
[NASA-TM-88931] N87-23934
HEAT OF FORMATION
Force-field parameters and molecular mechanics calculations for nitramines N87-23779
Heats of formation, structure and heteroatom ((17)O, (33)S) NMR studies of organosulfur molecules, radicals and ions
[DE87-006361] N87-24189
HEAT PUMPS
The fiber optic refrigeration cycle monitor
[DE87-006632] N87-24180
HEAT RESISTANT ALLOYS
Life prediction and constitutive models for engine hot section anisotropic materials
[NASA-CR-179594] N87-23622
Metals and Ceramics Division
[DE87-008548] N87-23697
Review of interactions of large solar fluxes with materials
[DE87-001156] N87-24024
HEAT STORAGE
Application of thermal and flywheel energy storage in orbiting nuclear burst power systems
[DE87-007882] N87-24021
Fluoride salts and container materials for thermal energy storage applications in the temperature range 973 to 1400 K
[NASA-TM-89913] N87-24026
HEAT TRANSFER
Behavior of simulated solid propellant flames in axial acoustic fields N87-23760
New ignition parameter correlations for predicting solid rocket motor ignition transients N87-23767
Theoretical influence of propellant packaging on tube erosion: model formulation and algorithm development N87-23784
Preliminary thermal analysis of transistor packages
[DE87-007708] N87-23898
Unsteady heat transfer resulting from the rapid charging of an evacuated tank with conducting walls
[AD-A179206] N87-23905
Heat transfer research for ocean thermal energy conversion
[DE87-001155] N87-24023
Solar cell concentrator system
[AD-A177981] N87-24025
HEAT TRANSFER COEFFICIENTS
Flow regimes of refrigerant mixtures condensing inside tubes
[ORNL/SUB/81-7762/4 AND 01] N87-23917
Computation of full-coverage film-cooled airfoil temperatures by two methods and comparison with high heat flux data
[NASA-TM-88931] N87-23934
HEAT TREATMENT
Influence of microstructure and microdamage processes on fracture at high loading rates
[AD-A179264] N87-23989
HEATING
Simultaneous radiative and convective heating of thin body in medium with variable temperature N87-23576
The energy source of the interplanetary medium and the helicsphere N87-24251
A simple two-component model for the far-infrared emission from galaxies N87-24314
A simple theory of bimodal star formation N87-24317
HEAVY IONS
Experiments and prospects for induction linac drivers
[DE87-006144] N87-23669
Heavy ion induced upsets in semiconductor devices
[ATR-86(8139)-3] N87-24205
Observations of heavy energetic ions for upstream from comet Halley
[DE87-003752] N87-24380
HEAVY NUCLEI
Measurements of ultraheavy cosmic rays with HEAO-3 N87-24256
HELICOPTER CONTROL
Helicopter anti-torque system using fuselage strakes
[NASA-CASE-LAR-13630-1] N87-23630
HELICOPTER DESIGN
Helicopter anti-torque system using fuselage strakes
[NASA-CASE-LAR-13630-1] N87-23630
HELICOPTERS
Aeroelasticity and mechanical stability report, 0.27 Mach scale model of the YAH-64 advanced attack helicopter
[NASA-CR-178284] N87-23596
Swashplate control system
[NASA-CASE-ARC-11633-1] N87-23631
Demonstration of frequency-sweep testing technique using a Bell 214-ST helicopter
[NASA-TM-89422] N87-23632
Visual and motion cueing in helicopter simulation N87-23634
Airborne simulation at the National Aeronautical Establishment of Canada N87-23659
Extension of Kirchhoff's formula to radiation from moving surfaces
[NASA-TM-89149] N87-24160
HELIOSEISMOLOGY
Vector array processor computer equipment
[AD-A179545] N87-24382
HELIOSPHERE
The energy source of the interplanetary medium and the helicsphere N87-24251
Studies of the interplanetary magnetic field: IMP's to Voyager N87-24253
Cosmic rays in the helicsphere N87-24254
Physics of the inner helicsphere: Mechanisms, models and observational signatures
[NASA-CR-181063] N87-24387
HELMETS
Visual display research tool N87-23635
HEMISPHERICAL SHELLS
Investigation of the buckling sensitivity of hemispherical containers with arbitrary liquid content
[MITT-31] N87-24008
HERMETIC SEALS
Pulsed Nd:YAG laser closure welding of the MC3593/3594 relay
[DE87-007825] N87-23967
HERTZSPRUNG-RUSSELL DIAGRAM
Modelling the IRAS colors of galaxies N87-24313
HETEROCYCLIC COMPOUNDS
Electronics and ionic transport in polymers
[AD-A178227] N87-23746
HETEROJUNCTIONS
Fabrication of AlGaAs/InGaAs pseudomorphic modulation doped field effect transistors with p-doped surface layers
[AD-A179230] N87-24201
HEWLETT-PACKARD COMPUTERS
DATA: A comprehensive data analysis environment for HP1000 computers
[DE87-007824] N87-24094
HIERARCHIES
Time slice manipulation in information hierarchy
[AD-A177949] N87-24237
HIGH ALTITUDE
Operation Everest 2: Importance of ventilation in defense of maximal oxygen uptake at extreme altitudes
[AD-A177874] N87-24082
HIGH ALTITUDE BREATHING
Pulmonary adaptation to high altitude
[AD-A179139] N87-24065
HIGH CURRENT
High current electron gun for space flight
[AD-A178467] N87-23875
High-current beam dynamics and transport, theory and experiment
[DE87-006154] N87-24172
HIGH ENERGY INTERACTIONS
Research in theoretical particle physics
[DE87-008240] N87-24169
The physics and a plan for a 45 GeV facility that extends the high-intensity capability in nuclear and particle physics
[LA-10720-MS] N87-24170
Data management for high energy physics experiments: Preliminary proposals
[DE87-006940] N87-24236
High energy gamma ray astronomy N87-24258
Infrared astronomy N87-24264
HIGH FREQUENCIES
Control considerations for high frequency, resonant, power processing equipment used in large systems
[NASA-TM-89926] N87-23690
HIGH POWER LASERS
University of Rochester, Laboratory for Laser Energetics
[DE87-005920] N87-23947

HIGH PRESSURE
Inelastic properties of ice I/sub h/ at low temperatures and high pressures
[DE87-007334] N87-23711
HIGH RESOLUTION
Medium- and long-wave infrared absorption spectra of carbon dioxide nitrous oxide at 800K
[AD-A179430] N87-23708
Holographic optical elements formed in light of reduced coherence
[AD-A179372] N87-23937
Development of ultrasonic thermometry for high-temperature high-resolution temperature profiling applications in LMFBR safety research
[SAND-84-1341] N87-24171
HIGH REYNOLDS NUMBER
High Reynolds Number tests of the NASA SC(2)-0012 airfoil in the Langley 0.3-meter transonic cryogenic tunnel
[NASA-TM-89102] N87-23594
HIGH SPEED
Extension of Kirchhoff's formula to radiation from moving surfaces
[NASA-TM-89149] N87-24160
HIGH TEMPERATURE
Medium- and long-wave infrared absorption spectra of carbon dioxide nitrous oxide at 800K
[AD-A179430] N87-23708
High temperature electrically conductive adhesives
[DE87-007020] N87-23747
Method of making a flexible diaphragm
[NASA-CASE-MSC-20797-1] N87-23981
Development of ultrasonic thermometry for high-temperature high-resolution temperature profiling applications in LMFBR safety research
[SAND-84-1341] N87-24171
HIGH TEMPERATURE ENVIRONMENTS
Development of a high temperature ceramic-to-metal seal for Air Force Weapons Laboratory Laser
[DE87-007711] N87-23949
HIGH TEMPERATURE GASES
Nuclear star formation on 100 parsec scales: 10' resolution radio continuum, HI and CO observations
N87-24322
Extremely Luminous Far-infrared Sources (ELFS)
N87-24323
HIGH VOLTAGES
A study of Schwarz converters for nuclear powered spacecraft
[NASA-TM-89911] N87-23903
HILBERT SPACE
Strong convergence and convergence rates of approximating solutions for algebraic Riccati equations in Hilbert spaces
[NASA-CR-178302] N87-24122
HISTORIES
Medical research programs, past and future, for designing atmospheres to retard fires
[AD-A178354] N87-24069
History of spaceflight
[AD-A178381] N87-24393
HMX
Low energy ignition of HMX using a foil bridge
[DE87-004211] N87-23754
AP/HMX composite propellant modeling N87-23776
Simultaneous thermogravimetric modulated beam mass spectrometry and time-of-flight velocity spectra measurements of thermal decomposition products from RDX and HMX N87-23780
The application of imaging laser induced fluorescence to the measurement of HMX and aluminized propellant ignition and deflagration flame structure N87-23782
HOLOGRAPHIC INTERFEROMETRY
Structural analysis of supersonic jet discharging from free-vortex nozzle by method of holographic interferometry with pulsed laser N87-23574
Holographic optical elements formed in light of reduced coherence
[AD-A179372] N87-23937
HOLOGRAPHY
Holographic correction of aberrations in optical systems employing synthetic apertures
[AD-A179107] N87-24173
HONEYCOMB STRUCTURES
Experimental evaluation of honeycomb/screen configurations and short contraction section for NASA Lewis Research Center's altitude wind tunnel
[NASA-TP-2692] N87-23662
Ceramic honeycomb structures and the method thereof
[NASA-CASE-ARC-11652-1] N87-23737
HOT STARS
Models for infrared emission from IRAS galaxies
N87-24286
HOT-FILM ANEMOMETERS
Crossflow vorticity sensor
[NASA-CASE-LAR-13436-1-CU] N87-23587
HOUSINGS
The T55-L-712 turbine engine compressor housing refurbishment project
[NASA-CR-179624] N87-23729
HTPB PROPELLANTS
AP/HMX composite propellant modeling N87-23776
HUBBLE DIAGRAM
Stellar bars and the spatial distribution of infrared luminosity N87-24293
Radio and infrared observations of (almost) one hundred non-Seyfert Markarian galaxies N87-24350
HUBS
Aeroelasticity and mechanical stability report, 0.27 Mach scale model of the YAH-64 advanced attack helicopter
[NASA-CR-178284] N87-23596
HUMAN BODY
International Symposium on In Vivo Body Composition Studies: Program and abstracts
[DE87-006750] N87-24080
HUMAN FACTORS ENGINEERING
Principles of data display in aviation instruments
N87-23572
Use of VDU's by flight simulator instructors
N87-23641
Text editing performance as a function of screen size
[AD-A179067] N87-24229
Research and Technology
[NASA-TM-89411] N87-24391
HUMAN PERFORMANCE
Operation Everest 2: Importance of ventilation in defense of maximal oxygen uptake at extreme altitudes
[AD-A177874] N87-24082
The review of a research proposal to study the effects of 130 torr oxygen on submarines held at Groton, Connecticut on September 4, 1986
[AD-A177976] N87-24083
Perception and structural analysis of morphologies
[ENST-86D004] N87-24086
HUMAN REACTIONS
Multipurpose visual display and eye movement recording system
[AD-A179620] N87-24068
HUMAN TOLERANCES
Annoyance response to simulated advanced turboprop aircraft interior noise containing tonal beats
[NASA-TP-2689] N87-24161
HYBRID CIRCUITS
Two-stage hybrid microcircuit amplifier
[DE87-009092] N87-23899
HYDRAULIC CONTROL
The development of the T-46 next generation trainer manned engineering simulator at the US Air Force Flight Test Center N87-23652
HYDRAULIC EQUIPMENT
A redefined hydraulic diameter for laminar flow
[AD-A179511] N87-23914
HYDRAZINES
In-situ analysis of hydrazine decomposition products
[NASA-TM-89916] N87-23693
HYDROCARBON FUELS
Novel application of topological indices. 2. Prediction of the threshold soot index for hydrocarbon fuels
[AD-A178001] N87-23716
Fuels from microalgae: Technology status, potential and research requirements
[DE86-010739] N87-23753
HYDRODYNAMICS
Compression and shear wave propagation in plain and filled elastomers
[AD-A178153] N87-23745
REZONE: A method for automatic rezoning in two-dimensional Lagrangian hydrodynamics problems
[DE87-006324] N87-23930
Squeeze film damper technology. Part 2. Extension of analysis and parametric study
[AD-A178094] N87-23974
Efficient star formation in the bright bar of M83
N87-24310
HYDROGEN
Effects of test facility contaminants on supersonic hydrogen-air diffusion flames N87-23790
Neutral hydrogen and star formation in irregular galaxies N87-24302
HYDROGEN CLOUDS
Cloud fluid models of gas dynamics and star formation in galaxies N87-24329
HYDROGEN EMBRITTLEMENT
Finite-difference program for hydrogen diffusion: Example problems manual
[DE87-007515] N87-23712
HYDROGENATION
Drift mobilities by time-of-flight methods and time-dependent phototransport in the nanosecond regime in amorphous semiconductors
[DE87-008021] N87-24208
HYDROXYL COMPOUNDS
New low temperature (hydroxylated) materials
[DE87-008530] N87-23749
HYDROXYL EMISSION
Extragalactic OH megamasers in strong IRAS sources
N87-24353
HYPERBOLIC DIFFERENTIAL EQUATIONS
Upwind and symmetric shock-capturing schemes
[NASA-TM-89464] N87-24145
HYPERBOLIC FUNCTIONS
Far field boundary conditions for time-dependent hyperbolic systems
[AD-A179361] N87-24123
HYPERSONIC FLOW
Hypersonic aerodynamic coefficients and convection flow estimation in a HERMES type project
[NASA-TT-20019] N87-23583
Optimal aerodynamic shapes for hypervelocity projectiles
[AD-A178367] N87-23672
HYPERSONIC SPEED
Mach 6 experimental and theoretical stability and performance of a cruciform missile at angles of attack up to 65 degrees
[NASA-TP-2733] N87-23592
Reactivation study for NASA Lewis Research Center's hypersonic tunnel facility
[NASA-TM-88918] N87-23664
HYPERTENSION
Hypertension in the aviator N87-24077
HYPERVELOCITY IMPACT
Application of a 100-kV electric gun for hypervelocity impact studies
[DE87-008730] N87-23976
HYPERVELOCITY PROJECTILES
Optimal aerodynamic shapes for hypervelocity projectiles
[AD-A178367] N87-23672
HYPOTHESES
Estimation of parameters in latent class models with constraints on the parameters
[AD-A178196] N87-24138
HYPOXIA
Pulmonary adaptation to high altitude
[AD-A179139] N87-24065
Pulmonary physiology and pulmonary function testing in aerospace medicine N87-24075
The review of a research proposal to study the effects of 130 torr oxygen on submarines held at Groton, Connecticut on September 4, 1986
[AD-A177976] N87-24083

I

ICE
Ice/frost/debris assessment for space shuttle Mission STS-32 (61-C)
[NASA-TM-89192] N87-23675
Inelastic properties of ice I/sub h/ at low temperatures and high pressures
[DE87-007334] N87-23711
ICE FORMATION
Icing of flow conditioners in a closed-loop wind tunnel
[NASA-TM-89824] N87-23591
IDEAL GAS
Unsteady heat transfer resulting from the rapid charging of an evacuated tank with conducting walls
[AD-A179206] N87-23905
IDENTIFYING
Highly integrated digital electronic control: Digital flight control, aircraft model identification, and adaptive engine control
[NASA-TM-86793] N87-23619
IGNITERS
Plasma torch igniter for scramjets N87-23789
IGNITION
Low power arcjet thruster pulse ignition
[NASA-TM-100123] N87-23691
Low energy ignition of HMX using a foil bridge
[DE87-004211] N87-23754
Effect of particle size on the shock sensitivity of pure porous HE (High Explosive)
[AD-A178206] N87-23814
Thermal ignition of pyrotechnics with lasers
[DE87-006245] N87-23955
IMAGE ANALYSIS
Automated radar image analysis research in support of military needs
[AD-A179615] N87-23627

Approximation errors and perceived similarity between approximated polygons
[TRITA-NA-8505] N87-24127

IMAGE ENHANCEMENT
Target segmentation and image enhancement through multisensor data fusion
[AD-A178875] N87-24178

IMAGE PROCESSING
Advanced visuals in mission simulators N87-23636
Holographic optical elements formed in light of reduced coherence
[AD-A179372] N87-23937
An atmospheric correction algorithm for remote identification of non-Lambertian surfaces and its range of validity
[DE87-006059] N87-24011
Utilizing remote sensing of thematic mapper data to improve our understanding of estuarine processes and their influence on the productivity of estuarine-dependent fisheries
[NASA-CR-180984] N87-24012
Intermediate level computer vision processing algorithm development for the content addressable array parallel processor
[AD-A179515] N87-24090
Recovering the orientation of textured surfaces in natural scenes
[AD-A179360] N87-24096
Edge focusing
[TRITA-NA-8518] N87-24099
Approximation errors and perceived similarity between approximated polygons
[TRITA-NA-8505] N87-24127
A PASCAL implementation of the image algebra
[AD-A177943] N87-24136
Target segmentation and image enhancement through multisensor data fusion
[AD-A178875] N87-24178
Nonlinear real-time optical signal processing
[AD-A178169] N87-24182

IMAGE RESOLUTION
Edge focusing
[TRITA-NA-8518] N87-24099

IMAGERY
Visual display research tool N87-23635
Image sensor data base for the DARPA ALV (Defense Advanced Research Projects Agency Autonomous Land Vehicle) program
[AD-A178117] N87-24246

IMAGES
A PASCAL implementation of the image algebra
[AD-A177943] N87-24136
Formation and stability of partially-neutralized plasma clumps
[AD-A179444] N87-24187

IMAGING TECHNIQUES
Effects on fuel spray characteristics and vaporization on energy release rates and flow field structure in a dump combustor N87-23804
Coherent multiple aperture optical imaging systems: Analysis and design
[AD-A179476] N87-24176

IMPACT
The impact damped harmonic oscillator in free decay
[NASA-TM-89697] N87-23978

IMPACT DAMAGE
Aircraft Dynamic Response to Damaged and Repaired Runways
[AGARD-R-739] N87-23609
Optimal aerodynamic shapes for hypervelocity projectiles
[AD-A178367] N87-23672
Investigation of the impact performance of various glass and ceramic systems
[AD-A178115] N87-23744

IMPACT LOADS
Optimal aerodynamic shapes for hypervelocity projectiles
[AD-A178367] N87-23672

IMPACT TESTS
Bird impact qualification test for A-10 windshield
[AD-A179263] N87-23599
Application of a 100-kV electric gun for hypervelocity impact studies
[DE87-006730] N87-23976

IMPLANTATION
Surface passivation of an implantable semiconductor multielectrode array
[AD-A178175] N87-24219

IMPURITIES
Characterization of material device structures
[AD-A178262] N87-24220

INCOHERENT SCATTER RADAR
A comparison of ionospheric model predictions with MITHRAS observations
[AD-A179374] N87-24036

INCOHERENT SCATTERING
Holographic optical elements formed in light of reduced coherence
[AD-A179372] N87-23937

INDENTATION
Thin film characterization using a mechanical properties microprobe
[DE87-006593] N87-24214

INDEXES (DOCUMENTATION)
Automating index preparation
[AD-A179327] N87-24231
Standardized procedure for system safety input to the Defense Technical Information Center (DTIC)
[AD-A178246] N87-24239

INDIAN OCEAN
Mixed layer and thermocline depth climatologies in the western Indian Ocean
[PB87-154613] N87-24060

INDIUM
Fabrication of AlGaAs/InGaAs pseudomorphic modulation doped field effect transistors with p-doped surface layers
[AD-A179230] N87-24201

INDIUM PHOSPHIDES
Solid state research
[AD-A178394] N87-24221

INDUSTRIAL SAFETY
Hazards evaluation of radiofrequency and microwave radiation
[DE87-006536] N87-24081

INELASTIC STRESS
Inelastic strain analogy for piecewise linear computation of creep residues in built-up structures
[NASA-TM-88813] N87-23995

INERTIAL CONFINEMENT FUSION
Experiments and prospects for induction linac drivers
[DE87-006144] N87-23669

INERTIAL PLATFORMS
Correlation between flight simulation and processing of flight tests based on inertial measurements N87-23655

INFORMATION MANAGEMENT
DOD (Department of Defense) Procedures for Management of Information Requirements
[PB87-155495] N87-24227

INFORMATION RETRIEVAL
Automating index preparation
[AD-A179327] N87-24231
Experiments on the cognitive aspects of information seeking and information retrieving
[PB87-157699] N87-24238
Standardized procedure for system safety input to the Defense Technical Information Center (DTIC)
[AD-A178246] N87-24239

INFORMATION SYSTEMS
Livermore risk analysis methodology: A quantitative approach to management of the risk associated with the operation of information systems
[DE87-006828] N87-24232
Energy Data Base: Subject categories and scope, a reference manual
[DE87-005547] N87-24235
Standardized procedure for system safety input to the Defense Technical Information Center (DTIC)
[AD-A178246] N87-24239

INFRARED ABSORPTION
Medium- and long-wave infrared absorption spectra of carbon dioxide nitrous oxide at 800K
[AD-A179430] N87-23708

INFRARED ASTRONOMY
Essays in Space Science
[NASA-CP-2464] N87-24247
Infrared astronomy N87-24264
Star Formation in Galaxies
[NASA-CP-2466] N87-24266
High mass star formation in the galaxy N87-24267
Diffuse infrared emission of the galaxy: Large scale properties N87-24268
The origin of the diffuse galactic IR/submm emission: Revisited after IRAS N87-24269
IRAS colors of VLA identified objects in the galaxy N87-24271
On the redistribution of OB star luminosity and the warming of nearby molecular clouds N87-24274
Maps of millimeter wave emission from three galactic star-forming regions N87-24275
Shock heated dust in L1551: L(IR) greater than 20 solar luminosities N87-24276
Diffuse infrared emission of the galaxy: Large scale properties N87-24279
The large scale gas and dust distribution in the galaxy: Implications for star formation N87-24280
A correlation between the IRAS infrared cirrus at 60 or 100 microns and neutral atomic hydrogen in the outer galaxy N87-24281
Infrared properties of dust grains derived from IRAS observations N87-24283
IRAS observations of the Pleiades N87-24284
CO observations of nearby galaxies and the efficiency of star formation N87-24291
Global properties of the nearby spiral M101 N87-24309
Modelling the IRAS colors of galaxies N87-24313
Infrared spectroscopy of star formation in galaxies N87-24320
Using SIRTF to study extragalactic star formation N87-24359
Spatial deconvolution of IRAS galaxies at 60 UM N87-24362
Detector arrays for low-background space infrared astronomy
[NASA-TM-88344] N87-24378

INFRARED DETECTORS
Detector arrays for low-background space infrared astronomy
[NASA-TM-88344] N87-24378

INFRARED IMAGERY
Target segmentation and image enhancement through multisensor data fusion
[AD-A178875] N87-24178
A fiber optic link for an infrared imaging camera system
[DE87-008346] N87-24181
Solid state research
[AD-A178394] N87-24221
A near-infrared study of the luminous merging galaxies NGC 2623 and ARP 148 N87-24339

INFRARED PHOTOMETRY
Star formation in the merging Galaxy NGC3256 N87-24340
Using SIRTF to study extragalactic star formation N87-24359

INFRARED RADIATION
Midwest free-electron laser program
[AD-A178106] N87-23953
Studies of infrared aurorae
[AD-A179539] N87-24037
Ultraluminous infrared galaxies N87-24327
The infrared morphology of galactic centers N87-24336
Properties of the unusual galaxy PSC 09104+4109 N87-24346
Optical and IR luminosity functions of IRAS galaxies N87-24348
Nuclear infrared emission and the colors of IRAS galaxies N87-24356
Enhanced star formation: The importance of bars in spiral galaxies N87-24357
Morphology of luminous IRAS galaxies: Summary talk N87-24376

INFRARED SPECTRA
Atmospheric radiance profile codes
[AD-A179258] N87-24035
Extragalactic infrared spectroscopy N87-24328
Using SIRTF to study extragalactic star formation N87-24359
Star formation in Seyfert galaxies N87-24364
Evidence for extended IR emission in NGC2798 and NGC6240 N87-24368
Structure in the nucleus of NGC 1068 at 10 microns N87-24370
Far-infrared properties of optically-selected quasars and Seyfert galaxies N87-24371
Infrared-ultraviolet spectra of active galactic nuclei N87-24372

INITIATORS (EXPLOSIVES)
Low energy ignition of HMX using a foil bridge
[DE87-004211] N87-23754

INJECTORS
Numerical and experimental studies of atomization and mixing from a coaxial injector element N87-23812

INJURIES
Training, muscle fatigue, and stress fractures
[AD-A178350] N87-24085

INLET NOZZLES
Investigation of shrouded nozzle exit pressure changes
[AD-A179477] N87-23911

INSTRUMENT FLIGHT RULES
Aircraft accident report: Southern Air Transport LOGAIR Flight 51, Lockheed L-382G, Kelly Air Force Base, Texas, October 4, 1986
[PB87-910404] N87-23604

INTEGRALS
Integral approximants for functions of higher monodromic dimension
[DE87-007508] N87-24129

INTEGRATED CIRCUITS
Plasma deposition of tungsten
[DE87-007390] N87-23724
Time domain wave propagation in multilayered integrated circuits
[AD-A178180] N87-23847

MIC technology for phased arrays N87-23866
Picosecond optical electronics [AD-A179061] N87-23868
VHDL (VHSIC (Very High Speed Integrated Circuits) Hardware Descriptive Languages) prototype simulator [AD-A179073] N87-23869
Research in VLSI systems [AD-A179227] N87-23872
Finite element analysis of slow-wave Schottky contact printed lines [AD-A179259] N87-23873
A VLSI CMOS circuit design technique to aid test generation [AD-A177934] N87-23887
Complexities of layouts in three-dimensional VLSI (Very Large-Scale Integration) circuits [AD-A178150] N87-23889
Computer-aided fabrication system implementation [AD-A178225] N87-24108
Report of the Second Workshop on Synchrotron Radiation Sources for X-ray Lithography [DE87-002155] N87-24179
Development of a theoretical model for annealing of radiation damage in semiconductor devices [NASA-CR-180394] N87-24211
Surface passivation of an implantable semiconductor multielectrode array [AD-A178175] N87-24219

INTERCEPTION
Satellite allocation for boost-phase missile intercepts [DE87-007719] N87-24155

INTERFACES
Techniques for implementing statically complete component mode synthesis for forced response [DE87-002698] N87-24002
Identification of structural interface characteristics using component mode synthesis [NASA-TM-88960] N87-24006
The development of a prototype intelligent user interface subsystem for NASA's scientific database systems [NASA-TM-87821] N87-24096
The structure of Al/GaAs interfaces [DE87-007181] N87-24206

INTERFEROMETRY
A study of the maximum entropy method of power spectrum estimation as applied to interferometer data [AD-A179403] N87-23707

INTERGALACTIC MEDIA
Using SIRTF to study extragalactic star formation N87-24359

INTERNAL COMBUSTION ENGINES
Synchronization trigger control system for flow visualization [NASA-TM-89902] N87-23902
Multidimensional modeling of convective heat transfer with application to I.C. engines [DE87-002939] N87-23922
A comparison of unburned fuel and aldehyde emissions from a methanol-fueled stratified charge and homogeneous charge engine [DE87-007793] N87-23966

INTERNATIONAL COOPERATION
Survey of environment related monitoring programs of international organizations and their contribution to international organizations [ETN-87-99913] N87-24033

INTERPLANETARY MAGNETIC FIELDS
The Magsat Bibliography [NASA-TM-87822] N87-24039
Particle propagation channels in the solar wind N87-24252
Studies of the interplanetary magnetic field: IMP's to Voyager N87-24253

INTERPLANETARY MEDIUM
The energy source of the interplanetary medium and the heliosphere N87-24251

INTERSTELLAR EXTINCTION
The HII regions in M51: Radio and optical observations N87-24295
Spectral classification of emission-line galaxies N87-24374

INTERSTELLAR GAS
Molecular gas and star formation in HI-deficient Virgo cluster galaxies N87-24307
Efficient star formation in the bright bar of M83 N87-24310

INTERSTELLAR MASERS
Extragalactic OH megamasers in strong IRAS sources N87-24353

INTERSTELLAR MATTER
The origin of the diffuse galactic IR/submm emission: Revisited after IRAS N87-24269
The large scale gas and dust distribution in the galaxy: Implications for star formation N87-24280
Infrared properties of dust grains derived from IRAS observations N87-24283
IRAS observations of the Pleiades N87-24284
IRAS and ground-based observations of star formation regions in the Magellanic clouds N87-24296
A simple theory of bimodal star formation N87-24317
Molecular gas in the starburt nucleus of M82 N87-24321
Cloud fluid models of gas dynamics and star formation in galaxies N87-24329
The azimuthal and radial distributions of HI and H2 in NGC 6946 N87-24335

INTERSTELLAR RADIATION
Star formation in Carina OB1: Observations of a giant molecular cloud associated with the eta Carinae Nebula N87-24272
On the origin of the 40-120 micron emission of galaxy disks: A comparison with H-alpha fluxes N87-24287
Characteristics of UGC galaxies detected by IRAS N87-24304
A simple two-component model for the far-infrared emission from galaxies N87-24314

INTERSTITIALS
Transient enhanced diffusion in ion-implanted silicon [DE87-007659] N87-24207

INVERSIONS
A unified direct-inverse procedure for two-dimensional boundary layers using spline/finite difference discretization [AD-A178223] N87-24140

INVESTIGATION
Flight investigation of the effects of an outboard wing-leading-edge modification on stall/spin characteristics of a low-wing, single-engine, T-tail light airplane [NASA-TP-2691] N87-23614
Flight test evaluation of techniques to predict longitudinal pilot induced oscillations [AD-A179229] N87-23629
Theoretical investigation of 3-D shock wave-turbulent boundary layer interactions, part 5 [AD-A179455] N87-23909

INVISCID FLOW
Application of the viscous-inviscid interaction method to the analysis of airfoil flows at low Reynolds numbers [AD-A177948] N87-23588
Viscous-inviscid interaction with higher-order viscous-flow equations: Applications to three-dimensional bodies [AD-A178264] N87-23924

IODINE
Functionalization of cubane using hypervalent iodine N87-23807

ION ACCELERATORS
Experiments and prospects for induction linac drivers [DE87-006144] N87-23669

ION BEAMS
EIRMA: An Energetic Ion Retarding Mass Analyzer for the BERT-1 (Beam Emission Rocket Test one) [AD-A178231] N87-23694
Generation of broadband noise in the magnetotail [AD-A179135] N87-24034
AXCEL: Interactive simulation program to compute two-dimensional potential distributions of electrostatic arrangements and of ion paths in electrostatic fields under consideration of space charging [DE87-007760] N87-24165
High-current beam dynamics and transport, theory and experiment [DE87-006154] N87-24172
Heavy ion induced upsets in semiconductor devices [ATR-86(8139)-3] N87-24205

ION CURRENTS
EIRMA: An Energetic Ion Retarding Mass Analyzer for the BERT-1 (Beam Emission Rocket Test one) [AD-A178231] N87-23694

ION DENSITY (CONCENTRATION)
Formation and stability of partially-neutralized plasma clumps [AD-A179444] N87-24187

ION ENGINES
Nuclear powered Mars cargo transport mission utilizing advanced ion propulsion [NASA-TM-100109] N87-23692

ION EXCHANGE MEMBRANE ELECTROLYTES
Electrochemical performance and transport properties of a Nafion membrane in a hydrogen-bromine cell environment [NASA-TM-89862] N87-23718

ION EXCHANGING
Electronics and ionic transport in polymers [AD-A178227] N87-23746

ION IMPLANTATION
Electrical behavior of Ge and (Ge + As) implanted gallium arsenide [AD-A179505] N87-24203
Transient enhanced diffusion in ion-implanted silicon [DE87 007659] N87-24207
Characterization of material device structures [AD-A178262] N87-24220

ION MOTION
AXCEL: Interactive simulation program to compute two-dimensional potential distributions of electrostatic arrangements and of ion paths in electrostatic fields under consideration of space charging [DE87-007760] N87-24165

ION PROPULSION
Nuclear powered Mars cargo transport mission utilizing advanced ion propulsion [NASA-TM-100109] N87-23692

ION SOURCES
Experiments and prospects for induction linac drivers [DE87-006144] N87-23669

IONIC DIFFUSION
Transient enhanced diffusion in ion-implanted silicon [DE87-007659] N87-24207

IONIC MOBILITY
Electronics and ionic transport in polymers [AD-A178227] N87-23746

IONIZATION
Comparison of CREME (Cosmic Ray Effects on Microelectronics) model LET (Linear Energy Transfer) spaceflight dosimetry data [AD-A177873] N87-23884

IONIZED GASES
Nuclear star formation on 100 parsec scales: 10' resolution radio continuum, HI and CO observations N87-24322
The initial mass function in HII galaxies N87-24332
Models relating the radio emission and ionised gas in Seyfert nuclei N87-24369

IONIZING RADIATION
Influence of ionizing radiations and electrical overstressings on MOS (Metal-Oxide Semiconductors) devices: A comparison [AD-A178214] N87-23891

IONOSPHERIC PROPAGATION
A new version of MODESRCH using interpolated values of the magnetoionic reflection coefficients [AD-A179094] N87-23822
An ELF (Extremely-Low-Frequency) transmitter experiment for the space shuttle. (The NASC-201 (Naval Air Space Command) experiment). Volume 1 [AD-A178237] N87-23849

IRON
Wavelengths of K X-rays of iron ions [IPPJ-AM-49] N87-24196

IRON ALLOYS
Al and Mg alloys for aerospace applications using rapid solidification and powder metallurgy processing [AD-A179547] N87-23721

IRRADIATION
A mechanistic study of the interaction of ultraviolet laser radiation with low density polymers [DE87-007846] N87-23734
A pulsed electron injector using a metal photocathode irradiated by an excimer laser [DE87-007499] N87-23877

IRREGULAR GALAXIES
IRAS observations of irregular galaxies N87-24299
Erratum: IRAS observations of irregular galaxies N87-24300
IUE observations of luminous blue star associations in irregular galaxies N87-24301
Neutral hydrogen and star formation in irregular galaxies N87-24302
Induced star formation in interacting galaxies N87-24325
Properties of the unusual galaxy PSC 09104+4109 N87-24346
Nuclear infrared emission and the colors of IRAS galaxies N87-24356

J

JET AIRCRAFT
DFVLR in-flight simulators ATTAS and ATTHES for flying qualities and flight control research N87-23657

JET ENGINE FUELS
Trends of petroleum fuels: Topical report [DE87-001237] N87-23755
Opposed jet burner studies of silane-methane, silane-hydrogen and hydrogen diffusion flames with air N87-23791
Functionalization of cubane using hypervalent iodine N87-23807

JET FLOW
Structural analysis of supersonic jet discharging from free-vortex nozzle by method of holographic interferometry with pulsed laser N87-23574
Opposed jet burner studies of silane-methane, silane-hydrogen and hydrogen diffusion flames with air N87-23791

JET MIXING FLOW
Compressibility of submerged supersonic jets
N87-23581

JOINTS (JUNCTIONS)
Development of a high temperature ceramic-to-metal seal for Air Force Weapons Laboratory Laser
[DE87-007711] N87-23949
Ultrasonic techniques for the evaluation of ceramic joints
[DE87-009104] N87-23986
Improved modeling of structural joint damping
[AD-A179111] N87-23988
Identification of structural interface characteristics using component mode synthesis
[NASA-TM-88960] N87-24006

JOSEPHSON JUNCTIONS
Experimental observation of the quantum behavior of a macroscopic degree of freedom
[DE87-008228] N87-24213

JUNCTION TRANSISTORS
Floating emitter solar cell
[NASA-CASE-NPO-16467-1-CU] N87-23879

K

KALMAN FILTERS
A new approach to multitarget tracking using probabilistic data association
[AD-A179437] N87-23825

KEROSENE
Antimisting Fuel (AMK) flight degrader development and aircraft fuel system investigation
[DOT/FAA/CT-86/6] N87-23816

KINEMATICS
Structure and kinematics of the molecular spiral arms in M51 N87-24312

KINETIC EQUATIONS
Polymer dynamics and gelation
[DE87-007578] N87-23748

KIRCHHOFF LAW OF RADIATION
Extension of Kirchhoff's formula to radiation from moving surfaces
[NASA-TM-89149] N87-24160

KNOWLEDGE
Research on knowledge representation, machine learning, and knowledge acquisition
[NASA-CR-180408] N87-24103

L

LABORATORIES
Engineering and instrumentation support of the AFGL (Air Force Geophysics Laboratory) Rocket Research Program
[AD-A179257] N87-23689
Federal laboratory nondestructive testing research and development applicable to industry
[DE87-006351] N87-23985
Sandia National Laboratories 34-meter diameter vertical axis wind turbine test bed
[DE87-003096] N87-24016

LABYRINTH SEALS
Three-step labyrinth seal for high-performance turbomachines
[NASA-TP-1848] N87-23921

LAGRANGE MULTIPLIERS
A consistent finite element formulation of nonlinear frictional contact problems
[AD-A179179] N87-23983

LAKES
Spatial characterization of acid rain stress in Canadian Shield lakes
[NASA-CR-180983] N87-24031
Spatial characterization of acid rain stress in Canadian Shield lakes
[NASA-CR-180982] N87-24032

LAMINAR BOUNDARY LAYER
On the breakdown of the wave packet trailing a turbulent spot in a laminar layer
[AD-A179607] N87-23915

LAMINAR FLOW
Three-dimensional structure of boundary layers in transition to turbulence
[AD-A178247] N87-23908
A redefined hydraulic diameter for laminar flow
[AD-A179511] N87-23914
On the breakdown of the wave packet trailing a turbulent spot in a laminar layer
[AD-A179607] N87-23915
Effective diffusion in laminar convective flows
[DE87-006054] N87-23920
Development of an explicit time marching procedure for laminar and turbulent flow N87-23926

LAMINATES
Fire and heat resistant laminating resins based on malemeido and citraconimido substituted 1 -2,4- and -2,6-diaminobenzenes
[NASA-CASE-ARC-11533-1] N87-23751
The Shock and Vibration Digest, Volume 19, No. 4
N87-23818
Recent advances in the nonlinear analysis of laminated composite plates and shells N87-23819
Time domain wave propagation in multilayered integrated circuits
[AD-A178180] N87-23847
Time-resolved picosecond reflectivity study of laser-excited layered compounds
[DE87-005115] N87-23952

LANDING AIDS
Efficient conduct of individual flights and air traffic or optimum utilization of modern technology for the overall benefit of civil and military airspace users
[AGARD-AR-236] N87-23808

LAPLACE EQUATION
An alternative Laplacian electrostatic field finite element formulation
[DE87-007031] N87-24158

LARGE SPACE STRUCTURES
An integrated, optimization-based approach to the design and control of large space structures
[AD-A179459] N87-23683
Control considerations for high frequency, resonant, power processing equipment used in large systems
[NASA-TM-89926] N87-23690
Modified independent modal space control method for active control of flexible systems
[NASA-CR-181065] N87-23980
Guidelines for noise and vibration levels for the space station
[NASA-CR-178310] N87-24162

LASER APPLICATIONS
A mechanistic study of the interaction of ultraviolet laser radiation with low density polymers
[DE87-007846] N87-23734
CARS approaches to simultaneous measurements of H2 and H2O concentration and temperature in H2-air combustion systems N87-23792
Computer simulation of the lasertron with a ring model
[DE87-007461] N87-23897
Light sheet visualization and velocity field measurements in seeded flows — YAG laser
[ISL-CO-225/86] N87-23935
Midwest free-electron laser program
[AD-A178106] N87-23953
Laser-enhanced electron attachment and its possible application for optical switching
[DE87-008787] N87-23957
Controlled nucleation and growth studies in metal oxide and alkoxide systems by dynamic laser-light-scattering methods
[DE87-009103] N87-23958
Multiplex electric discharge gas laser system
[NASA-CASE-NPO-16433-1] N87-23961

LASER DAMAGE
Laser hazards bibliography, 12 edition
[AD-A179220] N87-23945

LASER DOPPLER VELOCIMETERS
Laser Doppler velocimeter application in supersonic boundary-layer flow
[AD-A178395] N87-23590

LASER FUSION
University of Rochester, Laboratory for Laser Energetics
[DE87-005920] N87-23947

LASER HEATING
A model for silicon dendrite growth during laser/plasma deposition from a silane discharge
[DE87-007579] N87-23733
Midwest free-electron laser program
[AD-A178106] N87-23953
Thermal ignition of pyrotechnics with lasers
[DE87-006245] N87-23955

LASER INDUCED FLUORESCENCE
CN radical distributions in solid propellant flames
N87-23775
The application of imaging laser induced fluorescence to the measurement of HMX and aluminized propellant ignition and deflagration flame structure N87-23782

LASER MATERIALS
Epitaxial semiconductor optical interference devices
[DE87-006890] N87-24212

LASER OUTPUTS
Laser hazards bibliography, 12 edition
[AD-A179220] N87-23945
Experimental and theoretical studies of laser cooling and emittance control of neutral beams
[AD-A179226] N87-23946
Time-resolved picosecond reflectivity study of laser-excited layered compounds
[DE87-005115] N87-23952
Midwest free-electron laser program
[AD-A178106] N87-23953
Multiplex electric discharge gas laser system
[NASA-CASE-NPO-16433-1] N87-23961

LASER PLASMA INTERACTIONS
Role of cavitons in laser-plasma interactions
[DE87-008485] N87-24192

LASER PLASMAS
A model for silicon dendrite growth during laser/plasma deposition from a silane discharge
[DE87-007579] N87-23733
Double-diffraction X-ray imaging camera
[DE87-007936] N87-23940

LASER TARGETS
University of Rochester, Laboratory for Laser Energetics
[DE87-005920] N87-23947

LASER WELDING
Pulsed Nd:YAG laser closure welding of the MC3593/3594 relay
[DE87-007825] N87-23967

LASERS
Means for phase locking the outputs of a surface emitting laser diode array
[NASA-CASE-NPO-16542-1-CU] N87-23960

LATERAL CONTROL
Two blowing concepts for roll and lateral control of aircraft
[NASA-CR-180478] N87-23627
Swashplate control system
[NASA-CASE-ARC-11633-1] N87-23631

LATITUDE
A comparison of ionospheric model predictions with MITHRAS observations
[AD-A179374] N87-24036

LATTICES (MATHEMATICS)
On the existence and convergence of probability measures on continuous semi-lattices
[AD-A179267] N87-24148

LAYOUTS
Complexities of layouts in three-dimensional VLSI (Very Large-Scale Integration) circuits
[AD-A178150] N87-23689

LEAD ALLOYS
In situ HREM observation of interphase boundary motion in 95Pb-5Sn solder
[DE87-007616] N87-23817

LEADING EDGES
Evaluation of Navier-Stokes and Euler solutions for leading-edge separation vortices
[NASA-TM-89458] N87-23584
Flight investigation of the effects of an outboard wing-leading-edge modification on stall/spin characteristics of a low-wing, single-engine, T-tail light airplane
[NASA-TP-2691] N87-23614

LEARNING MACHINES
Research on knowledge representation, machine learning, and knowledge acquisition
[NASA-CR-180408] N87-24103

LEAST SQUARES METHOD
A study of the maximum entropy method of power spectrum estimation as applied to interferometer data
[AD-A179403] N87-23707
Computer programs for nonlinear least squares analysis of various three-dimensional geometrical elements
[DE87-006046] N87-24133
Multicomponent analysis using an array of piezoelectric crystal sensors
[AD-A178012] N87-24216

LEAVES
Error analysis of leaf area estimates made from allometric regression models
[NASA-TM-89220] N87-24010

LECTURES
Short Course on Cardiopulmonary Aspects of Aerospace Medicine
[AGARD-R-758] N87-24070

LEE WAVES
Study of lee-side flows over conically cambered delta wings at supersonic speeds, part 1
[NASA-TP-2680-PT-1] N87-23597

LESIONS
Training, muscle fatigue, and stress fractures
[AD-A178350] N87-24085

LIAPUNOV FUNCTIONS
Detumbling of two inter-connected rigid bodies using Liapunov methods for feedback control
[AD-A179207] N87-23679

LIFE (DURABILITY)
Environmental degradation of 316 stainless steel in high temperature low cycle fatigue
[NASA-TM-89931] N87-24007

A rapid prototyping approach to software validation [AD-A177939] N87-24106
LIFE SCIENCES
The 1986-87 NASA space/gravitational biology accomplishments [NASA-TM-89951] N87-24063
LIFT AUGMENTATION
Two blowing concepts for roll and lateral control of aircraft [NASA-CR-180478] N87-23627
LIGANDS
Metal alkoxides: Models for metal oxides: Alkoxide ligands in early transition metal organometallic chemistry [DE87-007309] N87-23715
LIGHT (VISIBLE RADIATION)
Holographic optical elements formed in light of reduced coherence [AD-A179372] N87-23937
LIGHT EMITTING DIODES
Means for phase locking the outputs of a surface emitting laser diode array [NASA-CASE-NPO-16542-1-CU] N87-23960
LIGHT SCATTERING
Controlled nucleation and growth studies in metal oxide and alkoxide systems by dynamic laser-light-scattering methods [DE87-009103] N87-23958
Geophysical monitoring for climatic change number 14 [PB87-162533] N87-24056
LIGHT TRANSMISSION
Fabry-Perot type optical interference filters [AD-A179394] N87-24174
Parametric frequency upconversion, optical fiber transmission and streak camera recording [DE87-005841] N87-24183
LIMB BRIGHTENING
Radiation transport in dust in disk geometry [NASA-CR-180995] N87-24157
LIMITS (MATHEMATICS)
A generalized procedure for constructing an upwind based TVD scheme [NASA-TM-88926] N87-24132
LINE SPECTRA
A study of the maximum entropy method of power spectrum estimation as applied to interferometer data [AD-A179403] N87-23707
The initial mass function in HII galaxies N87-24332
A dust scattered halo in starburst galaxy M82? N87-24334
A redshift survey of IRAS galaxies N87-24347
The correlation between far-IR and radio continuum emission from spiral galaxies N87-24349
Extragalactic OH megamasers in strong IRAS sources N87-24353
Near-infrared observations of IRAS minisurvey galaxies N87-24354
Ground-based follow up of IRAS galaxies N87-24355
The properties of highly luminous IRAS galaxies N87-24358
The relation between star formation and active nuclei N87-24360
Spectrophotometery of Brackett lines in very luminous IRAS galaxies N87-24367
Spectral classification of emission-line galaxies N87-24374
LINEAR ACCELERATORS
Experiments and prospects for induction linac drivers [DE87-006144] N87-23689
LINEAR ARRAYS
Means for phase locking the outputs of a surface emitting laser diode array [NASA-CASE-NPO-16542-1-CU] N87-23960
LINEAR ENERGY TRANSFER (LET)
Comparison of CREME (Cosmic Ray Effects on Microelectronics) model LET (Linear Energy Transfer) spaceflight dosimetry data [AD-A177873] N87-23884
LINEAR SYSTEMS
Inelastic strain analogy for piecewise linear computation of creep residues in built-up structures [NASA-TM-86813] N87-23995
LINEARITY
Reciprocating linear motor [NASA-CASE-GSC-12773-2] N87-23904
LININGS
Liner cooling research at NASA Lewis Research Center [NASA-TM-100107] N87-23624
LIPIDS
Fuels from microalgae: Technology status, potential and research requirements [DE86-010739] N87-23753
LIPOPROTEINS
Coronary risk factors in aerospace medicine N87-24078
LIQUEFIED GASES
Cost effective use of liquid nitrogen in cryogenic wind tunnels [NASA-CR-178279] N87-23663
LIQUID COOLING
Intercooled gas turbine [PB87-178042] N87-23972
LIQUID CRYSTALS
Electronics and ionic transport in polymers [AD-A178227] N87-23746
LIQUID FLOW
Catastrophic breakup of liquid jet by subsonic transverse gas stream N87-23578
LIQUID FUELS
Effects on fuel spray characteristics and vaporization on energy release rates and flow field structure in a dump combustor N87-23804
LIQUID NITROGEN
Cost effective use of liquid nitrogen in cryogenic wind tunnels [NASA-CR-178279] N87-23663
LIQUID ROCKET PROPELLANTS
Analytical prediction of combustion performance characteristics of bipropellant liquid rocket engine combustor N87-23810
Numerical and experimental studies of atomization and mixing from a coaxial injector element N87-23812
Noninfrusive temperature measurements in SSME preburner element flowfields N87-23813
LIQUID-SOLID INTERFACES
Apparatus and procedure to detect a liquid-solid interface during crystal growth in a bridgman furnace [NASA-CASE-LAR-13597-1-CU] N87-23713
LIQUID-VAPOR INTERFACES
Foam rheology: The linear viscoelastic response of a spatially periodic model [DE87-000960] N87-23731
LITHOGRAPHY
Report of the Second Workshop on Synchrotron Radiation Sources for X-ray Lithography [DE87-002155] N87-24179
LOAD TESTS
Thin film characterization using a mechanical properties microprobe [DE87-008593] N87-24214
LOADS (FORCES)
Training, muscle fatigue, and stress fractures [AD-A178350] N87-24065
LOCAL GROUP (ASTRONOMY)
Neutral hydrogen and star formation in irregular galaxies N87-24302
LOCKHEED AIRCRAFT
Aircraft accident report: Southern Air Transport LOGAIR Flight 51, Lockheed L-382G, Kelly Air Force Base, Texas, October 4, 1986 [PB87-910404] N87-23604
LOGARITHMS
The Shock and Vibration Digest, Volume 19, No. 6 N87-24125
On integrating a logarithmic or semilogarithmic piecewise linear PSD plot of a random variable X(T): Part 1 N87-24126
LOGIC CIRCUITS
Nonlinear real-time optical signal processing [AD-A178169] N87-24182
The development of a prototype CMOS (Complementary Metal Oxide Semiconductor) circuit simulator [AD-A177942] N87-24215
LOGISTICS
Experiments on the cognitive aspects of information seeking and information retrieving [PB87-157699] N87-24238
LONGITUDINAL CONTROL
Swashplate control system [NASA-CASE-ARC-11633-1] N87-23631
LONGITUDINAL STABILITY
An experimental investigation into methods for quantifying hang glider airworthiness parameters [CAR-8705] N87-23613
LOSSES
Measurements for rocket engine performance code verification N87-23811
LOUISIANA
Utilizing remote sensing of thematic mapper data to improve our understanding of estuarine processes and their influence on the productivity of estuarine-dependent fisheries [NASA-CR-180984] N87-24012
LOW ALTITUDE
Utilization of simulation to support F-14A low altitude high angle of attack flight testing N87-23649
LOW FREQUENCIES
Combustion instabilities in dump type ramjet combustors N87-23803
A new version of MODESRCH using interpolated values of the magnetoionic reflection coefficients [AD-A179094] N87-23822
LOW GRAVITY MANUFACTURING
Apparatus ad method for quiescent containerless processing of high temperature metals and alloys in low gravity [NASA-CASE-MFS-28087-1] N87-23944
LOW REYNOLDS NUMBER
Application of the viscous-inviscid interaction method to the analysis of airfoil flows at low Reynolds numbers [AD-A177948] N87-23588
LOW TEMPERATURE
Inelastic properties of ice I/sub h/ at low temperatures and high pressures [DE87-007334] N87-23711
Investigation of electromigration in thin film aluminum at low temperatures [AD-A179110] N87-23871
LOW THRUST PROPULSION
Strategy for exploration of the outer planets: 1986-1998 [NASA-CR-181021] N87-24381
LUMINESCENCE
Assembly and functionalization of supramolecular structures studied by luminescence techniques [AD-A178064] N87-24217
LUMINOSITY
Auroral particles N87-24249
Shock heated dust in L1551: L(IR) greater than 20 solar luminosities N87-24278
Star formation in normal galaxies N87-24285
IRAS and ground-based observations of star formation regions in the Magellanic clouds N87-24296
Star formation in the large Magellanic cloud N87-24297
Infrared emission and excitation in LMC HII regions N87-24298
Carbon monoxide emission from small galaxies N87-24303
Far-infrared properties of cluster galaxies N87-24305
Star formation rates as a function of galaxy mass N87-24308
Global properties of the nearby spiral M101 N87-24309
Modelling the IRAS colors of galaxies N87-24313
Starburst galaxies N87-24319
LUMINOUS INTENSITY
Spatial deconvolution of IRAS galaxies at 60 UM N87-24362
Star formation around active galactic nuclei N87-24363
Evidence for extended IR emission in NGC2798 and NGC6240 N87-24368
Summary of symposium: Low luminosity sources N87-24375
Morphology of luminous IRAS galaxies: Summary talk N87-24376
LUNAR SHADOW
Fifty year canon of solar eclipses: 1986-2035 [NASA-TM-89348] N87-24377
LYMAN ALPHA RADIATION
Infrared emission and excitation in LMC HII regions N87-24298
LYMAN BETA RADIATION
Erratum: IRAS observations of irregular galaxies N87-24300

M

MACH NUMBER
Mach 6 experimental and theoretical stability and performance of a cruciform missile at angles of attack up to 65 degrees [NASA-TP-2733] N87-23592
The supersonic through-flow turbofan for high Mach propulsion [NASA-TM-100114] N87-23626
MAGELLANIC CLOUDS
Star formation in the Magellanic clouds N87-24288
IRAS and ground-based observations of star formation regions in the Magellanic clouds N87-24296
Star formation in the large Magellanic cloud N87-24297
Infrared emission and excitation in LMC HII regions N87-24298
MAGNESIUM ALLOYS
Al and Mg alloys for aerospace applications using rapid solidification and powder metallurgy processing [AD-A179547] N87-23721
MAGNESIUM OXIDES
Sol-Gel synthesis of MgO-SiO2 glass compositions having stable liquid-liquid immiscibility [NASA-TM-89905] N87-23750

MAGNETIC FIELD CONFIGURATIONS
An ELF (Extremely-Low-Frequency) transmitter experiment for the space shuttle. (The NASC-201 (Naval Air Space Command) experiment). Volume 1
[AD-A178237] N87-23849

MAGNETIC FIELDS
The development of a containment vessel and Dewar for the particle astrophysics magnet facility (ASTROMAG)
[NASA-CR-181016] N87-23670
A comparison of ionospheric model predictions with MITHRAS observations
[AD-A179374] N87-24036
Architectural implications of a parallel computational approach to the vector wave equation
[AD-A179510] N87-24113
Auroral particles N87-24249
Mechanisms for the circular polarization of astrophysical OH masers in star-forming regions and the inferred magnetic fields N87-24277

MAGNETIC SIGNATURES
Magnetostatic surface field measurement facility
[AD-A178258] N87-23850

MAGNETOHYDRODYNAMIC STABILITY
Investigation of universal plasma instabilities
[DE87-008276] N87-24193

MAGNETOHYDRODYNAMIC WAVES
Physics of the inner heliosphere: Mechanisms, models and observational signatures
[NASA-CR-181063] N87-24387

MAGNETOHYDRODYNAMICS
Particle propagation channels in the solar wind N87-24252

MAGNETOIONICS
A new version of MODESRCH using interpolated values of the magnetoionic reflection coefficients
[AD-A179084] N87-23822

MAGNETOSPHERE
Comparison of CREME (Cosmic Ray Effects on Microelectronics) model LET (Linear Energy Transfer) spaceflight dosimetry data
[AD-A177873] N87-23884
Generation of broadband noise in the magnetotail
[AD-A179136] N87-24034
A comparison of ionospheric model predictions with MITHRAS observations
[AD-A179374] N87-24036
The joint NASA/Goddard-University of Maryland research program in charged particle and high energy photon detector technology
[NASA-CR-180996] N87-24166
Magnetospheres of the outer planets N87-24248
Particle acceleration in solar flares N87-24250

MAGNETOSTATIC FIELDS
Magnetostatic surface field measurement facility
[AD-A178258] N87-23850

MAGSAT SATELLITES
The Magsat Bibliography
[NASA-TM-87822] N87-24039

MAN MACHINE SYSTEMS
Use of VDU's by flight simulator instructors N87-23641
Trends in ground-based and in-flight simulators for development applications N87-23645
A multiple attribute decision analysis of manned airlock systems
[AD-A179241] N87-23682

MAN-COMPUTER INTERFACE
Text editing performance as a function of screen size
[AD-A179067] N87-24229

MANAGEMENT INFORMATION SYSTEMS
The success or failure of management information systems: A theoretical approach
[DE87-007802] N87-24233

MANEUVERABILITY
Evaluation of the angle of attack limiter of the F-16 C/D aircraft
[AD-A177941] N87-23612
Optimal continuous thrust orbital evasive maneuvers from geosynchronous orbit
[AD-A179413] N87-23668

MANEUVERABLE SPACECRAFT
A quantitative comparison of several orbital maneuvering vehicle configurations for satellite repair/replenishment
[AD-A179106] N87-23677

MANIPULATORS
Choosing sampling rates for robot control
[AD-A179447] N87-24118
Experimental evaluation of nonlinear feedback and feedforward control schemes for manipulators
[AD-A179449] N87-24119
Proposal for continued research in intelligent machines at the Center for Engineering Systems Advanced Research (CESAR) for FY 1988 to FY 1991
[DE87-007789] N87-24121

MANUAL CONTROL
Computer simulation studies on human control reliability in manual aircraft control: The origin of PIO N87-23644

MANUALS
DOD (Department of Defense) Procedures for Management of Information Requirements
[PB87-155495] N87-24227

MANUFACTURING
USSR report: Engineering and equipment
[JPRS-UEQ-87-005] N87-23570
Manufacturing processes for high-temperature structural ceramics: A patent trend analysis
[PB87-178059] N87-23742
Report of the Second Workshop on Synchrotron Radiation Sources for X-ray Lithography
[DE87-002155] N87-24179

MAPPING
The Arp Ring: Galactic or extragalactic? N87-24282
CO observations of galaxies with the Nobeyama 45-M telescope N87-24290
The HII regions in M51: Radio and optical observations N87-24295
Fifty year canon of solar eclipses: 1986-2035
[NASA-TM-89345] N87-24377

MAPS
Global distribution of total cloud cover and cloud type amounts over land
[DE87-006903] N87-24053

MARINE TECHNOLOGY
USSR report: Engineering and equipment
[JPRS-UEQ-87-005] N87-23570
Results of near field probe scanning tests for ultralow sidelobe arrays
[AD-A178141] N87-23846

MARS (PLANET)
Nuclear powered Mars cargo transport mission utilizing advanced ion propulsion
[NASA-TM-100109] N87-23692

MARSHLANDS
Utilizing remote sensing of thematic mapper data to improve our understanding of estuarine processes and their influence on the productivity of estuarine-dependent fisheries
[NASA-CR-180984] N87-24012

MASERS
Mechanisms for the circular polarization of astrophysical OH masers in star-forming regions and the inferred magnetic fields N87-24277

MASS
Star formation rates as a function of galaxy mass N87-24308

MASS BALANCE
Effectiveness of balancing flexible rotary compressor vanes on low-speed balancing machine N87-23580

MASS DISTRIBUTION
Optimization of payload mass placement in a dual keel space station
[NASA-TM-89051] N87-23687
Three-dimensional electric field predictions of an iron-copper galvanic couple
[AD-A178040] N87-23888

MASS FLOW
Starburst-driven superwinds from infrared galaxies N87-24330

MASS SPECTROMETERS
EIRMA: An Energetic Ion Retarding Mass Analyzer for the BERT-1 (Beam Emission Rocket Test one)
[AD-A178231] N87-23694

MASS SPECTROSCOPY
Simultaneous thermogravimetric modulated beam mass spectrometry and time-of-flight velocity spectra measurements of thermal decomposition products from RDX and HMX N87-23780

MASS TRANSFER
Heat transfer research for ocean thermal energy conversion
[DE87-001155] N87-24023

MATCHED FILTERS
Adaptive antennas N87-23865

MATERIALS RECOVERY
Full-scale test program for a shower wastewater recycling system: Technical evaluation
[AD-A178061] N87-24087
The field shower wastewater recycling system: Development of a program of instruction and preliminary analysis of its potential health implications
[AD-A178112] N87-24088

MATHEMATICAL MODELS
Mathematical model describing interaction of single nonsteady supersonic jet and movable barrier of finite dimensions N87-23575
Development of model describing unstable operation of turbocompressor and design of antisurging protection for gas turbine engine N87-23577
Aircraft Dynamic Response to Damaged and Repaired Runways
[AGARD-R-739] N87-23609
An experimental-analytical routine for the dynamic qualification of aircraft operating on rough runway surfaces N87-23611
The Shock and Vibration Digest, Volume 19, No. 5 N87-23620
Correlation between flight simulation and processing of flight tests based on inertial measurements N87-23655
An analysis of space station motion subject to the parametric excitation of periodic elevator motion
[AD-A179235] N87-23681
Foam rheology: The linear viscoelastic response of a spatially periodic model
[DE87-000960] N87-23731
Three-dimensional model for the linear elastic properties of a foam
[DE87-000984] N87-23732
Asymptotic models for solid propellant combustion and the onset of intrinsic instability N87-23764
Chemical kinetics combustion model of the NG/binder system N87-23773
Numerical simulation of combustion processes of mobile stick-propellant bundles N87-23785
Effects of test facility contaminants on supersonic hydrogen-air diffusion flames N87-23790
Downstream boundary effects on the frequency of self-excited oscillations in transonic diffuser flows N87-23794
Linear coupling of acoustics and entropy and acoustic stability in ramjet combustion chambers containing a plane flame N87-23795
Analysis of pressure oscillations in ramjets. Review of research: 1985-1986 N87-23796
Acoustic response of turbulent reacting recirculatory flows N87-23799
Computational studies of the effects of acoustics and chemistry on the flow field in an axisymmetric ramjet combustor N87-23801
Numerical simulations of cold flow in a ramjet dump combustor with a choked exit nozzle N87-23802
Combustion instabilities in dump type ramjet combustors N87-23803
Spray combustion: A driving mechanism for ramjet combustion instability N87-23805
Combustion, vaporization, and microexplosion of droplets of organic azides N87-23806
Analytical prediction of combustion performance characteristics of bipropellant liquid rocket engine combustor N87-23810
Numerical and experimental studies of atomization and mixing from a coaxial injector element N87-23812
Single and multiple electromagnetic scattering by dielectric obstacles from a resonance perspective
[DE87-007347] N87-23843
Complexities of layouts in three-dimensional VLSI (Very Large-Scale Integration) circuits
[AD-A178150] N87-23889
Preliminary thermal analysis of transistor packages
[DE87-007708] N87-23898
Turbulent boundary layer structure, drag reduction
[AD-A179246] N87-23907
Multidimensional modeling of convective heat transfer with application to I.C. engines
[DE87-002939] N87-23922
Modeling of dilute two-phase multispecies solid/gas flows
[DE87-009254] N87-23932
Thermomechanical effects in high-speed seal rubs
[NASA-CR-180418] N87-23979
Retardation effect in fatigue crack growth under stationary stochastic loading
[REPT-43/1986] N87-23999
An atmospheric correction algorithm for remote identification of non-Lambertian surfaces and its range of validity
[DE87-006059] N87-24011
The specification of lateral boundary conditions in three-dimensional mesoscale numerical models
[AD-A179185] N87-24046
Mid-latitude wind probability model
[AD-A179256] N87-24048
A preliminary evaluation of the performance of wind tunnel and numerical modeling simulations of the wind flow over a wind farm
[DE87-004634] N87-24051
User's manual for the convective cloud module version 1.0
[DE87-008343] N87-24058
Hardware synthesis from specification with polynomials
[TRITA-NA-8506] N87-24091
Numerical prediction of 1-D ablation using a finite control volume procedure with exponential differencing
[DE87-007947] N87-24130

Status of phenomenological modeling
[DE87-004922] N87-24143
Min-max bias robust M-estimates of scale
[AD-A179255] N87-24147
An introduction to structured modeling, revision
[AD-A179355] N87-24153
Semiempirical studies of atomic structure
[DE87-007320] N87-24164
Thermal fracture in selected nonlinear optical materials
[DE87-008213] N87-24209
Development of a theoretical model for annealing of radiation damage in semiconductor devices
[NASA-CR-180394] N87-24211
Systems model for natural gas vehicle fleets
[PB87-178083] N87-24245
Particle acceleration in solar flares N87-24250

MATRICES (MATHEMATICS)
Gaussian elimination with partial pivoting and load balancing on a multiprocessor
[DE87-007784] N87-24093
LU factorization algorithms on distributed-memory multiprocessor architectures
[DE87-007794] N87-24100
An extended set of FORTRAN basic linear algebra subprograms: Model implementation and test programs
[DE87-007913] N87-24101
Numerical prediction of 1-D ablation using a finite control volume procedure with exponential differencing
[DE87-007947] N87-24130
AMG (Algebraic Multigrid): Basic development, applications and theory
[AD-A178222] N87-24139

MATRIX MATERIALS
Ceramic fibre/glass matrix composites with outstanding mechanical performance
[AERE-R-12025] N87-23699

MAXIMUM ENTROPY METHOD
A study of the maximum entropy method of power spectrum estimation as applied to interferometer data
[AD-A179403] N87-23707

MAXIMUM LIKELIHOOD ESTIMATES
Estimation of parameters in latent class models with constraints on the parameters
[AD-A178196] N87-24138

MECHANICAL DEVICES
The Shock and Vibration Digest, Volume 19, No. 6
N87-24125

MECHANICAL ENGINEERING
Optimization of extended relational database systems
[AD-A179308] N87-24230

MECHANICAL PROPERTIES
Acta aeronautica et astronautica sinica
[AD-A179673] N87-23618
Ceramic fibre/glass matrix composites with outstanding mechanical performance
[AERE-R-12025] N87-23699
Mechanical properties of undirectional and fabric graphite/epoxy composites
[SAND-86-0784] N87-23702
Poly (pyrrolium anion) studies: Electrochemical synthesis and physical behavior
[AD-A178097] N87-23743
Thin film characterization using a mechanical properties microprobe
[DE87-008593] N87-24214

MECHANICAL SHOCK
The Shock and Vibration Digest, Volume 19, No. 5
N87-23620
The Shock and Vibration Digest, Volume 19, No. 3
N87-23996

MEDICAL SCIENCE
Medical research programs, past and future, for designing atmospheres to retard fires
[AD-A178354] N87-24089

MELTS (CRYSTAL GROWTH)
Microscale defect kinetics in melt-grown GaAs
[AD-A178158] N87-24218

MEMORY (COMPUTERS)
LU factorization algorithms on distributed-memory multiprocessor architectures
[DE87-007794] N87-24100
Investigations into the pattern processing capabilities of associative nets
[TRITA-NA-8601] N87-24114
Content-addressable memory: Applications, algorithms, and simulation
[AD-A177944] N87-24120

MESH
Intermediate level computer vision processing algorithm development for the content addressable array parallel processor
[AD-A179515] N87-24090

MESOSCALE PHENOMENA
The specification of lateral boundary conditions in three-dimensional mesoscale numerical models
[AD-A179185] N87-24046

MESSAGE PROCESSING
Communication-efficient parallel graph algorithms
[AD-A178266] N87-23853

METAL BONDING
Development of a high temperature ceramic-to-metal seal for Air Force Weapons Laboratory Laser
[DE87-007711] N87-23949

METAL FILMS
Corrosion sensing with acoustic wave devices
[DE87-003516] N87-23723
Plasma deposition of tungsten
[DE87-007390] N87-23724

METAL FOILS
Low energy ignition of HMX using a foil bridge
[DE87-004211] N87-23754

METAL FUELS
Metallized fuel burning characteristics in the solid fuel ramjet N87-23788

METAL JOINTS
The corrosion of Al 7075-T6 alloy coupled to Ti 6A 1-4V in wet air
[DE87-008347] N87-23726

METAL OXIDE SEMICONDUCTORS
Influence of ionizing radiations and electrical overstressings on MOS (Metal-Oxide Semiconductors) devices: A comparison
[AD-A178214] N87-23691
Noise characteristics of MOS (Metal-Oxide Semiconductors) devices degraded by electrical overstressings
[AD-A178217] N87-23892
Palladium-silver and gold alloys as catalytic gates on MIS gas sensors
[DE87-006959] N87-23943
Study of quantum mechanical effects in deep submicron, grating-gate field effect transistors
[AD-A179617] N87-24204
Solid state research
[AD-A178394] N87-24221

METAL OXIDES
Metal alkoxides: Models for metal oxides: Alkoxide ligands in early transition metal organometallic chemistry
[DE87-007309] N87-23715
Oxidation protection coatings for polymers
[NASA-CASE-LEW-14072-3] N87-23736

METAL SURFACES
Corrosion sensing with acoustic wave devices
[DE87-003516] N87-23723

METALLIC PLASMAS
Plasma deposition of tungsten
[DE87-007390] N87-23724

METALLIZING
Development of a high temperature ceramic-to-metal seal for Air Force Weapons Laboratory Laser
[DE87-007711] N87-23949

METALS
Metals and Ceramics Division
[DE87-008548] N87-23697
The use of molecular dynamics for the thermodynamic properties of simple and transition metals
[DE87-007718] N87-23725
Ultrasonic techniques for the evaluation of ceramic joints
[DE87-009104] N87-23986

METEOROLOGICAL CHARTS
Global distribution of total cloud cover and cloud type amounts over land
[DE87-006903] N87-24053

METEOROLOGY
Geophysical monitoring for climatic change number 14
[PB87-162533] N87-24056
Meso gamma-scale kinetic energy budgets of a thunderstorm within a squall-line derived from sesame dual-doppler data
[AD-A178119] N87-24057

METHOD OF MOMENTS
Evaluation of a thin-slot formalism for finite-difference time-domain electromagnetics codes
[DE87-008078] N87-23857

METHODOLOGY
Certification testing methodology for composite structure. Volume 1: Data analysis
[NADC-87042-60-VOL-1] N87-23705
Certification testing methodology for composite structure. Volume 2: Methodology development
[NADC-87042-60-VOL-2] N87-23706

METHYL ALCOHOL
A comparison of unburned fuel and aldehyde emissions from a methanol-fueled stratified charge and homogeneous charge engine
[DE87-007793] N87-23966

MICROANALYSIS
Multicomponent analysis using an array of piezoelectric crystal sensors
[AD-A178012] N87-24216

MICROELECTRONICS
Finite element analysis of slow-wave Schottky contact printed lines
[AD-A179259] N87-23873
Wetting properties of Au/Sn solders for microelectronics
[DE87-008519] N87-23883
Comparison of CREME (Cosmic Ray Effects on Microelectronics) model LET (Linear Energy Transfer) spaceflight dosimetry data
[AD-A177873] N87-23884
Two-stage hybrid microcircuit amplifier
[DE87-009092] N87-23899
Development of a theoretical model for annealing of radiation damage in semiconductor devices
[NASA-CR-180394] N87-24211

MICROHARDNESS
Thin film characterization using a mechanical properties microprobe
[DE87-008593] N87-24214

MICROMECHANICS
Three-dimensional model for the linear elastic properties of a foam
[DE87-000984] N87-23732

MICROORGANISMS
Fuels from microalgae: Technology status, potential and research requirements
[DE86-010739] N87-23753

MICROSTRIP TRANSMISSION LINES
Printed circuit antenna technology N87-23867

MICROSTRUCTURE
Study of the influence of metallurgical factors on fatigue and fracture of aerospace structural materials
[AD-A179268] N87-23720
Fundamentals of sol-gel thin film formation
[DE87-007387] N87-23738
In situ HREM observation of interphase boundary motion in 95Pb-5Sn solder
[DE87-007616] N87-23817

MICROWAVE AMPLIFIERS
High-powered, solid-state rf systems
[DE87-007457] N87-23896
Preliminary thermal analysis of transistor packages
[DE87-007708] N87-23898

MICROWAVE ANTENNAS
Microwave Antennas for Avionics
[AGARD-LS-151] N87-23859
Aircraft antennas/conformal antennas missile antennas N87-23862
Millimeter wave antennas for avionics N87-23864
MIC technology for phased arrays N87-23866
Printed circuit antenna technology N87-23867

MICROWAVE CIRCUITS
MIC technology for phased arrays N87-23866
Optically controlled microwave devices and circuits: Emerging applications in space communications systems
[NASA-TM-89869] N87-23900

MICROWAVE COUPLING
Microwave coupling inside complex systems
[DE87-003505] N87-23841

MICROWAVE EMISSION
Microwave production from a plasma driven by a high power relativistic electron beam
[DE87-003518] N87-24194

MICROWAVE EQUIPMENT
Finite element analysis of slow-wave Schottky contact printed lines
[AD-A179259] N87-23873
Optically controlled microwave devices and circuits: Emerging applications in space communications systems
[NASA-TM-89869] N87-23900

MICROWAVE FREQUENCIES
An evaluation of the communication system for the TAU mission study N87-23840

MICROWAVE SENSORS
A dual-processor multi-frequency implementation of the FINDS algorithm
[NASA-CR-178252] N87-23617

MICROWAVES
Microwave component time delays for the 70-meter antennas N87-23835
Hazards evaluation of radiofrequency and microwave radiation
[DE87-008536] N87-24061
Role of cavitons in laser-plasma interactions
[DE87-008485] N87-24192

MILITARY AIR FACILITIES
Otis ANGB (Air National Guard Base) visibility sensor field test study
[AD-A179176] N87-24045

MILITARY OPERATIONS
Automated radar image analysis research in support of military needs
[AD-A179615] N87-23827
Confidence interval for parameter n in a binomial distribution
[AD-A178325] N87-24151
MILITARY SPACECRAFT
Optimal continuous thrust orbital evasive maneuvers from geosynchronous orbit
[AD-A179413] N87-23668
MILITARY TECHNOLOGY
Aircraft Dynamic Response to Damaged and Repaired Runways
[AGARD-R-739] N87-23609
Spacecraft environment interaction investigation
[AD-A179183] N87-23678
Future directions of C3 research at DARPA (Defense Advanced Research Projects Agency)
[DE87-007501] N87-23948
Standardized procedure for system safety input to the Defense Technical Information Center (DTIC)
[AD-A178246] N87-24239
MILKY WAY GALAXY
Masses, luminosities and dynamics of galactic molecular clouds N87-24270
Survey of the galactic disk from 1 = -150 deg to 1 = 82 deg in the submillimeter range N87-24278
MILLIMETER WAVES
Measurement of solid-propellant burn rate using millimeter-wave techniques N87-23770
Research in millimeter wave techniques
[NASA-CR-181026] N87-23858
Millimeter wave antennas for avionics N87-23864
Printed circuit antenna technology N87-23867
Maps of millimeter wave emission from three galactic star-forming regions N87-24275
MIMD (COMPUTERS)
The hypercube as a supercomputer
[DE87-005029] N87-24092
MINICOMPUTERS
DATA: A comprehensive data analysis environment for HP1000 computers
[DE87-007824] N87-24094
MIS (SEMICONDUCTORS)
Palladium-silver and gold alloys as catalytic gates on MIS gas sensors
[DE87-006959] N87-23943
MISSILE ANTENNAS
Basic parameters of antennas for aircraft, satellites and missiles N87-23860
Aircraft antennas/conformal antennas missile antennas N87-23862
MISSILE DEFENSE
Satellite allocation for boost-phase missile intercepts
[DE87-007719] N87-24155
MISSILES
Mach 6 experimental and theoretical stability and performance of a cruciform missile at angles of attack up to 65 degrees
[NASA-TP-2733] N87-23582
MISSION PLANNING
Actions to implement the recommendations of the Presidential Commission on the Space Shuttle Challenger accident: Executive summary N87-23676
MIXERS
Research in millimeter wave techniques
[NASA-CR-181026] N87-23858
MIXING
Numerical and experimental studies of atomization and mixing from a coaxial injector element N87-23812
Direct numerical simulations of a temporally evolving mixing layer subject to forcing
[NASA-TM-88896] N87-23933
MIXTURES
Viscosity of synfuel compounds and mixtures
[DE87-006696] N87-23756
MOBILE COMMUNICATION SYSTEMS
Spread spectrum mobile radio communications
[AD-A179446] N87-23826
A multi user random access communication system for users with different priorities
[AD-A178372] N87-23854
MOBILITY
On autonomous terrain model acquisition by a mobile robot
[DE87-005719] N87-23964
MODELS
Preliminary performance characterizations of an engineering model multipropellant resistojet for space station application
[NASA-TM-100113] N87-23821
Analysis of jitter in a digital transmission system
[AD-A177945] N87-23844
MODFETS
Fabrication of AlGaAs/InGaAs pseudomorphic modulation doped field effect transistors with p-doped surface layers
[AD-A179230] N87-24201
MODULUS OF ELASTICITY
Foam rheology: The linear viscoelastic response of a spatially periodic model
[DE87-000960] N87-23731
Investigation of the impact performance of various glass and ceramic systems
[AD-A178115] N87-23744
MOISTURE
The corrosion of Al 7075-T6 alloy coupled to Ti 6A 1-4V in wet air
[DE87-008347] N87-23726
MOLECULAR BEAM EPITAXY
The structure of Al/GaAs interfaces
[DE87-007181] N87-24206
MOLECULAR CLOUDS
High energy gamma ray astronomy N87-24258
Infrared astronomy N87-24264
Star Formation in Galaxies
[NASA-CP-2466] N87-24266
Masses, luminosities and dynamics of galactic molecular clouds N87-24270
Star formation in Carina OB1: Observations of a giant molecular cloud associated with the eta Carinae Nebula N87-24272
Star forming regions of the southern galaxy N87-24273
On the redistribution of OB star luminosity and the warming of nearby molecular clouds N87-24274
Maps of millimeter wave emission from three galactic star-forming regions N87-24275
Diffuse infrared emission of the galaxy: Large scale properties N87-24279
The large scale gas and dust distribution in the galaxy: Implications for star formation N87-24280
Infrared properties of dust grains derived from IRAS observations N87-24283
IRAS observations of the Pleiades N87-24284
Models for infrared emission from IRAS galaxies N87-24286
CO observations of nearby galaxies and the efficiency of star formation N87-24291
Efficient star formation in the bright bar of M83 N87-24310
Large scale dissociation of molecular gas in the sprial arms of M51 N87-24311
Structure and kinematics of the molecular spiral arms in M51 N87-24312
A simple two-component model for the far-infrared emission from galaxies N87-24314
Detection of CO (J=1-0) in the dwarf elliptical galaxy NGC 185 N87-24315
A simple theory of bimodal star formation N87-24317
Star formation and dynamics in starburst nuclei N87-24324
The azimuthal and radial distributions of HI and H2 in NGC 6946 N87-24335
MOLECULAR ENERGY LEVELS
Force-field parameters and molecular mechanics calculations for nitramines N87-23779
Energy conversion processes based on molecular excited states
[DE87-007408] N87-24020
Heats of formation, structure and heteroatom ((17)O, (33)S) NMR studies of organosulfur molecules, radicals and ions
[DE87-006361] N87-24189
MOLECULAR EXCITATION
Energy conversion processes based on molecular excited states
[DE87-007408] N87-24020
MOLECULAR GASES
Large scale dissociation of molecular gas in the sprial arms of M51 N87-24311
Structure and kinematics of the molecular spiral arms in M51 N87-24312
Molecular gas in the starburt nucleus of M82 N87-24321
Ultraluminous infrared galaxies N87-24327
Interferometric CO observations of the ultraluminous IRAS galaxies ARP 220, IC 694/NGC 3690, NGC 6420 and NGC 7469 N87-24331
MOLECULAR IONS
Heats of formation, structure and heteroatom ((17)O, (33)S) NMR studies of organosulfur molecules, radicals and ions
[DE87-006361] N87-24189
MOLECULAR PHYSICS
The use of molecular dynamics for the thermodynamic properties of simple and transition metals
[DE87-007718] N87-23725
MOLECULAR SPECTRA
Detection of CO (J=1-0) in the dwarf elliptical galaxy NGC 185 N87-24315
MOLECULAR SPECTROSCOPY
Heats of formation, structure and heteroatom ((17)O, (33)S) NMR studies of organosulfur molecules, radicals and ions
[DE87-006361] N87-24189
MOLECULAR STRUCTURE
Poly (pyrrolium anion) studies: Electrochemical synthesis and physical behavior
[AD-A178097] N87-23743
Force-field parameters and molecular mechanics calculations for nitramines N87-23779
JSEP (Joint Services Electronics Program)
[AD-A177881] N87-23885
Heats of formation, structure and heteroatom ((17)O, (33)S) NMR studies of organosulfur molecules, radicals and ions
[DE87-006361] N87-24189
Evaluation of Tersoff's revised silicon potential in a molecular dynamic simulation of solid silicon
[AD-A179231] N87-24202
MOLTEN SALTS
Review of interactions of large solar fluxes with materials
[DE87-001156] N87-24024
Fluoride salts and container materials for thermal energy storage applications in the temperature range 973 to 1400 K
[NASA-TM-89913] N87-24026
MOMENTS OF INERTIA
An analysis of space station motion subject to the parametric excitation of periodic elevator motion
[AD-A179235] N87-23681
MOMENTUM TRANSFER
Experimental and numerical investigation of coherent structures
[AD-A179456] N87-23910
MONATOMIC GASES
The azimuthal and radial distributions of HI and H2 in NGC 6946 N87-24335
MONITORS
Corrosion sensing with acoustic wave devices
[DE87-003516] N87-23723
The fiber optic refrigeration cycle monitor
[DE87-006632] N87-24180
MONOCHROMATORS
SPECOL: A colorimetric measurement system
[BBC-RD-1987/4] N87-23942
MONOMERS
Synthesis of model polymers and related structures in support of vinyl monomer grafting studies
[DE87-007406] N87-23739
Assembly and functionalization of supramolecular structures studied by luminescence techniques
[AD-A178064] N87-24217
MONOPROPELLANTS
Chemical kinetics combustion model of the NG/binder system N87-23773
MONTE CARLO METHOD
Effective diffusion in laminar convective flows
[DE87-008054] N87-23920
MORPHOLOGY
Perception and structural analysis of morphologies
[ENST-86D004] N87-24086
IRAS colors of VLA identified objects in the galaxy N87-24271
Shock heated dust in L1551: L(IR) greater than 20 solar luminosities N87-24276
Stellar bars and the spatial distribution of infrared luminosity N87-24293
IUE observations of luminous blue star associations in irregular galaxies N87-24301
Large scale dissociation of molecular gas in the sprial arms of M51 N87-24311
Infrared spectroscopy of star formation in galaxies N87-24320
MOTION PERCEPTION
Simulator motion characteristics and perceptual fidelity N87-23639
The perception of the higher derivatives of visual motion
[AD-A179627] N87-24069
MOTION SICKNESS
An analysis of space station motion subject to the parametric excitation of periodic elevator motion
[AD-A179235] N87-23681
MOTION SIMULATION
Simulation of aircraft behaviour on and close to the ground: Summary of AGARD-lc6)ograph AG-285 N87-23640
Unusual airborne simulator applications N87-23656
Collected flight and simulation comparisons and considerations N87-23660

MOTION SIMULATORS
Flight Simulation
[AGARD-CP-408] N87-23833
Visual and motion cueing in helicopter simulation N87-23634
The application of optimal control techniques to the UTIAS research simulator N87-23637
Progress in the implementation of AGARD-AR-144 in motion system assessment and monitoring N87-23642
Piloted simulation in the development of the XV-15 tilt rotor research aircraft N87-23646

MOTOR VEHICLES
Systems model for natural gas vehicle fleets
[PB87-176083] N87-24245

MOUNTAINS
Radar as a complement to topographic maps for delineating marine terraces
[PB87-154597] N87-24013

MOUNTING
Adjustable mount for electro-optic transducers in an evacuated cryogenic system
[NASA-CASE-LAR-13100-1] N87-23962

MULTIBEAM ANTENNAS
Spacecraft multi-beam and contoured-beam antennas N87-23863

MULTIPLE BEAM INTERVAL SCANNERS
Spacecraft multi-beam and contoured-beam antennas N87-23863

MULTIPLEXING
Analysis of jitter in a digital transmission system
[AD-A177945] N87-23844

MULTIPROCESSING (COMPUTERS)
Flexible and high quality software on a multiprocessor computer system controlling a research flight simulator N87-23643
Gaussian elimination with partial pivoting and load balancing on a multiprocessor
[DE87-007784] N87-24093
Research aspects of rapid prototyping
[AD-A179007] N87-24097
LU factorization algorithms on distributed-memory multiprocessor architectures
[DE87-007794] N87-24100
Beyond Speedup: Performance analysis of parallel programs
[DE87-007954] N87-24115

MULTISENSOR APPLICATIONS
Target segmentation and image enhancement through multisensor data fusion
[AD-A178875] N87-24178

MUSCULAR FATIGUE
Training, muscle fatigue, and stress fractures
[AD-A178350] N87-24085

N

NASA PROGRAMS
National Aeronautics and Space Administration Authorization Act
[S-REPT-100-87] N87-24240
National Aeronautics and Space Administration — appropriations bill H.R. 2783 N87-24242
National Aeronautics and Space Administration Authorization Act, 1988
[S-REPT-100-87] N87-24243

NASA SPACE PROGRAMS
Research and technology
[NASA-TM-89193] N87-24392

NATIONAL AIRSPACE SYSTEM
Development of an air ground data exchange concept: Flight deck perspective
[NASA-CR-4074] N87-23607

NAVIER-STOKES EQUATION
Calculation of axisymmetric flow in swirlers by difference method N87-23579
Evaluation of Navier-Stokes and Euler solutions for leading-edge separation vortices
[NASA-TM-89458] N87-23584
Some aspects of vortex flows determined from the thin-layer Navier-Stokes equations
[NASA-TM-88375] N87-23595
Downstream boundary effects on the frequency of self-excited oscillations in transonic diffuser flows N87-23794
Acoustic response of turbulent reacting recirculatory flows N87-23799
Development of a finite volume time marching method
[JM/85-3] N87-23927
An explicit finite-volume time-marching procedure for turbulent flow calculations N87-23928
Explicit finite-volume time-marching calculations of total temperature distributions in turbulent flow N87-23929

NAVIGATION
On autonomous terrain model acquisition by a mobile robot
[DE87-005719] N87-23964
Proposal for continued research in intelligent machines at the Center for Engineering Systems Advanced Research (CESAR) for FY 1988 to FY 1991
[DE87-007789] N87-24121

NEAR INFRARED RADIATION
A near-infrared study of the luminous merging galaxies NGC 2623 and ARP 148 N87-24339
Near-infrared observations of IRAS minisurvey galaxies N87-24354
Ground-based follow up of IRAS galaxies N87-24355

NEBULAE
Star formation in Carina OB1: Observations of a giant molecular cloud associated with the eta Carinae Nebula N87-24272
Infrared emission and excitation in LMC HII regions N87-24298
IRAS observations of irregular galaxies N87-24299

NEODYMIUM LASERS
University of Rochester, Laboratory for Laser Energetics
[DE87-005920] N87-23947
Pulsed Nd:YAG laser closure welding of the MC3593/3594 relay
[DE87-007825] N87-23967

NEOPLASMS
Biomedical applications of the free electron laser
[AD-A179182] N87-24066

NEPTUNE (PLANET)
Magnetospheres of the outer planets N87-24248

NEURAL NETS
Investigations into the pattern processing capabilities of associative nets
[TRITA-NA-8601] N87-24114

NEUTRAL GASES
Neutral hydrogen and star formation in irregular galaxies N87-24302
Nuclear star formation on 100 parsec scales: 10' resolution radio continuum, HI and CO observations N87-24322

NEUTRAL SHEETS
Studies of the interplanetary magnetic field: IMP's to Voyager N87-24253

NEUTRON EMISSION
Neutron stars as cosmic neutron matter laboratories
[DE87-007468] N87-24379

NEUTRON STARS
High energy gamma ray astronomy N87-24258
Neutron stars as cosmic neutron matter laboratories
[DE87-007468] N87-24379

NICKEL HYDROGEN BATTERIES
Cost reductions in the nickel/hydrogen battery
[DE87-007576] N87-23881
Test results of a 60 volt bipolar nickel-hydrogen battery
[NASA-TM-89927] N87-24029

NICKEL IRON BATTERIES
Worldwide nickel/iron battery development for electric vehicle applications
[DE87-004822] N87-23876

NIGHT
A new version of MODESRCH using interpolated values of the magnetoionic reflection coefficients
[AD-A179094] N87-23822

NITRAMINE PROPELLANTS
Influence of two-phase flow in the deflagration of homogeneous solids N87-23777
Force-field parameters and molecular mechanics calculations for nitramines N87-23779
Quantum chemical calculations of the decomposition of nitramines: Thermochemistry and reaction pathways N87-23781
The application of imaging laser induced fluorescence to the measurement of HMX and aluminized propellant ignition and deflagration flame structure N87-23782
Thermal decomposition and ignition of a series of new nitramine lova propellants by CO2 laser N87-23783

NITRIC OXIDE
Laser studies of chemical dynamics at the gas-solid interface
[DE87-005950] N87-23710

NITRILES
Cellular monotectic model solidification
[NASA-CR-181027] N87-23717

NITROGEN
Multispecies CARS measurements in turbulent combustion N87-23808

NITROGEN POLYMERS
Spin-cast carbon films from polyacrylonitrile
[DE87-002489] N87-23703

NITROGLYCERIN
Chemical kinetics combustion model of the NG/binder system N87-23773

NITROUS OXIDES
Medium- and long-wave infrared absorption spectra of carbon dioxide nitrous oxide at 800K
[AD-A179430] N87-23708

NOISE
Guidelines for noise and vibration levels for the space station
[NASA-CR-178310] N87-24182

NOISE PREDICTION (AIRCRAFT)
Coupled aerodynamic and acoustical predictions for turboprops
[NASA-TM-87094] N87-23598

NOISE REDUCTION
Adaptive noise reduction in aircraft communication systems
[AD-A178267] N87-23851

NOISE TEMPERATURE
Use of a 2.3-GHz traveling-wave maser on the Usuda 64-meter antenna N87-23831

NONDESTRUCTIVE TESTS
Federal laboratory nondestructive testing research and development applicable to industry
[DE87-008351] N87-23985
Forced vibration as a method for determining structural integrity
[DE87-005878] N87-23992

NONLINEAR EQUATIONS
Selection principles and pattern formation in fluid mechanics and nonlinear shell theory
[NASA-CR-180941] N87-23916
Uniqueness of non-negative solutions of a class of semi-linear elliptic equations
[DE87-006966] N87-24128
Computer programs for nonlinear least squares analysis of various three-dimensional geometrical elements
[DE87-008046] N87-24133
Singularity structure of nonlinear ordinary and partial differential equations
[DE87-008242] N87-24134
Upwind and symmetric shock-capturing schemes
[NASA-TM-89464] N87-24145

NONLINEAR FEEDBACK
Experimental evaluation of nonlinear feedback and feedforward control schemes for manipulators
[AD-A179449] N87-24119

NONLINEAR OPTICS
Solid state research
[AD-A178394] N87-24221

NONLINEAR SYSTEMS
Selection principles and pattern formation in fluid mechanics and nonlinear shell theory
[NASA-CR-180941] N87-23916
PRONTO 2D: A two-dimensional transient solid dynamics program
[DE87-007823] N87-23993
The Shock and Vibration Digest, Volume 19, No. 3 N87-23996
Random vibration of nonlinear systems N87-23997

NONLINEARITY
Recent advances in the nonlinear analysis of laminated composite plates and shells N87-23819
A consistent finite element formulation of nonlinear frictional contact problems
[AD-A179179] N87-23963
A generalized procedure for constructing an upwind based TVD scheme
[NASA-TM-88926] N87-24132
Thermal fracture in selected nonlinear optical materials
[DE87-008213] N87-24209

NOZZLE DESIGN
Passive shear-flow control to minimize ramjet combustion instabilities N87-23798
Vortex-nozzle interactions in ramjet combustors N87-23800

NOZZLE FLOW
Structural analysis of supersonic jet discharging from free-vortex nozzle by method of holographic interferometry with pulsed laser N87-23574
Flow of gas through turbine stage with spherical nozzle segment N87-23582
Investigation of shrouded nozzle exit pressure changes
[AD-A179477] N87-23911

NOZZLE GEOMETRY
Effect of a trade between boattail angle and wedge size on the performance of a nonaxisymmetric wedge nozzle
[NASA-TP-2717] N87-23593
Experimental thrust performance of a high area-ratio rocket nozzle N87-23809

NOZZLE WALLS
Investigation of shrouded nozzle exit pressure changes
[AD-A179477] N87-23911

NUCLEAR ELECTRIC PROPULSION
Nuclear powered Mars cargo transport mission utilizing advanced ion propulsion
[NASA-TM-100109] N87-23692
NUCLEAR FUSION
Report to DOE of the fusion programs in applied plasma physics and development and technology at GA Technologies, Incorporated
[DE87-008882] N87-24197
Nucleosynthesis and astrophysical gamma ray spectroscopy N87-24259
Gamma ray transients N87-24260
NUCLEAR MAGNETIC RESONANCE
Heats of formation, structure and heteroatom ((17)O, (33)S) NMR studies of organosulfur molecules, radicals and ions
[DE87-006361] N87-24189
NUCLEAR POWER PLANTS
Finite-difference program for hydrogen diffusion: Example problems manual
[DE87-007515] N87-23712
NUCLEAR POWER REACTORS
USSR report: Engineering and equipment
[JPRS-UEQ-87-005] N87-23570
NUCLEAR RADIATION
Satellite observation of atmospheric nuclear gamma radiation
[AD-A177937] N87-24389
NUCLEAR REACTORS
A study of Schwarz converters for nuclear powered spacecraft
[NASA-TM-89911] N87-23903
NUCLEAR RESEARCH
Fusion Energy Postdoctoral Research Program and Professional Development Program
[DE87-006350] N87-24188
Report to DOE of the fusion programs in applied plasma physics and development and technology at GA Technologies, Incorporated
[DE87-008882] N87-24197
NUCLEATION
Investigation of the impact performance of various glass and ceramic systems
[AD-A178115] N87-23744
Controlled nucleation and growth studies in metal oxide and alkoxide systems by dynamic laser-light-scattering methods
[DE87-009103] N87-23958
NUCLEON-NUCLEON INTERACTIONS
Study of minimum bias trigger events in the p(p-) collider for the square root of s = 0.2 to 0.9 TeV
[NOTA-INTERNA-874] N87-24163
NUMERICAL ANALYSIS
On minimizing the number of calculations in design-by-analysis codes
[NASA-TP-2706] N87-23586
Numerical and experimental studies of atomization and mixing from a coaxial injector element N87-23812
Research in millimeter wave techniques
[NASA-CR-181026] N87-23658
Experimental and numerical investigation of coherent structures
[AD-A179456] N87-23910
Direct numerical simulations of a temporally evolving mixing layer subject to forcing
[NASA-TM-88896] N87-23933
Singularity structure of nonlinear ordinary and partial differential equations
[DE87-008242] N87-24134
AMG (Algebraic Multigrid): Basic development, applications and theory
[AD-A178222] N87-24139
Information based numerical practice
[AD-A178362] N87-24141
NUMERICAL CONTROL
Acta aeronautica et astronautica sinica
[AD-A179673] N87-23618
NUMERICAL WEATHER FORECASTING
Adaptive grid refinement for numerical weather prediction
[AD-A179393] N87-24049

O

O RING SEALS
Development of a high temperature ceramic-to-metal seal for Air Force Weapons Laboratory Laser
[DE87-007711] N87-23949
O STARS
High mass star formation in the galaxy N87-24267
On the origin of the 40-120 micron emission of galaxy disks: A comparison with H-alpha fluxes N87-24287
Infrared spectroscopy of star formation in galaxies N87-24320
OBSERVATION
TAF (Terminal Aerodrome Forecast) verification
[AD-A177931] N87-24055
OCEAN BOTTOM
Design of the shell project Seafloor Earthquake Measurement System (SEMS)
[DE87-007946] N87-24059
OCEAN DATA ACQUISITIONS SYSTEMS
Design of the shell project Seafloor Earthquake Measurement System (SEMS)
[DE87-007946] N87-24059
OCEAN MODELS
The specification of lateral boundary conditions in three-dimensional mesoscale numerical models
[AD-A179185] N87-24046
Ocean wind and wave model comparisons with GEOSAT (GEOdesy SATellite) satellite data
[AD-A178302] N87-24061
OCEAN SURFACE
Ocean wind and wave model comparisons with GEOSAT (GEOdesy SATellite) satellite data
[AD-A178302] N87-24061
OCEAN THERMAL ENERGY CONVERSION
Heat transfer research for ocean thermal energy conversion
[DE87-001155] N87-24023
ON-LINE SYSTEMS
On-line electron beam measurements for the Los Alamos Free-Electron Laser
[DE87-007452] N87-23956
OPERATING SYSTEMS (COMPUTERS)
DATA: A comprehensive data analysis environment for HP1000 computers
[DE87-007824] N87-24094
OPERATIONS RESEARCH
A multiple attribute decision analysis of manned airlock systems
[AD-A179241] N87-23682
Optimization of payload mass placement in a dual keel space station
[NASA-TM-89051] N87-23687
OPERATORS (MATHEMATICS)
Selection principles and pattern formation in fluid mechanics and nonlinear shell theory
[NASA-CR-180941] N87-23916
OPTICAL COMMUNICATION
An evaluation of the communication system for the TAU mission study N87-23840
OPTICAL CORRECTION PROCEDURE
Holographic correction of aberrations in optical systems employing synthetic apertures
[AD-A179107] N87-24173
OPTICAL DATA PROCESSING
Signal processing with degenerate 4-wave mixing
[AD-A179679] N87-24177
Nonlinear real-time optical signal processing
[AD-A178169] N87-24182
OPTICAL EQUIPMENT
Picosecond optical electronics
[AD-A179061] N87-23868
Holographic optical elements formed in light of reduced coherence
[AD-A179372] N87-23937
Holographic correction of aberrations in optical systems employing synthetic apertures
[AD-A179107] N87-24173
Coherent multiple aperture optical imaging systems: Analysis and design
[AD-A179476] N87-24176
Parametric frequency upconversion, optical fiber transmission and streak camera recording
[DE87-005841] N87-24183
Cornea Optical Topographical Scan System (COTSS)
[NASA-CR-179012] N87-24184
OPTICAL FILTERS
Fabry-Perot type optical interference filters
[AD-A179394] N87-24174
OPTICAL MEASURING INSTRUMENTS
SPECOL: A colorimetric measurement system
[BBC-RD-1987/4] N87-23942
OPTICAL PROPERTIES
White paper on nanocomposites as harmonic generation media
[DE87-008337] N87-23704
Picosecond optical electronics
[AD-A179061] N87-23868
Epitaxial semiconductor optical interference devices
[DE87-006890] N87-24212
OPTICAL RADAR
Horizontal variation of atmospheric extinction/backscatter coefficients
[AD-A178298] N87-23954
Shuttle Coherent Atmospheric Lidar Experiment (SCALE)
[NASA-TM-100307] N87-23959
LASA (Lidar Atmospheric Sounder and Altimeter) Earth observing system. Volume 2D: Instrument panel report
[NASA-TM-89356] N87-23962
OPTICAL REFLECTION
Fabry-Perot type optical interference filters
[AD-A179394] N87-24174
OPTICAL SWITCHING
Laser-enhanced electron attachment and its possible application for optical switching
[DE87-008787] N87-23957
OPTICAL WAVEGUIDES
Midwest free-electron laser program
[AD-A178106] N87-23953
Signal processing with degenerate 4-wave mixing
[AD-A179679] N87-24177
OPTIMAL CONTROL
The application of optimal control techniques to the UTIAS research simulator N87-23637
Modified independent modal space control method for active control of flexible systems
[NASA-CR-181065] N87-23980
OPTIMIZATION
An integrated, optimization-based approach to the design and control of large space structures
[AD-A179459] N87-23683
Coherent multiple aperture optical imaging systems: Analysis and design
[AD-A179476] N87-24176
Optimization of extended relational database systems
[AD-A179308] N87-24230
ORBIT CALCULATION
Simulation and analysis of a geopotential research mission
[NASA-CR-180695] N87-24042
ORBIT PERTURBATION
An analysis of geopotential effects on satellite constellations
[AD-A179507] N87-23684
ORBITAL MANEUVERING VEHICLES
A quantitative comparison of several orbital maneuvering vehicle configurations for satellite repair/replenishment
[AD-A179106] N87-23677
ORBITAL MANEUVERS
Optimal continuous thrust orbital evasive maneuvers from geosynchronous orbit
[AD-A179413] N87-23668
ORBITAL MECHANICS
An analysis of space station motion subject to the parametric excitation of periodic elevator motion
[AD-A179235] N87-23681
Inter-vehicle ranging system
[AD-A179492] N87-23938
ORBITAL POSITION ESTIMATION
COSPAS-SARSAT satellite orbit predictor, volume 9
[NASA-TM-85015] N87-23671
ORBITAL SERVICING
Human factors in space station architecture 2. EVA access facility: A comparative analysis of 4 concepts for on-orbit space suit servicing
[NASA-TM-86856] N87-24064
ORBITAL SPACE STATIONS
A systems analysis of emergency escape and recovery systems for the US space station
[AD-A179233] N87-23680
An analysis of space station motion subject to the parametric excitation of periodic elevator motion
[AD-A179235] N87-23681
A multiple attribute decision analysis of manned airlock systems
[AD-A179241] N87-23682
Space station WP-04 power system. Volume 1: Executive summary
[NASA-CR-179587] N87-23695
Space station WP-04 power system. Volume 2: Study results
[NASA-CR-179587] N87-23696
Application of advanced flywheel technology for energy storage on space station
[DE87-007657] N87-24028
National Aeronautics and Space Administration Authorization Act
[S-REPT-100-87] N87-24240
ORDER-DISORDER TRANSFORMATIONS
Ordered many-electron motions in atoms and X-ray lasers
[DE87-004731] N87-23951
ORGANIC COMPOUNDS
Storage and preservation of environmental samples
[DE87-004271] N87-24030
ORGANIC SULFUR COMPOUNDS
Heats of formation, structure and heteroatom ((17)O, (33)S) NMR studies of organosulfur molecules, radicals and ions
[DE87-006361] N87-24189

ORGANOMETALLIC COMPOUNDS
Metal alkoxides: Models for metal oxides: Alkoxide ligands in early transition metal organometallic chemistry [DE87-007309] N87-23715
Theoretical and experimental study of solid phase miscibility gaps in 3/5 quaternary alloys [DE87-008942] N87-24223
ORGANOMETALLIC POLYMERS
Energy conversion processes based on molecular excited states [DE87-007406] N87-24020
OSCILLATING FLOW
Numerical study of acoustic refraction and flow turning N87-23759
Vector array processor computer equipment [AD-A179545] N87-24382
OSCILLATIONS
Computer simulation studies on human control reliability in manual aircraft control: The origin of PIO N87-23644
Motion-dependent fluid forces acting on a tube row in crossflow [DE87-005574] N87-23923
OXIDATION
Oxidation protection coatings for polymers [NASA-CASE-LEW-14072-3] N87-23736
OXIDE FILMS
Oxidation protection coatings for polymers [NASA-CASE-LEW-14072-3] N87-23736
OXYGEN
Multispecies CARS measurements in turbulent combustion N87-23808
OXYGEN ATOMS
Radial density distribution of negative atomic oxygen in the oxygen positive column: An experiment [AD-A179212] N87-24186
OXYGEN CONSUMPTION
Operation Everest 2: Importance of ventilation in defense of maximal oxygen uptake at extreme altitudes [AD-A177874] N87-24062
The review of a research proposal to study the effects of 130 torr oxygen on submarines held at Groton, Connecticut on September 4, 1986 [AD-A177976] N87-24083

P

P-TYPE SEMICONDUCTORS
Fabrication of AlGaAs/InGaAs pseudomorphic modulation doped field effect transistors with p-doped surface layers [AD-A179230] N87-24201
PACIFIC ISLANDS
Station climatic summaries, Antarctica, Australia and Oceania [AD-A179242] N87-24047
PACKET SWITCHING
Future directions of C3 research at DARPA (Defense Advanced Research Projects Agency) [DE87-007501] N87-23948
PACKETS (COMMUNICATION)
Spread spectrum mobile radio communications [AD-A179446] N87-23826
PADE APPROXIMATION
Integral approximants for functions of higher monodromic dimension [DE87-007508] N87-24129
PALEONTOLOGY
The interpretation of crustal dynamics data in terms of plate motions and regional deformation near plate boundaries [NASA-CR-180938] N87-24038
PARABOLIC ANTENNAS
Spacecraft mass trade-offs versus radio-frequency power and antenna size at 8 GHz and 32 GHz N87-23830
Spacecraft multi-beam and contoured-beam antennas N87-23863
PARALLEL COMPUTERS
Solving the Cauchy-Riemann equations on parallel computers [NASA-CR-178307] N87-24107
Efficient graph algorithms for sequential and parallel computers [AD-A178403] N87-24110
PARALLEL FLOW
Efficient graph algorithms for sequential and parallel computers [AD-A178403] N87-24110
PARALLEL PROCESSING (COMPUTERS)
A dual-processor multi-frequency implementation of the FINDS algorithm [NASA-CR-178252] N87-23617
Intermediate level computer vision processing algorithm development for the content addressable array parallel processor [AD-A179515] N87-24090
The hypercube as a supercomputer [DE87-005029] N87-24092
LU factorization algorithms on distributed-memory multiprocessor architectures [DE87-007794] N87-24100
Efficient parallel algorithms for (delta+1)-coloring and maximal independent set problems [AD-A178287] N87-24109
Efficient graph algorithms for sequential and parallel computers [AD-A178403] N87-24110
Architectural implications of a parallel computational approach to the vector wave equation [AD-A179510] N87-24113
Investigations into the pattern processing capabilities of associative nets [TRITA-NA-8601] N87-24114
Beyond Speedup: Performance analysis of parallel programs [DE87-007954] N87-24115
Nonlinear real-time optical signal processing [AD-A178169] N87-24182
PARALLEL PROGRAMMING
Beyond Speedup: Performance analysis of parallel programs [DE87-007954] N87-24115
PARAMETER IDENTIFICATION
Correlation between flight simulation and processing of flight tests based on inertial measurements N87-23655
Measurements for rocket engine performance code verification N87-23811
PARAMETERIZATION
Squeeze film damper technology. Part 2. Extension of analysis and parametric study [AD-A178094] N87-23974
Estimation of parameters in latent class models with constraints on the parameters [AD-A178196] N87-24138
PARTIAL DIFFERENTIAL EQUATIONS
Singularity structure of nonlinear ordinary and partial differential equations [DE87-008242] N87-24134
Adaptive moving grid strategies for one-dimensional systems of partial differential equations [DE87-006824] N87-24144
PARTICLE ACCELERATION
Particle acceleration in solar flares N87-24250
PARTICLE ACCELERATORS
Rf control system for a rocket-borne accelerator [DE87-007459] N87-23873
Computer simulation of the lasertron with a ring model [DE87-007461] N87-23897
Study of minimum bias trigger events in the p(p-) collider for the square root of s = 0.2 to 0.9 TeV [NOTA-INTERNA-874] N87-24163
The physics and a plan for a 45 GeV facility that extends the high-intensity capability in nuclear and particle physics [LA-10720-MS] N87-24170
Heavy ion induced upsets in semiconductor devices [ATR-86(8139)-3] N87-24205
PARTICLE COLLISIONS
Study of minimum bias trigger events in the p(p-) collider for the square root of s = 0.2 to 0.9 TeV [NOTA-INTERNA-874] N87-24163
Theoretical studies in elementary particle physics [DE87-005895] N87-24167
PARTICLE DIFFUSION
Transport phenomena and interfacial kinetics in multiphase combustion systems [AD-A179544] N87-23709
PARTICLE EMISSION
Particle physics and cosmology [DE87-007308] N87-24388
PARTICLE ENERGY
Study of minimum bias trigger events in the p(p-) collider for the square root of s = 0.2 to 0.9 TeV [NOTA-INTERNA-874] N87-24163
PARTICLE MOTION
Microscopic modeling of sound waves in granular material [DE87-007400] N87-24159
Cosmic rays in the heliosphere N87-24254
PARTICLE SIZE DISTRIBUTION
Measurements of particulates in solid propellant rocket motors N87-23789
Effect of particle size on the shock sensitivity of pure porous HE (High Explosive) [AD-A178206] N87-23814
Modeling of dilute two-phase multispecies solid/gas flows [DE87-009254] N87-23932
Controlled nucleation and growth studies in metal oxide and alkoxide systems by dynamic laser-light-scattering methods [DE87-009103] N87-23958
PARTICLE THEORY
Research in theoretical particle physics [DE87-008240] N87-24169
PARTICLE TRAJECTORIES
AXCEL: Interactive simulation program to compute two-dimensional potential distributions of electrostatic arrangements and of ion paths in electrostatic fields under consideration of space charging [DE87-007760] N87-24165
PARTICLES
High temperature electrically conductive adhesives [DE87-007020] N87-23747
PASCAL (PROGRAMMING LANGUAGE)
A PASCAL implementation of the image algebra [AD-A177943] N87-24136
PASSENGER AIRCRAFT
Activities report of the German-Dutch wind tunnel [B6677593] N87-23665
Activities report of the German-Dutch wind tunnel [B6677594] N87-23666
PASSIVITY
Surface passivation of an implantable semiconductor multielectrode array [AD-A178175] N87-24219
PATENTS
Manufacturing processes for high-temperature structural ceramics: A patent trend analysis [PB87-178059] N87-23742
PATTERN RECOGNITION
Perception and structural analysis of morphologies [ENST-86D004] N87-24066
Recovering the orientation of textured surfaces in natural scenes [AD-A179360] N87-24098
Content-addressable memory: Applications, algorithms, and simulation [AD-A177944] N87-24120
Target segmentation and image enhancement through multisensor data fusion [AD-A178875] N87-24178
PAVEMENTS
Consequence of layer separation on pavement performance [DOT/FAA/PM-86/48] N87-23661
PAYLOADS
Engineering and instrumentation support of the AFGL (Air Force Geophysics Laboratory) Rocket Research Program [AD-A179257] N87-23689
PEACETIME
Training, muscle fatigue, and stress fractures [AD-A178350] N87-24085
PENUMBRAS
Fifty year canon of solar eclipses: 1986-2035 [NASA-TM-89348] N87-24377
PERFORMANCE PREDICTION
Analytical prediction of combustion performance characteristics of bipropellant liquid rocket engine combustor N87-23810
PERFORMANCE TESTS
Effect of a trade between boattail angle and wedge size on the performance of a nonaxisymmetric wedge nozzle [NASA-TP-2717] N87-23593
Certification testing methodology for composite structure. Volume 1: Data analysis [NADC-87042-60-VOL-1] N87-23705
Certification testing methodology for composite structure. Volume 2: Methodology development [NADC-87042-60-VOL-2] N87-23706
Trends of petroleum fuels: Topical report [DE87-001237] N87-23755
Solid fuel ramjet fuel regression rate/thrust modulation N87-23787
Preliminary performance characterizations of an engineering model multipropellant resistojet for space station application [NASA-TM-100113] N87-23821
Test plan for the 34 meter vertical axis wind turbine test bed located at Bushland, Texas [DE87-004777] N87-24017
Test results of a 60 volt bipolar nickel-hydrogen battery [NASA-TM-89927] N87-24029
Choosing sampling rates for robot control [AD-A179447] N87-24118
Experimental evaluation of nonlinear feedback and feedforward control schemes for manipulators [AD-A179449] N87-24119
Engineer in charge: A history of the Langley Aeronautical Laboratory, 1917-1958 [NASA-SP-4305] N87-24390

PERSONAL COMPUTERS
Personal computer based GOES data archive
[PB87-157517] N87-24384
PERSONNEL
Engineer in charge: A history of the Langley Aeronautical Laboratory, 1917-1958
[NASA-SP-4305] N87-24390
PERSONNEL SELECTION
Investigation of biochemical variation in operational aircrew
[AD-A179223] N87-24067
PERTURBATION
Random vibration of nonlinear systems N87-23997
An atmospheric correction algorithm for remote identification of non-Lambertian surfaces and its range of validity
[DE87-006059] N87-24011
PERTURBATION THEORY
Transport and photochemical modeling. Studies of atmospheric species
[NASA-CR-178311] N87-24040
Symbol manipulation and applied mathematics
[AD-A179571] N87-24124
PETN
Corrosion of gold bridgewire in electronic components
[DE87-000922] N87-23722
PETRI NETS
Colored stochastic Petri nets
[ENST-86C001] N87-24111
PHASE LOCKED SYSTEMS
Means for phase locking the outputs of a surface emitting laser diode array
[NASA-CASE-NPO-16542-1-CU] N87-23960
PHASE MATCHING
White paper on nanocomposites as harmonic generation media
[DE87-006337] N87-23704
PHASE TRANSFORMATIONS
Compression and shear wave propagation in plain and filled elastomers
[AD-A178153] N87-23745
PHASED ARRAYS
Results of near field probe scanning tests for ultralow sidelobe arrays
[AD-A178141] N87-23846
MIC technology for phased arrays N87-23866
PHENOMENOLOGY
Status of phenomenological modeling
[DE87-004922] N87-24143
PHOTOCATHODES
A pulsed electron injector using a metal photocathode irradiated by an excimer laser
[DE87-007499] N87-23877
PHOTOCHEMICAL REACTIONS
Energy conversion processes based on molecular excited states
[DE87-007408] N87-24020
Transport and photochemical modeling. Studies of atmospheric species
[NASA-CR-178311] N87-24040
Proceedings of the Tenth DOE Solar Photochemistry Research Conference
[DE87-006421] N87-24062
PHOTOCONDUCTIVITY
Solid state research
[AD-A178394] N87-24221
PHOTODETACHMENT
Radial density distribution of negative atomic oxygen in the oxygen positive column: An experiment
[AD-A179212] N87-24186
PHOTOELECTROCHEMICAL DEVICES
Energy conversion processes based on molecular excited states
[DE87-007408] N87-24020
PHOTOIONIZATION
Heats of formation, structure and heteroatom ((17)O, (33)S) NMR studies of organosulfur molecules, radicals and ions
[DE87-006361] N87-24189
PHOTOLITHOGRAPHY
Surface passivation of an implantable semiconductor multielectrode array
[AD-A178175] N87-24219
PHOTOLUMINESCENCE
Signal processing with degenerate 4-wave mixing
[AD-A179679] N87-24177
Drift mobilities by time-of-flight methods and time-dependent phototransport in the nanosecond regime in amorphous semiconductors
[DE87-006021] N87-24208
PHOTONS
High energy gamma ray astronomy N87-24258
PHOTOOXIDATION
Review of interactions of large solar fluxes with materials
[DE87-001156] N87-24024
PHOTOSENSITIVITY
Biomedical applications of the free electron laser
[AD-A179162] N87-24066
PHOTOSYNTHESIS
Proceedings of the Tenth DOE Solar Photochemistry Research Conference
[DE87-006421] N87-24062
PHOTOTHERMAL CONVERSION
Characterization of solar thermal concepts for electricity generation. Volume 1: Analyses and evaluation
[DE87-007161] N87-24019
PHOTOVOLTAIC CONVERSION
Space station WP-04 power system. Volume 1: Executive summary
[NASA-CR-179587] N87-23695
Space station WP-04 power system. Volume 2: Study results
[NASA-CR-179587] N87-23696
Issues in space photovoltaic research and technology
[NASA-TM-89922] N87-23901
PHYSICAL EXAMINATIONS
Cardiopulmonary screening for high-performance flying: Selection and retention issues N87-24079
PHYSIOLOGICAL EFFECTS
Laser hazards bibliography, 12 edition
[AD-A179220] N87-23945
PHYSIOLOGICAL RESPONSES
Laser hazards bibliography, 12 edition
[AD-A179220] N87-23945
PHYSIOLOGICAL TESTS
Short Course on Cardiopulmonary Aspects of Aerospace Medicine
[AGARD-R-758] N87-24070
Noninvasive methods for the detection of coronary artery disease in aviators: A stratified Bayesian approach N87-24072
Aeromedical aspects of mitral valve prolapse N87-24074
Pulmonary physiology and pulmonary function testing in aerospace medicine N87-24075
Cardiopulmonary screening for high-performance flying: Selection and retention issues N87-24079
PIEZOELECTRIC CRYSTALS
Multicomponent analysis using an array of piezoelectric crystal sensors
[AD-A178012] N87-24216
PIEZOELECTRIC TRANSDUCERS
Multicomponent analysis using an array of piezoelectric crystal sensors
[AD-A178012] N87-24216
PILOT INDUCED OSCILLATION
Flight test evaluation of techniques to predict longitudinal pilot induced oscillations
[AD-A179229] N87-23629
PILOT PERFORMANCE
Computer simulation studies on human control reliability in manual aircraft control: The origin of PIO N87-23644
Potential electron beam induced flashblindness in pilots
[AD-A178002] N87-24084
PILOT SELECTION
Coronary risk factors in aerospace medicine N87-24078
Cardiopulmonary screening for high-performance flying: Selection and retention issues N87-24079
PILOT TRAINING
Advanced visuals in mission simulators N87-23636
The application of optimal control techniques to the UTIAS research simulator N87-23637
Simulator motion characteristics and perceptual fidelity N87-23639
Use of VDU's by flight simulator instructors N87-23641
Radar simulators N87-23651
Operational training: Application and experience N87-23653
PIPE FLOW
Theoretical influence of propellant packaging on tube erosion: model formulation and algorithm development N87-23784
PIPELINING (COMPUTERS)
LU factorization algorithms on distributed-memory multiprocessor architectures
[DE87-007794] N87-24100
PIPES (TUBES)
Motion-dependent fluid forces acting on a tube row in crossflow
[DE87-005574] N87-23923
Energy-absorption capability and scalability of square cross section composite tube specimens
[NASA-TM-89067] N87-23991
PISTON ENGINES
Analysis of a mechanically simple external combustion engine with an unusual cycle
[DE87-007788] N87-23965
PITCH (INCLINATION)
Swashplate control system
[NASA-CASE-ARC-11633-1] N87-23631
PLANAR STRUCTURES
Results of near field probe scanning tests for ultralow sidelobe arrays
[AD-A178141] N87-23846
Finite element analysis of slow-wave Schottky contact printed lines
[AD-A179259] N87-23873
Recovering the orientation of textured surfaces in natural scenes
[AD-A179360] N87-24096
PLANETARY ATMOSPHERES
Strategy for exploration of the outer planets: 1986-1996
[NASA-CR-181021] N87-24381
PLANETARY RINGS
Strategy for exploration of the outer planets: 1986-1996
[NASA-CR-181021] N87-24381
PLASMA ACCELERATORS
Collective acceleration of protons by the plasma waves in a counterstreaming electron beam
[DE87-007493] N87-24196
PLASMA CONTROL
Investigation of universal plasma instabilities
[DE87-006276] N87-24193
Report to DOE of the fusion programs in applied plasma physics and development and technology at GA Technologies, Incorporated
[DE87-006882] N87-24197
PLASMA DENSITY
Role of cavitons in laser-plasma interactions
[DE87-006485] N87-24192
PLASMA DIAGNOSTICS
Semiempirical studies of atomic structure
[DE87-007320] N87-24164
The joint NASA/Goddard-University of Maryland research program in charged particle and high energy photon detector technology
[NASA-CR-180996] N87-24166
Report to DOE of the fusion programs in applied plasma physics and development and technology at GA Technologies, Incorporated
[DE87-006882] N87-24197
Activities report in plasma physics
[ETN-87-99588] N87-24199
PLASMA DRIFT
Formation and stability of partially-neutralized plasma clumps
[AD-A179444] N87-24187
Investigation of universal plasma instabilities
[DE87-006276] N87-24193
PLASMA FREQUENCIES
Generation of broadband noise in the magnetotail
[AD-A179136] N87-24034
PLASMA HEATING
Linear magnetized plasma response to an oblique electrostatic wave
[DE87-006194] N87-24191
Report to DOE of the fusion programs in applied plasma physics and development and technology at GA Technologies, Incorporated
[DE87-006882] N87-24197
Physics of the inner heliosphere: Mechanisms, models and observational signatures
[NASA-CR-181063] N87-24387
PLASMA INTERACTIONS
Linear magnetized plasma response to an oblique electrostatic wave
[DE87-006194] N87-24191
PLASMA JETS
Radial density distribution of negative atomic oxygen in the oxygen positive column: An experiment
[AD-A179212] N87-24186
PLASMA LAYERS
Extended potential drops preceding double layer formation in a triple plasma device
[TRITA-EPP-86-11] N87-24185
PLASMA PHYSICS
Report to DOE of the fusion programs in applied plasma physics and development and technology at GA Technologies, Incorporated
[DE87-006882] N87-24197
Activities report in plasma physics
[ETN-87-99588] N87-24199
PLASMA POTENTIALS
Extended potential drops preceding double layer formation in a triple plasma device
[TRITA-EPP-86-11] N87-24185
PLASMA RESONANCE
Linear magnetized plasma response to an oblique electrostatic wave
[DE87-006194] N87-24191

PLASMA TORCHES
Plasma torch igniter for scramjets N87-23789
PLASMA TURBULENCE
Investigation of universal plasma instabilities
[DE87-006276] N87-24193
PLASMA WAVES
Role of cavitons in laser-plasma interactions
[DE87-006485] N87-24192
Collective acceleration of protons by the plasma waves in a counterstreaming electron beam
[DE87-007493] N87-24196
PLASMAS (PHYSICS)
Formation and stability of partially-neutralized plasma clumps
[AD-A179444] N87-24187
Computer simulation of bounded plasma systems
[DE87-006193] N87-24190
PLASTIC DEFORMATION
Inelastic properties of ice I/sub h/ at low temperatures and high pressures
[DE87-007334] N87-23711
Thermomechanical effects in high-speed seal rubs
[NASA-CR-180418] N87-23979
Electrical resistivity response due to elastic-plastic deformations
[DE87-006826] N87-24222
PLASTIC PROPERTIES
Inelastic properties of ice I/sub h/ at low temperatures and high pressures
[DE87-007334] N87-23711
PLATES (STRUCTURAL MEMBERS)
The Shock and Vibration Digest, Volume 19, No. 3
N87-23996
PNEUMATIC PROBES
High-angle-of-attack pneumatic lag and upwash corrections for a hemispherical flow direction sensor
[NASA-TM-86790] N87-23616
PNEUMOTHORAX
Aeromedical disposition of pulmonary sarcoidosis, chronic obstructive lung disease, reactive airway disease and spontaneous pneumothorax N87-24076
POINT DEFECTS
Transient enhanced diffusion in ion-implanted silicon
[DE87-007659] N87-24207
POINT SOURCES
Systematic identification of IRAS point sources
N87-24343
A very deep IRAS survey at l(II) = 97 deg, b(II) = +30 deg N87-24344
What are cirrus point sources? N87-24345
Properties of the unusual galaxy PSC 09104+4109
N87-24346
A redshift survey of IRAS galaxies N87-24347
Optical and IR luminosity functions of IRAS galaxies
N87-24348
Ground-based follow up of IRAS galaxies N87-24355
IRAS observations of AGN candidates at low flux levels N87-24366
Evidence for extended IR emission in NGC2798 and NGC6240 N87-24368
IRAS observations of BL Lac objects N87-24373
POISSON DENSITY FUNCTIONS
Nonparametric estimation of the probability of a long delay in the M/G/1 queue
[AD-A178259] N87-24150
POISSON EQUATION
Computer simulation of bounded plasma systems
[DE87-006193] N87-24190
POLARIZED ELECTROMAGNETIC RADIATION
Reciprocating linear motor
[NASA-CASE-GSC-12773-2] N87-23904
POLLUTION MONITORING
Survey of environment related monitoring programs of international organizations and their contribution to international organizations
[ETN-87-99913] N87-24033
POLYAMIDE RESINS
Fire and heat resistant laminating resins based on maleimeido and citraconimido substituted 1 -2,4- and -2,6-diaminobenzenes
[NASA-CASE-ARC-11533-1] N87-23751
POLYCRYSTALS
A model for silicon dendrite growth during laser/plasma deposition from a silane discharge
[DE87-007579] N87-23733
POLYGONS
Approximation errors and perceived similarity between approximated polygons
[TRITA-NA-8505] N87-24127
The decomposition of an arbitrary three-dimensional planar polygon into a set of convex polygons
[AD-A177947] N87-24137
POLYIMIDE RESINS
Surface passivation of an implantable semiconductor multielectrode array
[AD-A178175] N87-24219
POLYIMIDES
Oxidation protection coatings for polymers
[NASA-CASE-LEW-14072-3] N87-23736
Adhesive evaluation of water-soluble LARC-TPI
[NASA-TM-89152] N87-23752
POLYMER CHEMISTRY
Fabrication of polymers for use under extreme conditions
[AD-A179458] N87-23730
POLYMERIC FILMS
Dielectric properties of styrene/acrylate copolymer coatings formed by electrophoretic deposition on gold, aluminum alloy, and porous anodized aluminum alloy substrates
[DE87-008885] N87-23741
POLYMERIZATION
Fabrication of polymers for use under extreme conditions
[AD-A179458] N87-23730
Fundamentals of sol-gel thin film formation
[DE87-007387] N87-23738
Electronics and ionic transport in polymers
[AD-A178227] N87-23746
Polymer dynamics and gelation
[DE87-007578] N87-23748
Fire and heat resistant laminating resins based on maleimeido and citraconimido substituted 1 -2,4- and -2,6-diaminobenzenes
[NASA-CASE-ARC-11533-1] N87-23751
POLYMERS
A mechanistic study of the interaction of ultraviolet laser radiation with low density polymers
[DE87-007846] N87-23734
Oxidation protection coatings for polymers
[NASA-CASE-LEW-14072-3] N87-23736
POLYNOMIALS
Hardware synthesis from specification with polynomials
[TRITA-NA-8506] N87-24091
POLYSTYRENE
A mechanistic study of the interaction of ultraviolet laser radiation with low density polymers
[DE87-007846] N87-23734
Dielectric properties of styrene/acrylate copolymer coatings formed by electrophoretic deposition on gold, aluminum alloy, and porous anodized aluminum alloy substrates
[DE87-008885] N87-23741
POROSITY
Effect of particle size on the shock sensitivity of pure porous HE (High Explosive)
[AD-A178206] N87-23814
PORPHYRINS
Biomedical applications of the free electron laser
[AD-A179182] N87-24066
POSITION (LOCATION)
Image sensor data base for the DARPA ALV (Defense Advanced Research Projects Agency Autonomous Land Vehicle) program
[AD-A178117] N87-24246
POSITIVE IONS
EIRMA: An Energetic Ion Retarding Mass Analyzer for the BERT-1 (Beam Emission Rocket Test one)
[AD-A178231] N87-23694
POSTMISSION ANALYSIS (SPACECRAFT)
Ice/frost/debris assessment for space shuttle Mission STS-32 (61-C)
[NASA-TM-89192] N87-23675
POTASSIUM HYDROXIDES
The inhibition effects of H2/O2/N2 flames seeded by potassium N87-23774
POTENTIAL ENERGY
Evaluation of Tersoff's revised silicon potential in a molecular dynamic simulation of solid silicon
[AD-A179231] N87-24202
POTENTIAL THEORY
Extended potential drops preceding double layer formation in a triple plasma device
[TRITA-EPP-86-11] N87-24185
POWDER (PARTICLES)
Modeling of dilute two-phase multispecies solid/gas flows
[DE87-009254] N87-23932
POWDER METALLURGY
Study of the influence of metallurgical factors on fatigue and fracture of aerospace structural materials
[AD-A179268] N87-23720
Al and Mg alloys for aerospace applications using rapid solidification and powder metallurgy processing
[AD-A179547] N87-23721
POWER CONDITIONING
Control considerations for high frequency, resonant, power processing equipment used in large systems
[NASA-TM-89926] N87-23690
A study of Schwarz converters for nuclear powered spacecraft
[NASA-TM-89911] N87-23903
POWER SPECTRA
A study of the maximum entropy method of power spectrum estimation as applied to interferometer data
[AD-A179403] N87-23707
POWER SUPPLIES
Investigations on the impact of voltage and current harmonics on end-use devices and their protection
[DE87-006018] N87-23878
PRANDTL NUMBER
Explicit finite-volume time-marching calculations of total temperature distributions in turbulent flow N87-23929
PRANDTL-MEYER EXPANSION
The freezing of flow deflection in Prandtl-Meyer expansion to vacuum
[ISL-CO-226/86] N87-23686
PREBURNERS
Nonintrusive temperature measurements in SSME preburner element flowfields N87-23813
PRECIPITATES
In situ HREM observation of interphase boundary motion in 95Pb-5Sn solder
[DE87-007616] N87-23817
PRECIPITATION HARDENING
Studies on age-hardening in spinodally modulated alloys: Experimental and theoretical
[DE87-008361] N87-23727
PREDICTION ANALYSIS TECHNIQUES
Life prediction and constitutive models for engine hot section anisotropic materials
[NASA-CR-179504] N87-23622
Noninvasive methods for the detection of coronary artery disease in aviators: A stratified Bayesian approach
N87-24072
PREDICTIONS
Environmental degradation of 316 stainless steel in high temperature low cycle fatigue
[NASA-TM-89931] N87-24007
Fifty year canon of solar eclipses: 1986-2035
[NASA-TM-89346] N87-24377
PREFLIGHT ANALYSIS
Ice/frost/debris assessment for space shuttle Mission STS-32 (61-C)
[NASA-TM-89192] N87-23675
PREPROCESSING
Utilizing remote sensing of thematic mapper data to improve our understanding of estuarine processes and their influence on the productivity of estuarine-dependent fisheries
[NASA-CR-180984] N87-24012
A PASCAL implementation of the image algebra
[AD-A177943] N87-24136
PRESERVING
Storage and preservation of environmental samples
[DE87-004271] N87-24030
PRESSURE DISTRIBUTION
Measurement of surface pressures caused by a projectile rotating band at supersonic speeds
[AD-A171082] N87-23585
On minimizing the number of calculations in design-by-analysis codes
[NASA-TP-2706] N87-23586
Experimental evaluation of honeycomb/screen configurations and short contraction section for NASA Lewis Research Center's altitude wind tunnel
[NASA-TP-2692] N87-23662
Behavior of simulated solid propellant flames in axial acoustic fields N87-23760
Surface roughness: Its effects on the performance of a two-dimensional compressor cascade
[AD-A179506] N87-23913
PRESSURE GRADIENTS
Unsteady heat transfer resulting from the rapid charging of an evacuated tank with conducting walls
[AD-A179206] N87-23905
Onset of Taylor vortices in flows with a circumferential pressure gradient: Application to the helical screw rheometer
[DE87-000453] N87-23918
PRESSURE MEASUREMENT
Investigation of shrouded nozzle exit pressure changes
[AD-A179477] N87-23911
PRESSURE OSCILLATIONS
Acoustic waveforms in statically tested space shuttle Solid Rocket Motors (SRM) N87-23758
Behavior of simulated solid propellant flames in axial acoustic fields N87-23760
Workshop report: Methods for measuring solid propellant combustion response N87-23762
Linear coupling of acoustics and entropy and acoustic stability in ramjet combustion chambers containing a plane flame N87-23795

Analysis of pressure oscillations in ramjets. Review of research: 1985-1986 N87-23796
Tones generated due to the impingement of two jets on each other N87-23797
Passive shear-flow control to minimize ramjet combustion instabilities N87-23798
Vortex-nozzle interactions in ramjet combustors N87-23800
Computational studies of the effects of acoustics and chemistry on the flow field in an axisymmetric ramjet combustor N87-23801
Numerical simulations of cold flow in a ramjet dump combustor with a choked exit nozzle N87-23802
Combustion instabilities in dump type ramjet combustors N87-23803
Spray combustion: A driving mechanism for ramjet combustion instability N87-23805

PRINTED CIRCUITS
Microwave Antennas for Avionics [AGARD-LS-151] N87-23859
Printed circuit antenna technology N87-23867
Finite element analysis of slow-wave Schottky contact printed lines [AD-A179259] N87-23873

PRIORITIES
A multi user random access communication system for users with different priorities [AD-A178372] N87-23854

PROBABILITY THEORY
Computer simulation studies on human control reliability in manual aircraft control: The origin of PIO N87-23844
A new approach to multitarget tracking using probabilistic data association [AD-A179437] N87-23825
Mid-latitude wind probability model [AD-A179256] N87-24048
Noninvasive methods for the detection of coronary artery disease in aviators: A stratified Bayesian approach N87-24072
On the existence and convergence of probability measures on continuous semi-lattices [AD-A179267] N87-24148
Nonparametric estimation of the probability of a long delay in the M/G/1 queue [AD-A178259] N87-24150

PROBLEM SOLVING
Research on knowledge representation, machine learning, and knowledge acquisition [NASA-CR-180408] N87-24103
Solving the Cauchy-Riemann equations on parallel computers [NASA-CR-178307] N87-24107
Efficient graph algorithms for sequential and parallel computers [AD-A178403] N87-24110
Asymptotic analysis of the roots of a certain transcendental equation [AD-A168315] N87-24131
AMG (Algebraic Multigrid): Basic development, applications and theory [AD-A178222] N87-24139
Upwind and symmetric shock-capturing schemes [NASA-TM-89464] N87-24145
An introduction to structured modeling, revision [AD-A179355] N87-24153
On the reliable and flexible solution of practical subset regression problems [NASA-TM-89442] N87-24156
Symmetry problems in particle physics [DE87-006369] N87-24168

PROCEDURES
Information based numerical practice [AD-A178362] N87-24141

PRODUCT DEVELOPMENT
Manufacturing processes for high-temperature structural ceramics: A patent trend analysis [PB87-178059] N87-23742

PRODUCTION ENGINEERING
Computer-aided fabrication system implementation [AD-A178225] N87-24108

PRODUCTIVITY
The success or failure of management information systems: A theoretical approach [DE87-007802] N87-24233

PROGRAM VERIFICATION (COMPUTERS)
A program maintenance aid using static data flow analysis techniques [AD-A179108] N87-24095
A rapid prototyping approach to software validation [AD-A177939] N87-24106

PROGRAMMING LANGUAGES
VHDL (VHSIC (Very High Speed Integrated Circuits) Hardware Descriptive Languages) prototype simulator [AD-A179073] N87-23869
Research aspects of rapid prototyping [AD-A179007] N87-24097

PROJECT MANAGEMENT
DOD (Department of Defense) Procedures for Management of Information Requirements [PB87-155495] N87-24227

PROJECT SETI
The Telecommunications and Data Acquisition Report [NASA-CR-181010] N87-23828

PROJECTILES
Measurement of surface pressures caused by a projectile rotating band at supersonic speeds [AD-A171082] N87-23585
Application of a 100-kV electric gun for hypervelocity impact studies [DE87-008730] N87-23976

PROJECTORS
Visual display research tool N87-23635

PROPAGATION VELOCITY
Formation and stability of partially-neutralized plasma clumps [AD-A179444] N87-24187

PROPELLANT ADDITIVES
Study of the suppression of rocket plume afterburning by chemical additives N87-23768
The inhibition effects of H2/O2/N2 flames seeded by potassium N87-23774

PROPELLANT BINDERS
Chemical kinetics combustion model of the NG/binder system N87-23773
AP/HMX composite propellant modeling N87-23776

PROPELLANT CHEMISTRY
The 23rd JANNAF Combustion Meeting, volume 1 [AD-A179158] N87-23757

PROPELLANT COMBUSTION
The 23rd JANNAF Combustion Meeting, volume 1 [AD-A179158] N87-23757
Chemical kinetics combustion model of the NG/binder system N87-23773
Quantum chemical calculations of the decomposition of nitramines: Thermochemistry and reaction pathways N87-23781
A hybrid closed bomb-strand burner for very high pressure burning rate measurements N87-23786
Analytical prediction of combustion performance characteristics of bipropellant liquid rocket engine combustor N87-23810
Nonintrusive temperature measurements in SSME preburner element flowfields N87-23813

PROPELLANT GRAINS
Modification of solid propellant deflagration rates due to random nonhomogeneities N87-23766
New ignition parameter correlations for predicting solid rocket motor ignition transients N87-23767
Measurements of particulates in solid propellant rocket motors N87-23769

PROPELLANT SENSITIVITY
Effect of particle size on the shock sensitivity of pure porous HE (High Explosive) [AD-A178206] N87-23814

PROPELLER FANS
Dynamic response of two composite prop-fan models on a nacelle/wing/fuselage half model [NASA-CR-179589] N87-23615

PROPELLERS
Coupled aerodynamic and acoustical predictions for turboprops [NASA-TM-87094] N87-23598
Extension of Kirchhoff's formula to radiation from moving surfaces [NASA-TM-89149] N87-24160

PROPULSION SYSTEM CONFIGURATIONS
Fuel cell powered propulsion systems for highway vehicles [DE87-007497] N87-24244

PROTECTIVE COATINGS
Oxidation protection coatings for polymers [NASA-CASE-LEW-14072-3] N87-23736

PROTOCOL (COMPUTERS)
Spread spectrum mobile radio communications [AD-A179446] N87-23826
Time slice manipulation in information hierarchy [AD-A177949] N87-24237

PROTON BEAMS
The physics and a plan for a 45 GeV facility that extends the high-intensity capability in nuclear and particle physics [LA-10720-MS] N87-24170

PROTON ENERGY
Satellite observation of atmospheric nuclear gamma radiation [AD-A177937] N87-24389

PROTOTYPES
VHDL (VHSIC (Very High Speed Integrated Circuits) Hardware Descriptive Languages) prototype simulator [AD-A179073] N87-23869
A single chip LSI high-speed functional tester [AD-A177886] N87-23886
Research aspects of rapid prototyping [AD-A179007] N87-24097
The development of a prototype intelligent user interface subsystem for NASA's scientific database systems [NASA-TM-87821] N87-24098
A rapid prototyping approach to software validation [AD-A177939] N87-24106

PROVING
A method for aircraft simulation verification and validation developed at the United States Air Force Flight Simulation Facility N87-23654
Symbol manipulation and applied mathematics [AD-A179571] N87-24124

PSYCHOLOGICAL EFFECTS
Annoyance response to simulated advanced turboprop aircraft interior noise containing tonal beats [NASA-TP-2689] N87-24161

PSYCHOLOGICAL FACTORS
Multipurpose visual display and eye movement recording system [AD-A179620] N87-24068

PULMONARY FUNCTIONS
Pulmonary physiology and pulmonary function testing in aerospace medicine N87-24075

PULSARS
High energy gamma ray astronomy N87-24258

PULSED JET ENGINES
Low power arcjet thruster pulse ignition [NASA-TM-100123] N87-23691

PULSED LASERS
University of Rochester, Laboratory for Laser Energetics [DE87-005920] N87-23947
Midwest free-electron laser program [AD-A178106] N87-23953
Pulsed Nd:YAG laser closure welding of the MC3593/3594 relay [DE87-007825] N87-23967

PYRAMIDS
Nonlinear real-time optical signal processing [AD-A178169] N87-24182

PYROLYSIS
Spin-cast carbon films from polyacrylonitrile [DE87-002489] N87-23703
Ceramic honeycomb structures and the method thereof [NASA-CASE-ARC-11652-1] N87-23737
Compression and shear wave propagation in plain and filled elastomers [AD-A178153] N87-23745

PYROTECHNICS
Thermal ignition of pyrotechnics with lasers [DE87-006245] N87-23955
Fully redundant mechanical release actuator [NASA-CASE-LAR-13198-1] N87-23983

PYRROLES
Poly (pyrrolium anion) studies: Electrochemical synthesis and physical behavior [AD-A178097] N87-23743
Electronics and ionic transport in polymers [AD-A178227] N87-23746

Q

QUALITY
Trends of petroleum fuels: Topical report [DE87-001237] N87-23755

QUANTUM CHROMODYNAMICS
Theoretical studies in elementary particle physics [DE87-005895] N87-24167
Research in theoretical particle physics [DE87-006240] N87-24169

QUANTUM EFFICIENCY
A pulsed electron injector using a metal photocathode irradiated by an excimer laser [DE87-007499] N87-23877

QUANTUM MECHANICS
Semiempirical studies of atomic structure [DE87-007320] N87-24164
Research in theoretical particle physics [DE87-006240] N87-24169

QUANTUM THEORY
JSEP (Joint Services Electronics Program) [AD-A177881] N87-23885
Experimental and theoretical studies of laser cooling and emittance control of neutral beams [AD-A179226] N87-23946
Study of quantum mechanical effects in deep submicron, grating-gate field effect transistors [AD-A179617] N87-24204
Experimental observation of the quantum behavior of a macroscopic degree of freedom [DE87-008228] N87-24213
Gauge invariant quantum cosmology [DE87-006685] N87-24226

QUASARS
Discrete X-ray sources and the X-ray background N87-24261
Far-infrared properties of optically-selected quasars and Seyfert galaxies N87-24371
QUATERNARY ALLOYS
Theoretical and experimental study of solid phase miscibility gaps in 3/5 quaternary alloys [DE87-006942] N87-24223

R

RADAR
Radar simulators N87-23651
RADAR ANTENNAS
Aircraft radar antennas N87-23861
RADAR APPROACH CONTROL
Efficient conduct of individual flights and air traffic or optimum utilization of modern technology for the overall benefit of civil and military airspace users [AGARD-AR-236] N87-23608
RADAR DETECTION
Analysis of space-based radar clutter spectra over different types of terrain and their effects on detection performance [AD-A178066] N87-23845
RADAR ECHOES
A comparison of ionospheric model predictions with MITHRAS observations [AD-A179374] N87-24036
RADAR IMAGERY
Automated radar image analysis research in support of military needs [AD-A179615] N87-23827
Radar as a complement to topographic maps for delineating marine terraces [PB87-154597] N87-24013
RADAR MEASUREMENT
Shuttle Coherent Atmospheric Lidar Experiment (SCALE) [NASA-TM-100307] N87-23959
RADAR TARGETS
A new approach to multitarget tracking using probabilistic data association [AD-A179437] N87-23825
RADAR TRACKING
A new approach to multitarget tracking using probabilistic data association [AD-A179437] N87-23825
RADIAL DISTRIBUTION
Radial density distribution of negative atomic oxygen in the oxygen positive column: An experiment [AD-A179212] N87-24186
The azimuthal and radial distributions of HI and H2 in NGC 6946 N87-24335
RADIAL FLOW
Flow of gas through turbine stage with spherical nozzle segment N87-23582
RADIANCE
Atmospheric radiance profile codes [AD-A179258] N87-24035
RADIANT COOLING
Experimental and theoretical studies of laser cooling and emittance control of neutral beams [AD-A179226] N87-23946
RADIANT FLUX DENSITY
Solar cell concentrator system [AD-A177981] N87-24025
A very deep IRAS survey at l(II) = 97 deg, b(II) = +30 deg N87-24344
What are cirrus point sources? N87-24345
Optical and IR luminosity functions of IRAS galaxies N87-24348
IRAS observations of AGN candidates at low flux levels N87-24366
RADIANT HEATING
Numerical simulation of a randomly heated, thermally unstable fluid [AD-A177888] N87-24225
RADIATION ABSORPTION
Fabry-Perot type optical interference filters [AD-A179394] N87-24174
RADIATION COUNTERS
The development of a containment vessel and Dewar for the particle astrophysics magnet facility (ASTROMAG) [NASA-CR-181016] N87-23670
RADIATION DAMAGE
Comparison of CREME (Cosmic Ray Effects on Microelectronics) model LET (Linear Energy Transfer) spaceflight dosimetry data [AD-A177873] N87-23884
Influence of ionizing radiations and electrical overstressings on MOS (Metal-Oxide Semiconductors) devices: A comparison [AD-A178214] N87-23891
Review of interactions of large solar fluxes with materials [DE87-001156] N87-24024
RADIATION DETECTORS
Apparatus and procedure to detect a liquid-solid interface during crystal growth in a bridgman furnace [NASA-CASE-LAR-13597-1-CU] N87-23713
Experimental bounds on beta beta-decay, cold dark matter and solar axions with an ultralow background Ge detector [DE87-002065] N87-24383
RADIATION DISTRIBUTION
Radiation transport in dust in disk geometry [NASA-CR-180995] N87-24157
The infrared morphology of galactic centers N87-24336
RADIATION DOSAGE
Comparison of CREME (Cosmic Ray Effects on Microelectronics) model LET (Linear Energy Transfer) spaceflight dosimetry data [AD-A177873] N87-23884
Status of phenomenological modeling [DE87-004922] N87-24143
RADIATION EFFECTS
A mechanistic study of the interaction of ultraviolet laser radiation with low density polymers [DE87-007846] N87-23734
Impulsive EMI (Electromagnetic Interference) radiated by Electrostatic Discharges (ESD) [AD-A178213] N87-23848
Heavy ion induced upsets in semiconductor devices [ATR-86(8139)-3] N87-24205
Development of a theoretical model for annealing of radiation damage in semiconductor devices [NASA-CR-180394] N87-24211
RADIATION HAZARDS
Hazards evaluation of radiofrequency and microwave radiation [DE87-006536] N87-24081
RADIATION PRESSURE
Numerical simulation of a randomly heated, thermally unstable fluid [AD-A177888] N87-24225
RADIATION PROTECTION
Hazards evaluation of radiofrequency and microwave radiation [DE87-006536] N87-24081
Status of phenomenological modeling [DE87-004922] N87-24143
RADIATION SOURCES
Report of the Second Workshop on Synchrotron Radiation Sources for X-ray Lithography [DE87-002155] N87-24179
RADIATION TRANSPORT
Radiation transport in dust in disk geometry [NASA-CR-180995] N87-24157
RADIATIVE HEAT TRANSFER
Simultaneous radiative and convective heating of thin body in medium with variable temperature N87-23576
RADIATIVE TRANSFER
Modelling of atmospheric effects on the angular distribution of a backscattering peak [DE87-006060] N87-24014
Transport and photochemical modeling. Studies of atmospheric species [NASA-CR-178311] N87-24040
RADIO ASTRONOMY
The Telecommunications and Data Acquisition Report [NASA-CR-181010] N87-23828
Dual-polarization 8.45 GHz traveling-wave maser N87-23838
An evaluation of the communication system for the TAU mission study N87-23840
Star Formation in Galaxies [NASA-CP-2466] N87-24266
Diffuse infrared emission of the galaxy: Large scale properties N87-24268
The origin of the diffuse galactic IR/submm emission: Revisited after IRAS N87-24269
IRAS colors of VLA identified objects in the galaxy N87-24271
Star forming regions of the southern galaxy N87-24273
The Arp Ring: Galactic or extragalactic? N87-24282
Star formation in normal galaxies N87-24285
CO observations of galaxies with the Nobeyama 45-M telescope N87-24290
Star formation and spiral structure in M81 N87-24294
The HII regions in M51: Radio and optical observations N87-24295
Far-infrared properties of cluster galaxies N87-24305
Starburst galaxies N87-24319
Infrared spectroscopy of star formation in galaxies N87-24320
RADIO BURSTS
The joint NASA/Goddard-University of Maryland research program in charged particle and high energy photon detector technology [NASA-CR-180996] N87-24166
Molecular gas in the starburt nucleus of M82 N87-24321
Star formation and dynamics in starburst nuclei N87-24324
Extragalactic infrared spectroscopy N87-24328
Cloud fluid models of gas dynamics and star formation in galaxies N87-24329
Starburst-driven superwinds from infrared galaxies N87-24330
A dust scattered halo in starburst galaxy M82? N87-24334
Far-infrared activity and starburst galaxies N87-24337
IRAS observations of starburst galaxies N87-24338
Star formation in the merging Galaxy NGC3256 N87-24340
The luminosity function of the brightest galaxies in the IRAS survey N87-24341
The relation between star formation and active nuclei N87-24360
Circumnuclear starbursts in Seyfert galaxies N87-24365
RADIO COMMUNICATION
Spread spectrum mobile radio communications [AD-A179446] N87-23826
RADIO EMISSION
Nuclear star formation on 100 parsec scales: 10' resolution radio continuum, HI and CO observations N87-24322
Induced star formation in interacting galaxies N87-24325
Ultraluminous infrared galaxies N87-24327
VLA continuum observations of barred spiral galaxies N87-24333
VLA observations of a sample of galaxies with high far-infrared luminosities N87-24342
Properties of the unusual galaxy PSC 09104+4109 N87-24346
The correlation between far-IR and radio continuum emission from spiral galaxies N87-24349
Radio and infrared observations of (almost) one hundred non-Seyfert Markarian galaxies N87-24350
The radio-far infrared correlation: Spiral and blue compact dwarf galaxies opposed N87-24351
Radio continuum, far infrared and star formation N87-24352
Ground-based follow up of IRAS galaxies N87-24355
Spectrophotometery of Brackett lines in very luminous IRAS galaxies N87-24367
Evidence for extended IR emission in NGC2798 and NGC8240 N87-24368
Models relating the radio emission and ionised gas in Seyfert nuclei N87-24369
Morphology of luminous IRAS galaxies: Summary talk N87-24376
RADIO FREQUENCIES
Rf control system for a rocket-borne accelerator [DE87-007459] N87-23673
Spacecraft mass trade-offs versus radio-frequency power and antenna size at 8 GHz and 32 GHz N87-23830
High-powered, solid-state rf systems [DE87-007457] N87-23896
RADIO FREQUENCY DISCHARGE
ESD (Electrostatic Discharge)/EOS (Electrical OverStress) susceptibility of a class of bipolar RF power transistors: Experimental studies on stripline-opposed emitter transistors [AD-A178212] N87-23890
RADIO GALAXIES
The frequency of enhanced star formation in interacting and isolated galaxies N87-24326
Ultraluminous infrared galaxies N87-24327
VLA observations of a sample of galaxies with high far-infrared luminosities N87-24342
RADIO INTERFEROMETERS
Atmospheric propagation effects on radio interferometry [AD-A178405] N87-23855
RADIO NAVIGATION
The Telecommunications and Data Acquisition Report [NASA-CR-181010] N87-23828
RADIO SOURCES (ASTRONOMY)
Extremely Luminous Far-Infrared Sources (ELFS) N87-24323

RADIO TRACKING
US Coast Guard SARSAT (Search And Rescue Satellite-Aided Tracking). Volume 2. Appendices [AD-A178307] N87-23600
US Coast Guard SARSAT (Search and Rescue Satellite-Aided Tracking). Volume 3. Programs and data listings [AD-A178308] N87-23601
RADIO TRANSMISSION
An ELF (Extremely-Low-Frequency) transmitter experiment for the space shuttle. (The NASC-201 (Naval Air Space Command) experiment). Volume 1 [AD-A178237] N87-23849
RADIO TRANSMITTERS
An ELF (Extremely-Low-Frequency) transmitter experiment for the space shuttle. (The NASC-201 (Naval Air Space Command) experiment). Volume i [AD-A178237] N87-23849
RADIOACTIVE DECAY
Nucleosynthesis and astrophysical gamma ray spectroscopy N87-24259
Experimental bounds on beta beta-decay, cold dark matter and solar axions with an ultralow background Ge detector [DE87-002065] N87-24383
RADOMES
Microwave Antennas for Avionics [AGARD-LS-151] N87-23859
RAILGUN ACCELERATORS
Application of a 100-kV electric gun for hypervelocity impact studies [DE87-006730] N87-23976
RAMAN SPECTROSCOPY
New concepts for cars diagnostics of solid propellant combustion N87-23771
CARS approaches to simultaneous measurements of H2 and H2O concentration and temperature in H2-air combustion systems N87-23792
Multispecies CARS measurements in turbulent combustion N87-23808
RAMJET ENGINES
Solid fuel ramjet fuel regression rate/thrust modulation N87-23787
Metallized fuel burning characteristics in the solid fuel ramjet N87-23788
Plasma torch igniter for scramjets N87-23789
Response of transonic diffuser flows to abrupt increases of back pressure: Wall pressure measurements N87-23793
Downstream boundary effects on the frequency of self-excited oscillations in transonic diffuser flows N87-23794
Linear coupling of acoustics and entropy and acoustic stability in ramjet combustion chambers containing a plane flame N87-23795
Analysis of pressure oscillations in ramjets. Review of research: 1985-1986 N87-23796
Tones generated due to the impingement of two jets on each other N87-23797
Passive shear-flow control to minimize ramjet combustion instabilities N87-23798
Acoustic response of turbulent reacting recirculatory flows N87-23799
Vortex-nozzle interactions in ramjet combustors N87-23800
Computational studies of the effects of acoustics and chemistry on the flow field in an axisymmetric ramjet combustor N87-23801
Numerical simulations of cold flow in a ramjet dump combustor with a choked exit nozzle N87-23802
Combustion instabilities in dump type ramjet combustors N87-23803
Effects on fuel spray characteristics and vaporization on energy release rates and flow field structure in a dump combustor N87-23804
Spray combustion: A driving mechanism for ramjet combustion instability N87-23805
Functionalization of cubane using hypervalent iodine N87-23807
RANDOM ACCESS
A multi user random access communication system for users with different priorities [AD-A178372] N87-23854
RANDOM ACCESS MEMORY
Spread spectrum mobile radio communications [AD-A179446] N87-23826
Communication-efficient parallel graph algorithms [AD-A178286] N87-23853
RANDOM PROCESSES
Numerical simulation of a randomly heated, thermally unstable fluid [AD-A177886] N87-24225
RANDOM VIBRATION
The Shock and Vibration Digest, Volume 19, No. 3 N87-23996
Random vibration of nonlinear systems N87-23997
RANGEFINDING
Z-corrections for DSN 70-meter antenna ranging calibration N87-23836
Inter-vehicle ranging system [AD-A179492] N87-23938
RAPID QUENCHING (METALLURGY)
Al and Mg alloys for aerospace applications using rapid solidification and powder metallurgy processing [AD-A179547] N87-23721
RARE EARTH COMPOUNDS
Novel fiber preforms: Rare earth doping [AD-A179454] N87-24175
RARE EARTH ELEMENTS
Novel fiber preforms: Rare earth doping [AD-A179454] N87-24175
RAYLEIGH SCATTERING
Finite difference simulations of Rayleigh wave scattering by 2-D rough topography [AD-A179190] N87-23824
RAYLEIGH WAVES
Finite difference simulations of Rayleigh wave scattering by 2-D rough topography [AD-A179190] N87-23824
RDX
Simultaneous thermogravimetric modulated beam mass spectrometry and time-of-flight velocity spectra measurements of thermal decomposition products from RDX and HMX N87-23780
REACTION KINETICS
Transport phenomena and interfacial kinetics in multiphase combustion systems [AD-A179544] N87-23709
Laser studies of chemical dynamics at the gas-solid interface [DE87-005950] N87-23710
Sandia cooperative group on the aerothermochemistry of turbulent combustion [DE87-006345] N87-23714
Chemical kinetics combustion model of the NG/binder system N87-23773
A hybrid closed bomb-strand burner for very high pressure burning rate measurements N87-23786
Effects of test facility contaminants on supersonic hydrogen-air diffusion flames N87-23790
Kinetic studies following state-selective laser excitation [DE87-007938] N87-23950
Thermal ignition of pyrotechnics with lasers [DE87-006245] N87-23955
The review of a research proposal to study the effects of 130 torr oxygen on submarines held at Groton, Connecticut on September 4, 1986 [AD-A177976] N87-24083
Microscale defect kinetics in melt-grown GaAs [AD-A178158] N87-24218
REACTOR SAFETY
Development of ultrasonic thermometry for high-temperature high-resolution temperature profiling applications in LMFBR safety research [SAND-84-1341] N87-24171
REACTOR TECHNOLOGY
USSR report: Engineering and equipment [JPRS-UEQ-87-005] N87-23570
Development of ultrasonic thermometry for high-temperature high-resolution temperature profiling applications in LMFBR safety research [SAND-84-1341] N87-24171
REAL TIME OPERATION
OASIS: A modern tool for real-time simulation N87-23638
JSEP (Joint Services Electronics Program) [AD-A177881] N87-23885
Automatic detection of electric power troubles (AI application) [NASA-TM-86593] N87-23893
Nonlinear real-time optical signal processing [AD-A178169] N87-24182
RECEIVERS
DSN advanced receiver: Breadboard description and test results N87-23833
Research in millimeter wave techniques [NASA-CR-181026] N87-23858
RECIPROCATION
Reciprocating linear motor [NASA-CASE-GSC-12773-2] N87-23904
RECIRCULATIVE FLUID FLOW
Acoustic response of turbulent reacting recirculatory flows N87-23799
Vortex-nozzle interactions in ramjet combustors N87-23800
RECLAMATION
The T55-L-712 turbine engine compressor housing refurbishment project [NASA-CR-179624] N87-23729
RECONSTRUCTION
Reconstruction of dynamic structural inputs in the presence of noise [DE87-006701] N87-24004
RECORDING
Parametric frequency upconversion, optical fiber transmission and streak camera recording [DE87-005841] N87-24183
RECOVERABLE SPACECRAFT
Detumbling of two inter-connected rigid bodies using Liapunov methods for feedback control [AD-A179207] N87-23679
RECRYSTALLIZATION
Cellular monotectic model solidification [NASA-CR-181027] N87-23717
A model for silicon dendrite growth during laser/plasma deposition from a silane discharge [DE87-007579] N87-23733
RECYCLING
Full-scale test program for a shower wastewater recycling system: Technical evaluation [AD-A178081] N87-24087
The field shower wastewater recycling system: Development of a program of instruction and preliminary analysis of its potential health implications [AD-A178112] N87-24088
RED SHIFT
What are cirrus point sources? N87-24345
A redshift survey of IRAS galaxies N87-24347
The properties of highly luminous IRAS galaxies N87-24358
REDUCTION
Smoothing and the second law [NASA-TM-86371] N87-24146
REFLECTANCE
A new version of MODESRCH using interpolated values of the magnetoionic reflection coefficients [AD-A179094] N87-23822
Time-resolved picosecond reflectivity study of laser-excited layered compounds [DE87-005115] N87-23952
Fabry-Perot type optical interference filters [AD-A179394] N87-24174
REFRACTOMETERS
The fiber optic refrigeration cycle monitor [DE87-006632] N87-24180
REFRACTORY MATERIALS
Metals and Ceramics Division [DE87-006548] N87-23697
Ceramic technology for advanced heat engines project [DE87-006538] N87-23740
Review of interactions of large solar fluxes with materials [DE87-001156] N87-24024
REFRIGERANTS
Flow regimes of refrigerant mixtures condensing inside tubes [ORNL/SUB/81-7762/4 AND 01] N87-23917
REFRIGERATING
The fiber optic refrigeration cycle monitor [DE87-006632] N87-24180
REGENERATIVE FUEL CELLS
Electrochemical performance and transport properties of a Nafion membrane in a hydrogen-bromine cell environment [NASA-TM-89662] N87-23718
REGRESSION ANALYSIS
Novel application of topological indices. 2. Prediction of the threshold soot index for hydrocarbon fuels [AD-A178001] N87-23716
Error analysis of leaf area estimates made from allometric regression models [NASA-TM-89220] N87-24010
On the reliable and flexible solution of practical subset regression problems [NASA-TM-89442] N87-24156
Multicomponent analysis using an array of piezoelectric crystal sensors [AD-A178012] N87-24216
REINFORCED PLATES
The Shock and Vibration Digest, Volume 19, No. 4 N87-23818
Recent advances in the nonlinear analysis of laminated composite plates and shells N87-23819
REINFORCED SHELLS
The Shock and Vibration Digest, Volume 19, No. 4 N87-23818
Recent advances in the nonlinear analysis of laminated composite plates and shells N87-23819
REINFORCEMENT (STRUCTURES)
The effect of reinforcement on the tear properties of flexible circuits [DE87-007022] N87-23895

RELATIVISTIC ELECTRON BEAMS
Potential electron beam induced flashblindness in pilots
[AD-A178002] N87-24084
Microwave production from a plasma driven by a high power relativistic electron beam
[DE87-003518] N87-24194
Collective acceleration of protons by the plasma waves in a counterstreaming electron beam
[DE87-007493] N87-24196
RELEASING
Fully redundant mechanical release actuator
[NASA-CASE-LAR-13198-1] N87-23983
RELIABILITY
A multiple attribute decision analysis of manned airlock systems
[AD-A179241] N87-23682
Otis ANGB (Air National Guard Base) visibility sensor field test study
[AD-A179176] N87-24045
On the reliable and flexible solution of practical subset regression problems
[NASA-TM-89442] N87-24156
REMOTE SENSING
High-angle-of-attack pneumatic lag and upwash corrections for a hemispherical flow direction sensor
[NASA-TM-86790] N87-23616
Shuttle Coherent Atmospheric Lidar Experiment (SCALE)
[NASA-TM-100307] N87-23959
Active and passive remote sensing of ice
[AD-A179481] N87-24009
Error analysis of leaf area estimates made from allometric regression models
[NASA-TM-89220] N87-24010
REMOTELY PILOTED VEHICLES
Unusual airborne simulator applications N87-23656
REMOVAL
Removable encapsulants for electronic devices
[DE87-005869] N87-23894
REPLENISHMENT
A quantitative comparison of several orbital maneuvering vehicle configurations for satellite repair/replenishment
[AD-A179106] N87-23677
REPORTS
Trends of petroleum fuels: Topical report
[DE87-001237] N87-23755
DOD (Department of Defense) Procedures for Management of Information Requirements
[PB87-155495] N87-24227
REPRESENTATIONS
Research on knowledge representation, machine learning, and knowledge acquisition
[NASA-CR-180408] N87-24103
REQUIREMENTS
LASA (Lidar Atmospheric Sounder and Altimeter) Earth observing system. Volume 2D: Instrument panel report
[NASA-TM-89356] N87-23962
RESCUE OPERATIONS
US Coast Guard SARSAT (Search And Rescue Satellite-Aided Tracking). Volume 2. Appendices
[AD-A178307] N87-23600
US Coast Guard SARSAT (Search and Rescue Satellite-Aided Tracking). Volume 3. Programs and data listings
[AD-A178308] N87-23601
A quantitative comparison of several orbital maneuvering vehicle configurations for satellite repair/replenishment
[AD-A179106] N87-23677
RESEARCH AND DEVELOPMENT
Metals and Ceramics Division
[DE87-006548] N87-23697
Manufacturing processes for high-temperature structural ceramics: A patent trend analysis
[PB87-178059] N87-23742
Worldwide nickel/iron battery development for electric vehicle applications
[DE87-004822] N87-23876
Electric and Hybrid Vehicles Program: 10th annual report to Congress for Fiscal Year 1986
[DE87-006350] N87-23965
Test plan for the 34 meter vertical axis wind turbine test bed located at Bushland, Texas
[DE87-004777] N87-24017
Results of the encouragement of basic research (1982-1986)
[ETN-87-99665] N87-24228
National Aeronautics and Space Administration — appropriations bill H.R. 2783 N87-24242
National Aeronautics and Space Administration Authorization Act, 1988
[S-REPT-100-87] N87-24243
Systems model for natural gas vehicle fleets
[PB87-178063] N87-24245
Research and Technology
[NASA-TM-89411] N87-24391
RESEARCH FACILITIES
A method for aircraft simulation verification and validation developed at the United States Air Force Flight Simulation Facility N87-23654
Reactivation study for NASA Lewis Research Center's hypersonic tunnel facility
[NASA-TM-89918] N87-23664
On-line electron beam measurements for the Los Alamos Free-Electron Laser
[DE87-007452] N87-23956
Proposal for continued research in intelligent machines at the Center for Engineering Systems Advanced Research (CESAR) for FY 1988 to FY 1991
[DE87-007789] N87-24121
The physics and a plan for a 45 GeV facility that extends the high-intensity capability in nuclear and particle physics
[LA-10720-MS] N87-24170
Results of the encouragement of basic research (1982-1986)
[ETN-87-99665] N87-24228
Engineer in charge: A history of the Langley Aeronautical Laboratory, 1917-1958
[NASA-SP-4305] N87-24390
Research and Technology
[NASA-TM-89411] N87-24391
Research and technology
[NASA-TM-89193] N87-24392
RESEARCH MANAGEMENT
Issues in space photovoltaic research and technology
[NASA-TM-89922] N87-23901
Medical research programs, past and future, for designing atmospheres to retard fires
[AD-A178354] N87-24089
Results of the encouragement of basic research (1982-1986)
[ETN-87-99665] N87-24228
Research and technology
[NASA-TM-89193] N87-24392
RESIDUAL STRESS
Study of the influence of metallurgical factors on fatigue and fracture of aerospace structural materials
[AD-A179268] N87-23720
RESIDUES
Inelastic strain analogy for piecewise linear computation of creep residues in built-up structures
[NASA-TM-86813] N87-23995
RESINS
High temperature electrically conductive adhesives
[DE87-007020] N87-23747
RESISTOJET ENGINES
Preliminary performance characterizations of an engineering model multipropellant resistojet for space station application
[NASA-TM-100113] N87-23821
RESOLUTION
Inter-vehicle ranging system
[AD-A179492] N87-23938
RESONANCE
Control considerations for high frequency, resonant, power processing equipment used in large systems
[NASA-TM-89926] N87-23690
Single and multiple electromagnetic scattering by dielectric obstacles from a resonance perspective
[DE87-007347] N87-23843
RESONANCE FLUORESCENCE
Experimental and theoretical studies of laser cooling and emittance control of neutral beams
[AD-A179226] N87-23946
RESONANT FREQUENCIES
Material damping measurements of 2D carbon-carbon composite beams
[AD-A179109] N87-23700
RESPIRATORY DISEASES
Short Course on Cardiopulmonary Aspects of Aerospace Medicine
[AGARD-R-758] N87-24070
Pulmonary physiology and pulmonary function testing in aerospace medicine N87-24075
Aeromedical disposition of pulmonary sarcoidosis, chronic obstructive lung disease, reactive airway disease and spontaneous pneumothorax N87-24076
Cardiopulmonary screening for high-performance flying: Selection and retention issues N87-24079
RESPIRATORY IMPEDANCE
Aeromedical disposition of pulmonary sarcoidosis, chronic obstructive lung disease, reactive airway disease and spontaneous pneumothorax N87-24076
RESPIRATORY PHYSIOLOGY
Pulmonary physiology and pulmonary function testing in aerospace medicine N87-24075
RESPIRATORY SYSTEM
Pulmonary adaptation to high altitude
[AD-A179139] N87-24065
RESPONSES
Annoyance response to simulated advanced turboprop aircraft interior noise containing tonal beats
[NASA-TP-2689] N87-24161
RETINAL IMAGES
The perception of the higher derivatives of visual motion
[AD-A179627] N87-24069
REVERSE FIELD PINCH
Compact toroid generation, lifetime, and stability studies in linear reverse field theta pinch geometries (TRX-2): Final report
[DE87-005094] N87-24195
REVISIONS
Flight investigation of the effects of an outboard wing-leading-edge modification on stall/spin characteristics of a low-wing, single-engine, T-tail light airplane
[NASA-TP-2691] N87-23614
Erratum: IRAS observations of irregular galaxies N87-24300
REYNOLDS NUMBER
Performance of two 10-lb/sec centrifugal compressors with different blade and shroud thicknesses operating over a range of Reynolds numbers
[NASA-TM-100115] N87-23623
RHEOLOGY
Inelastic properties of ice I/sub h/ at low temperatures and high pressures
[DE87-007334] N87-23711
Foam rheology: The linear viscoelastic response of a spatially periodic model
[DE87-000960] N87-23731
Improved beta" -alumina oxide electrolytes through transformation toughening
[DE87-007897] N87-23735
RHEOMETERS
Onset of Taylor vortices in flows with a circumferential pressure gradient: Application to the helical screw rheometer
[DE87-000453] N87-23918
RIGID STRUCTURES
Optimal aerodynamic shapes for hypervelocity projectiles
[AD-A178367] N87-23672
Detumbling of two inter-connected rigid bodies using Liapunov methods for feedback control
[AD-A179207] N87-23679
RISK
Coronary risk factors in aerospace medicine N87-24078
Livermore risk analysis methodology: A quantitative approach to management of the risk associated with the operation of information systems
[DE87-006828] N87-24232
ROBOTICS
Experimental evaluation of nonlinear feedback and feedforward control schemes for manipulators
[AD-A179449] N87-24119
ROBOTS
On autonomous terrain model acquisition by a mobile robot
[DE87-005719] N87-23964
Choosing sampling rates for robot control
[AD-A179447] N87-24118
Proposal for continued research in intelligent machines at the Center for Engineering Systems Advanced Research (CESAR) for FY 1988 to FY 1991
[DE87-007789] N87-24121
ROCKET ENGINE CONTROL
An approach of preventing combustion vibrations of rocket engine with lateral baffle
[AD-A179222] N87-23688
ROCKET ENGINES
Measurements for rocket engine performance code verification N87-23811
ROCKET EXHAUST
Study of the suppression of rocket plume afterburning by chemical additives N87-23768
The inhibition effects of H2/O2/N2 flames seeded by potassium N87-23774
ROCKET FIRING
TTCP non-linear instability program: US motor test data N87-23763
ROCKET NOZZLES
Experimental thrust performance of a high area-ratio rocket nozzle N87-23809
ROCKET PROPELLANTS
Preliminary performance characterizations of an engineering model multipropellant resistojet for space station application
[NASA-TM-100113] N87-23821
ROCKET THRUST
Experimental thrust performance of a high area-ratio rocket nozzle N87-23809

ROCKET-BORNE INSTRUMENTS
Rf control system for a rocket-borne accelerator
[DE87-007459] N87-23673
EIRMA: An Energetic Ion Retarding Mass Analyzer for the BERT-1 (Beam Emission Rocket Test one)
[AD-A178231] N87-23694
ROLL
Two blowing concepts for roll and lateral control of aircraft
[NASA-CR-180478] N87-23627
ROOT-MEAN-SQUARE ERRORS
On integrating a logarithmic or semilogarithmic piecewise linear PSD plot of a random variable X(T): Part 1 N87-24126
ROTARY STABILITY
Effectiveness of balancing flexible rotary compressor vanes on low-speed balancing machine N87-23580
ROTARY WING AIRCRAFT
Swashplate control system
[NASA-CASE-ARC-11633-1] N87-23631
Demonstration of frequency-sweep testing technique using a Bell 214-ST helicopter
[NASA-TM-89422] N87-23632
ROTATING BODIES
Measurement of surface pressures caused by a projectile rotating band at supersonic speeds
[AD-A171082] N87-23585
ROTATING CYLINDERS
Onset of Taylor vortices in flows with a circumferential pressure gradient: Application to the helical screw rheometer
[DE87-000453] N87-23918
ROTATING FLUIDS
Calculation of axisymmetric flow in swirlers by difference method N87-23579
ROTATING PLASMAS
Magnetospheres of the outer planets N87-24248
ROTATING SHAFTS
Rotary stepping device with memory metal actuator
[NASA-CASE-NPO-15482-1] N87-23970
ROTATION
Improved modeling of structural joint damping
[AD-A179111] N87-23986
ROTOR AERODYNAMICS
Squeeze film damper technology. Part 4. Design and application of squeeze film dampers
[AD-A177996] N87-23973
Research and Technology
[NASA-TM-89411] N87-24391
ROTOR BLADES (TURBOMACHINERY)
Dynamic response of two composite prop-fan models on a nacelle/wing/fuselage half model
[NASA-CR-179589] N87-23615
Squeeze film damper technology. Part 3. Experimental investigation of squeeze film dampers
[AD-A178095] N87-23975
ROTOR BODY INTERACTIONS
Squeeze film damper technology. Part 4. Design and application of squeeze film dampers
[AD-A177996] N87-23973
ROTORS
Aeroelasticity and mechanical stability report, 0.27 Mach scale model of the YAH-64 advanced attack helicopter
[NASA-CR-178284] N87-23596
Method for the determination of the three-dimensional aerodynamic field of a rotor-stator combination to compressible flow
[NASA-TM-100118] N87-23625
Swashplate control system
[NASA-CASE-ARC-11633-1] N87-23631
Squeeze film damper technology. Part 2. Extension of analysis and parametric study
[AD-A178094] N87-23974
Analysis and test results for an improved constant speed passive cyclic pitch wind turbine
[DE87-001135] N87-24022
Extension of Kirchhoff's formula to radiation from moving surfaces
[NASA-TM-89149] N87-24160
RUN TIME (COMPUTERS)
Efficient parallel algorithms for (delta+1)-coloring and maximal independent set problems
[AD-A178287] N87-24109
Beyond Speedup: Performance analysis of parallel programs
[DE87-007954] N87-24115
RUNWAY CONDITIONS
Consequence of layer separation on pavement performance
[DOT/FAA/PM-86/48] N87-23661
RUNWAYS
Aircraft Dynamic Response to Damaged and Repaired Runways
[AGARD-R-739] N87-23609
Interpretation in terms of the response of a one degree-of-freedom oscillator to two successive disturbances N87-23610
An experimental-analytical routine for the dynamic qualification of aircraft operating on rough runway surfaces N87-23611
Otis ANGB (Air National Guard Base) visibility sensor field test study
[AD-A179176] N87-24045

S

SAFETY
Medical research programs, past and future, for designing atmospheres to retard fires
[AD-A178354] N87-24089
Standardized procedure for system safety input to the Defense Technical Information Center (DTIC)
[AD-A178246] N87-24239
SAFETY MANAGEMENT
Actions to implement the recommendations of the Presidential Commission on the Space Shuttle Challenger accident: Executive summary N87-23676
Standardized procedure for system safety input to the Defense Technical Information Center (DTIC)
[AD-A178246] N87-24239
SAMPLES
Storage and preservation of environmental samples
[DE87-004271] N87-24030
SARSAT
US Coast Guard SARSAT (Search And Rescue Satellite-Aided Tracking). Volume 2. Appendices
[AD-A178307] N87-23600
US Coast Guard SARSAT (Search and Rescue Satellite-Aided Tracking). Volume 3. Programs and data listings
[AD-A178308] N87-23601
COSPAS-SARSAT satellite orbit predictor, volume 9
[NASA-TM-85015] N87-23671
SATELLITE ALTIMETRY
Ocean wind and wave model comparisons with GEOSAT (GEOdesy SATellite) satellite data
[AD-A178302] N87-24061
SATELLITE ANTENNAS
Basic parameters of antennas for aircraft, satellites and missiles N87-23860
SATELLITE ATTITUDE CONTROL
Detumbling of two inter-connected rigid bodies using Liapunov methods for feedback control
[AD-A179207] N87-23679
The freezing of flow deflection in Prandtl-Meyer expansion to vacuum
[ISL-CO-226/86] N87-23686
SATELLITE COMMUNICATION
An ELF (Extremely-Low-Frequency) transmitter experiment for the space shuttle. (The NASC-201 (Naval Air Space Command) experiment). Volume 1
[AD-A178237] N87-23849
SATELLITE IMAGERY
Utilizing remote sensing of thematic mapper data to improve our understanding of estuarine processes and their influence on the productivity of estuarine-dependent fisheries
[NASA-CR-180984] N87-24012
LANDSAT-based lineament analysis, East Texas Basin, and structural history of the Sabine Uplift area, East Texas and North Louisiana
[PB87-176327] N87-24043
Tactical weather expert system
[AD-A178605] N87-24050
SATELLITE NETWORKS
US Coast Guard SARSAT (Search And Rescue Satellite-Aided Tracking). Volume 2. Appendices
[AD-A178307] N87-23600
Future directions of C3 research at DARPA (Defense Advanced Research Projects Agency)
[DE87-007501] N87-23948
Satellite allocation for boost-phase missile intercepts
[DE87-007719] N87-24155
SATELLITE OBSERVATION
Satellite observation of atmospheric nuclear gamma radiation
[AD-A177937] N87-24389
SATELLITE ORBITS
COSPAS-SARSAT satellite orbit predictor, volume 9
[NASA-TM-85015] N87-23671
An analysis of geopotential effects on satellite constellations
[AD-A179507] N87-23684
SCALING LAWS
Energy-absorption capability and scalability of square cross section composite tube specimens
[NASA-TM-89087] N87-23991
SCANNING
Application of scanning acoustic microscopy to advanced structural ceramics
[NASA-TM-89929] N87-23987
SCATTERING
Spread spectrum mobile radio communications
[AD-A179446] N87-23826
Scattering by a truncated periodic array
[AD-A178285] N87-23852
SCATTERING COEFFICIENTS
Horizontal variation of atmospheric extinction/backscatter coefficients
[AD-A178298] N87-23954
Active and passive remote sensing of ice
[AD-A179461] N87-24009
Otis ANGB (Air National Guard Base) visibility sensor field test study
[AD-A179176] N87-24045
SCATTERING CROSS SECTIONS
A dust scattered halo in starburst galaxy M82?
N87-24334
Satellite observation of atmospheric nuclear gamma radiation
[AD-A177937] N87-24389
SCENE ANALYSIS
Edge focusing
[TRITA-NA-8518] N87-24099
SCHEDULING
Computer-aided fabrication system implementation
[AD-A178225] N87-24108
SCHOTTKY DIODES
Finite element analysis of slow-wave Schottky contact printed lines
[AD-A179259] N87-23873
Fabrication of AlGaAs/InGaAs pseudomorphic modulation doped field effect transistors with p-doped surface layers
[AD-A179230] N87-24201
The structure and electrical properties of metal contacts on GaAs
[DE87-008217] N87-24210
SCIENTIFIC SATELLITES
Satellite observation of atmospheric nuclear gamma radiation
[AD-A177937] N87-24389
History of spaceflight
[AD-A178381] N87-24393
SCREENS
Experimental evaluation of honeycomb/screen configurations and short contraction section for NASA Lewis Research Center's altitude wind tunnel
[NASA-TP-2692] N87-23662
SEA ICE
Active and passive remote sensing of ice
[AD-A179461] N87-24009
SEALS (STOPPERS)
Straight cylindrical seal for high-performance turbomachines
[NASA-TP-1850] N87-23936
Thermomechanical effects in high-speed seal rubs
[NASA-CR-180418] N87-23979
Experiments on dynamic stiffness and damping of tapered bore seals
[NASA-TM-89895] N87-23984
SEARCH PROFILES
Experiments on the cognitive aspects of information seeking and information retrieving
[PB87-157699] N87-24238
SEARCHING
US Coast Guard SARSAT (Search And Rescue Satellite-Aided Tracking). Volume 2. Appendices
[AD-A178307] N87-23600
US Coast Guard SARSAT (Search and Rescue Satellite-Aided Tracking). Volume 3. Programs and data listings
[AD-A178308] N87-23601
SEDIMENTS
Design of the shell project Seafloor Earthquake Measurement System (SEMS)
[DE87-007946] N87-24059
SEISMOLOGY
The interpretation of crustal dynamics data in terms of plate motions and regional deformation near plate boundaries
[NASA-CR-180938] N87-24038
Design of the shell project Seafloor Earthquake Measurement System (SEMS)
[DE87-007946] N87-24059
SELECTION
Information based numerical practice
[AD-A178362] N87-24141
SELF OSCILLATION
Stochastic excitation of acoustic waves in a combustion chamber N87-23761

SEMICONDUCTING FILMS
Superconducting electronic film structures
[AD-A179134] N87-24200
SEMICONDUCTOR DEVICES
Preliminary thermal analysis of transistor packages
[DE87-007708] N87-23898
Heavy ion induced upsets in semiconductor devices
[ATR-86(8139)-3] N87-24205
Development of a theoretical model for annealing of radiation damage in semiconductor devices
[NASA-CR-180394] N87-24211
Epitaxial semiconductor optical interference devices
[DE87-006890] N87-24212
SEMICONDUCTOR JUNCTIONS
The structure and electrical properties of metal contacts on GaAs
[DE87-006217] N87-24210
SEMICONDUCTOR LASERS
Solid state research
[AD-A178394] N87-24221
SEMICONDUCTORS (MATERIALS)
Apparatus and procedure to detect a liquid-solid interface during crystal growth in a bridgman furnace
[NASA-CASE-LAR-13597-1-CU] N87-23713
Floating emitter solar cell
[NASA-CASE-NPO-16467-1-CU] N87-23879
JSEP (Joint Services Electronics Program)
[AD-A177881] N87-23885
Surface passivation of an implantable semiconductor multielectrode array
[AD-A178175] N87-24219
Characterization of material device structures
[AD-A178262] N87-24220
SENSITIVITY
Investigation of the buckling sensitivity of hemispherical containers with arbitrary liquid content
[MITT-31] N87-24008
SEPARATED FLOW
Evaluation of Navier-Stokes and Euler solutions for leading-edge separation vortices
[NASA-TM-89458] N87-23584
Downstream boundary effects on the frequency of self-excited oscillations in transonic diffuser flows
N87-23794
Unsteady separated flows: Vorticity and turbulence
[AD-A179500] N87-23912
SEPARATORS
Electrochemical performance and transport properties of a Nafion membrane in a hydrogen-bromine cell environment
[NASA-TM-89662] N87-23718
SEQUENTIAL COMPUTERS
Efficient graph algorithms for sequential and parallel computers
[AD-A178403] N87-24110
SERVICE LIFE
Life prediction and constitutive models for engine hot section anisotropic materials
[NASA-CR-179594] N87-23622
Noise characteristics of MOS (Metal-Oxide Semiconductors) devices degraded by electrical overstressings
[AD-A178217] N87-23892
SET THEORY
On the reliable and flexible solution of practical subset regression problems
[NASA-TM-89442] N87-24156
SEYFERT GALAXIES
Extragalactic infrared spectroscopy N87-24328
Interferometric CO observations of the ultraluminous IRAS galaxies ARP 220, IC 694/NGC 3690, NGC 6420 and NGC 7469 N87-24331
Radio and infrared observations of (almost) one hundred non-Seyfert Markarian galaxies N87-24350
Ground-based 1- to 32-microns observations of ARP 220: Evidence for a dust-embedded AGN? N87-24361
Star formation in Seyfert galaxies N87-24364
Circumnuclear starbursts in Seyfert galaxies N87-24365
Models relating the radio emission and ionised gas in Seyfert nuclei N87-24369
Structure in the nucleus of NGC 1068 at 10 microns N87-24370
Far-infrared properties of optically-selected quasars and Seyfert galaxies N87-24371
SHAPE MEMORY ALLOYS
Rotary stepping device with memory metal actuator
[NASA-CASE-NPO-15482-1] N87-23970
SHAPES
Optimal aerodynamic shapes for hypervelocity projectiles
[AD-A178367] N87-23672
SHEAR LAYERS
Some aspects of vortex flows determined from the thin-layer Navier-Stokes equations
[NASA-TM-88375] N87-23595
SHEAR PROPERTIES
Compression and shear wave propagation in plain and filled elastomers
[AD-A178153] N87-23745
Techniques for implementing statically complete component mode synthesis for forced response
[DE87-002696] N87-24002
SHEAR STRAIN
A simplified computer solution for the flexibility matrix of contacting teeth for spiral bevel gears
[NASA-CR-179620] N87-23977
SHEAR STRENGTH
Compression and shear wave propagation in plain and filled elastomers
[AD-A178153] N87-23745
SHELL STABILITY
Investigation of the buckling sensitivity of hemispherical containers with arbitrary liquid content
[MITT-31] N87-24008
SHELL THEORY
Selection principles and pattern formation in fluid mechanics and nonlinear shell theory
[NASA-CR-180941] N87-23916
SHELLS (STRUCTURAL FORMS)
Collapse analysis of cylindrical composite panels with large cutouts under an axial load
[AD-A179112] N87-23701
SHIP HULLS
Thin-walled beam theories and their applications in the torsional strength analysis of ship hulls
[AD-A178296] N87-24001
SHOCK
The Shock and Vibration Digest, Volume 19, No. 6
N87-24125
SHOCK HEATING
Shock heated dust in L1551: L(IR) greater than 20 solar luminosities N87-24278
Physics of the inner heliosphere: Mechanisms, models and observational signatures
[NASA-CR-181063] N87-24387
SHOCK LOADS
Influence of microstructure and microdamage processes on fracture at high loading rates
[AD-A179264] N87-23989
SHOCK WAVE INTERACTION
Mathematical model describing interaction of single nonsteady supersonic jet and movable barrier of finite dimensions N87-23575
Theoretical investigation of 3-D shock wave-turbulent boundary layer interactions, part 5
[AD-A179455] N87-23909
SHOCK WAVE PROPAGATION
Cosmic rays in the heliosphere N87-24254
Origin and propagation of galactic cosmic rays N87-24257
SHOCK WAVES
Linear coupling of acoustics and entropy and acoustic stability in ramjet combustion chambers containing a plane flame N87-23795
GASPS: A time-dependent, one-dimensional, planar gas dynamics computer code
[DE87-008338] N87-23931
Upwind and symmetric shock-capturing schemes
[NASA-TM-89464] N87-24145
SHORT TAKEOFF AIRCRAFT
Development of in-flight simulation aircraft for research and training applications in UK N87-23658
SHROUDED NOZZLES
Investigation of shrouded nozzle exit pressure changes
[AD-A179477] N87-23911
SIGNAL DETECTION
Active and passive remote sensing of ice
[AD-A179461] N87-24009
SIGNAL GENERATORS
Block 3 X-band receiver-exciter N87-23837
SIGNAL MIXING
Signal processing with degenerate 4-wave mixing
[AD-A179679] N87-24177
SIGNAL PROCESSING
DSN advanced receiver: Breadboard description and test results N87-23833
Results of using the global positioning system to maintain the time and frequency synchronization in the Deep Space Network N87-23834
Perception and structural analysis of morphologies
[ENST-86D004] N87-24086
MVSE (Minimizes Variance Squared Error) adaptive filtering subject to a constraint on MSE (Mean Squared Error)
[DE87-007859] N87-24105
Signal processing with degenerate 4-wave mixing
[AD-A179679] N87-24177
Cornea Optical Topographical Scan System (COTSS)
[NASA-CR-179012] N87-24184
SIGNAL TO NOISE RATIOS
Adaptive antennas N87-23865
The perception of the higher derivatives of visual motion
[AD-A179627] N87-24089
SIGNAL TRANSMISSION
Block 3 X-band receiver-exciter N87-23837
SILANES
Sol-Gel synthesis of MgO-SiO2 glass compositions having stable liquid-liquid immiscibility
[NASA-TM-89905] N87-23750
SILICA GLASS
Sol-Gel synthesis of MgO-SiO2 glass compositions having stable liquid-liquid immiscibility
[NASA-TM-89905] N87-23750
SILICATES
Fundamentals of sol-gel thin film formation
[DE87-007387] N87-23736
SILICON
Development and analysis of silicon solar cells near 20% efficiency in the Flat Plate Solar Array Project
[NASA-CR-181005] N87-24018
Evaluation of Tersoff's revised silicon potential in a molecular dynamic simulation of solid silicon
[AD-A179231] N87-24202
Transient enhanced diffusion in ion-implanted silicon
[DE87-007659] N87-24207
SILICON ALLOYS
Al and Mg alloys for aerospace applications using rapid solidification and powder metallurgy processing
[AD-A179547] N87-23721
SILICON FILMS
A model for silicon dendrite growth during laser/plasma deposition from a silane discharge
[DE87-007579] N87-23733
SILICON TRANSISTORS
High-powered, solid-state rf systems
[DE87-007457] N87-23896
Preliminary thermal analysis of transistor packages
[DE87-007708] N87-23898
SIMULATION
Finite difference simulations of Rayleigh wave scattering by 2-D rough topography
[AD-A179190] N87-23824
Automatic detection of electric power troubles (AI application)
[NASA-TM-88593] N87-23893
Direct numerical simulations of a temporally evolving mixing layer subject to forcing
[NASA-TM-88896] N87-23933
A preliminary evaluation of the performance of wind tunnel and numerical modeling simulations of the wind flow over a wind farm
[DE87-004634] N87-24051
Numerical simulation of a randomly heated, thermally unstable fluid
[AD-A177888] N87-24225
SIMULATORS
Radar simulators N87-23651
VHDL (VHSIC (Very High Speed Integrated Circuits) Hardware Descriptive Languages) prototype simulator
[AD-A179073] N87-23869
The development of a prototype CMOS (Complementary Metal Oxide Semiconductor) circuit simulator
[AD-A177942] N87-24215
SINGLE CRYSTALS
Life prediction and constitutive models for engine hot section anisotropic materials
[NASA-CR-179594] N87-23622
Epitaxial semiconductor optical interference devices
[DE87-006890] N87-24212
SINGULARITY (MATHEMATICS)
Single and multiple electromagnetic scattering by dielectric obstacles from a resonance perspective
[DE87-007347] N87-23843
SINTERING
Improved beta'' -alumina oxide electrolytes through transformation toughening
[DE87-007897] N87-23735
SITES
A preliminary evaluation of the performance of wind tunnel and numerical modeling simulations of the wind flow over a wind farm
[DE87-004634] N87-24051
SIZE (DIMENSIONS)
A single chip LSI high-speed functional tester
[AD-A177886] N87-23886
Text editing performance as a function of screen size
[AD-A179067] N87-24229
SKIN (STRUCTURAL MEMBER)
Thermal stress analysis of space shuttle orbiter wing skin panel and thermal protection system
[NASA-TM-88276] N87-23994
SKIN FRICTION
Turbulent boundary layer structure, drag reduction
[AD-A179246] N87-23907

SKY BRIGHTNESS
IRAS colors of VLA identified objects in the galaxy N87-24271
A correlation between the IRAS infrared cirrus at 60 or 100 microns and neutral atomic hydrogen in the outer galaxy N87-24281
SLIDING FRICTION
Improved modeling of structural joint damping [AD-A179111] N87-23998
SLURRIES
Improved beta" -alumina oxide electrolytes through transformation toughening [DE87-007897] N87-23735
SMOKE ABATEMENT
Study of the suppression of rocket plume afterburning by chemical additives N87-23768
The inhibition effects of H2/O2/N2 flames seeded by potassium N87-23774
SMOOTHING
Smoothing and the second law [NASA-TM-88371] N87-24146
SNOW COVER
Active and passive remote sensing of ice [AD-A179461] N87-24009
SOCIAL FACTORS
The reality of the greenhouse effect [DE87-002383] N87-24041
SODIUM COOLING
Experimental and theoretical studies of laser cooling and emittance control of neutral beams [AD-A179226] N87-23946
SODIUM SULFUR BATTERIES
Low-resistivity glass electrolytes for sodium-sulfur cells [DE87-004837] N87-23880
SOFTWARE TOOLS
Colored stochastic Petri nets [ENST-88C001] N87-24111
Use of a DBMS to aid in the software conversion process [DE87-007863] N87-24234
SOL-GEL PROCESSES
Fundamentals of sol-gel thin film formation [DE87-007387] N87-23738
Polymer dynamics and gelation [DE87-007578] N87-23748
Sol-Gel synthesis of MgO-SiO2 glass compositions having stable liquid-liquid immiscibility [NASA-TM-89905] N87-23750
SOLAR ACTIVITY
Vector array processor computer equipment [AD-A179545] N87-24382
Solar-geophysical data number 509, January 1987. Part 1: (Prompt reports). Data for December 1986, November 1986 [PB87-162574] N87-24385
SOLAR ARRAYS
Space station WP-04 power system. Volume 1: Executive summary [NASA-CR-179587] N87-23695
Space station WP-04 power system. Volume 2: Study results [NASA-CR-179587] N87-23696
Development and analysis of silicon solar cells near 20% efficiency in the Flat Plate Solar Array Project [NASA-CR-181005] N87-24018
SOLAR CELLS
Floating emitter solar cell [NASA-CASE-NPO-16467-1-CU] N87-23879
Issues in space photovoltaic research and technology [NASA-TM-89922] N87-23901
Development and analysis of silicon solar cells near 20% efficiency in the Flat Plate Solar Array Project [NASA-CR-181005] N87-24018
Solar cell concentrator system [AD-A177981] N87-24025
SOLAR COLLECTORS
Characterization of solar thermal concepts for electricity generation. Volume 1: Analyses and evaluation [DE87-007161] N87-24019
Review of interactions of large solar fluxes with materials [DE87-001156] N87-24024
SOLAR CORONA
Numerical simulation of a randomly heated, thermally unstable fluid [AD-A177888] N87-24225
The energy source of the interplanetary medium and the heliosphere N87-24251
Physics of the inner heliosphere: Mechanisms, models and observational signatures [NASA-CR-181063] N87-24387
SOLAR CYCLES
A model for the low-latitude ionosphere with coefficients for different seasonal and solar cycle conditions [AD-A178207] N87-24044
SOLAR DIAMETER
Fifty year canon of solar eclipses: 1986-2035 [NASA-TM-89346] N87-24377
SOLAR DYNAMIC POWER SYSTEMS
Speculations on future opportunities to evolve Brayton powerplants aboard the space station [NASA-TM-89863] N87-23674
Space station WP-04 power system. Volume 1: Executive summary [NASA-CR-179587] N87-23695
Space station WP-04 power system. Volume 2: Study results [NASA-CR-179587] N87-23696
Issues in space photovoltaic research and technology [NASA-TM-89922] N87-23901
Fluoride salts and container materials for thermal energy storage applications in the temperature range 973 to 1400 K [NASA-TM-89913] N87-24026
SOLAR ECLIPSES
Fifty year canon of solar eclipses: 1986-2035 [NASA-TM-89346] N87-24377
SOLAR ENERGY
Solar Thermal Technology Program bibliography, 1973-1985 [DE86-010728] N87-24027
SOLAR ENERGY CONVERSION
Characterization of solar thermal concepts for electricity generation. Volume 1: Analyses and evaluation [DE87-007161] N87-24019
Proceedings of the Tenth DOE Solar Photochemistry Research Conference [DE87-006421] N87-24062
SOLAR FLARES
The joint NASA/Goddard-University of Maryland research program in charged particle and high energy photon detector technology [NASA-CR-180996] N87-24166
Particle acceleration in solar flares N87-24250
Particle propagation channels in the solar wind N87-24252
Cosmic rays in the heliosphere N87-24254
Solar-geophysical data number 509, January 1987. Part 2: (Comprehensive reports). Data for July 1986 [PB87-162582] N87-24386
SOLAR PROMINENCES
Solar-geophysical data number 509, January 1987. Part 2: (Comprehensive reports). Data for July 1986 [PB87-162582] N87-24386
SOLAR RADIATION
Modelling of atmospheric effects on the angular distribution of a backscattering peak [DE87-006060] N87-24014
Solar cell concentrator system [AD-A177981] N87-24025
SOLAR RADIO BURSTS
Solar-geophysical data number 509, January 1987. Part 2: (Comprehensive reports). Data for July 1986 [PB87-162582] N87-24386
SOLAR RADIO EMISSION
Solar-geophysical data number 509, January 1987. Part 1: (Prompt reports). Data for December 1986, November 1986 [PB87-162574] N87-24385
SOLAR SYSTEM
Measurements of ultraheavy cosmic rays with HEAO-3 N87-24256
SOLAR WIND
The joint NASA/Goddard-University of Maryland research program in charged particle and high energy photon detector technology [NASA-CR-180996] N87-24166
The energy source of the interplanetary medium and the heliosphere N87-24251
Particle propagation channels in the solar wind N87-24252
Studies of the interplanetary magnetic field: IMP's to Voyager N87-24253
Solar-geophysical data number 509, January 1987. Part 2: (Comprehensive reports). Data for July 1986 [PB87-162582] N87-24386
Physics of the inner heliosphere: Mechanisms, models and observational signatures [NASA-CR-181063] N87-24387
SOLDERED JOINTS
Wetting properties of Au/Sn solders for microelectronics [DE87-008519] N87-23883
SOLDERS
In situ HREM observation of interphase boundary motion in 95Pb-5Sn solder [DE87-007616] N87-23817
SOLID ELECTROLYTES
Improved beta" -alumina oxide electrolytes through transformation toughening [DE87-007897] N87-23735
Low-resistivity glass electrolytes for sodium-sulfur cells [DE87-004837] N87-23880
SOLID MECHANICS
PRONTO 2D: A two-dimensional transient solid dynamics program [DE87-007823] N87-23993
SOLID PHASES
Theoretical and experimental study of solid phase miscibility gaps in 3/5 quaternary alloys [DE87-006942] N87-24223
SOLID PROPELLANT COMBUSTION
Behavior of simulated solid propellant flames in axial acoustic fields N87-23760
Workshop report: Methods for measuring solid propellant combustion response N87-23762
TTCP non-linear instability program: US motor test data N87-23763
Asymptotic models for solid propellant combustion and the onset of intrinsic instability N87-23764
Role of combustion in the nonlinear combustion instability of composite solid propellants N87-23765
Modification of solid propellant deflagration rates due to random nonhomogeneities N87-23766
Study of the suppression of rocket plume afterburning by chemical additives N87-23768
Measurements of particulates in solid propellant rocket motors N87-23769
Measurement of solid-propellant burn rate using millimeter-wave techniques N87-23770
New concepts for cars diagnostics of solid propellant combustion N87-23771
CN radical distributions in solid propellant flames N87-23775
AP/HMX composite propellant modeling N87-23776
Numerical simulation of combustion processes of mobile stick-propellant bundles N87-23785
Solid fuel ramjet fuel regression rate/thrust modulation N87-23787
Metallized fusi burning characteristics in the solid fuel ramjet N87-23788
SOLID PROPELLANT IGNITION
The 23rd JANNAF Combustion Meeting, volume 1 [AD-A179158] N87-23757
New ignition parameter correlations for predicting solid rocket motor ignition transients N87-23767
Two techniques for measuring AP ignition delay N87-23772
The inhibition effects of H2/O2/N2 flames seeded by potassium N87-23774
A theoretical and numerical study of radiative ignition and deradiative extinction in solid propellants N87-23778
The application of imaging laser induced fluorescence to the measurement of HMX and aluminized propellant ignition and deflagration flame structure N87-23782
Thermal decomposition and ignition of a series of new nitramine lova propellants by CO2 laser N87-23783
Theoretical influence of propellant packaging on tube erosion: model formulation and algorithm development N87-23784
SOLID PROPELLANT ROCKET ENGINES
Acoustic waveforms in statically tested space shuttle Solid Rocket Motors (SRM) N87-23758
New ignition parameter correlations for predicting solid rocket motor ignition transients N87-23767
Measurements of particulates in solid propellant rocket motors N87-23769
SOLID STATE
High-powered, solid-state rf systems [DE87-007457] N87-23896
SOLID STATE DEVICES
Picosecond optical electronics [AD-A179061] N87-23868
Solid state research [AD-A178394] N87-24221
SOLIDIFICATION
Cellular monotectic model solidification [NASA-CR-181027] N87-23717
Al and Mg alloys for aerospace applications using rapid solidification and powder metallurgy processing [AD-A179547] N87-23721
Microscale defect kinetics in melt-grown GaAs [AD-A178158] N87-24218
SOLIDS
Evaluation of Tersoff's revised silicon potential in a molecular dynamic simulation of solid silicon [AD-A179231] N87-24202
SOLUBILITY
Sol-Gel synthesis of MgO-SiO2 glass compositions having stable liquid-liquid immiscibility [NASA-TM-89905] N87-23750
Adhesive evaluation of water-soluble LARC-TPI [NASA-TM-89152] N87-23752
Theoretical and experimental study of solid phase miscibility gaps in 3/5 quaternary alloys [DE87-006942] N87-24223

SOLUTIONS
Theoretical and experimental investigations of fluctuation thermodynamic properties of liquid solutions
[DE87-005681] N87-24224
SOLVENTS
Removable encapsulants for electronic devices
[DE87-005869] N87-23894
SOOT
Novel application of topological indices. 2. Prediction of the threshold soot index for hydrocarbon fuels
[AD-A176001] N87-23716
SOUND WAVES
Microscopic modeling of sound waves in granular material
[DE87-007400] N87-24159
SOUNDING ROCKETS
Engineering and instrumentation support of the AFGL (Air Force Geophysics Laboratory) Rocket Research Program
[AD-A179257] N87-23689
Atmospheric radiance profile codes
[AD-A179258] N87-24035
SOUTHERN HEMISPHERE
Star forming regions of the southern galaxy
N87-24273
SPACE CHARGE
Experiments and prospects for induction linac drivers
[DE87-006144] N87-23689
AXCEL: Interactive simulation program to compute two-dimensional potential distributions of electrostatic arrangements and of ion paths in electrostatic fields under consideration of space charging
[DE87-007760] N87-24165
SPACE COMMUNICATION
Optically controlled microwave devices and circuits: Emerging applications in space communications systems
[NASA-TM-89869] N87-23900
SPACE EXPLORATION
Strategy for exploration of the outer planets: 1986-1996
[NASA-CR-181021] N87-24381
History of spaceflight
[AD-A178381] N87-24393
SPACE FLIGHT
High-current electron gun for space flight
[AD-A179287] N87-23874
High current electron gun for space flight
[AD-A178467] N87-23875
Comparison of CREME (Cosmic Ray Effects on Microelectronics) model LET (Linear Energy Transfer) spaceflight dosimetry data
[AD-A177873] N87-23884
History of spaceflight
[AD-A178381] N87-24393
SPACE INFRARED TELESCOPE FACILITY
Using SIRTF to study extragalactic star formation
N87-24359
SPACE MAINTENANCE
A quantitative comparison of several orbital maneuvering vehicle configurations for satellite repair/replenishment
[AD-A179106] N87-23677
SPACE OBSERVATIONS (FROM EARTH)
Ground-based 1- to 32-microns observations of ARP 220: Evidence for a dust-embedded AGN? N87-24361
Strategy for exploration of the outer planets: 1986-1996
[NASA-CR-181021] N87-24381
SPACE PERCEPTION
The perception of the higher derivatives of visual motion
[AD-A179627] N87-24069
SPACE POWER REACTORS
Speculations on future opportunities to evolve Brayton powerplants aboard the space station
[NASA-TM-89863] N87-23674
Application of thermal and flywheel energy storage in orbiting nuclear burst power systems
[DE87-007882] N87-24021
SPACE SHUTTLE MAIN ENGINE
Nonintrusive temperature measurements in SSME preburner element flowfields N87-23813
Three-step labyrinth seal for high-performance turbomachines
[NASA-TP-1848] N87-23921
Straight cylindrical seal for high-performance turbomachines
[NASA-TP-1850] N87-23936
SPACE SHUTTLE MISSION 51-L
Actions to implement the recommendations of the Presidential Commission on the Space Shuttle Challenger accident: Executive summary N87-23676
SPACE SHUTTLE PAYLOADS
Design, development and test of shuttle/Centaur G-prime cryogenic tankage thermal protection systems
[NASA-TM-89825] N87-23685
Optimization of payload mass placement in a dual keel space station
[NASA-TM-89051] N87-23687
Shuttle Coherent Atmospheric Lidar Experiment (SCALE)
[NASA-TM-100307] N87-23959
SPACE SHUTTLES
Hypersonic aerodynamic coefficients and convection flow estimation in a HERMES type project
[NASA-TT-20019] N87-23583
Acoustic waveforms in statically tested space shuttle Solid Rocket Motors (SRM) N87-23758
High-current electron gun for space flight
[AD-A179287] N87-23874
High current electron gun for space flight
[AD-A178467] N87-23875
National Aeronautics and Space Administration Authorization Act
[S-REPT-100-87] N87-24240
SPACE STATION POWER SUPPLIES
Speculations on future opportunities to evolve Brayton powerplants aboard the space station
[NASA-TM-89863] N87-23674
Space station WP-04 power system. Volume 1: Executive summary
[NASA-CR-179587] N87-23695
Space station WP-04 power system. Volume 2: Study results
[NASA-CR-179587] N87-23696
SPACE STATIONS
Optimization of payload mass placement in a dual keel space station
[NASA-TM-89051] N87-23687
Control considerations for high frequency, resonant, power processing equipment used in large systems
[NASA-TM-89926] N87-23690
Preliminary performance characterizations of an engineering model multipropellant resistojet for space station application
[NASA-TM-100113] N87-23821
Guidelines for noise and vibration levels for the space station
[NASA-CR-178310] N87-24162
SPACE SUITS
Human factors in space station architecture 2. EVA access facility: A comparative analysis of 4 concepts for on-orbit space suit servicing
[NASA-TM-88856] N87-24064
SPACE TRANSPORTATION SYSTEM
National Aeronautics and Space Administration Authorization Act
[S-REPT-100-87] N87-24240
Research and technology
[NASA-TM-89193] N87-24392
SPACE WEAPONS
SDI (Strategic Defense Initiative) and the US defense posture
[DE87-006731] N87-24154
SPACECRAFT ANTENNAS
Spacecraft mass trade-offs versus radio-frequency power and antenna size at 8 GHz and 32 GHz
N87-23830
Spacecraft multi-beam and contoured-beam antennas
N87-23863
SPACECRAFT CHARGING
EIRMA: An Energetic Ion Retarding Mass Analyzer for the BERT-1 (Beam Emission Rocket Test one)
[AD-A178231] N87-23694
SPACECRAFT COMPONENTS
High-current electron gun for space flight
[AD-A179287] N87-23874
Identification of structural interface characteristics using component mode synthesis
[NASA-TM-88960] N87-24006
SPACECRAFT CONSTRUCTION MATERIALS
Potential Applications of Biotechnology to Aerospace Materials
[AD-A177875] N87-23667
Oxidation protection coatings for polymers
[NASA-CASE-LEW-14072-3] N87-23736
SPACECRAFT DESIGN
Actions to implement the recommendations of the Presidential Commission on the Space Shuttle Challenger accident: Executive summary N87-23676
Strategy for exploration of the outer planets: 1986-1996
[NASA-CR-181021] N87-24381
SPACECRAFT ENVIRONMENTS
Spacecraft environment interaction investigation
[AD-A179183] N87-23678
SPACECRAFT GUIDANCE
Inter-vehicle ranging system
[AD-A179492] N87-23938
SPACECRAFT INSTRUMENTS
Fully redundant mechanical release actuator
[NASA-CASE-LAR-13198-1] N87-23983
SPACECRAFT ORBITS
A quantitative comparison of several orbital maneuvering vehicle configurations for satellite repair/replenishment
[AD-A179106] N87-23677
SPACECRAFT POWER SUPPLIES
Control considerations for high frequency, resonant, power processing equipment used in large systems
[NASA-TM-89926] N87-23690
Issues in space photovoltaic research and technology
[NASA-TM-89922] N87-23901
A study of Schwarz converters for nuclear powered spacecraft
[NASA-TM-89911] N87-23903
Application of thermal and flywheel energy storage in orbiting nuclear burst power systems
[DE87-007882] N87-24021
Fluoride salts and container materials for thermal energy storage applications in the temperature range 973 to 1400 K
[NASA-TM-89913] N87-24026
Test results of a 60 volt bipolar nickel-hydrogen battery
[NASA-TM-89927] N87-24029
SPACECREWS
A quantitative comparison of several orbital maneuvering vehicle configurations for satellite repair/replenishment
[AD-A179106] N87-23677
SPACELAB PAYLOADS
Shuttle Coherent Atmospheric Lidar Experiment (SCALE)
[NASA-TM-100307] N87-23959
SPALLATION
Satellite observation of atmospheric nuclear gamma radiation
[AD-A177937] N87-24389
SPANWISE BLOWING
Two blowing concepts for roll and lateral control of aircraft
[NASA-CR-180478] N87-23627
SPARK IGNITION
A comparison of unburned fuel and aldehyde emissions from a methanol-fueled stratified charge and homogeneous charge engine
[DE87-007793] N87-23966
SPATIAL DISTRIBUTION
Experimental and numerical investigation of coherent structures
[AD-A179456] N87-23910
The perception of the higher derivatives of visual motion
[AD-A179627] N87-24069
Stellar bars and the spatial distribution of infrared luminosity N87-24293
IUE observations of luminous blue star associations in irregular galaxies N87-24301
SPATIAL RESOLUTION
Spatial deconvolution of IRAS galaxies at 60 UM
N87-24362
SPECIFICATIONS
Demonstration of frequency-sweep testing technique using a Bell 214-ST helicopter
[NASA-TM-89422] N87-23632
The specification of lateral boundary conditions in three-dimensional mesoscale numerical models
[AD-A179185] N87-24046
SPECTRAL BANDS
Atmospheric radiance profile codes
[AD-A179258] N87-24035
IRAS observations of BL Lac objects N87-24373
SPECTRAL EMISSION
Ground-based 1- to 32-microns observations of ARP 220: Evidence for a dust-embedded AGN? N87-24361
Star formation around active galactic nuclei
N87-24363
SPECTRAL ENERGY DISTRIBUTION
SPECOL: A colorimetric measurement system
[BBC-RD-1987/4] N87-23942
Properties of the unusual galaxy PSC 09104+4109
N87-24346
Star formation around active galactic nuclei
N87-24363
Infrared-ultraviolet spectra of active galactic nuclei
N87-24372
SPECTRAL RECONNAISSANCE
Analysis of space-based radar clutter spectra over different types of terrain and their effects on detection performance
[AD-A178066] N87-23845
SPECTRAL RESOLUTION
Analysis of space-based radar clutter spectra over different types of terrain and their effects on detection performance
[AD-A178066] N87-23845
SPECTRORADIOMETERS
SPECOL: A colorimetric measurement system
[BBC-RD-1987/4] N87-23942

SPECTRUM ANALYSIS
Analysis of space-based radar clutter spectra over different types of terrain and their effects on detection performance
[AD-A178066] N87-23845
Systematic identification of IRAS point sources N87-24343
SPEECH RECOGNITION
Adaptive noise reduction in aircraft communication systems
[AD-A176267] N87-23851
SPEED CONTROL
Analysis and test results for an improved constant speed passive cyclic pitch wind turbine
[DE87-001135] N87-24022
SPHERICAL SHELLS
Scattering from an open spherical shell having a circular aperture and enclosing a concentric dielectric sphere
[DE87-007099] N87-23842
SPIN
Flight investigation of the effects of an outboard wing-leading-edge modification on stall/spin characteristics of a low-wing, single-engine, T-tail light airplane
[NASA-TP-2691] N87-23814
SPIN DYNAMICS
Experimental bounds on beta beta-decay, cold dark matter and solar axions with an ultralow background Ge detector
[DE87-002065] N87-24383
SPIN STABILIZATION
Detumbling of two inter-connected rigid bodies using Liapunov methods for feedback control
[AD-A179207] N87-23679
SPIRAL GALAXIES
Star formation in normal galaxies N87-24285
On the origin of the 40-120 micron emission of galaxy disks: A comparison with H-alpha fluxes N87-24287
Present star formation in sprials of the Virgo cluster N87-24306
Molecular gas and star formation in HI-deficient Virgo cluster galaxies N87-24307
Star formation rates as a function of galaxy mass N87-24308
Global properties of the nearby spiral M101 N87-24309
The history of gas in sprial galaxies N87-24318
Nuclear star formation on 100 parsec scales: 10' resolution radio continuum, HI and CO observations N87-24322
Induced star formation in interacting galaxies N87-24325
Extragalactic infrared spectroscopy N87-24328
Cloud fluid models of gas dynamics and star formation in galaxies N87-24329
VLA continuum observations of barred spiral galaxies N87-24333
The correlation between far-IR and radio continuum emission from spiral galaxies N87-24349
The radio-far infrared correlation: Spiral and blue compact dwarf galaxies opposed N87-24351
Near-infrared observations of IRAS minisurvey galaxies N87-24354
SPLINE FUNCTIONS
A unified direct-inverse procedure for two-dimensional boundary layers using spline/finite difference discretization
[AD-A178223] N87-24140
SPRAYING
Effects on fuel spray characteristics and vaporization on energy release rates and flow field structure in a dump combustor N87-23804
Spray combustion: A driving mechanism for ramjet combustion instability N87-23805
SPREAD SPECTRUM TRANSMISSION
Spread spectrum mobile radio communications
[AD-A179446] N87-23826
SPRINGS (ELASTIC)
Rotary stepping device with memory metal actuator
[NASA-CASE-NPO-15482-1] N87-23970
SQUEEZE FILMS
Squeeze film damper technology. Part 4. Design and application of squeeze film dampers
[AD-A177996] N87-23973
Squeeze film damper technology. Part 2. Extension of analysis and parametric study
[AD-A178094] N87-23974
Squeeze film damper technology. Part 3. Experimental investigation of squeeze film dampers
[AD-A178095] N87-23975
SQUIBS
Low energy ignition of HMX using a foil bridge
[DE87-004211] N87-23754
STABILITY
Formation and stability of partially-neutralized plasma clumps
[AD-A179444] N87-24187
Compact toroid generation, lifetime, and stability studies in linear reverse field theta pinch geometries (TRX-2): Final report
[DE87-005094] N87-24195
STAINLESS STEELS
Environmental degradation of 316 stainless steel in high temperature low cycle fatigue
[NASA-TM-89931] N87-24007
STAR CLUSTERS
On the redistribution of OB star luminosity and the warming of nearby molecular clouds N87-24274
The Arp Ring: Galactic or extragalactic? N87-24282
The initial mass function in HII galaxies N87-24332
STAR FORMATION
Star Formation in Galaxies
[NASA-CP-2466] N87-24266
High mass star formation in the galaxy N87-24267
The origin of the diffuse galactic IR/submm emission: Revisited after IRAS N87-24269
Masses, luminosities and dynamics of galactic molecular clouds N87-24270
IRAS colors of VLA identified objects in the galaxy N87-24271
Star formation in Carina OB1: Observations of a giant molecular cloud associated with the eta Carinae Nebula N87-24272
Maps of millimeter wave emission from three galactic star-forming regions N87-24275
Mechanisms for the circular polarization of astrophysical OH masers in star-forming regions and the inferred magnetic fields N87-24277
The large scale gas and dust distribution in the galaxy: Implications for star formation N87-24280
The Arp Ring: Galactic or extragalactic? N87-24282
Star formation in normal galaxies N87-24285
Models for infrared emission from IRAS galaxies N87-24286
On the origin of the 40-120 micron emission of galaxy disks: A comparison with H-alpha fluxes N87-24287
Star formation in the Magellanic clouds N87-24288
Measuring star formation rates in blue galaxies N87-24289
CO observations of galaxies with the Nobeyama 45-M telescope N87-24290
CO observations of nearby galaxies and the efficiency of star formation N87-24291
Submm observations of IRAS galaxies N87-24292
Stellar bars and the spatial distribution of infrared luminosity N87-24293
Star formation and spiral structure in M81 N87-24294
The HII regions in M51: Radio and optical observations N87-24295
IRAS and ground-based observations of star formation regions in the Magellanic clouds N87-24296
Star formation in the large Magellanic cloud N87-24297
Infrared emission and excitation in LMC HII regions N87-24298
IRAS observations of irregular galaxies N87-24299
IUE observations of luminous blue star associations in irregular galaxies N87-24301
Neutral hydrogen and star formation in irregular galaxies N87-24302
Carbon monoxide emission from small galaxies N87-24303
Far-infrared properties of cluster galaxies N87-24305
Present star formation in sprials of the Virgo cluster N87-24306
Molecular gas and star formation in HI-deficient Virgo cluster galaxies N87-24307
Star formation rates as a function of galaxy mass N87-24308
Efficient star formation in the bright bar of M83 N87-24310
Large scale dissociation of molecular gas in the sprial arms of M51 N87-24311
Modelling the IRAS colors of galaxies N87-24313
A simple two-component model for the far-infrared emission from galaxies N87-24314
Star forming regions in gas-rich SO galaxies N87-24316
A simple theory of bimodal star formation N87-24317
The history of gas in sprial galaxies N87-24318
Starburst galaxies N87-24319
Infrared spectroscopy of star formation in galaxies N87-24320
Molecular gas in the starburt nucleus of M82 N87-24321
Nuclear star formation on 100 parsec scales: 10' resolution radio continuum, HI and CO observations N87-24322
Extremely Luminous Far-Infrared Sources (ELFS) N87-24323
Star formation and dynamics in starburst nuclei N87-24324
Induced star formation in interacting galaxies N87-24325
The frequency of enhanced star formation in interacting and isolated galaxies N87-24326
Ultraluminous infrared galaxies N87-24327
Extragalactic infrared spectroscopy N87-24328
Cloud fluid models of gas dynamics and star formation in galaxies N87-24329
Starburst-driven superwinds from infrared galaxies N87-24330
Interferometric CO observations of the ultraluminous IRAS galaxies ARP 220, IC 694/NGC 3690, NGC 6420 and NGC 7469 N87-24331
The initial mass function in HII galaxies N87-24332
VLA continuum observations of barred spiral galaxies N87-24333
The infrared morphology of galactic centers N87-24336
Far-infrared activity and starburst galaxies N87-24337
Star formation in the merging Galaxy NGC3256 N87-24340
Radio continuum, far infrared and star formation N87-24352
Enhanced star formation: The importance of bars in spiral galaxies N87-24357
Using SIRTF to study extragalactic star formation N87-24359
The relation between star formation and active nuclei N87-24360
Star formation around active galactic nuclei N87-24363
Star formation in Seyfert galaxies N87-24364
Circumnuclear starbursts in Seyfert galaxies N87-24365
IRAS observations of AGN candidates at low flux levels N87-24366
Spectrophotometery of Brackett lines in very luminous IRAS galaxies N87-24367
Evidence for extended IR emission in NGC2798 and NGC6240 N87-24368
Models relating the radio emission and ionised gas in Seyfert nuclei N87-24369
Far-infrared properties of optically-selected quasars and Seyfert galaxies N87-24371
Infrared-ultraviolet spectra of active galactic nuclei N87-24372
IRAS observations of BL Lac objects N87-24373
Summary of symposium: Low luminosity sources N87-24375
Morphology of luminous IRAS galaxies: Summary talk N87-24376
STATIC STABILITY
An experimental investigation into methods for quantifying hang glider airworithness parameters
[CAR-8705] N87-23613
STATIC TESTS
Three-step labyrinth seal for high-performance turbomachines
[NASA-TP-1848] N87-23921
STATISTICAL ANALYSIS
On the breakdown of the wave packet trailing a turbulent spot in a laminar layer
[AD-A179607] N87-23915
Three dimensional graphics in the statistical analysis of scientific data
[DE87-008151] N87-24104
Min-max bias robust M-estimates of scale
[AD-A179255] N87-24147
Changing time series
[AD-A178030] N87-24149
Systematic identification of IRAS point sources N87-24343
STATISTICAL DISTRIBUTIONS
Confidence interval for parameter n in a binomial distribution
[AD-A178325] N87-24151
STATISTICAL MECHANICS
The use of molecular dynamics for the thermodynamic properties of simple and transition metals
[DE87-007718] N87-23725
STATORS
Method for the determination of the three-dimensional aerodynamic field of a rotor-stator combination to compressible flow
[NASA-TM-100118] N87-23625
STEADY FLOW
A redefined hydraulic diameter for laminar flow
[AD-A179511] N87-23914

STEADY STATE
Far field boundary conditions for time-dependent hyperbolic systems
[AD-A179361] N87-24123
STEELS
Galvanic corrosion of Al-7075-T6 and Steel-4340 coupled to brass QQ-B-626, 360 and Al-7075-T6 coupled to Steel-4130 and Steel-4340: Exposure to aqueous NaCl and salt-fog environments
[AD-A179121] N87-23719
Investigation of tearing instability phenomena in ASTM steel
[AD-A177993] N87-24000
STEERING
The Shock and Vibration Digest, Volume 19, No. 4 N87-23818
Recent developments in vehicle dynamics N87-23820
STELLAR ACTIVITY
Far-infrared activity and starburst galaxies N87-24337
STELLAR COLOR
Diffuse infrared emission of the galaxy: Large scale properties N87-24268
Models for infrared emission from IRAS galaxies N87-24286
IRAS observations of irregular galaxies N87-24299
IRAS observations of starburst galaxies N87-24338
A near-infrared study of the luminous merging galaxies NGC 2623 and ARP 148 N87-24339
The luminosity function of the brightest galaxies in the IRAS survey N87-24341
A very deep IRAS survey at l(II) = 97 deg, b(II) = +30 deg N87-24344
A redshift survey of IRAS galaxies N87-24347
Nuclear infrared emission and the colors of IRAS galaxies N87-24356
Enhanced star formation: The importance of bars in spiral galaxies N87-24357
Star formation in Seyfert galaxies N87-24364
STELLAR LUMINOSITY
Star Formation in Galaxies
[NASA-CP-2466] N87-24266
On the redistribution of OB star luminosity and the warming of nearby molecular clouds N87-24274
Star formation in the Magellanic clouds N87-24288
Measuring star formation rates in blue galaxies N87-24289
CO observations of nearby galaxies and the efficiency of star formation N87-24291
Submm observations of IRAS galaxies N87-24292
Stellar bars and the spatial distribution of infrared luminosity N87-24293
Erratum: IRAS observations of irregular galaxies N87-24300
Characteristics of UGC galaxies detected by IRAS N87-24304
Molecular gas and star formation in HI-deficient Virgo cluster galaxies N87-24307
A simple two-component model for the far-infrared emission from galaxies N87-24314
Infrared spectroscopy of star formation in galaxies N87-24320
Extremely Luminous Far-infrared Sources (ELFS) N87-24323
Induced star formation in interacting galaxies N87-24325
The frequency of enhanced star formation in interacting and isolated galaxies N87-24326
Ultraluminous infrared galaxies N87-24327
Interferometric CO observations of the ultraluminous IRAS galaxies ARP 220, IC 694/NGC 3690, NGC 6420 and NGC 7469 N87-24331
Far-infrared activity and starburst galaxies N87-24337
IRAS observations of starburst galaxies N87-24338
A near-infrared study of the luminous merging galaxies NGC 2623 and ARP 148 N87-24339
Star formation in the merging Galaxy NGC3256 N87-24340
The luminosity function of the brightest galaxies in the IRAS survey N87-24341
VLA observations of a sample of galaxies with high far-infrared luminosities N87-24342
Properties of the unusual galaxy PSC 09104+4109 N87-24346
A redshift survey of IRAS galaxies N87-24347
Optical and IR luminosity functions of IRAS galaxies N87-24348
The correlation between far-IR and radio continuum emission from spiral galaxies N87-24349
The radio-far infrared correlation: Spiral and blue compact dwarf galaxies opposed N87-24351
Enhanced star formation: The importance of bars in spiral galaxies N87-24357
The properties of highly luminous IRAS galaxies N87-24358
Ground-based 1- to 32-microns observations of ARP 220: Evidence for a dust-embedded AGN? N87-24361
Spatial deconvolution of IRAS galaxies at 60 UM N87-24362
Star formation around active galactic nuclei N87-24363
Star formation in Seyfert galaxies N87-24364
STELLAR MASS
Measuring star formation rates in blue galaxies N87-24289
IUE observations of luminous blue star associations in irregular galaxies N87-24301
Efficient star formation in the bright bar of M83 N87-24310
STELLAR MASS ACCRETION
High mass star formation in the galaxy N87-24267
Star formation in Carina OB1: Observations of a giant molecular cloud associated with the eta Carinae Nebula N87-24272
STELLAR RADIATION
Molecular gas in the starburt nucleus of M82 N87-24321
The frequency of enhanced star formation in interacting and isolated galaxies N87-24326
STELLAR SPECTRA
Extremely Luminous Far-infrared Sources (ELFS) N87-24323
Extragalactic infrared spectroscopy N87-24328
Starburst-driven superwinds from infrared galaxies N87-24330
VLA continuum observations of barred spiral galaxies N87-24333
The azimuthal and radial distributions of HI and H2 in NGC 6946 N87-24335
A near-infrared study of the luminous merging galaxies NGC 2623 and ARP 148 N87-24339
Star formation in the merging Galaxy NGC3256 N87-24340
Systematic identification of IRAS point sources N87-24343
Extragalactic OH megamasers in strong IRAS sources N87-24353
Ground-based follow up of IRAS galaxies N87-24355
The properties of highly luminous IRAS galaxies N87-24358
The relation between star formation and active nuclei N87-24360
Circumnuclear starbursts in Seyfert galaxies N87-24365
STELLAR SPECTROPHOTOMETRY
Spectrophotometery of Brackett lines in very luminous IRAS galaxies N87-24367
STELLAR TEMPERATURE
The luminosity function of the brightest galaxies in the IRAS survey N87-24341
Nuclear infrared emission and the colors of IRAS galaxies N87-24356
STELLAR WINDS
Starburst-driven superwinds from infrared galaxies N87-24330
STIFFNESS
Motion-dependent fluid forces acting on a tube row in crossflow
[DE87-005574] N87-23923
Experiments on dynamic stiffness and damping of tapered bore seals
[NASA-TM-89895] N87-23984
STIFFNESS MATRIX
Calculation of eigenvector derivatives for structures with repeated eigenvalues
[DE87-006399] N87-24135
STIRLING ENGINES
Analysis of a mechanically simple external combustion engine with an unusual cycle
[DE87-007788] N87-23965
STOCHASTIC PROCESSES
Stochastic excitation of acoustic waves in a combustion chamber N87-23761
Retardation effect in fatigue crack growth under stationary stochastic loading
[REPT-43/1986] N87-23999
Colored stochastic Petri nets
[ENST-86C001] N87-24111
STORAGE
Storage and preservation of environmental samples
[DE87-004271] N87-24030
STORAGE BATTERIES
Test results of a 60 volt bipolar nickel-hydrogen battery
[NASA-TM-89927] N87-24029
STORAGE RINGS (PARTICLE ACCELERATORS)
Report of the Second Workshop on Synchrotron Radiation Sources for X-ray Lithography
[DE87-002155] N87-24179
STRAIN RATE
Acoustic waveforms in statically tested space shuttle Solid Rocket Motors (SRM) N87-23758
STRAKES
Helicopter anti-torque system using fuselage strakes
[NASA-CASE-LAR-13630-1] N87-23630
STRATOSPHERE
Transport and photochemical modeling. Studies of atmospheric species
[NASA-CR-178311] N87-24040
STREAK CAMERAS
Parametric frequency upconversion, optical fiber transmission and streak camera recording
[DE87-005841] N87-24183
STRESS ANALYSIS
Three-dimensional model for the linear elastic properties of a foam
[DE87-000984] N87-23732
Noise characteristics of MOS (Metal-Oxide Semiconductors) devices degraded by electrical overstressings
[AD-A178217] N87-23892
Thermal stress analysis of space shuttle orbiter wing skin panel and thermal protection system
[NASA-TM-88276] N87-23994
Recent studies in plate vibrations: 1981-1985. Part 2: Complicating effects N87-23998
Thin-walled beam theories and their applications in the torsional strength analysis of ship hulls
[AD-A178296] N87-24001
STRESS CONCENTRATION
Influence of microstructure and microdamage processes on fracture at high loading rates
[AD-A179264] N87-23989
STRESS CYCLES
Study of the influence of metallurgical factors on fatigue and fracture of aerospace structural materials
[AD-A179268] N87-23720
STRESS-STRAIN RELATIONSHIPS
Inelastic properties of ice /sub h/ at low temperatures and high pressures
[DE87-007334] N87-23711
Recent advances in the nonlinear analysis of laminated composite plates and shells N87-23819
Retardation effect in fatigue crack growth under stationary stochastic loading
[REPT-43/1986] N87-23999
The interpretation of crustal dynamics data in terms of plate motions and regional deformation near plate boundaries
[NASA-CR-180938] N87-24038
STRESSES
Training, muscle fatigue, and stress fractures
[AD-A178350] N87-24085
STRIP TRANSMISSION LINES
Rectangular microstrip patch antenna arrays
[AD-A179170] N87-23823
Finite element analysis of slow-wave Schottky contact printed lines
[AD-A179259] N87-23873
ESD (Electrostatic Discharge)/EOS (Electrical OverStress) susceptibility of a class of bipolar RF power transistors: Experimental studies on stripline-opposed emitter transistors
[AD-A178212] N87-23890
STRONG INTERACTIONS (FIELD THEORY)
The physics and a plan for a 45 GeV facility that extends the high-intensity capability in nuclear and particle physics
[LA-10720-MS] N87-24170
STRUCTURAL ANALYSIS
The Shock and Vibration Digest, Volume 19, No. 5 N87-23820
Consequence of layer separation on pavement performance
[DOT/FAA/PM-86/48] N87-23661
Collapse analysis of cylindrical composite panels with large cutouts under an axial load
[AD-A179112] N87-23701
Application of scanning acoustic microscopy to advanced structural ceramics
[NASA-TM-89929] N87-23987
Improved modeling of structural joint damping
[AD-A179111] N87-23988
Techniques for implementing statically complete component mode synthesis for forced response
[DE87-002698] N87-24002
LANDSAT-based lineament analysis, East Texas Basin, and structural history of the Sabine Uplift area, East Texas and North Louisiana
[PB87-176327] N87-24043
Perception and structural analysis of morphologies
[ENST-86D004] N87-24086
On integrating a logarithmic or semilogarithmic piecewise linear PSD plot of a random variable X(T): Part 1 N87-24126

Calculation of eigenvector derivatives for structures with repeated eigenvalues
[DE87-008399] N87-24135

STRUCTURAL DESIGN
Study of lee-side flows over conically cambered delta wings at supersonic speeds, part 1
[NASA-TP-2660-PT-1] N87-23597
The Shock and Vibration Digest, Volume 19, No. 5 N87-23820
Test plan for the 34 meter vertical axis wind turbine test bed located at Bushland, Texas
[DE87-004777] N87-24017

STRUCTURAL DESIGN CRITERIA
Dual-polarization 8.45 GHz traveling-wave maser N87-23838
Intercooled gas turbine
[PB87-178042] N87-23972

STRUCTURAL ENGINEERING
A consistent finite element formulation of nonlinear frictional contact problems
[AD-A179179] N87-23963

STRUCTURAL MEMBERS
Identification of structural interface characteristics using component mode synthesis
[NASA-TM-88960] N87-24006

STRUCTURAL PROPERTIES (GEOLOGY)
Radar as a complement to topographic maps for delineating marine terraces
[PB87-154597] N87-24013
LANDSAT-based lineament analysis, East Texas Basin, and structural history of the Sabine Uplift area, East Texas and North Louisiana
[PB87-176327] N87-24043

STRUCTURAL STABILITY
The influence of turbulence and deck section geometry on the aeroelastic behaviour of a cable-stayed bridge model
[NAE-AN-40] N87-23990
Forced vibration as a method for determining structural integrity
[DE87-005878] N87-23992
Thin-walled beam theories and their applications in the torsional strength analysis of ship hulls
[AD-A178296] N87-24001

SUBJECTS
Energy Data Base: Subject categories and scope, a reference manual
[DE87-005547] N87-24235

SUBMARINES
Medical research programs, past and future, for designing atmospheres to retard fires
[AD-A178354] N87-24089

SUBROUTINES
An extended set of FORTRAN basic linear algebra subprograms: Model implementation and test programs
[DE87-007913] N87-24101

SUBSONIC FLOW
Catastrophic breakup of liquid jet by subsonic transverse gas stream N87-23578

SUBSTRATES
The structure of Al/GaAs interfaces
[DE87-007181] N87-24206

SULFONATES
Electronics and ionic transport in polymers
[AD-A178227] N87-23746

SUMMARIES
Station climatic summaries, Antarctica, Australia and Oceania
[AD-A179242] N87-24047

SUN
Solar-geophysical data number 509, January 1987. Part 2: (Comprehensive reports). Data for July 1986
[PB87-162582] N87-24386

SUPERCOMPUTERS
The hypercube as a supercomputer
[DE87-005029] N87-24092

SUPERCONDUCTING MAGNETS
The development of a containment vessel and Dewar for the particle astrophysics magnet facility (ASTROMAG)
[NASA-CR-181016] N87-23670

SUPERCONDUCTIVITY
Superconducting electronic film structures
[AD-A179134] N87-24200

SUPERCONDUCTORS
Superconducting electronic film structures
[AD-A179134] N87-24200

SUPERCRITICAL AIRFOILS
High Reynolds Number tests of the NASA SC(2)-0012 airfoil in the Langley 0.3-meter transonic cryogenic tunnel
[NASA-TM-89102] N87-23594

SUPERCRITICAL FLOW
Response of transonic diffuser flows to abrupt increases of back pressure: Wall pressure measurements N87-23793

SUPERHIGH FREQUENCIES
DSS 13 frequency stability tests N87-23829
Microwave component time delays for the 70-meter antennas N87-23835
Block 3 X-band receiver-exciter N87-23837

SUPERNOVAE
Nucleosynthesis and astrophysical gamma ray spectroscopy N87-24259
Gamma ray transients N87-24260
A simple theory of bimodal star formation N87-24317

SUPERSONIC AIRCRAFT
The supersonic through-flow turbofan for high Mach propulsion
[NASA-TM-100114] N87-23626

SUPERSONIC COMBUSTION
Plasma torch igniter for scramjets N87-23789
CARS approaches to simultaneous measurements of H2 and H2O concentration and temperature in H2-air combustion systems N87-23792

SUPERSONIC CRUISE AIRCRAFT RESEARCH
The supersonic through-flow turbofan for high Mach propulsion
[NASA-TM-100114] N87-23626

SUPERSONIC FLOW
Experimental study of supersonic stream sliding at angle past one-step wedge with jaws N87-23573
Laser Doppler velocimeter application in supersonic boundary-layer flow
[AD-A178395] N87-23590
Study of lee-side flows over conically cambered delta wings at supersonic speeds, part 1
[NASA-TP-2660-PT-1] N87-23597
Investigation of shrouded nozzle exit pressure changes
[AD-A179477] N87-23911
Kinetic studies following state-selective laser excitation
[DE87-007938] N87-23950

SUPERSONIC JET FLOW
Structural analysis of supersonic jet discharging from free-vortex nozzle by method of holographic interferometry with pulsed laser N87-23574
Mathematical model describing interaction of single nonsteady supersonic jet and movable barrier of finite dimensions N87-23575
Compressibility of submerged supersonic jets N87-23581

SUPERSONIC SPEED
Measurement of surface pressures caused by a projectile rotating band at supersonic speeds
[AD-A171082] N87-23585

SUPERSONIC TURBINES
The supersonic through-flow turbofan for high Mach propulsion
[NASA-TM-100114] N87-23626

SUPPORTS
The influence of turbulence and deck section geometry on the aeroelastic behaviour of a cable-stayed bridge model
[NAE-AN-40] N87-23990

SUPPRESSORS
Microscale defect kinetics in melt-grown GaAs
[AD-A178158] N87-24218

SURFACE ACOUSTIC WAVE DEVICES
Corrosion sensing with acoustic wave devices
[DE87-003516] N87-23723

SURFACE FINISHING
Microwave component time delays for the 70-meter antennas N87-23835

SURFACE LAYERS
Fabrication of AlGaAs/InGaAs pseudomorphic modulation doped field effect transistors with p-doped surface layers
[AD-A179230] N87-24201

SURFACE NOISE INTERACTIONS
Extension of Kirchhoff's formula to radiation from moving surfaces
[NASA-TM-89149] N87-24160

SURFACE PROPERTIES
Measurement of surface pressures caused by a projectile rotating band at supersonic speeds
[AD-A171082] N87-23585
Acta aeronautica et astronautica sinica
[AD-A179673] N87-23618
Recovering the orientation of textured surfaces in natural scenes
[AD-A179360] N87-24096

SURFACE REACTIONS
A hybrid closed bomb-strand burner for very high pressure burning rate measurements N87-23786
Means for phase locking the outputs of a surface emitting laser diode array
[NASA-CASE-NPO-16542-1-CU] N87-23960

SURFACE ROUGHNESS
Surface roughness: Its effects on the performance of a two-dimensional compressor cascade
[AD-A179508] N87-23913

SURFACE ROUGHNESS EFFECTS
Effect of surface roughness on drag of aircraft N87-23571

SURFACE VEHICLES
Image sensor data base for the DARPA ALV (Defense Advanced Research Projects Agency Autonomous Land Vehicle) program
[AD-A178117] N87-24246

SURGES
Development of model describing unstable operation of turbocompressor and design of antisurging protection for gas turbine engine N87-23577

SUSPENSION SYSTEMS (VEHICLES)
The Shock and Vibration Digest, Volume 19, No. 4 N87-23818
Recent developments in vehicle dynamics N87-23820

SWEPT WINGS
Some aspects of vortex flows determined from the thin-layer Navier-Stokes equations
[NASA-TM-88375] N87-23595

SWITCHING CIRCUITS
Solid state research
[AD-A178394] N87-24221

SYMBOLS
Symbol manipulation and applied mathematics
[AD-A179571] N87-24124

SYMMETRICAL BODIES
High Reynolds Number tests of the NASA SC(2)-0012 airfoil in the Langley 0.3-meter transonic cryogenic tunnel
[NASA-TM-89102] N87-23594

SYMMETRY
Symmetry problems in particle physics
[DE87-006360] N87-24168

SYNCHRONISM
Synchronization trigger control system for flow visualization
[NASA-TM-89902] N87-23902
Time slice manipulation in information hierarchy
[AD-A177949] N87-24237

SYNCHRONOUS SATELLITES
Optimal continuous thrust orbital evasive maneuvers from geosynchronous orbit
[AD-A179413] N87-23668

SYNCHROTRON RADIATION
Report of the Second Workshop on Synchrotron Radiation Sources for X-ray Lithography
[DE87-002155] N87-24179

SYNCHROTRONS
The physics and a plan for a 45 GeV facility that extends the high-intensity capability in nuclear and particle physics
[LA-10720-MS] N87-24170
Report of the Second Workshop on Synchrotron Radiation Sources for X-ray Lithography
[DE87-002155] N87-24179

SYNTHESIS (CHEMISTRY)
Potential Applications of Biotechnology to Aerospace Materials
[AD-A177875] N87-23667
Preparation of B-trichloroborazine
[NASA-CASE-ARC-11643-1-SB] N87-23698
New low temperature (hydroxylated) materials
[DE87-008530] N87-23749
Functionalization of cubane using hypervalent iodine N87-23807

SYNTHETIC APERTURE RADAR
Automated radar image analysis research in support of military needs
[AD-A179615] N87-23827

SYNTHETIC APERTURES
Holographic correction of aberrations in optical systems employing synthetic apertures
[AD-A179107] N87-24173

SYNTHETIC FUELS
Fuels from microalgae: Technology status, potential and research requirements
[DE88-010739] N87-23753
Viscosity of synfuel compounds and mixtures
[DE87-008696] N87-23756

SYSTEM FAILURES
Failure detection and isolation for an asychronous digital flight control system
[AD-A178210] N87-23628
Investigation of electromigration in thin film aluminum at low temperatures
[AD-A179110] N87-23871

SYSTEMS ANALYSIS
Evaluation of the angle of attack limiter of the F-16 C/D aircraft
[AD-A177941] N87-23612

A systems analysis of emergency escape and recovery systems for the US space station
[AD-A179233] N87-23680
Engineering and instrumentation support of the AFGL (Air Force Geophysics Laboratory) Rocket Research Program
[AD-A179257] N87-23689
Research in VLSI systems
[AD-A179227] N87-23872
Random vibration of nonlinear systems N87-23997

SYSTEMS ENGINEERING
A quantitative comparison of several orbital maneuvering vehicle configurations for satellite repair/replenishment
[AD-A179106] N87-23677
Multiplex electric discharge gas laser system
[NASA-CASE-NPO-16433-1] N87-23961
Decaying confidence functions for aging knowledge in expert systems
[AD-A179328] N87-24152
Optimization of extended relational database systems
[AD-A179308] N87-24230
Standardized procedure for system safety input to the Defense Technical Information Center (DTIC)
[AD-A178246] N87-24239
Research and Technology
[NASA-TM-89411] N87-24391

SYSTEMS INTEGRATION
Trends in ground-based and in-flight simulators for development applications N87-23645

SYSTEMS MANAGEMENT
Using expert systems to manage distributed computer systems
[AD-A179329] N87-24112
Standardized procedure for system safety input to the Defense Technical Information Center (DTIC)
[AD-A178246] N87-24239

SYSTOLIC ARRAYS
Hardware synthesis from specification with polynomials
[TRITA-NA-8506] N87-24091

T

TAKEOFF
Aircraft accident report: Southern Air Transport LOGAIR Flight 51, Lockheed L-382G, Kelly Air Force Base, Texas, October 4, 1986
[PB87-910404] N87-23604
Interpretation in terms of the response of a one degree-of-freedom oscillator to two successive disturbances N87-23610
Simulation of aircraft behaviour on and close to the ground: Summary of AGARD•ic6)ograph AG-285 N87-23640

TAPERING
Experiments on dynamic stiffness and damping of tapered bore seals
[NASA-TM-89895] N87-23984

TARGET ACQUISITION
A new approach to multitarget tracking using probabilistic data association
[AD-A179437] N87-23825

TAXIING
Aircraft Dynamic Response to Damaged and Repaired Runways
[AGARD-R-739] N87-23609
Interpretation in terms of the response of a one degree-of-freedom oscillator to two successive disturbances N87-23610
An experimental-analytical routine for the dynamic qualification of aircraft operating on rough runway surfaces N87-23611

TAYLOR INSTABILITY
Onset of Taylor vortices in flows with a circumferential pressure gradient: Application to the helical screw rheometer
[DE87-000453] N87-23918

TEARING
The effect of reinforcement on the tear properties of flexible circuits
[DE87-007022] N87-23895
Investigation of tearing instability phenomena in ASTM steel
[AD-A177993] N87-24000

TECHNOLOGICAL FORECASTING
Speculations on future opportunities to evolve Brayton powerplants aboard the space station
[NASA-TM-89863] N87-23674

TECHNOLOGY ASSESSMENT
Manufacturing processes for high-temperature structural ceramics: A patent trend analysis
[PB87-178059] N87-23742
Fuels from microalgae: Technology status, potential and research requirements
[DE86-010739] N87-23753
Microwave Antennas for Avionics
[AGARD-LS-151] N87-23859
Characterization of solar thermal concepts for electricity generation. Volume 1: Analyses and evaluation
[DE87-007161] N87-24019
The effect of distributed computing technology on wide area network capacity requirements
[DE87-006229] N87-24117

TECHNOLOGY TRANSFER
Federal laboratory nondestructive testing research and development applicable to industry
[DE87-008351] N87-23985

TELECOMMUNICATION
Communication-efficient parallel graph algorithms
[AD-A178286] N87-23853
A multi user random access communication system for users with different priorities
[AD-A178372] N87-23854

TELEMETRY
Engineering and instrumentation support of the AFGL (Air Force Geophysics Laboratory) Rocket Research Program
[AD-A179257] N87-23689

TELEOPERATORS
A quantitative comparison of several orbital maneuvering vehicle configurations for satellite repair/replenishment
[AD-A179106] N87-23677

TEMPERATURE DEPENDENCE
The structure and electrical properties of metal contacts on GaAs
[DE87-008217] N87-24210

TEMPERATURE DISTRIBUTION
Explicit finite-volume time-marching calculations of total temperature distributions in turbulent flow N87-23929

TEMPERATURE EFFECTS
Effects of corona on heat transfer in an enclosure
[AD-A179209] N87-23906
Thermomechanical effects in high-speed seal rubs
[NASA-CR-180418] N87-23979

TEMPERATURE MEASUREMENT
CARS approaches to simultaneous measurements of H2 and H2O concentration and temperature in H2-air combustion systems N87-23792
Nonintrusive temperature measurements in SSME preburner element flowfields N87-23813
Development of ultrasonic thermometry for high-temperature high-resolution temperature profiling applications in LMFBR safety research
[SAND-84-1341] N87-24171
Star forming regions of the southern galaxy N87-24273
IRAS observations of the Pleiades N87-24284

TEMPERATURE MEASURING INSTRUMENTS
Development of ultrasonic thermometry for high-temperature high-resolution temperature profiling applications in LMFBR safety research
[SAND-84-1341] N87-24171

TEMPERATURE PROFILES
Development of ultrasonic thermometry for high-temperature high-resolution temperature profiling applications in LMFBR safety research
[SAND-84-1341] N87-24171

TENSILE DEFORMATION
Studies on age-hardening in spinodally modulated alloys: Experimental and theoretical
[DE87-008361] N87-23727

TERMINOLOGY
Energy Data Base: Subject categories and scope, a reference manual
[DE87-005547] N87-24235

TERRAIN
On autonomous terrain model acquisition by a mobile robot
[DE87-005719] N87-23964

TERRAIN ANALYSIS
Analysis of space-based radar clutter spectra over different types of terrain and their effects on detection performance
[AD-A178066] N87-23845

TEST EQUIPMENT
A single chip LSI high-speed functional tester
[AD-A177886] N87-23886

TEST FACILITIES
Reactivation study for NASA Lewis Research Center's hypersonic tunnel facility
[NASA-TM-89918] N87-23664
Magnetostatic surface field measurement facility
[AD-A178258] N87-23850
Modeling of dilute two-phase multispecies solid/gas flows
[DE87-009254] N87-23932
Sandia National Laboratories 34-meter diameter vertical axis wind turbine test bed
[DE87-003096] N87-24016

TETRAHEDRONS
Three-dimensional model for the linear elastic properties of a foam
[DE87-000984] N87-23732

TEXAS
LANDSAT-based lineament analysis, East Texas Basin, and structural history of the Sabine Uplift area, East Texas and North Louisiana
[PB87-176327] N87-24043

TEXTS
Text editing performance as a function of screen size
[AD-A179067] N87-24229

TEXTURES
Recovering the orientation of textured surfaces in natural scenes
[AD-A179360] N87-24096

THEMATIC MAPPING
Utilizing remote sensing of thematic mapper data to improve our understanding of estuarine processes and their influence on the productivity of estuarine-dependent fisheries
[NASA-CR-180984] N87-24012
Spatial characterization of acid rain stress in Canadian Shield lakes
[NASA-CR-180983] N87-24031

THEORETICAL PHYSICS
Research in theoretical particle physics
[DE87-008240] N87-24169

THERAPY
Hypertension in the aviator N87-24077

THERMAL ANALYSIS
Preliminary thermal analysis of transistor packages
[DE87-007706] N87-23898

THERMAL DECOMPOSITION
Simultaneous thermogravimetric modulated beam mass spectrometry and time-of-flight velocity spectra measurements of thermal decomposition products from RDX and HMX N87-23780
Quantum chemical calculations of the decomposition of nitramines: Thermochemistry and reaction pathways N87-23781
Thermal decomposition and ignition of a series of new nitramine lova propellants by CO2 laser N87-23783

THERMAL DEGRADATION
Theoretical influence of propellant packaging on tube erosion: model formulation and algorithm development N87-23784

THERMAL EMISSION
X-ray astronomical spectroscopy N87-24263
Infrared-ultraviolet spectra of active galactic nuclei N87-24372

THERMAL ENERGY
Unsteady heat transfer resulting from the rapid charging of an evacuated tank with conducting walls
[AD-A179206] N87-23905

THERMAL INSTABILITY
Numerical simulation of a randomly heated, thermally unstable fluid
[AD-A177888] N87-24225

THERMAL PROTECTION
Design, development and test of shuttle/Centaur G-prime cryogenic tankage thermal protection systems
[NASA-TM-89825] N87-23685
Thermal stress analysis of space shuttle orbiter wing skin panel and thermal protection system
[NASA-TM-88276] N87-23994

THERMAL RESISTANCE
Fire and heat resistant laminating resins based on malemeido and citraconimido substituted 1 -2,4- and -2,6-diaminobenzenes
[NASA-CASE-ARC-11533-1] N87-23751
Preliminary thermal analysis of transistor packages
[DE87-007706] N87-23898
Method of making a flexible diaphragm
[NASA-CASE-MSC-20797-1] N87-23981

THERMAL STABILITY
Thermal stress analysis of space shuttle orbiter wing skin panel and thermal protection system
[NASA-TM-88276] N87-23994

THERMAL STRESSES
Thermal stress analysis of space shuttle orbiter wing skin panel and thermal protection system
[NASA-TM-88276] N87-23994
Thermal fracture in selected nonlinear optical materials
[DE87-008213] N87-24209

THERMOCLINES
Mixed layer and thermocline depth climatologies in the western Indian Ocean
[PB87-154613] N87-24060

THERMODYNAMIC CYCLES
Analysis of a mechanically simple external combustion engine with an unusual cycle
[DE87-007788] N87-23965

Heat transfer research for ocean thermal energy conversion
[DE87-001155] N87-24023
THERMODYNAMIC EFFICIENCY
Intercooled gas turbine
[PB87-178042] N87-23972
THERMODYNAMIC PROPERTIES
The use of molecular dynamics for the thermodynamic properties of simple and transition metals
[DE87-007718] N87-23725
Theoretical and experimental investigations of fluctuation thermodynamic properties of liquid solutions
[DE87-005681] N87-24224
THERMODYNAMICS
Thermodynamic evaluation of transonic compressor rotors using the finite volume approach
[NASA-CR-180587] N87-23925
Meso gamma-scale kinetic energy budgets of a thunderstorm within a squall-line derived from sesame dual-doppler data
[AD-A178119] N87-24057
Smoothing and the second law
[NASA-TM-88371] N87-24146
THERMOELECTRIC GENERATORS
Speculations on future opportunities to evolve Brayton powerplants aboard the space station
[NASA-TM-89863] N87-23674
THERMOSPHERE
A comparison of ionospheric model predictions with MITHRAS observations
[AD-A179374] N87-24036
THETA PINCH
Compact toroid generation, lifetime, and stability studies in linear reverse field theta pinch geometries (TRX-2): Final report
[DE87-005094] N87-24195
THICK PLATES
Recent studies in plate vibrations: 1981-1985. Part 2: Complicating effects N87-23998
THICKNESS
Performance of two 10-lb/sec centrifugal compressors with different blade and shroud thicknesses operating over a range of Reynolds numbers
[NASA-TM-100115] N87-23623
THIN BODIES
Simultaneous radiative and convective heating of thin body in medium with variable temperature N87-23576
THIN FILMS
Spin-cast carbon films from polyacrylonitrile
[DE87-002489] N87-23703
Corrosion sensing with acoustic wave devices
[DE87-003516] N87-23723
Plasma deposition of tungsten
[DE87-007390] N87-23724
Fundamentals of sol-gel thin film formation
[DE87-007387] N87-23738
Investigation of electromigration in thin film aluminum at low temperatures
[AD-A179110] N87-23871
Superconducting electronic film structures
[AD-A179134] N87-24200
Thin film characterization using a mechanical properties microprobe
[DE87-006593] N87-24214
THIN PLATES
Thermal fracture in selected nonlinear optical materials
[DE87-006213] N87-24209
THIN WALLS
Thin-walled beam theories and their applications in the torsional strength analysis of ship hulls
[AD-A178296] N87-24001
THREE DIMENSIONAL BODIES
Viscous-inviscid interaction with higher-order viscous-flow equations: Applications to three-dimensional bodies
[AD-A178264] N87-23924
PRONTO 2D: A two-dimensional transient solid dynamics program
[DE87-007823] N87-23993
Computer programs for nonlinear least squares analysis of various three-dimensional geometrical elements
[DE87-006046] N87-24133
THREE DIMENSIONAL BOUNDARY LAYER
Three-dimensional structure of boundary layers in transition to turbulence
[AD-A179247] N87-23908
THREE DIMENSIONAL FLOW
Method for the determination of the three-dimensional aerodynamic field of a rotor-stator combination to compressible flow
[NASA-TM-100118] N87-23625
Investigation of shrouded nozzle exit pressure changes
[AD-A179477] N87-23911
Viscous-inviscid interaction with higher-order viscous-flow equations: Applications to three-dimensional bodies
[AD-A178264] N87-23924
THRUST
Low power arcjet thruster pulse ignition
[NASA-TM-100123] N87-23691
THRUST CHAMBERS
Measurements for rocket engine performance code verification N87-23811
THRUST CONTROL
Optimal continuous thrust orbital evasive maneuvers from geosynchronous orbit
[AD-A179413] N87-23668
An approach of preventing combustion vibrations of rocket engine with lateral baffle
[AD-A179222] N87-23688
THRUST VECTOR CONTROL
Development of in-flight simulation aircraft for research and training applications in UK N87-23658
The freezing of flow deflection in Prandtl-Meyer expansion to vacuum
[ISL-CO-226/86] N87-23686
THUNDERSTORMS
Tactical weather expert system
[AD-A178605] N87-24050
Meso gamma-scale kinetic energy budgets of a thunderstorm within a squall-line derived from sesame dual-doppler data
[AD-A178119] N87-24057
TILT ROTOR RESEARCH AIRCRAFT PROGRAM
Piloted simulation in the development of the XV-15 tilt rotor research aircraft N87-23646
TIME
Failure detection and isolation for an asychronous digital flight control system
[AD-A179210] N87-23628
Time domain wave propagation in multilayered integrated circuits
[AD-A178180] N87-23847
Decaying confidence functions for aging knowledge in expert systems
[AD-A179328] N87-24152
TIME DEPENDENCE
GASPS: A time-dependent, one-dimensional, planar gas dynamics computer code
[DE87-008338] N87-23931
Time-resolved picosecond reflectivity study of laser-excited layered compounds
[DE87-005115] N87-23952
Far field boundary conditions for time-dependent hyperbolic systems
[AD-A179361] N87-24123
Drift mobilities by time-of-flight methods and time-dependent phototransport in the nanosecond regime in amorphous semiconductors
[DE87-006021] N87-24208
TIME LAG
High-angle-of-attack pneumatic lag and upwash corrections for a hemispherical flow direction sensor
[NASA-TM-86790] N87-23616
Microwave component time delays for the 70-meter antennas N87-23835
TIME MARCHING
Thermodynamic evaluation of transonic compressor rotors using the finite volume approach
[NASA-CR-180587] N87-23925
Development of an explicit time marching procedure for laminar and turbulent flow N87-23926
Development of a finite volume time marching method
[JM/85-3] N87-23927
An explicit finite-volume time-marching procedure for turbulent flow calculations N87-23928
Explicit finite-volume time-marching calculations of total temperature distributions in turbulent flow N87-23929
TIME MEASUREMENT
Results of using the global positioning system to maintain the time and frequency synchronization in the Deep Space Network N87-23834
TIME OF FLIGHT SPECTROMETERS
Simultaneous thermogravimetric modulated beam mass spectrometry and time-of-flight velocity spectra measurements of thermal decomposition products from RDX and HMX N87-23780
TIME OPTIMAL CONTROL
Optimal continuous thrust orbital evasive maneuvers from geosynchronous orbit
[AD-A179413] N87-23668
TIME SERIES ANALYSIS
Automated radar image analysis research in support of military needs
[AD-A179615] N87-23827
Changing time series
[AD-A178030] N87-24149
TIN ALLOYS
Wetting properties of Au/Sn solders for microelectronics
[DE87-008519] N87-23883
TITANIUM ALLOYS
The corrosion of Al 7075-T6 alloy coupled to Ti 6A 1-4V in wet air
[DE87-008347] N87-23726
TOKAMAK DEVICES
Report to DOE of the fusion programs in applied plasma physics and development and technology at GA Technologies, Incorporated
[DE87-008882] N87-24197
TOLUENE
Viscosity of synfuel compounds and mixtures
[DE87-008696] N87-23756
TOPOGRAPHY
Finite difference simulations of Rayleigh wave scattering by 2-D rough topography
[AD-A179190] N87-23824
Radar as a complement to topographic maps for delineating marine terraces
[PB87-154597] N87-24013
Proposal for continued research in intelligent machines at the Center for Engineering Systems Advanced Research (CESAR) for FY 1988 to FY 1991
[DE87-007789] N87-24121
Cornea Optical Topographical Scan System (COTSS)
[NASA-CR-179012] N87-24184
TOPOLOGY
Novel application of topological indices. 2. Prediction of the threshold soot index for hydrocarbon fuels
[AD-A178001] N87-23716
TOROIDS
Compact toroid generation, lifetime, and stability studies in linear reverse field theta pinch geometries (TRX-2): Final report
[DE87-005094] N87-24195
TORQUE
Helicopter anti-torque system using fuselage strakes
[NASA-CASE-LAR-13630-1] N87-23630
Analysis and test results for an improved constant speed passive cyclic pitch wind turbine
[DE87-001135] N87-24022
TORSIONAL STRESS
Thin-walled beam theories and their applications in the torsional strength analysis of ship hulls
[AD-A178296] N87-24001
TORSIONAL VIBRATION
Turbomachine blade vibration N87-23621
TOUGHNESS
Investigation of the impact performance of various glass and ceramic systems
[AD-A178115] N87-23744
Influence of microstructure and microdamage processes on fracture at high loading rates
[AD-A179264] N87-23989
TOXICITY
Biomedical applications of the free electron laser
[AD-A179182] N87-24066
TRACE ELEMENTS
Transport and photochemical modeling. Studies of atmospheric species
[NASA-CR-178311] N87-24040
TRACKING (POSITION)
Advanced visuals in mission simulators N87-23636
A new approach to multitarget tracking using probabilistic data association
[AD-A179437] N87-23825
An evaluation of the communication system for the TAU mission study N87-23840
TRADEOFFS
Effect of a trade between boattail angle and wedge size on the performance of a nonaxisymmetric wedge nozzle
[NASA-TP-2717] N87-23593
Spacecraft mass trade-offs versus radio-frequency power and antenna size at 8 GHz and 32 GHz N87-23830
TRAFFIC
Nonparametric estimation of the probability of a long delay in the M/G/1 queue
[AD-A178259] N87-24150
TRAILING EDGES
Unsteady separated flows: Vorticity and turbulence
[AD-A179500] N87-23912
TRAINING AIRCRAFT
The development of the T-46 next generation trainer manned engineering simulator at the US Air Force Flight Test Center N87-23652
TRAINING EVALUATION
Training, muscle fatigue, and stress fractures
[AD-A178350] N87-24085
TRAJECTORY OPTIMIZATION
Optimal aerodynamic shapes for hypervelocity projectiles
[AD-A178367] N87-23672

TRANSCENDENTAL FUNCTIONS
Asymptotic analysis of the roots of a certain transcendental equation
[AD-A168315] N87-24131
TRANSDUCERS
Adjustable mount for electro-optic transducers in an evacuated cryogenic system
[NASA-CASE-LAR-13100-1] N87-23982
TRANSFORMATIONS (MATHEMATICS)
The decomposition of an arbitrary three-dimensional planar polygon into a set of convex polygons
[AD-A177947] N87-24137
TRANSIENT PRESSURES
Unsteady heat transfer resulting from the rapid charging of an evacuated tank with conducting walls
[AD-A179206] N87-23905
TRANSIENT RESPONSE
Impulsive EMI (Electromagnetic Interference) radiated by Electrostatic Discharges (ESD)
[AD-A178213] N87-23848
TRANSISTORS
Fabrication of AlGaAs/InGaAs pseudomorphic modulation doped field effect transistors with p-doped surface layers
[AD-A179230] N87-24201
TRANSITION METALS
Metal alkoxides: Models for metal oxides: Alkoxide ligands in early transition metal organometallic chemistry
[DE87-007309] N87-23715
The use of molecular dynamics for the thermodynamic properties of simple and transition metals
[DE87-007718] N87-23725
TRANSITION PROBABILITIES
Wavelengths of K X-rays of iron ions
[IPPJ-AM-49] N87-24198
TRANSMISSION
A study of Schwarz converters for nuclear powered spacecraft
[NASA-TM-89911] N87-23903
TRANSMISSION EFFICIENCY
DSS 13 frequency stability tests N87-23829
TRANSONIC FLOW
Response of transonic diffuser flows to abrupt increases of back pressure: Wall pressure measurements N87-23793
Downstream boundary effects on the frequency of self-excited oscillations in transonic diffuser flows N87-23794
Development of a finite volume time marching method
[JM/85-3] N87-23927
TRANSONIC WIND TUNNELS
High Reynolds Number tests of the NASA SC(2)-0012 airfoil in the Langley 0.3-meter transonic cryogenic tunnel
[NASA-TM-89102] N87-23594
TRANSPORT AIRCRAFT
DFVLR in-flight simulators ATTAS and ATTHES for flying qualities and flight control research N87-23657
TRANSPORT PROPERTIES
Transport phenomena and interfacial kinetics in multiphase combustion systems
[AD-A179544] N87-23709
Electrochemical performance and transport properties of a Nafion membrane in a hydrogen-bromine cell environment
[NASA-TM-89862] N87-23718
Electronics and ionic transport in polymers
[AD-A178227] N87-23746
TRANSPORT THEORY
High-current beam dynamics and transport, theory and experiment
[DE87-006154] N87-24172
TRAPPED PARTICLES
Magnetospheres of the outer planets N87-24248
TRAVELING WAVE MASERS
Use of a 2.3-GHz traveling-wave maser on the Usuda 64-meter antenna N87-23831
Dual-polarization 8.45 GHz traveling-wave maser N87-23838
TRENDS
Trends of petroleum fuels: Topical report
[DE87-001237] N87-23755
TRIGGER CIRCUITS
Synchronization trigger control system for flow visualization
[NASA-TM-89902] N87-23902
TROPICAL STORMS
Mid-latitude wind probability model
[AD-A179256] N87-24048
TUMBLING MOTION
Detumbling of two inter-connected rigid bodies using Liapunov methods for feedback control
[AD-A179207] N87-23679
TUNGSTEN
Plasma deposition of tungsten
[DE87-007390] N87-23724
TUNNEL DIODES
Palladium-silver and gold alloys as catalytic gates on MIS gas sensors
[DE87-006959] N87-23943
TURBINE BLADES
Acta aeronautica et astronautica sinica
[AD-A179673] N87-23618
TURBINE ENGINES
The T55-L-712 turbine engine compressor housing refurbishment project
[NASA-CR-179624] N87-23729
Antimisting Fuel (AMK) flight degrader development and aircraft fuel system investigation
[DOT/FAA/CT-86/6] N87-23816
TURBINE PUMPS
Straight cylindrical seal for high-performance turbomachines
[NASA-TP-1850] N87-23936
TURBINE WHEELS
Effectiveness of balancing flexible rotary compressor vanes on low-speed balancing machine N87-23580
TURBINES
USSR report: Engineering and equipment
[JPRS-UEQ-87-005] N87-23570
TURBOCOMPRESSORS
Development of model describing unstable operation of turbocompressor and design of antisurging protection for gas turbine engine N87-23577
Effectiveness of balancing flexible rotary compressor vanes on low-speed balancing machine N87-23580
Method for the determination of the three-dimensional aerodynamic field of a rotor-stator combination to compressible flow
[NASA-TM-100118] N87-23625
TURBOFAN ENGINES
The supersonic through-flow turbofan for high Mach propulsion
[NASA-TM-100114] N87-23626
TURBOMACHINE BLADES
The Shock and Vibration Digest, Volume 19, No. 5 N87-23620
Turbomachine blade vibration N87-23621
TURBOMACHINERY
Three-step labyrinth seal for high-performance turbomachines
[NASA-TP-1848] N87-23921
Straight cylindrical seal for high-performance turbomachines
[NASA-TP-1850] N87-23936
TURBOPROP AIRCRAFT
Coupled aerodynamic and acoustical predictions for turboprops
[NASA-TM-87094] N87-23598
TURBOPROP ENGINES
Dynamic response of two composite prop-fan models on a nacelle/wing/fuselage half model
[NASA-CR-179589] N87-23615
TURBULENCE
Unsteady separated flows: Vorticity and turbulence
[AD-A179500] N87-23912
On the breakdown of the wave packet trailing a turbulent spot in a laminar layer
[AD-A179607] N87-23915
Direct numerical simulations of a temporally evolving mixing layer subject to forcing
[NASA-TM-88896] N87-23933
TURBULENCE EFFECTS
Experimental evaluation of honeycomb/screen configurations and short contraction section for NASA Lewis Research Center's altitude wind tunnel
[NASA-TP-2692] N87-23662
TURBULENT BOUNDARY LAYER
Laser Doppler velocimeter application in supersonic boundary-layer flow
[AD-A178395] N87-23590
Turbulent boundary layer structure, drag reduction
[AD-A179246] N87-23907
Theoretical investigation of 3-D shock wave-turbulent boundary layer interactions, part 5
[AD-A179455] N87-23909
TURBULENT FLOW
Experimental evaluation of honeycomb/screen configurations and short contraction section for NASA Lewis Research Center's altitude wind tunnel
[NASA-TP-2692] N87-23662
Sandia cooperative group on the aerothermochemistry of turbulent combustion
[DE87-008345] N87-23714
Passive shear-flow control to minimize ramjet combustion instabilities N87-23798
Multispecies CARS measurements in turbulent combustion N87-23806
Three-dimensional structure of boundary layers in transition to turbulence
[AD-A179247] N87-23908
Experimental and numerical investigation of coherent structures
[AD-A179456] N87-23910
Thermodynamic evaluation of transonic compressor rotors using the finite volume approach
[NASA-CR-180567] N87-23925
Development of an explicit time marching procedure for laminar and turbulent flow N87-23926
An explicit finite-volume time-marching procedure for turbulent flow calculations N87-23928
Explicit finite-volume time-marching calculations of total temperature distributions in turbulent flow N87-23929
The influence of turbulence and deck section geometry on the aeroelastic behaviour of a cable-stayed bridge model
[NAE-AN-40] N87-23990
TURBULENT MIXING
Compressibility of submerged supersonic jets N87-23581
TURBULENT WAKES
Surface roughness: Its effects on the performance of a two-dimensional compressor cascade
[AD-A179506] N87-23913
TURING MACHINES
Hardware synthesis from specification with polynomials
[TRITA-NA-8506] N87-24091
TWO DIMENSIONAL BOUNDARY LAYER
A unified direct-inverse procedure for two-dimensional boundary layers using spline/finite difference discretization
[AD-A178223] N87-24140
TWO DIMENSIONAL FLOW
Two-dimensional aerodynamic characteristics of the AMES HI-120, HI-8, and LOW-12 airfoils
[NASA-CR-181018] N87-23589
Investigation of shrouded nozzle exit pressure changes
[AD-A179477] N87-23911
Effective diffusion in laminar convective flows
[DE87-008054] N87-23920
An explicit finite-volume time-marching procedure for turbulent flow calculations N87-23928
REZONE: A method for automatic rezoning in two-dimensional Lagrangian hydrodynamics problems
[DE87-006324] N87-23930
TWO PHASE FLOW
Catastrophic breakup of liquid jet by subsonic transverse gas stream N87-23578
Influence of two-phase flow in the deflagration of homogeneous solids N87-23777
Analysis of pressure oscillations in ramjets. Review of research: 1985-1986 N87-23796
Effects on fuel spray characteristics and vaporization on energy release rates and flow field structure in a dump combustor N87-23804
Modeling of dilute two-phase multispecies solid/gas flows
[DE87-009254] N87-23932

U

U.S.S.R.
USSR report: Engineering and equipment
[JPRS-UEQ-87-005] N87-23570
ULTRASONIC TESTS
Rapid quantification of an internal property — ultrasonic determination of bladder urine quantity
[NASA-CASE-LAR-13689-1-NP] N87-23941
Ultrasonic techniques for the evaluation of ceramic joints
[DE87-009104] N87-23966
ULTRASONIC WAVE TRANSDUCERS
Corrosion sensing with acoustic wave devices
[DE87-003516] N87-23723
ULTRASONICS
Development of ultrasonic thermometry for high-temperature high-resolution temperature profiling applications in LMFBR safety research
[SAND-84-1341] N87-24171
ULTRAVIOLET RADIATION
A mechanistic study of the interaction of ultraviolet laser radiation with low density polymers
[DE87-007846] N87-23734
Ordered many-electron motions in atoms and X-ray lasers
[DE87-004731] N87-23951
ULTRAVIOLET SPECTRA
Infrared-ultraviolet spectra of active galactic nuclei N87-24372
UMBRAS
Fifty year canon of solar eclipses: 1986-2035
[NASA-TM-89346] N87-24377

UNDERCARRIAGES
Aircraft Dynamic Response to Damaged and Repaired Runways
[AGARD-R-739] N87-23609
UNIQUENESS
Uniqueness of non-negative solutions of a class of semi-linear elliptic equations
[DE87-006966] N87-24128
UNITED STATES
Aircraft accident data: US air carrier operations calendar year 1984
[PB87-163992] N87-23603
Aircraft accident data: US air carrier operations calendar year 1983
[PB87-160628] N87-23605
Annual review of aircraft accident data, US general aviation: Calendar year 1984
[PB87-194791] N87-23606
Spatial characterization of acid rain stress in Canadian Shield lakes
[NASA-CR-180982] N87-24032
UNIVERSITY PROGRAM
Fusion Energy Postdoctoral Research Program and Professional Development Program
[DE87-006350] N87-24188
UNSTEADY FLOW
Mathematical model describing interaction of single nonsteady supersonic jet and movable barrier of finite dimensions N87-23575
Unsteady separated flows: Vorticity and turbulence
[AD-A179500] N87-23912
Numerical simulation of a randomly heated, thermally unstable fluid
[AD-A177888] N87-24225
UPLINKING
Block 3 X-band receiver-exciter N87-23837
An evaluation of the communication system for the TAU mission study N87-23840
UPWASH
High-angle-of-attack pneumatic lag and upwash corrections for a hemispherical flow direction sensor
[NASA-TM-86790] N87-23616
URANUS (PLANET)
Magnetospheres of the outer planets N87-24248
URINE
Rapid quantification of an internal property — ultrasonic determination of bladder urine quantity
[NASA-CASE-LAR-13689-1-NP] N87-23941
USER REQUIREMENTS
The development of a prototype intelligent user interface subsystem for NASA's scientific database systems
[NASA-TM-87821] N87-24098
The future of intersite networking
[DE87-007912] N87-24116
The effect of distributed computing technology on wide area network capacity requirements
[DE87-006229] N87-24117
Cornea Optical Topographical Scan System (COTSS)
[NASA-CR-179012] N87-24184
The success or failure of management information systems: A theoretical approach
[DE87-007602] N87-24233

V

VACUUM
The freezing of flow deflection in Prandtl-Meyer expansion to vacuum
[ISL-CO-226/86] N87-23686
VAPOR DEPOSITION
Transport phenomena and interfacial kinetics in multiphase combustion systems
[AD-A179544] N87-23709
Ceramic honeycomb structures and the method thereof
[NASA-CASE-ARC-11652-1] N87-23737
VAPOR PHASE EPITAXY
Epitaxial semiconductor optical interference devices
[DE87-006890] N87-24212
Solid state research
[AD-A178394] N87-24221
VAPOR PHASES
Quantum chemical calculations of the decomposition of nitramines: Thermochemistry and reaction pathways N87-23781
VAPORIZING
Combustion, vaporization, and microexplosion of droplets of organic azides N87-23806
VARIATIONS
Smoothing and the second law
[NASA-TM-88371] N87-24146
VECTOR ANALYSIS
Architectural implications of a parallel computational approach to the vector wave equation
[AD-A179510] N87-24113
The development of a prototype CMOS (Complementary Metal Oxide Semiconductor) circuit simulator
[AD-A177942] N87-24215
VECTORS (MATHEMATICS)
An extended set of FORTRAN basic linear algebra subprograms: Model implementation and test programs
[DE87-007913] N87-24101
VEHICLES
The Shock and Vibration Digest, Volume 19, No. 6 N87-24125
VELOCITY
Investigation of the impact performance of various glass and ceramic systems
[AD-A178115] N87-23744
VELOCITY DISTRIBUTION
Light sheet visualization and velocity field measurements in seeded flows — YAG laser
[ISL-CO-225/86] N87-23935
VELOCITY MEASUREMENT
Simultaneous thermogravimetric modulated beam mass spectrometry and time-of-flight velocity spectra measurements of thermal decomposition products from RDX and HMX N87-23780
VENTILATION
Operation Everest 2: Importance of ventilation in defense of maximal oxygen uptake at extreme altitudes
[AD-A177874] N87-24082
VERY LARGE SCALE INTEGRATION
A VLSI single chip (255,223) Reed-Solomon encoder with interleaver N87-23832
Research in VLSI systems
[AD-A179227] N87-23872
A VLSI CMOS circuit design technique to aid test generation
[AD-A177934] N87-23887
Complexities of layouts in three-dimensional VLSI (Very Large-Scale Integration) circuits
[AD-A178150] N87-23889
VERY LONG BASE INTERFEROMETRY
Atmospheric propagation effects on radio interferometry
[AD-A178405] N87-23855
VERY LOW FREQUENCIES
An ELF (Extremely-Low-Frequency) transmitter experiment for the space shuttle. (The NASC-201 (Naval Air Space Command) experiment). Volume 1
[AD-A178237] N87-23849
VHSIC (CIRCUITS)
VHDL (VHSIC (Very High Speed Integrated Circuits) Hardware Descriptive Languages) prototype simulator
[AD-A179073] N87-23869
VIBRATION
The Shock and Vibration Digest, Volume 19, No. 5 N87-23620
Analysis of jitter in a digital transmission system
[AD-A177845] N87-23844
Studies of infrared aurorae
[AD-A179539] N87-24037
The Shock and Vibration Digest, Volume 19, No. 6 N87-24125
Guidelines for noise and vibration levels for the space station
[NASA-CR-178310] N87-24162
VIBRATION DAMPING
Turbomachine blade vibration N87-23621
Material damping measurements of 2D carbon-carbon composite beams
[AD-A179109] N87-23700
Squeeze film damper technology. Part 4. Design and application of squeeze film dampers
[AD-A177996] N87-23973
Modified independent modal space control method for active control of flexible systems
[NASA-CR-181065] N87-23980
Experiments on dynamic stiffness and damping of tapered bore seals
[NASA-TM-89695] N87-23984
Forced vibration as a method for determining structural integrity
[DE87-005878] N87-23992
VIBRATION MEASUREMENT
Material damping measurements of 2D carbon-carbon composite beams
[AD-A179109] N87-23700
VIBRATION TESTS
Forced vibration as a method for determining structural integrity
[DE87-005878] N87-23992
Test plan for the 34 meter vertical axis wind turbine test bed located at Bushland, Texas
[DE87-004777] N87-24017
VIRGO GALACTIC CLUSTER
Present star formation in spirals of the Virgo cluster N87-24306
Molecular gas and star formation in HI-deficient Virgo cluster galaxies N87-24307
VISCOELASTICITY
Foam rheology: The linear viscoelastic response of a spatially periodic model
[DE87-000960] N87-23731
VISCOPLASTICITY
Thermomechanical effects in high-speed seal rubs
[NASA-CR-180418] N87-23979
VISCOSITY
Foam rheology: The linear viscoelastic response of a spatially periodic model
[DE87-000960] N87-23731
Synthesis of model polymers and related structures in support of vinyl monomer grafting studies
[DE87-007406] N87-23739
Viscosity of synfuel compounds and mixtures
[DE87-008696] N87-23756
Experimental and numerical investigation of coherent structures
[AD-A179456] N87-23910
VISCOUS FLOW
Application of the viscous-inviscid interaction method to the analysis of airfoil flows at low Reynolds numbers
[AD-A177948] N87-23588
Onset of Taylor vortices in flows with a circumferential pressure gradient: Application to the helical screw rheometer
[DE87-000453] N87-23918
Physics of pattern formation at liquid interfaces
[DE87-007540] N87-23919
Viscous-inviscid interaction with higher-order viscous-flow equations: Applications to three-dimensional bodies
[AD-A178264] N87-23924
Thermodynamic evaluation of transonic compressor rotors using the finite volume approach
[NASA-CR-180587] N87-23925
Development of an explicit time marching procedure for laminar and turbulent flow N87-23926
Development of a finite volume time marching method
[JM/85-3] N87-23927
An explicit finite-volume time-marching procedure for turbulent flow calculations N87-23928
Explicit finite-volume time-marching calculations of total temperature distributions in turbulent flow N87-23929
VISIBILITY
Otis ANGB (Air National Guard Base) visibility sensor field test study
[AD-A179176] N87-24045
Potential electron beam induced flashblindness in pilots
[AD-A178002] N87-24084
VISUAL PERCEPTION
Multipurpose visual display and eye movement recording system
[AD-A179620] N87-24068
The perception of the higher derivatives of visual motion
[AD-A179627] N87-24069
Potential electron beam induced flashblindness in pilots
[AD-A178002] N87-24084
VISUAL SIGNALS
Visual and motion cueing in helicopter simulation N87-23634
VOCODERS
Adaptive noise reduction in aircraft communication systems
[AD-A178267] N87-23851
VORTEX ALLEVIATION
Unsteady separated flows: Vorticity and turbulence
[AD-A179500] N87-23912
VORTEX BREAKDOWN
Evaluation of Navier-Stokes and Euler solutions for leading-edge separation vortices
[NASA-TM-89458] N87-23584
Selection principles and pattern formation in fluid mechanics and nonlinear shell theory
[NASA-CR-180941] N87-23916
VORTEX GENERATORS
Calculation of axisymmetric flow in swhirlers by difference method N87-23579
VORTEX SHEDDING
Unsteady separated flows: Vorticity and turbulence
[AD-A179500] N87-23912
VORTICES
Calculation of axisymmetric flow in swhirlers by difference method N87-23579
Evaluation of Navier-Stokes and Euler solutions for leading-edge separation vortices
[NASA-TM-89458] N87-23584
Some aspects of vortex flows determined from the thin-layer Navier-Stokes equations
[NASA-TM-88375] N87-23595
Study of lee-side flows over conically cambered delta wings at supersonic speeds, part 1
[NASA-TP-2680-PT-1] N87-23597

Acoustic response of turbulent reacting recirculatory flows N87-23799
Vortex-nozzle interactions in ramjet combustors N87-23800
Combustion instabilities in dump type ramjet combustors N87-23803
Turbulent boundary layer structure, drag reduction [AD-A179246] N87-23907
Onset of Taylor vortices in flows with a circumferential pressure gradient: Application to the helical screw rheometer [DE87-000453] N87-23918

VORTICITY
Crossflow vorticity sensor [NASA-CASE-LAR-13436-1-CU] N87-23587

VULNERABILITY
ESD (Electrostatic Discharge)/EOS (Electrical OverStress) susceptibility of a class of bipolar RF power transistors: Experimental studies on stripline-opposed emitter transistors [AD-A178212] N87-23890

W

WAFERS
Floating emitter solar cell [NASA-CASE-NPO-16467-1-CU] N87-23879
Study of quantum mechanical effects in deep submicron, grating-gate field effect transistors [AD-A179617] N87-24204

WAKES
Experimental and numerical investigation of coherent structures [AD-A179456] N87-23910

WALL PRESSURE
Response of transonic diffuser flows to abrupt increases of back pressure: Wall pressure measurements N87-23793

WALLS
Turbulent boundary layer structure, drag reduction [AD-A179246] N87-23907
Three-dimensional structure of boundary layers in transition to turbulence [AD-A179247] N87-23908

WASTE WATER
Full-scale test program for a shower wastewater recycling system: Technical evaluation [AD-A178061] N87-24087
The field shower wastewater recycling system: Development of a program of instruction and preliminary analysis of its potential health implications [AD-A178112] N87-24088

WATER
Adhesive evaluation of water-soluble LARC-TPI [NASA-TM-89152] N87-23752

WATER POLLUTION
Survey of environment related monitoring programs of international organizations and their contribution to international organizations [ETN-87-99913] N87-24033

WATER QUALITY
Spatial characterization of acid rain stress in Canadian Shield lakes [NASA-CR-180983] N87-24031
Spatial characterization of acid rain stress in Canadian Shield lakes [NASA-CR-180982] N87-24032
Full-scale test program for a shower wastewater recycling system: Technical evaluation [AD-A178061] N87-24087
The field shower wastewater recycling system: Development of a program of instruction and preliminary analysis of its potential health implications [AD-A178112] N87-24088

WATER RECLAMATION
Full-scale test program for a shower wastewater recycling system: Technical evaluation [AD-A178061] N87-24087
The field shower wastewater recycling system: Development of a program of instruction and preliminary analysis of its potential health implications [AD-A178112] N87-24088

WATER RESOURCES
The field shower wastewater recycling system: Development of a program of instruction and preliminary analysis of its potential health implications [AD-A178112] N87-24088

WATER TREATMENT
The field shower wastewater recycling system: Development of a program of instruction and preliminary analysis of its potential health implications [AD-A178112] N87-24088

WATER VAPOR
Single and multiple electromagnetic scattering by dielectric obstacles from a resonance perspective [DE87-007347] N87-23843

WATER WAVES
Ocean wind and wave model comparisons with GEOSAT (GEOdesy SATellite) satellite data [AD-A178302] N87-24061

WAVE ATTENUATION
Single and multiple electromagnetic scattering by dielectric obstacles from a resonance perspective [DE87-007347] N87-23843

WAVE EQUATIONS
Measurement of solid-propellant burn rate using millimeter-wave techniques N87-23770
Architectural implications of a parallel computational approach to the vector wave equation [AD-A179510] N87-24113

WAVE PACKETS
On the breakdown of the wave packet trailing a turbulent spot in a laminar layer [AD-A179607] N87-23915

WAVE PROPAGATION
Compression and shear wave propagation in plain and filled elastomers [AD-A178153] N87-23745
Numerical study of acoustic refraction and flow turning N87-23759
Time domain wave propagation in multilayered integrated circuits [AD-A178180] N87-23847
Finite element analysis of slow-wave Schottky contact printed lines [AD-A179259] N87-23873

WAVE REFLECTION
Numerical study of acoustic refraction and flow turning N87-23759
Finite difference simulations of Rayleigh wave scattering by 2-D rough topography [AD-A179190] N87-23824

WAVE SCATTERING
Finite difference simulations of Rayleigh wave scattering by 2-D rough topography [AD-A179190] N87-23824

WAVEGUIDE ANTENNAS
A new version of MODESRCH using interpolated values of the magnetoionic reflection coefficients [AD-A179094] N87-23322

WAVEGUIDES
Use of a 2.3-GHz traveling-wave maser on the Usuda 64-meter antenna N87-23831
Research in millimeter wave techniques [NASA-CR-181026] N87-23858

WEAPON SYSTEMS
Manned air to air combat simulation N87-23648
The use of Aeritalia flight simulator for the development of the AM-X weapon system N87-23650

WEAPONS
Microwave coupling inside complex systems [DE87-003505] N87-23841

WEATHER FORECASTING
Mid-latitude wind probability model [AD-A179256] N87-24048
Tactical weather expert system [AD-A178605] N87-24050
TAF (Terminal Aerodrome Forecast) verification [AD-A177931] N87-24055

WEATHER STATIONS
Station climatic summaries, Antarctica, Australia and Oceania [AD-A179242] N87-24047

WEDGE FLOW
Experimental study of supersonic stream sliding at angle past one-step wedge with jaws N87-23573

WEDGES
Effect of a trade between boattail angle and wedge size on the performance of a nonaxisymmetric wedge nozzle [NASA-TP-2717] N87-23593

WEIGHTLESSNESS
The 1986-87 NASA space/gravitational biology accomplishments [NASA-TM-89951] N87-24063

WELDED JOINTS
Pulsed Nd:YAG laser closure welding of the MC3593/3594 relay [DE87-007825] N87-23967

WELDING
Control of welding processes [AD-A177893] N87-23971

WETTING
Wetting properties of Au/Sn solders for microelectronics [DE87-008519] N87-23883

WIND (METEOROLOGY)
Mid-latitude wind probability model [AD-A179256] N87-24048
Ocean wind and wave model comparisons with GEOSAT (GEOdesy SATellite) satellite data [AD-A178302] N87-24061

WIND DIRECTION
Climatological observations in the Philip Smith Mountains of the North Slope, Alaska [DE87-008179] N87-24054

WIND MEASUREMENT
Shuttle Coherent Atmospheric Lidar Experiment (SCALE) [NASA-TM-100307] N87-23959

WIND SHEAR
The application of optimal control techniques to the UTIAS research simulator N87-23637

WIND TUNNEL CALIBRATION
Experimental evaluation of honeycomb/screen configurations and short contraction section for NASA Lewis Research Center's altitude wind tunnel [NASA-TP-2692] N87-23662

WIND TUNNEL MODELS
Aeroelasticity and mechanical stability report, 0.27 Mach scale model of the YAH-64 advanced attack helicopter [NASA-CR-178284] N87-23596
A preliminary evaluation of the performance of wind tunnel and numerical modeling simulations of the wind flow over a wind farm [DE87-004634] N87-24051

WIND TUNNEL TESTS
Experimental study of supersonic stream sliding at angle past one-step wedge with jaws N87-23573
Two-dimensional aerodynamic characteristics of the AMES HI-120, HI-8, and LOW-12 airfoils [NASA-CR-181018] N87-23589
Icing of flow conditioners in a closed-loop wind tunnel [NASA-TM-89824] N87-23591
High Reynolds Number tests of the NASA SC(2)-0012 airfoil in the Langley 0.3-meter transonic cryogenic tunnel [NASA-TM-89102] N87-23594
Aeroelasticity and mechanical stability report, 0.27 Mach scale model of the YAH-64 advanced attack helicopter [NASA-CR-178284] N87-23596
Activities report of the German-Dutch wind tunnel [B6677593] N87-23665
Activities report of the German-Dutch wind tunnel [B6677594] N87-23666
The influence of turbulence and deck section geometry on the aeroelastic behaviour of a cable-stayed bridge model [NAE-AN-40] N87-23990
A preliminary evaluation of the performance of wind tunnel and numerical modeling simulations of the wind flow over a wind farm [DE87-004634] N87-24051

WIND TUNNELS
Laser Doppler velocimeter application in supersonic boundary-layer flow [AD-A178395] N87-23590
Reactivation study for NASA Lewis Research Center's hypersonic tunnel facility [NASA-TM-89918] N87-23664
Activities report of the German-Dutch wind tunnel [B6677593] N87-23665
Activities report of the German-Dutch wind tunnel [B6677594] N87-23666
Engineer in charge: A history of the Langley Aeronautical Laboratory, 1917-1958 [NASA-SP-4305] N87-24390

WIND TURBINES
Wind energy systems: Program summary, fiscal year 1984 and 1985 [DE87-001109] N87-24015
Sandia National Laboratories 34-meter diameter vertical axis wind turbine test bed [DE87-003096] N87-24016
Test plan for the 34 meter vertical axis wind turbine test bed located at Bushland, Texas [DE87-004777] N87-24017
Analysis and test results for an improved constant speed passive cyclic pitch wind turbine [DE87-001135] N87-24022
A preliminary evaluation of the performance of wind tunnel and numerical modeling simulations of the wind flow over a wind farm [DE87-004634] N87-24051

WIND VELOCITY
A preliminary evaluation of the performance of wind tunnel and numerical modeling simulations of the wind flow over a wind farm [DE87-004634] N87-24051
Climatological observations in the Philip Smith Mountains of the North Slope, Alaska [DE87-008179] N87-24054

WINDPOWER UTILIZATION
Wind energy systems: Program summary, fiscal year 1984 and 1985
[DE87-001109] N87-24015
WINDPOWERED GENERATORS
Wind energy systems: Program summary, fiscal year 1984 and 1985
[DE87-001109] N87-24015
Sandia National Laboratories 34-meter diameter vertical axis wind turbine test bed
[DE87-003096] N87-24016
Test plan for the 34 meter vertical axis wind turbine test bed located at Bushland, Texas
[DE87-004777] N87-24017
A preliminary evaluation of the performance of wind tunnel and numerical modeling simulations of the wind flow over a wind farm
[DE87-004634] N87-24051
WINDSHIELDS
Bird impact qualification test for A-10 windshield
[AD-A179263] N87-23599
WING NACELLE CONFIGURATIONS
Dynamic response of two composite prop-fan models on a nacelle/wing/fuselage half model
[NASA-CR-179589] N87-23615
WING PANELS
Thermal stress analysis of space shuttle orbiter wing skin panel and thermal protection system
[NASA-TM-88276] N87-23994
WINGS
Flight investigation of the effects of an outboard wing-leading-edge modification on stall/spin characteristics of a low-wing, single-engine, T-tail light airplane
[NASA-TP-2691] N87-23614
WIRE WINDING
An interactive wire-wrap board layout program
N87-23839

X

X RAY ASTRONOMY
The joint NASA/Goddard-University of Maryland research program in charged particle and high energy photon detector technology
[NASA-CR-180996] N87-24166
Essays in Space Science
[NASA-CP-2464] N87-24247
Discrete X-ray sources and the X-ray background
N87-24261
The cosmic X-ray background N87-24262
X-ray astronomical spectroscopy N87-24263
A program of ground-based astronomy to complement Einstein observations
[AD-A179331] N87-24265
Far-infrared properties of cluster galaxies N87-24305
Starburst galaxies N87-24319
X RAY DIFFRACTION
Poly(pyrrolium anion) studies: Electrochemical synthesis and physical behavior
[AD-A178097] N87-23743
X RAY FLUORESCENCE
Special applications of the Debye Microdiffractometer
[RFP-3906] N87-23939
X RAY IMAGERY
Double-diffraction X-ray imaging camera
[DE87-007936] N87-23940
X RAY LASERS
Ordered many-electron motions in atoms and X-ray lasers
[DE87-004731] N87-23951
X RAY SOURCES
Discrete X-ray sources and the X-ray background
N87-24261
X RAY SPECTRA
A dust scattered halo in starburst galaxy M82?
N87-24334
X RAY SPECTROSCOPY
X-ray astronomical spectroscopy N87-24263
X RAYS
Report of the Second Workshop on Synchrotron Radiation Sources for X-ray Lithography
[DE87-002155] N87-24179
The cosmic X-ray background N87-24262
Solar-geophysical data number 509, January 1987. Part 2: (Comprehensive reports). Data for July 1986
[PB87-162582] N87-24386
XV-15 AIRCRAFT
Piloted simulation in the development of the XV-15 tilt rotor research aircraft N87-23646

Y

YAG LASERS
Light sheet visualization and velocity field measurements in seeded flows — YAG laser
[ISL-CO-225/86] N87-23935
Pulsed Nd:YAG laser closure welding of the MC3593/3594 relay
[DE87-007825] N87-23967
YAW
Analysis and test results for an improved constant speed passive cyclic pitch wind turbine
[DE87-001135] N87-24022
YF-16 AIRCRAFT
An experimental-analytical routine for the dynamic qualification of aircraft operating on rough runway surfaces N87-23611

Z

ZODIACAL LIGHT
Diffuse infrared emission of the galaxy: Large scale properties N87-24279

Typical Personal Author Index Listing

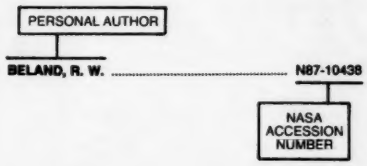

Listings in this index are arranged alphabetically by personal author. The NASA accession number denotes the number by which the citation is identified.

A

ABOELAZE, MOKHTAR A. N87-23689
ABOLINS, J. A. N87-24262
ABRAMZON, B. N87-23805
ACOSTA, WALDO A. N87-23624
ACTON, A. E. N87-23895
ADAMS, JAMES H., JR. N87-23684
AHLEN, S. P. N87-24383
ALLEN, C. N87-23747
ALLEN, J. J. N87-24002
ALLEN, M. G. N87-23804
ALLEN, R. J. N87-24311
ANDERSON, AUDIE N87-23693
ANDERSON, G. M. N87-24378
ANDERSON, G. R. N87-23654
ANDERSON, H. M. N87-23733
ANDERSON, K. A. N87-24252
ANDERSON, TORGER J. N87-23792
ANTCLIFF, RICHARD R. N87-23808
ANTONIAC, Z. A. N87-24019
ANTONIADIS, DIMITRI A. N87-24106
N87-24204
APPLETON, P. N. N87-24329
ARKHIPOV, A. I. N87-23582
ARMANDO, ARMANDO N87-23650
ARMSTRONG, ROBERT C. N87-23764
N87-23766
N87-23777
N87-23778
ARMUS, LEE N87-24330
ASHKENAS, IRVING L. N87-23660
AUSTIN, P. J., JR. N87-23934
AVIGNONE, F. T., III N87-24383
AXON, D. J. N87-24369

B

BABUSKA, I. N87-24141
N87-24142
BACON, L. D. N87-23841
N87-23857
BAER-RIEDHART, JENNIFER L. N87-23619
BAER, TOMAS N87-24189
BAILEY, A. D. N87-23694
BAKER, CLIFFORD C. N87-24229
BAKER, G. A., JR. N87-24129
BALASUBRAHMANYAN, V. K. N87-24255
BALDWIN, RICHARD S. N87-23718
BALLING, P. N87-23863
BALLY, JOHN N87-24303
BAME, S. J. N87-24380
BANDY, JOHN T. N87-24087
N87-24088
BANKS, BRUCE A. N87-23736
BANSAL, NAROTTAM P. N87-23750
BANTON, DAVID W. N87-23871
BARANOVSKIY, S. I. N87-23581
BARBER, B. N87-23635
BARBER, P. F. N87-24158
BARBER, PATRICK G. N87-23713
BARE, E. ANN N87-23593
BAREFOOT, JOHN C. N87-24067
BARGER, RAYMOND L. N87-23586
BARNARD, J. C. N87-24051
BARNES, A. G. N87-23640
BAROWY, WILLIAM M. N87-23708
BARRETT, J. W. N87-24270
BARSONY, MARY N87-24275
BARTON, M. Q. N87-24179
BARTON, P. N87-23865
BASH, FRANK N. N87-24294
BATEMAN, V. I. N87-24004
BATTLES, J. W. N87-23770
BAUM, JOSEPH D. N87-23759
BAUMANN, ROBERT H. N87-24012
BAUMGARDNER, R. W. N87-24043
BAWCOM, DWIGHT M. N87-23689
BAZ, A. N87-23980
BEAUCHAMP, R. L. N87-23881
BECK, SARA C. N87-24320
BECKER, DOROTHY L. N87-23757
BECKLIN, E. E. N87-24361
N87-24376
BEEBE, KENNETH R. N87-24216
BEEMAN, M. L. N87-23711
BEHRENS, RICHARD, JR. N87-23780
BEICHMAN, C. N87-24309
N87-24354
BEICHMAN, C. A. N87-24342
BELFORT, P. N87-24337
BELLANTONI, J. N87-23600
N87-23601
BELYAYEV, V. YA. N87-23571
BENNETT, G. A. N87-23898
BENOIT, J. N87-23638
BENSON, B. J. N87-24039
BERANEK, R. N87-23959
BERCHAK, M. J. N87-23589
BERGER, B. K. N87-24226
BERGEY, DANA J. N87-24176
BERGHOLM, FREDRIK N87-24099
BERK, H. L. N87-23920
BERNARD, J. N87-23820
BERRY, G. F. N87-23810
BERRY, ROBERT F., JR. N87-23713
BERTENSHAW, T. G. N87-23938
BHARATHAN, D. N87-24023
BHASIN, KUL B. N87-23900
BICAY, M. D. N87-24305
BICKER, C. J. N87-23770
BIEFELD, R. M. N87-24212
BILBRO, J. N87-23959
BINKLEY, J. S. N87-23781
BINNS, W. R. N87-24256
BIXLER, N. E. N87-23918
BJORKMAN, EILEEN A. N87-23629
BJUGSTAD, P. L. N87-23755
BLACKMON, ELEANOR W. N87-23661
BLACKWELL, B. F. N87-24130
BLALOCK, TRAVIS N87-23941
BLATT, PAUL E. N87-23645
BLOEMBERGEN, N. N87-23952
BLOMSHIELD, F. S. N87-23770
N87-23776
BLOOM, D. M. N87-23868
BLOOM, I. N87-23880
BLOSTEIN, DOROTHEA N87-24096
BOBER, LAWRENCE J. N87-23625
BOGAR, T. J. N87-23793
BOHM, MARTIN N87-24185
BOLAND N87-24241
BOLDT, ELIHU A. N87-24262
BORIS, J. P. N87-23801
BOSTICK, D. T. N87-24180
BOTHUN, G. D. N87-24304
BOTTINELLI, L. N87-24353
N87-24355
BOUCHET, P. N87-24355
BOULANGER, F. N87-24268
N87-24279
N87-24309
BOUWER, GERD N87-23657
BOWMAN, C. T. N87-23804
BOYLE, J. M. N87-24115
BRABY, L. A. N87-24143
BRADLEY, J. N87-23880
BRAGINSKI, A. I. N87-24200
BRAUN, J. D. N87-23722
BRAUSER, K. N87-23644
BRAY, RICHARD S. N87-23634
BREEMAN, J. H. N87-23655
BRIGGS, A. N87-23699
BRINK, K. N87-24314
BRINKER, C. J. N87-23738
BRODZINSKI, R. L. N87-24383
BROEMELING, LYLE N87-24149
BROOKS, BENNETT M. N87-23615
BROOME, R. D. N87-24061
BROWDER, JOAN A. N87-24012
BROWER, RONALD W. N87-24120
BROWN, D. H. N87-23833
BROWN, D. R. N87-24019
BROWN, G. V. N87-23978
BRUNSON, R. R. N87-23958
BRUNT, MARK A. N87-23641
BRYANT, R. A. N87-24234
BUCHANAN, BRUCE G. N87-24103
BUCHANAN, T. L. N87-23599
BUCKLEY, LEONARD J. N87-23743
BUECHTER, MARK J. N87-23684
BUHRMASTER, M. A. N87-24234
BUILTA, L. A. N87-23877
BULYCHEV, V. A. N87-23580
BURLEY, JAMES R., II N87-23593
BURLEY, RICHARD R. N87-23662
BURNHAM, D. N87-24045
BURNS, D. A. N87-24061
BUSSOLARI, STEVEN N87-24064
BYERS, C. H. N87-23958
BYRNES, H. STEWART N87-23815

C

CAGLAYAN, ALPER K. N87-23617
CAGLIOSTRO, DOMENICK E. N87-23737
CALLAHAN, ARTHUR B. N87-24083
CAMPBELL, ALISON W. N87-24332
CAMPBELL, D. H. N87-23775
CAMPBELL, W. H., JR. N87-23787
CAMPBELL, WILLIAM J. N87-24098
CANAVAN, G. H. N87-24155
CAREY, W. P. N87-24216
CARICO, DAVID P. N87-24354
CARLING, R. W. N87-23714
CARRAWAY, DEBRA L. N87-23587
CARSON, GEORGE T., JR. N87-23593
CASON, RANDALL W. N87-23632
CATALDO, RUSSELL L. N87-24029
CAUX, EMMANUEL N87-24278
CAVAGE, WILLIAM C. N87-23815
CAVALIER, AL N87-23941
CAVALLARO, JOSEPH H. N87-23677
CAVANAGH, R. R. N87-23710
CERULLO, L. J. N87-23953
CESARSKY, CATHERINE J. N87-24257
CHA, A. G. N87-23836
CHAMIS, ALICE N87-24238
CHAMPAGNE, F. H. N87-23910
CHAN, JOHN D. N87-23681
CHAN, KWAI S. N87-23720
CHANDRASHEKHARA, K. N87-23819
CHANG, S. H. N87-23969
CHARKEY, ALLEN N87-23870
CHAU, H. H. N87-23976
CHEN, E. P. N87-24005
CHEN, N. C. J. N87-23965
CHEN, PEHONG N87-24231
CHEN, PI-FUAY N87-23827
CHEN, S. S. N87-23923
CHEN, TIMOTHY S. N87-23698
CHENG, H. S. N87-23977
CHENG, LI-JEN N87-23879
CHENG, LOUIS Y. N87-23963
CHERVIN, R. M. N87-24053
CHIHKARA, R. S. N87-24010

CHIH, SAH N87-23879
CHINI, R. N87-24292
CHISHOLM, M. H. N87-23715
CHIU, H. H. N87-23810
CHLEWICKI, G. N87-24276
N87-24283
CHOW, C. T. S. N87-23955
CHRISTIAN, J. L. N87-24234
CHRISTOPHOROU, L. G. N87-23957
CHU, E. N87-24093
CHUN, K. S. N87-23902
CHUN, MING LEUNG N87-24157
CHURCHILL, GARY B. N87-23646
CICCONE, VINCENT J. N87-24067
CLARK, BRUCE J. N87-23598
CLARK, F. O. N87-24276
CLARK, I. O. N87-24263
CLARKE, CLIFTON A. N87-23856
CLARKE, J. N87-24213
CLAUS, RUSSELL W. N87-23933
CLEMENTS, P. A. N87-23634
CLINE, THOMAS L. N87-24247
N87-24260
CLOWES, R. G. N87-24343
N87-24358
COFFEY, H. E. N87-24385
N87-24386
COFFINBERRY, GEORGE A. N87-23816
COHEN, MARC M. N87-24064
COHEN, NORMAN S. N87-23765
COHEN, R. S. N87-24272
COLEGROVE, C. B. N87-23825
COLLINS, J. C. N87-24167
COMFORT, W. J., III N87-23931
COMPANION, JOHN N87-23941
CONDON, MICHAEL D. N87-24050
CONIGLIARO, P. N87-23649
COOK, M. V. N87-23613
COOVER, JOHN A., JR. N87-24057
CORDERO, R. N87-23705
N87-23706
COSTANTINO, MARC N87-23786
COULON, J. P. N87-23897
COWDREY, D. A. N87-23636
COWLEY, S. W. H. N87-24380
COX, P. N87-24269
N87-24284
CRAFT, B. N87-24179
CRAWFORD, E. A. N87-24195
CROKE, E. J. N87-23810
CROSSLEY, EDWARD A., JR. N87-23962
CROUCH, ROGER K. N87-23713
CRUTCHER, J. K. N87-23877
CULBERTSON, R. J. N87-24207
CULICK, F. E. C. N87-23795
N87-23796
CULICK, FRED E. C. N87-23761
CUNNINGHAM, LARRY N87-23689
CURLEE, T. R. N87-24233
CURLEY, WINIFRED N87-24088
CURRAN, FRANCIS M. N87-23693
CURTIS, L. J. N87-24164
CUTRI, ROC M. N87-24326
CYMERMAN, ALLEN N87-24082

D

DAHLBURG, R. B. N87-24225
DAHMANN, J. S. N87-23948
DAILY, J. W. N87-23800
DALEY, M. A. N87-23711
DALY, P. W. N87-24380
DANBERG, JAMES E. N87-23585
DANIEL, B. R. N87-23760
N87-23803
DANIELSON, G. E. N87-24327
DARLING, CLIFF N87-23729
DAVIDGE, R. W. N87-23699
DAVIDSON, DAVID L. N87-23720
DAVIS, J. A. N87-23799
DAVIS, J. L. N87-23855
DAWSON, D. M. N87-23699
DEBNAM, WILLIAM J., JR. N87-23713
DECHER, R. N87-24336
DEEVI, S. N87-23806
DEGRIJP, MARINUS H. K. N87-24366
DEGROOT, J. N87-24194
DEGUCHI, SHUJI N87-24277
DEJONG, T. N87-24314
DELEO, RICHARD V. N87-23616
DELGRANDE, J. MARK N87-24186
DEMPSEY, JEROME A. N87-24065
DENNEFELD, H. N87-24353
DENNEFELD, M. N87-24337
N87-24355
DENNIS, MICHAEL V. N87-24066
DEPOY, D. L. N87-24367
DESCHRYVER, F. C. N87-24217
DEUTSCH, L. J. N87-23832
DEVEREUX, NICHOLAS N87-24293
DEVORET, M. H. N87-24213
DIBBLE, R. W. N87-23714
DICAPUA, M. S. N87-24194
DICARLO, DANIEL J. N87-23614
DICKEY, JOHN M. N87-24349
DICKSON, C. L. N87-23755
DIEKMANN, VERNON L. N87-23632
DIKILITAS, ZEKI N87-23612
DIMOPOLOUS, S. N87-24383
DIRKS, J. A. N87-24019
DISALVO, F. J., JR. N87-23952
DOBBS, GREGORY M. N87-23792
DOLINSKI, KRZYSZTOF N87-23999
DONALDSON, J. C. N87-23590
DONGARRA, J. J. N87-24101
DOSS, E. D. N87-23932
DOUGHERTY, W. M. N87-24252
DOUVILLE, R. N87-23866
DOWNS, G. L. N87-23722
DOXAS, I. N87-23920
DOYLE, R. E. N87-24126
DRAKE, R. N87-24227
DRAKE, S. R. N87-24133
DRESSEL, LINDA L. N87-24350
DRITZ, K. W. N87-24115
DROST, M. K. N87-24019
DROTNING, W. D. N87-24094
DRUKIER, A. K. N87-24383
DRUMMOND, T. J. N87-24212
DUCROZ, J. N87-24101
DUGANOV, V. V. N87-23573
DUNN, ROBERT P. N87-23663
DURHAM, W. B. N87-23711
DUSENBERY, P. B. N87-24034
DWEK, E. N87-24280
DYER, DONALD D., JR. N87-23906
DYER, G. N87-23874
N87-23875
DYSON, J. E. N87-24369

E

EAGLES, S. A. N87-24342
ECKBRETH, A. C. N87-23771
ECKBRETH, ALAN C. N87-23792
EDELSON, R. A. N87-24371
N87-24372
EDWARDS, T. N87-23769
N87-23775
EGGERS, JAMES M. N87-23789
EGGERT, J. R. N87-24208
EHERNBERGER, L. J. N87-23616
EIMERL, D. N87-23704
N87-24209
ELIAS, J. H. N87-24327
N87-24354
ELIAS, JONATHAN H. N87-24296
ELLIOTT, J. C. N87-23877
ENGLAND, JAMES E. N87-23685
ENGLISH, ROBERT E. N87-23674
EPSTEIN, M. N87-23953
ERKELENS, L. J. J. N87-23655
ERNST, STEVEN P. N87-24219
ESKRIDGE, PAUL B. N87-24316
ESPENAK, FRED N87-24377
ESPINOSA, J. M. RODRIGUEZ N87-24364
ESPLIN, MARK P. N87-23708
ESTEVE, D. N87-24213
EVANS, DAVID S. N87-24249
EVANS, SLAYTON N87-24189
EWICK, D. W. N87-23754

F

FALGARONE, E. N87-24268
N87-24279
FARASSAT, F. N87-24160
FARLEY, GARY L. N87-23991
FASEL, H. N87-23910
FATOOHI, RAAD A. N87-24107
FAUBERT, D. N87-23845
FAURE, CLAUDIE N87-24086
FAZIO, G. G. N87-24370
FEINBERG, D. N87-23753
FEIVESON, A. H. N87-24010
FELDMAN, D. W. N87-23956
FELDMAN, R. B. N87-23956
FEREBEE, MELVIN J., JR. N87-23687
FERRARA, AUGUSTO M. N87-23815
FESTA, J. F. N87-24060
FICH, MICHEL N87-24271
N87-24281
FICHTEL, CARL E. N87-24258
FICKIE, K. D. N87-23784
FIELD, J. E. N87-23744
FIELD, M. E. N87-24171
FISHBANE, P. M. N87-24168
FISHER, S. C. N87-23813
FITZJARRALD, D. N87-23959
FLANAGAN, D. P. N87-23993
FLATHERS, G. W., II N87-23607
FLEMING, DAVID P. N87-23984
FLETCHER, JAY W. N87-23632
FLOOD, DENNIS J. N87-23901
FOLKARD, M. A. N87-24174
FORMAN, M. A. N87-24250
FOSTER, D. N87-24054
FOSTER, D. E. N87-23966
FOWLER, J. W. N87-24273
FOX, G. C. N87-24092
FOX, JANE L. N87-24037
FRANCIS, MICHAEL H. N87-23846
FRANCISCUS, LEO C. N87-23626
FRANCO, M. M. N87-23829
FRASER N87-23721
FREAR, D. N87-23817
FREDERICK, F., II N87-23775
FREDERICK, R. A., JR. N87-23772
FREYMANN, R. N87-23611
FRIEDMAN, MORTON L. N87-23671
FRIEDRICH, HEINZ N87-23653
FRIPP, ARCHIBALD L., JR. N87-23713
FROGEL, J. A. N87-24340
FROGEL, JAY A. N87-24288
N87-24296
FUCHS, E. F. N87-23878
FUERSCHBACH, P. W. N87-23967
FUJII, K. N87-23584
FULKERSON, E. S. N87-24194
FURCOLO, BERNARDO N87-23608
FUYUAN, XING N87-23688

G

GAHN, RANDALL F. N87-24029
GALECKI, DIANE L. N87-23692
GALLAGHER, J. N87-24299
GALLAGHER, J. S. N87-24300
GALLAGHER, J. S., III N87-24301
GALLAGHER, JOHN S., III N87-24289
GALOFF, PENELOPE K. N87-23945
GANJI, A. N87-23808
GARCIA-BARRETO, J. ANTONIO N87-24333
GARCIA, A. A. N87-24232
GARDINER, WILLIAM P. N87-24088
GARDNER, J. H. N87-23801
GARRARD, T. L. N87-24256
GARWOOD, ROBERT W. N87-24349
GATHERS, G. R. N87-23976
GATLEY, I. N87-24328
GATOS, HARRY C. N87-24218
GAVALER, J. R. N87-24200
GAVALI, S. N87-23584
GAVER, DONALD P. N87-24150
GEIST, G. A. N87-24100
GELMINI, G. N87-24383
GEMEINER, RUSSEL P. N87-24029
GEOFFRION, ARTHUR M. N87-24153
GEORGE, A. N87-24093
GEORGEN, W. M. N87-24245
GERBER, NATHAN N87-24131
GERSHWIN, STANLEY B. N87-24108
GERSTL, S. A. W. N87-24011
N87-24014
GEZARI, D. Y. N87-24370
GIACCONI, RICCARDO N87-24261
GIBSON, JERRY D. N87-24105
GILCHRIEST, C. E. N87-23830
GILCHRIST, GEORGE N87-23729
GILERSON, A. A. N87-23574
GILES, J. A. N87-23658
GILL, CHARLES W. N87-24173
GILLETT, F. N87-24299
GIORDANO, J. N87-23975
GIOVANELLI, R. N87-24305
GIOVANOLA, J. H. N87-23989
GLADDEN, H. J. N87-23934
GLEYZER, A. I. N87-23580
GLEZER, A. N87-23915
GODIWALA, PANKAJ M. N87-23617
GOEBEL, J. H. N87-24378
GOLDBERG, ANDREW V. N87-24109
N87-24110
GOLDOWSKY, MICHAEL P. N87-23904

GONZALEZ-SANABRIA, OLGA N87-24029
GOOD, J. C. N87-24267
GOODMAN, R. N87-23649
GOSSELINK, JAMES G. N87-24012
GOUGH, P. S. N87-23784
GOUGUENHEIM, L. N87-24353
N87-24355
GOURLEY, P. L. N87-24212
GRABELSKY, D. A. N87-24272
GRAHAM, E. K. N87-24209
GRAHAM, J. R. N87-24328
GRAHAM, JAMES R. N87-24340
GRAHAM, S. L. N87-24230
GRATZKI, A. N87-24011
GRAY, G. W. N87-24075
N87-24079
GRAY, STEVEN D. N87-24105
GREENBERG, K. E. N87-23724
GREGOREK, G. M. N87-23589
GRIMM, KENNETH R. N87-23846
GRISSOM, M. C. N87-24235
GRONSKY, R. N87-24206
GROSCH, CHESTER E. N87-24107
GROTCH, S. L. N87-24052
N87-24104
GROVES, BERTRON M. N87-24082
GRUBER, ROBERT P. N87-23691
GUARRO, S. B. N87-24232
GUERRA, ROSEMARY N87-23791
GUESS, T. R. N87-23702
GUIDERDONI, B. N87-24306
GUILLORY, JOHN N87-24187
GUM, DON R. N87-23645
GUPTA, S. C. N87-23826
GUPTA, Y. M. N87-23745
GUSTAFSSON, BERTIL N87-24123
GUTMARK, E. N87-23798

H

HAAG, THOMAS W. N87-23821
HAAS, JEFFREY E. N87-23684
HACKING, PERRY N87-24344
HAERTIG, J. N87-23935
HAFF, P. K. N87-24159
HAGEN, FLOYD W. N87-23616
HAHN, C. J. N87-24053
HALFORD, GARY R. N87-24007
HALL, D. N87-24117
HALLINAN, G. J. N87-23695
N87-23696
HALSTEAD, THORA W. N87-24083
HAMMARLING, S. N87-24101
HANDA, T. N87-24290
HANEY, THOMAS L. N87-24067
HANKE, DIETRICH N87-23657
HANSEN, JAMES R. N87-24390
HANSON, MILTON P. N87-23716
HANSON, R. J. N87-24101
HANSON, R. K. N87-23804
HANSONPARR, D. M. N87-23782
HARGIS, P. J., JR. N87-23733
N87-23734
HARITONIDIS, JOSEPH H. N87-23907
HARRINGTON, DOUGLAS E. N87-23682
HARRIS, H. H. N87-24024
HARRIS, JAMES S. N87-23885
HARRIS, M. T. N87-23958
HARRISON, MICHAEL N87-24231
HARTMAN, EDWARD R. N87-23592
HARTOP, R. N87-23835
HARVEY, PAUL M. N87-24297
N87-24339
HARWIT, MARTIN N87-24323
HATCH, R. L. N87-23773
HAUSER, M. G. N87-24280
HAUSER, MICHAEL G. N87-24264
HAWARDEN, T. G. N87-24357
HAY, STUART S. N87-23821
HAYASHI, M. N87-24290
HAYNES, DAVID P. N87-23982
HAYS, RICHARD A. N87-24000
HEARD, H. C. N87-23711
HEASLEY, J. N. N87-24358
HECKMAN, TIMOTHY M. N87-24330
HEEG, JENNIFER N87-23616
HEGDE, U. G. N87-23803
HEILES, CARL N87-24345
HELFAND, DAVID J. N87-24265
HELOU, GEORGE N87-24287
N87-24313
N87-24349
HENDRICKS, ROBERT C. N87-23921
N87-23936
HENNESSY, JOHN N87-23872
HERBERT, THORWALD N87-23908
HERNITER, BRUCE N87-24044
HEVENOR, RICHARD A. N87-23827
HEYMAN, JOSEPH S. N87-23941
HICKERSON, J. P. N87-24059
HICKMAN, JAMES R., JR. N87-24072
N87-24074
N87-24078
HILDEBRAND, GREGORY N87-23797
HILL, A. N87-23753
HILL, GARY J. N87-24356
HJALMARSON, A. N87-24312
HO, PAUL T. P. N87-24320
N87-24322
HOFFMAN, A. L. N87-24195
HOFFMAN, G. H. N87-24140
HOFFMAN, JOHN B. N87-23846
HOFFMANN, W. F. N87-24370
HOGEN-ESCH, T. E. N87-23739
HOHENEMSER, K. H. N87-24022
HOKENSON, GUSTAVE J. N87-23672
HOLLOWAY, W. A. N87-23938
HOLMES, BRUCE J. N87-23587
HOLMES, HARLAN K. N87-23587
HOLST, T. L. N87-23584
HOLT, STEPHEN S. N87-24263
HONNELL, R. E. N87-23949
HOOVER, S. M. N87-23719
HOROWITZ, MARK A. N87-23686
HORTON, K. G. N87-23769
HORTON, W. N87-23920
HOUCK, JAMES R. N87-24323
N87-24344
HSIEH, K. C. N87-23785
HSIEH, T. N87-23794
HSU, C. Y. N87-23977
HSU, I. S. N87-23832
HSU, MEICHUN N87-24237
HSU, MING-TA S. N87-23698
HUANG, C. Y. N87-23952
HUCHRA, J. P. N87-24347
HUCKELBRIDGE, A. A. N87-24006
HUFF, J. R. N87-24244
HUGHES, R. C. N87-23943
HULL, DAVID H. N87-24076
HUME, R. N87-24234
HUMMEL, E. N87-24325
N87-24352
HUMPHREY, JOSEPH W. N87-23795
HUNTER, D. N87-24299
HUNTER, D. A. N87-24300
N87-24301
HUNTER, DEIDRE A. N87-24289
HUNTER, S. R. N87-23957
HUNTLEY, A. F. N87-24234
HUPPI, RONALD J. N87-23706
HURD, A. J. N87-23738
HURD, W. J. N87-23833
HUSSEY, B. N87-23758
HUSTON, R. L. N87-23969
HUTCHINSON, M. N87-24117
HYLAND, A. R. N87-24297
HYNDS, R. J. N87-24360

I

IGNATYEV, V. N. N87-23579
ILLARIONOV, A. M. N87-23571
IMAMOTO, S. N87-24205
IMPEY, C. N87-24373
ISRAEL, M. H. N87-24256
ITO, KAZUFUMI N87-24122
ITOH, TATSUO N87-23873
IVANOV, O. K. N87-23573
IYENGAR, S. S. N87-23964
IYER, R. N. N87-23728

J

JACKSON, M. L. W. N87-24043
JACOBS, PATRICIA A. N87-24150
JACOBSON, ALLAN S. N87-24259
JAGODA, J. I. N87-23760
JAMES, P. A. N87-24368
JAMIESON, ROBERT S. N87-23970
JAMISON, DONALD K. N87-24087
JAMISON, SHERWIN W. N87-24055
JARRELL, JERRY D. N87-24048
JARRETT, OLIN, JR. N87-23808
JEANES, DENNIS P. N87-23682
JENDRZEJCZYK, J. A. N87-23923
JENKINS, B. K. N87-24182
JENKINS, JERALD M. N87-23994
N87-23995
JENNE, R. L. N87-24053
JENNINGS, M. J. N87-23922
JENSEN, DOUGLAS R. N87-23954
JENSEN, R. J. N87-23813
JIANG, T. L. N87-23810
JIH, R. S. N87-23824
JOHANSSON, L. E. B. N87-24312
JOHNS, C. E. N87-23637
JOHNSTON, PATRICK J. N87-23592
JOHNSTON, R. A. N87-23596
JOHNSTON, S. C. N87-23714
JOHNSTON, W. N87-24117
JONES, BARBARA N87-24364
JONES, HOWARD C. N87-23982
JONES, IRBY W. N87-23982
JONES, TERRY JAY N87-24297
JOSEPH, R. D. N87-24328
N87-24340
N87-24366
JOU, W.-H. N87-23602
JOY, MARSHALL N87-24339
JU, JIANN-WEN N87-23063
JUDY, M. M. N87-24066

K

KABIR, P. K. N87-24188
KACYNSKI, K. J. N87-23809
KAILASANATH, K. N87-23801
KAIN, K. E. N87-23712
KALLURI, SREERAMESH N87-24007
KAN, H. P. N87-23705
N87-23706
KANADE, TAKEO N87-24119
KANTOR, PAUL N87-24236
KAPER, H. G. N87-24128
KAROJI, H. N87-24355
KARSTENSEN, K. W. N87-23972
KASPER, ROLF G. N87-23686
KATILAUS, JAMES J. N87-23743
KATNIK, GREGORY N. N87-23675
KATO, TAKAKO N87-24198
KATZ, Y. N87-23915
KAUFMAN, K. C. N87-24140
KAUFMAN, L. N87-24069
KAUFMAN, MICHELE N87-24294
KAUKLER, WILLIAM F. N87-23717
KAUPPILA, T. J. N87-23677
KAZAKOS, P. P. N87-23854
KEEFE, D. N87-23689
KEEL, W. C. N87-24325
KEEL, W. G. N87-24346
KEEL, WILLIAM C. N87-24363
N87-24366
KEFFELER, D. R. N87-23673
KELCHNER, BRYAN L. N87-24203
KELLEY, HENRY L. N87-23630
KELLEY, J. J. N87-24054
KELLY, BRIAN K. N87-23680
KELLY, J. C. N87-24102
KENNEDY, FRANCIS E., JR. N87-23979
KENNEY, JEFFREY D. N87-24307
KENNICUTT, R. C. N87-24325
KENNICUTT, R. C., JR. N87-24295
KERR, C. N87-23747
KERR, F. J. N87-24280
KESTER, D. N87-24276
KESTIN, J. N87-23756
KETO, J. W. N87-23950
KHANDELWAL, SURESH N87-23625
KHOSLA, PRADEEP K. N87-24118
N87-24119
KHOSROWSHANI, JAFFAR S. N87-23807
KILKENNY, E. A. N87-23613
KIM, C. N87-23966
KIM, J. U. N87-23783
KING, D. S. N87-23710
KINZER, R. L. N87-24389
KINZEY, R. P. N87-24239
KIRBY, S. H. N87-23711
KIRCHNER, KEITH N87-23681
KIRK, A. N87-23834
KIRKPATRICK, MARC E. N87-23678
KLARMANN, J. N87-24256
KLATT, L. N. N87-24180
KLEIN, U. N87-24351
N87-24352
KLEINMANN, S. G. N87-24346
N87-24347
KLIMA, STANLEY J. N87-23987
KLIMAS, P. C. N87-24016
KNIEPP, N. N87-24239
KNIGHT, DOUGLAS R. N87-24083
N87-24089
KNIGHT, DOYLE D. N87-23909

KNOLL, RICHARD H. N87-23685
KO, B. N. N87-23787
KO, W. L. N87-23852
KO, WILLIAM L. N87-23994
KOGA, R. N87-24205
KOLASINSKI, W. A. N87-24205
KONG, J. A. N87-23847
KONG, JIN A. N87-24009
KOONS, HARRY C. N87-23849
KORNOTA, E. N87-23917
KOSZYKOWSKI, M. L. N87-23778
KOURTIDES, DEMETRIUS A. N87-23751
KOVALENKO, P. A. N87-23572
KOWALSKI, BRUCE R. N87-24216
KRAYNIK, A. M. N87-23731
N87-23732
N87-23918
KREITH, F. N87-24023
KREYSA, E. N87-24292
KRUEGEL, E. N87-24292
KRUYER, WILLIAM B. N87-24071
N87-24073
N87-24077
KUCERA, G. H. N87-23880
KUIPER, T. B. H. N87-24273
KUO, K. K. N87-23783
N87-23785
KUZNETSOV, A. V. N87-23575
KUZNETSOV, V. M. N87-23572
KWONG, M. K. N87-24126

L

LACY, LEWIS L. N87-23944
LAM, J. F. N87-23946
LAMB, G. M. N87-24370
LAMB, S. A. N87-24301
LAMPRU, PAUL D. N87-24050
LANDAHL, MARTEN T. N87-23907
LANDY, ROBERT J. N87-23619
LANGE, F. F. N87-23735
LANGEL, R. A. N87-24039
LANKFORD, JAMES N87-23720
LANSNER, ANDERS N87-24114
LARSEN, WILLIAM E. N87-23856
LARSON, TERRY J. N87-23616
LASHINSKY, H. N87-24193
LAUB, GEORGENE H. N87-23631
LAUBER, T. S. N87-24158
LAUDENSLAGER, JAMES B. N87-23961
LAURELIS, R. J. N87-24278
N87-24283
LAW, C. K. N87-23808
LAWING, PIERCE L. N87-23594
LAWRENCE, C. N87-24006
LAWSON, W. S. N87-24190
N87-24191
LEATHERWOOD, JACK D. N87-24161
LEE, A. N87-23806
LEE, C. N87-23974
LEE, C. S. N87-23627
LEE, J. H. N87-24378
LEE, R. S. N87-23976
LEE, S. N87-23800
LEENE, A. N87-24284
LEGGETT, S. G. N87-24336
LEGGETT, S. K. N87-24343
N87-24357
N87-24358
LEIKER, GREGORY L. N87-23988
LEISAWITZ, D. N87-24274
LEISERSON, CHARLES E. N87-23853
LEISSA, A. W. N87-23998
LEISSLER, GEORGE W. N87-23729
LEITH, E. N87-23937
LERMA, GUILLERMO N87-23981
LESH, JAMES R. N87-23960
LESQUEREN, A. M. N87-24353
LETAW, J. R. N87-24389
LETAW, JOHN R. N87-23884
LEVERANT, GERALD R. N87-23720
LEVINE, JAY H. N87-23759
LEVINE, L. O. N87-23742
LIANG, P. Y. N87-23612
LIANSHUN, DI N87-23688
LIBELO, L. F. N87-23842
LIEPA, V. V. N87-23850
LILEIKIS, DENNIS E. N87-23905
LILIENTAL-WEBER, Z. N87-24206
N87-24210
LIN, YU. N87-24393
LINASK, I. N87-23622
LINK, RICHARD E. N87-24000
LIOU, MENG-SING N87-24132
LISPER, BJOERN N87-24091
LITOVCHENKO, V. N87-24211
LIU, DICK L. N87-23887
LO, K. Y. N87-24321
LOGOWSKI, JACEK N87-24218
LOKEN, S. C. N87-24236
LOMBARD, DAVID S. N87-23663
LONDON, J. N87-24053
LOOK, DAVID C. N87-24220
LOPEZ, A. A. N87-24059
LORD, S. D. N87-24310
LOVE, W. N87-23642
LOW, F. J. N87-24347
LOW, FRANK J. N87-24362
LOWE, S. R. N87-23787
LOWRY, M. E. N87-24183
LUCY, MELVIN H. N87-23983
LUDEKE, R. N87-24206
LUMPKIN, A. H. N87-23956
LUQI N87-24097
LUTTGES, M. N87-23912
LYNCH, M. T. N87-23673
LYNCH, WILLIAM L., JR. N87-23869
LYNN, B. W. N87-24383
LYONS, LAWRENCE R. N87-24034

M

MABRY, J. N87-23959
MACCRACKEN, M. C. N87-24041
N87-24052
MACGILLIVRAY, H. T. N87-24343
N87-24358
MACNEIL, PETER N. N87-23685
MADNICK, STUART E. N87-24237
MADORE, B. F. N87-24327
N87-24341
MAGGS, BRUCE M. N87-23853
MAHER, J. V. N87-23919
MAILLOUX, ROBERT J. N87-23860
MAKINO, A. N87-23806
MAKSUTOVA, M. K. N87-23582
MALDER, N. N. N87-23730
MALKAN, M. A. N87-24371
N87-24372
MALONEY, PHILIP N87-24318
MALVEZZI, A. M. N87-23952
MANSON, S. STANFORD N87-24007
MANZO, MICHELLE A. N87-24029
MARGOLIS, STEPHEN B. N87-23764
N87-23766
N87-23777
MARHIC, M. E. N87-23953
MARION, J. N87-24209
MARISKA, J. T. N87-24225
MARMOLIN, HANS N87-24127
MARR, ROGER L. N87-23646
MARSLAND, D. P. N87-23842
MARSMAN, A. P. L. A. N87-23643
MARTIN, J. E. N87-23748
MARTIN, J. M. N87-24353
MARTIN, R. D. N87-24147
MARTIN, ROBERT N. N87-24322
MARTIN, S. J. N87-23723
MARTINDALE, DAVID L. N87-23663
MARTINEZ, F. E. N87-23741
MARTINEZ, R. J. N87-23747
MARTINIS, J. M. N87-24213
MARVEL, C. S. N87-23730
MARYNICK, DENNIS S. N87-23746
MASKARINEC, M. P. N87-24030
MATHES, H. B. N87-23763
N87-23770
MATTHEWS, J. L. N87-24066
MATTHEWS, K. N87-24327
N87-24354
MAY, L. NELSON, JR. N87-24012
MAY, M. M. N87-24154
MCCARTHY, PATRICK N87-24330
MCCARTHY, PATRICK J. N87-24345
MCCLUNG, R. W. N87-23966
MCCLUSKEY, EDWARD J. N87-23887
MCCONNELL, K. G. N87-24003
MCCORMICK, STEPHEN F. N87-24139
MCCREIGHT, C. R. N87-24370
N87-24378
MCFARLANE, R. A. N87-23946
MCGRATH, DANIEL T. N87-23823
MCHARGUE, C. J. N87-24214
MCINTOSH, GLEN E. N87-23663
MCINTOSH, R. N87-23753
MCINTYRE, J. F. N87-23719
MCKAY, D. W. N87-24189
MCKELVEY, M. E. N87-24378
MCLAUGHLIN, K. L. N87-23824
MCLAUGHLIN, THOMAS E. N87-24201
MCMANUS, K. R. N87-23804
MCMILLAN, R. W. N87-23858
MCMILLION, L. G. N87-23768
MCWHORTER, ALAN L. N87-24221
MEEKER, D. N87-24194
MEHTA, UNMEEL N87-23595
MEIKLE, W. P. S. N87-24340
MELIUS, C. F. N87-23781
MENDILLO, MICHAEL N87-24044
MENON, S. N87-23802
MENZEL, A. N87-24008
MERRIAM, MARSHAL L. N87-24148
METSCHER, B. D. N87-23840
METZLER, WILLIAM D. N87-24202
MEYER, T. G. N87-23622
MEYER, T. J. N87-24020
MEYER, W. A. N87-24245
MEZGER, P. G. N87-24289
N87-24292
MICCI, MICHAEL M. N87-23762
MIKROYANNIDIS, JOHN A. N87-23751
MILDICE, J. W. N87-23690
MILEY, G. N87-24373
MILEY, GEORGE K. N87-24330
N87-24366
MILEY, H. S. N87-24383
MILLER, C. N87-24246
MILLER, E. N87-23768
MILLER, G. C. N87-24061
MILLER, J. F. N87-23876
MILLER, K. T. N87-23735
MILLER, NORMA D. N87-24084
MILLS-CURRAN, W. C. N87-24135
MILROY, R. D. N87-24195
MINECK, RAYMOND E. N87-23594
MINEO, BETH N87-23941
MIRTICH, MICHAEL J. N87-23736
MISRA, AJAY K. N87-24026
MITTRA, R. N87-23852
MIYAMOTO, JUN-ICHI N87-23886
MOCHKOVITCH, R. N87-24337
MOHLER, J. H. N87-23955
MOIR, D. C. N87-23877
MOITRA, ANUTOSH N87-23586
MOLAVI, K. N87-23805
MOLINARI, R. L. N87-24060
MOODY, R. L. N87-24030
MOONEY, T. J. N87-24270
MOORE, JOAN G. N87-23925
N87-23928
N87-23929
MOORE, JOHN N87-23925
N87-23928
N87-23929
MOORE, N. L. N87-23985
MOORE, ROYCE D. N87-23623
MOORE, THOMAS C. N87-23587
MOREL, T. N87-23922
MORGAN, J. M. N87-23659
MORGAN, JAMES A. N87-24087
MORIARTY, ROBERT M. N87-23807
MORITA, SHIGERU N87-24198
MORREN, W. EARL N87-23821
MORRIS, J. W., JR. N87-23817
MORRISON, PHILIP N87-24334
MORSE, H. ANDREW N87-23631
MORSE, T. F. N87-24175
MOTE, M. W. N87-23726
MOUNTAIN, C. M. N87-24357
MULLER, ERNEST S. N87-23700
MULLINIX, DANIEL A. N87-23823
MUNCZEK, H. J. N87-24169
MURRAY, H. S. N87-24244
MURRAY, P. M. N87-23635
MUSSELMAN, K. A. N87-23719
MYERS, M. K. N87-24160

N

NADEAU, Y. N87-24001
NADVORSKIY, A. S. N87-23581
NAGLE-ESHLEMAN, JUDITH N87-23620
N87-23818
N87-23996
N87-24125
NAKAI, N. N87-24290
NATARAJAN, M. N87-24040
NAUMANN, K. W. N87-23686
NEALON, DON N87-24066
NEELAKANTASWAMY, PERAMBUR S. N87-23848
N87-23890
N87-23891
N87-23892
NEENAN, B. N87-23753
NEFF, D. N87-23831

NEIKIRK, DEAN P. N87-23673
NELSON, C. N87-24206
NELSON, P. A. N87-23880
NESS, NORMAN F. N87-24253
NETZER, D. W. N87-23769
N87-23757
N87-23788
NEUGEBAUER, G. N87-24327
N87-24341
N87-24354
N87-24373
NEWELL, ALLEN C. N87-23646
NEWHOUSE, M. N87-24018
NEWTON, JAMES E. N87-23591
NICHOLAS, O. P. N87-23658
NICHOLSON, STEPHEN N87-23925
N87-23927
N87-23928
N87-23929
NIEUWPOORT, A. M. H. N87-23655
NIGSLEY, D. M. N87-23622
NORBERG, TOMMY N87-24148
NORMAN, COLIN A. N87-24324
NORRIS, GEORGE E. N87-24220
NORRIS, P. P. N87-23622
NORTH, C. M. N87-23978
NORTHAM, G. B. N87-23791
NORTHAM, G. BURTON N87-23789
NOSSEIR, HAGY N87-23797

O

OBRIEN, WALTER F. N87-23789
OCONNELL, J. P. N87-24224
OLIGER, JOSEPH N87-24049
OLIVER, W. C. N87-24214
OLKEN, F. N87-24236
OLSEN, JAMES J. N87-23610
OLSZEWSKI, M. N87-24021
N87-24028
ORAN, E. S. N87-23801
ORMES, J. F. N87-24255
ORMES, JONATHAN F. N87-24247
N87-24257
ORNELLAS, DONALD N87-23766
OSBORN, J. E. N87-24142
OSBORN, J. R. N87-23772
OSHER, J. E. N87-23976
OSTERBROCK, DONALD E. N87-24374
OTOSHI, T. Y. N87-23629
OVERSKEI, D. O. N87-24197
OWNBY, MICHAEL R. N87-23644

P

PACALA, THOMAS J. N87-23961
PAIK, SEUNG W. N87-23588
PALKO, KEITH L. N87-23585
PALKO, R. L. N87-23811
PALMER, A. J. N87-23946
PALUMBO, GIORGIO G. C. N87-24323
PANCHENKO, V. I. N87-23574
PANITZ, J. K. G. N87-23741
PAQUETTE, MICHAEL P. N87-23679
PARKER, EUGENE N. N87-24251
PARKER, W. N87-23973
PARKINSON, D. N87-23642
PARKS, R. E. N87-24102
PARR, D. M. N87-23796
PARR, T. P. N87-23782
N87-23796
PASQUALE, JOSEPH N87-24112
N87-24152
PATEL, VIRENDRA C. N87-23924
PATIL, P. G. N87-23876
PATRICK, CLINT N87-23893
PATTERSON, MICHAEL J. N87-23692
PATTON, JAMES M., JR. N87-23614
PATUREL, G. N87-24953
PATZNER, PAUL A. N87-23648
PAUL, W. N87-24206
PAULSON, JAMES A. N87-24136
PAVLI, A. J. N87-23809
PEDLAR, A. N87-24369
PELED, URI N87-23797
PELLETT, G. L. N87-23791
PENFIELD, PAUL, JR. N87-24108
PENNYCOOK, S. J. N87-24207
PERAULT, M. N87-24268
N87-24279
PEREZ-BLANCO, H. N87-24180
PERRY, D. G. N87-23948
PERSSON, C. J. N87-24327
N87-24341
N87-24354
PERSSON, CAROL J. LONSDALE N87-24287
N87-24304
N87-24309
PERSSON, S. E. N87-24327
N87-24341
N87-24354
PETERSON, K. A. N87-23883
PETSCHEK, A. G. N87-24155
PETZOLD, L. R. N87-24144
PEYRAN, RICHARD J. N87-23631
PHILLIPS, M. M. N87-24340
PICK, JONATHAN C. N87-23652
PICKERING, H. W. N87-23728
PICKETT, R. L. N87-24061
PICONE, J. M. N87-24225
PIERCE, R. E. N87-23931
PIETREMENT, J. C. N87-23651
PIKE, ROSCOE A. N87-23752
PINES, D. N87-24379
PINKUS, O. N87-23973
N87-23974
N87-23975
PINNADUWAGE, L. A. N87-23957
PISANE, G. N87-23842
PISMIS, P. N87-24333
PISTER, KARL S. N87-23683
PLACE, J. L. N87-24013
PLOTKIN, SERGE A. N87-24109
PLUT, T. A. N87-23943
POGGE, RICHARD W. N87-24316
POH, S. N87-23980
POLAK, ELIJAH N87-23683
POLLAK, C. N87-23583
POMERANTZ, MARTIN N87-23746
POSNER, E. C. N87-23628
POSTHILL, J. B. N87-23817
POTTS, JEFFREY H. N87-24137
POULIN, J. R. N87-23913
POWERS, B. J. N87-24014
POWERS, J. P. N87-23769
POWERS, ROBERT B. N87-23687
PRAHARAJ, S. C. N87-23811
PRASSINOS, P. G. N87-24232
PREISSINGER, ROBERT D. N87-23668
PRESTON, R. F. N87-23699
PRESTWICH, A. H. N87-24328
PRICE, DONNA N87-23814
PROGAR, DONALD J. N87-23752
PUGET, J. L. N87-24268
N87-24279
PUXLEY, P. J. N87-24343
N87-24357
N87-24358
PYO, M. L. N87-23899

Q

QUINN, R. B. N87-23838

R

RAJESHWAR, KRISHNAN N87-23746
RALSTON, J. P. N87-24169
RAMACHANDRA, SRIDHAR M. N87-23625
RAMATY, R. N87-24250
RAMATY, REUVEN N87-24247
RAMSEY, B. D. N87-24336
RAO, J. S. N87-23621
RAO, N. S. V. N87-23984
RAPTIS, A. C. N87-23932
REACH, WILLIAM N87-24345
REDDY, J. N. N87-23819
REDMAN, D. N87-23769
REED, I. S. N87-23632
REEVES, J. H. N87-24383
REEVES, JOHN T. N87-24082
REID, D. W. N87-23896
REID, L. D. N87-23637
REISER, M. N87-24172
REINSCHLER, C. L. N87-23703
REUTER, D. N87-23803
REYNOLDS, JOHN R. N87-23748
REYNOLDS, PHILIP A. N87-23656
RHODES, C. K. N87-23951
RICCITIELLO, SALVATORE R. N87-23698
N87-23737
RICCO, A. J. N87-23723
RICE, W. N87-24299
N87-24304
N87-24309
RICE, W. L. N87-24282
N87-24341
RICHARDSON, I. G. N87-24380
RIEKE, G. H. N87-24360
RILEY, D. J. N87-23843
RISEMAN N87-24090
RIVA, G. N87-23805
RIVOLO, A. R. N87-24270
ROACH, J. F. N87-24244
ROBERTS, A. N87-23942
ROBERTS, L. N87-23627
ROBERTSON, D. N87-24117
ROBERTSON, N. A. N87-24368
ROBINSON, ANITA N87-23945
ROBINSON, MICHAEL B. N87-23944
ROCHE, M. F. N87-23880
ROCK, PAUL B. N87-24082
RODGERS, DOUGLAS C. N87-23911
RODRIGUEZ, J. L. N87-23943
RODRIGUEZ, JEFFREY J. N87-23851
ROELOFS, LARRY H. N87-24098
ROETTIGER, K. A. N87-24325
ROGERS, J. D. N87-23992
N87-24003
ROGERS, R. CLAYTON N87-23790
N87-23806
ROGERS, RICHARD L. N87-24106
ROHAN, MICHAEL N87-24334
ROHDE, FREDERICK W. N87-23827
ROMANISHIN, W. N87-24308
ROMINE, C. H. N87-24100
ROOK, B. J. N87-23845
ROSA, J. S. N87-23769
ROSENBLUM, M. N87-24117
ROSENBLUTH, M. N. N87-23920
ROSENTHAL, ALAN N87-24012
ROSNER, DANIEL E. N87-23709
ROSS, B. A. N87-24019
ROSS, L. M. N87-23898
ROTEM, D. N87-24236
ROTTER, M. D. N87-24183
ROUVRAY, D. H. N87-23716
ROWAN-ROBINSON, M. N87-24266
ROY, R. N87-23749
ROZANSKI, JAMES D. N87-23767
RUBIN, CLINTON T. N87-24065
RUBIN, J. B. N87-23769
RUDY, RICHARD J. N87-24364
RUDYAK, M. YE. N87-23578
RUSH, JODY N87-23945
RYDBECK, G. N87-24312
RYDBECK, GUSTAF N87-24315
RYDBECK, O. E. H. N87-24312
RYMER, W. Z. N87-23963

S

SADUN, ALBERTO N87-24334
SAETHER, E. S. N87-23705
N87-23706
SAGE, L. J. N87-24270
SAJBEN, M. N87-23793
SANDERS, D. B. N87-24327
N87-24331
N87-24341
SANDERSON, T. R. N87-24380
SANKAR, N. L. N87-23799
SANKAR, S. V. N87-23760
SARACEVIC, TEFKO N87-24238
SARGENT, A. I. N87-24331
SARMIENTO, CHARLES J. N87-23691
SATHER, DUANE P. N87-23918
SAUER, H. H. N87-24384
SAVAGE, A. N87-24343
N87-24358
SAVINA, T. F. N87-23581
SAWCHUK, A. A. N87-24182
SAYLORS, D. B. N87-24102
SCALO, JOHN M. N87-24329
SCHADOW, K. C. N87-23798
SCHAUBERT, DANIEL H. N87-23867
SCHIAVONE, REBECCA N87-23667
SCHLUTSMEYER, A. N87-23839
SCHNELL, R. C. N87-24056
SCHOLZE, RICHARD J. N87-24087
N87-24088
SCHRAMM, D. N. N87-24388
SCHRANK, HELMUT E. N87-23861
SCHREINER, K. E. N87-23890
SCHUBERT, W. K. N87-23943
SCHUNK, ROBERT W. N87-24036
SCHUTZ, B. E. N87-24042
SCHWARTZ, D. N87-24045
SCHWARTZ, ROBERT S. N87-24073
SCHWARZE, GENE E. N87-23903
SCHWERING, FELIX K. N87-23864
SCOTT, B. C. N87-24056
SCOTT, C. K., II N87-23788
SCOTT, JAMES R. N87-23598

SCOVILLE, N. Z. N87-24267
N87-24327
N87-24331
SCULL, N. N87-23966
SEDNEY, RAYMOND N87-24131
SEIFERT, R. N87-23644
SEITTER, KEITH L. N87-24046
SEKIGUCHI, KAZUHIRO N87-24336
SELLIS, TIMOLEON K. N87-24230
SENGIL, NEYSAN N87-24025
SENGUPTA, D. L. N87-23950
SENIOR, T. B. N87-23850
SERPEN, GURSEL N87-23628
SERRA, GUY N87-24278
SHAFFER, TIMOTHY D. N87-23746
SHAHIN, MOHAMED Y. N87-23861
SHAKIRYANOV, M. M. N87-23577
SHANNAN, J. N87-23820
SHARE, G. H. N87-24389
SHARP, D. J. N87-23741
SHAW, HAROLD N87-23689
SHELLMAN, C. H. N87-23822
SHERMAN, C. N87-23694
SHOCKEY, D. A. N87-23989
SHORT, NICHOLAS M., JR. N87-24098
SHOSHANI, A. N87-24236
SHU, FRANK H. N87-24375
SHU, P. K. N87-24370
SHUMINSKY, THOMAS K. N87-24215
SILBERBERG, R. N87-24389
SILK, J. N87-24317
SIMCHICK, RICHARD T. N87-23713
SIMON, M. N87-24348
SIMONS, RAINEE N. N87-23900
SIMPSON, W. A., JR. N87-23986
SINDLER, RONALD B. N87-24151
SINDORF, J. F. N87-23881
SINGH, TRILOCHAN N87-23774
SIRIGNANO, W. A. N87-23805
SJOBERG, WILLIAM F. N87-24047
SKAMAROCK, WILLIAM N87-24049
SKAVENSKI, ALEXANDER A. N87-24068
SKILLMAN, EVAN D. N87-24302
SKOCH, GARY J. N87-23623
SLINEY, DAVID H. N87-23945
SLOUGH, J. T. N87-24195
SMIGIELSKI, P. N87-23935
SMITH, ARTHUR F. N87-23615
SMITH, BEVERLY J. N87-24347
SMITH, D. S. N87-23707
SMITH, E. J. N87-24380
SMITH, ED D. N87-24088
SMITH, HENRY I. N87-24204
SMITH, S. A. N87-23985
SMITH, T. A. N87-23809
SODROSKI, T. J. N87-24280
SOFUE, Y. N87-24290
SOIFER, B. T. N87-24327
N87-24331
N87-24341
N87-24354
SOIFER, B. THOMAS N87-24323
SOLBACH, KLAUS N87-23862
SOLIMAN, S. S. N87-23826
SOLOMON, O. M., JR. N87-24004
SOLOMON, P. M. N87-24270
SOLOMON, SEAN C. N87-24038
SORENSEN, N. R. N87-23723
SORUM, L. N. N87-23673
SOVEY, JAMES S. N87-23736
N87-23821
SPEARS, K. G. N87-23953
SPEDTKE, P. N87-24165
SPEECE, ROBERT F. N87-23675
SPERGEL, D. N. N87-24383
SPINONI, MAURIZIO N87-23650
SRINIVASAN, M. G. N87-23932
STAPLES, K. J. N87-23642
STEEL, D. G. N87-23946
STEGEMAN, G. I. N87-24177
STEIN, W. E. N87-23956
STEINBERG, STANLY N87-24124
STEINHAUER, L. C. N87-24195
STEINMEYER, P. A. N87-23939
STEPHENSON, W. A. N87-24017
STERN, FREDERICK N87-23924
STEVENS, N. J. N87-23678
STEVENSON, CHARLES G. N87-23675
STEWART, H. E. N87-23800
STEWART, M. T. N87-24181
STODDARD, S. D. N87-23949
STOECKER, W. F. N87-23917
STONE, E. C. N87-24256
STOUGH, H. PAUL, III N87-23614
STOUT, R. B. N87-24222
STRAHLE, W. C. N87-23799
STRAUB, F. K. N87-23596
STRAUB, G. K. N87-23725
STRAUSS, JACK L. N87-24113
STRAUSS, MICHAEL A. N87-24345
STREET, ROBERT L. N87-24049
STREITMATTER, R. E. N87-24255
STRINGFELLOW, G. B. N87-24223
STROM, S. E. N87-24310
STRUCK-MARCELL, CURTIS N87-24329
STRUNKIN, YU. V. N87-23582
STUART, THOMAS A. N87-23903
STUFFLEBEAM, J. H. N87-23771
SUTHERLAND, BRUCE J. N87-23914
SUTTON, JOHN R. N87-24082
SUTTON, S. B. N87-23931
SWALLOW, J. C. N87-24080
SWANSON, G. A. N87-23622
SYLWESTER, A. P. N87-23703

T

TACCONI-GARMAN, LINDA J. N87-24335
TALLERICO, P. J. N87-23897
TAM, W. N87-23845
TANAKA, H. N87-23990
TANG, VICTOR K. N87-24151
TANIKAWA, T. N87-24192
TANIS, FRED J. N87-24031
N87-24032
TAVELLA, D. A. N87-23627
TAWARA, HIROYUKI N87-24198
TAYLOR, L. M. N87-23993
TAYLOR, ROBERT L. N87-23683
N87-23963
TEATES, H. B. N87-24050
TECZA, J. N87-23973
N87-23974
N87-23975
TELESCO, C. M. N87-24336
TEREBEY, SUSAN N87-24271
N87-24281
TERRY, K. N87-23753
THADDEUS, P. N87-24272
THEIS, WILLIAM M. N87-24220
THRONSON, HARLEY A., JR. N87-24303
TIBBITTS, E. E. N87-23722
TILANUS, R. P. J. N87-24311
TISCHLER, MARK B. N87-23632
TISLER, THOMAS W., JR. N87-23701
TITUS, CHRISTOPHER J. N87-24136
TO, C. W. S. N87-23997
TOMLINSON, B. N. N87-23639
TONG, A. N87-23805
TONG, CARL W. N87-24178
TONN, B. T. N87-24233
TOOMRE, JURI N87-24382
TORIKAI, T. N87-23783
TORVEN, STAFFAN N87-24185
TOTH, R. P. N87-23841
TOWNSEND, D. N87-23744
TRESCH-FIENBERG, R. N87-24370
TRIPPE, T. G. N87-24236
TRIVISON, DONNA N87-24238
TROXEL, DONALD E. N87-24108
TRUONG, T. K. N87-23832
TSAO, C. H. N87-24389
TUCKER, THOMAS M. N87-23816
TURKMAN, IBRAHIM R. N87-23890
N87-23891
N87-23892
TURLEY, R. S. N87-23946
TURNER, C. D. N87-23857
TURNER, JEAN L. N87-24320
N87-24322
TURNER, M. S. N87-24388
TZUANG, CHING-KUANG C. N87-23873

U

UNGER, S. W. N87-24369
UNGERER, V. N87-24298
UNQLAUB, R. N87-23834

V

VADER, J. PATRICIA N87-24348
VADROT, R. N87-23647
VALDES, A. N87-23728
VANALLEN, JAMES A. N87-24248
VANASSE, GEORGE A. N87-23708
VANBREUGEL, WIL N87-24330
VANDAM, THOMAS N87-23661
VANDERBORGH, N. E. N87-24244
VANDERGEEST, P. J. J. N87-23655
VANDERHULST, J. M. N87-24295
N87-24325
VANDERMUELEN, DAVID N87-24066
VANDERPLOEG, M. N87-23820
VANDSBURGER, U. N87-23804
VANOOSTEROM, W. N87-24278
VANOVERBECK, THOMAS N87-23808
VARMA, M. N87-23612
VARY, ALEX N87-23987
VEILLEUX, SYLVAIN N87-24374
VELSKO, S. N87-23704
VERHAEGEN, M. H. N87-24156
VERNON, THOMAS A. N87-24001
VIALLEFOND, F. N87-24298
N87-24309
VIDIN, YU. V. N87-23576
VINOGRADOV, B. S. N87-23574
VISWANATHAN, SIVASWAMY N87-23870
VLADIMIROFF, T. N87-23779
VOGT, GARY L. N87-23765

W

WADDINGTON, C. J. N87-24256
WADE, R. N87-24328
WAGNER, TIMOTHY C. N87-23789
WAH, BENJAMIN W. N87-23889
WALKER, K. P. N87-23622
WALKER, P. N87-23747
WALLICK, K. B. N87-23930
WALOWIT, J. N87-23974
WALSH, W. J. N87-23876
WALTERS, DENNIS C. N87-24220
WALTON, J. N87-23973
N87-23974
N87-23975
WANG, CAROLINE N87-23893
WARD, J. N87-24174
WARD, K. J. N87-23738
WARREN, S. G. N87-24053
WARREN, W. E. N87-23732
WASHBURN, J. N87-24206
WATSON, CAROLYN B. N87-23597
WATSON, WILLIAM D. N87-24277
WEAVER, D. P. N87-23775
WEAVER, DAVID P. N87-23774
WEBBER, WILLIAM R. N87-24254
WEBER, TIMOTHY S. N87-24095
WEEDMAN, DANIEL W. N87-24319
WEGLEY, H. L. N87-24051
WEINGART, R. C. N87-23978
WEISBIN, C. R. N87-23964
N87-24121
WENZEL, K. P. N87-24380
WESSELIUS, P. R. N87-24283
WEST, C. D. N87-23965
WHALEN, MARGARET V. N87-23693
WHEELER, THOMAS G. N87-24084
WHITEHEAD, R. S. N87-23705
N87-23706
WHITEOAK, J. B. N87-24273
WHITMORE, STEPHEN A. N87-23618
WHITTENBERGER, J. DANIEL N87-24026
WICHNER, R. P. N87-24021
WIELEBINSKI, R. N87-24352
WIKLIND, T. N87-24312
WIKLIND, TOMMY N87-24315
WILLIAMS, C. B. N87-23883
WILLIAMS, D. A. N87-23658
WILLIAMS, D. F. N87-23958
WILLIAMS, FORMAN A. N87-23777
WILLIAMS, G. P. N87-24179
WILLIAMS, REDFORD B., JR. N87-24067
WILLIAMS, ROBERT A. N87-23632
WILLIAMS, T. A. N87-24019
WILSON, ANDREW S. N87-24385
WILSON, JOHN C. N87-23630
WILSON, K. J. N87-23798
WILSON, L. G. N87-23791
WISCHMANN, K. B. N87-23894
WITHBROE, GEORGE L. N87-24387
WOLF, M. N87-24018
WOLFF, F. N87-23690
WOLSTENCROFT, R. D. N87-24336
N87-24343
N87-24358
WONG, A. Y. N87-24192
WOOD, C. C. N87-24232
WOOD, N. J. N87-23627
WOOD, RICHARD M. N87-23597
WOODWARD, P. W. N87-23755
WRIGHT, EDWARD L. N87-24359
WRIGHT, G. S. N87-24328
N87-24340
N87-24368

WUNDERLICH, E. N87-24351
N87-24352
WYGNANSKI, I. N87-23915
WYNN-WILLIAMS, C. G. N87-24285
N87-24342
N87-24361
WYSE, ROSEMARY F. G. N87-24317

Y

YAMADA, H. N87-23990
YAN, Y. T. N87-24196
YANG, VIGOR N87-23761
YAP, B. K. N87-24035
YEE, H. C. N87-24145
YEH, F. C. N87-23934
YOO, SUNGYUL N87-23924
YOON, S. C. N87-23769
YOUNG, J. S. N87-24310
YOUNG, JUDITH S. N87-24291
N87-24307
N87-24335
YU, K. N87-23800
YU, PHIL W. N87-24220

Z

ZACCARDELLI, CARLA N87-24163
ZACHOR, A. S. N87-23707
ZAKHAROV, N. N. N87-23573
ZAMAR, RUBEN H. N87-24147
ZAN, S. J. N87-23990
ZEANAH, HUGH N87-23893
ZENIE, ALEXANDRE N87-24111
ZHANG, C. Y. N87-24276
ZINKLE, S. J. N87-24214
ZINN, B. T. N87-23760
N87-23803
ZIOLKOWSKI, R. W. N87-23842
ZIPPERIAN, T. E. N87-23943
N87-24212
ZORZI, E. N87-23975
ZUBER, DAN N87-23730
ZUKAKISHVILI, R. I. N87-23571
ZWICKL, R. D. N87-24380

Typical Corporate Source Index Listing

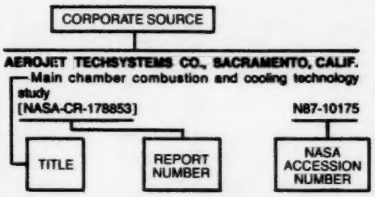

Listings in this index are arranged alphabetically by corporate source. The title of the document provides the user with a brief description of the subject matter. The report number helps to indicate the type of document cited (e.g., NASA report, translation, NASA contractor report). The NASA accession number denotes the number by which the citation is identified. The titles are arranged under each corporate source in ascending accession number order.

A

ADVISORY GROUP FOR AEROSPACE RESEARCH AND DEVELOPMENT, NEUILLY-SUR-SEINE (FRANCE).
Efficient conduct of individual flights and air traffic or optimum utilization of modern technology for the overall benefit of civil and military airspace users
[AGARD-AR-236] N87-23608
Aircraft Dynamic Response to Damaged and Repaired Runways
[AGARD-R-739] N87-23609
Flight Simulation
[AGARD-CP-408] N87-23633
Microwave Antennas for Avionics
[AGARD-LS-151] N87-23859
Short Course on Cardiopulmonary Aspects of Aerospace Medicine
[AGARD-R-758] N87-24070
Aeromedical evaluation and disposition of electrocardiographic abnormalities N87-24071
Noninvasive methods for the detection of coronary artery disease in aviators: A stratified Bayesian approach N87-24072
Valvular and congenital heart disease in the aviator N87-24073
Aeromedical aspects of mitral valve prolapse N87-24074
Pulmonary physiology and pulmonary function testing in aerospace medicine N87-24075
Aeromedical disposition of pulmonary sarcoidosis, chronic obstructive lung disease, reactive airway disease and spontaneous pneumothorax N87-24076
Hypertension in the aviator N87-24077
Coronary risk factors in aerospace medicine N87-24078
Cardiopulmonary screening for high-performance flying: Selection and retention issues N87-24079

AEG-TELEFUNKEN, ULM (WEST GERMANY).
Aircraft antennas/conformal antennas missile antennas N87-23862

AERITALIA S.P.A., TORINO (ITALY).
The use of Aeritalia flight simulator for the development of the AM-X weapon system N87-23650

AEROSPACE CORP., EL SEGUNDO, CALIF.
An ELF (Extremely-Low-Frequency) transmitter experiment for the space shuttle. (The NASC-201 (Naval Air Space Command) experiment). Volume 1
[AD-A178237] N87-23849
Generation of broadband noise in the magnetotail
[AD-A179136] N87-24034
Heavy ion induced upsets in semiconductor devices
[ATR-86(8139)-3] N87-24205

AIR FORCE ACADEMY, COLO.
Recent studies in plate vibrations: 1981-1985. Part 2: Complicating effects N87-23998

AIR FORCE ENVIRONMENTAL TECHNICAL APPLICATIONS CENTER, SCOTT AFB, ILL.
Station climatic summaries, Antarctica, Australia and Oceania
[AD-A179242] N87-24047

AIR FORCE FLIGHT TEST CENTER, EDWARDS AFB, CALIF.
The development of the T-46 next generation trainer manned engineering simulator at the US Air Force Flight Test Center N87-23652
A method for aircraft simulation verification and validation developed at the United States Air Force Flight Simulation Facility N87-23654

AIR FORCE GEOPHYSICS LAB., HANSCOM AFB, MASS.
EIRMA: An Energetic Ion Retarding Mass Analyzer for the BERT-1 (Beam Emission Rocket Test one)
[AD-A178231] N87-23694

AIR FORCE GLOBAL WEATHER CENTRAL, OFFUTT AFB, NEBR.
TAF (Terminal Aerodrome Forecast) verification
[AD-A177931] N87-24055

AIR FORCE INST. OF TECH., WRIGHT-PATTERSON AFB, OHIO.
Evaluation of the angle of attack limiter of the F-16 C/D aircraft
[AD-A177941] N87-23612
Failure detection and isolation for an asychronous digital flight control system
[AD-A179210] N87-23628
Flight test evaluation of techniques to predict longitudinal pilot induced oscillations
[AD-A179229] N87-23629
Optimal continuous thrust orbital evasive maneuvers from geosynchronous orbit
[AD-A179413] N87-23668
A quantitative comparison of several orbital maneuvering vehicle configurations for satellite repair/replenishment
[AD-A179106] N87-23677
Detumbling of two inter-connected rigid bodies using Liapunov methods for feedback control
[AD-A179207] N87-23679
A systems analysis of emergency escape and recovery systems for the US space station
[AD-A179233] N87-23680
An analysis of space station motion subject to the parametric excitation of periodic elevator motion
[AD-A179235] N87-23681
A multiple attribute decision analysis of manned airlock systems
[AD-A179241] N87-23682
An analysis of geopotential effects on satellite constellations
[AD-A179507] N87-23684
Material damping measurements of 2D carbon-carbon composite beams
[AD-A179109] N87-23700
Collapse analysis of cylindrical composite panels with large cutouts under an axial load
[AD-A179112] N87-23701
Analysis of jitter in a digital transmission system
[AD-A177945] N87-23844
VHDL (VHSIC (Very High Speed Integrated Circuits) Hardware Descriptive Languages) prototype simulator
[AD-A179073] N87-23869
Investigation of electromigration in thin film aluminum at low temperatures
[AD-A179110] N87-23871
Unsteady heat transfer resulting from the rapid charging of an evacuated tank with conducting walls
[AD-A178206] N87-23905
Effects of corona on heat transfer in an enclosure
[AD-A179209] N87-23906
Investigation of shrouded nozzle exit pressure changes
[AD-A179477] N87-23911
Surface roughness: Its effects on the performance of a two-dimensional compressor cascade
[AD-A179506] N87-23913
A redefined hydraulic diameter for laminar flow
[AD-A179511] N87-23914
Improved modeling of structural joint damping
[AD-A179111] N87-23988
Meso gamma-scale kinetic energy budgets of a thunderstorm within a squall-line derived from sesame dual-doppler data
[AD-A178119] N87-24057
A program maintenance aid using static data flow analysis techniques
[AD-A179106] N87-24095
A rapid prototyping approach to software validation
[AD-A177939] N87-24106
Architectural implications of a parallel computational approach to the vector wave equation
[AD-A179510] N87-24113
Content-addressable memory: Applications, algorithms, and simulation
[AD-A177944] N87-24120
A PASCAL implementation of the image algebra
[AD-A177943] N87-24136
Holographic correction of aberrations in optical systems employing synthetic apertures
[AD-A179107] N87-24173
Coherent multiple aperture optical imaging systems: Analysis and design
[AD-A179476] N87-24176
Target segmentation and image enhancement through multisensor data fusion
[AD-A178875] N87-24178
Radial density distribution of negative atomic oxygen in the oxygen positive column: An experiment
[AD-A179212] N87-24186
Fabrication of AlGaAs/InGaAs pseudomorphic modulation doped field effect transistors with p-doped surface layers
[AD-A179230] N87-24201
Evaluation of Tersoff's revised silicon potential in a molecular dynamic simulation of solid silicon
[AD-A179231] N87-24202
Electrical behavior of Ge and (Ge + As) implanted gallium arsenide
[AD-A179505] N87-24203
The development of a prototype CMOS (Complementary Metal Oxide Semiconductor) circuit simulator
[AD-A177942] N87-24215
Surface passivation of an implantable semiconductor multielectrode array
[AD-A178175] N87-24219

AIR FORCE ROCKET PROPULSION LAB., EDWARDS AFB, CALIF.
Role of combustion in the nonlinear combustion instability of composite solid propellants N87-23765
The inhibition effects of H2/O2/N2 flames seeded by potassium N87-23774
CN radical distributions in solid propellant flames N87-23775

AIR FORCE SYSTEMS COMMAND, WRIGHT-PATTERSON AFB, OHIO.
Acta aeronautica et astronautica sinica
[AD-A179673] N87-23618
An approach of preventing combustion vibrations of rocket engine with lateral baffle
[AD-A179222] N87-23688
History of spaceflight
[AD-A178381] N87-24393

AIR FORCE WRIGHT AERONAUTICAL LABS., WRIGHT-PATTERSON AFB, OHIO.
Interpretation in terms of the response of a one degree-of-freedom oscillator to two successive disturbances N87-23610
Trends in ground-based and in-flight simulators for development applications N87-23645

ALABAMA UNIV., HUNTSVILLE.
Cellular monotectic model solidification
[NASA-CR-181027] N87-23717

ALASKA UNIV., FAIRBANKS.
Climatological observations in the Philip Smith Mountains of the North Slope, Alaska
[DE87-006179] N87-24054

ALLIED BENDIX AEROSPACE, KANSAS CITY, MO.
Computer programs for nonlinear least squares analysis of various three-dimensional geometrical elements
[DE87-006048] N87-24133

AMDAHL CORP., SUNNYVALE, CALIF.
Evaluation of Navier-Stokes and Euler solutions for leading-edge separation vortices
[NASA-TM-89458] N87-23584
AMSTERDAM UNIV. (NETHERLANDS).
A simple two-component model for the far-infrared emission from galaxies N87-24314
ARECIBO IONOSPHERIC OBSERVATORY, PUERTO RICO.
Far-infrared properties of cluster galaxies N87-24305
ARGONNE NATIONAL LAB., ILL.
Analytical prediction of combustion performance characteristics of bipropellant liquid rocket engine combustor N87-23810
Worldwide nickel/iron battery development for electric vehicle applications
[DE87-004822] N87-23876
Low-resistivity glass electrolytes for sodium-sulfur cells
[DE87-004837] N87-23880
Motion-dependent fluid forces acting on a tube row in crossflow
[DE87-005574] N87-23923
Modeling of dilute two-phase multispecies solid/gas flows
[DE87-009254] N87-23932
An extended set of FORTRAN basic linear algebra subprograms: Model implementation and test programs
[DE87-007913] N87-24101
Beyond Speedup: Performance analysis of parallel programs
[DE87-007954] N87-24115
Uniqueness of non-negative solutions of a class of semi-linear elliptic equations
[DE87-006966] N87-24128
ARIZONA STATE UNIV., TEMPE.
Star formation rates as a function of galaxy mass N87-24308
ARIZONA UNIV., TUCSON.
Fabrication of polymers for use under extreme conditions
[AD-A179458] N87-23730
Experimental and numerical investigation of coherent structures
[AD-A179456] N87-23910
Signal processing with degenerate 4-wave mixing
[AD-A179679] N87-24177
The history of gas in sprial galaxies N87-24318
The frequency of enhanced star formation in interacting and isolated galaxies N87-24326
The relation between star formation and active nuclei N87-24360
Spatial deconvolution of IRAS galaxies at 60 UM N87-24362
ARMY ARMAMENT RESEARCH AND DEVELOPMENT COMMAND, DOVER, N. J.
Force-field parameters and molecular mechanics calculations for nitramines N87-23779
ARMY AVIATION RESEARCH AND DEVELOPMENT COMMAND, CLEVELAND, OHIO.
The T55-L-712 turbine engine compressor housing refurbishment project
[NASA-CR-179824] N87-23729
ARMY COMMUNICATIONS-ELECTRONICS COMMAND, FORT MONMOUTH, N.J.
Millimeter wave antennas for avionics N87-23864
ARMY CONSTRUCTION ENGINEERING RESEARCH LAB., CHAMPAIGN, ILL.
Consequence of layer separation on pavement performance
[DOT/FAA/PM-86/48] N87-23661
Full-scale test program for a shower wastewater recycling system: Technical evaluation
[AD-A178061] N87-24087
The field shower wastewater recycling system: Development of a program of instruction and preliminary analysis of its potential health implications
[AD-A178112] N87-24088
ARMY ENGINEER TOPOGRAPHIC LABS., FORT BELVOIR, VA.
Automated radar image analysis research in support of military needs
[AD-A179615] N87-23627
ARMY ENVIRONMENTAL HYGIENE AGENCY, ABERDEEN PROVING GROUND, MD.
Laser hazards bibliography, 12 edition
[AD-A179220] N87-23945
ARMY RESEARCH INST. OF ENVIRONMENTAL MEDICINE, NATICK, MASS.
Operation Everest 2: Importance of ventilation in defense of maximal oxygen uptake at extreme altitudes
[AD-A177874] N87-24082
ARNOLD ENGINEERING DEVELOPMENT CENTER, ARNOLD AIR FORCE STATION, TENN.
Laser Doppler velocimeter application in supersonic boundary-layer flow
[AD-A178395] N87-23590
Bird impact qualification test for A-10 windshield
[AD-A179263] N87-23599
ASSISTANT SECRETARY OF DEFENSE (COMPTROLLER), WASHINGTON, D. C.
DOD (Department of Defense) Procedures for Management of Information Requirements
[PB87-155495] N87-24227
ATMOSPHERIC RADIATION CONSULTANTS, ACTON, MASS.
A study of the maximum entropy method of power spectrum estimation as applied to interferometer data
[AD-A179403] N87-23707
ATOMIC WEAPONS RESEARCH ESTABLISHMENT, ALDERMASTON (ENGLAND).
High temperature electrically conductive adhesives
[DE87-007020] N87-23747
AVIONS MARCEL DASSAULT-BREGUET AVIATION, ISTRES (FRANCE).
OASIS: A modern tool for real-time simulation N87-23638

B

BALLISTIC RESEARCH LABS., ABERDEEN PROVING GROUND, MD.
Measurement of surface pressures caused by a projectile rotating band at supersonic speeds
[AD-A171082] N87-23585
Theoretical influence of propellant packaging on tube erosion: model formulation and algorithm development N87-23784
Asymptotic analysis of the roots of a certain transcendental equation
[AD-A168315] N87-24131
BATTELLE PACIFIC NORTHWEST LABS., RICHLAND, WASH.
Manufacturing processes for high-temperature structural ceramics: A patent trend analysis
[PB87-178059] N87-23742
BAYLOR UNIV., DALLAS, TEX.
Biomedical applications of the free electron laser
[AD-A179182] N87-24066
BELL TELEPHONE LABS., INC., MURRAY HILL, N. J.
Time-resolved picosecond reflectivity study of laser-excited layered compounds
[DE87-005115] N87-23952
BOEING COMMERCIAL AIRPLANE CO., SEATTLE, WASH.
Aircraft electromagnetic compatibility
[NASA-CR-181051] N87-23856
BONN UNIV. (WEST GERMANY).
The radio-far infrared correlation: Spiral and blue compact dwarf galaxies opposed N87-24351
BOSTON UNIV., MASS.
A model for the low-latitude ionosphere with coefficients for different seasonal and solar cycle conditions
[AD-A178207] N87-24044
Experimental bounds on beta beta-decay, cold dark matter and solar axions with an ultralow background Ge detector
[DE87-002065] N87-24383
BRITISH AEROSPACE PUBLIC LTD. CO., PRESTON (ENGLAND).
Simulation of aircraft behaviour on and close to the ground: Summary of AGARD•ic6)ograph AG-285 N87-23640
BRITISH BROADCASTING CORP., KINGSWOOD (ENGLAND).
SPECOL: A colorimetric measurement system
[BBC-RD-1987/4] N87-23942
BROOKHAVEN NATIONAL LAB., UPTON, N. Y.
International Symposium on In Vivo Body Composition Studies: Program and abstracts
[DE87-006750] N87-24080
Report of the Second Workshop on Synchrotron Radiation Sources for X-ray Lithography
[DE87-002155] N87-24179
BROWN UNIV., PROVIDENCE, R. I.
Novel fiber preforms: Rare earth doping
[AD-A179454] N87-24175
BUNDESMINISTERIUM FUER FORSCHUNG UND TECHNOLOGIE, BONN (WEST GERMANY).
Results of the encouragement of basic research (1982-1986)
[ETN-87-99665] N87-24228

C

CALIFORNIA INST. OF TECH., PASADENA.
Stochastic excitation of acoustic waves in a combustion chamber N87-23761
Linear coupling of acoustics and entropy and acoustic stability in ramjet combustion chambers containing a plane flame N87-23795
Analysis of pressure oscillations in ramjets. Review of research: 1985-1986 N87-23796
The hypercube as a supercomputer
[DE87-005029] N87-24092
Microscopic modeling of sound waves in granular material
[DE87-007400] N87-24159
High mass star formation in the galaxy N87-24267
Maps of millimeter wave emission from three galactic star-forming regions N87-24275
Diffuse infrared emission of the galaxy: Large scale properties N87-24279
On the origin of the 40-120 micron emission of galaxy disks: A comparison with H-alpha fluxes N87-24287
IRAS and ground-based observations of star formation regions in the Magellanic clouds N87-24296
Characteristics of UGC galaxies detected by IRAS N87-24304
Global properties of the nearby spiral M101 N87-24309
Modelling the IRAS colors of galaxies N87-24313
Molecular gas in the starburt nucleus of M82 N87-24321
Ultraluminous infrared galaxies N87-24327
Interferometric CO observations of the ultraluminous IRAS galaxies ARP 220, IC 694/NGC 3690, NGC 6420 and NGC 7469 N87-24331
The luminosity function of the brightest galaxies in the IRAS survey N87-24341
Near-infrared observations of IRAS minisurvey galaxies N87-24354
IRAS observations of BL Lac objects N87-24373
CALIFORNIA UNIV., BERKELEY.
An integrated, optimization-based approach to the design and control of large space structures
[AD-A179459] N87-23683
Vortex-nozzle interactions in ramjet combustors N87-23800
A consistent finite element formulation of nonlinear frictional contact problems
[AD-A179179] N87-23963
Using expert systems to manage distributed computer systems
[AD-A179329] N87-24112
Decaying confidence functions for aging knowledge in expert systems
[AD-A179328] N87-24152
Computer simulation of bounded plasma systems
[DE87-008193] N87-24190
Linear magnetized plasma response to an oblique electrostatic wave
[DE87-008194] N87-24191
Optimization of extended relational database systems
[AD-A179308] N87-24230
Automating index preparation
[AD-A179327] N87-24231
Particle propagation channels in the solar wind N87-24252
What are cirrus point sources? N87-24345
Summary of symposium: Low luminosity sources N87-24375
CALIFORNIA UNIV., BERKELEY. LAWRENCE BERKELEY LAB.
Experiments and prospects for induction linac drivers
[DE87-006144] N87-23669
In situ HREM observation of interphase boundary motion in 95Pb-5Sn solder
[DE87-007616] N87-23817
The future of intersite networking
[DE87-007912] N87-24116
The effect of distributed computing technology on wide area network capacity requirements
[DE87-008229] N87-24117
The structure of Al/GaAs interfaces
[DE87-007181] N87-24206
The structure and electrical properties of metal contacts on GaAs
[DE87-008217] N87-24210
Data management for high energy physics experiments: Preliminary proposals
[DE87-006940] N87-24236
Star formation in the merging Galaxy NGC3256 N87-24340
CALIFORNIA UNIV., DAVIS.
Combustion, vaporization, and microexplosion of droplets of organic azides N87-23806
Microwave production from a plasma driven by a high power relativistic electron beam
[DE87-003518] N87-24194
CALIFORNIA UNIV., IRVINE.
Spray combustion: A driving mechanism for ramjet combustion instability N87-23805
CALIFORNIA UNIV., LOS ANGELES.
An introduction to structured modeling, revision
[AD-A179355] N87-24153

Role of cavitons in laser-plasma interactions
[DE87-006485] N87-24192
Infrared-ultraviolet spectra of active galactic nuclei N87-24372

CALSPAN ADVANCED TECHNOLOGY CENTER, BUFFALO, N.Y.
Unusual airborne simulator applications N87-23656

CALSPAN FIELD SERVICES, INC., ARNOLD AFS, TENN.
Laser Doppler velocimeter application in supersonic boundary-layer flow
[AD-A178395] N87-23590
Bird impact qualification test for A-10 windshield
[AD-A179263] N87-23599

CAMBRIDGE UNIV. (ENGLAND).
Investigation of the impact performance of various glass and ceramic systems
[AD-A178115] N87-23744

CARLOW ASSOCIATES, INC., FAIRFAX, VA.
Text editing performance as a function of screen size
[AD-A179067] N87-24229

CARNEGIE INSTITUTION OF WASHINGTON, D. C.
IRAS observations of irregular galaxies N87-24299

CARNEGIE-MELLON UNIV., PITTSBURGH, PA.
Choosing sampling rates for robot control
[AD-A179447] N87-24118
Experimental evaluation of nonlinear feedback and feedforward control schemes for manipulators
[AD-A179449] N87-24119

CASE WESTERN RESERVE UNIV., CLEVELAND, OHIO.
Environmental degradation of 316 stainless steel in high temperature low cycle fatigue
[NASA-TM-89931] N87-24007

CATHOLIC UNIV. OF AMERICA, WASHINGTON, D.C.
The development of a containment vessel and Dewar for the particle astrophysics magnet facility (ASTROMAG)
[NASA-CR-181016] N87-23670
Modified independent modal space control method for active control of flexible systems
[NASA-CR-181065] N87-23980
Development of a theoretical model for annealing of radiation damage in semiconductor devices
[NASA-CR-180394] N87-24211

CENTER FOR NAVAL ANALYSES, ALEXANDRIA, VA.
Confidence interval for parameter n in a binomial distribution
[AD-A178325] N87-24151

CENTRE D'ESSAIS EN VOL, ISTRES (FRANCE).
Simulation of fly-by-wire control for civil transport aircraft at the French Centre d'Essais en Vol N87-23647

CENTRE NATIONAL DE LA RECHERCHE SCIENTIFIQUE, TOULOUSE (FRANCE).
Survey of the galactic disk from 1 = -150 deg to 1 = 82 deg in the submillimeter range N87-24278

CHARLES RIVER ANALYTICS, INC., CAMBRIDGE, MASS.
A dual-processor multi-frequency implementation of the FINDS algorithm
[NASA-CR-178252] N87-23617

CHICAGO UNIV., ILL.
The energy source of the interplanetary medium and the heliosphere N87-24251
Particle physics and cosmology
[DE87-007306] N87-24388

CHRYSLER CORP., HUNTSVILLE, ALA.
Advanced DC Motor Controller
[DE87-007756] N87-23882

CINCINNATI UNIV., OHIO.
Computer aided design and analysis of gear tooth geometry
[NASA-CR-179611] N87-23969

COHEN (NORMAN S.) PROFESSIONAL SERVICES, INC., REDLANDS, CALIF.
Role of combustion in the nonlinear combustion instability of composite solid propellants N87-23765

COLORADO STATE UNIV., FORT COLLINS.
AMG (Algebraic Multigrid): Basic development, applications and theory
[AD-A178222] N87-24139

COLORADO UNIV., BOULDER.
Investigations on the impact of voltage and current harmonics on end-use devices and their protection
[DE87-006018] N87-23878
Unsteady separated flows: Vorticity and turbulence
[AD-A179500] N87-23912
Selection principles and pattern formation in fluid mechanics and nonlinear shell theory
[NASA-CR-180941] N87-23916
Global distribution of total cloud cover and cloud type amounts over land
[DE87-006903] N87-24053
Vector array processor computer equipment
[AD-A179545] N87-24382

COLUMBIA UNIV., NEW YORK.
Singularity structure of nonlinear ordinary and partial differential equations
[DE87-006242] N87-24134
A program of ground-based astronomy to complement Einstein observations
[AD-A179331] N87-24265

COMMISSARIAT A L'ENERGIE ATOMIQUE, GIF-SUR-YVETTE (FRANCE).
Experimental observation of the quantum behavior of a macroscopic degree of freedom
[DE87-006228] N87-24213

COMMITTEE ON APPROPRIATIONS (U. S. HOUSE).
Department of Housing and Urban Development - Independent Agencies Appropriations Bill, 1988
[H-REPT-100-189] N87-24241
National Aeronautics and Space Administration N87-24242

COMMITTEE ON COMMERCE, SCIENCE, AND TRANSPORTATION (U. S. SENATE).
National Aeronautics and Space Administration Authorization Act
[S-REPT-100-87] N87-24240
National Aeronautics and Space Administration Authorization Act, 1988
[S-REPT-100-87] N87-24243

COMMUNICATIONS RESEARCH CENTRE, OTTAWA (ONTARIO).
Analysis of space-based radar clutter spectra over different types of terrain and their effects on detection performance
[AD-A178066] N87-23845
MIC technology for phased arrays N87-23866

CONSULTANTS CHOICE, INC., ATLANTA, GA.
Tactical weather expert system
[AD-A178605] N87-24050

CORNELL UNIV., ITHACA, N.Y.
Inelastic properties of ice I/sub h/ at low temperatures and high pressures
[DE87-007334] N87-23711
A very deep IRAS survey at l(II) = 97 deg, b(II) = +30 deg N87-24344

CRANFIELD INST. OF TECH., BEDFORD (ENGLAND).
An experimental investigation into methods for quantifying hang glider airworthiness parameters
[CAR-8705] N87-23613

CRYOLAB, INC., SAN LUIS OBISPO, CALIF.
Cost effective use of liquid nitrogen in cryogenic wind tunnels
[NASA-CR-178279] N87-23663

D

DARTMOUTH COLL., HANOVER, N.H.
Thermomechanical effects in high-speed seal rubs
[NASA-CR-180418] N87-23979

DAYTON UNIV., OHIO.
Potential Applications of Biotechnology to Aerospace Materials
[AD-A177875] N87-23667
CN radical distributions in solid propellant flames N87-23775

DEFENCE RESEARCH ESTABLISHMENT ATLANTIC, DARTMOUTH (NOVA SCOTIA).
Thin-walled beam theories and their applications in the torsional strength analysis of ship hulls
[AD-A178296] N87-24001

DEFENSE ADVANCED RESEARCH PROJECTS AGENCY, ARLINGTON, VA.
Future directions of C3 research at DARPA (Defense Advanced Research Projects Agency)
[DE87-007501] N87-23948

DEPARTMENT OF ENERGY, OAK RIDGE, TENN.
Energy Data Base: Subject categories and scope, a reference manual
[DE87-005547] N87-24235

DEPARTMENT OF ENERGY, WASHINGTON, D. C.
Worldwide nickel/iron battery development for electric vehicle applications
[DE87-004822] N87-23876
Electric and Hybrid Vehicles Program: 10th annual report to Congress for Fiscal Year 1986
[DE87-006350] N87-23968

DEUTSCHE FORSCHUNGS- UND VERSUCHSANSTALT FUER LUFT- UND RAUMFAHRT, BRUNSWICK (WEST GERMANY).
DFVLR in-flight simulators ATTAS and ATTHES for flying qualities and flight control research N87-23657

DEUTSCHE FORSCHUNGS- UND VERSUCHSANSTALT FUER LUFT- UND RAUMFAHRT, GOETTINGEN (WEST GERMANY).
An experimental-analytical routine for the dynamic qualification of aircraft operating on rough runway surfaces N87-23611

DORNIER-WERKE G.M.B.H., FRIEDRICHSHAFEN (WEST GERMANY).
Operational training: Application and experience N87-23653

DU PONT DE NEMOURS (E. I.) AND CO., AIKEN, S.C.
Finite-difference program for hydrogen diffusion: Example problems manual
[DE87-007515] N87-23712

DUITS-NEDERLANDSE WINDTUNNEL, NORTH EAST POLDER (NETHERLANDS).
Activities report of the German-Dutch wind tunnel
[B8677593] N87-23665
Activities report of the German-Dutch wind tunnel
[B8677594] N87-23666

DUKE UNIV., DURHAM, N. C.
Investigation of biochemical variation in operational aircrew
[AD-A179223] N87-24067

E

ECOLE NATIONALE SUPERIEURE DES TELECOMMUNICATIONS, PARIS (FRANCE).
Perception and structural analysis of morphologies
[ENST-86D004] N87-24086
Colored stochastic Petri nets
[ENST-86C001] N87-24111

ECOLE NORMALE SUPERIEURE, PARIS (FRANCE).
Diffuse infrared emission of the galaxy: Large scale properties N87-24268
Diffuse infrared emission of the galaxy: Large scale properties N87-24279

EDINBURGH UNIV. (SCOTLAND).
Enhanced star formation: The importance of bars in spiral galaxies N87-24357

ELECTRO-OPTICS CONSULTANTS, INC., HUNTSVILLE, ALA.
Cornea Optical Topographical Scan System (COTSS)
[NASA-CR-179012] N87-24184

ELECTRONICS RESEARCH LAB., ADELAIDE (AUSTRALIA).
A new approach to multitarget tracking using probabilistic data association
[AD-A179437] N87-23825
Fabry-Perot type optical interference filters
[AD-A179394] N87-24174

ENERGY RESEARCH CORP., DANBURY, CONN.
Aircraft battery state of charge and charge control system
[AD-A179066] N87-23870

ENVIRONMENTAL RESEARCH INST. OF MICHIGAN, ANN ARBOR.
Image sensor data base for the DARPA ALV (Defense Advanced Research Projects Agency Autonomous Land Vehicle) program
[AD-A178117] N87-24246

EUROPEAN RESEARCH OFFICE, LONDON (ENGLAND).
Assembly and functionalization of supramolecular structures studied by luminescence techniques
[AD-A178064] N87-24217

EUROPEAN SOUTHERN OBSERVATORY, LA SILLA (CHILE).
Star formation in Seyfert galaxies N87-24364

EUROPEAN SPACE AGENCY. EUROPEAN SPACE RESEARCH AND TECHNOLOGY CENTER, ESTEC, NOORDWIJK (NETHERLANDS).
Observations of heavy energetic ions for upstream from comet Halley
[DE87-003752] N87-24380

F

FEDERAL AVIATION AGENCY, ATLANTIC CITY, N.J.
Certification testing methodology for composite structure. Volume 1: Data analysis
[NADC-87042-60-VOL-1] N87-23705
Certification testing methodology for composite structure. Volume 2: Methodology development
[NADC-87042-60-VOL-2] N87-23706
Autogas in general aviation aircraft
[DOT/FAA/CT-87/05] N87-23815

FIVE-COLLEGE ASTRONOMY DEPT., AMHERST, MASS.
The azimuthal and radial distributions of HI and H2 in NGC 6946 N87-24335
A redshift survey of IRAS galaxies N87-24347

FLORIDA UNIV., GAINESVILLE.
Synthesis of model polymers and related structures in support of vinyl monomer grafting studies
[DE87-007406] N87-23739
Theoretical and experimental investigations of fluctuation thermodynamic properties of liquid solutions
[DE87-005681] N87-24224

FLOW RESEARCH, INC., KENT, WASH.
Numerical simulations of cold flow in a ramjet dump combustor with a choked exit nozzle N87-23802
FOM-INST. VOOR PLASMAFYSICA, RIJNHUIZEN, JUTPHAAS (NETHERLANDS).
Activities report in plasma physics
[ETN-87-99588] N87-24199

G

GA TECHNOLOGIES, INC., SAN DIEGO, CALIF.
Report to DOE of the fusion programs in applied plasma physics and development and technology at GA Technologies, Incorporated
[DE87-008882] N87-24197
GENERAL DYNAMICS CORP., SAN DIEGO, CALIF.
Control considerations for high frequency, resonant, power processing equipment used in large systems
[NASA-TM-89926] N87-23690
GENERAL ELECTRIC CO., CINCINNATI, OHIO.
Antimisting Fuel (AMK) flight degrader development and aircraft fuel system investigation
[DOT/FAA/CT-86/6] N87-23816
GEOLOGICAL SURVEY, MENLO PARK, CALIF.
Inelastic properties of ice I/sub h/ at low temperatures and high pressures
[DE87-007334] N87-23711
GEOLOGICAL SURVEY, RESTON, VA.
Radar as a complement to topographic maps for delineating marine terraces
[PB87-154597] N87-24013
GEORGE WASHINGTON UNIV., WASHINGTON, D.C.
The 1986-87 NASA space/gravitational biology accomplishments
[NASA-TM-89951] N87-24063
GEORGIA INST. OF TECH., ATLANTA.
Behavior of simulated solid propellant flames in axial acoustic fields N87-23760
Acoustic response of turbulent reacting recirculatory flows N87-23799
Combustion instabilities in dump type ramjet combustors N87-23803
Research in millimeter wave techniques
[NASA-CR-181026] N87-23858
GEORGIA UNIV., ATHENS.
Novel application of topological indices. 2. Prediction of the threshold soot index for hydrocarbon fuels
[AD-A178001] N87-23716
GESELLSCHAFT FUER SCHWERIONENFORSCHUNG M.B.H., DARMSTADT (WEST GERMANY).
AXCEL: Interactive simulation program to compute two-dimensional potential distributions of electrostatic arrangements and of ion paths in electrostatic fields under consideration of space charging
[DE87-007760] N87-24165
GESELLSCHAFT FUER STRAHLEN- UND UMWELTFORSCHUNG M.B.H., MUNICH (WEST GERMANY).
Survey of environment related monitoring programs of international organizations and their contribution to international organizations
[ETN-87-99913] N87-24033
GOUGH (PAUL) ASSOCIATES, INC., PORTSMOUTH, N.H.
Theoretical influence of propellant packaging on tube erosion: model formulation and algorithm development N87-23784
GRONINGEN RIJKSUNIVERSITEIT (NETHERLANDS).
Shock heated dust in L1551: L(IR) greater than 20 solar luminosities N87-24276
Infrared properties of dust grains derived from IRAS observations N87-24283
Infrared emission and excitation in LMC HII regions N87-24298
GRUMMAN AEROSPACE CORP., BETHPAGE, N.Y.
Utilization of simulation to support F-14A low altitude high angle of attack flight testing N87-23649

H

HAMILTON STANDARD, WINDSOR LOCKS, CONN.
Dynamic response of two composite prop-fan models on a nacelle/wing/fuselage half model
[NASA-CR-179589] N87-23615
HARRY DIAMOND LABS., ADELPHI, MD.
Scattering from an open spherical shell having a circular aperture and enclosing a concentric dielectric sphere
[DE87-007099] N87-23842
HARVARD COLL. OBSERVATORY, CAMBRIDGE, MASS.
Atmospheric propagation effects on radio interferometry
[AD-A178405] N87-23855
HARVARD-SMITHSONIAN CENTER FOR ASTROPHYSICS, CAMBRIDGE, MASS.
Nuclear star formation on 100 parsec scales: 10' resolution radio continuum, HI and CO observations N87-24322
Experimental bounds on beta beta-decay, cold dark matter and solar axions with an ultralow background Ge detector
[DE87-002065] N87-24383
HARVARD UNIV., CAMBRIDGE, MASS.
Time-resolved picosecond reflectivity study of laser-excited layered compounds
[DE87-005115] N87-23952
Drift mobilities by time-of-flight methods and time-dependent phototransport in the nanosecond regime in amorphous semiconductors
[DE87-008021] N87-24208
The initial mass function in HII galaxies N87-24332
Experimental bounds on beta beta-decay, cold dark matter and solar axions with an ultralow background Ge detector
[DE87-002065] N87-24383
HAWAII UNIV., HONOLULU.
Star formation in normal galaxies N87-24285
Stellar bars and the spatial distribution of infrared luminosity N87-24293
VLA observations of a sample of galaxies with high far-infrared luminosities N87-24342
Nuclear infrared emission and the colors of IRAS galaxies N87-24356
Ground-based 1- to 32-microns observations of ARP 220: Evidence for a dust-embedded AGN? N87-24361
Spectrophotometery of Brackett lines in very luminous IRAS galaxies N87-24367
Morphology of luminous IRAS galaxies: Summary talk N87-24376
HIGH TECHNOLOGY CORP., HAMPTON, VA.
On minimizing the number of calculations in design-by-analysis codes
[NASA-TP-2706] N87-23586
HOKENSON (GUSTAVE J.), LOS ANGELES, CALIF.
Optimal aerodynamic shapes for hypervelocity projectiles
[AD-A178367] N87-23672
HOUSTON UNIV., CLEAR LAKE, TEX.
Error analysis of leaf area estimates made from allometric regression models
[NASA-TM-89220] N87-24010
HUGHES HELICOPTERS, CULVER CITY, CALIF.
Aeroelasticity and mechanical stability report, 0.27 Mach scale model of the YAH-64 advanced attack helicopter
[NASA-CR-178284] N87-23596
HUGHES RESEARCH LABS., MALIBU, CALIF.
Experimental and theoretical studies of laser cooling and emittance control of neutral beams
[AD-A179226] N87-23946

I

IIT RESEARCH INST., BARTLESVILLE, OKLA.
Trends of petroleum fuels: Topical report
[DE87-001237] N87-23755
ILLINOIS INST. OF TECH., CHICAGO.
Theoretical studies in elementary particle physics
[DE87-005895] N87-24167
ILLINOIS UNIV., CHICAGO.
Functionalization of cubane using hypervalent iodine N87-23807
Analytical prediction of combustion performance characteristics of bipropellant liquid rocket engine combustor N87-23810
Ordered many-electron motions in atoms and X-ray lasers
[DE87-004731] N87-23951
ILLINOIS UNIV., URBANA.
Al and Mg alloys for aerospace applications using rapid solidification and powder metallurgy processing
[AD-A179547] N87-23721
Scattering by a truncated periodic array
[AD-A178285] N87-23852
Complexities of layouts in three-dimensional VLSI (Very Large-Scale Integration) circuits
[AD-A178150] N87-23889
Recovering the orientation of textured surfaces in natural scenes
[AD-A179360] N87-24096
Large scale dissociation of molecular gas in the sprial arms of M51 N87-24311
Neutron stars as cosmic neutron matter laboratories
[DE87-007468] N87-24379
ILLINOIS UNIV., URBANA-CHAMPAIGN.
Flow regimes of refrigerant mixtures condensing inside tubes
[ORNL/SUB/81-7762/4 AND 01] N87-23917
Mechanisms for the circular polarization of astrophysical OH masers in star-forming regions and the inferred magnetic fields N87-24277
IMPERIAL COLL. OF SCIENCE AND TECHNOLOGY, LONDON (ENGLAND).
Extragalactic infrared spectroscopy N87-24328
Evidence for extended IR emission in NGC2798 and NGC6240 N87-24368
Observations of heavy energetic ions for upstream from comet Halley
[DE87-003752] N87-24380
INDIAN INST. OF TECH., NEW DELHI.
Turbomachine blade vibration N87-23621
INDIANA UNIV., BLOOMINGTON.
Metal alkoxides: Models for metal oxides: Alkoxide ligands in early transition metal organometallic chemistry
[DE87-007309] N87-23715
INDUSTRIEANLAGEN-BETRIEBSGESELLSCHAFT M.B.H., OTTOBRUNN (WEST GERMANY).
Manned air to air combat simulation N87-23648
INSTITUT D'ASTROPHYSIQUE, PARIS (FRANCE).
Present star formation in sprials of the Virgo cluster N87-24306
Far-infrared activity and starburst galaxies N87-24337
Ground-based follow up of IRAS galaxies N87-24355
INSTITUT FRANCO-ALLEMAND DE RECHERCHES, ST. LOUIS (FRANCE).
The freezing of flow deflection in Prandtl-Meyer expansion to vacuum
[ISL-CO-226/86] N87-23686
Light sheet visualization and velocity field measurements in seeded flows
[ISL-CO-225/86] N87-23935
INTEGRAL TECHNOLOGIES, INC., WESTMONT, ILL.
Multidimensional modeling of convective heat transfer with application to I.C. engines
[DE87-002939] N87-23922
INTERNATIONAL BUSINESS MACHINES CORP., YORKTOWN HEIGHTS, N. Y.
The structure of Al/GaAs interfaces
[DE87-007181] N87-24206
IOWA STATE UNIV. OF SCIENCE AND TECHNOLOGY, AMES.
Recent developments in vehicle dynamics N87-23820
Cloud fluid models of gas dynamics and star formation in galaxies N87-24329
IOWA UNIV., IOWA CITY.
Viscous-inviscid interaction with higher-order viscous-flow equations: Applications to three-dimensional bodies
[AD-A178264] N87-23924
Magnetospheres of the outer planets N87-24248

J

JET PROPULSION LAB., CALIFORNIA INST. OF TECH., PASADENA.
The Telecommunications and Data Acquisition Report
[NASA-CR-181010] N87-23828
DSS 13 frequency stability tests N87-23829
Spacecraft mass trade-offs versus radio-frequency power and antenna size at 8 GHz and 32 GHz N87-23830
Use of a 2.3-GHz traveling-wave maser on the Usuda 64-meter antenna N87-23831
A VLSI single chip (255,223) Reed-Solomon encoder with interleaver N87-23832
DSN advanced receiver: Breadboard description and test results N87-23833
Results of using the global positioning system to maintain the time and frequency synchronization in the Deep Space Network N87-23834
Microwave component time delays for the 70-meter antennas N87-23835
Z-corrections for DSN 70-meter antenna ranging calibration N87-23836
Block 3 X-band receiver-exciter N87-23837
Dual-polarization 8.45 GHz traveling-wave maser N87-23838
An interactive wire-wrap board layout program N87-23839
An evaluation of the communication system for the TAU mission study N87-23840
Nucleosynthesis and astrophysical gamma ray spectroscopy N87-24259
Star forming regions of the southern galaxy N87-24273
Global properties of the nearby spiral M101 N87-24309
Observations of heavy energetic ions for upstream from comet Halley
[DE87-003752] N87-24380

JOHNS HOPKINS UNIV., BALTIMORE, MD.
Star formation and dynamics in starburst nuclei N87-24324

JOHNS HOPKINS UNIV., LAUREL, MD.
The 23rd JANNAF Combustion Meeting, volume 1 [AD-A179158] N87-23757
Numerical study of acoustic refraction and flow turning N87-23759

JOHNSON CONTROLS, INC., MILWAUKEE, WIS.
Cost reductions in the nickel/hydrogen battery [DE87-007576] N87-23881

JOINT PUBLICATIONS RESEARCH SERVICE, ARLINGTON, VA.
USSR report: Engineering and equipment [JPRS-UEQ-87-005] N87-23570
Effect of surface roughness on drag of aircraft N87-23571
Principles of data display in aviation instruments N87-23572
Experimental study of supersonic stream sliding at angle past one-step wedge with jaws N87-23573
Structural analysis of supersonic jet discharging from free-vortex nozzle by method of holographic interferometry with pulsed laser N87-23574
Mathematical model describing interaction of single nonsteady supersonic jet and movable barrier of finite dimensions N87-23575
Simultaneous radiative and convective heating of thin body in medium with variable temperature N87-23576
Development of model describing unstable operation of turbocompressor and design of antisurging protection for gas turbine engine N87-23577
Catastrophic breakup of liquid jet by subsonic transverse gas stream N87-23578
Calculation of axisymmetric flow in swirlers by difference method N87-23579
Effectiveness of balancing flexible rotary compressor vanes on low-speed balancing machine N87-23580
Compressibility of submerged supersonic jets N87-23581
Flow of gas through turbine stage with spherical nozzle segment N87-23582

K

KANSAS UNIV., LAWRENCE.
Research in theoretical particle physics [DE87-006240] N87-24169

KIMBALL PHYSICS, INC., WILTON, N.H.
High-current electron gun for space flight [AD-A179287] N87-23874
High current electron gun for space flight [AD-A178467] N87-23875

KITT PEAK NATIONAL OBSERVATORY, TUCSON, ARIZ.
Star formation in the Magellanic clouds N87-24288
Measuring star formation rates in blue galaxies N87-24289

L

LAS CAMPANAS OBSERVATORY (CHILE).
Ultraluminous infrared galaxies N87-24327
The luminosity function of the brightest galaxies in the IRAS survey N87-24341
Near-infrared observations of IRAS minisurvey galaxies N87-24354

LAWRENCE LIVERMORE NATIONAL LAB., CALIF.
White paper on nanocomposites as harmonic generation media [DE87-006337] N87-23704
Inelastic properties of ice I/sub h/ at low temperatures and high pressures [DE87-007334] N87-23711
A hybrid closed bomb-strand burner for very high pressure burning rate measurements N87-23786
Scattering from an open spherical shell having a circular aperture and enclosing a concentric dielectric sphere [DE87-007099] N87-23842
GASPS: A time-dependent, one-dimensional, planar gas dynamics computer code [DE87-006338] N87-23931
Thermal ignition of pyrotechnics with lasers [DE87-006245] N87-23955
Application of a 100-kV electric gun for hypervelocity impact studies [DE87-006730] N87-23976
The reality of the greenhouse effect [DE87-002383] N87-24041
The detection of CO2-induced climate change [DE87-006085] N87-24052
Hazards evaluation of radiofrequency and microwave radiation [DE87-006536] N87-24081
Three dimensional graphics in the statistical analysis of scientific data [DE87-006151] N87-24104
Adaptive moving grid strategies for one-dimensional systems of partial differential equations [DE87-006824] N87-24144
SDI (Strategic Defense Initiative) and the US defense posture [DE87-006731] N87-24154
Parametric frequency upconversion, optical fiber transmission and streak camera recording [DE87-005841] N87-24183
Role of cavitons in laser-plasma interactions [DE87-006485] N87-24192
Microwave production from a plasma driven by a high power relativistic electron beam [DE87-003518] N87-24194
Thermal fracture in selected nonlinear optical materials [DE87-006213] N87-24209
Experimental observation of the quantum behavior of a macroscopic degree of freedom [DE87-006228] N87-24213
Electrical resistivity response due to elastic-plastic deformations [DE87-006826] N87-24222
Gauge invariant quantum cosmology [DE87-006685] N87-24226
Livermore risk analysis methodology: A quantitative approach to management of the risk associated with the operation of information systems [DE87-006828] N87-24232

LEIDEN UNIV. (NETHERLANDS).
Star formation around active galactic nuclei N87-24363
IRAS observations of AGN candidates at low flux levels N87-24366

LICK OBSERVATORY, MOUNT HAMILTON, CALIF.
Star forming regions in gas-rich SO galaxies N87-24316
Spectral classification of emission-line galaxies N87-24374

LOCKHEED MISSILES AND SPACE CO., PALO ALTO, CALIF.
Auroral particles N87-24249

LONDON UNIV. (ENGLAND).
Models for infrared emission from IRAS galaxies N87-24286

LOS ALAMOS NATIONAL LAB., N. MEX.
Rf control system for a rocket-borne accelerator [DE87-007459] N87-23673
The use of molecular dynamics for the thermodynamic properties of simple and transition metals [DE87-007718] N87-23725
A pulsed electron injector using a metal photocathode irradiated by an excimer laser [DE87-007499] N87-23877
High-powered, solid-state rf systems [DE87-007457] N87-23896
Computer simulation of the lasertron with a ring model [DE87-007461] N87-23897
Preliminary thermal analysis of transistor packages [DE87-007708] N87-23898
REZONE: A method for automatic rezoning in two-dimensional Lagrangian hydrodynamics problems [DE87-006324] N87-23930
Future directions of C3 research at DARPA (Defense Advanced Research Projects Agency) [DE87-007501] N87-23948
Development of a high temperature ceramic-to-metal seal for Air Force Weapons Laboratory Laser [DE87-007711] N87-23949
Time-resolved picosecond reflectivity study of laser-excited layered compounds [DE87-005115] N87-23952
On-line electron beam measurements for the Los Alamos Free-Electron Laser [DE87-007452] N87-23956
An atmospheric correction algorithm for remote identification of non-Lambertian surfaces and its range of validity [DE87-006059] N87-24011
Modelling of atmospheric effects on the angular distribution of a backscattering peak [DE87-006060] N87-24014
Integral approximants for functions of higher monodromic dimension [DE87-007508] N87-24129
Satellite allocation for boost-phase missile intercepts [DE87-007719] N87-24155
AXCEL: Interactive simulation program to compute two-dimensional potential distributions of electrostatic arrangements and of ion paths in electrostatic fields under consideration of space charging [DE87-007760] N87-24165
The physics and a plan for a 45 GeV facility that extends the high-intensity capability in nuclear and particle physics [LA-10720-MS] N87-24170
Collective acceleration of protons by the plasma waves in a counterstreaming electron beam [DE87-007493] N87-24196
Fuel cell powered propulsion systems for highway vehicles [DE87-007497] N87-24244
Neutron stars as cosmic neutron matter laboratories [DE87-007468] N87-24379
Observations of heavy energetic ions for upstream from comet Halley [DE87-003752] N87-24380

LOUISIANA STATE UNIV., BATON ROUGE.
On autonomous terrain model acquisition by a mobile robot [DE87-005719] N87-23964
Utilizing remote sensing of thematic mapper data to improve our understanding of estuarine processes and their influence on the productivity of estuarine-dependent fisheries [NASA-CR-180964] N87-24012

LOWELL OBSERVATORY, FLAGSTAFF, ARIZ.
Erratum: IRAS observations of irregular galaxies N87-24300

LOWELL UNIV., MASS.
The specification of lateral boundary conditions in three-dimensional mesoscale numerical models [AD-A179185] N87-24048

LUFTFAHRT-BUNDESAMT, BRUNSWICK (WEST GERMANY).
Results of the specialized investigation of accidents involving German aircraft at home and abroad, and with foreign aircraft at home [ISSN-0178-8094] N87-23602

M

MANCHESTER UNIV. (ENGLAND).
Models relating the radio emission and ionised gas in Seyfert nuclei N87-24369

MARYLAND UNIV., COLLEGE PARK.
Viscosity of synfuel compounds and mixtures [DE87-006696] N87-23756
The Magsat Bibliography [NASA-TM-87822] N87-24039
Information based numerical practice [AD-A178362] N87-24141
Estimate for the errors in eigenvalue and eigenvector approximation by Galerkin methods, with particular attention to the case of multiple eigenvalues [AD-A178390] N87-24142
The joint NASA/Goddard-University of Maryland research program in charged particle and high energy photon detector technology [NASA-CR-180996] N87-24166
High-current beam dynamics and transport, theory and experiment [DE87-006154] N87-24172
Formation and stability of partially-neutralized plasma clumps [AD-A179444] N87-24187
Investigation of universal plasma instabilities [DE87-006276] N87-24193
Starburst-driven superwinds from infrared galaxies N87-24330
Circumnuclear starbursts in Seyfert galaxies N87-24365

MASSACHUSETTS INST. OF TECH., CAMBRIDGE.
Time domain wave propagation in multilayered integrated circuits [AD-A178180] N87-23847
Adaptive noise reduction in aircraft communication systems [AD-A178267] N87-23851
Communication-efficient parallel graph algorithms [AD-A178286] N87-23853
Turbulent boundary layer structure, drag reduction [AD-A179246] N87-23907
Active and passive remote sensing of ice [AD-A179461] N87-24009
The interpretation of crustal dynamics data in terms of plate motions and regional deformation near plate boundaries [NASA-CR-180938] N87-24038
Computer-aided fabrication system implementation [AD-A178225] N87-24106
Efficient parallel algorithms for (delta+1)-coloring and maximal independent set problems [AD-A178287] N87-24109
Efficient graph algorithms for sequential and parallel computers [AD-A178403] N87-24110

Study of quantum mechanical effects in deep submicron, grating-gate field effect transistors
[AD-A179617] N87-24204
Microscale defect kinetics in melt-grown GaAs
[AD-A178158] N87-24218
Time slice manipulation in information hierarchy
[AD-A177949] N87-24237
A dust scattered halo in starburst galaxy M82?
N87-24334

MASSACHUSETTS INST. OF TECH., LEXINGTON.
Solid state research
[AD-A178394] N87-24221

MASSACHUSETTS UNIV., AMHERST.
Printed circuit antenna technology N87-23867
Intermediate level computer vision processing algorithm development for the content addressable array parallel processor
[AD-A179515] N87-24090
CO observations of nearby galaxies and the efficiency of star formation N87-24291
Molecular gas and star formation in HI-deficient Virgo cluster galaxies N87-24307
Efficient star formation in the bright bar of M83
N87-24310
Properties of the unusual galaxy PSC 09104+4109
N87-24346

MAX-PLANCK-INST. FUER AERONOMIE, KATLENBURG-LINDAU (WEST GERMANY).
Observations of heavy energetic ions for upstream from comet Halley
[DE87-003752] N87-24380

MAX-PLANCK-INST. FUER RADIOASTRONOMIE, BONN (WEST GERMANY).
The origin of the diffuse galactic IR/submm emission: Revisited after IRAS N87-24269
IRAS observations of the Pleiades N87-24284
Submm observations of IRAS galaxies N87-24292
Radio continuum, far infrared and star formation
N87-24352

MCDONNELL-DOUGLAS CORP., ST. LOUIS, MO.
Response of transonic diffuser flows to abrupt increases of back pressure: Wall pressure measurements
N87-23793

MCDONNELL-DOUGLAS HELICOPTER CO., MESA, ARIZ.
Aeroelasticity and mechanical stability report, 0.27 Mach scale model of the YAH-64 advanced attack helicopter
[NASA-CR-178284] N87-23596

MECHANICAL TECHNOLOGY, INC., LATHAM, N. Y.
Squeeze film damper technology. Part 4. Design and application of squeeze film dampers
[AD-A177996] N87-23973
Squeeze film damper technology. Part 2. Extension of analysis and parametric study
[AD-A178094] N87-23974
Squeeze film damper technology. Part 3. Experimental investigation of squeeze film dampers
[AD-A178095] N87-23975

MESSERSCHMITT-BOELKOW-BLOHM G.M.B.H., MUNICH (WEST GERMANY).
Computer simulation studies on human control reliability in manual aircraft control: The origin of PIO N87-23644

MICHIGAN STATE UNIV., EAST LANSING.
Studies on age-hardening in spinodally modulated alloys: Experimental and theoretical
[DE87-006361] N87-23727

MICHIGAN UNIV., ANN ARBOR.
Magnetostatic surface field measurement facility
[AD-A178258] N87-23850
Holographic optical elements formed in light of reduced coherence
[AD-A179372] N87-23937

MIDWEST RESEARCH INST., GOLDEN, COLO.
Fuels from microalgae: Technology status, potential and research requirements
[DE86-010739] N87-23753
Wind energy systems: Program summary, fiscal year 1984 and 1985
[DE87-001109] N87-24015
Analysis and test results for an improved constant speed passive cyclic pitch wind turbine
[DE87-001135] N87-24022
Heat transfer research for ocean thermal energy conversion
[DE87-001155] N87-24023
Review of interactions of large solar fluxes with materials
[DE87-001156] N87-24024
Solar Thermal Technology Program bibliography, 1973-1985
[DE86-010728] N87-24027
Proceedings of the Tenth DOE Solar Photochemistry Research Conference
[DE87-006421] N87-24062

MILITARY ACADEMY, WEST POINT, N. Y.
An alternative Laplacian electrostatic field finite element formulation
[DE87-007031] N87-24158

MINNESOTA UNIV., MINNEAPOLIS.
Star formation in the large Magellanic cloud
N87-24297
Induced star formation in interacting galaxies
N87-24325
The correlation between far-IR and radio continuum emission from spiral galaxies N87-24349

MITRE CORP., BEDFORD, MASS.
Future directions of C3 research at DARPA (Defense Advanced Research Projects Agency)
[DE87-007501] N87-23948

MITRE CORP., MCLEAN, VA.
Development of an air ground data exchange concept: Flight deck perspective
[NASA-CR-4074] N87-23607

MORTON THIOKOL, BRIGHAM CITY, UTAH.
Acoustic waveforms in statically tested space shuttle Solid Rocket Motors (SRM) N87-23758
New ignition parameter correlations for predicting solid rocket motor ignition transients N87-23767
Study of the suppression of rocket plume afterburning by chemical additives N87-23768
Chemical kinetics combustion model of the NG/binder system N87-23773

MOUND LAB., MIAMISBURG, OHIO.
Corrosion of gold bridgewire in electronic components
[DE87-000922] N87-23722
Low energy ignition of HMX using a foil bridge
[DE87-004211] N87-23754
Thermal ignition of pyrotechnics with lasers
[DE87-006245] N87-23955

N

NAGOYA UNIV. (JAPAN).
Wavelengths of K X-rays of iron ions
[IPPJ-AM-49] N87-24198

NATIONAL ACADEMY OF SCIENCES - NATIONAL RESEARCH COUNCIL, WASHINGTON, D. C.
Control of welding processes
[AD-A177893] N87-23971
Guidelines for noise and vibration levels for the space station
[NASA-CR-178310] N87-24162
Strategy for exploration of the outer planets: 1986-1996
[NASA-CR-181021] N87-24381

NATIONAL AERONAUTICAL ESTABLISHMENT, OTTAWA (ONTARIO).
Airborne simulation at the National Aeronautical Establishment of Canada N87-23659
The influence of turbulence and deck section geometry on the aeroelastic behaviour of a cable-stayed bridge model
[NAE-AN-40] N87-23990

NATIONAL AERONAUTICS AND SPACE ADMINISTRATION, WASHINGTON, D.C.
Hypersonic aerodynamic coefficients and convection flow estimation in a HERMES type project
[NASA-TT-20019] N87-23583
Actions to implement the recommendations of the Presidential Commission on the Space Shuttle Challenger accident: Executive summary N87-23676
LASA (Lidar Atmospheric Sounder and Altimeter) Earth observing system. Volume 2D: Instrument panel report
[NASA-TM-89356] N87-23982
The 1986-87 NASA space/gravitational biology accomplishments
[NASA-TM-89951] N87-24063
Star Formation in Galaxies
[NASA-CP-2466] N87-24266
IUE observations of luminous blue star associations in irregular galaxies N87-24301

NATIONAL AERONAUTICS AND SPACE ADMINISTRATION. AMES RESEARCH CENTER, MOFFETT FIELD, CALIF.
Evaluation of Navier-Stokes and Euler solutions for leading-edge separation vortices
[NASA-TM-89458] N87-23584
Some aspects of vortex flows determined from the thin-layer Navier-Stokes equations
[NASA-TM-88375] N87-23595
High-angle-of-attack pneumatic lag and upwash corrections for a hemispherical flow direction sensor
[NASA-TM-86790] N87-23616
Highly integrated digital electronic control: Digital flight control, aircraft model identification, and adaptive engine control
[NASA-TM-86793] N87-23619
Swashplate control system
[NASA-CASE-ARC-11633-1] N87-23631
Demonstration of frequency-sweep testing technique using a Bell 214-ST helicopter
[NASA-TM-89422] N87-23632
Visual and motion cueing in helicopter simulation
N87-23634
Preparation of B-trichloroborazine
[NASA-CASE-ARC-11643-1-SB] N87-23698
Ceramic honeycomb structures and the method thereof
[NASA-CASE-ARC-11652-1] N87-23737
Fire and heat resistant laminating resins based on malemeido and citraconimido substituted 1 -2,4- and -2,6-diaminobenzenes
[NASA-CASE-ARC-11533-1] N87-23751
Thermal stress analysis of space shuttle orbiter wing skin panel and thermal protection system
[NASA-TM-86276] N87-23994
Inelastic strain analogy for piecewise linear computation of creep residues in built-up structures
[NASA-TM-86813] N87-23995
Human factors in space station architecture 2. EVA access facility: A comparative analysis of 4 concepts for on-orbit space suit servicing
[NASA-TM-86856] N87-24064
Upwind and symmetric shock-capturing schemes
[NASA-TM-89464] N87-24145
Smoothing and the second law
[NASA-TM-86371] N87-24146
On the reliable and flexible solution of practical subset regression problems
[NASA-TM-89442] N87-24156
Detector arrays for low-background space infrared astronomy
[NASA-TM-86344] N87-24378
Research and Technology
[NASA-TM-89411] N87-24391

NATIONAL AERONAUTICS AND SPACE ADMINISTRATION. GODDARD INST. FOR SPACE STUDIES, NEW YORK, N.Y.
Star formation in Carina OB1: Observations of a giant molecular cloud associated with the eta Carinae Nebula
N87-24272

NATIONAL AERONAUTICS AND SPACE ADMINISTRATION. GODDARD SPACE FLIGHT CENTER, GREENBELT, MD.
COSPAS-SARSAT satellite orbit predictor, volume 9
[NASA-TM-85015] N87-23671
Reciprocating linear motor
[NASA-CASE-GSC-12773-2] N87-23904
Spatial characterization of acid rain stress in Canadian Shield lakes
[NASA-CR-180983] N87-24031
Spatial characterization of acid rain stress in Canadian Shield lakes
[NASA-CR-180982] N87-24032
The Magsat Bibliography
[NASA-TM-87822] N87-24039
The development of a prototype intelligent user interface subsystem for NASA's scientific database systems
[NASA-TM-87821] N87-24098
Essays in Space Science
[NASA-CP-2464] N87-24247
Particle acceleration in solar flares N87-24250
Studies of the interplanetary magnetic field: IMP's to Voyager N87-24253
Antiprotons in cosmic rays N87-24255
Origin and propagation of galactic cosmic rays
N87-24257
High energy gamma ray astronomy N87-24258
Gamma ray transients N87-24260
The cosmic X-ray background N87-24262
X-ray astronomical spectroscopy N87-24263
Infrared astronomy N87-24264
On the redistribution of OB star luminosity and the warming of nearby molecular clouds N87-24274
The large scale gas and dust distribution in the galaxy: Implications for star formation N87-24280
Extremely Luminous Far-Infrared Sources (ELFS)
N87-24323
Structure in the nucleus of NGC 1068 at 10 microns
N87-24370
Fifty year canon of solar eclipses: 1986-2035
[NASA-TM-89346] N87-24377

NATIONAL AERONAUTICS AND SPACE ADMINISTRATION. JOHN F. KENNEDY SPACE CENTER, COCOA BEACH, FLA.
Ice/frost/debris assessment for space shuttle Mission STS-32 (61-C)
[NASA-TM-89192] N87-23675
Research and technology
[NASA-TM-89193] N87-24392

NATIONAL AERONAUTICS AND SPACE ADMINISTRATION. LYNDON B. JOHNSON SPACE CENTER, HOUSTON, TEX.
Method of making a flexible diaphragm
[NASA-CASE-MSC-20797-1] N87-23981

Error analysis of leaf area estimates made from allometric regression models
[NASA-TM-89220] N87-24010

NATIONAL AERONAUTICS AND SPACE ADMINISTRATION. LANGLEY RESEARCH CENTER, HAMPTON, VA.

On minimizing the number of calculations in design-by-analysis codes
[NASA-TP-2706] N87-23586

Crossflow vorticity sensor
[NASA-CASE-LAR-13436-1-CU] N87-23587

Mach 6 experimental and theoretical stability and performance of a cruciform missile at angles of attack up to 65 degrees
[NASA-TP-2733] N87-23592

Effect of a trade between boattail angle and wedge size on the performance of a nonaxisymmetric wedge nozzle
[NASA-TP-2717] N87-23593

High Reynolds Number tests of the NASA SC(2)-0012 airfoil in the Langley 0.3-meter transonic cryogenic tunnel
[NASA-TM-89102] N87-23594

Study of lee-side flows over conically cambered delta wings at supersonic speeds, part 1
[NASA-TP-2660-PT-1] N87-23597

Flight investigation of the effects of an outboard wing-leading-edge modification on stall/spin characteristics of a low-wing, single-engine, T-tail light airplane
[NASA-TP-2691] N87-23614

Helicopter anti-torque system using fuselage strakes
[NASA-CASE-LAR-13630-1] N87-23630

Optimization of payload mass placement in a dual keel space station
[NASA-TM-89051] N87-23687

Apparatus and procedure to detect a liquid-solid interface during crystal growth in a bridgman furnace
[NASA-CASE-LAR-13597-1-CU] N87-23713

Adhesive evaluation of water-soluble LARC-TPI
[NASA-TM-89152] N87-23752

Plasma torch igniter for scramjets N87-23789

Effects of test facility contaminants on supersonic hydrogen-air diffusion flames N87-23790

Opposed jet burner studies of silane-methane, silane-hydrogen and hydrogen diffusion flames with air N87-23791

Multispecies CARS measurements in turbulent combustion N87-23808

Rapid quantification of an internal property
[NASA-CASE-LAR-13689-1-NP] N87-23941

Adjustable mount for electro-optic transducers in an evacuated cryogenic system
[NASA-CASE-LAR-13100-1] N87-23982

Fully redundant mechanical release actuator
[NASA-CASE-LAR-13198-1] N87-23983

Energy-absorption capability and scalability of square cross section composite tube specimens
[NASA-TM-89087] N87-23991

Transport and photochemical modeling. Studies of atmospheric species
[NASA-CR-178311] N87-24040

Solving the Cauchy-Riemann equations on parallel computers
[NASA-CR-178307] N87-24107

Strong convergence and convergence rates of approximating solutions for algebraic Riccati equations in Hilbert spaces
[NASA-CR-178302] N87-24122

Extension of Kirchhoff's formula to radiation from moving surfaces
[NASA-TM-89149] N87-24160

Annoyance response to simulated advanced turboprop aircraft interior noise containing tonal beats
[NASA-TP-2689] N87-24161

Engineer in charge: A history of the Langley Aeronautical Laboratory, 1917-1958
[NASA-SP-4305] N87-24390

NATIONAL AERONAUTICS AND SPACE ADMINISTRATION. LEWIS RESEARCH CENTER, CLEVELAND, OHIO.

Icing of flow conditioners in a closed-loop wind tunnel
[NASA-TM-89824] N87-23591

Coupled aerodynamic and acoustical predictions for turboprops
[NASA-TM-87094] N87-23596

Performance of two 10-lb/sec centrifugal compressors with different blade and shroud thicknesses operating over a range of Reynolds numbers
[NASA-TM-100115] N87-23623

Liner cooling research at NASA Lewis Research Center
[NASA-TM-100107] N87-23624

Method for the determination of the three-dimensional aerodynamic field of a rotor-stator combination to compressible flow
[NASA-TM-100118] N87-23625

The supersonic through-flow turbofan for high Mach propulsion
[NASA-TM-100114] N87-23626

Experimental evaluation of honeycomb/screen configurations and short contraction section for NASA Lewis Research Center's altitude wind tunnel
[NASA-TP-2692] N87-23662

Reactivation study for NASA Lewis Research Center's hypersonic tunnel facility
[NASA-TM-89918] N87-23664

Speculations on future opportunities to evolve Brayton powerplants aboard the space station
[NASA-TM-89663] N87-23674

Design, development and test of shuttle/Centaur G-prime cryogenic tankage thermal protection systems
[NASA-TM-89825] N87-23685

Control considerations for high frequency, resonant, power processing equipment used in large systems
[NASA-TM-89926] N87-23690

Low power arcjet thruster pulse ignition
[NASA-TM-100123] N87-23691

Nuclear powered Mars cargo transport mission utilizing advanced ion propulsion
[NASA-TM-100109] N87-23692

In-situ analysis of hydrazine decomposition products
[NASA-TM-89916] N87-23693

Electrochemical performance and transport properties of a Nafion membrane in a hydrogen-bromine cell environment
[NASA-TM-89662] N87-23718

Oxidation protection coatings for polymers
[NASA-CASE-LEW-14072-3] N87-23736

Sol-Gel synthesis of MgO-SiO2 glass compositions having stable liquid-liquid immiscibility
[NASA-TM-89905] N87-23750

Multispecies CARS measurements in turbulent combustion N87-23808

Experimental thrust performance of a high area-ratio rocket nozzle N87-23809

Preliminary performance characterizations of an engineering model multipropellant resistojet for space station application
[NASA-TM-100113] N87-23821

Optically controlled microwave devices and circuits: Emerging applications in space communications systems
[NASA-TM-89889] N87-23900

Issues in space photovoltaic research and technology
[NASA-TM-89922] N87-23901

Synchronization trigger control system for flow visualization
[NASA-TM-89902] N87-23902

A study of Schwarz converters for nuclear powered spacecraft
[NASA-TM-89911] N87-23903

Three-step labyrinth seal for high-performance turbomachines
[NASA-TP-1848] N87-23921

Direct numerical simulations of a temporally evolving mixing layer subject to forcing
[NASA-TM-88896] N87-23933

Computation of full-coverage film-cooled airfoil temperatures by two methods and comparison with high heat flux data
[NASA-TM-88931] N87-23934

Straight cylindrical seal for high-performance turbomachines
[NASA-TP-1850] N87-23936

The impact damped harmonic oscillator in free decay
[NASA-TM-89897] N87-23978

Experiments on dynamic stiffness and damping of tapered bore seals
[NASA-TM-89895] N87-23984

Application of scanning acoustic microscopy to advanced structural ceramics
[NASA-TM-89929] N87-23987

Identification of structural interface characteristics using component mode synthesis
[NASA-TM-88960] N87-24006

Environmental degradation of 316 stainless steel in high temperature low cycle fatigue
[NASA-TM-89931] N87-24007

Fluoride salts and container materials for thermal energy storage applications in the temperature range 973 to 1400 K
[NASA-TM-89913] N87-24026

Test results of a 60 volt bipolar nickel-hydrogen battery
[NASA-TM-89927] N87-24029

A generalized procedure for constructing an upwind based TVD scheme
[NASA-TM-88926] N87-24132

NATIONAL AERONAUTICS AND SPACE ADMINISTRATION. MARSHALL SPACE FLIGHT CENTER, HUNTSVILLE, ALA.

Automatic detection of electric power troubles (AI application)
[NASA-TM-86593] N87-23693

Apparatus ad method for quiescent containerless processing of high temperature metals and alloys in low gravity
[NASA-CASE-MFS-28087-1] N87-23944

Shuttle Coherent Atmospheric Lidar Experiment (SCALE)
[NASA-TM-100307] N87-23959

The infrared morphology of galactic centers N87-24336

NATIONAL AERONAUTICS AND SPACE ADMINISTRATION. PASADENA OFFICE, CALIF.

Floating emitter solar cell
[NASA-CASE-NPO-16467-1-CU] N87-23879

Means for phase locking the outputs of a surface emitting laser diode array
[NASA-CASE-NPO-16542-1-CU] N87-23960

Multiplex electric discharge gas laser system
[NASA-CASE-NPO-16433-1] N87-23961

Rotary stepping device with memory metal actuator
[NASA-CASE-NPO-15482-1] N87-23970

NATIONAL AEROSPACE LAB., AMSTERDAM (NETHERLANDS).

Flexible and high quality software on a multiprocessor computer system controlling a research flight simulator N87-23643

Correlation between flight simulation and processing of flight tests based on inertial measurements N87-23655

NATIONAL BUREAU OF STANDARDS, WASHINGTON, D.C.

Laser studies of chemical dynamics at the gas-solid interface
[DE87-005950] N87-23710

NATIONAL CENTER FOR ATMOSPHERIC RESEARCH, BOULDER, COLO.

Global distribution of total cloud cover and cloud type amounts over land
[DE87-006903] N87-24053

A correlation between the IRAS infrared cirrus at 60 or 100 microns and neutral atomic hydrogen in the outer galaxy N87-24281

NATIONAL GEOPHYSICAL DATA CENTER, BOULDER, COLO.

Solar-geophysical data number 509, January 1987. Part 1: (Prompt reports). Data for December 1986, November 1986
[PB87-162574] N87-24385

Solar-geophysical data number 509, January 1987. Part 2: (Comprehensive reports). Data for July 1986
[PB87-162582] N87-24386

NATIONAL MARINE FISHERIES SERVICE, MIAMI, FLA.

Utilizing remote sensing of thematic mapper data to improve our understanding of estuarine processes and their influence on the productivity of estuarine-dependent fisheries
[NASA-CR-180984] N87-24012

NATIONAL OCEANIC AND ATMOSPHERIC ADMINISTRATION, BOULDER, COLO.

Geophysical monitoring for climatic change number 14
[PB87-162533] N87-24056

Auroral particles N87-24249

Personal computer based GOES data archive
[PB87-157517] N87-24384

NATIONAL OCEANIC AND ATMOSPHERIC ADMINISTRATION, MIAMI, FLA.

Mixed layer and thermocline depth climatologies in the western Indian Ocean
[PB87-154613] N87-24060

NATIONAL TRANSPORTATION SAFETY BOARD, WASHINGTON, D. C.

Aircraft accident data: US air carrier operations calendar year 1984
[PB87-183992] N87-23603

Aircraft accident report: Southern Air Transport LOGAIR Flight 51, Lockheed L-382G, Kelly Air Force Base, Texas, October 4, 1986
[PB87-910404] N87-23604

Aircraft accident data: US air carrier operations calendar year 1983
[PB87-160629] N87-23605

Annual review of aircraft accident data, US general aviation: Calendar year 1984
[PB87-194791] N87-23606

NAVAL AIR DEVELOPMENT CENTER, WARMINSTER, PA.

Certification testing methodology for composite structure. Volume 1: Data analysis
[NADC-87042-60-VOL-1] N87-23705

Certification testing methodology for composite structure. Volume 2: Methodology development
[NADC-87042-60-VOL-2] N87-23706

Poly (pyrrolium anion) studies: Electrochemical synthesis and physical behavior
[AD-A178097] N87-23743

NAVAL OCEAN RESEARCH AND DEVELOPMENT ACTIVITY, BAY ST. LOUIS, MISS.
Ocean wind and wave model comparisons with GEOSAT (GEOdesy SATellite) satellite data
[AD-A178302] N87-24061

NAVAL OCEAN SYSTEMS CENTER, SAN DIEGO, CALIF.
A new version of MODESRCH using interpolated values of the magnetoionic reflection coefficients
[AD-A179094] N87-23822
Horizontal variation of atmospheric extinction/backscatter coefficients
[AD-A178298] N87-23954

NAVAL POSTGRADUATE SCHOOL, MONTEREY, CALIF.
Application of the viscous-inviscid interaction method to the analysis of airfoil flows at low Reynolds numbers
[AD-A177948] N87-23588
Measurements of particulates in solid propellant rocket motors N87-23769
Solid fuel ramjet fuel regression rate/thrust modulation N87-23787
Metallized fuel burning characteristics in the solid fuel ramjet N87-23788
Solar cell concentrator system
[AD-A177981] N87-24025
Research aspects of rapid prototyping
[AD-A179007] N87-24097
The decomposition of an arbitrary three-dimensional planar polygon into a set of convex polygons
[AD-A177947] N87-24137
Nonparametric estimation of the probability of a long delay in the M/G/1 queue
[AD-A178259] N87-24150

NAVAL RESEARCH LAB., WASHINGTON, D. C.
Computational studies of the effects of acoustics and chemistry on the flow field in an axisymmetric ramjet combustor N87-23801
Numerical simulation of a randomly heated, thermally unstable fluid
[AD-A177888] N87-24225

NAVAL SAFETY CENTER, NORFOLK, VA.
Standardized procedure for system safety input to the Defense Technical Information Center (DTIC)
[AD-A178248] N87-24239

NAVAL SHIP RESEARCH AND DEVELOPMENT CENTER, ANNAPOLIS, MD.
Investigation of tearing instability phenomena in ASTM steel
[AD-A177993] N87-24000

NAVAL SUBMARINE MEDICAL RESEARCH LAB., GROTON, CONN.
The review of a research proposal to study the effects of 130 torr oxygen on submarines held at Groton, Connecticut on September 4, 1986
[AD-A177976] N87-24083
Medical research programs, past and future, for designing atmospheres to retard fires
[AD-A178354] N87-24089

NAVAL SURFACE WEAPONS CENTER, SILVER SPRING, MD.
Galvanic corrosion of Al-7075-T6 and Steel-4340 coupled to brass QQ-B-626, 360 and Al-7075-T6 coupled to Steel-4130 and Steel-4340: Exposure to aqueous NaCl and salt-fog environments
[AD-A179121] N87-23719
Downstream boundary effects on the frequency of self-excited oscillations in transonic diffuser flows N87-23794
Effect of particle size on the shock sensitivity of pure porous HE (High Explosive)
[AD-A178206] N87-23814

NAVAL UNDERWATER SYSTEMS CENTER, NEW LONDON, CONN.
Three-dimensional electric field predictions of an iron-copper galvanic couple
[AD-A178040] N87-23868

NAVAL WEAPONS CENTER, CHINA LAKE, CALIF.
TTCP non-linear instability program: US motor test data N87-23763
Measurement of solid-propellant burn rate using millimeter-wave techniques N87-23770
AP/HMX composite propellant modeling N87-23776
The application of imaging laser induced fluorescence to the measurement of HMX and aluminized propellant ignition and deflagration flame structure N87-23782
Passive shear-flow control to minimize ramjet combustion instabilities N87-23796

NETHERLANDS FOUNDATION FOR RADIO ASTRONOMY, DWINGELO.
The HII regions in M51: Radio and optical observations N87-24295
Neutral hydrogen and star formation in irregular galaxies N87-24302

NEVADA UNIV., RENO.
Study of the suppression of rocket plume afterburning by chemical additives N87-23768

NEW HAMPSHIRE UNIV., DURHAM.
Cosmic rays in the heliosphere N87-24254

NEW MEXICO STATE UNIV., LAS CRUCES.
Engineering and instrumentation support of the AFGL (Air Force Geophysics Laboratory) Rocket Research Program
[AD-A179257] N87-23689
IRAS observations of starburst galaxies N87-24338

NEW MEXICO UNIV., ALBUQUERQUE.
A model for silicon dendrite growth during laser/plasma deposition from a silane discharge
[DE87-007579] N87-23733
Symbol manipulation and applied mathematics
[AD-A179571] N87-24124

NEW YORK UNIV., NEW YORK.
The perception of the higher derivatives of visual motion
[AD-A179627] N87-24069

NORTH CAROLINA UNIV., CHAPEL HILL.
Energy conversion processes based on molecular excited states
[DE87-007408] N87-24020
On the existence and convergence of probability measures on continuous semi-lattices
[AD-A179267] N87-24148
Heats of formation, structure and heteroatom ((17)O, (33)S) NMR studies of organosulfur molecules, radicals and ions
[DE87-006361] N87-24189

NORTHEASTERN UNIV., BOSTON, MASS.
Multipurpose visual display and eye movement recording system
[AD-A179620] N87-24068
Infrared spectroscopy of star formation in galaxies N87-24320

NORTHROP CORP., HAWTHORNE, CALIF.
Certification testing methodology for composite structure. Volume 1: Data analysis
[NADC-87042-60-VOL-1] N87-23705
Certification testing methodology for composite structure. Volume 2: Methodology development
[NADC-87042-60-VOL-2] N87-23706

NORTHWESTERN UNIV., EVANSTON, ILL.
Midwest free-electron laser program
[AD-A178106] N87-23953
A simplified computer solution for the flexibility matrix of contacting teeth for spiral bevel gears
[NASA-CR-179620] N87-23977

O

OAK RIDGE ASSOCIATED UNIVERSITIES, INC., TENN.
Fusion Energy Postdoctoral Research Program and Professional Development Program
[DE87-006350] N87-24188

OAK RIDGE NATIONAL LAB., TENN.
Metals and Ceramics Division
[DE87-008548] N87-23697
Ceramic technology for advanced heat engines project
[DE87-008538] N87-23740
Laser-enhanced electron attachment and its possible application for optical switching
[DE87-008787] N87-23957
Controlled nucleation and growth studies in metal oxide and alkoxide systems by dynamic laser-light-scattering methods
[DE87-009103] N87-23958
On autonomous terrain model acquisition by a mobile robot
[DE87-005719] N87-23964
Analysis of a mechanically simple external combustion engine with an unusual cycle
[DE87-007788] N87-23965
A comparison of unburned fuel and aldehyde emissions from a methanol-fueled stratified charge and homogeneous charge engine
[DE87-007793] N87-23966
Ultrasonic techniques for the evaluation of ceramic joints
[DE87-009104] N87-23986
Application of thermal and flywheel energy storage in orbiting nuclear burst power systems
[DE87-007882] N87-24021
Application of advanced flywheel technology for energy storage on space station
[DE87-007657] N87-24028
Storage and preservation of environmental samples
[DE87-004271] N87-24030
Gaussian elimination with partial pivoting and load balancing on a multiprocessor
[DE87-007784] N87-24093
LU factorization algorithms on distributed-memory multiprocessor architectures
[DE87-007794] N87-24100
Proposal for continued research in intelligent machines at the Center for Engineering Systems Advanced Research (CESAR) for FY 1988 to FY 1991
[DE87-007789] N87-24121
The fiber optic refrigeration cycle monitor
[DE87-006632] N87-24180
Transient enhanced diffusion in ion-implanted silicon
[DE87-007859] N87-24207
Thin film characterization using a mechanical properties microprobe
[DE87-006593] N87-24214
The success or failure of management information systems: A theoretical approach
[DE87-007802] N87-24233
Use of a DBMS to aid in the software conversion process
[DE87-007863] N87-24234

OAKLAND UNIV., ROCHESTER, MICH.
Gauge invariant quantum cosmology
[DE87-006685] N87-24226

OBSERVATOIRE DE PARIS-MEUDON (FRANCE).
Extragalactic OH megamasers in strong IRAS sources N87-24353

OHIO STATE UNIV., COLUMBUS.
Two-dimensional aerodynamic characteristics of the AMES HI-120, HI-8, and LOW-12 airfoils
[NASA-CR-181018] N87-23589
Star formation and spiral structure in M81 N87-24294

OKLAHOMA STATE UNIV., STILLWATER.
Inter-vehicle ranging system
[AD-A179492] N87-23938
Changing time series
[AD-A178030] N87-24149

ONSALA SPACE OBSERVATORY (SWEDEN).
Structure and kinematics of the molecular spiral arms in M51 N87-24312
Detection of CO (J=1-0) in the dwarf elliptical galaxy NGC 185 N87-24315

OWENS VALLEY RADIO OBSERVATORY, PASADENA, CALIF.
Far-infrared properties of optically-selected quasars and Seyfert galaxies N87-24371

P

PACIFIC NORTHWEST LABS., RICHLAND, WASH.
Federal laboratory nondestructive testing research and development applicable to industry
[DE87-006351] N87-23985
Characterization of solar thermal concepts for electricity generation. Volume 1: Analyses and evaluation
[DE87-007161] N87-24019
A preliminary evaluation of the performance of wind tunnel and numerical modeling simulations of the wind flow over a wind farm
[DE87-004634] N87-24051
User's manual for the convective cloud module version 1.0
[DE87-008343] N87-24058
Status of phenomenological modeling
[DE87-004922] N87-24143
Experimental bounds on beta beta-decay, cold dark matter and solar axions with an ultralow background Ge detector
[DE87-002065] N87-24383

PARIS II UNIV., ORSAY (FRANCE).
Computer simulation of the lasertron with a ring model
[DE87-007461] N87-23897

PENNSYLVANIA STATE UNIV., STATE COLLEGE.
Stochastic excitation of acoustic waves in a combustion chamber N87-23761
A unified direct-inverse procedure for two-dimensional boundary layers using spline/finite difference discretization
[AD-A178223] N87-24140

PENNSYLVANIA STATE UNIV., UNIVERSITY PARK.
Nonuniform grain boundary corrosion and the local electrode potential in crevicing
[AD-A177889] N87-23728
New low temperature (hydroxylated) materials
[DE87-008530] N87-23749
Workshop report: Methods for measuring solid propellant combustion response N87-23762
Thermal decomposition and ignition of a series of new nitramine lova propellants by CO2 laser N87-23783
Numerical simulation of combustion processes of mobile stick-propellant bundles N87-23785

Thermal fracture in selected nonlinear optical materials
[DE87-008213] N87-24209
Starburst galaxies N87-24319

PENNSYLVANIA UNIV., PHILADELPHIA.
Development and analysis of silicon solar cells near 20% efficiency in the Flat Plate Solar Array Project
[NASA-CR-181005] N87-24018

PITTSBURGH UNIV., PA.
Physics of pattern formation at liquid interfaces
[DE87-007540] N87-23919

POLISH ACADEMY OF SCIENCES, WARSAW.
Retardation effect in fatigue crack growth under stationary stochastic loading
[REPT-43/1986] N87-23999

PORTLAND STATE UNIV., OREG.
Estimation of parameters in latent class models with constraints on the parameters
[AD-A178196] N87-24138

PRATT AND WHITNEY AIRCRAFT GROUP, EAST HARTFORD, CONN.
Life prediction and constitutive models for engine hot section anisotropic materials
[NASA-CR-179594] N87-23622

PRINCETON UNIV., N. J.
Influence of two-phase flow in the deflagration of homogeneous solids N87-23777

PURDUE UNIV., WEST LAFAYETTE, IND.
Two techniques for measuring AP ignition delay N87-23772

R

REDIFFUSION SIMULATION LTD., CRAWLEY (ENGLAND).
Visual display research tool N87-23635
Use of VDU's by flight simulator instructors N87-23841

REMTECH, INC., HUNTSVILLE, ALA.
Measurements for rocket engine performance code verification N87-23811

RENSSELAER POLYTECHNIC INST., TROY, N.Y.
Radiation transport in dust in disk geometry
[NASA-CR-180995] N87-24157

RICE UNIV., HOUSTON, TEX.
Radio and infrared observations of (almost) one hundred non-Seyfert Markarian galaxies N87-24350

RIT RESEARCH CORP., ROCHESTER, N.Y.
Impulsive EMI (Electromagnetic Interference) radiated by Electrostatic Discharges (ESD)
[AD-A178213] N87-23848
ESD (Electrostatic Discharge)/EOS (Electrical OverStress) susceptibility of a class of bipolar RF power transistors: Experimental studies on stripline-opposed emitter transistors
[AD-A178212] N87-23890
Influence of ionizing radiations and electrical overstressings on MOS (Metal-Oxide Semiconductors) devices: A comparison
[AD-A178214] N87-23891
Noise characteristics of MOS (Metal-Oxide Semiconductors) devices degraded by electrical overstressings
[AD-A178217] N87-23892

ROCHESTER UNIV., N. Y.
Double-diffraction X-ray imaging camera
[DE87-007936] N87-23940
University of Rochester, Laboratory for Laser Energetics
[DE87-005920] N87-23947

ROCKWELL INTERNATIONAL CORP., CANOGA PARK, CALIF.
Space station WP-04 power system. Volume 1: Executive summary
[NASA-CR-179587] N87-23695
Space station WP-04 power system. Volume 2: Study results
[NASA-CR-179587] N87-23696
Numerical and experimental studies of atomization and mixing from a coaxial injector element N87-23812
Nonintrusive temperature measurements in SSME preburner element flowfields N87-23813

ROCKWELL INTERNATIONAL CORP., GOLDEN, COLO.
Special applications of the Debye Microdiffractometer
[RFP-3906] N87-23939

ROCKWELL INTERNATIONAL CORP., THOUSAND OAKS, CALIF.
Improved beta" -alumina oxide electrolytes through transformation toughening
[DE87-007897] N87-23735

ROME AIR DEVELOPMENT CENTER, GRIFFISS AFB, N.Y.
Rectangular microstrip patch antenna arrays
[AD-A179170] N87-23823

ROME AIR DEVELOPMENT CENTER, HANSCOM AFB, MASS.
Basic parameters of antennas for aircraft, satellites and missiles N87-23860

ROME UNIV. (ITALY).
Study of minimum bias trigger events in the p(p-) collider for the square root of s = 0.2 to 0.9 TeV
[NOTA-INTERNA-874] N87-24183

ROSE-HULMAN INST. OF TECH., TERRE HAUTE, IND.
The impact damped harmonic oscillator in free decay
[NASA-TM-89897] N87-23978

ROYAL AIRCRAFT ESTABLISHMENT, BEDFORD (ENGLAND).
Simulator motion characteristics and perceptual fidelity N87-23639
Progress in the implementation of AGARD-AR-144 in motion system assessment and monitoring N87-23642
Development of in-flight simulation aircraft for research and training applications in UK N87-23658

ROYAL INST. OF TECH., STOCKHOLM (SWEDEN).
Hardware synthesis from specification with polynomials
[TRITA-NA-8506] N87-24091
Edge focusing
[TRITA-NA-8518] N87-24099
Investigations into the pattern processing capabilities of associative nets
[TRITA-NA-8601] N87-24114
Approximation errors and perceived similarity between approximated polygons
[TRITA-NA-8505] N87-24127
Extended potential drops preceding double layer formation in a triple plasma device
[TRITA-EPP-86-11] N87-24185

ROYAL OBSERVATORY, EDINBURGH (SCOTLAND).
Systematic identification of IRAS point sources N87-24343
The properties of highly luminous IRAS galaxies N87-24358

RUTGERS - THE STATE UNIV., NEW BRUNSWICK, N. J.
Theoretical investigation of 3-D shock wave-turbulent boundary layer interactions, part 5
[AD-A179455] N87-23909
Experiments on the cognitive aspects of information seeking and information retrieving
[PB87-157699] N87-24238

RUTHERFORD HIGH ENERGY LAB., CHILTON (ENGLAND).
The Arp Ring: Galactic or extragalactic? N87-24282

S

SAN DIEGO STATE UNIV., CALIF.
Tones generated due to the impingement of two jets on each other N87-23797

SANDIA LABS., LIVERMORE, CALIF.
Asymptotic models for solid propellant combustion and the onset of intrinsic instability N87-23764
Modification of solid propellant deflagration rates due to random nonhomogeneities N87-23766
Influence of two-phase flow in the deflagration of homogeneous solids N87-23777
A theoretical and numerical study of radiative ignition and deradiative extinction in solid propellants N87-23778
Simultaneous thermogravimetric modulated beam mass spectrometry and time-of-flight velocity spectra measurements of thermal decomposition products from RDX and HMX N87-23780
Quantum chemical calculations of the decomposition of nitramines: Thermochemistry and reaction pathways N87-23781

SANDIA NATIONAL LABS., ALBUQUERQUE, N. MEX.
Mechanical properties of undirectional and fabric graphite/epoxy composites
[SAND-86-0784] N87-23702
Spin-cast carbon films from polyacrylonitrile
[DE87-002469] N87-23703
Sandia cooperative group on the aerothermochemistry of turbulent combustion
[DE87-008345] N87-23714
Corrosion sensing with acoustic wave devices
[DE87-003516] N87-23723
Plasma deposition of tungsten
[DE87-007390] N87-23724
The corrosion of Al 7075-T6 alloy coupled to Ti 6A 1-4V in wet air
[DE87-008347] N87-23726
Foam rheology: The linear viscoelastic response of a spatially periodic model
[DE87-000960] N87-23731
Three-dimensional model for the linear elastic properties of a foam
[DE87-000984] N87-23732
A model for silicon dendrite growth during laser/plasma deposition from a silane discharge
[DE87-007579] N87-23733
A mechanistic study of the interaction of ultraviolet laser radiation with low density polymers
[DE87-007846] N87-23734
Fundamentals of sol-gel thin film formation
[DE87-007387] N87-23736
Dielectric properties of styrene/acrylate copolymer coatings formed by electrophoretic deposition on gold, aluminum alloy, and porous anodized aluminum alloy substrates
[DE87-008885] N87-23741
High temperature electrically conductive adhesives
[DE87-007020] N87-23747
Polymer dynamics and gelation
[DE87-007578] N87-23748
Microwave coupling inside complex systems
[DE87-003505] N87-23841
Single and multiple electromagnetic scattering by dielectric obstacles from a resonance perspective
[DE87-007347] N87-23843
Evaluation of a thin-slot formalism for finite-difference time-domain electromagnetics codes
[DE87-008078] N87-23857
Cost reductions in the nickel/hydrogen battery
[DE87-007576] N87-23881
Wetting properties of Au/Sn solders for microelectronics
[DE87-008519] N87-23883
Removable encapsulants for electronic devices
[DE87-005869] N87-23894
The effect of reinforcement on the tear properties of flexible circuits
[DE87-007022] N87-23895
Two-stage hybrid microcircuit amplifier
[DE87-009092] N87-23899
Onset of Taylor vortices in flows with a circumferential pressure gradient: Application to the helical screw rheometer
[DE87-000453] N87-23918
Palladium-silver and gold alloys as catalytic gates on MIS gas sensors
[DE87-006959] N87-23943
Pulsed Nd:YAG laser closure welding of the MC3593/3594 relay
[DE87-007825] N87-23967
Forced vibration as a method for determining structural integrity
[DE87-005878] N87-23992
PRONTO 2D: A two-dimensional transient solid dynamics program
[DE87-007823] N87-23993
Techniques for implementing statically complete component mode synthesis for forced response
[DE87-002696] N87-24002
Material damping from frequency analysis of driving point measurements
[DE87-005873] N87-24003
Reconstruction of dynamic structural inputs in the presence of noise
[DE87-006701] N87-24004
Dynamic brittle fracture analysis based on continuum damage mechanics
[DE87-006704] N87-24005
Sandia National Laboratories 34-meter diameter vertical axis wind turbine test bed
[DE87-003096] N87-24016
Test plan for the 34 meter vertical axis wind turbine test bed located at Bushland, Texas
[DE87-004777] N87-24017
Design of the shell project Seafloor Earthquake Measurement System (SEMS)
[DE87-007948] N87-24059
DATA: A comprehensive data analysis environment for HP1000 computers
[DE87-007824] N87-24094
CADCAM-005: An introduction to the data exchange process using IGES
[DE87-008079] N87-24102
MVSE (Minimizes Variance Squared Error) adaptive filtering subject to a constraint on MSE (Mean Squared Error)
[DE87-007959] N87-24105
Numerical prediction of 1-D ablation using a finite control volume procedure with exponential differencing
[DE87-007947] N87-24130
Calculation of eigenvector derivatives for structures with repeated eigenvalues
[DE87-008399] N87-24135
Development of ultrasonic thermometry for high-temperature high-resolution temperature profiling applications in LMFBR safety research
[SAND-84-1341] N87-24171
Epitaxial semiconductor optical interference devices
[DE87-006890] N87-24212

SANDIA NATIONAL LABS., LIVERMORE, CALIF.
A fiber optic link for an infrared imaging camera system
[DE87-008346] N87-24181
SANTA FE CORP., ALEXANDRIA, VA.
Systems model for natural gas vehicle fleets
[PB87-178063] N87-24245
SCIENCE APPLICATIONS INTERNATIONAL CORP., MONTEREY, CALIF.
Mid-latitude wind probability model
[AD-A179256] N87-24048
SELENIA S.P.A., ROME (ITALY).
Efficient conduct of individual flights and air traffic or optimum utilization of modern technology for the overall benefit of civil and military airspace users
[AGARD-AR-236] N87-23608
SEVERN COMMUNICATIONS CORP., SEVERNA PARK, MD.
Comparison of CREME (Cosmic Ray Effects on Microelectronics) model LET (Linear Energy Transfer) spaceflight dosimetry data
[AD-A177873] N87-23884
Satellite observation of atmospheric nuclear gamma radiation
[AD-A177937] N87-24389
SINGER-LINK-MILES LTD., LANCING (ENGLAND).
Advanced visuals in mission simulators N87-23636
SMITHSONIAN ASTROPHYSICAL OBSERVATORY, CAMBRIDGE, MASS.
Physics of the inner heliosphere: Mechanisms, models and observational signatures
[NASA-CR-181063] N87-24387
SMITHSONIAN INSTITUTION, CAMBRIDGE, MASS.
Studies of infrared aurorae
[AD-A179539] N87-24037
SOLAR TURBINES INTERNATIONAL, SAN DIEGO, CALIF.
Intercooled gas turbine
[PB87-178042] N87-23972
SOUTH CAROLINA UNIV., COLUMBIA.
Experimental bounds on beta beta-decay, cold dark matter and solar axions with an ultralow background Ge detector
[DE87-002065] N87-24383
SOUTHERN METHODIST UNIV., DALLAS, TEX.
Spread spectrum mobile radio communications
[AD-A178446] N87-23826
SOUTHWEST RESEARCH INST., SAN ANTONIO, TEX.
Study of the influence of metallurgical factors on fatigue and fracture of aerospace structural materials
[AD-A179268] N87-23720
SPACE TELESCOPE SCIENCE INST., BALTIMORE, MD.
Discrete X-ray sources and the X-ray background N87-24261
A simple theory of bimodal star formation N87-24317
Star formation and dynamics in starburst nuclei N87-24324
SPECTRA TECHNOLOGY, INC., BELLEVUE, WASH.
Compact toroid generation, lifetime, and stability studies in linear reverse field theta pinch geometries (TRX-2): Final report
[DE87-005094] N87-24195
SRI INTERNATIONAL CORP., MENLO PARK, CALIF.
Influence of microstructure and microdamage processes on fracture at high loading rates
[AD-A179264] N87-23969
ST SYSTEMS CORP., HAMPTON, VA.
Transport and photochemical modeling. Studies of atmospheric species
[NASA-CR-178311] N87-24040
STANDARD TELEPHONES AND CABLES LTD., PAIGNTON (ENGLAND).
Adaptive antennas N87-23865
STANFORD UNIV., CALIF.
Two blowing concepts for roll and lateral control of aircraft
[NASA-CR-180478] N87-23627
Effects on fuel spray characteristics and vaporization on energy release rates and flow field structure in a dump combustor N87-23804
Picosecond optical electronics
[AD-A179061] N87-23868
Research in VLSI systems
[AD-A179227] N87-23872
JSEP (Joint Services Electronics Program)
[AD-A177881] N87-23885
A single chip LSI high-speed functional tester
[AD-A177886] N87-23886
A VLSI CMOS circuit design technique to aid test generation
[AD-A177934] N87-23887
Adaptive grid refinement for numerical weather prediction
[AD-A179393] N87-24049
Research on knowledge representation, machine learning, and knowledge acquisition
[NASA-CR-180408] N87-24103
Far field boundary conditions for time-dependent hyperbolic systems
[AD-A179361] N87-24123
Experimental bounds on beta beta-decay, cold dark matter and solar axions with an ultralow background Ge detector
[DE87-002065] N87-24383
STATE UNIV. OF NEW YORK, STONY BROOK.
Masses, luminosities and dynamics of galactic molecular clouds N87-24270
SVERDRUP TECHNOLOGY, INC., CLEVELAND, OHIO.
The T55-L-712 turbine engine compressor housing refurbishment project
[NASA-CR-179624] N87-23729
Environmental degradation of 316 stainless steel in high temperature low cycle fatigue
[NASA-TM-89931] N87-24007
SYSTEMS TECHNOLOGY, INC., HAWTHORNE, CALIF.
Collected flight and simulation comparisons and considerations N87-23660

T

TECHNISCHE UNIV., HANOVER (WEST GERMANY).
Investigation of the buckling sensitivity of hemispherical containers with arbitrary liquid content
[MITT-31] N87-24008
TECHNOLOGY SERVICE CORP., SILVER SPRING, MD.
Results of near field probe scanning tests for ultralow sidelobe arrays
[AD-A178141] N87-23846
TEL-AVIV UNIV. (ISRAEL).
On the breakdown of the wave packet trailing a turbulent spot in a laminar layer
[AD-A179607] N87-23915
TELEDYNE GEOTECHNICAL, ALEXANDRIA, VA.
Finite difference simulations of Rayleigh wave scattering by 2-D rough topography
[AD-A179190] N87-23824
TEXAS A&M UNIV., COLLEGE STATION.
Potential electron beam induced flashblindness in pilots
[AD-A178002] N87-24084
TEXAS UNIV., ARLINGTON.
Electronics and ionic transport in polymers
[AD-A178227] N87-23748
TEXAS UNIV., AUSTIN.
Finite element analysis of slow-wave Schottky contact printed lines
[AD-A179259] N87-23873
Effective diffusion in laminar convective flows
[DE87-008054] N87-23920
Kinetic studies following state-selective laser excitation
[DE87-007938] N87-23950
Simulation and analysis of a geopotential research mission
[NASA-CR-180695] N87-24042
LANDSAT-based lineament analysis, East Texas Basin, and structural history of the Sabine Uplift area, East Texas and North Louisiana
[PB87-176327] N87-24043
A near-infrared study of the luminous merging galaxies NGC 2623 and ARP 148 N87-24339
TEXTRON BELL HELICOPTER, FORT WORTH, TEX.
Piloted simulation in the development of the XV-15 tilt rotor research aircraft N87-23646
THOMSON-CSF, TRAPPES (FRANCE).
Radar simulators N87-23651
TICRA A/S, COPENHAGEN (DENMARK).
Spacecraft multi-beam and contoured-beam antennas N87-23863
TOKYO UNIV. (JAPAN).
CO observations of galaxies with the Nobeyama 45-M telescope N87-24290
TOLEDO UNIV., OHIO.
Semiempirical studies of atomic structure
[DE87-007320] N87-24164
TORONTO UNIV., DOWNSVIEW (ONTARIO).
The application of optimal control techniques to the UTIAS research simulator N87-23637
TRANSPORTATION SYSTEMS CENTER, CAMBRIDGE, MASS.
US Coast Guard SARSAT (Search And Rescue Satellite-Aided Tracking). Volume 2. Appendices
[AD-A178307] N87-23600
US Coast Guard SARSAT (Search and Rescue Satellite-Aided Tracking). Volume 3. Programs and data listings
[AD-A178308] N87-23601
Otis ANGB (Air National Guard Base) visibility sensor field test study
[AD-A179175] N87-24045
TRW SPACE TECHNOLOGY LABS., REDONDO BEACH, CALIF.
Spacecraft environment interaction investigation
[AD-A179183] N87-23678
TUFTS UNIV., MEDFORD, MASS.
Training, muscle fatigue, and stress fractures
[AD-A178350] N87-24085

U

UNITED KINGDOM ATOMIC ENERGY AUTHORITY, HARWELL (ENGLAND).
Ceramic fibre/glass matrix composites with outstanding mechanical performance
[AERE-R-12025] N87-23699
UNITED TECHNOLOGIES RESEARCH CENTER, EAST HARTFORD, CONN.
New concepts for care diagnostics of solid propellant combustion N87-23771
CARS approaches to simultaneous measurements of H2 and H2O concentration and temperature in H2-air combustion systems N87-23792
UNIVERSIDAD NACIONAL AUTONOMA DE MEXICO, ENSENADA.
VLA continuum observations of barred spiral galaxies N87-24333
UNIVERSITY OF SOUTHERN CALIFORNIA, LOS ANGELES.
Nonlinear real-time optical signal processing
[AD-A178169] N87-24182
Using SIRTF to study extragalactic star formation N87-24359
UNIVERSITY OF WESTERN ONTARIO, LONDON.
Random vibration of nonlinear systems N87-23997
UTAH STATE UNIV., BEDFORD, MASS.
Medium- and long-wave infrared absorption spectra of carbon dioxide nitrous oxide at 800K
[AD-A179430] N87-23708
UTAH STATE UNIV., LOGAN.
A study of the maximum entropy method of power spectrum estimation as applied to interferometer data
[AD-A179403] N87-23707
Atmospheric radiance profile codes
[AD-A179258] N87-24035
A comparison of ionospheric model predictions with MITHRAS observations
[AD-A179374] N87-24036
Studies of infrared aurorae
[AD-A179539] N87-24037
UTAH UNIV., SALT LAKE CITY.
Theoretical and experimental study of solid phase miscibility gaps in 3/5 quaternary alloys
[DE87-008942] N87-24223

V

VIBRATION INST., CLARENDON HILLS, ILL.
The Shock and Vibration Digest, Volume 19, No. 5 N87-23620
The Shock and Vibration Digest, Volume 19, No. 4 N87-23818
The Shock and Vibration Digest, Volume 19, No. 3 N87-23996
The Shock and Vibration Digest, Volume 19, No. 6 N87-24125
VIRGINIA POLYTECHNIC INST. AND STATE UNIV., BLACKSBURG.
Plasma torch igniter for scramjets N87-23789
Recent advances in the nonlinear analysis of laminated composite plates and shells N87-23819
Three-dimensional structure of boundary layers in transition to turbulence
[AD-A179247] N87-23908
Thermodynamic evaluation of transonic compressor rotors using the finite volume approach
[NASA-CR-180587] N87-23925
Development of an explicit time marching procedure for laminar and turbulent flow N87-23926
Development of a finite volume time marching method [JM/85-3] N87-23927
An explicit finite-volume time-marching procedure for turbulent flow calculations N87-23928
Explicit finite-volume time-marching calculations of total temperature distributions in turbulent flow N87-23929
VIRGINIA UNIV., CHARLOTTESVILLE.
A multi user random access communication system for users with different priorities
[AD-A178372] N87-23854
Symmetry problems in particle physics
[DE87-006369] N87-24168

W

WASHINGTON STATE UNIV., PULLMAN.
Compression and shear wave propagation in plain and filled elastomers
[AD-A178153] N87-23745
WASHINGTON UNIV., SEATTLE.
Global distribution of total cloud cover and cloud type amounts over land
[DE87-006903] N87-24053
Min-max bias robust M-estimates of scale
[AD-A179255] N87-24147
Multicomponent analysis using an array of piezoelectric crystal sensors
[AD-A178012] N87-24218
IRAS colors of VLA identified objects in the galaxy
N87-24271
WASHINGTON UNIV., ST. LOUIS, MO.
Analysis and test results for an improved constant speed passive cyclic pitch wind turbine
[DE87-001135] N87-24022
Measurements of ultraheavy cosmic rays with HEAO-3
N87-24256
WAYNE STATE UNIV., DETROIT, MICH.
The inhibition effects of H2/O2/N2 flames seeded by potassium N87-23774
WESTINGHOUSE ELECTRIC CORP., BALTIMORE, MD.
Aircraft radar antennas N87-23861
WESTINGHOUSE RESEARCH AND DEVELOPMENT CENTER, PITTSBURGH, PA.
Superconducting electronic film structures
[AD-A179134] N87-24200
WINDSOR UNIV. (ONTARIO).
Proceedings of the Tenth DOE Solar Photochemistry Research Conference
[DE87-006421] N87-24062
WISCONSIN UNIV., MADISON.
A comparison of unburned fuel and aldehyde emissions from a methanol-fueled stratified charge and homogeneous charge engine
[DE87-007793] N87-23966
Pulmonary adaptation to high altitude
[AD-A179139] N87-24065
WRIGHT STATE UNIV., DAYTON, OHIO.
Characterization of material device structures
[AD-A178262] N87-24220
WYLE LABS., INC., HUNTSVILLE, ALA.
On integrating a logarithmic or semilogarithmic piecewise linear PSD plot of a random variable X(T): Part 1 N87-24126
WYOMING UNIV., LARAMIE.
Carbon monoxide emission from small galaxies
N87-24303

Y

YALE UNIV., NEW HAVEN, CONN.
Transport phenomena and interfacial kinetics in multiphase combustion systems
[AD-A179544] N87-23709
Optical and IR luminosity functions of IRAS galaxies
N87-24348
YAP ANALYTICS, INC., LEXINGTON, MASS.
Atmospheric radiance profile codes
[AD-A179258] N87-24035

Typical Contract Number Index Listing

Listings in this index are arranged alphanumerically by contract number. Under each contract number the NASA accession numbers denoting documents that have been produced as a result of research done under that contract are arranged in ascending order. The NASA accession number denotes the number by which the citation is identified.

AF PROJ. 2688 ..... N87-24045
AF-AFOSR-0007-82 ..... N87-23730
AF-AFOSR-0012-85 ..... N87-23937
AF-AFOSR-0014-82 ..... N87-24265
AF-AFOSR-0029-84 ..... N87-24036
AF-AFOSR-0034-84 ..... N87-23709
AF-AFOSR-0036-86 ..... N87-23873
AF-AFOSR-0040-82 ..... N87-23909
AF-AFOSR-0055-86 ..... N87-24187
AF-AFOSR-0057-85 ..... N87-24947
AF-AFOSR-0070-85 ..... N87-24382
AF-AFOSR-0062-84 ..... N87-23760
AF-AFOSR-0092-85 ..... N87-24124
AF-AFOSR-0139-84 ..... N87-23868
AF-AFOSR-0146-85 ..... N87-23910
AF-AFOSR-0181-84 ..... N87-24182
AF-AFOSR-0183-86 ..... N87-23867
AF-AFOSR-0191-85 ..... N87-23721
AF-AFOSR-0240-82 ..... N87-24139
AF-AFOSR-0277-84 ..... N87-24177
AF-AFOSR-0303-85 ..... N87-24122
AF-AFOSR-0304-85 ..... N87-24175
AF-AFOSR-0309-82 ..... N87-23826
AF-AFOSR-0312-84 ..... N87-24088
AF-AFOSR-0317-82 ..... N87-24096
AF-AFOSR-0329-85 ..... N87-24089
AF-AFOSR-0333-84 ..... N87-23915
AF-AFOSR-0361-83 ..... N87-23663
AF-AFOSR-0376-85 ..... N87-24204
AF-AFOSR-0396-84 ..... N87-24122
ARPA ORDER 4871 ..... N87-24112
N87-24230
N87-24231
AT(40-1)-3405 ..... N87-24193
DA PROJ. W05-13-CC N87-24048
DA PROJ. 1L1-61102-AF-43 ..... N87-24131
DA PROJ. 1L1-61102-AH-45 ..... N87-23729
DA PROJ. 1L1-61102-SH-57 ..... N87-23744
DA PROJ. 1L1-62618-AH-80 ..... N87-23585
DA PROJ. 1L1-62716-AH-70 ..... N87-24229
DA PROJ. 3M1-61102-BS-10 ..... N87-24085
N87-24086
DAAA14-85-C-0014 ..... N87-23784
DAAA15-86-D-0005 ..... N87-24229
DAAD07-86-C-0100 ..... N87-24050
DAAG29-85-K-0048 ..... N87-23885
DAAK11-83-C-0051 ..... N87-23784
DAAK29-83-K-0081 ..... N87-23785
DAJA45-84-C-0012 ..... N87-24217
DAJA45-85-C-0021 ..... N87-23744
DAMD17-82-C-2259 ..... N87-24085
DAMD17-86-C-6088 ..... N87-24085
DARPA ORDER-3773-6 ..... N87-23872
DASG60-86-C-0062 ..... N87-23872
DE-AC02-76CH-00016 ..... N87-24080
N87-24179
DE-AC02-80RA-50150 ..... N87-23876
DE-AC02-81ER-10942 ..... N87-23727
DE-AC02-83CH-10093 ..... N87-23753
N87-24015
N87-24022
N87-24023
N87-24024
N87-24027
N87-24062
DE-AC02-83ER-13137 ..... N87-23951
DE-AC03-76SF-00098 ..... N87-23869
N87-23735
N87-23817
N87-24116
N87-24117
N87-24206
N87-24210
N87-24213
N87-24236
N87-24340
DE-AC03-76SF-00515 ..... N87-24383
DE-AC03-81ER-40050 ..... N87-24092
DE-AC03-84ER-53158 ..... N87-24197
DE-AC04-76DP-00053 ..... N87-23722
N87-23754
N87-23955
DE-AC04-76DP-00613 ..... N87-24133
DE-AC04-76DP-00789 ..... N87-23702
N87-23703
N87-23723
N87-23724
N87-23731
N87-23732
N87-23733
N87-23734
N87-23738
N87-23741
N87-23747
N87-23748
N87-23841
N87-23843
N87-23857
N87-23881
N87-23883
N87-23894
N87-23895
N87-23899
N87-23918
N87-23943
N87-23967
N87-23992
N87-23993
N87-24002
N87-24003
N87-24004
N87-24005
N87-24016
N87-24017
N87-24059
N87-24094
N87-24102
N87-24105
N87-24130
N87-24171
N87-24212
N87-23939
DE-AC04-76DP-03533 ..... N87-23714
DE-AC04-76DR-00789 ..... N87-23726
N87-24181
DE-AC04-86AL-33163 ..... N87-23922
DE-AC05-76OR-00033 ..... N87-24188
DE-AC05-84OR-21400 ..... N87-23897
N87-23740
N87-23917
N87-23957
N87-23958
N87-23964
N87-23966
N87-23988
N87-24021
N87-24028
N87-24030
N87-24093
N87-24100
N87-24121
N87-24180
N87-24207
N87-24214
N87-24233
N87-24234
DE-AC05-85ER-40216 ..... N87-24172
DE-AC06-76RL-01830 ..... N87-23985
N87-24019
N87-24051
N87-24058
N87-24143
N87-24383
DE-AC08-80ER-53096 ..... N87-24195
DE-AC08-83NV-10336 ..... N87-23882
DE-AC09-76SR-00001 ..... N87-23712
DE-AI01-82ER-60085 ..... N87-24053
DE-AI05-84ER-13150 ..... N87-23710
DE-AS03-76ET-53064 ..... N87-24190
N87-24191
DE-AS05-80ER-10641 ..... N87-24189
DE-AS05-80ER-10676 ..... N87-24184
DE-AS05-80RA-50159 ..... N87-24158
DE-AS08-84DP-40197 ..... N87-23940
DE-FC08-85DP-40200 ..... N87-23947
DE-FC22-83FE-60149 ..... N87-23755
DE-FG02-84ER-13190 ..... N87-24134
DE-FG02-84ER-45060 ..... N87-23727
DE-FG02-84ER-45061 ..... N87-24223
DE-FG02-84ER-45070 ..... N87-24208
DE-FG02-84ER-45131 ..... N87-23919
DE-FG02-85ER-40214 ..... N87-24189
DE-FG02-85ER-40234 ..... N87-24388
DE-FG02-85ER-40235 ..... N87-24167
DE-FG02-85ER-45204 ..... N87-23749
DE-FG02-86ER-13570 ..... N87-23715
DE-FG03-85ER-25009 ..... N87-24092
DE-FG05-80ET-53088 ..... N87-23920
DE-FG05-84ER-13191 ..... N87-23950
DE-FG05-84ER-40157 ..... N87-24168
DE-FG05-84ER-45104 ..... N87-23739
DE-FG05-85ER-13362 ..... N87-24224
DE-FG05-86ER-13633 ..... N87-24020
DE-FG06-84ER-60269 ..... N87-24054
DE-FG22-85PC-80505 ..... N87-23756
DE-FG22-86PC-90959 ..... N87-24159
DTFA03-83-C-00018 ..... N87-23816
F04611-84-C-0024 ..... N87-23765
F04611-84-0019 ..... N87-23772
F04611-86-X-0006 ..... N87-23769
F04701-85-C-0086 ..... N87-23849
N87-24034
F19628-81-K-0051 ..... N87-24044
F19628-82-C-0111 ..... N87-23689
F19628-83-C-0056 ..... N87-23707
N87-23708
N87-24035
N87-24037
F19628-84-C-0038 ..... N87-23678
F19628-85-C-0002 ..... N87-23851
N87-24221
F19628-85-C-0006 ..... N87-23938
F19628-85-C-0035 ..... N87-23624
F19628-85-C-0090 ..... N87-23875
F19628-85-C-0101 ..... N87-23874
F19628-85-K-0006 ..... N87-24046
F29601-82-K-0024 ..... N87-23850
F33615-79-C-2050 ..... N87-23973
N87-23974
N87-23975
F33615-82-D-0627 ..... N87-24067
F33615-83-D-0602 ..... N87-24084
F33615-84-C-1423 ..... N87-24220
F33615-84-C-2435 ..... N87-23870
F49620-82-C-0004 ..... N87-23946
F49620-83-C-0019 ..... N87-23907
F49620-83-K-0009 ..... N87-23912
F49620-84-K-0002 ..... N87-23908
F49620-85-C-0043 ..... N87-24200
F49620-85-C-0144 ..... N87-24148
F49620-86-C-0024 ..... N87-23720
F49620-86-C-0041 ..... N87-24090
F49620-86-K-0010 ..... N87-23989
GR/B94953 ..... N87-23613
GRI-5082-211-0706 ..... N87-24043
GRI-5084-233-1039 ..... N87-23972
GRI-5085-800-1191 ..... N87-23742

GRI-5086-410-1230 ..... N87-24245
JPL-97582 ..... N87-24373
JPL-956290 ..... N87-24018
JPL-957249 ..... N87-24325
JPL-957317 ..... N87-24306
MDA903-80-C-0432 ..... N87-23672
MDA903-83-C-0335 ..... N87-23672
N87-23686
N87-23687
MDA903-84-K-0062 ..... N87-23672
MDA903-86-K-0220 ..... N87-23971
NAGW-249 ..... N87-24367
NAGW-577 ..... N87-24157
NAGW-761 ..... N87-24323
NAG1-517 ..... N87-24122
NAG2-134 ..... N87-24303
NAG2-276 ..... N87-23916
NAG2-315 ..... N87-24359
NAG2-401 ..... N87-23589
NAG3-337 ..... N87-24007
NAG3-553 ..... N87-24007
NAG3-593 ..... N87-23925
NAG3-3143 ..... N87-23977
NAG5-376 ..... N87-24252
NAG5-404 ..... N87-24301
NAG5-520 ..... N87-23980
NAG5-528 ..... N87-24042
NAG5-536 ..... N87-23855
NAG5-548 ..... N87-24010
NAG5-749 ..... N87-23980
NAG5-814 ..... N87-24038
NAG5-843 ..... N87-23670
NAG5-884 ..... N87-24211
NAG5-27571 ..... N87-23855
NAG8-089 ..... N87-23717
NAG8-498 ..... N87-24256
NAG8-500 ..... N87-24256
NAG8-502 ..... N87-24256
NASA ORDER L-76724-B N87-24162
NASA ORDER S-56107-D N87-24012
NASW-3166 ..... N87-24063
NASW-3502 ..... N87-24390
NASW-4005 ..... N87-23583
NAS1-16458 ..... N87-24040
NAS1-16475 ..... N87-23596
NAS1-17070 ..... N87-24107
N87-24122
NAS1-17719 ..... N87-23617
NAS1-17974 ..... N87-23607
NAS1-18107 ..... N87-24107
N87-24122
NAS1-18216 ..... N87-23663
NAS2-11125 ..... N87-24248
NAS2-12261 ..... N87-23856
NAS3-22901 ..... N87-23685
NAS3-23939 ..... N87-23622
NAS3-24068 ..... N87-23615
NAS3-24105 ..... N87-23729
NAS3-24666 ..... N87-23695
N87-23696
NAS5-28779 ..... N87-24031
N87-24032
NAS7-100 ..... N87-24018
NAS7-918 ..... N87-24305
NAS8-27976 ..... N87-24256
NAS8-27977 ..... N87-24256
NAS8-27978 ..... N87-24256
NAS8-34659 ..... N87-24184
NAS8-36548 ..... N87-23611
NATO-82-0592 ..... N87-24295
NATO-83/584 ..... N87-24322
NATO-0592/82 ..... N87-24325
NCC2-271 ..... N87-23627
NCC2-274 ..... N87-24103
NGL-14-001-001 ..... N87-24251
NGR05-002-160 ..... N87-24256
NGR21-002-316 ..... N87-24166
NGR24-005-050 ..... N87-24256
NGR26-008-001 ..... N87-24256
NSF AST-81-11711 ..... N87-24325
NSF AST-82-12252 ..... N87-24291
N87-24310
NSF AST-83-12699 ..... N87-24354
NSF AST-84-03054 ..... N87-24275
NSF AST-84-12473 ..... N87-24267
N87-24275
N87-24331
NSF AST-84-18197 ..... N87-24265
N87-24342
N87-24356
N87-24361
NSF AST-84-20374 ..... N87-24295
NSF AST-85-09907 ..... N87-24322
NSF AST-86-09907 ..... N87-24320
NSF DMS-84-10324 ..... N87-24142
NSF DMS-85-16191 ..... N87-24142
NSF ECS-83-20364 ..... N87-24119
NSF IST-87-05411 ..... N87-24238
NSF PHY-82-15249 ..... N87-24383
NSF PHY-83-06693 ..... N87-24383
NSF PHY-83-10654 ..... N87-24383
NSF PHY-84-05654 ..... N87-24383
NSG-3188 ..... N87-23969
NSG-5012 ..... N87-23858
NSG3-253 ..... N87-23979
N00014-75-C-0536 ..... N87-24216
N00014-75-C-0570 ..... N87-24153
N00014-75-C-0661 ..... N87-24109
N00014-76-C-0016 ..... N87-24248
N00014-79-C-0762 ..... N87-23783
N00014-80-C-0822 ..... N87-23853
N87-24109
N87-24110
N00014-81-K-0564 ..... N87-24138
N00014-81-K-0640 ..... N87-23745
N00014-82-K-0292 ..... N87-24149
N00014-82-K-0335 ..... N87-24049
N87-24123
N00014-83-C-0671 ..... N87-23846
N00014-83-F-0180 ..... N87-23846
N00014-83-G-0047 ..... N87-23799
N00014-83-K-0136 ..... N87-23924
N00014-83-K-0258 ..... N87-24009
N00014-83-K-0581 ..... N87-24218
N00014-84-C-0149 ..... N87-23852
N87-23889
N00014-84-C-0169 ..... N87-24147
N00014-84-C-0359 ..... N87-23802
N00014-84-K-0201 ..... N87-23728
N00014-84-K-0267 ..... N87-24049
N87-24123
N00014-84-K-0365 ..... N87-23715
N00014-84-K-0372 ..... N87-23800
N00014-84-K-0383 ..... N87-23804
N00014-84-K-0434 ..... N87-23795
N87-23796
N00014-84-K-0470 ..... N87-23803
N00014-84-K-0532 ..... N87-23848
N87-23890
N87-23891
N87-23892
N00014-84-K-0700 ..... N87-23806
N00014-85-C-2200 ..... N87-23884
N87-24389
N00014-85-K-0169 ..... N87-24141
N87-24142
N00014-85-K-0213 ..... N87-24108
N00014-85-K-0658 ..... N87-23805
N00014-86-F-0049 ..... N87-24385
N87-24386
N00014-86-K-0186 ..... N87-24066
N00014-86-K-0188 ..... N87-23953
N00014-86-K-0533 ..... N87-23847
N00014-86-K-0742 ..... N87-23854
N00014-86-K-0769 ..... N87-23748
N00014-86-WR-2C034 ..... N87-23782
N00014-87-C-0001 ..... N87-24151
N00019-84-WR-41049 ..... N87-23787
N00019-85-WR-51139 ..... N87-23787
N00024-85-C-5301 ..... N87-23757
N00039-83-C-0483 ..... N87-24237
N00039-84-C-0089 ..... N87-24112
N87-24152
N87-24230
N87-24231
N00039-85-C-0571 ..... N87-24237
N00228-84-C-3142 ..... N87-24048
N60530-83-C-0166 ..... N87-23793
N60530-86-WR-30021 ..... N87-23787
N87-23788
N62269-84-C-0243 ..... N87-23705
N87-23706
N62583-86-M-T167 ..... N87-23963
ONR-2-536403-SDI-1986 ..... N87-23807
USAFETAC/DS-87-036 ..... N87-24047
U0230 ..... N87-23997
W-31-109-ENG-38 ..... N87-23810
N87-23876
N87-24101
N87-24128
W-7405-ENG-36 ..... N87-23673
N87-23725
N87-23877
N87-23896
N87-23897
N87-23898
N87-23930
N87-23948
N87-23949
N87-23952
N87-23956
N87-24011
N87-24014
N87-24129
N87-24155
N87-24165
N87-24196
N87-24244
N87-24379
N87-24380
W-7405-ENG-48 ..... N87-23704
N87-23711
N87-23786
N87-23842
N87-23931
N87-23955
N87-23976
N87-24041
N87-24052
N87-24081
N87-24104
N87-24144
N87-24154
N87-24183
N87-24192
N87-24194
N87-24209
N87-24222
N87-24226
N87-24232
W-31109-ENG-38 ..... N87-23880
N87-23923
N87-23932
N87-24115
W7405-ENG-36 ..... N87-24170
YR0-2303 ..... N87-23963
199-13-46-1 ..... N87-24162
481-54-02 ..... N87-23690
485-40-02 ..... N87-23695
N87-23696
505-43-31 ..... N87-23616
505-45-58 ..... N87-23596
505-53-51 ..... N87-23994
505-60 ..... N87-23584
N87-24146
505-61-01-02 ..... N87-23594
N87-23663
505-61-41-01 ..... N87-23614
505-61-51-10 ..... N87-23596
505-62-3A N87-23662
505-62-3B N87-23664
505-62-11 ..... N87-23902
505-62-21 ..... N87-23921
N87-23933
N87-23936
N87-24132
505-62-22 ..... N87-23934
505-62-61-07 ..... N87-23592
N87-23597
505-62-91-01 ..... N87-23593
505-63-01 ..... N87-23729
505-63-01-01 ..... N87-23752
505-63-01-06 ..... N87-23991
505-63-11 ..... N87-23978
N87-23984
N87-24006
505-63-51 ..... N87-23969
N87-23977
505-66-11 ..... N87-24156
505-66-41-02 ..... N87-23607
505-66-41-05 ..... N87-23617
505-68-11 ..... N87-23591
505-68-91-09 ..... N87-23586
505-69-61 ..... N87-23626
505-90-21-01 ..... N87-24107
N87-24122
505-41-3A N87-24026
506-41-11 ..... N87-23901
506-41-21 ..... N87-23718
N87-24029
506-41-31 ..... N87-23903
506-42-31 ..... N87-23691
N87-23692
N87-23693
N87-23821
506-43-61 ..... N87-23995
506-44-21 ..... N87-23900
506-45-31 ..... N87-24378
506-49-31-01 ..... N87-23687
533-02-21 ..... N87-23619
533-04-11 ..... N87-23622
533-43-11 ..... N87-23987
535-03-01 ..... N87-23625
535-03-11-01 ..... N87-24160
535-03-11-03 ..... N87-24161
535-05-01 ..... N87-23623
N87-23624
553-13-80 ..... N87-24007

673-62-02-70 ..... N87-24040
674-26-05 ..... N87-23760
917-60-01 ..... N87-23665
992-21-01 ..... N87-23632

Typical Report Number Index Listing

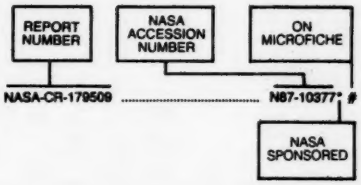

Listings in this index are arranged alphanumerically by report number. The NASA accession number denotes the number by which the citation is identified. An asterisk (*) indicates that the item is a NASA report. A pound sign (#) indicates that the item is available on microfiche.

A-1642 ..... N87-23858* #
A-86037 ..... N87-24064* #
A-86424 ..... N87-24146* #
A-87031 ..... N87-24391* #
A-87073 ..... N87-23632* #
A-87158 ..... N87-24156* #
A-87202 ..... N87-23584* #
A-87236 ..... N87-24145* #

AD-A168315 ..... N87-24131 #
AD-A171082 ..... N87-23585 #
AD-A177873 ..... N87-23884 #
AD-A177874 ..... N87-24062 #
AD-A177875 ..... N87-23667 #
AD-A177881 ..... N87-23885 #
AD-A177886 ..... N87-23866 #
AD-A177888 ..... N87-24225 #
AD-A177889 ..... N87-23728 #
AD-A177893 ..... N87-23971 #
AD-A177931 ..... N87-24055 #
AD-A177934 ..... N87-23887 #
AD-A177937 ..... N87-24389 #
AD-A177939 ..... N87-24106 #
AD-A177941 ..... N87-23612 #
AD-A177942 ..... N87-24215 #
AD-A177943 ..... N87-24136 #
AD-A177944 ..... N87-24120 #
AD-A177945 ..... N87-23844 #
AD-A177947 ..... N87-24137 #
AD-A177948 ..... N87-23586 #
AD-A177949 ..... N87-24237 #
AD-A177976 ..... N87-24063 #
AD-A177981 ..... N87-24025 #
AD-A177993 ..... N87-24000 #
AD-A177996 ..... N87-23973 #
AD-A178001 ..... N87-23716 #
AD-A178002 ..... N87-24084 #
AD-A178012 ..... N87-24216 #
AD-A178030 ..... N87-24149 #
AD-A178040 ..... N87-23888 #
AD-A178061 ..... N87-24087 #
AD-A178064 ..... N87-24217 #
AD-A178066 ..... N87-23845 #
AD-A178094 ..... N87-23974 #
AD-A178095 ..... N87-23975 #
AD-A178097 ..... N87-23743 #
AD-A178106 ..... N87-23953 #
AD-A178112 ..... N87-24088 #
AD-A178115 ..... N87-23744 #
AD-A178117 ..... N87-24246 #
AD-A178119 ..... N87-24057 #
AD-A178141 ..... N87-23846 #
AD-A178150 ..... N87-23889 #
AD-A178153 ..... N87-23745 #
AD-A178158 ..... N87-24218 #
AD-A178169 ..... N87-24182 #
AD-A178175 ..... N87-24219 #
AD-A178180 ..... N87-23847 #
AD-A178196 ..... N87-24138 #
AD-A178206 ..... N87-23814 #
AD-A178207 ..... N87-24044 #

AD-A178212 ..... N87-23890 #
AD-A178213 ..... N87-23848 #
AD-A178214 ..... N87-23891 #
AD-A178217 ..... N87-23892 #
AD-A178222 ..... N87-24139 #
AD-A178223 ..... N87-24140 #
AD-A178225 ..... N87-24106 #
AD-A178227 ..... N87-23746 #
AD-A178231 ..... N87-23694 #
AD-A178237 ..... N87-23849 #
AD-A178246 ..... N87-24239 #
AD-A178258 ..... N87-23850 #
AD-A178259 ..... N87-24150 #
AD-A178262 ..... N87-24220 #
AD-A178264 ..... N87-23924 #
AD-A178267 ..... N87-23851 #
AD-A178285 ..... N87-23852 #
AD-A178286 ..... N87-23853 #
AD-A178287 ..... N87-24109 #
AD-A178296 ..... N87-24001 #
AD-A178298 ..... N87-23954 #
AD-A178302 ..... N87-24061 #
AD-A178307 ..... N87-23600 #
AD-A178308 ..... N87-23601 #
AD-A178325 ..... N87-24151 #
AD-A178350 ..... N87-24085 #
AD-A178354 ..... N87-24089 #
AD-A178362 ..... N87-24141 #
AD-A178367 ..... N87-23672 #
AD-A178372 ..... N87-23854 #
AD-A178381 ..... N87-24393 #
AD-A178390 ..... N87-24142 #
AD-A178394 ..... N87-24221 #
AD-A178395 ..... N87-23590 #
AD-A178403 ..... N87-24110 #
AD-A178405 ..... N87-23855* #
AD-A178467 ..... N87-23875 #
AD-A178605 ..... N87-24050 #
AD-A178875 ..... N87-24178 #
AD-A179007 ..... N87-24097 #
AD-A179061 ..... N87-23868 #
AD-A179067 ..... N87-24229 #
AD-A179073 ..... N87-23869 #
AD-A179086 ..... N87-23870 #
AD-A179094 ..... N87-23822 #
AD-A179106 ..... N87-23677 #
AD-A179107 ..... N87-24173 #
AD-A179108 ..... N87-24095 #
AD-A179109 ..... N87-23700 #
AD-A179110 ..... N87-23871 #
AD-A179111 ..... N87-23968 #
AD-A179112 ..... N87-23701 #
AD-A179121 ..... N87-23719 #
AD-A179134 ..... N87-24200 #
AD-A179136 ..... N87-24034 #
AD-A179139 ..... N87-24065 #
AD-A179158 ..... N87-23757 #
AD-A179170 ..... N87-23823 #
AD-A179176 ..... N87-24045 #
AD-A179179 ..... N87-23963 #
AD-A179182 ..... N87-24066 #
AD-A179183 ..... N87-23678 #
AD-A179185 ..... N87-24048 #
AD-A179190 ..... N87-23824 #
AD-A179206 ..... N87-23905 #
AD-A179207 ..... N87-23679 #
AD-A179209 ..... N87-23906 #
AD-A179210 ..... N87-23628 #
AD-A179212 ..... N87-24186 #
AD-A179220 ..... N87-23945 #
AD-A179222 ..... N87-23888 #
AD-A179223 ..... N87-24067 #
AD-A179226 ..... N87-23946 #
AD-A179227 ..... N87-23672 #
AD-A179229 ..... N87-23629 #
AD-A179230 ..... N87-24201 #
AD-A179231 ..... N87-24202 #
AD-A179233 ..... N87-23680 #
AD-A179235 ..... N87-23681 #
AD-A179241 ..... N87-23682 #
AD-A179242 ..... N87-24047 #
AD-A179246 ..... N87-23907 #
AD-A179247 ..... N87-23908 #

AD-A179255 ..... N87-24147 #
AD-A179256 ..... N87-24048 #
AD-A179257 ..... N87-23689 #
AD-A179258 ..... N87-24035 #
AD-A179259 ..... N87-23873 #
AD-A179263 ..... N87-23599 #
AD-A179264 ..... N87-23989 #
AD-A179267 ..... N87-24148 #
AD-A179268 ..... N87-23720 #
AD-A179287 ..... N87-23874 #
AD-A179306 ..... N87-24230 #
AD-A179327 ..... N87-24231 #
AD-A179328 ..... N87-24152 #
AD-A179329 ..... N87-24112 #
AD-A179331 ..... N87-24265 #
AD-A179355 ..... N87-24153 #
AD-A179360 ..... N87-24096 #
AD-A179361 ..... N87-24123 #
AD-A179372 ..... N87-23937 #
AD-A179374 ..... N87-24036 #
AD-A179393 ..... N87-24049 #
AD-A179394 ..... N87-24174 #
AD-A179403 ..... N87-23707 #
AD-A179413 ..... N87-23668 #
AD-A179430 ..... N87-23708 #
AD-A179437 ..... N87-23825 #
AD-A179444 ..... N87-24187 #
AD-A179446 ..... N87-23826 #
AD-A179447 ..... N87-24118 #
AD-A179449 ..... N87-24119 #
AD-A179454 ..... N87-24175 #
AD-A179455 ..... N87-23909 #
AD-A179456 ..... N87-23910 #
AD-A179458 ..... N87-23730 #
AD-A179459 ..... N87-23683 #
AD-A179461 ..... N87-24009 #
AD-A179476 ..... N87-24176 #
AD-A179477 ..... N87-23911 #
AD-A179492 ..... N87-23938 #
AD-A179500 ..... N87-23912 #
AD-A179505 ..... N87-24203 #
AD-A179506 ..... N87-23913 #
AD-A179507 ..... N87-23684 #
AD-A179510 ..... N87-24113 #
AD-A179511 ..... N87-23914 #
AD-A179515 ..... N87-24090 #
AD-A179539 ..... N87-24037 #
AD-A179544 ..... N87-23709 #
AD-A179545 ..... N87-24382 #
AD-A179547 ..... N87-23721 #
AD-A179571 ..... N87-24124 #
AD-A179607 ..... N87-23915 #
AD-A179615 ..... N87-23827 #
AD-A179617 ..... N87-24204 #
AD-A179620 ..... N87-24068 #
AD-A179627 ..... N87-24069 #
AD-A179673 ..... N87-23618 #
AD-A179679 ..... N87-24177 #

AD-E950921 ..... N87-23728 #
AD-E950921 ..... N87-23885 #
AD-E950921 ..... N87-23886 #
AD-E950921 ..... N87-23971 #
AD-E950921 ..... N87-24225 #
AD-E950935 ..... N87-24216 #

AE-85-2 ..... N87-23915 #

AEDC-TR-86-44 ..... N87-23590 #

AEDC-TSR-86-V57 ..... N87-23599 #

AERE-R-12025 ..... N87-23699 #

AFGL-IP-332 ..... N87-23694 #

AFGL-TR-86-242 ..... N87-23689 #
AFGL-TR-86-0011 ..... N87-24045 #
AFGL-TR-86-0162 ..... N87-23707 #
AFGL-TR-86-0214 ..... N87-23678 #
AFGL-TR-86-0217 ..... N87-23874 #
AFGL-TR-86-0243 ..... N87-23855* #
AFGL-TR-86-0260 ..... N87-24044 #

AFGL-TR-86-0269 ..... N87-23824 #
AFGL-TR-87-0009 ..... N87-24035 #
AFGL-TR-87-0010 ..... N87-24037 #
AFGL-TR-87-0015 ..... N87-24046 #
AFGL-TR-87-0016 ..... N87-23708 #
AFGL-TR-87-0030 ..... N87-23938 #
AFGL-TR-860109 ..... N87-23694 #

AFGWC/TN-86/002 ..... N87-24055 #

AFIT/CI/NR-87-28T ..... N87-24057 #

AFIT/GA/AA/86D-2 ..... N87-23681 #
AFIT/GA/AA/86D-4 ..... N87-23906 #
AFIT/GA/AA/86D-9 ..... N87-23905 #
AFIT/GA/AA/86D-11 ..... N87-23679 #
AFIT/GA/AA/86D-12 ..... N87-23668 #

AFIT/GAE/AA/86D-9 ..... N87-23968 #
AFIT/GAE/AA/86D-10 ..... N87-23700 #
AFIT/GAE/AA/86D-13 ..... N87-23913 #
AFIT/GAE/AA/86D-15 ..... N87-23911 #
AFIT/GAE/AA/86D-17 ..... N87-23914 #
AFIT/GAE/AA/86D-18 ..... N87-23701 #
AFIT/GAE/AA/86J-1 ..... N87-23629 #

AFIT/GCE/ENG/86D-1 ..... N87-24120 #
AFIT/GCE/ENG/86D-10 ..... N87-24106 #

AFIT/GCS/ENG/86D-15 ..... N87-23669 #
AFIT/GCS/ENG/87M-1 ..... N87-24095 #

AFIT/GE/ENG/86D-5 ..... N87-24219 #
AFIT/GE/ENG/86D-9 ..... N87-23612 #
AFIT/GE/ENG/86D-11 ..... N87-24201 #
AFIT/GE/ENG/86D-21 ..... N87-23671 #
AFIT/GE/ENG/86D-39 ..... N87-24215 #
AFIT/GE/ENG/86D-54 ..... N87-23844 #
AFIT/GE/ENG/86D-55 ..... N87-24178 #
AFIT/GE/ENG/86D-59 ..... N87-24135 #
AFIT/GE/ENG/87M-1 ..... N87-24176 #
AFIT/GE/ENG/87M-5 ..... N87-24113 #
AFIT/GE/ENG/87M-6 ..... N87-23628 #

AFIT/GEP/ENP/86D-3 ..... N87-24186 #
AFIT/GEP/ENP/86D-6 ..... N87-24203 #

AFIT/GNE/ENP/87M-3 ..... N87-24173 #
AFIT/GNE/ENP/87M-5 ..... N87-24202 #

AFIT/GSO/AA/86D-1 ..... N87-23664 #
AFIT/GSO/AA/86D-2 ..... N87-23677 #
AFIT/GSO/AA/86D-5 ..... N87-23680 #

AFIT/GSO/ENS/86D-3 ..... N87-23682 #

AFOSR-85-0376-001 ..... N87-24204 #
AFOSR-87-0082TR ..... N87-24182 #
AFOSR-87-0166TR ..... N87-23667 #
AFOSR-87-0234TR ..... N87-24139 #
AFOSR-87-0294TR ..... N87-23668 #
AFOSR-87-0310TR ..... N87-23720 #
AFOSR-87-0313TR ..... N87-23969 #
AFOSR-87-0314TR ..... N87-24200 #
AFOSR-87-0315TR ..... N87-23907 #
AFOSR-87-0316TR ..... N87-23908 #
AFOSR-87-0336TR ..... N87-24148 #
AFOSR-87-0339TR ..... N87-23946 #
AFOSR-87-0364TR ..... N87-23912 #
AFOSR-87-0366TR ..... N87-23915 #
AFOSR-87-0395TR ..... N87-23909 #
AFOSR-87-0402TR ..... N87-23683 #
AFOSR-87-0405TR ..... N87-24124 #
AFOSR-87-0409TR ..... N87-23730 #
AFOSR-87-0421TR ..... N87-23721 #
AFOSR-87-0424TR ..... N87-23910 #
AFOSR-87-0433TR ..... N87-24204 #
AFOSR-87-0435TR ..... N87-24069 #
AFOSR-87-0453TR ..... N87-24090 #
AFOSR-87-0477TR ..... N87-24187 #
AFOSR-87-0478TR ..... N87-23937 #
AFOSR-87-0481TR ..... N87-23673 #
AFOSR-87-0497TR ..... N87-24362 #
AFOSR-87-0503TR ..... N87-24265 #
AFOSR-87-0512TR ..... N87-23826 #
AFOSR-87-0522TR ..... N87-24036 #
AFOSR-87-0523TR ..... N87-23709 #
AFOSR-87-0533TR ..... N87-24068 #
AFOSR-87-0548TR ..... N87-24177 #
AFOSR-87-0556TR ..... N87-24175 #

AFWAL-TR-82-2112-PT-2 ..... N87-23974 #
AFWAL-TR-82-2112-PT-3 ..... N87-23975 #
AFWAL-TR-82-2112-PT-4 ..... N87-23973 #
AFWAL-TR-86-1181 ..... N87-24220 #
AFWAL-TR-86-2114 ..... N87-23870 #

AFWL-TN-86-29 ..... N87-23850 #

AGARD-AR-236 ..... N87-23608 #

AGARD-CP-406 ..... N87-23633 #

AGARD-LS-151 ..... N87-23859 #

AGARD-R-739 ..... N87-23609 #
AGARD-R-758 ..... N87-24070 #

AIAA-PAPER-85-1877 ..... N87-23619* #

AIAA-87-0355 ..... N87-24132* #
AIAA-87-1557 ..... N87-23685* #
AIAA-87-1742 ..... N87-23625* #
AIAA-87-1745 ..... N87-23623* #
AIAA-87-1828 ..... N87-23624* #
AIAA-87-1886 ..... N87-23684* #
AIAA-87-1903 ..... N87-23692* #
AIAA-87-2050 ..... N87-23626* #
AIAA-87-2120 ..... N87-23621* #
AIAA-87-2122 ..... N87-23693* #
AIAA-87-9226 ..... N87-24026* #
AIAA-87-9262 ..... N87-24029* #
AIAA-87-9314 ..... N87-23903* #
AIAA-87-9353 ..... N87-23690* #

ANL-86-48 ..... N87-23923 #
ANL-87-7 ..... N87-24115 #

ANL/FE-86-5 ..... N87-23932 #

ANL/MCS-TM-81 ..... N87-24101 #

APR-2 ..... N87-24193 #

AR-10 ..... N87-23966 #

ASR-2 ..... N87-23622* #

ATR-86(B139)-3 ..... N87-24205 #

AVSCOM-TM-87-A-1 ..... N87-23632* #
AVSCOM-TM-87-B-3 ..... N87-23991* #

AVSCOM-TR-87-C-8 ..... N87-23624* #
AVSCOM-TR-87-C-13 ..... N87-23969* #
AVSCOM-TR-87-C-16 ..... N87-23977* #
AVSCOM-TR-87-C-20 ..... N87-23729* #
AVSCOM-TR-87-C-21 ..... N87-23623* #

A86409 ..... N87-23595* #

BBC-RD-1987/4 ..... N87-23942

BDX-613-3741 ..... N87-24133 #

BN-1056 ..... N87-24142 #
BN-1059 ..... N87-24141 #

BNL-38789 ..... N87-24179 #
BNL-39426 ..... N87-24060 #

BRL-MR-3532 ..... N87-23585 #

BRL-TR-2727 ..... N87-24131 #

B8677593 ..... N87-23685 #
B8677594 ..... N87-23686 #

CAL-1629 ..... N87-24265 #

CAR-8705 ..... N87-23613 #

CERL-N-87/06 ..... N87-24087 #

CERL-TR-N-87/07 ..... N87-24088 #

CESAR-86/59 ..... N87-23964 #
CESAR-87/09P ..... N87-24121 #

CISR-M010-8702-21 ..... N87-24237 #

CLASSIC-87-15 ..... N87-24049 #
CLASSIC-87-16 ..... N87-24123 #

CMU-RI-TR-87-4 ..... N87-24119 #
CMU-RI-TR-87-5 ..... N87-24118 #

CMW-87-P-2 ..... N87-23873 #

CONF-860510-17-REV ..... N87-23669 #
CONF-860529-69 ..... N87-24172 #
CONF-860758-2 ..... N87-24104 #
CONF-860829-41 ..... N87-23817 #

CONF-861068-18 ..... N87-23880 #
CONF-861207-93 ..... N87-23724 #
CONF-861207-94 ..... N87-23733 #
CONF-861207-95 ..... N87-24206 #
CONF-861207-96 ..... N87-23734 #
CONF-861207-97 ..... N87-23952 #
CONF-861230-6 ..... N87-23754 #
CONF-861240-15 ..... N87-23841 #
CONF-861240-16 ..... N87-24194 #
CONF-861264-2 ..... N87-24379 #
CONF-870132-102 ..... N87-24209 #
CONF-870134-2 ..... N87-23964 #
CONF-870163-1 ..... N87-24143 #
CONF-870167-1 ..... N87-24210 #
CONF-870249-4 ..... N87-24236 #
CONF-870254-3 ..... N87-23738 #
CONF-870271-1 ..... N87-23948 #
CONF-870277-1 ..... N87-24117 #
CONF-870302-30 ..... N87-23897 #
CONF-870302-45 ..... N87-23673 #
CONF-870302-48 ..... N87-23956 #
CONF-870302-49 ..... N87-23896 #
CONF-870302-61 ..... N87-23877 #
CONF-870302-63 ..... N87-24196 #
CONF-870304-5 ..... N87-24023 #
CONF-870307-16 ..... N87-24016 #
CONF-870385-4 ..... N87-24212 #
CONF-870385-7 ..... N87-24207 #
CONF-870388-5 ..... N87-24214 #
CONF-870410-3 ..... N87-23703 #
CONF-870410-11 ..... N87-24030 #
CONF-870414-1 ..... N87-24041 #
CONF-870416-5 ..... N87-24244 #
CONF-870446-1 ..... N87-24002 #
CONF-870482-2 ..... N87-23992 #
CONF-870486-2 ..... N87-23883 #
CONF-870492-1 ..... N87-24129 #
CONF-870513-3 ..... N87-23723 #
CONF-870516-7 ..... N87-23957 #
CONF-870533-1 ..... N87-23918 #
CONF-870533-2 ..... N87-23731 #
CONF-870533-3 ..... N87-23732 #
CONF-870567-1 ..... N87-24092 #
CONF-870576-1 ..... N87-24014 #
CONF-870576-2 ..... N87-24011 #
CONF-870584-1 ..... N87-24180 #
CONF-870637-2 ..... N87-24222 #
CONF-870665-1 ..... N87-24003 #
CONF-870665-3 ..... N87-24004 #
CONF-870668-1 ..... N87-23955 #
CONF-870674-1 ..... N87-23894 #
CONF-870674-2 ..... N87-23747 #
CONF-870674-3 ..... N87-23895 #
CONF-870676-1 ..... N87-23943 #
CONF-870677-1 ..... N87-24144 #
CONF-870697-1 ..... N87-24005 #
CONF-8604292-2 ..... N87-24183 #
CONF-8605182-4 ..... N87-24383 #
CONF-8606157-4 ..... N87-23951 #
CONF-8606279 ..... N87-24062 #
CONF-8606292-1 ..... N87-24213 #
CONF-8607113-2 ..... N87-24226 #
CONF-8607121-1 ..... N87-24226 #
CONF-8608102-SUMM ..... N87-24179 #
CONF-8608153-3 ..... N87-23722 #
CONF-8608164-1 ..... N87-24128 #
CONF-8608172-1 ..... N87-24154 #
CONF-8609203 ..... N87-24060 #
CONF-8609269-1 ..... N87-23711 #
CONF-8610122-11 ..... N87-23876 #
CONF-8610138 ..... N87-24116 #
CONF-8610207-3 ..... N87-24380 #
CONF-8610255-1 ..... N87-24232 #
CONF-8610268-1 ..... N87-23976 #
CONF-8611146-1 ..... N87-24052 #
CONF-8703110-1 ..... N87-24105 #
CONF-8704101-1 ..... N87-24028 #
CONF-8704101-2 ..... N87-23881 #

CPIA-PUBL-457 ..... N87-23757

CRC-1408 ..... N87-23845 #

CRM-86-265 ..... N87-24151 #

CSE/86-108 ..... N87-23707 #
CSE/86-120 ..... N87-24035 #
CSE/86-139 ..... N87-24037 #

CSG-63 ..... N87-23689 #

DE86-010728 ..... N87-24027 #
DE86-010739 ..... N87-23753 #
DE87-000453 ..... N87-23918 #
DE87-000922 ..... N87-23722 #
DE87-000960 ..... N87-23731 #

DE87-000984 ..... N87-23732 #
DE87-001109 ..... N87-24015 #
DE87-001135 ..... N87-24022 #
DE87-001155 ..... N87-24023 #
DE87-001156 ..... N87-24024 #
DE87-001237 ..... N87-23755 #
DE87-002065 ..... N87-24383 #
DE87-002155 ..... N87-24179 #
DE87-002383 ..... N87-24041 #
DE87-002489 ..... N87-23703 #
DE87-002898 ..... N87-24002 #
DE87-002939 ..... N87-23922 #
DE87-003096 ..... N87-24016 #
DE87-003505 ..... N87-23841 #
DE87-003516 ..... N87-23723 #
DE87-003518 ..... N87-24194 #
DE87-003752 ..... N87-24380 #
DE87-004211 ..... N87-23754 #
DE87-004271 ..... N87-24030 #
DE87-004634 ..... N87-24051 #
DE87-004731 ..... N87-23951 #
DE87-004777 ..... N87-24017 #
DE87-004822 ..... N87-23876 #
DE87-004837 ..... N87-23880 #
DE87-004922 ..... N87-24143 #
DE87-005029 ..... N87-24092 #
DE87-005094 ..... N87-24195 #
DE87-005115 ..... N87-23952 #
DE87-005547 ..... N87-24235 #
DE87-005574 ..... N87-23923 #
DE87-005681 ..... N87-24224 #
DE87-005719 ..... N87-23964 #
DE87-005841 ..... N87-24183 #
DE87-005869 ..... N87-23894 #
DE87-005873 ..... N87-24003 #
DE87-005878 ..... N87-23992 #
DE87-005895 ..... N87-24167 #
DE87-005920 ..... N87-23947 #
DE87-005950 ..... N87-23710 #
DE87-006059 ..... N87-24011 #
DE87-006060 ..... N87-24014 #
DE87-006085 ..... N87-24052 #
DE87-006117 ..... N87-24018* #
DE87-006144 ..... N87-23669 #
DE87-006154 ..... N87-24172 #
DE87-006245 ..... N87-23955 #
DE87-006324 ..... N87-23930 #
DE87-006350 ..... N87-24188 #
DE87-006361 ..... N87-24189 #
DE87-006369 ..... N87-24168 #
DE87-006421 ..... N87-24062 #
DE87-006632 ..... N87-24180 #
DE87-006685 ..... N87-24226 #
DE87-006701 ..... N87-24004 #
DE87-006704 ..... N87-24005 #
DE87-006750 ..... N87-24080 #
DE87-006824 ..... N87-24144 #
DE87-006826 ..... N87-24222 #
DE87-006828 ..... N87-24232 #
DE87-006890 ..... N87-24212 #
DE87-006903 ..... N87-24053 #
DE87-006940 ..... N87-24236 #
DE87-006959 ..... N87-23943 #
DE87-006968 ..... N87-24128 #
DE87-007020 ..... N87-23747 #
DE87-007022 ..... N87-23895 #
DE87-007031 ..... N87-24158 #
DE87-007099 ..... N87-23842 #
DE87-007161 ..... N87-24019 #
DE87-007181 ..... N87-24206 #
DE87-007308 ..... N87-24388 #
DE87-007309 ..... N87-23715 #
DE87-007320 ..... N87-24164 #
DE87-007334 ..... N87-23711 #
DE87-007347 ..... N87-23843 #
DE87-007387 ..... N87-23738 #
DE87-007390 ..... N87-23724 #
DE87-007400 ..... N87-24159 #
DE87-007406 ..... N87-23739 #
DE87-007408 ..... N87-24020 #
DE87-007452 ..... N87-23956 #
DE87-007457 ..... N87-23896 #
DE87-007459 ..... N87-23673 #
DE87-007461 ..... N87-23897 #
DE87-007468 ..... N87-24379 #
DE87-007493 ..... N87-24196 #
DE87-007497 ..... N87-24244 #
DE87-007499 ..... N87-23877 #
DE87-007501 ..... N87-23948 #
DE87-007508 ..... N87-24129 #
DE87-007515 ..... N87-23712 #
DE87-007540 ..... N87-23919 #
DE87-007576 ..... N87-23881 #
DE87-007578 ..... N87-23748 #
DE87-007579 ..... N87-23733 #
DE87-007616 ..... N87-23817 #
DE87-007657 ..... N87-24028 #
DE87-007659 ..... N87-24207 #
DE87-007708 ..... N87-23898 #
DE87-007711 ..... N87-23949 #
DE87-007718 ..... N87-23725 #
DE87-007719 ..... N87-24155 #
DE87-007756 ..... N87-23882 #
DE87-007760 ..... N87-24165 #
DE87-007784 ..... N87-24093 #
DE87-007788 ..... N87-23965 #
DE87-007789 ..... N87-24121 #
DE87-007793 ..... N87-23966 #
DE87-007794 ..... N87-24100 #
DE87-007802 ..... N87-24233 #
DE87-007823 ..... N87-23993 #
DE87-007824 ..... N87-24094 #
DE87-007825 ..... N87-23967 #
DE87-007846 ..... N87-23734 #
DE87-007859 ..... N87-24105 #
DE87-007882 ..... N87-24021 #
DE87-007883 ..... N87-24234 #
DE87-007897 ..... N87-23735 #
DE87-007912 ..... N87-24116 #
DE87-007913 ..... N87-24101 #
DE87-007936 ..... N87-23940 #
DE87-007938 ..... N87-23950 #
DE87-007946 ..... N87-24059 #
DE87-007947 ..... N87-24130 #
DE87-007954 ..... N87-24115 #
DE87-008018 ..... N87-23878 #
DE87-008021 ..... N87-24208 #
DE87-008046 ..... N87-24133 #
DE87-008054 ..... N87-23920 #
DE87-008078 ..... N87-23857 #
DE87-008079 ..... N87-24102 #
DE87-008151 ..... N87-24104 #
DE87-008179 ..... N87-24054 #
DE87-008193 ..... N87-24190 #
DE87-008194 ..... N87-24191 #
DE87-008213 ..... N87-24209 #
DE87-008217 ..... N87-24210 #
DE87-008228 ..... N87-24213 #
DE87-008229 ..... N87-24117 #
DE87-008240 ..... N87-24169 #
DE87-008242 ..... N87-24134 #
DE87-008276 ..... N87-24193 #
DE87-008337 ..... N87-23704 #
DE87-008338 ..... N87-23931 #
DE87-008343 ..... N87-24058 #
DE87-008345 ..... N87-23714 #
DE87-008346 ..... N87-24181 #
DE87-008347 ..... N87-23726 #
DE87-008350 ..... N87-23966 #
DE87-008351 ..... N87-23985 #
DE87-008361 ..... N87-23727 #
DE87-008399 ..... N87-24135 #
DE87-008485 ..... N87-24192 #
DE87-008519 ..... N87-23883 #
DE87-008530 ..... N87-23749 #
DE87-008536 ..... N87-24081 #
DE87-008538 ..... N87-23740 #
DE87-008548 ..... N87-23697 #
DE87-008593 ..... N87-24214 #
DE87-008696 ..... N87-23756 #
DE87-008730 ..... N87-23976 #
DE87-008731 ..... N87-24154 #
DE87-008787 ..... N87-23957 #
DE87-008882 ..... N87-24197 #
DE87-008885 ..... N87-23741 #
DE87-008942 ..... N87-24223 #
DE87-009092 ..... N87-23899 #
DE87-009103 ..... N87-23958 #
DE87-009104 ..... N87-23986 #
DE87-009254 ..... N87-23932 #

DOD-7750.5-M ..... N87-24227 #

DOE/AL-33183/T1 ..... N87-23922 #

DOE/CE-0179 ..... N87-23968 #

DOE/CH-10093/3 ..... N87-24015 #

DOE/DP-40197/1 ..... N87-23940 #
DOE/DP-40200/37 ..... N87-23947 #

DOE/ER-10641/5 ..... N87-24189 #
DOE/ER-10676/9 ..... N87-24164 #
DOE/ER-10942/T1 ..... N87-23727 #
DOE/ER-13150/3 ..... N87-23710 #
DOE/ER-13190/3 ..... N87-24134 #
DOE/ER-13191/7 ..... N87-23950 #
DOE/ER-13362/2 ..... N87-24224 #
DOE/ER-13570/1 ..... N87-23715 #
DOE/ER-13633/1 ..... N87-24020 #
DOE/ER-25009/391 ..... N87-24092 #
DOE/ER-40157/T1 ..... N87-24168 #
DOE/ER-40214/2 ..... N87-24169 #
DOE/ER-40234/2 ..... N87-24386 #
DOE/ER-40235/T2 ..... N87-24167 #
DOE/ER-45061/1 ..... N87-24223 #
DOE/ER-45070/2 ..... N87-24208 #
DOE/ER-45104/3 ..... N87-23739 #
DOE/ER-45131/4 ..... N87-23919 #
DOE/ER-45204/T1 ..... N87-23749 #
DOE/ER-53096/T1 ..... N87-24195 #
DOE/ER-60065/H1 ..... N87-24053 #
DOE/ER-60269/5 ..... N87-24054 #

DOE/ET-53068/261 ..... N87-23920 #

DOE/JPL-7006117 ..... N87-24018* #

DOE/NBM-7008276 ..... N87-24193 #

DOE/NV-10336/1 ..... N87-23882 #

DOE/OR-00033/T285 ..... N87-24188 #

DOE/PC-80505/T6 ..... N87-23756 #
DOE/PC-90959/T1 ..... N87-24159 #

DOE/RA-50150/23 ..... N87-23878 #
DOE/RA-50159/T2 ..... N87-24158 #

DOE/TIC-4584-R7 ..... N87-24235 #

DOT-TSC-CG-85-3-VOL-2 ..... N87-23600 #
DOT-TSC-CG-85-3-VOL-3 ..... N87-23601 #

DOT/FAA/CT-86/6 ..... N87-23816 #
DOT/FAA/CT-86/39-VOL-1 ..... N87-23705 #
DOT/FAA/CT-86/39-VOL-2 ..... N87-23706 #
DOT/FAA/CT-86/40 ..... N87-23858* #
DOT/FAA/CT-87/05 ..... N87-23815 #

DOT/FAA/PM-86/48 ..... N87-23661 #

DPST-87-203 ..... N87-23712 #

DREA-TM-87/202 ..... N87-24001 #

DTNSRDC/SME-86-31 ..... N87-24000 #

D6-53840 ..... N87-23856* #

E-2688 ..... N87-23598* #
E-3142 ..... N87-23662* #
E-3184 ..... N87-23936* #
E-3186 ..... N87-23921* #
E-3313 ..... N87-23933* #
E-3364 ..... N87-24132* #
E-3372 ..... N87-23934* #
E-3415 ..... N87-24006* #
E-3449 ..... N87-23902* #
E-3473 ..... N87-23685* #
E-3474 ..... N87-23591* #
E-3529 ..... N87-23718* #
E-3530 ..... N87-23674* #
E-3543 ..... N87-23900* #
E-3552 ..... N87-23984* #
E-3563 ..... N87-24026* #
E-3571 ..... N87-23729* #
E-3587 ..... N87-23978* #
E-3588 ..... N87-23903* #
E-3599 ..... N87-23750* #
E-3609 ..... N87-23693* #
E-3614 ..... N87-23664* #
E-3620 ..... N87-23901* #
E-3629 ..... N87-23690* #
E-3631 ..... N87-24029* #
E-3632 ..... N87-23967* #
E-3636 ..... N87-24007* #
E-3641 ..... N87-23892* #
E-3645 ..... N87-23691* #
E-3647 ..... N87-23624* #
E-3657 ..... N87-23821* #
E-3659 ..... N87-23626* #
E-3660 ..... N87-23623* #
E-3662 ..... N87-23625* #

ENST-86C001 ..... N87-24111 #
ENST-86D004 ..... N87-24086 #

ER-6129 ..... N87-23972 #

ERIM-189400-21-L ..... N87-24032* #
ERIM-193600-1-F ..... N87-24246 #
ERIM-198400-19-L ..... N87-24031* #

ERL-0300-TR ..... N87-24174 #
ERL-0381-TR ..... N87-23825 #

ESD-T-86-096 N87-23851 #
ESD-TR-86-99 N87-24221 #
ESD-5-606 N87-24045 #
ETN-87-99588 N87-24199 #
ETN-87-99590 N87-23665 #
ETN-87-99591 N87-23666 #
ETN-87-99606 N87-24111 #
ETN-87-99608 N87-24086 #
ETN-87-99642 N87-23935 #
ETN-87-99643 N87-23686 #
ETN-87-99645 N87-24008 #
ETN-87-99665 N87-24226 #
ETN-87-99666 N87-23602 #
ETN-87-99767 N87-24163 #
ETN-87-99785 N87-24185 #
ETN-87-99913 N87-24033 #
FR-2 N87-23617* #
FSR-DR-15 N87-23695* #
FSR-DR-15 N87-23696* #
FTD-ID(RS)T-0012-87 N87-23688 #
FTD-ID(RS)T-1218-86 N87-24393 #
FTD-ID(RS)T-1246-85 N87-23618 #
GA-A-18692 N87-24197 #
GPO-74-463 N87-24241 #
GPO-74-470 N87-24243 #
GRI-86/0166 N87-23972 #
GRI-86/0195 N87-23742 #
GRI-87/0019 N87-24245 #
GRI-87/0077 N87-24043 #
H-REPT-100-189 N87-24241 #
H-1314 N87-23616* #
H-1318 N87-23619* #
H-1355 N87-23995* #
H-1382 N87-23994* #
HAC-REF-E9915 N87-23946 #
HSER-11058 N87-23615* #
ICASE-87-31 N87-24122* #
ICASE-87-34 N87-24107* #
IFSR-261 N87-23920 #
IIHR-307 N87-23924 #
INTEGRAL-35 N87-24127 #
INTEGRAL-46 N87-24099 #
IPPJ-AM-49 N87-24198 #
ISBN-0-947767-58-4 N87-23613 #
ISBN-92-835-0394-5 N87-23633 #
ISBN-92-835-0409-7 N87-23609 #
ISBN-92-835-1544-7 N87-24070 #
ISBN-92-835-1547-1 N87-23859 #
ISL-CO-225/86 N87-23935 #
ISL-CO-226/86 N87-23686 #
ISSN-0073-0300 N87-24008 #
ISSN-0178-8094 N87-23602 #
ISSN-0208-5658 N87-23999 #
ISSN-0348-7539 N87-24185 #
ISSN-0751-1337 N87-24111 #
ISSN-0751-1345 N87-24086 #
JE535 N87-23665 #
JE535 N87-23666 #
JIAA-TR-75 N87-23627* #
JM/85-3 N87-23927* #
JM/87-4 N87-23925* #
JPL-TDA-PR-42-89 N87-23628* #
JPRS-UEQ-87-005 N87-23570 #
L-16184 N87-24161* #
L-16192 N87-23597* #
L-16226 N87-23586* #
L-16243 N87-23614* #
L-16248 N87-23593* #
L-16259 N87-23594* #
L-16287 N87-23592* #
LA-TR-87-5 N87-24165 #
LA-UR-86-4331 N87-24380 #
LA-UR-87-72 N87-23952 #
LA-UR-87-416 N87-23673 #
LA-UR-87-502 N87-23896 #
LA-UR-87-517 N87-23897 #
LA-UR-87-571 N87-24011 #
LA-UR-87-572 N87-24014 #
LA-UR-87-709 N87-24379 #
LA-UR-87-805 N87-23948 #
LA-UR-87-810 N87-23877 #
LA-UR-87-820 N87-24244 #
LA-UR-87-870 N87-24196 #
LA-UR-87-925 N87-23956 #
LA-UR-87-1096 N87-24129 #
LA-10720-MS N87-24170 #
LA-10829-MS N87-23930 #
LA-10884-MS N87-23949 #
LA-10905-MS N87-23898 #
LA-10926-MS N87-24155 #
LA-10959-MS N87-23725 #
LBL-21345-REV N87-23669 #
LBL-22353 N87-23735 #
LBL-22460 N87-24116 #
LBL-22581 N87-24206 #
LBL-22879 N87-23817 #
LBL-22883 N87-24236 #
LBL-22948 N87-24117 #
LBL-23016 N87-24210 #
LBL-23119 N87-24213 #
MDHC-150-V-1003 N87-23596* #
MIT/LCS/TM-318 N87-23853 #
MIT/LCS/TM-320 N87-24109 #
MIT/LCS/TR-374 N87-24110 #
MITT-31 N87-24008 #
MLM-3393(OP) N87-23722 #
MLM-3413(OP) N87-23754 #
MTI-87TR15-PT-2 N87-23974 #
MTI-87TR16-PT-3 N87-23975 #
MTI-87TR17-PT-4 N87-23973 #
MTR-87W21 N87-23607* #
NADC-86117-60 N87-23743 #
NADC-87042-60-VOL-1 N87-23705 #
NADC-87042-60-VOL-2 N87-23706 #
NAE-AN-40 N87-23990 #
NAS 1.15:85015 N87-23671* #
NAS 1.15:86593 N87-23893* #
NAS 1.15:86790 N87-23616* #
NAS 1.15:86793 N87-23619* #
NAS 1.15:86813 N87-23995* #
NAS 1.15:86856 N87-24064* #
NAS 1.15:87094 N87-23598* #
NAS 1.15:87821 N87-24096* #
NAS 1.15:87822 N87-24039* #
NAS 1.15:88276 N87-23994* #
NAS 1.15:88344 N87-24378* #
NAS 1.15:88371 N87-24146* #
NAS 1.15:88375 N87-23595* #
NAS 1.15:88896 N87-23933* #
NAS 1.15:88926 N87-24132* #
NAS 1.15:88931 N87-23934* #
NAS 1.15:88960 N87-24006* #
NAS 1.15:89051 N87-23687* #
NAS 1.15:89087 N87-23991* #
NAS 1.15:89102 N87-23594* #
NAS 1.15:89149 N87-24160* #
NAS 1.15:89152 N87-23752* #
NAS 1.15:89192 N87-23675* #
NAS 1.15:89193 N87-24392* #
NAS 1.15:89220 N87-24010* #
NAS 1.15:89346 N87-24377* #
NAS 1.15:89356 N87-23962* #
NAS 1.15:89411 N87-24391* #
NAS 1.15:89422 N87-23632* #
NAS 1.15:89442 N87-24156* #
NAS 1.15:89458 N87-23584* #
NAS 1.15:89464 N87-24145* #
NAS 1.15:89624 N87-23591* #
NAS 1.15:89825 N87-23685* #
NAS 1.15:89862 N87-23718* #
NAS 1.15:89863 N87-23674* #
NAS 1.15:89869 N87-23900* #
NAS 1.15:89895 N87-23984* #
NAS 1.15:89897 N87-23978* #
NAS 1.15:89902 N87-23902* #
NAS 1.15:89905 N87-23750* #
NAS 1.15:89911 N87-23903* #
NAS 1.15:89913 N87-24026* #
NAS 1.15:89916 N87-23693* #
NAS 1.15:89918 N87-23664* #
NAS 1.15:89922 N87-23901* #
NAS 1.15:89926 N87-23690* #
NAS 1.15:89927 N87-24029* #
NAS 1.15:89929 N87-23987* #
NAS 1.15:89931 N87-24007* #
NAS 1.15:89951 N87-24063* #
NAS 1.15:100107 N87-23624* #
NAS 1.15:100109 N87-23692* #
NAS 1.15:100113 N87-23821* #
NAS 1.15:100114 N87-23626* #
NAS 1.15:100115 N87-23623* #
NAS 1.15:100118 N87-23625* #
NAS 1.15:100123 N87-23691* #
NAS 1.15:100307 N87-23959* #
NAS 1.21:4305 N87-24390* #
NAS 1.26:4074 N87-23607* #
NAS 1.26:178252 N87-23617* #
NAS 1.26:178279 N87-23663* #
NAS 1.26:178284 N87-23596* #
NAS 1.26:178302 N87-24122* #
NAS 1.26:178307 N87-24107* #
NAS 1.26:178310 N87-24162* #
NAS 1.26:178311 N87-24040* #
NAS 1.26:179587 N87-23695* #
NAS 1.26:179587 N87-23696* #
NAS 1.26:179589 N87-23615* #
NAS 1.26:179594 N87-23622* #
NAS 1.26:179611 N87-23969* #
NAS 1.26:179620 N87-23977* #
NAS 1.26:179624 N87-23729* #
NAS 1.26:180394 N87-24211* #
NAS 1.26:180406 N87-24103* #
NAS 1.26:180418 N87-23979* #
NAS 1.26:180478 N87-23627* #
NAS 1.26:180587 N87-23925* #
NAS 1.26:180695 N87-24042* #
NAS 1.26:180938 N87-24038* #
NAS 1.26:180941 N87-23916* #
NAS 1.26:180962 N87-24032* #
NAS 1.26:180983 N87-24031* #
NAS 1.26:180984 N87-24012* #
NAS 1.26:180995 N87-24157* #
NAS 1.26:180996 N87-24166* #
NAS 1.26:181005 N87-24018* #
NAS 1.26:181010 N87-23828* #
NAS 1.26:181016 N87-23670* #
NAS 1.26:181018 N87-23589* #
NAS 1.26:181021 N87-24381* #
NAS 1.26:181026 N87-23858* #
NAS 1.26:181027 N87-23717* #
NAS 1.26:181051 N87-23856* #
NAS 1.26:181063 N87-24387* #
NAS 1.26:181065 N87-23980* #
NAS 1.55:2464 N87-24247* #
NAS 1.55:2466 N87-24266* #
NAS 1.60:1848 N87-23921* #
NAS 1.60:1850 N87-23936* #
NAS 1.60:2660-PT-1 N87-23597* #
NAS 1.60:2689 N87-24161* #
NAS 1.60:2691 N87-23614* #
NAS 1.60:2692 N87-23662* #
NAS 1.60:2706 N87-23586* #
NAS 1.60:2717 N87-23593* #
NAS 1.60:2733 N87-23592* #
NAS 1.71:ARC-11652-1 N87-23737* #
NAS 1.71:LAR-13689-1 N87-23941* #
NAS 1.77:20019 N87-23583* #
NAS 1.179012 N87-24184* #
NASA-CASE-ARC-11533-1 N87-23751*
NASA-CASE-ARC-11633-1 N87-23631*
NASA-CASE-ARC-11643-1-SB N87-23696*
NASA-CASE-ARC-11652-1 N87-23737* #
NASA-CASE-GSC-12773-2 N87-23904*
NASA-CASE-LAR-13100-1 N87-23962*
NASA-CASE-LAR-13196-1 N87-23983*
NASA-CASE-LAR-13436-1-CU N87-23587* #
NASA-CASE-LAR-13597-1-CU N87-23713* #
NASA-CASE-LAR-13630-1 N87-23630* #
NASA-CASE-LAR-13689-1-NP N87-23941* #
NASA-CASE-LEW-14072-3 N87-23736*
NASA-CASE-MFS-28087-1 N87-23944*

NASA-CASE-MSC-20797-1 ..... N87-23981*

NASA-CASE-NPO-15482-1 ..... N87-23970*
NASA-CASE-NPO-16433-1 ..... N87-23961*
NASA-CASE-NPO-16467-1-CU N87-23679*
NASA-CASE-NPO-16542-1-CU N87-23960*

NASA-CP-2464 ..... N87-24247* #
NASA-CP-2466 ..... N87-24266* #

NASA-CR-4074 ..... N87-23607* #
NASA-CR-178252 ..... N87-23617* #
NASA-CR-178279 ..... N87-23663* #
NASA-CR-178284 ..... N87-23596* #
NASA-CR-178302 ..... N87-24122* #
NASA-CR-178307 ..... N87-24107* #
NASA-CR-178310 ..... N87-24162* #
NASA-CR-178311 ..... N87-24040* #
NASA-CR-179012 ..... N87-24184* #
NASA-CR-179587 ..... N87-23695* #
NASA-CR-179587 ..... N87-23696* #
NASA-CR-179589 ..... N87-23615* #
NASA-CR-179594 ..... N87-23622* #
NASA-CR-179611 ..... N87-23969* #
NASA-CR-179620 ..... N87-23977* #
NASA-CR-179624 ..... N87-23729* #
NASA-CR-180394 ..... N87-24211* #
NASA-CR-180408 ..... N87-24103* #
NASA-CR-180418 ..... N87-23979* #
NASA-CR-180478 ..... N87-23627* #
NASA-CR-180587 ..... N87-23925* #
NASA-CR-180695 ..... N87-24042* #
NASA-CR-180938 ..... N87-24038* #
NASA-CR-180941 ..... N87-23916* #
NASA-CR-180962 ..... N87-24032* #
NASA-CR-180983 ..... N87-24031* #
NASA-CR-180984 ..... N87-24012* #
NASA-CR-180995 ..... N87-24157* #
NASA-CR-180996 ..... N87-24166* #
NASA-CR-181005 ..... N87-24018* #
NASA-CR-181010 ..... N87-23828* #
NASA-CR-181016 ..... N87-23670* #
NASA-CR-181018 ..... N87-23589* #
NASA-CR-181021 ..... N87-24381* #
NASA-CR-181026 ..... N87-23858* #
NASA-CR-181027 ..... N87-23717* #
NASA-CR-181051 ..... N87-23856* #
NASA-CR-181063 ..... N87-24387* #
NASA-CR-181065 ..... N87-23980* #

NASA-SP-4305 ..... N87-24390* #

NASA-TM-85015 ..... N87-23671* #
NASA-TM-86593 ..... N87-23893* #
NASA-TM-86790 ..... N87-23616* #
NASA-TM-86793 ..... N87-23619* #
NASA-TM-86813 ..... N87-23995* #
NASA-TM-86856 ..... N87-24064* #
NASA-TM-87094 ..... N87-23598* #
NASA-TM-87821 ..... N87-24098* #
NASA-TM-87822 ..... N87-24039* #
NASA-TM-88276 ..... N87-23994* #
NASA-TM-88344 ..... N87-24378* #
NASA-TM-88371 ..... N87-24146* #
NASA-TM-88375 ..... N87-23595* #
NASA-TM-88896 ..... N87-23933* #
NASA-TM-88926 ..... N87-24132* #
NASA-TM-88931 ..... N87-23934* #
NASA-TM-88960 ..... N87-24006* #
NASA-TM-89051 ..... N87-23687* #
NASA-TM-89087 ..... N87-23991* #
NASA-TM-89102 ..... N87-23594* #
NASA-TM-89149 ..... N87-24160* #
NASA-TM-89152 ..... N87-23752* #
NASA-TM-89192 ..... N87-23675* #
NASA-TM-89193 ..... N87-24392* #
NASA-TM-89220 ..... N87-24010* #
NASA-TM-89346 ..... N87-24377* #
NASA-TM-89356 ..... N87-23962* #
NASA-TM-89411 ..... N87-24391* #
NASA-TM-09422 ..... N87-23632* #
NASA-TM-89442 ..... N87-24156* #
NASA-TM-89458 ..... N87-23584* #
NASA-TM-89464 ..... N87-24145* #
NASA-TM-89824 ..... N87-23591* #
NASA-TM-89825 ..... N87-23685* #
NASA-TM-89862 ..... N87-23718* #
NASA-TM-89863 ..... N87-23674* #
NASA-TM-89869 ..... N87-23900* #
NASA-TM-89895 ..... N87-23984* #
NASA-TM-89897 ..... N87-23978* #
NASA-TM-89902 ..... N87-23902* #
NASA-TM-89905 ..... N87-23750* #
NASA-TM-89911 ..... N87-23903* #
NASA-TM-89913 ..... N87-24026* #
NASA-TM-89916 ..... N87-23693* #

NASA-TM-89918 ..... N87-23664* #
NASA-TM-89922 ..... N87-23901* #
NASA-TM-89926 ..... N87-23690* #
NASA-TM-89927 ..... N87-24029* #
NASA-TM-89929 ..... N87-23987* #
NASA-TM-89931 ..... N87-24007* #
NASA-TM-89951 ..... N87-24063* #
NASA-TM-100107 ..... N87-23624* #
NASA-TM-100109 ..... N87-23692* #
NASA-TM-100113 ..... N87-23821* #
NASA-TM-100114 ..... N87-23626* #
NASA-TM-100115 ..... N87-23623* #
NASA-TM-100118 ..... N87-23625* #
NASA-TM-100123 ..... N87-23691* #
NASA-TM-100307 ..... N87-23959* #

NASA-TP-1848 ..... N87-23921* #
NASA-TP-1850 ..... N87-23936* #
NASA-TP-2660-PT-1 ..... N87-23597* #
NASA-TP-2689 ..... N87-24161* #
NASA-TP-2691 ..... N87-23614* #
NASA-TP-2692 ..... N87-23662* #
NASA-TP-2706 ..... N87-23586* #
NASA-TP-2717 ..... N87-23593* #
NASA-TP-2733 ..... N87-23592* #

NASA-TT-20019 ..... N87-23583* #

NCAR-TN/STR-273 ..... N87-24053 #

NCEL-CR-87.006 ..... N87-23963 #

NEPRF-CR-86-06 ..... N87-24048 #

NIPER-224 ..... N87-23755 #

NMAB-421 ..... N87-23971 #

NOAA-TM-ERL-AOML-64 ..... N87-24060 #

NOAA-TM-ERL-SEL-74 ..... N87-24384 #

NORDA-168 ..... N87-24061 #

NOSC/TD-1042 ..... N87-23954 #

NOSC/TR-1143 ..... N87-23822 #

NOTA-INTERNA-874 ..... N87-24163 #

NPS52-87-006 ..... N87-24097 #
NPS55-86-022 ..... N87-24150 #
NPS72-86-002 ..... N87-24025 #

NRC-26190 ..... N87-23990 #

NRL-MR-5911 ..... N87-24225 #

NSMRL-MEMO-87-2 ..... N87-24089 #

NSMRL-MR-87-1 ..... N87-24083 #

NSWC/TR-86-26 ..... N87-23719 #
NSWC/TR-86-336 ..... N87-23814 #

NTSB-AAR-87-04 ..... N87-23604 #

NTSB/ARC-87/01 ..... N87-23605 #
NTSB/ARC-87/02 ..... N87-23603 #

NTSB/ARG-87/02 ..... N87-23606 #

NUSC-TR-7849 ..... N87-23886 #

ORNL-6350 ..... N87-23986 #
ORNL-6358 ..... N87-23697 #
ORNL-6365 ..... N87-24234 #

ORNL/SUB-86-97366/1 ..... N87-23966 #

ORNL/SUB/81-7762/4 AND 01 ..... N87-23917 #

ORNL/TM-10194 ..... N87-24021 #
ORNL/TM-10285 ..... N87-23958 #
ORNL/TM-10306 ..... N87-23740 #
ORNL/TM-10320 ..... N87-24233 #
ORNL/TM-10323 ..... N87-24093 #
ORNL/TM-10351 ..... N87-23965 #
ORNL/TM-10383 ..... N87-24100 #
ORNL/TM-10388 ..... N87-24121 #

PB87-154597 ..... N87-24013 #
PB87-154613 ..... N87-24060 #
PB87-155495 ..... N87-24227 #
PB87-157517 ..... N87-24384 #
PB87-157699 ..... N87-24238 #

PB87-158556 ..... N87-24381* #
PB87-160828 ..... N87-23605 #
PB87-162533 ..... N87-24056 #
PB87-162574 ..... N87-24385 #
PB87-162582 ..... N87-24386 #
PB87-176327 ..... N87-24043 #
PB87-178042 ..... N87-23972 #
PB87-178059 ..... N87-23742 #
PB87-178083 ..... N87-24245 #
PB87-183992 ..... N87-23603 #
PB87-194791 ..... N87-23606 #
PB87-910404 ..... N87-23604 #

PNL-SA-14385 ..... N87-24383 #
PNL-SA-14591 ..... N87-24143 #

PNL-6105 ..... N87-24051 #
PNL-6128-VOL-1 ..... N87-24019 #
PNL-6143 ..... N87-23985 #
PNL-6188 ..... N87-24058 #

PWA-5968-47 ..... N87-23622* #

Q-2 ..... N87-24211* #

QPR-6 ..... N87-23756 #

QTR-2 ..... N87-23748 #

R-8610 ..... N87-23617* #

RADC-TR-86-151 ..... N87-23823 #
RADC-TR-86-184 ..... N87-23875 #

REPT-43/1986 ..... N87-23999 #
REPT-87-B-0266 ..... N87-24098* #
REPT-87-B-0289 ..... N87-23671* #
REPT-87-B-0293 ..... N87-24039* #
REPT-87-1 ..... N87-24066 #
REPT-87-909-SUPER-R1 ..... N87-24200 #
REPT-87B0055 ..... N87-24247* #
REPT-1986-3 ..... N87-24221 #

RFP-3906 ..... N87-23939 #

RITRC-002 ..... N87-23890 #
RITRC-009 ..... N87-23846 #
RITRC-010 ..... N87-23892 #
RITRC-011 ..... N87-23891 #

RU-TR-165-MAE-F ..... N87-23909 #

R86AEB565 ..... N87-23816 #

S-REPT-100-87 ..... N87-24240 #
S-REPT-100-87 ..... N87-24243 #

SAE-PAPER-870450 ..... N87-23902* #

SAND-84-1341 ..... N87-24171 #
SAND-85-2604 ..... N87-24059 #
SAND-85-2873 ..... N87-23741 #
SAND-86-0594 ..... N87-23993 #
SAND-86-0784 ..... N87-23702 #
SAND-86-1169C ..... N87-23733 #
SAND-86-1222C ..... N87-24016 #
SAND-86-1290C ..... N87-23734 #
SAND-86-1299C ..... N87-23724 #
SAND-86-1431C ..... N87-24005 #
SAND-86-1589C ..... N87-24002 #
SAND-86-1607C ..... N87-24004 #
SAND-86-1623 ..... N87-24017 #
SAND-86-1785C ..... N87-23841 #
SAND-86-1904C ..... N87-23883 #
SAND-86-2169C ..... N87-23731 #
SAND-86-2196 ..... N87-23857 #
SAND-86-2281C ..... N87-23918 #
SAND-86-2347C ..... N87-23732 #
SAND-86-2535C ..... N87-23703 #
SAND-86-2564 ..... N87-24102 #
SAND-86-2714C ..... N87-23723 #
SAND-86-2904 ..... N87-23899 #
SAND-87-0011 ..... N87-23843 #
SAND-87-0014C ..... N87-24003 #
SAND-87-0050 ..... N87-24135 #
SAND-87-0077C ..... N87-23894 #
SAND-87-0206 ..... N87-24130 #
SAND-87-0295C ..... N87-23747 #
SAND-87-0296C ..... N87-23895 #
SAND-87-0336C ..... N87-23992 #
SAND-87-0354 ..... N87-23967 #
SAND-87-0369 ..... N87-24094 #
SAND-87-0386C ..... N87-24212 #
SAND-87-0402C ..... N87-23738 #
SAND-87-0582C ..... N87-23943 #
SAND-87-0691C ..... N87-23748 #

SAND-87-0823C ..... N87-24105 #
SAND-87-7100C ..... N87-23881 #
SAND-87-8205 ..... N87-24181 #
SAND-87-8208 ..... N87-23726 #
SAND-87-8213 ..... N87-23714 #

SAPR-4 ..... N87-24012* #
SAPR-10 ..... N87-24387* #
SAPR-11 ..... N87-24387* #

SASR-1 ..... N87-24038* #

SCC-86-01 ..... N87-23884 #

SD-TR-87-03-VOL-1 ..... N87-23849 #
SD-TR-87-12 ..... N87-24034 #

SERI/CP-233-2959 ..... N87-24062 #

SERI/SP-231-2550 ..... N87-23753 #
SERI/SP-255-3046 ..... N87-24024 #
SERI/SP-272-3008 ..... N87-24027 #

SERI/STR-217-3002 ..... N87-24022 #

SERI/TP-250-3119 ..... N87-24023 #

SGD-509-PT-1 ..... N87-24385 #
SGD-509-PT-2 ..... N87-24386 #

SR-1 ..... N87-23855* #
SR-2 ..... N87-23938 #
SR-3 ..... N87-23624 #
SR-18 ..... N87-23707 #
SR-19 ..... N87-24035 #
SR-20 ..... N87-24037 #
SR-21 ..... N87-23708 #

SWRI-06-8972 ..... N87-23720 #

TGAL-86-9 ..... N87-23824 #

THC-02GH87021A ..... N87-23672 #

TR-1-JSSC ..... N87-24239 #
TR-2 ..... N87-23890 #
TR-9 ..... N87-23848 #
TR-10 ..... N87-23892 #
TR-11 ..... N87-23891 #
TR-35 ..... N87-24216 #
TR-40 ..... N87-23716 #
TR-72 ..... N87-24147 #
TR-86-1 ..... N87-24138 #
TR-87-001 ..... N87-24140 #
TR-148 ..... N87-24148 #
TR-756 ..... N87-23851 #
TR-0066(6940-06)-10-VOL-1 ..... N87-23849 #
TR-0066(6940-06)-12 ..... N87-24034 #

TRITA-EPP-86-11 ..... N87-24185 #

TRITA-NA-8505 ..... N87-24127 #
TRITA-NA-8506 ..... N87-24091 #
TRITA-NA-8518 ..... N87-24099 #
TRITA-NA-8601 ..... N87-24114 #

TRW-43543-6011-UE-00 ..... N87-23678 #

TSC-W41-405/KKS ..... N87-23846 #

UCB/ERL-M-86/94 ..... N87-24191 #
UCB/ERL-M-87/14 ..... N87-24190 #

UCB/ERL-M86/58 ..... N87-24230 #

UCID-20907 ..... N87-23704 #
UCID-20978 ..... N87-24081 #
UCID-21029 ..... N87-23931 #

UCRL-15900 ..... N87-24192 #
UCRL-94113 ..... N87-24104 #
UCRL-94639 ..... N87-24194 #
UCRL-94736 ..... N87-24222 #
UCRL-94740 ..... N87-23955 #
UCRL-94746 ..... N87-24226 #
UCRL-94835 ..... N87-24154 #
UCRL-95133 ..... N87-24232 #
UCRL-95464 ..... N87-23976 #
UCRL-95580 ..... N87-24041 #
UCRL-95914 ..... N87-24052 #
UCRL-95941 ..... N87-23711 #
UCRL-95999 ..... N87-24183 #
UCRL-96074 ..... N87-23842 #
UCRL-96190 ..... N87-24144 #
UCRL-96256 ..... N87-24209 #

UILU-ENG-86-4004 ..... N87-23917 #
UILU-ENG-87-2212 ..... N87-23889 #
UILU-ENG-87-2217 ..... N87-23852 #
UILU-ENG-87-2219 ..... N87-24096 #

US-PATENT-APPL-SN-003676 ..... N87-23587* #
US-PATENT-APPL-SN-006199 ..... N87-23713* #
US-PATENT-APPL-SN-008242 ..... N87-23737* #
US-PATENT-APPL-SN-008895 ..... N87-23630* #
US-PATENT-APPL-SN-526739 ..... N87-23970*
US-PATENT-APPL-SN-641147 ..... N87-23751*
US-PATENT-APPL-SN-729704 ..... N87-23983*
US-PATENT-APPL-SN-771537 ..... N87-23981*
US-PATENT-APPL-SN-781812 ..... N87-23960*
US-PATENT-APPL-SN-790594 ..... N87-23961*
US-PATENT-APPL-SN-805010 ..... N87-23944*
US-PATENT-APPL-SN-809851 ..... N87-23904*
US-PATENT-APPL-SN-831377 ..... N87-23982*
US-PATENT-APPL-SN-834977 ..... N87-23736*
US-PATENT-APPL-SN-836648 ..... N87-23879*
US-PATENT-APPL-SN-846439 ..... N87-23631*
US-PATENT-APPL-SN-901496 ..... N87-23696*
US-PATENT-APPL-SN-929669 ..... N87-23941* #

US-PATENT-CLASS-60-634 ..... N87-23983*
US-PATENT-CLASS-60-638 ..... N87-23983*
US-PATENT-CLASS-62-514-R N87-23962*
US-PATENT-CLASS-89-1.14 ..... N87-23983*
US-PATENT-CLASS-136-249 ..... N87-23879*
US-PATENT-CLASS-136-255 ..... N87-23879*
US-PATENT-CLASS-156-87 ..... N87-23981*
US-PATENT-CLASS-156-286 ..... N87-23981*
US-PATENT-CLASS-156-289 ..... N87-23981*
US-PATENT-CLASS-156-298 ..... N87-23981*
US-PATENT-CLASS-156-307.1 ..... N87-23981*
US-PATENT-CLASS-156-307.3 ..... N87-23981*
US-PATENT-CLASS-156-307.7 ..... N87-23981*
US-PATENT-CLASS-250-238 ..... N87-23982*
US-PATENT-CLASS-250-352 ..... N87-23982*
US-PATENT-CLASS-290-1-R N87-23904*
US-PATENT-CLASS-310-15 ..... N87-23904*
US-PATENT-CLASS-310-30 ..... N87-23904*
US-PATENT-CLASS-310-306 ..... N87-23970*
US-PATENT-CLASS-337-393 ..... N87-23970*
US-PATENT-CLASS-350-3.73 ..... N87-23960*
US-PATENT-CLASS-350-3.81 ..... N87-23960*
US-PATENT-CLASS-357-30 ..... N87-23879*
US-PATENT-CLASS-357-35 ..... N87-23879*
US-PATENT-CLASS-372-18 ..... N87-23960*
US-PATENT-CLASS-372-43 ..... N87-23960*
US-PATENT-CLASS-372-68 ..... N87-23961*
US-PATENT-CLASS-372-81 ..... N87-23961*
US-PATENT-CLASS-372-103 ..... N87-23960*
US-PATENT-CLASS-373-10 ..... N87-23944*
US-PATENT-CLASS-373-15 ..... N87-23944*
US-PATENT-CLASS-416-114 ..... N87-23631*
US-PATENT-CLASS-416-158 ..... N87-23631*
US-PATENT-CLASS-423-276 ..... N87-23696*
US-PATENT-CLASS-423-284 ..... N87-23696*
US-PATENT-CLASS-428-421 ..... N87-23736*
US-PATENT-CLASS-428-422 ..... N87-23736*
US-PATENT-CLASS-428-447 ..... N87-23736*
US-PATENT-CLASS-428-473.5 ..... N87-23736*
US-PATENT-CLASS-428-702 ..... N87-23736*
US-PATENT-CLASS-548-413 ..... N87-23751*

US-PATENT-4,664,980 ..... N87-23736*
US-PATENT-4,665,277 ..... N87-23879*
US-PATENT-4,665,334 ..... N87-23970*
US-PATENT-4,669,354 ..... N87-23983*
US-PATENT-4,669,958 ..... N87-23631*
US-PATENT-4,670,565 ..... N87-23751*
US-PATENT-4,672,202 ..... N87-23962*
US-PATENT-4,675,583 ..... N87-23904*
US-PATENT-4,676,853 ..... N87-23981*
US-PATENT-4,676,962 ..... N87-23696*
US-PATENT-4,677,629 ..... N87-23960*
US-PATENT-4,677,636 ..... N87-23961*
US-PATENT-4,677,642 ..... N87-23944*

USAETL-R-092 ..... N87-23827 #

USAFETAC/DS-81-060 ..... N87-24047 #

USAFSAM-TR-85-56 ..... N87-24067 #
USAFSAM-TR-86-31 ..... N87-24084 #

USCG-D-29-85-VOL-2 ..... N87-23600 #
USCG-D-29-85-VOL-3 ..... N87-23601 #

USGS/OFR-86/010 ..... N87-24013 #

UVA/525415/EE87/104 ..... N87-23854 #

WP-338-REV ..... N87-24153 #

WSU-SDL-0106-FTR ..... N87-23745 #

FEDERAL REGIONAL DEPOSITORY LIBRARIES

ALABAMA

AUBURN UNIV. AT MONTGOMERY LIBRARY
Documents Department
Montgomery, AL 36193
(205) 271-9650

UNIV. OF ALABAMA LIBRARY
Documents Dept.-Box S
University, AL 35486
(205) 348-6046

ARIZONA

DEPT. OF LIBRARY, ARCHIVES AND PUBLIC RECORDS
Third Floor—State Cap.
1700 West Washington
Phoenix, AZ 85007
(602) 255-4121

UNIVERSITY OF ARIZONA LIB.
Government Documents Dept.
Tucson, AZ 85721
(602) 621-6433

ARKANSAS

ARKANSAS STATE LIBRARY
One Capitol Mall
Little Rock, AR 72201
(501) 371-2326

CALIFORNIA

CALIFORNIA STATE LIBRARY
Govt. Publications Section
P.O. Box 2037
Sacramento, CA 95809
(916) 324-4863

COLORADO

UNIV OF COLORADO LIB.
Government Pub. Division
Campus Box 184
Boulder, CO 80309
(303) 492-8834

DENVER PUBLIC LIBRARY
Govt. Pub. Department
1357 Broadway
Denver, CO 80203
(303) 571-2131

CONNECTICUT

CONNECTICUT STATE LIBRARY
Government Documents Unit
231 Capitol Avenue
Hartford, CT 06106
(203) 566-7029

FLORIDA

UNIV. OF FLORIDA LIBRARIES
Library West
Documents Department
Gainesville, FL 32611
(904) 392-0367

GEORGIA

UNIV. OF GEORGIA LIBRARIES
Government Reference Dept.
Athens, GA 30602
(404) 542-8949

HAWAII

UNIV. OF HAWAII LIBRARY
Govt. Documents Collection
2550 The Mall
Honolulu, HI 96822
(808) 948-8230

IDAHO

UNIV. OF IDAHO LIBRARY
Documents Section
Moscow, ID 83843
(208) 885-6344

ILLINOIS

ILLINOIS STATE LIBRARY
Information Services Branch
Centennial Building
Springfield, IL 62756
(217) 782-5185

INDIANA

INDIANA STATE LIBRARY
Serials Documents Section
140 North Senate Avenue
Indianapolis, IN 46204
(317) 232-3686

IOWA

UNIV. OF IOWA LIBRARIES
Govt. Documents Department
Iowa City, IA 52242
(319) 353-3318

KANSAS

UNIVERSITY OF KANSAS
Doc. Collect—Spencer Lib.
Lawrence, KS 66045-2800
(913) 864-4662

KENTUCKY

UNIV. OF KENTUCKY LIBRARIES
Govt. Pub. Department
Lexington, KY 40506-0039
(606) 257-3139

LOUISIANA

LOUISIANA STATE UNIVERSITY
Middleton Library
Govt. Docs. Dept.
Baton Rouge, LA 70803
(504) 388-2570

LOUISIANA TECHNICAL UNIV. LIBRARY
Documents Department
Ruston, LA 71272-0046
(318) 257-4962

MAINE

UNIVERSITY OF MAINE
Raymond H. Fogler Library
Tri-State Regional Documents Depository
Orono, ME 04469
(207) 581-1680

MARYLAND

UNIVERSITY OF MARYLAND
McKeldin Lib.—Doc. Div.
College Park, MD 20742
(301) 454-3034

MASSACHUSETTS

BOSTON PUBLIC LIBRARY
Government Docs. Dept.
Boston, MA 02117
(617) 536-5400 ext.226

MICHIGAN

DETROIT PUBLIC LIBRARY
Sociology Department
5201 Woodward Avenue
Detroit, MI 48202-4093
(313) 833-1409

MICHIGAN STATE LIBRARY
P.O. Box 30007
Lansing, MI 48909
(517) 373-1593

MINNESOTA

UNIVERSITY OF MINNESOTA
Government Pubs. Division
409 Wilson Library
309 19th Avenue South
Minneapolis, MN 55455
(612) 373-7870

MISSISSIPPI

UNIV. OF MISSISSIPPI LIB.
Documents Department
University, MS 38677
(601) 232-5857

MONTANA

UNIV. OF MONTANA
Mansfield Library
Documents Division
Missoula, MT 59812
(406) 243-6700

NEBRASKA

UNIVERSITY OF NEBRASKA - LINCOLN
Love Library
Documents Department
Lincoln, NE 68588-0410
(402) 472-2562

NEVADA

UNIVERSITY OF NEVADA LIB.
Govt. Pub. Department
Reno, NV 89557-0044
(702) 784-6579

NEW JERSEY

NEWARK PUBLIC LIBRARY
5 Washington Street
Newark, NJ 07101-0630
(201) 733-7812

NEW MEXICO

UNIVERSITY OF NEW MEXICO
Zimmerman Library
Government Pub. Dept.
Albuquerque, NM 87131
(505) 277-5441

NEW MEXICO STATE LIBRARY
Reference Department
325 Don Gaspar Avenue
Santa Fe, NM 87503
(505) 827-3826

NEW YORK

NEW YORK STATE LIBRARY
Empire State Plaza
Albany, NY 12230
(518) 474-5563

NORTH CAROLINA

UNIVERSITY OF NORTH CAROLINA AT CHAPEL HILL
Davis Library
BA/SS Documents Division
Chapel Hill, NC 27515
(919) 962-1151

NORTH DAKOTA

UNIVERSITY OF NORTH DAKOTA
Chester Fritz Library
Documents Department
Grand Forks, ND 58202
(701) 777-4629
In cooperation with North Dakota State Univ. Library

OHIO

STATE LIBRARY OF OHIO
Documents Department
65 South Front Street
Columbus, OH 43266-0334
(614) 462-7051

OKLAHOMA

OKLAHOMA DEPT. OF LIB.
Government Documents
200 NE 18th Street
Oklahoma City, OK 73105
(405) 521-2502, ext. 252

OKLAHOMA STATE UNIV. LIB.
Documents Department
Stillwater, OK 74078
(405) 624-6546

OREGON

PORTLAND STATE UNIV. LIB.
Documents Department
P.O. Box 1151
Portland, OR 97207
(503) 229-3673

PENNSYLVANIA

STATE LIBRARY OF PENN.
Government Pub. Section
P.O. Box 1601
Harrisburg, PA 17105
(717) 787-3752

TEXAS

TEXAS STATE LIBRARY
Public Services Department
P.O. Box 12927—Cap. Sta.
Austin, TX 78711
(512) 475-2996

TEXAS TECH. UNIV. LIBRARY
Govt. Documents Department
Lubbock, TX 79409
(806) 742-2268

UTAH

UTAH STATE UNIVERSITY
Merrill Library, U.M.C. 30
Logan, UT 84322
(801) 750-2682

VIRGINIA

UNIVERSITY OF VIRGINIA
Alderman Lib.—Public Doc.
Charlottesville, VA 22903-2498
(804) 924-3133

WASHINGTON

WASHINGTON STATE LIBRARY
Documents Section
Olympia, WA 98504
(206) 753-4027

WEST VIRGINIA

WEST VIRGINIA UNIV. LIB.
Documents Department
Morgantown, WV 26506-6069
(304) 293-3640

WISCONSIN

MILWAUKEE PUBLIC LIBRARY
814 West Wisconsin Avenue
Milwaukee, WI 53233
(414) 278-3065

ST. HIST LIB. OF WISCONSIN
Government Pub. Section
816 State Street
Madison, WI 53706
(608) 262-4347

WYOMING

WYOMING STATE LIBRARY
Supreme Ct. & Library Bld.
Cheyenne, WY 82002
(307) 777-5919

National Aeronautics and
Space Administration
Code NTT-4
Washington, D.C.
20546

Official Business

Penalty for Private Use, $300

SPECIAL FOURTH-CLASS RATE
POSTAGE & FEES PAID
NASA
PERMIT No. G 27

NASA

POSTMASTER: If Undeliverable (Section 158
Postal Manual) Do Not Return